Regional Geology Reviews

Megh Raj Dhital

Geology of the Nepal Himalaya

Regional Perspective of the Classic Collided Orogen

Springer

Regional Geology Reviews

For further volumes:
http://www.springer.com/series/8643

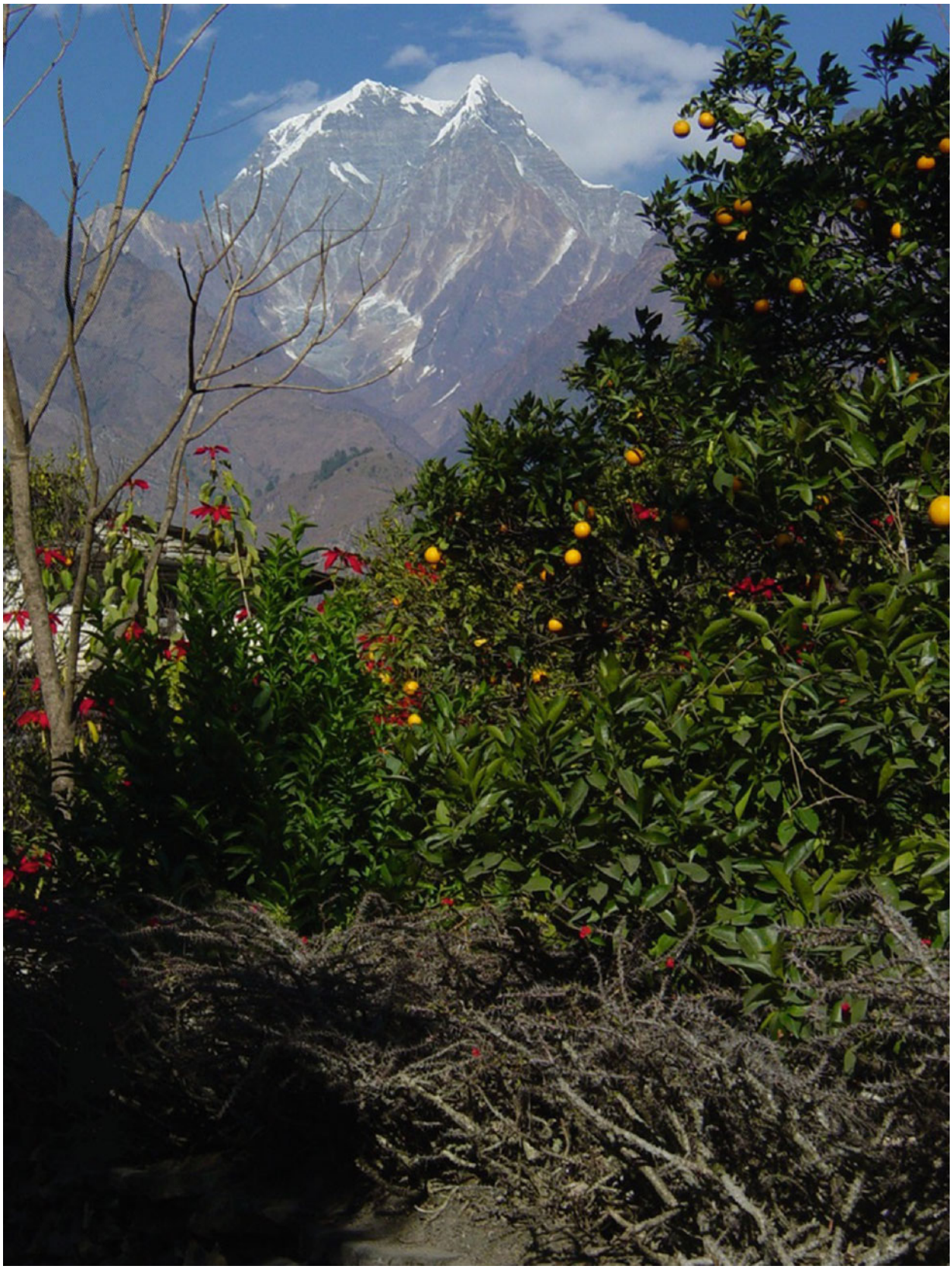

View of Mt Nilgiri from Tatopani

Megh Raj Dhital

Geology of the Nepal Himalaya

Regional Perspective of the Classic Collided Orogen

Springer

Megh Raj Dhital
Central Department of Geology
Tribhuvan University
Kirtipur, Kathmandu
Nepal

ISBN 978-3-319-02495-0 ISBN 978-3-319-02496-7 (eBook)
DOI 10.1007/978-3-319-02496-7
Springer Cham Heidelberg New York Dordrecht London

Library of Congress Control Number: 2014949333

Cover illustration: Photo by Megh Raj Dhital
South face of Mt Nilgiri, viewed from Tatopani.

Printed on acid-free paper

Springer is part of Springer Science+Business Media (www.springer.com)

This book is dedicated to the memory of Toni Hagen

Foreword

Perhaps no sector in the Himalaya is endowed with so exciting a geological setup as Nepal. Forming a bridge between the Western and Eastern Himalaya, Nepal occupies a pivotal and significant place in the geology of the Himalaya. Stretching from the low lying foothill in south to the highest peak of Sagarmatha (Mt. Everest) in the north and covering a vast time span from the Proterozoic to Holocene, the Nepal Himalaya preserves unique geological events. Varied kinds of igneous rocks, metamorphosed sequences and sedimentary rocks of disparate environments make a captivating geological mosaic.

Yet this fascinating terrain did not receive the attention of geologists as it deserved. The early contributions were restricted to isolated sectors, leaving many gaps in the understanding of the geology of Nepal. It is thus fitting that these gaps are being filled by Prof. Megh Raj Dhital—son of the soil, in this book. I have been in touch with him for quite some time and have held several discussions. He has painstakingly compiled the data scattered in numerous publications and arranged these into several chapters with informative maps, charts and figures with his own inputs. To begin, the reader is introduced to the role of plate tectonics in the creation of the Himalaya. The most fascinating aspect of the Himalaya to one and all is its charming scenery; naturally the physiographic subdivisions have to be dealt in a book on geology as the topography is controlled by the rocks. Political boundaries were created much after the Himalaya came into existence; the geological elements of Nepal, therefore, should find continuity in the adjoining Western and Southeast Himalaya and the Peninsular India. An elaboration of this aspect forms a basis for regional understanding of the geology of the Himalaya. The geology of the Lesser Himalaya constituted of unfossiliferous rocks that have been tectonically disrupted is nightmare to any stratigrapher; seven chapters are devoted to their exhaustive account. Elaboration of complicated geology of the Higher Himalaya and the enigma of inverted grade of metamorphism in the Himalaya is of interest to one and all. Richly fossiliferous rocks of the Tethyan Himalaya evoke curiosity even amongst layman and no book on geology of Nepal could be complete without their description. Siwalik rocks, representing almost the final phase of the mountain building, find copious place. The Terai and intermontane basins are unique to the Nepal Himalaya; their genesis makes an interesting reading. Neotectonics having environmental significance should be a must to the planners and administrators. The plethora of information of 36 chapters has been summarised with conclusions in the final chapter.

One may differ with Prof. Dhital's conclusions, but the narrative is exhaustive and makes an absorbing reading. He has succeeded in his task and discharged the debt he owes to the Nepal geology. This book completes the panorama of the Himalayan geology stretching from the West to the East.

Panchkula — O. N. Bhargava

Preface

With the exception of the work carried out by a handful of early explorers, intensive geological investigations in Nepal began only in 1951, exactly 100 years after the establishment of the Geological Survey of India. But, soon after, the geological literature on Nepal began to grow exponentially, and presently the number of publications has become too numerous, and the information is scattered worldwide through various books, periodicals, and unpublished reports in more than seven languages. Therefore, it is desirable to gather, amidst many details, the important geological knowledge of the Nepal Himalaya and to go through the prevailing concepts, behind the formation and development of this towering mountain range of the world.

This book has ensued from my research into the existing geological literature as well as its developmental trend in the Himalaya. While preparing the book, I have also drawn on my own geological investigations over the length and breadth of Nepal as well as its surrounding regions. Consequently, I felt it necessary to preface this book also with a few words on the epistemic aspect of geological research in the Himalaya. Geological investigation in the Himalaya, not unlike in any other part of the earth's crust, has to deal primarily with information gathering, based on some conceptual connotations. Indeed, to trace even a simple geological contact, some theoretical background is necessary. However, one of the distinctive attributes of Himalayan geology is the proliferation of views on various geological phenomena, operating in this majestic mountain realm. The geological literature of the Himalaya is beset with the origin, evolution, and demise of such diverse concepts and ideas. At first glance, the geological literature of the Himalaya may seem to be overwhelmed with such conundrums or contradictions and the science of geology in a state of disorder. However, a deeper insight into the subject matter may bring out an order out of the chaos. These theoretical discourses were so vital that they provided ample impetus to carry out intensive research in this classic collided orogen. As a result, albeit gradually, a clearer and more beautiful geological picture of the whole Himalayan Range has come into sight.

The centrally located Nepal Himalaya is expediently circumstanced for the study of Himalayan geology with its diverse dimensions. It is in the Nepal Himalaya, where most theories and concepts have flourished in the past 60 years of time. Though it is a relatively short interval, if we take into account the last 200 years of intense and exhaustive investigation of the Himalaya by a gamut of researchers from various countries of the world, the outcomes have proved to be astonishingly fruitful in their application to the whole Himalayan Range and also beyond its borders.

Geologists do not spend whole of their life in theoretical discourses alone, but they do produce a range of geological maps, immensely useful to the governmental as well as private organisations in their endeavour to develop construction material- or mineral-based industries, hydropower projects, or road networks, to extract groundwater, and ameliorate land with irrigation facilities. Such scrupulously drawn maps are also inevitable for petroleum exploration, urban planning, natural hazards assessment, and environmental protection. Therefore, many detailed geological maps of some particular areas are included in this book. Since more than two-thirds of the total area of Nepal is hitherto unmapped on a large scale, there remains much research work to be carried out in the future. In fact, one of the root causes of many

contradictory opinions on various geological processes is the state of poor geological mapping. Ironically, some earlier maps portray the field reality more accurately and vividly than those heavily laden with specific theoretical conjectures.

It is endeavoured to bring together, through this book, the geology of the whole Himalayan Range of Nepal, i.e., from the graceful grasslands of the Ganga basin on the south to the towering Tethyan zone on the north. Though many writers have chosen to discuss the geology of the Himalaya from south to north, this book is arranged somewhat differently. It is because, the limits of various broad geological divisions are not always distinct, and it is desirable to follow the geological convention of dealing with the oldest units first. Hence, after giving introduction to the Himalaya and neighboring regions, the book describes the oldest sequence of the Lesser Himalaya, and it is followed by the Higher Himalaya, Tethys Himalaya, Siwaliks, and the youngest Terai and intermontane basins.

It is my belief that without a comprehensive look at the various Himalayan terranes, it is practically impossible to grasp fully the process, operating behind the formation and development of the spectacular Himalaya. However, it is not intended merely to document all the scientific ontology, but an attempt is made to reveal a sound basis to the prevailing concepts. It is anticipated that the book will help the reader to move forward from a cognitive approach to a constructive one with the praxis of linking a variety of knowledge, including the earlier inferences or views and contemporary theories or models, where the intent of both the past and present researchers is more or less the same, but their investigation process can be different.

Kathmandu, July 2014 Megh Raj Dhital

Acknowledgments

Tribhuvan University generously granted me a year-long sabbatical leave to carry out this research. The Central Department of Geology, Tribhuvan University, not only provided me with library and laboratory facilities, but also supported my fieldwork in various parts of Nepal. The University of Natural Resources and Applied Life Sciences (BOKU), the University of Vienna, and the Geological Survey of Austria offered library and laboratory facilities. Information was also gathered from Tübingen University and ETH Zürich libraries. I also received a 4-month-long research fellowship from Hokkaido University. Nepal Academy of Science and Technology as well as Indian National Science Academy facilitated my 3-month-long research in Kolkata. The library of the Geological Survey of India, as well as the Presidency University, Kolkata, and Tongji University, Shanghai, were inevitable for gathering much needed information. Maps, data and reports were also acquired from the Department of Mines and Geology, the Department of Survey, and the Department of Irrigation, Kathmandu, Nepal. International Centre for Integrated Mountain Development (ICIMOD) assisted me with GIS and related tools.

It would have been impossible to write this book without an enormous amount of technical as well as intellectual help from my seniors, colleagues, friends and students. I thank all of them, and especially the following individuals for their cooperation: Madhav Prasad Sharma, Ramesh Prasad Bashyal, Toran Sharma, Bishal Nath Upreti, Dibya Ratna Kansakar, Krishna Prasad Kaphle, Prakash Chandra Adhikary, Sarbjit Prasad Mahato, Vishnu Dangol, Ram Bahadur Sah, Pradeep Kumar Mool, Samjwal Ratna Bajracharya, Suresh Das Shrestha, Madhav Belbase, Ananta Prasad Gajurel, Dinesh Pathak, Lila Nath Rimal, Lalu Prasad Paudel, Khum Narayan Paudayal, Naresh Kazi Tamrakar, Subas Chandra Sunuwar, Soma Nath Sapkota, Sudhir Rajaure, Rajendra Prasad Khanal, Prem Bahadur Thapa, Kamal Raj Regmi, Ranjan Kumar Dahal, Subesh Ghimire, Motilal Ghimire, Kamala Kant Acharya, Sunil Dwivedi, Basanta Raj Adhikari, Prabin Kayastha, Amardeep Regmi and Gautam Khanal.

Jean Friedrich Schneider kindly invited me to research for 9 months at BOKU. Hermann Häusler allocated space and computer facilities, whereas Bernhard Grasemann granted permission to library and equipment access at Vienna University. Thomas Hofmann from the Geological Survey of Austria made available various books and journals as well as published and unpublished reports. Many stimulating and fruitful discussions with Gerhard Fuchs and Wolfgang Frank clarified several issues related to tectonics and stratigraphy. Hisao Ando, Kazunori Arita, Erwin Appel, Yuichiro Tanioka, Florimond De Smedt, Bai Yun, Pitambar Gautam and Sumit Kumar Ray helped substantially in my research endeavour.

I am indebted to Om Narain Bhargava for critically reviewing the manuscript and making painstaking corrections as well as for giving many practical suggestions. He also facilitated my field observations in Solan and Simla.

I am grateful to all the authors and publishers, who kindly gave permission to use their material. I thank the staff of Springer for their enthusiastic and unfailing help throughout the production of this book, and particularly Dörthe Mennecke-Bühler and Ashok Arumairaj for editorial advice, guidance and speedy correction. Errors of commission and omission are my own. Last but not least, I am grateful to my wife and children for their understanding and encouragement.

Megh Raj Dhital

Contents

Part VI Siwaliks

Introduction

1

Knowledge, after all, is of human creation; and, as a rule, the knowledge of the structure of a mountain chain comes as the reward of glorious struggle, both physical and mental.

—E.B. Bailey (1935, p. 1)

The enduring geological beauty and arresting grandeur of the Himalaya (*hima* = snow, *álaya* = abode in Sanskrit) have attracted investigators from far and wide, especially for the last two centuries. Despite the fact that their knowledge was derived from a limited source or observations were confined to a few isolated regions, some of the pioneers were successful in making astonishingly accurate geological predictions by dint of their ingenious insight into the natural phenomena operating in this immense and insurmountable mountain range. As the rigor of investigation as well as regional coverage steadily increased, newer theories and hypotheses also became prolific.

The resplendently located Himalayan Range (Fig. 1.1) with its unparalleled altitude and complex geological history (Fig. 1.2) is considered to be a perfect archetype of continent–continent collision (Argand 1924; Powell and Conaghan 1973; Molnar and Tapponnier 1975). The Himalayan belt is also well known for its diverse textures and structures as well as for inverted metamorphism—another outstanding phenomenon.

This world's loftiest orogenic system exhibits evidence of the complete Wilson cycle from the Mesozoic to the Eocene, followed by still ongoing post-collisional deformation (Windley 1995, p. 134). After the break-up of the Gondwanaland about 250 Ma, the inexorable flight of the Indian plate towards the north began in the Cretaceous, and this process continues even today. The flight resulted in a collision with the Eurasian plate (Figs. 1.3 and 1.4). The collision took place obliquely and the northwest portion of Kohistan–Ladakh came into contact with the Eurasian plate about 65 Ma (Jaeger et al. 1989) or 55 Ma (Klootwijk 1984), followed by an anticlockwise rotation of the Indian plate and collision around 50 Ma (Besse et al. 1984) or 45 Ma (Dewey et al. 1989). Le Pichon and Heirtzler (1968), and Le Pichon et al. (1973) investigated the motion of the Indian plate and concluded that its movement is a rotation whose center has shifted from about 2°N, 26°E to 29°N, 27°E. On the other hand, Zhu et al. (2005) deny the diachroneity of collision and state that the India–Asia collision took place synchronously in the western and eastern Tethyan Himalaya at 50.6 ± 0.2 Ma.

The convergence velocity between Eurasia and India changed significantly (from 15 to 4 cm/a) about 50–35 Ma (Fig. 1.5) and this decrease also coincided with the onset of the India–Eurasia collision. Crustal thickening leading to mountain building in Tibet was the main cause of the Cenozoic slowdown of the Indian plate (Copley et al. 2010).

The Himalayan realm contains a mosaic of Paleoproterozoic to Cenozoic rocks with heterogeneous composition and tectonic style. These rocks are telescoped by long-distance tectonic transport (Brookfield 1993).

1.1 Early Investigations

The eighteenth- and early nineteenth-century geological investigations in the Himalaya were sporadic and sketchy. New theories and hypotheses emerged right from the Neptunistic views on the origin of different rock and mineral groups to the Plutonistic views on the origin of granites. Some of the early researchers (called the naturalists) focused their attention on mineral wealth and physical geology; others were interested in fauna, flora, topography, or climate; whereas a few of them described various Himalayan rock types in terms of Abraham G. Werner's stratigraphic scheme of Primary, Secondary, and Tertiary strata.

There were very early views on the central crystalline axis (Stoliczka 1866) as a barrier comprising metamorphic or igneous core versus sedimentary cover underlain by the Indian shield rocks; there were unrelenting debates on the geosynclinal origin of the Himalaya versus its development from a reactivated platform, and contracting earth versus expanding earth. All kinds of such hypotheses ultimately faded away when the plate tectonic paradigm prevailed in the 1960s.

M.R. Dhital, *Geology of the Nepal Himalaya*, Regional Geology Reviews,
DOI 10.1007/978-3-319-02496-7_1

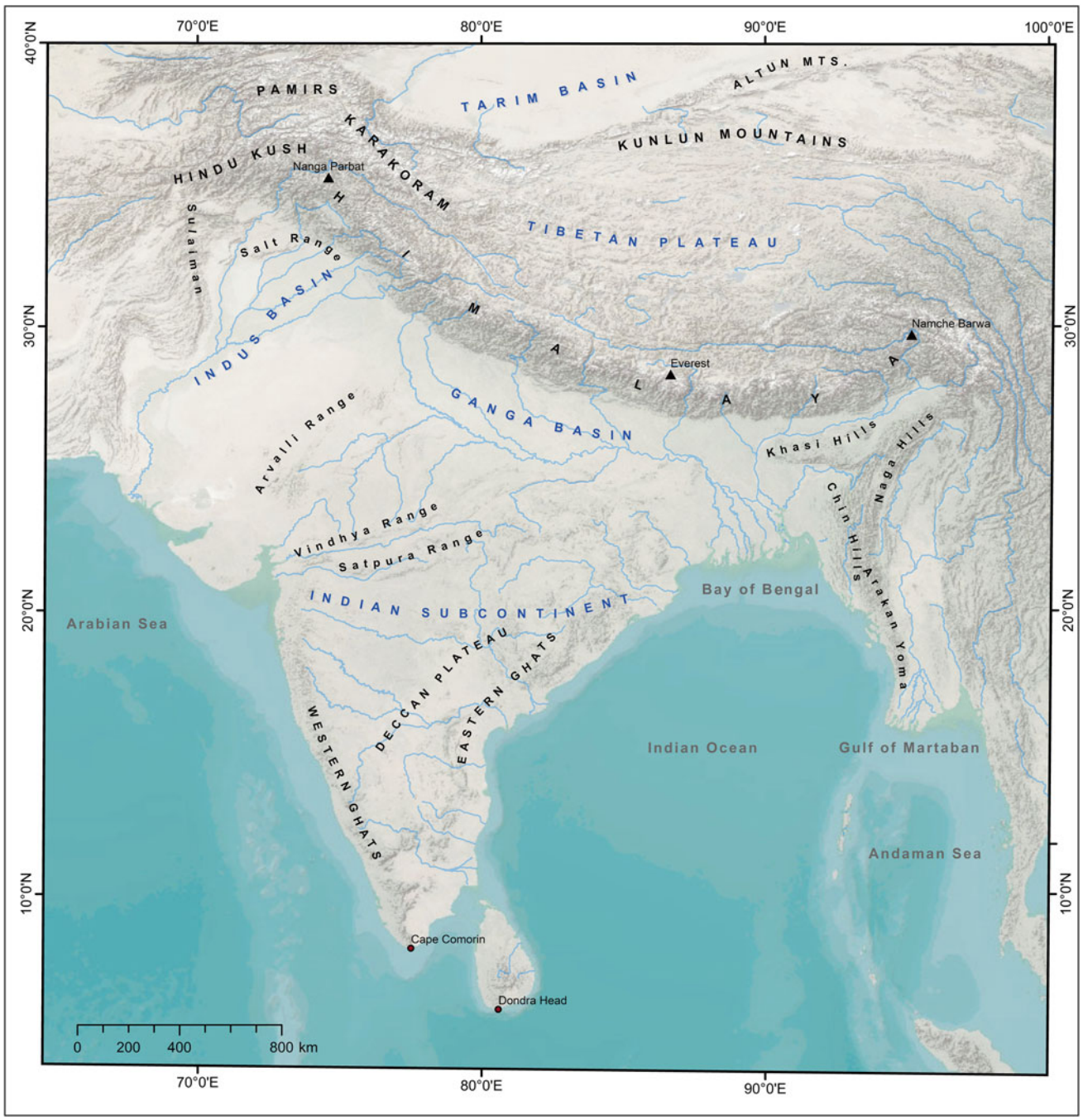

Fig. 1.1 Tibetan Plateau, Indian Subcontinent, Himalaya, and neighboring mountain ranges. *Source* Compiled from SRTM DEM, USGS, NOAA, USDA, and GIS User Community

Calder (1832) and Herbert (1842) were some of the earlier investigators expressing their views on various rock units of the Himalaya. After the establishment of the Geological Survey of India in 1851, H.B. Medlicott excelled with his superb geological observations and very many innovative and far-reaching views on Himalayan mountain building and the development of the Siwalik trough. Middlemiss (1890) fully developed the Main Boundary Fault concept postulated by Medlicott (1864). In the history of Himalayan geology, the notion of large-scale recumbent folding came from von Lóczy in 1878 (Chap. 5). In contrast to the "fixistic" views of Eduard Suess (1885) and his concept of foredeep (Chap. 35), "mobilist" Argand (1924) proposed the revolutionary idea of the India–Eurasia collision (Fig. 1.3). But, it was Suess who distinguished the Tethys Sea and denied the permanency of oceans, as

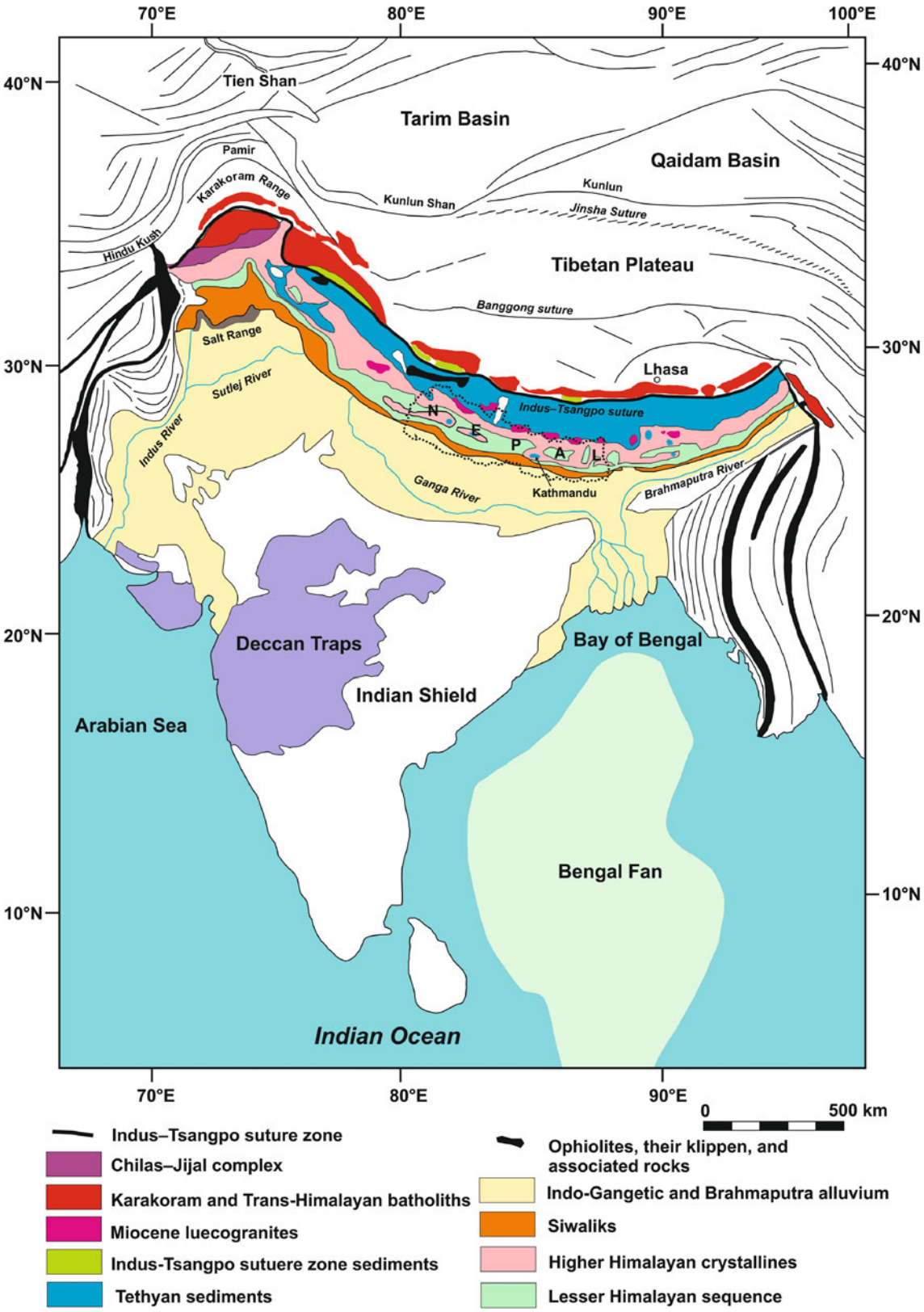

Fig. 1.2 Simplified geological map of Himalaya and position of Nepal. *Source* Modified from Stöcklin (1980), Gansser (1981), and Sorkhabi and Stump (1993)

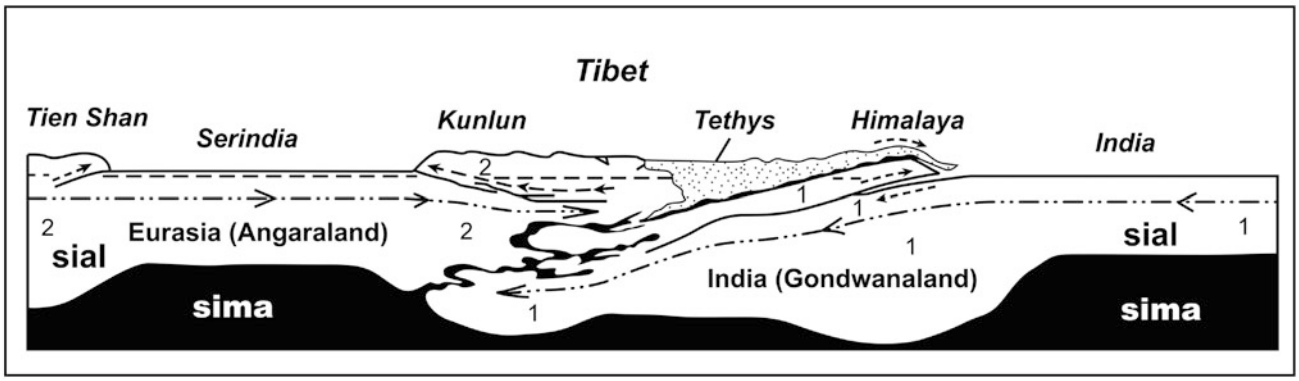

Fig. 1.3 Collision between India and Asia as visualized by Argand. *Source* Modified from Argand (1924, p. 349)

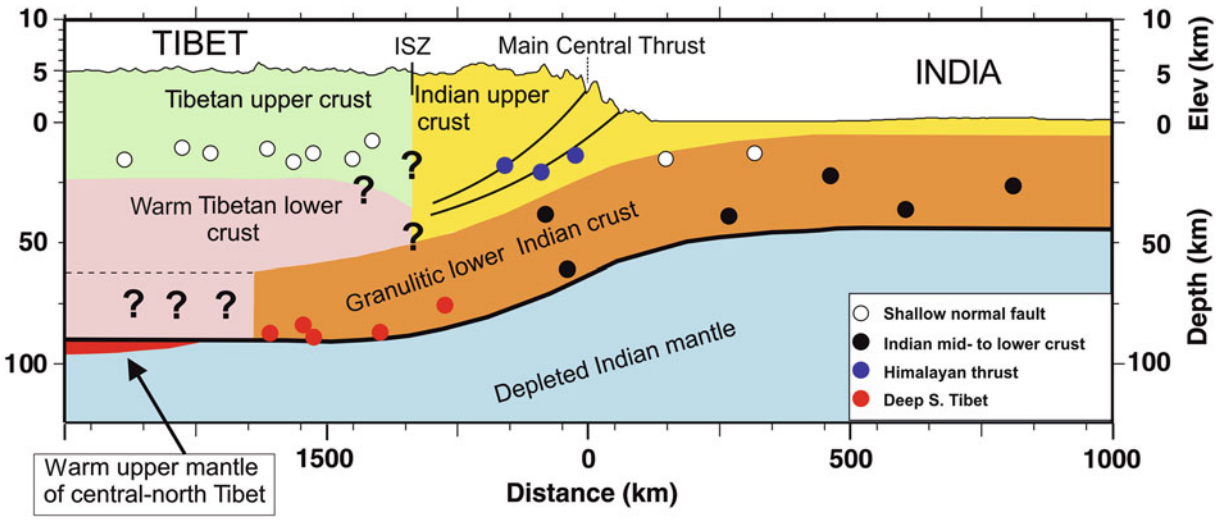

Fig. 1.4 Schematic cross-section through the Himalaya to illustrate the relations between structure and earthquake distribution. *Black dots* are earthquakes within the underthrusting Indian shield, and occur down to the Moho. *White dots* are shallow normal faulting events, mostly in Tibet but also at the top of the flexing Indian shield beneath the Ganga foreland basin. Blue dots are shallow-dipping thrusts at ~15 km depth on the main underthrusting interface(s) beneath the Himalaya. The rigid, strong, granulitic lower crust of India is underthrust beneath the Himalaya, and to an unknown distance farther north, indicated by question marks. This Indian lower crust helps support the elevation of Tibet, because the only way Tibet can collapse is by the flow of the warm, weak lower Tibetan crust over this rigid base, which is a slow dissipative process. The precise configurations of geological boundaries indicated by question marks beneath the Indus–Tsangpo suture zone (ISZ) are unknown. *Source* Jackson et al. (2008). © Geological Society of London. Used by permission

regarded by Dana (1873). Following the observations of Auden (1937), Heim and Gansser (1939) defined the Main Central Thrust as a major intracrustal dislocation. As in the Alps, they also contemplated the Main Boundary Thrust as a phenomenon of relief thrusting.

In the Russian literature, Rezvoi (1964), a diehard "fixist," gave a general account of the geology of the Himalaya, and he especially referred to the work of von Lóczy (1907), Lombard (1953), Hagen (1954), and Bordet (1961), who proposed various nappes or thrust sheets (such as the Darjeeling, Kathmandu, and Nawakot nappes) in the Himalaya. But Rezvoi denied such interpretations and believed in some short-distant thrusts developed in the reactivated Indian platform.

The iconic Nepal Himalaya had remained virtually virgin to geoscientists until 1950. But soon after, a truly international endeavor of geologists, taking part in mountaineering expeditions, and especially the 9-year-long untiring investigations of Toni Hagen, made "mysterious" Nepal one of the most enticing and extensively investigated segments of the Himalayan arc.

1.2 Classification Schemes

There have been various attempts to classify the Himalaya. For example, Strachey (1851) identified the following divisions in the Himalaya and surrounding region (from south to north).

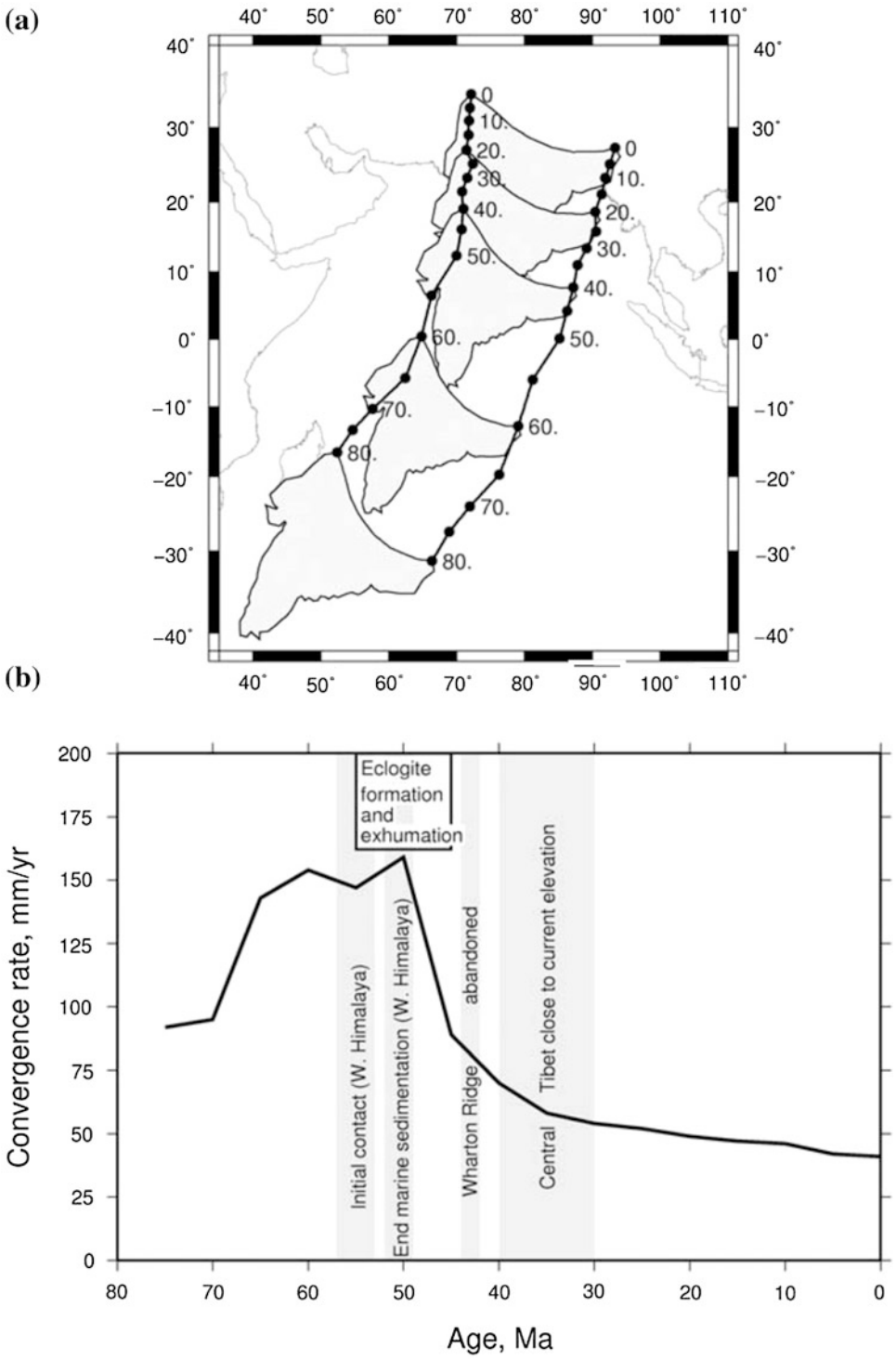

Fig. 1.5 **a** Flight of India and collision with the rest of Asia. The *black lines* show the positions since 80 Ma, in a Eurasia-fixed reference frame. Positions are labeled with the time in million years. The reconstructed locations of the present-day outline of the Indian subcontinent are shown at 20 Ma increments. **b** The *black line* shows the rate of convergence between India and Asia since 75 Ma (at a point currently located at 28° N, 80° E). The *gray* bands show the timings of notable events in the history of the India–Asia collision. Also shown are the timings of eclogite formation and exhumation, which probably record the end of subduction in the region. The collision is thought to have begun at the western part of the plate boundary (i.e., the dates shown indicate the time of initial contact of the continental margins and the end of marine sedimentation) and propagated eastwards over the subsequent 5–10 Ma. *Source* Copley et al. (2010). © John Wiley and Sons Ltd. Used by permission

- Alluvial plain of Ganga and Indus, called the Terai
- Siwalik or Sub-Himalayan Range with dip of beds to the north
- Longitudinal valleys within the Siwaliks
- Metamorphic strata without fossils (with granites and volcanic rocks)
- Crystalline schists
- Azoic slates
- Paleozoics
- Secondary rocks
- Tertiary rocks.

Medlicott and Blanford (1879) divided the Himalayan region into three longitudinal zones: the Sub-Himalaya, Lower Himalaya, and the Central or Tibetan Himalaya. Burrard and Hayden (1908, p. 5) subdivided the Himalayan Range into the following four sections.

- The Punjab Himalaya from the Indus to the Sutlej
- The Kumaun Himalaya from the Sutlej to the Kali
- The Nepal Himalaya from the Kali to the Tista
- The Assam Himalaya from the Tista to the Brahmaputra.

They published the first geological map of the Himalaya and physiographically classified the ranges into the Great Himalaya, rising above the limits of perpetual snow; the Lesser Himalaya, a series of ranges closely related to the Great Himalaya; and the Siwalik ranges, which intervene between the Lesser Himalaya and the plains (Burrard and Hayden 1908, p. 75). Their geological subdivisions of the Himalaya include (p. 207) an outer or Sub-Himalayan zone of Tertiary rocks, a central or Himalayan zone of Lesser Himalaya and line of high peaks, and the northern or Tibetan zone lying mostly behind the high peaks with abundantly fossiliferous (from Cambrian to Tertiary) rocks.

Hagen (1954, 1956) divided up the Nepal Himalaya into the following 10 zones: Tibetan plateau; granites of Mustang–Mugu: massive tourmaline granites; Khumbu nappes; Tibetan synclinorium with Langu–Kagbeni–Manangbhot; Kathmandu nappes; Hiunchuli zone; Piuthan nappes (in west Nepal); Nawakot nappes; Pokhara zone; and the Siwaliks. He also stated that the roots of the Kathmandu nappes lie in the Himalayan main range. Around Kathmandu, they contain Silurian limestones and other older rocks that have moved about 65 km to the south and are forming a half-klippe. The Kathmandu nappes also reappear south of Jumla. The intrusions of granites, pegmatites, and aplites are seen in the Kathmandu nappes, even in their southern frontal part. He also identified the Manaslu granite intruded in the Kathmandu nappes, amphibolites in the Nawakot nappes northwest of Pokhara, and basic intrusions in the frontal parts of the Nawakot and Piuthan nappes. He recorded the intrusives (i.e., nepheline syenites) of the Ampipal area, west of Gorkha (near Luintel Bhanjyang), and mapped them as granites within the Nawakot nappes. He also stated that to the north of the Annapurna and Dhaulagiri ranges, a complexly deformed synclinorium with Mesozoic filling is located and intruded by the Mustang granite on the Tibetan border.

Hashimoto et al. (1973) divided the Nepal Himalaya into the Arun River, Ramechhap–Okhaldhunga, Chautara, Kathmandu, Buri Gandaki, Pokhara–Gurkha, Dhaulagiri, and Karnali regions, respectively, from east to west.

1.3 Proposed Subdivisions

The Nepal Himalaya together with the Terai belt (Fig. 1.6) is classified into the following essentially longitudinal geological zones distributed from south to north, respectively (Gansser 1964; Fuchs and Frank 1970; Stöcklin 1980).

- Terai and Bhabar zone
- Siwaliks and intermontane basins
- Lesser Himalaya
- Higher Himalaya
- Tethys Himalaya.

The Terai or Active Himalayan foreland basin, Siwaliks (Sub-Himalaya), Lesser Himalaya (Lesser Himalayan Sequence), Higher Himalaya (Greater Himalayan Crystalline Complex), and Tethys Himalaya (Tethyan Himalayan Sequence) correspond to the major subdivisions (Yin 2006) of the North Indian Sequence (Brookfield 1993) in Nepal, and hereafter they are treated as main geological subdivisions, rather than physiographic units.

Here, it is proposed to divide the country into the following six transverse physiographic regions, delimited primarily by the watersheds of major river systems (Fig. 1.7).

- Mahakali–Seti region
- Karnali–Bheri region
- Gandaki region
- Bagmati–Gosainkund region
- Koshi region
- Arun–Tamar region.

The major elements of each region are summarized in Table 1.1. Because detailed geological investigations are confined to some specific tracts, and most of the country remains yet to be explored, the geology in the following chapters is presented in accordance with the precedence of the work carried out by various researchers as far as practicable. Most of the early research was either confined to central Nepal or of general nature. However, the work of Heim and Gansser (1939) in the Mahakali region remains an exception. On the other hand, regional geological investigations of Hagen (1969) and Hashimoto et al. (1973) with contrasting tectonic interpretation stand out as rare examples. Although Talalov (1977) also covered most parts of Nepal, he was not concerned with the stratigraphy of various rock successions.

This book comprises seven Parts and 36 chapters. This chapter provides the introduction, featuring general background to the Himalaya, including its origin, extent, and global tectonic context.

Part 1 (Chaps. 2 and 3) is devoted to the geological setting of the Himalaya and physiography of Nepal, whereas Part 2 (Chaps. 4 and 5) deals, respectively, with the northwest and southeast neighboring tracts. A comparison clearly shows the contrasting lithology and stratigraphy of these two segments of the Himalaya. Consequently, the Nepal Himalaya lying between these two regions shares some geological elements of both areas.

Part 3 (Chaps. 6–12) describes the Lesser Himalaya in its diversity of lithology, stratigraphy, and structure. Detailed descriptions of a few specific regions are also presented in

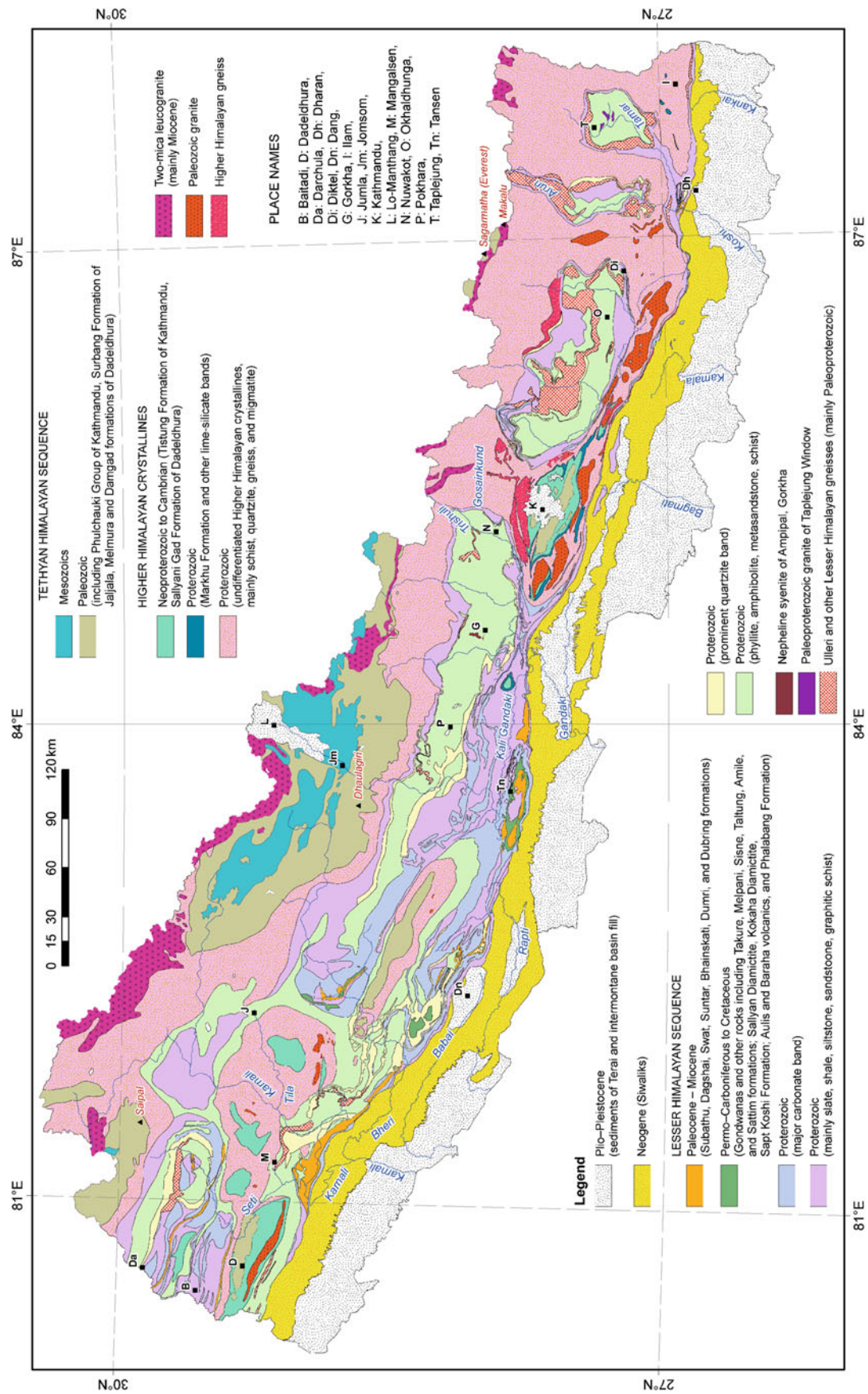

Fig. 1.6 Simplified geological map of Nepal. *Source* Compiled from Tater et al. (1983), Shrestha and Shrestha (1984), Shrestha et al. (1985, 1986, 1987), ESCAP (1993), Amatya and Jnawali (1994), and several others as well as author's observations

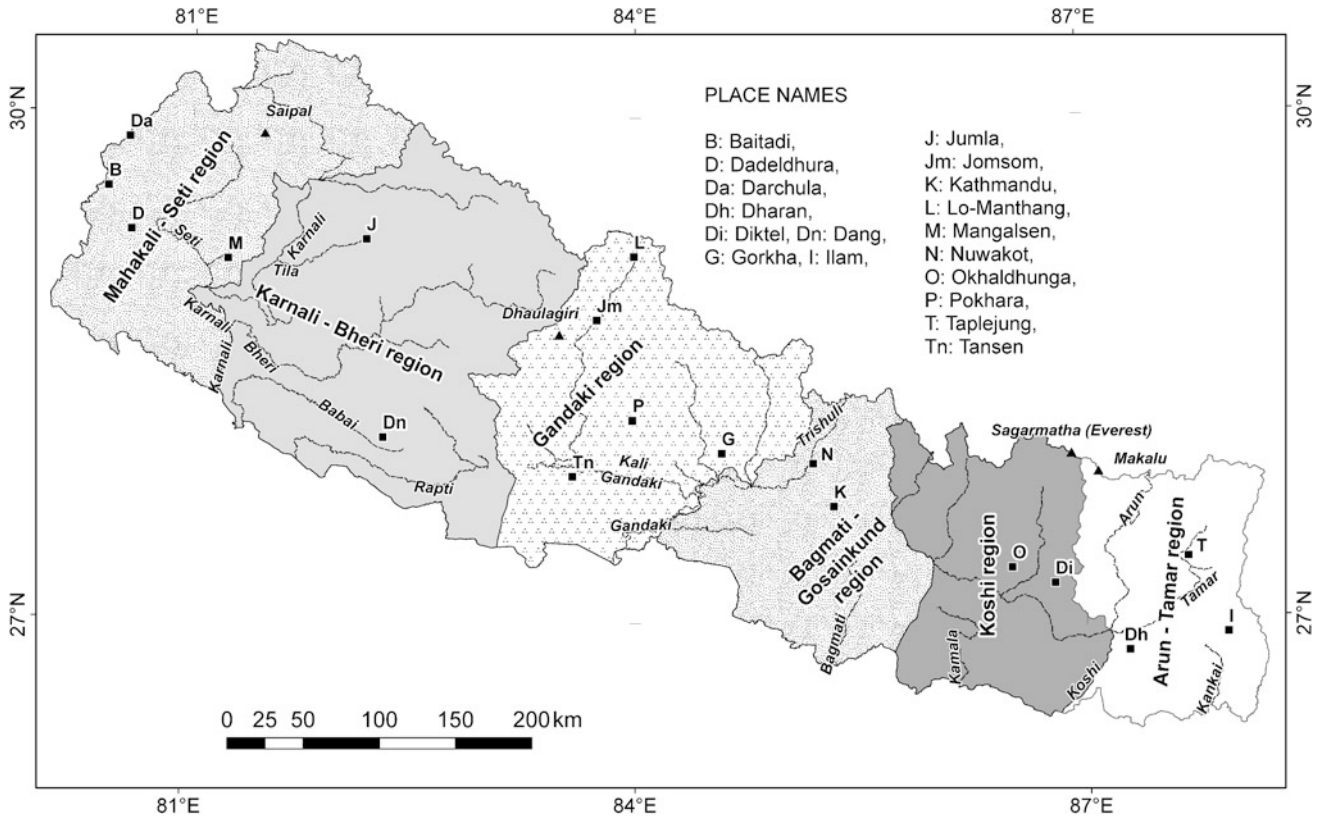

Fig. 1.7 Six transverse divisions of the Nepal Himalaya. *Source* Compiled from the maps of the Survey Department of Nepal

Table 1.1 Some important areas or features within the six transverse regions of Nepal and corresponding geological zones

Geological zone/ physiographic region	Mahakali–Seti region	Karnali–Bheri region	Gandaki region	Bagmati–Gosainkund region	Koshi region	Arun–Tamar region
Terai and Bhabar zones		Partly absent	Partly absent		Dharan	
Siwaliks	Two belts	Plunging folds and three belts	Folded and faulted	Two belts	Two belts	A narrow frontal belt
Intermontane basins	Puntura Khola, Rangun Khola	Dang, Deukhuri, Surkhet	Thakkhola, Pokhara, Chitwan	Kathmandu, Hetaunda, Marin Khola	Sindhuli, Katari, Gaighat	None
Lesser Himalaya	Darchula, Baitadi, Patan, Pancheshwar, Narrow Budar zone	Widest sedimentary belt, Bheri River, North Dang, Rolpa, Sallyan, Piuthan	Pokhara, Syangja, Gorkha, Marsyangdi River, Kali Gandaki River, Palpa	Discontinuous Lesser Himalayan zone, Marin Khola	Tama Koshi River, Okhaldhunga window, Narrow frontal sedimentary belt, Katari outliers	Arun window, Tamar window, Barahakshetra, Dharan–Dhankuta
Higher Himalaya	Darchula, Dadeldhura, Gaira	Jumla, Jajarkot	Dana and Lete, Modi Khola	Rasuwa Gadhi, Kathmandu and central Mahabharat Range, Melamchi, Panchkhal	Tama Koshi River, Mount Everest, and neighborhood	Mount Makalu and neighborhood
Tethys Himalaya	Mahakali River	Dolpa, Jaljala klippe	Thakkhola, Manang	Phulchauki	Mount Everest and neighborhood	

Source Author's observations

this section. Some typical stratigraphic and structural features of this essentially unfossiliferous belt give clues to regional correlation.

Part 4 (Chaps. 13–20) discusses the Higher Himalayan rocks with their rather vague stratigraphy and intense metamorphism. The last chapter of this section deals with various metamorphic models explaining the inverted metamorphism in the Himalaya.

Part 5 (Chaps. 21–26) is devoted to the Tethys Himalaya where stratigraphy is clearer owing to the occurrence of fossils, but this belt also experienced severe deformation, manifested by intricate folds and faults.

The Siwalik belt, characterized by its relatively simple lithology and spectacular sedimentary structures, is presented in Part 6 (Chaps. 27–33). This zone has also undergone significant compression and shortening, as revealed by many folds and imbricate thrusts.

Part 7 (Chaps. 34 and 35) deals with the geology of the Terai and a few intermontane basins. Neotectonics and active faults are also described in this section. Conclusions are given in Chap. 36, where the main geological aspects of Nepal are summarized. In this chapter, the Nepal Himalaya is also compared and contrasted with other parts of the orogen.

References

Amatya KM, Jnawali BM (1994) Geological map of Nepal, Scale: 1:1,000,000. Department of Mines and Geology, International Centre for Integrated Mountain Development, Carl Duisberg Gesellschaft e. V., and United Nations Environment Programme

Argand E (1924) La tectonique de l'Asie. Congrès Géologique International, Belgique, Comptes Rendues de la 13ème Session, en Belgique 1922. H. Vaillant-Carmanne, Liège, pp 171–372

Auden JB (1937) The geology of the Himalaya in Garhwal. Rec Geol Surv India 71(Part 4):407–433 (with 3 plates including a long cross-section on the scale of 1 inch = 2 miles)

Bailey EB (1935) Tectonic essays. Oxford at the Clearendon Press, Mainly Alpine 200 pp

Besse J, Courtillot V, Pozzi JP, Westphal M, Zhou YX (1984) Palaeomagnetic estimates of crustal shortening in the Himalayan thrusts and Zangbo suture. Nature 311:621–626

Bordet P (1961) Recherches Géologiques dans L'Himalaya du Népal, Région du Makalu, Expéditions Françaises a l'Himalaya 1954–1955, Edition du Centre National de la Recherche Scientifique (C. N. R. S.), 275 pp. (with geological maps in colors)

Brookfield ME (1993) The Himalayan passive margin from Precambrian to Cretaceous times. Sed Geol 84:1–35

Burrard SG, Hayden HH (1908) A sketch of the geography and geology of the Himalaya mountains and Tibet. Calcutta, 308 pp (with a geological map of the Himalaya in colors, scale 1 inch = 40 miles, and many other maps in colors from various parts of the Himalaya)

Calder J (1832) General observations on the geology of India. Asiat Res Comprising Hist Antiq Arts Sci Lit Asia VIII:1–22

Copley A, Avouac J-P, Royer J-Y (2010) India–Asia collision and the Cenozoic slowdown of the Indian plate: Implications for the forces driving plate motions. J Geophys Res 115:B03410, 1–14. doi:10.1029/2009JB006634

Dana JD (1873) On some results of the Earth's contraction from cooling, including a discussion of the origin of mountains and the nature of the Earth's interior. Am J Sci Ser 3, 5:423–443; 6:6–14, 104–115, 161–171

Dewey JF, Cade S, Pitman WC (1989) Tectonic evolution of the India/Eurasia collision zone. Eclogae Geol Helv 82:717–734

ESCAP (Economic and Social Commission for Asia and the Pacific) (1993) Geology and mineral resources of Nepal, atlas of mineral resources of the ESCAP region, vol 9. United Nations, New York, 107 pp (with a geological map in colors, scale: 1:1,000,000)

Fuchs G, Frank W (1970) The geology of West Nepal between the rivers Kali Gandaki and Thulo Bheri. Jahrbuch der Geologischen Bundesanstalt, vol 18, pp 1–103 (with a geological map and cross-sections)

Gansser A (1964) Geology of the Himalayas. Interscience, New York, 289 pp

Gansser A (1981) The geodynamic history of the Himalaya. In: Gupta HK, Delany FM (eds) Zagros Hindu Kush Himalaya. American Geophysical Union, Geodynamics series, vol 3, pp 111–121

Hagen T (1954) Über die räumliche Verteilung der Intrusionen im Nepal-Himalaya. Schweizerische Mineralogische und Petrographische Mitteilungen, Band 34, pp 300–308 (with English summary and 2 plates of a tectonic map and cross-sections)

Hagen T (1956) Das Gebirge Nepals. In: Die Alpen (Zeitschrift des Schweizer Alpenclub), Bern, vol XXXII, Jahrgang, No. 1, Hefte 5–7 und 11, pp 124–130; pp 162–177; 295–303

Hagen T (1969) Report on the geological survey of Nepal. Volume 1: Preliminary Reconnaissance. Denkschiiften der Schweizerischen Naturforschenden Gesellschaft, Band LXXXVI/1, 185 pp (with a geological map)

Hashimoto S, Ohta Y, Akiba C (1973) Geology of the Nepal Himalayas. Saikon Publishing Co Ltd, Tokyo, 292 pp (with 6 plates including a geological map of Nepal (Plates 1 and 2) in colors, scale: 1:500,000)

Heim A, Gansser A (1939) Central Himalaya: geological observations of the Swiss expedition 1936. Denkschriften der Schweizerischen Naturforschenden Gesellschaft, Band LXXIII, Abh. 1, 245 pp (with geological maps in colors, sections, and plates)

Herbert GD (1842) Report of the Mineralogical survey of the Himalaya mountains lying between the rivers Satlej and Kali, with a geological map. J Asiat Soc Bengal XI:1–13

Jackson J, McKenzie D, Priestley K, Emmerson B (2008) New views on the structure and rheology of the lithosphere. J Geol Soc Lond 165:453–465

Jaeger J, Courtillot V, Tapponnier P (1989) Paleontological view of the ages of the Deccan Traps, The Cretaceous/Tertiary boundary, and the India-Asia collision. Geology 17:316–319

Klootwijk C (1984) A review of the Indian Phanerozoic paleomagnetism: implications for the India-Asia collision. Tectonophysics 105:331–353

Le Pichon X, Heirtzler JR (1968) Magnetic anomalies in the Indian Ocean and sea-floor spreading. J Geophys Res 73:2101–2117

Le Pichon X, Francheteau J, Bonin J (1973) Plate tectonics. Elsevier, Amsterdam, 300 pp

Lombard A (1953) La tectonique du Népal Oriental. Un profil de l'Everest à la plaine du Gange. Bulletin de la Société Géologique de France, Série 6(III):321–327 (with a cross-section)

Medlicott HB (1864) On the geological structure and relations of the southern portion of the Himalayan Range between the rivers Ganges

and Ravee. Mem Geol Surv India III(4):1–206 (with a geological map in colors; scale: 1 inch = 8 miles)
Medlicott HB, Blanford WT (1879) A manual of the geology of India, Part II: extra-peninsular area. Published by order of the Government of India, Calcutta, pp 445–817 (with 21 plates and a map in colors)
Middlemiss CS (1890) Physical geology of the Sub-Himalaya of Garhwál and Kumaun. Mem Geol Surv India XXIV(Part 2):59–200 (with 3 plates of cross-sections and a plate of geological map in colors; scale 1 inch = 4 miles)
Molnar P, Tapponnier P (1975) Cenozoic tectonics of Asia: effects of a continental collision. Science 189:419–426
Powell C McA, Conaghan PJ (1973) Plate tectonics and the Himalayas. Earth Planet Sci Lett 20:1–12
Rezvoi DP (1964) Tectonics of the Himalayas (evolution of concepts and the present state of the problem). In: Mouratov MV, Puscharovsky YM, Khain VE, Mazarovich OA (eds) Folded areas of Eurasia (proceeding of the conference on the problems of Tectonics, held in Moscow), 376 pp. Nauka, Moscow, pp 348–365 (in Russian)
Shrestha SB, Shrestha JN (1984) Geological map of Eastern Nepal. Scale: 1:250,000. Department of Mines and Geology, Kathmandu
Shrestha SB, Shrestha JN, Sharma SR (1985) Geological map of Far-Western Nepal. Scale: 1:250,000. Department of Mines and Geology, Kathmandu
Shrestha SB, Shrestha JN, Sharma SR (1986) Geological map of Central Nepal. Scale: 1:250,000. Department of Mines and Geology, Kathmandu
Shrestha SB, Shrestha JN, Sharma SR (1987) Geological map of Mid-Western Nepal. Scale: 1:250,000. Department of Mines and Geology, Kathmandu
Sorkhabi RB, Stump E (1993) Rise of the Himalaya: a geochronologic approach. GSA Today 3(4):85–92
Stöcklin J (1980) Geology of Nepal and its regional frame. J Geol Soc Lond 137:1–34
Stoliczka F (1866) Geological sections across the Himalayan Mountains, from Wangtu-Bridge on the river Sutlej to Sungdo on the Indus: with an account of the formations in Spiti; accompanied by a revision of all known fossils from that district. Mem Geol Surv India V(Part 1):1–154 (with 1 map, 6 sections in colors, and 10 plates of fossils)
Strachey R (1851) On the geology of part of the Himalaya Mountains and Tibet. Q J Geol Soc Lond 7:292–310 (with a geological map and two cross-sections in colors)
Suess E (1885) Das Antlitz der Erde. Prag and Leipzig vol I, 778 pp
Talalov VA (1977) Main features of magmatism and metallogeny of the Nepalese Himalayas. Colloques internationaux du C. N. R. S. No. 268 –Écologie et Géologie de l'Himalaya, Paris, pp 409–430
Tater JM, Shrestha SB, Shrestha JN (1983) Geological map of Western Central Nepal. Scale: 1:250,000. Department of Mines and Geology, Kathmandu
von Lóczy L (1907) Megfigyelések a Keleti-Himalájában. Földrajzi Közlemények, XXXV Kötet, 7 Füzet, pp 293–310
Windley BF (1995) The evolving continents, 3rd edn. Wiley, New York, 526 pp
Yin A (2006) Cenozoic tectonic evolution of the Himalayan orogen as constrained by along-strike variation of structural geometry, exhumation history, and foreland sedimentation. Earth Sci Rev 76:1–131
Zhu B, Kidd WSF, Rowley DB, Currie BS, Shafique N (2005) Age of Initiation of the India-Asia Collision in the East-Central Himalaya. J Geol 113:265–285

Part I

Geological Setting and Physiography

Geological Setting of Himalaya

2

The Himalayas have no direct continuation either towards the west or to the east. The singular syntaxial bends on both extremes preclude a straightforward continuation of the Himalayan elements.

—A. Gansser (1964, p. 256)

The conspicuous continental climax on earth, the Himalaya, is situated on the south edge of the elevated Tibetan Plateau. The extensive alluvial plains of Indus (Sindh or Sindhu), Ganga (Ganges), and Brahmaputra or Yarlung Tsangpo (or *Zangbo* = river in Tibetan) delimit this mountain range from the south. Together with the Karakoram mountains, bordering the Himalaya on the northwest, this orogenic belt meets and fuses with the Pamirs, from where several other Asiatic mountain chains diverge (Figs. 1.1 and 2.1). The Himalayan Range abruptly encounters an impressive syntaxial bend around Mount Nanga Parbat (8,125 m) at its northwest extremity, from where the Hindu Kush, Sulaiman, and Kirthar ranges continue to the south or southwest. There is another similar sharp syntaxial twist around Mount Namche Barwa (7,756 m) at the southeast end of the Himalaya, from where the Arakan mountains swing to the south or southwest.

The three great antecedent rivers—Indus, Ganga, and Brahmaputra—have been witnessing the Himalayan evolution and rise since the time of its embryonic growth about 50 Ma (Patriat and Achache 1984). The Brahmaputra and Ganga embrace this majestic mountain range from the north and south, respectively, and make a thousands-of-kilometers–long detour before ultimately merging and debouching into the Bay of Bengal. Although, like the Brahmaputra, the Indus also collects its waters from the environs of twin shimmering lakes—Manasarovar (*Mapam Yumco* in Tibetan) and Rakas (*La'nga Co* in Tibetan) in Tibet—it flows at first towards the opposite direction (i.e., to the west), and then comes very close to the tributaries of the Ganga, with a trifling aerial distance in the dead levels of their common alluvial plain, and briskly conveys its waters and sediments into the Arabian Sea near the Gulf of Oman.

2.1 Tibetan Plateau

The Tibetan Plateau with the Himalaya and neighboring ranges constitutes by far the widest and highest orogenic system on earth. The changes in its orography and earth's climate are intimately linked to this collisional event (Rowley 1996). The south face of the Himalaya is characterized by verdant vegetation, however, the plateau (Fig. 2.1) is essentially a vast (about 2.5 million sq km) cold desert with an altitude variation from 4,000 to 5,000 m. The plateau attained its altitude as a result of underthrusting of the Indian plate below Asia (Argand 1924).

Tibet is neither a mere "high plateau" nor just a "median mass," but an intensely folded mountain country with several east–west trending fold belts (Stöcklin 1980). Its crustal thickness frequently exceeds 70 km (Fig. 2.2), which is almost double the normal thickness of the continental crust. It is assumed that the Indian lower crust is underplated below Tibet. In this process the lower crust experienced multiple slicing and stacking leading to the anomalous crustal thickness of Tibet, whereas the decoupled Indian upper crust was thrust towards the south, forming the Himalaya. The Tibetan Plateau is made up of a number of microcontinents, flysch complexes, and island arcs. These smaller younger plates were gradually broken down from the ancient large Indian plate and they moved towards Asia. In this process, the microcontinents successively collided with the Eurasian plate and were subducted beneath it from the Paleozoic Era (Chang and Cheng 1973, p. 264). The most important of them are the Qilian Shan, eastern Kunlun–Qaidam, Songpan–Ganzi, Qiangtang, and Lhasa terranes, distributed from north to south, respectively (Fig. 2.2).

M.R. Dhital, *Geology of the Nepal Himalaya*, Regional Geology Reviews,
DOI 10.1007/978-3-319-02496-7_2

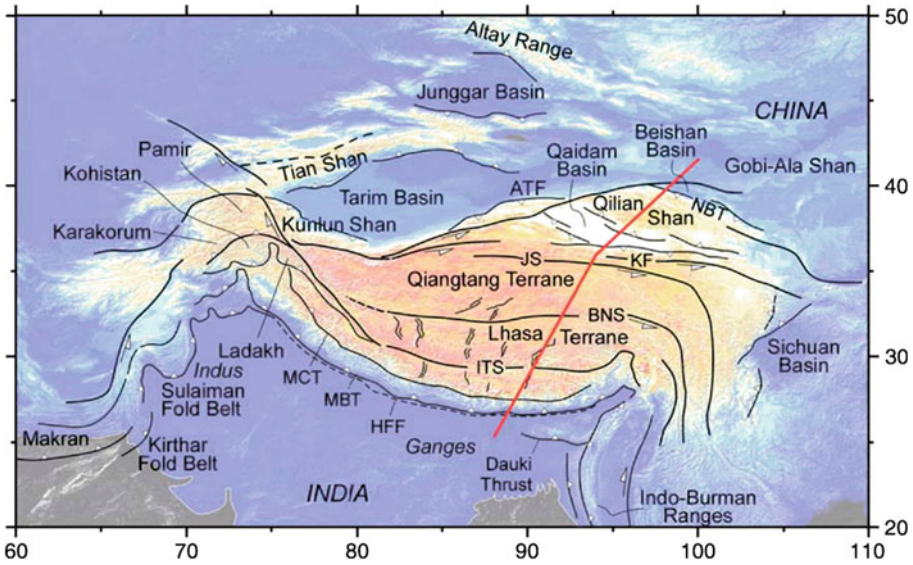

Fig. 2.1 Tectonic map of the Tibetan Plateau and surrounding regions. Color shades show elevation. *Red line* shows the position of the profile (Fig. 2.2). *ATF* Altyn Tagh Fault, *HFF* Himalayan Frontal Fault, *MBT* Main Boundary Thrust of Himalaya, *MCT* Main Central Thrust, *ITS* Indus–Tsangpo Suture, *BNS* Banggong–Nujiang Suture, *JS* Jinsha Suture, *KF* Kunlun Fault, *NBT* North Border Thrust. *Source* Jiménez-Munt et al. (2008). © Elsevier. Used by permission

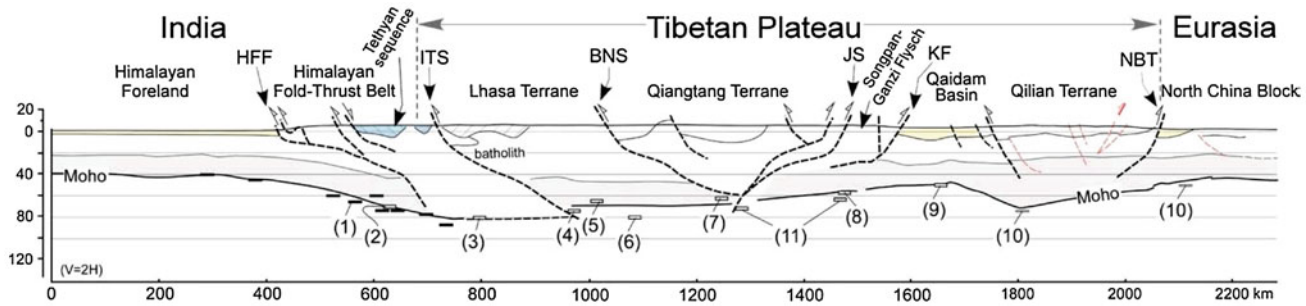

Fig. 2.2 Crustal structure along the profile inferred from geological and geophysical data. Bars show some Moho depth. *Source* Jiménez-Munt et al. (2008). © Elsevier. Used by permission

The northernmost Qilian Shan terrane is constituted of complexly deformed early Paleozoic arcs, which were formed at the south margin of the North China craton, and they were subsequently offset by the Altyn Tagh fault in the Cenozoic (Yin and Harrison 2000).

The eastern Kunlun–Qaidam terrane is bounded to the north by the southern Qilian suture and to the south by the Anyimaqen–Kunlun–Muztagh suture. It consists of the Kunlun batholith of Meso- to Neo-Proterozoic gneisses, schists, and marbles, which were unconformably overlain by Neoproterozoic stromatolitic strata and Cambrian to Ordovician carbonates (Yin and Harrison 2000).

The triangular Songpan–Ganzi terrane lies north of the Jinsha suture and south of the Anyimaqen–Kunlun–Muztagh suture. The terrane is positioned between the eastern Kunlun–Qaidam terrane to the north and the Qiangtang terrane to the south. It mainly comprises a thick, deep marine turbidity succession of Triassic age, generally named the Songpan–Ganzi flysch complex, which is actually distributed in a much wider area than the Songpan–Ganzi terrane (Dewey et al. 1988; Yin and Harrison 2000).

The Qiantang terrane is delimited by the Jinsha suture from the north and the Banggong–Nujiang suture from the south. It is made up of metamorphic rocks of eclogite and blueschist facies, belonging to an Early Triassic age. These rocks are separated from the overlying Paleozoic–Mesozoic sedimentary sequence by low-angle normal faults. The Paleozoic rocks contain a tillitic sequence, like the Talchirs in the Indian subcontinent, as well as Permian limestones alternating with volcanic rocks, whereas the Triassic rocks are represented by carbonates interbedded with continental siliciclastic and volcanic rocks. The Jurassic succession

unconformably overlies the last sequence and is made up of volcanics and limestones (Dewey et al. 1988; Yin and Harrison 2000; Mascle et al. 2012).

The Lhasa terrane is the southernmost microcontinent, whose north boundary corresponds to the Banggong–Nujiang suture and the south border is the Indus–Tsangpo suture. The Lhasa terrane is composed mainly of Ordovician and Carboniferous to Triassic shallow marine clastic deposits, resting on the Mesoproterozoic to Early Cambrian basement (Yin and Harrison 2000, p. 218). The Permian strata contain some tillite beds similar to the Talchirs. Presumably, the Lhasa terrane drifted away from the north part of Gondwana during the Triassic, and collided with the south margin of the Qiangtang terrane between the Late Jurassic and middle Cretaceous epochs (Dewey et al. 1988). The Cretaceous to Tertiary Gangdese batholith, intruding into the rocks of the Lhasa terrane, and constituting its south margin, is related to the north-dipping subduction of the Indian plate (Chang and Cheng 1973).

2.2 Indus–Tsangpo Suture Zone

The Indus–Tsangpo or Yarlung Zangbo suture zone is the north tectonic boundary between the Himalaya (Indian plate) and Tibetan Plateau (Lhasa terrane). The boundary is generally marked by a topographic depression, along which the Indus and Zangbo rivers flow in opposite directions (Heim and Gansser 1939).

The Indus–Tsangpo suture zone is a narrow (less than 15 km) belt of oceanic rocks, representing obducted remnants of the Tethys Sea (Ding et al. 2005). The suture zone consists of almost vertical tectonic slices (called exotic blocks) that are intensely deformed and dislocated (Diener 1895, 1898; von Krafft 1902; Heim and Gansser 1939). At a few places, these rocks constitute klippen over the south-lying Tethyan sequence. The suture is rather a discontinuous zone consisting of a wild flysch containing blocks of Permian limestone, Early Triassic pelagic limestone, lenses of serpentinite, Late Cretaceous pelitic calcschist, and pillow and massive alkali basaltic lava. This zone also comprises ophiolites as thin sheets and obducted masses, radiolarites with basic lavas, and some blueschists, recording a pressure of about 1 GPa and a temperature range of 350–450 °C (Mascle et al. 2012). Along the central segment of the suture, Mesozoic sediments of the Tethys Himalaya are metamorphosed. There are post-metamorphic granitic intrusions aligned south of the suture (Gansser 1977). To the east of the Kailas Valley, the metamorphic flysch overlies the non-metamorphic and almost horizontal Kailas Conglomerate along the Great Counterthrust (Heim and Gansser 1939, p. 188). The complex geometry of the Indus–Tsangpo suture zone resulted from the following sequence of events: (1) nappe movements, (2) shortening and isoclinal folding, and (3) backfolding (Burg 1992, p. 42).

2.3 Himalayan Orogen

The 2,400 km long and from 250 to 400 km wide Himalayan fold-and-thrust belt occupies about 600,000 sq km of area. It is positioned between 75° and 95° east longitude, and 27° and 35° north latitude. The Himalaya frequently surpasses 6,000 m contour level, and out of 14 eminent summits exceeding 8,000 m, 11 of them stand on this range, and the remaining three also belong to the neighboring Karakoram mountains. Most of these stupendous Himalayan peaks are congregated towards the center of the range from where the ridgeline altitude gradually decreases to the east and west (Mingtao 1982, p. 10). But this decline is halted abruptly by the two mighty marginal peaks: Nanga Parbat anchoring the Himalaya on the west where the Indus River drains its waters, and Namche Barwa standing at the east tip where the Brahmaputra flows through its foot and creates many gorges and forced meanders. To the southeast, the snow-clad Himalayan ridgeline lies at a distance of about 100 km from the alluvial plains (foreland) and that distance gradually increases to the northwest and reaches about 150 km. The Himalayan topography exhibits self-affine characteristics. An analysis of roughness of this landscape exhibits signs of multifractality as a result of the many intertwined processes shaping the landscape's form (Rodríguez-Iturbe and Rinaldo 2001, p. 233).

The Himalayan mountain range displays a perfect southwards-convex arcuate bulge (Heim and Gansser 1939, p. 1) with a radius of about 1,500 km and the center around 90° east longitude and 42° north latitude. Its present festooning curves are exactly opposite to those of the Alps with which it is connected by the transitional ranges of Iran and Hindu Kush. As compared to all other mountain belts resulting from subduction or collision, the Himalaya with its associated ranges is unique in that it lies on the subducting portion of the plate (Argand 1924). The Himalayan arc is comparable with an island arc, but it is located on land and is linked with the other arcs between Indonesia on the southeast to the Mediterranean on the northwest. It is intriguing why the Himalayan arc should result from simple underthrusting, its size and radius be comparable to those of island arcs, and be part of the island arc chain (Ollier and Pain 2000, p. 131).

The Himalaya—the young and restless giant (Valdiya 1998)—stands splendidly between the Lhasa terrane to the north and the Indian craton to the south. The north portion of the Indian shield with some Gondwana continental deposits formed the south border of the Tethys Sea. The Himalayan orogen incorporated all three elements, that is, the Tethys

sediments, Indian shield, and Gondwanas. After the collision along the Indus–Tsangpo suture zone, the tectonic activity was partially transferred towards the south. The subsequent major event was the formation of the Main Central Thrust, a deep intracrustal fracture in the Himalaya. The next large event occurred still farther south, where the frontal faults developed, respectively, in the Lesser Himalaya and Siwaliks. They represent a shallower intracrustal feature. As do many other mountain belts, the Himalaya displays a relay of orogenic activity from the deeper inner belt to the shallower outer belt (Gansser 1977). Thus, the Himalayan orogen has evolved from intense continental deformation, leading to extensive crustal shortening and thickening, large-scale thrusting and folding, polyphase metamorphism, anatexis, and granite intrusion, together with cryptic and fleeting episodes of exhumation, uplift, and erosion.

2.4 Ganga Foreland Basin

The immense alluvial level plains of the Ganga extend between the mighty Himalaya to the north and the ancient Indian tableland to the south. Early attempts to obtain the thickness of alluvium were unsuccessful (Box 2.1). Based on aeromagnetic and gravity studies, Sen Gupta (1964) found Bouguer and isostatic anomalies to be largely negative over the Gangetic plains, but they become increasingly positive over the high (5,000 m) Himalayan peaks. He found the basement depth in the alluvium to vary from about 1,500 m near the northern fringe of the Indian shield to about 9,000 m near the Himalayan foothills. Seismic surveys revealed an unconformity marking the base of the Tertiaries and underlying limestones at a depth of 1,800 m near Bareli. Positive anomalies are also recorded to the south of the Gangetic Plains, in the northern Indian shield. In other words, the Ganga Basin is flanked on the north and south sides by positive anomalies and the situation is similar to the gravity profile across the Pacific-type arcs and deep oceanic trenches. In this case, the gravity minima of the Ganga Basin correspond to those over deep trenches and the Himalayan positive anomaly to the positive gravity over the island arcs (Sen Gupta 1964, p. 324). Gutenberg and Richter (1954, p. 66) also compared the Himalaya with the Pacific arc based on their investigation on the depth of earthquake foci. They noted that the foredeep of the Himalayan arc is represented by the very deep alluvial depression of the Ganga.

Box 2.1: Early Boreholes in the Ganga Basin

Oldham (1893, pp. 432, 434) described a borehole sunk at Lucknow, in the Ganga Basin, to a depth of 407 m, or about 300 m below sea level. It passed through the alluvium with alternations of sand and sandy silt with occasional bands of calcrete without approaching the bedrock. A similar borehole driven at Kolkata, between 1835 and 1840 down to a depth of 140 m below sea level, also passed through the alluvium without reaching the hard rock.

2.5 Basement Structure of Ganga Basin

The Ganga Basin uniformly dips towards the northeast, where the overlying sediments reach a thickness of 9–10 km (Misra and Phukan 2005). The Bouguer anomaly map also shows a relatively uniform regional slope towards the north with its values ranging from 60 mGal in the south to a maximum of 210 mGal near the Nepal border. The basin becomes shallow to the east and west (Ahmad and Alam 1978; Singh 1999). The basement configuration reveals a gradual increase in thickness from south to north, indicating a maximum thickness of about 8,000 m in the extreme north margin of the basin (Fig. 2.3). The following main tectonic divisions are found in the Ganga Basin from east to west, respectively (Ahmad and Alam 1978, pp. 586–589).

The Monghyr–Saharsa Ridge (Fig. 2.4) forms a NNE–SSW trending structural high and could be the northwards extension of the Satpura Range. The sedimentary cover (mainly the Siwaliks) on the ridge is less than 3,000 m thick.

The East Uttar Pradesh Shelf lies between the Monghyr–Saharsa Ridge to the east and the Faizabad Ridge to the west. To the south of it the Vindhyan and Satpura groups of rocks crop out, and to the north the shelf seems to merge with the Gandak Depression. The inferred rocks to be met with are the Satpura Crystallines, Vindhyans, and Siwaliks.

The Gandak Depression (or Deep) lies between the East Uttar Pradesh Shelf and the Himalayan frontal ranges (Siwaliks). In this depression are found more than 6,000 m of Vindhyan, Mesozoic, Paleocene, and Neogene deposits on the Satpura Crystalline base. The Raxaul well drilled in the northern zone of the depression encountered some basement gneisses (? Satpura and Bundelkhand). They are overlain by a succession of purple shales, slates, and quartzites (? Vindhyan). This unit was unconformably followed by the Lower, Middle, and Upper Siwaliks which were finally succeeded by the Gangetic alluvium.

The NE–SE trending Faizabad Ridge (Fig. 2.4) is the most prominent structure of the Ganga Basin. It is made up of Bundelkhand Granitoids and inferred to have a thin Neogene cover. Six boreholes drilled in the West Uttar Pradesh Shelf revealed a complex structure with folds and faults (e.g., the Moradabad Fault). To the west of the Moradabad Fault, the shelf is made up of the Delhi Group

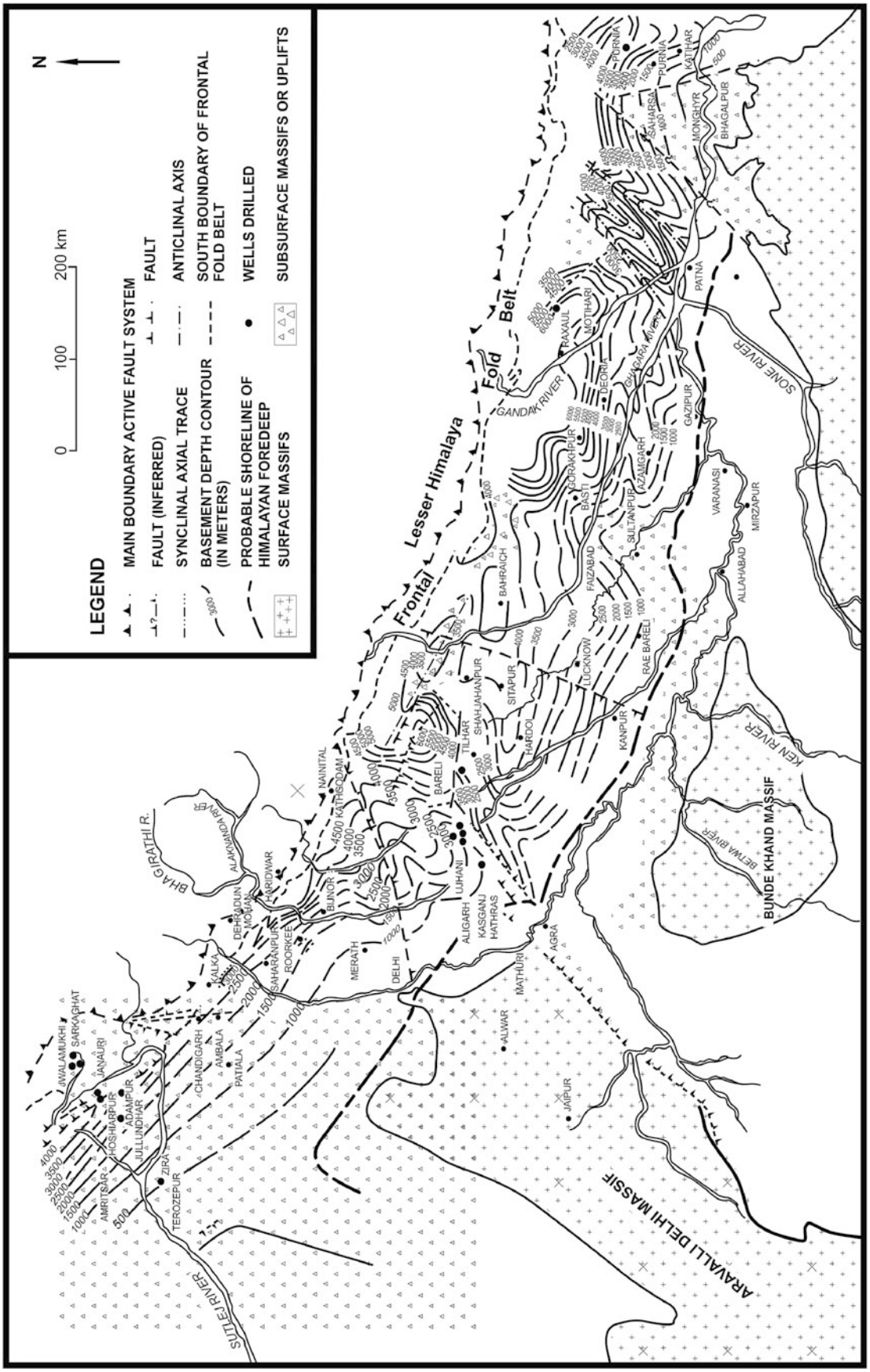

Fig. 2.3 Basement depth map of Ganga Basin. *Source* Modified from Ahmed and Alam (1978). © Wadia Institute of Himalayan Geology. Used by permission

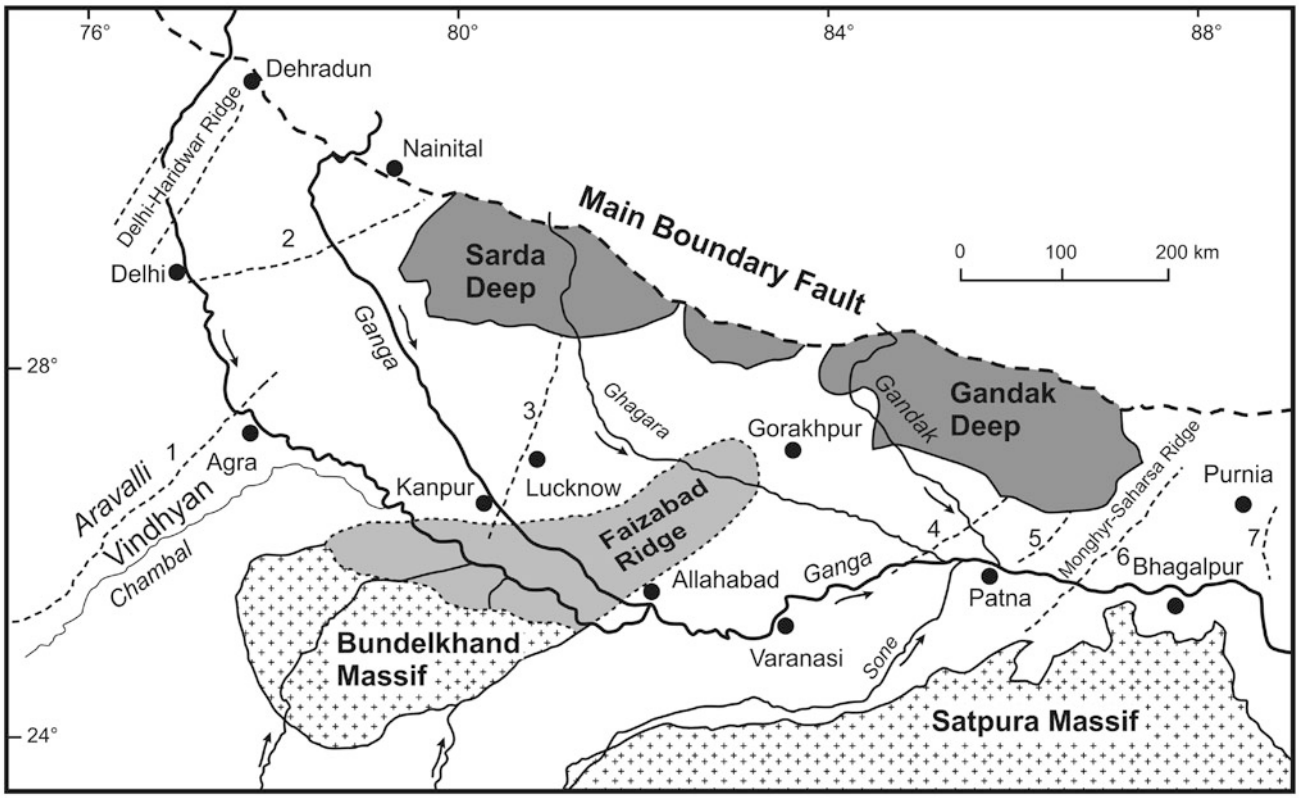

Fig. 2.4 Subsurface geology and tectonic framework of the Ganga Basin. Numbers indicate the major subsurface faults identified from geophysical investigations. *1* Great Boundary Fault, *2* Delhi–Moradabad Fault, *3* Lucknow Fault, *4* West Patna Fault, *5* East Patna Fault, *6* Monghyr–Saharsa Ridge Fault, *7* Malda–Kishanganj Fault. *Source* Modified from Sinha et al. (2005). © Wadia Institute of Himalayan Geology. Used by permission

(Basement) unconformably overlain by a Lesser Himalayan sequence. It is again followed with an unconformity by the Middle and Upper Siwaliks grading into the Gangetic alluvium. To the east of the fault are the basement rocks of the Aravalli Group, which are unconformably followed by a Lesser Himalayan sequence, and again with an unconformity by the Middle and Upper Siwaliks, respectively. The Upper Siwaliks gradually pass into the overlying alluvium. In this shelf, the pre-Siwalik unconformity constitutes a northeasterly dipping homocline, varying in depth from 620 (to the south) to 4,200 m (near the Indo–Nepal border).

The Sarda Depression is the north extension of the West Uttar Pradesh Shelf. It contains more than 6,000 m of sediments represented by Vindhyan, Mesozoic, and Paleogene and Neogene sediments.

The Delhi–Haridwar Ridge is the northward extension of the Delhi fold belt and marks the western limit of the Ganga Basin.

The basement is represented by metamorphic and igneous rocks, which can be followed southwards to meet the Bundelkhand massif (Misra and Phukan 2005). These rocks are succeeded with an unconformity by the Vindhyans. The deposition over the crystalline basement took place in the Mesoproterozoic. Then there was a gap until 600 Ma. At that time, the sediments were transformed to low-grade metamorphic rocks. During the Mesoproterozoic–early Paleozoic, shallow marine mixed siliciclastic and carbonate sequences of passive margin were accumulated. Throughout the early Paleozoic, between the ridges in the Sarda and Gandak depressions, thick shallow marine glauconitic sediments were also deposited. These sediments were laid down in a peritidal platform, with spatial variation of lithofacies from supratidal to subtidal as well as from shallow offshore shoal to fluvial. In the Ordovician, there was a regional uplift followed by a major rift phase during the Permo–Carboniferous era. Subsequently, thick Gondwana sediments were deposited in the depression between Purnia and east of the Monghyr–Saharsa Ridge (Sinha 2005). Then, the region experienced a long hiatus until an important Cretaceous transgression. The hiatus caused widespread erosion, and some basic intrusives were also emplaced at the base of the sedimentary sequence, near Raxaul, towards the northern margin of the Gandak Depression. They can be correlated with the Rajmahal volcanics (Fuloria 1969). The transgression, in turn, was followed by another hiatus that lasted up to the onset of the Tertiary.

Owing to progressive flexing of the Indian plate, the south margin of the foredeep migrated southwards. In this process the north margin of the foredeep was deformed and the foredeep wedges were accreted to the south. The general trend of the foredeep is parallel to the Himalayan front. The sediments accumulated in the foredeep consist of the Tertiary siliciclastics. Except the Paleogene marine Subathu, the rest of the Tertiary sediments are fluvial and consist of many fining-upwards sequences (Sinha 2005).

During the India–Asia collision, a major inversion took place and the pre-existing basement faults were reactivated. The displacement along these faults resulted in the development of linear highs and lows. In the Neogene foredeep area, during the Mesozoic and early Paleogene the region experienced denudation and peneplanation; as a result the sediments were removed from the highs and survived only in the areas of linear lows across the basin. The wedge-shaped Tertiary package gently dips due north and it attains a thickness of about 6,000 m in the proximity of the foothills (Sinha 2005).

2.6 Unstable River Courses

Many and great have been the alterations in the drainage lines of the Indus, Ganga, Brahmaputra, and their tributaries. For example, in Vedic times, the portion of the river that flowed to the Punjab was known as the Saraswati, and that which joined the Ganga was called the Yamuna (Oldham 1886; Radhakrishna and Merh 1999). At the beginning of the nineteenth century, the Brahmaputra broke away from its old course and flowed west of the Madhopur jungle to join the Ganga, and the new channel was named the Jamuna (Oldham 1886, p. 341). In August 1787, the Tista River deserted the Ganga and joined the Brahmaputra (Shillingford 1893).

The Koshi (Kosi or Kusi, *Kaushiki* in Sanskrit) River is the most devastating one. The river has frequently shifted its channel (Fig. 2.5) and formed a megafan. In the past 250 years, it has migrated westwards by about 150 km via more than 12 channels. In the past, before the construction of the Koshi barrage in 1963, there were some attempts to train the river (Box 2.2). The main cause of channel shifting is the deposition of an enormous amount of sediment load on the Ganga Basin from denudation of the Himalayan ranges. The main channel of the Koshi River oscillates between the Brahmaputra to the east and Gandak (Gandaki) to the west, and the pivot is at Chatra, in Nepal (Fergusson 1863). The oscillation periods are long and slow towards the west whereas they are sudden and devastating while moving towards the east. In the late 1880s and early 1890s, the Koshi River suddenly shifted its main channel on the borders of Nepal and much of the floodwater was thrown eastwards, towards Purnia and Dinajpur. During the rainy season of 1893, severe floods occurred in the Koshi River (Shillingford

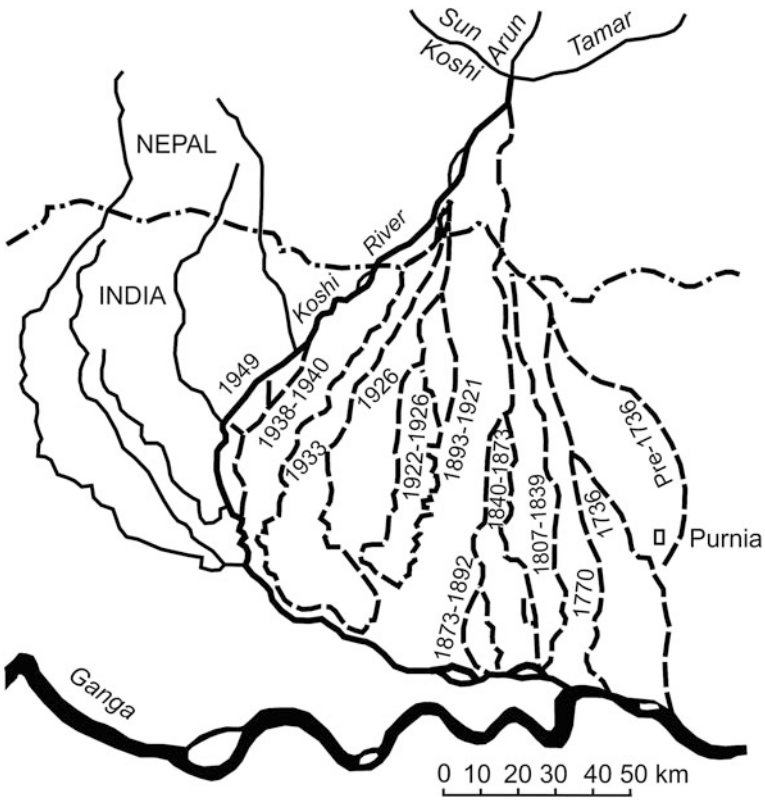

Fig. 2.5 Channel shifting by the Koshi River. *Source* Modified from Duff (1992)

1893, pp. 1–2). The waters in the Ganga and Brahmaputra rivers interact in a complex manner during flooding (Box 2.3).

Box 2.2: Past Attempts to Train the Koshi

Shillingford (1893, p. 14) described the following case of river training works:

> In North Bhagalpur, there is an extensive embankment of earth in places some 5–10 m high, called the Bīr Bandh, extending from the foot of the Belkār (Beltar) or outer range of hills in Nepal southwards into Bhagalpur district, about 80 km in length, it runs nearly parallel with the present course of the Kusī (Koshi) which approaches it towards its south end. Dr. Buchanan Hamilton and others considered it to be a fortification, a theory shown by Dr. Hunter to be highly improbable, but it may possibly be a dyke to prevent Kusī (Koshi) overflows from flooding the lower country to the west and carving out fresh channels … . Dr. Buchanan Hamilton conjectures that this earth-work was constructed by Lakṣmaṇa II, about the close of the 12th century, the only reasons assigned for the supposition being that tradition stated it to have been built by a Lakṣmaṇa and "as the works were never completed and have the appearance of having been suddenly deserted, it is probable that they were erected by Lakṣmaṇa the second, who in the year 1207, was subdued and expelled from Nadiya by the Moslems." Probably he refers to the detached portions at its southern end, cut away by river action, when alluding to its incomplete and abandoned appearance. This extensive embankment cuts off the sources of the Ḍimrā and Tīljugā (Trijuga) rivers from the Kusī (Koshi), and intercepts all flood-waters of the latter river from entering the channels.

Box 2.3: Backflows in Ganga and Brahmaputra

In the first month of inundation when there is much water in the Brahmaputra River, the Ganga above Jaffirgunj flows backwards, and the Echamati at Pubna flows into the Ganga, instead of flowing out of it. During that period there is a considerable amount of deposit in its bed. But, during the last month of the rainy season, when the water in the Brahmaputra River has nearly run off, an immense water body previously spread over the floodplains rushes into the partially deserted bed of the Brahmaputra, which acts as a wastewater reservoir, and clears out the sediments deposited in the earlier months (Fergusson 1863, p. 337).

After the construction of the Koshi barrage, the river was trained to some extent. However, in 2008, the Koshi breached its embankments and followed an earlier course towards the east, bringing about much devastation in Nepal and India.

References

Ahmad A, Alam JM (1978) The Ganga Basin, its subsurface sequences, their affinity, sedimentological and tectonic implications. Himalayan Geol 8(Part I):583–608 (Wadia Institute of Himalayan Geology, Dehradun)

Argand E (1924) La tectonique de l'Asie. Congrès Géologique International, Belgique, Comptes Rendues de la 13ème Session, en Belgique 1922. H. Vaillant-Carmanne, Liège, pp 171–372

Burg JP (1992) Himalayan orogeny and global tectonics seen from the Tsangpo suture zone of Tibet (China). In: Sinha AK (ed) Himalayan orogeny and global tectonics, Publication No. 197 of the International Lithosphere Programme. Oxford & IBH Publishing Co., New Delhi, (343 pp), pp 35–44

Chang C-F, Cheng H-L (1973) Some tectonic features of the Mt. Jolmo Lungma area, Southern Tibet, China. Scientia Sinica XVI(2):257–265

Dewey JF, Shackleton RM, Chang C, Sun Y (1988) The tectonic evolution of the Tibetan plateau. Philos Trans R Soc Lond, Ser A 327:379–413

Diener C (1895) Ergebnisse einer geologischen expedition in den Central-Himalaya von Johar, Hundes, und Painkhanda. Denkschriften der Kaiserlichen Akademie der Wissenschaften, Wien 62:533–608

Diener C (1898) Notes on the geological structure of the Chitichun region. Mem Geol Surv India XXVIII(Part 1):1–27

Ding L, Kapp P, Wan XQ (2005) Paleocene–Eocene record of ophiolite obduction and initial India–Asia collision, south central Tibet. Tectonics, vol 24, TC3001. doi: 10.1029/2004TC001729

Duff P, McL D (1992) Holmes' principles of physical geology, 4th edn. ELBS, London, 791 pp

Fergusson J (1863) On recent changes in the delta of the Ganges. Q J Geol Soc Lond XIX(Part 1):321–354 (with 1 plate)

Fuloria RC (1969) Geological framework of Ganga Basin. In: Selected lectures on petroleum exploration, vol 1. Petroleum Geology, Geophysics & Geochemistry, pp 170–186 (with a geological sketch map), Institute of Petroleum Exploration, Oil and Natural Gas Commission, Dehradun, India

Gansser A (1964) Geology of the Himalayas. Interscience, New York, 289 pp

Gansser A (1977) The great suture zone between Himalaya and Tibet, a preliminary account. Colloques internationaux du C.N.R.S., No. 268—Écologie et Géologie de l'Himalaya, pp 181–191

Gutenberg B, Richter CF (1954) Seismicity of the earth and associated phenomena, 2nd edn. Princeton University Press, Princeton, 310 pp

Heim A, Gansser A (1939) Central Himalaya: geological observations of the Swiss expedition 1936. Denkschriften der Schweizerischen Naturforschenden Gesellschaft, Band LXXIII, Abh. 1, 245 pp (with geological maps in colors, sections, and plates)

Jiménez-Munt I, Fernàndez M, Vergés J, Platt JP (2008) Lithosphere structure underneath the Tibetan Plateau inferred from elevation, gravity and geoid anomalies. Earth Planet Sci Lett 267:276–289

Mascle G, Pêcher A, Guillot S, Rai SM, Gajurel AP (2012) The Himalaya–Tibet collision. Nepal Geological Society and Société Géologique de France, Paris, 264 pp

Mingtao Z (1982) The roof of the world. Harry N. Abrams, Incorporated, New York, 227 pp

Misra R, Phukan RK (2005) Search for hydrocarbon in Ganga Basin: south-eastern part of Gandak depression merits further probe. In: Bhattacharya AR, Agarwal KK (eds) Himalayan orogen—Foreland interaction, vol 2. Palaeontological Society of India, Lucknow, pp 11–21

Oldham RD (ed) (1893) A manual of the geology of India: stratigraphic and structural geology, 2nd edn. Geological Survey of India, Calcutta, 543 pp (with a geological map of India in colors, scale: 1 inch = 96 miles)

Oldham RD (1886) On probable changes in the geography of the Punjab and its rivers: an historico-geographical study. J Asiatic Soc Bengal, Calcutta LV:(Part II, 4):322–343 (with a map)

Ollier CD, Pain CF (2000) The origin of mountains. Routledge, London, 345 pp

Patriat P, Achache J (1984) India-Asia collision chronology has implications for crustal shortening and driving mechanism of plates. Nature 311:615–621

Radhakrishna BP, Merh SS (eds) (1999) Vedic Sarasvati: evolutionary history of a lost river of Northwestern India, vol 42. Geological Society of India, Bangalore, 329 pp

Rodríguez-Iturbe I, Rinaldo A (2001) Fractal River Basins: chance and self-organization. Cambridge University Press, Cambridge, 547 pp

Rowley DB (1996) Age of initiation of collision between India and Asia: a review of stratigraphic data. Earth Planet Sci Lett 145:1–13

Sen Gupta S (1964) Possible subsurface structures below the Himalayas and the gangetic plains. In: International geological Congress, report of the Twenty-Second session, part XI, proceedings of section 11: Alpine and Himalayan orogeny, New Delhi, pp 334–352

Shillingford FA (1893) On changes in the course of the Kusī River, and the probable dangers arising from them. J Asiat Soc Bengal, Calcutta LXIV(Part I, 1):1–25 (with a map)

Singh IB (1999) Tectonic control on sedimentation in Ganga Plain Foreland basin: constraints on Siwalik sedimentation models. In: Jain AK, Manickavasagam RM (eds) Geodynamics of the NW Himalaya, vol 6. Gondwana Research Group Memoir, Osaka, pp 247–262

Sinha YB (2005) Hydrocarbon prospectivity of the Ganga Basin and the Frontal Thrust—fold belt of the Himalayas: some thoughts. In: Bhattacharya AR, Agarwal KK (eds) Himalayan orogen—Foreland interaction, vol 2. Palaeontol Society of India, Lucknow, pp 1–9

Sinha R, Tandon SK, Gibling MR, Bhattacharjee PS, Dasgupta AS (2005) Late Quaternary geology and alluvial stratigraphy of the Ganga basin. Himalayan Geol 26(1):223–240

Stöcklin J (1980) Geology of Nepal and its regional frame. J Geol Soc Lond 137:1–34

Valdiya KS (1998) Dynamic Himalaya. Universities Press (India) Limited, Hyderabad, 178 pp

von Krafft A (1902) Notes on the "Exotic Blocks" of Malla Johar in the Rhot Mahals of Kumaon. Mem Geol Surv India XXXII(Part 3):127–183 (with map and sections)

Yin A, Harrison TM (2000) Geologic evolution of the Himalayan-Tibetan orogen. Ann Rev Earth Planet Sci 28:211–280

Physiography of Nepal

3

The great elevation of these peaks is scarcely more striking than the depth of the valleys or hollows which separate them, and which are always the beds of the rivers.

—J.D. Herbert (1842, p. xxvi)

The territory of Nepal (Fig. 3.1) falls in the central portion of the Himalayan arc and extends between 80°04′ and 88°12′ east longitude, and 26°22′ and 30°27′ north latitude. The country approximates an oblong and occupies an area of 147,181 sq km. Its maximum length is about 825 km, and its width varies between 250 and 170 km from west to east, respectively. About 80 % of Nepal's land is occupied by mountains.

Nepal, sometimes remembered as "heaven on earth," is one of the most fascinating places in the world. It is also a country of great contrasts (Hagen 1969, p. 16). Its altitude ranges from 64 m (at Kechana in the plains of southeast Nepal) to 8,848 m (Mount Everest, the world's highest summit) both within an aerial distance of about 150 km, where the climate quickly changes from subtropical to arctic conditions. It also has the Kali Gandaki Gorge, the deepest defile on earth. Apart from the third pole (i.e., Mt. Everest), the Nepal Himalaya is also symbolized by the highest number of great dazzling snow-clad summits exceeding 8,000 m as well as a diverse range of landforms.

The territory of Nepal is divided into the following roughly parallel physiographic regions (Fig. 3.2) from south to north, respectively (Hagen 1969, p. 18). A profile across the Himalaya illustrates the subdivisions (Fig. 3.3).

- Terai
- Siwalik Range (or briefly Siwaliks) with dun valleys
- Mahabharat Range
- Midlands
- Fore Himalaya
- Great Himalaya
- Inner Himalayan valleys
- Tibetan marginal ranges.

3.1 Terai

The Terai Plain is represented by Pleistocene to Holocene sediments and is part of the Ganga foreland basin. In Nepal there are three separate areas where the alluvium is observed south of the Siwalik hills (Fig. 3.2). Its width varies from about 30 km in west Nepal to about 40 km in central Nepal, and from 25 to 50 km in east Nepal. Its altitude fluctuates from about 100–200 m from east to west, respectively. Generally, the Terai slopes towards the south and the altitudinal difference between the Siwalik foothills and the Indian border ranges from 100 to 200 m. The Terai is subdivided into the three zones, respectively, from north to south.

3.1.1 Upper Terai or Bhabar Zone

The Bhabar (or Bhabhar) zone is observed at the foot of the Siwaliks and it is made up of coalescing alluvial fans, which are crosscut by major rivers and streams. It is 10–15 km wide. The Bhabar zone gently (a few degrees) slopes towards the south and consists of poorly sorted boulders, cobbles, pebbles, and sand derived from the Siwalik or older rocks. It is the zone of groundwater recharge for the Terai. But in the monsoon season, debris flows, gully erosion, and abrupt river channel shifting affect this region.

3.1.2 Middle Terai or Marshy Land

The middle Terai lies at the distal end of the coalescing alluvial fans of the Bhabar zone. Most of the region is made

M.R. Dhital, *Geology of the Nepal Himalaya*, Regional Geology Reviews,
DOI 10.1007/978-3-319-02496-7_3

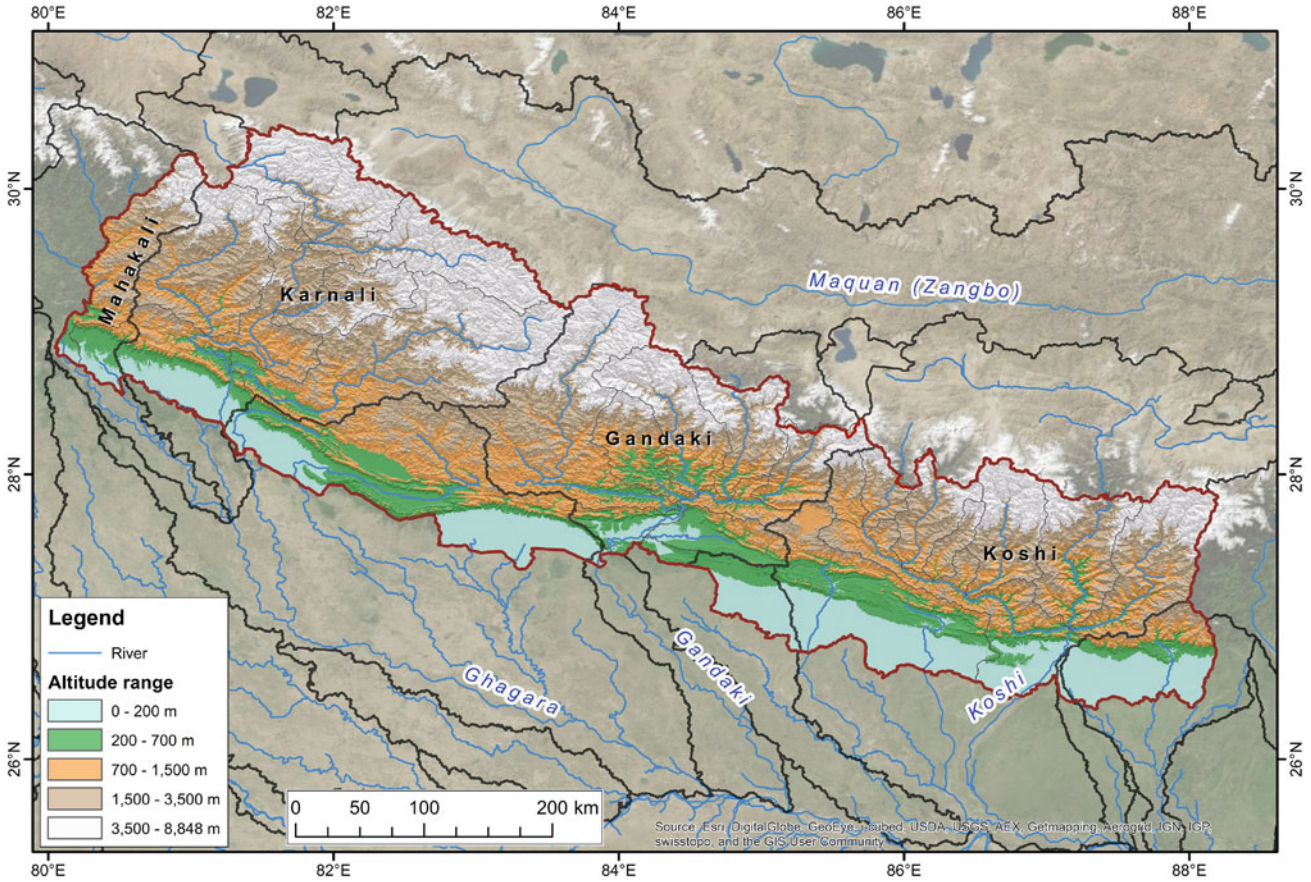

Fig. 3.1 Nepal and its main river basins. *Source* Compiled from ESRI, DigitalGlobe, GeoEye, i-cubed, USDA, USGS, AEX, Getmapping, Aerogrid, IGN, IGP, swisstopo, and the GIS user community

up of fine silt and clay but there are also alternating beds of sand and fine gravel. The beds are very gently (less than 1°) tilted to the south. Frequently, a spring line separates the middle Terai from the Bhabar zone (Fig. 3.4).

3.1.3 Lower Terai or Gangetic Alluvium

Most of the lower Terai lies in the zone of interaction between the Gangetic alluvium and the deposits of its meandering and braided tributaries. It is almost flat and the gradient is less than 0.1 %. The sediments are represented by sand, silt, and clay with some pebbles.

3.2 Siwaliks and Dun Valleys

The first topographic rise north of the Terai is called the Siwaliks or Chure (Churia) hills in Nepal. The Siwalik hills range in altitude from about 300 m to 2,000 m and they are generally higher than 1,000 m. Most of the Siwalik ridges extend in the east–west direction, parallel to the Himalayan trend. There have been contradictory opinions on the existence of a single, essentially longitudinally flowing, trunk river or various large transverse debauchers during Siwalik time (Box 3.1).

Box 3.1: Indobrahm or Siwalik River

Pascoe (1919, p. 145) noted that many Himalayan rivers have northwestward pointing V's in their course where they cross the Siwalik foothills or where they enter the plain. Such sharp bends were thought to be the remnants of a former northwest-flowing main river called by Pascoe as the Indobrahm, of which these rivers were tributaries. They were later captured by the southeast-flowing main river (the Ganga). Pilgrim (1919) had similar ideas and proposed the name Siwalik to the trunk river. He argued that since there is an unconformity between the boulderbeds and the underlying Siwaliks, there was a river flowing from

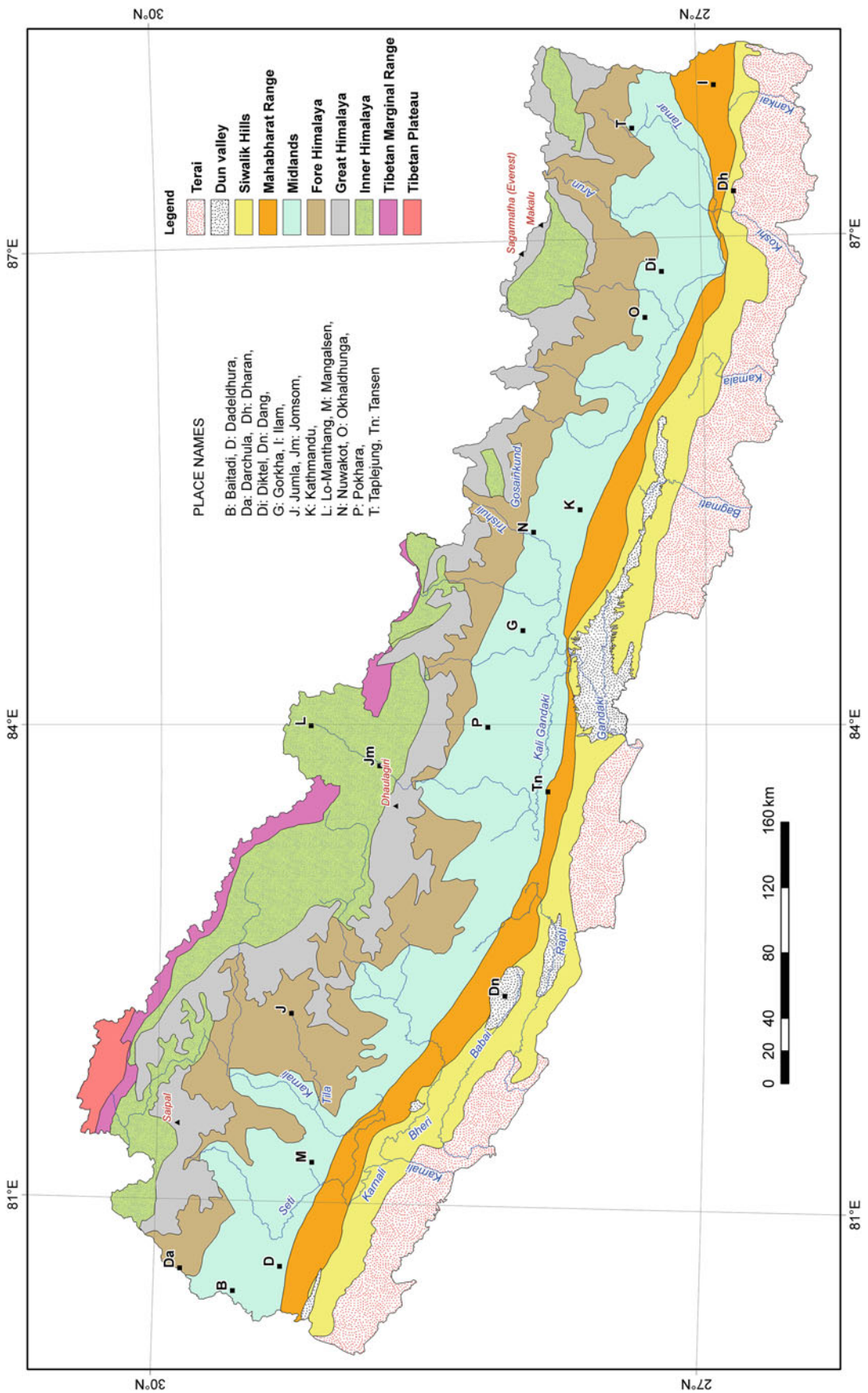

Fig. 3.2 Physiographic divisions of Nepal. *Source* Modified from Hagen (1969)

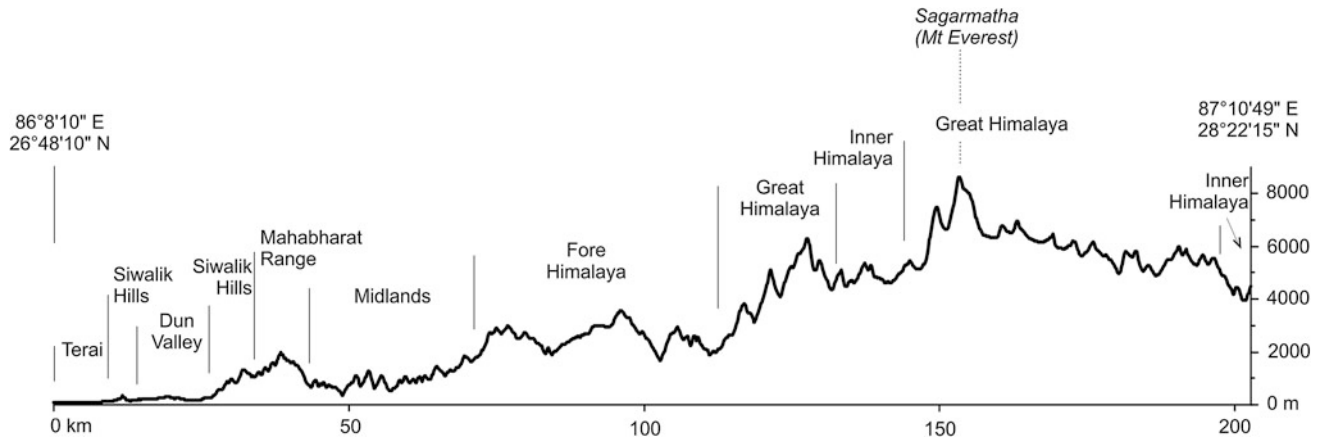

Fig. 3.3 Profile of the Himalaya through east Nepal and position of physiographic regions. *Source* Generated from the SRTM DEM

southeast to northwest (toward the Eocene sea). The river was dammed by torrents coming from the Himalayas and produced boulderbeds more than 1,500 m thick. Between the end of the Eocene and recent times, the drainage of that part of India must have been reversed. The erosive power of the river could not keep pace with the rapidly rising Himalaya and the river was elbowed off to the west. As a result, the boulder-conglomerates were formed.

On the other hand, Krishnan and Aiyengar (1940, p. 15) remark that such a hypothesis of river capture is not required. The tectonic movements of appreciable magnitude have caused great changes in the river courses that existed during the time of deposition of the Siwaliks. The Siwaliks themselves have been uplifted to about 1,200 m in post-Siwalik times and these movements were responsible for the changes in drainage pattern. However, the investigations of Burbank (1992) lend some support to this hypothesis.

The Siwalik Range, also known as the Sub-Himalaya, continues throughout the Himalaya with a few short gaps in Bhutan (Chap. 5). Medlicott and Blanford (1879, p. 521) noted that the Sub-Himalayan hills are easily distinguishable everywhere from the much higher mountains to their north by the abrupt difference of elevation and by contour. They very commonly exhibit a steep face (scarp slope) to the south and a gentle inner dip slope (Fig. 3.5) and, as a general rule, they consist of two ranges, separated by a broad flat valley, called the "dún" (doon) in India or "mári" in Nepal (Strachey 1851, p. 296).

Generally, the Siwalik belt is 10–15 km wide. However, it occupies a wider (more than 50 km) zone in the western Himalaya of Pakistan (Potwar Plateau) and India (Jammu and Himachal Pradesh). It is about 20 km wide at the western border (i.e., the Mahakali River) of Nepal and less than 1 km near its eastern extremity (i.e., the Mechi River). On the other hand, it is from 30 to 50 km wide in the areas with intermontane valleys.

The Siwalik hills west of Karnali are made up of two ranges around the Rangun Khola, at the west border of Nepal with India. There is a single belt between Budar and the Karnali River, around Butwal, and between Dharan and Ilam. In the other places, there are two or more chains, the northernmost of which sometimes mingles with the Mahabharat Range.

When there are multiple Siwalik ranges, they are not parallel to each other, but converge or diverge here and there. These ranges are broadly concave or convex towards the foreland. As a result, some space is left between them and that space is occupied by tectonic (or dun) valleys (Hagen 1969, p. 20). This kind of divergence or convergence is related mainly to the orientation of branching imbricate faults.

The dun or intermontane valleys are confined between the Karnali River to the west and the Koshi River to the east. There is also a small valley in the Kankai River basin. The most important intermontane valleys are the Surkhet, Dang, Deukhuri, Chitwan, Hetaunda, Marin, Udaipur, Katari, and the Gaighat–Beltar. The altitude of these valleys ranges from about 700 m (Dang) to about 100 m (near Beltar). Sometimes, the two valleys (such as Dang and Deukhuri) are arranged in an en echelon fashion (Fig. 3.2).

One of the remarkable features of frontal Siwalik hills is their abrupt disappearance in the Terai Plain (Fig. 3.6). This is observed east of Karnali, around the bend of the Rapti River (east of Nepalgunj), west of Amiliya, north of Mirchaiya, and south of Beltar. These are the closures of the Siwalik beds forming plunging anticlines or synclines.

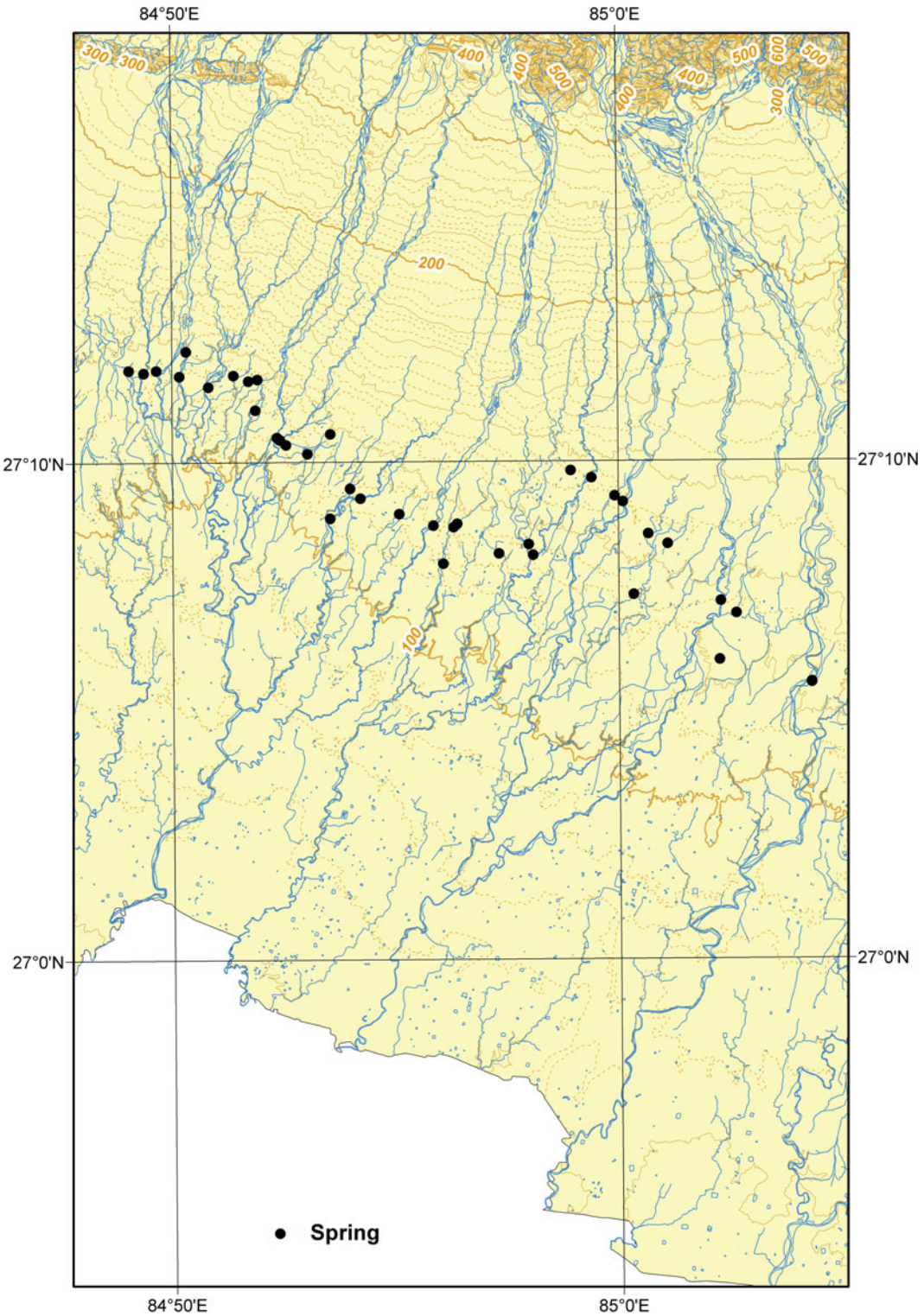

Fig. 3.4 Spring line marking the boundary between the Bhabar zone and middle Terai in central Nepal. *Source* Compiled from the data of DoI (1993)

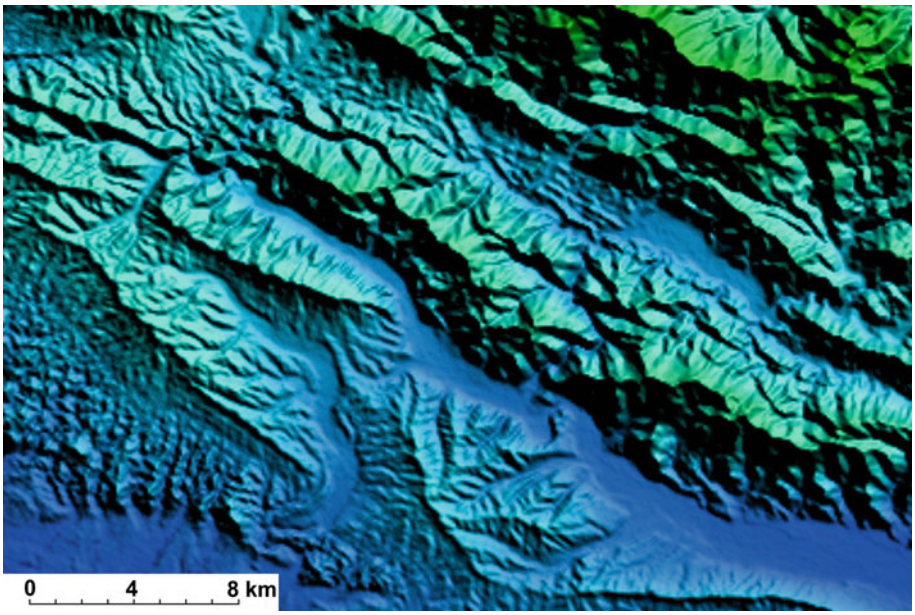

Fig. 3.5 Dip slopes and scarp slopes observed in Siwaliks of east Nepal. *Source* Generated from SRTM DEM

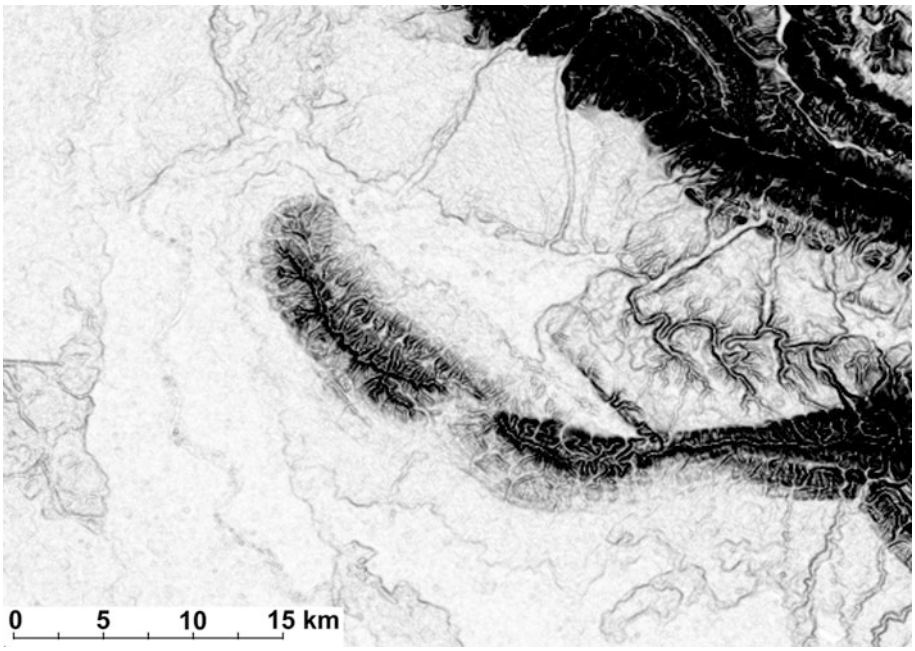

Fig. 3.6 Disappearing Siwalik hills in the neighborhood of the Rapti River in west Nepal. *Source* Generated from SRTM DEM

The landforms of the Siwaliks are controlled predominantly by tectonic processes and subordinately by weathering and mass wasting. Parallel and rectangular drainage patterns (controlled by bedding and joints) are frequent in the Siwaliks. Centripetal and rectangular drainage patterns are common in the core of synclines and a radial pattern is characteristic of an anticlinal core. The hills are characterized by hogback and cuesta structures with south-facing escarpments. A hogback structure is observed basically in very thick sandstone successions, whereas a cuesta is characteristic of conglomerate beds. Interbedded competent (sandstone) and incompetent (mudstone) beds have given rise to alternating ridges and furrows. Most of the streams on scarp slopes flow essentially due south, against the strike of beds, whereas those originating on dip slopes flow from south to north.

Rainwater significantly affects the soft and loose Siwalik strata leading to flash floods and debris flows (Box 3.2). Flashy overland flows on Siwalik shingles and sands generate alluvial fans, but some deep gullies result when such flows erode loose sand or soft mud beds. Consequently, there are rugged hills, deep gorges, cliffs, and active gullies representing the erosional landforms, whereas river terraces, alluvial fans, and talus cones are the examples of

Fig. 3.7 Large granite boulders at the west end of Hetaunda, on the upper terrace of the Burhi Rapti River. View to west. *Source* Photo by author

depositional landforms. On the other hand, owing to the deposition of an excessive amount of bed load and the pervious nature of strata, the Siwalik valleys and hills are dry most of the time.

Box 3.2: Debris Flow in the Siwalik Belt

Medlicott (1875, p. 100) went to Hetaunda on his way to Kathmandu and noted the large boulders around Hetaunda (Fig. 3.7) and inferred them to be of glacial origin. Most probably, such boulders were deposited from the past debris flows similar to those incurred during the hydrological disaster of 1993 in south-central Nepal. Heim and Gansser (1939, p. 9) describe some boulders of extraordinary size (nearly 100 cubic metres) from the Murti River, east of the Tista, and attribute them to the erosive power of the river owing to very high (10–12 m per year) rainfall.

3.3 Mahabharat Range

The Mahabharat (named after the great Hindu epic, *the Mahabharata*) is the next high mountain range lying north of the Terai and overlooking the Midlands. The Main Boundary active fault system frequently delimits the Mahabharat Range from the Siwaliks. The Mahabharat Range rises higher than the Siwalik hills and reaches an altitude of 3,000 m, but most of it is less than 2,000 m. Different from the Siwaliks, this range is discontinuous and includes a variety of Lesser and Higher Himalayan rocks. The geomorphic classification of mountains into the Siwalik and Mahabharat ranges does not always coincide with the geological subdivisions.

The Mahabharat Range is divisible into three main segments, separated by two major antecedent rivers. The stretch west of the Karnali (near the Seti confluence) as well as the portion east of the Narayani (Gandaki) is constituted mainly of metamorphic and crystalline rocks, whereas the central portion extending between the Karnali and Narayani is composed of sedimentary or slightly metamorphosed sequences. The east and west segments are not only identical in their rock composition, but also possess a similar synformally folded crest, which is interrupted only by some antecedent rivers. Although the Bagmati River seems to be an exception, as it cuts through the Chandragiri hills, it too does not cross the crest of Shivapuri (Sheopuri) positioned north of Kathmandu. However, the central segment encounters a variety of folds and faults. The Mahabharat Range is rather discontinuous, dissected also by the rivers originating from the south face of the Himalaya, and relatively subdued in topography. Intense erosion in the central segment of the Mahabharat Range exposed the underlying rock sequences when the region was denuded of the metamorphic cover.

The Mahabharat Range acts as a barrier to the rivers originating from the Midlands or farther north and flowing into the Ganga. It is evident from their abrupt orientation change while approaching the range: those flowing essentially perpendicular to it suddenly take a parallel course.

Even antecedent rivers are deflected to the east or west by this range and they make narrow and deep gorges while crossing it. All these observations point to a recent upheaval of the Mahabharat Range.

3.4 Midlands

The Midlands, the heart of Nepal, compose the scenic lowlands between the Mahabharat Range to the south and the high mountains to the north (Hagen 1969, p. 21). Their altitude varies between 600 and 2,000 m, and they are generally covered with alluvial, colluvial, and residual soils. Most of the densely populated valleys are located within the Midlands. Chaurjahari, Kusma, Pokhara, Kathmandu, Panchkhal, and Tumling Tar are some of the valleys in the Midlands.

The Midlands display diverse drainage patterns including trellis, rectangular, parallel, and dendritic. The Kathmandu Valley (Fig. 3.8) is a textbook example of the centripetal drainage pattern. The main longitudinally or transversely aligned rivers, such as the Trishuli, Sun Koshi, Tama Koshi, Dudh Koshi, Arun, and Tamar in central and east Nepal follow the antiformal cores (Hagen 1969, p. 22). However, such an alignment is not evident in west Nepal. In many areas, river trends agree very well with the strikes of the joints in the region (Scheidegger 1999).

The Midlands have been bestowed a variety of alluvial terraces suitable for agriculture. They were produced by constant lateral channel shifting and vertical incision of the snaking rivers. A range of sedimentary, low-grade metamorphic, and crystalline rocks belonging mainly to the Higher and Lesser Himalayan sequences constitutes the Midlands. When a rock is exposed to prolonged sunshine for tens of thousands to hundreds of thousands of years in a humid subtropical region of the Midlands, a residual red soil develops. The red color is due to oxidation of iron-containing minerals (viz., pyrite, chlorite, biotite, hornblende) of the bedrock. Such a soil is almost like a laterite found in South India and tropical regions. The red soil ranges from a few meters to tens of meters deep and is distributed in foothills, ridges, spurs, and convex slopes of the Midlands. Similar soils are also infrequently observed in the Siwalik foothills, dun valleys, and Mahabharat Range.

3.5 Fore Himalaya

The Midlands region exceeding the average altitude of 3,000 m is defined as the Fore Himalaya (Hagen 1969, p. 22). This region lies in the inner belt of the Midlands, that is, at the foot of the Great Himalayan Range. This portion of the Himalaya falls within the crystalline thrust sheets or in

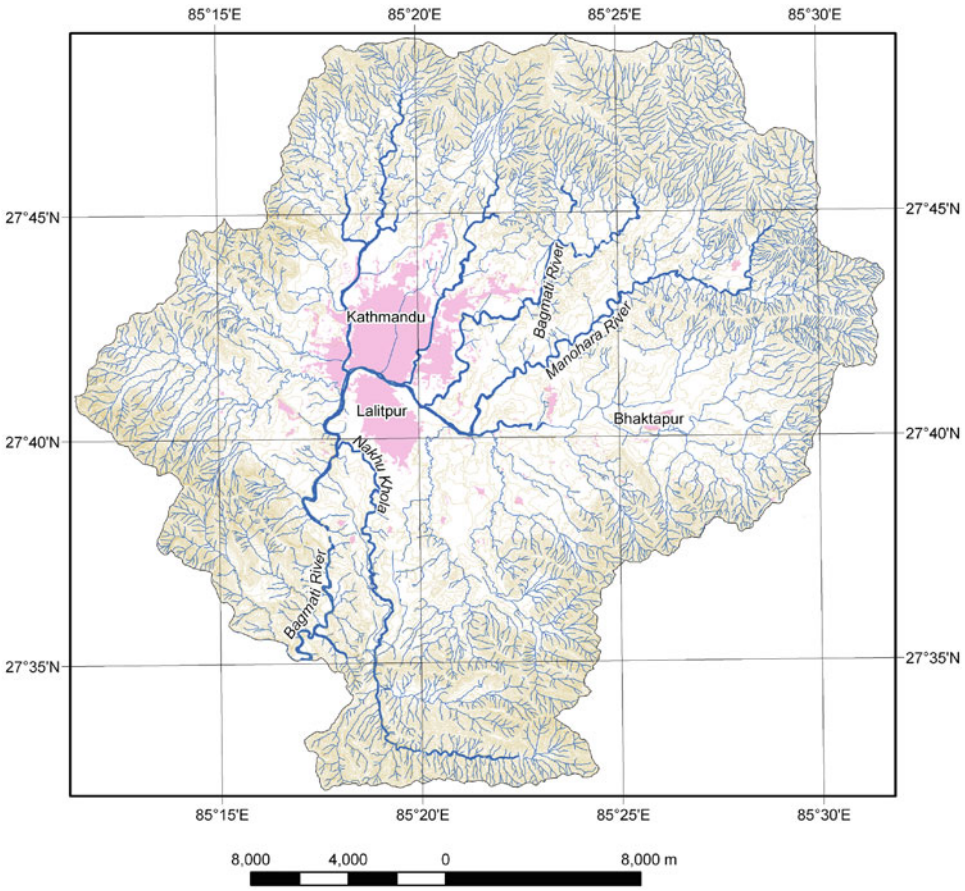

Fig. 3.8 Kathmandu Valley: an example of centripetal drainage pattern. *Source* Compiled from the maps of Survey Department of Nepal

the valleys surrounded by them. It is also marked by an increased microseismic activity. The valleys of Jumla in west Nepal and Solu in east Nepal are two examples. This highland, where the altitude may exceed 4,000 m, is covered with thick snow in winter and gets some rain in summer.

3.6 Great Himalayan Range

The Great Himalayan Range is the showpiece of Nepal where there are eight summits exceeding 8,000 m (Table 3.1). The region is made up of metamorphic rocks and crystallines capped by sedimentary rocks with some granite intrusions. Generally, the south face of the Great Himalaya is steeper and shorter than its north slope. A peculiar feature of the Great Himalayan Range is that although it stands as a barrier to the humid air coming from the Indian Ocean and prevents the moisture from entering the Tibetan Plateau, the range allows the passage of some deep trans-Himalayan rivers through it. These mighty rivers originate in the Tibetan marginal mountains with an altitude of less than 6,000 m but cross a range whose altitude exceeds 8,000 m (Wager 1934, p. 328; Hagen 1969, p. 19).

The transverse gorges (Box 3.3) of Himalaya are no less impressive than its summits. The great Himalayan Range is not a single continuous chain but is interrupted by gorges thousands of meters deep, which occur very close to the summits standing at the border of the precipices (Wager 1937, p. 239). The Great Himalayan Range incorporates a number of massifs, such as the Kanjiroba, Dhaulagiri, Annapurna, Langtang, Khumbu, and Kanchenjunga.

Box 3.3: 'Anomalous' Arun River

The antecedent nature of trans-Himalayan rivers was first established by studying the morphology of the Arun River. Heron believed that the Arun River had cut back through the Himalayan range and had captured an east-flowing river in Tibet. The Arun River flows essentially from west to east and meanders through the broad plain of Tibet until it sharply turns southwestwards and southwards through the main Himalayan range. While flowing through the Higher Himalayan Zone, it encounters the upper gorge. Before entering the gorge, the river flows through a fairly open valley with extensive terraces of boulders and gravel. Then it abruptly turns at a right angle (Fig. 3.9) into the core of a high mountain of hard gneiss forming a canyon called the Yo Ri gorge, with almost vertical walls. It continues to flow southwards through this gorge for about 5 km, then swings again and flows west for about 6 km, and finally emerges from the gorge following the same trend as before entering the canyon (Heron 1922, p. 219). This anomalous phenomenon was later explained by Wager (1937, p. 248) as a typical act of an antecedent river.

Most of the landscape is carved by rivers, glaciers, snow, ice, and wind. The glaciers are the reservoirs of frozen water that feeds a number of large rivers of Nepal. Cirques, lateral and terminal moraines, hanging valleys, and terraces of fluvio-glacial or lacustrine origin are the common landforms. There are also numerous glacier lakes posing a threat of outburst flood to the community living in the Midlands. Snow and rock avalanches as well as various other glacial disasters have struck this region. The event of May 5, 2012 in the Annapurna region of west Nepal devastated the Seti River valley. The Great Himalayan Range contains some giant rockslides such as the Tsergo Ri (Scott and Drever 1953; Masch and Preuss 1977) and Lete.

3.7 Inner Himalayan Valleys

Because there is no single continuous Great Himalayan Range, the intermediate areas are occupied by the Inner Himalayan valleys (Hagen 1969, p. 23). Such valleys are surrounded by the Great Himalayan and Tibetan marginal

Table 3.1 Eight summits of Nepal exceeding 8,000 m

S. N.	Summit	Altitude (m)	North latitude	East longitude
1	Everest	8,848	27°59′17″	86°55′31″
2	Kanchenjunga	8,586	27°42′09″	88°08′51″
3	Lhotse	8,516	27°57′45″	86°56′03″
4	Makalu	8,463	27°53′23″	87°05′20″
5	Cho Oyu	8,201	28°05′39″	86°39′39″
6	Dhaulagiri	8,167	28°41′46″	83°29′36″
7	Manaslu	8,163	28°2′58″	84°33′35″
8	Annapurna I	8,091	28°35′45″	83°49′13″

Source Topographic maps of Nepal

Fig. 3.9 The upper gorge of Arun with a right-angle turn. *Source* Google earth, DigitalGlobe 2013

ranges. The rivers flowing through the valleys make deep gorges while breaking the lofty Himalayan barrier. Such gorges facilitate the inflow of moisture-laden warm winds from the south and the valleys get some precipitation. The Thakkhola, Manang, and Khumbu are some examples. In the Khumbu region, Pleistocene and Holocene terraces and fans are made up of matrix- and clast-supported diamicts originating from hyperconcentrated flows and coarse-grained debris flows (Barnard et al. 2006).

3.8 Tibetan Marginal Ranges

The Tibetan marginal ranges constitute the northern boundary of the Inner Himalaya (Hagen 1969, p. 35). The major Himalayan rivers originating from these ranges flow towards the Indian subcontinent (Fig. 3.1). Some of the important mountains in Tibet are the Lhagoi Kangri Range and the Kailash (Gangdise)—Nyainqentanglha ranges (Mingtao 1982, p. 11). The highland north of the Tibetan marginal ranges belongs to the extensive Tibetan Plateau. It is basically a tableland with many lakes and river valleys.

References

Barnard PL, Owen LA, Finkel RC (2006) Quaternary fans and terraces in the Khumbu Himal south of Mount Everest: their characteristics, age and formation. J Geol Soc London 163:383–399

Burbank DW (1992) Causes of recent Himalayan uplift deduced from deposited patterns in the Ganges basin. Nature 357:680–683

DoI (Department of Irrigation) (1993) Feasibility study on expanding groundwater development for irrigation in the Birganj area of the Terai. Nippon Koei Co., Ltd. and Nepalconsult (P) Ltd., Kathmandu, vol. II, Annexes, p I-27 (unpublished)

Hagen T (1969) Report on the geological survey of Nepal. Volume 1: Preliminary Reconnaissance. Denkschiiften der Schweizerischen Naturforschenden Gesellschaft, Band LXXXVI/1, 185 pp (with a geological map)

Heim A, Gansser A (1939) Central Himalaya: geological observations of the swiss expedition 1936. Denkschriften der Schweizerischen Naturforschenden Gesellschaft, Band LXXIII, Abh. 1, 245 pp (with geological maps in colors, sections, and plates)

Herbert JD (1842) Report of the mineralogical survey of the Himmalaya mountains lying between the rivers Sutlej and Kalee. Illustrated by a Geological Map. J Asiatic Soc Bengal, Calcutta XI (126*) (Extra number), pp i–clv

Heron AM (1922) Geological results of the Mount Everest reconnaissance expedition. Rec Geol Surv India LIV(2):215–234 (with a geological map in colors)

Krishnan MS, Aiyengar NKN (1940) Did the Indobrahm or Siwalik River exist? Records of the Geological Survey of India, vol LXXV, Professional Paper No. 6, pp 1–24

Masch L, Preuss E (1977) Das Vorkommen des Hyalomylonits von Langtang, Himalaya (Nepal). Neues Jahrb Mineral Abh 129:292–311

Medlicott HB, Blanford WT (1879) A manual of the geology of India, part II: extra-peninsular area. Published by Order of the Government of India, Calcutta, pp 445–817 (with 21 plates and a map in colors)

Medlicott HB (1875) Note of the geology of Nepal. Records of the Geological Survey of India, vol. VIII, Part 4, pp 93–101 (with a geological map on 1 inch = 6 miles)

Mingtao Z (1982) The roof of the world. Harry N. Abrams, Incorporated, New York, 227 pp

Pascoe EH (1919) The early history of the Indus, Ganges, and the Brahmaputra. Q J Geol Soc LXXV:138–155

Pilgrim GE (1919) Suggestions concerning the history of the drainage of northern India, arising out of a study of the Siwalik boulder conglomerate. J Asiatic Soc Bengal, New Series, XV:81–99 (with 2 plates)

Scheidegger AE (1999) Morphotectonics of Eastern Nepal. Indian J Landscape Syst Ecol Stud Calcutta 22(2):1–9

Scott JS, Drever HI (1953) Frictional fusion along a Himalayan thrust. In: Proceedings of the Royal Society of Edinburgh, section B, vol 65, Part 2, No. 10, pp 121–142

Strachey R (1851) On the geology of part of the Himalaya Mountains and Tibet. Q J Geol Soc London 7:292–310 (with a geological map and two cross-sections in colors)

Wager LR (1934) A review of the geology and some new observations. In: Ruttledge H (ed) Everest 1933. Hodder and Stoughton Limited, London, pp 312–336

Wager LR (1937) The Arun River drainage pattern and the rise of the Himalaya. Geogr J London LXXXIX(3):239–250 (with a map and profile of the Arun and Tista rivers)

Part II

Geology of Neighboring Regions

Northwest Himalaya

4

In General Strachey's paper on this part of the Himalayas a very important observation is recorded, that the trap-rock of the Lower Himalayas enters the sandstone of the Sub-Himalayan zone. The position is in the Gola river south of Bhimtál. No fact of the kind has been noticed elsewhere.

—Medlicott and Blanford (1879, p. 543)

Simla, Krol, Shali, Jaunsar, and neighboring regions of Northwest India have played a pivotal role in the development of Himalayan geology. Under the auspices of the Geological Survey of India, many brilliant investigators have devoted much of their time and effort to this tract of the Himalaya. Medlicott (1864) undertook the mammoth task of surveying a vast hitherto unexplored ground between the rivers Ganga and Ravi. He heralded a revolution in the geological investigation of the Himalaya by enunciating various lithostratigraphic and tectonic units of permanent significance. Following his footsteps, Oldham (1883, 1888), Middlemiss (1887, 1890), Holland (1908), Pilgrim and West (1928), West (1939), and Auden (1934, 1937) mapped most of the rock succession of the Northwest Himalaya. This time-honored tradition of detailed field investigation was continued by many others, including Heim and Gansser (1939), Bhargava (1972, 1976, 1980), Bhargava and Srikantia (2014), Srikantia and Sharma (1976), and Valdiya (1964, 1980). Owing to the dearth of fossils, frequent lithofacies variations, and strata thrown into complex contortions and diverse dislocations, there still remain unsolved many stratigraphic and structural riddles. Inasmuch as the geological structures and lithostratigraphic classifications of this region are inevitable for regional correlation and comparison, a brief account of them is presented below as perceived by various researchers, and hence the description of some lithostratigraphic units is repeated purposely.

4.1 Medlicott's Classification

Medlicott (1861, 1864, p. 17) classified the Himalaya of Northwest India into the Himalayan and Sub-Himalayan series. His Himalayan series is separated from the Sub-Himalayan series to the south by the Main Boundary Fault, and is further subdivided into the metamorphic and unmetamorphic successions (Table 4.1). The main rock types representing the metamorphic succession are slates, siliceous and micaceous schists, hornblende schists, and quartzites. There also frequently occur banded gneisses assuming a granitoid aspect, and some basic rocks are found in association with the slates and schists (Medlicott 1864, p. 21).

An extensive area north of the Sub-Himalaya is represented by sedimentary rocks comprising the unmetamorphic succession. It is remarkable that Medlicott formulated this lithostratigraphic unit in such a way that it straddles not only the sedimentary but also some transitionally overlying metamorphic rocks of the Simla area. In doing so, he argued that stratigraphic relations of a rock succession are more important than its metamorphic grade. The main lithostratigraphic units mapped by Medlicott are the following.

4.1.1 Infra-Blaini or Simla Slates

This formation consists of a discontinuously laminated slate or indurated shale, occupying the lower part of the Blaini beds. It is a very thick succession of fines, represented by shaly slates, "*grits*", and thin, fine, earthy sandstones, which are well exposed at Simla. The slates are generally devoid of carbonaceous material (Medlicott 1864, p. 33).

4.1.2 Blaini Formation

The Blaini Formation has two peculiar features, following which this marker horizon can be traced to a great distance. The principal component of the Blaini Formation is a pure limestone, which is very dense and oftentimes compact or subcrystalline. It shows frequently in pale pink colors, but also in blue and greenish yellow. The limestone is well bedded and massive, forming thick bands. Its thickness varies from 5 to 6 m. The limestone is regularly underlain by matrix-supported conglomerate. The base of the conglomerate is made up of a fine, *gritty* slate of dull green or blue color, whereas its top contains the same colored thinly

M.R. Dhital, *Geology of the Nepal Himalaya*, Regional Geology Reviews,
DOI 10.1007/978-3-319-02496-7_4

Table 4.1 Medlicott's classification of the Northwest Himalaya

Sub-Himalayan series		
Upper	Sivâlik (Middle and Upper Siwalik)	Conglomerates, sandstones, clays
Middle	Nahun (Nahan, Lower Siwalik)	Lignite, sandstones, clays
Lower	Subathu	Kasaoli (Kasauli): gray and purple sandstones
		Dugshai (Dagshai): purple sandstones and red clays
		Subathu: fine silty clays, with limestone *(Nummulites)*
Himalayan series		
1. Unmetamorphic		Krol: limestones
		Infra-Krol: carbonaceous shales or slates
		Blini (Blaini): limestone and conglomerate
		Infra-Blini (Simla): slates
2. Metamorphic		Crystalline and sub-crystalline rocks

bedded rock. Throughout the base of the conglomerate, well-rounded pebbles of quartz are scattered and there could be areas where such pebbles are absent or scarce. For the most part, subangular slate clasts may prevail, giving the rock a much brecciated appearance. This pebble-conglomerate is frequently thick-bedded and sometimes massive, and its total thickness ranges from 3 to more than 30 m (Medlicott 1864, pp. 30–31).

Later, Oldham (1887, p. 144) added that underlying the "conglomerate" bed are carbonaceous slates, which generally weather white on the bedding surface, and below them is another "conglomerate." The total thickness of this sequence is about 60 m. The "conglomerate" is not a conglomerate at all, but a fine-grained silty matrix, in which are scattered blocks of slate and quartzite. These clasts are angular to subangular and, sometimes, attain a volume of 0.2–0.3 m^3. Hence, these and other larger fragments were dropped into a comparatively calm sea, in which the silt was gradually deposited. The facts that the rock preserves its characteristics for a long distance, there frequently occur well-rounded pebbles, and there are no accompanying lavas or volcanic ashes, lead to the hypothesis that the clasts were deposited by floating ice.

McMahon (1877) described the Blaini Formation from the Simla neighborhood as well as various other localities. In the Ussan (Ashni or Ashmi) River gorge, there are several almost vertical beds that are sparsely to abundantly conglomeratic. In them, subangular to partially rounded blocks of slaty *grit* are absent, but white quartz "eggs" are quite abundant. At times, the conglomerate contains very fine clasts and it presumably passes into the Blaini quartzose sandstone. This type of Blaini conglomerate is, sometimes, much flowered over and pierced by white quartz veins, which do not pass into the matrix, demonstrating clearly that the pebbles were derived from some metamorphic rocks. These rounded pebbles of dark gray or purple quartzite are randomly scattered among the quartz eggs (McMahon 1877, p. 205).

4.1.3 Infra-Krol Formation

One of the most characteristic features of the Infra-Krol Formation is its carbonaceous nature. These dark colored carbonaceous shales and slates show a gradual disappearance of the black ingredient. When weathered, the carbonaceous matter disappears and the shales acquire a light gray tint. The Infra-Krol Formation also contains thin-bedded, carbonaceous, *gritty* slates with a few intercalations of thicker, fine sandstone of brown and iron-stained colors. Some sporadic lenticular limestone beds are also present in this formation. The Infra-Krol Formation is about 300–600 m thick (Medlicott 1864, pp. 28–30).

4.1.4 Krol Formation

To the west of Solan, overlying the shaly slates, is a pale yellow colored, coarse, quartzose sandstone with ochrous clay cement. The rock decomposes into a sharp, coarse, dusty sand. The thin-bedded to very thick-bedded and massive sandstone succession has a variable thickness (from 5 to 30 m) within a short distance. This coarse sandstone is everywhere overlain by a limestone with inconsistent thickness, color, and composition. There are 100 to 125 m thick, clear, blue, compact limestones, which exhibit very regular, thin (10–20 cm) beds, characterized by irregularly distributed nodules and regularly disposed chert strings. Stratigraphically upwards, some shaly clays set in, which frequently have a light but bright pink, and sometimes mottled green color. The uppermost beds of the Krol Formation are made up of thick-bedded, dense, blue, subcrystalline limestone. The last limestone is impregnated by irregular and angular chert nodules and strings. There also occur some thin partings of pink and blue shale between the thick beds of hard limestone. This last upper limestone succession is more than 250 m thick (Medlicott 1864, pp. 23–25).

4.1.5 Metamorphic Equivalents of Infra-Krol and Krol Formations

Towards the upper part of the Simla Slates, at Boileaugunge, Jako (Jakko), and their vicinity of Simla hills, there are highly foliated schists, mica schists, and hornblende–garnet

schists. They are very frequently traversed by large quartz veins and seams (Medlicott 1864, p. 34).

The schists of Jakko could be the equivalents of the black slates of the Infra-Krol Formation, as there are carbonaceous bands in the schistose rocks. Similarly, the schistose quartzites of Boileaugunge, which stratigraphically overlie the carbonaceous rocks, could be the equivalents of the Krol sandstone (Medlicott 1864, pp. 34–35).

On the southwest spur of the Jutogh hill, above the very gently dipping quartzites, is a considerable thickness of dark blue limestone, alternating with graphitic schist bands. It is followed upwards by schists, gneisses, and thick-bedded, blue limestones with much irregularly distributed chert. They are followed by garnetiferous schists up to the summit of Jutogh. Their lithological characteristics resemble those of the Krol Formation (Medlicott 1864, p. 35).

Subsequently, Oldham (1887, pp. 147–148) classed the above three metamorphic units, overlying the Simla slates, into the Jakko carbonaceous slates, Boileaugunge quartzites, and Jutogh carbonaceous slates and limestones. He also claimed that the uppermost or Jutogh carbonaceous slates and limestones are the youngest rocks within this succession and contain three distinct limestone beds, separated by schists and quartzites. He further noted that one of the most enigmatic features in the geology of Simla was the metamorphism of the higher sequences accompanied by the absence of metamorphism in the lower strata. To explain this anomalous phenomenon, he refers to the unpublished paper of Medlicott on the geology of the Punjab where the author has suggested that the heat may have been applied from above by the intrusion of a granite sheet, since removed by denudation. Oldham (1887, p. 149) also postulated an alternative hypothesis that there could also be a core of an igneous body having been intruded into the country rock but not yet exposed by denudation.

Medlicott's Sub-Himalayan series occupies the hills south of the Main Boundary Fault, and comprises the following formations, successively in ascending order.

4.1.6 Subathu Formation

The Subathu Formation forms the base of the foreland basin of the Northwest Sub-Himalaya. It also overlies the Lesser Himalayan rocks with a sharp unconformity. Major Vicary (1853) first described the Nummulitic strata of the Subathu area and his fossil collection was studied by D'Archiac and Haime (1853, p. 175). Medlicott (1864, pp. 11 and 74) remarked that the prevalent character of this formation is calcaro–argillaceous. There are thick beds of silty clay, exhibiting a very fine texture and subdued natural colors. They weather in splinters of acicular, subcubical, sporadically shaly, or laminated shapes. The calcareous rocks appear as irregular, subconcretionary, earthy beds, but at times as thin beds of hard limestone. Coarse siltstones to fine sandstones of the same dull color as the clays also appear occasionally. Towards the top, the thickness as well as frequency of sandstones increases and the rock has a prevailing purplish tint; with them are intercalated strong beds of lumpy, *gritty* clays, of bright and deep red colors. These clays are slightly gypsiferous. Thus, the mineralogical and textural characteristics of the lower beds are completely lost and the contact with the overlying Dagshai Formation is perfectly transitional and arbitrary. The fossils in the Subathu Formation are frequently very abundant, although ill preserved, and wanting in the upper formation.

4.1.7 Dagshai and Kasauli Formations

The Dagshai Formation is characterized by the deep red color of the clays and the corresponding dark purple of the sandstones. The Kasauli Formation contains gray and purple sandstones and shales with fossil leaves, seeds, and stems of various species. The Subathu–Dagshai–Kasauli succession represents one uninterrupted sequence deposited in tranquil and deeper waters being transitionally followed by sands and fines accumulated on land (Medlicott 1864, p. 12).

4.1.8 Siwaliks

The Lower Siwaliks are made up of clear bright red clays and soft sandstones. The overlying younger Siwalik rocks are represented by regularly alternating beds of unconsolidated, brown, earthy conglomerate and brown clay, resting unconformably over the Lower Siwaliks (Medlicott 1864, pp. 13–14).

4.2 Oldham's Investigations in Jaunsar and Bawar

Based on the work of Medlicott, Oldham (1883) continued mapping in the Northwest Himalaya. While extending his investigations in Jaunsar and Bawar, he came across with a variety of sedimentary rocks and identified the following main lithostratigraphic units.

4.2.1 Jaunsars and Chakrata Formation

Oldham (1883, p. 193) noted that, with the exception of a great limestone sequence (possibly equivalent to the Krol), no representative of any of the subdivisions established on the Simla section was to be recognized in the Jaunsar

district. Therefore, he designated the Chakrata series (Formation) for these rocks. The Chakrata Formation is made up of gray slates and quartzites, underlain by a band of limestone, generally some 100 or 125 m thick, which is again underlain by a great succession of slates and quartzites, marked by the prevalence of red and mottled beds. The quartzites also include a few meter-thick conglomerate bands. In several parts of Jaunsar, volcanic rocks are exposed in the Chakrata Formation. In a few places, gray-green volcanic rocks underlie the Deoban Limestone, whereas several beds of volcanic breccia and ash are found both above and below a thick band of blue limestone exposed to the east of Chakrata (Oldham 1883, p. 194).

4.2.2 Deoban Formation

Overlying the Chakrata Formation, is a very thick limestone and dolomite succession, very similar to the Krol Formation, but which, as its relation to the underlying beds is very different from what has been described on the Simla section, Oldham called it the Deoban Limestone. This succession is mainly dolomitic and contains stromatolites (Box 4.1). The dolomites are intercalated with slates, which are frequently gray, but sporadically colored.

Box 4.1: Discovery of Stromatolites

Quite early in the geological investigation of the Northwest Himalaya, researchers have noticed the stromatolites from various carbonate rocks of the Lesser Himalaya. McClelland (1834) reported presumable fossils from the valley of Ponar River, a small stream, which rises in the mountains between Lohughat (Lohaghat) and Almorah (Almora) at an altitude of about 450 m. Though he misidentified them as *Dentalium annulata, it* was the first find of fossil stromatolites. Medlicott (1864, p. 55) described flat circular-shaped structures in the Kukurhutti (Kakarhatti) Limestone within the Simla slates. Similarly, in the carbonate rocks of the Deoban Formation, Oldham (1883, p. 195) noticed

> …a peculiar structure seen in some of the beds makes them resemble an accumulation of some closely-chambered shells interbedded in a matrix of calcareous mud, so organic looking that it is difficult to believe that they are not obscured fossils.

Oldham (1888, p. 133) further clarified the matter by stating that the Deoban Formation exposed in Jaunsar comprises a pale gray, bedded limestone, which is sporadically oolitic, oftentimes mephitic and contains some cherty concretions. Some of the beds of the limestone exhibiting black specks on a white ground display pseudo-organic structures and they are generally imbedded in a brown-weathering matrix, while the structures retain their blue-gray color. Such structures are also abundant in various places such as in Sirmur and west and south of the Giri River.

Concerning similar structures observed in Kulu, Sherborn (1888, p. 255) wrote,

> The concentric structure occupying nearly the whole of the surface of the slab … touches one side; and only the corners of the slab show the undisturbed bluish matrix. The rings are of many shades of gray, with a few of an orange-pink color passing into brown. On two sides of the face of the slab are indications of other concentric masses, and with one of these the example in question appears to have been joined, as it shows a tendency to assume a pear shape; with a 'point below' the root or starting point of growth—as in the description of the figures of the American form.

Valdiya (1969) and Tewari (2003) present a detailed classification of stromatolites. The stromatolites are characterized by the prolific occurrence of columnar and branching varieties. Raha and Sastry (1973) studied the stromatolites from the Jammu Limestone. They discovered several Proterozoic forms, such as *Collonella* Komar, *Conophyton cylindricus* Maslov, *Baicalia baicalica* Krylov, and *Masloviella* (*Collenia*) *columnaris*.

4.2.3 Mandhali and Bawar Formations

According to Oldham (1883), above the Deoban Limestone occur conglomeratic beds of the Mandhali. They contain intraformational pebbles of quartzite and limestone in a slaty matrix. They also include gray and colored slates and shales. Oldham also recognized the Mandhalis near Nainital and Bhimtal as well as in the Giri River.

Oldham (1883, p. 197) Wrote

> In northeastern Jaunsar, occupying a considerable tract of country is a series of fine-grained glassy quartzites with interbedded schists, some of the beds containing granules of blue quartz, which in the Tons descend to the level to the river, but southwards merely cap the ridges; they lie almost undisturbed and nearly horizontal on the eroded edges of the intensely disturbed older rocks, and are evidently far newer than any of the other formations in Northern Jaunsar, or Bawar as it is locally called; yet, though so much newer and so much less disturbed, the rocks are far more metamorphosed than those of the older series, the siliceous beds being everywhere converted into glassy quartzites, and the argillaceous bands being, in Bawar, uniformly schistose, while across the Tons, in Garhwal, they occasionally become almost gneiss. I propose to call this the Bawar series.

The lithologically similar Kuncha Formation in central Nepal also contains blue quartz (Chap. 6).

4.3 Proposal of Nappes in Simla Area by Pilgrim and West

Pilgrim and West (1928) explained the superposition of high-grade metamorphic rocks over low-grade ones in terms of folded nappes (Box 4.2) that were frequently recumbent. They based their stratigraphic classification and structural interpretation on the degree of metamorphism and differentiated the rocks of the Simla area into the following formations in order of superposition upwards (Table 4.2).

Box 4.2: Recognition of Nappes or Thrust Sheets

It was an enigmatic situation for Medlicott (1864, p. 51), Oldham (1883), and Middlemiss (1887), to observe metamorphosed sequences overlying sedimentary suites in the Northwest Himalaya. The observation led to the discovery of thrusts in the Northwest Himalaya. Oldham (1893) recognized reverse faults in the frontal ranges, and, subsequently, Hayden (1913, p. 147) proposed to convert the reverse faults of Oldham and Fischer into overthrusts. The work of Pilgrim and West (1928), Wadia (1934), and West (1939) substantiated the nappes and thrust sheets in the Northwest Himalaya. On the other hand, Auden (1937) reinterpreted the work of Middlemiss in west Garhwal and proposed a thrust sheet. The seminal work of Heim and Gansser (1939) established the existence of the Main Central Thrust and the Higher Himalayan metamorphic thrust sheet in the Kumaun Himalaya and in the Mahakali section of Nepal. Gansser (1964) and Le Fort (1975) remarked that the thrusts relay in time from the hinterland to the foreland.

4.3.1 Thrusts and Nappes

In the neighborhood of Simla, Pilgrim and West (1928, pp. 9–10) identified the following four faults: (1) crossing the northeast foot of Jakko and passing through Annadale and north of Jutogh; (2) north of Kathlighat railway station; (3) south of Kathlighat railway station; and (4) on the ridge above Kiarighat. The first two join to form a folded thrust sheet. Thus, there are three overlapping thrusts that produce, respectively, the following rock sequences.

- The uppermost Jutogh Thrust separates the underlying Chail Formation from the overlying Jutogh Formation.
- The Chail Thrust is an intermediate dislocation between the underlying Jaunsar Formation and the overlying Chail Formation.
- The Jaunsar Thrust is the lowest fault between the underlying Blaini Formation or the Simla Slates and the overlying Jaunsar Formation.

Field investigations by West (1939) and Auden (1934) showed that the Chail Thrust is the most convincing of all other thrusts in the area around Simla and Chor (Chaur). They reported a crushed zone below the thrust and stated that the Deoban Limestone is intensely deformed and folded near the fault but it exhibits steady northerly dips, away from the thrust (Fermor 1931, p. 130).

Pilgrim and West (1928) were unable to follow the stratigraphy proposed by Medlicott in the Simla area and they recognized the following new units.

4.3.2 Jutogh Formation

They argued that because the Jutogh Formation is the most metamorphosed, it must be the oldest, whereas the Simla Slates should be the youngest as they are the least affected by metamorphism. Different from Medlicott (1864), they included all the metamorphic rocks of the Simla hills in their metamorphosed units, and regarded them as a folded thrust sheet.

4.3.3 Chaur Gneissose Granite

The porphyritic Chaur granite consists of orthoclase, quartz, biotite, and albite. The granite also has abundant inclusions of zircon and some apatite. In certain parts, xenoliths of quartzite and garnetiferous schist are frequent. The foliation in the granite is concordant with the country rock. Pilgrim and West (1928, p. 55) concluded that the foliation developed at the time of intrusion and crystallization of the granite. There also occur dikes of olivine-dolerite crosscutting the granite and also the country rock. While approaching the Chaur granite, the garnet zone is followed by the staurolite zone, but near the granite the staurolite zone disappears (Pilgrim and West 1928, p. 65). The zoned metamorphism around the granite led the authors to infer that the granite was intruded contemporaneously both with the metamorphism and recumbent folding. Hence, these granites must not be Tertiary, but older in age (Pilgrim and West 1928, p. 137).

Table 4.2 Classification of rocks in the Simla area

Dagshai Formation	Purple sandstones and clays
?Unconformity	
Upper Subathu Beds	Purple sandstone and '*grits*'
Unconformity	
Subathu Formation	Shales, limestones, carbonaceous beds
	Basal pisolitic laterite
Krol Formation	Massive blue limestone
	Red shale
	Limestone and shale
Krol Sandstone	Sandstone, readily decomposing into dusty sand
Infra-Krol Beds	Shaly slates, with beds and lenticles of hard brown quartzitic '*grit*'
Blaini Limestone	Pale pink magnesian limestone
Blaini Conglomerate	Boulderbeds; slates with pebbles (glacial)
Shali Limestone and Slates	(Position uncertain)
Simla Slates (Infra-Blaini)	Dark unaltered slates, and micaceous sandstones
	Limestone with pseudo-organic structure (Kakarhatti and Naldera limestone)
Jagas (Jaunsar) Formation	Pale, sub-schistose slates
	Much crushed micaceous slates and phyllites
	Purple phyllites and conglomerate
	Purple, green, and gray quartzites, pebbly in their upper portion
	Slates with slaty cleavage and vein quartz
Chail Formation	Light gray and brown schistose slates and quartz-schists
	Slightly talcose flaggy quartzites and quartz-schists
	Talc-schist bed (10–12 m thick)
	Slightly puckered gray phyllites
	Gray slates with interbedded banded crushed limestone
Intrusion of Chor granite accompanied by intense folding and high-grade metamorphism. Olivine dolerites are intruded both into the granite as well as into the Jutogh Formation	
Jutogh Formation (order of superposition uncertain)	Quartzites and schists
	Crushed and banded dolomitic limestone, generally carbonaceous and often containing actinolite
	Carbonaceous slates and phyllites (often garnetiferous) (Jakko slates)
	Quartzites and mica schists (Boileaugunge beds); hornblende schists and gneisses are frequently intruded

Source Pilgrim and West (1928, pp. 3–4)
?: Unconfirmed unconformity

4.3.4 Chail Formation

Pilgrim and West (1928, p. 17) defined this "series" (formation) as a succession of talcose quartzites, quartz-schists, and phyllites, and regard it as older than the Blaini and Jagas formations. In the Jagas Formation, the quartzites display a clastic structure and the constituent grains are not recrystallized. They are either sandstones or *grits*. In the Chail Formation, the quartzites are recrystallized and the quartz grains form a mosaic without any cementing material. The Chail Formation is more schistose owing to the development of new sericite or muscovite between the quartz grains. There is a marker band of talc-quartz-schist ranging in thickness from 10 to 15 m and persistent over an extensive area. It is characterized by a bright silvery color seen from afar. It is a relatively soft and friable (due to the presence of thin quartz lenses) rock with scattered tiny magnetite grains.

4.3.5 Jagas (Jaunsar) Formation

Between Dudham and Jagas the following sequence (Table 4.3) is observed (Pilgrim and West 1928, pp. 14–15).

Table 4.3 Stratigraphic succession described by Pilgrim and West (1928)

Jagas (Jaunsar) Formation	Light yellow and lavender phyllites, carbonaceous in places
	Purple phyllites and crushed conglomerates
	Massive white quartzites
	Brown slates
	Massive white quartzites
	Light green-brown slates
	Dark slates
	Quartzites
	Light and dark slates
Jaunsar Thrust	
Blaini Beds	Red shales
	Blaini limestone
	Upper boulderbed
	Bleach slates
	Lower boulderbed
Simla Slates	

The conglomerates observed by McMahon (1877) in the gorge of Ashni (see above) with white quartz "eggs" belong to their Jaunsar Formation. Inasmuch as this formation varies rapidly in composition from place to place, it is difficult to define the exact stratigraphic position of the conglomerates (Pilgrim and West 1928, p. 15). Similarly, in the Chakrata area, these authors were unable to find the volcanic beds in the Jaunsar Formation of Oldham. They also examined the rock specimens collected by Oldham and found that there were just hornblende schists (Pilgrim and West 1928, p. 42). The two authors also correlate, with some reservations, the conglomerate beds and an overlying cream limestone of the Mandhali Formation with the Blaini Formation. On the other hand, the Mandhali boulderbed, resting directly over the Deoban Formation, contains some pebbles derived from it. Hence, it is impossible to correlate the Deoban Formation with the Krol Formation. Also, the stromatolites so frequently observed in the Deoban limestone are not characteristic of the Krol limestone (Pilgrim and West 1928, p. 44).

4.3.6 Naldera Limestone and Simla Slates

Pilgrim and West (1928, pp. 44–45) describe about 30 m thick, clear blue limestone from the Naldera Ridge located to the north of Simla, where the limestone is interbedded with the Simla Slates presumably at their base. This limestone also contains stromatolites and is identical with the Kakarhatti limestone of Medlicott. Hence, these two limestones may be homotaxial with the Deoban Formation. However, the stromatolites observed in them are dissimilar and so are their lithologies. On the other hand, Pilgrim and West (1928) are tempted to correlate the Deoban Formation with the Shali Limestone (see below), acknowledging the fact that there is even less lithological resemblance between the Shali limestone and Deoban limestone than there is between the Naldera limestone.

4.3.7 Shali Limestone

The Shali Limestone is made up of a blue colored intensely hard variety, which is frequently dolomitic. It weathers dirty white and includes a number of black chert bands, ranging in thickness from 3 mm to 5 cm, and sometimes up to 10 cm and more. The uppermost part of this formation is composed of a cream colored limestone, which is generally free from chert and contains a few thin beds of quartzose sandstone. Its total thickness is more than 350 m (Pilgrim and West 1928, p. 120).

The Madhan Slates comprise jointed slates interbedded with gray to light gray quartzose sandstones which frequently pass into a massive white quartzose sandstone. Purple *gritty* quartzites and purple shales as well as cream and lavender slates occur at several horizons (Pilgrim and West 1928, pp. 120–121).

4.3.8 Opinions at Variance

After the work of Pilgrim and West (1928), West continued mapping the Jutogh Formation and allied rocks farther to the north and east, where he showed that the recumbent folds in the Jutogh series do not exist (Pascoe 1929, p. 164).

Kumar and Pande (1972) described the folds and faults of the Simla area in terms of gravity structures. They are of the opinion that there is no Krol Thrust, but many imbricate faults in this parautochthonous unit lying below the Chail–Jutogh nappe. They assume that the Chail–Jutogh nappe is essentially a single unit. On the other hand, Naha and Ray (1972) discussed recumbent folding in the Jutogh series forming the Simla Klippe. They base their argument solely on the structural analysis of the Simla Klippe. However, none of these authors above took the entire Jutogh–Chail–Simla–Krol succession for their analysis, which extends for several tens of kilometers farther southeast. To explain recumbent folding, Naha and Ray (1972) combined the two carbonaceous bands in the Jutogh series mapped by Pilgrim and West (1928) into a single one. However, they also noted that it is difficult to delineate the Jutogh–Chail contact owing to deformation and metamorphism. Like Pilgrim and West (1928), they were also unable to locate in the field any large-scale fold hinges and presumed that all such closures were eroded away. According to Frank et al. (1977), the so-called Lower Crystalline nappe or the Jutogh Thrust is part of the Lesser Himalaya. It contains blue quartz and acid volcanics, as in the Berinags. Bhargava and Srikantia

Table 4.4 Classification of rocks in the Krol belt by Auden (1934)

Solan neighborhood			Tons River neighborhood		
Nahans (Only at Kalka)			Nahans		
Kasauli					
Dagshai			Dagshai		
Subathu (Nummulitic)			Subathu (Nummulitic)		
Absent			*Never in contact*		
			Tal	Upper Tal	
				Lower Tal	
Krol Formation	Krol limestone	Krol E	Krol Formation	Krol limestone	Upper Krol limestone
		Krol D			
		Krol C			
		Krol B (Red Shale)			Red Shales
		Krol A			Lower Krol limestone
	Krol sandstone				
	Infra-Krol			Infra-Krol	
Blaini			Blaini		
Jaunsar with possible Mandhali			Nagthat	Jaunsar Formation	
			Chandpur		
			Mandhali		
Simla Slates with Kakarhatti limestone			Deoban limestone		
			Simla Slates (Morar–Chakrata beds)		
Dolerites					

(2014) observed that recumbent folds are confined only to the basal part of the Jutogh Thrust sheet. They have also recorded hinges of recumbent folds, the most prominent being the Rajgarh Fold.

4.4 Auden on the Krol Belt

In the Krol Belt, Auden (1934) subdivided the Jaunsars into the Mandhali, Chandpur, and Nagthat stages (formations). He argued that the Krol Belt moved along the Krol–Tons Thrust. He was the first to recognize the difficulties in correlating various rocks based on metamorphic grade. According to him, the sediments of the Nummulitic sea (i.e., the Subathu Formation) were deposited on the Simla Slates as the basement. Auden (1937, p. 421) further emphasized that there is a lateral variation in metamorphism within the same rock unit.

After Medlicott (1864) first identified the Krol series in the Simla Himalaya, Auden (1934) carried out a more detailed investigation of that tract of the Lesser Himalaya. His classification scheme is summarized in Table 4.4.

4.4.1 Simla Slates

The Simla Slates exhibit dark and subdued colors with gray-blue tints. They are composed of micaceous shales, bleaching shales and slates, pencil slates, clay slates, sporadic phyllites, sandstones, and predominant graywackes. Generally, fracture cleavage is characteristic and parting is parallel to bedding. Their bed thickness varies from 1 to 3 cm and the rock is massive (Auden 1934, p. 366). The Chhaosa Slates are equivalent to the Simla Slates. In the vicinity of Subathu, the Simla Slates are represented by crenulated phyllites, but they also contain some massive quartzites, shaly quartzites with fine ripple marks, and green nodular micaceous siltstones. The Simla Slates range in thickness from 350 to 450 m.

The Kakarhatti limestone is intercalated in these slates. The limestone is pale gray, blue-gray, and purple; it is microcrystalline and sporadically oolitic, contains chert in irregular patches aligned parallel to the bedding, and is interbedded with green bleaching slates and shales characterized by pencil cleavage (Auden 1934, p. 367). The Simla Slates are succeeded by the Jaunsars, which Auden divided up into the Mandhali, Chandpur, and Nagthat formations.

4.4.2 Mandhali Formation (Lower Jaunsar)

Its lower part is composed of the Kalsi quartzites and bleaching slates. The quartzites are light gray to white and intensely veined with quartz. These quartzites are followed by the Kalsi limestones exhibiting a highly banded nature and interbedded with slates or phyllites. The limestones are of gray-blue, green, purple, and other variegated varieties. They are followed upwards by quartzites, *grits*, conglomerates, and pebble beds. The pebble beds are pale green, gray, and purple, and commonly contain clasts of vein-quartz and purple slate or phyllite. Sometimes, these pebble beds are metamorphosed to yield schistose quartzites and pebble-schists. The boulderbed occurs above these pebbly quartzites and below the Dhaira limestone (Auden 1934, p. 369). The clasts in the boulderbed are composed of limestone, dark slate, pale and dark sheared quartzites, and vein-quartz. The limestone clasts range from fine-grained to marmorized types and some pink-weathering varieties. There are also thin (5 cm) lenticular beds of dark limestone ranging in length up to 1.5 m. Immediately below the Dhaira limestone a graphitic schist or slate is infrequently present. The Dhaira limestone comprises thinly interbedded, dark, microcrystalline, lenticular limestones and dark pyritic slates (Auden 1934, p. 370). Between the Dhaira and Bansa limestones are found silvery black, sheeny phyllites and pale green, slightly talcose phyllites. The Bansa limestone weathers to deep blue-black granular surfaces, displaying a profusion of sand grains. The limestone is blue to gray and purple, and is thinly to thickly bedded and massive. Towards the upper part, the Bansa limestone is interbedded with a pale quartzite or quartz schist, and thus transitionally passes into the overlying Chandpur Formation (Auden 1934, p. 371).

4.4.3 Chandpur Formation (Middle Jaunsar)

A conspicuous feature of the Chandpur Formation is its highly laminated association of quartzite and phyllite, and the occurrence of abundant green beds. There are as many as 24 laminae in 2 cm. In these laminae, quartzite predominates and the rock as a whole is strongly crenulated (Auden 1934, p. 371). Apart from these rocks, there also occur more massive, cross-bedded quartzites and an extensive succession of chlorite-tuffs, slates, and quartzites. Sporadically, amygdaloidal basic lavas and dolerites are also found. The Chandpur Formation is more than 1,400 m thick (Auden 1934, p. 372).

4.4.4 Nagthat Formation (Upper Jaunsar)

The Nagthat Formation is represented by sandstones, arkoses, quartzites, *grits*, conglomerates, clay-slates, and phyllites exhibiting purple and green colors. Generally, the arenaceous rocks are strongly cross-bedded and ripple-marked, whereas the conglomerates have pebbles derived from vein-quartz, purple and pale quartzite, and purple and green slate or phyllite. Some green tuffaceous sandstones are also encountered. Sporadic boulderbeds and dark micaceous slates are also present (Auden 1934, p. 373).

4.4.5 Blaini Formation

The Blaini Formation succeeds the Jaunsars. Although it contains the limestone and boulderbed, their distribution is variable, and either only the limestone or the boulderbed alone or in various combinations of these two associations are found. There may be several boulderbeds with or without limestones. The boulderbeds and limestones frequently die out along their strike and are followed by black slates akin to the Infra-Krols. The boulderbeds exhibit dark gray-brown colors and contain angular, subangular, and rounded boulders dispersed in a fine-grained clayey or *gritty* matrix. The boulder size varies from granules to 1 m across (Auden 1934, p. 375).

The associated pink carbonate is microcrystalline, does not react with dilute HCl, and is laminated to thin-bedded. There is also a limestone that is sandy and soft, and weathers to dark brown crusts. The limestone grades upwards to calcareous slates and shales of purple or pink color. The Blaini Formation varies in thickness from 0 m to more than 80 m (Auden 1934, p. 375).

4.4.6 Infra-Krol Formation

This formation is composed mainly of dark shales and slates interbedded with thin (5 mm to 10 cm), buff-weathering impure slaty quartzites. There also set in occasional thicker beds of gray quartzite. Black carbonaceous shales or slates appear towards the upper part of the Infra-Krol Formation. Its minimum thickness is about 150 m (Auden 1934, pp. 378–439).

4.4.7 Krol Sandstone

The Krol Sandstone shows in a soft crumbling type, without distinct bedding, and it is stained an orange color with iron. There is a conspicuous horizon of sandstone containing from 2–5 cm long black shale fragments. In some places, the sandstone is interbedded with carbonaceous shale and in some other localities is lenticular and pebbly. The sand grains are frequently well rounded and cemented by silica. The rounding of grains may have been caused by wind

action. The total thickness of the Krol Sandstone varies widely and ranges from 10 to 100 m and it also dies out in many areas (Auden 1934, pp. 379–380).

4.4.8 Krol Limestones

There is a variety of limestones and shales in this unit and they can be divided into the following five members. These subdivisions, though persistent, have not been delineated over the entire Krol Belt.

Krol A (Lower Krol Limestone) contains a thinly (2–10 cm) interbedded sequence of limestone and shale. Their weathered bed surfaces exhibit subdued gray-green colors, whereas the fresh ones are essentially dark blue. They are characterized by a rapid alternation of shaly limestone and calcareous shale or slate with parallel as well as lenticular and discontinuous bedding, incorporating lenses and pillows of limestone. Its top part is made up of a massive dolomitic limestone of about 5–15 m thickness, which displays current bedding and sporadic ripples (Auden 1934, p. 381). There are thin black chert bands and pillows, gypsum, and anhydrite intercalated in this member. The total thickness of the Krol A member varies widely and generally ranges from 100 to 200 m (Auden 1934, p. 382).

Krol B consists of soft, thinly laminated, purple and red shales with patches and intercalations of green shale. This unit also frequently contains thin dolomitic and cherty limestone beds. There also appear sporadic ripples and near the top of this member appear very incompetent, parallel-bedded, shaly limestones. This member is about 100 m thick (Auden 1934, pp. 382–383).

Krol C is is a massive, dark blue, crystalline limestone, which generally stinks on fracture and develops plane surfaces on weathering. It is excellently exposed near Solan, and is about 100 m thick (Auden 1934, p. 385).

Although Krol D consists of chert, limestone, and shale, cherty limestone predominates, and it frequently alternates with shale. A limestone succession is from 3 to 10 m thick and consists of pale or dark and mephitic varieties. The chert is light colored and comes in thin discontinuous bands and wisps of up to 5 cm thickness, whereas the intercalated shales are black, red, green, and orange. There also appear some soft white sandstones and infrequent conglomerates, containing pebbles of vein-quartz and chert. Intraformational breccias are developed in some of the limestones, and pockets of gypsum in the limestone are found in a few places. The Krol D member is more than 200 m thick (Auden 1934, p. 383).

Krol E constitutes rugged peaks and ridges of limestone made up of beds from 30 cm to 1.5 m in thickness. The limestone is microcrystalline with banded gray to pale cream white colors. Stratigraphically upwards, these limestones pass by increase of quartz grains, respectively, to pale sandy limestones and pale calcareous sandstone. There also occur rare bands of saccharoidal crystalline limestone and cream white limestone with calcite veins. Red, black, and orange shales are present in subordinate amounts. The total thickness of Krol C, D, and E is about 1,000 m (Auden 1934, pp. 383–384).

4.4.9 Tal Formation

Middlemiss (1887, pp. 33–34) described these rocks from Garhwal and divided them into the Lower Tal and Upper Tal formations. According to Auden (1937, p. 385), the Lower Tal is made up of a thick succession of black carbonaceous slates and graywackes, akin to the Infra-Krol Formation. Frequently, the graywackes are calcareous and their upper surfaces contain ripples. The Lower Tal Formation varies in thickness from 500 to 100 m.

The Upper Tal is composed mainly of pale green to white arkosic quartzites in which cross-bedding and ripple marks are in profusion. Infrequent purple sandstone beds are also present. The arkosic quartzites contain pebbles of vein-quartz, green slate, and pink feldspar. The interbedded purple, red, and green micaceous shales contain many sun cracks. The intercalated limestones are dark, sandy, and cross-laminated. The Lower Tal member is about 600 m thick (Auden 1937, pp. 385–386). Subsequently, the Tal was raised to a group level, and subdivided into the Shaliyan, Sankholi, and Koti Dhaman formations (Bhargava et al. 1998).

The occurrence of various Early Cambrian fossils, including trilobites, has settled the age of this formation (Singh 1979; Rai and Singh 1983; Azmi and Pancholi 1983; Brasier and Singh 1987; Mathur and Joshi 1989).

4.4.10 Subathu Formation

In the Krol Belt, this formation comprises olive-green and purple oily looking shales, green and white sandstones, iron-stained quartzites, and infrequent shaly sandstones with ripples. There are compact fossils mainly of oysters and sporadic *Nummulites*. There are two other facies of restricted distribution: ferruginous pisolitic laterite and carbonaceous beds with total carbon of 60 %. Very infrequently, conglomerates are also encountered with pale microcrystalline limestone. The Subathu sandstones are composed of rock fragments of phyllite, carbonaceous slate, and sandstone. The sandstones also contain detrital tourmaline, garnet, plagioclase, and kyanite (Auden 1937, p. 387).

A metamorphosed sequence of the Subathu Formation is found in a few localities of the Krol Belt, where the purple

and green shales have changed into phyllites and the carbonaceous shales are converted into dark bleaching slates (Auden 1937, p. 387).

4.4.11 Dagshai Formation

Between the Subathu and overlying Dagshai Formation is present a white quartzose sandstone. On top of it are alternations of purple, cindery, sandy shales, and purple or green sandstones reaching in thickness up to 4.5 m. In the sandstone beds, cross-bedding and ripple marks are common. There are several conglomerate beds very similar to those of the Subathu Formation and they contain intraformational shale clasts. The Dagshai Formation is about 600 m thick (Auden 1937, p. 388).

4.4.12 Kasauli Formation

The Kasauli Formation differs from the underlying Dagshai Formation in its general lack of purple color. The massive and hard sandstones strongly predominate over the shales which are less cindery and greener. They are commonly soft or hard clay-slates with palm leaves. The Kasauli sandstones frequently contain detrital garnets (Auden 1937, p. 388).

4.4.13 Lower Siwaliks (Nahans)

The Lower Siwaliks comprise a regular alternation of sandstone and shale. The green-brown sandstones are generally very thick-bedded, massive, and coarsely cross-bedded whereas the shales are brown and green in color (Auden 1937, p. 388).

4.4.14 Dolerites and Associated Rocks

These rocks are found in the Jaunsar, Infra-Krol, the A, B, D members of the Krol Formation, and the Subathu Formation. The Dolerites in the Tertiaries contain sporadic augite, some chlorite, uralite, magnetite, pyrite, and calcite (Auden 1937, pp. 389–390).

4.5 Shali Window: West's Version

West (1939) mapped in detail the Shali tectonic window lying to the north of Simla. He summarized the lithostratigraphic successions as shown in Table 4.5.

He also mentioned that, except for the Subathu beds, all other rocks are devoid of fossils and recent work suggests that the Chail Formation is probably equivalent to a metamorphosed portion of the Simla Slates. On the other hand, the Shali Formation could be homotaxial with the Krol Formation but with some reservations (West 1939, pp. 137–138).

4.5.1 Shali Thrust

The Shali Thrust makes more than three-quarters of a circle and the area bounded by the thrust marks a dome. The rocks above the Shali Thrust belong to the Chail Formation and those below the thrust are a variety of sedimentary succession. After the Chail Formation moved horizontally for several kilometers over the younger rocks to the southwest, they were folded together to constitute the dome. Subsequently, denudation wore away the hanging wall and the tectonic window with younger rocks was exposed (West 1939, p. 140).

4.5.2 Lower Shali Limestone

The Lower Shali limestone in its lowest part is represented by a pink, thin-bedded, pure variety and above it is a massive, gray dolomitic limestone.

4.5.3 Shali Slates and Chail Formation

The Shali slates are generally dull black colored and splintery; they bleach to a light gray color and pass downwards into a banded slaty limestone, and upwards into earthy thin limestones (West 1939, p. 141). They are partly clay-slates with distinct cleavage. On the other hand, the overlying Chail Formation separated from the Shali slates by the Shali Thrust is made up of phyllites or silky schistose slates full of vein-quartz (West 1939, p. 142).

4.5.4 Upper Shali Limestone

The Upper Shali limestone attains a thickness of more than 750 m and is made up of massive gray colored dolomitic limestone.

4.6 Further Investigations in Simla–Krol Belt

The Geological Survey of India made further investigations in the Northwest Himalaya to resolve the stratigraphic and structural problems of the region. Srikantia and Sharma (1976) carried out detailed mapping in the Shali, Jutogh, Chail, and Simla areas. They extended their map between Simla to the east and the Ravi River to the west. Their

Table 4.5 Lithostratigraphy of the Shali window, north of Simla

Tertiary	Dagshai beds	Purple shales, with interbedded purple and green sandstones
	Subathu beds	Jointed shales, with thin beds of limestone containing nummulites
Madhan slates		Rusty brown sandy slates, finely jointed, and slightly micaceous
Shali Formation	Shali quartzite	Pure white quartzite, sometimes containing chert
	Upper Shali limestone	Massive, gray, dolomitic limestone, full of parallel sheets of chert
	Shali slates	A variety of slates and slaty limestones
	Lower Shali limestone	Massive, gray, dolomitic limestone, with only occasional chert Pink limestone with no chert, banded at the base
	Khaira quartzites	White and purple quartzites
Chail Formation		Dark silky slates and phyllites, with interbedded dark limestone, frequently banded

Source West (1939, p. 137)

detailed mapping clearly shows the absence of any recumbent folding in the Jutogh series. They also demonstrate that the Shali limestone is older than the Krol limestone. They do not distinguish the Chail Thrust and include the Chails under the Simla Group. In other words, they differentiate the following groups or formations in descending order.

- Kasauli, Dagshai, Subathu, and so on
- Blaini, Infra-Krol, Krol, Tal, and so on
- Simla Group (including Jaunsar Group or separately Mandhali, Chandpur, or Nagthat)
- Shali Group
- Jutogh Group.

They correlate the Jutogh Formation with the Shalkhalas and Dogras and give a regional importance to the Jutogh Thrust. There is no perceptible break between the Subathus and the overlying Dagshai beds. They noted that the Dharamsalas (i.e., the Dagshai and Kasauli formations) occur even north of the Main Boundary Fault, and within the south Siwalik belt, there are thrust-bound inliers of the Dharamsalas. Therefore, there is no particular significance of the term, "Main Boundary Fault" (Srikantia and Sharma 1976, p. 97).

Columnar stromatolites are found in the Shali dolomite. Apart from the stromatolitic dolomite, there are red-purple shales, cherty dolomites, black slates, and pale yellow quartzites, with ripple marks and sun cracks in shales and slates. The whole sequence is very similar to the Chappani–Khoraidi and Hapurkot–Dhorbang Khola formations in west Nepal (Chaps. 8 and 9). There is a saliferous horizon in the Shali schuppen zone north of Mandi (Srikantia and Sharma 1976, p. 107).

Salt is extensively distributed in the lower part of the Shali Formation (their Lokhan Member) and there are saline springs. The salt layer facilitated extensive thrusting. Many dolerite and diorite dikes also appear in the Shali Formation.

Bhargava (1972, 1976) identified the Tiuni, Deoban, Mandhali, Chandpur, Nagthat, Blaini, Infra-Krol, Krol, and Tal formations in the Krol Belt. He correlated the Shali dolomite with the Deoban Formation based on similar stromatolites and lithostratigraphic resemblance.

4.6.1 Tiuni Formation

The Tiuni Formation (later upgraded to the Atal Group) is green-gray in color, and contains shales, slates, and quartzites with sporadic limestone lenses. Basic flows (with vesicular structures) are also interstratified with the Tiuni Formation.

4.6.2 Deoban Formation

The Deoban Formation extends towards the Kumaun Himalaya as the Calc series of Tejam and Pithoragarh (Gansser 1964). To the north, it is supposed to be continued below the thrust sheets and merge with the Shali Formation.

The Deoban Formation is made up primarily of carbonates. The lower part of the Deoban Formation contains a basal quartzite of dull maroon to gray color. It is intruded by doleritic dikes. Ripples and cross-bedding (up to 60 cm thick) are very common in the quartzite. The quartzite is followed by some limestones and dolomites. The limestone is bluish gray, pink, or green-gray, whereas the dolomite is light bluish gray. These carbonates are cherty at places and enclose badly preserved stromatolites. This sequence is succeeded by gray shales, slates, limestones, and dolomites with phosphorite. The last beds are overlain by dark limestones and dolomites, containing columnar stromatolites. A gray-green shale occurs at the top of the formation.

4.6.3 Simla Group

The Deoban Formation in the south part is succeeded by the Simla Group (Bhargava 1972), consisting of green splintery shales interbedded with limestone beds, containing incomplete stromatolites. They are followed by rapid alternations of graywacke, siltstone, and shale of maroon and olive green to dark gray colors. Flute casts, graded bedding, load casts, and cross-laminae are seen in the sandstone. Generally, the

cross laminated beds are less than 6 cm thick. The topmost part of the Simla Group is made up of ferruginous quartzites, micaceous quartzites, shales, and lenticular conglomerate beds with vein-quartz and green quartzite pebbles.

4.6.4 Mandhali Formation

The Mandhali Formation forms the basal part of the Jaunsar Group. This formation consists of quartzites, shales, slates, and platy limestones of gray-green color. There are also a few boulderbeds within this formation. The Mandhali Formation also contains some carbonaceous bands as well as pyritiferous, and sporadically phosphatic zones. It rests over the Deban Formation in the north part along an unconformity (Bhargava 1972).

It is important to note that the Deoban Limestone belt and the Shali Limestone belt are widely separated by the intervening Jutogh Thrust.

Bhargava and Bhattacharrya (1975) mapped all the Blaini outcrops in Himachal Pradesh and in part of Uttarakhand. The mapping revealed that the Blaini rests over six different formations of the Simla and Jaunsar groups, thereby establishing an unconformable relationship between the Blaini and its basement rocks. In ascending stratigraphic order, they described: Member A, lower boulderbed; Member B, a sequence of quartzite, shale, and siltstone; Member C, upper boulderbed; and Member D, pinkish dolomite with interbedded red, green, and gray shales, with varvites. These authors regarded Members A and C as representing glaciomarine deposits, and Member B as interglacial deposits.

The Krol sequence occurs in two tectonic belts; the inner and outer. The former, bounded by the Krol–Giri Thrust, is deposited over the Simla Group, whereas the latter, framed by the synformally folded Tons Thrust, rests over the Jaunsar Group (Bhargava 1972, 1976). The Tal Group is confined to the Inner Krol Belt. These Krol and Tal sequences have been described as superficial nappes (Bhargava 1972). Jiang et al. (2002) have proposed hiatuses within the Krol sequence.

4.7 Pre-Tertiary Outliers in the Sub-Himalaya

Auden (1934) mapped these rocks at first as within the Subathu Formation but subsequently (Auden 1948, p. 81) revised his earlier view and considered them to be "the wedges between the Eocene, younger Tertiaries and the Krol rocks." Raina (1964) mapped a number of detached outcrops of limestone, dolomite, and shale along the Sub-Himalaya, lying sometimes between the Siwaliks and Subathu series marking the Main Boundary Thrust and, sometimes, within the Subathu. He suggested that they could occur as "klippen" or "detached masses." Later, Vohra et al. (1976) described these rocks under the Sataun Formation. There are some discontinuous strips of limestone outcrops between Tundapathar and Sataun with the Eocene succession restricted to the zone of thrust with the Siwaliks. The limestones are thickly bedded with stromatolitic structures. They belong to intertidal to mud flat and shoal deposits, in which stromatolites prevailed. There are numerous faults and basic dikes making a network. Their large-scale geological map shows imbricate faults at the front.

4.8 Lithostratigraphic Correlation and Other Issues

Chaterji and Swami Nath (1976) discuss a number of problems in the Simla Himalaya, such as the correlation of carbonate rocks (i.e., Shali, Deoban, Krol, and Larji Formations), stratigraphic position of Jaunsar and Simla Slates, status of Blaini Formation and other boulderbeds, distribution of the pre-Tertiary carbonate rocks in the Sub-Himalaya, and the structure of various thrust sheets.

4.8.1 Correlation of Simla Slates and Allied Rocks

Wadia and West jointly visited parts of Hazara and the Simla hills in 1930 in order to compare and correlate their geological work (Fermor 1931, p. 125). They conclude that the Shalkhala series of Hazara is equivalent to the Jutogh series of the Simla hills. Both these formations contain carbonaceous schists and carbonates with the characteristic pure white marbles. The marbles are associated with quartzites, quartz schists, and mica schists in both formations. Although the Chail series in the Simla hills is separated from the overlying Jutogh series by a thrust, there is no tectonic break in Hazara, where both units are intimately associated and hence are inseparable. The Jaunsar series is younger, but not older as previously considered, than the Simla Slates, and intervenes between them and the Blaini boulderbeds. Owing to an unconformity at the base of the Blaini boulderbeds, the Jaunsars are absent in the Simla hills (Fermor 1931, p. 126).

The Simla Group of Bhargava (1972, 1976), Srikantia and Sharma (1976) as well as Chaterji and Swami Nath (1977) includes parts of the Chail series, Simla Slates, and Jaunsar series of earlier workers. It lies unconformably over the Shali and Deoban formations. The redefined Jaunsar Group includes the erstwhile Chail series (Bhargava 1972, 1976; Chaterji and Swami Nath 1977).

4.8.2 Correlation of Blaini Boulderbeds and Other Unfossiliferous Lesser Himalayan Rocks

Holland (1908, pp. 129–130) described a boulder from the Simla neighborhood exhibiting conspicuous striations and confirmed the views of Oldham on the glacial origin of the Blaini boulderbeds. However, he differed from Oldham's view on the late Paleozoic age of this formation, and hence its correlation with the Talchir boulderbeds (Oldham 1888, p. 142). Holland concluded that the unfossiliferous outer Himalayan rocks are parts of the Peninsular systems, and thus are Precambrian in age.

Auden (1934), Bhargava (1972, 1976), Srikantia and Sharma (1976), and Chaterji and Swami Nath (1977) state that the Blaini and Mandhali boulderbeds occur in two distinct stratigraphic horizons where the former is younger and the latter is older.

Valdiya (1964) attempted to correlate various unfossiliferous rocks of the Lesser Himalaya on the basis of their tectonic and lithological characteristics. He grouped them broadly under two tectonic subdivisions: the parautochthonous unit (Great limestone of Jammu, Larji, Shali, Pokhara window of Hagen, etc.) and nappe unit (Krol nappe system, Shali and Giri thrusts, Hiunchuli, Piuthan, and Nawakot nappes of Hagen). His correlation scheme of lithological subdivisions is based on the identification of the following two groups: the Argillo-Calcareous Group and the Arenaceous Group. In the calcareous group, there is a rich development of *Collenia*-like stromatolites. He correlates these Lesser Himalayan rocks with the peninsular Indian Vindhyan and other older series of rocks.

4.8.3 Correlation of Carbonate Sequences

After the work of Medlicott (1864), many investigators began to correlate every limestone with the Krol Formation. For example, West (1939) correlated the Shali with the Krol, and Auden (1948, p. 81) correlated the carbonate sequence of Larji with the Krol series. Such correlations were found incompatible with the actual stratigraphy and structure (Chaterji and Swami Nath 1976). The Shali, Larji, and Deoban formations could be coeval and are Proterozoic in age, whereas the Krol and Shali (Deoban) formations are different. The Naldera and Kakarhatti carbonate rocks are stratigraphically younger and structurally higher than the Shali Formation (Chaterji and Swami Nath 1977).

Auden (1937) correlated the Jhiku carbonates and Benighat Slates of Udaipur in east Nepal with the Blaini and Krol series. The phyllites of Daling are correlated with the schistose phyllites of the main Garhwal nappe. According to Vohra et al. (1976), the outer belt of pre-Tertiary carbonate rocks is more likely to be "wedges" than klippen and could be correlated with the Shali and Deoban formations. Srikantia and Sharma (1976) argue that because Gansser (1964, p. 15) had described the Vindhyan rocks from Peninsular India of similar lithology with stromatolites, the Shali Formation could be coeval with them.

4.8.4 Depositional Environment of Simla Slates and Allied Rocks

Rupke (1974) based his observations on aerial photographs and field verifications. He studied a few outcrops in the field and declared that the Simla Slates were of turbiditic origin. His view was followed by many subsequent investigators. Valdiya (1980) also firmly believes that the Simla Slates are of very deep-water origin. However, it is remarkable that Singh and Merajuddin (1978) carried out detailed sedimentological investigation of the Chhaosa Formation (Simla Slates) in the Simla Hills and concluded that the sediments were accumulated in a shallow tidal environment. Their investigations in the field failed to discover any trace of the Bouma cycle and hence they conclude that the Simla Slates do not belong to the turbidites.

4.8.5 Depositional Environment of Krol Formation and Related Rocks

Singh and Rai (1978) studied the Krol Formation in Nainital and concluded that it is of intertidal, tidal flat, and subtidal origin. Singh (1978) reported that Infra-Krol Formation was deposited in a lagoonal environment.

4.8.6 Subathu–Dagshai Passage-Beds

Oldham (1893, pp. 350–351) described the Subathu–Dagshai passage-beds. The Subathu is conformably overlain by a very thick sequence of hard gray sandstones, interbedded with bright red nodular clays belonging to the Dagshai Formation. The transition from the Subathu to Dagshai is marked by a group of passage-beds, composing a peculiar pisolitic marl with small calcareous concretions set in a red clay matrix, a white sandstone containing irregular ferruginous concretions with dark purple or brown shales. The overlying Dagshai Formation consists predominantly of two rock types: one is a bright red or purple clay, weathering into rounded nodular lumps; and the other is a fine-grained, hard, gray-to-purplish sandstone. The clays strongly predominate in the lower portion where the 3–15 m thick sandstone beds constitute a minor portion of the total thickness. But the proportion of sandstone imperceptibly increases upwards, at

the expense of the claystones, and the top 50–100 m of the Dagshai Formation comprises sandstones with thin red clay beds. Similarly, there is a perfect transition between the Dagshai Formation and the overlying Kasauli Formation. The bright red nodular clays are absent in the Kasauli Formation and it is essentially a sandstone-predominating sequence. The sandstones are gray to gray-green in color; most of them are softer, coarser, more micaceous, and in places distinctly micaceous, whereas the interbedded dull green clay beds are *gritty* and micaceous.

Notwithstanding a prolonged history of investigation, the complex geology of the Northwest Himalaya is not yet fully understood. The Proterozoic Lesser Himalayan sequence has been classified into some well-established formations, which extend laterally at least for a few hundred kilometers and continue in west Nepal. However, this segment of the Himalaya also suffers from two problems: attributing various formation names to the same stratigraphic unit and including different stratigraphic units in a single formation name. The last circumstances severely limit further extension of these formation names.

References

Auden JB (1934) The geology of the Krol Belt, Part 4. Rec Geol Surv India LXVII:357–454 (with 9 plates, including a geological map in colors, scale: 1 inch = 2 miles)

Auden JB (1937) The geology of the Himalaya in Garhwal, Part 4. Rec Geol Surv India 71:407–433 (with 3 plates, including a long cross-section on the scale of 1 inch = 2 miles)

Auden JB (1948) Some new limestone and dolomite occurrences in northern India. Indian Miner II(2):77–91

Azmi RJ, Pancholi CP (1983) Early Cambrian (Tommotian) and other shelly microfauna from the upper Krol of the Mussoorie Syncline, Garhwal lesser Himalaya with remarks on the Precambrain-Cambrian boundary. Himalayan Geol 11:360–372

Bhargava ON (1972) A reinterpretation of the Krol belt. Himalayan Geol 2:47–81

Bhargava ON (1976) Geology of the Krol belt and associated formations: a reappraisal, Part I. Mem Geol Surv India 106:167–234 (with a map)

Bhargava ON (1980) Outline of the stratigraphy of eastern Himachal Pradesh with special reference to the Jutogh group. In: Valdiya KS, Bhatia SB (eds) Stratigraphy and correlation of lesser Himalayan formations. Hindustan Publishing Corporation, Delhi, pp 117–125

Bhargava ON, Bhattacharya BK (1975) The Blaini formation of Himachal Pradesh and Uttar Pradesh. Bull Indian Geolo Assoc 8 (2):71–99

Bhargava ON, Singh I, Hans SK, Bassi UK (1998) Early Cambrian trace and trilobite fossils from the Nigali Dhar Syncline (Sirmaur District, Himachal Pradesh): lithostratigraphic correlation and fossil contents of the Tal group. Himalayan Geol 19(1):89–108

Bhargava ON, Srikantia SV (2014) Geology and age of metamorphism of the Jutogh and Vaikrita thrust sheets, Himachal Himalaya. Himalayan Geol 35(1):1–15 (with a map in colors)

Brasier MD, Singh P (1987) Microfossils and Precambrian-Cambrian boundary stratigraphy at Maldeota, lesser Himalaya. Geol Mag 124:323–345

Chaterji GC, Swami Nath J (1976) Problems of stratigraphy and structure of parts of the Simla Himalaya—an assessment, Part I. Mem Geol Surv India 106:1–16

Chaterji GC, Swami Nath J (1977) The stratigraphy and structure of parts of the Simla Himalaya—a synthesis, Part II. Mem Geol Surv India 106:408–488

D'Archiac E, Haime J (1853) *Description des animaux fossiles du groupe nummulitique de l'Inde, précédée d'un résumé géologique et d'une monographie des nummulites*. Gide & J. Baudry, Paris, 373 pp

Fermor LL (1931) General report of the geological survey of India, Part I. Rec Geol Surv India LXV:1–160

Frank W, Thöni M, Purtscheller F (1977) Geology and petrography of Kulu–Rampur area. Colloques internationaux du C. N. R. S. no. 268—Écologie et Géologie de l'Himalaya, Paris, pp 147–172

Gansser A (1964) Geology of the Himalayas. Interscience, New York, 289 pp

Hayden HH (1913) Notes on the relationship of the Himalaya to the Indo-Gangetic plain and the Indian Peninsula, Part 2. Rec Geol Sur India XLIII:138–167

Heim A, Gansser A (1939) Central Himalaya: geological observations of the Swiss Expedition 1936. Denkschriften der Schweizerischen Naturforschenden Gesellschaft, Band LXXIII, Abh. 1, 245 pp (with geological maps in colors, sections, and plates)

Holland TH (1908) On the occurrence of striated boulders in the Blaini formation of Simla, with a discussion of the geological age of the beds, Part 1. Rec Geol Surv India XXXVII:129–135 (with one plate)

Jiang G, Christie-Blick N, Kaufman AJ, Banerjee DM, Rai V (2002) Sequence stratigraphy of the Neoproterozoic infra Krol formation and Krol group, lesser Himalaya, India. J Sed Res 72(4):524–542

Kumar R, Pande IC (1972) Deformation of the rocks of Simla hills, Part 2. Geologische Rundschau 61:430–441

Le Fort P (1975) Himalayas, the collided range: present knowledge of the continental arc. Am J Sci 275:1–44

Mathur VK, Joshi A (1989) Record of Redlichiid Trilobite from the lower Tal formation, Mussoorie Syncline, lesser Himalaya, India. J Geol Soc India 33:268–270

McClelland J (1834) Notice of some fossil impressions occurring in the transition limestone of Kamaon. J Asiatic Soc Bengal III:628–631 (with a plate containing 4 figures)

McMahon CA (1877) The Blaini group and the "Central Gneiss" in the Simla Himalayas, Part 4. Rec Geol Surv India X:204–223

Medlicott HB (1861) On the sub-Himalayan rocks between the Ganges and the Jumna. J Asiatic Soc Bengal Calcutta XXX(1):22–31

Medlicott HB (1864) On the geological structure and relations of the southern portion of the Himalayan range between the rivers Ganges and Ravee. Mem Geol Surv India 3(4):1–206 (with a geological map in colors; scale: 1 inch = 8 miles)

Medlicott HB, Blanford WT (1879) A manual of the geology of India, Part II: extra-peninsular area. Published by order of the Government of India, Calcutta, pp 445–817 (with 21 plates and a map in colors)

Middlemiss CS (1887) Physical geology of West British Garhwal; with notes on a route traverse through Jaunsar Bawar and Tiri-Garhwal. Rec Geol Surv India XX:26–40 (with 1 plate and two maps in colors; scales 1 inch = 4 miles and 1 inch = 1 mile)

Middlemiss CS (1890) Physical geology of the sub-Himalaya of Garhwál and Kumaun, Part 2. Mem Geol Surv India XXIV:59–200 (with 3 plates of cross-sections and a plate of geological map in colors; scale 1 inch = 4 miles)

Naha K, Ray SK (1972) Structural evolution of the Simla Klippe in the lower Himalayas, Part 3. Geologische Rundschau 61:1050–1086

Oldham RD (1883) Note on the geology of Jaunsar and lower Himalayas, Part 4. Rec Geol Surv India XVI:193–198 (with a geological sketch of Jaunsar Bawar, scale: 1 inch = 5 miles, in colors)

Oldham RD (1887) Preliminary sketch of the geology of Simla and Jutogh. Rec Geol Surv India, Part 3 XX:143–152 (with a map)

Oldham RD (1888) The sequence and correlation of the pre-tertiary sedimentary formations of the Simla region of the lower Himalayas. Rec Geol Surv India XXI:130–143

Oldham RD (ed) (1893) A manual of the geology of India: stratigraphic and structural geology, 2nd edn. Geological Survey of India, Calcutta, 543 pp (with a geological map of India in colors, scale: 1 inch = 96 miles)

Pascoe E (1929) General report for 1928, Part 1. Rec Geol Surv India LXII:1–184

Pilgrim GE, West WD (1928) The structure and correlation of the Simla rocks. Mem Geol Surv India LIII:1–140 (with a geological map in colors; scale: 1 inch = 2 miles)

Raha PK, Sastry MVA (1973) Stromatolites from the Jammu limestone, district Udhampur, Jammu, and their stratigraphic and palaeogeographic significance. Himalayan Geol 3:135–147

Rai V, Singh IB (1983) Discovery of trilobite impressions in the Arenaceous member of Tal formation, Mussoorie area, India. J Palaeontol Soc India 28:114–117

Raina BN (1964) A note on the occurrences of some detached outcrops of limestones in the sub-Himalayas of Simla hills. In: International geological congress, report of the twenty-second session, India, Part XI. Proceedings of session 11. Himalayan and Alpine Orogeny, New Delhi, pp 59–78

Rupke J (1974) Stratigraphic and structural evolution of the Kumaon lesser Himalaya. Sediment Geol 11(Special Issue):81–265 (with two map sheets in colors)

Sherborn CD (1888) On a limestone with concentric structure from Kulu, North India. Geol Mag Lond New Series, Decade III, vol V (VI):255–257

Srikantia SV, Sharma RP (1976) Geology of the Shali belt and the adjoining areas, Part I. Mem Geol Surv India 106:31–166 (with 2 maps)

Singh IB (1978) Sedimentological evolution of the Krol Belt sediments. Himalayan geology, Part II, vol 8. Wadia Institute of Himalayan Geology, Dehra Dun, pp 657–682

Singh IB (1979) Environment and age of the Tal formation of Mussoorie and Nilkanth areas of Garhwal Himalaya. J Geol Soc India 20:214–225

Singh IB, Merajuddin (1978) Some sedimentological observations of the Chhaosa Formation (Simla Slates) in the Simla hills. Himalayan Geology, Part II, vol 8. Wadia Institute of Himalayan Geology, Dehra Dun, pp 683–700

Singh IB, Rai V (1978) Some observations on the depositional environment of the Krol formation in Nainital area. Himalayan Geology, Part II, vol 8. Wadia Institute of Himalayan Geology, Dehra Dun, pp 633–656

Tewari VC (2003) Correlation and palaeobiology of Vindhyan and lesser Himalayan stratigraphic successions. J Palaeontol Soc India 48:155–165

Valdiya KS (1964) The unfossiliferous formations of the Lesser Himalaya and their correlation. In: International geological congress, report of the twenty-second session, India, Part XI, proceedings of session 11: Himalayan and Alpine Orogeny, New Delhi, pp 15–36

Valdiya KS (1969) Stromatolites of the lesser Himalayan carbonate formations and the Vindhyans. J Geol Soc India 10:1–25

Valdiya KS (1980) Geology of Kumaun lesser Himalaya. Wadia Institute of Himalayan Geology, Dehra Dun, 291 pp (with a map in colors)

Vicary M (1853) On the geology of a part of the Himalayan mountains, near Subathoo. Q J Geol Soc IX:70–73

Vohra CP, Raina AK, Dua KJS, Khanna PC (1976) The outer pre-tertiary limestone belt between Tundapathar and Sataun, Part I. Mem Geol Surv India 106:17–30 (with a map)

Wadia DN (1934) The Cambrian-Trias sequence of North Western Kashmir (parts of Muzaffarabad and Barumula districts), Part 2. Rec Geol Surv India 68:121–176

West WD (1939) The structure of the Shali 'window' near Simla, Part 1. Rec Geol Surv India 74:133–163 (with 4 plates and a geological map in colors; scale: 1 inch = 2 miles)

Southeast Himalaya and Adjacent Indian Peninsula

5

The Tertiaries fringe the older rocks continuously from close to the Mechi eastward nearly as far as Dálingkot.
—F.R. Mallet (1874, p. 45)

East Nepal shares many geological attributes with the neighboring regions of Darjeeling, Sikkim, and Bhutan. The three tectonic windows, respectively, of Arun and Tamar in Nepal, and Rangit in Sikkim are positioned in similar geological settings (Ghosh 1956). The uninterrupted Higher Himalayan thrust sheet covers an extensive tract of east Nepal and contiguous regions of Darjeeling, Bhutan, and Arunachal Pradesh. In East Nepal as well as in the vicinity of Darjeeling and Sikkim, there is a narrow belt of Lesser Himalayan sedimentary and low-grade metamorphic rocks just south of the Higher Himalayan crystallines. Nautiyal et al. (1964, p. 2) and Gansser (1983, p. 13) state that the greater portion of Bhutan is represented by the crystalline rocks of the Higher Himalaya containing, towards the north, large masses of Tertiary granites. These Higher Himalayan crystallines encroach upon a narrow Lesser Himalayan fringe zone of sedimentary rocks.

5.1 Gondwanas of Indian Peninsula

The Gondwanas and allied successions so widespread in the Indian Peninsula are incompletely distributed at the front of the Lesser Himalaya as a few narrow and discontinuous slivers. But their occurrence alone signifies that the Indian Shield rocks were directly involved in the Himalayan orogeny, without a substantial development of a foredeep or geosynclinal trough, so conspicuous in the Alps (Gansser 1966, p. 840). This world-renowned plant-bearing succession (Box 5.1) is classified into two or three divisions.

Box 5.1 Gondwanas

Oldham (1893) as well as Holland and Tipper (1913) give a historical background to the term *Gondwana*. Since this eminent plant-bearing succession of India was previously described under multifarious local names such as Talchir, Damuda, Mahadeva, and Rajmahal, it was felt necessary to embrace them in a unified classification, and Medlicott (1873) implicitly proposed the name while describing the plant-bearing beds from the Satpura coal basin in August 1872. Subsequently, Feistmantel (1876, p. 82) formally designated them to the Gondwana series or system. He also mentioned that the name was informally introduced by Medlicott and applied by F. Blanford in his work on physical geology of India. In his annual report for the year 1880, Medlicott (1881, p. 2) explicitly uses the term Gondwana, referring to his omitted passage of text in the earlier publication of 1873:

> …For this purpose, the name Gondwana would seem to be suitable, from the country of the most wide-spread aboriginal tribe of Central India, inhabiting a large portion of the ground formed by these plant-bearing rocks, including the Sátpura basin where the series is apparently found most complete.

Suess (1888, p. 318) from the University of Vienna, Austria, applied this term to designate a supercontinent Gondwanaland where similar plant and other fossils prevail.

5.1.1 Lower Gondwanas (?Carboniferous–Permian: 280–245 Ma)

The Lower Gondwanas of Peninsular India are generally classified into the Talchir Formation (Blanford et al. 1856, p. 35) and the overlying Damudas (Oldham 1856, p. ix). Fox (1934) presents a regional perspective to the Lower Gondwana coalfields of India with an excellent geological description of various lithological units. While providing a detailed account of the Gondwanas of India, Krishnan (1958) separates the Gondwana coal, boulderbeds, and volcanics. He also describes marine and plant fossils from

M.R. Dhital, *Geology of the Nepal Himalaya*, Regional Geology Reviews,
DOI 10.1007/978-3-319-02496-7_5

this succession and presents a global synthesis of Gondwanas based on an elaborate correlation table.

Blanford et al. (1856) investigated the Talchir Formation (? late Carboniferous—early Permian), containing a boulderbed, which in places assumes the form of a conglomerate. The rounded boulders, frequently reaching up to 1.5 m in diameter, are derived essentially from granite and gneiss, and embedded in a matrix of coarse sandstone to very fine shale (Blanford et al. 1856, p. 47). The matrix is commonly represented by fine-grained, bluish gray, rippled, sandy shale. The boulders were transported by floating ice (Box 5.2) into a tranquil lake with a sluggish current, where the deposition of silt was taking place (Blanford et al. 1856, p. 49).

Box 5.2 Glacial Origin of Boulderbeds

The definitive proof of glacial origin of the boulderbeds was found by Fedden in January 1872. In the Godavari valley, T. Oldham had excavated the ground (*Footnote* in Blanford 1872, p. 324) and from there Fedden picked out a beautiful block of granite one side of which was excellently polished, scoured, and striated. The sample is exhibited in the Indian Museum, Kolkata (Fedden 1875, p. 17; Waagen 1888, p. 90). These boulderbeds rest unconformably over the Precambrian rocks of the Indian Peninsula. But sometimes about 5–10 m thick very coarse sandstone intervenes between the Precambrian gneisses and the usual boulderbed of about 30 m or so in thickness (Blanford et al. 1856, p. 48).

The Talchir Formation is consistent in composition over a very wide area (Blanford 1872, pp. 321–322). Its lower part regularly comprises a boulderbed of generally less than 15–20 m thickness, consisting of striated and faceted pieces of rock brought by moving ground-ice from various sources. The boulderbeds are overlain by 150–275 m thick pale yellow to green laminated shales and soft fine sandstones (Fox 1934, p. 11). The shales frequently break up into thin tessellated splinters. On the upper surfaces of some of the sandstones, conspicuous bioturbation (tracks) is observed, and some sandstones also include many intraformational rip-up mud clasts. The last shale and sandstone sequence is succeeded by about 125 m thick blue nodular shales, containing occasional dropstones and sandy beds (Blanford et al. 1856, pp. 52–55). The sandstones contain fresh feldspar grains, suggesting the prevalence of land-ice and the disruptive action of frost (Wadia 1976, p. 172).

In the Auranga Coalfield (GSI 1999), the Talchir beds are discontinuous. They were unconformably deposited on an eroded and uneven basement.

About 150–200 m thick coal-bearing strata of the Karharbari Formation (early Permian) succeed the Talchir Formation (Blanford 1865, p. 30). They are made up of *grits*, conglomerates, and sandstones. There are mainly gray, mottled, medium- to coarse-grained, laminated feldspathic sandstones and a few shales with dull clean coal seams (Wadia 1976, p. 172).

5.1.2 Damudas (Permian)

Before embarking on a long voyage in the hitherto unexplored Himalaya, as long ago as January 1848, Hooker (1854, p. 8) visited the plant-bearing beds of Damuda, India. McClelland (1850) had identified from these beds more than 30 fossil plant species such as *Zamia, Glossopteris* and *Tæniopteris.* Some of these genera, together with the stem of *Glossopteris* called *Vertebraria*, are also found in the coalfields of Sindh and Australia.

Blanford (1865) gave the first detailed stratigraphic and paleontological description of the Raniganj (Damuda) coalfields. He also elaborated upon the previous work related to the discovery of coal and mentions that the continuous coal fire in that area was earlier thought to be related to volcanic eruptions. Oldham (1865) mapped a large tract of coalfields in central India and Bengal, and attempted to correlate various coal-bearing successions based on known vertebrate and plant fossils.

The Karharbari Formation is followed up-section by the Damudas (Blanford 1885), the most famous coal-bearing rock succession in India. It is further subdivided into the following formations (Wadia 1976, p. 174; GSI 1999):

- Raniganj Formation (late Permian)
- Barren Measures (late Permian)
- Barakar Formation (early Permian).

The Barakar Formation (Blanford 1885; GSI 1999) rests conformably upon the older formations. It contains a cyclic deposition of coarse- to very coarse-grained, white to grayish white, massive, soft sandstone, medium-grained arkosic sandstone, pebbly sandstone; debris flow deposits; ferruginous sandstones with interbeds of siltstone, claystone, shale, fireclay, and gray shale, with thin ironstone shale bands and coal seams. The Barakar Formation is about 600 m thick.

The Barren Measures (Ironstone and Shales) are made up of a very thick sequence of carbonaceous gray shale, with ironstone concretions and bands, and medium-grained

sandstones. This formation is rather inconsistently developed, as evidenced from its varying (from 0 to 400 m) thickness.

The overlying Raniganj Formation is composed of massive, cross-bedded, coarse and fine, greenish to greenish-yellow sandstones, sandy shales, and micaceous shales, with infrequent micaceous siltstones, and red, brown, and black shales, with many interbedded coal seams. This formation is about 1,500 m thick.

Frequently, the coalfields of east India are invaded by dikes and sills of dolerite and ultrabasic rocks, exhibiting clear contact metamorphic effects (Blanford 1865 p. 59; Wadia 1976, p. 175).

5.1.3 Middle Gondwanas (Triassic: 245–208 Ma)

The Middle Gondwanas (Vredenburg 1907) are represented by massive red and yellow coarse-grained sandstones, conglomerates, siltstones, and shales. This unit is generally free of coal seams or carbonaceous matter. The Middle Gondwanas are further classified into the following formations:

- Maleri Formation (Late Triassic)
- Mahadeva Formation (Late Triassic)
- Panchet Formation (Early Triassic).

The Panchet Formation (Blanford 1865, p. 30, pp. 126–131; Blanford 1872, pp. 327–328) rests over the Lower Gondwanas with a disconformity. It is made of red, chocolate, and green clays interbedded with coarse, micaceous and feldspathic, soft, highly cross-bedded sandstones, sporadically enclosing reworked fragments of Damuda rocks. It contains many plant fossils, such as *Schizoneura gondwanensis, Glossopteris, Vertebraria indica,* and *Cyclophlebis.* It also contains vertebrate fossils, including fish, reptiles, and amphibians (Waagen 1888, p. 95; Wadia 1976, pp. 182–183). The Panchet Formation is about 450 m thick.

The Mahadeva Formation (Oldham 1856, p. ix) is the most extensive sequence in the Middle Gondwanas, and attains a thickness of 1,200 m. It is comprised of variegated massive sandstones, alternating with ferruginous and micaceous clays, siltstones, and conglomerates. They are occasionally associated with bands of impure earthy limestone. This formation contains leaves and seeds of ferns and remains of many amphibians (Wadia 1976, p. 184).

The Maleri Formation conformably overlies the Mahadeva Formation. It is composed mainly of thick, bright red clay beds with a few soft sandstone intercalations. Locally the Maleri Formation attains a thickness of about 600 m, however, it is generally considerably thinner (King 1881, p. 270). In this formation, the remains of reptiles and fish are abundant.

5.1.4 Upper Gondwanas (Jurassic–Early Cretaceous: 208–110 Ma)

The Upper Gondwanas are distributed in distant and isolated places, such as the Rajmahal Hills and Damuda Valley (Ball 1877). They are composed of massive sandstones and shales, akin to those of the Middle Gondwanas. Yet they are distinguished from the Middle Gondwanas by the occurrence of coal seams and lignites as well as the extensive development of limestones.

The Upper Gondwanas cropping out in the Rajmahal Hills consist of a succession of basaltic lava flows or traps with interstratifications of shale and sandstone. The sediments were deposited during the intervals of volcanic eruption and their upper part is affected by contact metamorphism. The sedimentary rocks are made up primarily of hard, white and gray shale, carbonaceous shale, white and gray sandstone, and hard quartzose *grit*. The Rajmahal trap rocks contain dark, very hard, amygdaloidal basalt containing much olivine. The amygdales are composed of quartz, agate, chalcedony, and zeolites. The basalt flows generally range in thickness between 20 and 75 m, but there are also some flows less than 20 m thick as well as others up to 200 m in thickness, whereas the interbedded shale and sandstone beds are significantly thinner (0.5–15 m) and discontinuous (Ball 1877, p. 215). In the northern part of the Rajmahal hills, there are pinkish trachytes, displaying porphyritic to vesicular textures. The volcanics of Rajmahal are also associated with a number of sills and dikes of ultrabasic composition (Ball 1877, p. 220; Dhara et al. 1999). The Rajmahal traps with their associated sedimentary beds attain a thickness of more than 600 m, and of which the sedimentary rocks constitute less than 30 m in the aggregate (Oldham 1893, p. 176). This formation contains quite different plant fossils from the older formations. The important ones are *Equisetum rajmahalense*, *Cyclopteris oldhami*, *Pterophyllum distans*, *Pterophyllum rajmahalense*, and *Ptilophyllum acutifolium* (Feistmantel 1877, p. 143).

5.2 Lesser Himalayan Sequence

Gansser (1939, pp. 16–17) subdivided the Lesser Himalayan rocks of the Darjeeling area into the Dalings (schists with quartzites) and garnetiferous mica schists. The Gondwanas are well observed in the Rangit window of Sikkim, and they also crop up as a narrow strip thrust over the Siwaliks of Sikkim and Darjeeling (Ghosh 1956). These rocks also occur in the Bhutan Himalaya as highly sheared bands of carbonaceous shale, and irregular beds and lenses of anthracite (Gansser 1983, p. 21). The geology of the Bhutan Himalaya

is presented in detail by Bhargava (1995). The narrow belt of Lesser Himalayan rocks of Darjeeling, Sikkim, and Bhutan is represented primarily by the following successions.

5.2.1 Daling and Shumar Groups

Mallet (1874, pp. 40–41) defined the Daling series (Formation) as light green, slightly greasy slates, which are sometimes interbedded with dark green-gray varieties. The slates are often laminated and highly cleaved with two sets of joints, causing the rock to break into small splinters. There also occur some bands of flaggy quartzite and hornblende schist. The schist is slightly calcareous and contains some actinolite. But such calcareous beds are extremely insignificant and the Daling Formation as a whole is characterized by an almost complete absence of lime. It is also distinguished from the Baxa Formation by the scarcity of bright-colored alternations of slates. The Daling slates are somber-colored and monotonous.

While moving from the lower part (i.e., the Tista River) to the upper horizons (towards Darjeeling), Gansser (1939, pp. 16–17) reported that the characteristic rocks of the Daling Schists are clay-slates, alternating with greenish-gray metasandstones. Another rock type is sericite–chlorite quartzite. It contains small rounded quartz grains as well as some large grains in a fine ground mass of sericite with almost colorless chlorite. The next rock type is biotite–chlorite schist with epidote. In the rock, quartz is very fine-grained and forms thin layers where biotite is partly altered to chlorite. This last sequence passes upwards to the garnetiferous mica schists.

The garnetiferous mica schists are characterized by diverse rock types. There are quartzites, containing muscovite and biotite; quartzites with garnet, muscovite, and biotite; highly micaceous quartzites; and garnet–muscovite–biotite schists. These rocks are followed by kyanite–staurolite–garnet–muscovite–biotite schists with porphyroblasts of kyanite and staurolite.

Jangpangi (1974) and Gansser (1983, pp. 29–30) noted that the Shumar Formation in Bhutan is represented mainly by white and green-gray quartzites. In this formation, coarse- to fine-grained, light gray to white, thin, platy quartzites grade upwards into thicker bands.

5.2.2 Baxa Formation

Mallet (1874, p. 34) defined the Baxa series in Bhutan as a massive dolomite succession, also containing beds of variegated soft slate, quartzite, and schist. Gansser (1983, p. 23) restricted the term Baxa Formation to the dolomites, limestones, and calcareous shales with locally developed pockets of gypsum and nests of largely crystalline calcite. The dolomite is of light gray color and exhibits a saccharoid structure. It also contains stromatolites and oncolites (Raha and Das 1989; Tangri 1995, p. 51).

5.2.3 Diuri Formation

Nautiyal et al. (1964) identified a sequence of pebbly shales and slates as the Diuri boulderbed in Bhutan. At the base of this formation, Gansser (1983, p. 22) recorded pebbles mainly of white to dark gray quartzite and subordinately of white vein-quartz, pale yellow siliceous dolomite, black slate, perthitic alkali feldspar, and quartz. They vary in size from 0.5 to 5 cm, are angular to rounded, and embedded in a fine sericitic quartzite matrix. Above this conglomerate band are more than 2,000 m thick black to dark ash-gray slates and pebbly shales, alternating with silty and quartzitic bands. The pebble beds have a matrix of phyllite with disseminated sericite, muscovite, chlorite, a minor proportion of quartz and calcite, and rather abundant graphite. The Diuri Formation is separated from the underlying Damudas by a thrust fault.

5.2.4 Setikhola Formation (Permian)

The Setikhola Formation of southeast Bhutan is characterized by the occurrence of Permian marine fossils. Joshi (1990, 1995) classified these rocks under Member A (400 m thick) of pink, maroon, white, and sporadically green sandstones interbedded with green and maroon shales. This unit is dominated by red beds; it is intensely bioturbated and contains sandstone dikes, flute casts, and flame structures. This member was deposited on a beach or mudflat. Member B (140 m thick) is a rhythmically interbedded sequence of black, gray, and greenish-gray carbonaceous shale and calcareous quartzwacke. The sandstones are calcareous, contain asymmetric ripples and cross-laminae, whereas the mudstone contains sandstone dikes, sun cracks, and slump folds. Member B was accumulated in a semi-isolated basin. Member C (550 m thick) represents a sequence of gray to light gray and brown sandstone, carbonaceous shale, and diamictite. The sandstone is frequently calcareous. Most of Member C was deposited in a reducing environment of a lagoon. But there is also a 25 m thick diamictite bed, occurring 190 m below the top of Member C. Within Member C, Joshi (1995, p. 36) recognized four levels, yielding early Permian fossils.

From the Rangit tectonic window of Sikkim, Sahni and Srivastava (1956) describe *Eurydesma* and many other fossils of late Carboniferous–early Permian age, found in a blue conglomeratic sandstone, lying below the Gondwana sandstones. The fossiliferous horizon is about 1.2 m thick

and also contains *Fenestella* in profusion at its upper 15 cm. The boulderbeds underlie the fossiliferous horizon. On the other hand, from the topmost Gondwana beds they recognized *Glossopteris* and *Vertebraria* as well as other stems. They also recovered *Conularia* and an allied fauna from the Subansiri area of Assam. They compare both these fossiliferous rocks with the Agglomeratic Slates of Kashmir.

5.2.5 Damudas

On his way back to Darjeeling in March 1849, Hooker (1854) discovered some thin coal beds near Pankhabari (southwest of Darjeeling), where the bedrock is made up of steeply (65°) dipping, *gritty*, and micaceous sandstones, interbedded with indurated shale and clay, and thin seams of brown lignite with a rhomboidal cleavage. In the intercalated carbonaceous shale he observed obscure impressions of fern leaves, of *Trizygia*, and *Vertebraria*. The carbonaceous beds at the Pankhabari spur steeply dip due north and are intercalated with soft white and pink micaceous sandstones. Both of these fossils are characteristic of the Damuda coalfields (Hooker 1854, p. 403).

Medlicott (1865) explored the coal of Assam for the first time, whereas Mallet (1874) extended these studies to Darjeeling and Bhutan. His detailed investigations of the coal beds around Pankhabari confirmed the prevalence of well-preserved plant remains, of which *Glossopteris* was the most dominant species (Mallet 1874, p. 17). He also reported abundant occurrence of *Vertebraria* from a few other localities of the Darjeeling district. On the other hand, while carrying out detailed investigations in northeast Assam, Hayden (1910) explained the apparent inversion of coal-bearing beds by introducing a reverse fault.

In an illustrative short paper on the Gondwanas of Sikkim and Darjeeling, Ghosh (1952) gave the lithological, stratigraphic, and structural details of the Lower Gondwana coal measures of Sikkim and Darjeeling. These coal measures are found in the metamorphic terrain of the Lesser Himalaya, and are isolated from the Gondwanas, composing the south foothills of the Outer Himalaya. They appear in the Rangit window and are surrounded by Baxa and Daling sequences. The coal measures consist of light to dark gray, *gritty*, and feldspathic sandstones, carbonaceous slates, and semi-anthracitic coal. They have tillite and varved slates at their base, where scattered rounded, elliptical, and subangular pebbles and boulders of gneiss, granite, quartzite, phyllite, chert, and limestone are frequent. He also pointed out the diverse distribution of pebble beds, such as the Lachi series of Wager (1939), which lies at an altitude of over 5,500 m, and others observed at the base of the Gondwanas in the Outer Himalaya. These pebble beds are generally regarded as equivalents of the Talchir boulderbed occupying the base of the Lower Gondwana of the Indian Peninsula. Hence he demonstrated that the widespread unconformity at the base of the Gondwanas in the Himalayan region is not in conformity with the earlier suggestions that the Dalings represent a metamorphosed portion of the Gondwanas (Ghosh 1952, p. 179).

In the Rangit window, there are a number of coal seams that range in thickness from about 1 m to nearly 8 m. Their chemical composition is akin to that of the Gondwana coal elsewhere. The coal measures are either crosscut by or alternating with mica-lamprophyre dikes and sills, respectively. These igneous bodies have been subjected to considerable alteration by serpentinization. As a result, the coal seam in contact with such bodies is converted into a natural coke. He also remarks that similar dikes are also observed in the Raniganj and Jharia coalfields as well as in those of Outer Himalaya of Sikkim and Darjeeling (Ghosh 1952, p. 179). Therefore, the Gondwanas together with the older schists and gneisses simultaneously experienced the post-Gondwana orogenic movements that folded the rocks together first, and then overturned them (Ghosh 1952, p. 180).

In the Bhutan Himalaya, Pilgrim (1906, p. 24) found the total thickness of the Gondwanas to be about 150 m and their lowest beds represented by very soft fine sandstones, which weather into numerous small crags and pinnacles. These sandstones are interbedded with various coal seams that have experienced intense shearing and crushing. The upper 100 m of the succession is made up of hard quartzitic sandstones with thin carbonaceous shale partings and infrequent shale beds. Lakshminarayana (1995, pp. 30–31) recognized the Damuda Subgroup made up of feldspathic sandstone, siltstone, shale, carbonaceous shale, and coal. The beds are lenticular and represent fining-upwards sequences. The friable to weakly indurated light gray to white and subordinately light brown sandstones comprise medium- to coarse-grained, moderately sorted, subangular grains of quartz, K-feldspar, mica, garnet, zircon, and apatite. Frequently, the sandstones are cross laminated. The upper part of the sandstone succession is gradually replaced by siltstone and shale, containing Lower Gondwana plant fossils.

5.3 Higher Himalayan Crystallines

The Higher Himalayan succession in Darjeeling is represented by the Darjeeling Gneiss (Mallet 1874). It contains garnetiferous psammitic gneiss and injected garnetiferous muscovite–biotite gneiss as well as sillimanite–biotite gneiss (Gansser 1939, pp. 18–19).

5.3.1 Lime-Silicate Inclusions in Darjeeling Gneiss

The lime-silicate inclusions are confined to the lower horizons of the Darjeeling Gneiss. They form 20–25 cm thick lenticular bodies with bent or crumpled ends. They also form concordantly folded bands with the surrounding gneiss. The following mineral associations are generally characteristic of the lime-silicate rocks (Gansser 1939, p. 21): quartz + oligoclase-andesine + biotite + garnet; quartz + a little andesine + a little biotite + garnet + titanite; bytownite + green hornblende + garnet + quartz + titanite; bytownite +, garnet + diopside + quartz + titanite; bytownite + quartz + fine garnet. There are also some lenticular inclusions of basic rocks rich in hornblende.

5.3.2 Pegmatites and Basic Sills

Pegmatite and aplite dikes frequently crisscross the gneisses in various directions. Such dikes are also found in the garnetiferous mica schist of the Daling–Shumar Group. The pegmatites rich in muscovite and tourmaline are up to 5 m thick. There also occur some pegmatite sills.

5.4 Inverted Metamorphism

Auden (1935, p. 163) noticed a progressive increase in metamorphism upwards in the Dalings and Darjeeling Gneiss. Subsequently, Ray (1947) carried out a detailed investigation in that area and identified the following rock units in Darjeeling from top to bottom, respectively: coarse micaceous Darjeeling Gneiss, flaggy garnetiferous mica schist, carbonaceous schists and calc-silicates, golden and silver mica schists, graywacke schists, slates, and Damudas. Mallet (1874) had noted two layers of graphitic schist, but Ray (1947, p. 120) found four of them. They occur persistently for about 15 km and lie below the garnetiferous schist. His metamorphic zones are as follows: sillimanite zone, kyanite–staurolite zone, garnet zone, biotite zone, and chlorite zone. The Gondwanas show very low-grade metamorphism. Mohan et al. (1989) estimated the *P–T* conditions of metamorphism in the Darjeeling–Sikkim region, where temperatures varied from 580 °C for the garnet zone to a maximum of 770 °C for the sillimanite zone, whereas the corresponding pressure values ranged from 0.5 to 0.77 GPa. Neogi et al. (1998) noted that both pressure and temperature increase progressively towards the upper structural levels from the Main Central Thrust zone, which indicates an inverted Barrovian succession. They also discuss the complex history of polyphase metamorphism, dehydration, melting, and generation of migmatites in the Higher Himalaya of Sikkim. Swapp and Hollister (1991) interpreted the inverted metamorphism in Bhutan as a polymetamorphic process, where there was an early high-pressure metamorphic event and a later, low-pressure—high-temperature episode affecting mainly the upper part of the Higher Himalaya.

5.5 Proposition of a Huge Recumbent Fold

The earliest champions of field investigation from the Geological Survey of India, such as Medlicott (1864) and Mallet (1874) were unable to explain the superposition of metamorphosed sequences over sedimentary suites. Mallet (1874, p. 42) pointed out that even though the comparatively more metamorphosed Darjeeling Gneiss overlies the Daling Formation, the latter is not inverted, contrary to the proposition of some earlier (and also later) investigators. For example, L. von Lóczy, a Hungarian professor, had taken geological traverses in the Darjeeling area in 1878 and presented his observations in a lecture in 1883; he postulated such a regional-scale inversion of beds in his publication that came out only in 1907. He had discovered there highly metamorphosed crystallines overlying low-grade metamorphics. To explain this "anomalous" phenomenon, he surmised for the first time an enormous recumbent fold or nappe (Fig. 5.1) with a displacement of 150–200 km to the south (Lóczy 1907).

Although subsequent studies by Auden (1935, p. 162) and Gansser (1964) failed to recognize such a huge nappe, the investigations by Frank et al. (1977) in the Northwest Himalaya and Searle and Rex (1989) in the Zanskar Himalaya have revealed some large recumbent folds and nappes in those regions.

5.6 Folded Tethyan Rocks

Gansser (1983) mapped a number of isolated Tethyan rocks in the Bhutan Himalaya. The Phulchauki klippe in central Nepal and the Jaljala klippe in west Nepal also occupy a similar position. The Tethyan rocks of Bhutan occur over the Higher Himalayan crystallines in the following isolated synclinoria (Bhargava 1995, p. 14): Linghshi, Gurpola, Black Mountain, Sakteng, and one located to the north of Lake Lunana. Of all the known Tethyan rocks of the Himalaya, those composing Black Mountain are nearest to the Indian craton.

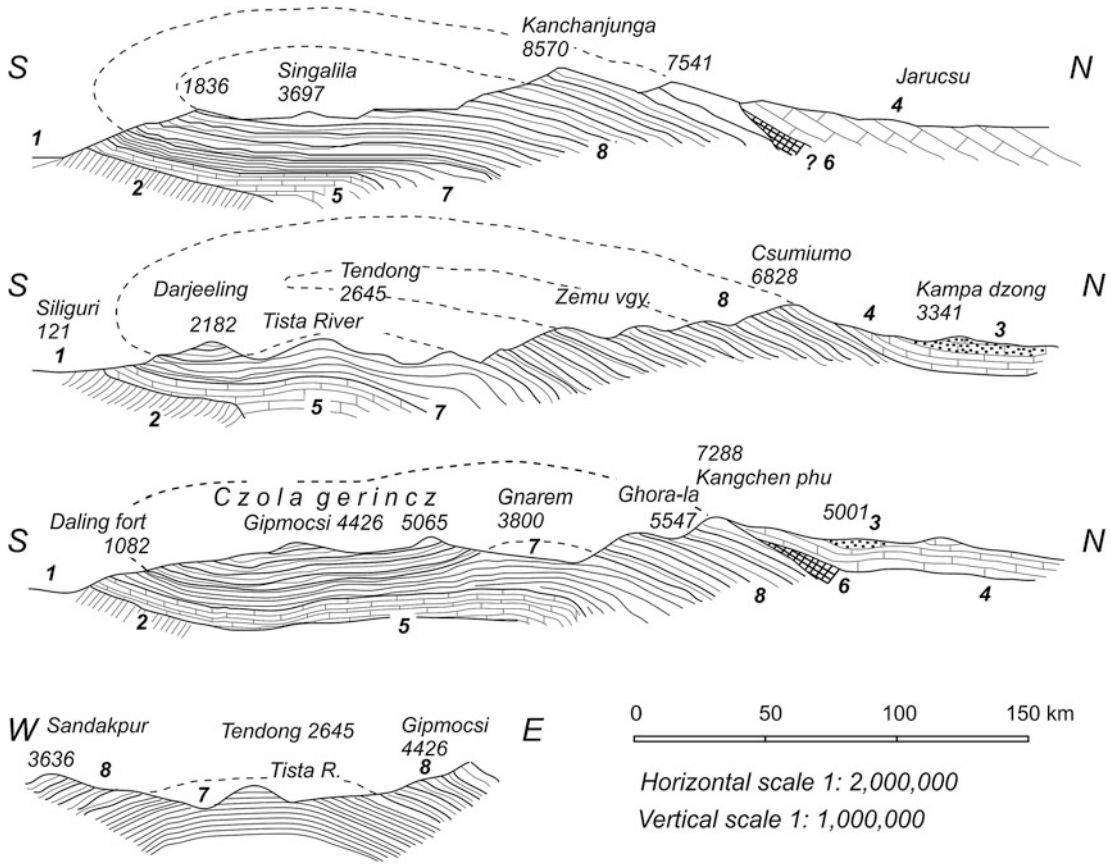

Fig. 5.1 A large recumbent fold (nappe) proposed by von Lóczy. *Source* Modified from von Lóczy (1907, p. 306)

5.7 Interrupted Siwalik Belt

A unique feature of the Siwalik belt in Bhutan is that they are missing in a few places. As identified first by Godwin-Austen (1865, p. 106, 1868, p. 122) and further discussed by Medlicott (1865, p. 436), Mallet (1874, p. 48), Heim (1938), Heim and Gansser (1939, p. 6), and Gansser (1983, p. 16), there is a small gap between the Chel and Jaldhoka Rivers in southwest Bhutan (Fig. 5.2). The rocks are also interrupted for about 50 km in the Hattisar (Geylegphug) embayment, between the Sankosh and Manas Rivers.

The Siwalik Range that extends due ENE and dips towards the mountains abruptly disappears between the Chel and Jaldhoka Rivers, whereas the older Dalings of the Lesser Himalaya protrude towards the plains. In this area, the Lesser Himalayan rocks have come over the alluvial deposits for about 5 km through a 15 km gap in the Siwaliks (Mallet 1874; Gansser 1983).

5.8 South-Tilted Alluvial Terraces

Nakata (1972) identified the southwards-dipping alluvial terraces in Bhutan, at the Hattisar embayment (Fig. 5.3). He attributed this tilt to the movement along the Himalaya Front Tectonic Line. Locally, the Siwalik rocks have also moved over the Pleistocene–Holocene alluvial terraces (Bhargava 1995).

5.9 Frontal Anticline

Godwin-Austen (1875) described the east Himalayan rocks, constituting the outer belt of the Dafla Hills in India. The cross-section (Fig. 5.4) is most remarkable, as it clearly shows a frontal anticline in the Tertiaries. The anticline is partly eroded away. Probably, it is the first identification of a fold at the foothills.

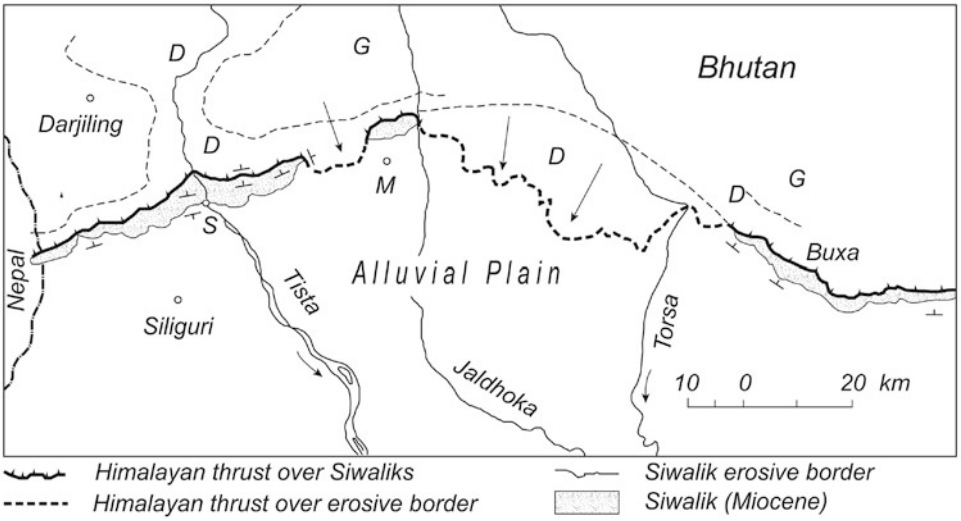

Fig. 5.2 Sketch map of the Himalayan belt through the Siwalik gaps east of the Tista. *G* gneiss; *D* Daling series; in the western part including Damudas (Carboniferous); *B* Baxa series; *S* Sivok railway station; *M* Matiali. *Source* Modified from Heim (1938, p. 419)

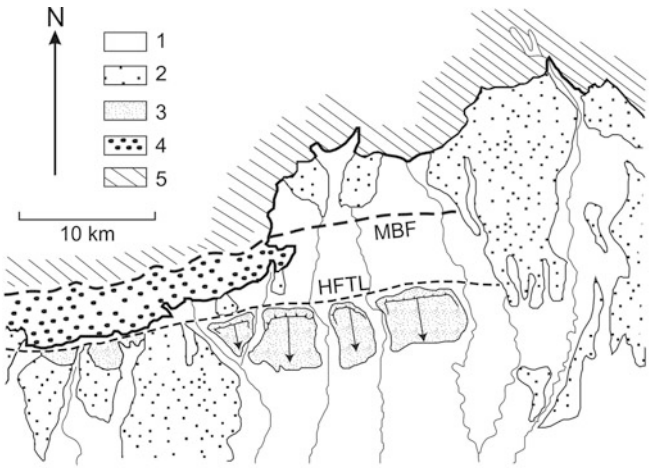

Neotectonics at the Hattisar (Geylegphu) embayment
1- Alluvial fill, 2- main terraces, 3- tilted and faulted terraces, 4: Siwaliks, 5: Pre-Siwaliks
MBF- Main Boundary Fault, HFTL- Himalaya Front Tectonic Line

Fig. 5.3 Disrupted Siwalik succession at Hattisar embayment (Bhutan). Note the tilted terraces to the south and steep escarpment to the north. *Source* Modified from Nakata (1972) and Gansser (1983)

The frontal anticline is well exposed in the Burroi Gorge, where the Tertiary sandstones crop out on its left bank. They dip about 50° towards the plains and they constitute a 2.5–3 m high exposure with an undulating and smooth denuded surface. About 400 m farther upstream to the next large pool, the same succession continues, where the upper surface of denuded sandstone is 5–6 m above the river, indicating a high gradient of the paleo-river channel. On top of this unconformity rest 15–20 m thick iron-colored sands and gravels, which are almost horizontal, but show a very slight incline towards the south (Godwin-Austen 1875, p. 39). In that area, he also identified the Damudas with coal seams, akin to those described by Mallet (1874) from the Pankhabari area of Darjeeling. The contact between the Damudas and the Tertiaries is highly crushed.

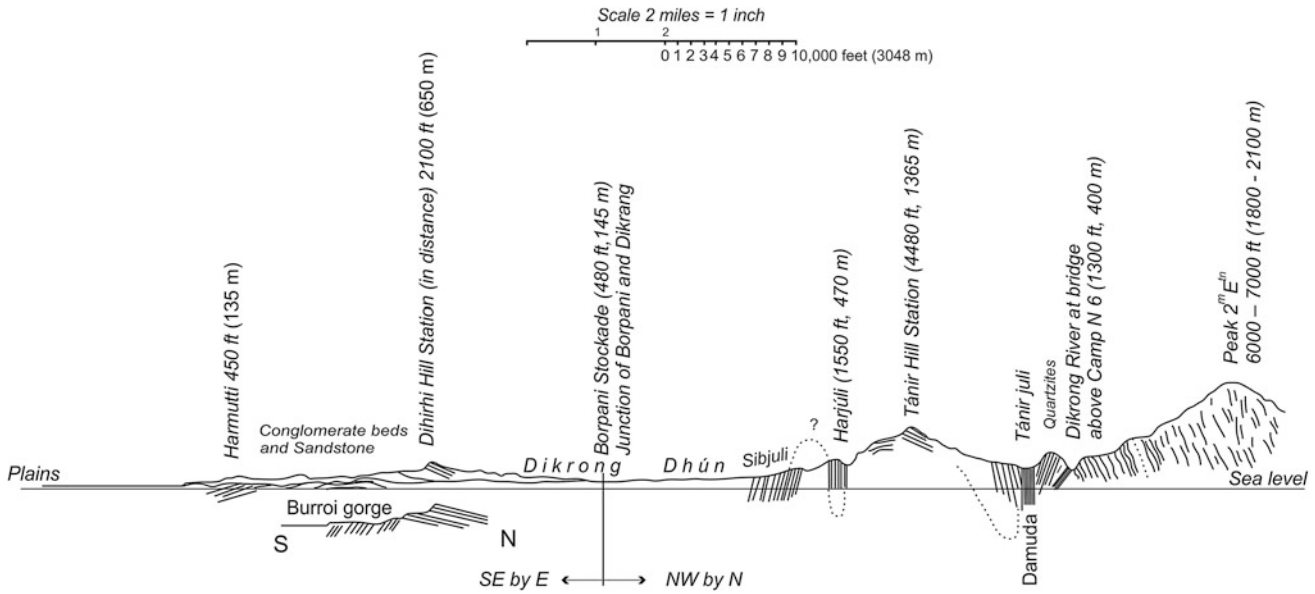

Fig. 5.4 Partly eroded frontal anticline observed in the outer Dafla hills of east Himalaya. *Source* Modified from Godwin-Austen (1875)

References

Auden JB (1935) Traverses in the Himalaya. Rec Geol Surv India LXIX(Part 2):123–167 (with 6 plates including a geological sketch map)

Ball V (1877) Geology of the Rajmehal Hills. Mem Geol Surv India XIII(Part 2):155–248 (with 6 plates and 5 maps in colors; scale: 1 in = 1 mile)

Bhargava ON (ed) (1995) The Bhutan Himalaya: a geological account. Geol Surv India, Special Publication 39:245 (with a geological map in colors, 1:500,000 scale)

Blanford WT (1865) On the geological structure and relations of the Raniganj coal field, Bengal. Mem Geol Surv India III(Part I): 1–195

Blanford WT (1872) Description of the geology of Nágpúr and its neighbourhood. Mem Geol Surv India IX(Part 2):295–330 (with a geological map in colors; scale: 1 in = 4 miles)

Blanford WT (1885) Homotaxis, as illustrated from Indian formations (Presidential address to the geological section of the British association, at Montreal, 1884). Rec Geolo Surv India XVIII(Part 1):32–57

Blanford WT, Blanford HF, Theobald W (1856) On the geological structure and relations of the Talcheer coal field, in the district of Cuttack. Mem Geol Surv India I(Part 1):33–89 (with two plates and a geological map on a scale of 1 in to 4 miles in colors)

Dhara MK, Basu SK, Bandyopadhyay RK, Roy B, Pal AK (eds) (1999) Geology and mineral resources of the states of India, Part I, West Bengal. Geological Survey of India, Calcutta, Miscellaneous Publication no. 30, pp 1–42 (with a geological and mineral map in colors, scale: 1:2,000,000)

Fedden F (1875) On the evidence of 'ground-ice' in tropical India, during the Tálchír period. Rec Geol Surv India VIII(Part 1):16–18

Feistmantel O (1876) Note on the age of some fossil floras of India. Rec Geol Surv India IX:28–42

Feistmantel O (1877) Jurassic (Liassic) Flora of the Rajmahal group in the Rajmahal Hills. Palaeontologia Indica, series ii, xi, and xii, vol. 1, part 2, 143 pp

Fox CS (1934) The Lower Gondwana coalfields of India. Mem Geol Surv India LIX:1–386 (with 15 plates including a geological map in colors; scale: 1 inch = 1 mile)

Frank W, Thöni M, Purtscheller F (1977) Geology and petrography of Kulu–Rampur area. Colloques internationaux du C. N. R. S. No. 268 –Écologie et Géologie de l'Himalaya, Paris, pp 147–172

Gansser A (1939) The rock types of Darjeeling. In: Heim A, Gansser A (eds) Central Himalaya: geological observations of the Swiss expedition 1936. Denkschriften der Schweizerischen Naturforschenden Gesellschaft, Band LXXIII, Abh. 1, pp 16–24

Gansser A (1964) Geology of the Himalayas. Interscience, New York, 289 pp

Gansser A (1966) The Indian Ocean and the Himalayas—a geological interpretation. Eclogae Geol Helv 59(2):831–848

Gansser A (1983) Geology of the Bhutan Himalaya. Denkschriften der Schweizerischen Naturforschenden Gesellschaft 96:181 (with 4 plates: a geological map in colors; scale: 1:2,000,000; cross-sections in colors and black, and a panorama of mountains)

Ghosh AMN (1952) A new coalfield in the Sikkim Himalaya. Curr Sci XXI(7):179–180

Ghosh AMN (1956) Recent advances of geology and structure of Eastern Himalaya. Presidential address to Indian science congress. In: Proceedings of the forty-third session, Agra, part II, Section V, pp 85–99

Godwin-Austen HH (1865) Notes on the Sandstone formation, &c. near Buxa Fort, Bhootan Dooars. J Asiatic Soc Bengal, Calcutta XXXIV (Part II, No. 2):106–107 (with a plate of geological cross-section in colors)

Godwin-Austen HH (1868 Notes on geological features of the country near foot of hills in the Western Bhootan Dooars. J Asiatic Soc Bengal, Calcutta XXXVII(Part II, No. 2):117–123 (with 1 plate)

Godwin-Austen HH (1875) Notes on the geology of part of the Dafla Hills, Assam; lately visited by the force under Brigadier-General Stafford, C. B. J Asiatic Soc Bengal XLIV(1):35–41 (with one plate showing two cross-sections)

Geological Survey of India (GSI) (1999) Geological map of Auranga Coalfield, North Koel River Valley, Bihar, India (map in colors, scale: 1:50, 000)

Hayden HH (1910) Some coal-fields in North-Eastern Assam. Rec Geol Surv India XL(Part 4):283–319 (with 6 plates including one geological map; scale: 1 inch = 8 miles)

Heim A (1938) The Himalayan border compared with the Alps. Rec Geol Surv India LXXII(Part 4):413–421

Heim A, Gansser A (1939) Central Himalaya: geological observations of the Swiss expedition 1936. Denkschriften der Schweizerischen Naturforschenden Gesellschaft, Band LXXIII, Abh. 1, 245 pp (with geological maps in colors, sections, and plates)

Holland TH, Tipper GH (1913) Indian geological terminology. Mem Geol Surv India XLIII(Part 1):1–127 (with 5 maps)

Hooker JD (1854) Himalayan Journals; or, notes of a naturalist (in Bengal, the Sikkim and Nepal Himalayas, the Khasia Mountains, &c. Published by the Grand Colosseum Warehouse Co, Glasgow, vol 1, 408 pp (with 2 maps)

Jangpangi BS (1974) Stratigraphy and tectonics of parts of Eastern Bhutan. Himalayan Geol 4(Part I):117–136

Joshi A (1990) Marine Permian fossils from foothills of Bhutan Himalaya. Curr Sci 59(6):318–321

Joshi A (1995) Setikhola Formation. In: Bhargava ON (ed) The Bhutan Himalaya: a geological account. Geol Surv India, Special Publication 39:34–37

King W (1881) The geology of the Pránhita-Godavári Valley. Mem Geol SurvIndia XVIII(Part 3):151–300

Krishnan MS (1958) Some problems in the geology of the Gondwana formations. Rec Geol Surv India 85(Part 4):409–436

Lakshminarayana G (1995) Damuda Subgroup. In: Bhargava ON (ed) The Bhutan Himalaya: a geological account. Geol Surv India, Special Publication 39:29–33

Lóczy L von (1907) Megfigyelések a Keleti-Himalájában. Földrajzi Közlemények, XXXV Kötet, 7 Füzet, pp 293–310

Mallet FR (1874) On the geology and mineral resources of the Dárjíling District and the Western Duárs. Mem Geol Surv India XI(Part 1):1–96 [with two colored geological maps (of Darjeeling Hill Territory and Western Bhootan Dooars) of 1 inch = 4 miles scale]

McClelland J (1850) Report of the geological survey of India, for the season of 1848–1849. Geological survey of India. J. C. Sherriff, Military Orphan Press, Calcutta, 92 pp (with maps and plates)

Medlicott HB (1864) On the geological structure and relations of the southern portion of the Himalayan Range between the rivers Ganges and Ravee. Mem Geol Surv India III(Art. 4):1–206 (with a geological map in colors; scale: 1 inch = 8 miles)

Medlicott HB (1865) The coal of Assam; results of a brief visit to the coal-fields of that province in 1865; with geological notes on Assam and the hills to the south of it. Mem Geol Surv India IV:387–442 (with 1 geological map in colors; scale: 1 inch = 80 miles)

Medlicott HB (1873) Note on the Sátpúrá coal-basin. Mem Geol Surv India X(Art. 2):133–188 (with a map; scale 1 inch = 12 miles)

Medlicott HB (1881) Annual report of the geological survey of India, and of the geological museum, Calcutta, for the year 1880. Rec Geol Surv India XIV(Part 1):i–xiii

Mohan A, Windley BF, Searle MP (1989) Geothermobarometry and development of inverted metamorphism in the Darjeeling-Sikkim region of the eastern Himalaya. J Metamorph Geol 7:95–110

Nakata T (1972) Geomorphic history and crustal movements of the foot-hills of the Himalayas. Science Reports of Tohoku University, 7th Series (Geography), vol. 22, no. 1, pp 39–177

Nautiyal SP, Jangpangi BS, Pushkar S, Guha Sarkar TK, Bhate VD, Raghavan MR, Sahai TN (1964) A preliminary note on the geology of Bhutan Himalaya. In: International geological congress, report of the twenty-second session, part XI, proceedings of section 11. Alpine and Himalayan Orogeny, New Delhi, pp 1–14

Neogi S, Dasgupta S, Fukuoka M (1998) High P-T polymetamorphism, dehydration melting, and generation of migmatites and granites in the High Himalayan Crystalline Complex, Sikkim, India. J Petrol 39 (1):61–66

Oldham RD (ed) (1893) A manual of the geology of India: stratigraphic and structural geology, 2nd edn. Geological Survey of India, Calcutta, India, 543 pp (with a geological map of India in colors, scale: 1 inch = 96 miles)

Oldham T (1856) Preface. Mem Geol Surv India I(Part I):i–x

Oldham T (1865) Additional remarks on the geological relations and probable geological age of the several systems of rocks in Central India and Bengal. Mem Geol Surv India III(Part I, Art II):197–213 (with a map in colors; scale: 1 inch = 1 mile)

Pilgrim GE (1906) Notes on the geology of a portion of Bhutan. Rec Geolo Surv India XXXIV(Part 1):22–30 (with a geological map in colors; scale: 1 inch = 8 miles and 2 geological cross-sections on 1 inch = 1 mile)

Raha PK, Das DP (1989) Correlation of stromatolite-bearing Upper Proterozoic basins of India and palaeogeographic significance. Himalayan Geol 13:119–142

Ray (1947) Zonal metamorphism in the eastern Himalaya and some aspects of local geology. Q J Geol Min Metall Soc India XIX (4):117–140 (with two plates: geological map and zones of metamorphism)

Sahni MR, Srivastava JP (1956) Discovery of *Eurydesma* and *Conularia* in the Eastern Himalaya and description of associated faunas. J Palaeontol Soc India Inaugural Number 1:202–214

Searle MP, Rex DC (1989) Thermal model for the Zanskar Himalaya. J Metamorph Geol 7(1):127–134

Suess E (1888) Das Antlitz der Erde. Prag, Wien, and Leipzig, vol. II, 703 pp

Swapp SM, Hollister LS (1991) Inverted metamorphism within the Tibetan slab of Bhutan: evidence for a tectonically transported heat source. Can Mineral 29:1019–1041

Tangri SK (1995) Baxa Group. In: Bhargava ON (ed) The Bhutan Himalaya: a geological account. Geological Survey of India, Special Publication 39, pp 38–58

Vredenburg EW (1907) A summary of the geology of India. Thacker, Spink & Co, 67 pp

Waagen W (1888) The Carboniferous glacial period. Rec Geol Surv India XXI(Part 3):89–130 (with one plate)

Wadia DN (1976) Geology of India. Tata McGraw-Hill Publishing Co, New Delhi, 508 + p

Wager LR (1939) The Lachi series of North Sikkim and the age of the rocks forming Mount Everest. Rec Geol Surv India 74(Part 2):171–188 (with 5 plates)

Part III

Lesser Himalaya

Introduction to Lesser Himalaya

6

Barren of fossils, affected by tectonism and transformed to various degrees by metamorphism, these rocks remain the impressive but unpaged historic manuscript of the Himalaya.

—K.S. Valdiya (1964, p. 15)

The distorted and dislocated rocks of the Lesser (or Lower) Himalaya comprise most of the ruggedly youthful Mahabharat Range and they also form relatively mature but subtle midlands hidden behind it. The four antecedent river systems: Mahakali (or Kali), Karnali, Gandaki, and Koshi have incised into the Higher Himalayan thrust sheet so deeply that the entombed Lesser Himalayan succession is revealed in transverse river valleys as well as in the deeply dissected inner zone (Fig. 6.1). An overwhelming majority of these rocks (Box 6.1) are of Proterozoic age and they previously constituted the north portion of the Indian craton (Holland 1908; Gansser 1964). There are also some Paleocene–Eocene sediments of the trespassing Tethys Sea and overlying Oligocene to Early Miocene continental deposits, distributed not only in the outer zone but also in the inner windows of Darchula, Bajhang, and Jajarkot. This fact itself points to the existence of the more than 200 km wide Early Miocene foreland basin, a greater portion of which was affected subsequently by the Himalayan orogeny. The foreland was much wider than the Siwalik basin, as Early Paleocene–Oligocene strata extend under the Ganga Basin, where they rapidly pass into the succeeding Siwaliks (Johnson 1994; Friedenreich et al. 1994; Raiverman 2002). In pace with the upheaving Himalaya and retreating shallow Eocene sea, the foreland basin was formed either directly on the contemporaneous deposits or on the adjoining Indian craton. The foreland basin was gradually transformed into the Siwalik basin, which again continued to grow to the south, on the Indian craton. The last inference is based on the observation of Proterozoic tectonic slices in central and east Nepal, where there is a disconformity separating these older strata from the overlying Siwaliks. The Indo-Gangetic alluvium is the latest version of the foreland basin, developed in front of the Himalayan arc.

Box 6.1: General Features of Lesser Himalaya

- The Lesser Himalaya is composed basically of Proterozoic rocks. The apparent paucity of fossils in the Lesser Himalaya is related to its old age.
- In most parts of the Lesser Himalaya, there is a colossal depositional gap between the Proterozoic rocks and the overlying Paleocene–Eocene beds, indicating a prolonged history of denudation (or non-deposition).
- No other large unconformities have been identified in the Proterozoic sequence.
- Tight to overturned folds, mostly north-dipping but also some south-dipping imbricate faults, and detached outliers characterize the Lesser Himalayan belt. The tectonic transport was mostly towards the foreland with some instances of movement towards the hinterland.
- Practically the entire Lesser Himalayan sequence was previously concealed under the Higher Himalayan crystalline thrust sheet.
- The thrust sheet moved over the Lesser Himalayan sequence, which was deformed to yield various folds and faults. In this process, the Higher Himalayan sequence was also passively contorted.
- Though mostly composed of sedimentary and low-grade metamorphic rocks, some granites, augen gneisses, amphibolites, and volcanic rocks are also present at various stratigraphic levels.
- A few nepheline syenite bodies are intruded in the Lesser Himalaya of central Nepal, whereas old granites are found in east Nepal.

M.R. Dhital, *Geology of the Nepal Himalaya*, Regional Geology Reviews,
DOI 10.1007/978-3-319-02496-7_6

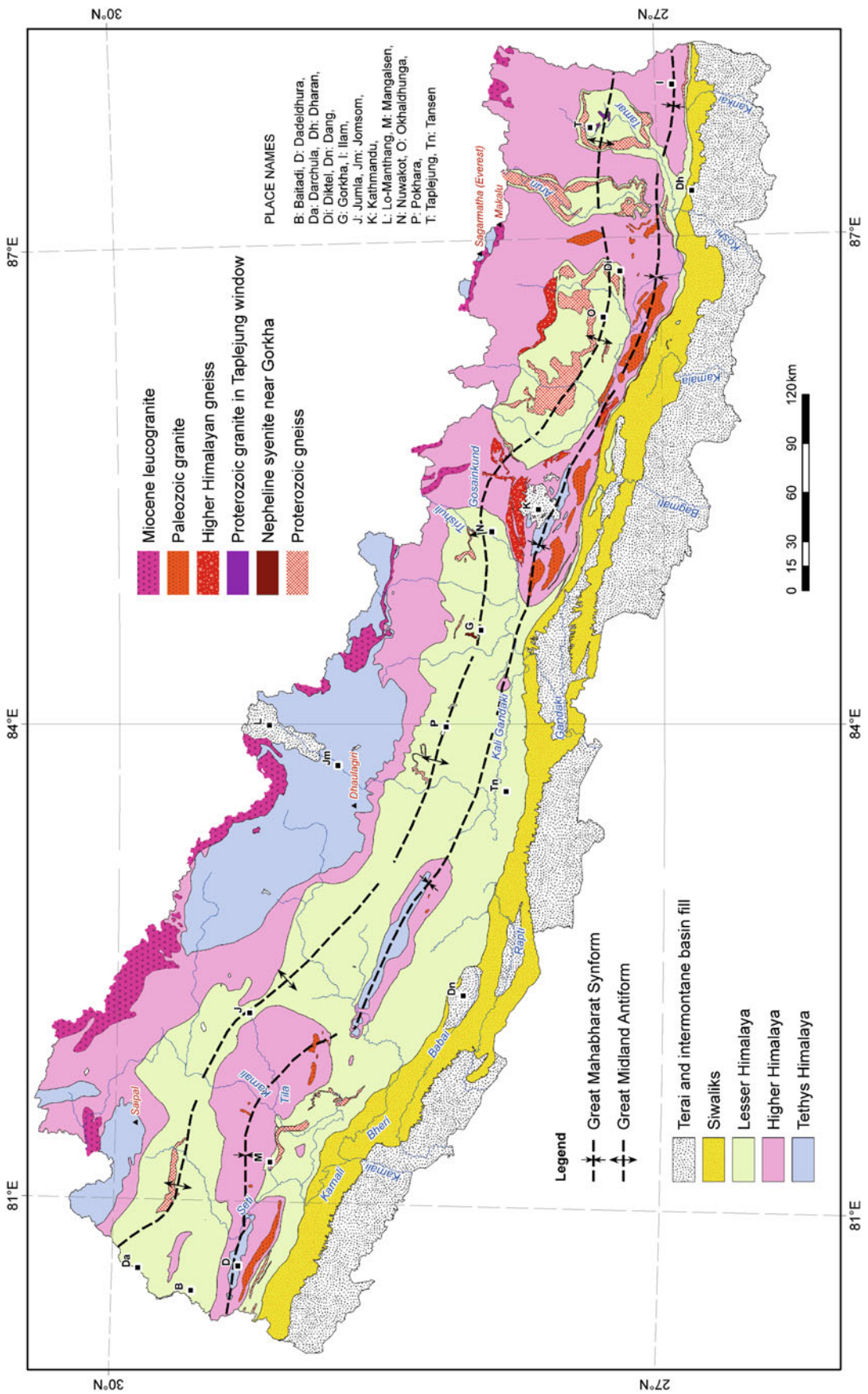

Fig. 6.1 Generalized geological map of Nepal showing main geological divisions and two broad folds. *Source* Based on Hagen (1969), ESCAP (1993), Amatya and Jnawali (1994), and several other published maps

- There are carbonate beds containing a variety of stromatolites straddling different stratigraphic rungs.
- Diamictites of various ages are distributed within the Lesser Himalaya.
- Like the carbonate rocks, redbeds and black slates are also not confined to a single stratigraphic horizon.
- Generally, the grade of metamorphism increases from foreland (south) to hinterland (north).
- Himalayan metamorphism may affect a given sedimentary rock unit to such an extent that its primary sedimentological and petrographic details are obliterated. Consequently, the rock seems to represent a completely different succession.

The Lesser Himalaya, so termed by Burrard and Hayden (1908, pp. 75, 86), is essentially made up of sedimentary and mildly metamorphosed strata. Medlicott (1879, p. 519) defined the Lower Himalaya as a broad zone lying between the snowy peaks on the north and the Sub-Himalaya on the south. He also remarked that although the most accessible and the most frequented part of the mountains, it is the least understood and structurally extremely complex. Similarly, Oldham (1883, p. 193) made the following remarks:

> This is but part of the great Himalayan puzzle, that newer beds almost always seem to dip under older, that faults are generally reversed, and that the dip of the beds in their neighbourhood is precisely the reverse of what would be expected on à priori grounds. The total thickness of these beds is indeterminable, partly on account of their intense disturbance, and partly from the fact that neither their base nor summit has been seen … .

These remarks are equally valid to date. Despite more than 60 years of indefatigable investigation by an array of foreign and national geologists, this tract remains the most enigmatic within the entire mountain range of Nepal. The crux of the Lesser Himalayan problem may be formulated in terms of a dilemma that the structure of this predominantly unfossiliferous zone can be unraveled after its stratigraphic reconstruction, whereas the stratigraphy can be worked out after investigating its structural details. Consequently, the history of investigation in this part is impregnated with controversies on the age of certain rock groups and their structural position.

6.1 Pioneer Investigations in Nepal

Kathmandu and its surrounding regions of central Nepal have been the hub of geological research since very early days. At the invitation of the Nepal Government, Medlicott visited the Kathmandu Valley and the neighboring tract of this secluded country of that period in May 1875. He was able to identify the Sheopuri gneisses made up of coarse feldspar, silvery mica, and schorl. He also reported schists and calcareous rocks of Nagarjun surrounding the gneisses (Medlicott 1875, p. 97), and the fossiliferous sedimentary sequence of the Chandragiri Hills (Chap. 21). After his reconnaissance, Nepal had to wait for a long 60 years to receive J. B. Auden, another outstanding authority from the Geological Survey of India. In connection with the assessment of the damage incurred by the Great Nepal–Bihar earthquake of February 15th, 1934, Auden (1935) was granted permission to follow the same route to the Kathmandu Valley as that permitted to Medlicott, but he also traveled to Udaipur and Taplejung on his way to Darjeeling. He was the first to notice the superposition of high-grade metamorphic rocks including the Sheopuri gneisses over the sedimentary succession of the Lesser Himalaya in the Kathmandu region. He prepared a regional geological map of the area between Kathmandu and Darjeeling and opined that the anomalous superposition could be analogous to that observed between the Darjeeling Gneiss and underlying Daling schists in the Southeast Himalaya.

Toni Hagen entered Nepal for the first time in October 1950 and completed his fieldwork in April 1958. He came to Nepal with a background of geology, geomorphology, and photogeology, specialized in three-dimensional block diagram construction (e.g., Hagen 1950a, b) in the Swiss Alps, and superbly applied his skills to the preparation of various cross-sections and diagrams in Nepal.

6.2 The Great Controversy

Hagen (1969) was deeply impressed by the discovery of nappes in the Northwest Himalaya and Darjeeling. Also, guided by his research experience in the Alps, he envisioned various nappes in the Nepal Himalaya.

During his first trip to the Kathmandu Valley, Trishuli Valley, and surrounding areas, Hagen (1951) had already come across the superposition of medium- to high-grade metamorphic rocks over sedimentary and low-grade metamorphic sequences. Founded on these and other observations, he distinguished the Nawakot and overlying Kathmandu nappes. These nappes have their roots near Rasuwa Gadhi, and constitute a very big antiform in the vicinity of Gosainkund. Farther to the south, the nappes make a vast synform around Kathmandu. Due to the axial plunge towards the east, the fold closes west of Kathmandu. He also discovered that the Kathmandu nappes lie concordantly on the Nawakot nappes, whose south portion has experienced thrusting and late phase folding (Hagen 1951, p. 134). He compared the two nappe systems, respectively,

with the Garhwal and Krol nappes of Auden (1937) in Kumaun. Hagen also favored the correlation of the Sheopuri gneisses with those of Darjeeling.

Lombard (1952) introduced the term "*dalle du Tibet*" (Tibetan slab) in the geological literature for the Higher Himalayan succession. Lombard (1953a, b) and Lombard and Bordet (1956) constructed a few cross-sections across east Nepal and correlated the Higher and Lesser Himalayan sequences, respectively, with the Kathmandu and Nawakot nappes of Hagen.

Hashimoto (1959) investigated the rocks of central and west Nepal during the Mount Manaslu expedition and he also observed the inverted metamorphism. But he was deeply sceptical about the occurrence of any nappe. Similarly, Bordet (1961), Gansser (1964), and others also cast some doubt upon Hagen's multiple nappe hypothesis.

In the meantime, Hashimoto et al. (1973) carried out further geological investigations in Nepal, and came up with a proposition of vertical block faults instead of various horizontally disposed nappes. In the capacity of a UNDP expert, Talalov explored the mineral deposits of Nepal between 1969 and 1972. In line with the above critiques, he also had a quite contrary view. When Hagen assumed many nappes and surmised meager ore deposits, Talalov (1972, 1977) inferred bountiful mineral deposits but failed to find any nappe. Sharma (1973, 1990) also denied the existence of any thrust of significant displacement.

A group of experts from the Geological Survey of India, including Nadgir, Nanda, and Powde, carried out detailed mapping in west and central Nepal in the late 1960s. Their work (Fig. 6.2) was fundamental in defining the stratigraphy of this region.

These investigators also did not believe in large-scale thrusting and proposed a continuous succession in central Nepal. Nadgir (1976) described the lithostratigraphy of Kathmandu and the surrounding region, and assigned a Mesoproterozoic age to the stromatolites of the Nawakots. He also drew a transitional contact between the Nawakots and overlying Bhimphedis. His Nawakot succession contains a lower group of *gritty* phyllites, quartzites, and basic effusives; a thick middle group of laminated phyllites, redbeds, and shallow-water algal (stromatolitic) dolomites; and a thick upper group of black, variegated, carbonaceous shales and limestones with some concretionary quartzites. He inferred that the plutonic activities around Kathmandu metamorphosed the Bhimphedis. The Lesser Himalayan rocks of the Nawakots have a close affinity to the Vindhyan rocks of the Indian craton. The rocks similar to the Nawakots were met with in a borehole under about 4,000 m of Siwalik cover near Raxaul, only 60 km south of the nearest exposure in the Mahabharat Range.

Stöcklin came to Nepal as a UNDP expert in July 1975 and led a photogeological survey in central Nepal, primarily for the purpose of mineralogical exploration. His two-year–long geological investigations were immensely valuable for the establishment of stratigraphy and solving intriguing confusion regarding thrusting, block faulting, and metamorphism in the Lesser and Higher Himalaya of central Nepal. Equipped with past experience in other mountain belts, he made painstaking field observations and mapped about 5,000 km^2 of central Nepal for the first time on a scale of 1 inch to a mile. As a result, he confirmed the Mahabharat Thrust between the Kathmandu Complex and the underlying Nawakot Complex and concluded that the fault is the southern continuation of the Main Central Thrust (Stöcklin 1980).

6.3 Distribution of Lesser Himalayan Sequence

The Lesser Himalayan rocks are exposed predominantly between the Siwaliks to the south and the Higher Himalayan crystallines to the north. In Kumaun, Valdiya (1964) subdivided the Lesser Himalayan sequence into the parautochthonous and nappe units. In west Nepal, Fuchs and Frank (1970) grouped these rocks under the parautochthonous sequence, comprising the outer zone or tectonic windows, and the Chail nappes thrust over them. In Nepal, the Lesser Himalayan rocks show intermittently in about a 100 km wide belt that narrows down to a few kilometers in the Mahabharat foothills of east and west Nepal. The rocks are exposed in the following zones (Fig. 6.1):

- Tectonic windows surrounded by the Higher Himalayan crystallines
- Inner zone of low-grade metamorphic and sedimentary rocks
- Intermediate transition zone between the inner and outer zones
- Outer Lesser Himalayan zone predominated by sedimentary rocks
- Sedimentary slices of Lesser Himalayan rocks within the Sub-Himalayan belt

The Lesser Himalayan rocks may straddle these zones without any sharp structural break. Similarly, the distinction between the tectonic windows and the inner zone is primarily of tectonic nature.

6.3.1 Tectonic Windows

The interplay among thrusting, erosion, and folding has created a complex pattern of tectonic windows and klippen in west Nepal, around Baitadi, Darchula, Bajhang, and Jumla (Figs. 1.6 and 6.1). The folded and fragmented Higher Himalayan thrust sheet approaches the Siwaliks near Budar

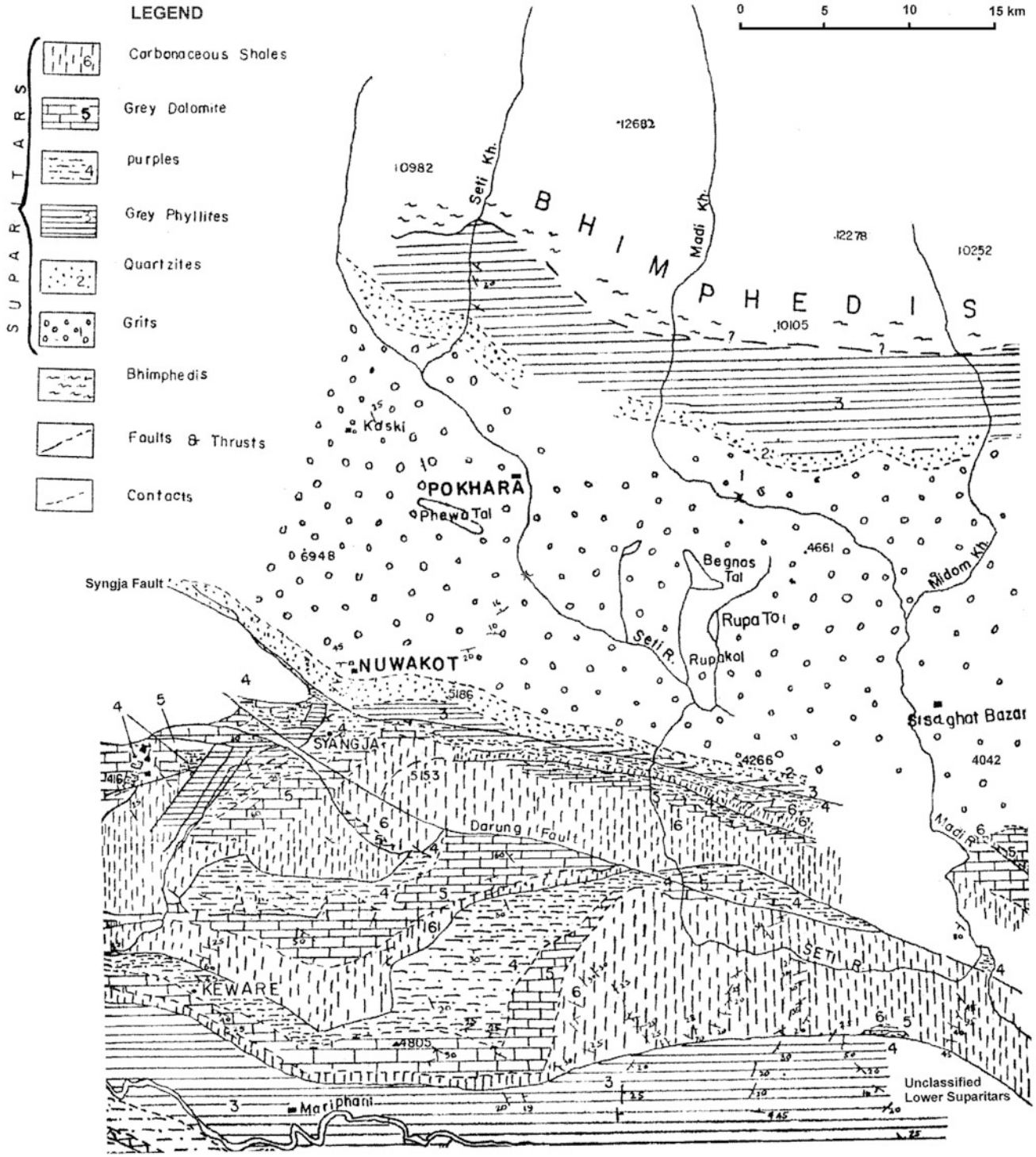

Fig. 6.2 Part of the geological map of west Nepal prepared by Nanda (1966). The stratigraphy is similar to that proposed by Stöcklin and Bhattarai (1977) for central Nepal

and the Karnali River. The main rocks representing this part of the Lesser Himalaya are the Proterozoic phyllites, quartzites, amphibolites, and slates, together with a huge succession of carbonates. One of the important aspects of this zone is the occurrence of Early Miocene rocks within some imbricate slices.

The Okhaldhunga, Arun, and Tamar windows occur in east Nepal, where they are surrounded by the Higher

Himalayan thrust sheet (Brunel and Andrieux 1977). These tectonic windows are developed in longitudinally as well as transversely folded Higher Himalayan antiformal culminations. Some of them contain Paleoproterozoic phyllites and quartzites with a few bands of gneiss and some granite intrusions. As a rule, towards the top of the windows, the grade of metamorphism increases and indiscernibly passes into the overlying Higher Himalayan sequence.

6.3.2 Inner Zone

This zone primarily belongs to the north part of the vast tectonic windows of the past, which were widened so extensively that there remain but a few large and some small Higher Himalayan klippen near their south margin. In fact, this zone lies within the eroded portion of the Great Midland Antiform (Chap. 13) first described by Hagen (1969). This fold begins at the Chamoli window in the Northwest Himalaya of Kumaun (Fuchs and Sinha 1978), enters Nepal near Darchula, and extends over Bajhang and Jumla. Then it continues towards the Thuli Bheri River, Baglung, Pokhara, Gorkha, and the Trishuli River for about 425 km (Fig. 6.1). The rocks representing the inner zone also do not differ much from those of the tectonic windows.

6.3.3 Intermediate Zone

There is a tract of transition from the inner to the outer zone. The intermediate zone lies roughly within the vanished Higher Himalayan core of the Great Mahabharat Synform (Chap. 13) or in its vicinity, and assumes a special tectonic position. The area between Baitadi and Dadeldhura, the Chhera Khola area southwest of Jajarkot, the region north of the Kali Gandaki and south of Galyang, and the middle reach of the Trishuli River, south of Mugling, are placed in the intermediate zone. Sedimentary and low- to medium-grade metamorphic rocks constitute this zone.

6.3.4 Outer Zone

The grade of metamorphism in the Lesser Himalayan sequence gradually diminishes from the hinterland towards the foreland, and the sedimentary rocks preponderate to the south. A narrow belt between the west border of Nepal and the Bheri River, an extensive region between the Bheri and Narayani, and some discontinuous patches composing the Mahabharat Range between the Narayani and Mechi belong to this zone. In the outer zone, one finds tectonic klippen of sedimentary or low-grade metamorphic rocks resting directly on the youngest sedimentary rocks of the Lesser Himalaya.

6.3.5 Older Sedimentary Slices in the Siwalik Belt

Proterozoic sedimentary slices are distributed in the Bagmati River, north of Marin Khola, and the area between Sindhuli Madi and the Tawa Khola. These rocks make many irregular, thin slices in the Sub-Himalayan belt. Generally, there is a conspicuous disconformity between the two contrasting units, representing the older Lesser Himalayan sequence and the younger Siwaliks.

6.4 Classifying Lesser Himalayan Rocks

Because it had been a formidable task to classify the immensely thick (more than 15 km) pile of the Lesser Himalayan Proterozoic succession (Box 6.2), Valdiya (1964) proposed a simple threefold division of arenaceous, calcareous, and pelitic units, respectively, from the bottom upwards. Sharma (1973) applied this notion throughout Nepal.

Fuchs and Frank (1970) developed the lithostratigraphy based on a single major limestone unit (Krol or Shali) and only one major quartzite unit (Nagthat), and they interpreted the reappearance of similar lithologies not as possible facies recurrences, but as tectonic repetitions forming many nappes (Stöcklin 1980).

Hashimoto et al. (1973) identified the Midland Metasediment Group, containing four subgroups. The Lowermost Subgroup is represented mostly by black slates in the Sun Koshi Valley and around Okhaldhunga as well as in the Chautara and Marsyangdi areas. The Lower Subgroup forms the core of the Kunchha–Gorkha–Nawakot antiform, and it is made up of medium- to coarse-grained sandstones and chlorite-sericite-phyllites. The sandstones are characterized by opalescent clastic quartz grains of subrounded shape. The grains frequently show beautiful blue schlieren. Some conglomeratic layers also occur in this subgroup. The Middle Subgroup consists of pale orange or white quartzites with conspicuous ripple marks. The subgroup is well developed in the middle and southern parts of the Midlands. There are also some amphibolite bands in the Middle Subgroup. The Upper Subgroup contains stromatolitic carbonate rocks with a subordinate amount of slates. It occurs in the northern and southern parts of east Nepal, especially in the vicinity of Tumlingtar and in the Arun window. The subgroup also appears in the eastern part of the Dhaulagiri region and in the Piuthan zone (Akiba et al. 1973, pp. 238–241). Their investigation helped to recognize wide sedimentary zones, some granites, and a prominent NNE–SSW trending lineation throughout the Nepal Himalaya. Bordet (1961) had noticed the lineation first in east Nepal.

In central Nepal, Stöcklin and Bhattarai (1977) identified the Nawakot Complex, whereas Colchen et al. (1986) grouped these rocks under the Midland formations, which are developed mainly in the inner zone.

The Department of Mines and Geology published five geological maps on a scale of 1:250,000. In them, the Lesser Himalayan rocks are classified into the Midland Group and the Surkhet Group. The Midland Group is subdivided into the Pokhara or Dailekh Subgroup, Lakharpata Subgroup, and the unconformably overlying Gondwana Subgroup (Tater et al. 1983; Shrestha et al. 1987).

The Pokhara or Dailekh Subgroup contains the Kushma Formation (medium- to fine-grained, massive, green-gray to white quartzites), Seti or Ranimatta Formation (gray to green-gray *gritty* phyllites and metasandstones with metabasics), Naudanda Formation (fine- to medium-grained, massive, white quartzites), and the Ghanpokhara Formation (black carbonaceous phyllites, slates, and shales with white limestones).

The Lakharpata Subgroup begins with the Galyang Formation (black slates with some carbonates), and is followed upwards, respectively, by the Sangram Formation (black laminated shales with thin limestone and quartz arenite interbeds), Syangja Formation (white, pale orange, and pink calcareous quartzites and dolomitic limestones with dark gray, purple, and pale green shales), and the Lakharpata Formation (fine-grained, gray limestones, dolomitic limestones, and dolomites, containing stromatolites, with thin intercalations of black to dark gray shale or purple and green shale).

The Gondwana Subgroup contains the Takure Formation of black shales, psammitic schists, and phyllites.

The Surkhet Subgroup (Cretaceous–Eocene) comprises the Melpani Formation (white, gray, ferruginous quartzites with gray, black, and reddish brown shales and sporadic conglomerates; some gray fossiliferous limestones with gastropods and pelecypods), the Swat Formation (gray to dark gray, soft, carbonaceous shales with beds and lenses of fine-grained limestone containing *Nummulites* and *Assilina*), and the topmost Suntar Formation (fine- to medium-grained, green-gray sandstones with purple shales (Shrestha et al. 1987).

ESCAP (1993) published a regional geological map of the country and classified the Lesser Himalayan rocks into the Lesser Himalayan metasediments and the Lesser Himalayan crystallines. Their first sequence is subdivided into the Kuncha Group of phyllites, quartzites, and metasandstones; the Nawakot Group of variegated quartzites, carbonates, slates, and phyllites; and the Tansen Group of Permo–Carboniferous to Early Miocene rocks. Their Lesser Himalayan crystallines are equivalent to the Kathmandu Complex of Stöcklin and Bhattarai (1977).

Box 6.2: Early Views on Unfossiliferous Strata

For a long time, it was puzzling why the Lesser Himalayan sequence so promising to be fossiliferous is devoid of them, whereas the nearby Tibetan-Tethyan sequence is so rich in organic remains. In this connection, (Holland 1908, p. 132) made the following remarks,

> … on the Tibetan side of the snowy peaks, every period from the Lower Paleozoic to the top of the Mesozoic is marked by highly fossiliferous strata, while to the south great thicknesses of strata are absolutely devoid of fossils, one naturally wonders whether these two sets of strata do in reality correspond in age, whether, in fact, it is possible that the waters in which the southern beds were formed were always devoid of living beings, while only a few miles away the ocean always was teeming with life.

Though he justifiably inferred that the Lesser Himalayan rocks could basically belong to the Proterozoic, many prominent geoscientists were unable to follow his line of thought, and postulated various Paleozoic and Mesozoic age ranges. Special attention was given to the Blaini boulderbeds, supposedly to be equivalent to the Permo–Carboniferous Talchir boulderbeds of Peninsular India (Chap. 5). Later investigations revealed a Proterozoic age for the Blaini Formation too.

6.4.1 Augen Gneisses

Pêcher and Le Fort (1977) studied the Ulleri-type of augen gneisses from west Nepal and inferred their volcano-sedimentary origin. Stöcklin (1980) remarked that the Lesser Himalayan gneisses occur at various stratigraphic levels and hence cannot be attributed to the volcano-sedimentary origin for all of them. Sharma and Kizaki (1988) investigated the augen gneisses and granitoids of the Jajarkot area and remarked that some of them could be of granitic affinity whereas others could be of metasomatic origin. Regmi and Arita (2008) studied the augen gneisses from the Lesser and Higher Himalaya of east Nepal, and concluded that they have similar geochemical characteristics, and most of them could be old S-type granites or their equivalents.

Brunel and Andrieux (1977) discovered large crystalline nappes covering almost the whole of east Nepal. They also observed inverted metamorphism in the Higher and Lesser Himalayan rocks, where they mapped a distinct mineral stretching lineation (Fig. 6.3) in the Lesser Himalayan augen gneisses. The lineation is characteristic of plastic deformation associated with the Main Central Thrust movement for more than 100 km. Pêcher (1977) investigated the C/S

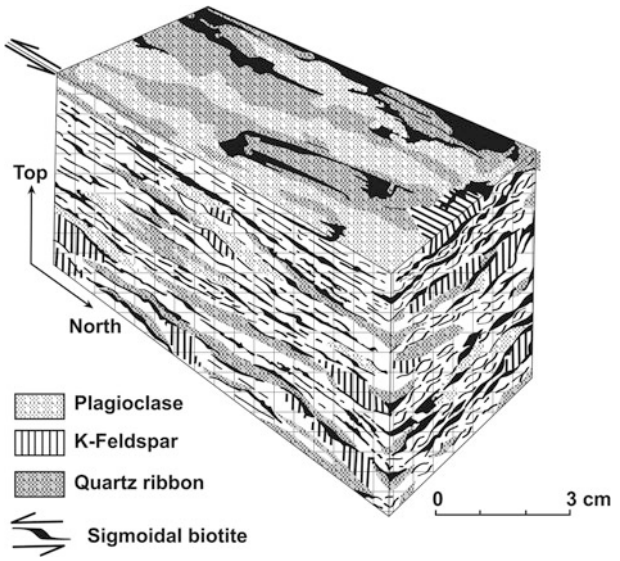

Fig. 6.3 Lesser Himalayan augen gneisses with stretched grains. *Source* Modified from Brunel and Andrieux (1977)

penetrative fabric (Fig. 6.4) of the shear zone linked with the Main Central Thrust. Bouchez and Pêcher (1981) further elaborated upon this ubiquitous fabric (Fig. 6.5). Pêcher (1991) investigated the deformation in the Main Central Thrust zone and prepared a map of stretching lineations from west Nepal (Fig. 6.6), and noticed a top-to-south sense of shearing in the Lesser and Higher Himalaya as well as significant dextral shearing in the Higher Himalayan sequences. Le Fort and Raï (1999) obtained an age of 1.74 Ga (Rb–Sr isotopic dates) for the Ulleri augen gneiss of west Nepal, whereas Kohn et al. (2010) obtained an age of about 1.88 Ga (U–Pb isotopic dates) on the zircons extracted from the augen gneisses of the Langtang area.

6.4.2 Igneous Rocks

Proterozoic granites, orthogneisses, and metabasics are the main rocks of igneous origin in the Lesser Himalaya. There also occur some isolated slices of Cretaceous volcanic rocks

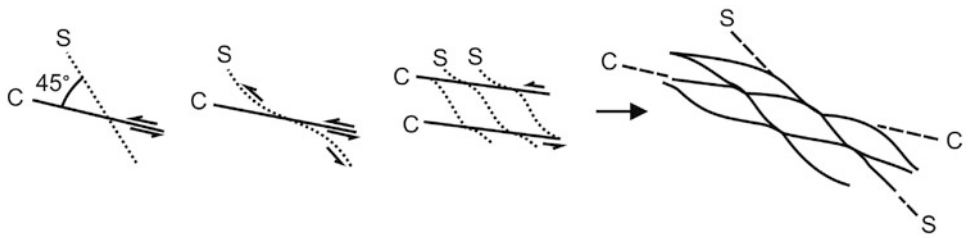

Fig. 6.4 Formation of C/S "almonds," in the shear zone of main central Thrust, in the section perpendicular to cleavage. *Source* Modified from Pêcher (1977)

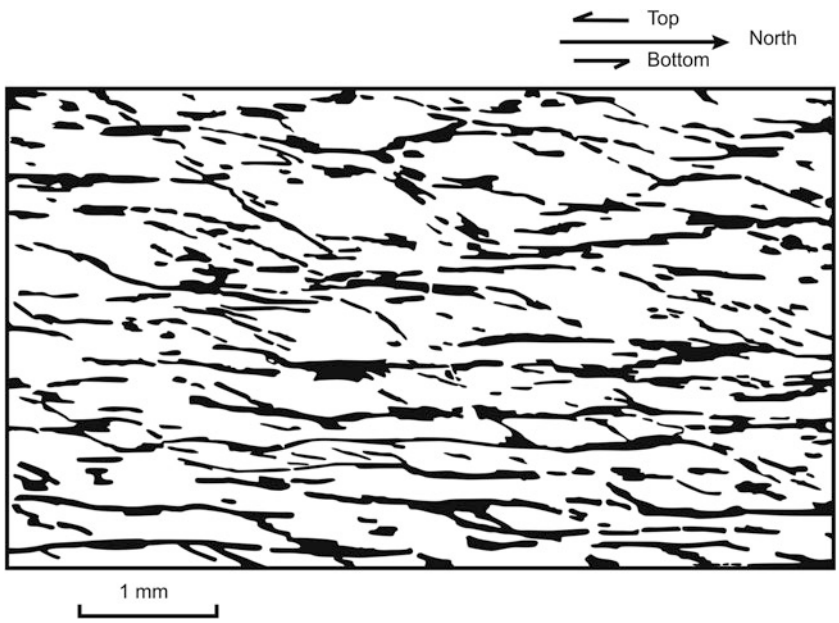

Fig. 6.5 Sketch of C/S "almonds" in the shear zone of the main central Thrust, depicting a top-to-south sense of shear. *Source* Modified from Bouchez and Pêcher (1981)

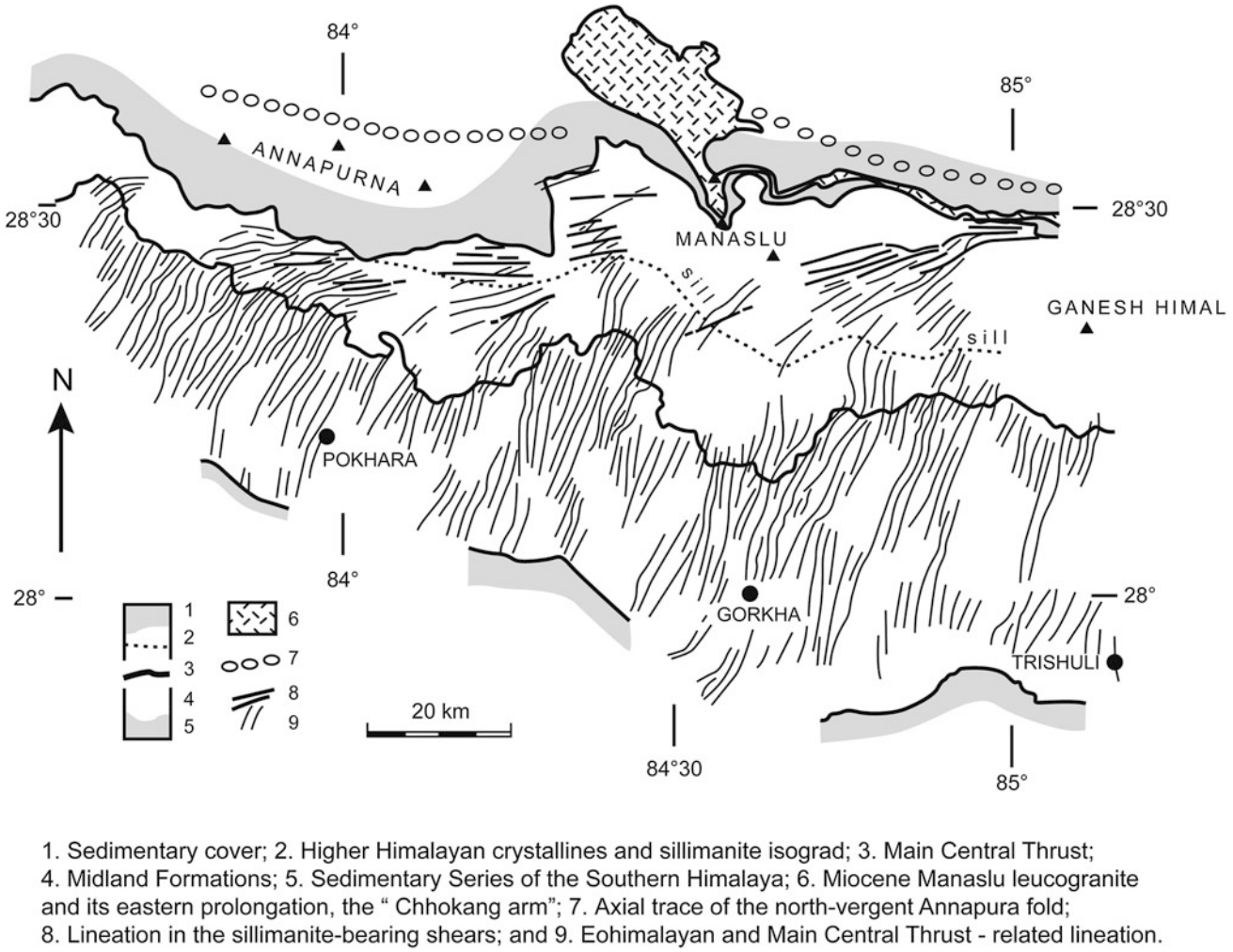

Fig. 6.6 Dextral shearing in the Higher Himalaya of west Nepal. *Source* Modified from Pêcher (1991). © John Wiley and Sons Ltd. Used by permission

in west Nepal. In the Larji–Rampur window of the Northwest Lesser Himalaya of India, there are some phyllites, quartzites, stromatolitic dolomites, amphibolites, and acid metavolcanics with blue quartz. The metarhyolites and granite–gneisses of 1.84 ± 0.7 Ga age occur in the core of an antiform (Frank et al. 1977). Bhat and Le Fort (1992) obtained a Paleoproterozoic (2.51 ± 0.09 Ga) Sm–Nd whole-rock isochron age for the Rampur metavolcanics. Miller et al. (2000) applied a single zircon evaporation method to date these rocks, and obtained an age of 1.80 Ga. Similarly, Upreti et al. (2003) obtained an age older than 1.6 Ga for the granites of east Nepal (Chap. 12).

6.4.3 Carbonate Sequences

Heim and Gansser (1939) mapped a huge carbonate sequence west of the Mahakali River. A continuation of this sequence is found between Darchula and Patan, and also to the east in Bajhang and Dhorpatan. The carbonates represent the Bajhang nappes of Hagen and the Krol or Shali Formation of Fuchs and Frank (1970), or the Lakharpata Formation of Shrestha et al. (1987). These rocks are similar to the Dhading Dolomite of Stöcklin and Bhattarai (1977) in central Nepal. The Proterozoic carbonates as well as redbeds and black slates occur at several stratigraphic levels. There is a complex structural relationship among various carbonate sequences cropping out in west Nepal (Chaps. 8 and 9).

6.5 Correlation of Unfossiliferous Sequences

Auden (1935) reasoned that the sedimentary rocks of the Udaipur region could be homotaxial with the Krol belt, whereas the coal-bearing beds of the Barahakshetra area

could be correlated with the Gondwanas of Darjeeling. Auden and Saha (1952) correlated the carbonates of central Nepal with the Krol and Deoban formations of northwest India and also described the granites of the Kulekhani area.

Hagen (1969, p. 158) telecorrelated some Lesser Himalayan rocks and their major structures with those of the Alps. He also inferred that the sedimentary and low-grade metamorphic rocks, comprising his Piuthan Zone and the area around Tansen, could be an extension of the Krol belt in Nepal. His observations attracted the attention of Fuchs and Frank, who worked out in detail the geology of the region between the rivers Kali Gandaki and Thulo Bheri in west Nepal. They borrowed a number of formation names from Northwest Himalaya, and demonstrated the eastward extension of the Krol belt in Nepal (Fuchs and Frank 1970; Frank and Fuchs 1970). It was an attempt to simplify the various names given to the seemingly identical lithostratigraphic unit. In this process, they were successful in identifying the main thrust sheets as well as other major faults and folds. Further investigations in this area (Chaps. 8 and 9) have brought to attention an intensely folded and imbricate-faulted zone, consisting of the rocks akin to the Krol belt and other older sequences. Detailed investigations in Tansen, the Kali Gandaki region of Ramdighat, Syangja, and the Dang–Sallyan area have demonstrated profound lithofacies changes across the belt.

6.6 Gondwanas and Coal

After S. Bowman's investigation of the coal-bearing Gondwanas of Barahakshetra in east Nepal, Auden (1935) portrayed them on a geological sketch. Later, Gansser (1964) extended them from east to west Nepal on his geological map. Bashyal (1980a, b) provided further information regarding their extension and the chemical composition of volcanics associated with them. Fuchs and Frank (1970) observed some carbonaceous beds in the Sallyan area of west Nepal and attributed them to the Lower Gondwanas. On the other hand, detailed study by Sakai (1983) proved the existence of the Upper Gondwanas in the Tansen area of west Nepal (Chap. 9). Recently, some coal is being extracted from the pre-Eocene strata in Dang and Palpa.

6.7 Inverted Metamorphism

Inverted metamorphism has significantly altered the Lesser Himalayan sedimentary sequence. Generally, there is a steady increase in metamorphic grade from south to north (Fig. 6.7). Sometimes the sediments are metamorphosed so strongly that their original appearance is almost obliterated, and the rocks look totally different from their counterparts exposed in the neighborhood. The Barikot window to the north of Jajarkot, the inner zones of Marsyangdi and Trishuli, and the tectonic windows of east Nepal are some areas of such alteration.

Most of the time, the metamorphic isograds are parallel to the trends of Lesser and Higher Himalayan sequences, however, in a few instances, the inverted metamorphic isograds crosscut the sequences obliquely.

Chakrabarti et al. (2004) investigated the marbles, quartzites, and graphitic schists of the Ganesh Himal polymetallic (zinc and lead) mineral deposit and reported strongly folded rocks of the Lesser Himalaya. The rocks contain garnet, staurolite, and kyanite. The lead isotope data gave an age of 875–785 Ma for these ore deposits.

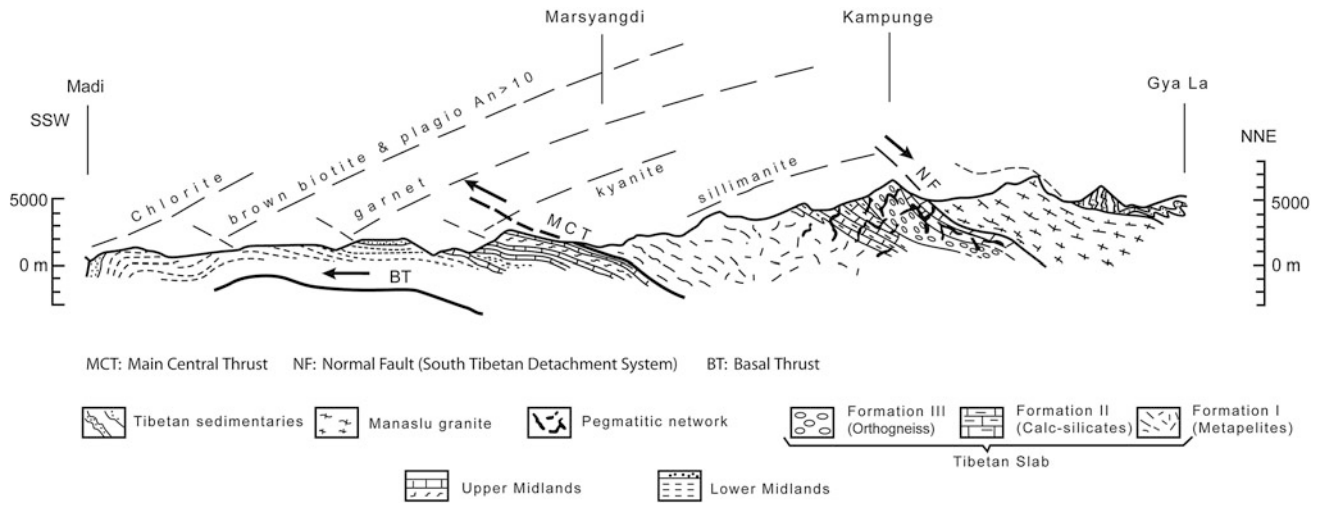

Fig. 6.7 Inverted metamorphism in the Lesser and higher Himalaya of central Nepal, across the Manaslu massif. *Source* Modified from Pêcher (1989). © John Wiley and Sons Ltd. Used by permission

6.8 Structure of Inner Zone

Lombard (1952) inferred a schuppen zone below his Tibetan slab. In west Nepal, Fuchs and Frank (1970) identified three Chail nappes and a Rukum nappe, which originated from below the Main Central Thrust.

The schuppen zone is well reflected in the work of Hashimoto et al. (1973), where they drew a number of faults (supposed to be the Main Central Thrust equivalents) between various schists, quartzites, and gneisses (e.g., Akiba et al. 1973, p. 21). Arita et al. (1973, p. 116, 1982), and Arita (1983) have proposed more than one Main Central Thrust.

On the other hand, Bodenhausen and Egeler (1971) did not find any thrust sheet, such as the Chail nappe of Fuchs and Frank (1970) between Beni and Dana in west Nepal. Pêcher and Le Fort (1986, p. 296) also argue that the Lesser Himalayan Ulleri-type augen gneisses in west Nepal do not represent tectonic slices. In some instances, the metamorphic isograds crosscut the gneisses. The gneisses display a gradational contact with the contiguous rock, both of them contain rounded blue quartz, and both are associated with volcanics (amphibolites). The intense deformation in the Ulleri gneisses is striking, whereas the metasedimentary formations adjoining the gneisses lack suitable markers to elucidate the deformation. But the orientation of the quartz C-axis does not imply any significant tectonic break across the metasedimentary rocks and the gneisses (Boucher and Pêcher 1981).

6.9 Structure of Intermediate Zone

Superposed folding characterizes the deformation in this zone. Apart from the Higher Himalayan thrust sheet, some Lesser Himalayan thrusts had also covered most of the area in the past (Fuchs 1981). Presumably, the superposed folds are synchronous with the movement of these thrusts. On the other hand, the backthrusts moving over Early Miocene rocks demonstrate subsequent hinterland-directed movement of the imbricate faults.

6.10 Structure of Outer Zone

Middlemiss (1890, p. 124) observed that, like the Alps, the Himalayan front was characterized by imbricate structures. But the thrust arrangement in these two ranges was very different. He explained his observations in the following words:

> … we ascend from the plains over blocks of strata all dipping away from the present region of deposition, and, though each step or disturbance zone is older as a whole, the individual members are arranged in the opposite manner to what they are in England.

His detailed investigations also revealed continuous deposition of strata along one line, and their gradual and simultaneous crushing up along another adjacent line. For example, he observed to the south of the Sanguri Sot, north and east sides of the Kohat dun, and north of the Sara River, the uppermost Siwalik conglomerates occurring in a conspicuous unconformity on the upturned edges of the Lower Siwaliks. However, in other parts of the country, such as in the Ramganga–Pelani section, he recorded a normal ascending series of strata without break from the base of the Nahans up to the top of the Siwalik conglomerate. Hence it was the evidence of progressive and successional folding and faulting taking place throughout the Sub-Himalayan belt (Middlemiss 1890, p. 124). Thus he had worked out the fundamental lithostratigraphic, structural, and tectonic details of the Sub-Himalaya and adjoining Himalayan frontal ranges more than a century ago. The investigations in Nepal reconfirmed his observations and interpretations (Chap. 28).

Remy (1975a, b) mapped a large portion of west Nepal and drew attention to imbricate faults in the frontal belt. The imbricate faults in the Lesser Himalaya and Siwaliks are generally north-dipping and rather parallel to each other. But, some of them also dip to the south, forming hinterland-vergent thrusts, and others merge with each other giving rise to a number of branch lines. Such imbricate faults predominate in the inner Lesser Himalayan belt lying south of Pokhara (Dhital et al. 2002), in the outer Lesser Himalaya of Dang, Sallyan, and Piuthan (Dhital and Kizaki 1987), as well as in the Siwaliks of west Nepal (Dhital et al. 1995). They represent a complex duplex system in the Lesser Himalaya and an imbricate stack in the Siwaliks. DeCelles et al. (1998) applied the duplex concept throughout the west Nepal Lesser Himalaya. The Lesser Himalayan imbricate faults were eventually exposed after erosion of their roof thrust. Such fault zones are sometimes rich in carbonaceous matter (Box 6.3).

The Chail nappes of Fuchs and Sinha (1978) and Fuchs (1981) override the Siwaliks near Amritpur in the Kumaun Lesser Himalaya. These authors have extended the nappes towards Nepal, essentially as a single thrust sheet below the Almora crystallines of the Higher Himalaya. Robinson et al. (2006) have assigned the Ramgarh thrust to the Chail nappes of Fuchs (1981). Based on balanced cross-sections, they reckoned the shortening in the Himalaya of far-west Nepal. Ironically, Bhargava (1972, 1976) as well as Srikantia and Sharma (1976) were unable to trace the Chail nappe from its type locality near Simla. Similarly, Raina and Dungrakoti (1975) did not find any thrust fault of earlier workers around Ramgarh.

Box 6.3: Carbonaceous Matter in Fault Zones

Medlicott (1864, p. 29) gives a detailed account of the carbonaceous matter occurring in fault zones. Such fault zones can be located even far away in the interior of the Lesser Himalaya. The carbonaceous matter in such zones is in greater proportion than anywhere in the country rock, and sometimes such fault zones are far removed from black slates from which the carbonaceous material could have been derived. The carbonaceous matter has a brilliant jet-black color, is flaky, breaks up into scales, and is highly lustrous. It contains about 25 % of fixed carbon, volatiles about 10 % (mainly sulfurous fumes and a small proportion of hydrocarbons), and 65 % of ash.

6.11 Main Boundary Thrust

The Main Boundary Thrust (Box 6.4) has been conventionally considered to be an uninterrupted tectonic line that extends throughout the Himalayan arc and separates the Lesser Himalaya from the Sub-Himalaya, and in several instances it also acts as a "relief thrust" (Box 6.5). The thrust experienced significant movements, and presently it is overriding the Siwaliks. However, there have been many instances where the fault is no longer considered to be a single continuous boundary.

In the Northwest Himalaya as well as in Nepal, the Siwalik–Lesser Himalayan boundary is not a single fault; there are, instead, a number of overlapping thrusts that have moved over the Siwaliks, and their frontal part has been commonly designated as the Main Boundary Thrust (Box 6.6). There are also several active faults running intermittently through this frontal belt. Although the active faults mostly coincide with the emergent tips of the earlier thrusts, in some instances the thrusts and active faults deviate from each other (Chap. 28). In the Northwest Himalaya, the Subathu, Dagshai, and Kasauli formations are frequently thrust over the Siwaliks. However, in the frontal belt of Nepal, mainly Proterozoic rocks are juxtaposed with the Siwaliks. On the other hand, the Siwaliks or their equivalents disconformably overlie the older sequences extending below the Terai alluvium (Friedenreich et al. 1994).

To accommodate the immense shortening across the Himalaya, Hagen (1969) drew 22 nappes. Fuchs and Frank (1970) denied the existence of such a large number of nappes; they mapped a few Chail nappes in the Lesser Himalaya and a crystalline nappe in the Higher Himalaya. In the outer zone, many researchers have delineated one or two "boundary" thrusts supposedly encompassing the entire Himalayan Range, whereas several other Lesser Himalayan and Siwalik thrusts have received a somewhat secondary status. Most probably, all these imbricate frontal faults originate from the Main Himalayan Thrust (Nelson et al. 1996; Brown et al. 1996), or a similar very low-angle detachment fault at depth, and their collective contribution to shortening is significantly higher than that of any particular thrust.

Box 6.4: Locating Boundary Thrusts

It all began with geological investigations in the Northwest Himalaya between the rivers Ganga and Ravi in 1857–1858 by Medlicott (1861, 1864), from where he described in detail the striking vertical contact between the Sub-Himalayan and Lesser Himalayan rocks. He observed there the following four rock sequences: the Nahun (Lower Siwalik), Siwalik (Middle and Upper), Nummulitic, and older Lesser Himalayan. He postulated a boundary fault between the Nahuns and Nummulitics (Medlicott 1864, p. 112) and opined that the fault was almost the depositional limit of the Siwaliks, as these rocks are absent to the north, beyond that boundary (p. 102). In the Sub-Himalayan zone between the Ganga and Nepal frontiers, Middlemiss (1890, p. 118) identified the following five longitudinal tectonic boundaries arranged respectively from south to north: (a) Upper Siwalik–Middle Siwalik, (b) Middle Siwalik–Nahan (Lower Siwalik), (c) Nahan–Nummulitic, (d) Nummulitic—Lesser Himalayan massive limestone, and (e) limestone–other metamorphic rocks. Middlemiss (1890) reiterated that the Main Boundary Fault corresponded to the northern limit of deposition in the Siwalik basin and also envisioned that these other faults too were approximate boundary faults, indicating local limits of deposition of successive rock groups.

Heim (1938, p. 413) proposed to call the Main Boundary Fault a thrust plane, which brings the Himalayan formations over the Siwalik Tertiaries. His main argument was that, like in the Alps, the Main Boundary Thrust is a single large thrust sheet that continues throughout the Himalayan belt. The "relief thrust" (Box 6.5) in Bhutan is the evidence of such a large and continuous displacement up to the present.

Box 6.5: Relief Thrusting

Heim (1938, p. 418) and Gansser (1964, p. 82; 1983) described "relief thrusting" from Bhutan and Nainital, while Bhargava (1976, p. 218) reported a similar case from the Krol Belt. This phenomenon is well known in the Subalpine molasse belt of the Alps, where the thrust sheet moves on the weathered surface of foreland. However, the situation in Nepal differs significantly from the observations made by these authors, as there are Lower as well as Middle Siwalik rocks bordering the Lesser Himalayan sequence on the north. Sporadically, some Upper Siwalik rocks are also encountered.

Box 6.6: Legacy of Boundary Faults

Wadia (1926) writes that the Main Boundary Fault (MBF) is no more the limit of deposition between the Murrees and successive Siwalik zones to the west of the Ravi River. The Tertiary rocks attain a thickness of about 6,000 m in the Jammu hills and overlie the Murrees. Similarly, at their type area, the Eocene Subathu sediments rest unconformably over the Simla Slates and fall within the Lesser Himalayan zone, above the MBF. Here, the Lesser Himalayan Subathu has been juxtaposed against the Sub-Himalayan Subathu along the Main Boundary Thrust (Raiverman 2002). Later work also indicated that the MBF is not a simple fault making the cliff face of the northern limit of the Siwalik basin.

While discussing the geology and structure of the Garhwal area, Auden (1937, p. 416) made the following remarks,

> The Main Boundary Fault, in the sense originally used by Medlicott, separates the Siwaliks from the older Tertiaries which have been thrust upon them. East of Longitude 78°, the Dagshai rocks (Murrees) are very seldom seen, and the chief fault is the Krol Thrust which has brought pre-Tertiaries forward so as to rest directly on Siwaliks. This Krol Thrust has been called the Main Boundary Fault both by Middlemiss and myself, but, although it does in fact form the northern boundary of the Siwaliks over some of the area between Dehra and Naini Tal, it is not the same fault as that to which Medlicott originally assigned the term.

At the 25th Session of the Indian Science Congress (1938), the problem was discussed by Evans, Wadia, and Auden (*in* Wadia 1938), and it was decided that the "Main Boundary Fault" is a misnomer since the faults are thrust planes inclined northwards and, therefore, the actual boundary of the Siwalik basin should have been further north of the present trace of the fault on the ground and may be concealed below the overthrust unit. Thus the emphasis was shifted from the paleogeographic bias to one of structure (Chaterji and Swami Nath 1976).

Heim and Gansser (1939) presented their view on the Main Boundary Thrust (MBT) in the following words:

> Similarly to the discoveries in the Alps at the beginning of this century, the younger generation of the geologists of India have recognized that the so-called "main boundary fault" … at the interior contact of the Siwaliks is a thrust plane, the older Himalayan formations overriding the Tertiaries of the border zone. The question to our mind was to find out the true nature of this thrust plane, no special studies of the kind having apparently been made. Wherever an abnormal contact was found, the older authors have drawn a fault line on maps and sections. We cannot, therefore, refer to them as a reliable source, and new investigations are necessary.

For Hagen, the Main Boundary Thrust marked the common south limit of various nappes approaching the Siwalik belt. The Main Boundary Thrust represented the foot of his nappes, where he also noted some recent tectonic movements along the thrust.

Concerning the faults observed in the Himalaya, Le Fort (1975, p. 23) wrote,

> …thrusts are not always made of one single plane but may consist of a series of more or less parallel accidents that sometimes relieve one another. This is particularly evident in the case of the MBT… MCT (Main Central Thrust) is made of several thrusts with an en-échelon pattern at a Himalayan scale.

Valdiya (1978, pp. 2–3) stated that the Lesser Himalaya is demarcated against the Siwalik subprovince by what is commonly described as the "Main Boundary Fault." But in actuality the MBF, originally defined as the tectonic feature separating the Siwalik from the pre-Siwalik Tertiaries, is exposed only in the extreme western sector roughly between the Yamuna and Tons valleys. East of the Yamuna, the higher Krol Thrust has overlapped the Eocene Subathu and has completely concealed the MBF; the only exception is seen near Durgapipal in the east where a narrow belt of Subathu is exposed between the Siwalik and the overthrust Krol rocks. The Krol Thrust, which has brought various lithological units of the Krol nappe over the Siwaliks, constitutes the real southern boundary of the Lesser Himalaya.

Srikantia and Sharma (1976, p. 97) remarked that there is no perceptible break between the Subathus and the overlying Dagshai beds. They noted that the

Siwaliks are seen to overlie the Dharamsalas (i.e., the Dagshai and Kasauli) even north of the fault and, within the southern Siwalik belt, there are thrust-bound inliers of the Dharamsalas. Therefore, there is no particular significance to the term Main Boundary Fault.

Chaterji and Swami Nath (1977, p. 441) conclude,

> The 'Main Boundary Fault' or 'Thrust' is not a single plane of dislocation between Upper and Lower Tertiary or pre-Tertiary formations. Different thrust sheets successively and tectonically overlap the one preceding and rest over the Siwalik system. The term 'Main Boundary Fault' or 'Thrust' does not convey the same connotation as was originally intended and it should be abandoned.

References

Akiba C, Amma S, Ohta Y (1973) Arun River region. In: Hashimoto S, Ohta Y, Akiba C (eds) Geology of the Nepal Himalayas. Himalayan Committee of Hokkaido University, Japan, pp 13–33

Amatya KM, Jnawali BM (1994) Geological map of Nepal, Scale: 1:1,000,000. Department of Mines and Geology, International Centre for Integrated Mountain Development, Carl Duisberg Gesellschaft e. V., and United Nations Environment Programme, Berlin

Arita K (1983) Origin of the inverted metamorphism of the lower Himalayas, central Nepal. Tectonophysics 95:43–60

Arita K, Hayashi D, Yoshida M (1982) Geology and structure of the Pokhara–Piuthan area, central Nepal. J Geol Soc Nepal 2(Special Issue):5–29

Arita K, Ohta Y, Akiba C, Maruo Y (1973) Kathmandu Region. In: Hashimoto S, Ohta Y, Akiba C (eds) Geology of the Nepal Himalayas. Himalayan Committee of Hokkaido University, Japan, pp 99–145

Auden JB (1935) Traverses in the Himalaya. Rec Geol Surv India LXIX(part 2):123–167 (with 6 plates including a geological sketch map)

Auden JB (1937) The geology of the Himalaya in Garhwal. Rec Geol Surv India 71(part 4):407–433 (with 3 plates including a long cross-section on the scale of 1 inch = 2 miles)

Auden JB, Saha AK (1952) Geological notes on central Nepal. Rec Geol Surv India 82(part 2):354–357

Bashyal RP (1980a) Gondwana type of formation with phosphatic rocks in S.E. Nepal. J Geol Soc India, Bangalore 21:489–491

Bashyal RP (1980b) Potassic volcanics from the Permo-Carboniferous Nepal Himalayas. Mem Geol Soc India, Bangalore 3:472–474

Bhargava ON (1972) A reinterpretation of the Krol belt. Himalayan Geol 2:47–81

Bhargava ON (1976) Geology of the Krol belt and associated formations: a reappraisal. Mem Geol Surv India 106(part I):167–234 (with a map)

Bhat MI, Le Fort P (1992) Sm-Nd age and petrogenesis of Rampur metavolcanic rocks, NW Himalaya: Late Archean relics in the Himalayan belt. Precambr Res 56:191–210

Bodenhausen JWA, Egeler CG (1971) On the geology of the upper Kali Gandaki valley, Nepalese Himalayas I and II. In: Proceedings of the Koninklijke Nederlandse Akademie van Wetensohappen—Amsterdam. Series B 74(5):526–546

Bordet P (1961) Recherches Géologiques dans L'Himalaya du Népal, Région du Makalu, Expéditions Françaises a l'Himalaya 1954–1955, Edition du Centre National de la Recherche Scientifique (C. N. R. S.), 275 pp (with two geological maps in colors)

Bouchez J-L, Pêcher A (1981) The Himalayan Main Central Thrust pile and its quartz-rich tectonites in central Nepal. Tectonophysics 78:23–50

Brown LD, Zhao W, Nelson KD, Hauck M, Alsdorf D, Ross A, Cogan M, Clark M, Liu X, Che J (1996) Bright spots, structure, and magmatism in Southern Tibet from INDEPTH seismic reflection profiling. Science 274:1688–1690

Brunel M, Andrieux J (1977) Déformations superposées et mécanismes associes au chevauchement central Himalayan «M. C. T.»: Népal Oriental. Colloques internationaux du C. N. R. S. No. 268—Écologie et Géologie de l'Himalaya, Paris, pp 69–83

Burrard SG, Hayden HH (1908) A sketch of the geography and geology of the Himalaya mountains and Tibet. Calcutta, 308 pp (with a geological map of the Himalaya in colors, scale 1 inch = 40 miles, and many other maps in colors from various parts of the Himalaya)

Chakrabarti CK, Upreti BN, Ghosh AK (2004) Geochemistry of the Ganesh Himal zinc–lead deposits, central Nepal Himalaya. J Nepal Geol Soc 30:39–54

Chaterji GC, Swami Nath J (1976) Problems of stratigraphy and structure of parts of the Simla Himalaya—An assessment. Mem Geol Surv India 106(part I):1–16

Chaterji GC, Swami Nath J (1977) The stratigraphy and structure of parts of the Simla Himalaya—a synthesis. Mem Geol Surv India 106(part II):408–488

Colchen M, Le Fort P, Pêcher A (1986) Annapurna–Manaslu–Ganesh Himal. Centre National de la Recherches Scientifique, Special Publication, Paris, 136 pp (with one geological map, 1:200,000)

DeCelles PG, Gehrels GE, Quade J, Ojha TP (1998) Eocene-Early Miocene foreland basin development and the history of Himalayan thrusting, western and central Nepal. Tectonics 17:741–765

Dhital MR, Kizaki K (1987) Structural aspect of the Northern Dang, Lesser Himalaya. Bull Coll Sci Univ Ryukyus Okinawa 45:159–182

Dhital MR, Gajurel AP, Paudel LP, Kizaki K (1995) Geology and structure of the Siwaliks and Lesser Himalaya in Surai Khola—Bardanda Area, Mid Western Nepal. Bull Dept Geol Tribhuvan Univ 4(Special Issue):1–70

Dhital MR, Thapa PB, Ando H (2002) Geology of the inner Lesser Himalaya between Kusma and Syangja in western Nepal. Bull Dept Geol Tribhuvan Univ 9(Special Issue):1–60

ESCAP (Economic and Social Commission for Asia and the Pacific) (1993) Geology and mineral resources of Nepal, atlas of mineral resources of the ESCAP region, vol 9. United Nations, New York, 107 pp. (with a geological map in colors)

Frank W, Fuchs GR (1970) Geological investigations in west Nepal and their significance for the geology of the Himalayas. Geol Rundsch 59:552–580

Frank W, Thöni M, Purtscheller F (1977) Geology and petrography of Kulu–Rampur area. Colloques Internationaux du C. N. R. S. No 268—Écologie et Géologie de l'Himalaya, Paris, pp 147–172

Friedenreich OR, Slind OL, Pradhan UMS, Shrestha RB (1994) Petroleum geology of Nepal. Can J Explor Geophys 30(2):103–114

Fuchs G (1981) Geologic–tectonical map of the Himalaya, scale: 1:2,000,000. Geologische Bundesanstalt, Wien

Fuchs G, Frank W (1970) The geology of West Nepal between the rivers Kali Gandaki and Thulo Bheri. Jahrbuch der Geologischen Bundesanstalt 18:1–103 (with a geological map and cross-sections)

Fuchs G, Sinha AK (1978) The tectonics of the Garhwal–Kumaun Lesser Himalaya. Jahrbuch der Geologischen Bundesanstalt, Wien, Band 121, Heft 2, pp 219–241 (with 1 plate containing geological map in colors, Scale: 1:500,000)

Gansser A (1964) Geology of the Himalayas. Interscience, New York, 289 pp

Gansser A (1983) Geology of the Bhutan Himalaya. Denkschriften der Schweizerischen Naturforschenden Gesellschaft 96:181 (with 4 plates: a geological map in colors; scale: 1:2,000,000; cross-sections in colors and black, and a panorama of mountains)

Hagen T (1950a) Moderne Kartierungsmethoden. Photogeologie. Separatabdruck aus der "Neuen Zürcher Zeitung" Nr. 1038 (29), vol 18. Mai 1950, pp 1–7

Hagen T (1950b) Wissenschaftliche luftbild-interpretation. Ein methodischer Versuch. Mitteilung aus dem Geologischen Institut an der Eidgenössischen Technischen Hochschule in Zürich. Sonderabdruck aus "Geographica Helvetica", Nr. 4, pp 209–276 (with 19 red-and-blue color-separated 3-D images and a pair of red-and-blue spectacles)

Hagen T (1951) Preliminary note on the geological structure of central Nepal. Verhandlungen der Schweizerischen Naturforschenden Gesellschaft, Luzern, pp 133–134

Hagen T (1969) Report on the geological survey of Nepal. Volume 1: Preliminary Reconnaissance. Denkschiiften der Schweizerischen Naturforschenden Gesellschaft, Band LXXXVI/1, 185 pp (with a geological map)

Hashimoto S (1959) Some notes on the geology and petrography of the southern approach to Mt. Manaslu in the Nepal Himalaya. J Fac Sci X(1):95–110 (Hokkaido University, Sapporo, Japan, Series IV, Geology and Mineralogy)

Hashimoto S, Ohta Y, Akiba C (1973) Geology of the Nepal Himalayas. Saikon Publishing Co. Ltd., Tokyo, 292 pp (with 6 plates including a geological map of Nepal (Plates 1 and 2) in colors, scale: 1:500,000)

Heim A (1938) The Himalayan border compared with the Alps. Rec Geol Surv India LXXII(part 4):413–421

Heim A, Gansser A (1939) Central Himalaya: geological observations of the swiss expedition 1936. Denkschriften der Schweizerischen Naturforschenden Gesellschaft, Band LXXIII, Abh. 1, 245 pp (with geological maps in colors, sections, and plates)

Holland TH (1908) On the occurrence of striated boulders in the Blaini Formation of Simla, with a discussion of the geological age of the beds. Rec Geol Surv India XXXVII(part 1):129–135 (with one plate)

Johnson MRW (1994) Volume balance of erosional loss and sediment deposition related to Himalayan uplifts. J Geol Soc Lond 151:217–220

Kohn MJ, Paul SK, Corrie SL (2010) The lower lesser Himalayan sequence: a Paleoproterozoic arc on the northern margin of the Indian plate. Geol Soc Am Bull 122:323–35

Le Fort P (1975) Himalayas, the collided range: present knowledge of the continental arc. Am J Sci 275-A:1–44

Le Fort P, Rai SM (1999) Pre-Tertiary felsic magmatism of the Nepal Himalaya: recycling of continental crust. J Asian Earth Sci 17:607–628

Lombard A (1952) Les grandes lignes de la géologie du Népal Oriental. Bulletin de la Société Belge de Géologie de Paléontologie et d'Hydrologie, Bruxelles, vol LXI, Fascicule 3, pp 260–264

Lombard A (1953a) Présentation d'un profil géologique du mont Everest à la plaine du Gange (Népal Oriental). Bulletin de la Société Belge de Géologie de Paléontologie et d'Hydrologie, Bruxelles, vol LXII, Fascicule 1, pp 123–129 (with a cross-section)

Lombard A (1953b) La tectonique du Népal Oriental. Un profil de l'Everest à la plaine du Gange. Bulletin de la Société Géologique de France, Série 6, vol III, pp 321–327 (with a cross-section)

Lombard A, Bordet P (1956) Une coupe géologique dans la région d'Okhaldunga (Népal Oriental). Bulletin de la Société géologique de France, Paris, vol 6, sér 6, pp 21–25

Medlicott HB (1879) Sub-Himalayas. In: Medlicott HB, Blanford WT (eds) A Manual of the Geology of India, Part II: Extra-Peninsular Area. Published by order of the Government of India, Calcutta, pp 517–571

Medlicott HB (1861) On the Sub-Himalayan rocks between the Ganges and the Jumna. J Asiatic Soc Bengal, Calcutta XXX(1):22–31

Medlicott HB (1864) On the geological structure and relations of the southern portion of the Himalayan Range between the rivers Ganges and Ravee. Mem Geol Surv India III(Art. 4):1–206 (with a geological map in colors; scale: 1 inch = 8 miles)

Medlicott HB (1875) Note of the geology of Nepal. Rec Geol Surv India VIII(Part 4):93–101 (with a geological map on 1 inch = 6 miles)

Middlemiss CS (1890) Physical geology of the Sub-Himalaya of Garhwál and Kumaun. Mem Geol Surv India XXIV(Part 2):59–200 (with 3 plates of cross-sections and a plate of geological map in colors; scale 1 inch = 4 miles)

Miller C, Klötzli U, Frank W, Thöni M, Grasemann B (2000) Proterozoic crustal evolution in the NW Himalaya (India) as recorded by circa 1.80 Ga mafic and 1.84 Ga granitic magmatism. Precambr Res 103:191–206

Nadgir BB (1976) Tectonics of Nepal Himalaya. Geol Soc India 43 (Part 1):109–118 (Miscellaneous Publication)

Nanda MM (1966) Report on geological mapping in western Nepal (parts of Lumbini, Tansen, Gulmi, West Nos. 3 and 4 districts). Geological Survey of India, Kathmandu, with a map (unpublished)

Nelson KD, Zhao Wenjin, Brown LD, Kuo J, Che Jinkai, Liu Xianwen, Kiemperer SL, Makovsky Y, Meissner R, Mechie J, Kind R, Wenzel F, Ni J, Nabelek J, Leshou Chen, Tan Handong, Wei Wenbo, Jones AG, Booker J, Unsworth M, Kidd WSF, Hauck M, Alsdorf D, Ross A, Cogan M, Changde Wu, Sandvol E, Edwards M (1996) Partially molten middle crust beneath southern Tibet: synthesis of project INDEPTH results. Science 274:1684–1688

Oldham RD (1883) Note on the geology of Jaunsar and lower Himalayas. Rec Geol Surv India XVI(part 4):193–198 (with a Geological Sketch of Jaunsar Bawar, scale: 1 inch = 5 miles, in colors)

Pêcher A (1977) Geology of the Nepal Himalaya: deformation and petrography in the Main Central Thrust zone. Colloques internationaux du C. N. R. S. No. 268, Écologie et Géologie de l'Himalaya, Paris, pp 301–318

Pêcher A (1989) The metamorphism in the central Himalaya. J Metamorph Geol 7:31–41

Pêcher A (1991) The contact between the higher Himalaya Crystallines and the Tibetan sedimentary series: Miocene large-scale dextral shearing. Tectonics 10(3):587–598

Pêcher A, Le Fort P (1977) Origin and significance of the Lesser Himalaya augen gneisses. Colloques internationaux du C. N. R. S. No. 268, Écologie et Géologie de l'Himalaya, Paris, pp 319–329

Pêcher A, Le Fort P (1986) The metamorphism in central Nepal Himalaya, its relations with the thrust tectonic. In: Le Fort P, Colchen M, Montenat C (eds) Évolution des domaines orogéniques d'Asie méridionale (de la Turquie à l'Indonésie), Livre jubilaire Pierre Bordet, Sciences de la Terre, Mémoire no. 47, Nancy, pp 285–309

Raina BN, Dungrakoti BD (1975) Geology of the area between Naini Tal and Champawat, Kumaun Himalaya, Uttar Pradesh, vol 5. Himalayan Geology, Wadia Institute of Himalayan Geology, Dehra Dun, pp 1–27

Raiverman V (2002) Foreland sedimentation in Himalayan tectonic regime: a relook at the orogenic process. Bishen Singh Mahendra Pal Singh (Publishers), Dehra Dun, India, 378 pp (with maps)

Regmi KR, Arita K (2008) Major and trace element geochemistry of augen gneisses from the higher Himalayan crystalline zone, main central Thrust zone and lesser Himalayan dome in Tamakoshi-Likhu Khola area, East Nepal. Himalayan Geol 29(2):95–108

Remy JM (1975a) Géologie du Népal ouest du Népal Himalaya. Éditions du Centre National de la Recherche Scientifique, Paris, 69 pp (with a geological map in colors; Scale: 1:506,880)

Remy JM (1975b) An introduction to the geology of the Western Nepal. Himalayan Geol 5:280–301

Robinson DM, DeCelles PG, Copeland P (2006) Tectonic evolution of the Himalayan thrust belt in Western Nepal: Implications for channel flow models. GSA Bull 118(7/8):865–885

Sakai H (1983) Geology of the Tansen group of the lesser Himalaya in Nepal. Mem Fac Sci Kyushu Univ Fukuoka Ser D 25:27–74

Sharma CK (1973) Geology of Nepal. Mani Ram Sharma, Educational Enterprises, Kathmandu, 164 pp

Sharma CK (1990) Geology of Nepal Himalaya and adjacent countries. Sangeeta Sharma, 479 pp

Sharma T, Kizaki K (1988) The granitoid rocks of the Dailekh and the Jajarkot regions in the lesser Himalaya of central West Nepal. J Nepal Geol Soc 5(1):47–67

Shrestha SB, Shrestha JN, Sharma SR (1987) Geological map of Mid-Western Nepal. Department of Mines and Geology, Kathmandu

Srikantia SV, Sharma RP (1976) Geology of the Shali belt and the adjoining areas. Mem Geol Surv India 106(part I):31–166 (with 2 maps)

Stöcklin J (1980) Geology of Nepal and its regional frame. J Geol Soc Lond 137:1–34

Stöcklin J, Bhattarai KD (1977) Geology of Kathmandu area and central Mahabharat Range, Nepal Himalaya. HMG/UNDP mineral exploration project, technical report, 86 pp (with 15 maps), unpublished

Talalov VA (1972) Geology and ores of Nepal. UNDP report, Department of Mines and Geology, Kathmandu, 4 volumes (unpublished)

Talalov VA (1977) Main features of magmatism and metallogeny of the Nepalese Himalayas. Colloques internationaux du C. N. R. S. No. 268—Écologie et Géologie de l'Himalaya, Paris, pp 409–430

Tater JM, Shrestha SB, Shrestha JN (1983) Geological map of Western central Nepal. Scale: 1:250,000. Department of Mines and Geology, Kathmandu

Upreti BN, Rai SM, Sakai H, Koirala DR, Takigami Y (2003) Early Proterozoic granite of the Taplejung window, far eastern lesser Nepal Himalaya. J Nepal Geol Soc 28:9–18

Valdiya KS (1964) The unfossiliferous formations of the lesser Himalaya and their correlation. In: International geological congress, report of the twenty-second session, India, Part XI, Proceedings of session 11: Himalayan and Alpine Orogeny, New Delhi, pp 15–36

Valdiya KS (1978) Outline of the structure of Kumaun lesser Himalaya. In: Saklani PS (ed) Tectonic Geology of the Himalaya. Today and Tomorrow's Publishers, India, (340 p), pp 1–13

Wadia DN (1926) Geology of India (for students), Revised edn. Macmillan and Co. Limited, London, 400 pp

Wadia DN (1938) The structure of the Himalayas and of the North Indian Foreland. In: Proceedings of the Indian science congress association, 25th session, part 2, pp 91–118 (Discussions in Part 4, pp 18–20)

Lesser Himalaya of Mahakali–Seti Region

7

At the base of the Crystalline Nappe, the Chail Nappes are passively dragged to the S.
—G. Fuchs and W. Frank (1970, p. 99)

Albeit the well-studied Lesser Himalayan rocks of Kumaun uninterruptedly continue in this region of Nepal, yet they remain one of the least investigated sequences, whose stratigraphy is sketchy and structures are obscure. This portion of the Lesser Himalaya constitutes the tectonic windows of predominantly Proterozoic carbonate rocks with subordinate slates, quartzites, and metabasics (Fig. 7.1). There also occur some thin and discontinuous slices of Paleocene–Early Miocene rocks.

7.1 Carbonates and Allied Rocks in Tectonic Windows of Darchula

The Deoban–Tejam belt of Kumaun is exposed in a large tectonic window, which extends to the Darchula area of west Nepal. This belt consists of extremely thick dolomites, limestones, and quartzites. Gansser (1964) described these rocks under the southerly Badolisera–Pithoragarh zone and the northerly Chamoli–Tejam zone. Fuchs and Sinha (1978) placed them under the Infra-Krol and carbonates of Shali or Deoban. On the other hand, Valdiya (1980) included these zones under his Deoban and Mandhali formations. The Badolisera–Pithoragarh zone is characterized by extensive overturning of beds and the two belts are separated by the synformally folded Baijanth–Askot crystalline klippen (Gansser 1964).

The Berinag Quartzites (Fig. 7.2) in the Badolisera–Pithoragarh zone are represented by thick-bedded and locally conglomeratic (with quartz pebbles up to 25 cm size), coarse-grained, pink varieties. In them are intercalations of sericite schist, green chlorite schist, and thick bodies of limestone and dolomitic limestone.

At the north border of the Almora–Dudatoli crystallines, Heim and Gansser (1939) observed thin bands of quartzite with dark gray slates, passing upwards into red to green-gray varieties. Farther higher, thin beds of light gray and white dolomite and limestone appear above green sericite schists. The carbonate rocks contain columnar stromatolites depicting overturned dips (Misra and Valdiya 1961; Valdiya 1962). In these carbonates, an approximately 50 m thick horizon of very coarse-crystalline magnesite regularly occurs and it is associated with some talcose layers. Farther up-section, some limestones alternate with quartzites. Various doleritic amphibolite bands are intercalated in the slates and quartzites (Fig. 7.2). These sills of Badolisera are made up of a highly altered diabase. In them, plagioclase laths are replaced by epidote and zoisite. There are also xenomorphic hornblende, sporadic clear andesine, and some tourmaline (Heim and Gansser 1939, p. 59).

In the Badolisera–Pithoragarh zone, there are two detrital sedimentary sections: the lower one, which is rich in variegated schists and sericitic quartzites, and an upper one, separated by the limestones and dolomites, which is more uniformly quartzitic and frequently contains quartz pebble horizons. The lower quartzite horizon is exposed in the Berinag region where the metamorphic grade increases upwards, as indicated by sericitization and the appearance of biotite (Gansser 1964, p. 95).

Compared to the Badolisera–Pithoragarh zone, the carbonates of the Chamoli–Tejam zone are more uniformly constituted, contain less argillaceous and quartzitic intercalations, and are considerably thicker (Gansser 1964, p. 97). Their lower part is represented by thick-bedded dolomites and crystalline limestones (Fig. 7.3). Near Kapkot, in the dolomites a conglomerate bed is intercalated, containing boulders and pebbles of quartzite, limestone, and reddish sericitic sandstone (Heim and Gansser 1939, p. 40). The conglomerate is overlain by marbles and dolomites, regularly interbedded with dark argillaceous slates or phyllites (Gansser 1964, p. 97). These dolomites of the Tejam zone frequently enclose sericitic quartzites with phyllite partings and alternations. Some basic rocks alternate with quartzites south of Karnaprayag (in the Ata Gad) and Chamoli. The

M.R. Dhital, *Geology of the Nepal Himalaya*, Regional Geology Reviews,
DOI 10.1007/978-3-319-02496-7_7

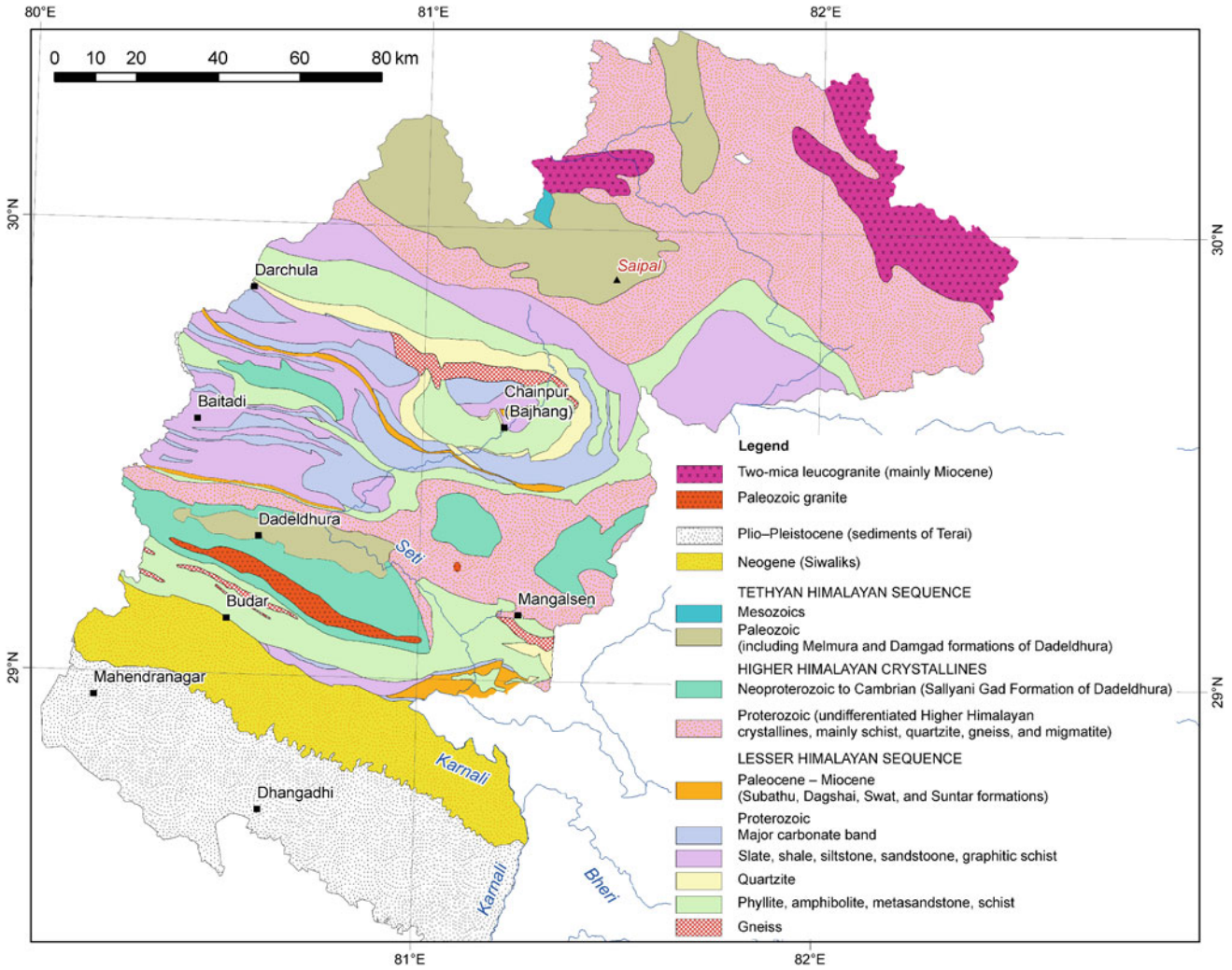

Fig. 7.1 Simplified geological map of the Mahakali–Seti region. *Source* Based on Shrestha et al. (1985), ESCAP (1993), Amatya and Jnawali (1994), other published maps, and author's observations

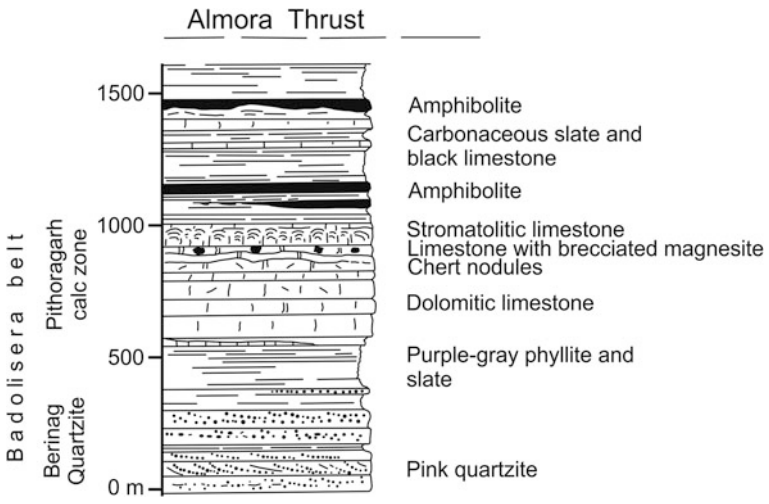

Fig. 7.2 Stratigraphy of the Badolisera–Pithoragarh zone. *Source* Modified from Gansser (1964)

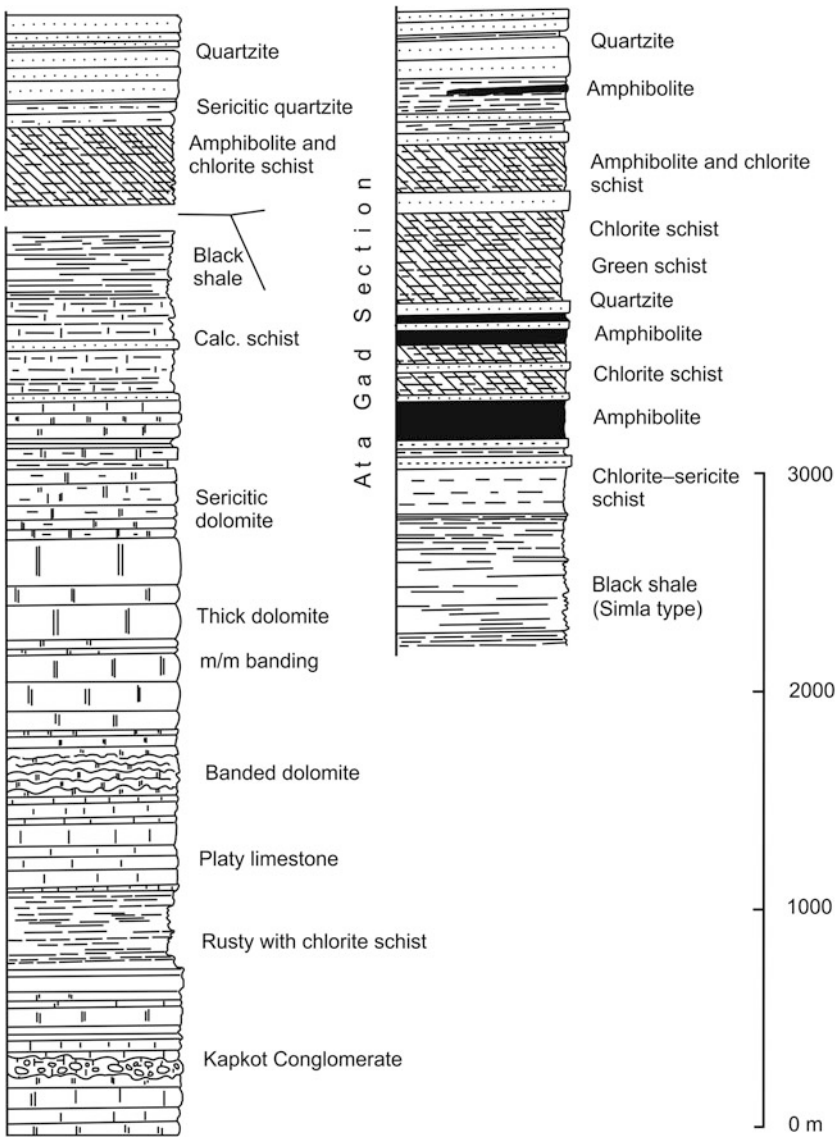

Fig. 7.3 Stratigraphy of the Chamoli–Tejam zone. *Source* Modified from Gansser (1964)

amphibolite intercalations are followed up-section by chlorite–sericite schists, and then a most conspicuous section of black clay-slates, some types akin to the Simla Slates (Gansser 1964, p. 98).

Fuchs and Sinha (1978) and Fuchs (1981) have distinguished the Chail nappe from this area, which includes the chlorite–sericite schists and amphibolites of Badolisera and Ata Gad.

Heim and Gansser (1939, pp. 91–92) describe the kyanite-bearing sericite quartzite of Girgaon. The rocks also contain cobalt-blue lazurite scales. These Lesser Himalayan rocks are exposed to the north of Tejam, below their Main Central Thrust. This is probably one of the earliest records of kyanite appearing below the Main Central Thrust. Their documentation also entails that these authors demarcate the overthrust not according to the metamorphic grade of constituent rocks, but based on stratigraphic and structural differences.

7.2 Investigations Between Darchula and Budar

In this westernmost segment of Nepal, Bashyal (1982, 1986) identified regionally folded Higher and Lesser Himalayan thrust sheets. He also recorded many other folds and north- as well as south-dipping faults in the Lesser Himalaya. He distinguished the Baitadi Metasedimentary Unit, Banku Quartzite, as well as Bajhang and Parchuni klippen in the inner zone; and the Dadeldhura Crystalline Unit, Budar Metasedimentary Unit, and the Karnali Sedimentary Unit in the outer Lesser Himalaya. He correlated these rocks with those of Kumaun.

The Baitadi Metasedimentary Unit consists of the Patan slates with some variegated quartzites and the Baitadi carbonates. The carbonates are represented by stromatolitic dolomites with some chert, limestones, and black slates or variegated calcareous slates. The Parchuni Klippe occupies an identical position to that of Askot (Gansser 1964; Fuchs and Sinha 1978) in Kumaun. It is made up of two mica schists and augen gneisses, whereas there are amphibolites just below the thrust contact on either side. The Banku Quartzite is composed of pale green to white quartzites with chlorite schist and amphibolite alternations. It is equivalent to the Berinag Quartzites of Kumaun. The Bajhang klippe lies north of Chainpur, and its structural position is similar to that of the Chhiplakot Klippe of Kumaun (Valdiya 1980). The klippe contains gneisses, schists, and quartzites.

The Dadeldhura Crystalline Unit is the continuation of the Almora nappe of Valdiya (1980) and it is equivalent to the Kathmandu nappe of Hagen (1969). It consists of garnetiferous mica schists, quartzites, gneisses, and granites. The Dadeldhura Phyllites occur in the core of the synform.

The Budar Metasedimentary Unit is made up of quartzites and slates with some amphibolites. Bashyal (1986) has also included the augen gneisses of Goganpani in this unit. These rocks are equivalent to the Bhimtal Formation of Raina and Dungrakoti (1975).

The Karnali Sedimentary Unit borders the Siwaliks, and is made up of Proterozoic dolomites and limestones with quartzites. The younger rocks are represented by sandstones, shales, and conglomerates of the Bet Khola Formation, Nummulitic limestones of the Swat Formation, and the Early Miocene Suntar Formation of red-purple shales and green sandstones (Bashyal 1986).

7.2.1 Malikarjun Thrust and Early Miocene Strata

About a few hundred meters north of Malikarjun, a south-dipping abrupt thrust separates the Early Miocene beds from the overlying Proterozoic succession (Fig. 7.4). It can be a backthrust or the north limb of a synformally folded thrust sheet. The thrust enters Nepal from Kumaun (across the Mahakali River) and runs through Baskot, north of Gwani, and Agar. Then, it crosses the Nau Gad and the Chameliya River (Fig. 7.4), and continues to the southeast. There is a sharp disconformity between the gray to light gray dolomites

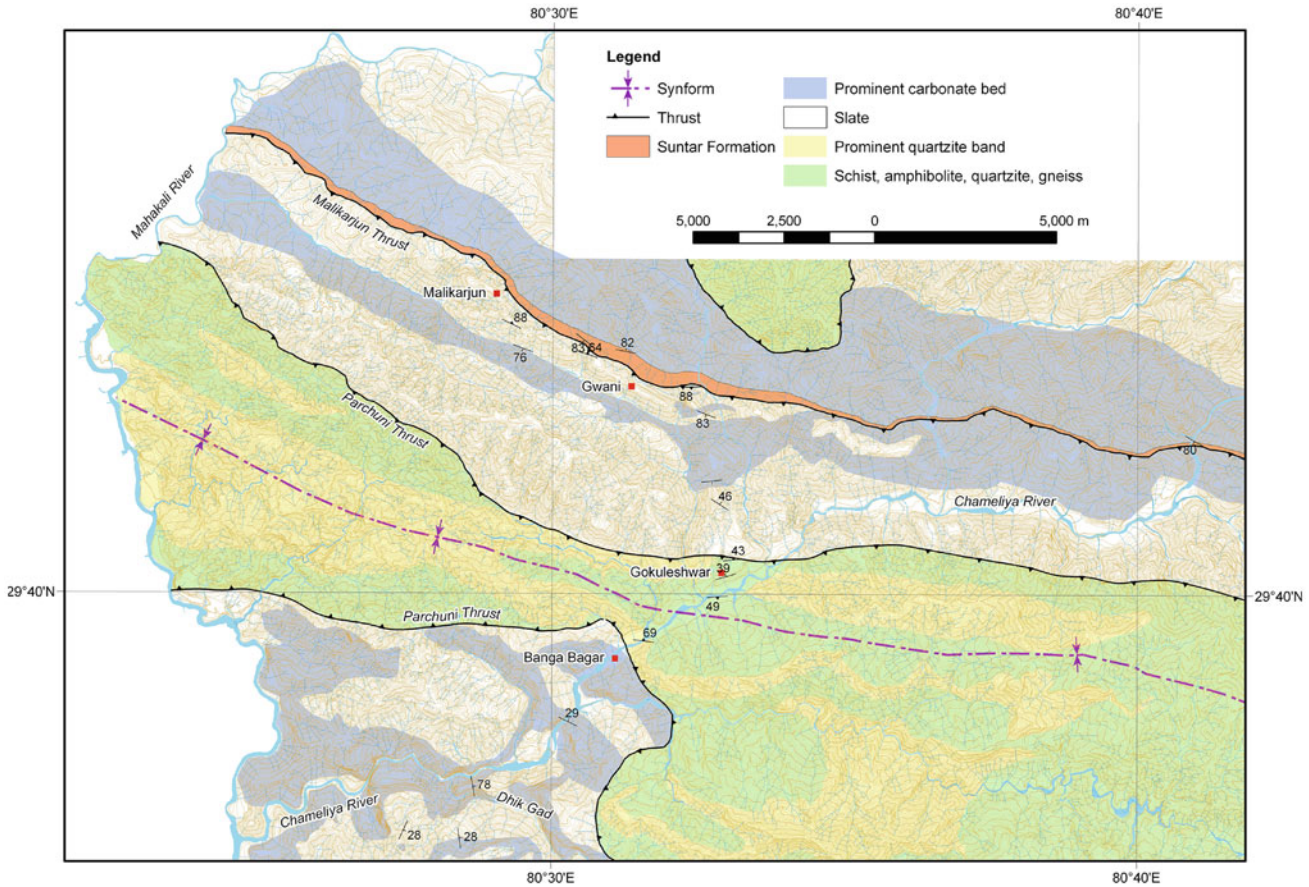

Fig. 7.4 Malikarjun Thrust and Early Miocene strata of the Suntar Formation. *Source* Author's observations

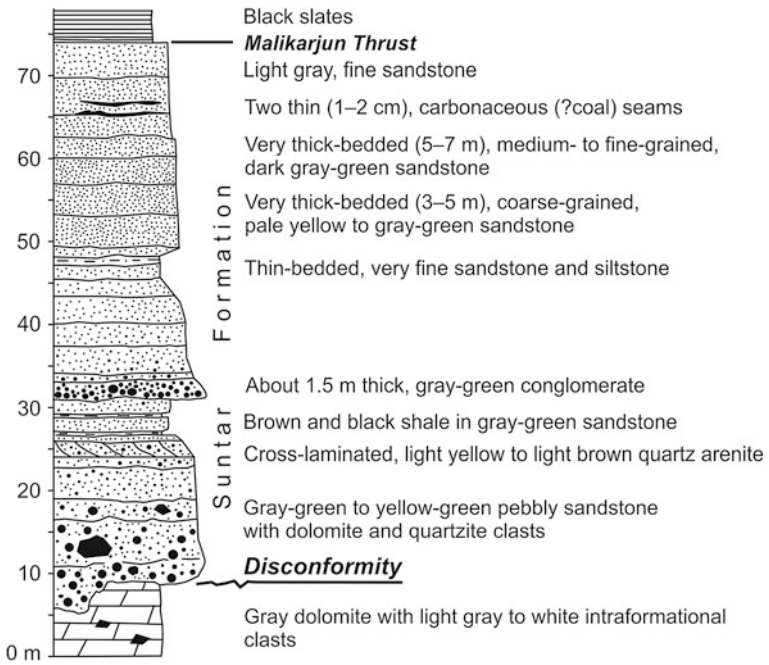

Fig. 7.5 Columnar section from the Chameliya River, showing the disconformity between the Suntar formation and the Gray Dolomite. The Malikarjun Thrust truncates the Early Miocene strata of the Suntar formation. *Source* Author's observations

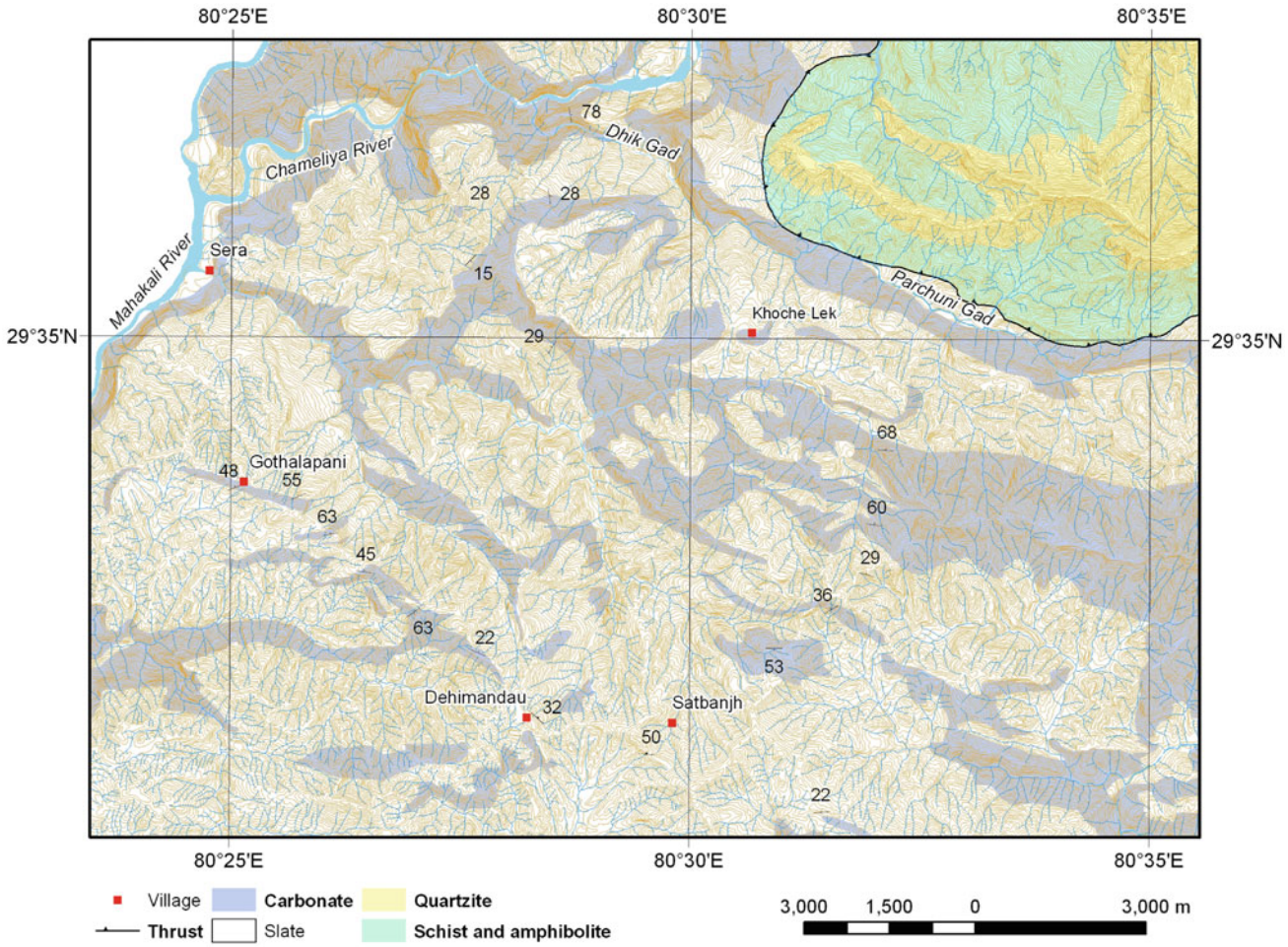

Fig. 7.6 Intensely folded Baitadi carbonates exposed between Gothalapani and Satbanjh. *Source* Author's observations

and overlying gray-green pebbly sandstones or conglomerates. The sequence is followed upwards by red-purple shales or mudstones. At the fault zone, Mesoproterozoic gray stromatolitic dolomites and black slates rest over the Early Miocene succession of red-purple shales and gray-green sandstones (Fig. 7.5). This youngest Lesser Himalayan succession varies in thickness from less than 50 m to more than 400 m. Owing to subsequent south-vergent deformation, the beds are frequently overturned and steeply dip due north. These beds belong to the Suntar Formation of Shrestha et al. (1985) and are homotaxial with the Dagshai Formation of Fuchs (1981).

Shrestha et al. (1985) traced the thrust between the Mahakali and Seti Rivers. In Nepal, the thrust continues for about 100 km and disappears under the North Dadeldhura Thrust in Bajhang (Fig. 7.1). It is difficult to work out the kinematics accurately, but it is inferred that there have been at least the following four events of tectonic deformation:

- Movement along the Main Central Thrust
- Movement of the Banku Quartzite unit
- Forward thrusting and folding or backthrusting of Lesser Himalayan strata
- Overturning of south-dipping Early Miocene beds.

7.2.2 Superposed Folding in Baitadi Carbonates and Patan Formation

The dolomites and black slates exposed between Satbanjh, Baitadi, and Gokuleshwar exhibit a complex pattern of superposed folding (Fig. 7.6). These folds are characterized by tight hinges and long axial traces essentially parallel to the faults and can be classed as the refolded folds. The carbonates northeast of Satbanjh contain deposits of talc and magnesite, whereas the columnar stromatolite-bearing cherty dolomites in the vicinity of the Parchuni Gad are rich in phosphorite (Bashyal 1985).

A sharp thrust separates the Baitadi Carbonates (to the north) from the Patan Formation of slates and quartzites (Fig. 7.7). The slates and quartzites are also intensely folded.

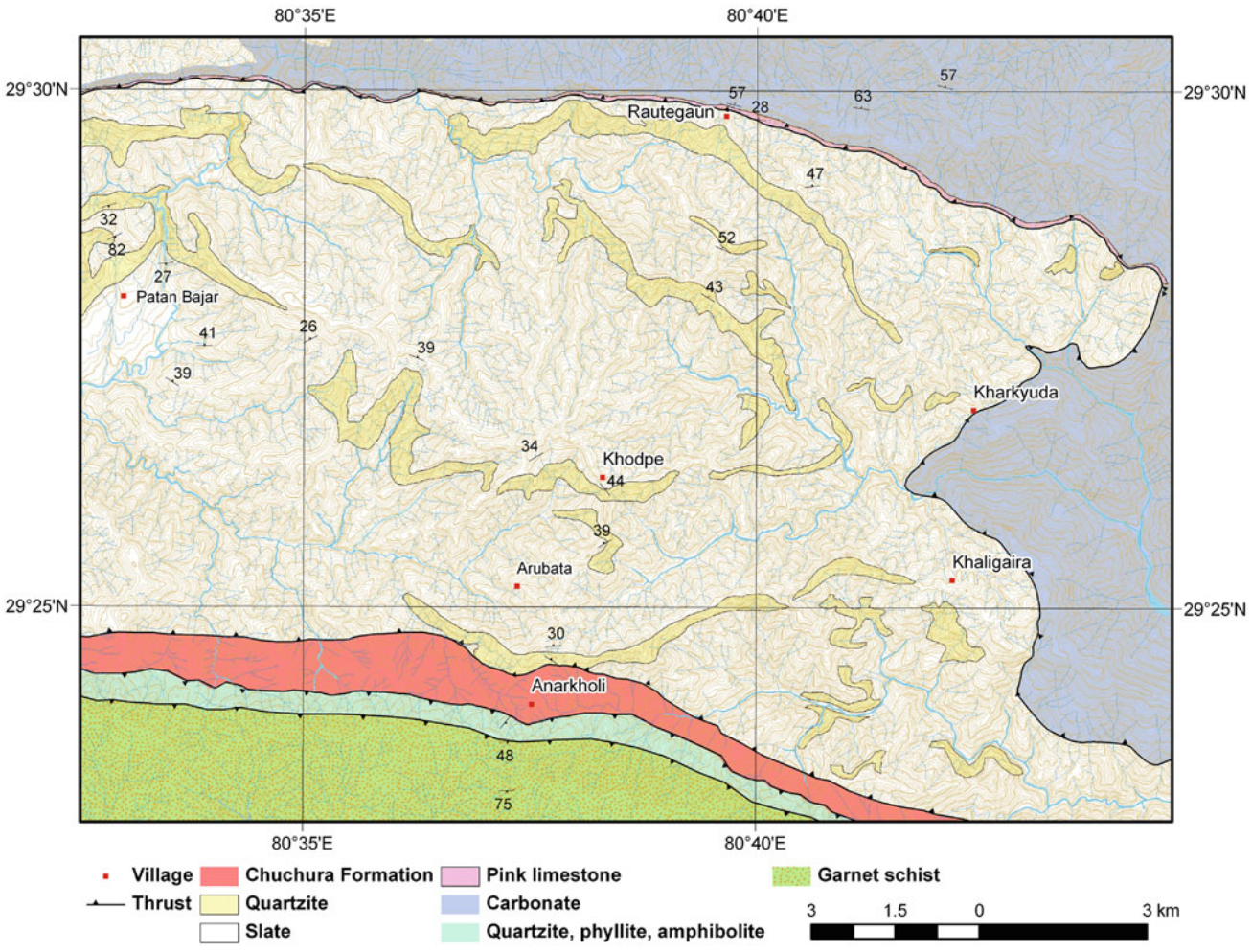

Fig. 7.7 Superposed folds in the quartzites of the Patan Formation. *Source* Author's observations

To the south, there are Early Miocene beds and the North Dadeldhura Thrust, bringing Higher Himalayan rocks over the Lesser Himalayan sequence. The superposed folding was presumably related to the movement of the thrust sheets.

7.2.3 Early Tertiary Beds of Patan–Pancheshwar

The Eocene–Early Miocene beds are exposed to the north of the Dadeldhura Crystalline Unit. They are sandwiched between the south-dipping Anarkholi Thrust, containing the Ranimatta Formation in its hanging wall, and the north-dipping Pachkora Thrust whose hanging wall is made up of the Patan Formation of slates and quartzites (Dhital 2008). In this area too, the Patan Formation is intensely deformed and exhibits the features of superposed folding (Fig. 7.8).

In the adjoining Kumaun Himalaya, the Chail nappe of Fuchs and Sinha (1974, 1978) contains the rocks equivalent to the Ranimatta Formation, whereas the Anarkholi Thrust seems to be the eastwards extension of the Ramgarh Thrust (Valdiya 1980; Robinson et al. 2003, 2006). The North Dadeldhura Thrust brings with it the Higher Himalayan schists and gneisses of the Dadeldhura Group over the Ranimatta Formation, and the group as well is the eastwards continuation of the Almora or Garhwal thrust sheet in India.

The early Tertiary succession is represented by the Chuchura Formation (Fig. 7.8) made up of red-purple or brown mudstone and shale interbedded with gray-green sandstone. There are also some medium to thick (30 cm to 1 m), light gray lenticular Nummulitic limestone beds intercalated in green-gray feeble shale with lenses of compact bivalves. These fossils indicate an Eocene age.

Detailed field mapping in the border region of west Nepal and the adjoining Indian territory (Fig. 7.8) revealed that the red-purple and gray-green sandstone and shale beds of the Chuchura Formation continue in the Indian territory and join with the Rautgara Formation (Valdiya 1980) at its type locality near Pancheshwar, and the rock succession contains shallow marine deposits overlain by fining-upwards fluvial cycles.

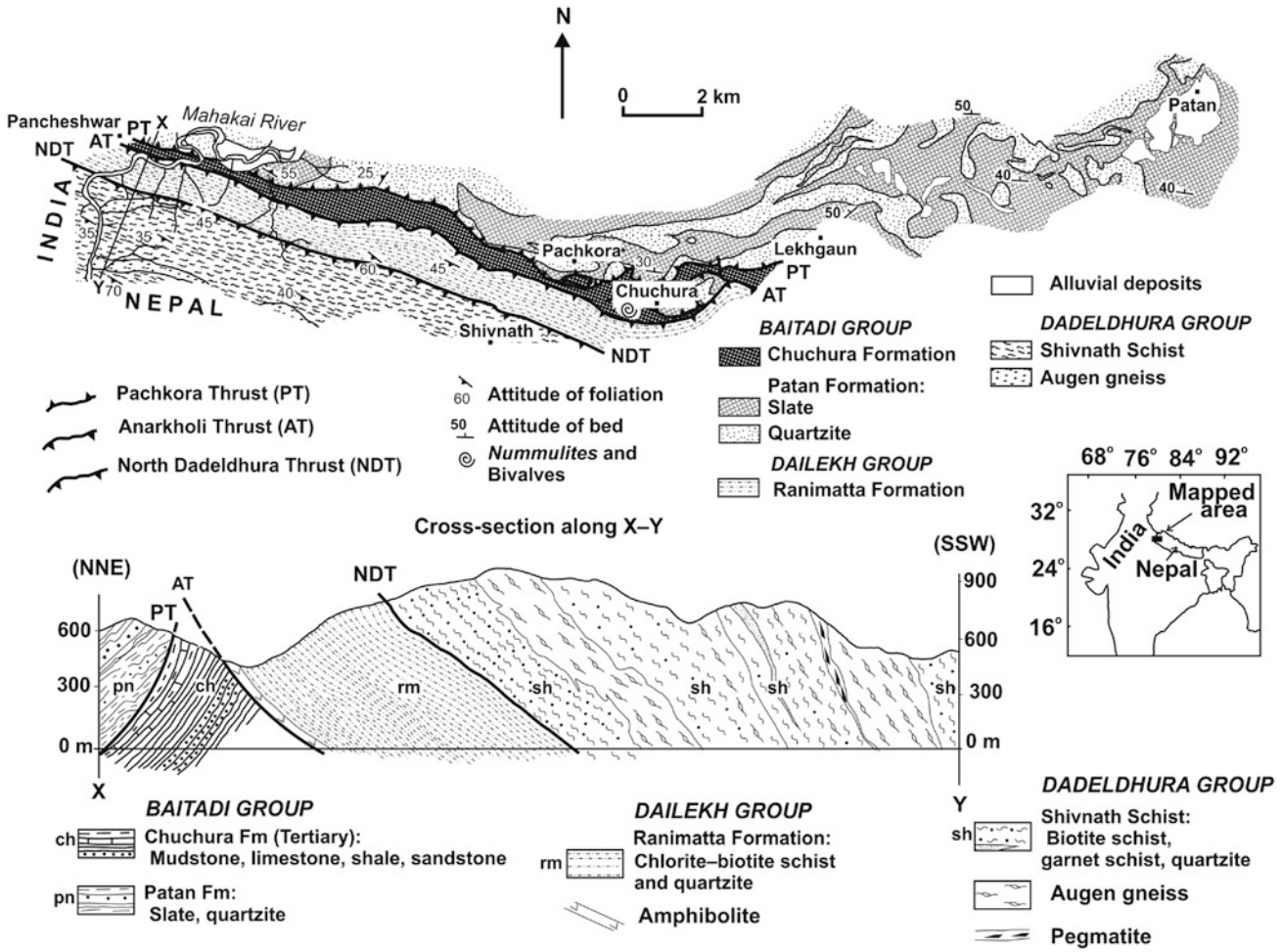

Fig. 7.8 Geological map and cross-section of Pancheshwar area in west Nepal, showing the Tertiary beds of the Chuchura Formation sandwiched between the Melauli Thrust and the Pachkora Thrust. *Source* Modified from Dhital (2008)

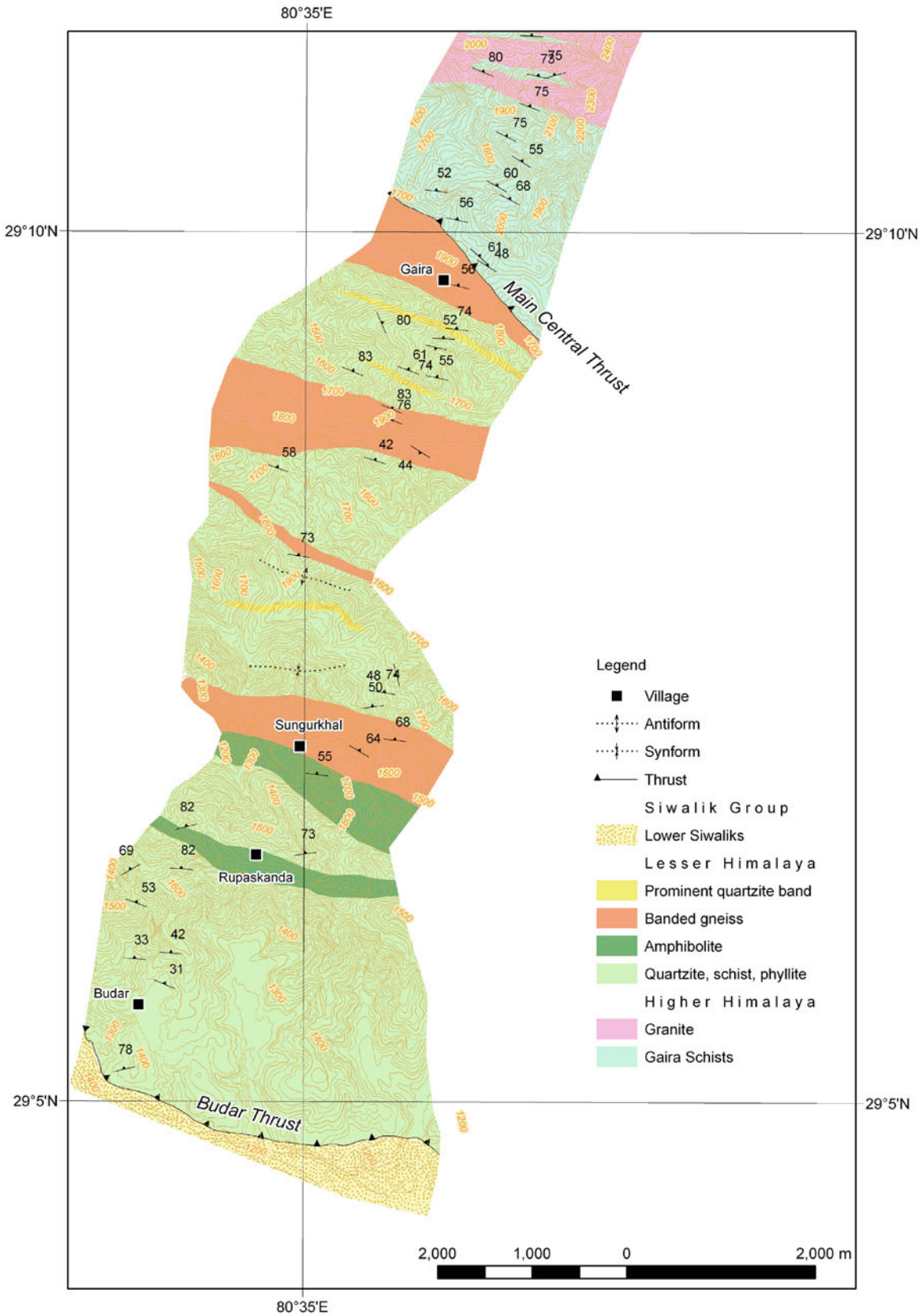

Fig. 7.9 Geological transect between Budar and Gaira. *Source* Author's observations

7.2.4 Budar–Gaira Transect

The Lesser Himalayan rocks are thrust over the Lower Siwaliks at Budar along the Budar Thrust (Fig. 7.9). The thrust was later affected by the Main Boundary Active Fault System, which is a normal fault marked by many sag ponds (Chap. 28). The Budar Thrust continues from India (where it is variously positioned and called the Krol Thrust, Main Boundary Thrust, Chail nappe, or Ramgarh Thrust), crosses the Mahakali River, and extends eastwards up to Budar and beyond (Chap. 8). There are pale green to white quartzites alternating with green phyllites just above the fault. North of Budar, light pink to pale yellow quartzites occur with wave ripples. Some of them are also purple, light green, or white. Most of them are medium- to very thick-banded (2–3 m), medium- to fine-grained, and contain sericite or muscovite flakes. There are also 1 mm to 30 cm thick infrequent bands of purple, green-gray to dark green slates and phyllites with sporadic sun cracks. In a few places, the gray-green phyllite is mottled with purple and red patches. Some pale yellow to white quartzite successions are up to 50 m thick.

The rock becomes more pelitic towards the top (south of Rupaskanda), where dark gray-green phyllites are succeeded by purple and dark gray-green mottled varieties. This unit gives way upwards to a light green to white quartzite band with a minor proportion of pink quartzite and red-purple or gray-green mottled phyllite. Towards the upper part of the last phyllite unit, there is a zone of dark gray-green chlorite schist, and above it is approximately 25 m thick blue-green amphibolite (Fig. 7.10).

The above section extends stratigraphically upwards with some more amphibolite and quartzite alternations for a few hundred meters, where a light gray banded gneiss with green-gray tinge appears first. Feldspar-rich pegmatite veins area are injected in the gneiss, whose lower part is affected by contact metamorphism.

The gneisses continue northwards and, at Sungurkhal, they show in massive and hard bands, where dark gray-green, medium-grained (1–3 mm long) feldspar laths define indistinct foliation. The gneissic bands are from 30 cm to 2–3 m thick and separated by 20 cm to 2 m thick, dark green chlorite schist and quartzite alternations. While continuing structurally upwards, the gneisses gradually pass into amphibolite-like bands. Farther north, dark green chlorite schists and quartzites (thinly banded) are encountered, and in them are 5 to 50 cm thick dark gray-green feldspar-rich quartzite and gneiss bands. Farther upwards appear gray to green-gray (when weathered) banded gneisses with sporadic (5 %) dark gray-green schist and quartzite alternations. The dark schist is very fine-grained. With the appearance of large pegmatite veins in banded gneisses, the Lesser Himalayan sequence terminates at Gaira.

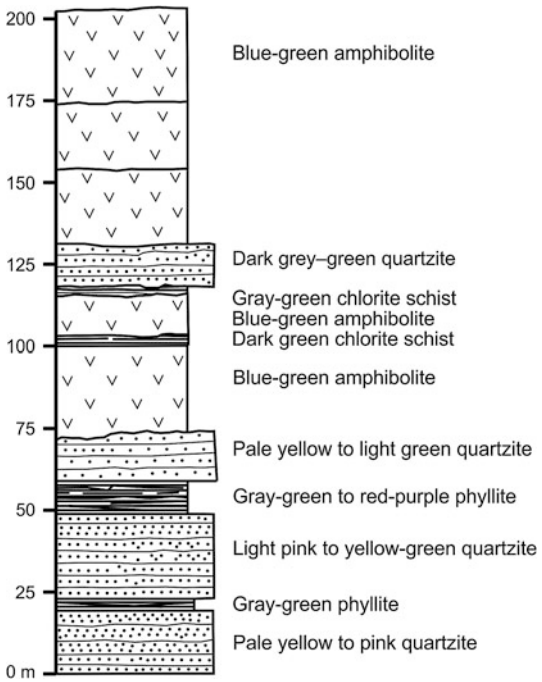

Fig. 7.10 Columnar section at Rupaskanda showing the alternation of quartzite, phyllite, and amphibolite. *Source* Author's observations

In the Budar–Gaira transect, the grade of metamorphism steadily increases upwards. North of Rupaskanda, at first gray biotite schists, quartzites, and feldspathic schists are seen, and then there are zones of schist with some tiny (less than 1 mm) garnets.

In the adjoining Kumaun Lesser Himalaya, Raina and Dungrakoti (1975) identified the Bhimtal Formation of variegated quartzites containing Bhowali Volcanics, Ramgarh Porphyry, and Amritpur Granite. Nautiyal and Rawat (1990) investigated in detail the Proterozoic Amritpur Granite. The granite is thrust over the Siwaliks, and there is also a Lower Siwalik wedge in the granite.

The South Dadeldhura Thrust (equivalent to the Main Central Thrust) passes through the saddle of Gaira. Although the thrust brings the Higher Himalayan crystallines over the Lesser Himalayan succession, the fault is difficult to delineate in the field. The Higher Himalayan rocks, represented by dark gray-green schists, appear north of Gaira. They are strongly sheared and contain snowball garnets. The Dadeldhura Granite is intruded into the schists and it is of early Paleozoic age (Einfalt et al. 1993). In the bordering Kumaun Himalaya, Raina and Dungrakoti (1975) have included these Higher Himalayan rocks under their Garhwal Group consisting of schists, gneisses, and granites.

The Paleozoic granites and gneisses are strongly deformed. Generally, the Dadeldhura Granite is coarse-grained and

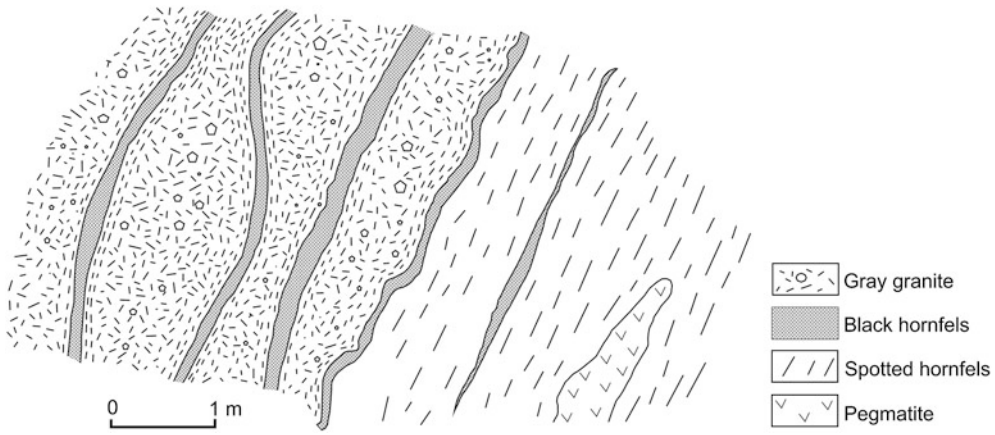

Fig. 7.11 Boudinaged granite and hornfels bands near the intrusive contact, north of Gaira. *Source* Author's observations

contains feldspar, muscovite, some biotite, and tourmaline. There are zones of granite porphyry. Talalov (1977, p. 411) included these rocks under his Dandeldhura gabbro–granite series, containing topaz and lithium mica, whereas Kaphle (1991) attributed them to the tin granites.

About 3 km north of Gaira, one finds dark gray to black hornfelsic quartzites, metasiltstones, and graphitic schists in the granite. The exposed band is about 25 m wide. It is thinly to thickly (10–50 cm) foliated. There also appear dark green-gray schists and hard quartzites (thinly banded) with spotted hornfelses. The hornfelsic schists and quartzites continue farther north. Wide boudins of granite are seen in the hornfelses (Fig. 7.11) with some large pegmatite veins.

Beyssac et al. (2004) applied Raman spectroscopy of carbonaceous material to investigate the thermal metamorphism in this region and obtained a large-scale inverted thermal gradient in the Lesser Himalaya and a rather uniform gradient in the Higher Himalaya. Temperature in the Lesser Himalaya decreases from 540 °C at the top to less than 330 °C at the lower part, whereas the Higher Himalayan rocks record a uniform temperature of about 540 °C.

References

Amatya KM, Jnawali BM (1994) Geological map of Nepal, scale: 1:1,000,000. Department of Mines and Geology, International Centre for Integrated Mountain Development, Carl Duisberg Gesellschaft e. V., and United Nations Environment Programme

Bashyal RP (1982) Geological framework of Far Western Nepal. Himalayan Geol Wadia Inst Himalayan Geol Dehra Dun 12:40–50

Bashyal RP (1985) A preliminary appraisal of Baitadi phosphorite, Far Western Nepal. J Nepal Geol Soc 3(1, 2):13–19

Bashyal RP (1986) Geology of Lesser Himalaya, far Western Nepal. In: Le Fort P, Colchen M, Montenat C (eds) Évolution des domaines orogéniques d'Asie méridionale (de la Turquie à l'Indonésie), Livre jubilaire Pierre Bordet, Sciences de la Terre, Mémoire no. 47, Nancy, pp 31–42

Beyssac O, Bollinger L, Avouac J-P, Goffé B (2004) Thermal metamorphism in the Lesser Himalaya of Nepal determined from Raman spectroscopy of carbonaceous material. Earth Planet Sci Lett 225:233–241

Dhital MR (2008) Lesser Himalayan Tertiary rocks in west Nepal and their extension in Kumaun, India. J Nepal Geol Soc 37:11–24

Einfalt HC, Hoehndorf A, Kaphle KP (1993) Rediometric age determination of the Dadeldhura granite, Lesser Himalaya, Far Western Nepal. Schweiz Miner Petrogr Mitt 73:97–106

ESCAP (Economic and Social Commission for Asia and the Pacific) (1993) Geology and mineral resources of Nepal, atlas of mineral resources of the ESCAP region, vol 9. United Nations, New York, 107 pp (with a geological map in colors)

Fuchs G (1981) Geologic–tectonical map of the Himalaya, scale: 1:2,000,000. Geologische Bundesanstalt, Wien

Fuchs G, Frank W (1970) The geology of West Nepal between the rivers Kali Gandaki and Thulo Bheri. Jahrbuch der Geologischen Bundesanstalt 18:1–103 (with a geological map and cross-sections)

Fuchs G, Sinha AK (1974) On the geology of Naini-Tal (Kumaun Himalaya). Himalayan Geol 4:563–580

Fuchs G, Sinha AK (1978) The tectonics of the Garhwal–Kumaun Lesser Himalaya. Jahrbuch der Geologischen Bundesanstalt, Wien, Band 121, Heft 2, pp 219–241 (with 1 plate containing geological map in colors, Scale: 1:500,000)

Gansser A (1964) Geology of the Himalayas. Interscience, New York, 289 pp

Hagen T (1969) Report on the geological survey of Nepal. Preliminary reconnaissance, vol 1. Denkschiiften der Schweizerischen Naturforschenden Gesellschaft, Band LXXXVI/1, 185 pp (with a geological map)

Heim A, Gansser A (1939) Central Himalaya: geological observations of the Swiss Expedition 1936. Denkschriften der Schweizerischen Naturforschenden Gesellschaft, Band LXXIII, Abh. 1, 245 pp (with maps, sections, and plates)

Kaphle KP (1991) Geochemistry of Dadeldhura granite and its mineral potential. J Nepal Geol Soc 7:21–38

Misra RC, Valdiya KS (1961) The calc zone of Pithoragarh, with special reference to the occurrence of stromatolites. J Geol Soc India 2:78–90

Nautiyal SP, Rawat RS (1990) Nature and preliminary petrochemistry of the Amritpur Granites, Nainital District, Kumaun Himalaya, Uttar Pradesh, India. J Himalayan Geol 1(2):199–208

Raina BN, Dungrakoti BD (1975) Geology of the area between Naini Tal and Champawat, Kumaun Himalaya, Uttar Pradesh. Himalayan Geol Wadia Inst Himalayan Geol Dehra Dun 5:1–27

Robinson DM, DeCelles PG, Copeland P (2006) Tectonic evolution of the Himalayan thrust belt in western Nepal: Implications for channel flow models. GSA Bull 118(7/8):865–885

Robinson DM, DeCelles PG, Patchett J, Garzione CN (2003) Kinematic model for the main central thrust in Nepal. Geology 31:359–362

Shrestha SB, Shrestha JN, Sharma SR (1985) Geological map of Far-Western Nepal. Department of Mines and Geology, Kathmandu

Talalov VA (1977) Main features of magmatism and metallogeny of the Nepalese Himalayas. Colloques internationaux du C. N. R. S. No 268—Écologie et Géologie de l'Himalaya, Paris, pp 409–430

Valdiya KS (1962) Note on the discovery of stromatolitic structure from the lower Shali Limestone of Tatapani near Simla. UP Curr Sci 31:64–65

Valdiya KS (1980) Geology of Kumaun Lesser Himalaya. Wadia Institute of Himalayan Geology, Dehra Dun, 291 pp (with a geological map in colors)

Lesser Himalaya of Karnali–Bheri Region

8

In its prolongation to the eastward, according to Colonel Kirkpatrick, it is called Humla to the north of Zumila, and beyond the Arun, according to Hamilton's map, appended to the History of the Goorka war, the Harpala mountains.

—W. Jameson (1839, pp. 1039–1040)

In about 150 km wide expanse, a variety of sedimentary and low-grade metamorphic rocks of the Lesser Himalaya is distributed within the watersheds of the Karnali, Bheri, and Rapti Rivers (Fig. 8.1). Whereas in the Mahakali–Seti region, the Proterozoic low-grade metamorphic pile overrides the Siwaliks, in this area a discontinuous belt of Lesser Himalayan sedimentary sequence is juxtaposed with them. This region is also characterized by the abundance of quartzites and metabasics. Although the past extent of the Higher Himalayan crystalline sheet is difficult to surmise, there were at least two other large thrusts (i.e., the Budar Thrust in the west and Kapurkot Thrust in the east), which covered almost the entire younger Lesser Himalayan sedimentary succession. Numerous small and large klippen of phyllite, quartzite, and carbonates bear witness to recent widespread erosion.

In this area, Hagen (1969) has drawn a complex nappe system and some autochthonous (such as the Piuthan zone) as well as parautochthonous units. His Nawakot nappes continue up to the Piuthan zone. Hagen has also mapped a schuppen structure in the outer zone of this region and described the Nummulitic horizons of Dang and Surkhet.

8.1 Galwa Tectonic Window

The Galwa tectonic window (Hagen 1959) developed in the core of the Great Midland Antiform, which was denuded of the Higher Himalayan thrust sheet at its west end (Figs. 8.2 and 8.3). In this window, Fuchs (1974, 1977) distinguished the phyllites and quartzites of his "Chail nappe 3." These rocks are thrust over a sedimentary succession of laminated black slates and siltstones (Simla Slates); thin- to thick-bedded, coarse- to fine-grained, pink, white, and green quartzites with sporadic conglomerates (Nagthats); and thin-bedded, white, pink, gray, cherty dolomites, marbles, phyllites, and diamictites, containing boulders of dolomite, quartzite, vein-quartz, and argillite (Blainis). The Blaini Formation is also rich in hematitic schists and quartzites. This formation is followed upwards by black slates passing into white, gray, and blue stromatolitic dolomites and limestones (Shalis).

The Chail nappes are made up of thick-bedded, white, green, and gray quartz arenites with cross-bedding and ripple marks, schistose conglomerates, phyllites, and psammitic schists. There also set in medium- to coarse-grained basic metavolcanics exhibiting an ophitic texture. Although the metavolcanics are partly altered to chlorite schists or amphibolites, they do contain many amygdales. The Chail nappes also comprise coarse-grained, two-mica granite–gneisses and some aplites with tourmaline (Fig. 8.2). The surrounding Higher Himalayan rocks are represented by ortho- and paragneisses, marbles, schists, and quartzites (Chap. 15).

A conspicuous antiformal core is exposed between Sinja and Lake Rara (Fig. 8.4). The core is made up of black slates and is surrounded by gray stromatolitic dolomites. The dolomites are succeeded upwards by white quartzites with amphibolites and gray phyllites, chlorite schists, or garnet schists.

8.2 Surkhet–Dailekh Tract

Fuchs (1977) mapped a large portion of the Lesser Himalaya between Surkhet and Dailekh, where he identified Early Miocene beds (Dagshai or Suntar Formation) at the foot of the Mahabharat Range, north of Surkhet (Fig. 8.5). He also recognized a thin bed of carbonates (Lakharpata Group) thrust over the Paleocene–Early Eocene strata of the Surkhet Group. The Surkhet Group begins with white, gray, green, thick-bedded quartz arenites or quartzose sandstones, containing shaly intercalations (Melpani Formation). This primarily medium- to coarse-grained arenaceous succession is followed up-section by 150–170 m thick fissile shales, at the top of which is an approximately 10 cm thick bed containing gastropods and bivalves. The fossils indicate a Paleocene–

M.R. Dhital, *Geology of the Nepal Himalaya*, Regional Geology Reviews,
DOI 10.1007/978-3-319-02496-7_8

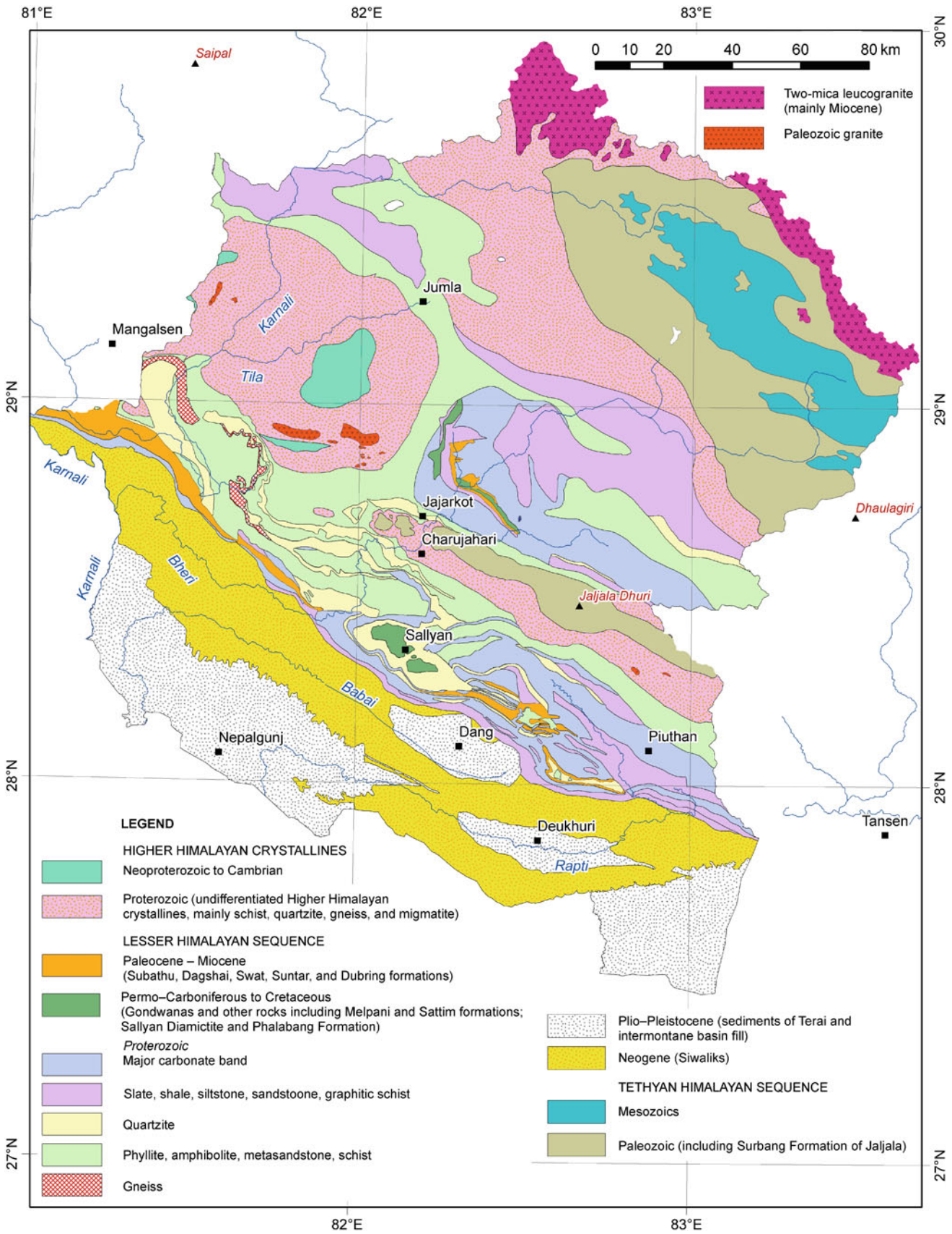

Fig. 8.1 Simplified geological map of the Karnali–Bheri region. *Source* Based on Fuchs and Frank (1970), Tater et al. (1983), Shrestha et al. (1987), ESCAP (1993), Amatya and Jnawali (1994), other published maps, and author's observations

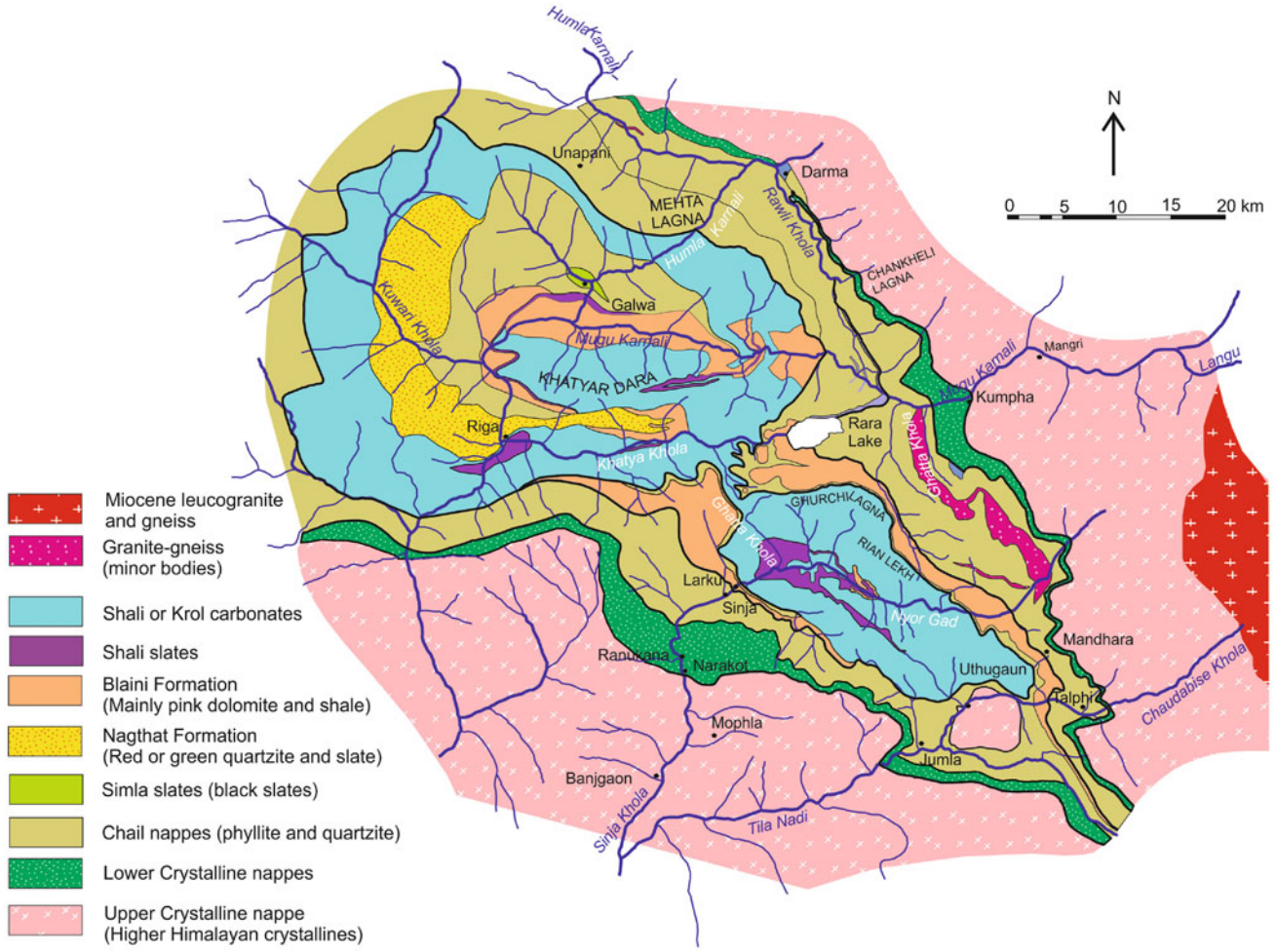

Fig. 8.2 Geological map of the Galwa tectonic window. *Source* Modified from Fuchs (1977)

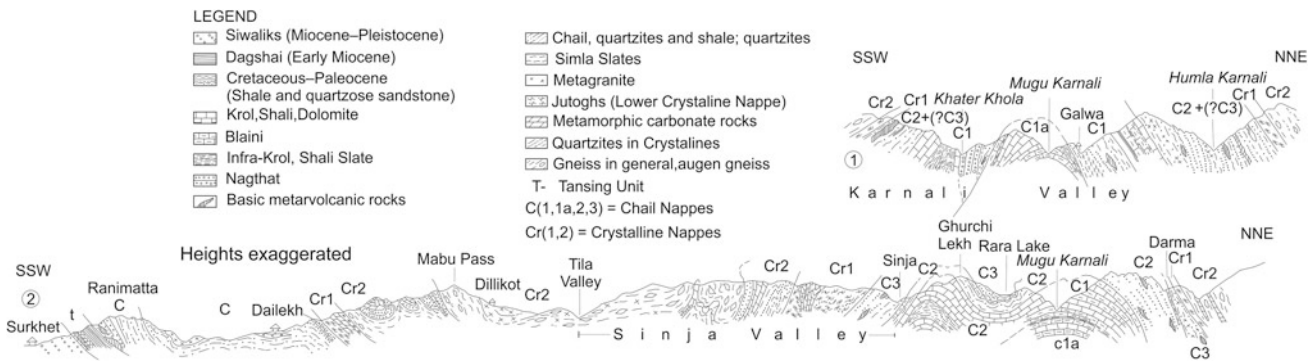

Fig. 8.3 Geological cross-sections through the Karnali region. *Source* Modified from Fuchs (1977)

Eocene age (Swat or Subathu Formation). Above the fossiliferous horizon are thick-bedded, medium-grained, compact, gray-green sandstones, regularly alternating with silty and micaceous purple shales or shaly sandstones (Suntar or Dagshai Formation). The sandstones frequently contain intraformational shale clasts.

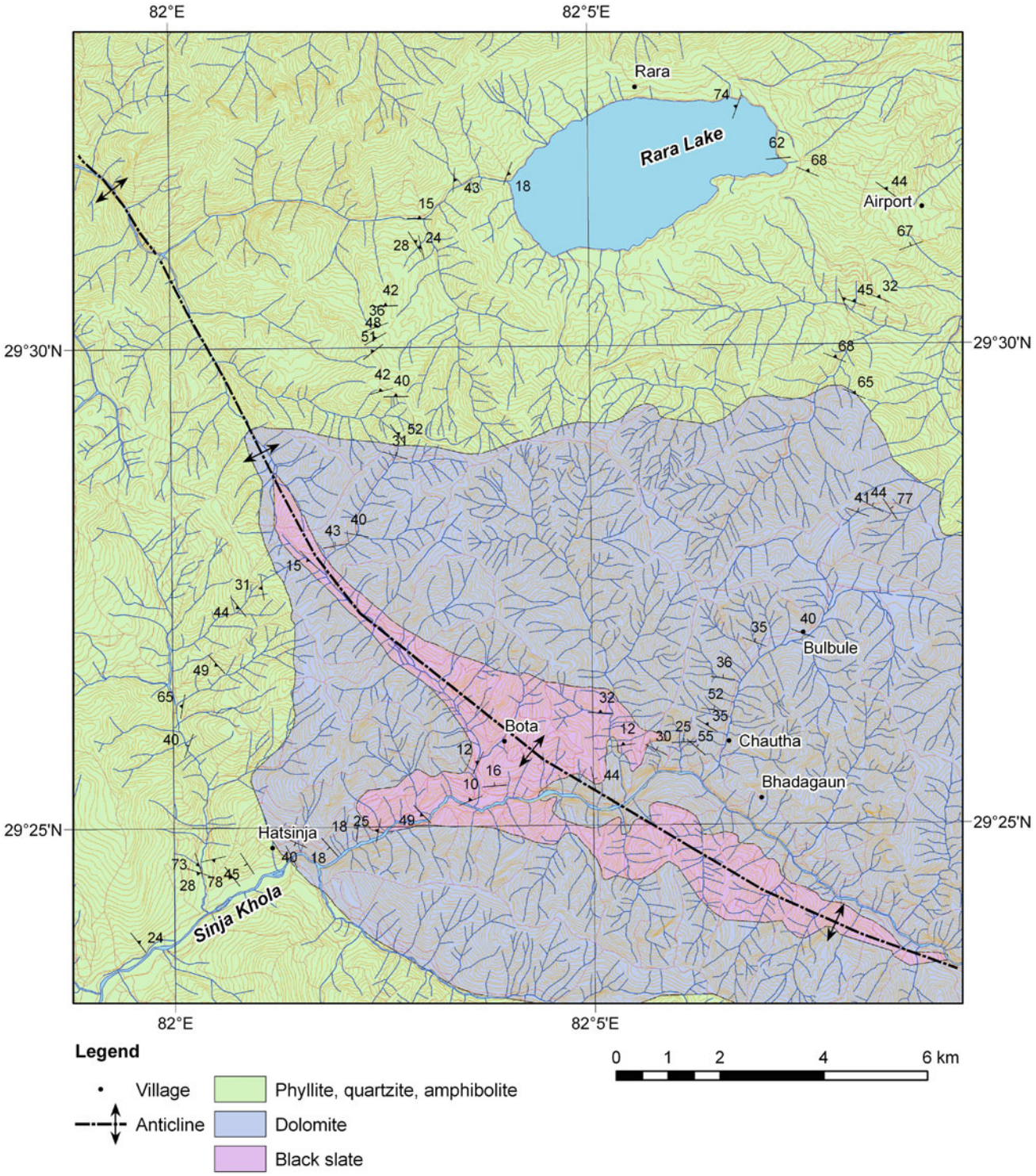

Fig. 8.4 Anticlinal core of Bota, exposed between Sinja and Lake Rara. *Source* Author's observations

In this area, the Ranimatta Formation is represented by a moderately to steeply north-dipping sequence of metabasics, alternating mainly with white or some pink quartzites. These rocks continue from the Mahakali River, and in this area, they are thrust over the youngest Lesser Himalayan sedimentary rocks along the Budar Thrust. After crossing the Karnali River, the Budar Thrust follows the upper slopes of the Mahabharat Range and passes through the north part of Surkhet (Fig. 8.5).

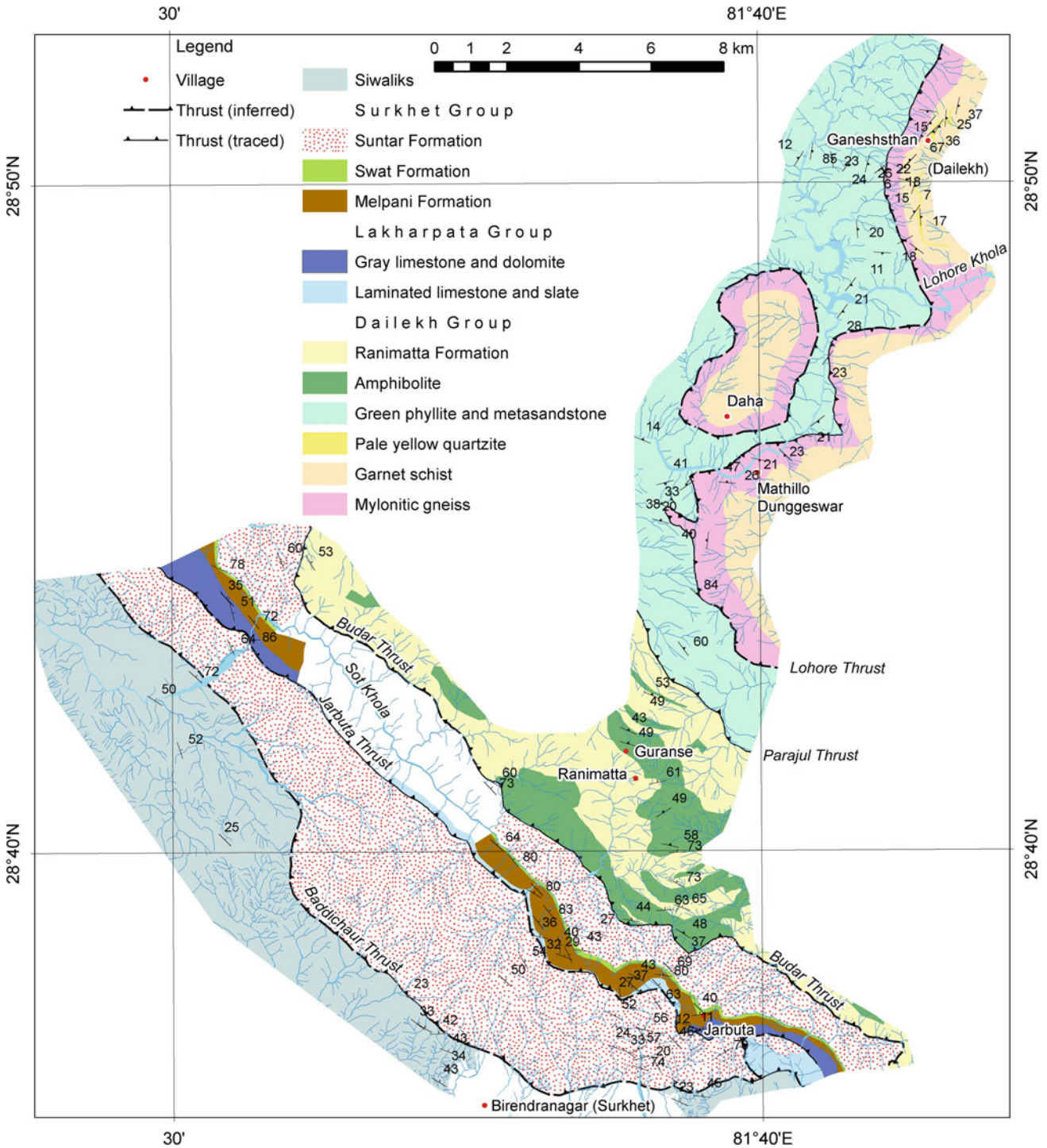

Fig. 8.5 Thrust sheets and imbricate faults. *From north to south* Lohore Thrust, Parajul Thrust, Budar Thrust, Jarbuta Thrust, and Baddichaur Thrust. *Note* the two *branch lines* near Jarbuta and that the Baddichaur Thrust terminates against another thrust at the extreme southeast corner of the mapped area. *Source* Author's observations

The medium- to coarse-grained, basic rocks, cropping out north of Surkhet, commonly show an ophitic texture. They contain euhedral and twinned augite, slender pseudomorphs of sericite–albite aggregates (developed from alteration of a more basic plagioclase) and secondary sphene, chlorite, and opaque minerals. In certain zones, the schistosity is well developed, and the basic rocks are altered to chlorite schists. Medium- to coarse-grained quartzites with local pebbly bands

alternate with the basic rocks. This lithology resembles that of the Nagthat Formation, particularly that cropping out in the Bhowali–Bhimtal area of Kumaun (Fuchs 1977, p. 169).

The metasedimentary rocks of the Ranimatta Formation exposed north of Ranimatta (Fig. 8.5) are made up of white to green, massive or schistose quartzites, psammitic schists, and sericite–chlorite schists with some metavolcanics. The Parajul Thrust brings gray-green phyllites and metasandstones over these rocks in the north. The gas and oil seeps of Dailekh are located within the last succession of gently folded phyllite and metasandstone.

Coarse augen gneisses and granitoids appear in the Lohore Khola, where the rocks dip essentially due east and form a broad east-plunging synform. Presumably, these gneisses are thrust over the gray-green phyllites (Sharma and Kizaki 1988) along the Lohore Thrust. The augen gneisses are made up of large deformed microcline phenocrysts. There are also many pegmatite veins penetrating the phyllites (Fuchs 1977, p. 170). Around the town of Dailekh are distributed black graphitic schists, white quartzites, and some gray garnet schists, sporadically alternating with thin, gray marble bands.

8.3 Fossiliferous Beds of Barikot Window

The Barikot window occupies the core of a complex antiform in the area north of Jajarkot (Chap. 15). The vast window is made up mainly of carbonates with subordinate slates, phyllites, and quartzites, including some metabasics. From this window, Fuchs and Frank (1970, p. 31) reported about 25 m thick dark gray shales, containing lenses of *Nummulites* and *Assilina* with indeterminate gastropods and bivalves in the upper part (Subathus). The fossils include *Assilina placentula* Dehayes. The last shale bed is overlain with an erosional contact by a massive bed of green pebbly sandstone, followed by a rhythmic interbedding of red-purple or green mottled shales and gray-green sandstones (Early Miocene Dagshais). This sequence is about 50 m thick and is terminated by a thrust fault at the top. These Tertiary strata lie about 95 km north of the Siwalik belt, and over them the Lesser Himalayan thrust had moved for more than 100 km (Frank and Fuchs 1970, p. 577). Sakai et al. (1999) identified slightly metamorphosed Early Miocene beds (Dumri Formation) from the same area and dated the metamorphism at 16–17 Ma. They also inferred an approximately 300 km wide pre-Siwalik foreland basin.

8.4 Region Between Jajarkot and Botechaur

In this region, quartzites and metabasics preponderate (Kansakar 1991) in the Ranimatta Formation of the Dailekh Group, which makes its widest appearance in the environs of the Bheri River and the area farther west (Fig. 8.6). This group continues uninterruptedly from the Mahakali River, passes through Ranimatta (Fig. 8.5), and extends towards the east for several kilometers before disappearing under a thick carbonate pile east of the Bheri River.

There are essentially three overlapping Lesser Himalayan thrust sheets that are exposed due to incision by the Bheri and Sharda rivers. The structurally lowest discontinuity is the Budar Thrust, carrying the Dailekh Group of rocks; the second fault is the Chaklighat Thrust, producing the Kubhinde Complex; and the uppermost one is the Kapurkot Thrust, transporting phyllites and quartzites of the Sharda Group. To the north, the Higher Himalayan crystallines interrupt the Lesser Himalayan sequence of this tract by overriding the Sharda Group of rocks along the Main Central Thrust (Figs. 8.6 and 8.7).

8.4.1 Kapurkot Thrust

In this area, the Kapurkot Thrust (Dhital and Kizaki 1987a) passes through the east and northeast parts of the Lesser Himalayan sequence (Fig. 8.6). The thrust has traveled for more than 30 km towards the foreland. The Kapurkot Thrust generally overrides the Kumak Carbonates of the Kubhinde Complex, but in the Chhera Khola area, it rests over the Dailekh Group.

8.4.2 Sharda Group

In this area, the Sharda Group (Dhital and Kizaki 1987b) is represented by the Dangri Formation and Raira (or Balle) Quartzite (Figs. 8.6 and 8.7). The lower part of the Dangri Formation contains light to dark gray (fresh) or gray-green (weathered) phyllites, alternating with some subordinate bands of thick- to very thick-bedded, medium-grained, white to light gray, dense, hard, and massive quartzite. The light gray quartzite bands display parallel laminae as well as planar cross-laminae. This formation passes upwards to very thick bands of gray to green-gray biotite schist, alternating

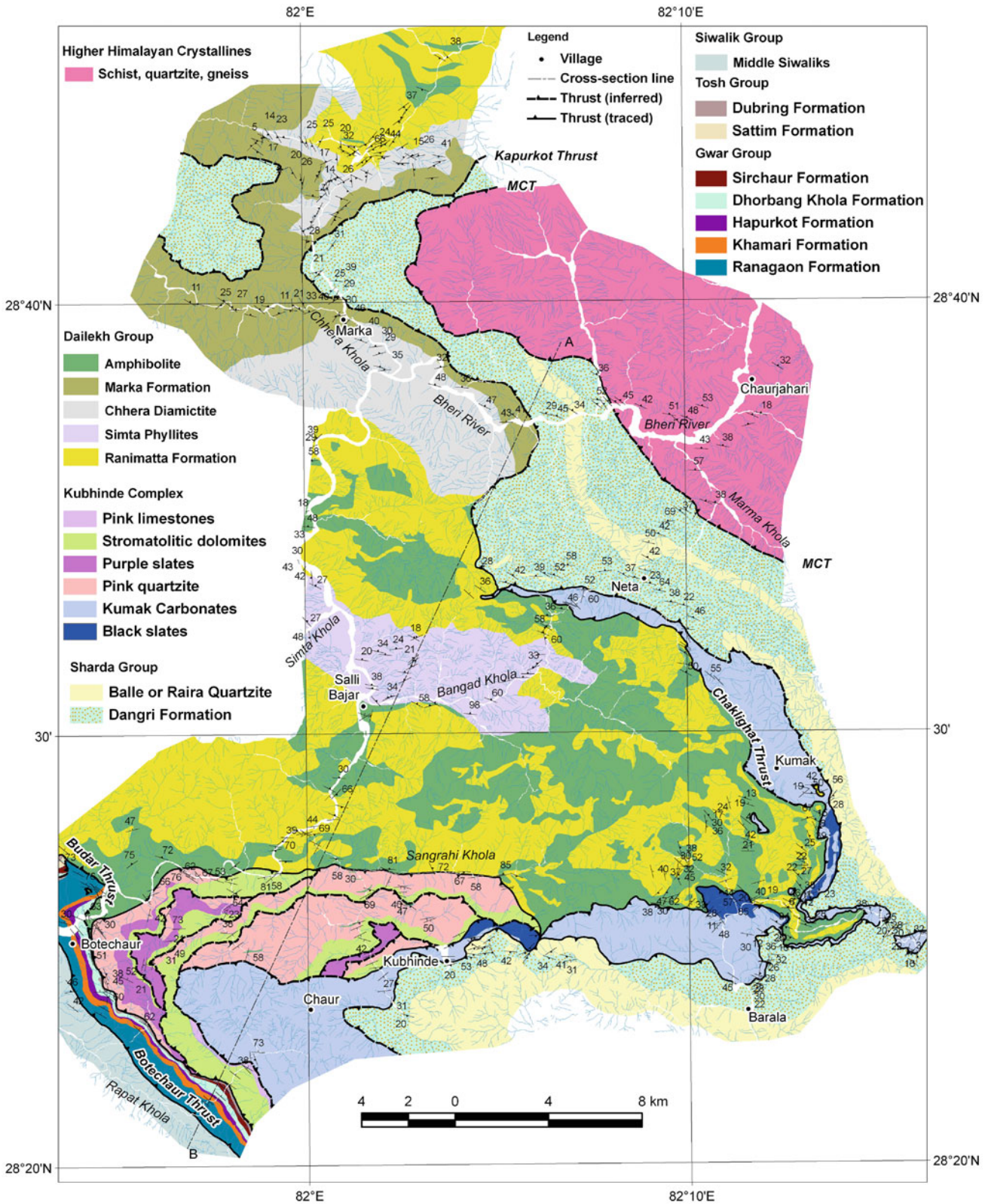

Fig. 8.6 Geological map of the Bheri River and the region between Jajarkot and Botechaur showing four main thrusts: The MCT (Main Central Thrust), Kapurkot Thrust, and Chaklighat Thrust. The Botechaur Thrust overrides the Siwaliks. *Note* prolific development of metabasics in the Ranimatta Formation. *Source* Author's observations

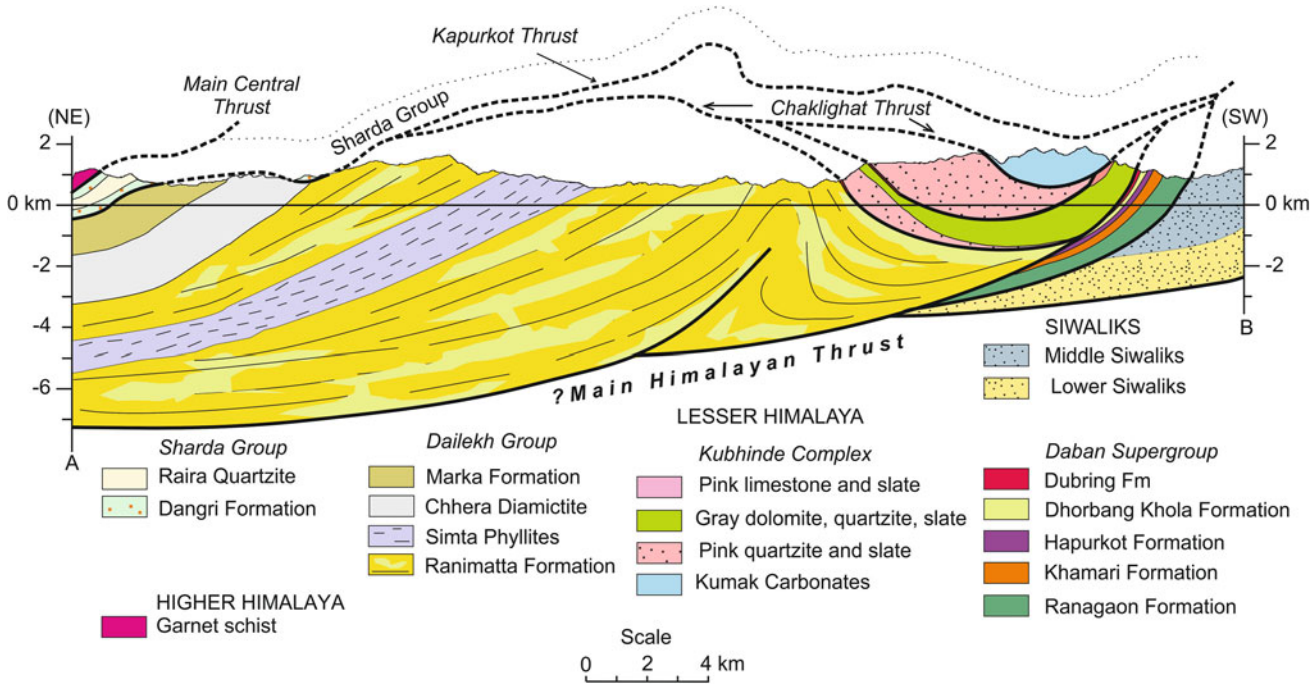

Fig. 8.7 Geological cross-section along the *line A–B* (Fig. 8.6) showing imbricate faults and the Main Himalayan Thrust. *Source* Author's observations

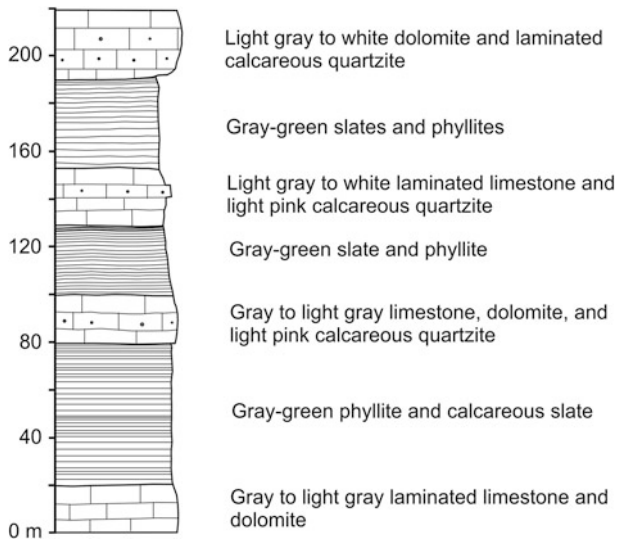

Fig. 8.8 Columnar section depicting interbedding between slates and carbonates of the Kubhinde Complex, at Rame Khola. *Source* Author's observations

with pale yellow quartzite and psammitic schist. East of Neta, there are also rare thin pegmatite veins and micro-granite dikes (Sharma and Kizaki 1988). About 200–400 m thick Raira Quartzite (Adhikary and Sharma 1983) appears towards the upper part of the Dangri Formation. The Raira Quartzite is made up of a pale yellow to white or light gray-green laminated variety with partings of gray-green phyllite, black graphitic schist, and biotite schist. Farther upwards, the Dangri Formation continues with gray-green biotite schists, containing tiny garnets and alternating with medium- to thick-bedded white quartzites. The last schist-predominating band is interrupted rather abruptly by an approximately 100 m thick zone of gray mylonitic banded gneiss, followed by a very thick succession of garnet schist or graphitic schist with thin marble bands as well as kyanite schist and gneiss alternations. This crystalline sequence is designated as the Chaurjhari Formation (Sharma et al. 1984) of the Higher Himalaya, and the Main Central Thrust is drawn at the base of the mylonitic gneiss.

8.4.3 Kubhinde Complex

The Kubhinde Complex lies in the footwall of the Kapurkot Thrust. This rock succession is truncated by many folded imbricate faults and the Chaklighat Thrust from the underlying Dailekh Group (Fig. 8.7). The Kubhinde Complex is tentatively divided up into the following units from bottom to top, respectively.

Black slates are frequent at the base of the Kubhinde Complex. In the Mokhla Khola, Chaklighat, and Rame Khola as well as south of Chaur, the Kubhinde Complex begins with dark gray to black slates with gray limestone beds and thin partings (Fig. 8.8). Generally, the Chaklighat Thrust moves along the black slates and there is a gradual

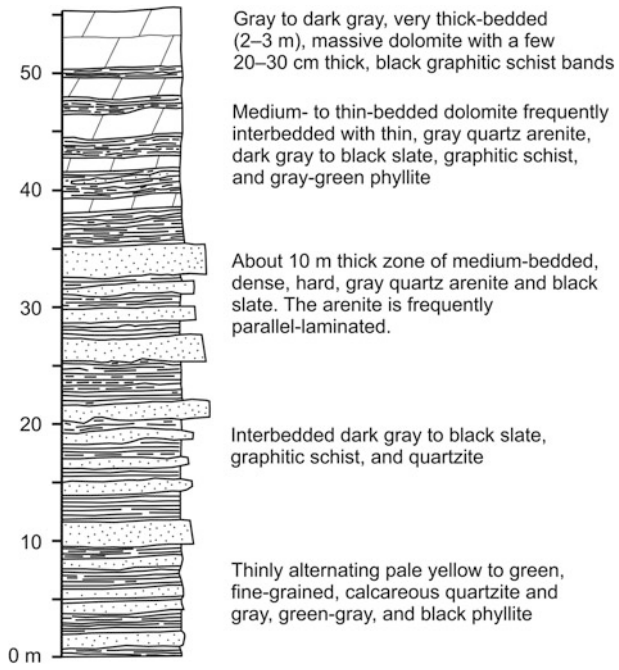

Fig. 8.9 Transitional contact between slates and dolomites of the Kubhinde Complex, exposed in the road cut south of Neta. *Source* Author's observations

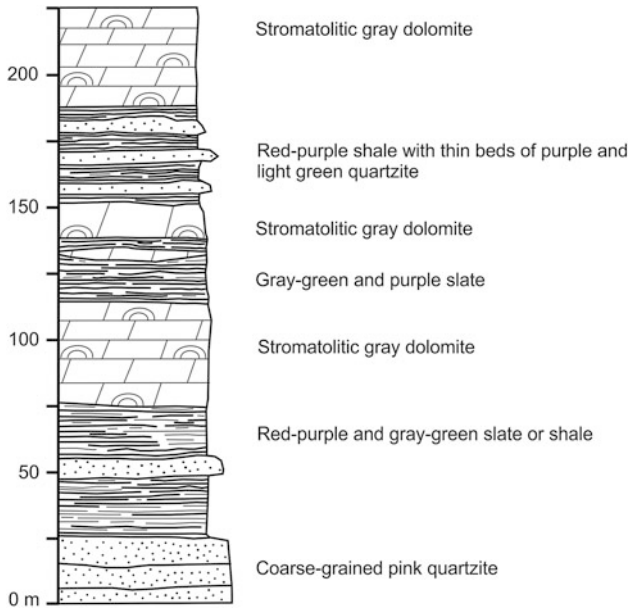

Fig. 8.10 Occurrence of stromatolites in the dolomites of the Kubhinde Complex, exposed west of Chaur. *Source* Author's observations

transition from slate to overlying dolomite (Fig. 8.9). While moving upwards, the sequence becomes more calcareous and passes into the Kumak Carbonates.

The Kumak Carbonates (Sharma et al. 1984) constitute the main portion of the Kubhinde Complex. They contain very thick (1–5 m) beds of gray dolomite with columnar stromatolites (Kansakar 1991). These carbonate rocks are continuously exposed along about 75 km long stretch. They also form various klippen farther east (see below).

Pink quartzites are found at the lower portion of the folded imbricate slices between Botechaur, Chaur, and Sangrahi Khola. They contain thick to very thick (1–3 m) beds of medium- to fine-grained, dense quartz arenite with phyllite partings and sporadic amphibolite bands. Their upper surfaces are marked by numerous wave and current ripples, and the interbedded red-purple and gray-green slates contain sun cracks. There also occur some coarse- to very coarse-grained, massive, dense, very thick, gray quartzites.

Purple slates generally overlie the pink quartzite unit. Their distribution is rather limited and patchy. Most of them are confined to the west slope of Chaur and east of Botechaur. They are made up of purple and gray slates or shales with thin quartz arenite bands. There are also infrequent intercalations of thin limestone.

The stromatolitic dolomites (Fig. 8.10) are the most conspicuous rocks. Thick to very thick beds of gray dolomite contain various columnar as well as domed stromatolites. But their relationship with the Kumak Carbonates or similar dolomites of the Gwar Group is not clear. A few quartzites as well as gray-green and red-purple shales or slates are also intercalated in this unit.

Pink limestones represent the upper part of the gray stromatolitic dolomite. They compose a relatively thin sequence of laminated pink-purple and light green limestone and calcareous slate. To the south of Chaur, this unit is truncated by the Chaklighat Thrust, encompassing gray dolomites of the Kumak Carbonates in its hanging wall (Fig. 8.7).

8.4.4 Antiformal Closure of Mokhla

The slates and carbonates, sandwiched between the Kapurkot Thrust and the Chaklighat Thrust, form a narrow (about 1.5 km wide and 4.5 km long) antiformal closure at Mokhla (Fig. 8.11). There is also a smaller (about 1 km^2) window of the Kumak Carbonates surrounded by the Dangri Formation. These carbonate rocks reappear farther east as large masses and blocks, which Fuchs and Frank (1970) have included under their Shali or Krol Formation. The top part of the carbonates is strongly sheared, and several mesoscopic recumbent folds are observed near the contact zone with the Kapurkot Thrust.

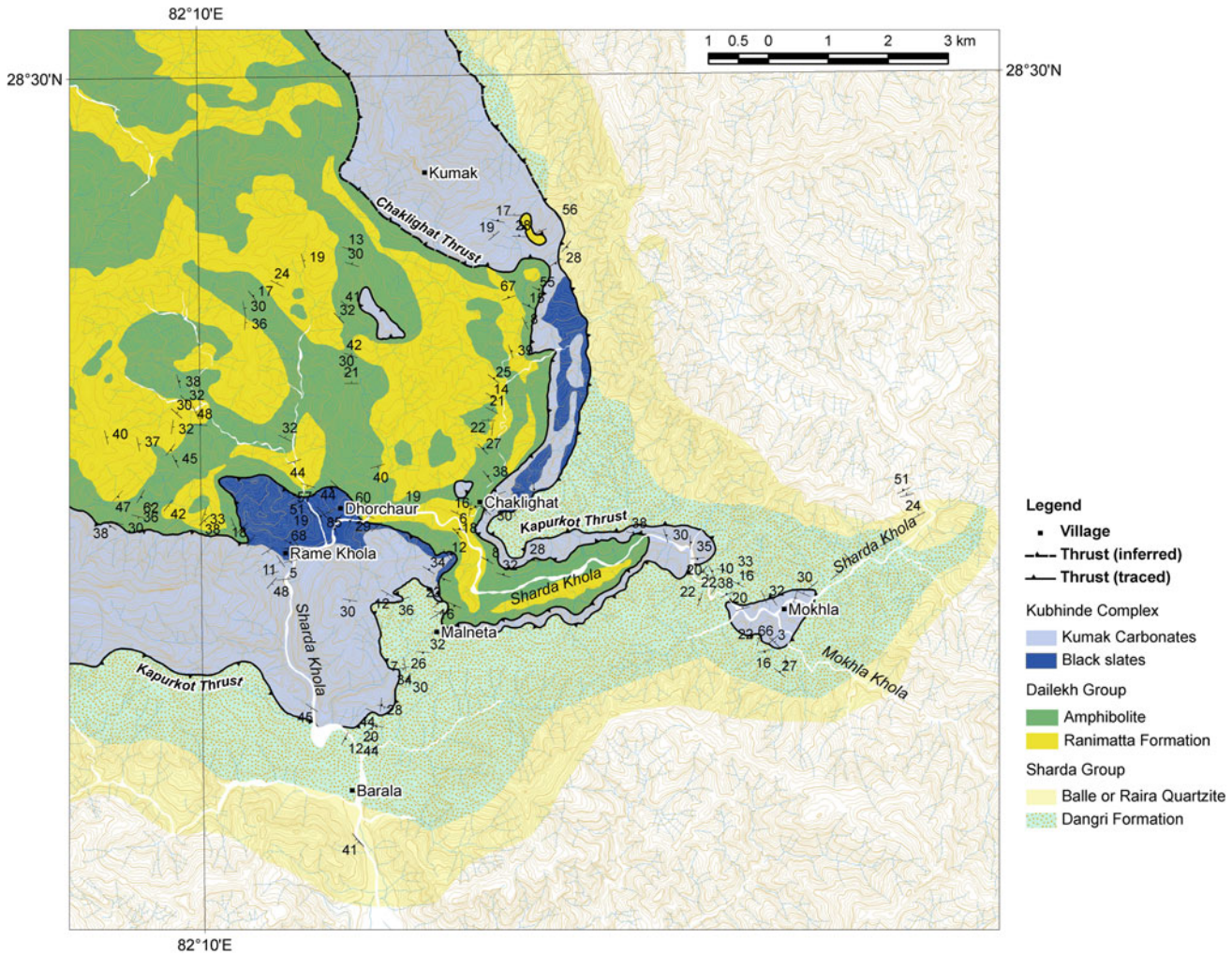

Fig. 8.11 Geological map showing the Kapurkot Thrust, Chaklighat Thrust, and antiformal closure around Mokhla. *Source* Author's observations

8.4.5 Dailekh Group

The Dailekh Group commences with the Ranimatta Formation, which occupies a wide area between Botechaur, Salli Bajar, and Chaklighat. It comprises mainly parallel-laminated, infrequently plane cross-laminated, pale gray, yellow, or white quartzites. Sporadic green to light blue-green bands also exist. Some quartzite beds are granular to pebbly. Metabasic rocks (mainly amphibolites) are abundant in this formation and constitute about 30 % of its total thickness.

The rocks exposed in the upper reach of the Chhera Khola, north of Jyula (Fig. 8.12), consist of an alternating sequence of blue-green phyllite or garnet schist and light gray to green-gray quartzite. In their lower section, the proportion of schist predominates over quartzite, and there are also very thick (more than 25 m) bands of amphibolite. Towards the upper part of this formation, are medium- to coarse-grained, pale yellow, white, light gray, or light green-gray quartzites, which are generally medium- to thick-banded, blocky, and have gray to green-gray schist partings and bands.

The Simta Phyllites (Kansakar and Chitrakar 1984) appear as a distinct member within the Ranimatta Formation. They crop out north of Salli Bajar and in the Simta Khola. In this member, blue-green phyllites abound, whereas quartzites and amphibolites are absent or extremely rare. Its lower contact exposed at Salli Bajar is rather sharp, but the upper limit is a gradual transition (Fig. 8.13).

The Chhera Diamictite is found farther north in the Chhera Khola, especially between Chhera Chaur and Marka, north of Baluwa, and in the Bheri River (Figs. 8.6 and 8.12). This formation has a rather sharp lower contact with the Ranimatta Formation and the contact is inferred to be a disconformity. The diamictite is usually calcareous and metamorphosed to a garnet grade. The meta-diamictite contains angular to subrounded clasts of gray dolomite, pale yellow quartzite, gray gneiss, and black schist. The clasts are

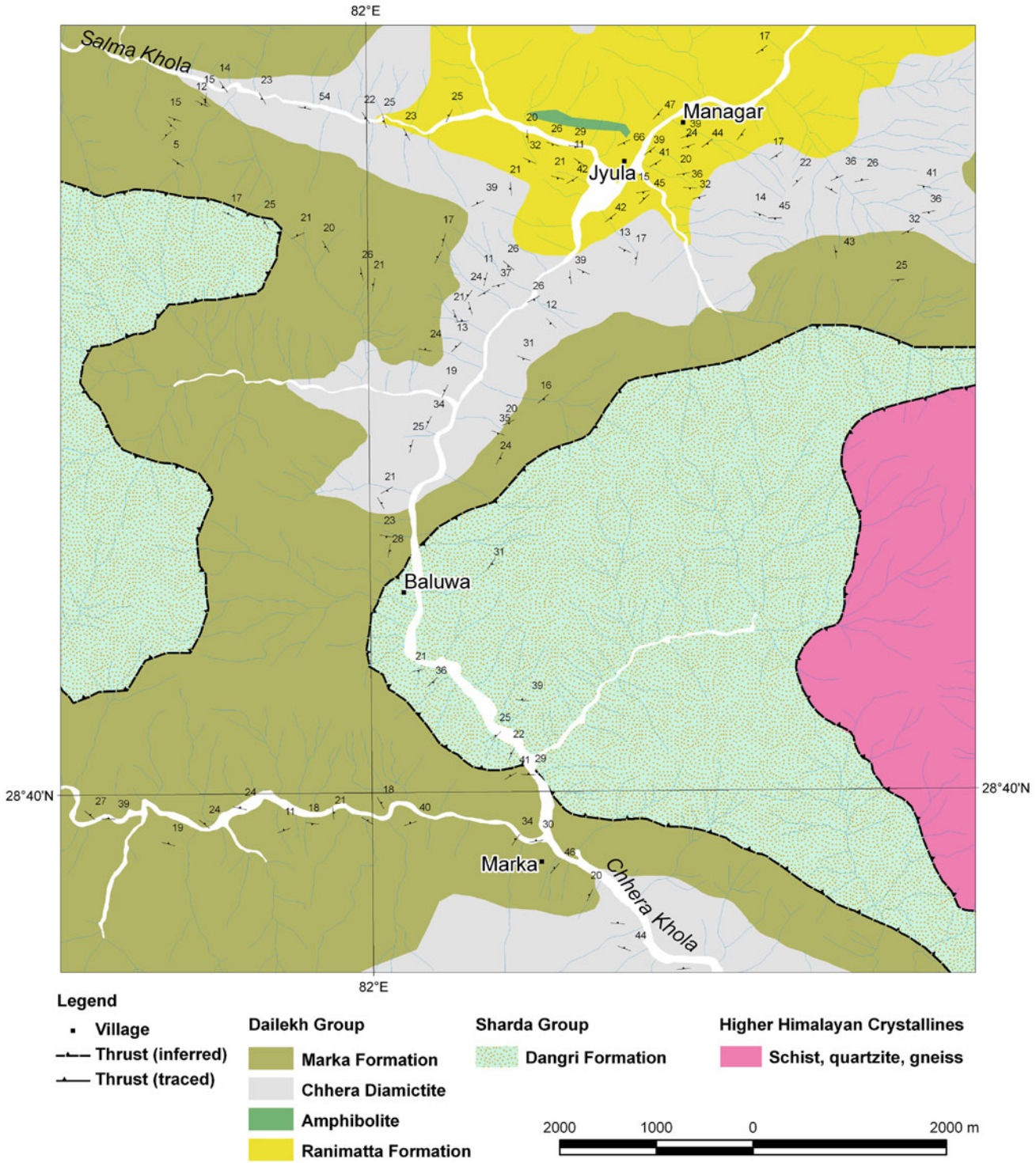

Fig. 8.12 Dome–basin structures seen in the Chhera Khola neighborhood. *Source* Author's observations

generally strongly stretched parallel to foliation, and they are also distorted or crenulated. The proportion of clasts in the metadiamictite varies widely and ranges from less than 1 % to about 10 %. The metadiamictite is repeated to the northeast and southwest, where it constitutes the core of two open synforms (Fig. 8.12).

There is a gradational contact between the Chhera Diamictite and overlying Marka Formation (Fig. 8.14). The Marka

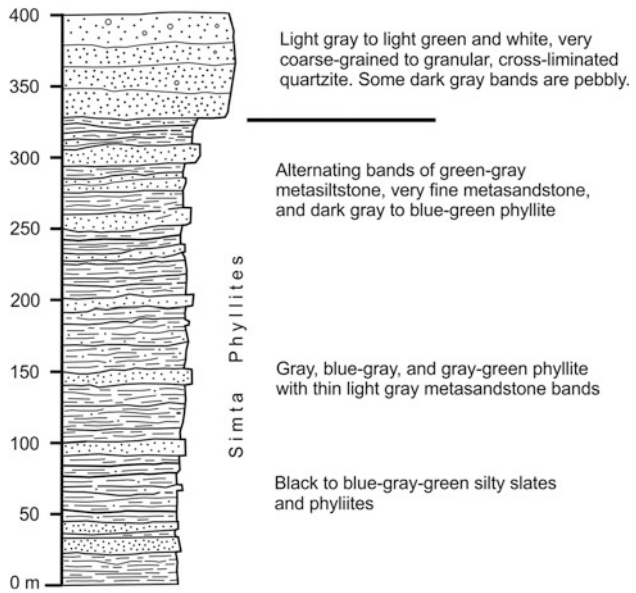

Fig. 8.13 A transitional passage from the Simta Phyllites to the overlying quartzites, exposed to the north of Salli Bajar. *Source* Author's observations

Formation is made up mainly of light gray to pale quartzites with gray to blue-gray garnet schist or phyllite interbands.

8.4.6 Folds of Chhera Khola

The intermediate zone of the Lesser Himalaya in the Chhera Khola, southwest of Jajarkot, lies within the eroded core of the Jaljala Synform. The rocks have undergone superposed folding, giving rise to dome–basin-like structures, where a small domal culmination at Baluwa is surrounded by four wide synformal depressions. The noncylindrical nature of folds is evident from the geological map (Fig. 8.12) as well as stereographic projection of foliations and lineations (Fig. 8.15).

8.4.7 Budar Thrust Termination

The Budar Thrust has in its hanging wall the Dailekh Group of rocks, whereas the footwall is represented by limestones, slates, and shales of the Lakharpata or Gwar Group with some younger rocks of the Surkhet or Tosh Group. The thrust comes very close to the Siwaliks and terminates against the imbricate slices of the Kubhinde Complex, just east of the Bheri River, near Botechaur (Fig. 8.16).

8.4.8 Frontal Imbricate Zone

On the right bank of the Bheri River, immediately north of the Middle Siwaliks, there is a zone of imbricate thrusts making a network of splays, emerging presumably from the Main Himalayan Thrust. In this zone, a variety of rocks, including stromatolitic dolomites, pink quartz arenites, phyllites, and Early Miocene strata is juxtaposed (Fig. 8.16). These rocks make a narrow (less than 3 km) belt, which expands significantly farther east (see below). The region east of the Bheri River is represented by a single splay designated as the Botechaur Thrust.

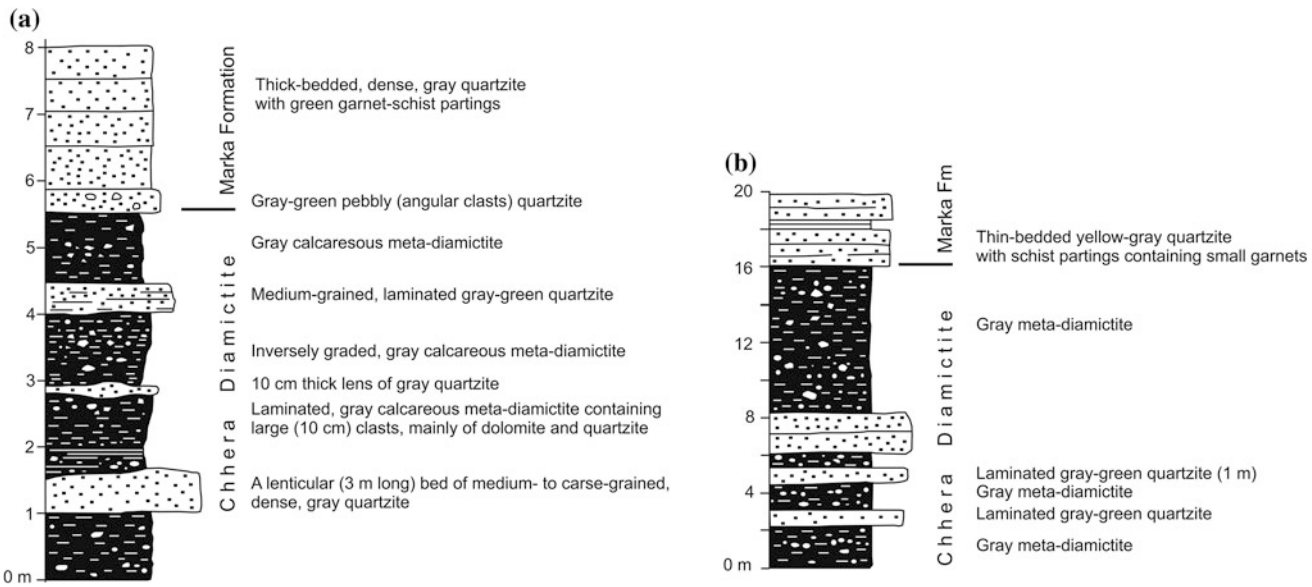

Fig. 8.14 Transitional contact between the Chhera Diamictite and the Marka Formation observed, **a** near Raijobra, on the way to Ahale and, **b** at Ratmata. *Source* Author's observations

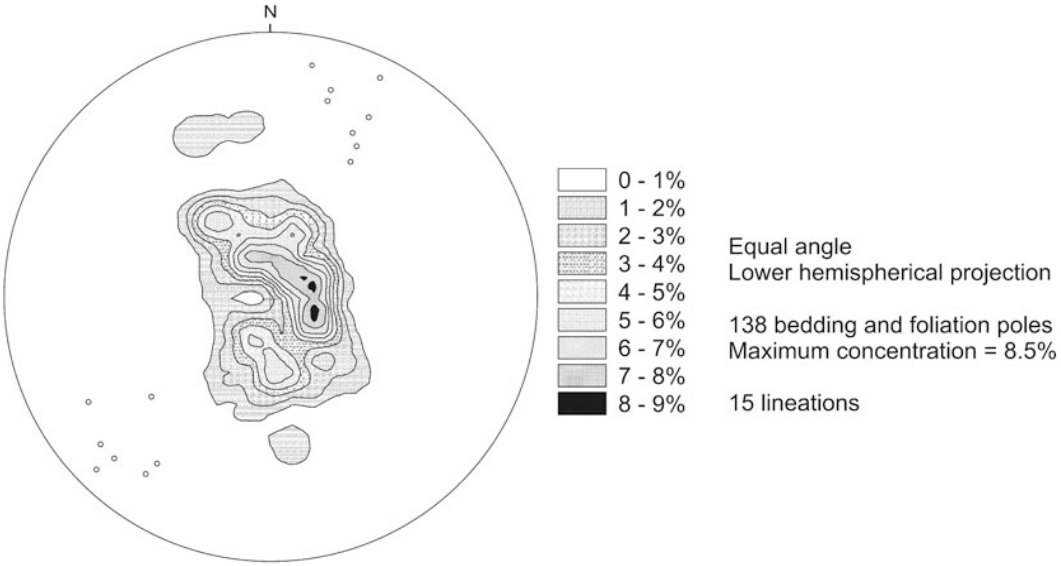

Fig. 8.15 Stereographic plot of foliations and lineations from the Chhera Khola area. Non-cylindrical nature of folds is evident. *Source* Author's observations

8.4.9 Daban Supergroup

A narrow strip of the Daban Supergroup (Dhital and Kizaki 1987b) is seen to the north of the Botechaur Thrust. The Main Boundary active fault coincides with this thrust. The active fault crosses the Bheri River at Botechaur where it records some left lateral strike-slip displacement (Nakata et al. 1984).

The Proterozoic Gwar Group, composing the lower part of the Daban Supergroup, begins with black laminated slates of the Ranagaon Formation (Fig. 8.16). They form a few hundred meter-wide zone in the hanging wall of the Botechaur Thrust. The black slates or shales facilitated the movement of the hanging wall flat of the Botechaur Thrust for tens of kilometers. The slates transitionally pass upwards to the Khamari Formation, comprising light pink and pale yellow coarse-grained quartz arenites with red-purple and gray-green shale partings or thin beds. The transitionally succeeding Hapurkot Formation is made up of quartz arenites, shales, and dolomites with many short columnar stromatolites. The Hapurkot Formation gives way to the domed stromatolite-bearing Dhorbang Khola Formation and then to the Sirchaur Formation, containing interlaminated gray-green or pink-purple limestones. The Sirchaur Formation is separated by a disconformity from the overlying gray to brown sandstones and black shales of the Sattim Formation. This formation is followed upwards by red-purple mudstones or shales and gray-green sandstones of the Dubring Formation. In the Beteni Khola, the gray dolomites of the Dhorbang Khola Formation are disconformably overlain by the Dubring Formation of sandstones and shales with a few hematite beds (Fig. 8.17).

8.5 Outer Lesser Himalaya of Dang, Sallyan, and Piuthan

The Botechaur Thrust and Main Boundary active fault, alias the Main Boundary Thrust, run along the north foothills of the Dang Valley, where they juxtapose the Lesser Himalayan rocks with the Siwaliks or deformed fluvial sediments. The rocks bounded by the Botechaur Thrust and Kapurkot Thrust belong to the Daban Supergroup, whereas those resting over the Kapurkot Thrust constitute the Sharda Group (Fig. 8.18). In this region, the Kapurkot Thrust propagated towards the foreland as a passive roof thrust, whereas the Botechaur Thrust played the role of a floor thrust. Both of these major thrusts constituted a large duplex with many horses bound within them (Dhital and Kizaki 1987a). Frequently, a thick Kumak Carbonate band appears as a detached horse, which is concordantly folded with the roof thrust. The intricate distribution of outliers and klippen throughout the region is the consequence of recent widespread erosion of the roof as well as the underlying horses.

8.5.1 Sharda Group

The low-grade metamorphic rocks of the Sharda Group occupy the northwest part of the Mahabharat Range in Dang and Sallyan. They also extend towards the Bheri River and farther northeast in the Midlands of west Nepal (Figs. 8.18 and 8.19). The Sharda Group consists of the following formations, respectively, from bottom upwards (Dhital and Kizaki 1987b; Dhital 1992).

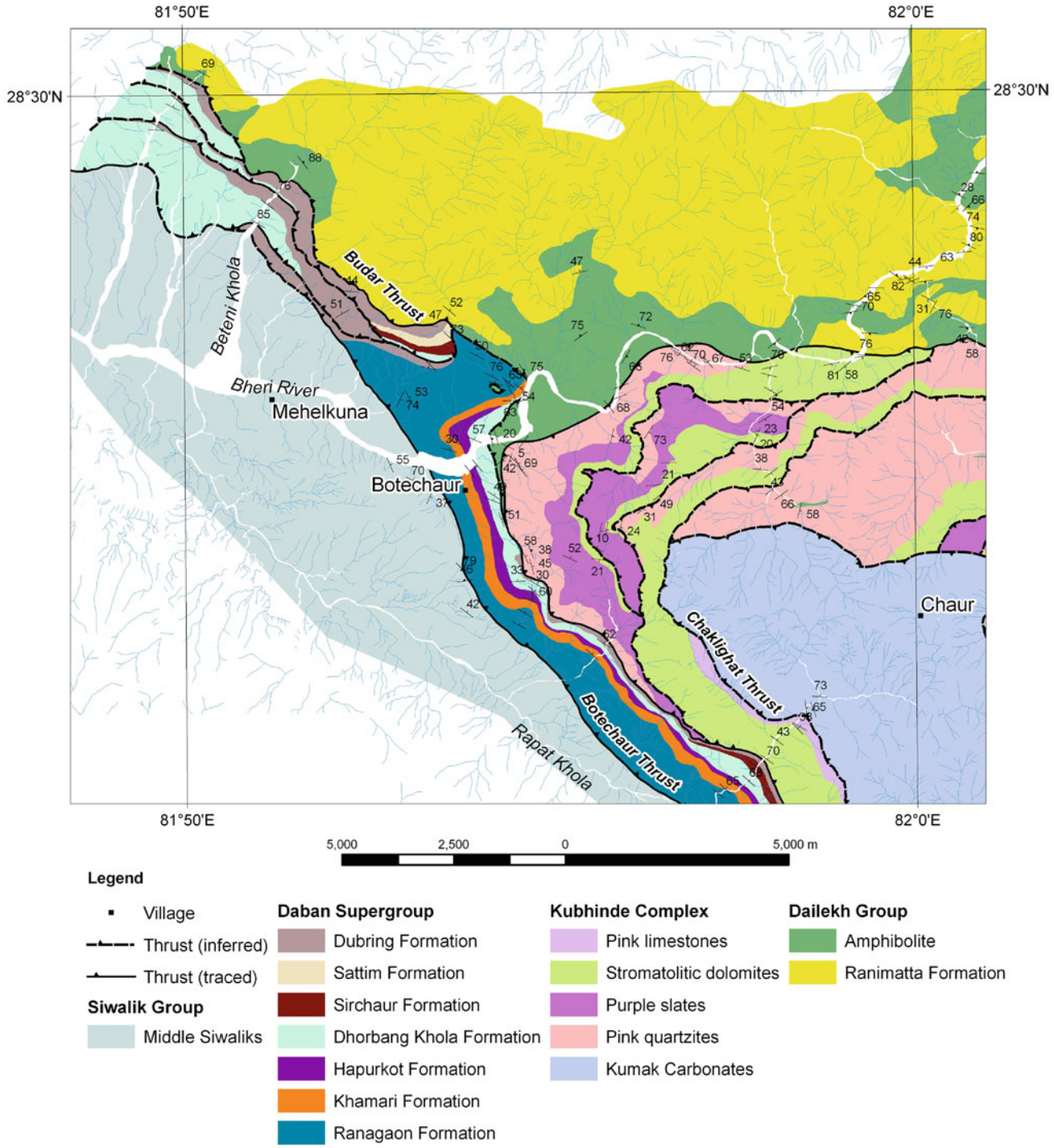

Fig. 8.16 Frontal faults around Botechaur. *Source* Author's observations

The lowest unit of the Sharda Group is represented by the Dangri Formation (Fig. 8.20). It is made up of parallel-laminated, gray and gray-green phyllite or slate bands (2–30 m) alternating with very thick-bedded, coarse-grained, gray, yellow, and white quartzites. As a rule, the phyllites dominate (about 75 %) over the quartzites. Frequently, the quartzite–phyllite transition is gradual, and marked by thin (1 mm to 1 cm) parallel and continuous laminae of quartzite, alternating with thin (1–3 mm) phyllite laminae. In the phyllite, there are also some medium- to fine-grained silty laminae that grade into the clayey laminae. On the other hand, the phyllite–quartzite transition is rather abrupt. The

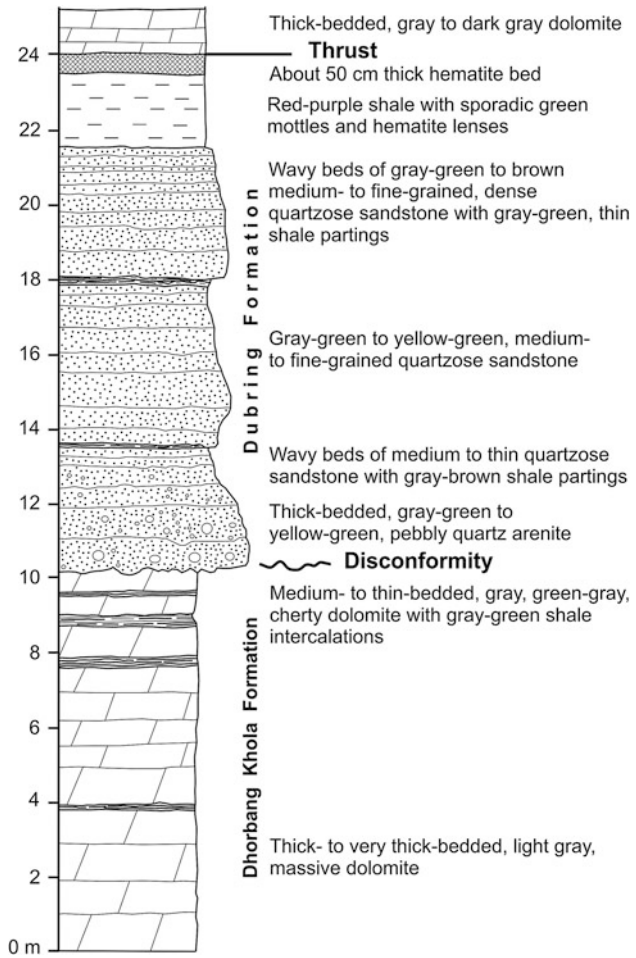

Fig. 8.17 Disconformity between the Proterozoic dolomites and Eocene Dubring Formation in the Beteni Khola. *Source* Author's observations

quartzites are represented mainly by coarse- to fine-grained quartz arenites or subarkoses. In the vicinity of the Kapurkot Thrust, the grains are stretched parallel to foliation, and the quartz grains display conspicuous pressure shadows.

Towards the upper section, the quartzite bands gradually become thicker at the expense of the phyllite bands, and finally they grade into the overlying Balle Quartzite. Towards the upper contact, extremely rare, thin bands of conglomerate are also found in the Dangri Formation. The clay and sand beds constituting the Dangri Formation were presumably deposited in a transitional zone between the sandy beach and continental shelf. The Dangri Formation is more than 500 m thick (Fig. 8.20).

The transitionally overlying Balle Quartzite (Fig. 8.20) shows in thick- to very thick-bedded white, light gray, and green-gray bands, which are coarse- to very coarse-grained and infrequently pebbly. They are made up of quartz arenites and subarkoses, and commonly alternating with up to 20 m thick dark green and gray-green phyllites. The proportion of phyllite varies from place to place and generally oscillates between less than 10 and 50 % of the total thickness. Towards the upper part of the Balle Quartzite appear very thick quartzite beds with a red tint (Fig. 8.21). The conglomerate beds have a sharp scoured lower contact with the underlying gray quartzites. The pebbles in the conglomerate are frequently made up of dark gray to black, light gray, and green-gray quartzites. The pebbles are about 3 cm wide, 10 cm long, and sometimes they are stretched parallel to foliation. The conglomerate beds also contain thin lenses of granular to very coarse-grained sandstone. The conglomerates, parallel- and cross-laminated quartzites with ripples, and overlying phyllites constitute fining-upwards cyclic sequences. Also sporadically present in the quartzites are granular and pebbly lenses. Under the microscope, the quartz grains composing the quartzite exhibit concavo-convex and sutured contacts, they display conspicuous pressure shadows, and near their grain boundaries are concentrated clusters or stringers of sericite. On the other hand, the alternating phyllites are made up essentially of chlorite and sericite.

The Balle Quartzite was deposited on sandy beaches, but its upper part, made up of conglomerates, quartzites, and phyllites, was the product of a fluvial environment. The Balle Quartzite is about 1,000 m thick and it is disconformably succeeded by the Sallyan Diamictite (Fig. 8.20).

The gray-green Sallyan Diamictite contains clasts of diverse composition. Generally, they range in size from 2 to 70 cm, and they are composed of gray limestone or dolomite; white, pink, gray, green-gray, and black quartzite; black chert; white marble; black slate; light gray granite; and infrequent green-gray schist. The proportion of matrix and clasts varies widely in the diamictite. Generally, the matrix is as much as 70–90 % of the rock by volume and rarely is it less than 20 %. The matrix is also represented by poorly sorted green-gray to dark brown granules as well as sand and silt grains of quartz, feldspar, dolomite, and lithic fragments, floating in a cryptocrystalline sericitic mass constituting more than 80 % of the total. The foliation in the diamictite is often oblique to the bedding. The clasts are frequently deformed to yield lens-shaped grains, oriented parallel to foliation. The roundness of clasts larger than 4 mm varies from 0.2 to 0.6 (i.e., subangular to rounded), and the length/width ratio changes from 2 (parallel to foliation) to 5 (perpendicular to foliation).

Another important aspect of the Sallyan Diamictite is that the average size of clasts decreases stratigraphically upwards and the green-gray matrix gradually becomes dark gray to black. There is a 30 cm thick band of gray-green sandstone towards the upper part, and its upper contact is marked as the boundary between the Sallyan Diamictite and overlying Phalabang Formation. The Sallyan Diamictite is about 500 m thick, but its thickness varies widely. It invariably grades into the overlying Phalabang Formation.

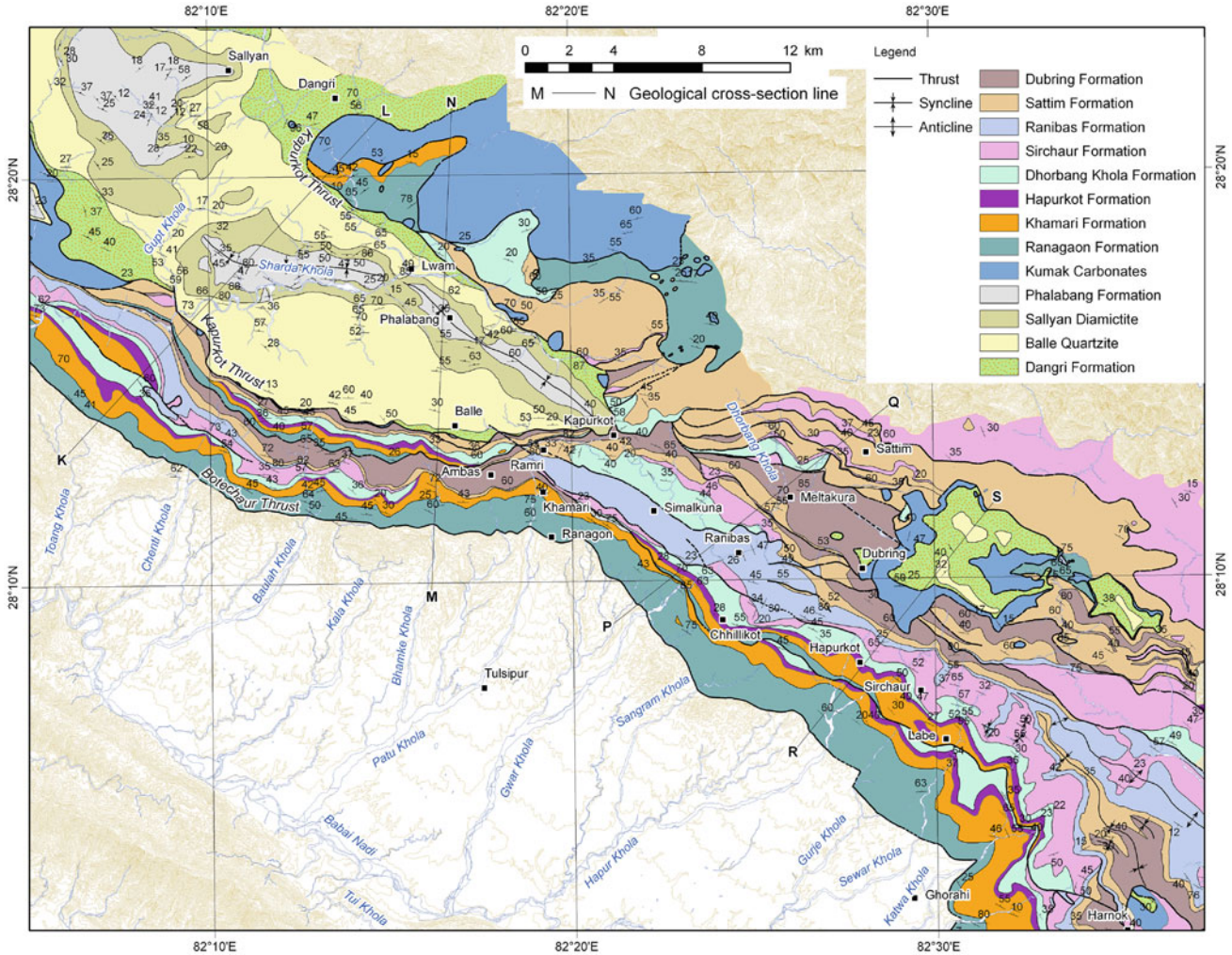

Fig. 8.18 Geological map of north Dang, Sallyan, and Piuthan, Lesser Himalaya in west Nepal. *Source* Author's observations

The Phalabang Formation mainly occupies the synclinal cores, and is comprised of black carbonaceous slates and phyllites. There is about a 60 m thick succession of green-gray, dark gray to black sandstone at its basal part. In the slates, their pelitic matrix constitutes about 50 % and in it are 0.02 to 0.1 mm long sericite and chlorite flakes arranged parallel to the foliation. The slates also contain 0.04 to 1.5 mm long and 0.01 to 0.03 mm wide detrital quartz and feldspar lenses, which are most likely the previous laminae disrupted by the foliation. The carbonaceous matter is dispersed in the slates as a very fine dark brown to gray mass, and occasionally includes irregular carbonaceous fragments of about 0.01 mm in size. A weathered variety of carbonaceous slate is gray-brown to green-gray in color. There are also areas where gray-brown to dark green slates or phyllites and micaceous metasandstones alternate with each other.

The Phalabang Formation was presumably deposited in a fluvio-glacial to lacustrine environment. Its thickness varies from less than 75 m to more than 450 m.

8.5.2 Correlation and Comparison of Sharda Group

From the Phalabang Formation, Fuchs and Frank (1970, p. 43) reported approximately 20 m thick bleaching black slates, which yielded a relatively well-preserved spore of the genus *Vittatina*, and based on this finding, they considered it to belong to the Lower Gondwanas.

The Sallyan Diamictite is somewhat similar to the Sisne Formation (Chap. 9). But the latter is resting disconformably over the Kerabari Formation of dolomite and limestone,

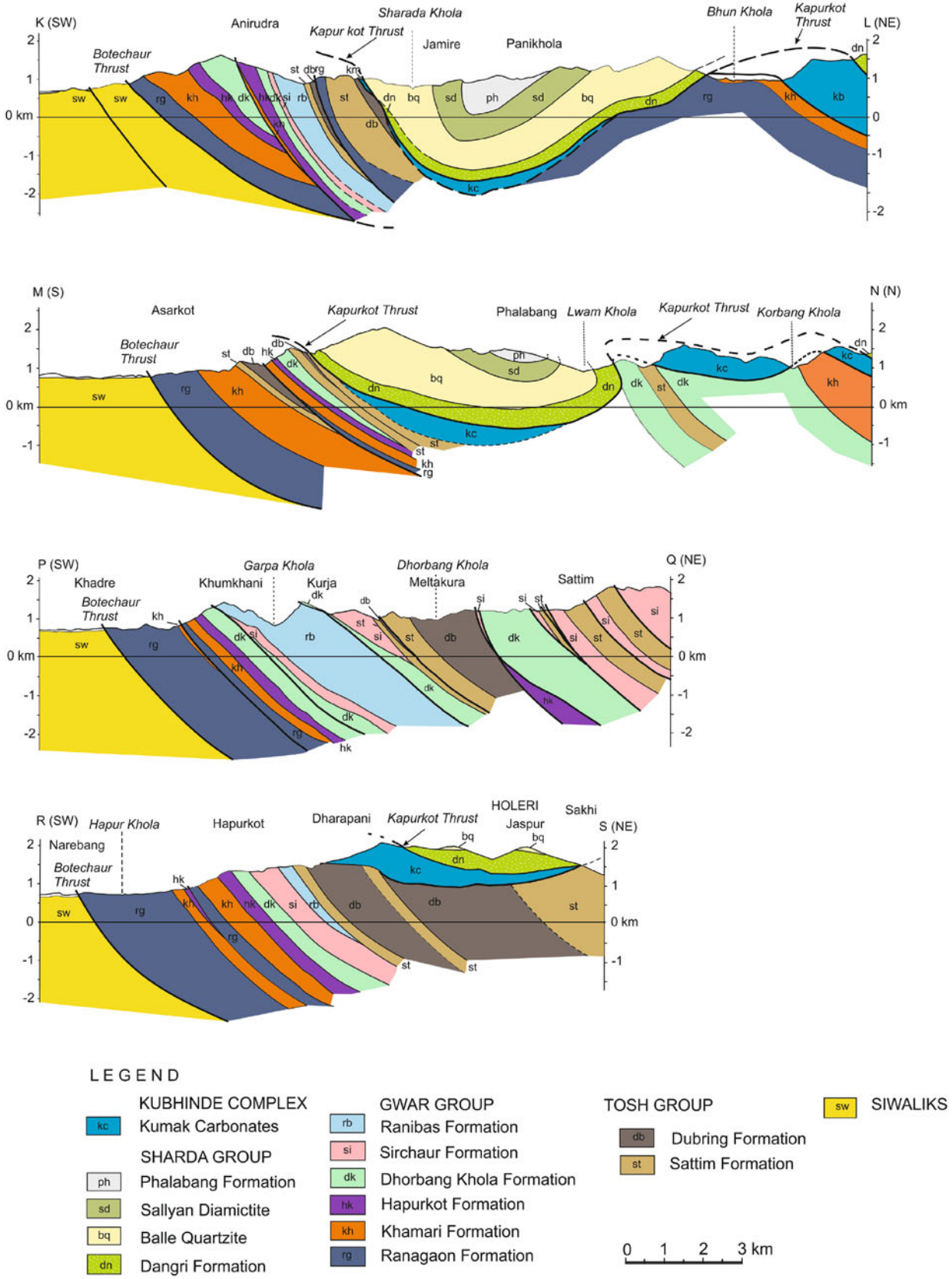

Fig. 8.19 Geological cross-section across the Lesser Himalaya of north Dang and Sallyan. *Section lines* are shown in Fig. 8.18. *Source* Author's observations

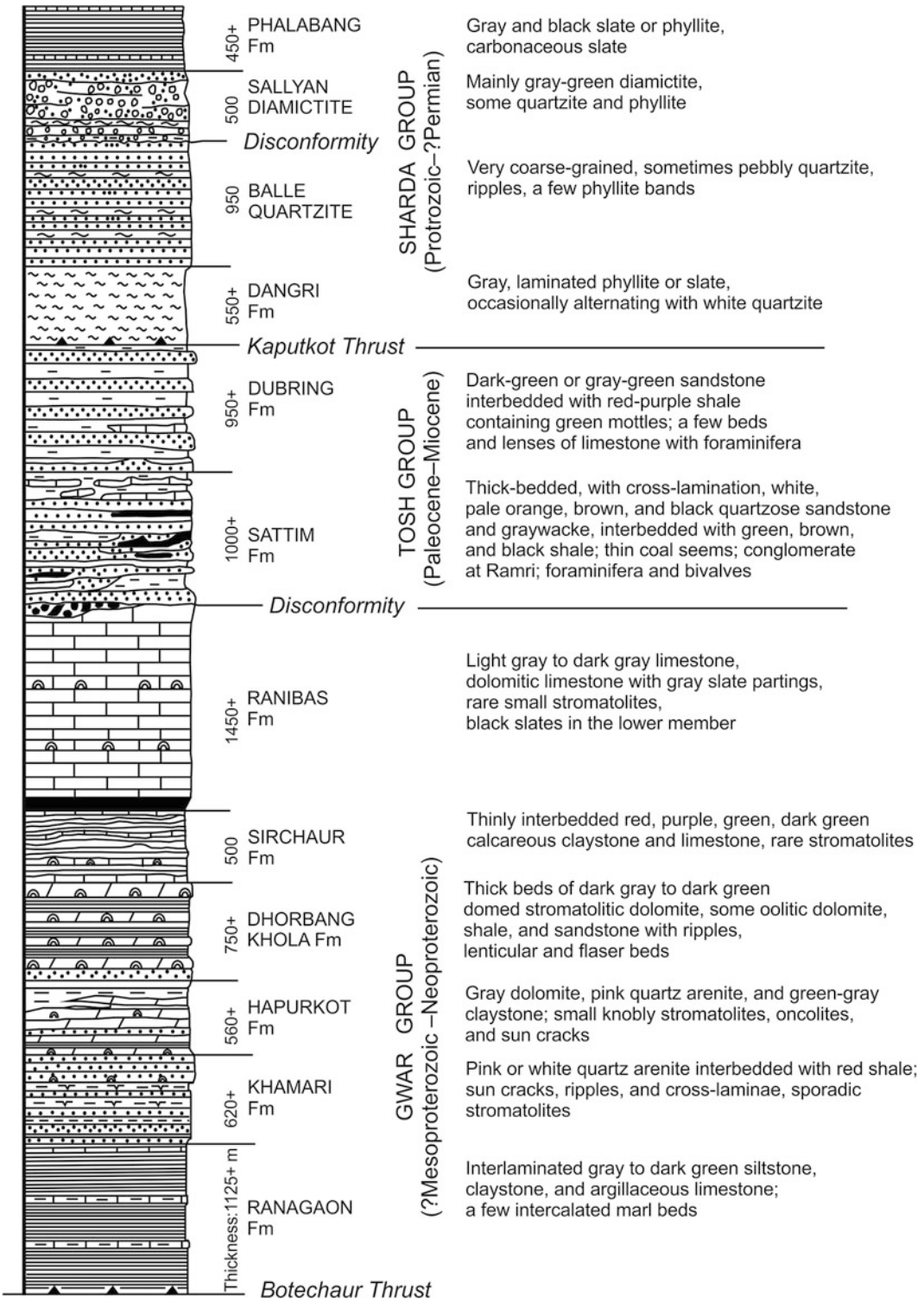

Fig. 8.20 Generalized tectonostratigraphic column of the Lesser Himalaya in north Dang, Sallyan, and Piuthan. *Source* Modified from Dhital and Kizaki (1987b). © University of the Ryukyus. Used by permission

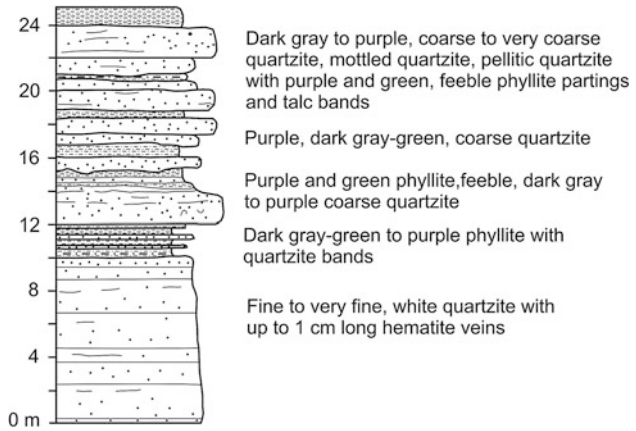

Fig. 8.21 The upper section of the Balle Quartzite containing pink and purple phyllites and quartzites. *Source* Author's observations

equivalent to the Ranibas Formation in the present area. The Sisne Formation is overlain by the Taltung Formation, containing plant fossils of Upper Gondwana age. The Sallyan Diamictite is distinct from the Blaini Formation, in that it is free of limestones (Brookfield 1987). The Sisne Formation rests unconformably on the Kerabari Formation, whereas the Ramri Conglomerate and other members of the Sattim Formation (presumably equivalent to the Amile Formation) overlie the Ranibas Formation disconformably.

The Sallyan Diamictite is found in the roof thrust of essentially low-grade metamorphic rocks, whereas the Sisne Formation lies in the sedimentary sequence of the frontal ranges. Therefore, if the Sallyan Diamictite and Sisne Formation are homotaxial in origin, the former must have been subsequently metamorphosed and also distributed in the more inner part of the Lesser Himalaya. On the other hand, the Chhera Diamictite is metamorphosed to a garnet grade and it is covered by the Sharda Group of rocks. Hence, its position is uncertain. Because there are many Proterozoic diamictite sequences, the Sallyan Diamictite and the Chhera Diamictite could be one of them, and the scanty plant remains in the Phalabang Formation need further investigation.

8.5.3 Gwar Group

The Proterozoic Gwar Group consists essentially of shales, sandstones, and carbonates. It is separated from the overlying Tosh Group by a ubiquitous disconformity with erosional surface and a basal conglomerate, whereas its lower part is delimited by the Botechaur Thrust. The Gwar Group attains a thickness of more than 5,000 m and comprises the following six formations (Fig. 8.20).

The Ranagaon Formation uninterruptedly extends throughout the north edge of the Dang Valley for over 60 km and constitutes the foothills of the Mahabharat Range. In fact, these rocks continue tens of kilometers farther to the southeast and northwest of the valley and override the Siwaliks along the Botechaur Thrust or the Main Boundary active fault.

The Ranagaon Formation is a rather monotonous sequence of dark gray to green-gray laminated siltstones, claystones, argillaceous limestones, and slates, which weather into yellow and brown tinges (Fig. 8.22). They are feeble, intensely fractured, and injected by many quartz and calcite veins. Slaty cleavage is prominent near the thrust, but gradually disappears farther upwards. This formation is further classified into the following two members.

A 5 to 25 m wide zone of dark gray to black fault gouge marks the base of the Lower Member, composing the hanging wall of the thrust. Frequently, it is carbonaceous and occasionally slightly calcareous. Moving away from the thrust, the gouge gives way to the fault breccia, containing up to 2 mm wide and 1–2 cm long parallel and lenticular bands with quartz, feldspar, and lithic fragments less than 1 mm across. In the carbonaceous cryptocrystalline matrix of the fault gouge as well as in the bands, abundant minute sericite crystals and a few prismatic quartz grains are oriented parallel to the foliation.

The zone of fault gouge and breccia is followed by a sequence of thinly (0.5–2 mm) interlaminated, very coarse- to medium-grained (0.02–0.06 mm) siltstone and calcareous siltstone, with quartz as a dominant (75 %) mineral and subordinately occurring feldspar, calcite, chert, and carbonaceous matter in their descending order. The moderately sorted, subangular to subrounded grains display sutured to concavo-convex contacts, and they are cemented by calcite and clay or surrounded by carbonaceous veinlets. In them, lighter-colored fine laminae contain more microspar cement than the darker ones. Infrequent sparry calcite patches are present in the calcareous laminae, where many quartz grains are partly or fully replaced by calcite. There also occur tiny sericite crystals and authigenic quartz overgrowths around some grains. The rock is well cleaved and the grains are slightly elongated parallel to the cleavage.

Farther up-section, this member continues as a laminated (less than 1 mm to 2 cm) sequence of siltstone, calcareous claystone, and argillaceous limestone, where dark gray to black and light gray to green-gray laminae regularly alternate and extend for more than 2 m. They are commonly graded (from very coarse silt to clay) and exhibit sharp lower contacts. A few thick to very thick (0.5–1 m), massive, argillaceous limestone and marl beds are also intercalated. An approximately 70 cm thick topmost bed of them is designated as the upper limit of this more than 1,075 m thick Lower Member (Fig. 8.23).

The Upper Member of the Ranagaon Formation is composed principally of 10 to 15 cm thick, light gray to white

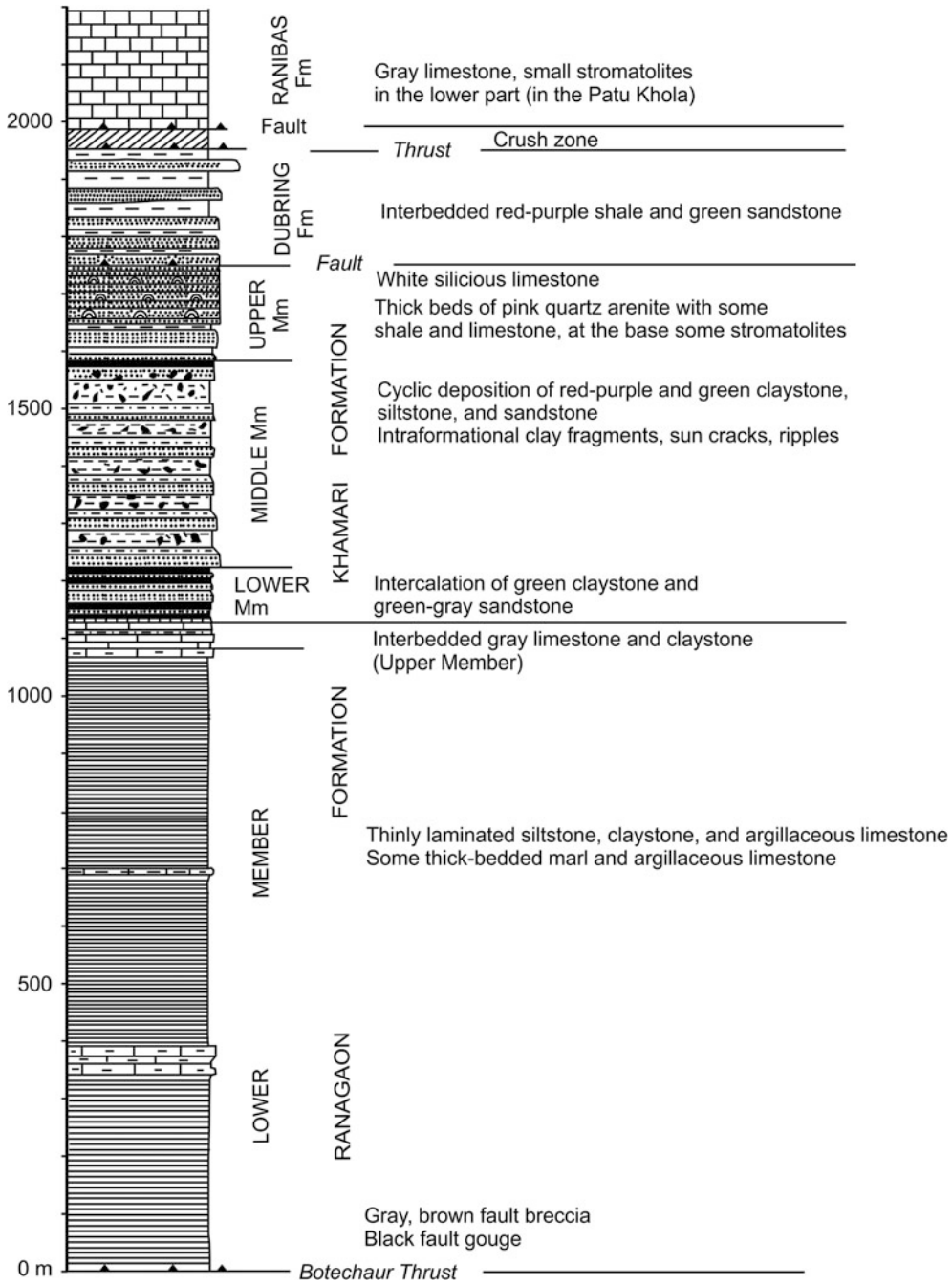

Fig. 8.22 Columnar section, measured along the Patu Khola, showing the contact between the Ranagaon Formation and the overlying Khamari Formation. The lower parts of the Dubring and Ranibas Formation are cut out by imbricate faults. *Source* Modified from Dhital and Kizaki (1987b). © University of the Ryukyus. Used by permission

limestones, interbedded with dark yellow to light green, laminated, calcareous siltstones, and argillaceous limestones (Fig. 8.23). The siltstones are well cleaved, and display textural features akin to those of the Lower Member, but are more calcareous and contain a micritic matrix. The limestones consist of finely crystalline (0.06–0.08 mm) pseudosparite with a hypidiotopic texture. They also contain a trifling quantity (1–2 %) of tiny (0.02–0.05 mm) quartz, feldspar, and sparry calcite grains in about 0.6 mm wide patches. The pseudosparite infrequently includes lenticular to curved, thin (0.8 mm) laminae, comprising very coarse to fine silt of quartz and feldspar with sporadic sericite flakes. Most of the detrital grains are "floating" in a fine sparite matrix, but some exhibit point contacts.

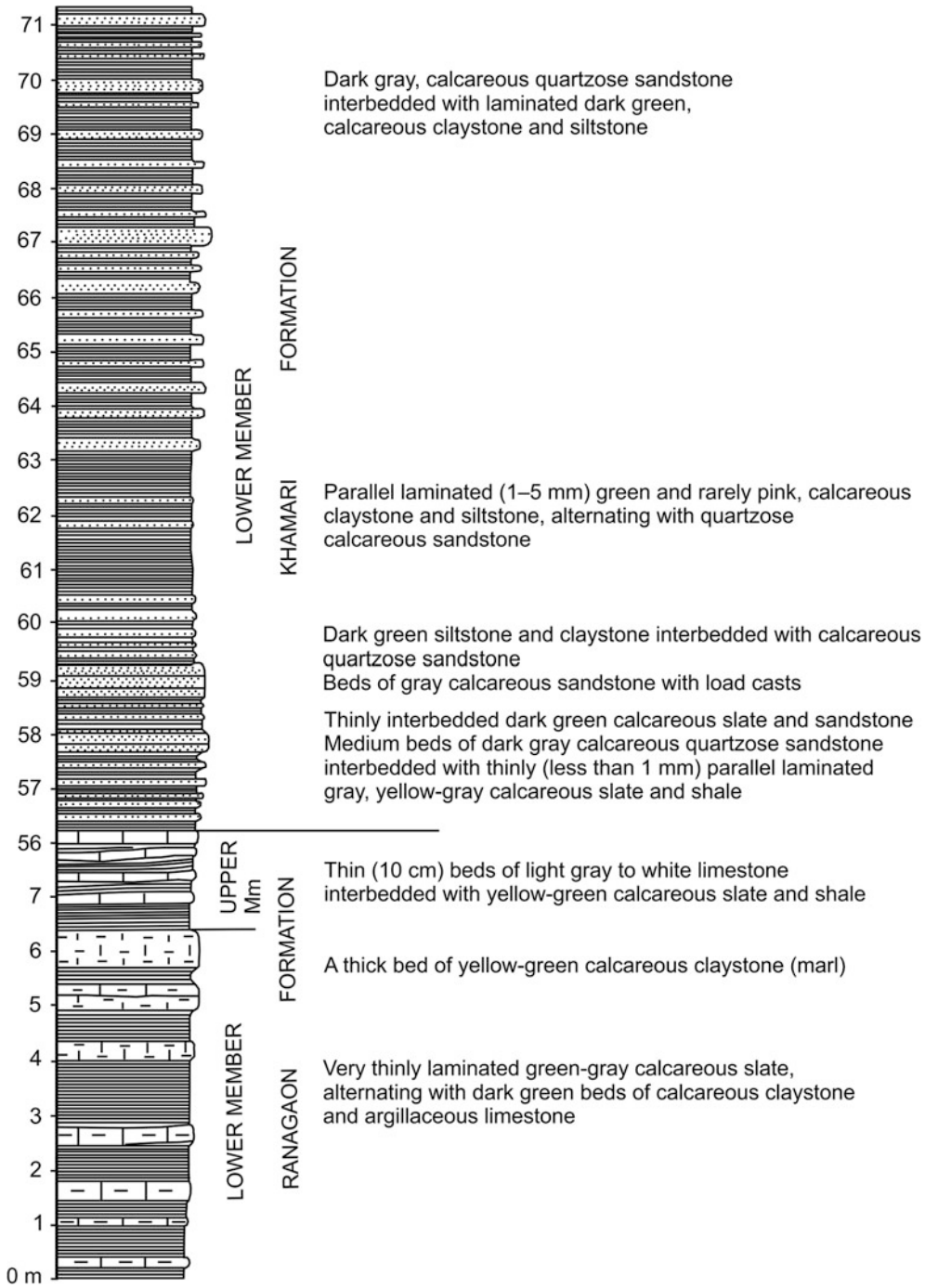

Fig. 8.23 Detailed columnar section, measured along the Patu Khola, exhibiting the contacts between the lower and upper members of the Ranagaon Formation, and between the upper member of the Ranagaon Formation and the lower member of the Khamari Formation. *Source* Modified from Dhital and Kizaki (1987b) © University of the Ryukyus. Used by permission

This member is predominantly parallel-laminated, although extremely rare trough cross-laminated limestones do occur. It is about 50 m thick, and grades transitionally into the overlying Khamari Formation (Fig. 8.23).

The Khamari Formation is distinguished from the underlying argillaceous Ranagaon Formation by the appearance of quartz arenites. Generally, the Khamari Formation represents an interbedded succession of pale orange, yellow, and pink quartz arenites; calcareous sandstones; and red, purple, and green shales or slates with a few argillaceous limestone beds. It is further split into the following three members (Fig. 8.22).

The Lower Member of the Khamari Formation begins with an interbedding of gray to dark green, medium- to thin-bedded calcareous sandstones and dark green to olive green thinly laminated claystones, siltstones, and argillaceous limestones (Fig. 8.23), quite similar to those from the underlying Ranagaon Formation. The Lower Member also contains a few thick (0.5–l m) calcareous sandstone and quartz arenite beds with load casts at their bases, whereas some others preserve beautiful wave ripples on their upper bounding surfaces. There are also a number of wavy and lenticular beds of sandstone and siltstone. The calcareous sandstone beds become successively thicker stratigraphically upwards.

The very fine calcareous sandstones and very coarse siltstones consist of quartz (60–80 %), plagioclase, microcline, and a few lithic fragments (chert and sparite). They are cemented by microspar (30–40 %) and cryptocrystalline mass. Their grains are subangular, moderately sorted, and exhibit tangential as well as concavo-convex contacts. In some sandstone beds, very thin (0.3 mm) laminae of claystone may be present. In some calcareous sandstones are infrequently present intraformational shale fragments, which become more abundant in the Middle Member. The Lower Member is 100 m thick.

The basal portion of the Middle Member contains an approximately 10 m thick sequence of light pink to white, very thick (2–4 m), massive, coarse-grained quartz arenite with indistinct thin laminae. The beds are wavy and non-parallel, and each of them is separated by a thin (1–2 mm) parting of green claystone. Ripples are very characteristic of this member and their index (length/height) is about 20.

The horizon is followed by a 6 m thick succession of very thin-bedded (1–2 cm), yellow-white quartz arenite with green calcareous claystone and siltstone. The siltstone and claystone are thinly laminated and the grain size decreases upwards.

The above sandstone sequence passes into a 4 m thick red-purple silty claystone bed, made up of thin, irregular, and discontinuous laminae. The claystone includes numerous intraformational shale fragments of the same composition and color, and is succeeded by an 11 cm thick gray sandstone bed with a sharp lower contact. The last bed is further overlain by many other sandstone and shale sequences. One such cyclic deposition (Fig. 8.24) contains the following rocks.

1. Quartzose sandstone: From 10 to 50 cm but exceptionally up to 2 m thick, white, pink, and pale yellow, infrequently green-gray, coarse- to medium-grained quartz arenites and sublitharenites contain intraformational shale fragments less than 1 mm to 1 cm in length; their upper surfaces are full of ripples. Under the microscope, some of the sand grains display an imbrication-like arrangement, they are well sorted, most of them are rounded, and a few are well rounded. The grains exhibit concavo-convex and sutured contacts, and constitute indistinct laminae. They also contain many detrital tourmaline and zircon grains.
2. Interbedded sequence: Red-purple or rarely green claystone and pink to yellow-gray siltstone and sandstone represent this sequence. Beds from 5 cm thick to thinly laminated are frequently wavy and lenticular, whereas the intercalated claystones contain intraformational shale fragments, sun cracks, and display convolute lamination.
3. Shale: Mainly red and purple, in places green, thick-bedded (1.5 m and more) mottled claystones and fine siltstones contain abundant intraformational shale fragments. They also contain conspicuously large (up to 1 cm wide) and many smaller secondary sun cracks. The rock is slightly calcareous and displays graded bedding as well as thin lamination. Its grain size decreases upwards from coarse silt to clay. Some laminae contain flat-lying shale fragments, and others display contrasting color banding. There may be present from 14 to 20 laminae within a centimeter-thick bed, and such laminae are frequently contorted to yield convolute and flame structures.

The Middle Member is about 350 m thick and gradationally passes into the overlying Upper Member.

The Upper Member of the Khamari Formation is similar to the Middle Member in many respects, but it contains many thick to very thick (up to 4 m) cycles of quartzose sandstone and calcareous quartzose sandstone, which are succeeded by thinner (generally less than 1 m) sandstone and shale cycles. It also contains three or four stromatolitic horizons, a few algal mats, and some dolosparite as well as pseudosparite beds. Owing to the presence of hard quartzose sandstones, composing more than 75 % of the total thickness, this member forms gorges and cliffs.

At the base of this member is a 75 cm thick bed of light green thinly (0.5–2 mm) laminated argillaceous limestone with purple mottles. This bed, with rather wavy and continuous laminae, gives way to a 2.5 m thick interbedded succession of pink siltstone and red claystone, followed by a 2 m thick, mottled, laminated, green argillaceous limestone. The last argillaceous limestone bed is overlain, respectively, by a 30 cm thick, coarse-grained, pink calcareous sandstone, and a 3 m thick, light pink, massive quartz arenite, grading into a succession of interbedded sandstone, siltstone, and shale.

Stromatolites first appear in this member on the upper surface of dolomitic quartzose sandstone beds (Fig. 8.25). The stromatolites contain some peloids and intraclasts (0.01–0.02 mm long) of microspar in their basal part, where tiny (0.04–0.08 mm) quartz grains are dispersed in a very finely (0.04–0.06 mm) crystalline dolosparite. The stromatolites also have some irregular and discontinuous laminae roughly parallel to each other. Their algal structure is marked by 1–2 cm thick alternating sparry and pseudosparry laminae. But there also set in some thin silty laminae. The stromatolite bioherms are approximately 15–50 cm in diameter and are

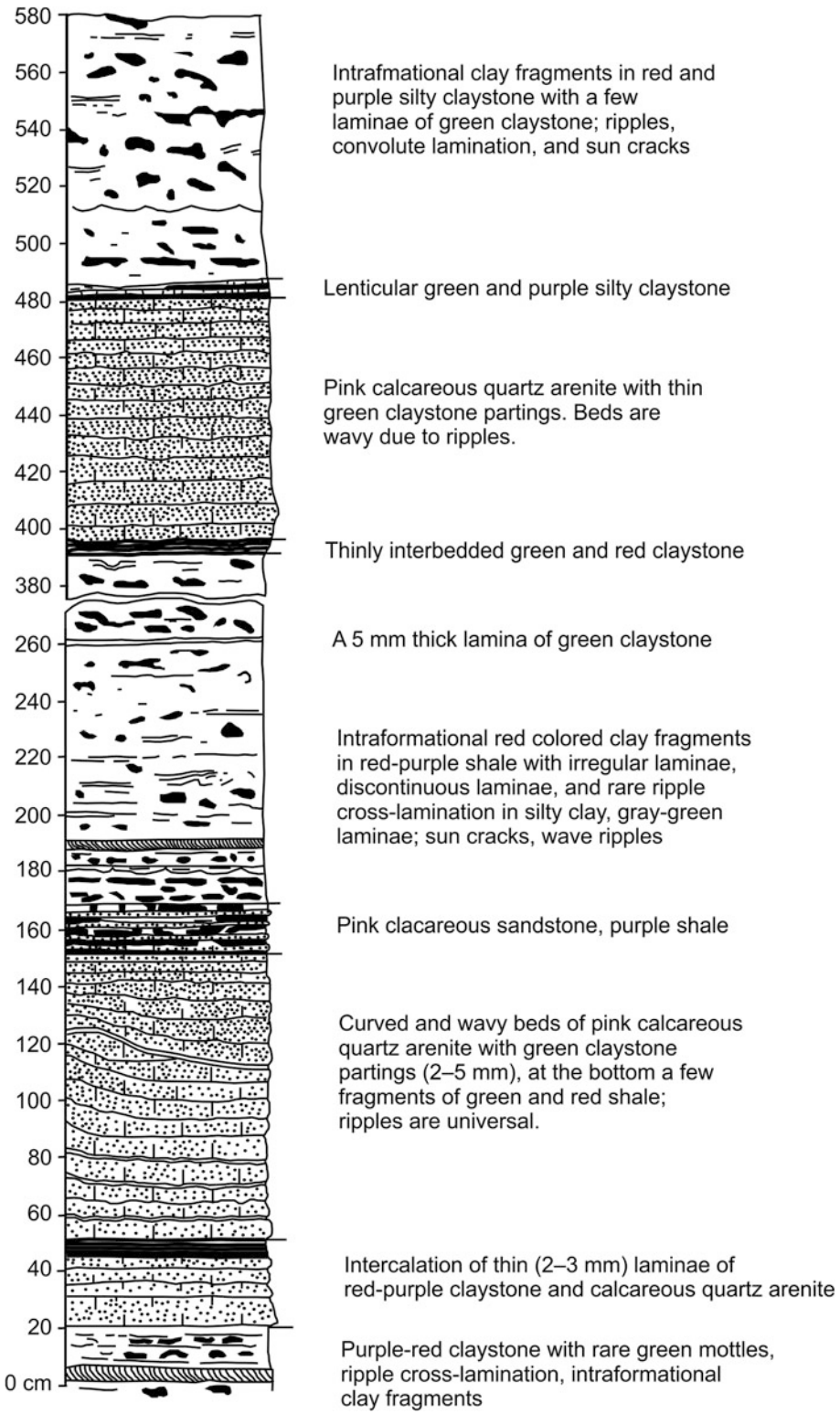

Fig. 8.24 Cyclic deposition in the Middle Member of the Khamari Formation, the Sisnya Khola. *Source* Modified from Dhital and Kizaki (1987b). © University of the Ryukyus. Used by permission

irregularly spaced. The domes are frequently 15–20 cm apart, circular in plan view, and 5–25 cm high. The stromatolites of higher horizons are flatter (height: 5–15 cm; diameter: 40–60 cm), and elongated to elliptical in plan view.

The last stromatolitic horizon is followed up-section by very thick (up to 3 m) and very coarse-grained quartzose sandstone beds, displaying a variety of current and wave ripples on their upper surfaces. There are also a few very

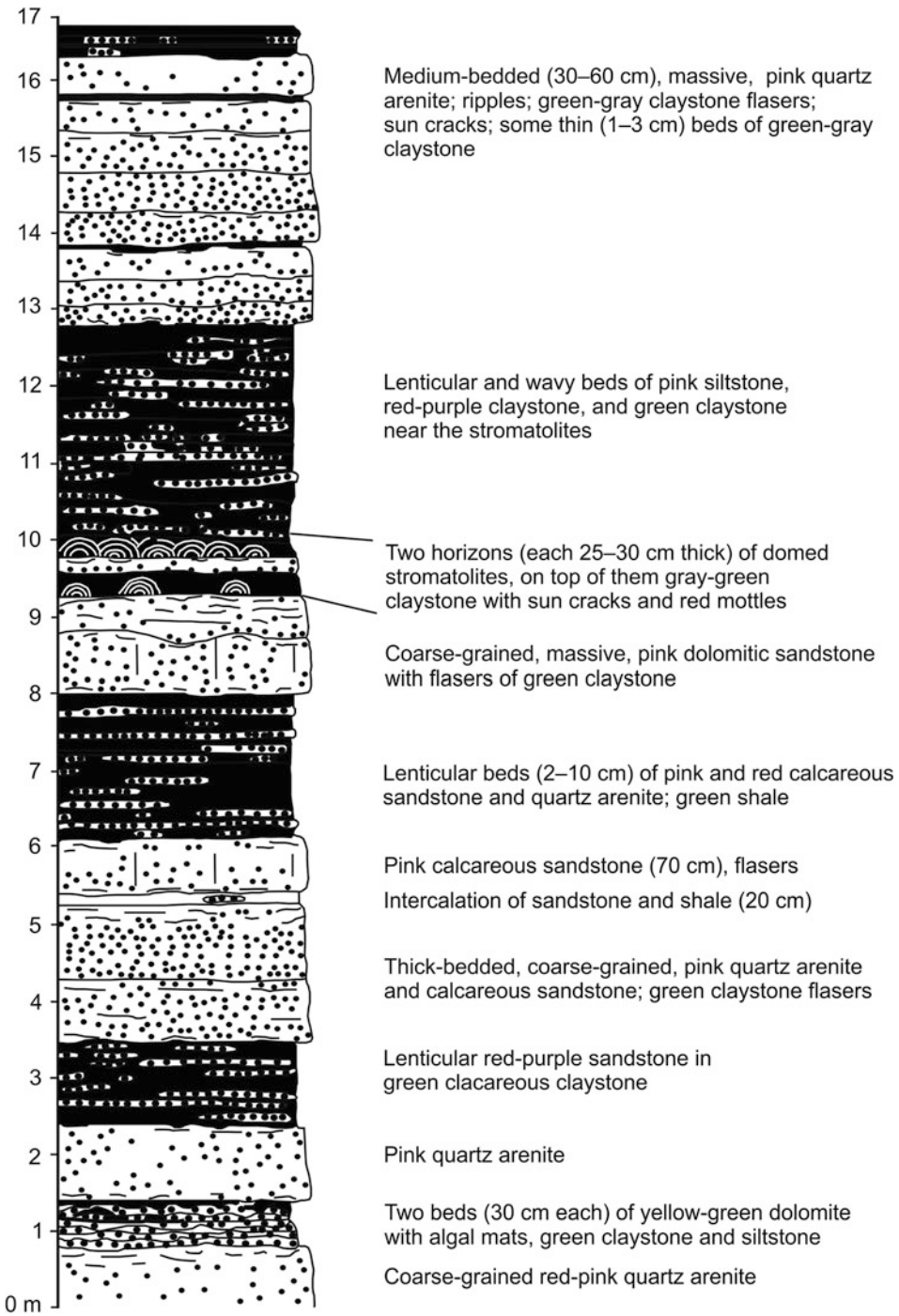

Fig. 8.25 Detailed columnar section showing the position of the lower stromatolite beds in the upper member of the Khamari Formation, the Patu Khola. *Source* Modified from Dhital and Kizaki (1987b). © University of the Ryukyus. Used by permission

coarse sublitharenite beds, containing red shale pebbles and sand grains of agate. The sandstones alternate with red and green mottled shales containing very wide sun cracks.

Within the upper 50 m of this member are a number of thick (30–70 m) white and light green lenticular silty dolomite beds, which are interbedded with green and red shales. The limestones are made up primarily of pseudosparite with sporadic microsparite spots and a trifling amount (5 %) of quartz silt. Apart from them, several beds of medium- to fine-grained pink calcareous sublitharenite are alternating with very coarse- to coarse-grained siltstone with tiny sericite grains oriented parallel to lamination. The Upper Member attains a thickness of 170 m and imperceptibly grades into the Hapurkot Formation.

The Hapurkot Formation has a mixed lithology of the underlying terrigenous and overlying carbonate rocks. It consists mainly of red or pink quartzose sandstones, calcareous sandstones, red-purple and dark green shales, and

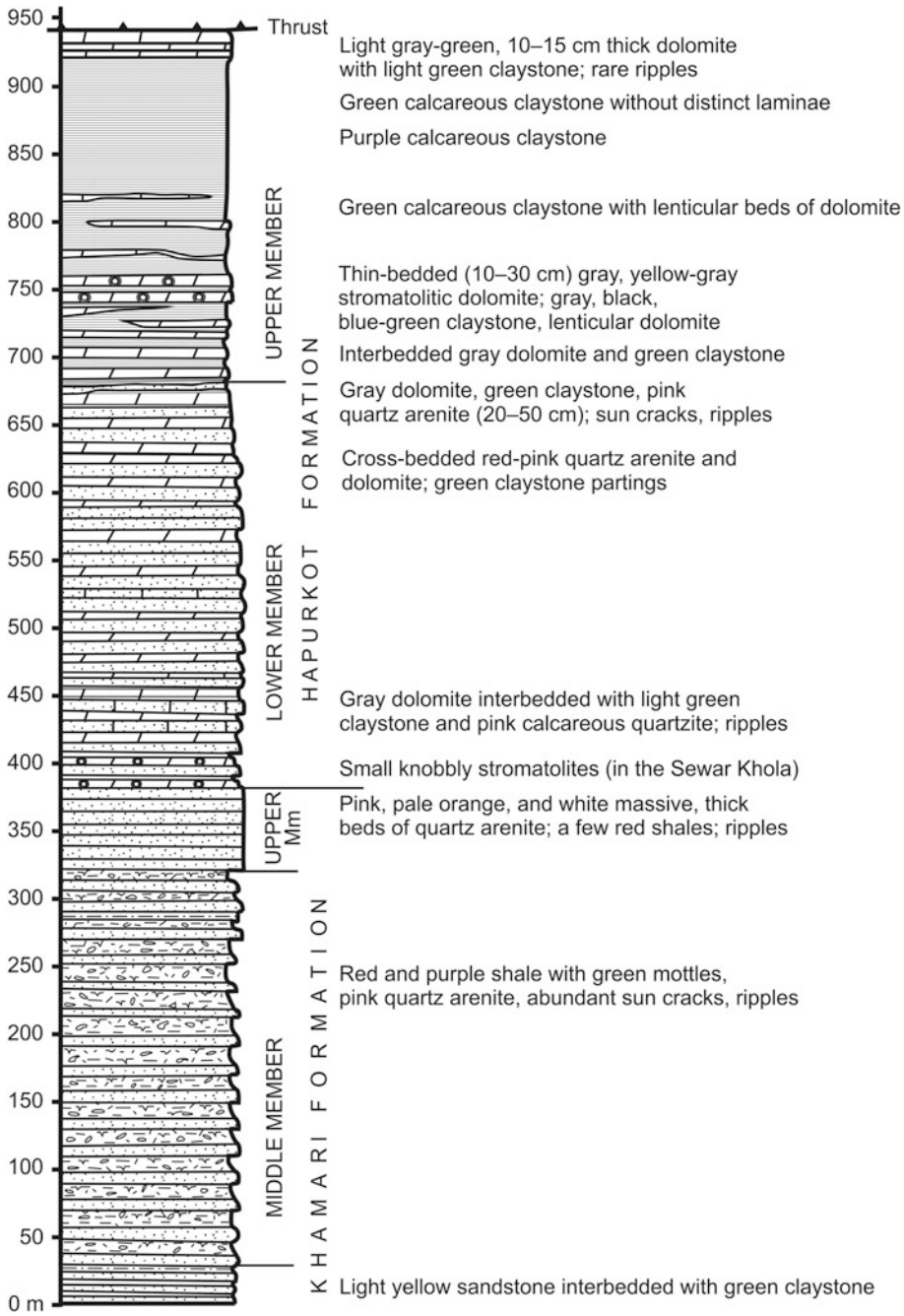

Fig. 8.26 Stratigraphic column depicting the transitional contact between the Khamari and Hapurkot formations. *Source* Modified from Dhital and Kizaki (1987b). © University of the Ryukyus. Used by permission

gray dolomites with small stromatolites. The Hapurkot Formation is divided up into the following two members.

The uppermost thick (50–70 cm) bed of light pink to white quartz arenite, representing the Khamari Formation, gives way to the rocks of the Lower Member of the Hapurkot Formation (Fig. 8.26), consisting of 10–20 cm thick green to dark green calcareous siltstone and gray-green dolomite beds alternating with red, green, and purple silty (0.01–0.02 mm) calcareous argillites, containing random sericite flakes.

To the south of Labe, this member begins with an intercalation of 10–20 cm thick gray-green dolomite and dark green calcareous siltstone together with dark red and green claystone. It is further succeeded by an interbedded sequence of purple calcareous shale with subordinate light green claystone and white to purple calcareous siltstone and sandstone. The calcareous shales contain thin (0.5–2 mm), wavy, parallel, and continuous laminae, whereas in the silty sandstones climbing ripple laminae predominate, and in the upper portions of claystones convolute laminations, isolated

sandstone pillows, and flame structures are conspicuous. Moving farther up-section, the proportion of purple and green calcareous shales varies considerably, and their purple varieties frequently contain intraformational shale clasts.

In the purple and violet calcareous claystones and pale yellow to gray calcareous quartzose sandstones are intercalated blue-gray dolomite beds, containing small (10–12 cm wide) domed stromatolites, whose average height does not exceed 4 cm and are covered by green-gray thinly laminated calcareous claystone and siltstone. This sequence is followed upwards by a 1.5 m thick gray dolomite, containing rounded to elliptical oncolites whose size ranges from 15 to 45 mm.

The algal laminae in stromatolites and oncolites are composed of dolosparite or its patches and clusters in dolomicrite. The dolosparite is made up of 0.01–0.02 mm long anhedral to subhedral grains, and its patches range in size from 0.02 to 0.06 mm. Infrequently, the stromatolitic laminae contain rounded peloids (0.1 mm) in a dolospar cement, and they are crosscut by a variety of thin (0.03–0.3 mm) dolomite veins and black zigzag or irregular stylolites, containing very fine quartz silt.

The Lower Member is about 300 m thick at its type section. It progressively becomes finer-grained towards its top part, where lenticular sandstones predominate, and finally grades into the dolomites and shales of the overlying Upper Member.

The Upper Member of the Hapurkot Formation commences with an interbedding of thick (30–50 cm), green shales and gray dolomites with subordinate lenticular siltstone beds, where the proportion of claystone increases steadily upwards and there appear yellow-gray lenticular dolomite beds intercalated in thin (2–5 cm), dark gray to black or dark green claystones. The dolomites contain small (2–5 cm across) columnar stromatolites. They are 15–20 cm high and subcircular to irregular in cross-section, and grow from a point upwards in the form of unbranching, turbinate to conical bioherms. The separate bioherms are joined upwards with each other by thin (1 mm) and wavy algal laminae. The stromatolitic dolomite rests over a blue-green calcareous claystone with indistinct parallel and convolute laminae, and the stromatolites are capped with a 7 cm thick green-purple claystone. The sequence continues upwards with lenticular medium (10–30 cm) beds of yellow-gray dolomite, containing small (1–2 cm high and 2–5 cm across) domed stromatolites and intercalated in 2–5 cm thick gray-black claystones, which finally change upwards into green and purple claystones.

At Hapurkot, the Upper Member appears as a monotonous succession of green-gray claystones with sporadic 10–15 cm thick dolomite beds displaying ripple marks, and it transitionally passes into the overlying Dhorbang Khola Formation. But, east of Ramri, the uppermost sequence of the Upper Member continues as a thinly interbedded succession of pink quartzose sandstone and dark gray to black slate. The last sequence is followed by a 30 m thick zone of thick-bedded (up to 1 m), occasionally thinly laminated to cross-laminated, pink and gray quartz arenites, containing current ripple marks on their upper surfaces and interbedded with dark green calcareous slates. This zone again grades into very thick (up to 2 m) beds of pink and orange quartzose sandstone and calcareous quartzose sandstone, alternating with 5–10 cm thick dark green thinly laminated dolomite and dolomitic slate bands, which alternate at an interval of 1–6 m. Ultimately, this zone grades into the predominantly dolomitic sequence of the Dhorbang Khola Formation. The Upper Member exceeds 260 m at Hapurkot.

The Dhorbang Khola Formation is characterized by the prolific occurrence of stromatolites and consists mainly of thick to very thick dolomites, sandstones, and shales. It is subdivided into the following two members. To the east of Ramri, the Lower Member begins with an approximately 18 m thick cyclic sequence of 25 cm to 2 m thick, gray dolomite and 1–50 cm thick, green slate intercalation, containing infrequent dolomite laminae. The last slate intercalation appears at an interval of 2–4 m. There are also a few calcareous sandstone and fine sublitharenite beds, alternating with thick dolomite, containing stromatolites. The sandstones have silica cement, they are cross-laminated, and their grains exhibit sutured contacts. On top of this sequence appears another 20 m thick succession of thick-bedded gray dolomite with current ripples and thin (2–15 cm) dark green shale with sun cracks. A 3 m thick massive bed of gray dolomite, including large domed stromatolites, rests over the latter succession. The stromatolites assume a semicircular to slightly irregular shape in transverse section; they are up to 50 cm across, and about 5 cm high. The larger stromatolites are covered with three or four beds of thin (5 cm) red shale or green claystone. Farther upwards, similar stromatolite-bearing sequences recur a number of times.

On the Kapurkot–Mulpani road, the Lower Member contains gray stromatolitic dolomites, oolitic dolomites, and thick white and pink quartzose sandstones. These thick (60 cm to 1 m) dolomite and sandstone beds are separated from each other by thin (1 cm), green claystone partings. The sandstones belong to quartz arenite and sublitharenite varieties, and consist of rounded to subrounded (infrequently well-rounded), coarse quartz grains (85–95 %), feldspar (microcline and plagioclase: 2–3 %), chert (5–10 %), and other lithic components (2–3 %). The grains are well-sorted, authigenic quartz fills their interstices, and they are slightly elongated parallel to indistinct bedding. The oodolosparite comprises about 60 % of ooids ranging in diameter from 0.2 to 1 mm and having circular to slightly elliptical sections. They are embedded in a medium to fine (0.04–0.3 mm) dolosparite having equant crystals of hypidiotopic texture.

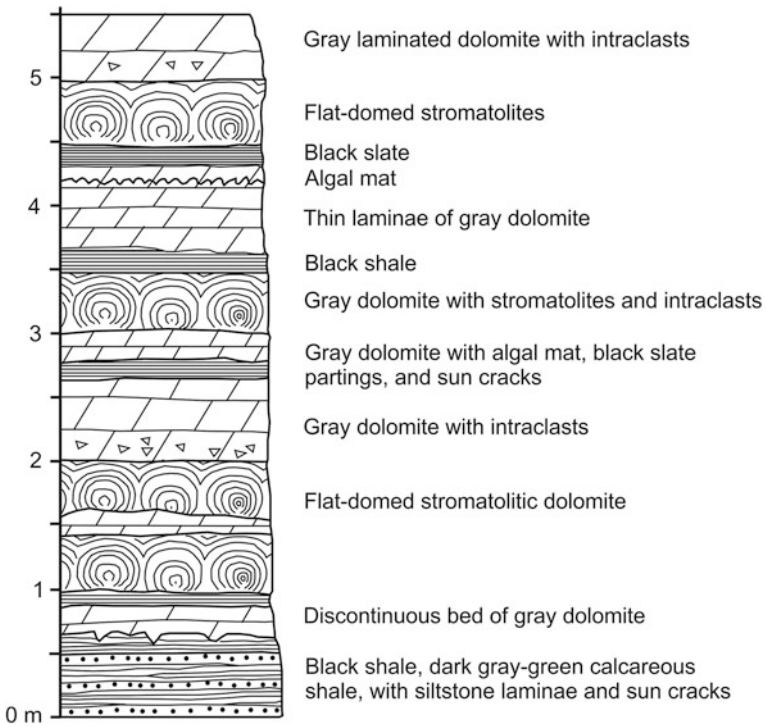

Fig. 8.27 Stratigraphic column of the Dhorbang Khola Formation showing various sedimentary structures and stromatolites. *Source* Author's observations

The ooids have 5–15 (frequently 7–12) laminae whose thickness varies from 0.02 to 0.06 mm, and in them micritic and microsparry laminae (some of them with radial fabric) alternate. About 50 % of the ooids are single, but the remaining 50 % are larger (0.5–1 mm) compound varieties with two to five ooids bound together. The nucleus of ooids is either an euhedral quartz grain or dolosparite, and the radial cracks present in some of the ooids are filled with microspar, whereas some of them are partly or completely replaced by chert or dolospar.

There are several stromatolite-bearing horizons in the Lower Member, exposed on the Kapurkot–Mulpani road (Fig. 8.27). This member also contains algal mats and laterally linked columnar biostromes. The domed stromatolites are generally isolated and grow from a point and display a cabbage-head structure (Fig. 8.28); the smaller ones are hemispherical, whereas the larger ones are flatter. The stromatolites contain rhythmically alternating thin (0.05–0.5 mm) laminae of fine (0.02–0.04) pseudosparite and microsparite (about 0.001 mm), where the subhedral dolospar crystals constitute hypidiotopic and xenotopic textures. The microsparite laminae are generally discontinuous and contain thin stylolites.

Apart from the stromatolitic dolomites, there also occur dolomicrites with thin (less than 1 mm) laminae of fibrous silica, which are interbedded with laminated sandy and silty pelmicrosparite. Some other dolomites are composed of microsparite with plentiful intraclasts. They frequently appear as gray, blue-gray, and pink cross-laminated dolomites with intraclasts and sinuous-crested ripples on their upper surfaces. The third type is represented by a rhythmic alternation of thin, gray-green, and pink dolomicrosparite and calcareous claystone, where the laminae are frequently wavy and continuous, but occasionally discontinuous. Some other carbonate beds in the Lower Member are composed of a red and pink interlaminated succession of microsparite and pseudosparite. There are also some black slates, alternating sequences of claystone, siltstone, and sandstone, and lenticular calcareous quartzose sandstone beds. The Lower Member is more than 700 m thick.

The Upper Member of the Dhorbang Khola Formation overlies the dolomitic succession of the Lower Member rather abruptly, and is composed principally of dark gray to black monotonous slates devoid of any visible laminae. Moving upwards, these slates contain 5–10 cm thick dark green feebly calcareous claystone intercalations, and transitionally grade over the Sirchaur Formation. The Upper Member varies in thickness from 50 to 100 m.

The Sirchaur Formation sets in as a predominantly fine-grained, thin-bedded to interlaminated sequence of light green, red, and purple calcareous claystone and limestone. It consists of the following two members.

The dark gray to black slates of the Dhorbang Khola Formation transitionally grade over dark green calcareous argillites, belonging to the Lower Member of the Sirchaur Formation (Fig. 8.20). The Lower Member also contains lenticular blue-gray dolomite beds of up to 20 cm thickness, which appear at an interval of 10 cm to 1.5 m. There

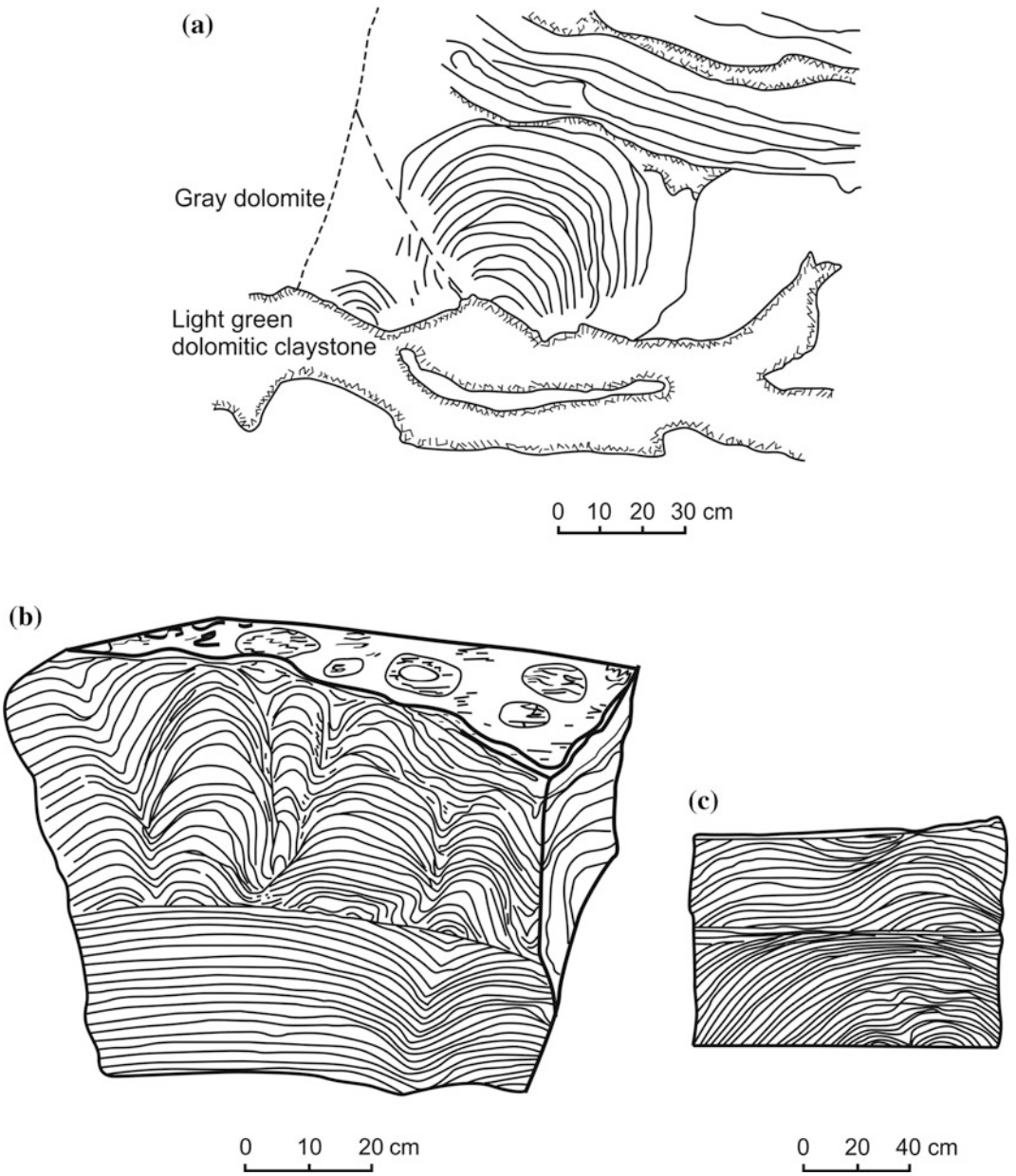

Fig. 8.28 Various stromatolites found in the Dhorbang Khola Formation. **a** single stromatolite dome; **b** columnar stronatolites; **c** two stromatelite domes separated by an erosional surface. *Source* Modified from Dhital and Kizaki (1987b). © University of the Ryukyus. Used by permission

sporadically occur about 2 cm thick zones of light green, discontinuously laminated shale. The lenticular dolomites are composed mainly of pseudodolosparite with equant to bladed crystals (0.08–0.25 mm) of hypidiotopic texture and a little (10 %) of terrigenous quartz silt (0.01–0.04 mm), concentrated in 0.8–1 mm thick indistinct laminae of finer-grained (0.04–0.08 mm) dolospar. Generally, the quartz grains are replaced by dolomite, but there are also some wavy, thin (1–1.5 mm) silty laminae with a higher (up to 20 %) quartz concentration. The green calcareous argillite comprises finely (0.02–0.04 mm) crystalline equant grains of sparite (about 5 %), coarse (0.01–0.03 mm) quartz silt (25 %), and some lithic fragments (5 %) cemented in a calcareous clay matrix (60 %). In the argillite, a few chlorite and sericite flakes are also found arranged parallel to the bedding. The thickness of the Lower Member generally varies from 40 to 60 m.

The green calcareous argillite of the Lower Member imperceptibly grades over the Upper Member consisting of an intercalation of white, pink, and light green laminated

limestone in red-purple and dark green laminated (1 mm to 1 cm) calcareous claystone. The limestone contains slightly wavy laminae where they display gradational contacts with the underlying claystone laminae. The red-purple claystones contain green irregular mottles. Extremely rare, small knobbly stromatolites are present in some sections. The stromatolites are about 4 cm high, circular to elliptical in cross-section, contain from 8 to 10 laminae within 1 cm, and are covered by red-purple calcareous claystone. There also infrequently occur ripples and sun cracks.

Interlaminated dark green claystone and light green limestone appear in the middle part of the Upper Member. It also contains subordinate, 10–15 cm thick, zones of red-purple claystones, reappearing at 30–50 cm intervals. The limestone consists of microsparite or argillaceous microsparite, not different from that of the Lower Member. The top portion of the Upper Member comprises mainly evenly laminated dark green argillites (50 %) and the same colored lenticular limestones (about 50 %). The green argillites further pass upwards into dark green calcareous argillites (about 70 %), interbedded with thin (2 mm–2 cm) lenticular beds of gray limestone (about 30 %). With the appearance of dark gray to black claystones or slates, the Sirchaur Formation transitionally passes into the overlying Ranibas Formation. The thickness of the Upper Member is about 450 m.

The Ranibas Formation forms imposing rides and peaks of gray limestone. It also includes very subordinate black slates or parallel-laminated shales and is further differentiated into the following two members.

The Lower Member begins with an approximately 27 m thick succession of black slates, containing a few thick to very thick (up to 5 m) lenticular (4–5 m long) gray limestones. Farther up-section, the sequence continues as a 7 m thick zone of black slates, followed by about 8-m-thick zone of alternating lenticular gray limestone and black slate. The last alternating sequence gradually gives way to evenly laminated (1–6 mm) black slates and hard, medium to thin (5–25 cm) limestones, and finally passes into the Upper Member of gray to black limestones with black slate partings. The Lower Member is 95 m thick.

With the onset of laminated (1–6 mm), gray dolomitic limestone, the Upper Member continues upwards as a slightly siliceous variety. In a few sections, there are laterally linked, small (5–10 cm high, 2–3 cm across) columnar stromatolites made up of 1–3 mm thick laminae. The gray dolomite continues upwards with about 100 m thick light gray to white siliceous dolomitic limestone, comprising microsparite with spots of sparite and some peloids or intraclasts of 0.2–0.5 mm in size. This sequence continues with gray to black laminated (1–3 mm) limestone, containing intraformational angular clasts of limestone ranging from 2 mm to 2 cm (exceptionally up to 10 cm) in length. Some limestone beds also contain penecontemporaneous deformational structures, such as chevron folds with randomly oriented hinges. Some dark to light gray laminated limestones contain current ripples on their upper surfaces, and others include small stromatolites capped by calcareous argillites with sun cracks. The laminated limestone comprises finely crystalline (0.1–0.3 mm) pseudosparite with irregular to slightly elongated spots of microspar and pseudospar with scattered quartz silt.

While moving upwards, the Upper Member continues with very thick (up to 1.5 m), pink to light gray siliceous limestones, separated by thin (1 cm), dark green argillite and slate bands. At the upper end of the Member, near the disconformity, are present from 10 cm to 1m thick gray limestones, on top of which is a basal conglomerate, containing subangular to rounded pebbles of gray limestone; gray, pale yellow, or white quartzite; and light gray chert. The pebbles are set in a light gray to blue-green silty sand matrix, which is generally weathered and occasionally calcareous. The irregular erosional contact, below the basal conglomerate, marks the boundary between the Gwar Group and the overlying Tosh Group (Fig. 8.29). The Upper Member exceeds 1,350 m in thickness.

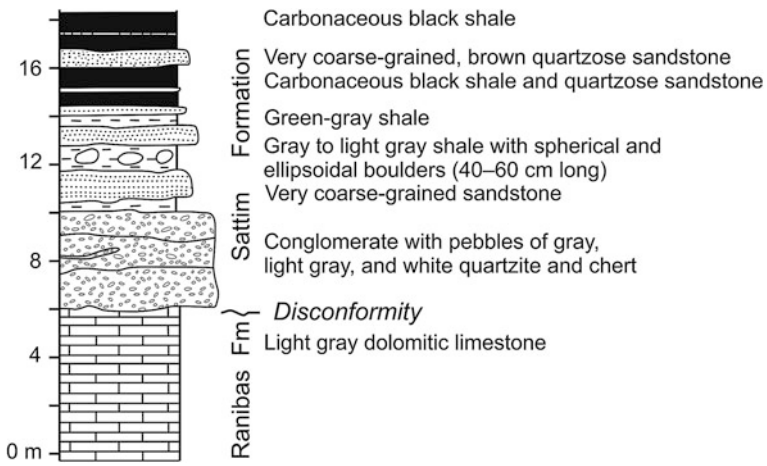

Fig. 8.29 Disconformity between the Gwar Group and overlying Tosh Group. *Source* Author's observations

8.5.4 Tosh Group

The Tosh Group comprises conglomerates, sandstones, and shales with coal seams, and many fossiliferous horizons. Presumably, this group ranges in age from the Paleocene to Miocene, and it is classified into the following formations.

In the Sattim Formation, thick- to very thick-bedded, white, pale orange, brown, and black quartzose sandstones and graywackes regularly alternate with dark green, brown, black, and red shale including some thin coal seams, and a few limestone beds with many fossils. It is subdivided into the following three members.

Its Lower Member is represented by the Ramri Conglomerate. The disconformity (Figs. 8.29 and 8.30) is followed up-section by dark brown to red or green shale. The shale above the disconformity is succeeded by a cross-bedded, thick, white quartzose sandstone with a sharp lower contact and some conglomerate lenses in its lower part. This sandstone bed is followed upwards by many very thick conglomerate beds of yellow, gray, and white colors. They also include some thin, discontinuous sandstone lenses, and exhibit scoured and irregular lower contacts. The well-rounded to angular pebbles in conglomerates are principally of white, gray, light green, and pink quartzite, black chert, and agate. Their size varies from 1 to 22 cm and they are sometimes embedded in a matrix of fines, having a composition similar to those of pebbles. The conglomerates gradationally pass upwards to an interbedded sequence of quartzites and shales with coal seams. The Ramri Conglomerate is about 50 m thick, occurs intermittently, and is absent in most parts of the area.

The Middle Member of the Sattim Formation includes the Coal Measures of Dang. The coal measures occur as thin beds, lenses, and stringers at various levels within this member, composed mainly of many quartz arenite and shale cycles. In the road cut east of Ramri, the disconformity is marked by an approximately 6 m thick, fining-upwards conglomerate lens resting with a sharp and scoured contact on thinly (2–10 cm) bedded white quartzose sandstone with green claystone partings (Fig. 8.30). The conglomerate represents a channel fill, and the pebbles (2–10 cm in diameter) are made up primarily of light gray to white quartzite or black chert; the matrix of conglomerate contains medium- to coarse-grained sublitharenite with quartz (70 %), chert (25 %), and feldspar (5 %). The sand grains are well sorted, display concavo-convex to sutured contacts, and are associated with some quartz silt with secondary sericite. The Lower and Middle members of the Sattim Formation can be homotaxial with the Melpani and Amile formations (Chap. 9).

The Upper member of the Sattim Formation corresponds to the Sewar Khola Beds, containing the first Nummulitic horizon. This horizon lies in the gray rock succession, and it is similar in many aspects to the situation in the Northwest Himalaya, where two Nummulitic horizons are found. At Tosh, in the upper part of the succession, there are very thick-bedded (up to 3 m), massive, light gray quartzose sandstones. From 0.5 to 1 m thick, gray-green and pink-gray, mottled argillaceous limestones appear in the uppermost part of the sandstone sequence. The limestones transitionally grade over a succession of purple and green calcareous argillite with *Nummulites* and *Assilina* fossils, and very feeble, crumbly, brown shale including many dispersed bivalves. There also appear a few lenses of compact bivalves and gastropods. The topmost part of the sequence is composed of dark green and pink argillaceous limestones, containing scattered foraminifera.

The Dubring Formation is the youngest formation of the region, and it is extensively distributed to the south of Dubring and Harnok as well as around Mulpani and Meltakura. Most of the Dubring Formation is a cyclic deposition of green-gray sandstone and red-purple mudstone with a minor proportion of green, brown, and black shale. In the Dhorbang Khola, the thick-bedded gray to black carbonaceous quartzose sandstones of the Sattim Formation grade over a very thick dark gray-green sandstone bed of the Dubring Formation. The last sandstone bed is followed by a red-purple mudstone bed, and this sequence is repeated several times. The Dubring Formation is divided up into the following two members.

The Lower Member is designated as the Meltakura Beds, containing the second Nummulitic horizon (Fig. 8.31). Although this is primarily a red facies, there also appear some green sandstones. Within this member, several wavy and lenticular beds of pink, red, and purple limestone also occur, interbedded between the same colored calcareous argillites. The limestones yield *Nummulites* and *Assilina* fossils. Some very feeble, brown to tan colored shale beds with compact bivalve lenses also occur. Some shells are also scattered in the brown shale. The Upper Member of the Sattim Formation and the Lower Member of the Dubring Formation can both be correlated with the Eocene Subathu, Swat, and Bhainskati formations.

The Upper Member of the Dubring Formation is made up of fluvial cycles of gray-green sandstone and red-purple shale. The sandstones contain a considerable amount (up to 20 %) of phyllite clasts. The clasts are strongly deformed and have a sigmoidal shape. There are also a few biotite flakes (which are altered to chlorite), some chert fragments, and feldspar grains. The clasts are cemented by clay or silica. The quartz grains infrequently display welded and sutured contacts. This member is lithologically identical with the Miocene beds, mapped elsewhere as the Dagshai, Melpani, or Dumri Formation.

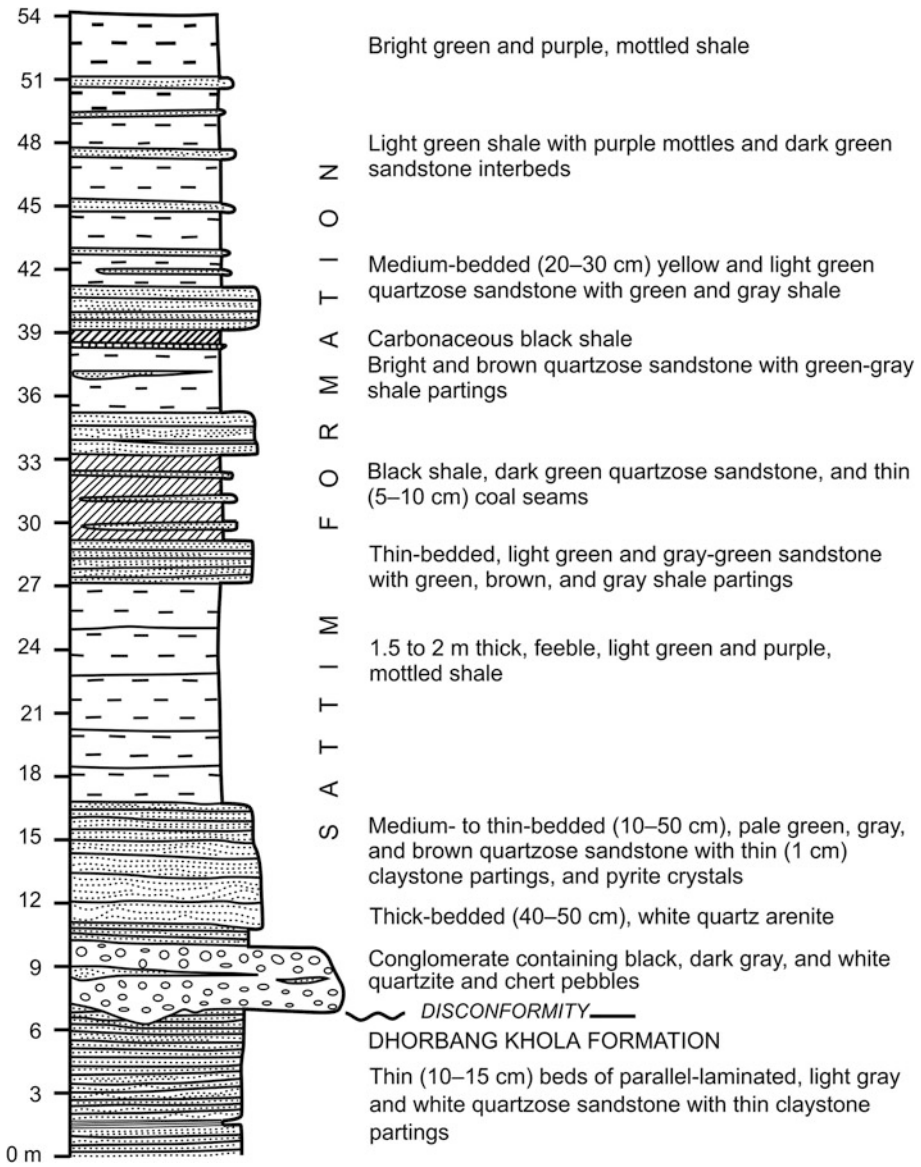

Fig. 8.30 Stratigraphic column depicting the disconformity between the Dhorbang Khola Formation and overlying Sattim Formation from east of Ramri. *Source* Author's observations

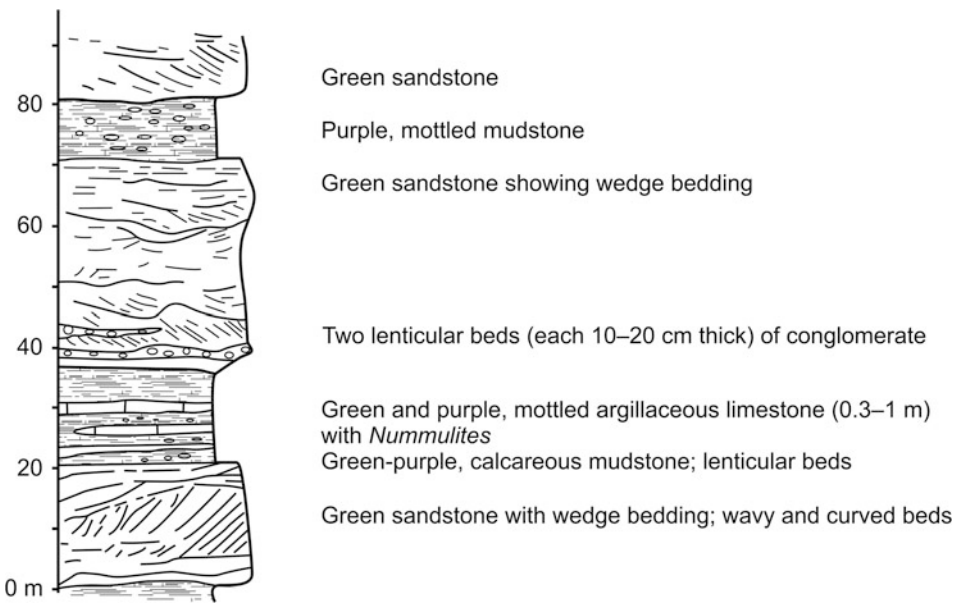

Fig. 8.31 Fossil occurrences in red-purple shale, green sandstone, and limestone. *Source* Author's observations

References

Adhikary TP, Sharma T (1983) Geological report of Marma, Chaurjhari, and Jajarkot area (Far Western Nepal). Unpublished report submitted to the Department of Mines and Geology, Kathmandu, 41 pp

Amatya KM, Jnawali BM (1994) Geological map of Nepal, scale: 1:1,000,000. Department of Mines and Geology, International Centre for Integrated Mountain Development, Carl Duisberg Gesellschaft e. V., and United Nations Environment Programme

Brookfield ME (1987) Lithostratigraphic correlation of Blaini Formation (Late Proterozoic, Lesser Himalaya India) with other Late Proterozoic tillite sequences. Geologisches Rundschau 76:477–484

Dhital MR, Kizaki K (1987a) Structural aspect of the Northern Dang, Lesser Himalaya, vol 45. Bulletin of the College of Science, University of Ryukyus, Okinawa, pp 159–182

Dhital MR, Kizaki K (1987b) Lithology and stratigraphy of the Northern Dang, Lesser Himalaya, vol 45. Bulletin of the College of Science, University of Ryukyus, Okinawa, pp 183–244

Dhital MR (1992) Lithostratigraphy of low-grade metamorphic rocks of Sharda Group in the West Nepal Lesser Himalaya, vol 2, no 1, Special Issue. Bulletin of Department of Geology, Tribhuvan University, pp 45–55

ESCAP (Economic and Social Commission for Asia and the Pacific) (1993) Geology and mineral resources of Nepal, atlas of mineral resources of the ESCAP region, vol 9. United Nations, New York, 107 pp (with a geological map in colors, scale: 1:1,000,000)

Frank W, Fuchs GR (1970) Geological investigations in west Nepal and their significance for the geology of the Himalayas. Geol Rundsch 59:552–580

Fuchs G (1974) On the geology of the Karnali and Dolpo Regions, west Nepal. Mitteilungen der Geologischen Gesellschaft in Wien, Wien, 66–67 Band, 1973–1974, pp 21–32 (with 3 plates)

Fuchs G (1977) The geology of the Karnali and Dolpo Regions, western Nepal. Jahrbuch der Geologischen Bundesanstalt, Wien, Band 120, Heft 2, pp 1–103 (with 9 plates)

Fuchs G, Frank W (1970) The geology of west Nepal between the rivers Kali Gandaki and Thulo Bheri. Jahrbuch der Geologischen Bundesanstalt, vol 18, pp 1–103 (with a geological map and cross-sections)

Hagen T (1959) Über den Geologischen Bau des Nepal-Himalaya mit besonderer Berücksichtigung der Siwalik-Zone und der Talbildung. Jahrbuch der St. Gallischen Naturwissenchaftlichen Gesellschaft, vol 76, pp 3–48 (with 10 figures and 9 plates)

Hagen T (1969) Report on the geological survey of Nepal. Volume 1: preliminary reconnaissance. Denkschiiften der Schweizerischen Naturforschenden Gesellschaft, Band LXXXVI/1, 185 pp (with a geological map)

Jameson W (1839) Remarks on the geology, &c. of the country extending between Bhar and Simla. J Asiat Soc Bengal, Calcutta VIII(96):1037–1057

Kansakar DR (1991) Geology and structural evolution in the Bheri River region, southwest Nepal. J Nepal Geol Soc 7:59–80

Kansakar DR, Chitrakar GR (1984) Report on geological investigation in Dang–Sallyan region, western Nepal. Unpublished report submitted to the Department of Mines and Geology, Kathmandu, 43 pp

Nakata T, Iwata S, Yamanaka H, Yagi H, Maemoku H (1984) Tectonic landforms of several active faults in the western Nepal Himalayas. J Nepal Geol Soc 4(Special Issue):177–200

Sakai H, Takigami Y, Nakamura Y, Nomura H (1999) Inverted metamorphism in the Pre-Siwalik foreland basin sediments beneath the crystalline nappe, western Nepal Himalaya. J Asian Earth Sci 17:727–739

Sharma T, Kizaki K (1988) The granitoid rocks of the Dailekh and the Jajarkot regions in the Lesser Himalaya of Central West Nepal. J Nepal Geol Soc 5(1):47–67

Sharma T, Kansakar DR, Kizaki K (1984) Geology and tectonics of the region between Kali Gandaki and Bheri Rivers in Central West Nepal, vol 38. Bulletin of College of Science, University of the Ryukyus, Okinawa, Japan, pp 57–102

Shrestha SB, Shrestha JN, Sharma SR (1987) Geological map of Mid-Western Nepal. Scale: 1:250,000. Department of Mines and Geology, Kathmandu

Tater JM, Shrestha SB, Shrestha JN (1983) Geological map of Western Central Nepal. Scale: 1:250,000. Department of Mines and Geology, Kathmandu

Lesser Himalaya of Gandaki Region

9

After a common Precambrian story, the Higher and Lesser Himalayas separate in two basins, the northern one on a continental thinned margin, the southern one intracratonic under shallow marine and continental influences.

—P. Le Fort (1975, p. 1)

The Gandaki region includes the widest Lesser Himalayan belt in Nepal, encompassing the inner, intermediate, and outer zones (Fig. 9.1). The oldest Lesser Himalayan rocks constitute the lowest stratigraphic rung in the antiformal cores of the inner zone, whereas younger sedimentary sequences are copiously developed in the outer zone. Notwithstanding the fact that the weathering of ages has removed the Higher Himalayan thrust sheet from almost the whole Gandaki region, investigations in the Kali Gandaki Valley (Le Fort 1975), Modi Khola area (Arita 1983; Paudel and Arita 2000, 2006), Manaslu neighborhood (Pêcher 1989), and Gorkha have demonstrated that the Lesser Himalayan rocks of the intermediate and inner zones have retained inverted metamorphism. As with all other occurrences of the Lesser Himalayan rocks, this region, too, experienced intense compression, leading to the proliferation of folds and faults.

9.1 Inner Zone of Gorkha

The inner zone is made up essentially of the Kuncha Formation, exposed in the core of the Great Midland Antiform, also known as the Kunchha–Gurkha anticlinorium (Ohta et al. 1973) or Pokhara–Kunchha–Gorkha anticlinorium (Pêcher 1977, Fig. 9.2). In this region, nepheline syenites and kindred rocks merit special attention, as they are extremely rare in the Himalaya. So far, such rocks are known only from two distant places: at Ampipal in west Nepal and in Sikkim. In both cases, they crop out in the core of a metasedimentary sequence, representing the lowest portion of the Lesser Himalaya. In Sikkim, the alkali syenite dikes with a NW–SE trend, are from a few meters to over 200 m long, and some of them exhibit chilled borders with the country rock (Singh et al. 1983).

The Gorkha–Ampipal area of west Nepal is made up of a variety of metamorphic rocks, such as phyllites, schists, marbles, quartzites, and gneisses. The broad lithological subdivisions (Dhital 1995) making up the region are the following (Fig. 9.3).

9.1.1 Kuncha Formation

In this area, the Kuncha Formation (Chap. 10) appears as an immensely thick (more than 4 km) and fairly monotonous succession of green-gray, dark gray, and bluish gray phyllite, phyllitic metasandstone, *gritty* phyllite, and quartzite. Infrequently occurring muscovite flakes (0.5–1 mm) are aligned parallel to foliation in phyllites and metasandstones. There are also sporadic granular and pebbly phyllites (Fig. 9.4) with stretched clasts and amphibolite bands, such as those found south of Manakamana. As an exception, a band of about 20 m thick white quartzite is intercalated in the Kuncha Formation to the north of Manakamana.

Light green to white calcareous quartzite, siliceous crystalline limestone, and marble compose the upper portion of the Kuncha Formation. To the north of Harmi Bhanjyang, an approximately 500 m thick band of impure marble and siliceous crystalline limestone appears above a large nepheline syenite intrusion. In some other sections, impure marble and green phyllite alternations are subordinately present. These calcareous rocks are presumably equivalent to the Banspani Member (Stöcklin and Bhattarai 1977).

9.1.2 Garnetiferous Schists and Gneisses

The Kuncha Formation is somewhat abruptly followed upsection by a sequence of gray to dark gray garnet–biotite–muscovite schist, where the size of garnets may exceed 6 mm. At Ratmate, snowball garnets of 2–5 mm in diameter are surrounded by about 1 cm long lens-shaped biotite and muscovite envelopes. In this succession, generally from 10 to 30 cm and rarely 5 m thick gray and dark gray schists and quartzites frequently alternate. There also occur a few very thick (1–2 m) bands of graphitic schist and white quartzite. Many stretched, boudinaged, and folded quartz veins as well as a few tourmaline-rich pegmatite veins are injected in the rock. Amphibolite bands reaching 10 m in thickness

M.R. Dhital, *Geology of the Nepal Himalaya*, Regional Geology Reviews,
DOI 10.1007/978-3-319-02496-7_9

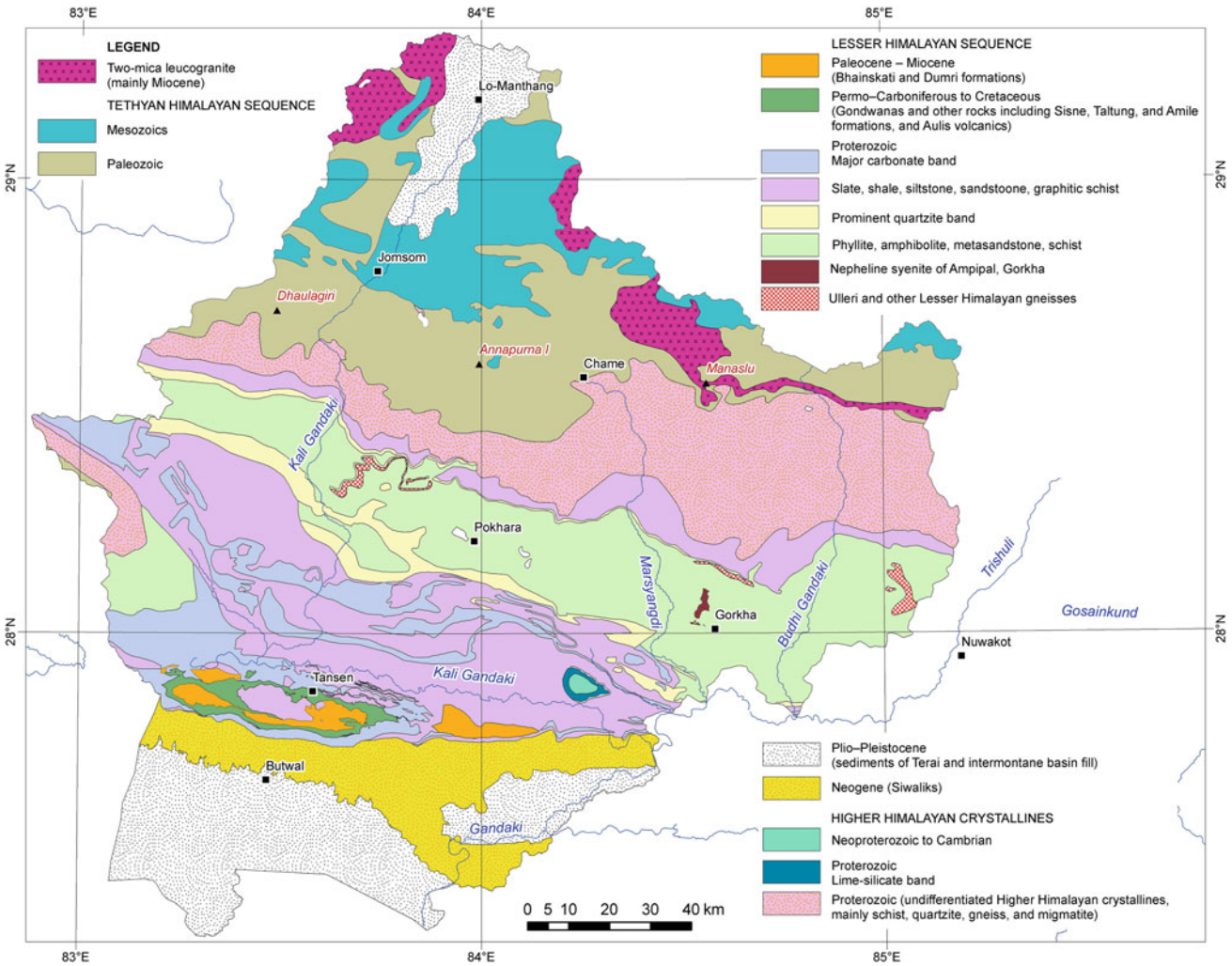

Fig. 9.1 Simplified geological map of the Gandaki region. *Source* Based on Tater et al. (1983), Shrestha et al. (1986), ESCAP (1993), Amatya and Jnawali (1994), other published maps, and author's observations

infrequently alternate with up to 20 m thick white quartzite bands. Towards the higher part of this sequence, 50–100 m thick augen and banded gneisses alternate with 5–10 m thick gray and dark gray schists. The gneisses are strongly lineated, and the augen in them range from 2 mm to 2 cm in size.

9.1.3 Graphitic Schists and Marbles

This unit succeeds the last succession again with a quite sharp contact, and comprises green-gray, light gray, and white calcareous schists, alternating with light gray, green-gray, pink, and white calcareous quartzites, dolomitic marbles, and dark gray to black graphitic schists. There are also some alternations of actinolite schist, feldspathic schist, and garnetiferous schist. Quartz and calcite veins of several generations crisscross these rocks.

In the lower part, 10 cm–1.5 m thick calcareous quartzites and dolomites alternate with 1 mm–50 cm thick schist bands. Up to 5 m thick, light gray, white, and cream colored quartzites display ripple marks. Schist and marble bands alternate thinly (1–5 mm) towards the upper section, where a few bands of green-gray or dark gray to black graphitic schist and garnetiferous schist also occur. Towards the top of this sequence, a prominent marble band continues for several kilometers.

In the west part, this succession contains dark gray slates, phyllites, and garnetiferous schists, alternating with crystalline dolomites, marbles, and calcareous quartzites. The metamorphic grade steadily increases eastwards, where one finds long (5–7 cm) kyanite blades together with quartz in dark gray graphitic schists.

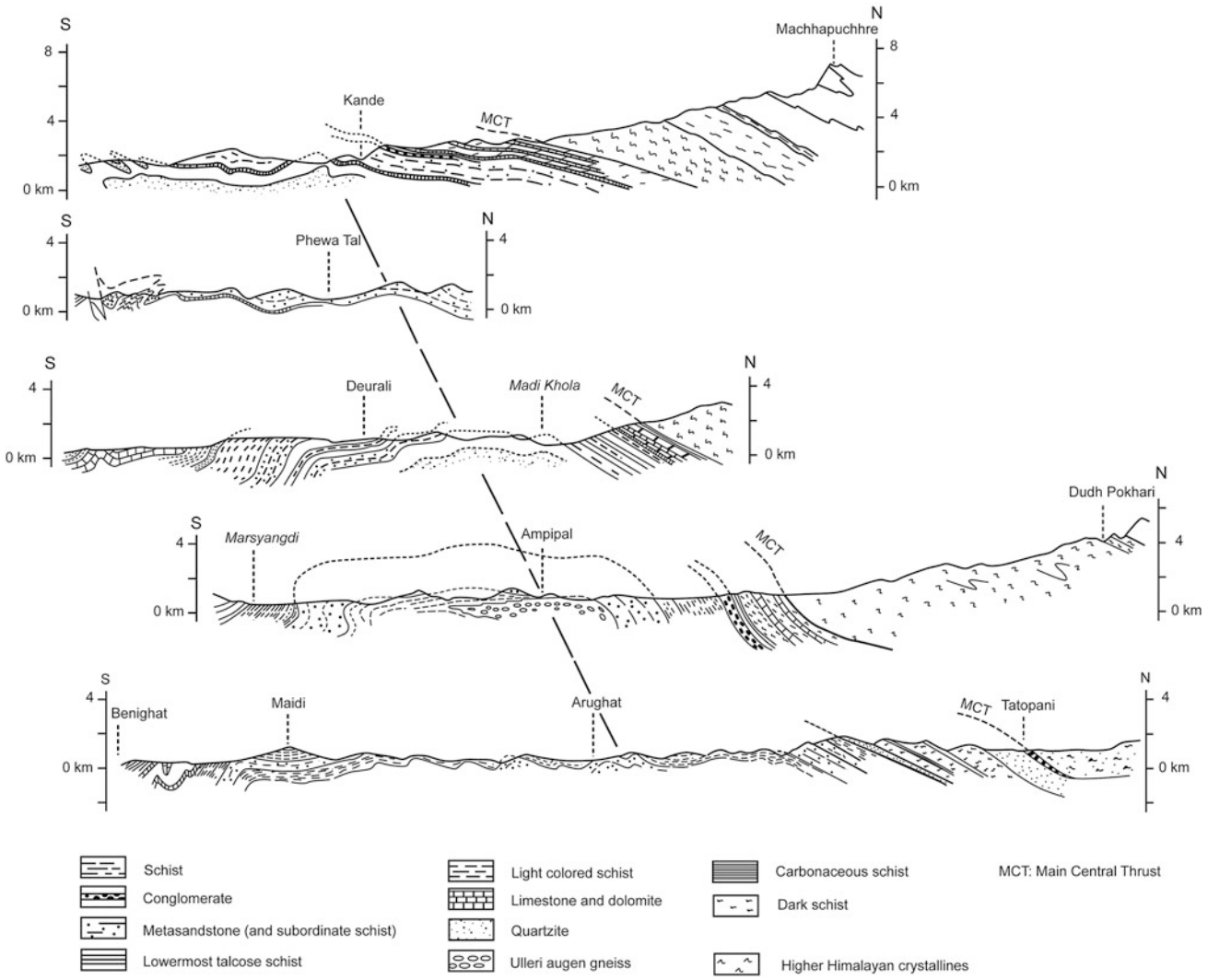

Fig. 9.2 Cross-section through the Gorkha anticlinorium. *Source* Modified from Pêcher (1977). © Centre National de la Recherche Scientifique, Paris, France. Used by permission

9.1.4 Higher Himalayan Sequence

Over the graphitic schists and marbles, the Main Central Thrust brings the Higher Himalayan rocks, represented by coarse-grained gray to dark gray schists, pale quartzites, gray banded gneisses, augen gneisses, and mylonitic gneisses. The schists and gneisses contain sillimanite, kyanite, garnet, biotite, K-feldspar, muscovite, and quartz. Up to 1.5 m thick pegmatite veins, containing large (1–2 cm) muscovite, biotite, kyanite, and K-feldspar crystals, crosscut the gneisses and schists. Within the massive to blocky augen and banded gneisses, several thick (20 m) zones, rich in gray kyanite schist, are conspicuous.

9.1.5 Structure of Inner Zone

Stretching and mineral lineations are excellently developed in the Kuncha Formation. Their statistical analysis reveals a NNE or SSW trend (peak trend = N 18°E), with a gentle plunge in either direction, and they are distributed concordantly to regional-scale folding. The lineations consistently record a similar trend in a wide area of this region (Ohta et al. 1973; Pêcher 1991), and they also coincide with the direction of anisotropy of magnetic remanence in the Ampipal massif (Gautam 1990).

In the Gorkha–Ampipal area, the Kuncha Formation is warped into doubly plunging to dome- and basin-like, en

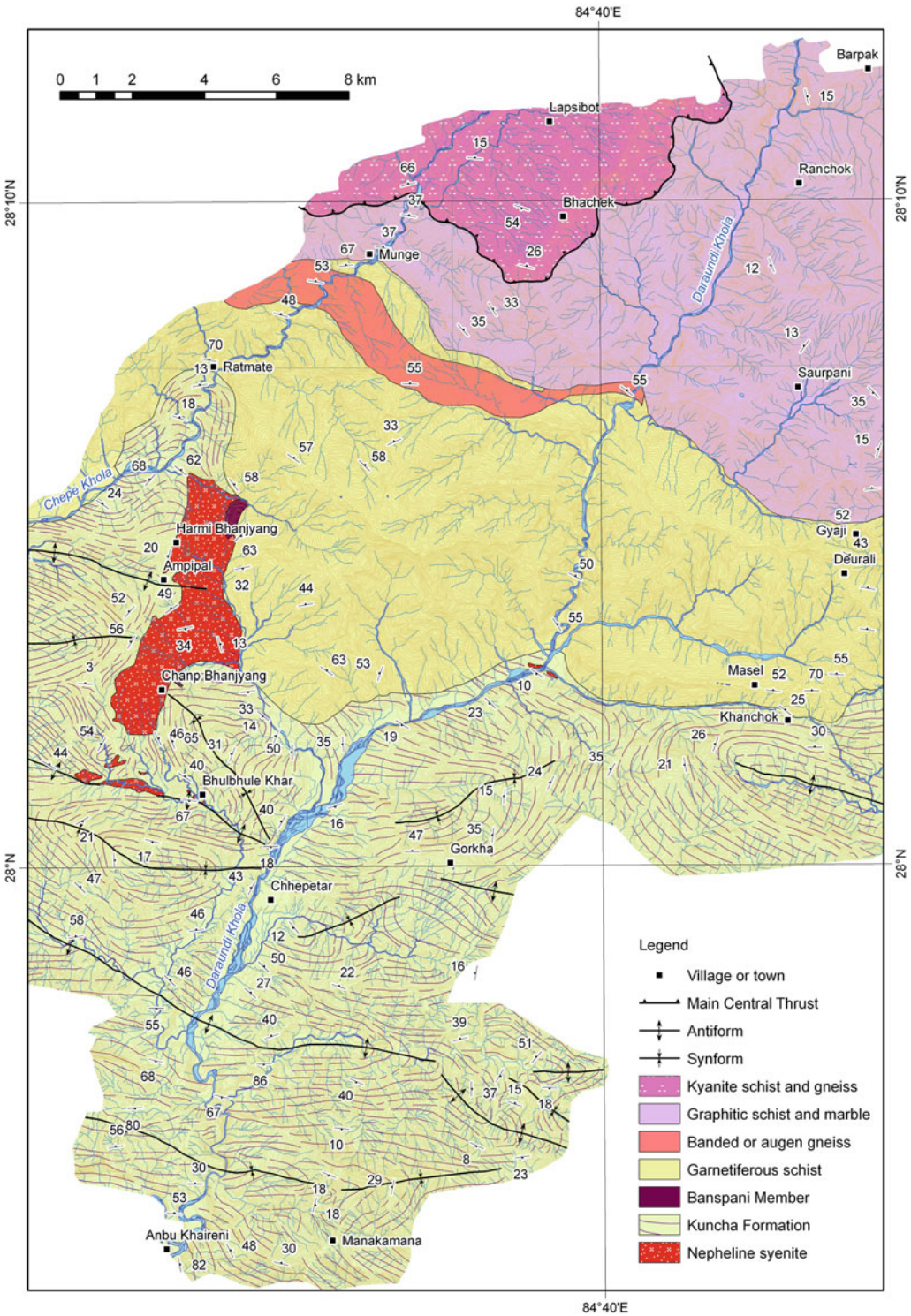

Fig. 9.3 Geological map of the Gorkha–Ampipal area, Central Nepal Lesser Himalaya. *Source* Modified from Dhital (1995)

echelon types of noncylindrical fold. They are from 2 to 20 km long, essentially in the northwest–southeast direction, and their wavelength reaches up to a few kilometers. On the other hand, the rocks overlying the Kuncha Formation make up a steeply dipping homocline. A variety of small-scale folds occurs within the graphitic schists and marbles,

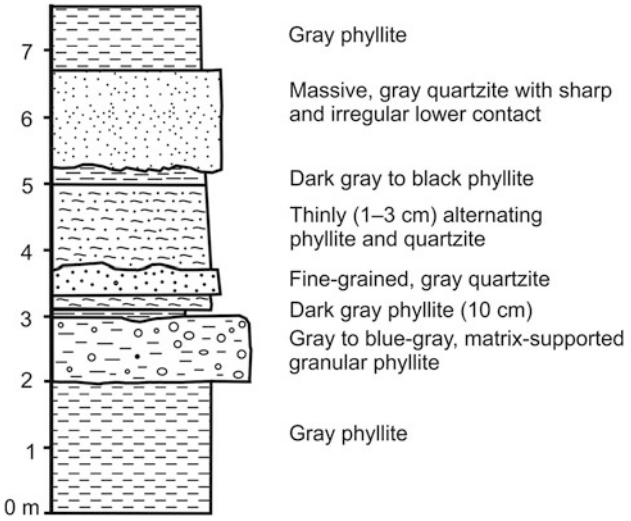

Fig. 9.4 Columnar section of the Kuncha Formation, about 1 km north of Anbu Khaireni. *Source* Author's observations

especially on approaching the Main Central Thrust. They represent isoclinal to polyclinal, disharmonic, convolute, and ptygmatic types in the laminated calcareous quartzites and schists, and they assume the aspects of parallel to polyclinal folds in the thicker marble bands.

The Main Central Thrust sharply overrides the graphitic schists and marbles, and its hanging wall is represented by gently dipping sillimanite–kyanite schists, mylonitic gneisses, and quartzites. Towards the west, it covers most of the graphitic schists and marbles, living behind only a narrow band in the Chepe Khola (Fig. 9.3). The folds in the gneisses are often completely disrupted, and may be categorized under intrafolial, ptygmatic, and strongly boudinaged types.

9.1.6 Nepheline Syenites

A. Pêcher and P. Le Fort discovered the alkaline gneisses of Ampipal (Lasserre et al. 1975; Pêcher 1977), whereas Lasserre (1977) and Le Fort and Raï (1999) carried out their geochemical analysis (Tables 9.1 and 9.2), and classed them under miaskitic nepheline syenites. They also found that the nepheline syenites are crosscut by basic and ultrabasic dikes, representing melteigites and jacupirangites.

Koide et al. (1992) further subdivided the igneous bodies into olivine clinopyroxenites, shonkinites, nepheline syenites, and malignites. They are characterized by a high alkaline content. The olivine clinopyroxenites have 0.63 wt% of Na_2O and 1.1 wt% of K_2O, shonkinites include 4.4 and 3.1 %, and nepheline syenites contain 6.4 and 6.5 %, respectively.

The nepheline syenite intrusions vary widely in their shape, size, and orientation. The largest pluton is about 7.5 km long in the NNE–SSW direction and about 2 km wide. The second largest intrusion is about 2.5 km long approximately in the east–west direction and 300 m wide. Numerous other smaller bodies, ranging in size from hundreds of meters to a few centimeters, also occur. The nepheline syenite bodies have sharp and irregular contacts with the country rock, they are crosscut by a great number of dikes, and their contact metamorphic effects are conspicuous in the country rock.

The secondary mineralization in the marbles is represented by magnetite, actinolite, biotite, and chlorite. There exist a few old iron mine workings in the magnetite mineralization zones. Similar minerals are also seen in the nepheline syenite. The mineralization seems to be the result of metasomatism in the country rock (marble) and the

Table 9.1 Major element content (in percent) in the nepheline syenites from Ampipal massif (Lasserre 1977)

Component	1	2	3	4	5
SiO_2	56.13	56.22	55.24	56.85	57.80
$A1_2O_3$	22.21	21.77	21.59	19.83	21.41
Fe_2O_3 total	4.31	4.80	3.92	3.53	2.61
MnO	0.14	0.20	0.17	0.12	0.08
MgO	0.56	0.43	0.33	0.41	0.20
CaO	1.62	1.19	1.32	1.97	1.52
Na_2O	5.96	6.11	6.63	5.91	6.70
K_2O	6.23	6.85	6.90	7.47	6.90
TiO_2	0.23	0.10	0.14	0.37	0.14
P_20_5	n.d.	n.d.	n.d.	n.d.	n.d.
L. I.	2.42	2.64	2.79	2.73	2.06
Total	99.81	100.31	99.03	99.19	99.42

Table 9.2 Trace element content (in ppm) in the nepheline syenites from Ampipal massif (Lasserre 1977)

Component	1	2	3	4	5
Ba	586	307	331	570	1,037
Co	10	10	10	19	10
Cr	16	10	10	307	10
Cu	10	10	10	26	10
Ni	10	10	10	55	10
Sr	587	273	514	284	1,377
V	14	10	10	154	10
U	n.d.	n.d.	n.d.	5.7	n.d.
Th	n.d.	n.d.	n.d.	74.0	n.d.
Th/U	–	–	–	13.0	–
K/Ba	88.2	185.3	173.1	108.7	55.2
Ca/Sr	19.7	31.1	18.3	49.5	7.9

nepheline syenite by the development of skarns. It also indicates a direct relationship between the mineralization in the nepheline syenite and the marbles on top of them. Inasmuch as the nepheline syenite bodies exhibit the same attitudes of foliation and lineation as those of the country rock, they must have been intruded prior to the development of foliation and lineation.

The intrusives of the study area are represented by biotite–hornblende–clinopyroxene nepheline syenites, alkaline syenitic gneisses, and clinopyroxenites. The nepheline syenites consist of microperthitic alkali feldspar and nepheline. Their minor and accessory minerals are biotite, garnet, apatite, zircon, magnetite, and allanite. The secondary minerals are cancrinite, quartz, and albite. The nepheline syenites have undergone intense cataclasis and recrystallization, leading to the formation of alkaline (syenitic) gneisses. The rocks are also sporadically mylonitized (Koide et al. 1992).

Although the alkaline gneisses are represented by banded and augen varieties, the banded gneisses predominate. The gneisses are composed of microperthitic alkali feldspar, lepidomelane, alkaline amphiboles (which are frequently rimmed by biotite and riebeckite), and nepheline. Biotite, garnet, apatite, zircon, magnetite, and allanite occur as minor and accessory minerals, whereas biotite, cancrinite, quartz, and albite represent secondary minerals.

The clinopyroxenites are made up of plagioclase, clinopyroxene with a hornblende rim, and hornblende with a biotite rim. Other minerals are magnetite, apatite, and ilmenite (Koide et al. 1992).

The alkali syenites of Sikkim are mesocratic to melanocratic and generally medium-grained. They contain some megacrysts of K-feldspar, and there are also riebeckite, kataphorite, and aegirine–augite. They are represented by saturated peralkaline, perpotassic plutons with anomalously high concentrations of Th (0.01–0.04 % of ThO_2) and U (0.003–0.01 % of U_3O_8). The radioactive minerals, constituting some anomalous zones in phyllites and chlorites, are represented by uraninite, davidite, leucoxene, and cyrtolite (Singh et al. 1983).

Goswami and Bhattacharya (2008) described the nepheline syenites from Chhotanagpur in east India. The Proterozoic two nepheline syenite bodies occurring in the northeast part of Puruliya District have distinct principal mafic minerals. One has biotite and the other has amphibole, but both exhibit identical chemical composition. Granulite-facies metamorphism of the biotite-bearing nepheline syenites could have produced amphiboles from biotite.

Lasserre (1977) opined that the nepheline syenites resulted from rapid crystallization of a very fluid residual magma, the product of differentiation of a greater volume of a basic magma in a tectonically stable continental region. He also compared the nepheline syenites with the Deccan Traps, and inferred an Early Oligocene age of their emplacement during rifting of the Indian craton in an island arc setting. Similarly, Adhikari (1993) found a primary magnetic remanence age range of 54–49 Ma (Early Eocene) for the ultrabasic and basic dikes. However, based on fission-track dating, Gautam and Koshimizu (1991) obtained exhumation rates of 2.00–2.22 mm/a and the corresponding cooling rates of 80°/Ma for the period between 2.81 Ma and the present. Bordet et al. (1981) refer to preliminary Rb–Sr dating that has yielded a much older (Proterozoic) age. At Bhulbhule Khar, many hot springs issue through the strongly altered nepheline syenites. Their water is alkaline and saturated with H_2S gas and sulfur. The occurrence of banded and augen gneisses, pegmatites, amphibolites, and nepheline syenites with crosscutting dikes probably points to a prolonged magmatic activity in the past, whereas the development of copper and other secondary ore mineralization zones as well as the prevalence of several generations of quartz and calcite

veins indicates a continued hydrothermal activity in that area. On the other hand, the occurrence of hot springs may be attributed to some recent tectonic activities.

9.2 Intermediate Zone of Kusma–Syangja

This region lies in the synclinal core of the Great Mahabharat Synform, made up of the Nawakot nappes of Hagen (1969). Nanda (1966) carried out detailed geological investigations in this portion of west Nepal and his lithostratigraphic units were subsequently formalized by Stöcklin and Bhattarai (1977), while working in central Nepal (Chap. 10). Sakai (1986) defined many lithostratigraphic units from this area. Hirayama et al. (1988) mapped a number of vertical faults and thrusts.

The sedimentary and low-grade metamorphic rocks of the Kusma–Syangja area are classified into the Lower Nawakot Group, Upper Nawakot Group, and Sirkot Group (Dhital et al. 2002). There is also a thin and discontinuous succession of the Tansen Group. Owing to inherent structural complexities leading to difficulties in correlation, some new formation names were introduced within the Nawakot Group.

The Lower Nawakot Group (Chap. 10) is developed in the north and central parts of the region. It is represented by the following formations, from bottom to top, respectively (Figs. 9.5 and 9.6).

9.2.1 Kuncha Formation

The Kuncha Formation occupies the north portion of the area where it makes two belts. It is a very thick and rather monotonous sequence of alternating blue-green to gray-green phyllites or chlorite schists; gray-green to light gray *gritty* phyllites; fine-grained, massive, olive green quartzites; gray-green metasandstones; and sporadically occurring coarse-grained metaconglomerates and thick (up to 5 m) lenses of massive, dark green amphibolite. The phyllite is very fine-grained, thinly foliated, and crenulated. It includes tiny (0.5–1 mm) sericite or muscovite flakes, arranged parallel to foliation.

The Kuncha Formation, constituting the core of a large synform, possesses gray-green thin- to medium- (10–50 cm) banded metasandstones as well as some colored *gritty* phyllites with a subordinate amount of thinly laminated light gray to white micaceous quartzite and sporadic bands of conglomerate. Very thick (3–4 m) bands of medium- to coarse-grained metasandstone comprise the upper part of the synform in the lower reaches of the Malyangdi Khola.

Frequently occurring coarse-grained *gritty* phyllites contain pelitic matrix, and some of them grade into white quartzites. Their angular to subrounded clasts are generally less than 5 mm in diameter, and they are made up of bluish-gray quartz, smoky quartz, or feldspar. The quartz grains are frequently polycrystalline, indicating their metamorphic provenance. Occasional metaconglomerate bands occur up to 6 m thick and contain strongly stretched (up to 6 cm long) pebbles of quartzite and vein-quartz. With a rapid transition from phyllites and metasandstones, this formation grades into the overlying Naudanda Quartzite. In the Syangja area, the Kuncha Formation exceeds 2,000 m in thickness, and its base is nowhere exposed.

9.2.2 Naudanda Quartzite

The Naudanda Quartzite forms steep, bare, and rugged cliffs and ridges, constituting the north portion of the region. It consists of medium- to coarse-grained, medium- to very thick-bedded (50 cm–5 m), massive, pale yellow, light gray, white, and light green quartzites, alternating with thin bands of blue-gray to green-gray phyllite. The quartzite contains excellent wave and current ripples, parallel laminae, and various types of cross-laminae.

Its lower part comprises thick- to very thick-bedded (2–3 m), blocky to massive, medium- to coarse-grained, light gray to white quartzites. They are frequently recrystallized, and their grains are stretched parallel to foliation. The middle portion of the Naudanda Quartzite is constituted of medium- to very thick-bedded (0.5–2 m), pale yellow to light gray or green-gray quartzites, alternating with gray-green phyllites. Up to 20 m thick bands of massive, medium- to fine-grained, dark green amphibolite are sporadically distributed in the middle portion. The upper portion contains alternating bands of dark gray phyllite and light green to white laminated quartzite. The Naudanda Quartzite contains many mesoscopic and small-scale folds, which frequently plunge due east or northeast. With an increase in the proportion of phyllite, the Naudanda Quartzite passes into the overlying Nayagaun Formation. A massive bed of light green quartzite, containing metamorphosed mud clasts, is intercalated at the contact between them. The Naudanda Quartzite is about 1,300 m thick at Naudanda, but its thickness varies widely.

9.2.3 Nayagaun Formation

The stratigraphic position of this formation is rather uncertain, and it is assumed to be equivalent to the Dandagaon Phyllites of Stöcklin and Bhattarai (1977). The phyllites, which constitute more than 75 % of the Nayagaun Formation, are somber to dark green-colored, and they are generally free of *grits*. They are oftentimes fine-grained, regularly parallel-laminated, and alternating with thin to thick (a few cm to 1 m), wavy to lenticular bands of gray to green-gray, fine quartzites. However, there are also infrequent bands of

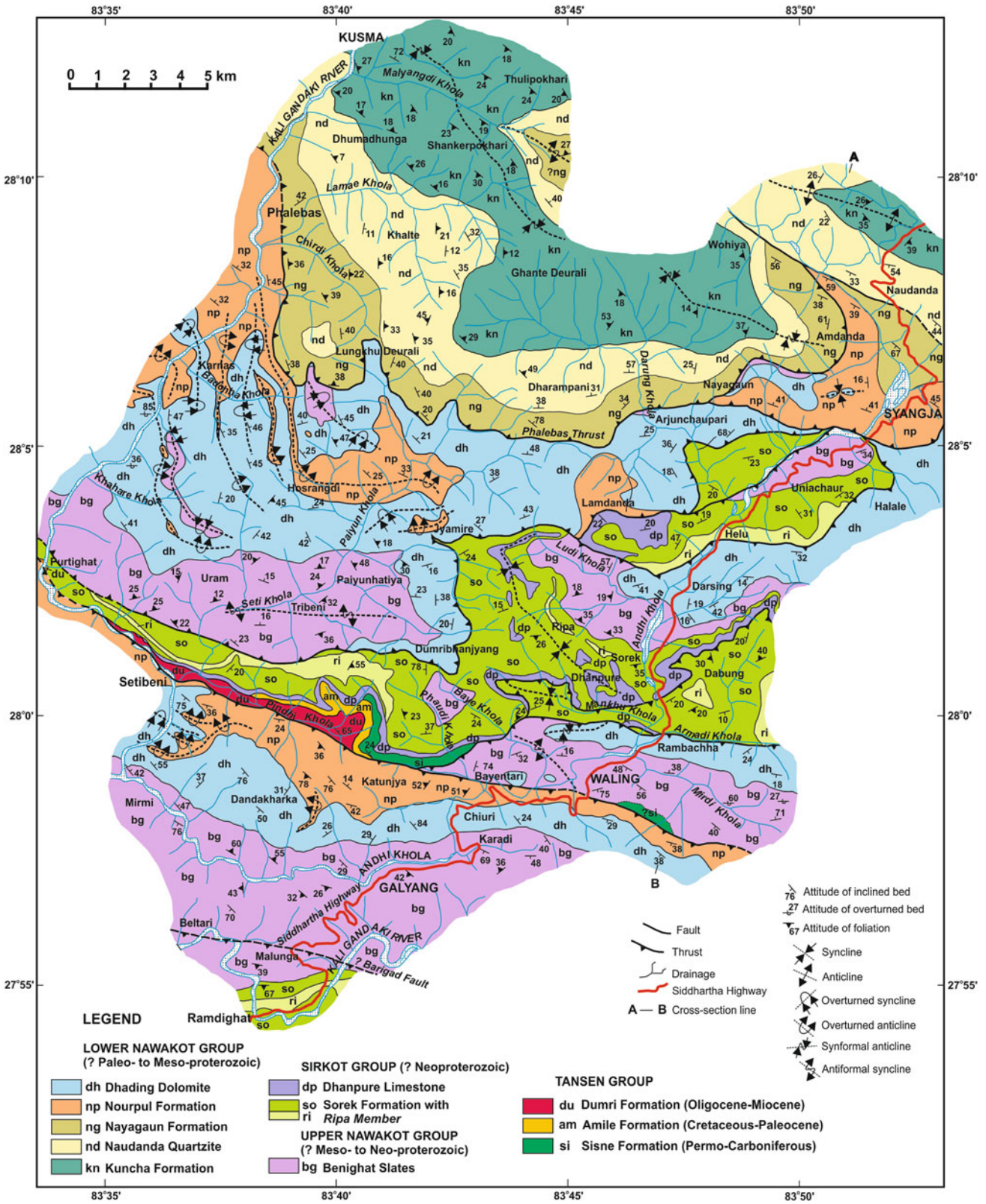

Fig. 9.5 Geological map of Kusma–Syangja area in west Nepal. *Source* Modified from Dhital et al. (2002). © Central Department of Geology, Tribhuvan University. Used by permission

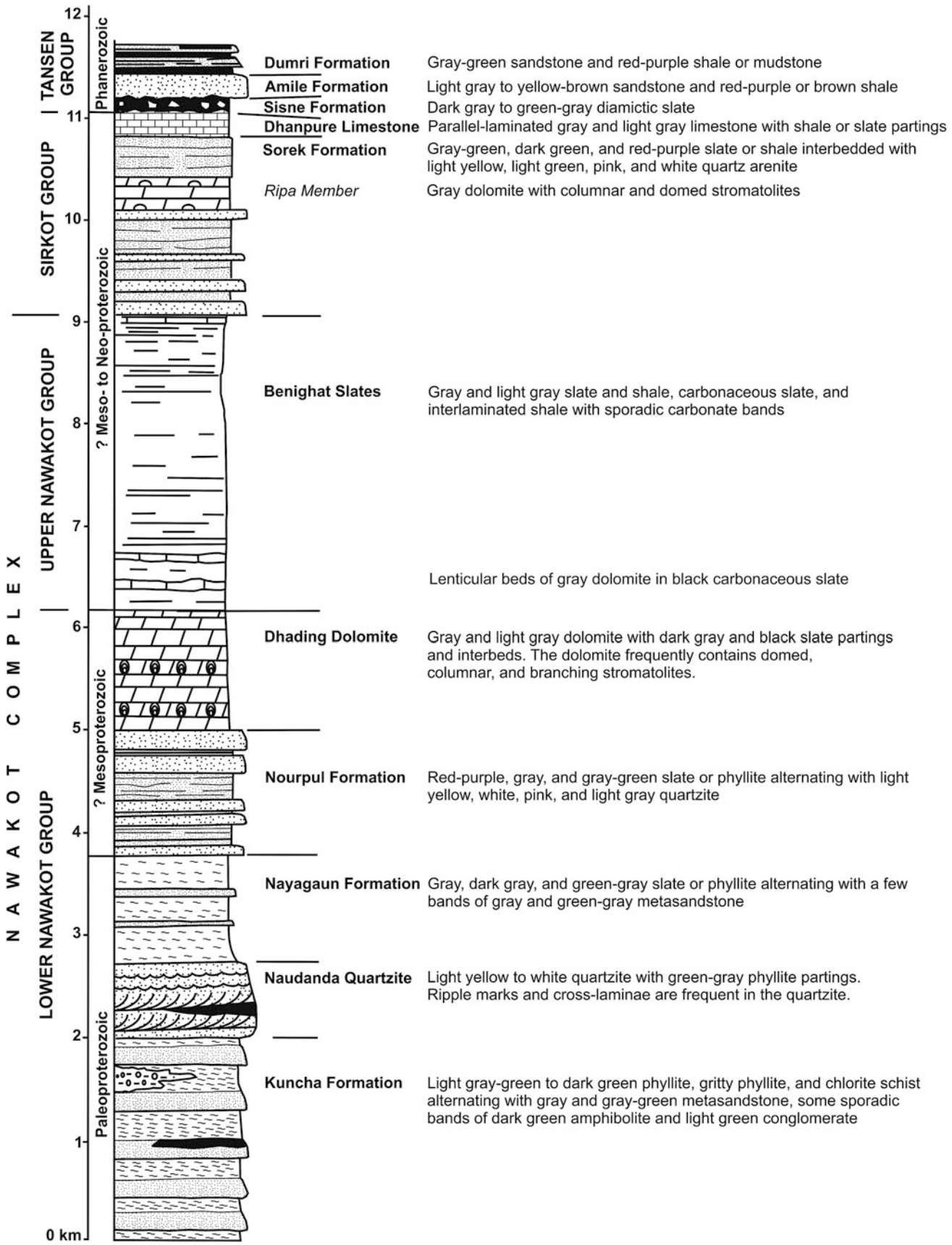

Fig. 9.6 Generalized lithostratigraphic column of the Lesser Himalayan rocks in the Kusma–Syangja area. *Source* Modified from Dhital et al. (2002). © Central Department of Geology, Tribhuvan University. Used by permission

coarse-grained green-gray quartzite. Their strongly deformed varieties exhibit a conspicuous crenulation cleavage. There also occasionally occur lenticular carbonate beds and dark gray to black calcareous quartzites. The black slates in the Lamae Khola alternate with thinly (10–30 cm) banded, fine-grained, dark gray calcareous metasandstones. The thinly alternating dark green phyllites and quartzites of the Nayagaun Formation transitionally pass into the overlying Nourpul Formation, which is about 100 m thick in the Darung Khola, and about 1,200 m in the vicinity of Haripala.

9.2.4 Nourpul Formation

The Nourpul Formation begins with a few centimeter- to decimeter-thick, gray-green and purple phyllites, slates, and quartzites. Although the rocks composing this formation display variegated (green, red, purple, pale yellow, gray, and black) colors, they are predominantly red-purple. Their color is vivid, especially when the rocks are slightly weathered, whereas the fresh outcrops exhibit somewhat darker tones.

To the south of Syangja, the lower part of the Nourpul Formation contains medium- to very thick-bedded, medium- to coarse-grained, dense, light gray and pink quartzite, alternating with red-purple and gray-green slates. Its middle portion is made up primarily of thick- to very thick-bedded, gray quartzites with prolific ripples and cross-laminae. The quartzites are intercalated in 5–25 cm thick bands of gray, dark gray, red-purple, and green-gray slates. The upper part is made up of pink, light gray, green-gray, and white quartzites, alternating with similar colored mottled slates of almost equal proportions. These slates frequently contain polygonal sun cracks and intraformational mud clasts, whereas the alternating quartzites are wavy to lenticular in shape.

A few sporadic beds of calcareous quartzite and dolomite are initially set in the middle sections of the formation, however, they become more frequent in its upper part. A gradational contact between the Nourpul Formation and the overlying Dhading Dolomite is represented by an alternation of pink quartzite, purple siliceous dolomite, and gray dolomite with black slate partings or interbeds. The Nourpul Formation attains a thickness of 12,000 m south of Syangja, and it is about 600 m thick near Bayentari.

9.2.5 Dhading Dolomite

The Dhading Dolomite constitutes almost all the precipitous peaks and ridges, occupying the middle and southern parts of the region. It is the lowermost prominent carbonate sequence, primarily made up of very thick, massive, and dense varieties of gray dolomite. The dolomite contains from 1 mm to 1 cm thick, continuous, plane to wavy, parallel to subparallel, light gray to blue-gray laminae. Generally, a dolomite sequence is from 1 to 5 m thick and displays typical splintery fractures. With the dolomite are regularly intercalated dark gray to black slate bands, ranging in thickness from a few milli meter to 1 cm and rarely exceeding 1 m. Some dolomites contain detrital quartz grains.

The lower part of this formation comprises very thick-bedded, massive, blue-gray dolomites with gray slate partings and interbeds, whereas its middle part consists of thick to very thick gray dolomite beds, containing stromatolites, intraclasts, and chert nodules (Fig. 9.7). The stromatolites are represented by about 1 m long and 10 cm wide columnar and branching varieties. There are also some small domed stromatolites together with algal mats, intraclasts, and chert in the middle and upper parts of this formation.

The dolomites are made up primarily of dolomicrite and pseudospar, which frequently contain cavities and vugs filled up with chert and quartz. There are calcite veins of various generations as well as stylolites and pressure solution strips within the dolomites. Owing to intense folding, downward-facing stromatolites are observed at a number of places, such as to the northwest of Waling and in the Paiyun Khola. Some dolomites in the Paiyun Khola contain elongated chert nodules, arranged essentially parallel to the wavy bedding and range in size from several milli meter to 20 cm. A few beds of medium- to coarse-grained, gray-green and white quartzite (3 cm–2 m) and gray slate (1–50 cm) are also intercalated in the dolomites.

The transitional contact between the Dhading Dolomite and the overlying Benighat Slates is marked by about 25 m thick, gray limestone band. The Dhading Dolomite is about 1,200 m thick.

The Upper Nawakot Group is represented here by the Benighat Slates alone, whereas in place of the overlying Malekhu Limestone found in central Nepal (Chap. 10), the Sorek Formation is developed.

9.2.6 Benighat Slates

The Benighat Slates contain very thinly (less than 1 mm) cleaved varieties. They sometimes contain thin strips of carbonaceous matter, best visible in fresh outcrops. On the other hand, their weathered varieties appear green-gray and light gray to brown. Another noticeable feature of these slates is that they display well-developed lamination, especially in the upper part of the formation. The plane, continuous, and parallel laminae range in thickness from less than 0.5 mm–2 cm. The conspicuous color banding in the laminated slates is due essentially to micrograding of the lamina, consisting of very fine sand (light gray), silt (gray), and clay (dark gray), respectively, from bottom to top.

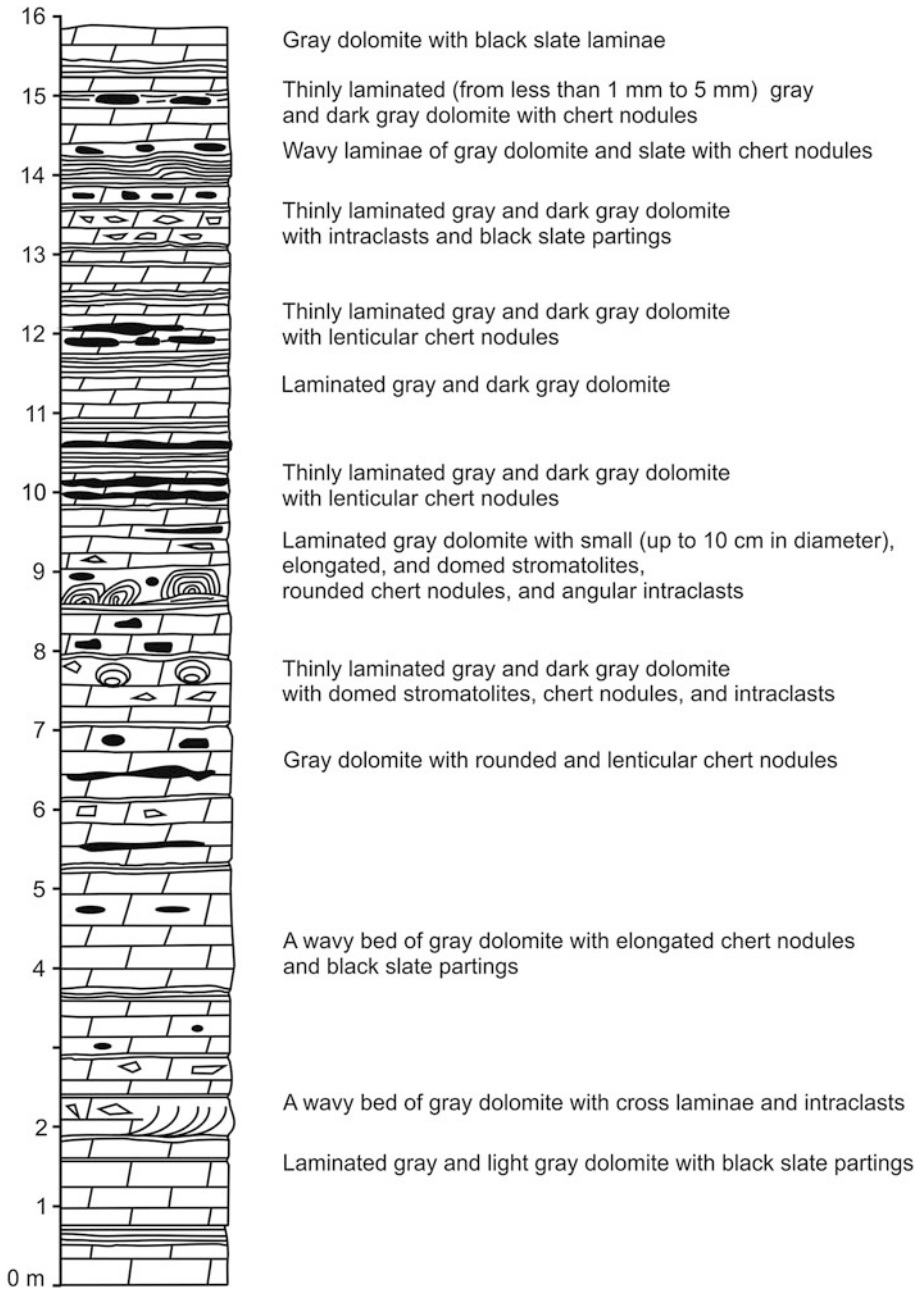

Fig. 9.7 Detailed column showing the position of stromatolites and some sedimentary structures from the lower part of the Dhading Dolomite. *Source* Modified from Dhital et al. (2002). © Central Department of Geology, Tribhuvan University. Used by permission

In the vicinity of Paiyunhatiya and Beulibas, and at Karadi, a carbonate band is observed within the slates, about 200 m above the contact with the Dhading Dolomite. Exceptionally rare, thin, very fine, dark gray quartzite bands are also intercalated in the slates. As a result of intense deformation, the slates are thrown into polyclinal and chevron folds. With the appearance of medium- to fine-grained pale yellow quartzite and red-purple and green slates, the Benight Slates transitionally pass into the overlying Sorek Formation of the Sirkot Group. The Benighat Slates are about 3,000 m thick in the neighborhood of Galyang and Malunga.

The lithological succession overlying the Benighat Slates is represented by the Sirkot Group, which is distributed in the middle portion of the region. The group is differentiated into the following formations.

9.2.7 Sorek Formation

The Sorek Formation begins with the appearance of gray-green and red-purple mottled slates, exhibiting fine laminae. There are also a few gray-green quartzite or calcareous quartzite intercalations. Wave as well as current ripples

abound on the upper surfaces of the quartzites, whereas conspicuous sun cracks prevail in the slates. The calcareous quartzites have a calcite cement, and in them quartz grains display irregular shapes, owing basically to their dissolution and overgrowth. This sequence is succeeded upwards by an alternating succession of red-purple to gray-green shale or slate and pale yellow, pink, or gray quartzite. This formation also contains some coarse-grained, gray to green-gray calcareous quartzites, with gray-green claystone partings and interbeds. The quartzites commonly display ripples, whereas sun cracks and intraformational shale clasts are discernible in the claystone. Although a few thick (50 cm–1 m) beds of gray dolomite occur at various stratigraphic levels, they become important towards the upper part of the Sorek Formation and are classified under the Ripa Member.

The Ripa Member comprises medium- to thick-bedded, gray to light gray dolomites, containing short columnar to domed stromatolites. The dolomites also frequently include many intraclasts (microbreccia) and are intercalated between gray-green and purple shales or slates, light gray to pink calcareous quartzites, and gray-green siltstones. The lenticular to discontinuous Ripa Member varies in thickness from 200 to 500 m, and it may be absent in some sections.

In the Seti Khola, near the confluence with the Pindhi Khola, the Ripa Member contains dark gray laminated slates, alternating with thick- to very thick-bedded, gray dolomite, containing short columnar as well as domed stromatolites. This sequence transitionally grades into the overlying Dhanpure Limestone. However, in some other locations, the Ripa Member grades into a succession of gray-green, dark gray to black, and red-purple shales with light gray, light green, and pink quartz arenites or calcareous quartzites. The upper part of the Sorek Formation is made up predominantly of black slates, transitionally passing into the overlying Dhanpure Limestone. The Sorek Formation is about 1,700 m thick, but it may be considerably thinner in some parts of the region.

9.2.8 Dhanpure Limestone

The Dhanpure Limestone occurs as a marker horizon in the study area, and frequently begins with a thick (25 m) band of gray-green to black carbonaceous shale or slate (Fig. 9.5), which is followed up-section by gray to green-gray parallel-laminated limestones with dark gray to black shale or slate partings and intercalations. The limestone is constituted mainly of micrite and pseudospar laminae, separated by a thin strip of dark claystone, and the rock is regularly ramified by various generations of crosscutting calcite veins. Generally, the Dhanpure Limestone is intensely deformed, and polyclinal to chevron folds are notable.

The Dhanpure Limestone sporadically contains about 1 m thick blue-gray laminated dolomite and thin (less than 10 cm) beds of laminated red-purple shale. Towards its upper section, the gray-green laminated limestones with black slate partings give way to a few pale yellow to light gray quartzite beds. The Dhanpure Limestone is 200–400 m thick, and a sharp disconformity separates it from the overlying Sisne Formation.

The Tansen Group, which represents the youngest rock succession in the intermediate zone, is confined to a narrow strip in the vicinity of Setibeni and the Pindhi Khola. It consists of the following formations.

9.2.9 Sisne Formation

The Sisne Formation overlies the Dhanpure Limestone, with a sharp disconformity. It is constituted of dark gray to gray-green diamictic slates with angular clasts (from 2 mm to 20 cm across) of gray dolomite, dark gray to black slate, and pale yellow to gray quartzite. There also set in dark gray to black (carbonaceous) slates and light gray or dark gray to green-gray quartzites. Nevertheless, the predominating lithology is a dark gray slate, with sparsely disseminated fine (less than 4 mm) clasts. The Sisne Formation is about 200 m thick in the Phaudi Khola, and a sharp disconformity separates it from the succeeding Amile Formation.

9.2.10 Amile Formation

This formation is confined mainly to the middle and upper reaches of the Phaudi Khola, where it rests either over the Sisne Formation or the Dhanpure Limestone, and is represented by medium- to coarse-grained, massive, yellow-gray quartzite with a few gray or brown shale beds. In a small tributary of the Pindhi Khola, there are dark gray-green sandstones, with partings and interbeds of laminated gray-green siltstone and shale. They are followed upwards by very thick-bedded dark gray to brown sandstones. These rocks also presumably belong to the Amile Formation. The Amile Formation is about 200 m thick.

9.2.11 Dumri Formation

The Dumri Formation, the youngest rock of the region, is distributed as a continuous band between Setibeni and the Pindhi Khola. There is a small outcrop of this formation at Purtighat. This formation rests disconformably over the Sorek Formation, Dhanpure Limestone, and Amile Formation. The Dumri Formation contains very thick (up to 20 m)

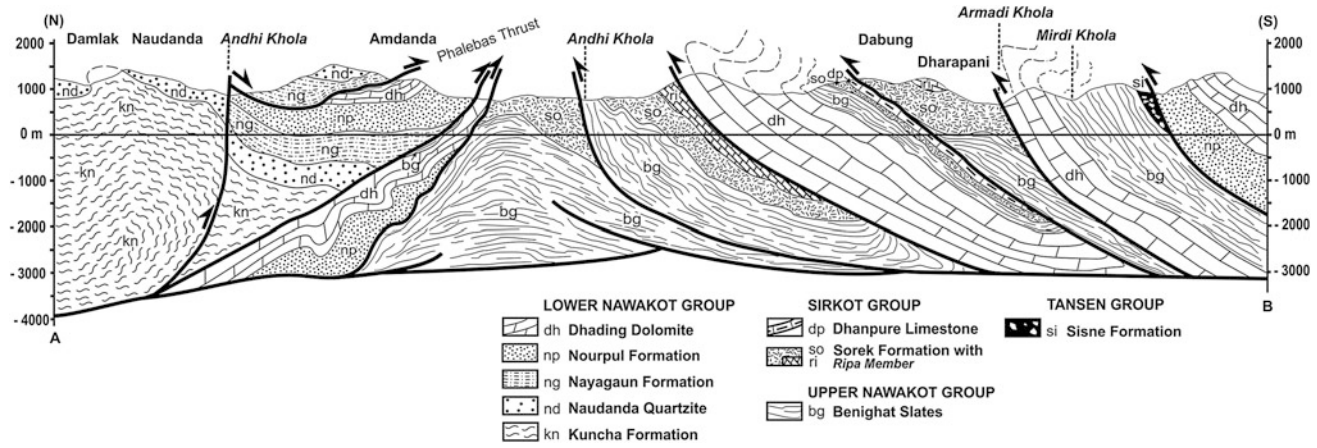

Fig. 9.8 Geological cross-section across the line A–B (Fig. 9.5) depicting north- and south-dipping faults and a triangle zone in the middle. *Source* Modified from Dhital et al. (2002). © Central Department of Geology, Tribhuvan University. Used by permission

fining-upwards cycles of gray-green soft sandstone and green or red-purple mottled shale or mudstone. A sequence of very thick-bedded, massive (5–10 m), pebbly (2–5 mm across) sandstone; parallel- and cross-laminated green sandstone; and very thick-bedded (up to 15 m) red-purple shale, crops out on the left bank of the Kali Gandaki River. In it, the rounded to subangular pebbles are composed of vein-quartz, red chert, and pink quartzite. The Dumri Formation attains a maximum thickness of about 400 m in the Pindhi Khola.

9.2.12 Structure of Intermediate Zone

The Phalebas Thrust divides this region into the low-grade metamorphic rocks of the north unit and sedimentary rocks of the south unit (Upreti et al. 1980). The area also contains numerous north- as well as south-dipping imbricate faults, constituting a triangle zone (Fig. 9.8). Folds of various sizes, some of them with overturned limbs, are found in the western part of the area, where their curved axial traces imply superposed folding.

9.3 Outer Zone of Kali Gandaki and Palpa

In this part of the Lesser Himalaya, Fuchs and Frank (1970) determined major stratigraphic units, including the fossiliferous beds of Palpa. However, the comprehensive investigations of Sakai (1983, 1985) revealed its complex stratigraphic and structural aspects. In this area, he recognized the Kali Gandaki Supergroup consisting of the Lower, Middle, and Upper groups. His Lower Kali Gandaki Group constitutes part of the Nawakot Complex discussed above, and the other two groups are described below.

The Middle Kali Gandaki Group is distributed primarily between the Kali Gandaki River and the north slopes of the Mahabharat Range (Fig. 9.9). Its age is assumed to range between the Mesoproterozoic and Neoproterozoic, based on the relationship of these rocks with the underlying rocks of the Dhading Dolomite and Benighat Slates (Dhital et al. 2002). The Middle Kali Gandaki Group includes the following formations.

9.3.1 Heklang Formation

The Heklang Formation is made up essentially of dark gray-green slates and phyllites. When weathered, they exhibit brown and gray tints. The phyllites frequently alternate with up to 10 m thick bands, incorporating calcareous laminae. There also appear some dark brown weathering subordinate beds of calcareous sandstone, marl, and dolomite. The Heklang Formation is more than 800 m thick at its type locality (Sakai 1985, p. 346). It transitionally passes into the overlying Virkot Formation.

9.3.2 Virkot Formation

The Virkot Formation is represented by light pink to white quartzites and red-purple slates or phyllites. Owing to the intercalation of these white and red-purple rocks, this formation manifests a characteristic color banding (Sakai 1985, p. 348). The contact between the Virkot Formation and underlying Heklang Formation is placed at the first appearance of red-purple slate. The Virkot Formation is about 510 m thick and further subdivided into the following two members.

Most of the Lower Member (Fig. 9.10) is a monotonous succession of red-purple shale or slate with well-developed crenulation cleavage. This member also contains some calcareous laminae at various stratigraphic levels. The shale is frequently variegated, finely mottled, and bioturbated. There also appear a few irregular beds of gray-green shale, ranging

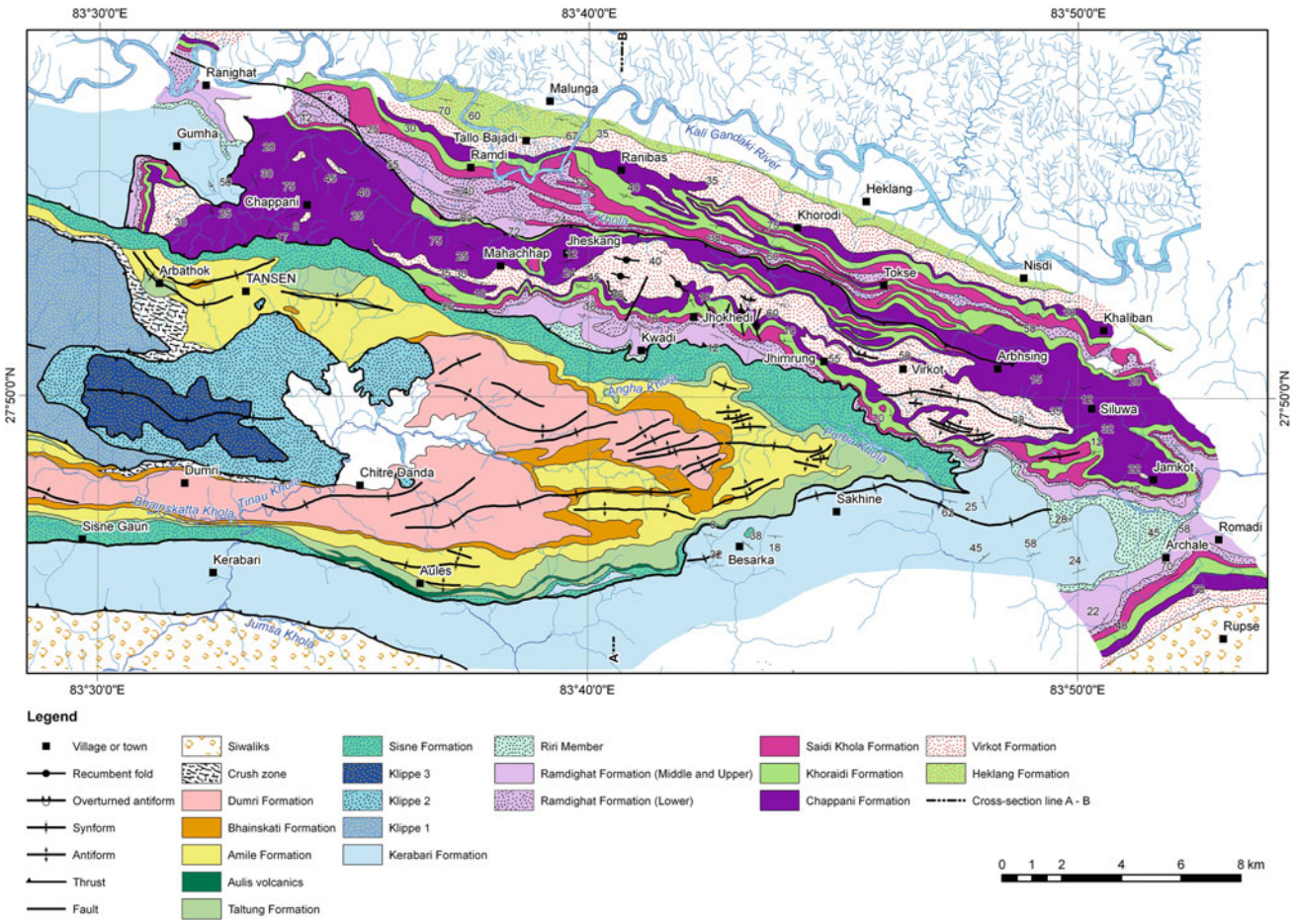

Fig. 9.9 Geological Map of the Kali Gandaki area. *Source* Modified from Sakai (1983, 1985)

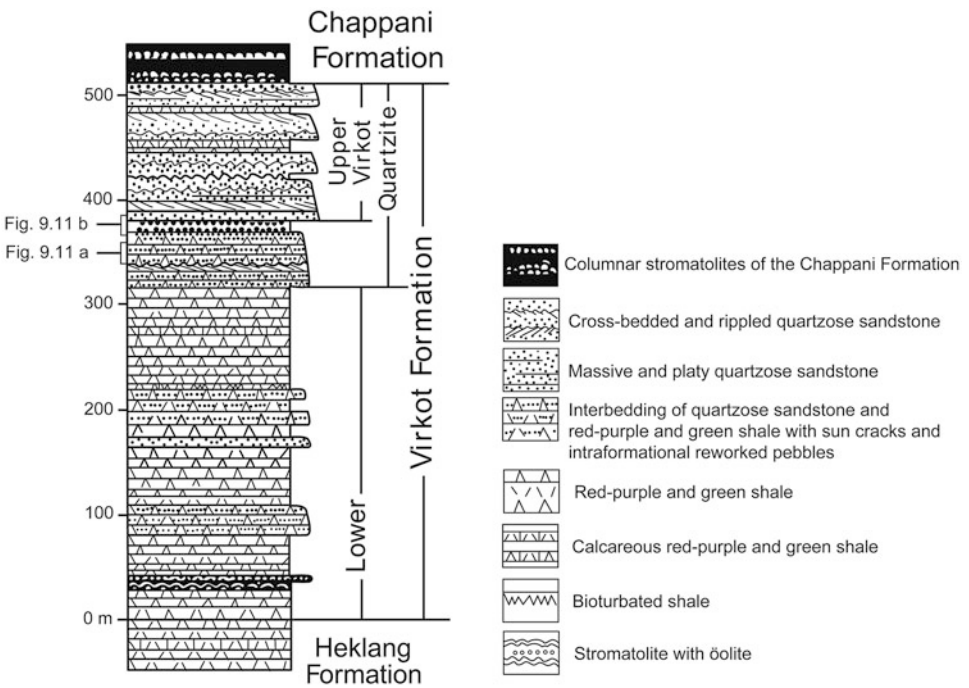

Fig. 9.10 Columnar section of the Virkot Formation with its two members. *Source* Modified from Sakai (1985). © H Sakai. Used by permission

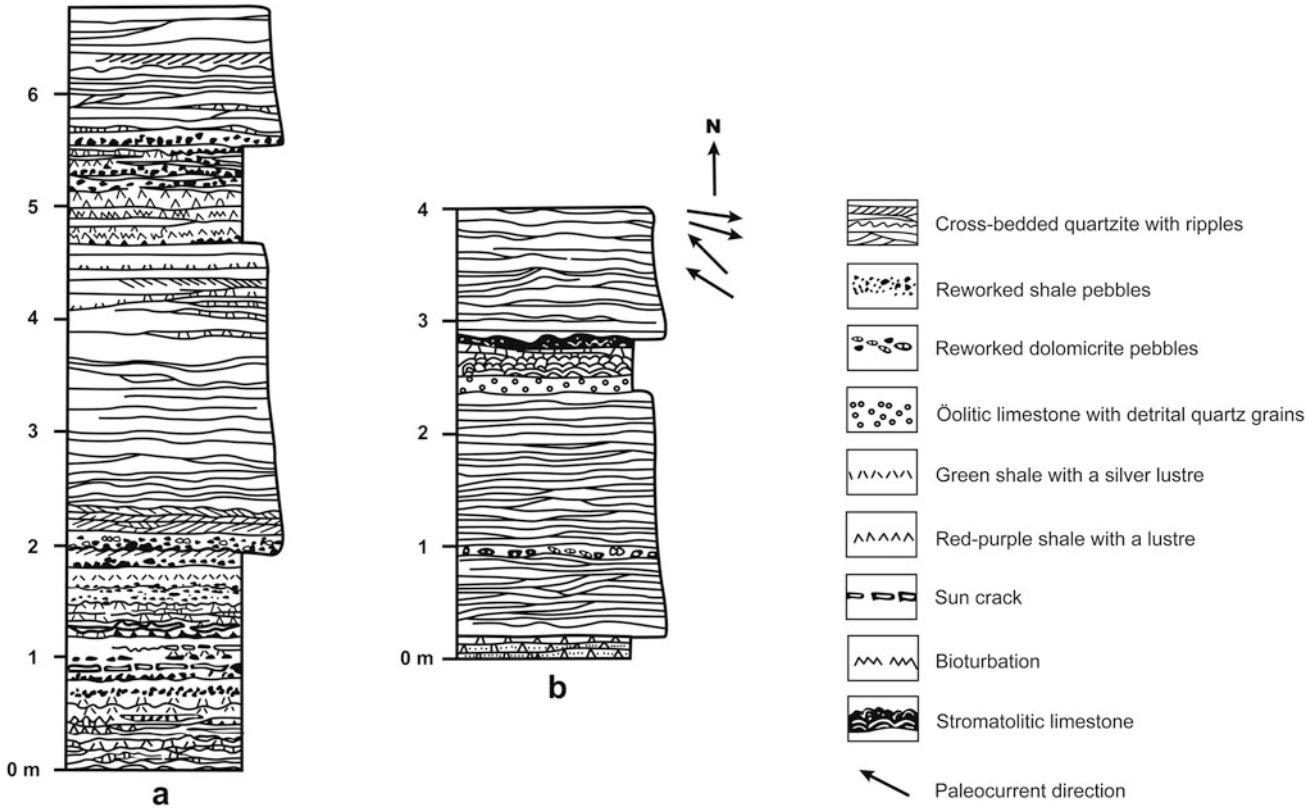

Fig. 9.11 Detailed columnar section from the lower part of the Virkot Formation (see Fig. 9.10) depicting various sedimentary structures. *Source* Modified from Sakai (1985). © H Sakai. Used by permission

in thickness from less than a meter to 10 m. In the type area, there are two stratigraphic horizons, where intercalations of banded shale and quartzite repeat at 1–10 m intervals. Some of the shales depict sun cracks and intraformational shale pebbles, whereas the quartzites include sporadic dolomite pebbles. In the lower portion of this member, an approximately 2 m thick stromatolitic dolomite bed is intercalated, and it shows gently undulating regular algal laminae. The stromatolitic dolomite rests over a green shale, with a sharp lower contact, and is followed up-section by rhythmically interbedded red-purple shale and quartzose sandstone. It is the lowermost stromatolitic horizon encountered in the Kali Gandaki Supergroup (Sakai 1985, p. 348). The Lower Member is about 300 m thick.

Pink, white, and light green quartz arenites regularly alternate with red or green shales or slates in the lower portion of the Upper Member. The individual beds range in thickness from a few centimeters to 5 m. In the type section, from 10 to 20 cm thick quartzite beds display wavy and planar bedding, and sporadically contain thin red or green sericite-bearing slate partings (Fig. 9.11). The quartzites exhibit a bimodal distribution of grains: the well-rounded quartz grains are from 0.5 to 0.8 mm in diameter, whereas the subangular to subrounded ones vary from 0.05 to 0.3 mm in size. Apart from quartz, some well-rounded, medium to coarse grains of micrite and tourmaline are sporadically observed in the quartzite. In the quartzite, cross-bedding and ripple marks are frequent, whereas ripple cross-lamination and asymmetric ripple marks are infrequently observed. There are also variegated shale flasers. The shale beds also occur as thin partings and from 1 to 5 cm thick interbeds, containing conspicuous polygonal sun cracks and intraformational shale pebbles.

A 25 cm thick oolitic limestone bed is followed by a 15 cm thick stromatolitic limestone bed towards the top part of the Upper Member (Fig. 9.11). These beds serve as a marker horizon, as they extend for a long distance. The oolitic limestone is made up of ooids (0.5–1 mm in diameter), some peloids (less than 0.5 mm in length), and a minor amount of detrital quartz grains in a micritic matrix. Most of the ooids exhibit a concentric pattern (? oncolites), they are radially cracked, and some are broken into smaller fragments. The columnar and domed stromatolites in the limestone are from 3 to 8 cm wide, 10 to 15 cm high, and tightly packed. They consist of thinly (0.5–1 mm) alternating light and dark laminae, and within the dark ones, there is also very fine (as thin as 0.01 mm) internal lamination (Sakai 1985, p. 350). The last bed of stromatolitic limestone is covered by a 1 m

thick bed of laminated gray shale and quartzite containing some rain imprints.

The uppermost part of the Upper Member is characterized by the abundance of very thick (tens of meters) pink quartzites. They display striking planar as well as wedge cross-laminations and a variety of ripple marks. Their petrographic characteristics are akin to those occurring in the lower part of the Upper Member. A stromatolitic dolomite bed lies about 40 m above the base of the upper part in the Angha Khola and Virkot areas. Its maximum thickness is about 80 m and it rests on a red quartzite bed. The diameter of domed to bulbous stromatolites ranges from 10 cm to more than 50 cm. The stromatolitic dolomite is frequently interbedded with about 2 cm thick lenticular beds of subrounded to well-rounded, fine-grained, quartzose sandstone with dolomitic matrix (Sakai 1985, p. 851).

The Virkot Formation was deposited in arid conditions. The thick quartzite beds were formed as sand dunes. The wavy and planar bedforms with cross-bedding, herringbone cross-bedding, and ripple marks indicate a mixed origin of tidal and eolian environments near the shoreline. On the other hand, red-purple and green shales, predominating in the Lower Member, were deposited from suspension in a lagoonal environment, whereas the three stromatolitic horizons observed in the Upper Member indicate the deposition of these and associated rocks in an intertidal zone (Sakai 1985, p. 351).

9.3.3 Chappani Formation

The Chappani Formation rests conformably over the Virkot Formation and is represented mainly by fine-grained sediments, containing small stromatolites at various levels. This formation is 400 m thick at its type locality and divided up into the following three members (Sakai 1985, p. 353).

The Lower Member commences with a several meter-thick, silicified, columnar stromatolitic bed. The bed is overlain by a thick succession of gray slates, containing light green, thin, and parallel clay laminae at different stratigraphic rungs. There are also intercalated small columnar stromatolites, occupying various stratigraphic positions (Fig. 9.12). The stromatolitic beds are from 0.1 to 1 m thick and alternate with micritic limestone beds or lenses (Sakai 1985, p. 353). The stromatolite bodies display columnar and branching morphologies. The columns range in diameter from 5 to 15 cm. They are of a uniform diameter at the base, but become wider and less curved upwards, and their branching occurs a little after widening of the columns. The stromatolitic lamination is represented by 0.1–1 mm thick

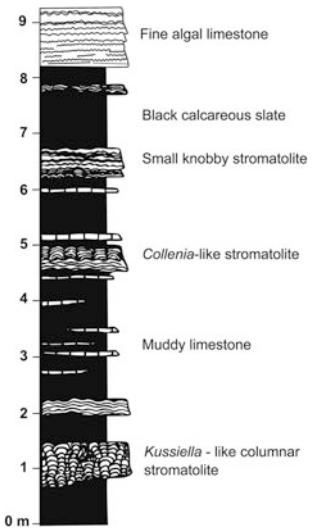

Fig. 9.12 Position of various stromatolitic beds in the Chappani Formation. *Source* Modified from Sakai (1985). © H Sakai. Used by permission

dark and light gray alternating bands. There also occur stromatolitic laminae, comprising laterally linked and closely spaced vertical columns. The columns are up to 1 m high and their diameter varies from 10 to 20 cm. There also occur tabular to slightly undulating stromatolitic biostromes (Sakai 1985, p. 354).

The Middle Member is a sequence of rhythmically alternating red-purple and green calcareous clay-slate. Its thickness ranges from 50 to 70 m, and it sporadically contains 5 to 10 cm thick, cream colored micritic limestone beds (Sakai 1985, p. 354).

The Upper Member comprises white, light pink, and light green quartzose sandstones, intercalated in the same colored shales or slates. In the type section, it commences with a 10 m thick succession of quartzose sandstone, the lower part of which is characterized by an alternation of 3–10 m thick, fine sandstone and light green shale beds. Various ripples, cross-laminae, and wedge bedding are present in the sandstone beds of the Upper Member. Red-purple and green reworked flat pebbles of shale frequently constitute interstratifications. One of the remarkable aspects of the Upper Member is the appearance of eolian sand beds and disseminated sand grains in dolomite beds (Sakai 1985, p. 355).

The clay-slates comprising the Lower Member of the Chappani Formation were deposited from suspension in the tranquil water of a lagoon, whereas the graded laminae presumably resulted from the turbidity currents related to sporadic flooding in an arid environment. The basal silicified stromatolites could have been formed in an intertidal zone.

On the other hand, the small stromatolites, appearing in the Lower Member, were formed in supratidal ponds, marshes, or lagoons. Similarly, most of the Upper Member was deposited in lagoonal beaches and eolian dune complexes (Sakai 1985, p. 356).

9.3.4 Khoraidi Formation

The Khoraidi Formation begins with a large stromatolite-bearing dolomite bed, resting over the quartzites of the Chappani Formation. This formation consists predominantly (more than 80 %) of stromatolitic dolomites. Apart from them, there also occur a few strata made up of oolites and others, represented by quartzites, and rhythmites. Its thickness at the type locality is about 350 m (Sakai 1985, p. 356).

Sakai (1985, p. 357) classified the stromatolites, occurring in the Khoraidi Formation in the following morphological types:

- Flat to undulatory laminated sheet forms
- Tabular forms
- Columnar and conical forms
- Subspherical to domed forms
- Oncolites.

In the Khoraidi Formation, subspherical to domed stromatolites predominate, and they are generally followed upsection by tabular bodies (Fig. 9.13). The stromatolites are laterally linked to yield 0.5–1 m thick biostromes. The domed and subspherical forms have a diameter ranging from 10 cm to 1 m, and the succeeding tabular forms reach 4 m. The stromatolites are from 30 to 70 cm high and frequently densely grow without interspaces. If such interspaces between the columns do occur, they are filled up with oolites, dolomite breccias, and broken stromatolite pieces (Sakai 1985, p. 358).

The stromatolites are made up of 1–2 mm thick black organic laminae and light dolomicritic laminae stacked at an interval of 1–2 cm. There also occur several oncolite beds, intercalated with calcareous sandstones and oolitic horizons, found in between the stromatolite biostromes (Sakai 1985, p. 359).

The oolitic rocks are represented mainly by pure oodolosparite or its arenaceous varieties, whose interspaces are filled up with sparry dolomite, and their nuclei are made up of detrital quartz grains, sometimes displaying idiomorphic overgrowth. From a few decimeters to 3 m, thick, fine- to medium-grained, light gray quartzose sandstone beds are commonly intercalated in the Khoraidi Formation. Some gypsum pseudomorphs are also scattered in these sandstone beds at various stratigraphic rungs (Sakai 1985, p. 360).

Sporadically occurring rhythmites are constituted of thinly laminated shale and sandstone. They are from 5 cm to a few meters thick with sharp lower and upper bounds. These beds sometimes record bioturbation, represented by small sand pipes and tubules (Sakai 1985, p. 360). The Khoraidi Formation was deposited in intertidal sandy flats, algal flats, sandy beaches, tidal channels, and lagoons in an arid shoreline environment (Sakai 1985, p. 361).

9.3.5 Saidi Khola Formation

The Saidi Khola Formation (Fig. 9.14) is represented mainly by a rhythmic interbedding of sandstones and shales. It is 180 m thick at its type section in the Saidi Khola, and in turn subdivided into the following three parts (Sakai 1985, p. 362).

A 2–3 m thick basal bed of the Saidi Khola Formation rests conformably over the last stromatolitic dolomite bed of the Khoraidi Formation. The basal bed comprises a 1–4 mm (exceptionally up to 1 cm) thick interlaminated sequence of quartzose sandstone and black shale. The shale is infrequently bioturbated and contains the tubules of quartzose sandstone.

The above basal bed is followed upwards by a succession of thickly (up to 50 cm) interbedded sandstone and shale. In this part, the sandstone-to-shale ratio gradually increases upsection, and towards the middle portion of the Saidi Khola Formation, some thick-bedded coarse sandstone beds appear (Sakai 1985, p. 362). Excluding their light green, green, or light purple colors, the shales occurring in the middle portion are otherwise similar to those found in the upper part. In the lower and middle portions of the formation, the thickness of shales and sandstones generally ranges from 2 to 10 cm. There are many rhythmites where quartzose sand laminae are from 1 to 5 mm thick. Some thin (up to 5 cm) sandstone beds extend for more than 10 m laterally, whereas others as thick as 20 cm wedge out at a distance of just 2 m (Sakai 1985, p. 363).

The beds of the Saidi Khola Formation gradually become thinner upwards, and finally at the top appear bioturbated rhythmites. The last rhythmite sequence is from 5 to 10 m thick and passes upwards into the slates of the overlying Ramdighat Formation. The rhythmites of the Saidi Khola Formation were deposited in an intertidal environment (Sakai 1985, p. 363).

The Upper Kali Gandaki Group is predominated by fine terrigenous rocks and carbonates. It is distributed in the tight synclinal cores as well as in the Mahabharat Range, bordering on the Siwaliks. This group is divided up into the following two formations.

9.3.6 Ramdighat Formation

The Ramdighat Formation (Fig. 9.14) comprises basically calcareous argillites, with a minor proportion of thin limestone. Coarse-grained terrigenous rocks are characteristically absent in this formation. It attains a thickness of about 750 m in its reference section of the Nisti Khola and is subdivided into the following members (Sakai 1985, p. 365).

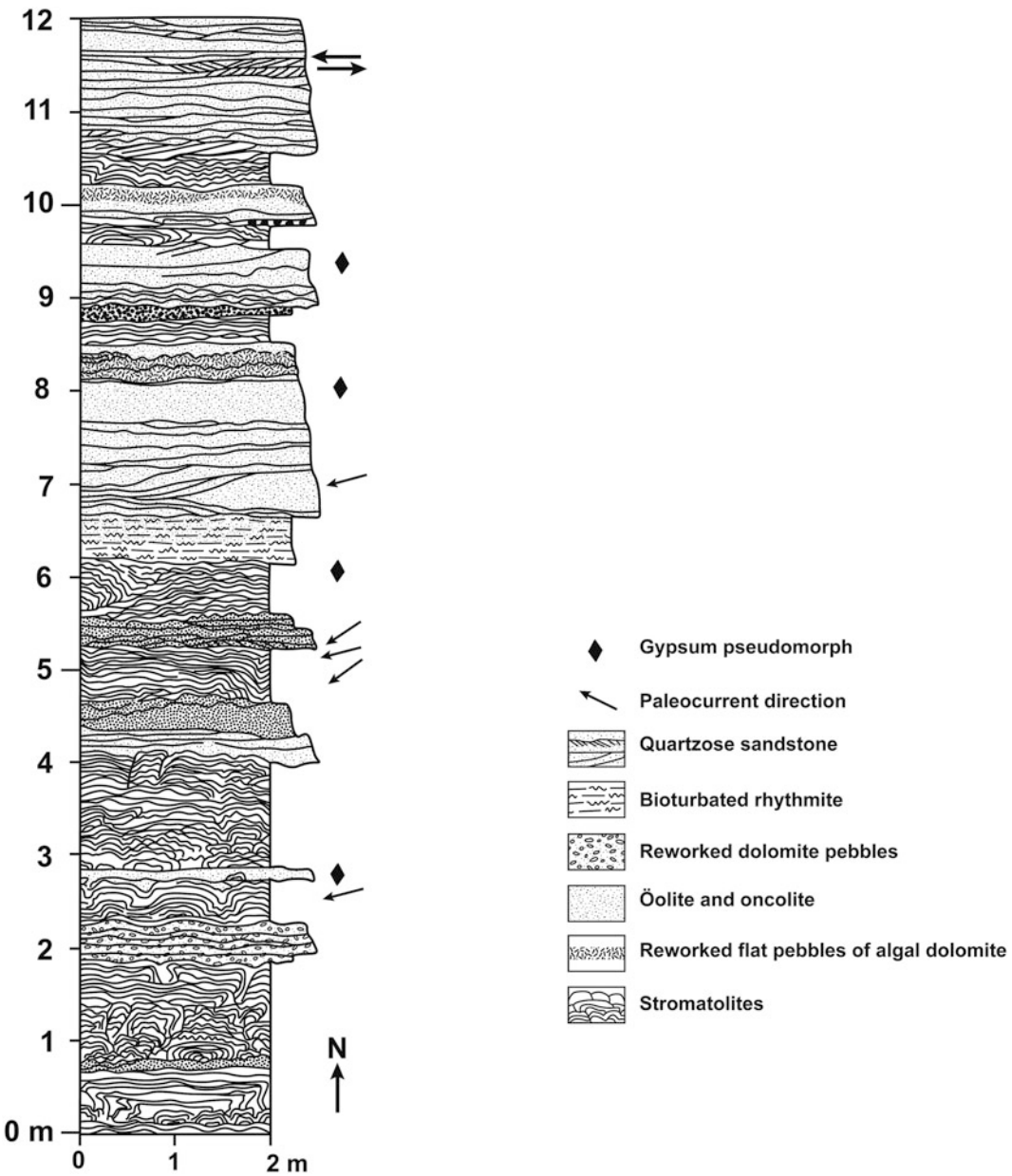

Fig. 9.13 Detailed column of the Khoraidi Formation showing various stromatolites. *Source* Modified from Sakai (1985). © H Sakai. Used by permission

The approximately 80 to 90 m thick Lower Member begins with black slates that form two-thirds of the total thickness, and they grade into the green slates, constituting the upper one-third of the member. Their bedding surface can be discerned by sporadically occurring fine sandstone laminae. Well-developed clay cleavage forms sharp-edged angular plates, coated with fibrous sericite (Sakai 1985, p. 365).

The Middle Member comprises calcareous slates, characterized by a few meter-thick conspicuous red-purple, pink, and green varieties. These slates are regularly and thinly interbedded with white limestones. The individual slate and limestone beds or laminae range from 1 mm to 5 cm in thickness. The limestone contains light microsparite and dark micrite laminae, whereas the variegated slates incorporate angular to rounded silt- to clay-sized quartz grains in a dirty microsparite matrix (Sakai 1985, p. 366).

The Upper Member begins with a rhythmite of thinly interbedded white limestone and gray calcareous slate. Its middle portion is represented by green to gray-green and brown calcareous slate and rhythmite, consisting of lenticular white limestone and brown calcareous slate. The interbedded slate bands are from 2 mm to 5 cm thick and infrequently

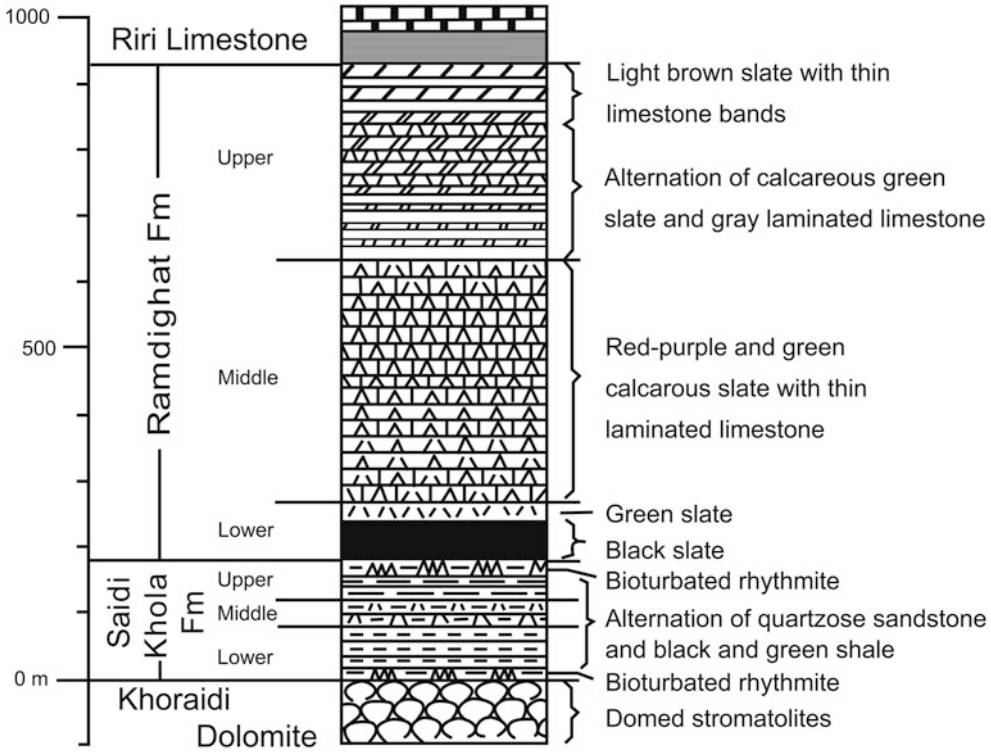

Fig. 9.14 Stratigraphic column of the Saidi Khola and Ramdighat formations. *Source* Modified from Sakai (1985). © H Sakai. Used by permission

bioturbated. There is also a 5 to 7 mm thick graded bed of intraclastic limestone, intercalated in the slate. It contains intraclasts of oolite, peloids, and rounded sand-sized micrite in a sparry calcite matrix. The proportion of limestone beds and laminae decreases upwards, and the upper part is made up of finely laminated dark brown calcareous slate with a few black carbonaceous laminae (Sakai 1985, p. 366). The Ramdighat Formation was deposited in a lagoon or a large bay that bordered an intertidal flat with an algal marsh zone (Sakai 1985, p. 367).

9.3.7 Kerabari Formation

The Kerabari Formation (Fig. 9.15), the youngest sequence of the Kali Gandaki Supergroup, rests conformably on the Ramdighat Formation. At its type section, the Kerabari Formation is more than 2,100 m thick and subdivided into the following two members (Sakai 1985, p. 367).

The Riri Limestone Member, occurring at the bottom of the Kerabari Formation, contains platy, black, argillaceous limestones of 100–150 m thickness. They begin with decimetric beds of black calcareous and carbonaceous slate and limestone. Under the microscope, the limestone is represented by sparite, with some fine quartz grains. The dark color of the rock results from very fine (0.02–0.05 mm thick) carbonaceous laminae. The uppermost section of the member is composed of black limestone (mainly pure sparite), alternating with thin black shale (Sakai 1985, pp. 367–369).

The main part of this member is comprised of the Kerabari Dolomite, which is thick- to very thick-bedded, laterally persistent and monotonous, light gray rock. This member is roughly subdivided into the following three parts.

The thickly interbedded black slates and limestones of the Riri Member gradually grade upwards into the thin-bedded black shales and gray dolomites. These last couples attain a thickness of 100–200 m and may partly comprise rhythmites. Sporadic knobbly algal structures are found in the dolomite. Farther upwards, there are thinly (up to 10 cm) bedded dolomites, containing ripple marks or parallel laminae, and they constitute from 100 to 200 m of the stratigraphic succession, whereas the uppermost 200 to 300 m of the lower part is composed of bedded dolomicrite with intraformational dolomicrite pebbles and sporadic oscillation ripple marks or flute casts (Sakai 1985, p. 369).

The middle portion is represented principally by thinly to thickly (5–50 cm) plane-parallel bedded dolomicrite. A bed of laterally linked domed stromatolitic dolomite constitutes its lower limit. There are also some thin (1–5 cm), platy to lenticular or nodular, dark gray to black chert beds in its lower and upper parts. Some of the chert beds are rhythmically interbedded with platy dolomite beds.

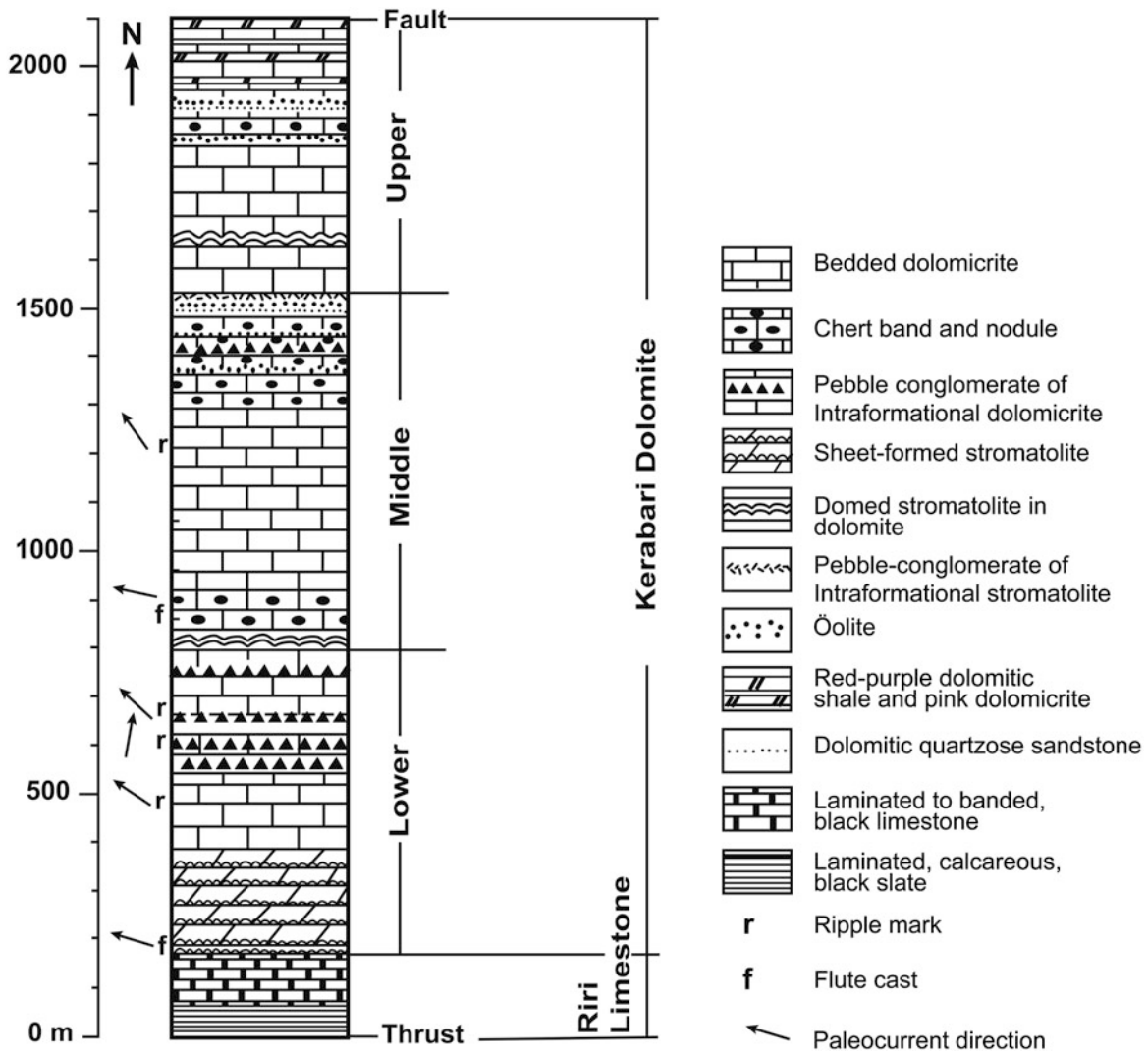

Fig. 9.15 Columnar section of the Kerabari Formation showing its two members. *Source* Modified from Sakai (1985). © H Sakai. Used by permission

There also occur intraformational dolomicrite, chert, and sandstone pebble-bearing conglomerate beds, some of which are graded and contain flute casts. A few of such conglomerates contain clasts of stromatolite. Towards the upper part of it are found several thin oolitic beds (Sakai 1985, p. 370).

The upper portion comprises platy- to wedge-shaped dolomicrite beds, with varying thickness. There also occur light pink to purple shale, dolomite, and conglomerate, containing agate granules (Sakai 1985, p. 370). The Kerabari Formation was deposited in shallow marine conditions of an inner shelf, intertidal zone, and lagoon. Subrounded quartz grains could have been originated from wind-blown sands (Sakai 1985, p. 372). The Kerabari Formation is succeeded by the overlying Sisne Formation of the Tansen Group with a disconformity, marked by a basal conglomerate (Sakai 1983).

9.4 Stratigraphy of Tansen Group

Sakai (1983) investigated the Tansen Group of predominantly clastic sedimentary rocks from the Lesser Himalaya of west Nepal. The Tansen Group (Figs. 9.16 and 9.17) attains a maximum thickness of 2,400 m, and is divided up into the following formations, respectively, from the bottom upwards.

9.4.1 Sisne Formation

The Sisne Formation is the lowest unit of the Tansen Group. It disconformably overlies the Kerabari Formation of the Kali Gandaki Supergroup. The disconformity exposed at

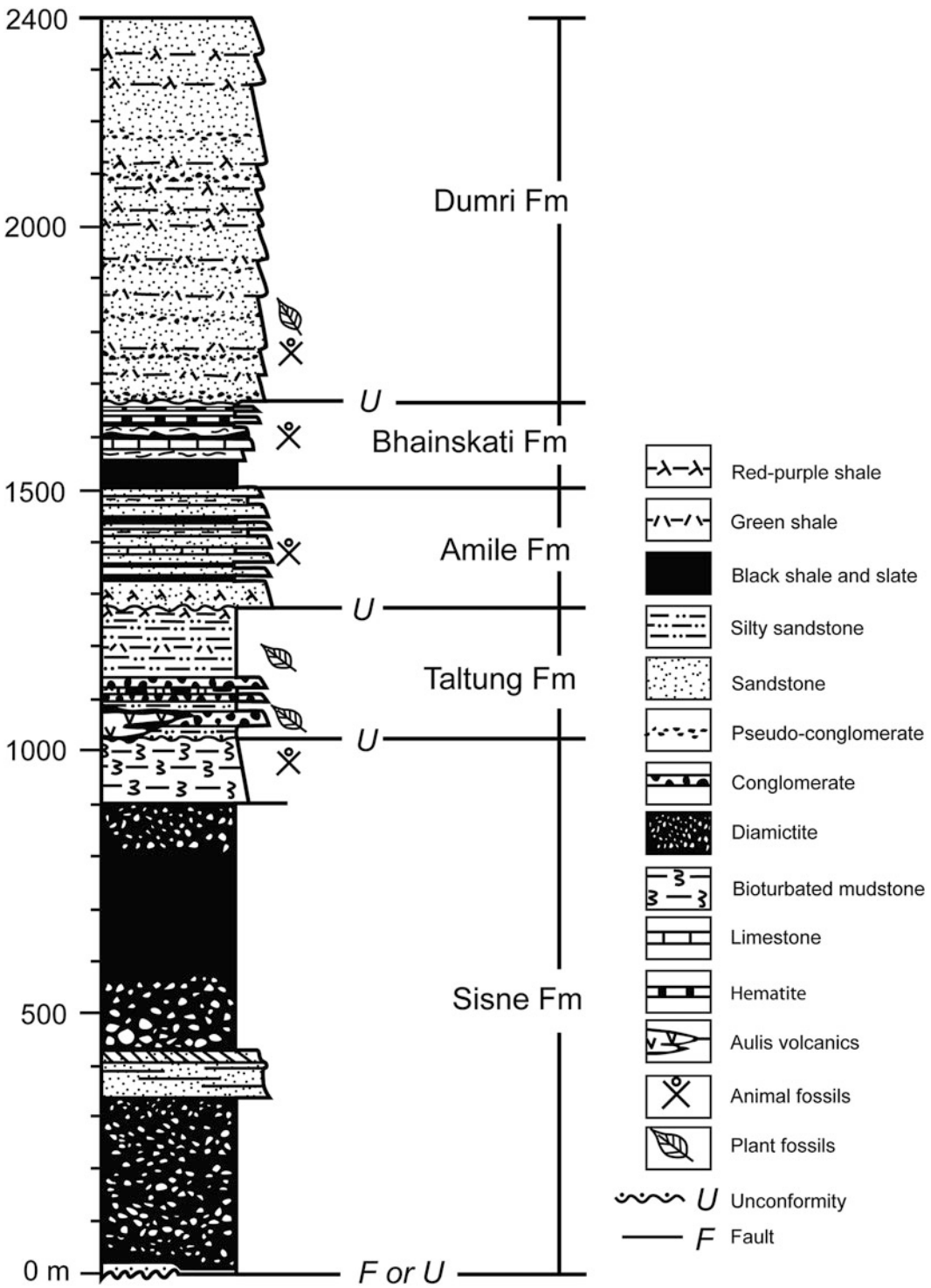

Fig. 9.16 Generalized lithostratigraphic column of the Tansen Group. *Source* Modified from Sakai (1983). © H Sakai. Used by permission

Besarka is marked by about 20 cm thick basal conglomerate, containing angular clasts of algal, oolitic, and massive dolomite and chert, derived primarily from the Kerabari Formation. The top part of the conglomerate also exhibits a limonitic weathered surface (Sakai 1983, p. 35). The basal conglomerate is succeeded, respectively, by a 50 cm thick micaceous shale bed with plant remains, a 4–5 m thick, black, micaceous shale, and a 6 m thick mudstone, containing unsorted sand and granules.

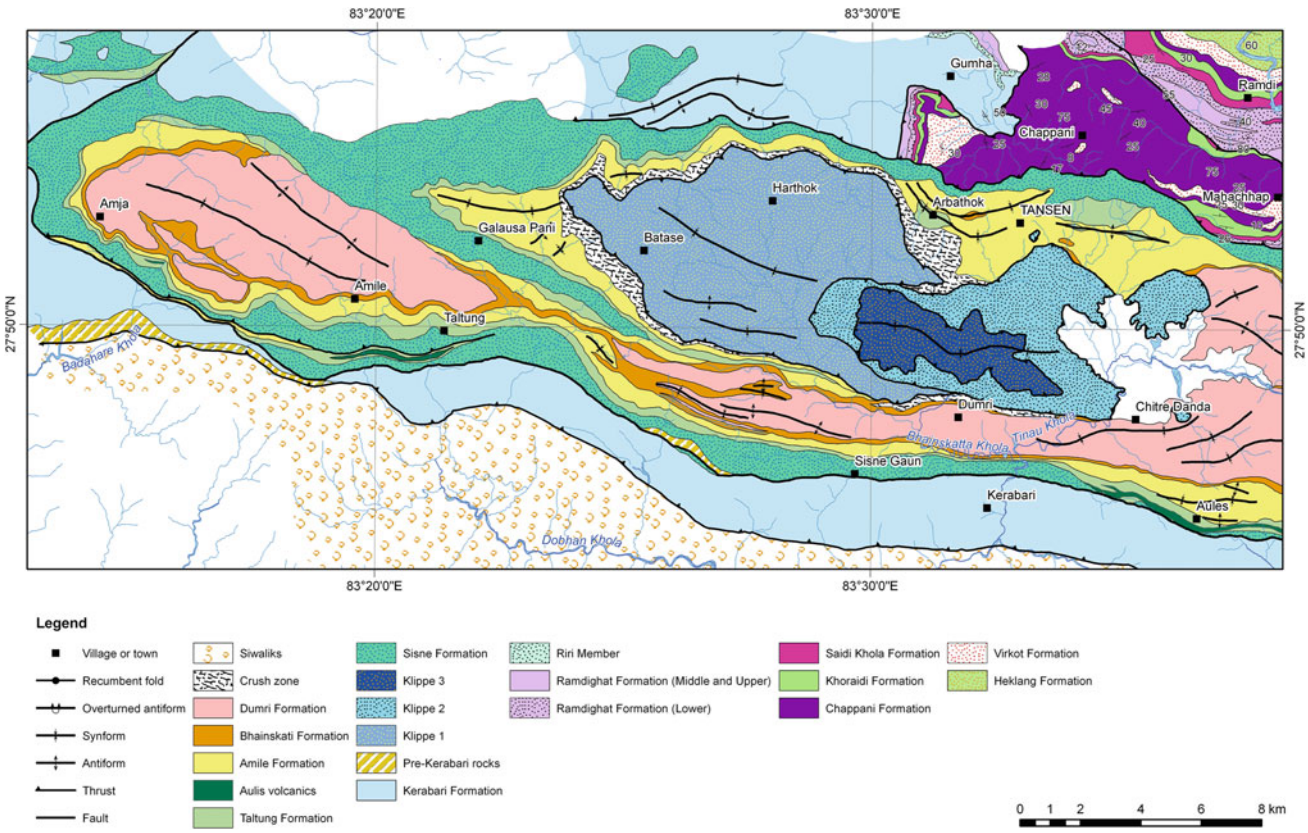

Fig. 9.17 Geological map of Tansen area. *Source* Modified from Sakai (1983, 1985)

The Sisne Formation comprises a thick succession of diamictite (300 m) in its lower levels, followed upwards by sandstones (80 m) and another diamictite sequence (80 m). Its upper part is made up of black shale with some diamictite beds and an approximately 100 m thick highly bioturbated top sequence of alternating sandstone and mudstone. The maximum thickness of the Sisne Formation is 1,020 m (Sakai 1983, p. 34).

The proportion of clasts and matrix varies widely in the diamictite. Most of it is unstratified and unsorted, and contains a structureless clayey matrix with randomly scattered clasts of varying sizes and shapes. The clast-to-matrix ratio varies significantly, that is, from several pieces/m^2 to 500 pieces/m^2 (Sakai 1983, p. 37). Most of the clasts are of granite, gneiss, limestone, dolomite, and sandstone. There also occur clasts of slate and phyllite as well as some sporadic volcanic rock fragments.

Dark gray to black claystones are the predominating rock in the Sisne Formation. Generally, the claystones are massive but infrequently laminated, and in them pencil cleavage is well developed. A few sandstone beds and sandy diamictite or conglomerate horizons are interbedded between the claystones (Sakai 1983, p. 37).

The Ritung Bioturbated Mudstone Member (Fig. 9.16) comprises the uppermost part of the Sisne Formation (Sakai 1983, p. 38). It is about 130 m thick and includes a few millimeter- to a few centimeter-thick mudstone beds, rhythmically alternating with up to 10 cm thick fine-grained sandstones. From 2 to 5 m thick lenticular diamictite beds also occur in the upper part of the member. The Ritung Member is strongly bioturbated and contains sinuous, straight, vertical, and oblique tubules of up to 2 cm across, formed by burrowing animals. It has a calcareous cement and is frequently mottled (Sakai 1983, p. 38).

Most of the Sisne Formation is inferred to be of glacial origin. But the occurrence of thick sandstone beds with climbing ripple lamination and scour-and-fill marks, and the presence of thin conglomerates exhibiting imbricate pebbles indicate the influence of water current. The bioturbated upper member seems to have originated in a shallow marine (tidal flat) environment (Sakai 1983, p. 39).

From some floats of shale, derived from the upper part of the Sisne Formation, Sakai (1983, p. 40) discovered various bryozoan fossils belonging to the genera *Fenestella*, *Polypora*, and *Acanthocladia*. Because the genera *Fenestella* and *Polypora* range in age from the Ordovician to Permian, whereas the distribution of *Acanthocladia* is known to span from the Carboniferous to Permian, Sakai assigned a Carboniferous to Permian age for the Sisne Formation.

9.4.2 Taltung Formation

The Sisne Formation is followed upwards by the Taltung Formation (Fig. 8.16) with a distinct disconformity marked by a basal conglomerate bed, containing clasts derived from the underlying Sisne Formation (Sakai 1983, p. 41). The Taltung Formation is about 200 m thick and further divided up into the following two members.

The Lower Member of the Taltung Formation begins with a basal bed designated as the Charchare Conglomerate, and it is followed by other cyclic deposits of conglomerate and sandstone. There are also a few lava flows, called the Aulis volcanics (Sakai 1983, p. 42) in its lower part.

The Charchare Conglomerate serves as an ubiquitous marker horizon in Tansen. It is from 13 to 20 m thick and rests upon the Sisne Formation with a conspicuous erosional surface. This basal horizon is represented essentially by two fining-upwards sequences, containing mainly alternating coarse-grained sandstone beds, followed by thin conglomerates at their top. Most of the Charchare Conglomerate is made up of densely packed and well-sorted pebbles and cobbles. More than 75 % of them are well-rounded to rounded, and they are overwhelmingly composed of volcanic rocks and quartzites. The volcanic pebbles were derived mainly from the Aulis volcanics (Sakai 1983, p. 43). The Charchare Conglomerate is also characterized by imbricate pebbles which show a flow direction from SE to NW. The conglomerate beds also sporadically contain silicified or calcified wood fragments, ranging up to 1 m in length (Sakai 1983, p. 44).

Trachytic to basaltic lava flows, called the Aulis volcanics, are associated with the Lower Member of the Taltung Formation. In the Tansen area, there are mainly three such lava flows. One of them rests directly on the Charchare Conglomerate, whereas the other two flows occupy higher levels in the lower portion of the Lower Member (Sakai 1983, p. 45). These concordant lava flows typically have one or two intercalations of sandstones and conglomerates, made up of volcanic clasts or those derived from quartzites. One of the prominent lava flows is from 30 to 200 m thick and extends over 13 km in the vicinity of Aulis. In the Amile and Badahare rivers, the flows are from 40 to 50 m thick and contain at least two clastic intercalations. The two lava flows with the clastic intercalations attain a maximum thickness of 100 m and extend for 7 km (Sakai 1983, p. 45).

The lava flows are dark gray-green in color; they are generally massive but exhibit pillow structures at their base and top. The upper portions of such pillows are amygdaloidal with cylindrical vesicles, ranging up to 2 cm in diameter and 6 cm in length. Most of the flows are massive but some are porphyritic, having plagioclase phenocrysts (0.2–0.8 cm) in the ground mass of plagioclase microlites (less than 0.2 mm) and granular clinopyroxene, exhibiting an intersertal texture. Most of the plagioclase phenocrysts and some microlites have altered into saussurite, whereas nearly all clinopyroxene is altered into chlorite. The Aulis volcanics are intimately related to the Upper Gondwana plant fossils, occurring from a level 7 m above the base of the Taltung Formation, and hence must belong to the same age (Sakai 1983, p. 46).

The main portion of the Lower Member is represented by a number of fining-upwards fluvial cycles, each commencing with conglomerate, followed by sandstone, and ending in siltstone. There are about eight such cycles, each of which varies in thickness from 7 to 20 m. Generally, their base is made up of a conglomerate bed, resting on the underlying sequence with a sharp scoured contact. The conglomerate beds are from 3 to 15 m and exceptionally up to 55 m thick, and contain mainly volcanic and quartzite clasts, not much different from those of the Charchare Conglomerate. Each conglomerate bed passes upwards into trough and tabular cross-laminated coarse- to very coarse-grained sandstone, grading upwards into planar lamination. The topmost part of the cycle is generally represented by finely laminated sandy siltstone or unstructured mudstone with carbonaceous seams. Hence, these sequences can be attributed to the fluvial deposits where the conglomerates presumably were laid down by braided channels, the overlying cross-bedded sandstones were accumulated on point bars, and the top siltstone beds may represent floodplain deposits (Sakai 1983, p. 47).

In the lower part of the Lower Member, there are as many as eight intercalated beds of tuff, tuffaceous shale, and sandstone, where the sandstone beds contain large (from 0.5 to 1 m in diameter) calcareous concretions.

The Upper Gondwana (Jurassic–Cretaceous) plant fossils abound in several siltstone beds as well as thin silty horizons within conglomerates. The plant fossils (Kimura et al. 1985) include *Ptilophyllum* cf. *P. cutchense* Morris, *Pterophyllum* sp., *Cladophlebis indica* (Oldham and Morris), and *Elatocladus tenerrimus* (Feistmantel). Some large (40 cm in diameter and 60 cm long) silicified trunks are also encountered in some of the conglomerate beds (Sakai 1983, p. 47).

The Upper Member of the Taltung Formation contains fining-upwards rhythmic cycles of sandstone and shale, where each sequence is from 8 to 20 m thick. Medium- to very coarse-grained, cross-bedded, olive green sandstone constitutes its lower part. Generally, the sandstones are massive but some of them exhibit scour-and-fill structures at their base, and they also include carbonaceous seams. These sandstone beds transitionally pass upwards into silty sandstone beds, followed by carbonaceous siltstone and shale (Sakai 1983, p. 47). The siltstones include hematite speckles and calcareous concretions, whereas the carbonaceous siltstones are intensely bioturbated. The uppermost portion of this member is made up of 7 to 8 m thick, red-purple silty shale with green-gray irregular reduction spots. Hence, like the Lower Member, this member too is of fluvial origin (Sakai 1983, p. 48).

9.4.3 Amile Formation

The Amile Formation is widely distributed in the Tansen Synclinorium. It is made up of sandstones, shales, and limestones in varying proportions. It is mainly a nonmarine sequence with some marine fossiliferous beds in its middle part. The Amile Formation is more than 230 m thick and divided up into the following three members (Sakai 1983, p. 49).

The Lower Member of the Amile Formation commences with an approximately 10 m thick white pebbly quartz arenite bed, resting with a scoured contact on the red-purple shale of the Taltung Formation. The contact marks a distinct disconformity. In its type section of Amile (Fig. 9.18), the basal bed consists of 20–30 cm thick white quartzose sandstones with a few intercalations of back shale (Sakai 1983, p. 49). The sandstones also contain some scattered pebbly zones and stringers. The subrounded to well-rounded pebbles are represented by quartzite, chert, and agate, and they are generally less than 5 cm in diameter. Another distinctive feature of the sandstones is their prolific mottling by ferruginous matter, which gives light pink to dark brown or red-purple colors (Sakai 1983, p. 51). The Lower Member also includes up to 1.5 m thick dark gray to black carbonaceous shale beds, laminated calcareous beds, sideritic horizons, and pyritous wood fragments (Fig. 9.18).

The occurrence of fossiliferous siltstones and limestones, and rhodochrosite-bearing siltstones are some of the distinctive features of the Middle Member. These marker horizons are well discernible throughout the Tansen Synclinorium. The fossiliferous beds represented by argillaceous limestones contain bivalves, gastropods, echinoids, corals, and vertebrate bones, and attain a thickness of 20 m. They are strongly bioturbated and overlain by pink colored limestones. The last limestone bed is up to 5 m thick and contains 5–20 cm thick bedded micrite with thin partings and lenses of calcareous sandstone (Sakai 1983, p. 51). Another important aspect of the Middle Member is the occurrence of

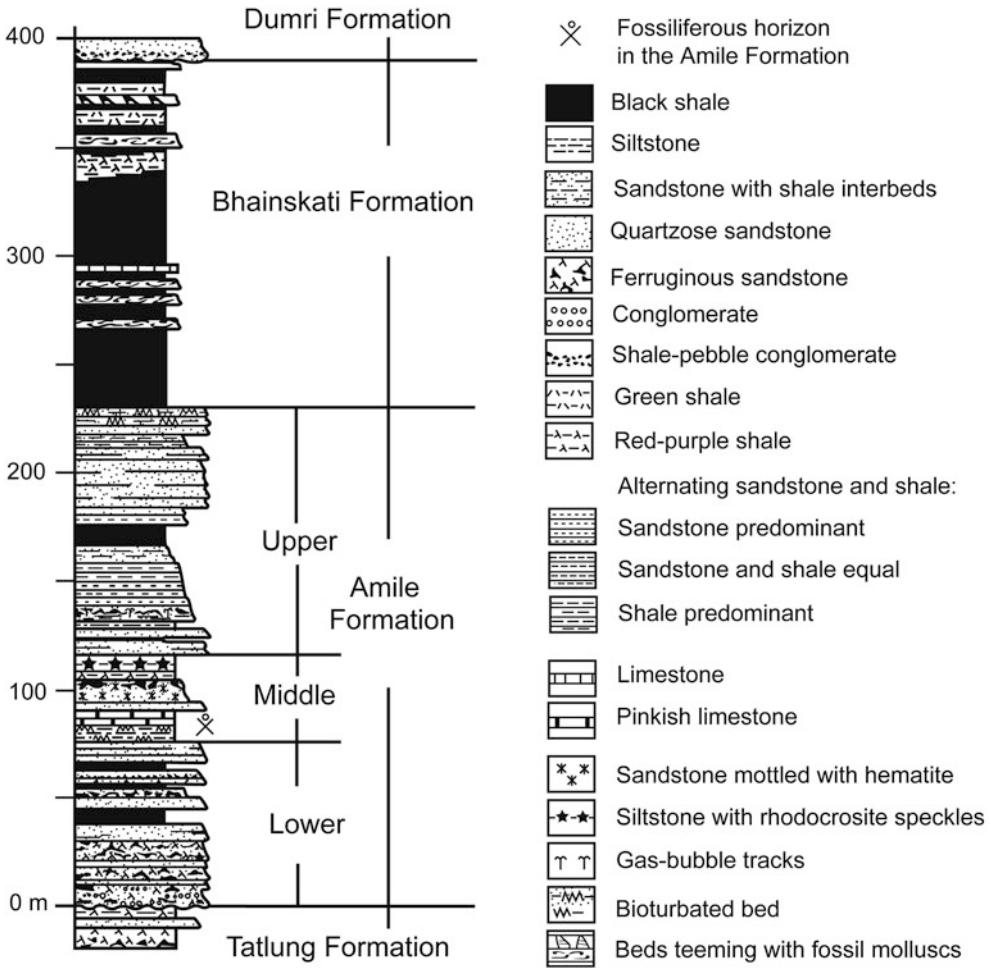

Fig. 9.18 Lithostratigraphic sequence of the Amile and Bhainskati formations. *Source* Modified from Sakai (1983). © H Sakai. Used by permission

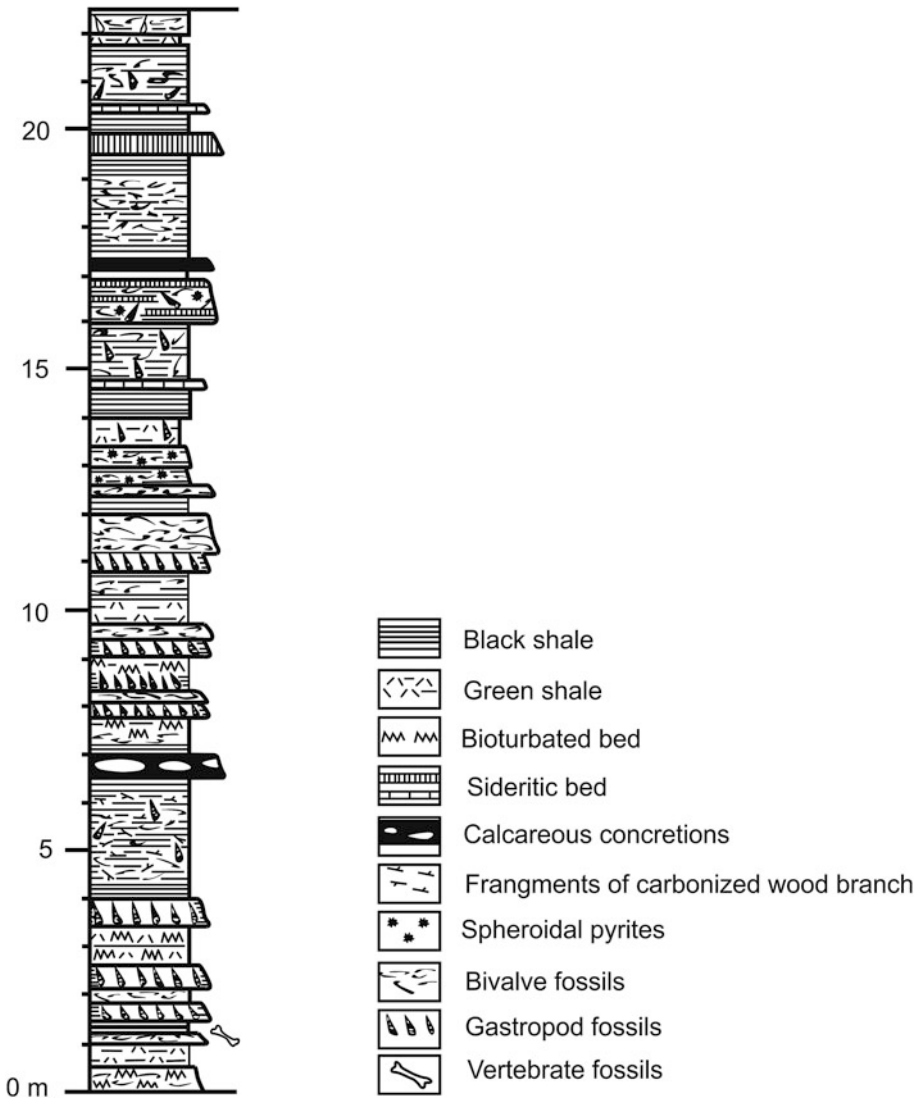

Fig. 9.19 Detailed stratigraphic column of the middle part of the Bhainskati Formation. *Source* Modified from Sakai (1983). © H Sakai. Used by permission

dark gray hematitic pisolites and speckles, ranging in size from 0.5 to 1 cm. The uppermost bed of the Middle Member is made up of a 4 m thick siltstone, profusely impregnated by rhodochrosite speckles to the extent that they form a massive bed in some locality (Sakai 1983, p. 51).

The Upper Member consists predominantly of quartzose sandstone with a minor amount of thin-bedded carbonaceous muddy sandstone and carbonaceous shale intercalations. Because these muddy sandstone beds are rich in siderite or hematite, they give rise to reddish brown weathered colors. Sometimes, the muddy carbonaceous sandstones enclose gas-bubble tracks (Fig. 9.18). The top portion of the Upper Member is made up of an intensely bioturbated carbonaceous muddy sandstone with coalified wood fragments and some very large (45 cm wide and over 3 m long) trails on its upper surface (Sakai 1983, p. 51).

9.4.4 Bhainskati Formation

The Bhainskati Formation (Figs. 9.18 and 9.19) is the most conspicuous stratigraphic unit in the Tansen area, characterized by the prolific occurrence of marine fossils in a black shale succession. The Bhainskati Formation overlies the Amile Formation conformably but with a sharp contact and attains a thickness of about 160 m in its type locality.

The main part of the Bhainskati Formation (Fig. 9.18) is comprised of black shales with thin alternations of calcareous and fossiliferous horizons in its middle part. The upper portion of the Bhainskati Formation contains gray-green and red-purple shale and hematite beds. The black shales are frequently bioturbated, and contain coalified wood fragments and carbonaceous flakes. Many fossil-bearing horizons are present between 40 and 90 m above the base of the

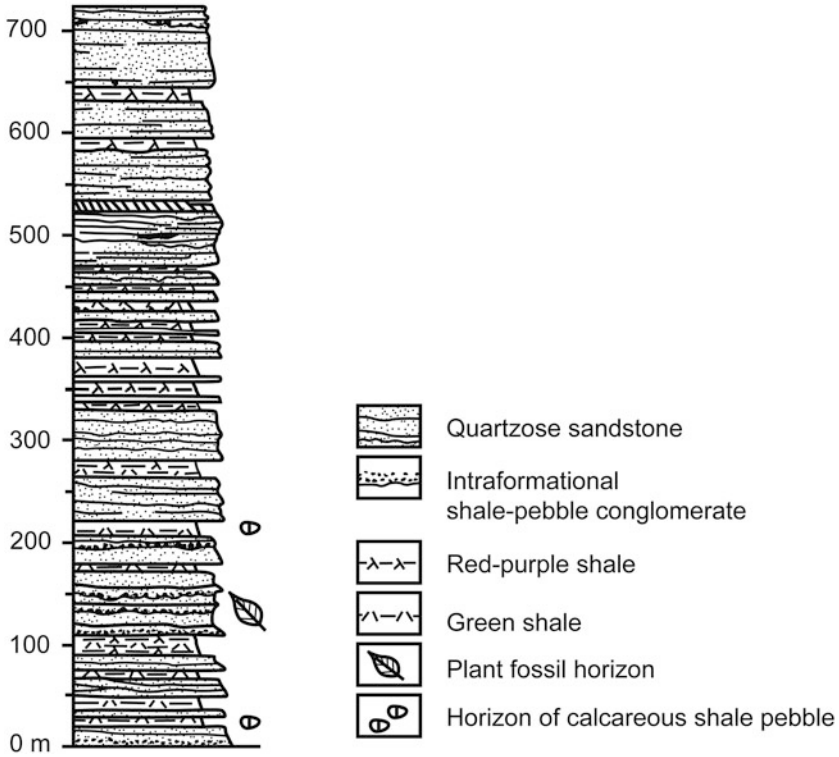

Fig. 9.20 Lithostratigraphic column of the Dumri Formation. *Source* Modified from Sakai (1983). © H Sakai. Used by permission

Bhainskati Formation (Fig. 9.19), and a number of them can be classified as coquinites (Sakai 1983, p. 53). The fossils are represented by a large number of a single species densely packed together. There are also some vertebrate bones and lens-shaped concretionary calcareous nodules that are up to 30 cm thick and 3 m long.

The upper part of the Bhainskati Formation is represented by green and red-purple shales with some hematite beds. At the type locality in the Bhainskatta Khola, there are up to six oolitic hematite beds, varying in thickness from 5 cm to 2 m, whereas, towards the west end, there are some sideritic oolites, containing gastropods and bivalves. The middle portion of the upper part includes some highly bioturbated sandstones of up to 1 m in thickness, containing sinuous red-pigmented sandpipes (Sakai 1983, pp. 54–55).

Sakai (1983, p. 56) obtained *Nummulites beaumonti* D'Archiac and Heime and *Assilina papillata* Nuttal from 30 to 50 m above the base of the Bhainskati Formation. As these fossil finds indicate a Middle Eocene age, this formation may range in age from the Middle to Late Eocene. The occurrence of land mammals together with marine fish is another noteworthy feature of the Bhainskati Formation.

9.4.5 Dumri Formation

The Dumri Formation occupies the topmost stratigraphic rung in the Tansen Group and exhibits a disconformable contact with the underlying Bhainskati Formation. It is represented by a thick succession of medium-grained, bluish-gray quartzose sandstone and red-purple and green shale with a total thickness of about 725 m (Fig. 9.20). The amount of shale gradually increases from its lower to upper horizons. The sandstones belong to the quartzose wacke with a minor amount of carbonaceous matter. Their thickness ranges from 10 cm to 6 m; generally they are massive, but some of them display large-scale wedge bedding. Load casts are sporadic at their base, whereas ripples are frequent at the top surfaces of thin beds (Sakai 1983, pp. 57–58).

The lower 1–4 m of the Dumri Formation contain angular clasts of calcareous shale. There also occur many intraformational shale-pebble conglomerates and conglomeratic sandstones, containing tabular shale clasts that are up to a few decimeters across and set in a sandy matrix. The shale-pebble-bearing conglomerates are frequent generally at the lower part of a sandstone, filling a scoured channel in the underlying shale or sandstone. Some coalified branches and trunks (up to 6 m long and 60 cm across) are also found embedded in the sandstone (Sakai 1983, p. 58).

Red and green colors are characteristic of the fines composing the Dumri Formation. Green tints predominate in its lower horizons, whereas the upper beds are vividly red colored. Some beds in its middle portion are mottled red and green owing to the prevailing reducing conditions during diagenesis and also resulting from strong bioturbation, marked by sinuous tubes of varying colors (Sakai 1983, p. 58).

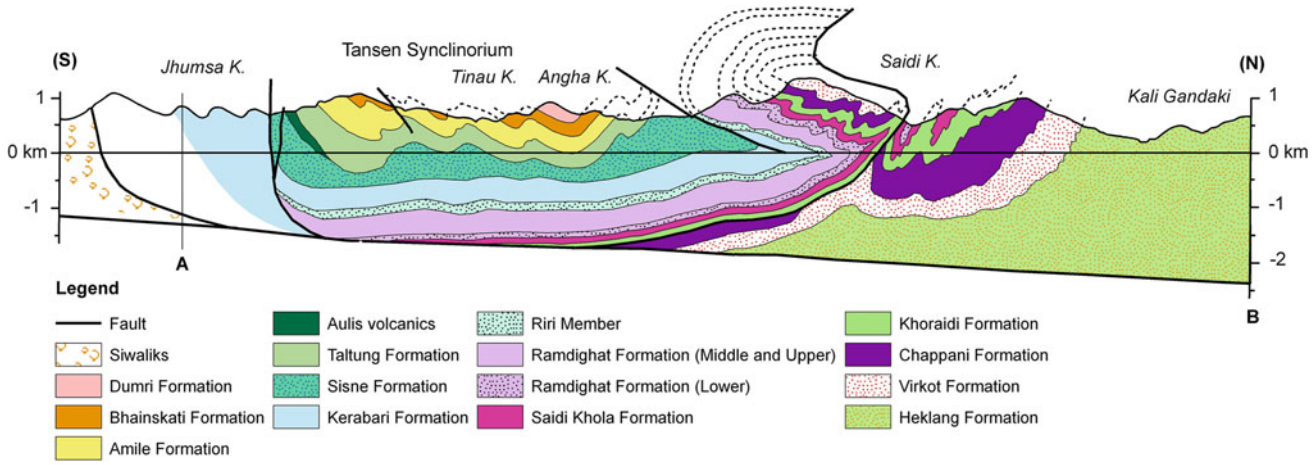

Fig. 9.21 Geological cross-section across the Kali Gandaki Supergroup and the Tansen Group. The line A–B is depicted in Fig. 9.9. *Source* Modified from Sakai (1985)

The fluvial Dumri Formation was deposited in Early Miocene time, after the Eocene marine transgression. Its source area was lying to the north as indicated by cross-bedding and imbricate pebbles (Sakai 1983, p. 59).

9.5 Structure of Outer Zone

The Lesser Himalayan fold-and-thrust belt of the Gandaki region is characterized by intense folding, thrusting, and backthrusting. Various klippen are found in the synclinal core, whereas tight to overturned folds are found in the north limb of the syncline (Figs. 9.9, 9.17, and 9.21).

References

Adhikari DP (1993) Paleomagnetism of the dyke rocks of the Ampipal Massif, Lesser Himalaya, Central Nepal. Unpublished M. Sc. thesis, submitted to the Central Department of Geology, Tribhuvan University, Kathmandu, 70 pp

Amatya KM, Jnawali BM (1994) Geological map of Nepal, Scale: 1:1 000 000. Department of Mines and Geology, International Centre for Integrated Mountain Development, Carl Duisberg Gesellschaft e. V., and United Nations Environment Programme

Arita K (1983) Origin of the inverted metamorphism of the lower Himalayas, Central Nepal. Tectonophysics 95:43–60

Bordet P, Colchen M, Le Fort P, Pêcher A (1981) The geodynamic evolution of the Himalaya. Ten years of research in Central Nepal Himalaya and some other regions. In: Gupta HK, Delany FM (eds) Zagros-Hindu Kush-Himalaya geodynamic evolution. Geodynamic series, vol 3. American Geophysical Union, Washington, DC, pp 149–168

Dhital MR (1995) Mode of occurrence of nepheline syenites in the Gorkha–Ampipal area, Central Nepal Lesser Himalaya. J Nepal Geol Soc 11(Special Issue):159–170

Dhital MR, Thapa PB, Ando H (2002) Geology of the inner Lesser Himalaya between Kusma and Syangja in western Nepal. Bull Dep Geol Tribhuvan Univ 9(Special Issue):1–60

ESCAP (Economic and Social Commission for Asia and the Pacific) (1993) Geology and mineral resources of Nepal, atlas of mineral resources of the ESCAP region, vol 9. United Nations, New York, 107 pp (with a geological map in colors)

Fuchs G, Frank W (1970) The geology of west Nepal between the rivers Kali Gandaki and Thulo Bheri. Jahrbuch der Geologischen Bundesanstalt 18:1–103 (with a geological map and cross-sections)

Gautam P, Koshimizu S (1991) Zircon and apatite fission-track dating of the Ampipal Alkaline Massif, the Nepal Lesser Himalaya. J Nepal Geol Soc 7:1–8

Gautam P (1990) Paleomagnetic study of the Lesser Himalaya in Nepal. Unpublished D.Sc. thesis submitted to the Hokkaido University, Sapporo, Japan, 165+ pp

Goswami B, Bhattacharya C (2008) Metamorphism of nepheline syenite gneisses from Chhotanagpur Granite Gneiss complex, Northeastern Puruliya district, Eastern India. J Geol Soc India 71:209–213

Hagen T (1969) Report on the geological survey of Nepal. Volume 1: Preliminary Reconnaissance. Denkschiiften der Schweizerischen Naturforschenden Gesellschaft, Band LXXXVI/1, 185 pp (with a geological map)

Hirayama J, Nakajima T, Shrestha SB, Adhikari TP, Tuladhar RM, Tamrakar JM, Chitrakar GR (1988) Geology of southern part of the Lesser Himalaya, west Nepal. Bull Geol Surv Jpn 39(4):205–249

Kimura T, Bose MN, Sakai H (1985) Fossil plant remains from Taltung Formation, Palpa district, Nepal Lesser Himalaya. Bull Natl Sci Mus Tokyo Ser C 11(4):141–153

Koide Y, Arita K, Toyoshima T, Sharma MP (1992) Geochemistry of Ampipal pluton, preliminary report. Bull Dep Geol Tribhuvan Univ Kathmandu 2(1):11–23

Lasserre JL (1977) Amphibolites and alkaline gneisses in the Midland formations of Nepal: petrography, geochemistry—geodynamic involvements. Colloques internationaux du CNRS, no 268—Écologie et Géologie de l'Himalaya, pp 213–236

Lasserre JL, Pêcher A, Le Fort P (1975) An occurrence of nepheline syenite and alkaline gneisses at Ampipal, Lesser Himalaya of Central Nepal, preliminary note. Chayanica Geol 2(1):71–78

Le Fort P (1975) Himalayas, the collided range: present knowledge of the continental arc. Am J Sci 275-A:1–44

Le Fort P, Raï SM (1999) Pre-Tertiary felsic magmatism of the Nepal Himalaya: recycling of the continental crust. J Asian Earth Sci 17:607–628

Nanda MM (1966) Report on geological mapping in western Nepal (Parts of Lumbini, Tansen, Gulmi, West Nos. 3 and 4 Districts). Report submitted to the Geological Survey of India (unpublished) (with a map)

Ohta Y, Akiba C, Arita K, Maruo Y (1973) Pokhara–Gorkha Region. In: Ohta Y, Akiba C (eds) Hashimoto, S. (supervisor): Geology of the Nepal Himalayas. Himalayan Committee of Hokkaido University, Sapporo, pp 159–188

Paudel LP, Arita K (2000) Tectonic and polymetamorphic history of the Lesser Himalaya in Central Nepal. J Asian Earth Sci 18:561–584

Paudel LP, Arita K (2006) Thermal evolution of the Lesser Himalaya, Central Nepal: insights from K-white micas compositional variation. Gondwana Res 9:409–425

Pêcher A (1977) Geology of the Nepal Himalaya: deformation and petrography in the Main Central Thrust Zone. In: Colloques internationaux du CNRS, no 268, Écologie et Géologie de l' Himalaya, pp 301–318

Pêcher A (1989) The metamorphism in the Central Himalaya. J Metamorph Geol 7:31–41

Pêcher A (1991) The contact between the higher Himalaya crystallines and the Tibetan sedimentary series: miocene large-scale dextral shearing. Tectonics 10(3):587–598

Sakai H (1983) Geology of the Tansen Group of the Lesser Himalaya in Nepal. Mem Fac Sci Kyushu Univ Ser D Geol 25(1):27–74

Sakai H (1985) Geology of the Kali Gandaki Supergroup of the Lesser Himalaya in Nepal. Mem Fac Sci Kyushu Univ Ser D Geol 25(3): 337–397

Sakai H (1986) Stratigraphic equivalence and lithofacies comparison of the Kali Gandaki Supergroup between the inner and outer Lesser Himalayas. Mem Fac Sci Kyushu Univ Ser D Geol 26(1):69–79

Shrestha SB, Shrestha JN, Sharma SR (1986) Geological map of Central Nepal. Scale: 1:250 000. Department of Mines and Geology, Kathmandu

Singh J, Saxena DN, Varma HM, Dhana Raju R (1983) Rare radioactive perpotassic alkali syenites from parts of South Sikkim. India Curr Sci 52(4):162–164

Stöcklin J, Bhattarai KD (1977) Geology of Kathmandu area and central Mahabharat Range, Nepal Himalaya. HMG/UNDP Mineral Exploration Project, technical report, 86 pp (unpublished), (with 15 maps)

Tater JM, Shrestha SB, Shrestha JN (1983) Geological map of Western Central Nepal. Scale: 1:250 000. Department of Mines and Geology, Kathmandu

Upreti BN, Sharma T, Merh SS (1980) Structural geology of Kusma-Sirkang section of the Kali Gandaki Valley and its bearing on the tectonic framework of Nepal Himalaya. Tectonophysics 62:155–164

Lesser Himalaya of Bagmati–Gosainkund Region

10

Two different main nappe groups were found in Central Nepal. The lower one was called by the author as Nawakot nappe system, the overlying one the Kathmandu Nappe system.

—Toni Hagen (1951)

The Lesser Himalayan rocks of the Bagmati–Gosainkund region compose a relatively wide portion of the Great Midland Antiform in the inner zone between Nuwakot and Dhunche, and they also form an open fold representing the Great Mahabharat Synform in the intermediate zone around Mugling and Narayanghat (Figs. 6.1 and 10.1). The rocks reappear in the Okhaldhunga tectonic window (Chap. 11), which is separated from the inner zone by the Gosainkund tectonic bridge. A narrow and discontinuous Lesser Himalayan strip stretches along the foothills of the Mahabharat Range, and a few of its slivers crop up amid the Siwaliks in the Bagmati River and north of the Marin Khola. In the Bagmati–Gosainkund region too, the grade of metamorphism steadily increases from the foreland to the hinterland (Beyssac et al. 2004). As a result, the black slates of the outer zone pass into the inner zone as graphitic schists containing kyanite blades (Chap. 17).

10.1 Intermediate Zone and Mahabharat Range

The rocks of central Nepal are differentiated into the Nawakot Complex, representing the Lesser Himalayan sequence and the physically overlying Kathmandu Complex (Stöcklin and Bhattarai 1977; Stöcklin 1980), belonging to the Higher Himalayan crystallines and Tethyan Himalayan sequence (Chap. 17). The two complexes differ basically in their lithostratigraphic characteristics and are separated from each other by the Mahabharat Thrust, which is the southern continuation of the Main Central Thrust (Stöcklin et al. 1982). On the other hand, the Lesser Himalayan rocks are thrust over the Siwaliks along the Narayani alias Main Boundary Thrust.

The Nawakot Complex represents a sedimentary to low-grade metamorphic sequence, comprising phyllites, metasandstones, quartzites, slates, shales, and carbonate rocks. Its total thickness is more than 8 km and is further classified into the Lower Nawakot Group and the overlying Upper Nawakot Group (Table 10.1).

The Lower Nawakot Group represents probably the oldest rock succession in the Lesser Himalaya of Nepal. These rocks cover an extensive area north and west of Kathmandu as well as to the east of the valley. The Upper Nawakot Group represents a broad unit of slates, limestones, phyllites, quartzites, and amphibolites. It generally occurs below the Mahabharat Thrust (Main Central Thrust) and hence has undergone intense deformation. Inverted metamorphism too has significantly affected its upper end.

10.1.1 Kuncha Formation

Bordet (1961) introduced the term *Série de Kunchha* for this enormous and monotonous succession akin to a flysch, which extends eastwards from the Gandaki region (Chap. 9). The rocks of this formation are weakly metamorphosed, have a silky luster with green-gray, blue-gray, and yellow-gray shades. They are composed of phyllites, phyllitic quartzites, and phyllitic *gritstones*, resembling a graywacke. The Kuncha Formation is generally devoid of carbonates. Although the phyllites are frequently argillaceous, they do include very fine and dense siliceous laminae. The quartzites are impure and show an oily luster and olive green color. As in the Gandaki region, here too occur *gritty* phyllites with detrital grains mostly of blue and smoky quartz, and sporadically of feldspar, tourmaline, and other minerals disseminated in a phyllitic matrix. Similar clasts are also present in the Bawar Formation of the Northwest Himalaya (Chap. 4). The Kuncha Formation also contains some quartz conglomerates with pebbles of less than 1 cm in diameter (Stöcklin and Bhattarai 1977, p. 14). There are also a few meter-thick concordant basic rock layers in the Kuncha Formation (Figs. 10.2 and 10.3).

The Kuncha Formation is quite monotonous, however, Stöcklin and Bhattarai (1977) have distinguished an

M.R. Dhital, *Geology of the Nepal Himalaya*, Regional Geology Reviews,
DOI 10.1007/978-3-319-02496-7_10

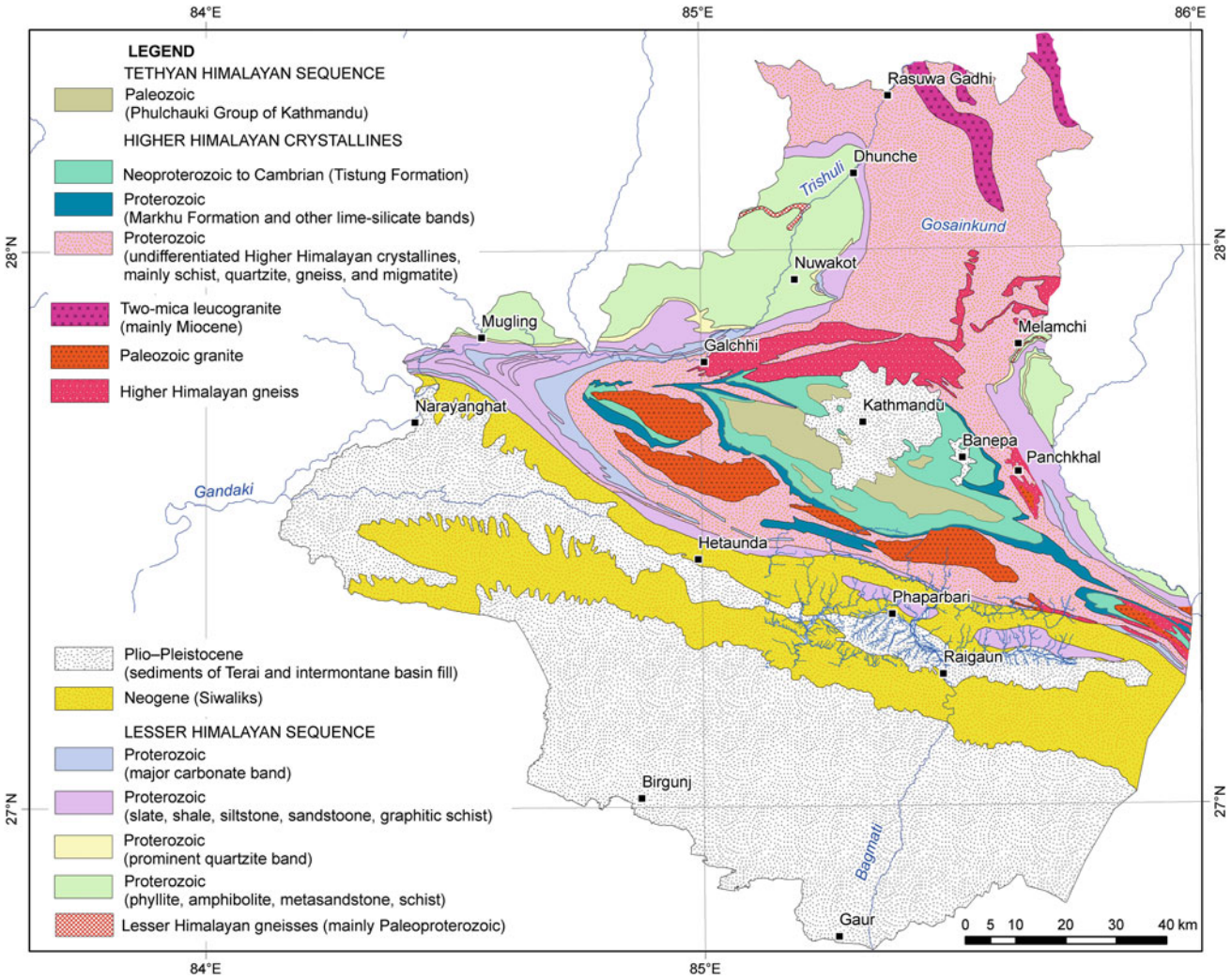

Fig. 10.1 Simplified geological map of the Bagmati–Gosainkund region. *Source* Based on Stöcklin and Bhattarai (1977), Stöcklin et al. (1982), Shrestha et al. (1986), other published maps, and author's observations

approximately 200 m thick Banspani Quartzite Member towards its upper end. This member is feebly calcareous, and displays light gray-green colors when fresh and pink to purple tints when weathered. It is generally thinly banded and cross-laminated. They have also identified the Labdi Phyllite Member, which is fine-grained and argillaceous. It is of blue-green color, but it also sporadically displays vivid yellow, pink, purple, and violet shades in weathered condition. The Labdi Phyllite Member is about 200 m thick, occurs just below the Fagfog Quartzite, and shows gradational contacts with the overlying and underlying quartzite sequences.

Generally, the Kuncha Formation has sericite and chlorite as metamorphic minerals. But its metamorphic grade varies from place to place. Biotite abounds at Betrawati, whereas garnet is present at Barhabise and around Syaphrubensi. The Kuncha Formation is also characterized by well-developed lineation, frequently oriented due northeast–southwest. The Kuncha Formation is more than 3,000 m thick in central Nepal, and its base is nowhere exposed. Its depositional age is estimated between 1.9 and 1.8 Ga (Martin et al. 2011).

10.1.2 Fagfog Quartzite

Arita et al. (1973, p. 107) defined this formation as white quartzites, ranging from colloidal varieties of fine chert to impure coarse quartz arenites with infrequent reddish and pale orange tints. The Fagfog Quartzite shows graded bedding, cross-lamination, and spectacular wave and current ripple marks. It also includes some thin (10–20 cm) gray-green phyllite and black slate intercalations. In many places, there are three quartzite bands separated by phyllites. Nanda (1973) reported some thin metabasic bands in the Fagfog Quartzite. With a thin zone of alternating phyllites and

Table 10.1 Tectonostratigraphic subdivisions of the Nawakot Complex

Lithostratigraphic unit	Main lithology	Approximate thickness (m)	Era
KATHMANDU COMPLEX			
Mahabharat Thrust (Main Central Thrust)			
2. Upper Nawakot Group			
Robang Phyllites with Dunga Quartzites	Phyllite, quartzite	200–1,000	? Neoproterozoic
Malekhu Limestone	Limestone, dolomite	800	? Mesoproterozoic
Benighat Slates with Jhiku carbonate beds	Slate, argillaceous dolomite	500–3,000	? Mesoproterozoic
? Disconformity			
1. Lower Nawakot Group			
Dhading Dolomite	Metasandstone, phyllite	500–1,000	? Mesoproterozoic
Nourpul Formation	Marble, schist	800	? Mesoproterozoic
Dandagaon Phyllites	Quartzite, schist	1,000	Paleoproterozoic
Fagfog Quartzite	White quartzite	400	Paleoproterozoic
Kuncha Formation with Banspani Quartzite and Labdi Phyllites		3,000+	Paleoproterozoic
Narayani alias Main Boundary Thrust			
Siwaliks (Neogene)			

Source Based on Stöcklin and Bhattarai (1977)
?: An uncertain (approximate) date or thickness, or any other measurement

quartzites, the Fagfog Quartzite grades into the overlying Dandagaon Phyllites. The Fagfog Quartzite is about 350 m thick at its type locality, but its thickness varies widely. This formation was deposited round 1.7 Ga (Martin et al. 2011).

10.1.3 Dandagaon Phyllites

This formation is composed of rather uniform argillaceous to finely quartzitic phyllites of dark blue-green color, and these rocks often display reddish-weathering tints. A millimeter- to a centimeter-thick green quartzite bands containing sericite and chlorite are also present. There also set in very infrequent thin bands of dense dolomite and calc-phyllite exhibiting fine lamination. These calc-phyllites exhibit brown calcareous laminae, alternating with green chlorite laminae. Some lenses and nodules of quartz are also present in the Dandagaon Phyllites. The Dandagaon Phyllites exhibit a sharp but gradational contact with the overlying Nourpul Formation, and they are about 1,000 m thick.

10.1.4 Nourpul Formation

The Nourpul Formation represents an assorted succession, comprising quartzites, phyllites, and calcareous rocks. It is further subdivided into the following three members.

The Purebesi Quartzite Member follows the predominantly phyllitic Dandagaon Phyllites and forms the basal portion of the Nourpul Formation. It is represented by fine- to coarse-grained arkosic quartzites, displaying colors ranging from pure white to pink, pale yellow, and green. Infrequently rounded quartz grains of up to 2 mm in diameter occur in its lowermost horizons. Oftentimes, the quartzites display cross-lamination and ripple marks. The Purebesi Quartzite is about 300 m thick at its type locality.

The Purebesi Quartzite is succeeded by the prominently phyllitic Middle Member, with a variable proportion of quartzitic and calcareous intercalations. The phyllites commonly display gray-green to blue-gray coloration in fresh outcrops, but they show vivid red tints in weathered conditions. The regularly alternating impure micaceous quartzites are frequently dark green or green-gray and sporadically pink. Similarly, there are regularly intercalated carbonate beds composed of dense and microcrystalline siliceous dolomite. Some of these beds are composed of fine quartz grains, whereas some others range from siliceous dolomite to dolomitic quartzite. The variegated carbonate beds show light gray, yellow, and pale green colors in fresh conditions but intense buff, orange, pink, carmine, and violet colors when weathered. The phyllite–quartzite and phyllite–dolomite alternations range in thickness from tens of meters to about 100 m between the thicker intervals of pure phyllite (Stöcklin and Bhattarai 1977, pp. 16–17).

The dolomite and dolomitic quartzite intercalations become more abundant in the Upper Member of the Nourpul Formation. A regular alternation of decimetric green phyllite and buff or orange siliceous dolomite frequently results in

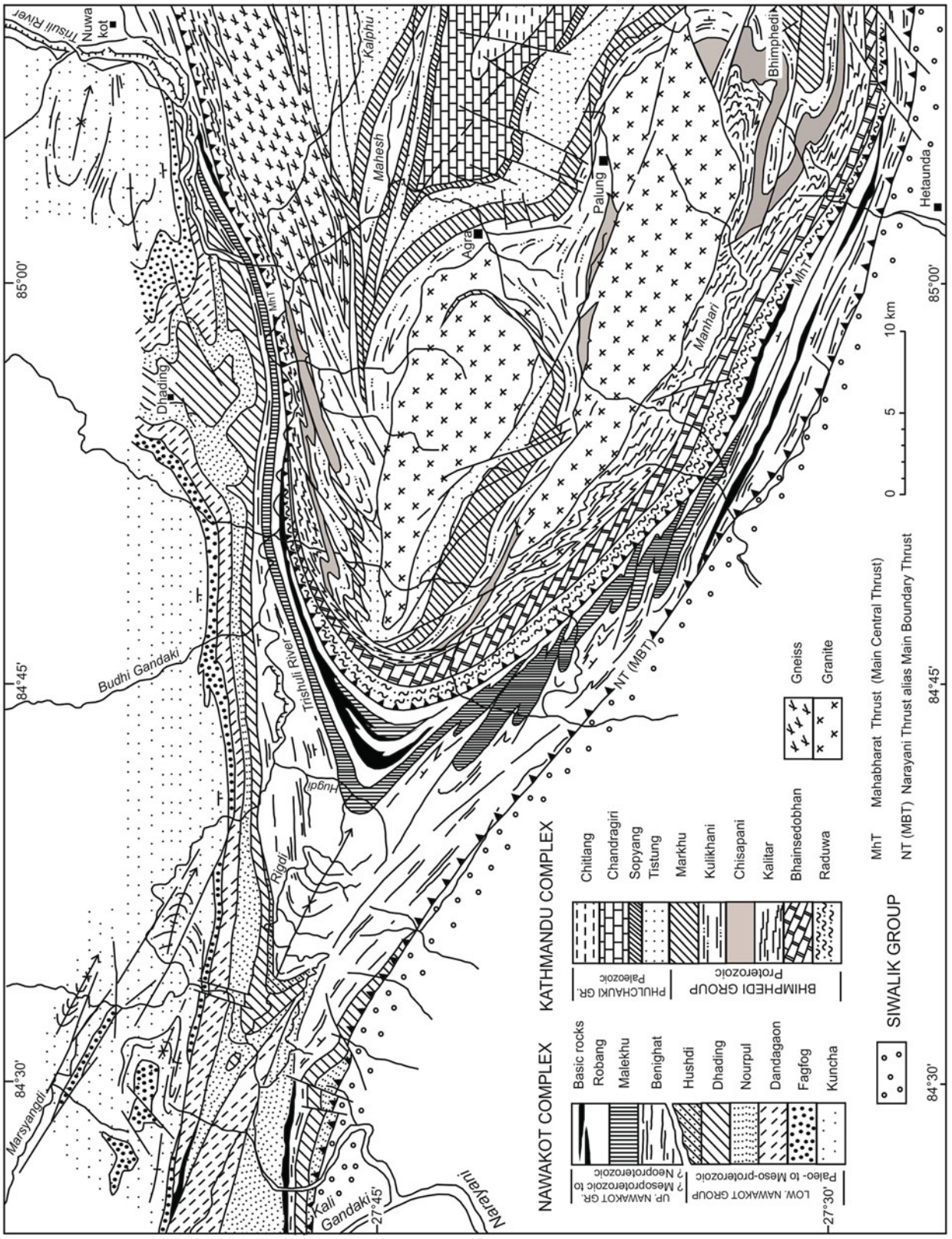

Fig. 10.2 Geological map of central Nepal. *Source* Modified from Stöcklin (1980)

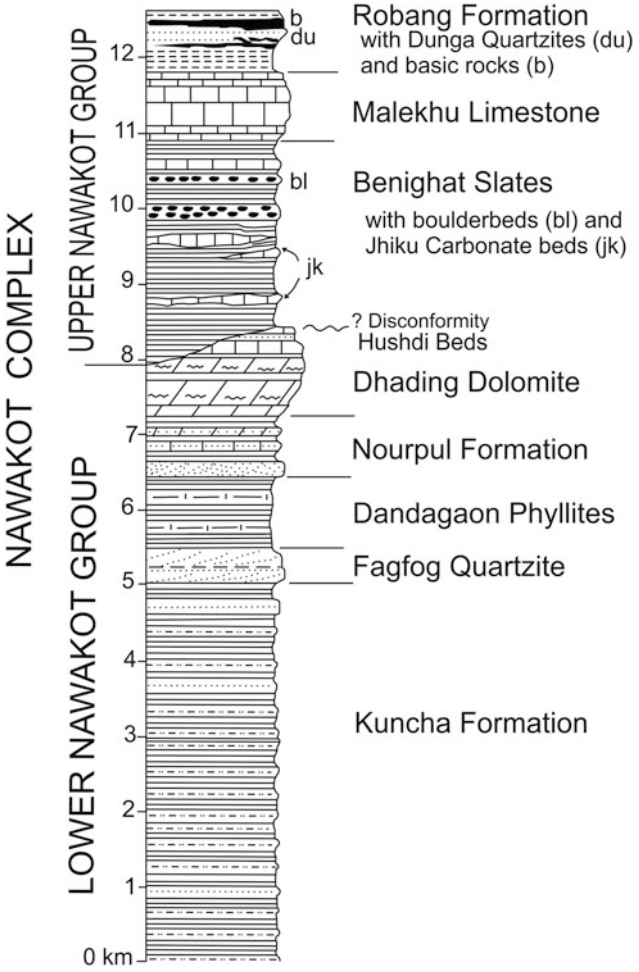

Fig. 10.3 Lithostratigraphy of the Nawakot Complex in central Nepal. *Source* Modified from Stöcklin (1980)

beautiful color banding. With a decrease in the phyllite content, the Upper Member transitionally passes into the overlying Dhading Dolomite. The Nourpul Formation is about 800 m thick in its type locality, but its thickness varies widely in other places due mainly to tectonic causes (Stöcklin and Bhattarai 1977, p. 17).

10.1.5 Dhading Dolomite

The Dhading Dolomite forms prominent hills and ridges around Dhading. It is essentially a microcrystalline and dense dolomite, exhibiting light gray color and splintery fractures (Stöcklin and Bhattarai 1977, p. 17). It is thick-bedded and massive in the main part, but is thinner-bedded to platy in its basal portion. There are thin lenticular and nodular chert bands at various levels. In some places, the upper, rather darker dolomite contains black siliceous and argillaceous slate bands of up to 20 m in thickness.

Although the dolomite appears massive from afar, it is generally finely laminated. Frequently, such laminae are of algal nature and pass into stromatolites. The stromatolites are distributed in almost all levels of the Dhading Dolomite. Generally, they are of columnar and branching types, resembling *conophyton* and *collenia* reported from the Northwest Himalaya (Chap. 4). The Dhading Dolomite varies in thickness from 500 to 1,000 m.

The contact of the Dhading Dolomite with the overlying Benighat Slates is quite abrupt in the Budhi Gandaki section of central Nepal, where the black Benighat slates override the dolomites without any transitional zone. At the base of the Benighat Slates, there is an approximately 50–100 cm thick weathered zone alluding to an erosional unconformity (Stöcklin and Bhattarai 1977, pp. 17–18). However, in west Nepal and in other parts of the country, such a sharp disconformity is not observed. In places, the dolomites and slates are interbedded and this formation transitionally passes into the black slates of Benighat (Chap. 9).

10.1.6 Benighat Slates

Dark bluish-gray to black, soft-weathering, and highly cleaved slates and phyllites represent this formation. The rocks are mainly argillaceous, but there are also subordinate bands of siliceous or finely quartzitic composition. Generally the formation is devoid of quartzites. When weathered, these rocks may display dark green colors due to the presence of chlorite. But such colors are more typical of the Robang Formation. Also, the weathered exposures and scree may display silver-gray, light gray to white, pale green, pinkish, and orange colors. There are some specific zones rich in carbonate content, where they are classified as the Jhiku carbonates or calcareous beds (Stöcklin and Bhattarai 1977, p. 18).

The black carbonaceous slates contain much (30–40 %) graphitic matter with some quartz and light mica. They form up to tens of meters thick zones. These graphitic slates weather into limonitic crust, exhibiting yellow, orange, and ochrous colorations, and they are covered with powdery sulfur, presumably from the decomposition of pyrite so common in these rocks. Especially on riverbanks, one encounters white powdery encrustations of bittersalt (Stöcklin and Bhattarai 1977, p. 19). The thickness of the Benighat Slates varies significantly and generally ranges from 500 to 3,000 m.

Stöcklin and Bhattarai (1977, p. 19) discovered two boulderbeds within the Benighat Slates in the Hugdi Khola. One of them occurs about 30 m below the base of the Malekhu Limestone. It is a lenticular bed with a thickness varying from 5 to 10 m. In it, the rounded and unsorted boulders range in diameter from 7 to 30 or 40 cm, are composed exclusively of quartzite, and are embedded in a green quartzitic or orange to brown calcareous

matrix. The second boulderbed lies about 600 m below the base of the Malekhu Limestone and it is 20–30 m thick. The boulders are again made up of poorly sorted quartzite, but they display distinct bedding, and their matrix is quartzitic. The lower boulderbed passes upwards into 30 m of massive quartzitic phyllite and subsequently to ordinary dark phyllite.

Occurring within the Benighat Slates, the Jhiku carbonates are represented by a variety of lithotypes. Some of them are thinly bedded, very fine-grained, dense, dark gray to black siliceous dolomite interbedded with black slates, whereas others are thin-bedded, platy, fine-grained, yellowish gray to pale green siliceous limestones and dolomites. Others are represented by buff-colored finely quartzitic carbonates, alternating with blue-green phyllite of tens of centimeters in thickness. There also occur a few beds of dark laminated siliceous limestone.

10.1.7 Malekhu Limestone

The Malekhu Limestone is one of the conspicuous units of the Upper Nawakot Group. It is constituted of thin-bedded, platy dolomitic and siliceous limestones of pale yellow color. It is microcrystalline to dense, and hard with green sericite–chlorite partings and thin intercalations. Especially, its lower and upper parts comprise platy limestone, whereas the middle portion is rather thick-bedded dark gray dolomite or dolomitic limestone with bands of black chert and intercalations of black siliceous and carbonaceous slates. Frequently, there is an approximately 50 m thick basal limestone zone and it is separated by about 150 m thick black slates from the main limestone body. At Malekhu, sporadic domed stromatolites are observed in its middle part. The Malekhu Limestone exhibits perfectly gradational contacts with the underlying and overlying slate bands, belonging, respectively, to the Benighat and Robang Formations. The transition is generally marked by an approximately 20–30 m thick alternation of calcareous and argillaceous rocks. The Malekhu Limestone assumes a thickness of about 800 m at its type locality (Stöcklin and Bhattarai 1977, p. 20) and is presumably older than 1.3 Ga (Martin et al. 2011).

10.1.8 Robang Formation (Robang Phyllites with Dunga Quartzites)

The Robang Phyllites comprise primarily green-gray sericite–chlorite phyllites and some darker slates akin to those of the Benighats. There also occur bands of dark green chloritic phyllites and associated with them are metamorphosed basic tuffs, metadiabases, and metagabbros. The tuff-like bands sometimes alternate with light green, soapy, talcose phyllites.

There are also sporadic intercalations of thin calcareous beds. A boulderbed of about 2 m thickness and similar to those found in the Benighat Slates was observed in the Hugdi Khola (Stöcklin and Bhattarai 1977, p. 21). But, different from the Benighat Slates, the Robang Formation frequently contains thin to thick alternations of light green to white quartzites. The more prominent quartzite bands are included in the Dunga Quartzite Beds. They are generally medium-grained, clean, white quartzites with minor phyllite intercalations, and they may attain a thickness of 500 m. But there also appear varieties that are thinly bedded and very fine-grained, almost like the bedded chert. The thickness of the Robang formation ranges from 200 m to more than 1,000 m.

10.1.9 Main Central Thrust

The Mahabharat Thrust or the Main Central Thrust (Figs. 10.2 and 10.4) has in its hanging wall the rocks of the Kathmandu Complex (Chap. 17). At the thrust contact, the

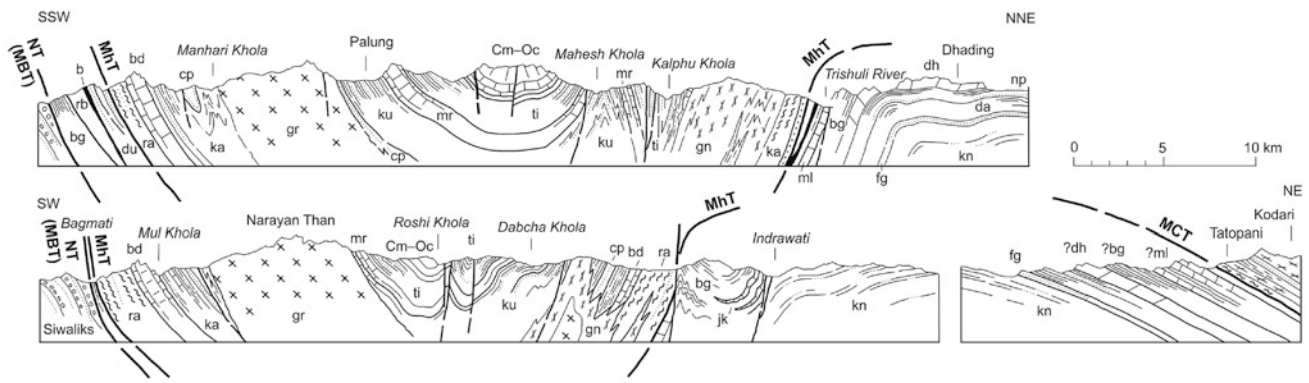

kn: Kuncha Fm; fg: Fagfog Quartzite; da: Dandagaon Phyllites; np: Nourpul Fm; dh: Dhading Dolomite; bg: Benighat Slates; jk: Jhiku carbonates; ml: Malekhu Limestone; rb: Robang Fm; du: Dunga Quartzites; b: basic rocks; ra: Raduwa Fm; bd: Bhainsedobhan Marble; ka: Kalitar Fm; cp: Chisapani Quartzite; ku: Kulikhani Fm; mr: Markhu Fm; ti: Tistung Fm; Cm–Oc: Chandragiri Limestone (Cambro–Ordovician); gn: gneiss; gr: granite; MCT: Main Central Thrust; Mht: Mahabharat Thrust; NT(MBT): Narayani Thrust alias Main Boundary Thrust

Fig. 10.4 Geological cross-sections through the Great Mahabharat Synform in central Nepal. *Source* Modified from Stöcklin (1980)

phyllites of the Robang Formation or chloritized Benighat Slates rapidly pass upwards into lustrous chlorite schists where tiny garnets appear; these rocks then pass into the abundantly garnetiferous coarse mica-schists of the Raduwa or Kalitar Formation of the Kathmandu Complex. The coarse crystallinity of the Higher Himalayan rocks at the fault contact is enhanced by a profusion of segregationary quartz and nodular schistosity planes, which impart a gneissic appearance to these rocks (Stöcklin 1980, p. 23).

10.2 Proterozoic Lesser Himalayan Slices in the Siwalik Belt

Acharyya (1971) reported several imbricate slices of Daling, Baxa, and Damuda from east Darjeeling, where they occur within the Siwalik belt of Kumai. Hérail et al. (1986) discovered a few discontinuous Lesser Himalayan slivers within the Siwalik belt of central and east Nepal, and described them as substratum outcrops made up of red-purple and green-gray sandstones and shales with dolerite dikes or sills. These investigators correlated the basic rocks with the Gondwanas and the sedimentary rocks with the Murrees of Pakistan and Dharamsala beds of the Northwest Himalaya. Based on paleomagnetic dating, Gautam et al. (1995) assigned an Eocene–Early Oligocene age to the basic volcanics and the Lesser Himalayan sediments. This Lesser Himalayan succession was designated the Bagmati Group by Adhikary and Rimal (1996), who inferred it to be older than the Eocene. On the other hand, Takigami et al. (2002) carried out ^{40}Ar–^{39}Ar dating of the volcanics and obtained an age range of 1.5–1.7 Ga.

There are two separate areas where the Bagmati Group of rocks is exposed in the region. The west belt is located a few kilometers north of Phaparbari and the east belt crops out in the Basan Khola and Dwar Khola (Fig. 10.5). The rocks are bounded to the south by the Basan Thrust (Adhikary and Rimal 1996), whereas its northern limit is a sharp disconformity (Fig. 10.6), exposed at several locations. The Lesser Himalayan rocks of this area are strongly deformed and thrown into mesoscopic tight and isoclinal folds. They primarily contain the following three sequences with basic rocks.

10.2.1 Red-Purple Sandstone and Shale

In the west belt, these rocks form two almost parallel bands, extending along the lower and upper bounds of the Bagmati Group, but in the east belt their distribution is rather limited to the upper part (Fig. 10.5). The rocks are constituted of medium- to thick-bedded, medium- to fine-grained, dense sandstones, quartz arenites, and micaceous quartzites of red-purple, brown, and gray to white colors. Some massive sandstone beds are hematitic, contain thin shale partings, and are interbedded between gray-green shales and siltstones. Medium- to coarse-grained, thick to very thick, pale yellow, soft sandstones also sporadically occur. Fine-grained, soft, mottled (pink-purple and gray-green) sandstones are generally interbedded with red-purple and brown shales and siltstones. Most of the succession is either parallel-laminated or cross-laminated. Generally, the sandstone and shale form an interbedded sequence of 5–25 m thickness, which is succeeded by a few meter- to tens of meter-thick finer-grained sequence of siltstone and shale. Current as well as wave ripples are frequent in the sandstones, and sun cracks are infrequently noticed in the shales. There are also intraformational shale fragments in the lower parts of some sandstone beds.

In the upper part of the east belt, red-purple, brown, pink, and pale green sandstones are regularly interbedded with red-purple and gray-green shales. The sandstones are medium- to thick-bedded, fine-grained, parallel- as well as cross-laminated, and infrequently mottled. Basic lava flows or sills and dikes are present in the red sandstone and shale sequence (Fig. 10.7) of both belts.

10.2.2 Gray-Green Shale and Sandstone

This shale-predominating succession occupies the central part of the west belt, and it is also exposed in the lower part of the east belt in the Dwar Khola and its vicinity. It is made up primarily of thick-bedded, fine- to very fine-grained, green-gray, soft sandstones. The sandstones are parallel- as well as cross-laminated and thinly interbedded with similar colored siltstones and shales. The sandstone–shale sequences attain a thickness of 10–25 m, and they also include some basic dikes, sills, and lava flows (Fig. 10.5).

10.2.3 Gray Shale

This succession is confined to the east belt, in the Dwar Khola and its vicinity. It is comprised of laminated to thin-bedded, dark green-gray to blue-gray, feeble shale, siltstone, and very fine sandstone with basic volcanic rocks. The rock is intensely deformed, giving rise to various tight to isoclinal and chevron folds.

10.2.4 Basic Rocks

The basic rocks are represented by coarse- to fine-grained varieties with plagioclase (andesine and labradorite), augite, and glass exhibiting subophitic to intergranular textures. Based on petrological and geochemical investigations of the

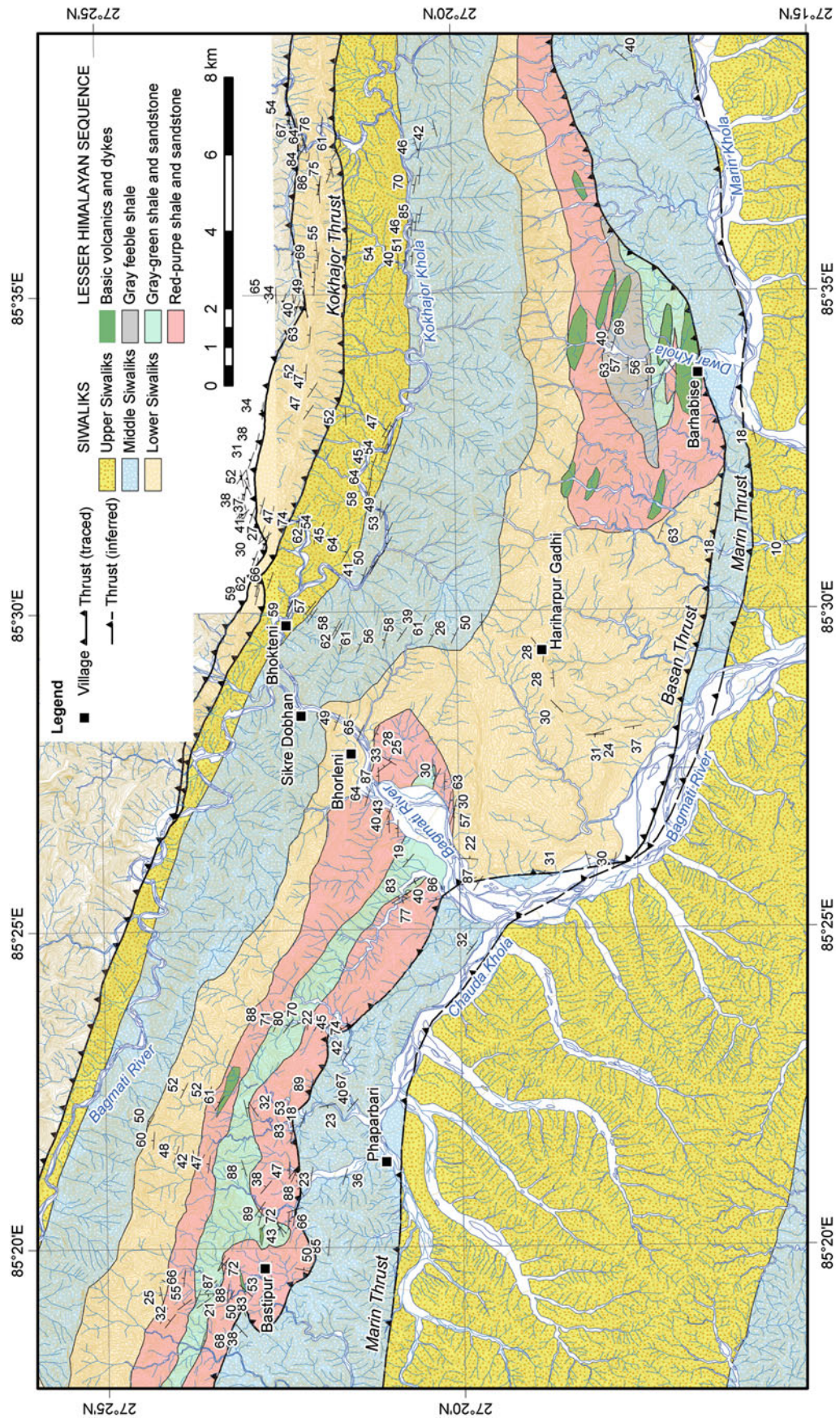

Fig. 10.5 Geological map of the Phaparbari–Marin Khola area, depicting the Bagmati Group of the Lesser Himalayan sequence within the Siwalik belt. *Source* Based on field survey in 2013 by MR Dhital and A Regmi, and data of Adhikary and Rimal (1996)

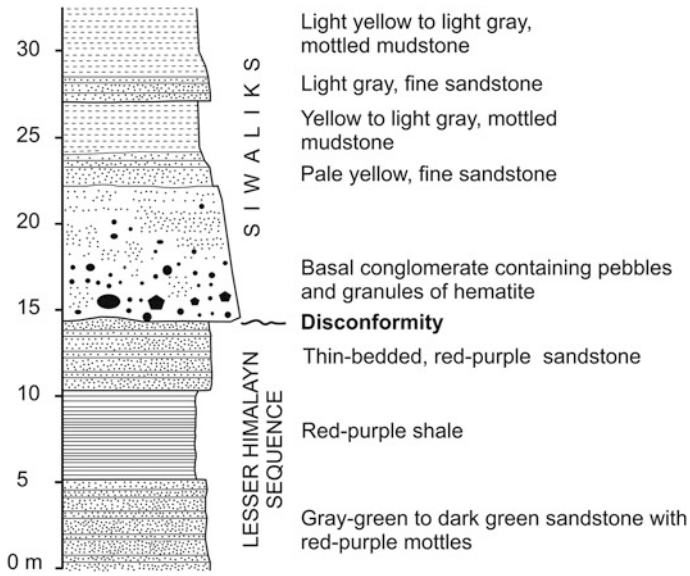

Fig. 10.6 The disconformity between the Proterozoic Bagmati Group and the Siwaliks exposed on the left bank of the Bagmati River. *Source* Author's observations

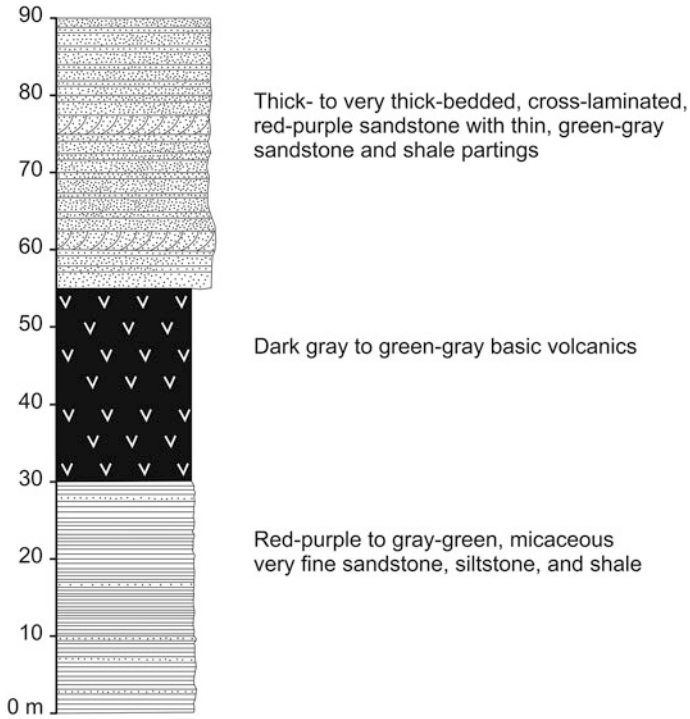

Fig. 10.7 Occurrence of basic volcanic rocks within the Bagmati Group. The exposure is located northwest of Bastipur. *Source* Author's observations

volcanites, Kaphle and Einfalt (1992) grouped them under basalts with a tendency to basaltic andesite and Hawaiite. Gautam et al. (1995) studied their petrochemistry and concluded that they belonged to tholeiitic type within-plate basalts, similar to continental flood basalts.

Proterozoic Lesser Himalayan slivers are also found in the Siwalik belt farther east (Chap. 11), where carbonate and shale beds predominate. On the other hand, the stratigraphic and lithological characteristics of the present succession are similar to the Khamari Formation (Chap. 8) or the Virkot Formation (Chap. 9) in west Nepal.

References

Acharyya SK (1971) Unique occurrence of *klippen* structure with the Siwalik belt, Eastern Darjeeling hill, West Bengal. Indian Miner 25:387–388

Adhikary TP, Rimal LN (1996) Stratigraphy and structural framework of the Sub-Himalaya, Bagmati River Region, Central Nepal. J Nepal Geol Soc 13:37–50

Arita K, Ohta Y, Akiba C, Maruo Y (1973) Kathmandu region. In: Hashimoto S, Ohta Y, Akiba C (eds) Geology of the Nepal Himalayas. Himalayan Committee of Hokkaido University, Sapporo, pp 99–145

Beyssac O, Bollinger L, Avouac J-P, Goffé B (2004) Thermal metamorphism in the Lesser Himalaya of Nepal determined from Raman spectroscopy of carbonaceous material. Earth Planet Sci Lett 225:233–241

Bordet P (1961) Recherches Géologiques dans L'Himalaya du Népal, Région du Makalu, Expéditions Françaises a l'Himalaya 1954–1955, Edition du Centre National de la Recherche Scientifique (C. N. R. S.), 275 pp (with two geological maps in colors)

Gautam P, Upreti BN, Arita K (1995) Paleomagnetism and petrochemistry of the Dowar Khola volcanics, central Nepal Sub Himalaya. J Nepal Geol Soc 11(Special Issue):179–195

Hagen T (1951) Preliminary note on the geological structure of central Nepal. Verhandlungen der Schweizerischen Naturforschenden Gesellschaft, Luzern, pp 133–134

Hérail G, Mascle G, Delcaillau B (1986) Les Siwaliks de L'Himalaya Du Népal: un exemple d'évolution géodynamique d'un prisme d'accrétion intracontinental. Sciences de la Terre, Nancy, Mémoire 47:155–182

Kaphle KP, Einfalt HC (1992) Occurrence of volcanites in the lower Siwalik formation, an evidence of late tertiary igneous activity in the central Siwaliks of Nepal. J Nepal Geol Soc 8:11–19

Martin AJ, Burgya KD, Kaufmann BA, Gehrels GE (2011) Stratigraphic and tectonic implications of field and isotopic constraints on depositional ages of Proterozoic Lesser Himalayan rocks in central Nepal. Precambr Res 185:1–17

Nanda MM (1973) Progress report on geological mapping of Trisuli-Bazar area, Nuwakot and Dhading Districts, Bagmati Anchal, Nepal. Report, submitted to the Geological Survey of India. 31 pp (with maps), unpublished

Shrestha SB, Shrestha JN, Sharma SR (1986) Geological map of Central Nepal. Scale: 1:250 000. Department of Mines and Geology, Kathmandu

Stöcklin J (1980) Geology of Nepal and its regional frame. J Geol Soc London 137:1–34

Stöcklin J, Bhattarai KD (1977) Geology of Kathmandu area and central Mahabharat Range, Nepal Himalaya. HMG/UNDP Mineral Exploration Project, Technical Report, 86 pp (with 15 maps), unpublished

Stöcklin J, Bhattarai KD, Chhetri VS, Bhandary AN (1982) Photogeological map of part of central Nepal. Department of Mines and Geology, Nepal, and the UNDP. Scale: 1:100,000; in colors, with explanatory notes

Takigami Y, Sakai H, Orihashi Y (2002) 1.5 to 1.7 Ga rocks discovered from the Lesser Himalaya and Siwalik belt: ^{40}Ar–^{39}Ar ages and their significances in the evolution of Himalayan orogen. Geochim Cosmochim Acta 66(S1):A762

Lesser Himalaya of Koshi Region

11

In questions of science, the authority of a thousand is not worth the humble reasoning of a single individual.
—Galileo Galilei (1632)

The Koshi region includes the largest tectonic window of Nepal, where the Lesser Himalayan rocks occupy the core of the Great Midland Antiform (Fig. 11.1). In continuation with the Kathmandu–Gosainkund region, the rocks are also distributed along the foothills of the Mahabharat Range, and some of their sedimentary slices are preserved in the Siwalik Hills of Katari and Kampu Ghat.

Lombard (1952, 1958) and Hagen (1959) made an early reconnaissance of this window and constructed a few cross-sections through Mount Everest, Okhaldhunga, and the Mahabharat Range. Ishida (1969) as well as Ishida and Ohta (1973) carried out preliminary structural and petrographic studies in the Lesser Himalaya of this tract. Stöcklin and Bhattarai (1977) mapped its northwest extremity and included the rocks under the Nawakot Complex, whereas Schelling (1992) identified the Khare Phyllite, Melung–Salleri augen gneiss, Ramechhap Group, and many other sequences. This region is characterized by the prevalence of augen gneisses in the Lesser Himalaya as well as the Higher Himalaya. The Lesser Himalayan augen gneisses are distributed between Kharidhunga and Okhaldhunga, where they constitute an approximately 2 to 5 km thick and about 100 km long body (Fig. 11.1). Its marginal part is phyllonitic, but the inner portion is a typical augen gneiss with large (2–20 cm in diameter), sometimes euhedral, megacrysts of K-feldspar in a foliated matrix. The augen gneiss body grades into a porphyritic granite towards its core (Kano 1984).

11.1 Kharidhunga Area

The Kharidhunga area (Fig. 11.2) lies in the northwest corner of the Okhaldhunga window, where the Proterozoic rocks of the Nawakot Complex represent the Lesser Himalayan sequence. The Nawakot Complex covers an extensive tract of country in the west (Chaps. 9 and 10) and also extends farther east, towards the Tama Koshi and Dudh Koshi Rivers (Fig. 11.1).

In this area too, the Kuncha Formation comprises a very thick (more than 2,500 m) succession of gray to green-gray phyllites, *gritty* phyllites, and metasandstones (Dahal and Adhikary 2001). There are some sections predominated by phyllites and others rich in metasandstones, whereas, occasionally, gray-green quartzites are intercalated in its upper part. Many quartz veins are injected in the rock and most of them are aligned parallel to foliation. Tiny garnets appear towards the northern upper sections of this formation. The rocks of the Kuncha Formation are thrown into doubly plunging mesoscopic folds, and they also display a conspicuous lineation trending due NE–SW.

The Fagfog Quartzite sets in rather abruptly over the Kuncha Formation, and it consists of fine- to coarse-grained light gray, pale yellow, and white quartz arenites with thin gray-green phyllite alternations or partings. Generally, its thickness varies from less than 250–800 m, but in some sections it thins out and disappears (Dahal and Adhikary 2001).

Above the Fagfog Quartzite occur the Dandagaon Phyllites with a gradational contact. They mainly constitute a thinly alternating sequence of gray-green and dark gray phyllites, however, there also occur sporadic beds of gray to light gray, siliceous, laminated dolomites with micaceous partings. The Dandagaon Phyllites range in thickness from 300 to 800 m (Dahal and Adhikary 2001).

The Nourpul Formation follows the Dandagaon Phyllites with a yellow quartz arenite band that gives way upwards to a variety of dark gray carbonaceous slates and phyllites with many quartz veins, oriented essentially parallel to foliation. This formation also subordinately includes calcareous phyllite and quartzite bands towards its upper end. Infrequently occurring white quartzites contain micaceous partings or thin bands. In some locations, pink, green, and white quartzites alternate with gray or green-gray garnet–biotite–chlorite schists. Banded, augen, and granitic gneisses occupy a wide portion within the Nourpul Formation. They are more abundant towards the east and in them augen gneisses

M.R. Dhital, *Geology of the Nepal Himalaya*, Regional Geology Reviews,
DOI 10.1007/978-3-319-02496-7_11

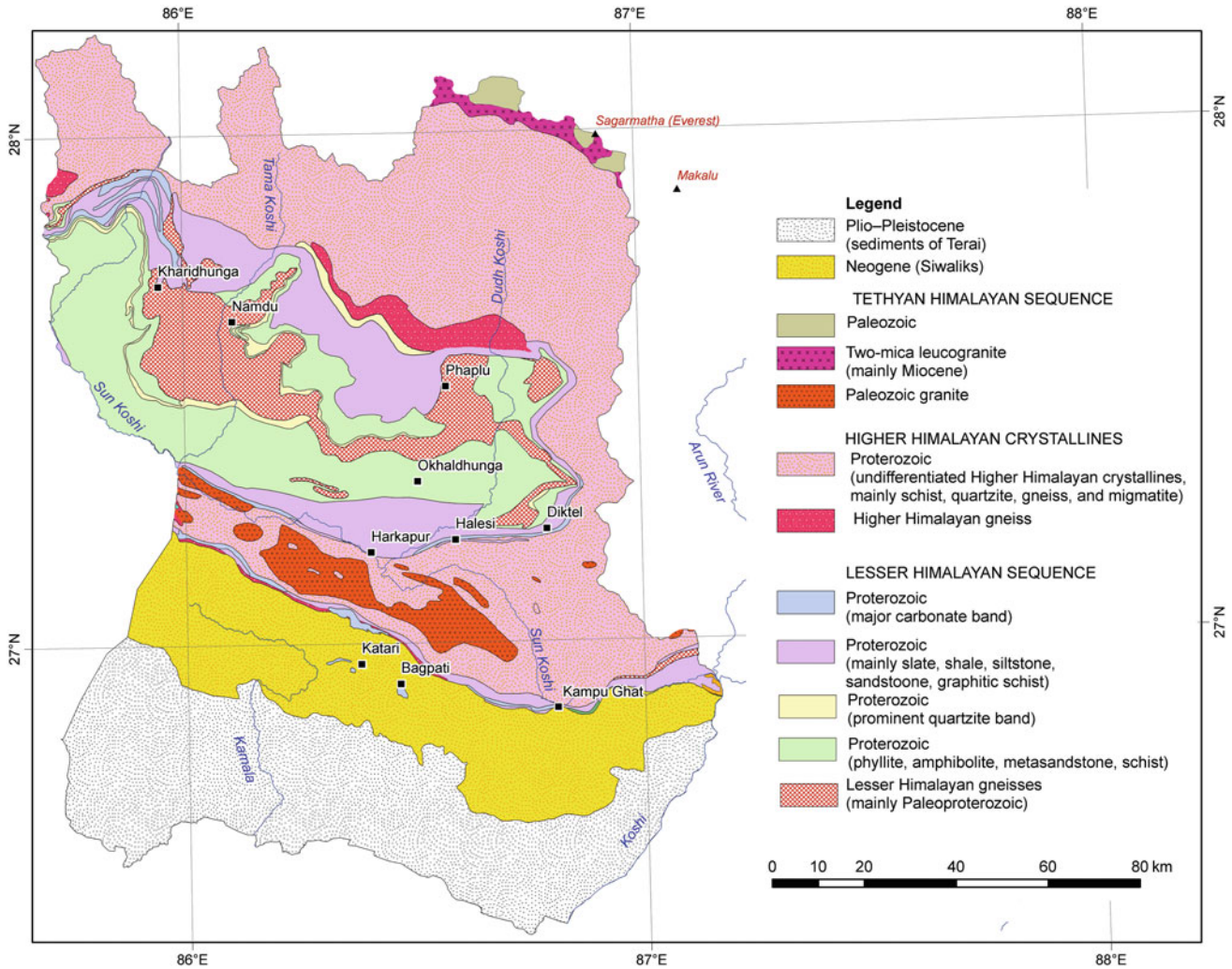

Fig. 11.1 Simplified geological map of the Koshi region. *Source* Based on Stöcklin (1980), Shrestha and Shrestha (1984), Shrestha et al. (1986), ESCAP (1993), Amatya and Jnawali (1994), other published maps, and author's observations

strongly predominate over the other two varieties. Feldspar augen are up to 2 cm long and occur in association with quartz, biotite, and muscovite. The gneisses frequently display sharp and irregular contacts with some presumable chilled effects. The Nourpul Formation (including the gneisses) attains a thickness of 1,500–2,000 m (Dahal and Adhikary 2001).

The Dhading Dolomite transitionally succeeds the Nourpul Formation and consists principally of dolomites, with subordinate phyllites and a few quartzite bands. This formation also includes many massive beds of dolomite, magnesite, and talc, representing one of the largest magnesite and talc deposits of Nepal. The Dhading dolomite is from 200 to 300 m thick (Dahal and Adhikary 2001). Columnar stromatolites are observed in the altered magnesite and talc bands of the Kharidhunga area. These ores are confined to the core of a syncline that contains gneisses in its lower part. The ores have been referred to either of sedimentary or hydrothermal (with metasomatic replacement) origin. Dangol (1992) revealed that neither the trace elements nor their associations in the ores have anomalous concentrations with the exception of Sr and Ba, which have a relatively high content as compared with the ultrabasic rocks. Hence, his data allude to the sedimentary origin of magnesite and talc. Nevertheless, their link with the underlying Proterozoic orthogneisses cannot be ruled out, as the rocks were affected by regional metamorphism and folding, which could have significantly altered the distribution of elements. The irregular ore bodies are confined to certain pockets, akin to those resulting from hydrothermal and metasomatic alterations. Farther north, beyond the present map area, there are black graphitic schists, which could have played the role of a seal above the dolomites to produce the ores.

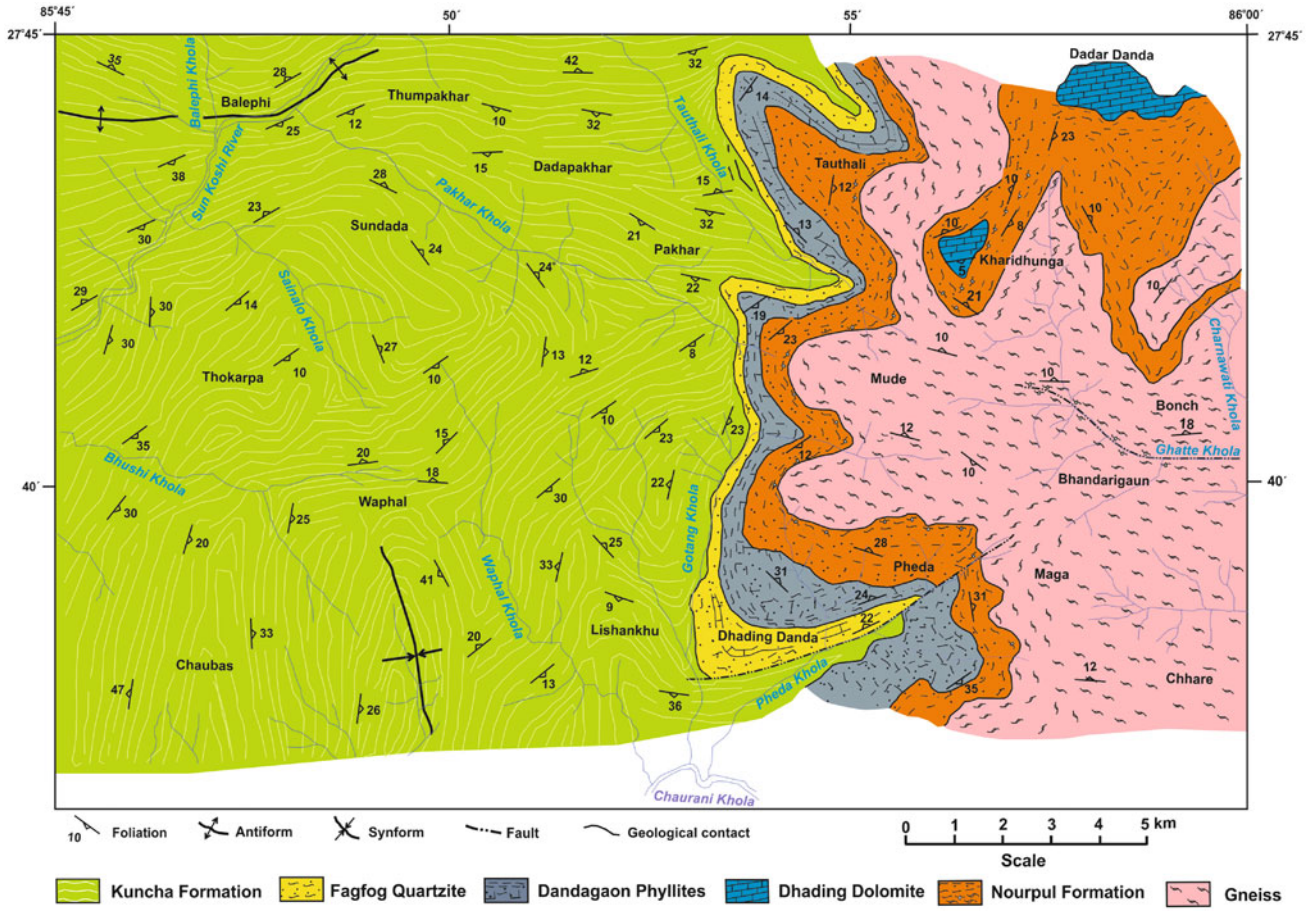

Fig. 11.2 Geological map of the Kharidhunga area. *Source* Modified from Dahal and Adhikary (2001). © Nepal Geological Society. Used by permission

11.2 Namdu–Gairimudi Area

Lithological correspondence between the Namdu–Gairimudi (Fig. 11.3) and Kharidhunga areas is evident in their common occurrence of graphitic schists or slates and stromatolitic dolomites, containing magnesite and talc. Owing to the proximity of the Main Central Thrust, the rocks of the Namdu–Gairimudi area were subjected to a greater degree of metamorphism. Although these rocks primarily belong to the Nawakot Complex, some lithological variations attest to their further classification.

The Maina Pokhari Gneiss constitutes the north, central, south, and west parts of the map area. It is represented regularly by a quite foliated, stretched, and banded variety and subordinately by a strongly lineated type. There also occur some augen gneisses where the augen are of K-feldspar and their matrix is composed mainly of quartz, feldspar, and biotite. Infrequent protoliths also occur in the gneisses, especially near the contact with schists and phyllites.

The gneisses principally occupy three broad regions (i.e., around Maina Pokhari, Gairimudi, and in the Gopi Khola), and form gently dipping flanks of a large open syncline (Fig. 11.3). Chilled effects are conspicuous in the gray augen gneisses and strongly lineated banded gneisses exposed at Thulachaur, where they display sharp and irregular contacts with the surrounding schist (Fig. 11.4). In the Gopi Khola, gray to green-gray, strongly lineated banded and augen gneisses (Fig. 11.5) occupy both of its banks. The gneisses form a narrow zone on the east that abruptly widens to the west (Fig. 11.3). The field observations allude to the magmatic origin of gneisses that were subsequently foliated and metamorphosed. The thickness of the Maina Pokhari Gneiss is more than 400 m.

The Maina Pokhari Gneiss was emplaced mainly in the Khani Khola Formation, which is widely distributed in the west, south, and northeast parts; a few small patches of the gneiss also occur in the north-central part (Fig. 11.3). The rocks of the Khani Khola Formation are represented by dark gray, green-gray (when weathered), and bright green garnet–chlorite schists; black biotite schists; medium- to thin-bedded,

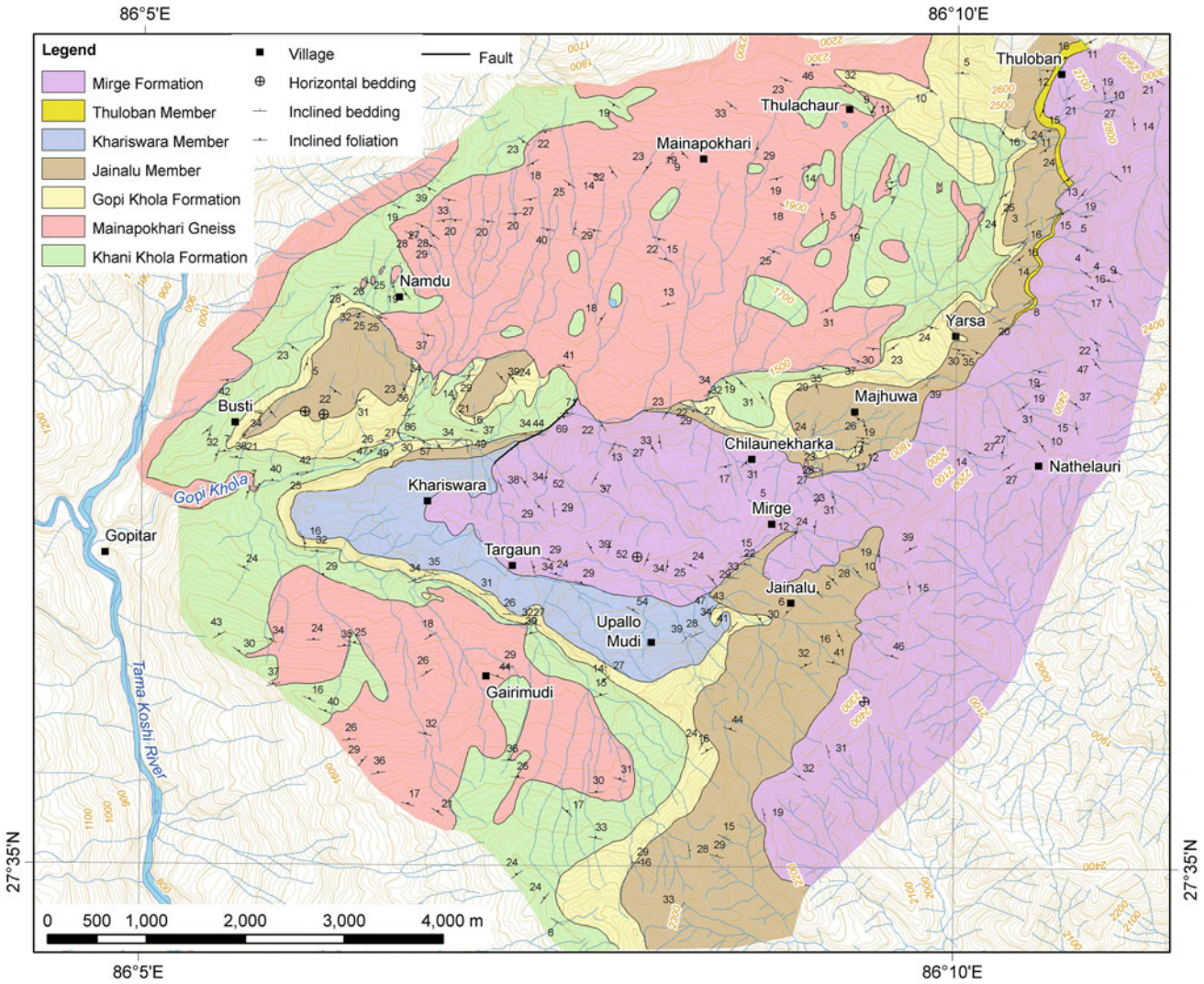

Fig. 11.3 Geological map of the Namdu–Gairimudi area in the inner Lesser Himalayan zone. *Source* Based on field survey in 1997 by MR Dhital and KR Regmi

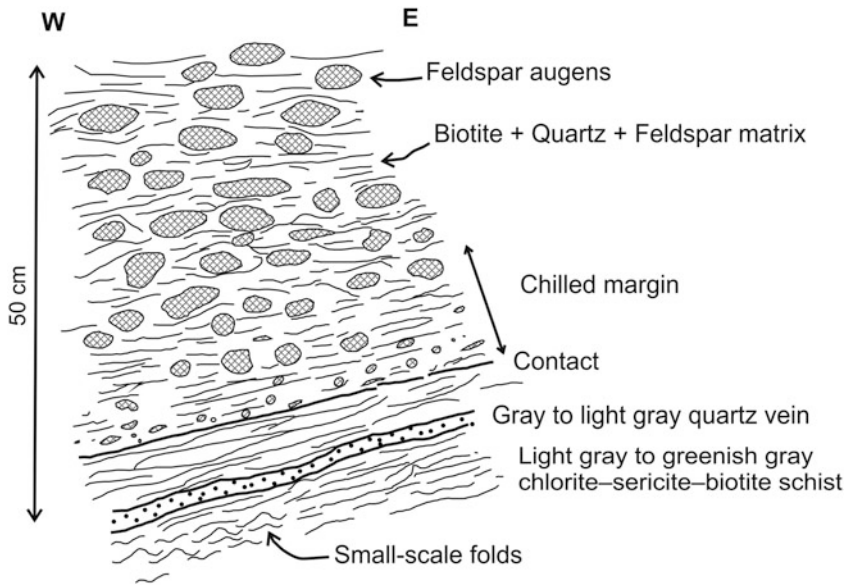

Fig. 11.4 Chilled contact between augen gneiss and schist. *Source* Author's observations

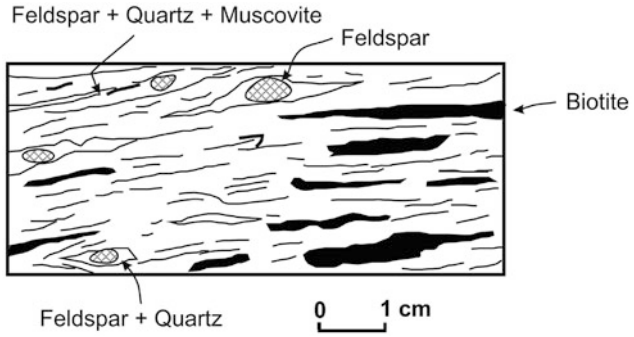

Fig. 11.5 Strongly stretched and lineate augen gneiss in the Gopi Khola. *Source* Author's observations

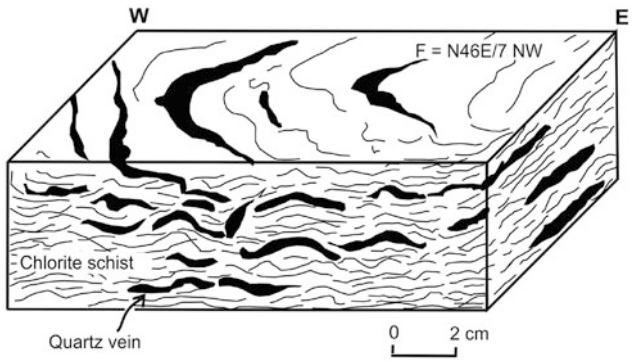

Fig. 11.6 Deformed quartz veins in the chlorite schist of the Khani Khola Formation. *Source* Author's observations

evenly laminated, blocky to flaggy, light gray to yellow-gray, fine-grained quartzites; green to light green quartzites; and metasandstones. In the schists, the size of garnets varies from 1 to 3 mm, and they are idioblastic to subrounded in shape. Many quartz veins crosscut the garnet–chlorite schist. These veins are frequently sigmoid to lenticular and sheared (Fig. 11.6). Some deformed and boudinaged tourmaline-bearing pegmatites are also present within the schist. The schists of this formation are strongly deformed and crenulated. The Khani Khola Formation reaches 250 m in thickness.

The Gopi Khola Formation transitionally overlies the Khani Khola Formation. Here are mainly medium- to thick-bedded, sporadically laminated, blocky to platy, gray-green, pale yellow, light gray, and white quartzites with infrequent schist or phyllite parting and thin bands. These quartzites are occasionally calcareous and strongly lineated parallel to the dip of bedding. In most parts of the area, the rocks of the Gopi Khola Formation form high cliffs. The Gopi Khola Formation is 200 m thick.

The Gopi Khola Formation transitionally passes into the overlying Majhuwa Formation. It is subdivided into the following three members.

The rocks of the Jainalu Member crop out around Jainalu and Majhuwa. They are represented by dark gray, green-gray (when weathered), green, and bright green chlorite–biotite schists, gray-green phyllites, and thinly laminated, medium- to thick-bedded gray dolomites. The dolomites sporadically contain columnar stromatolites. The Jainalu Member is about 100 m thick.

In the Khariswara Member, light gray to white, medium- to very thick-bedded magnesite and talc-bearing beds abound. At the bottom of this unit, gray dolomites (metasomatically altered to magnesite and talc) are observed. The columnar stromatolites are well developed in the cliff south of Targaun. Good exposures of magnesite and talc are also seen in the stream east of Chilaunekharka.

The rocks of the Thuloban Member are exposed in the northeast part and are represented by interlaminated gray to white calcareous quartzites, gray dolomites, and dark gray schists. The Thuloban Member is about 50 m thick and it is absent in the southern part of the map area.

The Mirge Formation is present in the northeast, east, and central sectors. Gray to dark gray garnetiferous schists, gray to black graphitic schists with abundant quartz veins, gray metasandstones, and green-gray amphibolites are the main constituents. The size of garnets in the schists reaches 1 cm and they are predominantly idioblastic, whereas others are rounded and display beautiful pressure shadows around them. The Mirge Formation is about 400 m thick.

A gently east-plunging, open syncline passes through the Gopi Khola, Khariswara, and Mirge (Fig. 11.3). The graphitic schists of the Mirge Formation occupy the core of this major fold with gently (up to 35°) dipping limbs. Apart from it, there is also a complementary anticline, the core of which is made up of the quartzites of the Gopi Khola Formation. Pinch and swell structures, crenulation cleavage, stretching lineation, and various small-scale folds are frequent in the Namdu–Gairimudi area. Crenulation cleavage is well developed, mainly in the rocks of the Khani Khola Formation. A prominent lineation trends due SW (S9°W, S18°W) and its plunge varies from 10° to 35°. The small-scale folds are of S-type, M-type, and Z-type (Fig. 11.7). The minor asymmetric folds indicate a top-to-south sense of movement, which is typical for the rocks close to the Main Central Thrust.

The metamorphic grade in the Namdu–Gairimudi area steadily increases towards the Main Central Thrust, as evidenced from the appearance, respectively, of chlorite, biotite, and garnet. A comparison between these rocks and those of central Nepal (Table 11.1) shows that the Dandagaon Phyllites and Nourpul Formation of the Nawakot Complex are not typically developed in this part of the Lesser Himalaya.

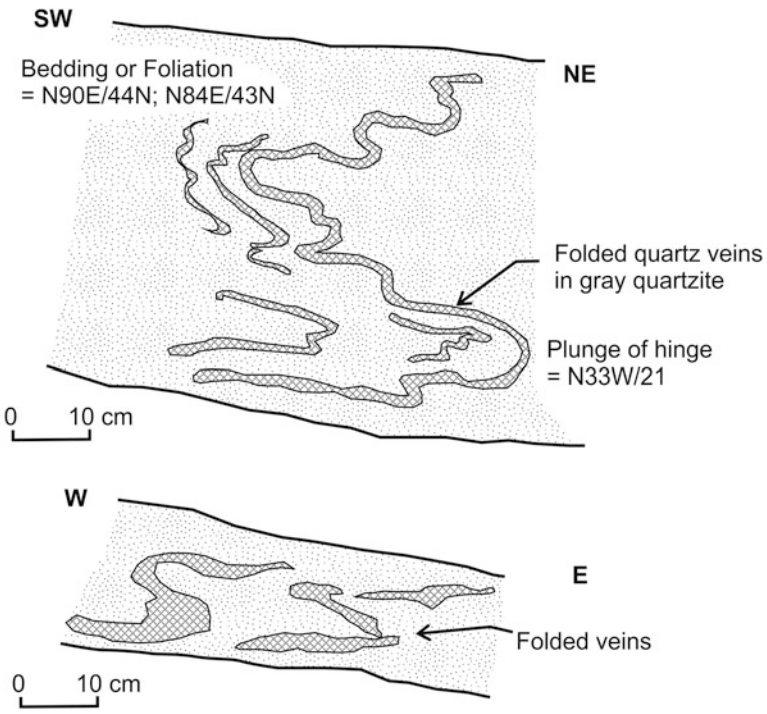

Fig. 11.7 Small-scale folds in the quartzites of the Jainalu Member exposed in the Khani Khola. *Source* Author's observations

Table 11.1 Correlation of rocks from Namdu–Gairimudi with those from Central Nepal Lesser Himalaya

Central Nepal (Stöcklin and Bhattarai 1977)		Namdu–Gairimudi area
Upper Nawakot Group	Benighat Slates	Mirge Formation
Lower Nawakot Group	Dhading Dolomite Nourpul Formation	Majhuwa Formation
	Dandagaon Phyllites Fagfog Quartzite	Gopi Khola Formation
	Kuncha Formation	Khani Khola Formation

Source Author's observations

11.3 Metasediments and Mylonitic Gneisses of Phaplu

Towards the north margin of the Okhaldhunga window, a succession similar to that of the Namdu–Gairimudi and Kharidhunga areas is observed at Phaplu and its vicinity in east Nepal. Strongly lineated augen and banded gneisses with a well-developed C/S fabric occupy the upper reach of the Solu Khola (Fig. 11.8), where they were mapped as the Melung–Salleri augen gneisses (Schelling 1992). Different from the Namdu–Gairimudi area, passage from gneisses to schists or quartzites appears perfectly transitional, without any trace of contact metamorphism. Similar features are also characteristic of the Ulleri gneisses found in west Nepal (Chap. 6). In the mylonitic gneisses, rounded augen of feldspar and quartz are up to 2 cm in diameter. The gneisses infrequently alternate with gray-green feldspathic schists or quartzites. Sporadic amphibolite bands are also found in this sequence. An approximately 50–150 m thick quartzite band appears towards the top of the succession. These pale yellow to white quartzites are also strongly lineated and contain subordinate bands of schist and gneiss. Generally, the quartzites are massive, very thick-banded, and display rare parallel laminae. This succession resembles the Fagfog Quartzite of the Nawakot Complex, and it is transitionally followed by abundantly garnetiferous graphitic schists, alternating with calcareous quartzite or marble bands. There are also intercalated a few very fine, white quartzite and blue-green amphibolite bands. The last succession, which strongly resembles the Benighat Slates, is abruptly followed by a thick sequence of kyanite schist and banded gneiss, representing the Higher Himalayan crystallines.

11.4 Harkapur–Mane Bhanjyang Area

The tract of country between Harkapur and Mane Bhanjyang provides a glimpse of the rocks constituting the footwall of the Main Central Thrust on the south edge of the Okhaldhunga tectonic window (Fig. 11.9). On the left bank of the Sun Koshi River, a few hundred meter-wide Lesser Himalayan belt is milled and shattered, resulting in the development of large landslips. The Proterozoic Lesser Himalayan

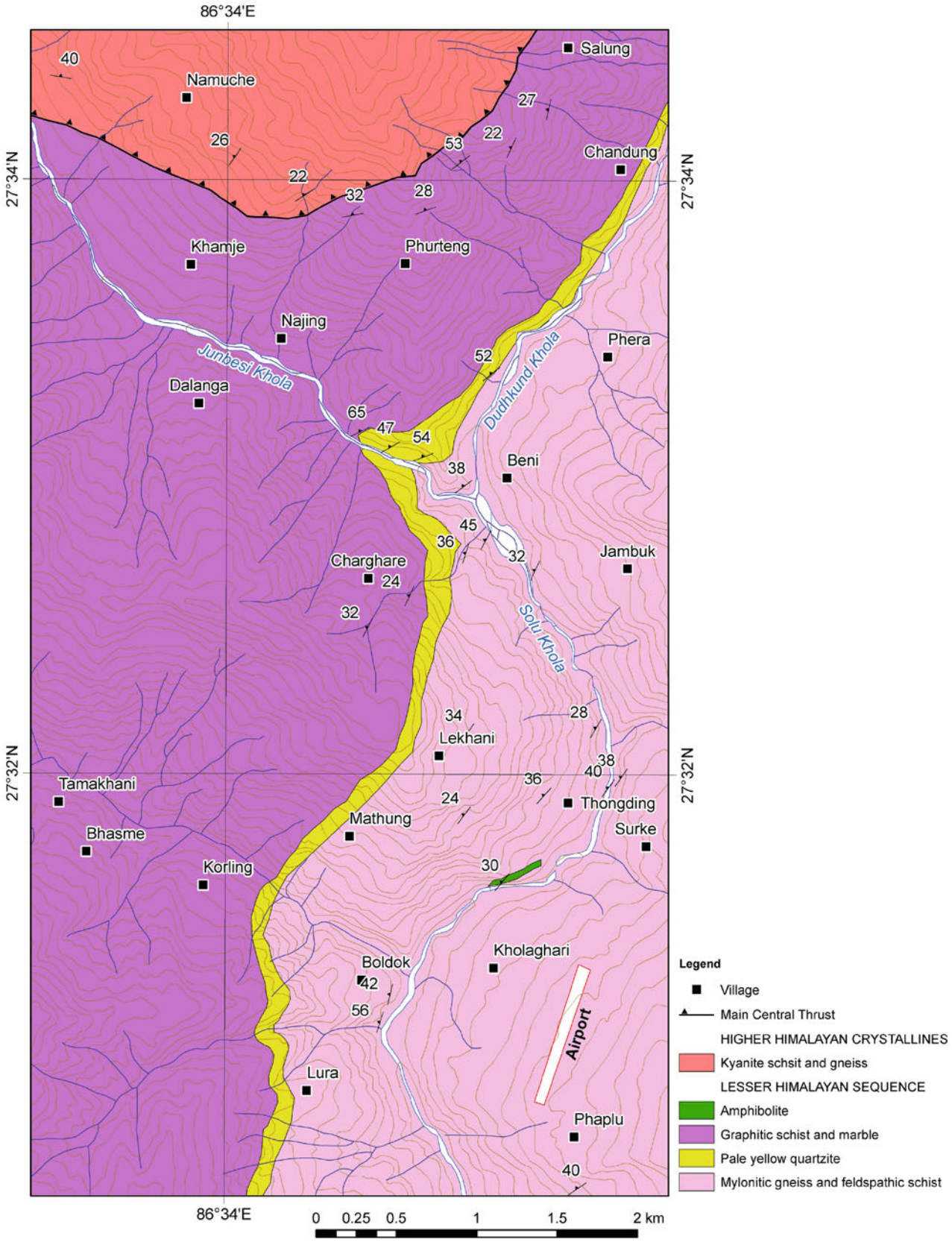

Fig. 11.8 Metasediments and gneisses of the Lesser Himalaya developed near the north margin of the Okhaldhunga window. *Source* Based on field survey in 2009 by MR Dhital, KK Acharya, and N Regmi

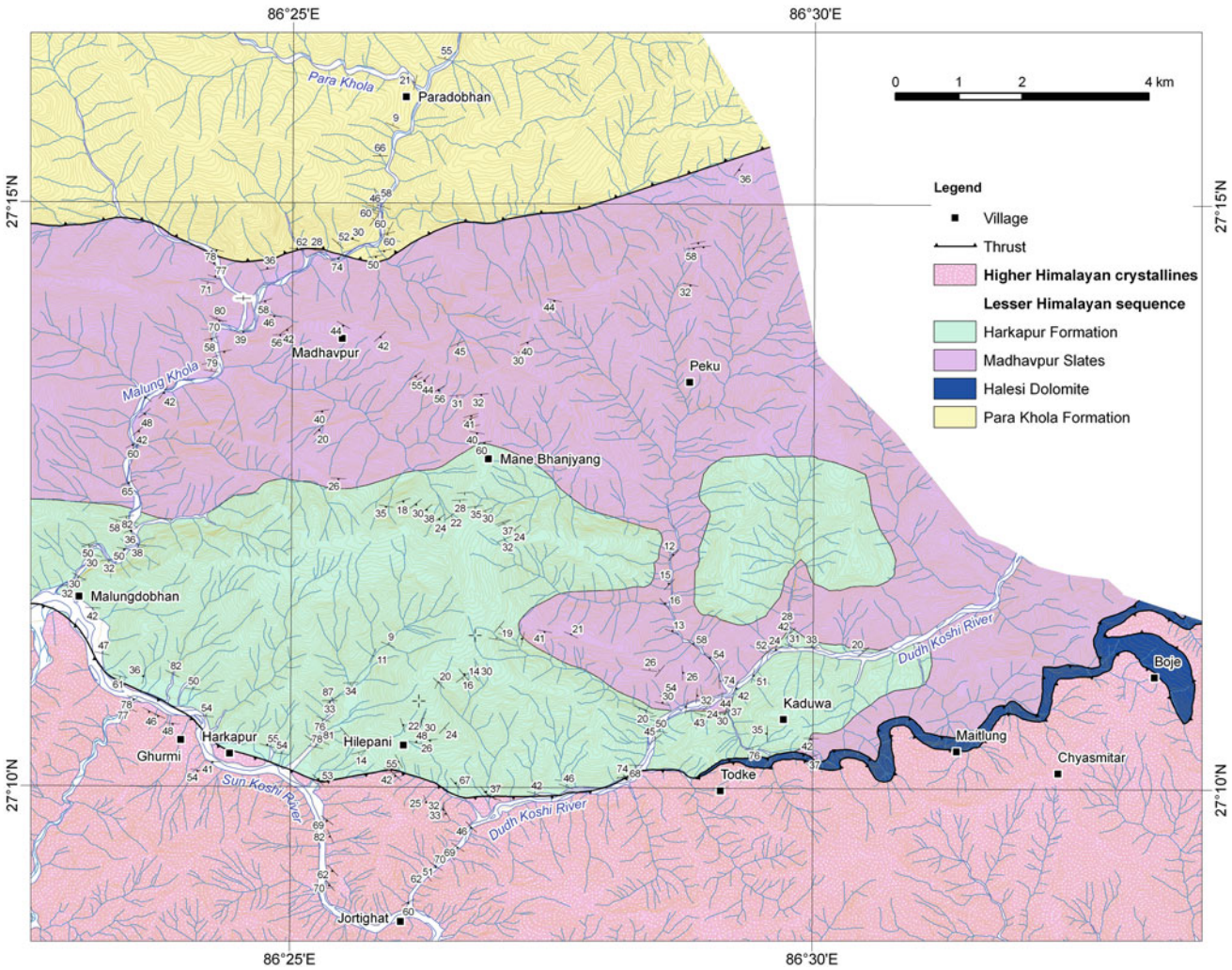

Fig. 11.9 Geological map of the Harkapur–Mane Bhanjyang area. *Source* Based on Dhital (2006), Bijukchhen (2011), Gyawali (2011), and author's observations in 2011

rocks of this area are classified into the following formations (Bijukchhen 2011; Gyawali 2011).

The Para Khola Formation (Figs. 11.9 and 11.10) is made up predominantly of thick to very thick beds of medium- to coarse-grained, massive, pink and purple quartzite, interbedded with red-purple and gray-green, mottled slate partings or thin bands. A few amphibolite bands are also encountered sporadically. Spectacular ripples and cross-laminae are characteristic of this formation. The Para Khola Formation is thrust over the younger Madhavpur Slates along the Dhad Khola Thrust (Fig. 11.9).

The Halesi Dolomite (Dhital 2006) composes the footwall of the Main Central Thrust for a distance of about 18 km (Fig. 11.11). It is made up of gray to dark gray, medium- to thick-bedded, crystalline dolomite with sporadic stromatolites. The formation is more than 200 m thick near Halesi. The Para Khola Formation and the Halesi Dolomite are never in contact with each other. Nonetheless, it is an assumption that the Halesi Dolomite is younger than the Para Khola Formation but older than the Madhavpur Slates.

The Madhavpur Slates occupy the footwall of the Dhad Khola Thrust (Fig. 11.9). In the lower part of this formation occur dark gray to black, parallel-laminated graphitic slates with abundant quartz veins. Its middle part contains black graphitic slates with bands of thinly foliated, gray, calcareous quartzite. Thin interbeds of gray-green to dark gray slate and dark gray dolomite are frequent. In the upper part, the Madhavpur Slates comprise thinly laminated or foliated, black, calcareous slates or phyllites, and siltstones. The calcareous slates transitionally pass into the overlying Harkapur Formation.

The lower part of the Harkapur Formation comprises light gray, medium- to thick-bedded dolomites intercalated in gray, green-gray to dark gray slates, green-gray phyllites, or thin-bedded, dark gray, graphitic slates. There also occur thin beds of light gray to green-gray, parallel-laminated,

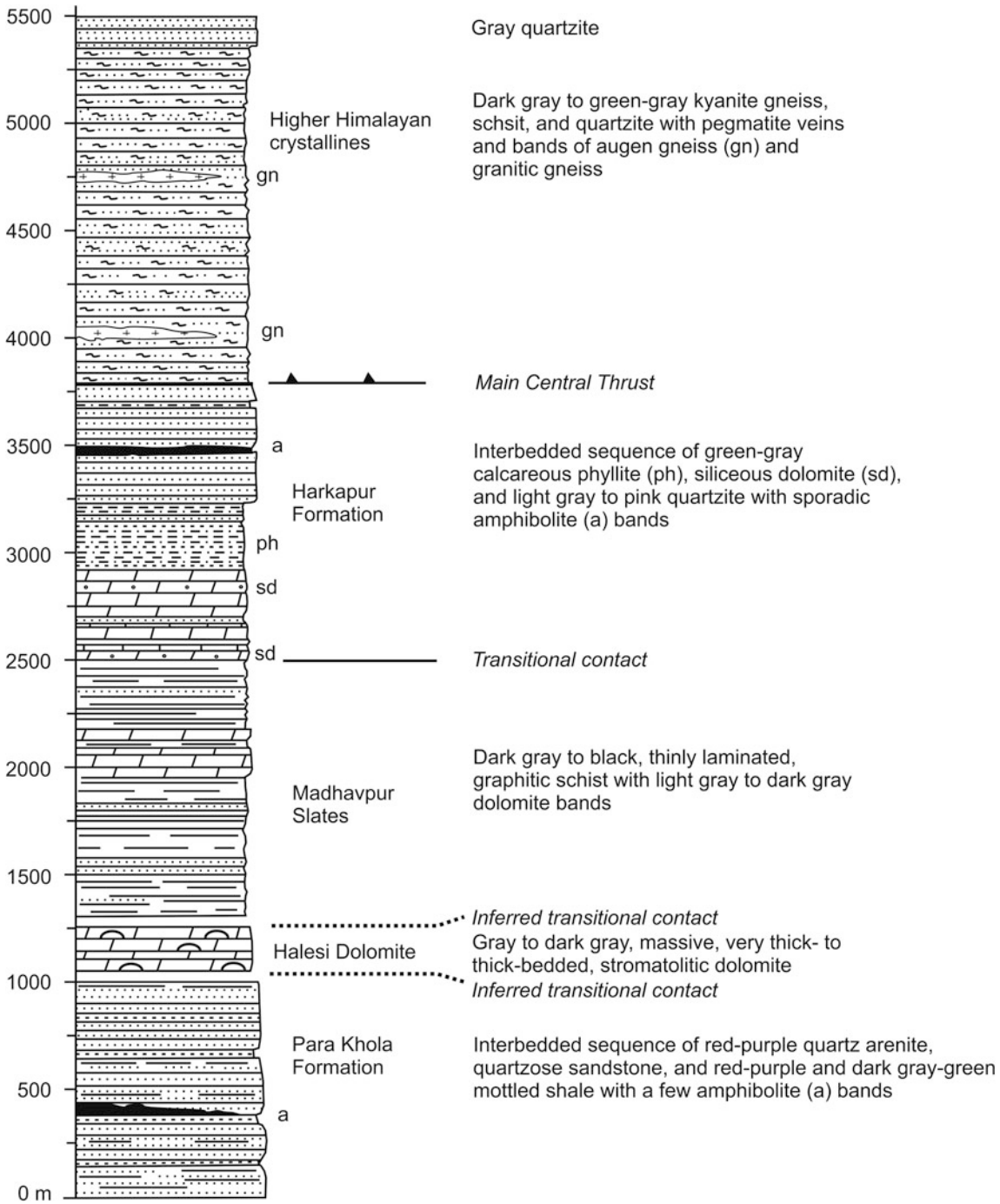

Fig. 11.10 Tectonostratigraphic column of the Harkapur–Mane Bhanjyang area. *Source* Modified from Gyawali (2011)

fine- to medium-grained, calcareous quartzite with gray-green phyllite or slate partings and some light gray to white, thickly bedded, fine- to medium-grained dolomite. The upper part of the Harkapur Formation consists of an interbedded succession of greenish gray calcareous phyllite and siliceous dolomite with sporadic amphibolite bands. In the Sun Koshi and Dudh Koshi Rivers, the last sequence is sharply truncated by the Main Central Thrust (Fig. 11.9).

Although the Para Khola Formation resembles the Nourpul Formation in lithology, some minor differences are apparent. The Para Khola Formation is more arenaceous, thick- to very thick-bedded, and massive. The Halesi Dolomite is similar to the Dhading Dolomite, and the Madhavpur Slates, with thin carbonate beds, are akin to the Benighat Slates with Jhiku carbonates, whereas the transitionally overlying phyllites, quartzites, and carbonates of the

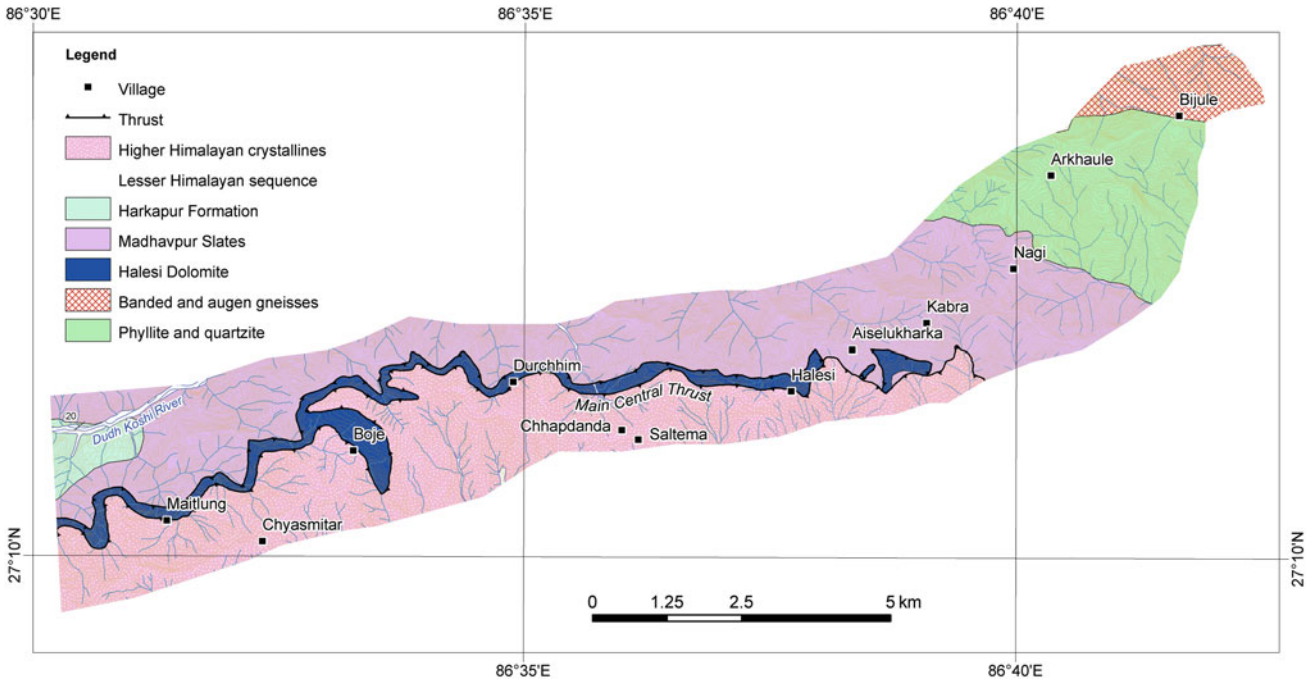

Fig. 11.11 Geological map of the Halesi area showing the distribution of dolomite below the Main Central Thrust. *Source* Modified from Dhital (2006)

Harkapur Formation might be homotaxial with the Malekhu Limestone and the Robang Formation of the Upper Nawakot Group (Chap. 10).

11.5 Imbricate Slices of Katari–Bagpati Area

In the Siwalik belt of the Koshi region, a number of imbricate slices of the Lesser Himalayan sequence crop up mainly in two separate segments (Fig. 11.12). The first segment discontinuously appears south of Katari, to the east in the Bagpati area, and to the west along the right bank of the Tawa Khola. The second segment is well developed between the Kakur Khola, Maruwa Khola, and the Tawa Khola.

The Kakur Khola Formation is found at the base of various imbricate slices (Fig. 11.13). It is made up of medium- to thin-bedded, parallel- and cross-laminated, fine-grained, pink quartz arenites and red-purple shales containing sporadic sun cracks. The quartz arenites are cross-laminated, contain wave as well as current ripples on their upper bounding surfaces, and in them well-rounded quartz grains are cemented by silica. This formation also includes infrequent partings or thin beds of gray-green shale and light gray, laminated siliceous dolomite. In this sequence, a few basic lava flows or sills are discernible (Adhikari 2013a). Based on lithological characteristics and occurrence of basic rocks, this sequence is assumed to be homotaxial with the Bagmati Group (Chap. 10).

The Dhaduwa Quartzite transitionally overlies the Kakur Khola Formation and is represented mainly by thick- to very thick-bedded, white quartz arenites with sporadic dolomite bands and gray-green shale partings (Fig. 11.13).

In the Kakur Khola, the Dhaduwa Quartzite passes upwards into the Maruwa Khola Formation. This formation is relatively well exposed in the Maruwa Khola gorge, where it begins with pink, red-purple, and gray dolomite interbeds, containing sporadic domed as well as short columnar stromatolites. Intercalated in the dolomite are pink, light gray, and pale yellow quartz arenites (Fig. 11.14). Towards the upper end of this formation appear some cherty dolomite beds, which are interbedded between gray dolomite and gray-green shale. In the Maruwa Khola, this formation is frequently truncated by a sharp disconformity, repeatedly exposed in various imbricate slices. But, in the Bagpati and Simaltar areas, the Maruwa Khola Formation transitionally grades over the Simaltar Formation.

The Simaltar Formation is the main source of cement-grade limestone found in the area. It crops up at Bagpati as well as near Patana Bhanjyang and Simaltar. It is composed of a thinly interbedded to laminated sequence of light green, pink, and purple limestone and calcareous shale or argillite. The rock is intensely deformed and its upper part is truncated by a disconformity. The Proterozoic Kakur Khola Formation, Dhaduwa Quartzite, Maruwa Khola Formation, and the Simaltar Formation are comparable with the Gwar Group in the Karnali–Bheri region (Chap. 8) as well as the Middle and Upper Kali Gandaki groups in the Gandaki region (Chap. 9).

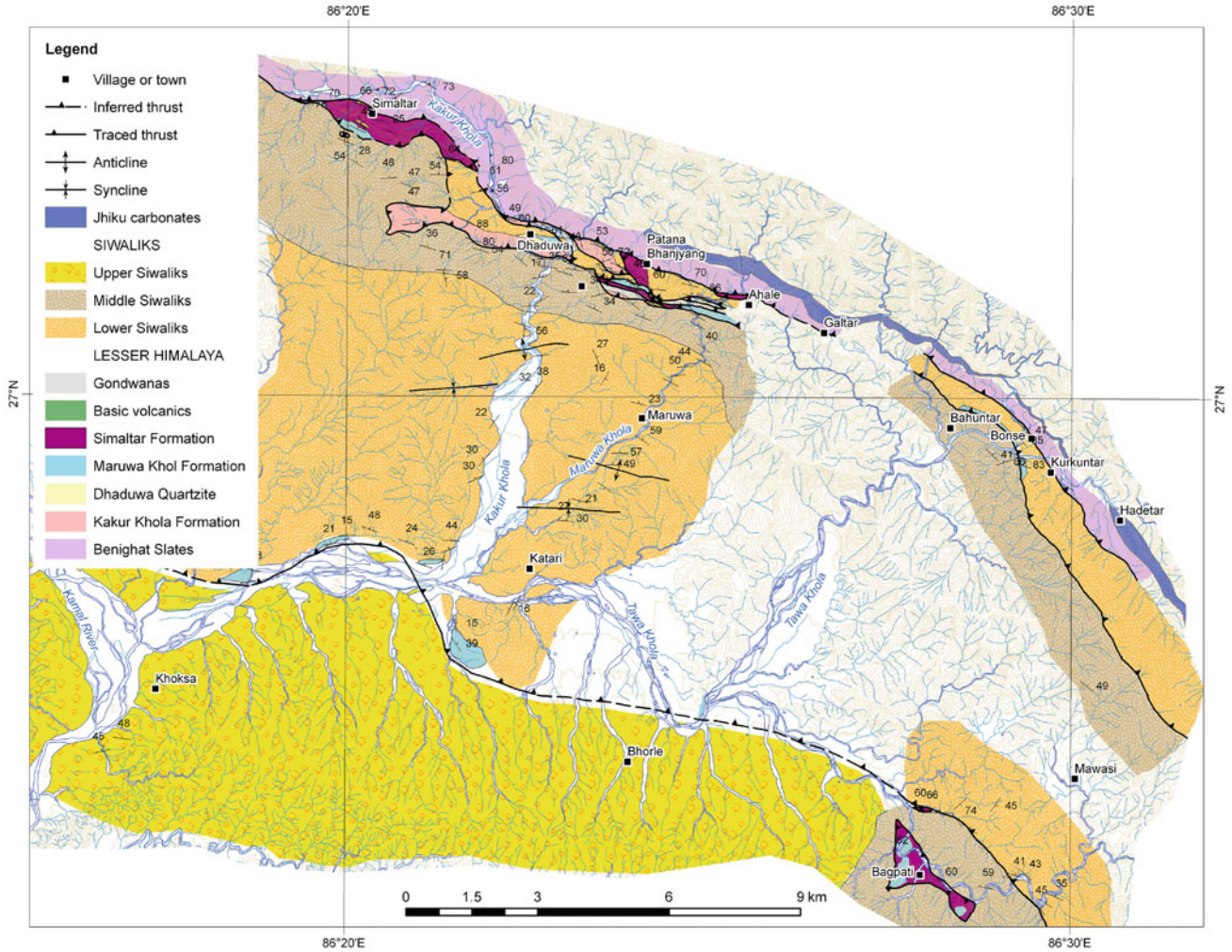

Fig. 11.12 Geological map of the Katari–Tawa Khola–Bagpati area depicting the distribution of Proterozoic rocks in the Siwalik belt. *Source* Based on field survey in 2006, 2009 and 2012 by MR Dhital, and data of Adhikari (2013a, b)

The presumable Gondwanas rest over the above formations with a sharp disconformity marked by a basal conglomerate bed, containing rounded, subrounded, to angular casts of dolomite and quartz arenite. The Gondwana sequence continues upwards with an interbedded succession of gray to dark gray carbonaceous quartzite, ferruginous quartzite, and shale with thin coal seams (Fig. 11.14). Another sharp disconformity with a basal conglomerate separates the Gondwanas from the overlying Siwaliks. The Siwaliks are represented by soft sandstone and mudstone beds.

11.6 Kampu Ghat Area

Kampu Ghat lies on the right bank of the Sun Koshi River, a few kilometers downstream from its conspicuous L-bend (Fig. 11.15). The Lesser Himalayan succession occurs essentially in two imbricate slices containing low-grade metamorphic rocks and carbonates of Proterozoic age as well as Neogene Siwalik outliers. There is also a thin and discontinuous strip of presumed Gondwanas. In this area, the Higher Himalayan crystallines cross the Sun Koshi River and override the Lesser Himalayan succession, with a trifling gap between them and the Siwaliks.

The hanging wall of the Main Central Thrust is made up of garnetiferous schists (Fig. 11.15). The gently dipping schists cross the Sun Koshi River at the Kapuwa Khola confluence and form the Siddhipur ridge, from where the Siwaliks are just a few hundred meters away. The schists contain garnet, mica, biotite, tremolite, actinolite, and hornblende. The garnetiferous schists are followed by a few graphitic bands with many quartz veins. These rocks are succeeded upwards by highly lineated, massive, gray quartzites, alternating with schists or sporadic marble bands. The last sequence is followed by kyanite schists and fine- to medium-grained banded gneisses and granites (West 1950, p. 26). The banded

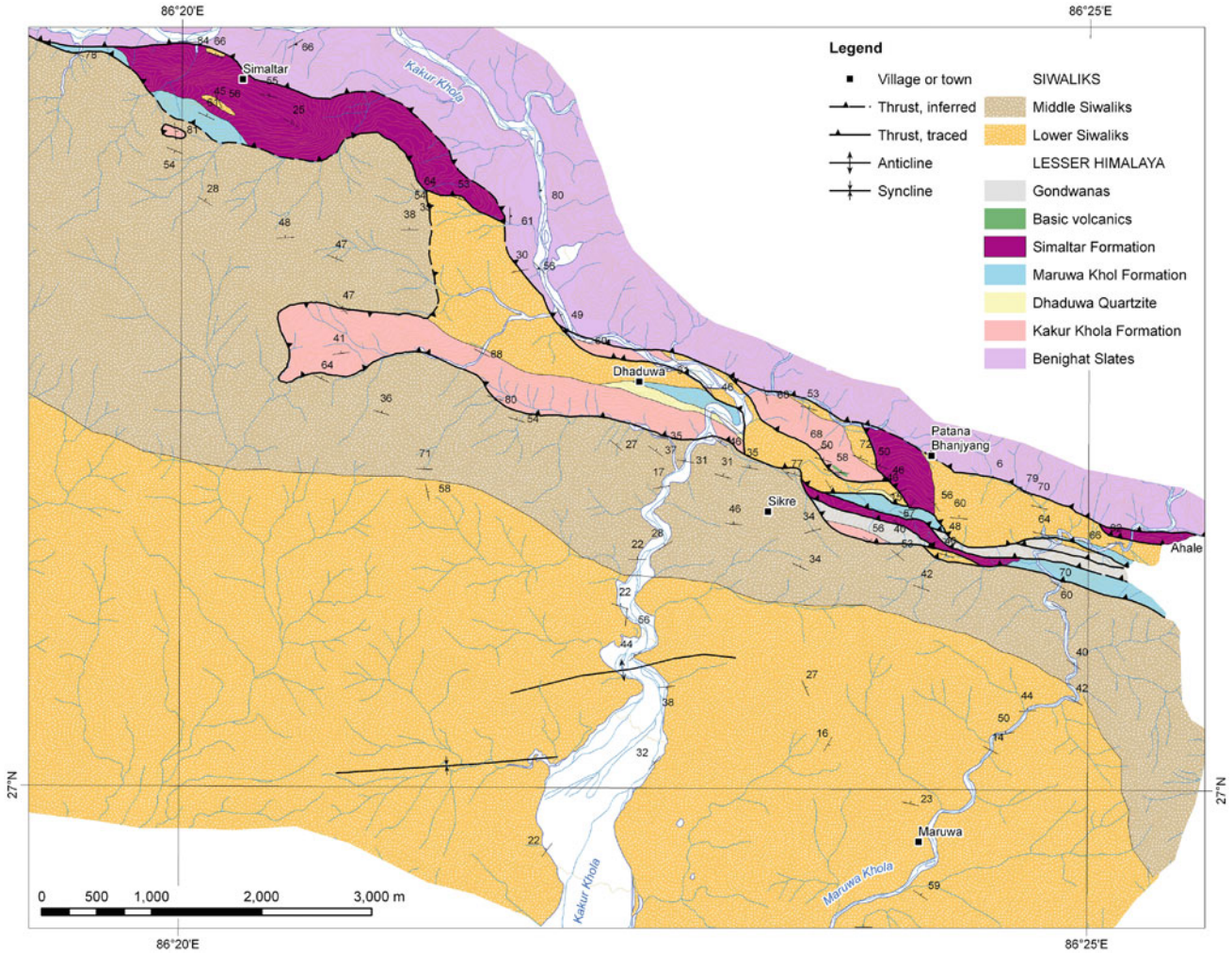

Fig. 11.13 Geological map of the Kakur Khola–Maruwa Khola area. *Source* Based on field survey in 2006, 2009 and 2012 by MR Dhital, and data of Adhikari (2013a, b)

gneisses are quite heterogeneous and contain schistose, quartzitic, and feldspathic varieties with many quartz veins and pegmatites (Chaudhary 1997).

The Lesser Himalayan metasedimentary rocks are represented by bluish and greenish gray phyllites and light gray quartzites, consisting of muscovite, biotite, and quartz. They are thrust over other Lesser Himalayan sedimentary rocks and Siwaliks.

In both banks of the Sun Koshi River, the Kampu Ghat Formation (Chaudhary 1997) of gray dolomites is intermittently distributed, but it persistently extends to the west, towards the Baruwa Khola (Fig. 11.15). In the Sun Koshi River, a few pockets of magnesite are found in the Kampu Ghat Formation, where it is sandwiched between the Siwaliks and the Lesser Himalayan low-grade metamorphic rocks. Sometimes, the dolomites turn cherty at the basal part of the formation. A few thick beds of highly fractured, blue-gray dolomite succeed the magnesite-bearing succession and they contain domed stromatolites together with many intraclasts.

The dolomite is disconformably overlain by the presumed Gondwanas, belonging to the Dhungre Formation (Chaudhary 1997). They are exposed at the mouth of the Dhungre Khola, where it meets the Sun Koshi River. The Dhungre Formation is represented by a gray to dark gray, calcareous shale. The thin-bedded shale is fragile, and its contact with the underlying Kampu Ghat Formation is sharp.

The Lower Siwaliks cropping out in this area are made up predominantly of interbedded red, purple, green, brown, and orange mudstones and gray, greenish gray, and purple sandstones.

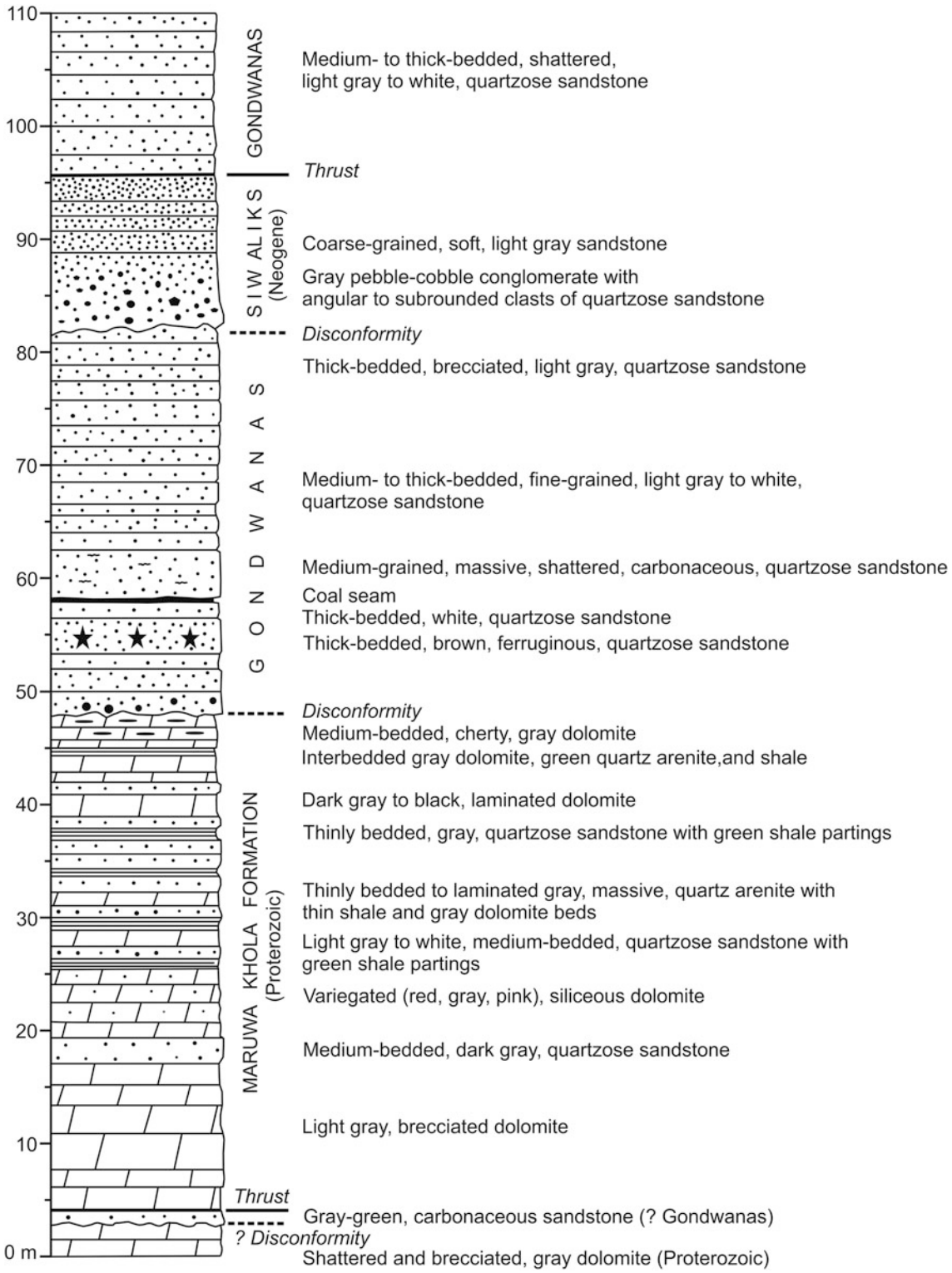

Fig. 11.14 Tectonostratigraphic column of the rocks exposed in the Maruwa Khola. *Source* Modified from Adhikari (2013a)

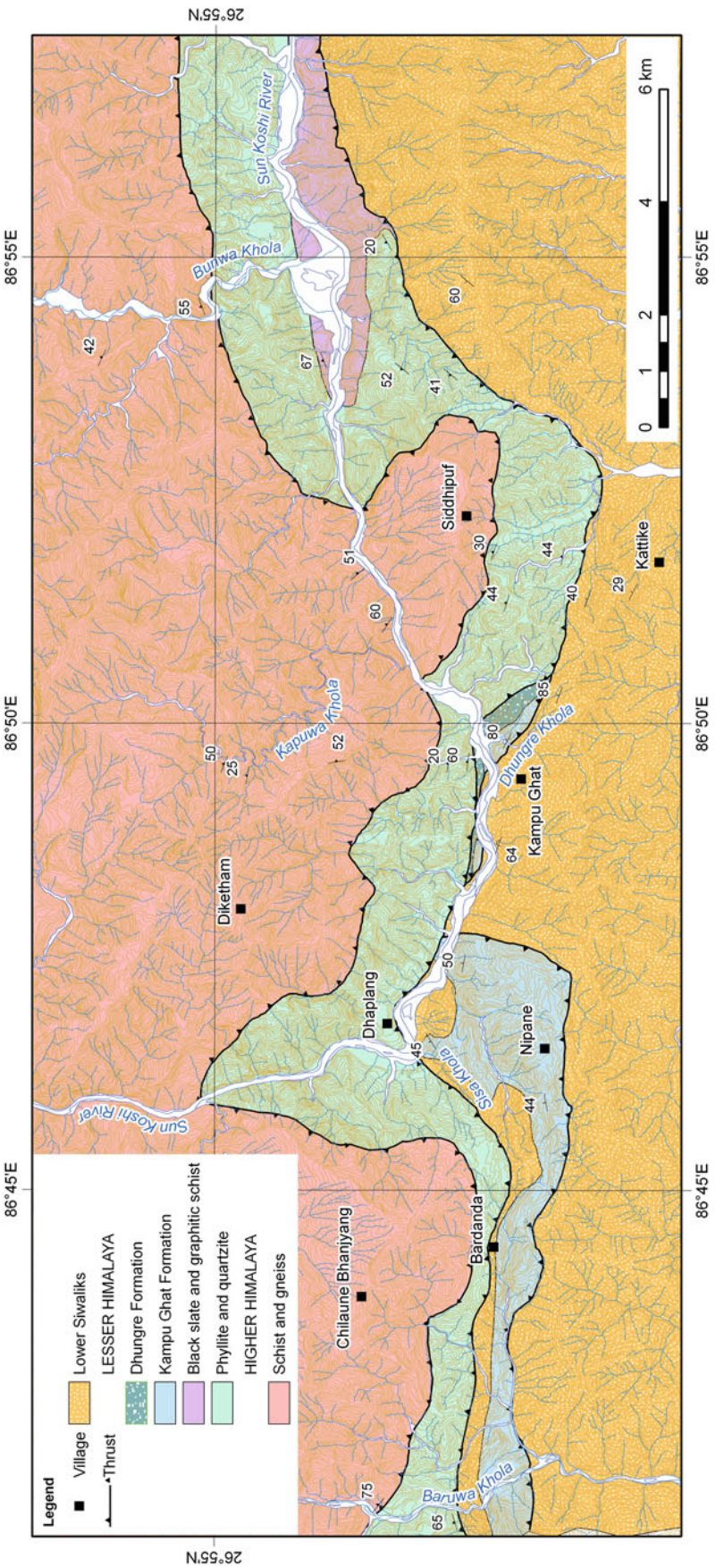

Fig. 11.15 Geological map of the Kampu Ghat area showing the distribution of Gondwanas. *Source* Based on field survey in 1994 and 1997 by MR Dhital, and data of Chaudhary (1997)

References

Adhikari N (2013a) Lithology and stratigraphy of the Pre-Siwalik rocks around Katari–Patana Bhanjyang area, Udayapur district, eastern Nepal. Unpublished M.Sc. Thesis, submitted to the Central Department of Geology, Tribhuvan University, Kirtipur, Kathmandu, Nepal, 72 pp

Adhikari S (2013b) Geology of Katari–Patana Bhanjyang area, eastern Nepal, with special reference to petrography of Pre-Siwalik rocks. Unpublished M.Sc. Thesis, submitted to the Central Department of Geology, Tribhuvan University, Kirtipur, Kathmandu, Nepal, 76 pp

Amatya KM, Jnawali BM (1994) Geological map of Nepal, Scale: 1:1,000,000. Department of Mines and Geology, International Centre for Integrated Mountain Development, Carl Duisberg Gesellschaft e. V., and United Nations Environment Programme

Bijukchhen SM (2011) Landslide susceptibility mapping of the Ghurmi–Dhad Khola area in eastern Nepal. Unpublished M.Sc. Thesis, submitted to the Central Department of Geology, Tribhuvan University, Kirtipur, Kathmandu, Nepal, 84 pp

Chaudhary BNR (1997) Geology of the Kampughat–Chisapani area, Udayapur and Khotang Districts, Eastern Nepal Himalaya. Unpublished M.Sc. Thesis, submitted to the Central Department of Geology, Tribhuvan University, Kirtipur, Kathmandu, Nepal, 41 pp

Dahal RK, Adhikary PC (2001) Geology of the Kharidhunga–Thokarpa area, Central Nepal, Lesser Himalaya. J Nepal Geol Soc 23:19–26

Dangol V (1992) Results of preliminary geochemical studies in the Kharidhunga Magnesite Deposit, Dolakha District, Nepal. Bulletin of the Department of Geology, Tribhuvan University, Kathmandu, Nepal, vol 2, no 1. Proceedings of the symposium: Geodynamics of the Nepal Himalaya, pp 141–148

Dhital MR (2006) Impact of July 2004 high-intensity rain on Hilepani–Jayaramghat–Diktel environment friendly road in East Nepal. J Nepal Geol Soc 34:81–94

ESCAP (Economic and Social Commission for Asia and the Pacific) (1993) Geology and mineral resources of Nepal, atlas of mineral resources of the ESCAP region, vol 9. United Nations, New York, 107 pp (with a geological map in colors, scale: 1:1,000,000)

Galileo G (1632) Dialogue concerning the two chief world systems. Translated by Stillman Drake, Berkeley: University of California Press, 1967

Gyawali BR (2011) Geology of Ghurmi–Dhad Khola area in east Nepal with reference to strain analysis of MCT zone. Unpublished M.Sc. Thesis, submitted to the Central Department of Geology, Tribhuvan University, Kirtipur, Kathmandu, Nepal, 64 pp

Hagen T (1959) Über den Geologischen Bau des Nepal-Himalaya mit besonderer Berücksichtigung der Siwalik-Zone und der Talbildung. Jahrbuch der St. Gallischen Naturwissenchaftlichen Gesellschaft 76:3–48. (with 10 figures and 9 plates)

Ishida T (1969) Petrography and structure of the area between the Dudh Kosi and the Tamba Kosi, East Nepal. J Geol Soc Jpn 75:115–125

Ishida T, Ohta Y (1973) Ramechhap-okhaldhunga region. In: Hashimoto S, Ohta Y, Akiba C (eds) Geology of the Nepal Himalayas. Himalayan Committee of Hokkaido University, Japan, pp 25–68

Kano T (1984) Occurrence of augen gneisses in the Nepal Himalayas. J Nepal Geol Soc 4(Special Issue):121–139

Lombard A (1952) Les grandes lignes de la géologie du Népal Oriental. Bulletin de la Société Belge de Géologie de Paléontologie et d'Hydrologie, Bruxelles LXI(Fascicule 3):260–264

Lombard A (1958) Un itinéraire géologique dans l'Est du Népal (Massif du Mont Everest). Mémoires Société Helvétique Sciences Naturelles 82:1–107

Schelling D (1992) The tectonostratigraphy and structure of the eastern Nepal Himalaya. Tectonics 11(5):925–943

Shrestha SB, Shrestha JN (1984) Geological map of Eastern Nepal. Scale: 1:250,000. Department of Mines and Geology, Kathmandu

Shrestha SB, Shrestha JN, Sharma SR (1986) Geological map of central Nepal. Scale: 1:250,000. Department of Mines and Geology, Kathmandu

Stöcklin J, Bhattarai KD (1977) Geology of Kathmandu area and central Mahabharat Range, Nepal Himalaya. HMG/UNDP mineral exploration project, Technical report, 86 pp (with 15 maps), unpublished

Stöcklin J (1980) Geology of Nepal and its regional frame, London. J Geol Soc 137:1–34

West WD (1950) General report of the Geological Survey of India for the year 1949. Rec Geol Surv India 83(Part 1):1–397

Lesser Himalaya of Arun–Tamar Region

12

Immediately above Chingtam, the Tambur is joined by a large affluent from the west, the Mywa, which is crossed by an excellent iron bridge, formed of loops hanging from two parallel chains; along which is laid a plank of sal timber.

—Joseph Dalton Hooker (1854, p. 137)

The transverse domal culminations of Arun and Tamar (Tamur or Tamor) have been transformed into impressive tectonic windows, enclosing the low-grade metamorphic rocks of the Lesser Himalaya within their eroded cores (Fig. 12.1). In this region, the Lesser Himalayan rocks of the outer zone continuously extend from the Sapt Koshi River to the Mechi River, and farther east along the foothills of Darjeeling. Although the Lesser Himalayan sequence bears many similarities with the succession composing the Koshi region, some differences in lithology and structure are evident from the geology of a few areas summarized below.

12.1 Arun Window

Bordet and Latreille (1955) mapped the Arun window, whereas Hagen (1969) gave a fairly detailed account of the Arun transverse antiform (Fig. 12.1). Akiba et al. (1973) included this area under their Tumlingtar autochthonous window. Bordet (1961) classified the metamorphic rocks of the Arun Valley and its neighborhood into the Lower Himalayan and Higher Himalayan successions. The Higher Himalayan rocks, constituting the *dalle du Tibet* (Tibetan slab) overlie the Lesser Himalayan *séries de couverture* (thrust sheet) along the Main Central Thrust. His Lesser Himalayan sequence comprises the following lithological units (Bordet 1961, pp. 250–251).

The Migmatites or migmatitic gneisses occur at the base and have a variable thickness, often reaching several thousand meters. They are either banded or augen-shaped and contain large feldspar, biotite, and muscovite grains with red garnet and blue or green kyanite. These rocks also include some amphibolite bands, and are intersected by many pegmatite and aplite veins.

The Migmatites give way to the Mica Schists with garnet, tourmaline, and infrequently appearing staurolite and kyanite. They also enclose sporadic graphitic layers. The thickness of the Mica Schists varies from hundreds of meters to a few meters.

The Mica Schists are followed by the Lower Quartzites, containing biotite, garnet, and kyanite. There are frequent alternations of white bands with thicker bands colored gray or red-brown. Within these quartzites are also found graphitic black slates and blue impure graphitic marbles. This unit is from tens of meters to 500 m thick.

The Lower Phyllites rest over the Lower Quartzites. These blue-gray phyllites contain numerous grains of idiomorphic red garnet and sericite, as well as quartz. Near the top, there is a horizon of black graphitic slate. This succession is 300–400 m thick.

The overlying Upper Quartzites are composed of white or green varieties, which frequently include some chlorite, and their thickness varies from 10 to 100 m.

The Calc-Schists appear on top of the Upper Quartzites, and are represented by yellow or red phyllites rich in yellowish gray carbonate bands, and bright green or pale amphibolites. This unit is about 150 m thick.

The Calc-Schists gradually pass upwards to the Upper Phyllites, which are generally pale yellow colored, sometimes sandy, and with irregular joints. They are about 300 m thick and succeeded by 100–200 m thick, lustrous, gray phyllites with quartz veins.

The above *séries de couverture* measures from 1,000 to 2,000 m in thickness. It is very incompetent and strongly deformed.

12.2 Sabha Khola Area

Andrews (1985) examined a portion of the Arun window during her survey of gemstone deposits. She identified the Lesser Himalayan and Higher Himalayan successions in the Sabha Khola area (Fig. 12.2) and mapped in detail various lithological units (Table 12.1). Here, a minor modification is

M.R. Dhital, *Geology of the Nepal Himalaya*, Regional Geology Reviews,
DOI 10.1007/978-3-319-02496-7_12

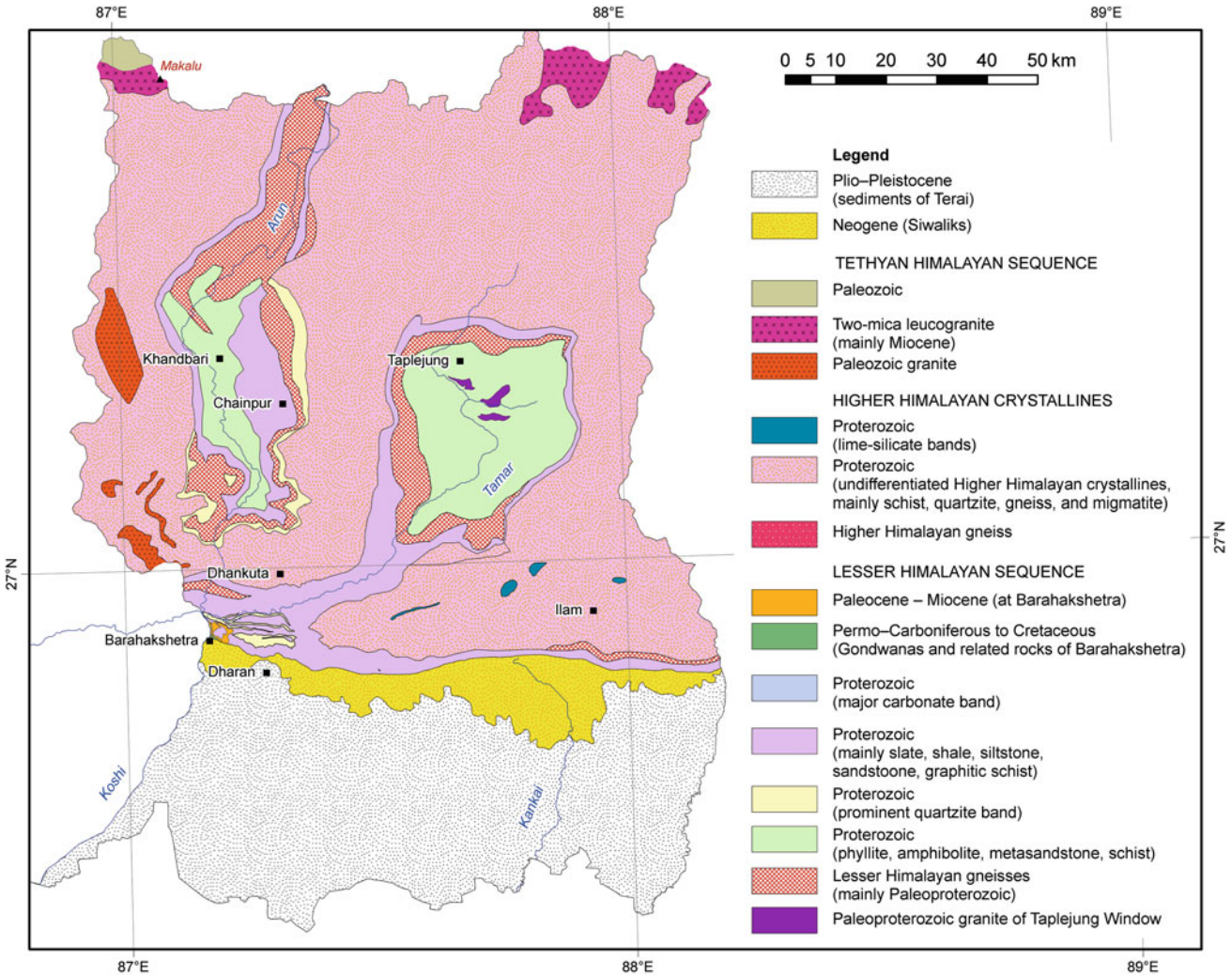

Fig. 12.1 Simplified geological map of the Arun–Tamar region. *Source* Based on Shrestha and Shrestha (1984), ESCAP (1993), Amatya and Jnawali (1994), other published maps, and author's observations

made in her tectonostratigraphic subdivisions, and the Tumlingtar Group is introduced from Akiba et al. (1973) instead of her Nawakot Complex.

The Tumlingtar Group begins with the green-gray Hinuwan Phyllite, consisting predominantly of fine sericite and chlorite with abundant quartz grains (less than 1 mm in diameter). Minor bands of quartzite and graphitic phyllite also occur sporadically. The phyllites also contain a minor amount of biotite and feldspar with some accessory minerals, including tourmaline, apatite, sphene, and epidote. The alternating medium-grained, white quartzites with mica partings are just a few meters thick. Frequently, the quartzites show a well-developed lineation parallel to the dip direction of foliation.

The Lower Hokse Quartzite is rich in mica and chlorite, it is strongly lineated, and predominantly exhibits a green color. There are also a few green-gray phyllites, similar to the Hinuwan Phyllite. These phyllite bands and partings range in thickness from a few millimeters to a meter. Small-scale folds are also well developed in the quartzite. The lineation is generally parallel to the dip of beds. The fine- to medium-grained quartzite infrequently contains quartz veins.

The Khekuwa Phyllite is almost identical to the Hinuwan Phyllite and can be traced continuously along the entire map area. The above three formations (i.e., the Hinwan Phyllite, Lower Hokse Quartzite, and Khekuwa Phyllite) belong to Unit A of Meier and Hiltner (1993). This unit also contains subordinate bands of thin basic sills. Way-up criteria testify to an upwards younging direction for the sediments.

The Upper Hokse Quartzite closely resembles the Lower Hokse Quartzite in composition and texture. It displays a slightly paler color, ranging from pale green to yellow-white. Thin bands and partings of green phyllite are frequent in the quartzite. A prominent lineation is parallel to the dip of foliation.

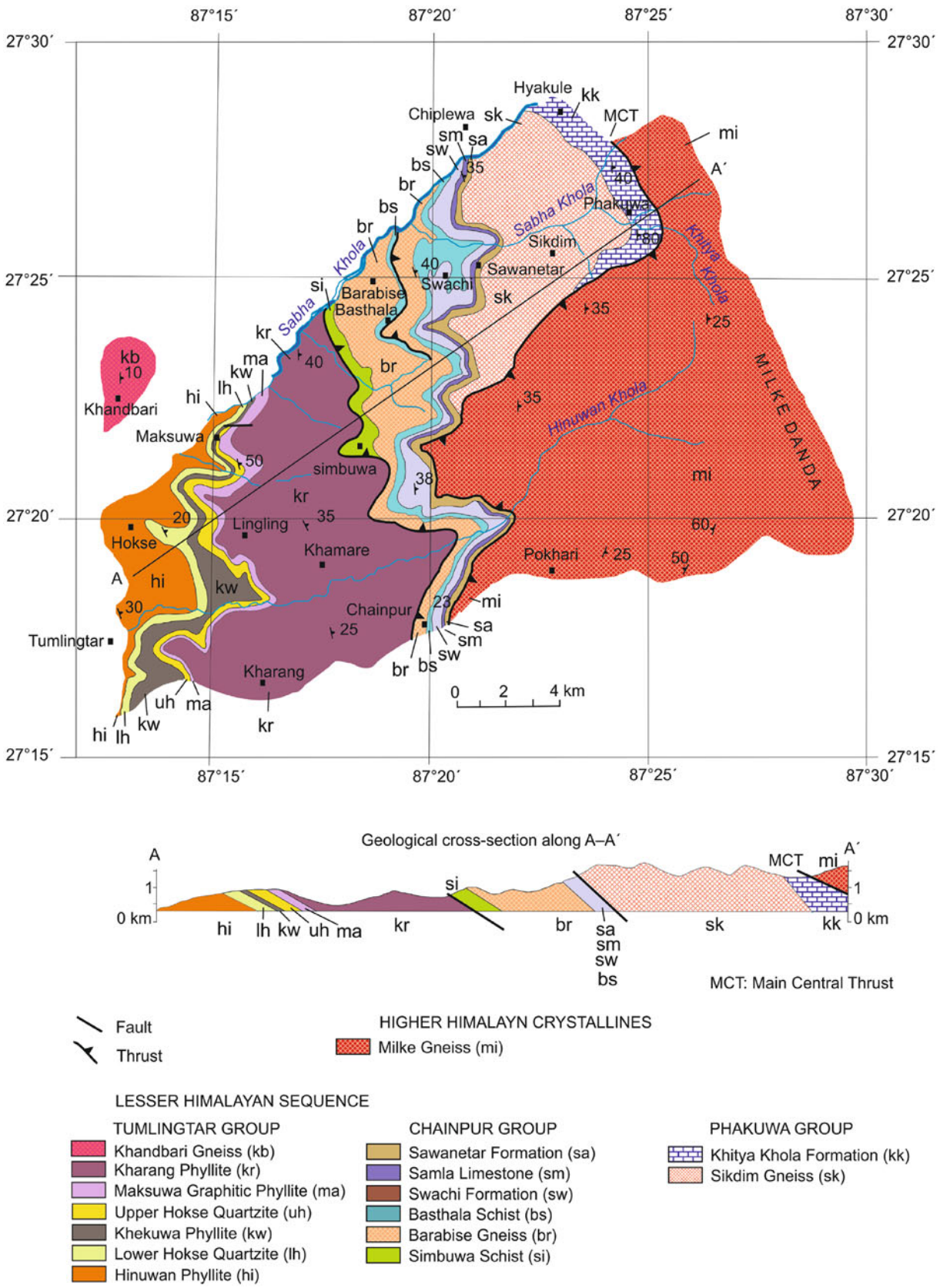

Fig. 12.2 Geological map of the Sabha Khola area, east Nepal. *Source* Modified from Andrews (1985). © Nepal Geological Society. Used by permission

Table 12.1 Tectonostratigraphic subdivisions of the rocks in the Sabha Khola area

Name of unit	Main lithology	Thickness (m)	Synonymy (Bordet 1961)
Higher Himalayan Crystallines			
Milke Gneiss	Biotite gneiss	3,500+	Barun Gneiss
Main Central Thrust			
Lesser Himalayan Sequence			
Phakuwa Group			
Khitya Khola Formation	Marble, quartzite, schist	900	
Sikdim Gneiss	Biotite gneiss	2,500	Migmatites
Thrust			
Chainpur Group			
Sawanetar Formation	Quartzite, schist	100	Mica Schists and Upper Quartzites
Samla Limestone	Marble, calcareous schist	50	
Swachi Formation	Mica schist, quartzite, phyllite	150	Lower Phyllites and Lower Quartzites
Basthala Schist	Mica schists	100	Mica Schists
Barabise Gneiss	Biotite gneiss	1,500	Migmatites
Simbuwa Schist	Mica schist	250	Mica Schists
Khandbari Gneiss			Migmatites
Thrust			
Tumlingtar Group			
Kharang Phyllite	Phyllite, amphibolite, carbonate	3,000	Calc-Schists, Upper Phyllites, and Lower Phyllites
Maksuwa Graphitic Phyllite	Graphitic phyllite	240	Calc-Schists and Upper Phyllites
Upper Hokse Quartzite	Argillaceous quartzite	270	Upper Quartzites
Khekuwa Phyllite	Green phyllite	150	Upper Quartzites
Lower Hokse Quartzite	Argillaceous quartzite	290	Upper Quartzites
Hinwan Phyllite	Green phyllite	800	Lower Phyllites

Source Modified from Andrews (1985)

The Maksuwa Graphitic Phyllite contains a number of bands rich in graphite, which are commonly alternating with gray chlorite–sericite phyllites. The gray phyllite also contains small (less than 1 mm) garnets. Under the microscope, the graphitic phyllites exhibit a fine-grained matrix of quartz (50 %), graphite (40 %), phlogopite (8 %), and carbonates (2 %).

The Kharang Phyllite is composed of green-gray and silver phyllites with a few lenses of amphibolite and carbonate rocks. The phyllite is similar to the Hinuwan Phyllite, but commonly contains garnets ranging from less than 1 to 3 mm in diameter. The green-gray phyllite frequently grades in and out of the silver phyllite, both being equally dominant. Amphibolites constitute discontinuous lenses of a few meters to a few tens of meters in extent, and generally less than a couple of meters in thickness. They are fine- to medium-grained, dark gray or dark green, and weather into blocks and slabs. This formation also contains some discontinuous carbonate bands, which are a few meters thick and several hundred meters to a kilometer or more in extent. They are typically fine-grained, crystalline, sugary gray and white, laminated rock, with intercalations of coarsely crystalline white marble. The last three units (i.e., the Upper Hokse Quartzite, Maksuwa Graphitic Phyllite, and Kharang Phyllite) belong to Unit B of Meier and Hiltner (1993). These rocks record stronger deformation than those of Unit A and also contain many quartz lenses whose frequency increases structurally upwards.

The Khandbari Gneiss appears to be thrust over the Tumlingtar Group, but it is not included in the map area. It forms a thin wedge beginning at Khandbari, and then it widens to the north. It is primarily an augen gneiss, and shows a strong lineation and foliation, with angular or lenticular augen of K-feldspar averaging 2 cm in diameter. The rock is intersected by quartz and pegmatite veins.

The Chainpur Group commences with the Simbuwa Schist, which is thrust over the Tumlingtar Group. It is a garnet–biotite–muscovite schist with abundant quartz in veins and lenses. It is a fine- to medium-grained rock with a wavy foliation.

The Barabise Gneiss is primarily a banded variety of pelitic biotite gneiss with sporadic mica schist lenses. The main almandine garnet deposits of the area are confined to

the chlorite schist lenses, present in the upper part of this formation. The gneiss is made up of lighter bands containing mainly quartz and feldspar, and darker ones formed by biotite with sporadic muscovite and pyroxene. Some garnets and irregular K-feldspar porphyroblasts are also found within the gneiss. Towards the upper part, the rock often takes the character of a granitic gneiss.

The Basthala Schist consists of a variety of mica schists, ranging from a muscovite schist to a chlorite–biotite–muscovite–phlogopite schist. The schists are quartz-rich, and sometimes contain garnets. A few amphibolite lenses are also found within the Basthala Schist.

The Swachi Formation is represented mainly by micaceous quartzites, schists, and phyllites. The quartzites are generally pale yellow to white, but some of them are also of dark gray color. The schists contain muscovite, biotite, and phlogopite. Some dark gray to black phyllites are present in the northern part of the map area. The gray-green muscovite–sericite–chlorite schists and phyllites may or may not contain garnets.

The Samla Limestone forms a thin but persistent band of coarse-crystalline calcite marble. There are infrequent alternations of laminated and fine-grained magnesian limestone. To the north, near the village of Chiplewa, this formation contains thinly bedded, gray dolomites and black schists.

The Sawanetar Formation is made up of alternating schists and quartzites, having a gradational contact with the underlying Samla Limestone. However, they are separated from the overlying Phakuwa Group by a thrust fault. In the lower part of the Sawanetar Formation, occur white quartzites with paper-thin muscovite partings. The quartzites commonly alternate with muscovite–biotite schists and graphitic schists. Meier and Hiltner (1993) reported frequently occurring staurolite and kyanite from their Unit C, which corresponds to the Chainpur Group of Andrews (1985), but does not include the gneisses.

The Phakuwa Group commences with the Sikdim Gneiss, which is very similar to the Barabise Gneiss. The Sikdim Gneiss contains about 5 mm thick gray bands rich in biotite and other dark minerals, and light bands containing quartz and feldspar. It also contains tiny garnets.

The Sikdim Gneiss is succeeded by the Khitya Khola Formation, containing gem-bearing pegmatites rich in tourmaline (elbaite), beryl, and grossular. This formation includes schists, quartzites, and marbles. The quartzites are dense and recrystallized, foliated, and schistose. The alternating schist bands are composed of muscovite and biotite with abundant quartz and some garnets. Black graphitic schists and kyanite schists are also present. The marbles are represented by dolomite as well as calcite. The dolomite tends to be dark and fine-grained with a sugary texture. There are also a few thin (5 cm) layers of foliated tremolite marble. The calcite marble is light colored and coarse-crystalline. Contact metamorphism is noticed near pegmatite intrusions, and it results in a variety of hornblende schists, actinolite–tremolite schists, kyanite gneisses, diopside, and pure hedenbergite.

The Higher Himalayan crystallines are represented by the Milke Gneiss. It is an evenly banded, medium-grained gneiss that contains light strips made up of quartz and feldspar, and dark strips containing biotite. In the rock, euhedral and poikilitic garnets are abundant; kyanite and sillimanite also infrequently occur. In the Milke Gneiss, sporadic hornblende gneiss and quartzite bands are also encountered. Small bodies of tourmaline granite and pegmatites are frequently intruded into the Milke Gneiss. Meier and Hiltner (1993) also include the Khandbari Gneiss, Barabise Gneiss, Sikdim Gneiss, and Khitya Khola Formation under the Higher Himalayan crystallines. Their Main Central Thrust lies under the Khandbari or Barabise Gneiss of Andrews (1985). The very large orthogneiss bodies of this area, including the Sikdim Gneiss, contain granite protoliths of early Paleozoic age (Kai 1981) and hence are similar to the granites of the Kathmandu Complex (Chap. 17).

12.3 Taplejung Window

The Tamar River's prolonged and powerful erosive action developed the oval Taplejung window (Figs. 12.1 and 12.3). Within the window are confined the Proterozoic low-grade metamorphic rocks of the Taplejung Group (Schelling and Arita 1991). Green-gray phyllites, chlorite schists, some *gritty* phyllites, and gray metasandstones compose the lower Lesser Himalayan sequence of the window. These rocks are similar to the Kuncha Formation (Chaps. 9 and 10). Ghimire (2001) noticed a steady increase in the proportion of quartzites at the expense of phyllites, while moving from the lower to middle stratigraphic levels. As a result, in the Henwa Khola and its vicinity, the proportion of phyllite and quartzite is almost equal. This stratigraphic section contains 10–25 m thick, quite persistent, pale yellow to white quartzite bands, intercalated in gray-green crenulated phyllites or chlorite schists. The last quartzite and phyllite succession is succeeded upwards by another pelitic rock sequence of biotite–chlorite schists (Fig. 12.3). The biotite–chlorite schists of the Taplejung Group are sharply overlain by mylonitic augen gneisses, very similar to those found in the Arun window. The gneisses contain quartz, feldspar, biotite, and muscovite, and in them a C/S fabric is well developed. They could be homotaxial with the Ulleri gneisses of west Nepal (Chap. 6).

In the south, thin bands of garnetiferous schist and hornblende–actinolite schist appear at the upper contact with the augen gneisses, whereas in the north, the augen gneisses and overlying garnetiferous schists become very thick, but the phyllite and quartzite unit as well as the succeeding

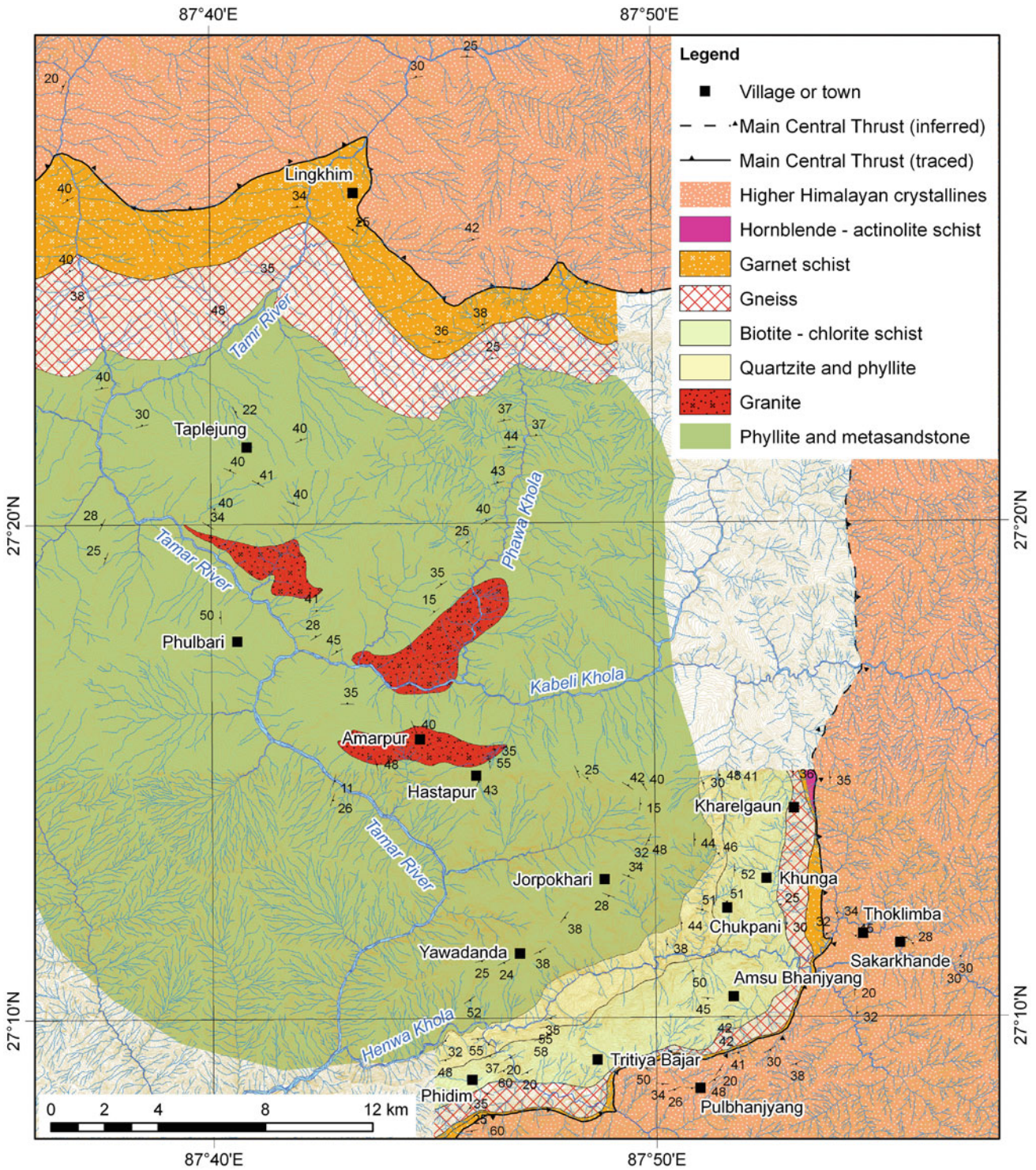

Fig. 12.3 Geological map of the Taplejung tectonic window. *Source* Compiled from Ghimire (2001) and Upreti et al. (2003)

pelitic sequence become imperceptible (Fig. 12.3). The Higher Himalayan crystallines of the area sharply override the Lesser Himalayan succession, and are comprised of banded gneisses, quartzites, quartzose gneisses, and schists with kyanite and sillimanite.

Auden (1935) identified sheared granites and granitic gneisses in the core of the Taplejung window. Upreti et al. (2003) mapped three large granite bodies (Fig. 12.3) and many other smaller intrusives. The three granite bodies have a strongly deformed and mylonitized outer zone and an

undeformed core. Their peripheral part also contains some xenoliths and sporadic hornfelses. The rocks of the outer zone are converted into orthogneisses and display a porphyritic texture, whereas those constituting the core generally show a granular texture. The smaller bodies are invariably converted to orthogneisses. The granites consist of quartz, microcline, plagioclase, biotite, muscovite, and tourmaline. The ^{40}Ar–^{39}Ar muscovite plateau age of the Kabeli Khola granite is older than 1.6 Ga. Hence, these granites as well as the augen gneisses could be of similar age and origin (Upreti et al. 2003).

12.4 Tribeni–Dharan–Dhankuta Area

The sedimentary and low-grade metamorphic rocks of the Tribeni–Dharan–Dhankuta area are categorized under the Leoti Group and the overlying Bhendetar Group. The Chimra Thrust obliquely cuts through these strata and displaces the Phongsawa Group of rocks towards the foothills of the Mahabharat Range, from where they extend farther east, over the Siwaliks (Fig. 12.4). On the other hand, a network of frontal faults exists in the Barahakshetra neighborhood, where the Gondwanas compose a few shreds.

The Leoti Group (Table 12.2) begins with the Raguwa Formation of thinly alternating dark gray to black phyllites, carbonaceous black slates, and green-gray quartzites. There are also a few calcareous phyllite bands. The slates range in thickness from a few centimeters to several meters, and they become predominant towards the upper part.

The succeeding Phalametar Quartzite shows mainly in thick, medium- to coarse-grained, white to light gray, massive bands, which alternate with thin bands of green phyllite or dark gray to black slate. At the basal part of this formation, partings of green phyllite also sporadically occur. Thin bands of green phyllite, thick bands of light gray to white quartzite, and thick bands of laminated, dark gray slate compose its middle portion. This formation ends with very thick, massive, white quartzites.

In the overlying Chiuribas Formation, dark green, gray-green, and red-purple phyllites alternate with similar colored metasandstones and quartzites. There also appear a few amphibolite layers. Bordet (1961, pp. 50–51) described this formation under his Varicolored Phyllites, consisting of blue-gray, yellowish, sometimes variegated, greenish and reddish phyllites at the base, near the contact with the Siwaliks. The rocks form a thinly to thickly banded and monotonous sequence with a few carbonate intercalations. Towards the west, in the vicinity of Tribeni, the Chiuribas Formation contains very thick (several hundred meter) bands of pale yellow to white quartzite, resembling the Phalametar Quartzite or the Sanguri Quartzite. The transitional contact between the Chiuribas Formation and the underlying Phalametar Quartzite is marked by about 20 m thick alternation of green-gray, shiny, laminated phyllite and medium-banded, white quartzite.

The Bhendetar Group commences with the Sanguri Quartzite (Bordet 1961) of white, yellowish, or pink variety. This formation is made up mainly of thick beds of medium- to fine-grained, dense, massive, milky white quartz arenite, pink quartzite, and pale green quartzite, alternating with red-purple and dark green phyllite partings and thin bands. The quartzites have preserved conspicuous ripple marks on their top surfaces, whereas a few coarse- to very coarse-grained quartzites contain sporadic granules and pebbles of white and pink quartz.

The Karkichhap Formation succeeds the Sanguri Quartzite with a sharp contact, and it is confined to the core of a tight syncline (Fig. 12.4). This formation comprises a thinly alternating sequence of dark gray slates and gray quartzites. Strongly deformed and distorted sun cracks regularly occur in the slates, which are also ramified by many quartz veins. Wave and interference ripples are conspicuous on the upper surfaces of the quartzites.

The hanging wall of the Chimra Thrust is made up of dark gray to black slates, belonging to the Mulghat Formation. Its lower part is designated as the Ukhudanda Member, which is discontinuous and disappears in the south slopes of the Mahabharat Range. This member is represented mainly by gray, green-gray to dark gray, thin- to thick-banded, crenulated, mylonitic schists, with numerous quartz veins and a few bands of amphibolite. Feldspar and quartz augen of less than 1 cm in diameter are distributed throughout the rock. They are intensely sheared and their size gradually decreases towards the upper portion, where a few dark green, medium- to coarse-grained, hard, and massive amphibolite bands are found in the north slopes of the Mahabharat Range.

The Mulghat Formation continues upwards with dark gray to black, soft-weathering, laminated, and thinly foliated graphitic slates alternating with thin bands of medium- to fine-grained, gray quartzite or carbonate. The contrast between a fresh black rock and its weathered variety, resembling a gray-green phyllite, is outstanding. Quartz veins occur in profusion and are oriented essentially parallel to foliation. In the Mulghat area, this formation is about 1,500 m thick and its thickness gradually increases towards the east.

The Okhre Formation (Rai 2012) transitionally overlies the Mulghat Formation. It is represented by greenish gray to light gray, thinly foliated, crenulated, and shiny chlorite–garnet–biotite schists and actinolite schists. Quartz boudins are widely distributed concordantly within the schist. Generally, medium- to thick-bedded, fine- to coarse-grained quartzites with gray schist partings form approximately 25 m thick bands. The quartzites of this formation are strongly lineated parallel to the dip of beds and appear gneissic due to the schist partings. Thin to medium bands of dark green

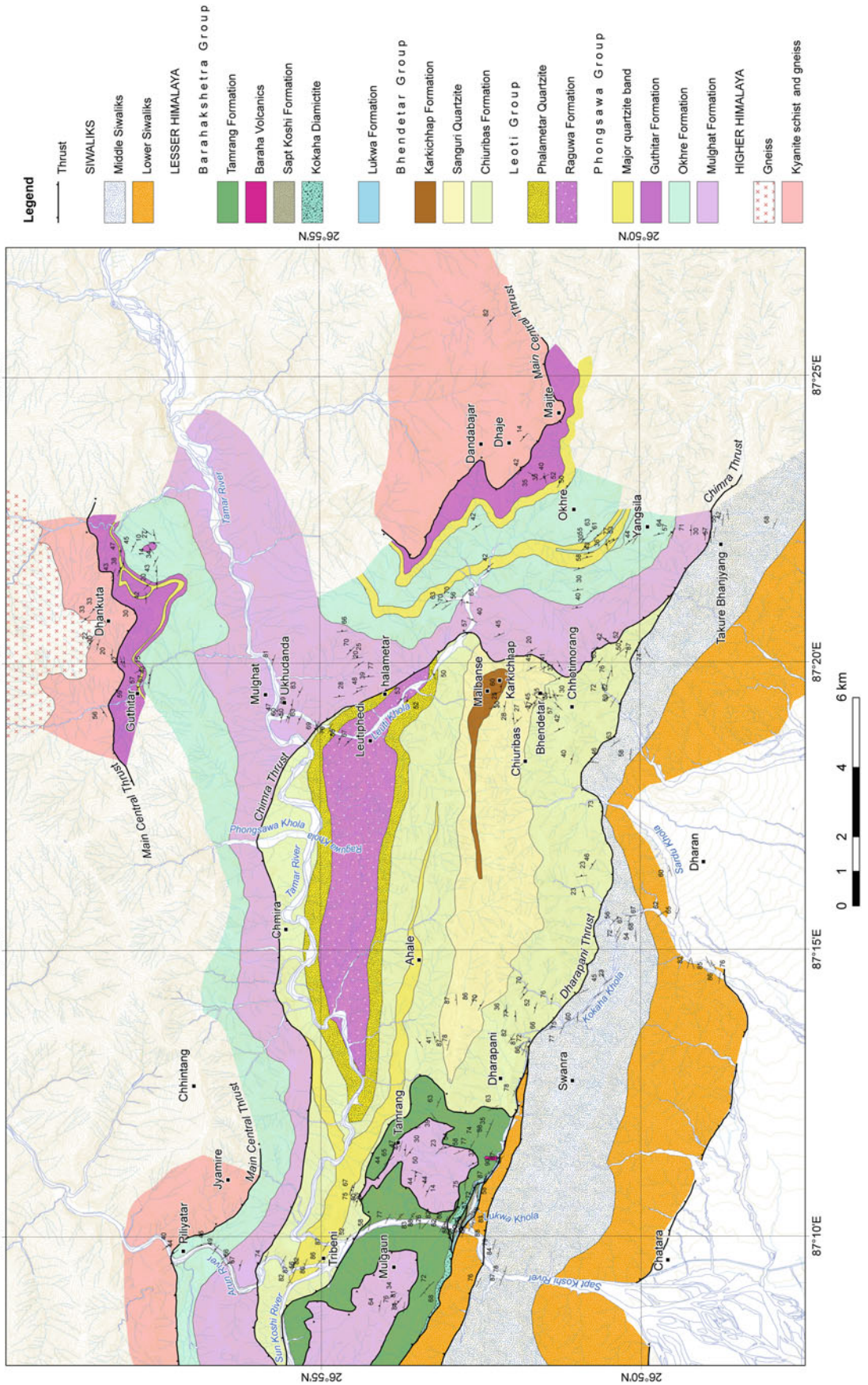

Fig. 12.4 Geological map of Tribeni–Dharan–Dhankuta area. *Source* Based on author's observations and data of Dhital (1992), Sunuwar (1993), Rai (2012), and Timsina (2011)

Table 12.2 Tectonostratigraphic subdivisions of the Tribeni–Dharan–Dhankuta area

Group	Formation	Lithology
Higher Himalayan crystallines		Dark gray, blue-gray, and green-gray kyanite schists, garnetiferous schists, actinolite schists, and quartzites, with banded and augen gneisses
		Main Central Thrust
Phongsawa	Guthitar	Dark gray to black graphitic schists, garnet schists, and fine-grained, white quartzites
	Okhre	Gray-green phyllites, chlorite schists, actinolite schists, or garnet schists with bands of amphibolite and quartzite
	Mulghat	Dark gray, muscovite–biotite schists with numerous stretched quartz veins and augen-shaped lenses
		Ukhudanda Member: Gray, mylonitic schists containing infrequent bands of amphibolite, and numerous sheared quartz veins and lenses
		Chimra Thrust
Bhendetar	Karkichhap	An alternation of gray quartzites with ripples and dark gray or green-gray slates with sun cracks
	Sanguri Quartzite	Medium- to fine-grained, massive, dense, thick-bedded, milky white and pink quartzites with abundant ripple marks and cross-laminae; infrequent intercalations of purple slate and phyllite
Leoti	Chiuribas	Dark green, gray-green, and red-purple phyllites alternating with similar colored metasandstones or quartzites and sporadic amphibolites
	Phalametar Quartzite	Medium- to fine-grained, massive, dense, white, light gray, and cream colored quartzites with phyllite partings and intercalations
	Raguwa	Dark gray and black carbonaceous phyllites and slates with gray quartzite alternations and calcareous phyllite bands

Source Modified from Dhital (1992), Sunuwar (1993), Timsina (2011), and Rai (2012)

amphibolite are distributed throughout the formation. To the south, there are also some thin bands of graphitic schist and garnet schist.

The transitionally succeeding Guthitar Formation (Timsina 2011) is composed essentially of thin-banded graphitic schists, alternating with green-gray garnet schists and medium- to coarse-grained, gray to milky white quartzites. Infrequently gray-green amphibolites also occur with garnet or actinolite schist partings.

The Main Central Thrust rather sharply overrides the graphitic schists of the Guthitar Formation and brings the Higher Himalayan crystallines over the Lesser Himalayan sequence. The Higher Himalayan rocks commence with light to dark gray, thin- to medium-banded, feldspar–garnet–biotite schists and gray to pale yellow, medium- to thick-banded, medium- to coarse-grained quartzites. Banded and augen gneisses are the main constituents of the Higher Himalayan crystallines, where the kyanite-bearing banded gneisses and schists predominate at the base and the augen gneisses prevail towards the upper section.

The rocks, appearing on either side of the Chimra Thrust, allude to their inherent similarity. The Raguwa Formation is comparable with the Mulghat Formation, and the Phalametar Quartzite together with the overlying Chiuribas Formation and the Sanguri Quartzite could be homotaxial with the Okhre Formation. Similarly, the Karkichhap Formation bears some resemblance to the Guthitar Formation. Hence, it is speculated that these rocks belonged to the same stratigraphic unit, which was repeated twice owing to subsequent displacements along the Chimra Thrust.

12.5 Barahakshetra

Just north of Barahakshetra, the Sapt Koshi River makes a narrow and straight gorge (Fig. 12.5), which has been a favored site for constructing a high dam. For this purpose, some geological investigations were carried out in the past (Box 12.1). In the Barahakshetra area, the Proterozoic Lukwa Formation lies at the base of the Gondwanas. It is made up essentially of light to dark gray, cherty dolomites, containing intraclasts and columnar as well as domed stromatolites. The Lukwa Formation is thrust over the Lower Siwaliks and a sharp disconformity separates the dolomites from the overlying Gondwana sequence (Fig. 12.6).

Box 12.1: Attempts at Damming the Sapt Koshi River

According to West (1950, p. 25), Damodaran and Mitra visited Barahakshetra in 1949 to find cement-grade limestone for the Sapt Koshi dam to be constructed there. They took a traverse from Barahakshetra to Kathmandu following the Sun Koshi River via Tribeni. They recorded the Nahans (Lower Siwaliks), Krols (dolomites), Damudas (coal-bearing beds), and quartzites in the vicinity of Barahakshetra. They also observed massive white quartzbites at Tribeni, and black slates and Dalings (phyllites) in the lower reaches of the Sun Koshi River.

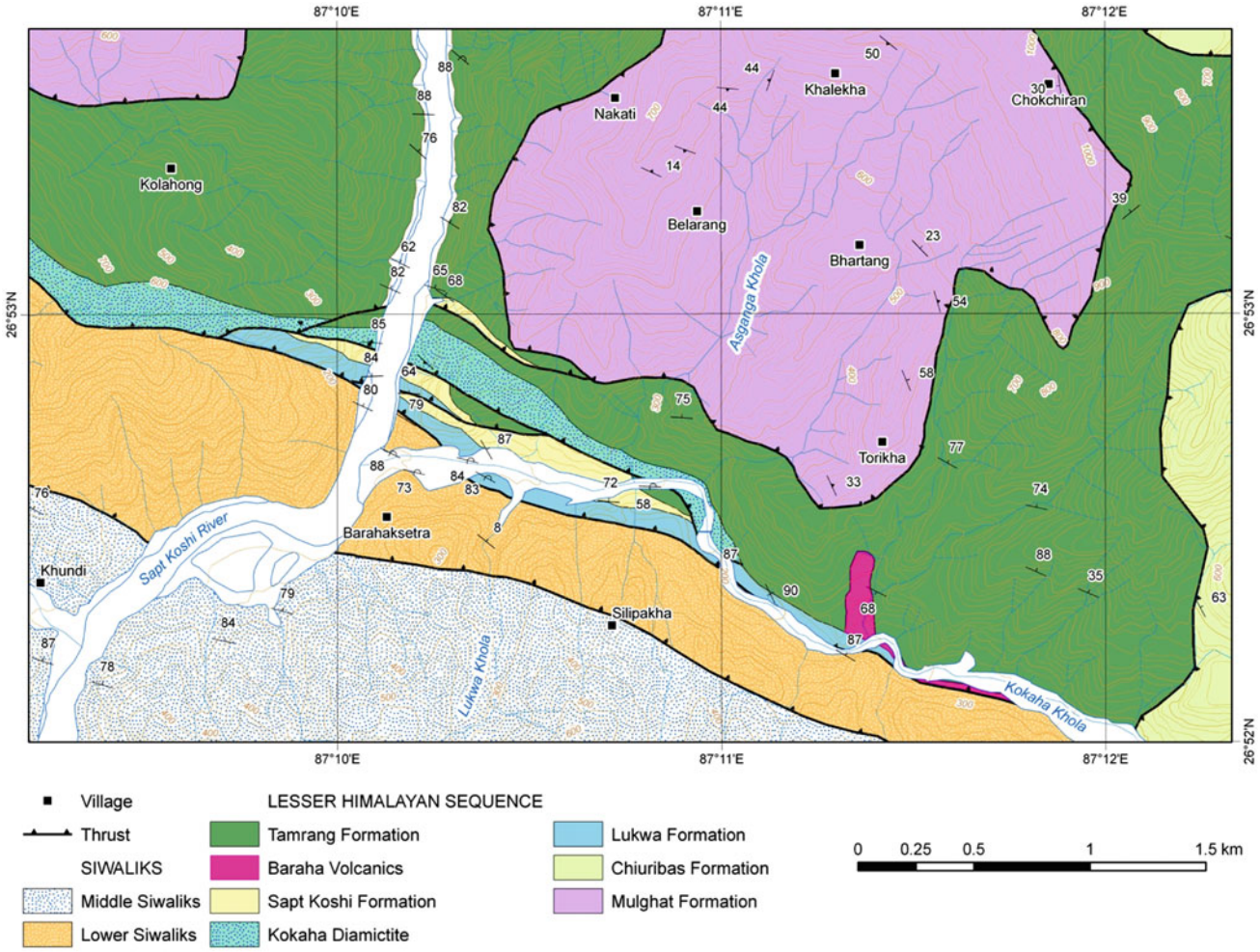

Fig. 12.5 Geological map of Barahakshetra area. *Source* Author's observations

Bashyal (1980a, b) designated the Barahakshetra Formation to the Gondwanas and identified five lithostratigraphic units. The Barahakshetra Group (Dhital 1992) crops out discontinuously due to intense deformation and imbricate faulting, and varies in thickness from tens of meters to several kilometers. It can be subdivided into the following formations.

The Kokaha Diamictite has a faulted lower contact with the underlying strata, and hence its stratigraphic position is rather uncertain. However, this formation is inferred to be resting disconformably over the Proterozoic rocks, based on its contrasting lithofacies and the occurrence of similar rocks elsewhere (Chaps. 8 and 9). The Kokaha Diamictite contains subangular to subrounded clasts of quartzite, dolomite, schist, gneiss, granite, shale, and sandstone. Their maximum size reaches 1 m and they are embedded in a dark gray silty clay matrix.

The Sapt Koshi Formation overlies a sharp disconformity, marked by an irregular erosional surface (Fig. 12.6). This formation comprises medium- to very thick-bedded, gray and dark gray carbonaceous quartzites, dark gray to black carbonaceous shales or conglomerates with some light gray, dark gray, and red chert and quartzite pebbles. Lenses and seams of coal are also characteristic of this formation (Fig. 12.7).

The Baraha Volcanics are represented by interlayered tuffs and agglomerates. They occur below the Tamrang Formation, in the eastern sector of the Barahakshetra area (Fig. 12.5). Brown, tan, dark green to gray tuffs are made up of poorly sorted lithic volcanic clasts of varying sizes. In the clasts are observed phenocrysts and microlites of K-feldspar. Quartz and sodic plagioclase with some biotite and pyroxene are also present (Bashyal 1980b, p. 473).

The tuffs are succeeded upwards by the Tamrang Formation of green-gray to dark gray calcareous sandstones, gray limestones, and dark gray or green-gray shales (Fig. 12.8). The soft calcareous sandstones contain quartz, ankerite, calcite, muscovite, and plagioclase in an argillo–calcareous matrix (Bashyal 1980a). Indeterminate plant remains (Carbonaceous patches and stringers) occur in the

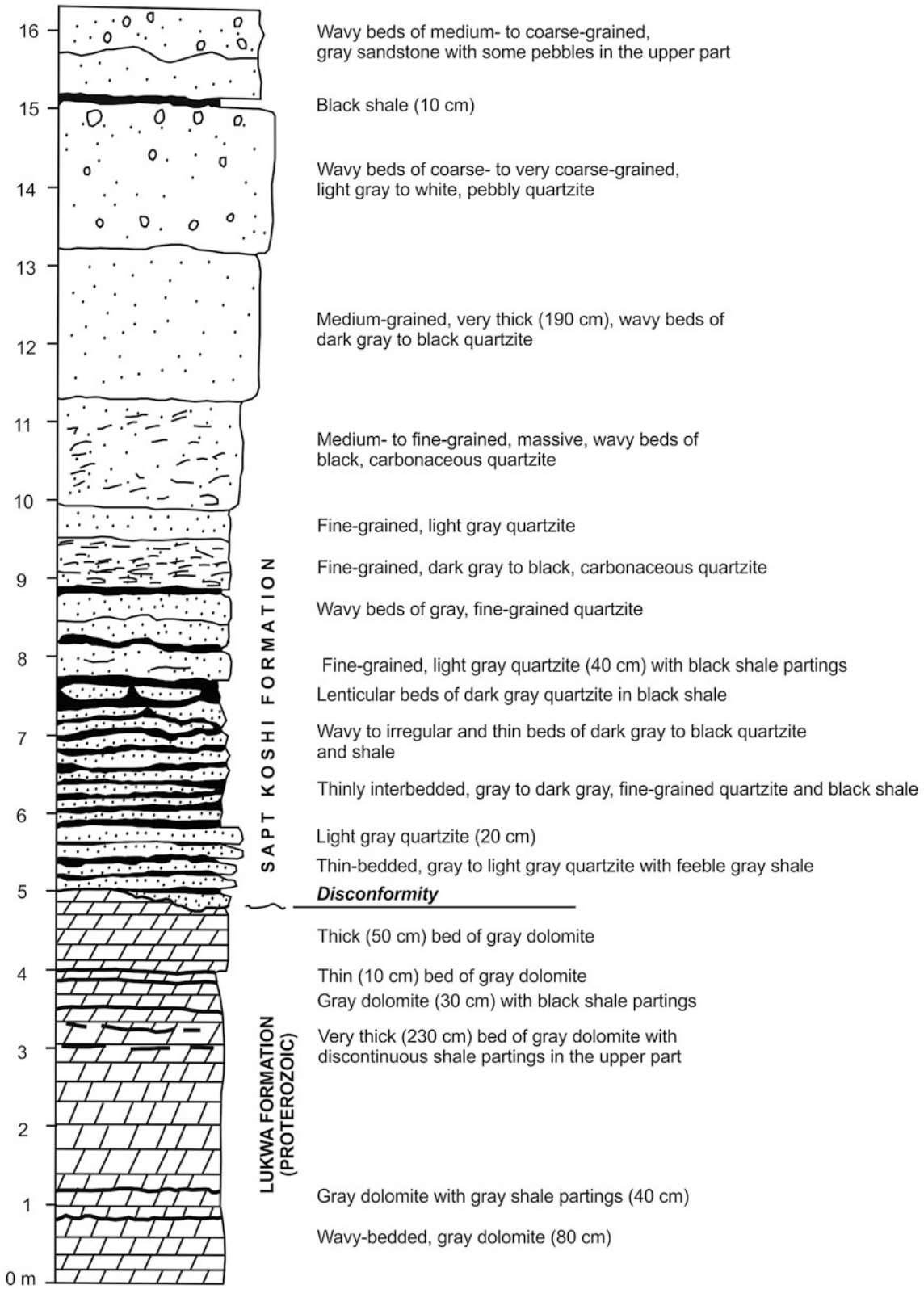

Fig. 12.6 Columnar section depicting a disconformable contact between the Lukwa Formation and the Sapt Koshi Formation (Lower Gondwanas) in the Sapt Koshi River. *Source* Author's observations

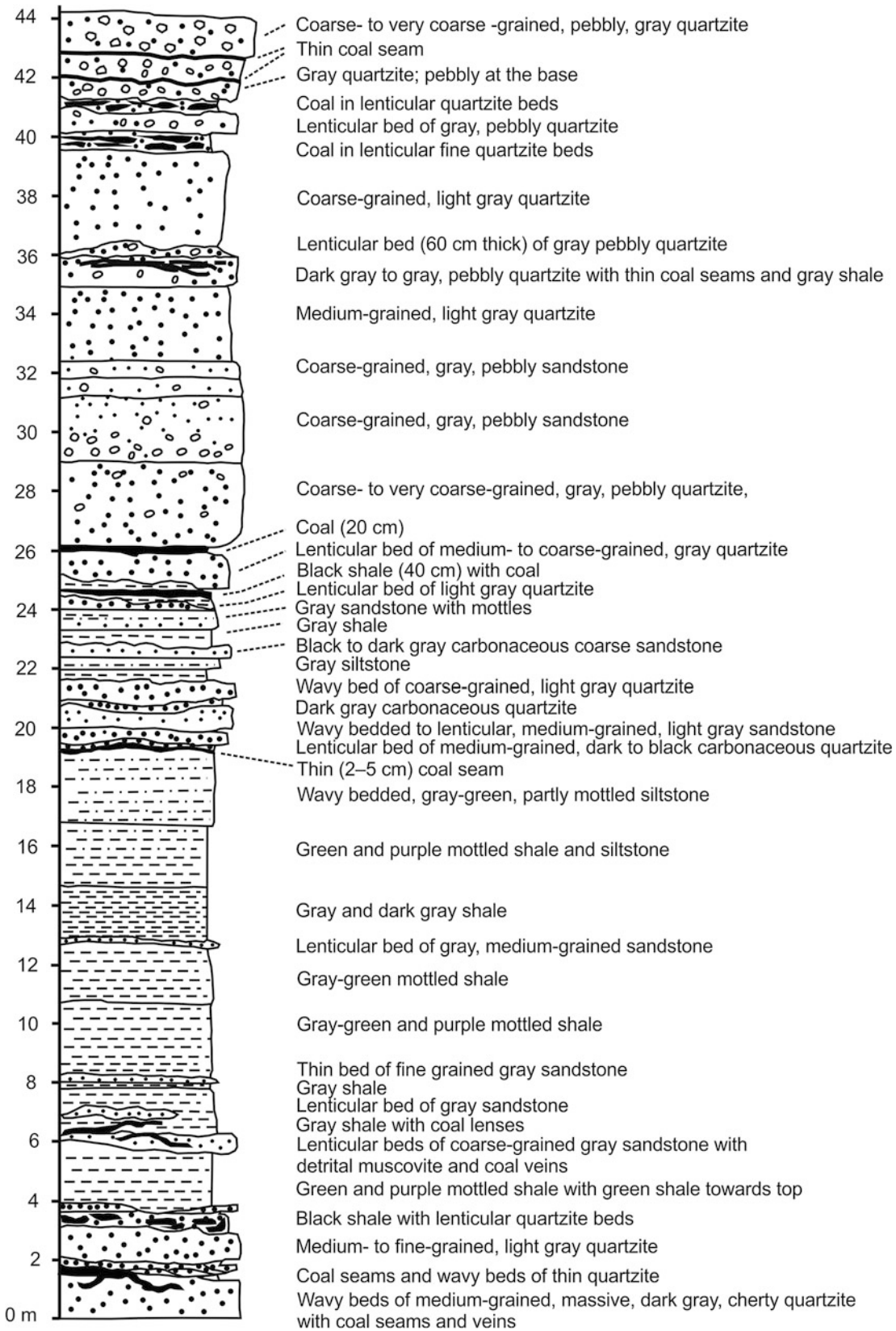

Fig. 12.7 Columnar section representing the middle part of the Sapt Koshi Formation in the Kokaha Khola. *Source* Author's observations

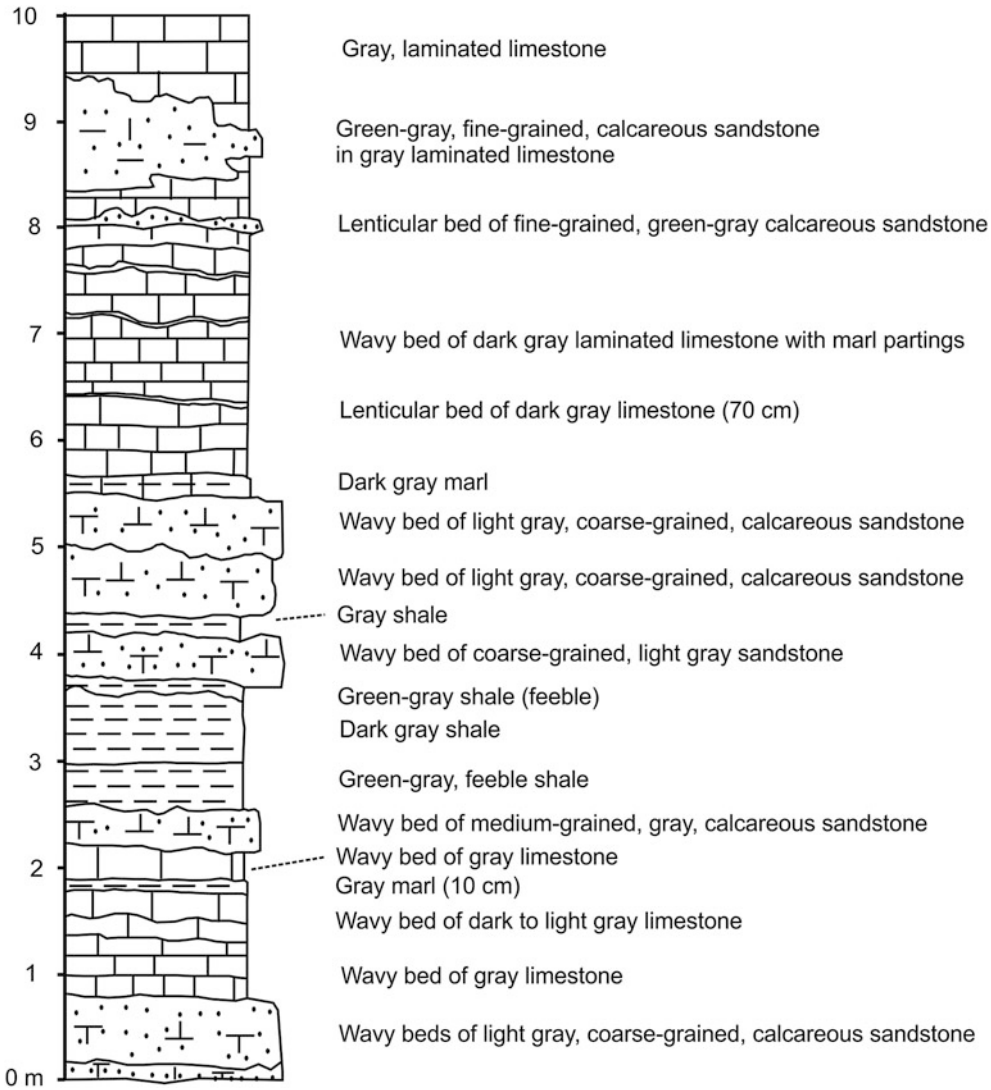

Fig. 12.8 Detailed columnar section from the lower part of the Tamrang Formation in the Kokaha Khola. *Source* Author's observations

middle and upper parts of this formation. In the Barahakshetra area, a greater portion of the Tamrang Formation is covered by two large klippen of black slates, apparently belonging to the Mulghat Formation (Figs. 12.4 and 12.5). To the east of Barahakshetra, the Dharapani Thrust truncates the Tamrang Formation by juxtaposing green-gray phyllites and quartzites of the Chiuribas Formation.

The Kokaha Diamictite is comparable with the boulder-beds in the Rangit window of Sikkim, the Diuri Boulderbed of Bhutan, and the Talchir Formation of the Indian Peninsula (Chap. 5). Presumably, this formation is homotaxial with the Sisne Formation of the Tansen area (Chap. 9). In the Takure Khola, east of Dharan, Bashyal (1980a, 2001) recovered *Schizoneura gondwanensis* Feistmantel from the rocks, similar to those of the Sapt Koshi Formation. The plant fossil belongs to the Damuda flora of Permian age. He also reported some well-preserved radiolarian fossils from the gray-green calcareous sandstone, resembling the Tamrang Formation. The Tamrang Formation is comparable with the upper portion of the Setikhola Formation (Permian) in southeast Bhutan (Chap. 5). However, the Sapt Koshi Formation also closely resembles the Amile and Sattim formations, whereas the middle and upper sections of the Tamrang Formation do not differ much from the Dumri and Dubring formations of west Nepal (Chaps. 8 and 9).

12.6 Mechi Transect

The Proterozoic Lesser Himalayan sequence also crops out along the right bank of the Mechi River, which constitutes the east border of Nepal with India. This section comprises mainly gray-green phyllites, black graphitic schists, and pale yellow to white quartzites (Fig. 12.9).

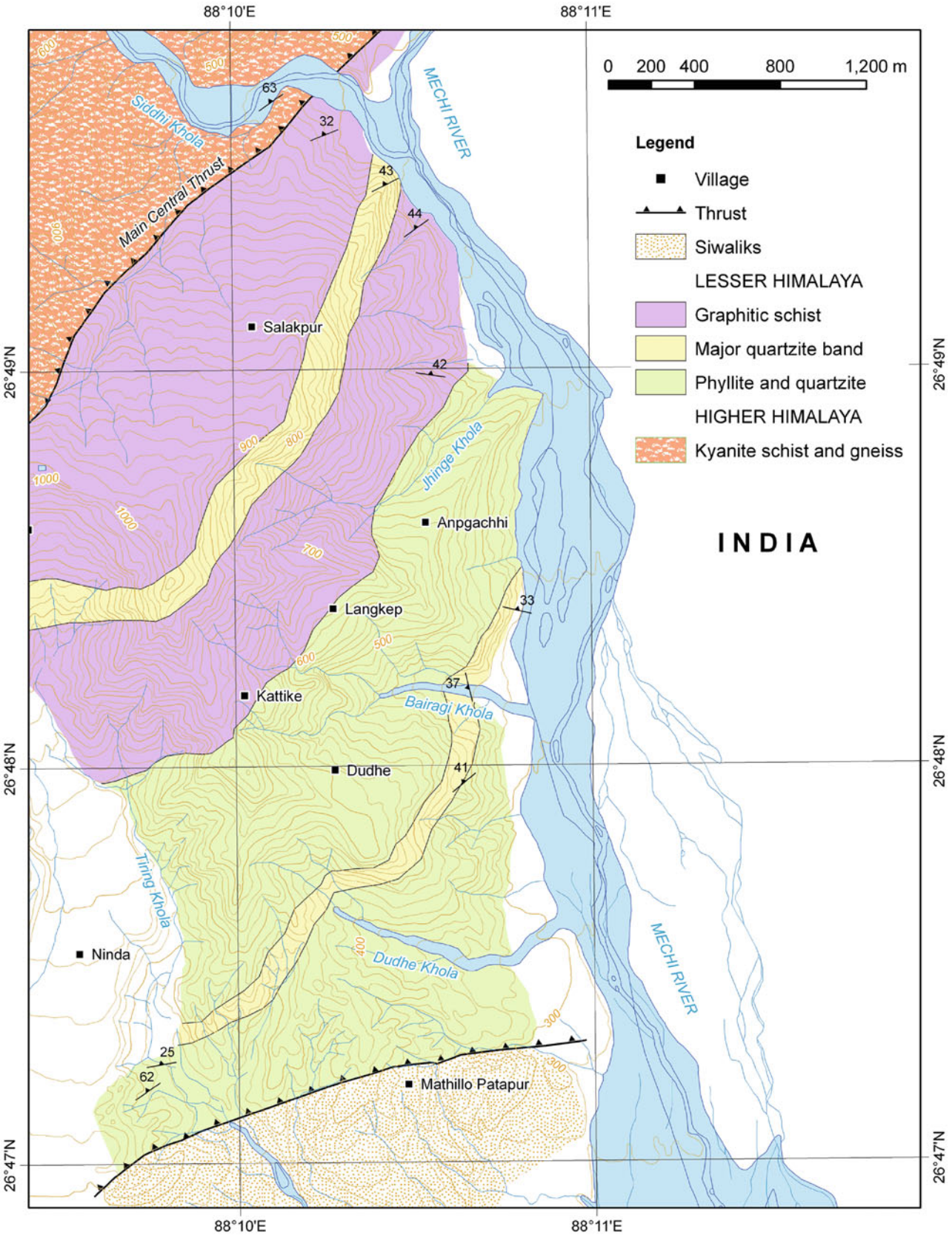

Fig. 12.9 Geological transect of the Mechi River, between the Dudhe Khola and Siddhi Khola. *Source* Author's observations

The section between the Tiring Khola and Dudhe Khola contains thinly alternating bands of gray-green phyllite and pale yellow to white quartz arenite. In this stretch, phyllites strongly predominate over quartzites. The area between the Dudhe Khola and the Jhinge Khola is represented mainly by gray-green phyllites. In the Bairagi Khola, there are two thick (25–50 m) quartzite bands, and between them occur 10–20 m thick green-gray phyllites. This pale yellow to white quartzite-predominating sequence can be traced for a long distance (Fig. 12.9). The quartzites are generally medium-bedded and very fine-grained. They are massive and may or may not include thin (1 mm) phyllite partings. Several mesoscopic folds are observed in the white quartzites.

The metamorphic grade gradually increases stratigraphically upwards, and the area between the Jhinge Khola and the Siddhi Khola contains mainly green-gray to dark gray biotite schists, graphitic schists, and garnetiferous schists. Near the confluence of the Siddhi Khola and the Mechi River, there is an approximately 125 m thick quartzite-dominant sequence, where the quartzites are clustered within 1–15 m thick bands. These gray, gray-green, and white, fine-grained quartz arenites are regularly parallel-laminated, thin-bedded, and alternating with dark gray graphitic schists. The schist bands range in thickness from several centimeters to 25 m and they contain many disrupted quartz veins. From 1–2 m thick amphibolite bands are sporadically found in the dark gray schists. In the Siddhi Khola, the Higher Himalayan crystallines appear above the Lesser Himalayan sequence with a relatively obscure contact, marked by the appearance of feldspathic schists, kyanite schists, and gneisses.

A lithological comparison between the Lesser Himalayan rocks and those of the Tribeni–Dharan–Dhankuta area reveals many similarities with the Mulghat, Okhre, and Guthitar formations. The Higher Himalayan crystallines of this part are the direct continuation of the Darjeeling Gneiss (Chap. 5); the phyllite, schist, quartzite, and graphitic schist bands can also be compared with similar alternations present in the Dalings.

References

Akiba C, Amma S, Ohta Y (1973) Arun river region. In: Hashimoto S, Ohta Y, Akiba C (eds) Geology of the Nepal Himalayas. Himalayan Committee of Hokkaido University, Japan, pp 13–33

Amatya KM, Jnawali BM (1994) Geological map of Nepal, Scale: 1:1,000,000. Department of Mines and Geology, International Centre for Integrated Mountain Development, Carl Duisberg Gesellschaft e. V., and United Nations Environment Programme

Andrews E (1985) Stratigraphy of the Sabhaya Khola region, Sankhuwa Sabha District, Eastern Nepal. J Nepal Geol Soc 2 (2):12–35

Auden JB (1935) Traverses in the Himalaya. Rec Geol Surv India LXIX(Part 2):123–167 (with 6 plates including a geological sketch map)

Bashyal RP (1980a) Gondwana type of formation with phosphatic rocks in S.E. Nepal. J Geol Soc India, Bangalore 21:489–491

Bashyal RP (1980b) Potassic volcanics from the Permo-Carboniferous Nepal Himalayas. Mem Geol Soc India, Bangalore 3:472–474

Bashyal RP (2001) Gondwana formations of Nepal Himalayas and their regional significance. Gondwana Res 4(4):572–573

Bordet P (1961) Recherches Géologiques dans L'Himalaya du Népal, Région du Makalu, Expéditions Françaises a l'Himalaya 1954–1955, Edition du Centre National de la Recherche Scientifique (C. N. R. S.), 275 pp (with a Geological Sketch Map of Everest and Makalu, scale 1:50,00, in colors; and the Geological Sketch Map of Arun and Everest Region, scale 1:250,000, in colors; and 5 large plates showing the panoramic geological view of Himalayan peaks)

Bordet P, Latreille M (1955) La Géologie de L'Himalaya de l'Arun. Bulletin de la Société géologique de France, Paris, vol 5, ser 6, pp 529–542

Dhital MR (1992) Lithostratigraphic comparison of three diamictite successions of Nepal Lesser Himalaya. J Nepal Geol Soc 8:43–54

ESCAP (Economic and Social Commission for Asia and the Pacific) (1993) Geology and mineral resources of Nepal, atlas of mineral resources of the ESCAP region (vol 9, 107 pp). United Nations, New York (with a geological map in colors, scale: 1:1,000,000.)

Ghimire S (2001) Geological mapping in the Taplejung window, Panchthar District, Far Eastern Nepal Himalaya with special emphasis on the metamorphism and tectonics. Unpublished M.Sc. Thesis, submitted to the Central Department of Geology, Tribhuvan University, Kirtipur, Kathmandu, Nepal, 90 pp

Hagen T (1969) Report on the geological survey of Nepal. Volume 1: Preliminary Reconnaissance. Denkschiiften der Schweizerischen Naturforschenden Gesellschaft, Band LXXXVI/1, 185 pp (with a geological map)

Hooker JD (1854) Himalayan Journals; or, notes of a naturalist (in Bengal, the Sikkim and Nepal Himalayas, the Khasia Mountains, & c (vol 1, 408 pp). Grand Colosseum Warehouse Co., Glasgow (with 2 maps)

Kai K (1981) Rb–Sr geochronology of the rocks of the Himalayas, Eastern Nepal. I. The metamorphic age of the Himalayan Gneiss. Memoirs of the Faculty of Science, Kyoto University, Series Geology and Mineralogy, vol XLVII, no 2, pp 135–148

Meier K, Hiltner E (1993) Deformation and metamorphism within the Main Central Thrust zone, Arun Tectonic Window, eastern Nepal. In: Treloar PJ, Searle, MP (eds). Himalayan Tectonics. Geological Society Special Publication No 74, pp 511–523

Rai LK (2012) Geology of Dharan–Mulghat area in east Nepal, with special reference to microstructure and strain analysis. Unpublished M.Sc. Thesis, submitted to the Central Department of Geology, Tribhuvan University, Kirtipur, Kathmandu, Nepal, 61 pp

Schelling D, Arita K (1991) Thrust tectonics, crustal shortening, and the structure of the far-eastern Nepal Himalaya. Tectonics 10 (5):851–862

Shrestha SB, Shrestha JN (1984) Geological map of Eastern Nepal. Scale: 1:250,000. Department of Mines and Geology, Kathmandu

Sunuwar SC (1993) Geology of Tribeni–Barahakshetra area, Sunsari–Dhankuta District, Eastern Nepal. Unpublished M.Sc. Thesis, submitted to the Central Department of Geology, Tribhuvan University, Kirtipur, Kathmandu, Nepal, 94 pp

Timsina C (2011) Seismic hazard assessment of the Dhankuta Municipality, Eastern Nepal. Unpublished M.Sc. Thesis, submitted to the Central Department of Geology, Tribhuvan University, Kirtipur, Kathmandu, Nepal, 89 pp

Upreti BN, Rai SM, Sakai H, Koirala DR, Takigami Y (2003) Early Proterozoic granite of the Taplejung window, far eastern Lesser Nepal Himalaya. J Nepal Geol Soc 28:9–18

West WD (1950) General report of the geological survey of India for the year 1949. Rec Geol Surv India 83(Part 1):1–396 (with a geological map)

Part IV

Higher Himalaya

Introduction to Higher Himalaya

13

We only see what we know.

—Johann Wolfgang von Geothe

As in many other parts of the Himalaya, the Higher (or Greater) Himalayan rocks (Box 13.1) in Nepal comprise a shredded and perforated, but essentially continuous and broadly undulating crystalline thrust sheet. Owing to deep erosion and denudation of this gigantic carapace, its aberrant outliers are also encountered in west Nepal. To the north, the Higher Himalayan crystallines display stark, rugged, and lofty uplands, interrupted by abrupt and craggy U-shaped valleys of mighty glaciers, and abysmal transverse gorges and defiles of roaring rivers. As the thrust sheet approaches the Siwaliks to the south, intense and deep weathering upsets its ruggedness, and relatively wider valleys with smoother spurs and ridges clothed with dense and lush vegetation constitute parts of the Midlands and the Mahabharat Range.

Box 13.1: Basic Features of Higher Himalaya

The Higher Himalaya possesses the following main characteristics.

- The main Himalayan rampart as well as an extensive tract of the Midlands and Mahabharat Range is composed of the Proterozoic Higher Himalayan crystallines forming the hanging wall of the Main Central Thrust.
- Though the Higher Himalayan crystallines are composed primarily of augen and banded gneisses, there are also migmatites, schists, quartzites, and marbles, alternating with or injected by these gneisses and intruded by Paleozoic granites and Tertiary leucogranites.
- The gneisses are not confined to a single stratigraphic horizon, but are distributed in a wide zone with varying thickness.
- About 10–20 km thick metamorphic thrust sheet of the Higher Himalaya is resting over the multifarious Lesser Himalayan succession. The southwards-leaning thrust sheet is passively folded in the Midlands, and most of its antiformal region is eroded away, leaving behind the synformal outliers and klippen distributed in various parts of the Midlands and Mahabharat Range.
- The Paleozoic granites that have survived erosion are found in the synforms, where they frequently grade into orthogneisses, indicating intense tectonic and metamorphic activity after their emplacement.
- The Tertiary leucogranites show sharp and chilled contacts with the gneisses and migmatites. Generally, these granite bodies have a concordant floor and an irregular roof.
- In central Nepal, the Higher Himalayan thrust sheet reaches the Siwaliks and makes the Lesser Himalayan zone discontinuous.
- The Higher Himalayan crystallines are characterized by inverted metamorphism towards their base and normal Barrovian type of metamorphism towards their top.
- The grade of metamorphism in the Higher Himalayan crystallines decreases progressively from the hinterland towards the foreland (Siwaliks). Also, their metamorphic grade sharply diminishes towards the Tethyan sedimentary succession.
- The Higher Himalayan crystallines are frequently truncated to the north by a system of normal faults called the South Tibetan Detachment System. At the surface, the detachment is a discontinuous fault system with one or more splays. In some instances, it is represented just by a shear zone.

Calder (1832, pp. 2–3) was awestruck by the grand and extensive mountain ranges forming the principal boundaries of the Indian subcontinent. He reported that on the north the stupendous rampart of the Himalaya contains a vast accumulation of sublime peaks, the pinnacles of our globe.

M.R. Dhital, *Geology of the Nepal Himalaya*, Regional Geology Reviews,
DOI 10.1007/978-3-319-02496-7_13

These elevated portions preponderate in gneisses along with mica schists, hornblende schists, chlorite slates, and crystalline limestones. The rest is represented by clay slates and flinty slates, and towards the base, we find sandstones composing the southern steps of the chain.

Joseph Dalton Hooker visited Darjeeling and the Tamar River valley in 1848, Sikkim in 1849, and the Khasi Mountains in 1850. He pioneered the investigations of geology, flora, fauna, and other details of this part of the Himalaya. He recorded the occurrence of high-grade metamorphic rocks over low-grade schists. He also observed the boulders of gneiss and granite in the Tamar River (Hooker 1854, pp. 137–139).

In the Lesser Himalaya of Darjeeling, Mallet (1874, pp. 39–42) observed a sudden lithological change between the Damudas and the overlying Dalings. The latter rocks contain light green greasy slates, quartzites, and some calcareous hornblende schists with actinolite and passing into dolomites. He remarked that the Dalings underlie the Darjeeling Gneiss without any indication of faulting, and the superposition records a phenomenon of metamorphic inversion. Von Lóczy explained this anomalous distribution by drawing a huge recumbent fold (Chap. 5). Similarly, between Almora and Mussooree of Kumaun, Oldham (1883, p. 164) noted a gradual passage from gneisses to underlying schists and then to slates.

Hagen (1969) showed that the crystalline rocks corresponding to the Tibetan slab of Lombard (1952) compose a prominent portion of the Himalayan Range in Nepal. These rocks are also marked by a distinct topographic break, above which are disposed the Himalayan peaks. However, most of the peaks are capped by the Tethyan sedimentary rocks. But, unlike Lombard's Tibetan slab, representing a single huge homocline, Hagen considered the Higher Himalayan crystallines to represent his various nappes that extend to the south, over the Lesser Himalaya. In central Nepal, Hagen (1951, p. 134) included the Higher Himalayan rocks under the Kathmandu nappe system, which is thrust over the Nawakot nappe system of the Lesser Himalaya. The Kathmandu nappe is made up of gneisses, schists, quartzites, and phyllites, with different degrees of metamorphism. There also crop out sandstones and limestones of Ordovician age. Granites, pegmatites, and aplites are intruded in the lower part of the Kathmandu nappe.

Kruparz (1953) visited the Kathmandu Valley and went to Tibet via Banepa, Chautara, and Kodari. His geological section across the Kathmandu Valley and Nyalam Dzong (Tibet) astonishingly accurately depicts a major thrust sheet with gneisses as well as underlying slates and phyllites (Fig. 13.1). Investigations of Fuchs and Frank (1970) and Fuchs (1977) led to the recognition of a thin Lower and a thick Upper Crystalline nappe in west Nepal. Their Upper Crystalline nappe includes medium- to fine-grained, banded, two-mica gneisses, quartzites, marbles, and paragneisses. The nappe also contains migmatites, granitic gneisses, and augen gneisses with kyanite and sillimanite. Hashimoto et al. (1973) carried out detailed petrographic and microstructural studies of the Higher Himalayan rocks, designated by them as the Himalayan gneisses, which are thrust southwards onto their Midland metasediments (Ohta 1973, pp. 242–243).

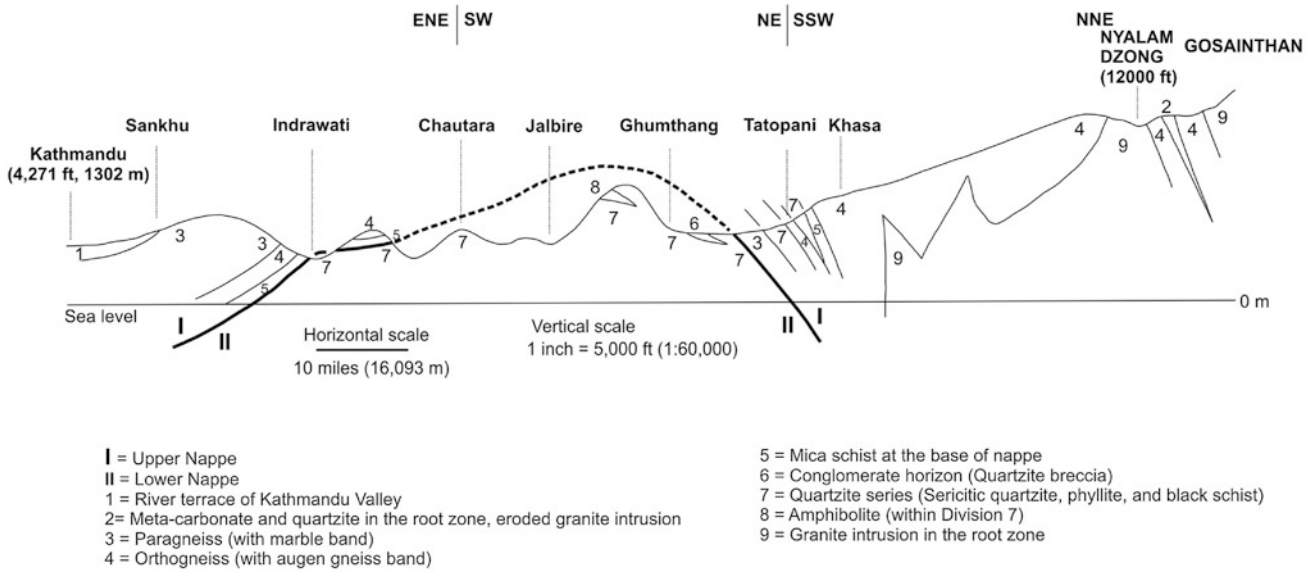

Fig. 13.1 Cross-section through Kathmandu–Indrawati–Kodari–Nyalam Dzong (Tibet). *Source* Modified from Kruparz (1953)

13.1 Main Central Thrust

In the Northwest Himalaya, Heim and Gansser (1939) separated the Higher Himalayan crystallines (also called the Central Crystallines or "central gneiss"; Box 13.2) from the overlying Tethyan sedimentary sequence and underlying faintly metamorphosed Lesser Himalayan succession. The crystallines form a large thrust sheet, which overrides the Lesser Himalayan succession along the Main Central Thrust (Box 13.3). These crystallines are about 10 km thick in the Mahakali River section. In that tract, the Main Central Thrust is gently folded and brings in its hanging wall medium- to high-grade schists and gneisses, which rest on the Lesser Himalayan slates, phyllites, quartzites, and carbonates. Following Heim and Gansser, the Main Central Thrust has been traced throughout the Himalayan Range, and it is considered to be one of the fundamental structures. However, there remain some controversies regarding its nature and position (Box 13.4).

Box 13.2: Gneisses Versus Granites

Strachey (1851) reported granites and gneisses from the Northwest Himalaya and Stoliczka (1866, p. 15) described well banded gneisses from this region under the title of "central gneiss." He found these rocks on the ascent from the Sutlej Valley to the Babeh pass. In parallel with the Alps, he believed the gneisses to constitute the principal geological axis of the Himalayan Range, on either side of which the subsequent sediments were deposited. The failure to observe such a disposition by subsequent investigators made the term no more tenable (Oldham 1893, p. 42). McMahon (1877, 1882, 1883) mapped the "central gneiss" from various parts of Northwest Himalaya and utilized a microscope for the first time to investigate these rocks. He classed them as "gneissose-granite". Oldham (1883) investigated the "central gneiss" in Almora where he found these rocks concordantly lying over schists. Hence, there arose a dispute over the origin and age of these rocks. Stoliczka and Oldham believed that these gneisses were homotaxial with the Precambrian paragneisses of the Indian craton, but McMahon (1882, 1887) favoured that they were much younger (Tertiary) intrusives. However, he also admitted that not all of them were of granite origin (McMahon 1883, p. 143; Odell 1983).

Box 13.3: Discovery of Main Central Thrust

In his classic work on the geology of west Garhwal, Middlemiss (1887, p. 34) observed that the schists and gneisses (comprising his Inner formation) are enclosed in an elongated trough (synform) and are surrounded by sedimentary rocks (representing his Outer formations) from all sides. Since the concept of large-scale thrusting was unconceivable at that time, he had to postulate a reverse fault encircling his Inner formation. Exactly after 50 years, Auden (1937) carried out further investigations in that region and remarked (p. 412) that though Middlemiss imagined it a ring-shaped reverse fault everywhere dipping inwards, centripetally below the schistose series, his two accurately-drawn geological maps clearly depicted a thrust sheet. Auden mapped in detail the Krol and Garhwal nappes as well as many tectonic windows, exposing Nummulitic rocks together with metamorphic outliers resting on the Lesser Himalayan sedimentary sequence. He also thoroughly investigated the Higher Himalayan rocks represented by schists, gneisses, and pegmatites, which were separated from the underlying little metamorphosed shales, phyllites, limestones, and quartzites of the Lesser Himalaya by a thrust fault whose minimum distance of translation was about 80 km (Auden 1937, p. 432). Soon after, Heim and Gansser (1939, pp. 78, 225) designated that fault the Main Central Thrust.

13.2 Higher Himalayan Crystallines

In Nepal, the Higher Himalayan rocks (Fig. 6.1) are truncated by the Main Central Thrust from below, whereas the South Tibetan Detachment System frequently delimits them from the overlying sedimentary rocks. Their age is generally estimated to range from Neoproterozoic to Ordovician (Parrish and Hodges 1996; DeCelles et al. 2000). Around Kathmandu, the Cambro–Ordovician sedimentary strata of the Tethys Himalaya conformably overlie the Higher Himalayan sequence (Stöcklin 1980). Similar conditions are also observed in the Jaljala and Karnali synformal klippen of west Nepal (Fuchs and Frank 1970; Fuchs 1977).

The Higher Himalayan crystallines (Box 13.1) are made up of medium- to high-grade schists, quartzites, and marbles together with augen and banded gneisses, migmatites, and granites. In the banded gneisses, dark biotite-rich strips alternate with light bands of granitic and tourmaline-rich pegmatitic material, whereas the augen gneisses contain large feldspar laths. Lateral and vertical distribution of the gneisses is inconsistent and irregular. For example, they are less common or absent in the southern part but are abundant in the north. In the vicinity of Kathmandu, they are found in the north flank of the Mahabharat Synclinorium where they link up with the gneisses of Hagen's "tectonic bridge" of Gosainkund, and

through this the Central Crystalline zone. In vertical distribution, they are also not bound to a specific horizon but appear or disappear within the Bhimphedi Group and the immediately overlying Tistung Formation (Stöcklin 1980, p. 21).

Box 13.4: Problems in Defining Main Central Thrust

Ever since Heim and Gansser (1939) documented the Main Central Thrust from the region between Nainital and Darchula (west border of Nepal), this fault has not been without controversies. Various investigators have followed primarily three different approaches while mapping the Main Central Thrust (Yin 2006): it marks the lithological difference between the Lesser Himalayan rocks (below) and the Higher Himalayan rocks (above) as proposed by Heim and Gansser (1939); it denotes an abrupt change in metamorphic grade (Le Fort 1975); and the fault defines the top or basal surface of several kilometer-thick shear zone across the lowermost part of the Higher Himalayan rocks and the uppermost part of the Lesser Himalayan sequence (Arita 1983; Searle et al. 2003, 2008). For ideal conditions, all these three criteria should hold true (Le Fort 1996); however that is not the case in most instances. Consequently, locating the Main Central Thrust has become a matter of personal choice (Stöcklin 1980). There are some researchers who have drawn more than one Main Central Thrust straddling the Lesser and Higher Himalayan sequences (Maruo and Kizaki 1983; Arita 1983) and others have proposed various thrusts within the Higher Himalayan metamorphic pile. For example, Valdiya (1977) distinguishes the Main Central Thrust (or the Munsiari Thrust sheet) and overlying Vaikrita Thrust in Kumaun, whereas Goscombe et al. (2006) have identified many faults in the Higher Himalayan sequence. On the other hand, Shrestha and Shrestha (1984), ESCAP (1993), Upreti and Le Fort (1999), Rai et al. (1998), and Hodges (2000) have proposed a separate thrust sheet for the Kathmandu Complex. But Johnson et al. (2001) have strongly opposed such a proposal, which is based solely on metamorphic considerations and violates structural relationships. Martin et al. (2005) did not detect any significant mixing of the Higher and Lesser Himalayan rocks in the Main Central Thrust zone of west Nepal.

Bordet (1961) was the first to map the Main Central Thrust in the Arun Valley of east Nepal, where he placed the thrust along a prominent kyanite-bearing zone within the sillimanite gneisses. In the same region, Hubbard (1989) mapped this fault further down, below the Num orthogneiss, near Tumlingtar. Goscombe et al. (2006) remarked that the Main Central Thrust of previous workers is in fact an unconformity (designated by them the Himalayan unconformity), and shifted this fault further south, beneath the Ulleri–Phaplu augen gneiss. They also mapped a second fault called the High Himal Thrust near the Main Central Thrust of Bordet. In west Nepal Le Fort (1971, 1975), Pêcher (1991), and Colchen et al. (1986) have placed the Main Central Thrust on the basis of the occurrence of highly deformed augen gneisses characterized by a strongly developed stretching lineation.

To overcome the difficulty of separating the metamorphosed Lesser Himalayan and Higher Himalayan sequences, many researchers have used the differences in U–Pb detrital zircon ages (e.g. Parrish and Hodges 1996; Ahmad et al. 2000; DeCelles et al. 2000) or differences in Nd isotope compositions (e.g. Robinson et al. 2001; Martin et al. 2005; Richards et al. 2005, 2006). Others have used young U–Pb and Th–Pb monazite ages (e.g. Harrison et al. 1997; Catlos et al. 2001, 2002). None of these methods in themselves can be used independently to define a thrust fault. Lithology, detrital zircon ages, and Nd isotopes give information on stratigraphy, not structural relationships. Isograds and monazite ages give information on metamorphic reactions, fluids, and timing of mineral growth, not structure (Searle et al. 2008).

Searle et al. (2008) redefine the Main Central Thrust in terms of a high-strain zone lying below the ductile shear zone and inverted metamorphic sequence. They include the entire inverted metamorphic zone within the Higher Himalayan sequence. This definition too suffers from some difficulties, such as the youngest Early Miocene strata may also record inverted metamorphism (e.g. Sakai et al. 1999) and a sedimentary sequence (e.g. the Benighat Slates in central Nepal) may experience, without interruption, progressively higher (i.e., from chlorite to kyanite) metamorphic grades.

While addressing this problem, Stöcklin (1980, p. 13) made the following remarks:

> One should expect again that tectonic interpretations of these crystalline masses be preceded by, and based upon, a necessary minimum of stratigraphic work. In Nepal, most authors confined themselves to listing the various crystalline rock types and describing their petrography, elaborating mainly on the gneisses to emphasize the contrast in metamorphic grade with the (meta-) sedimentary belts.

In the Arun tectonic window of east Nepal, Brunel (1986) and Brunel and Kienast (1986) used various strain markers (e.g., C/S fabrics, stretching lineations, and snowball garnets) to map deformation in the Main Central Thrust zone and showed a high-strain zone with a dominant top-to-south simple shear component. Further investigations of Grasemann et al. (1999), Law et al. (2004), and Jessup et al. (2006) based on mean kinematic vorticity numbers revealed that the deformation in the Main Central Thrust zone also includes a significant component of pure shear, which ranges from 44 to 58 % in the Mount Everest region.

13.3 Folded Higher Himalayan Thrust Sheet

The broad undulations of the 10–20 km thick (less than 5 km in the Kali Gandaki Valley) Higher Himalayan thrust sheet (with some Tethyan outliers) can be approximated to two arc-parallel folds named the Great Midland Antiform, occupying the inner zone, and the Great Mahabharat Synform, extending along the outer zone (Fig. 6.1). The antiform is equivalent to the Midland Anticline and Himalayan Fore-Anticline of Hagen, whereas the synform belongs to his Mahabharat Syncline as well as the Dandeldhura zone (Hagen 1969, p. 40), and it also includes the Mahabharat Synclinorium (Stöcklin 1980) in central Nepal. Apart from the two megafolds, there also appear some en echelon longitudinal synforms and antiforms in west and east Nepal. Erosion has almost completely removed the core of the Great Midland Antiform. The sole survivor is the Gosainkund antiformal culmination in central Nepal. Intense erosion has also converted the Great Mahabharat Synform into various elongated klippen and half-klippen. Some of the important ones are the Almora–Dadeldhura–Karnali Synform and Jaljala Synform in west Nepal, the Mahabharat Synclinorium in Central Nepal, and the Ilam–Darjeeling Synform in east Nepal. Except for these roughly longitudinal folds, the Higher Himalayan thrust sheet is also affected by many late transverse antiforms (Brunel and Adnrieux 1977; Brunel 1986) that have evolved along major rivers of Nepal. The transversely folded thrust sheet has formed many dome–basin-like structures. These structures are well known from east Nepal where the uninterrupted Higher Himalayan thrust sheet exceeds 100 km in width. For example, the large Okhaldhunga window represents a complex dome or antiformal culmination, which is surrounded on three sides by three interlocking elongated synformal depressions. Its remaining northern portion is marked by the Melung–Salleri synformal depression and the Dudh Koshi antiformal culmination. The transverse antiformal culminations and synformal depressions may reflect the effect of lateral ramps that caused hanging-wall thickening and the development of horses in the Lesser Himalayan sequence (Johnson 1994).

The deformation pattern in the Higher Himalayan thrust sheet and the underlying Lesser Himalayan sequence is quite contrasting. Owing to continued convergence of the Indian and Eurasian plates, a variety of subsidiary thrust sheets and duplexes developed at shallower depth in the concealed Lesser Himalaya, whereas the Higher Himalayan crystallines were too massive and competent to be significantly affected by these processes. Nevertheless, the sheet was passively folded in response to the stresses, overall erosion, and isostatic adjustments. In central Nepal, the Higher Himalayan rocks override the Siwaliks, indicating quite young movements along their south front, where the relatively incompetent Siwaliks and Lesser Himalayan rocks are still being underthrust beneath the Higher Himalayan sheet.

13.4 Root Zone

Hagen attributed the Central Crystallines to the root zone of his various crystalline nappes. However, Gansser (1964, p. 157) denied the occurrence of such a large-scale root zone in the Himalaya. On the other hand, rapid removal of the lithospheric root beneath the thickened crust of Tibet can be responsible for the current elevation of the plateau, its lack of surface slope, and pattern of present deformation (Jiménez-Munt et al. 2008).

In the Trishuli–Rasuwa Gadhi area of central Nepal, Hagen and Hunger (1952) differentiated phyllites, conglomerates, graphitic schists, and quartzites in the Nawakot nappe; and two-mica schists, garnet schists, quartzites, pegmatites, migmatitic gneisses, and augen gneisses in the Kathmandu nappe. They also distinguished younger pegmatites and intrusives. The grade of metamorphism is higher in the root zone (between Rasuwa Gadhi and Syaphrubensi) than in the frontal part lying south of Kathmandu. In the sillimanite-bearing gneisses of the Rasuwa Gadhi area, belonging to the root zone of the Kathmandu nappe, they found large (about 1 m thick), almost vertical, crosscutting dikes of microgranite with straight walls, indicating their intrusion after the main phase of deformation (Fig. 13.2). Hagen (1969) showed the Kathmandu nappes being thrust over the Nawakot nappes in his beautiful block diagram (Fig. 13.3).

Schelling and Arita (1991) have inferred a root zone making a footwall ramp in east Nepal, whereas Robinson et al. (2003) depicted a root zone in the Darchula and Bajhang area as a hanging wall and footwall flat. In central Nepal, it is believed that the relatively steep ramp is characterized by intense microseismicity owing to stress concentration or fluid pressure (Pandey et al. 1999; Avouac 2003). On the other hand, Cattin and Avouac (2000) have modeled a gently dipping Main Himalayan Thrust in the same region.

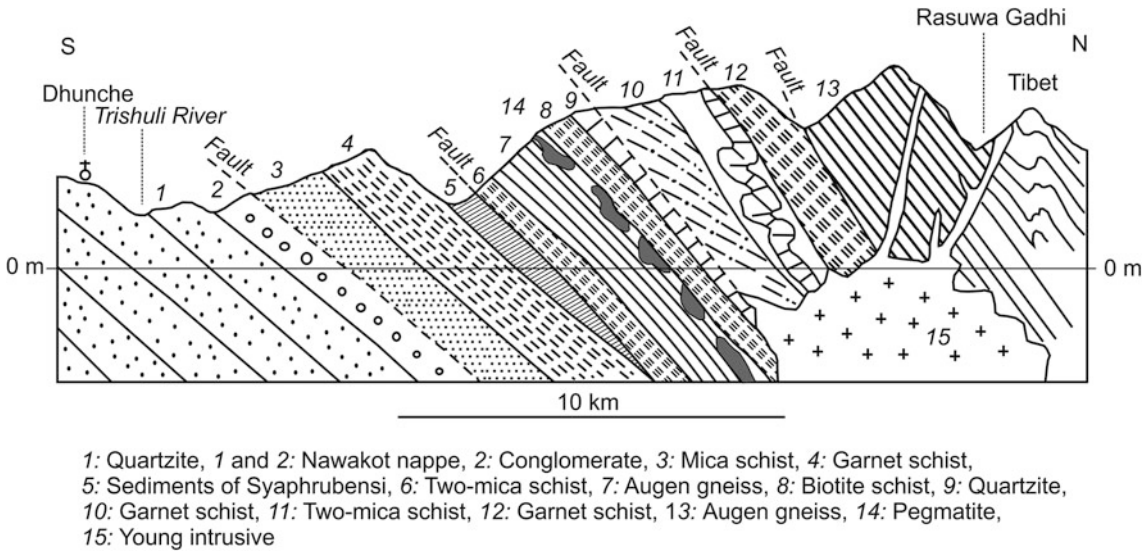

Fig. 13.2 Geological section across the "root zone" of the Kathmandu nappes in central Nepal (the Trishuli River valley, Rasuwa Gadhi). *Source* Modified from Hagen and Hunger (1952)

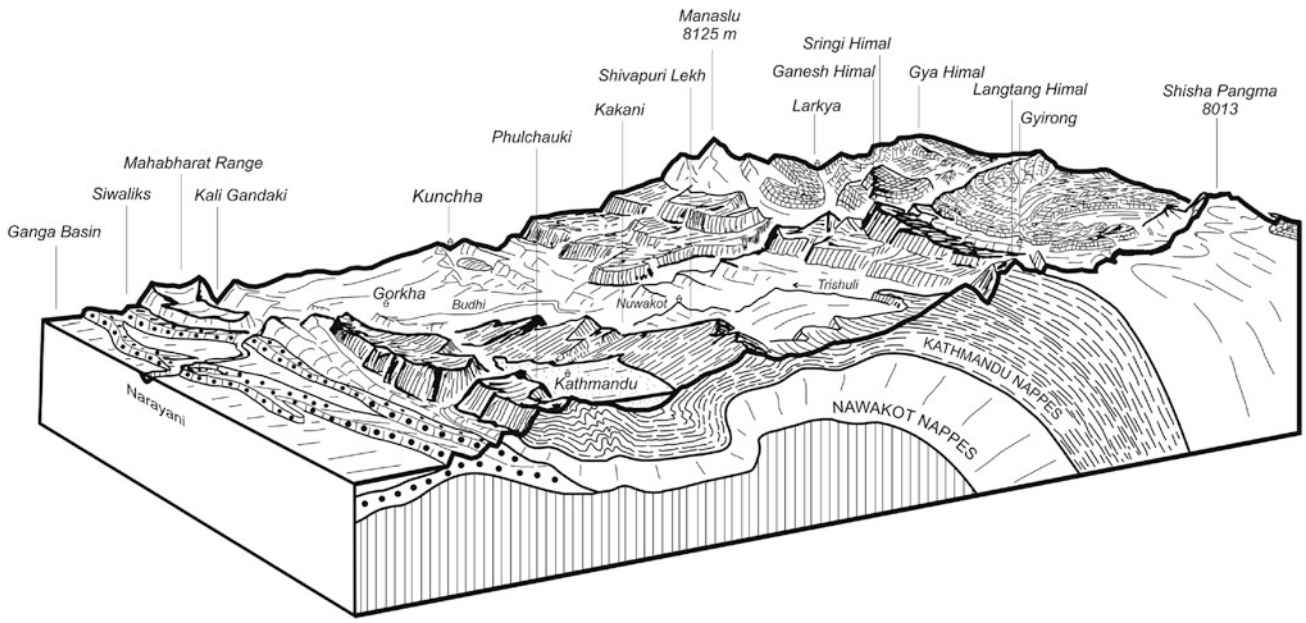

Fig. 13.3 Block diagram showing the superposition of the Kathmandu nappes over the Nawakot nappes in central Nepal. *Source* Modified from Hagen (1969)

13.5 Slip Along Main Central Thrust

A rough estimate of the displacement along the Main Central Thrust can be obtained by applying the klippe-to-window method in central, west, and east Nepal. It gives an estimate of more than 100 km of displacement along the thrust (Dhital et al. 2002). Balanced cross-section–based slip estimates along the Main Central Thrust vary from 140 to 210 km in east Nepal (Schelling and Arita 1991), and several hundred kilometers in west Nepal in the Dadeldhura area (Robinson et al. 2006).

The Main Central Thrust cooled below 350 °C in the Dadeldhura area of west Nepal about 21 Ma (DeCelles et al. 2001). The thrust was active around 22–17 Ma in central Nepal (Johnson and Rogers 1997; Johnson et al. 2001), whereas the shear zone of the Main Central Thrust around Kathmandu was cooled below 350 °C between 21 and

14 Ma and its southern portion became stationary around 14 Ma (Arita et al. 1997). Investigations of Catlos et al. (2001) in the Main Central Thrust zone of central Nepal revealed its prolonged and discontinuous movement ranging from 41 to 13 Ma. Monazite dating in the Langtang area revealed that the root zone of the Main Central Thrust was reactivated between 8 and 3 Ma, whereas its frontal portion was inactive during the same period (Harrison et al. 1997). Inasmuch as metamorphic isograds across the Main Central Thrust zone have been compressed or telescoped into a 1–2 km thick section (Searle and Rex 1989; Hubbard 1996), shearing postdates peak metamorphism (Searle et al. 2008).

13.6 South Tibetan Detachment System

The South Tibetan Detachment System separates the medium- to high-grade metamorphic rock of the Higher Himalaya from the overlying sedimentary or low-grade metamorphic succession of the Tethys Himalaya. Detailed investigations in south Tibet (Burg et al. 1984; Burchfield et al. 1992) have shown it as a system of normal faults (Box 13.5). In Nepal, the South Tibetan Detachment System occupies a few kilometer-wide zone, where there are a number of longitudinal faults or shear zones with a complex alternating history of top-north and top-south motion (Hodges et al. 1996; Carosi et al. 1998; Searle et al. 2003). Although most of these faults lie north of the Great Himalayan peaks, the Annapurna Detachment lies on the south slopes, and it exhibits top-north as well as top-south shear fabrics (Godin et al. 1999). In the same area, the Deorali Detachment was active and coeval with the Main Central Thrust at 22.2 Ma (Godin et al. 2001). The top-north Modi Khola shear zone was active between 22.5 and 18.5 Ma, and the south-lying Machhapuchhre Detachment was active after 18.5 Ma (Hodges et al. 1996). Because the Higher Himalayan sequence shows upwards-younging ages from 15 to 12 Ma, the motion on the Annapurna Detachment ceased by about 22.5 Ma, and these rocks were exhumed to mid-crustal levels about 15–12 Ma (Godin et al. 1999). In central Nepal, some detachment faults also exhibit right-lateral shear (Brun et al. 1985; Pêcher 1991; Coleman 1996) along the South Tibetan Detachment System in the Manaslu Himal and Upper Marsyangdi region.

Box 13.5: Early Records of Normal Faults

Odell (1925) was the first to notice some normal faults in the Everest region. Subsequently, Wager (1939, p. 175) made the following observations:

> At the entrance to the Rongbuk valley the lower part of the Mount Everest limestone series is injected by granite sills yet, a hundred feet above, the only obvious metamorphic effect is a slight hardening, and veining by granite does not occur… No signs of a basement bed to the limestone series are to be seen, nor weathering of the upper part of the gneiss. On the other hand, there are abundant signs of violent movement, so that I regard the junction, which dips north at about 45°, as a fault plane. The Mount Everest limestone is at least a thousand feet thick in Lhonak, to the west, and probably the same at Dothak in the Chumbi valley, to the east, and it is likely therefore, that on Lachi the fault cuts out much of the limestone. It is noteworthy that the postulated fault is apparently a normal one and not a thrust although it has a relatively low dip.

13.7 Thin-Skinned Tectonics

Although the thin-skinned tectonic concepts of cross-section balancing have been applied quite extensively, some limitations to their use are evident in the Himalayan region with the deepest crust. There are no accurate criteria to decide at what depth to draw the basal detachment, or at what angle the sole thrust dips north beneath the Himalaya (Searle 1989). Inhomogeneous deformation precludes the prerequisite of plane strain (Ramsay and Huber 1987, p. 545) in most parts of the Himalaya. Deeply eroded imbricate slices also complicate the matter further (Dhital and Kizaki 1987). On the other hand, centrifuged orogen models (Ramberg 1967, p. 148) have been developed with some success to simulate the tectonic features of many mountain belts.

13.8 Polyphase Metamorphism

Krummenacher (1961, 1966) carried out the first age determinations on rocks from the Siwaliks to the Tethys Himalaya of Nepal. A quartzite from the Nawakot nappes in Central Nepal containing presumably a detrital muscovite was analyzed by the K–Ar method and it yielded 728 ± 12 Ma. Based on a number of age determinations on various rocks, he concluded that there were two main metamorphic events: the Proterozoic and one between 25 and 11 Ma.

The metamorphic events in the Himalayan orogen have been divided up into the Eo-Himalayan (Middle Eocene to Early Oligocene: 45–30 Ma) or M1 type (Caby et al. 1983; Le Fort 1989) and the Neo-Himalayan (Early to Middle Miocene: 23–15 Ma) or M2 type (Hodges 1993). It is believed that the Eo-Himalayan metamorphism took place prior to the initiation of the Main Central Thrust. It is a "normal" Barrovian type of metamorphism. The Neo-Himalayan metamorphism is synkinematically linked with the activity of the Main Central Thrust, characterized by

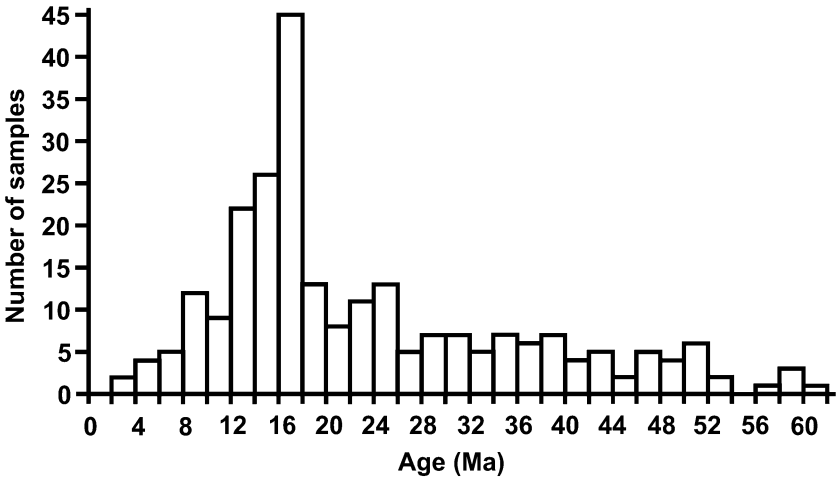

Fig. 13.4 Cenozoic cooling ages of the Higher Himalayan crystallines. *Source* Modified from Sorkhabi and Stump (1993)

inverted metamorphism. Except for these two metamorphic episodes, there are several other prior or posterior events and it becomes difficult to pigeonhole them within the two types. For example, in the Namche Barwa region of the east syntaxis, Plio–Pleistocene metamorphic overprinting is found in the Proterozoic rocks, constituting the Indian plate (Burg et al. 1997). Sorkhabi and Stump (1993) compiled 247 Cenozoic cooling ages corresponding to paleotemperatures of 300–350 °C from the Higher Himalaya and its klippen (Fig. 13.4). These ages depict a rapid cooling and a major pulse of exhumation around 18 to 16 Ma, whereas the younger (less than 8 Ma) ages correspond mainly to the Main Central Thrust zone.

13.9 Subduction Metamorphism and Eclogites

The Higher Himalayan sequence includes some high- and ultra-high-pressure rocks. Ultra-high-pressure eclogites occur in the Kaghan Valley of Pakistan (Pognante and Spencer 1991; Tonarini et al. 1993) and in the Tso Morari dome of Ladakh, India (de Sigoyer et al. 1997, 2000). These eclogites lie close to the Indus–Tsangpo suture zone (O'Brien et al. 2001) and are believed to be related to the subduction of the leading edge of the Indian continental crust during the early stage of the India–Asia collision, before the formation of the Main Central Thrust. The eclogites record temperatures of 725 ± 25 °C and pressures of 2.8–3.0 GPa (Mukherjee and Sachan 2001; O'Brien et al. 2001). Dating of accessory zircon (Kaneko et al. 2003; Parrish et al. 2006) and garnet (Tonarini et al. 1993) has given an age of about 46 Ma in the Kaghan Valley, and a garnet isochron has given an age of about 54 Ma for Tso Morari (de Sigoyer et al. 2000).

Eclogites are also found in the Ama Drime massif, located about 30 km east of Mt. Makalu in the north Arun Valley, in the Kharta region of Tibet (Lombardo and Rolfo 2000), and the Makalu–Everest region of the Arun River valley in east Nepal (Parkinson and Kohn 2002). These eclogites are different from those of Pakistan and India, as they did not reach the ultra-high-pressure metamorphism and they are strongly overprinted by subsequent metamorphism, leaving meager evidence for eclogitization. The Ama Drime massif represents a north–south trending horst between two normal faults: the Ama Drime and Nyönno Ri detachments on the western and eastern sides (Armijo et al. 1986). It contains migmatites and orthogneisses with some metabasic layers and pods. The Ama Drime paragneisses overlie the orthogneisses and they also contain pelitic schists. The migmatitic orthogneisses contain a few hundred meter-thick boudins of metabasics, recording eclogite facies metamorphism (Groppo et al. 2007). The orthogneisses are dated at 1.8 Ga, similar to the Ulleri orthogneisses of the Lesser Himalaya in west Nepal (Robinson et al. 2001; Liu et al. 2007; Cottle et al. 2009). These high-pressure granulites contain garnet, clinopyroxene, orthopyroxene, plagioclase, quartz, and biotite. These rocks record pressures ranging from 1.5 to 1.8 GPa and temperatures of 800 °C. These conditions were followed by isothermal decompression down to a pressure of about 0.3 GPa. The peak metamorphism occurred around 30 Ma, whereas their isothermic decompression took place from 20 to 12 Ma (Lombardo and Rolfo 2000; Liu et al. 2007; Groppo et al. 2007; Kali et al. 2010).

Corrie et al. (2010) used garnet geochronology to measure the timing of eclogitization in the Arun Valley, and they obtained an age of 20.7 ± 0.4 Ma, significantly younger than ultra-high–pressure eclogites from the western Himalaya. The P–T calculations in the Arun eclogites indicate three

metamorphic episodes: (i) eclogite-facies metamorphism at about 670 °C and ≥1.5 GPa at 23–16 Ma; (ii) a peak-T granulite event at about 780 °C and 1.2 GPa; and (iii) late-stage amphibolite-facies metamorphism at about 675 °C and 0.6 GPa at about 14 Ma. Langille et al. (2010) obtained significant west-directed displacement along the Ama Drime detachment.

13.10 Barrovian Metamorphism

According to Frank et al. (1977), in the Himalaya, a crystalline basement, separated by a pronounced unconformity from the overlying sediments, is practically missing. However, Bhargava (1980) and Bhargava et al. (2011) have regarded the Jeori–Wangtu–Bandal Gneissic Complex in the Northwest Himalaya as the basement, over which the Rampur–Berinag sequences were deposited in a rifted basin. In Central Nepal, the Higher Himalayan rocks display a steady increase in metamorphic grade from top to bottom. The Devonian limestones, constituting the peak of Phulchauki, are basically unmetamorphosed. While moving stratigraphically downwards, very fine sericite and chlorite appear in the Silurian slates and they become prominent in the Cambrian Tistung Formation. Biotite appears first in its lower part and becomes prominent throughout the Bhimphedi Group. Garnet usually shows first as tiny crystals in the middle Kalitar Formation, becomes larger and plentiful in the lower Kalitar, where it frequently occurs with amphiboles, and is most conspicuous in the Raduwa Formation, constituting the base of the Bhimphedi Group. This metamorphism, which increases with depth and shows a clear zonation roughly concordant with stratigraphy, is considered the primary regional metamorphism (Stöcklin 1980; Johnson et al. 2001). Thus, normal-way-up Barrovian metamorphism is observed in the Kathmandu region (Morrison and Oliver 1993). At the base of the Main Central Thrust in the Kathmandu Complex, peak metamorphism was recorded at temperatures of 500–600 ± 50 °C and pressures of 0.8–1.1 ± 0.15 GPa in the Early Miocene (Johnson et al. 2001). Rai et al. (1998) measured a peak metamorphic pressure of about 0.75 GPa and a temperature of about 500 °C at the front of the Mahabharat Synclinorium, and a pressure ranging between 0.70 and 0.80 GPa and a temperature of about 675 °C at its back.

The Kangmar massif is one of a series of gneiss domes situated in the North Himalayan (or Lhagoi Kangri) belt of south Tibet within the Tethys Himalaya. It lies south of the Indus–Tsangpo suture zone and north of the South Tibetan Detachment System. It is an example of Himalayan metamorphism that affects the upper part of the Higher Himalayan crystallines and the lower part of the Tibetan Tethys zone. In this area, an orthogneiss occupies the core of the dome, which displays an intermediate high-pressure type Himalayan metamorphism, ranging in age from 40 to 20 Ma (Burg et al. 1984). The orthogneiss is dated at 485 ± 6 Ma and 484 ± 7 Ma with the Rb–Sr whole rock method and at 585 + 16 or −12 Ma by the U–Pb method on zircons (Xu et al. 1983). An emplacement age of 508 ± 1 Ma is interpreted on the basis of concordant single zircon analysis (Lee et al. 2000). The grade of metamorphism increases downwards and the highest grade rocks are found in the center of the dome. Colorless chloritoid, zoned garnet, biotite, staurolite, and kyanite successively wrap around the core (Burg et al. 1984). Their mica cooling ages, which range from 15 to 10 Ma, increase with depth and decrease northwards within a single structural horizon across the dome (Lee et al. 2000).

13.11 Inverted Metamorphism

While moving stratigraphically upwards, the inverted metamorphism generally attains a maximum temperature and pressure gradient and then quite rapidly declines into a normal lithostratigraphic gradient. The inverted metamorphism (Fig. 13.5) has become one of the distinctive aspects of the Himalaya (Harrison et al. 1999). A steady increase in the grade of metamorphism is discernible from the upper part of the Lesser Himalaya (i.e., the footwall of the Main Central Thrust) to the lower end of the Higher Himalaya (i.e., the hanging wall of the Main Central Thrust). Since the investigation of this phenomenon from the Northwest Himalaya (Heim and Gansser 1939), many studies have been carried out in west Nepal (Le Fort 1975; Arita 1983; Pêcher 1989), around Kathmandu (Johnson et al. 2001; Rai et al. 1998), in the Langtang Valley (Macfarlane et al. 1992; Macfarlane 1995), and in the Everest–Makalu region of east Nepal (Bordet 1961; Hubbard 1989; Corrie et al. 2010, Goscombe and Hand 2000). The inverted metamorphism in Nepal is supposed to be a Neo-Himalayan event. On the other hand, Harrison et al. (1997) propose a very young age of inverted metamorphism and attribute it to the reactivation of the Main Central Thrust (Chap. 20).

13.12 Cambro–Ordovician Granites and Gneisses

Cambro–Ordovician granites are intruded in the Higher Himalayan succession of Dadeldhura in west Nepal and the Kathmandu Complex in central and east Nepal. The granites are made up of biotite-rich and tourmaline-rich varieties. They are closely associated with the adjacent gneisses, which display a similar mineral composition. At Sindhuli Gadhi in east Nepal, augen gneisses occupy the peripheral

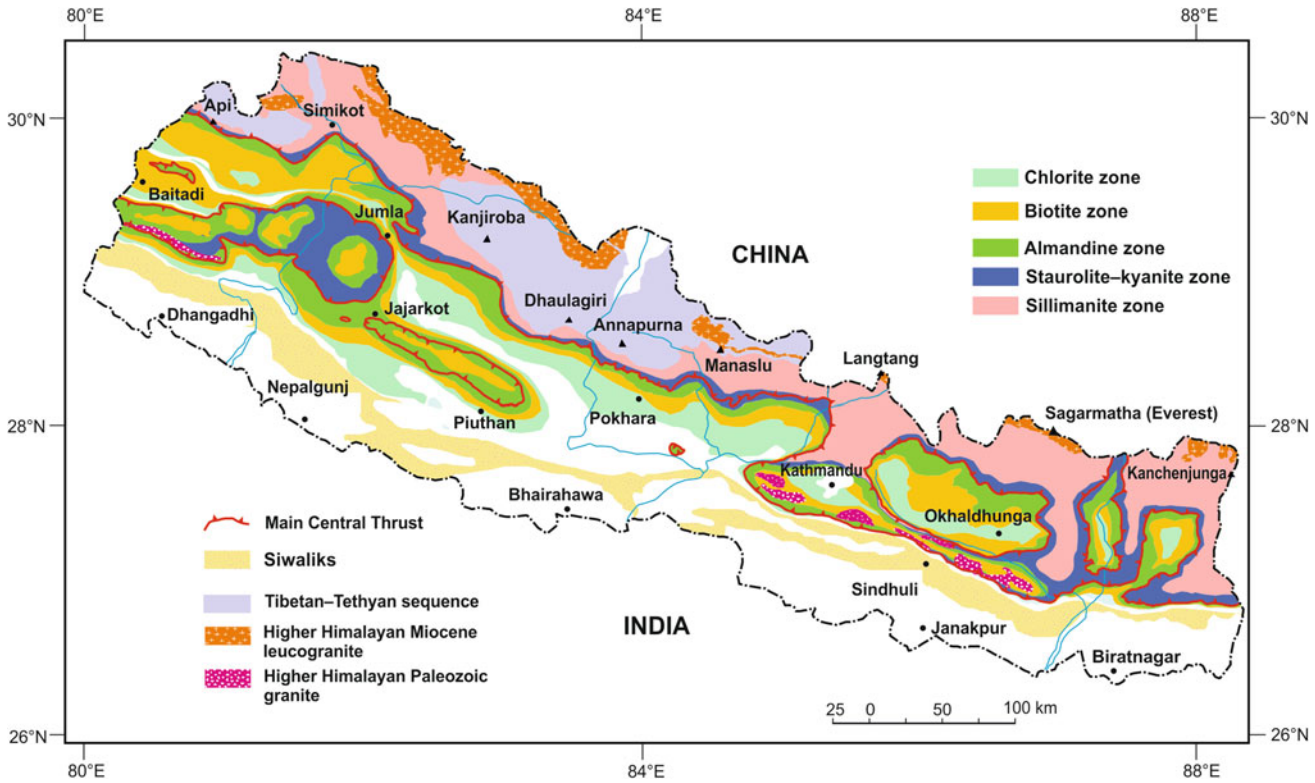

Fig. 13.5 Generalized metamorphic zones in the Lesser and Higher Himalaya of Nepal. Note a small klippe of Higher Himalayan rocks southeast of Pokhara and kyanite appearing below the Main Central Thrust at a few places. Not depicted in the figure is slight (anchizonal) metamorphism (however, sometimes reaching up to the biotite zone), which affects the lower portion of the Tibetan–Tethyan sequence and rapidly decreases structurally upwards. *Source* Compiled from Hagen (1969), Hashimoto et al. (1973), Stöcklin and Bhattarai (1977), Stöcklin (1980), Pêcher and Le Fort (1986), Amatya and Jnawali (1994), and author's observations

part of a large synform, and they imperceptibly change into granites by disappearance of crystal orientation and schistosity. Several concordant, tabular granite bodies, up to 200 m thick, are intruded in the metasediments. Contact metamorphic effect of granite intrusion on the host rock is rather limited, and the metamorphic grade of the country rock increases *away* from the granites, where "away" means down-section (Stöcklin 1980, p. 22).

The Cambro–Ordovician granitoids are not confined to the south margin of the Higher Himalaya in Nepal. They constitute a discontinuous belt, which stretches for more than 1,700 km in the Higher Himalayan crystallines, and frequently forms klippen and half-klippen. In this belt, there are also numerous augen gneisses of almost similar composition, age, and distribution. In Tibet, there is the Lhagoi Kangri plutonic belt (Debon et al. 1983), extending for some 900 km with similar rocks. In the northern part of the Lhasa block, there are orthogneisses with K-feldspar and biotite. These granites and gneisses could be the product of late Pan-African orogeny (Le Fort et al. 1980). Some age determinations of the granites are summarized in Table 13.1.

13.13 Tertiary Leucogranites

In the Swat and Nayan region (west of Nanga Parbat in the Northwest Himalaya of Pakistan), post-collisional leucogranites range in age from 50 to 35 Ma (Zeitler and Chamberlain 1991). These granites could have resulted from melting of the lower crust during tectonic thickening of the Indian plate.

In the Higher Himalayan sequence of Nepal, Early to Middle Miocene leucogranites (Heim and Gansser 1939; Gansser 1964; Le Fort 1975; Hagen 1969) occur as several plutons, very many dikes, and veins. These igneous rocks are mainly concentrated towards the top part of the migmatitic gneisses in the Tibetan slab (Le Fort et al. 1987). They are found in the Annapurna–Manaslu region, where the floor of these intrusives is generally concordant with the underlying rocks. This relationship is well seen in the Manaslu granite and its eastern extension called the Chhokang arm (Fig. 6.6) as well as in the Shisha Pangma granite. The Manaslu granite has a less than 100 m wide

Table 13.1 Some dated Cambro–Ordovician granites, granitoids, and gneisses of Nepal

Locality	Age in Ma	Method	Author(s)
Dadeldhura granite	470 ± 5.6	Rb–Sr	Einfalt et al. (1993)
Augen gneiss, Formation III, Tibetan slab, central Nepal	517 ± 62	Rb–Sr	Le Fort et al. (1982)
Gosainkund orthogneiss	486 ± 9	U–Pb	Rai et al. (2011)
Simchar granite	466 ± 40 511 ± 55	Rb–Sr	Le Fort et al. (1983)
Palung granite	486 ± 10	Rb–Sr	R. Beckinsale *in* Mitchell (1981)
Palung and Simchar granites (combined)	493 ± 11	Rb–Sr	Le Fort et al. (1983)
Paragneisses, Mt. Lhotse, Mt. Everest region	449 ± 56	Rb–Sr	Ferrara et al. (1983)
Migmatitic orthogneiss, Dudh Koshi Valley	550 ± 16	Rb–Sr	Ferrara et al. (1983)
Barun migmatite, East Nepal	525 ± 20	Rb–Sr	Kai (1981)
Barun and Irkhua gneisses, East Nepal	512 ± 20	Rb–Sr	Kai (1981)

contact metamorphic aureole in a garnet–staurolite metamorphic assemblage. It records a pressure of about 0.4 GPa and a temperature of 550 ± 40 °C and requires a corresponding emplacement depth of about 9 to 13 km (Guillot et al. 1995). The granite was intruded around 25–18 Ma. Its roof is rather irregular and it intrudes into the Tethys Himalayan sedimentary sequence up to the Cretaceous rocks. These granites are injected by a network of aplite and pegmatite vein (Le Fort et al. 1987). They are generally medium- to very fine-grained with an equigranular texture. They have a quite uniform mineral composition of anhedral quartz (32 %), slightly zoned subhedral plagioclase (37 %), perthitic K-feldspar 21 %), essentially euhedral muscovite (7 %), and biotite (3 %). Sillimanite–fibrolite frequently occurs at the base of the plutons. Cordierite and pink andalusite also occur infrequently. Tourmaline is so frequent in the granite that they are sometimes called the tourmaline granites, where the mineral is generally concentrated in veins and pegmatite margins. Owing to intense deformation, the granites are sometimes transformed into augen gneisses. The C/S fabric shows a top-to-north or northeast sense of shear (Le Fort et al. 1987). A similar situation prevails in the Everest–Makalu granites.

The North Himalayan or Lhagoi Kangri leucogranite belt lies on the north border of Nepal, in the Tibetan marginal ranges. These plutons are located about 60 km south of and parallel to the Indus–Tsangpo suture zone. There are about 20 domes, and the two well-known bodies are the Mugu and Mustang granites, first mapped by Hagen (1969). These granite plutons are injected into the Tethyan sediments. Their composition is similar to those of the Higher Himalayan leucogranites. Most of them were intruded after the emplacement of the Higher Himalayan leucogranites and they range in age from approximately 20–10 Ma (Schärer et al. 1986; Debon et al. 1986).

13.14 Other Younger Leucogranites

In the Northwest Himalaya, Zeitler and Chamberlain (1991) have documented a few leucogranite dikes from the Nanga Parbat–Haramosh massif of Pakistan. Their age ranges from 7 to 2.3 Ma (U–Pb analyses of zircons). These observations indicate a protracted but episodic magmatic activity in the Himalaya, which is very similar to the metamorphism affecting this orogen.

References

Ahmad T, Harris N, Bickle M, Chapman H, Bunbury J, Prince C (2000) Isotopic constraints on the structural relationships between Lesser Himalayan series and High Himalayan crystalline series, Garhwal Himalaya. Tectonophysics 112:467–477

Amatya KM, Jnawali BM (1994) Geological map of Nepal, scale: 1:1,000,000. Department of Mines and Geology, International Centre for Integrated Mountain Development, Carl Duisberg Gesellschaft e. V., and United Nations Environment Programme

Arita K (1983) Origin of the inverted metamorphism of the lower Himalayas, central Nepal. Tectonophysics 95:43–60

Arita K, Dallmeyer RD, Takasu A (1997) Tectonothermal evolution of the Lesser Himalaya, Nepal: constraints from Ar/Ar ages from the Kathmandu Nappe. Island Arc 6:372–385

Armijo R, Tapponnier P, Mercier JL, Han TL (1986) Quaternary extension in southern Tibet: field observations and implications. J Geophys Res 91(B14):13801–13872

Auden JB (1937) The geology of the Himalaya in Garhwal. Rec Geol Surv India 71(Part 4):407–433 (with 3 plates including a long cross-section on the scale of 1 in. = 2 miles)

Avouac J-P (2003) Mountain building, erosion, and the seismic cycle in the Nepal. Adv Geophys 46:1–80. doi:10.1016/S0065-2687(03)46001-9

Bhargava ON (1980) The tectonic windows of the Lesser Himalaya. Himalayan Geol 10:135–155

Bhargava ON, Kaur G, Deb M (2011) Paleoproterozoic paleosol in the Lesser Himalaya. J Asian Earth Sci 42(6):1371–1380

Bordet P (1961) Recherches Géologiques dans L'Himalaya du Népal, Région du Makalu, Expéditions Françaises a l'Himalaya 1954–1955. Edition du Centre National de la Recherche Scientifique (C. N. R. S.), 275 pp (with the geological sketch map of Everest and Makalu, scale 1:50,000, in colors; and the geological sketch map of Arun and Everest region, scale 1:250,000, in colors; and 5 large plates showing the panoramic geological view of Himalayan peaks)

Brun JP, Burg JP, Ming CG (1985) Strain trajectories above the Main Central Thrust (Himalaya) in southern Tibet. Nature 313:388–390

Brunel M, Adnrieux J (1977) Déformations superposées et mécanismes associes au chevauchement central himalayen «M. C. T.»: Népal oriental. Colloques internationaux du C. N. R. S., No. 268. Écologie et Géologie de l'Himalaya, pp 69–83

Brunel M (1986) Ductile thrusting in the Himalayas: shear sense criteria and stretching lineations. Tectonics 5(2):247–265

Brunel M, Kienast J-R (1986) Etude pétro-structurale des chevauchements ductiles himalayens sur la transversale de l'Everest–Makalu (Népal oriental). Can J Earth Sci 23:1117–1137

Burchfield BC, Chen Z, Hodges KV, Liu Y, Royden LH, Deng C, Xu J (1992) The South Tibetan detachment system, Himalayan orogen: extension contemporaneous with and parallel to shortening in a collisional mountain belt. Geol Soc Am Spec Pap 269:1–41

Burg JP, Davy P, Nievergelt P, Oberli F, Seward D, Diao Z, Meier M (1997) Exhumation during crustal folding in the Namche Barwa syntaxis. Terra Nova 9:117–123

Burg JP, Guiraud M, Chen GM, Li GC (1984) Himalayan metamorphism and deformations in the North Himalayan Belt (southern Tibet, China). Earth Planet Sci Lett 69:391–400

Caby R, Pêcher A, Le Fort P (1983) Le grand chevauchement central himalayen: nouvelles données sur le métamorphisme inverse à la base de la Dalle du Tibet. Rev Géol Dynam Géog Phys 24:89–100

Calder J (1832) General observations on the geology of India. Asiatic Researches comprising history and antiquities, the arts, sciences, and literature of Asia, vol VIII, pp 1–22

Carosi R, Lombardo B, Molli G, Musumeci G, Pertusati PC (1998) The South Tibetan detachment system in the Rongbuk valley, Everest region. Deformation features and geological implications. J Asian Earth Sci 16:299–311

Catlos EJ, Harrison TM, Kohn MJ, Grove M, Ryerson FJ, Manning CE, Upreti BN (2001) Geochronologic and thermobarometric constraints on the evolution of the Main Central Thrust, central Nepal Himalaya. J Geophys Res 106:16177–16204

Catlos EJ, Harrison TM, Manning CE, Grove M, Rai SM, Hubbard MS, Upreti BN (2002) Records of the evolution of the Himalayan orogen from in situ Th–Pb ion microprobe dating of monazite: Eastern Nepal and western Garhwal. J Asian Earth Sci 20:459–479

Cattin R, Avouac JP (2000) Modeling mountain building and the seismic cycle in the Himalaya of Nepal. J Geophys Res 105 (B6):13389–13407

Colchen M, Le Fort P, Pêcher A (1986) Annapurna–Manaslu–Ganesh Himal. Centre National de la Recherches Scientifique, Special Publication, Paris, 136 pp (with a geological map, 1:200,000)

Coleman ME (1996) Orogen-parallel and orogen-perpendicular extension in the central Nepalese Himalayas. Geol Soc Am Bull 298:553–571

Corrie SL, Kohn MJ, Vervoort JD (2010) Young eclogite from the Greater Himalayan sequence, Arun valley, eastern Nepal: P–T–t path and tectonic implications. Earth Planet Sci Lett 289:406–416

Cottle JM, Jessup MJ, Newell DL, Horstwood MSA, Noble SR, Parrish RR, Waters DJ, Searle MP (2009) Geochronology of granulitized eclogite from the Ama Drime Massif: implications for the tectonic evolution of the South Tibetan Himalaya. Tectonics 28:TC1002. doi:10.1029/2008TC002256

de Sigoyer J, Chavagnac V, Blichert-Toft J, Villa IM, Luais B, Guillot S, Cosca M, Mascle G (2000) Dating the Indian continental subduction and collisional thickening in the northwest Himalaya: multichronology of the Tso Morari eclogites. Geology 28:487–490

de Sigoyer J, Guillot S, Lardeaux J-M, Mascle G (1997) Glaucophane-bearing eclogites in the Tso Morari dome (eastern Ladakh, NW Himalaya). Eur J Mineral 9:1073–1083

Debon F, Le Fort P, Sheppard SMF, Sonet J (1986) The four plutonic belts of the Transhimalaya–Himalaya: a chemical, mineralogical, isotopic, and chronological synthesis along a Tibet-Nepal section. J Petrol 27(1):219–250

Debon F, Sonet J, Liu GH, Jin CW, Xu RH (1983) Chemical-mineralogical typology and Rb–Sr dating of the three plutonic belts in Southern Tibet. Terra Cognita 3:265

DeCelles PG, Gehrels GE, Quade J, Lareau B, Spurlin M (2000) Tectonic implications of U-Pb zircon ages of the Himalayan orogenic belt in Nepal. Science 288:497–499

DeCelles PG, Robinson DM, Quade J, Ojha TP, Garzione CN, Copeland P, Upreti BN (2001) Stratigraphy, structure and tectonic evolution of the Himalayan fold–thrust belt in western Nepal. Tectonics 20:487–509

Dhital MR, Kizaki K (1987) Structural aspect of the Northern Dang, Lesser Himalaya, vol 45. Bulletin of the College of Science, University of Ryukyus, Okinawa, pp 159–182

Dhital MR, Thapa PB, Ando H (2002) Geology of the inner Lesser Himalaya between Kusma and Syangja in western Nepal, vol 9, special issue. Bulletin of the Department of Geology, Tribhuvan University, Kathmandu, pp 1–60

Einfalt HC, Hoehndorf A, Kaphle KP (1993) Rediometric age determination of the Dadeldhura granite, Lesser Himalaya, Far Western Nepal. Schweizerische Mineralogische und Petrographische Mitteilungen 73:97–106

ESCAP (Economic and Social Commission for Asia and the Pacific) (1993) Geology and mineral resources of Nepal, atlas of mineral resources of the ESCAP region, vol 9. ESCAP, New York, 107 pp (with a geological map in colors)

Ferrara G, Lombardo B, Tonarini S (1983) Rb/Sr geochronology of granites and gneisses from the Mount Everest region, Nepal Himalaya. Geologisches Rundschau 72:119–136

Fuchs G, Frank W (1970) The geology of West Nepal between the Rivers Kali Gandaki and Thulo Bheri, vol 18. Jahrbuch der Geologischen Bundesanstalt, Wien, Sonderband, pp 1–103 (with 9 plates)

Frank W, Thöni M, Purtscheller F (1977) Geology and petrography of Kulu–Rampur area. Colloques internationaux du C. N. R. S. No. 268 - Écologie et Géologie de l'Himalaya, Paris, pp 147–172

Fuchs G (1977) The geology of the Karnali and Dolpo regions, Western Nepal, vol 120, Heft 2. Jahrbuch der Geologischen Bundesanstalt, Wien, Band, pp 1–103 (with 9 plates)

Gansser A (1964) Geology of the Himalayas. Interscience, New York, 289 pp

Godin L, Brown RL, Hanmer S (1999) High strain zone in the hanging wall of the Annapurna detachment, central Nepal Himalaya. In: Macfarlane A, Sorkhabi RB, Quade J (eds) Himalaya and Tibet: mountain roots to mountain tops, vol 328. Geological Society of America Special Paper, London, pp 199–210

Godin L, Parrish RR, Brown RL, Hodges KV (2001) Crustal thickening leading to exhumation of the Himalayan metamorphic core of central Nepal: Insights from U-Pb geochronology and 40Ar/39Ar thermochronology. Tectonics 20:729–747

Goscombe BD, Hand M (2000) Contrasting P–T paths in the Eastern Himalaya, Nepal: inverted isograds in a paired metamorphic belt. J Petrol 41:1673–1719

Goscombe B, Gray D, Hand M (2006) Crustal architecture of the Himalayan metamorphic front in eastern Nepal. Gondwana Res 10:232–255

Grasemann B, Fritz H, Vannay J-C (1999) Quantitative kinematic flow analysis from the Main Central Thrust zone (NW Himalaya):

implications for a decelerating strain path and the extrusion of orogenic wedges. J Struct Geol 21:837–843
Groppo C, Lombardo B, Rolfo F, Pertusati P (2007) Clockwise exhumation path of granulitized eclogites from the Ama Drime Range (eastern Himalayas). J Metamorph Geol 25:51–75
Guillot S, Le Fort P, Pêcher A, Roy Barman M, Aprahamian J (1995) Contact metamorphism and depth of emplacement of the Manaslu granite (central Nepal). Implications for Himalayan orogenesis. Tectonophysics 241:99–119
Hagen T (1951) Preliminary note on the geological structure of Central Nepal. Verhandlungen der Schweizerischen Naturforschenden Gesellschaft, Luzern, pp 133–134
Hagen T (1969) Report on the geological survey of Nepal. Volume 1: Preliminary reconnaissance. Denkschiiften der Schweizerischen Naturforschenden Gesellschaft. Band LXXXVI/1, 185 pp (with a geological map)
Hagen T, Hunger JP (1952) Über geologisch-petrographische Untersuchungen in Zentral-Nepal. Schweiz Mineral Petrogr Mitt 32:309–333
Harrison TM, Grove M, Lovera OM, Catlos EJ, D'Andrea J (1999) The origin of Himalayan anatexis and inverted metamorphism: models and constraints. J Asian Earth Sci 17:755–772
Harrison TM, Ryerson FJ, Le Fort P, Yin A, Lovera OM, Catlos EJ (1997) A Late Miocene-Pliocene origin for the central Himalayan inverted metamorphism. Earth Planet Sci Lett 146:E1–E7
Hashimoto S, Ohta Y, Akiba C (1973) Geology of the Nepal Himalayas. Saikon Publishing Co. Ltd., Tokyo, 292 pp (with 6 plates including a geological map of Nepal (Plates 1 and 2) in colors, scale: 1:500,000)
Heim A, Gansser A (1939) Central Himalaya: geological observations of the Swiss expedition 1936. Denkschriften der Schweizerischen Naturforschenden Gesellschaft. Band LXXIII, Abh. 1, 245 pp (with maps, sections, and plates)
Hodges KV (1993) Tectonic evolution of the eastern Himalayan orogen. Geol Soc Am Abst Programme 25:A-39
Hodges KV (2000) Tectonics of the Himalaya and southern Tibet from two perspectives. Geol Soc Am Bull 112:324–350
Hodges KV, Parrish RR, Searle MP (1996) Tectonic evolution of the central Annapurna Range, Nepalese Himalaya. Tectonics 15:1264–1291
Hooker JD (1854) Himalayan Journals; or, notes of a naturalist (in Bengal, the Sikkim and Nepal Himalayas, the Khasia Mountains, & c, vol 1. Grand Colosseum Warehouse Co., Glasgow, 408 pp (with 2 maps)
Hubbard MS (1989) Thermo-barometric constraints on the thermal history of the Main Central Thrust zone and the Tibetan slab, Eastern Nepal Himalaya. J Metamorph Petrol 7:19–30
Hubbard MS (1996) Ductile shear as a cause of inverted metamorphism: example from the Nepal Himalaya. J Geol 104:493–499
Jessup MJ, Law RD, Searle MP, Hubbard MS (2006) Structural evolution and vorticity of flow during extrusion and exhumation of the Greater Himalayan Slab, Mount Everest Massif, Tibet/Nepal: implications for orogen-scale flow partitioning. In: Law RD, Searle MP, Godin L (eds) Channel flow, ductile extrusion and exhumation in continental collision zones, vol 268. Geological Society, Special Publications, London, pp 379–413
Jiménez-Munt I, Fernàndez M, Vergés J, Platt JP (2008) Lithosphere structure underneath the Tibetan Plateau inferred from elevation, gravity and geoid anomalies. Earth Planet Sci Lett 267:276–289
Johnson MRW (1994) Culminations and domal uplifts in the Himalaya. Tectonophysics 239:139–147
Johnson MRW, Rogers G (1997) Rb–Sr ages of micas from the Kathmandu complex, Central Nepalese Himalaya: implications for the evolution of the Main Central Thrust. J Geol Soc London 154:863–869
Johnson MRW, Oliver GJH, Parrish RR, Johnson SP (2001) Synthrusting metamorphism, cooling, and erosion of the Himalayan Kathmandu Complex, Nepal. Tectonics 20(3):394–415
Kai K (1981) Rb–Sr geochronology of the rocks of the Himalayas, Eastern Nepal. II. The age and the origin of the granite on the Higher Himalayas, vol XLVII, no. 2. Memoirs of the Faculty of Science, Kyoto University, Series Geology and Mineralogy, Kyoto, pp 149–157
Kali E, Leloup PH, Arnaud N, Mahéo G, Liu D, Boutonnet E, VanderWoerd J, Xiaohan L, Liu-Zeng J, Haibing L (2010) Exhumation history of the deepest central Himalayan rocks (Ama Drime range): key P-T-D-t constraints on orogenic models. Tectonics 29:1–31
Kaneko Y, Katayama I, Yamamoto H, Misawa K, Ishikawa M, Rehman HU, Kausar AB, Shiraishi K (2003) Timing of Himalayan ultrahigh-pressure metamorphism: sinking rate and subduction angle of the Indian continental crust beneath Asia. J Metamorph Geol 21(6):589–599
Krummanacher D (1961) Détermination d'âge isotopique faites sur quelque roches de l'Himalaya du Népal par la méthode potassium-argon. Bulletin de suisse Minéralogie et Pétrologie 41:273–283
Krummanacher D (1966) Népal Central: géochronométrie des séries de l'Himalaya. Bulletin de suisse Minéralogie et Pétrologie 46:43–54
Kruparz H (1953) Das Profil Kathmandu (Nepal)-Nyalam Dzong (Süd-Tibet). In: Küpper H, Exner Ch, Grubinger H (eds) Skizzen zum Antlitz der Erde. Verlag Bruder Hollinek, Wien, pp 60–71
Langille JM, Jessup MJ, Cotte JM, Newell D, Seward G (2010) Kinematic evolution of the Ama Drime detachment: insights into orogen-parallel extension and exhumation of the Ama Drime Massif, Tibet-Nepal. J Struct Geol 32:900–919
Law RD, Searle MP, Simpson RL (2004) Strain, deformation temperatures and vorticity of flow at the top of the Greater Himalayan slab, Everest massif, Tibet. J Geol Soc London 161:305–320
Le Fort P (1971) Les formations cristallophylliennes de la Thakkhola. In: Bordet P, Colchen M, Krummenacher D Le Fort P, Mouterde R, Rémi M (eds) Recherches géologiques dans l'Himalaya du Népal, région de la Thakkhola. Centre National de la Recherche Scientifique, Paris, pp 41–81
Le Fort P (1975) Himalayas, the collided range: present knowledge of the continental arc. Am J Sci 275-A:1–44
Le Fort P, Pecher A, Vidal Ph (1982) Les gneiss oeilles de la Dalle du Tibet: un episode magmatique au Paleozoique inferieur en Himalaya du Nepal. 9eme Reun Annu Sci de la Terre, Paris, Soc Geol Fr ed, p 369
Le Fort P (1989) The Himalayan orogenic segment. In: Sengör AMC (ed) Tectonic evolution of the Tethyan region. Kluwer, Dordrecht, pp 289–386
Le Fort P (1996) Evolution of the Himalaya. In: Yin A, Harrison TM (eds) The tectonics of Asia. Cambridge University Press, New York, pp 95–106
Le Fort P, Cuney M, Deniel C, France-Lanord C, Sheppard SMF, Upreti BN, Vidal P (1987) Crystal generation of the Himalayan leucogranites. Tectonophysics 134:39–57
Le Fort P, Debon F, Sonet J (1980) The "Lesser Himalayan" cordierite granite belt: typology and age of the pluton of Manserah (Pakistan), vol 13, Geological Bulletin (Special Issue). University of Peshawar, Peshawar, pp 51–61
Le Fort P, Debon F, Sonet J (1983) The lower Paleozoic "Lesser Himalayan" granitic belt: emphasis on the Simchar pluton of central Nepal. In: Shams FA (ed) Granites of Himalaya, Karakorum, and Hindu-Kush. Institute of Geology, Punjab University, Lahore, pp 235–255
Lee J, Hacker BR, Dinklage WS, Wang Y, Gans P, Calvert A, Wan J-L, Chen W, Blythe AE, McClelland W (2000) Evolution of

Kangmar Dome, southern Tibet: structural, petrologic, and thermochronologic constraints. Tectonics 19(5):872–895
Liu Y, Siebel W, Massonne H-J, Xiao X (2007) Geochronological and petrological constraints for tectonic evolution of the central Greater Himalayan sequence in the Kharta area, southern Tibet. J Geol 115:215–230
Lombard A (1952) Les grandes lignes de la géologie du Népal Oriental, vol LXI, Fascicule 3. Bulletin de la Société Belge de Géologie de Paléontologie et d'Hydrologie, Bruxelles, pp 260–264
Lombardo B, Rolfo F (2000) Two contrasting eclogite types in the Himalayas: implications for the Himalayan orogeny. J Geodyn 30:37–60
Macfarlane AM (1995) An evaluation of the inverted metamorphic gradient at Langtang National Park. J Metamorph Petrol 13:595–612
Macfarlane AM, Hodges KV, Lux D (1992) A structural analysis of the Main Central Thrust Zone, Langtang National Park, Central Nepal Himalaya. Geol Soc Am Bull 104:1389–1402
Mallet FR (1874) On the geology and mineral resources of the Dárjíling District and the Western Duárs. Mem Geol Surv India XI(Part 1):1–96 (with two colored geological maps (of Darjeeling Hill Territory and Western Bhootan Dooars) of 1 in. = 4 miles scale)
Martin AJ, DeCelles PG, Gehrels GE, Patchett PJ, Isachsen C (2005) Isotopic and structural constraints on the location of the Main Central Thrust in the Annapurna Range, central Nepal Himalaya. Geol Soc Am Bull 117:926–944
Maruo Y, Kizaki K (1983) Thermal structure in the nappes of Eastern Nepal Himalayas. In: Shams FA (ed) Granites of Himalaya, Karakorum and Hindu-Kush. Institute of Geology, Punjab University, Lahore, pp 271–286
McMahon CA (1877) The Blaini Group and the "Central Gneiss" in the Simla Himalayas, Rec Geol Surv India X:204–223
McMahon CA (1882) The Geology of Dalhousie, North-West Himalaya. Rec Geol Surv India XV:34–51
McMahon CA (1883) On the microscopic structure of some Dalhousie rocks. Rec Geol Surv India XVI:129–144 (with 2 plates)
McMahon CA (1887) Some remarks on pressure metamorphism with reference to the foliation of the Himalayan gneissose-granite. Rec Geol Surv India XX:203–205
Middlemiss CS (1887) Physical Geology of West British Garhwal; with notes on a route traverse through Jaunsar-Bawar and Tiri-Garhwal. Rec Geol Surv India XX:26–40 (with 1 plate and two maps in colors; scales 1 in. = 4 miles and 1 in. = 1 mile)
Mitchell AHG (1981) Himalayan and Transhimalayan granitic rocks in and adjacent to Nepal and their mineral potential. J Nepal Geol Soc 1(1):41–52
Morrison CWK, Oliver GJH (1993) A study of illite crystallinity and fluid inclusions in the Kathmandu Klippe and the Main Central Thrust zone, Nepal. In: Treloar PJ, Searle MP (eds.) Himalayan tectonics, No. 74. Geological Society Special Publication, London, pp 525–540
Mukherjee BK, Sachan HK (2001) Discovery of coesite from Indian Himalaya: a record of ultra-high pressure metamorphism in Indian continental crust. Curr Sci 81:1358–1361
O'Brien PJ, Zotov N, Law R, Khan MA, Jan MQ (2001) Coesite in Himalayan eclogite and implications for models of India-Asia collision. Geology 29:435–438
Odell NE (1925) Observation on the rocks and glaciers of Mount Everest. Geograph J LXVI(4):289–315 (with a map in colors on 1:25,000 scale)
Odell NE (1983) On the occurrence of granites in the Himalayan mountains. In: Shams FA (ed) Granites of Himalayas, Karakorum, and Hindu Kush. Punjab University, Lahore, pp 1–10
Ohta Y (1973) Geology of the Nepal Himalayas. In: Hashimoto S, Ohta Y, Akiba C (eds) Geology of the Nepal Himalayas, Saikon Publishing Co. Ltd., Tokyo, pp 235–259
Oldham RD (1883) Note on a traverse between Almora and Mussooree made in October 1882. Rec Geol Surv India XVI:162–164
Oldham RD (ed) (1893) A manual of the Geology of India: stratigraphic and structural geology, 2nd edn. Geological Survey of India, Calcutta, 543 pp (with a geological map of India in colors, scale: 1 in. = 96 miles)
Pandey MR, Tandukar RP, Avouac J-P, Vergne J, Héritier T (1999) Seismotectonics of Nepal Himalayas from a local seismic network. J Asian Earth Sci 17:703–712
Parkinson CD, Kohn MJ (2002) A first record of eclogite from Nepal and consequences for the tectonic evolution of the Greater Himalayan sequence. Eos Trans Am Geophys Union 83(19): V42A–11
Parrish RR, Hodges KV (1996) Isotopic constraints on the age and provenance of the Lesser and Greater Himalayan sequences, Nepalese Himalaya. Geol Soc Am Bull 108:904–911
Parrish RR, Gough SJ, Searle MP, Waters DJ (2006) Plate velocity exhumation of ultrahigh-pressure eclogites in the Pakistan Himalaya. Geology 34:989–992
Pêcher A (1989) The metamorphism in the Central Himalaya. J Metamorph Geol 7:31–41
Pêcher A (1991) The contact between the Higher Himalaya Crystallines and the Tibetan sedimentary series: Miocene large-scale dextral shearing. Tectonics 10(3):587–598
Pêcher A, Le Fort P (1986) The metamorphism in central Nepal Himalaya, its relations with the thrust tectonic. In: Le Fort P, Colchen M, Montenat C (eds) Évolution des domaines orogéniques d'Asie méridionale (de la Turquie à l'Indonésie), no. 47. Livre jubilaire Pierre Bordet, Sciences de la Terre, Mémoire, Nancy, pp 285–309
Pognante U, Spencer DA (1991) First report of eclogites from the Himalayan belt, Kaghan valley (northern Pakistan). Eur J Mineral 3:613–618
Rai SM, Guillot S, Le Fort P, Upreti BN (1998). Pressure–temperature evolution in the Kathmandu and Gosainkund regions, Central Nepal. J Asian Earth Sci 16(2–3):283–298
Rai SM, Upreti BN, Parrish R, Copeland P, Le Fort P (2011) U–Pb ages of Nardanda Pegmatite of the Kathmandu Crystalline Nappe and augen gneisses of the Gosainkund Crystalline Nappe, central Nepal Himalaya. J Nepal Geol Soc 43(Special Issue):37–44
Ramberg H (1967) Gravity, deformation, and the earth's crust. Academic Press, New York, 214 pp
Ramsay JG, Huber MI (1987) The techniques of modern structural geology, vol 2. Academic Press, London, pp 309–700
Richards A, Argles T, Harris N, Parrish R, Ahmad T, Darbyshire F, Draganits E (2005) Himalayan architecture constrained by isotopic tracers from clastic sediments. Earth Planet Sci Lett 236:773–796
Richards A, Parrish R, Harris N, Argles T, Zhang L (2006) Correlation of lithotectonic units across the eastern Himalaya, Bhutan. Geology 34:341–344
Robinson DM, DeCelles PG, Copeland P (2006) Tectonic evolution of the Himalayan thrust belt in western Nepal: implications for channel flow models. Geol Soc Am Bull 118:865–885
Robinson DM, DeCelles PG, Garzione CN, Pearson ON, Harrison TM, Catlos EJ (2001) The kinematic evolution of the Nepalese Himalaya interpreted from Nd isotopes. Earth Planet Sci Lett 192:507–521
Robinson DM, DeCelles PG, Patchett J, Garzione CN (2003) Kinematic model for the Main Central thrust in Nepal. Geology 31:359–362
Sakai H, Takigami Y, Nakamura Y, Nomura H (1999) Inverted metamorphism in the Pre-Siwalik foreland basin sediments beneath the crystalline nappe, western Nepal Himalaya. J Asian Earth Sci 17:727–739
Schärer U, Xu R, Allègre CJ (1986) U–(Th)–Pb systematics and age of Himalayan leucogranites, south Tibet. Earth Planet Sci Lett 77:35–48

Schelling D, Arita K (1991) Thrust tectonics, crustal shortening, and the structure of the far-eastern Nepal Himalaya. Tectonics 10 (5):851–862

Searle MP (1989) Structural evolution and sequence of thrusting in the High Himalayan, Tibetan-Tethys and Indus suture zones of Zanskar and Ladakh, Western Himalaya. J Struct Geol 8(8):923–936

Searle MP, Rex AJ (1989) Thermal model for the Zanskar Himalaya. J Metamorph Geol 7:127–134

Searle MP, Simpson RL, Law RD, Parrish RR, Waters DJ (2003) The structural geometry, metamorphic and magmatic evolution of the Everest massif, High Himalaya of Nepal–south Tibet. J Geol Soc London 160:345–366

Searle MP, Law RD, Godin L, Larson KP, Streule MJ, Cottle JM, Jessup MJ (2008) The Himalayan Main Central Thrust in Nepal. J Geol Soc London 165:523–534

Shrestha SB, Shrestha JN (1984) Geological map of Eastern Nepal. Department of Mines and Geology, Kathmandu

Sorkhabi RB, Stump ES (1993) Rise of Himalaya: a geochonologic approach. GSA Today 3(4):85–92

Stöcklin J (1980) Geology of Nepal and its regional frame. J Geol Soc London 137:1–34

Stöcklin J, Bhattarai KD (1977) Geology of Kathmandu area and central Mahabharat Range, Nepal Himalaya. HMG/UNDP mineral exploration project, technical report, 86 pp (with 15 maps), unpublished

Stoliczka F (1866) Geological sections across the Himalayan Mountains, from Wangtu-Bridge on the river Sutlej to Sungdo on the Indus: with an account of the formations in Spiti; accompanied by a revision of all known fossils from that district. Mem Geol Surv India V(Part 1):pp 1–154 (with 1 map, 6 sections in colors, and 10 plates of fossils)

Strachey R (1851) On the geology of part of the Himalaya Mountains and Tibet. Q J Geol Soc London 7:292–310 (with a geological map and two cross-sections in colors)

Tonarini S, Villa I, Oberli F, Meier M, Spencer DA, Pognante U, Ramsay JG (1993) Eocene age of eclogite metamorphism in the Pakistan Himalaya: implications for India-Eurasia collision. Terra Nova 5:13–20

Upreti BN, Le Fort P (1999) Lesser Himalayan crystalline nappes of Nepal: problems of their origin. In: Macfarlane AM, Sorkhabi RB (eds) Himalaya and Tibet: mountain roots to mountain tops, vol 328. Geological Society of America, Special Papers, pp 225–238

Valdiya KS (1977) Structural set-up of the Kumaun Lesser Himalaya. Colloques internationaux du C.N.R.S., no. 268. Écologie et Géologie De L'Himalaya, Paris, pp 449–462

Wager LR (1939) The Lachi series of North Sikkim and the age of the rocks forming Mount Everest. Rec Geol Surv India 74(Part 2):pp 171–188 (with 5 plates)

Xu RH, Schärer U, Allègre CJ (1983) U/Pb dating of the orogenic events in the Himalayas and in the Tibetan Plateau. Terra Cognita 3 (2/3):273

Yin A (2006) Cenozoic tectonic evolution of the Himalayan orogen as constrained by along-strike variation of structural geometry, exhumation history, and foreland sedimentation. Earth Sci Rev 76:1–131

Zeitler PK, Chamberlain CP (1991) Petrogenetic and tectonic significance of young leucogranites from the northwestern Himalaya, Pakistan. Tectonics 10(4):729–741

Higher Himalaya of Mahakali–Seti Region 14

The basis of the 30 km thick crust, pushed from the northeast, slipped easily forward on the fluid substratum.
—A. Heim and A. Gansser (1939, p. 225)

Heim and Gansser (1939) established the stratigraphy and structure of the Higher Himalayan crystallines for the first time from Kumaun of India and the contiguous west border of Nepal. They showed that the Higher Himalayan rocks, belonging to the Central Crystalline Zone as well as the Chhiplakot, Askot, and Almora klippen in Kumaun, continue towards Nepal. Gansser (1964) slightly differed from their earlier interpretations, and inferred an out-of-sequence thrust between the Main Central Thrust and the Almora Thrust, encompassing all the above klippen. Fuchs and Sinha (1978) followed the interpretation of Heim and Gansser (1939), however, Valdiya (1980) included these klippen under his Almora Group of rocks, forming a separate thrust sheet. Hagen (1969) questioned the continuity of the Almora crystalline klippe in Nepal, and considered the Dadeldhura zone as a parautochthonous unit. Subsequently, Bashyal (1986) mapped these tectonic outliers in Nepal, respectively, as the Bajhang, Parchuni, and Dadeldhura klippen.

14.1 Darchula Neighborhood

The Main Central Thrust appears to the north of Darchula as a sharp fault, where it overrides crystalline limestones and slates. It exhibits an almost flat (about 10°) hanging wall and a more steeply dipping footwall. Farther to the west, the footwall also encloses amphibolites of gabbro–dioritic composition injected in quartzites (Gansser 1964, p. 104). In the Mahakali section, the hanging wall is made up of gneisses, represented by uniformly coarse-grained biotite and alkali feldspar with sporadic plagioclase. There are large perthitic grains of orthoclase, quartz with strong undulatory extinction, intensely pleochroic biotite, and a groundmass of quartz and sericite. The thick basal gneiss bodies pass upwards to more schistose augen gneisses, containing large grains of amethyst (Gansser 1939, p. 78). Some lenticular bodies (reaching up to 300 m in thickness) of augen gneisses contain very coarse biotite and very big (up to 16 cm in length) feldspar augen, exposed to the north of Phangu. These rocks are frequently minutely folded and occur within biotite–sericite schists.

The above biotite–sericite schists observed at the village of Soso are followed by a conspicuous white quartzite band with amphibolite of about 100 m in thickness. They constitute the base of the sedimentary zone of Sirdang (Fig. 14.1). The main green, massive, body of amphibolite at Soso is a coarse biotite–amphibolite with dispersed large hornblende grains (Gansser 1939, p. 79).

The sedimentary zone of Sirdang begins with a thick succession of dark gray phyllitic slates with thin marble intercalations. The slates are abundantly graphitic and also contain small scales of biotite and sericite, but they are devoid of lime. In them, quartz forms small polygonal grains, whereas small idiomorphic tourmaline and rather large zoisite grains are present as accessories. The black graphitic slates are followed upwards by muscovite-bearing gray marbles. The marble band above the village of Sirdang is about 20 m thick, and in it the main mineral is tabular calcite, whereas some quartz and muscovite flakes are arranged parallel to the cleavage (Gansser 1939, p. 81).

The upper crystalline zone is observed north of Sirdang. Its base is marked by thick snow-white sericite quartzites, which overlie an amphibolite band. There is also a thin amphibolite band just below the Main Central Thrust (Figs. 14.1 and 14.2). The Higher Himalayan rocks, comprising its hanging wall, dip at an angle of 30–60°, and are transitionally followed upwards by the Paleozoic rocks of the Tethys Himalaya. The upper crystalline zone (including its passage zone to the lowermost Tethyan rocks) is subdivided into the following units (Gansser 1939, pp. 82–88).

(h) Calcareous zone of Garbyang (of the Tethys Himalaya) follows the Budhi Schists.
(g) Towards Budhi, the pegmatites die out, metamorphism decreases, and biotite porphyroblast-bearing schists appear.
(f) Fine-grained gneisses and calc-silicate layers with profuse pegmatite dikes.
(e) Migmatitic gneisses.

M.R. Dhital, *Geology of the Nepal Himalaya*, Regional Geology Reviews,
DOI 10.1007/978-3-319-02496-7_14

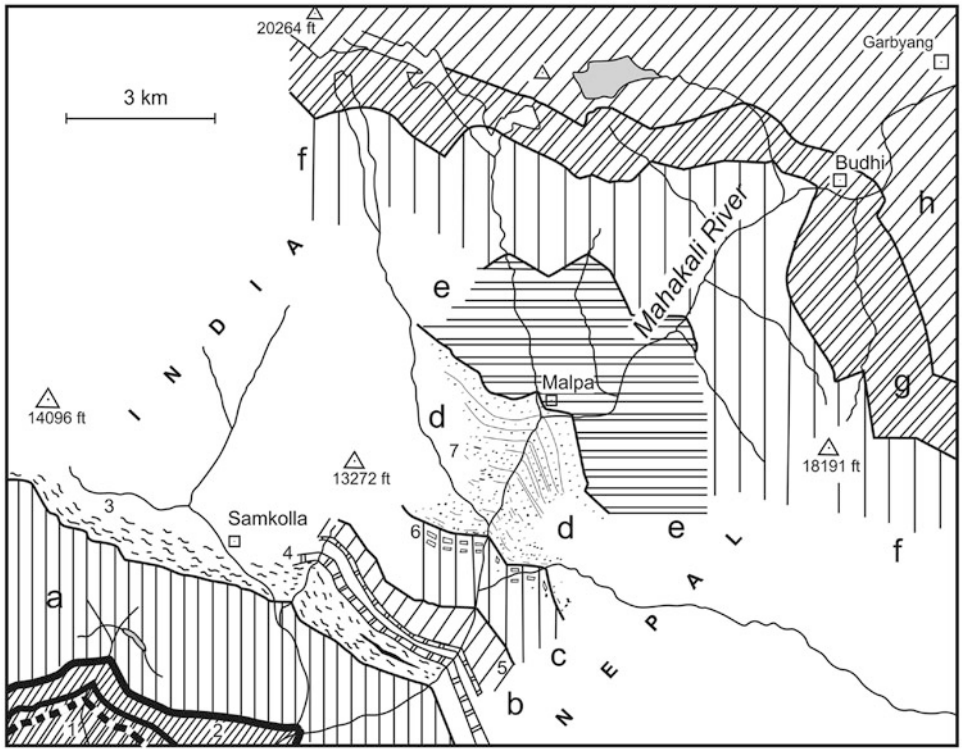

Fig. 14.1 Geological sketch of the Higher Himalayan rocks cropping out north of Darchula. *1*. Graphitoid schists with marbles. *2*. Quartzite with amphibolite sills: *a* muscovite–biotite gneiss, partly injected; *b* schists (*3*) with orthogneiss (*4*) and injected gneiss (*5*); *c* injection gneiss with some calc-silicate layers (*6*); *d* quartzite with kyanite–garnet schists (*7*); *e* injection gneisses with some pegmatite dikes; *f* complex zone of biotite–psammite gneiss with calc-silicate marble layers both pierced by dikes of pegmatite; *g* biotite porphyroblast zone of Budhi; *h* zone of Garbyang. *Source* Modified from Gansser (1939)

(d) Quartzite and mica schist.
(c) Migmatitic gneisses with the first lime-silicate layers in their upper part.
(b) Schists with minor gneiss injections.
(a) Large mass of injected muscovite-biotite gneiss.

Based on tectonic and petrographic investigations, Heim and Gansser (1939) reconfirmed the primary sedimentary source of the Higher Himalayan crystallines. Their thickness varies from 10 km in the Mahakali River section to about 20 km in west Kumaun. The magmatic injections, intrusions, and dikes are all younger than the original sedimentary deposits. These crystallines must be older than the overlying Garbyang or Martoli Formation as well as other younger Paleozoic and Mesozoic rocks of the Tethys Himalaya.

14.1.1 Zone a

Above the thin amphibolite sill, observed north of Sirdang, overlies a large injected (migmatitic) gneiss body. It is a strongly micaceous, garnet-bearing, biotite–muscovite gneiss of irregular banding. Under the microscope, the gneiss exhibits slightly undulatory, lobate quartz, twinned oligoclase, highly pleochroic biotite, bluish gray tourmaline, and less abundant muscovite. There is also a relictic idiomorphic garnet and apatite as an accessory mineral. Apart from oligoclase, alkali feldspar (mainly orthoclase with some obliterated microcline) is also abundant. At some localities, the rock is like greisen due to incipient mobilization of the gneisses.

14.1.2 Zone b

The migmatitic gneisses are followed upwards by dark garnetiferous biotite–psammite gneisses, containing quartz and oligoclase–andesine, xenomorphic garnet, and apatite as an accessory mineral. They are succeeded by a variety of rock types, including staurolite–garnet–biotite phyllites (with small idiomorphic dark red-brown garnets without inclusions, and large ones with abundant quartz and magnetite inclusions in the core).

14.1.3 Zone c

In its lower part are migmatitic gneisses, consisting of gray psammitic layers and white aplite bands. They are succeeded upwards by thin bands of lime-silicate rocks. Fine red garnets appear in the quartzose aplite bands, which are covered by a few centimeter-thick zoisite stalks. These stalks again alternate with garnet zones and some calcite-rich portions.

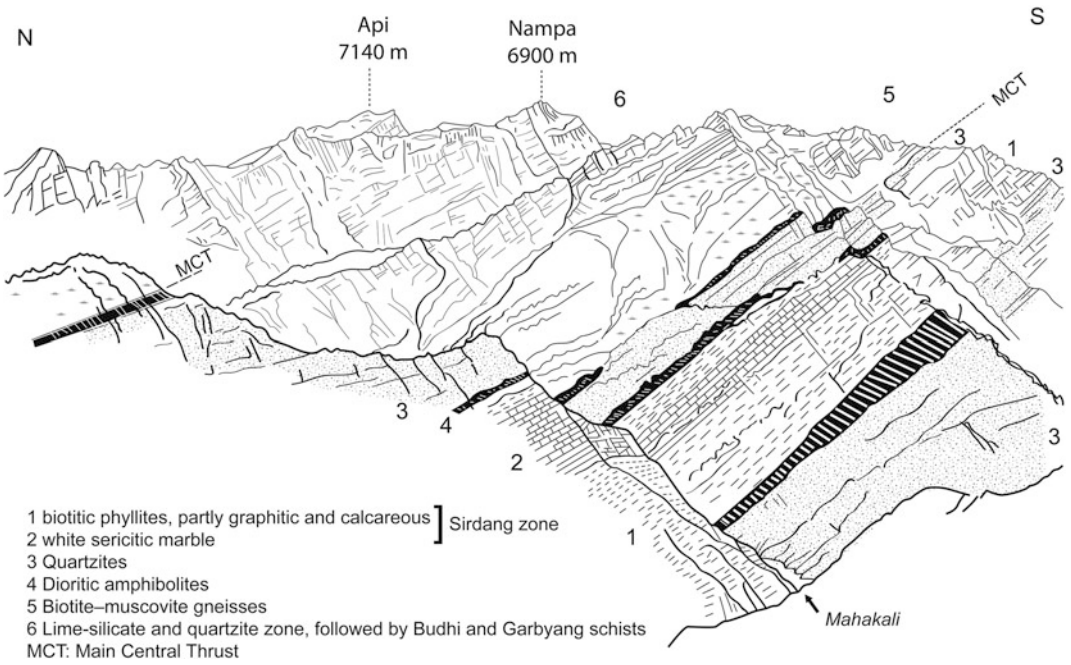

Fig. 14.2 The sedimentary Sirdang zone with the north branch of the Main Central Thrust. *Source* Modified from Gansser (1939).

14.1.4 Zone d

This zone consists of kyanite–garnet–biotite gneisses at the base and is overlain by a thick quartzite succession. The kyanite forms large stalks, whereas biotite appears as large brown sheets, and subordinate plagioclase represented by albite–oligoclase shows distinct twinned lamellas. There are also some large rutile grains in biotite and kyanite. This rock succession gradually passes into the sericite–quartzite of great thickness. It includes some sericite schists with vivid blue kyanite crystals of up to 8 cm in length, garnet, and tourmaline. The first pegmatite dikes are encountered in the middle portion of this zone, where they crosscut the quartzite bands. In the Alaknanda Valley, there is a huge (about 9 km thick) quartzite succession of Pandukeshwar, corresponding to this zone in the Mahakali River (Gansser 1939, p. 93). In these quartzites Auden (1935, p. 134) recorded conspicuous large planar cross-bedding. Similar very thick quartzite bands are also present in the Higher Himalayan succession of the Rasuwa Gadhi area in central Nepal (Chap. 17).

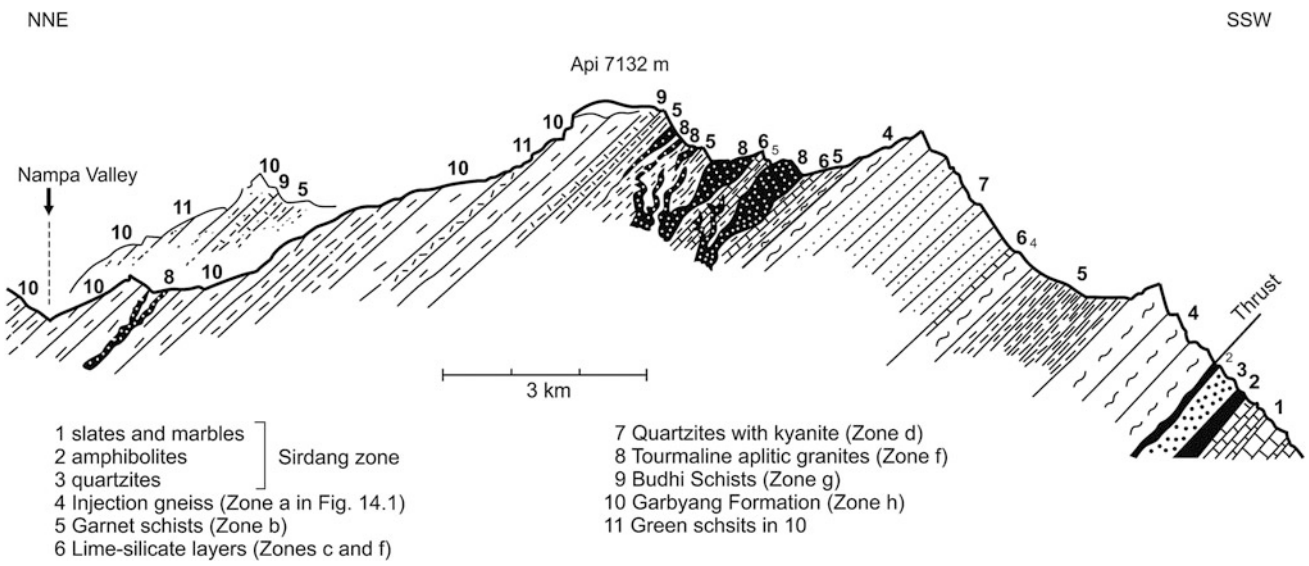

Fig. 14.3 Section across Mount Api with tourmaline-granite intrusions. *Source* Modified from Gansser (1939)

14.1.5 Zone e

This zone is characterized by the increasing abundance in number as well as size of pegmatite and aplite dikes. There also occur augen gneisses around Malpa, where some augen are up to 10 cm in length. The several-meter-thick pegmatite dikes contain plentiful crystals of zoned tourmaline. There also appear some large granite dikes and smaller stocks of a fine-grained muscovite granite, and very characteristic muscovite–tourmaline–aplite granites. Such granite bodies are well exposed in the vicinity of Api Himal (Gansser 1964, p. 106; Figs. 14.3 and 14.4). Their typical chemical composition is summarized in Table 14.1.

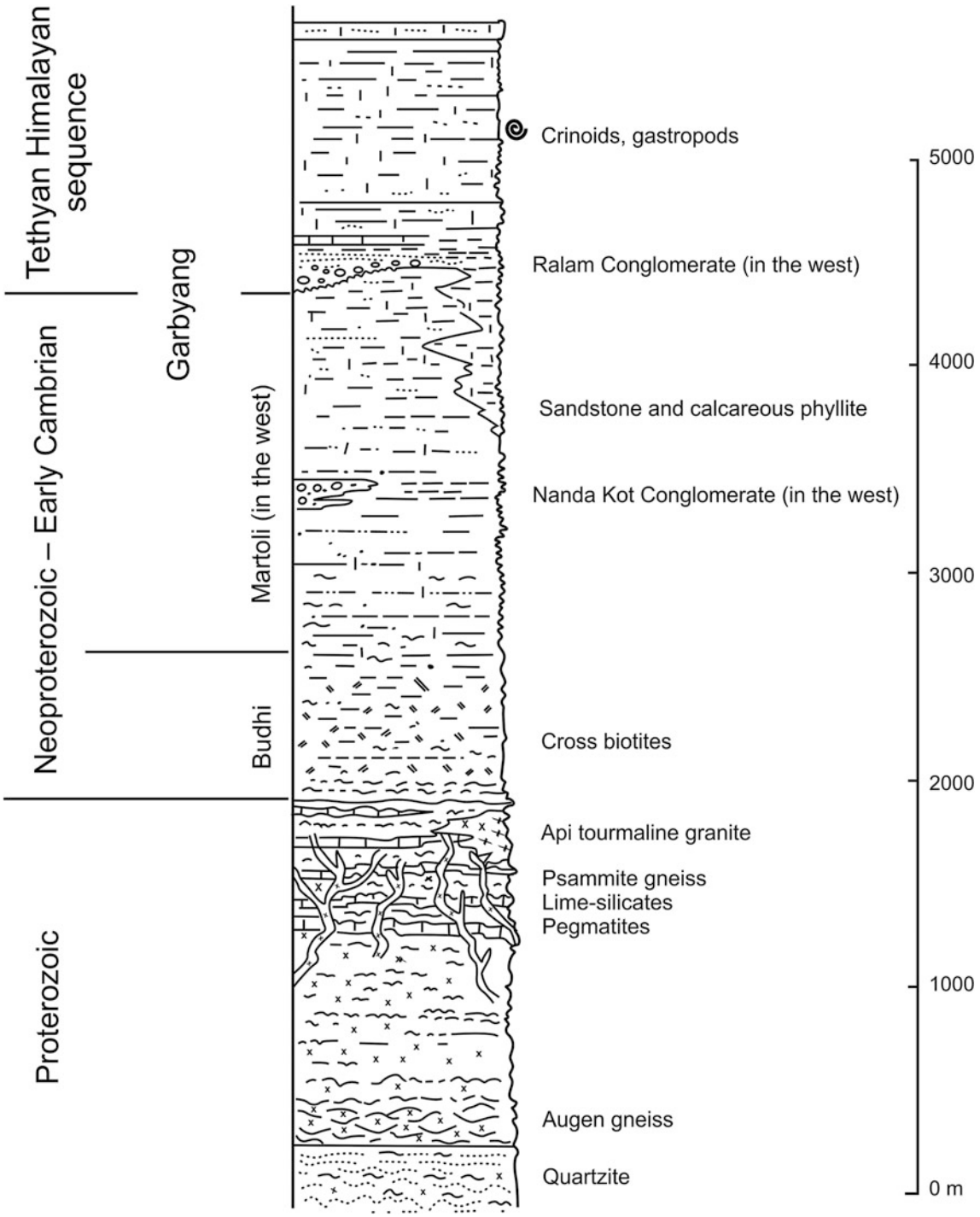

Fig. 14.4 Stratigraphy of Higher Himalayan crystallines exposed in the Mahakali River section. *Source* Modified from Gansser (1964)

Table 14.1 Chemical composition of granite from Api Himal

Component	Percent
SiO_2	71.90
Al_2O_3	15.41
Fe_2O_3	–
FeO	0.78
MgO	0.16
CaO	0.75
Na_2O	5.26
K_2O	3.82
TiO_2	0.11
P_2O_5	0.27
H_2O	0.95
B_2O_3	0.64
Total	100.05

Source Gansser (1939)

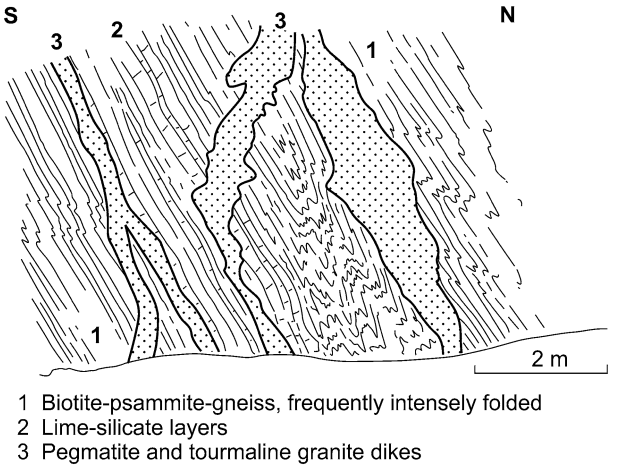

Fig. 14.5 Details of lime-silicate and psammite gneisses with pegmatites and granitic dikes. Small-scale folds are well developed in the gneiss. *Source* Modified from Gansser (1939)

14.1.6 Zone f

This zone extends almost throughout the western Higher Himalaya. It is very complex and petrographically diverse. In this zone, highly metamorphosed lime-silicate marble bands (up to 20 m thick) alternate with finely stratified psammitic gneisses. The rock is minutely folded and injected by a swarm of pegmatite and aplite dikes and veins, which traverse the rock in all directions. Some dikes of granite reach a thickness of 20 m. Mostly well-banded lime-silicate horizons vary considerably in composition. There are variations from lime-silicate gneisses to large diopside calc-marbles and coarse-crystalline scapolite-bearing phlogopite marbles. Some intercalated plagioclases are of labradorite or even more basic type (Gansser 1964, p. 107).

14.1.7 Zone g: Budhi Schists

With a decrease in metamorphism, the dikes characteristic of the last zone gradually disappear and so do the marbles. Although the decrease in metamorphism corresponds to the disappearance of dikes, no direct relationship between metamorphism and dike intrusion exists, inasmuch as the pegmatite and granite dikes crosscut the metamorphic rock without any visible trace of tectonic disturbance, and the surrounding rocks are intensely folded (Fig. 14.5). The regional metamorphism has a more deep-seated cause, and the dike intrusions are a possible follow-up (Gansser 1964, p. 107).

The distinctive feature of this zone is the occurrence of schists with biotite porphyroblasts. They are called the Budhi Schists, and constitute the passage zone from the underlying comparatively more metamorphosed psammitic gneiss to the overlying slightly metamorphic sequence of Garbyang. The Budhi Schists include large biotite porphyroblasts with sieve-like quartz inclusions, and some of the biotite flakes lie obliquely to foliation, indicating their subsequent rotation (Gansser 1939, p. 88).

14.1.8 Zone h: Garbyang Formation

The low-grade metamorphic rocks of the Garbyang Formation overlie the Budhi Schists. They are very fine-grained, slightly sericitic, arenaceous to calcareous phyllites with dolomitic and green chloritic bands.

The Martoli Formation (about 5 km thick) and Ralam Conglomerate replace the Garbyang Formation in the Northwest Higher Himalaya of Kumaun. The Martoli Formation consists of little metamorphosed calcareous and noncalcareous phyllites with quartzite alternations. It is joined to the underlying crystalline rocks not only by a passage in decreasing metamorphism upwards, but also by some of the last pegmatite dikes. The Martoli Formation is about 5 km thick (Heim and Gansser 1939, p. 202).

The Ralam Conglomerate is exposed on both flanks of the Ralam Pass, and consists primarily of quartzite pebbles, cobbles, and boulders in black or red quartzitic groundmass. At a few places, it has an erosional contact with the underlying Martoli Formation. The conglomerate passes gradually into a gray to purple and green, very hard and massive quartzite (500–800 m), followed by yellow to orange, weathered, massive dolomite (50–100 m). This formation is not represented in the Mahakali River section (Heim and Gansser 1939, p. 202).

14.2 Dadeldhura Klippe

The Higher Himalayan crystallines of the Dadeldhura area form a large klippe (Fig. 7.1), which is an east continuation of the Almora klippe in Kumaun. Its lower part consists of gray-green garnet schists, quartzites, and gneisses. They are variously named the Sallyani Gad Formation (Shrestha et al. 1985) or the Gaira schist and Saukharka granite–gneiss (Bashyal 1986). The Paleozoic Dadeldhura Granite is intruded into this unit (Chap. 7). The synclinal core of the Dadeldhura klippe is composed predominantly of green-gray to dark gray phyllites or schists with or without bands of quartzite, calcareous quartzite, and crystalline limestone. They belong to the Melmura and Damgad formations (Shrestha et al. 1985) of presumable early Paleozoic age. These strongly lineated and crenulated rocks occasionally contain a number of mesoscopic folds. Some pegmatite veins and sporadic amphibolite bands also appear in this formation (Upreti 1990). This chiefly pelitic succession is comparable with the Garbyang Formation.

References

Auden JB (1935) Traverses in the Himalaya. Rec Geol Surv India LXIX(Part 2):123–167 (with 6 plates including a geological sketch map)

Bashyal RP (1986) Geology of Lesser Himalaya, far western Nepal. In: Le Fort P, Colchen M, Montenat C (eds) Évolution des domaines orogéniques d'Asie méridionale (de la Turquie à l'Indonésie), Livre jubilaire Pierre Bordet, Sciences de la Terre, Mémoire no 47, Nancy, pp 31–42

Fuchs G, Sinha AK (1978) The tectonics of the Garhwal–Kumaun Lesser Himalaya. Jahrbuch der Geologischen Bundesanstalt, Wien, Band 121, Heft 2, pp 219–241 (with 1 plate containing geological map in colors, Scale: 1:500 000)

Gansser A (1939) The Central High Range (Nampa–Nanda Devi–Badrinath). In: Heim A, Gansser A (eds) Central Himalaya: Geological Observations of the Swiss Expedition 1936. Denkschriften der Schweizerischen Naturforschenden Gesellschaft, Band LXXIII, Abh 1, pp 62–97

Gansser A (1964) Geology of the Himalayas. Interscience, New York, 289 pp

Hagen T (1969) Report on the geological survey of Nepal. Volume 1: Preliminary reconnaissance. Denkschiiften der Schweizerischen Naturforschenden Gesellschaft, Band LXXXVI/1, 185 pp (with a geological map)

Heim A, Gansser A (1939) Central Himalaya: Geological Observations of the Swiss Expedition 1936. Denkschriften der Schweizerischen Naturforschenden Gesellschaft, Band LXXIII, Abh 1, 245 pp (with geological maps in colors, sections, and plates)

Shrestha SB, Shrestha JN, Sharma SR (1985) Geological map of Far-Western Nepal. Scale: 1:250 000. Department of Mines and Geology, Kathmandu

Upreti BN (1990) An outline geology of far western Nepal. J Himalayan Geol 1:93–102

Valdiya KS (1980) Geology of Kumaun Lesser Himalaya. Wadia Institute of Himalayan Geology, Dehra Dun, 291 pp (with a geological map in colors)

Higher Himalaya of Karnali–Bheri Region 15

In my report for February, I mentioned that General Jung Bahadur had sent us a large collection of ninety-six kinds of rocks and ores.

—H. Piddington (1854, p. 170)

The Higher Himalayan crystallines that form the south slopes of the Great Himalayan Range enter this territory from the Mahakali–Seti region and continue farther east in the Gandaki region with a rather diminished thickness. The Almora–Dadeldhura–Karnali klippe extends up to this region as an open synform with crystallines grading upwards into the Tethyan Himalayan sequence (Fig. 8.1). Concentrated erosion of yesteryear has dissociated the synform from the adjacent Jaljala klippe, which too is analogously folded and contains some Tethyan outliers.

15.1 Crystallines Around Galwa Window

The Galwa tectonic window (Fig. 8.2) is surrounded by the Higher Himalayan rocks, comprising two-mica gneisses, quartzitic gneisses, quartzites, garnet–kyanite–mica schists or gneisses, amphibolites, and calc-gneisses. This rock assemblage is succeeded upwards by a several thousand-meter-thick complex of granite–gneiss, migmatite, paragneiss, and carbonate rocks. Kyanite, commonly occurring in the lower part of the sequence, is replaced by sillimanite towards the top (Fuchs 1974). The Mugu Granite (Hagen 1969) is intruded in the north part of the Higher Himalayan crystallines.

The Mugu Granite is a medium-grained rock with a hypidiomorphic texture. It contains twinned and zoned microcline phenocrysts of up to 1 cm in length, and they enclose plagioclase, biotite, muscovite, and some sillimanite, whose long axis is parallel to the zoned rims of K-feldspar (Fuchs 1977).

There is no hard and fast boundary between the Mugu Granite and the migmatite complex. Migmatization was only in part brought about by the Mugu Granite, because the migmatites contain older augen gneisses and some paragneisses, which are crosscut by folded granite veins. On the other hand, the granite contains many augen gneiss xenoliths (Fuchs 1977). A succession of calc-gneiss, marble, calc-schist, and calc-phyllite constitutes the roof of the granite. These rocks belong to the lower part of the Dhaulagiri Limestone, and in them the grade of metamorphism decreases stratigraphically upwards. The Higher Himalayan crystallines of this area are more than 10 km thick (Fuchs 1974).

15.2 Karnali Klippe and Underlying Sequences

The Higher Himalayan rocks of the Karnali klippe are thrust over the metasediments of the Lesser Himalaya. Yoneshiro and Kizaki (1996) give a fairly detailed account of stratigraphy, structure, and metamorphism of this area. The synformal Karnali klippe consists mainly of gneisses, which are thrust over the low-grade metamorphic rocks of the Lesser Himalaya along the Main Central Thrust. Fuchs and Frank (1970) mapped these crystalline rocks as their Upper Crystalline nappe, which is thrust over their Lower Crystalline nappe.

The Siwalik belt, with soft sandstones and mudstones, is thrust over by the sedimentary rocks of the Lesser Himalaya, consisting mainly of dolomites, quartz arenites, and shales. They belong broadly to the Lakharpata Group and are unconformably succeeded by the Surkhet Group (Fig. 15.1; Chap. 8) of rocks, comprising gray-green sandstones, black shales, and red-purple shales. The quartzites and amphibolites of the Ranimatta Formation override these youngest sedimentary rocks of the Lesser Himalaya along the Budar Thrust. The quartzites are fine- to coarse-grained, white, gray, and occasionally pink in color, and contain several interbands of amphibolite and phyllite at various levels. The Parajul Thrust produces the Ranimatta Formation, a sequence of pelitic phyllites, pelitic schists, quartzites, and mylonitic augen gneisses of the Dailekh Group (Fig. 15.1). The phyllites show well-developed foliation and lineation,

M.R. Dhital, *Geology of the Nepal Himalaya*, Regional Geology Reviews,
DOI 10.1007/978-3-319-02496-7_15

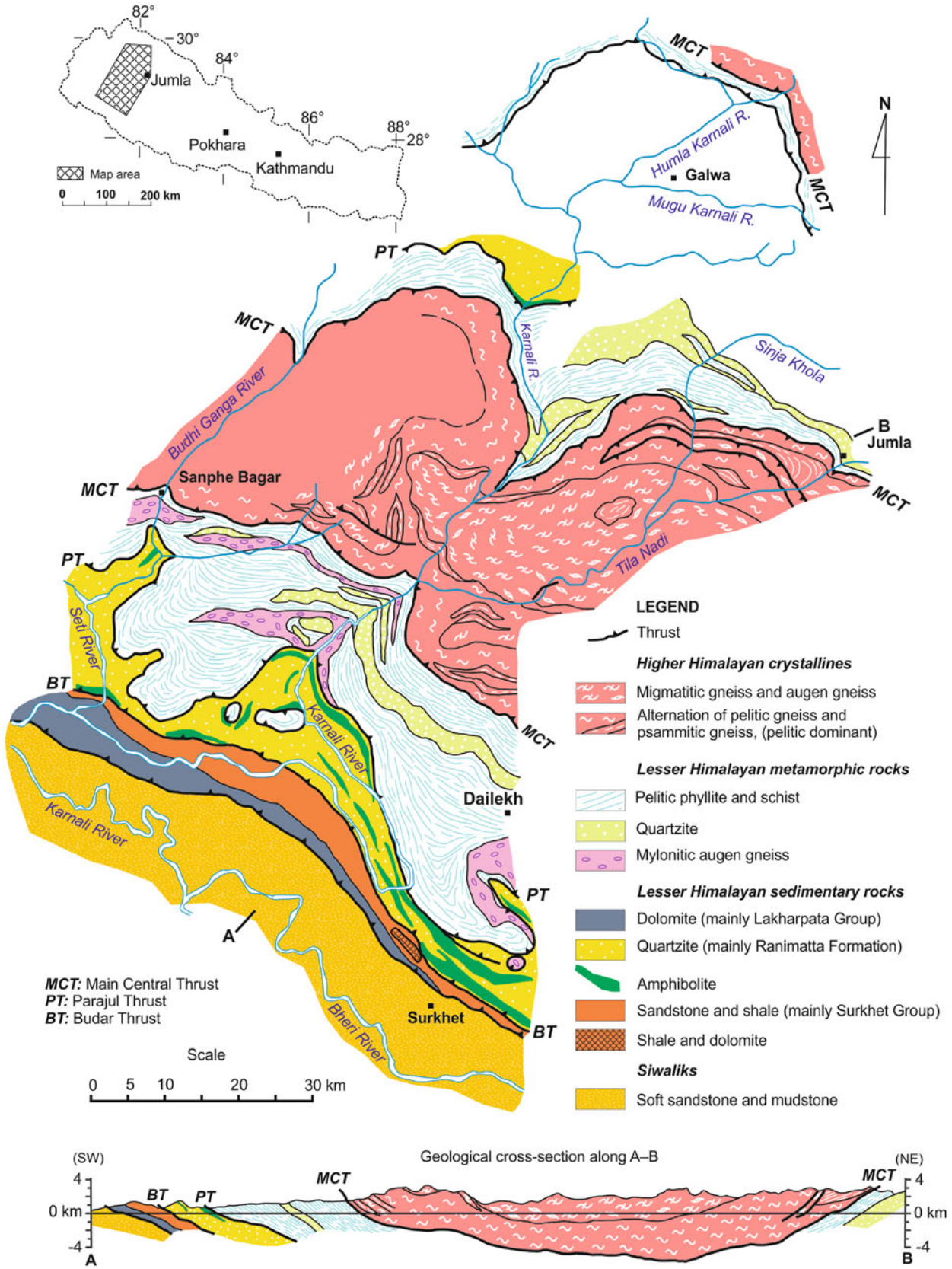

Fig. 15.1 Geology of Karnali klippe and neighborhood. *Source* Modified from Yoneshiro and Kizaki (1996). © Central Department of Geology, Tribhuvan University. Used by permission

and they also contain many quartz lenses and veins, especially near the Main Central Thrust. Also, in their middle and upper sections garnets become progressively abundant and their size increases from less than 1–10 mm. A few quartzite interbands found in the middle and upper parts contain sericite, whereas their less metamorphosed varieties preserve some wave ripples on their upper surfaces, which indicate a right-way-up sequence. The mylonitic augen gneisses have abundant K-feldspar porphyroblasts, and exhibit well-developed foliation and lineation.

The Higher Himalayan crystallines occupy the north and central portions, and they are represented by various kinds of gneisses, which can be subdivided into the lower pelitic and psammitic gneisses, and upper alternations of migmatitic gneisses and calc-silicate gneisses. Garnet and kyanite abound primarily in the pelitic gneisses of the lower part. The upper part of the crystallines contains a few scapolite-bearing calc-silicate bands. On the other hand, the migmatitic gneisses occupy mainly the core of the synformal Karnali klippe.

15.2.1 Metamorphic Mineral Assemblage

The Higher Himalayan pelitic gneisses contain mainly the following mineral assemblages: garnet–biotite–muscovite–plagioclase–quartz, kyanite–garnet–biotite–plagioclase–quartz ± muscovite, staurolite–garnet–biotite–muscovite–plagioclase–quartz, and kyanite–staurolite–garnet–biotite–muscovite–plagioclase–quartz. Among them, the first two are the most common assemblages. The rocks include a minor proportion of zircon, tourmaline, ilmenite, apatite, and rutile. Poikiloblastic garnet contains quartz, muscovite, and ilmenite. A snowball texture is observed in the garnet core, but it is absent in the rim.

The Higher Himalayan psammitic gneisses mainly include the following two assemblages: garnet–biotite–muscovite–plagioclase–quartz and biotite–muscovite–plagioclase–quartz. Out of these, the first assemblage is the most common one.

The low-grade metamorphic rocks of the Lesser Himalaya, constituting the footwall of the Main Central Thrust, show a variety of mineral assemblages, and the most frequent ones are: chlorite–muscovite–quartz, biotite–chlorite–muscovite–quartz ± plagioclase, cordierite–muscovite–quartz, cordierite–biotite–muscovite–plagioclase–quartz ± chlorite, garnet–biotite–cordierite–muscovite–plagioclase–quartz, staurolite–garnet–biotite–muscovite–plagioclase–quartz ± chlorite, and kyanite–garnet–biotite–muscovite–plagioclase–quartz. In contrast to the Higher Himalayan crystallines, these rocks are finer grained and well foliated. Most of the poikiloblastic garnets of this zone display a snowball texture. Many garnets are replaced by chlorites along their outer rim or cracks. Staurolite is arranged parallel to foliation, whereas the kyanite crystals of this zone are smaller than those found in the Higher Himalayan crystallines. The metasediments of the Ranimatta Formation contain a single assemblage of chlorite–muscovite–quartz ± plagioclase.

15.2.2 Metamorphic Zonation

Yoneshiro and Kizaki (1996) identified the following five metamorphic zones in the Karnali klippe. The zones are symmetrically distributed across the synform (Fig. 15.2).

Zone I is defined by a chlorite–muscovite assemblage, although unstable biotite appears close to Zone II. The following reactions are probable while passing from Zone I to II.

$$\text{Chlorite} + \text{K-feldspar} = \text{biotite} + \text{muscovite} + H_2O$$

$$\text{Phengite} + \text{chlorite} = \text{biotite} + \text{muscovite} + H_2O, \text{ or}$$

$$\text{Phengite} + \text{chlorite} = \text{biotite} + \text{chlorite} + \text{quartz}$$

In Zone II, an assemblage of biotite–chlorite–muscovite occurs widely, where chlorite is still stable (Yoneshiro and Kizaki 1996). The upper limit of Zone II is marked by the first appearance of the garnet–biotite association; on the other hand, Zone III contains basically a garnet-predominating assemblage, in which chloritoid occurs in its lower part. The higher-grade part of Zone III is defined by the breakdown of the chloritoid–biotite tie line to form a garnet–chlorite association.

Staurolite first appears in Zone IV, where it is present in chloritoid-bearing rocks, forming an assemblage of staurolite–garnet–biotite–chlorite–cordierite. Staurolite was formed at the expense of chloritoid. The higher-grade part in Zone IV is defined by the disappearance of the garnet–chlorite tie line and the appearance of the staurolite–biotite tie line.

Zone V begins with the first appearance of kyanite. Staurolite persists with kyanite in its lower part, but it disappears in the upper higher-grade portion.

The metamorphic isograds (Fig. 15.2) are arranged essentially parallel to the trend of main geological structures, such as fold axes and faults. The mineral assemblage composing the center of the Karnali klippe shows the highest grade. Thus, in this area, the metamorphic grade increases stratigraphically and structurally upwards, signifying the inverted metamorphism (Yoneshiro and Kizaki 1996, p. 10).

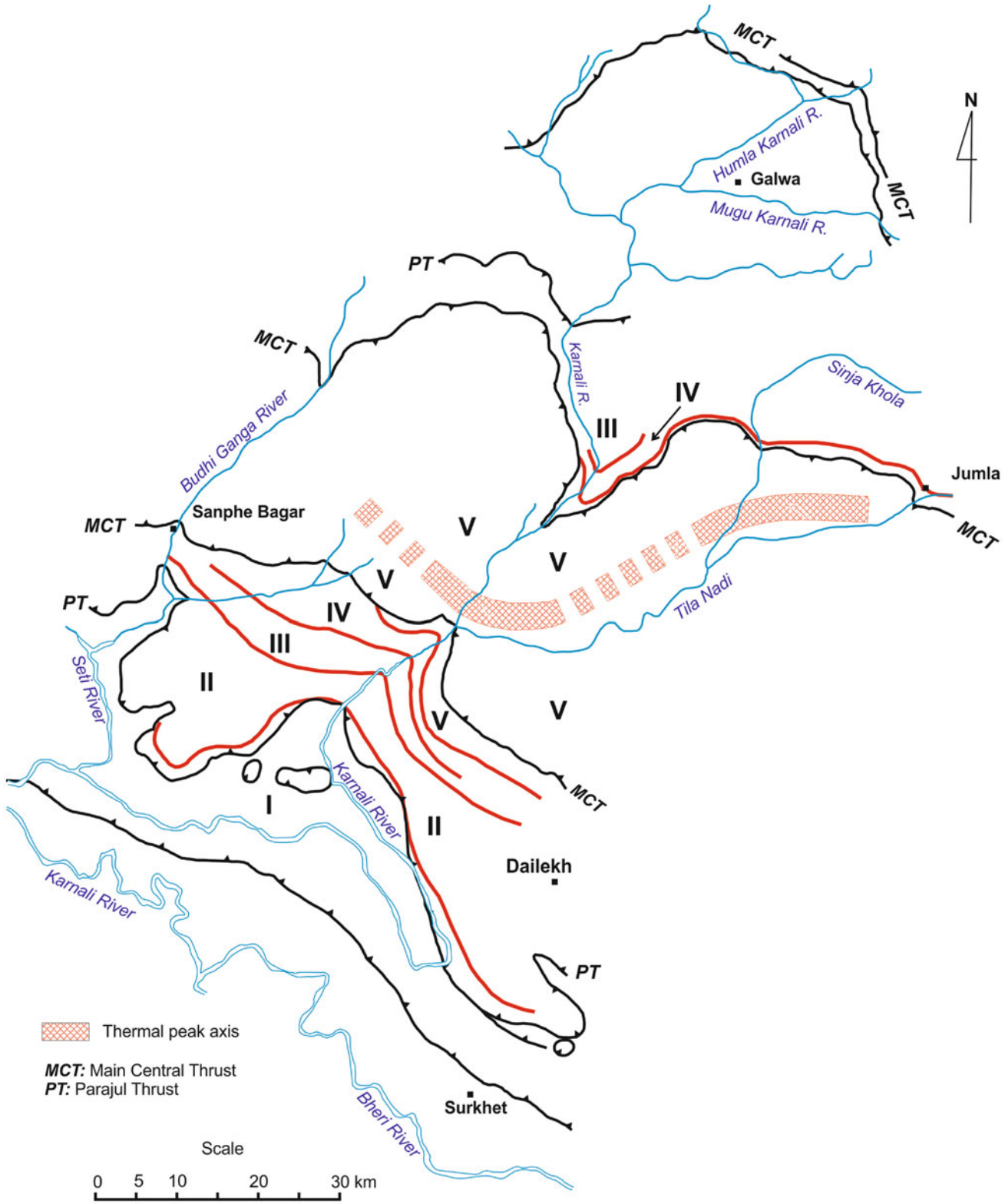

Fig. 15.2 Metamorphic zonation map of the Karnali klippe. The metamorphic thermal peak axis is also indicated. *Source* Modified from Yoneshiro and Kizaki (1996). © Central Department of Geology, Tribhuvan University. Used by permission

15.2.3 Mineral Chemistry and P–T Conditions

Garnets are present successively from Zones III to V, and most of them display distinct chemical zoning. Garnets from Zones II and IV show typical normal zoning. In them, Mn has a bell-shaped chemical profile, and Mg increases from their core to the rim. The Mg/Fe ratio invariably rises from their core to the rim, and the zoning pattern shows almost the same behavior as the Mg. The Ca profiles of garnets are rather constant. The upper part of Zone V contains some garnets without zoning. The value of Mg/(Mg + Fe) in the biotite from kyanite-bearing rocks is the highest, and the staurolite-bearing rock has the next highest value, whereas other rocks show a lesser and variable value.

The temperatures ranged from 470 to 570 °C in Zone III, and from 480 to 620 °C in Zone IV. On the other hand, Zone V experienced temperatures ranging from 560 to 720 °C, respectively, from the lower to upper parts of this zone. The pressures in the lower part of Zone V ranged from 0.62 to 0.7 GPa and 0.82 to 1.11 GPa in the higher part. The peak thermal axis of metamorphism extends essentially parallel to the axial trace of the synform forming the Karnali klippe, and it corresponds to the upper part of the klippe.

15.3 Crystallines South of Kanjiroba

Frank and Fuchs (1970) as well as Fuchs and Frank (1970) classed the Higher Himalayan crystallines of the Jaljala klippe under the Upper Crystalline nappe (Fig. 15.3), which is thrust over the Lower Crystalline nappe of metasediments (belonging mainly to the Lesser Himalayan sequence) along the Main Central Thrust. The Lower Crystalline nappe is a few hundred meters thick, and it contains very fine-grained, brown-gray, biotite–muscovite–plagioclase gneisses with thin phyllite lenses. Also very characteristic are dark gray to black graphite–garnet phyllite interbands in the gneisses. The garnets reach 5 mm in size. This unit also contains calc-mica associated with muscovite and biotite, some phyllite lenses, and coarse-grained and thin-banded micaceous quartzites with biotite. Fine-grained epidote–amphibolite bodies also occur infrequently. The metamorphic grade of the Lower Crystalline nappe corresponds primarily to the albite–epidote–almandine subfacies of the greenschist facies (Fuchs and Frank 1970, p. 45).

The Upper Crystalline nappe is much thicker than the Lower Crystalline nappe, and together with the overlying Dhaulagiri Limestone, attains a thickness of about 12 km (Fig. 15.3). The Upper Crystalline nappe includes a lower gneiss complex, which is partly migmatitic and contains some lime-silicate rocks. These rocks become more abundant towards the top, and grade into the overlying metamorphic carbonate complex, where the metamorphic grade gradually decreases upwards, and dies out in the basal part of the Dhaulagiri Limestone (Fuchs and Frank 1970, p. 46).

The gneisses of the Upper Crystalline nappe are represented by coarse-grained biotite–garnet–kyanite gneiss grading into mica schists and fine-grained, gray, biotite–garnet (kyanite)–gneiss. There are also some fine-grained, gray, migmatitic gneisses, which are presumably the homogenization products of flaky gneiss. They alternate with the garnet–kyanite gneiss. In some areas, light-colored, augen gneisses are abundant, where the microcline forms the augen which may be up to 5 cm in size. Coarse-grained, biotite–garnet quartzites and amphibolites poor in plagioclase also infrequently occur. Sporadic interbands of calcite marble, lime-silicate marble, calc-mica schist, and fine-grained, biotite–calc–silicate gneisses are also found in the gneiss complex. A few fine-grained calc-silicate layers contain vesuvianite and wollastonite, whereas some coarse-grained calc-silicate layers contain muscovite, biotite, garnet, diopside, hornblende, scapolite, and microcline (Fuchs and Frank 1970, p. 48).

The crystalline nappes were one of the most active tectonic elements of the Himalayan orogen. Their movement caused the dragging and more passive tectonics of the Chail nappes or the Rukum nappes (Frank and Fuchs 1970, p. 577). The crystallines were metamorphosed at the beginning of the Alpine orogeny. Then they were thrust onto the Chail nappes, and this caused metamorphism of the latter. In a final tectonic episode, both units were thrust over the unmetamorphosed foreland, made up of the Tertiaries (Fuchs and Frank 1970, p. 49).

15.4 Jaljala Klippe

The basal beds of the Dhaulagiri Limestone in the Thabang Valley contain a thick quartzite succession. It is a fine-grained, gray, micaceous quartzite, occasionally containing parallel laminae. The overlying carbonate rocks of the Jaljala Dhuri (Fig. 15.3) closely resemble those of the Kanjiroba area. Fuchs and Frank (1970, p. 53) reported crinoid fragments from these rocks and correlate them with the Garbyang Formation (Chap. 14). Sharma et al. (1984) and Sharma and Kizaki (1989) investigated the rocks of the Jaljala area. They classified the Higher Himalayan rocks of the klippe into the following formations.

The Chaurjhari Formation is made up of muscovite–biotite schists and garnetiferous mica schist with subordinate bands of micaceous quartzite, garnetiferous graphitic schist, and feldspathic schist. The gray garnet-bearing graphitic schists are tens of meters thick, and they are interbedded with mica schists. The feldspathic schists occur as sporadic bands containing K-feldspar, and plagioclase. The white micaceous quartzite interbands characteristically break into centimeter-thick slabs. But these quartzites become more

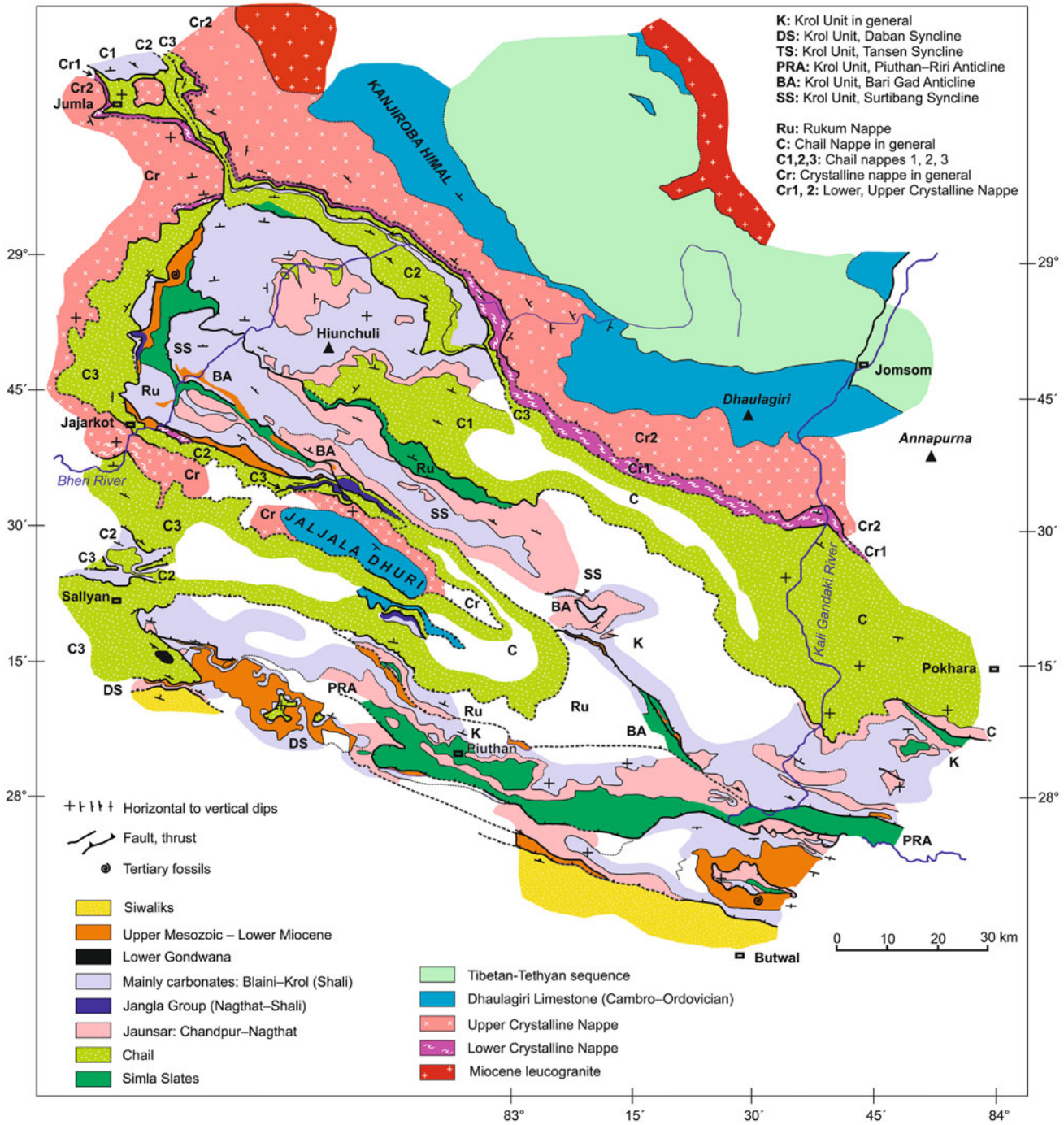

Fig. 15.3 Generalized geological map of the area between the rivers Bheri and Kali Gandaki. *Source* Modified from Frank and Fuchs (1970)

massive to the east. There are also extremely rare marble bands in this formation (Sharma et al. 1984).

The Chaurjhari Formation is gradationally followed upwards by the Thabang Formation represented mainly by impure marbles alternating with mica schists. The marble bands also contain quartz, muscovite, biotite, amphibolite, and garnet as impurities. Their metamorphism gradually decreases stratigraphically upwards and passes into the overlying Jaljala Formation.

The Jaljala Formation consists of a regularly interbedded sequence of medium- to fine-grained calcareous sandstone and calcareous siltstone. Silver to green-gray phyllites also occur frequently. In the upper part of the Jaljala Formation gray silty limestones interbedded with gray-green slates are

present. This formation is equivalent to the Dhaulagiri Limestone of Fuchs and Frank (1970).

15.4.1 Metamorphism

Sporadic garnets make their first appearance in the pelitic and semipelitic rocks of the Lesser Himalaya composing the footwall of the Main Central Thrust. The main mineral assemblages are garnet–biotite–chlorite–muscovite–quartz ± epidote ± albite and garnet–chlorite–muscovite–quartz ± epidote ± albite. Garnets are very few and less than 1 mm in size.

In the overlying Chaurjhari Formation, the pelitic and semipelitic rocks contain the following mineral assemblages.

$$\text{Garnet}-\text{biotite}-\text{chlorite}-\text{muscovite}-\text{quartz} \pm \text{epidote} \pm \text{albite}$$

$$\text{Garnet}-\text{chlorite}-\text{muscovite}-\text{quartz} \pm \text{epidote} \pm \text{albite}$$

$$\text{Garnet}-\text{chloritoid}-\text{chlorite}-\text{muscovite}-\text{quartz} \pm \text{epidote} \pm \text{albite}$$

$$\text{Biotite}-\text{chlorite}-\text{muscovite}-\text{quartz} \pm \text{epidote} \pm \text{albite}$$

In the Chaurjhari Formation, the garnet porphyroblasts are larger (up to 1 cm) and more abundant than in the underlying Lesser Himalayan succession. Blastomylonitic augen gneisses are found in some sections. Towards the middle part of the Thabang Formation, the garnet isograd is succeeded by the biotite isograd and the new mineral assemblage contains biotite–chlorite–muscovite–quartz ± epidote ± albite.

The carbonate bands are made up mainly of dolomite and calcite. Towards the upper end of the Thabang Formation, the biotite isograd is followed by the chlorite isograd.

Hence, in this area, the metamorphic grade at first steadily increases structurally upwards and attains its highest value near the Main Central Thrust. Then, the grade progressively decreases, and sedimentary rocks prevail in the Jaljala Formation. A peak metamorphic temperature of about 550 °C was reckoned in the Jajarkot section of the Chaurjhari Formation (Sharma and Kizaki 1989).

References

Fuchs G (1974) On the geology of the Karnali and Dolpo regions, West Nepal. Mitteilungen der Geologischen Gesellschaft in Wien, Wien, 66–67 Band, 1973–1974, pp 21–32 (with 3 plates)

Fuchs G (1977) The geology of the Karnali and Dolpo regions, western Nepal. Jahrbuch der Geologischen Bundesanstalt, Wien, Band 120, Heft 2, pp 1–103 (with 9 plates)

Fuchs G, Frank W (1970) The geology of west Nepal between the rivers Kali Gandaki and Thulo Bheri. Jahrbuch der Geologischen Bundesanstalt, Wien, Sonderband 18, pp 1–103 (with 9 plates)

Frank W, Fuchs GR (1970) Geological investigations in west Nepal and their significance for the geology of the Himalayas. Geol Rundsch 59:552–580

Hagen T (1969) Report on the geological survey of Nepal. Volume 1: Preliminary reconnaissance. Denkschiiften der Schweizerischen Naturforschenden Gesellschaft, Band LXXXVI/1, 185 pp (with a geological map)

Piddington H (1854) On nepaulite; a new mineral from the neighbourhood of Kathmandoo. J Asiat Soc Bengal Calcutta XXIII(2):170–173

Sharma T, Kansakar DR, Kizaki K (1984) Geology and tectonics of the region between Kali Gandaki and Bheri rivers in central west Nepal. Bull Coll Sci Univ Ryukyus Okinawa Jpn 38:57–102

Sharma T, Kizaki K (1989) Metamorphism and thermal history of the Jaljala Synclinorium, central west Nepal Himalaya. J Nepal Geol Soc 6:21–36

Yoneshiro T, Kizaki K (1996) Metamorphism and thermal structure of the Karnali Klippe, western Nepal Himalaya. Bull Dept Geol Tribhuvan Univ Kathmandu 5:1–20

Higher Himalaya of Gandaki Region

16

One fundamental geological approach to the problem of the MCT has so far been unduly neglected in Nepal: systematic large-scale mapping of the MCT region.

—J. Stöcklin (1980, p. 24)

Although most of the Higher Himalayan crystallines in the Gandaki region are confined to the south slopes of the Great Himalayan Range, a solitary small synformal klippe (Fig. 6.1), resting on the Lesser Himalayan sequence almost towards its south end, provides the missing link between the crystallines and their past extent. Colchen et al. (1981, 1986) studied the Tethyan, Higher Himalayan, and Lesser Himalayan successions between the rivers Kali Gandaki on the west and Budhi Gandaki on the east, and delineated the Main Central Thrust within the inverted metamorphic gradient of this tract. Apart from the Main Central Thrust, the South Tibetan Detachment System (Chap. 13) is another important structure investigated thoroughly in this region. This region has also been a testing ground for various Himalayan tectonometamorphic (Chap. 20) as well as some other orogenic models.

16.1 Kali Gandaki Area

The Higher Himalayan metamorphic rocks, which constitute the base of the Tethyan succession, are brought into relief in the steep and torturous gorge of Kali Gandaki, between Dana and Lete (Fig. 16.1). The gigantic Tibetan slab (Lombard 1952) dips due north at an angle of about 30°, and is thrust over the Lesser Himalayan sequence of garnetiferous schists and graphitic schists (Fig. 16.2) along the Main Central Thrust (Le Fort 1971). The Higher Himalayan crystallines are classified into the following three formations (Le Fort 1975).

The lowest rock succession, appearing north of Dana, is included in Formation I. It begins with banded mylonitic quartzites liberally alternating with gneisses, which are intermittently highly micaceous. There is also a rare passage of impure (cipolin-like) marbles with the above rocks, while moving north (towards the top). The lenses of segregated quartz are frequent within this succession (Le Fort 1971).

The previous sequence is followed up-section by the kyanite zone of about 1,400 m in thickness. At its lower levels, the quartzites rapidly disappear together with the micaceous horizons, and there appear large garnets with kyanite. Importantly, sillimanite occurs towards the top of this succession.

Formation II begins with a zone of calcareous gneisses, including white, yellow, and blue impure marbles (about 2,000 m thick), which follow the kyanite zone. The principal minerals found here are calcite, quartz, hornblende, plagioclase, epidote, almandine, phlogopite, and diopside. There is also a small amount of scapolite, anorthite, and vesuvianite. Metasomatism is observed near the contact of gneiss and marble.

A succession of banded gneiss (about 1,600 m) appears above the calcareous gneisses. It is characterized by many, very fine and perfectly regular, dark bands of biotite, alternating with less than a centimeter-thick, light bands. The calcareous nature of the previous succession does not abruptly disappear, but persists in the banded gneisses as thin carbonate bands. However, the carbonates seldom occur in the overlying succession.

Formation III commences with a succession of augen gneiss. A minor migmatite zone is observed upstream from Ghasa. Within the pegmatites in the augen gneiss, Le Fort (1971, p. 63) discovered a number of ruby crystals (1–2 mm in diameter) as well as a few pink andalusite grains in some other pegmatites.

The final gneisses and calcareous schists constitute a zone of about 300 m in thickness. The contact between the augen gneisses and the succession of sandstone, calcareous sandstone, and calcareous schist is perfectly concordant. It is well exposed west of Dhampu, above a large alluvial cone, and the contact dips at an angle of about 45° due north (Le Fort 1971, p. 65). Farther north, there are two prominent alternating bands of banded gneiss, within the zone of calcareous gneisses.

M.R. Dhital, *Geology of the Nepal Himalaya*, Regional Geology Reviews,
DOI 10.1007/978-3-319-02496-7_16

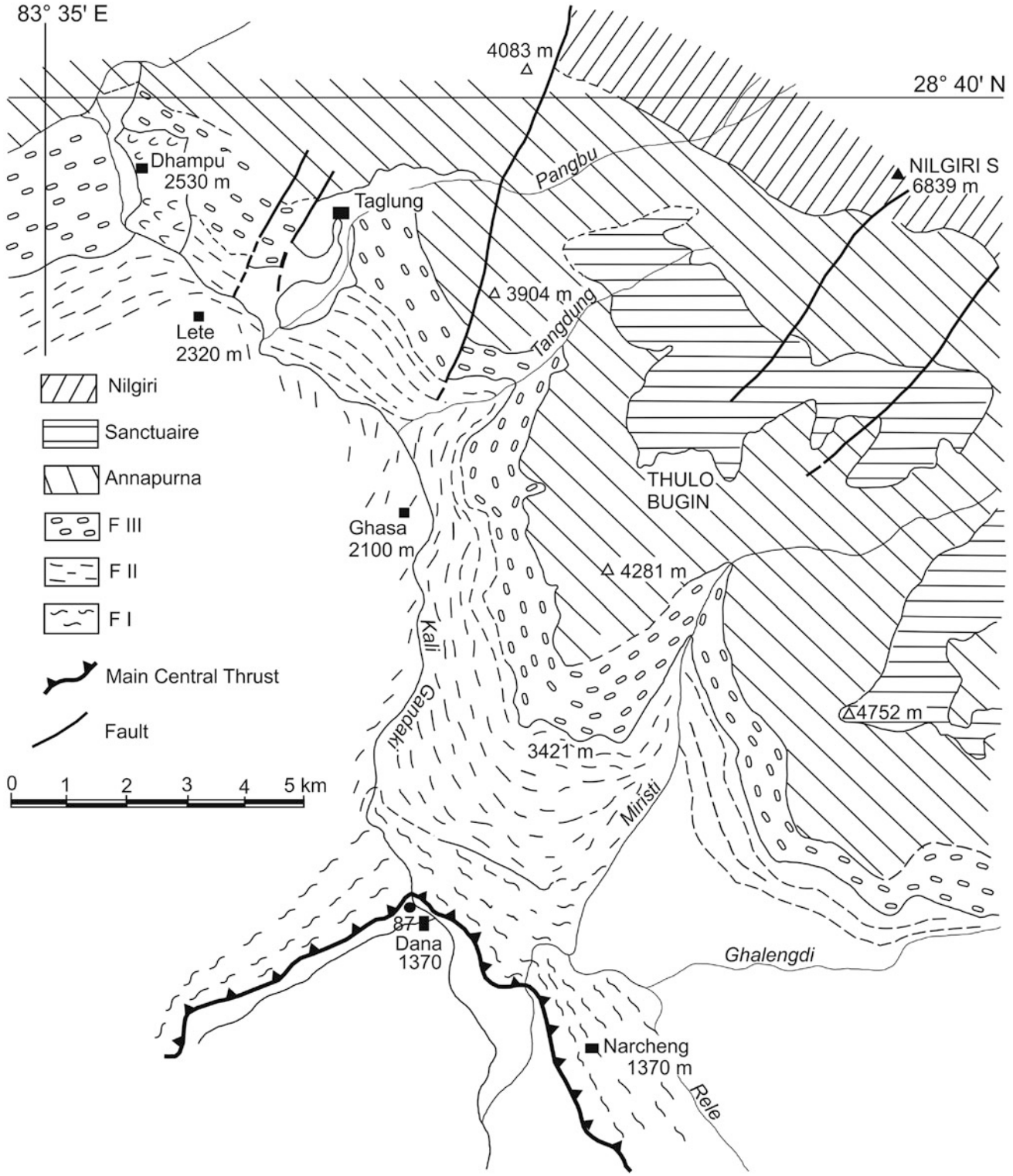

Fig. 16.1 Simplified geological map of the Kali Gandaki and Miristi Valley. *Source* Modified from Le Fort et al. (1986). © Centre National de la Recherche Scientifique, Paris, France. Used by permission

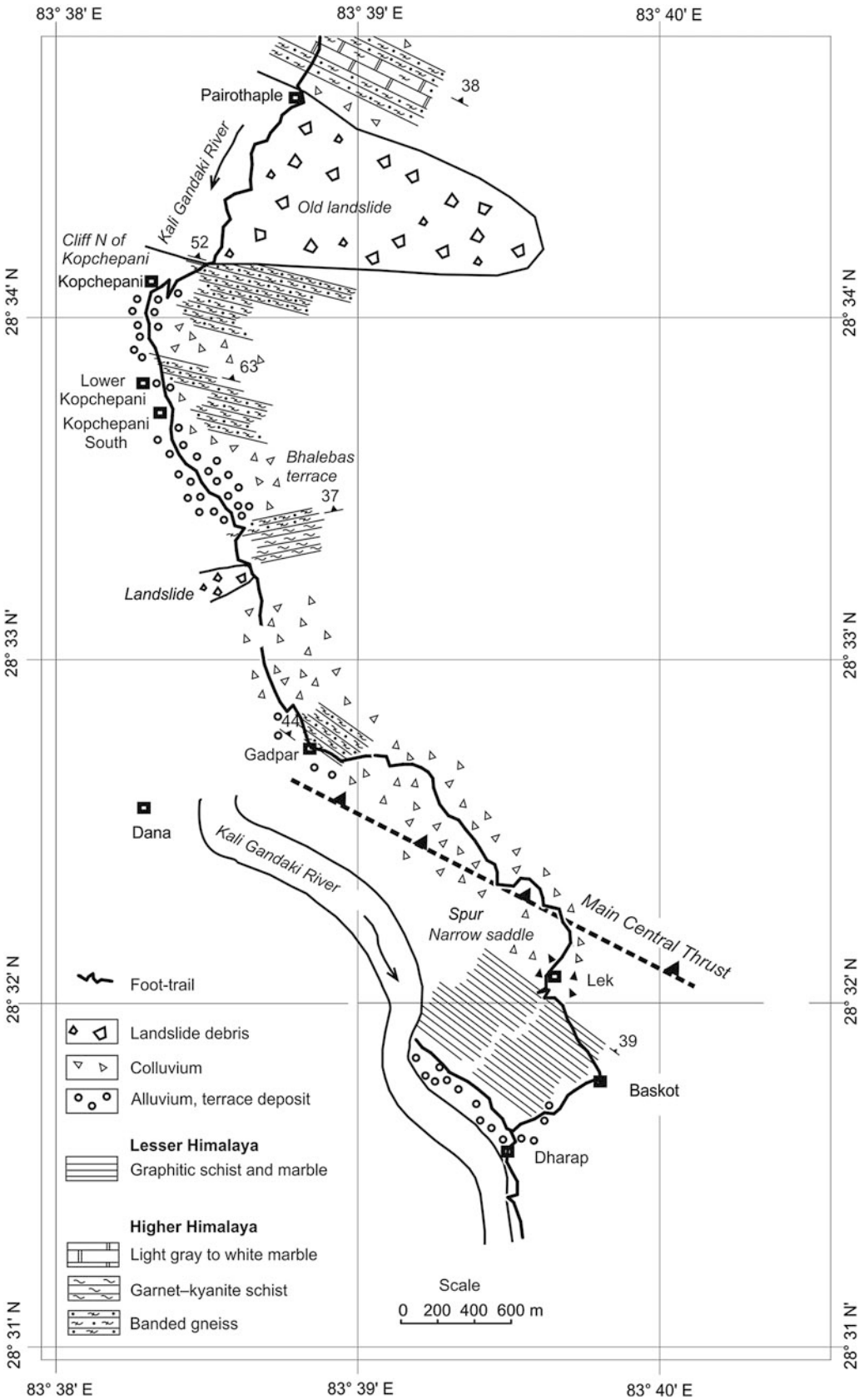

Fig. 16.2 Position of the Main Central Thrust east of Dana. *Source* Author's observations

One of the characteristic features of this area is the preponderance of pegmatites, crosscutting all the aforementioned units, whereas lamprophyres are missing, with an exception of their single appearance in the calcareous Ordovician rocks, observed farther north, about 1 km above Tukuche (Le Fort 1971, p. 44).

16.2 Annapurna–Manaslu–Ganesh Himal Area

In this extensive area, the Lesser Himalayan Kuncha Formation occupies the core of the Gorkha anticlinorium. The formation contains *gritty* phyllites and metasandstones, which attain a thickness of more than 5,000 m. In its lower part, a white quartzite band is present in the area southwest of Pokhara. The Kuncha Formation also includes the Ulleri augen gneisses, which form an approximately 20 km long and up to 1,500 m wide lenticular body. The Kuncha Formation is overlain by the pale yellow to white Fagfog Quartzite. The quartzite is frequently interbedded with phyllites or schists (Colchen et al. 1986, p. 98).

The south limb of the anticlinorium continues with the rocks akin to the Dhading Dolomite, Benighat Slates, Malekhu Limestone, and Robang Formation (Chap. 10). On the other hand, the thickness of the north limb is variable. It is less than 2,000 m in the Chepe Khola, but exceeds 5,000 m in the Daraundi Khola. The north limb continues with a succeeding sequence of light colored schists (200–700 m) with chlorite, quartz, and muscovite. They continue to include thin quartzite beds and up to 1 m thick dolomitic interbands. In a few sections of the north limb, sun cracks are preserved (Colchen et al. 1986, p. 99). These variegated rocks are followed upwards by two thin (a few meters) dolomite or limestone beds, which are presumably equivalent to the Dhading Dolomite of the south limb. These carbonate rocks are succeeded by a thick (1,000–1,400 m) succession of dark gray to black graphitic schists. Towards their upper end, another thick (100 m) carbonate band persists. The Lesser Himalayan sequence ends with the occurrence of a light colored quartzite zone, containing some schist and carbonate bands. This last sequence could be equivalent to the Robang Formation (Chap. 10). Amphibolite sills of varying thickness (up to several meters) and extent (several kilometers) are not confined to a single horizon, but are distributed at various levels of the Lesser Himalayan sequence. Especially, they are abundant in the Fagfog Quartzite equivalents (Colchen et al. 1986, p. 101).

The Tibetan slab of the Higher Himalayan crystallines overrides the above sequence (Figs. 16.3 and 16.4). In this area, inverted metamorphism is clearly discernible in the Lesser Himalayan as well as overlying Higher Himalayan succession. The chlorite and biotite isograds lie within the core of the Gorkha anticlinorium, and the garnet isograd is found in the north limb of the fold. Locally, the kyanite isograd crosscuts the Lesser Himalayan rocks in the Marsyangdi River. On the other hand, the sillimanite isograd is developed towards the top part of the slab, particularly in the areas where it is thick, such as the neighborhood east of Mount Annapurna (Colchen et al. 1986, p. 155).

16.3 Annapurna Detachment

The upper end of the Higher Himalayan crystallines is frequently bordered by a north-dipping normal fault or shear zone, indicating a top-to-northeast sense of movement, and it is part of the regional South Tibetan Detachment System (Burg et al. 1984; Burchfield et al. 1992). From the Kali Gandaki Valley, Brown and Nazarchuk (1993) reported the Annapurna Detachment (Figs. 16.3 and 16.4), which is correlated with the South Tibetan Detachment System. The structures in the hanging wall of the detachment record both extensional and compressional movements. The detachment is well exposed in the Kali Gandaki River. Its footwall contains migmatitic quartz–feldspar gneisses and calc-silicates, intruded by sheets of two-mica leucogranite. Kinematic indicators, such as C/S fabrics, shear bands, rotated and nonrotated porphyroclasts with tails, asymmetric folds with tails, and pegmatite dike arrays that have been extended or shortened depending on their orientation, record the sense of movement (Brown and Nazarchuk 1993, p. 464). These shear sense indicators are found in the footwall, from 5 to 100 m below the fault.

The northeast-verging folds (Fig. 16.4), including the Nilgiri nappe in the hanging wall of the Annapurna Detachment, have a well-developed axial plane cleavage, defined by the preferred orientation of biotite, and hence predate normal faulting. These structures are considered to be the result of early crustal thickening (Brown and Nazarchuk 1993, p. 471).

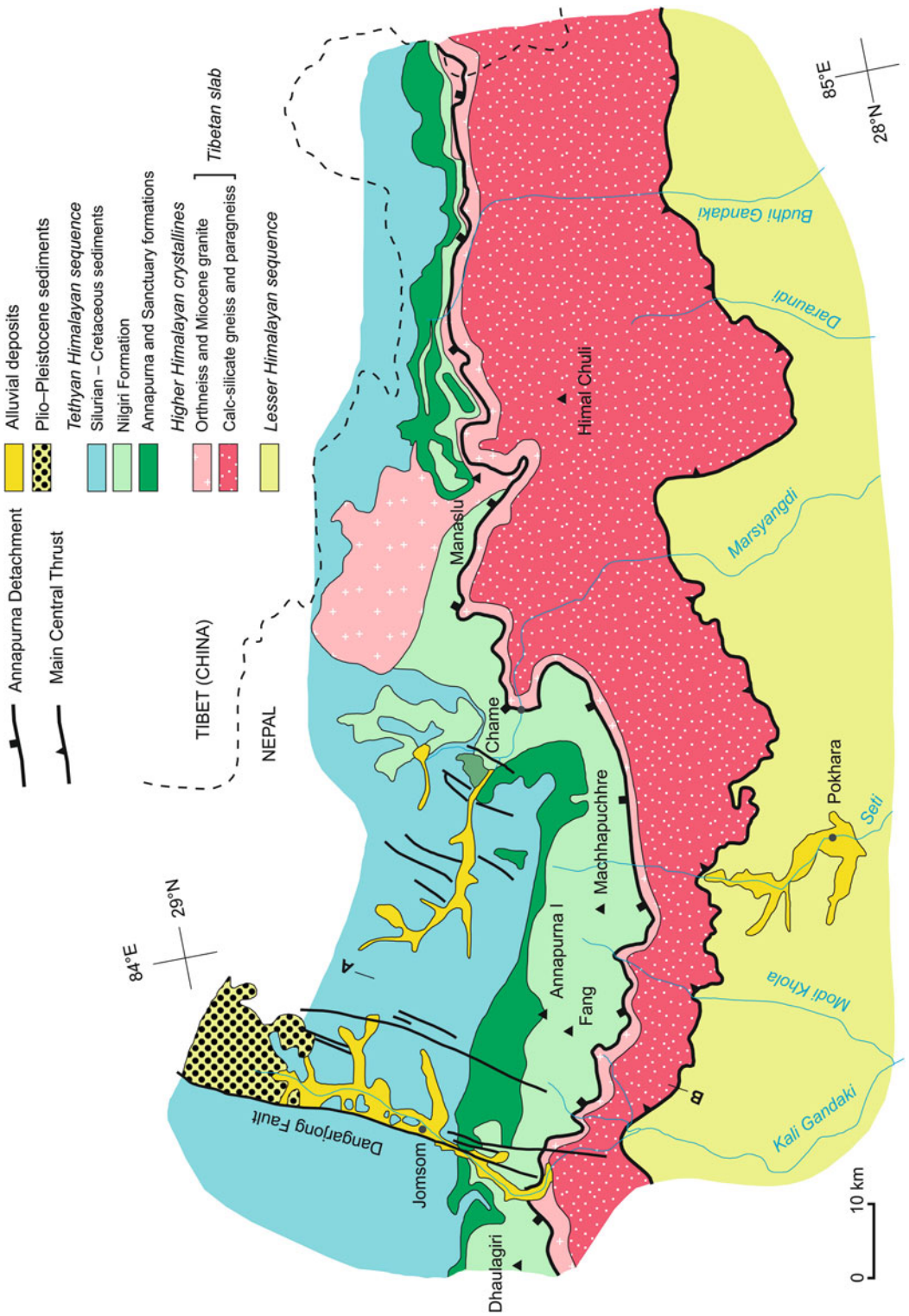

Fig. 16.3 Generalized geological map of central Nepal showing the Main Central Thrust and Annapurna detachment fault in the area between the Kali Gandaki and Marsyangdi. *Cross-section line A–B* (Fig. 16.4) is also indicated. *Source* Modified from Colchen et al. (1986) and Brown and Nazarchuk (1993)

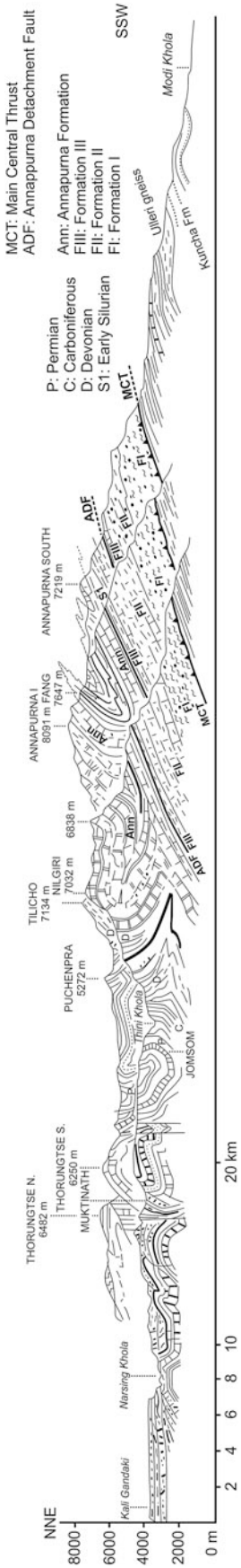

Fig. 16.4 A composite geological cross-section along A–B (Fig. 16.3) showing main structural features of the Higher Himalayan crystallines and the Tethyan Himalayan sequence in the Kali Gandaki–Budhi Gandaki area. *Source* Modified from Colchen et al. (1986)

Different from Brown and Nazarchuk (1993), who put the normal fault between the orthogneiss of Formation III and the Larjung Marble of the Tethyan Himalayan sequence, Vannay and Hodges (1996, p. 639) did not identify any brittle or ductile fabrics indicative of top-to-northeast extension. Also, petrographic and geothermobarometric data indicated no major disruption of the P–T field gradient across the Formation III–Larjung contact. These authors also propose that the Annapurna Detachment corresponds to a relatively thick, ductile shear zone that lies between the amphibolite-facies calc-silicate gneiss of the Larjung Formation and the greenschist-facies crystalline limestones of the lowermost Annapurna Formation. They also identified the Kalopani shear zone in the upper part of the Higher Himalayan crystallines. Godin et al. (1999) found that the immediate hanging wall of the Annapurna Detachment has an approximately 1,500 m thick extensional shear zone, which transposes the southwest-verging structures.

16.4 Neighborhood of Ngadi–Marsyangdi Confluence

This area occupies the north flank of the Great Midland Antiform or the Gorkha anticlinorium, where the Kuncha Formation is extensively distributed in its core, lying several kilometers south of the map area. This formation is made up of a very thick (several kilometers), sequence of green-gray to blue-gray phyllite and metasandstone. Scarce amphibolite bands are also found in it. The Kuncha Formation is delimited from the north by pale yellow quartzites, containing interbands of gray-green garnetiferous schist or quartzite.

The metamorphic grade steadily increases from the south to the north, and the quartzites are succeeded up-section by the garnet schist unit (Fig. 16.5), comprising gray garnet–muscovite–biotite schists and quartzites. The size of garnets in the schist varies widely. Often, the garnets are from 1 to 2 mm in diameter, but may exceed 6 mm. Frequently, garnets of 2–5 mm in diameter display snowball structures. They are surrounded by about 1 cm long biotite and muscovite envelopes. Generally, 10–30 cm (rarely, more than 5 m) thick, gray, and dark gray schist and quartzite bands alternate with each other. There also occur a few bands (1–2 m thick) of graphitic schist and white quartzite. Numerous generations of quartz vein are common in the schist, and they are often stretched and boudinaged. Rare pegmatite veins with tourmaline are also present.

The succession of garnetiferous schists is overlain by an intensely deformed and gently dipping zone of graphitic schist (Fig. 16.5). In this unit, gray, green-gray, light gray, and white calcareous schists alternate with light gray, green-gray, and white calcareous quartzites, dolomitic marbles, and dark gray to black graphitic schists. Quartz and calcite veins of several generations ramify the rock. In the area northwest of Ngadi Bajar, kyanite blades are frequent in graphitic schists.

A several hundred-meter-thick carbonate succession is observed in the vicinity of Kaule (Fig. 16.5) and Usta. The calcareous quartzite and dolomite bands occurring within this unit are from 10 cm to 1.5 m thick, and they alternate with 1 mm–50 cm thick schist bands. Very thick (up to 5 m) light gray, white, and cream colored quartzite bands also occur. Generally, schist, quartzite, and marble bands alternate. This unit also sporadically contains gray calcareous schists, intersected by pink calcite veins. The schists alternate with light gray calcareous gneisses as well as some augen or banded gneisses. There are also sparse dolomitic gneiss and marble bands (30 cm–1 m thick).

The Main Central Thrust abruptly overrides the carbonates (Fig. 16.5) and brings with it gray and dark gray, parallel-banded, coarse-grained, schist and quartzite alternations, containing kyanite, garnet, biotite, K-feldspar, muscovite, and quartz. Generally, the rock is massive to blocky. In the schist, kyanite and garnet crystalloblasts range in size from less than 1 to 5 mm.

A remarkable feature of the area is the occurrence of thick (from 50 to about 200 m) debris flow deposits (Fig. 16.5). The deposits are distributed on both banks of the Ngadi River, especially south of Bhirpustung, around Dingding as well as in the vicinity of Bahundanda and at Tarachok (Fig. 16.5). They contain large (exceeding 5 m) subangular boulders of augen gneiss, banded gneiss, and marble. Very large (15 m) boulders of banded gneiss, granitic gneiss, and quartzite are also sporadically present. The sediments contain a moderately compact, fine (sandy to silty), light gray to white matrix. In them, the proportion of matrix and clasts varies widely. Generally, the matrix constitutes 50–60 % of the total volume. Dark gray mudstone lumps are sporadically present in the debris flow deposits, especially in the area west of Bahundanda.

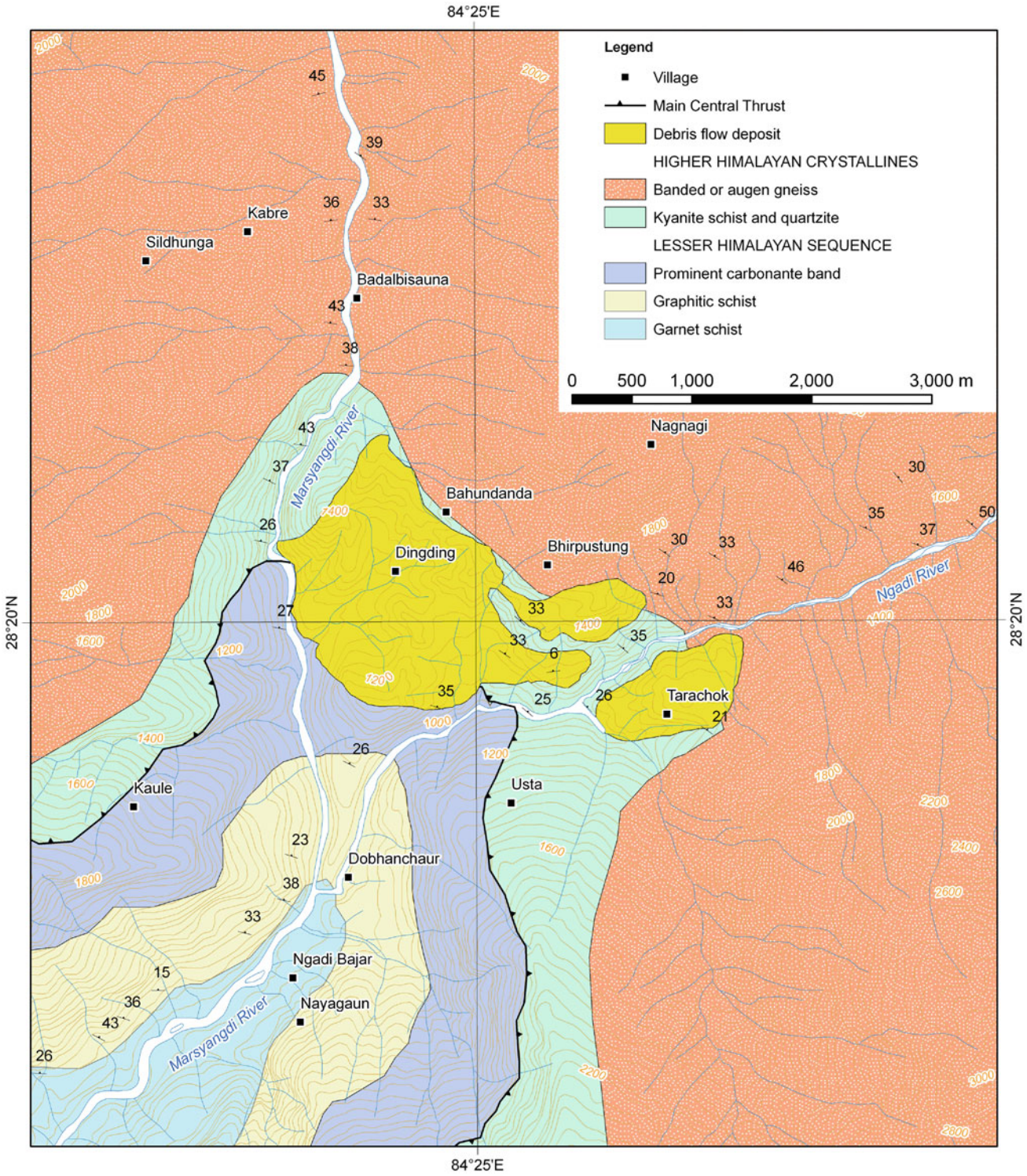

Fig. 16.5 Geological map of the area around the Marsyangdi–Ngadi confluence. *Source* Based on field survey in 2009 by MR Dhital, SC Sunuwar, and D Laudari

References

Brown RL, Nazarchuk JH (1993) Annapurna detachment fault in the Greater Himalaya of central Nepal. In: Treloar PJ, Searle MP (eds) Himalayan tectonics, vol 74. Geological Society Special Publication, London, pp 461–473

Burchfield BC, Chen Z, Hodges KV, Liu Y, Royden LH, Deng C, Xu J (1992) The South Tibetan detachment system, Himalayan orogen: extension contemporaneous with and parallel to shortening in a collisional mountain belt. Geol Soc Am Spec Pap 269:1–41

Burg JP, Guiraud M, Chen GM, Li GC (1984) Himalayan metamorphism and deformations in the North Himalayan Belt (southern Tibet, China). Earth Planet Sci Lett 69:391–400

Colchen M, Le Fort P, Pêcher A (1981) Carte géologique Annapurna–Manaslu–Ganesh Himalaya du Népal. Échelle 1:200,000. Népal central. In: Gupta HK, Delany FM (eds) Zagros–Hindu Kush–Himalaya geodynamic evolution. American Geophysical Union, Washington, DC

Colchen M, Le Fort P, Pêcher A (1986) Annapurna–Manaslu–Ganesh Himal. Centre National de la Recherches Scientifique. Special Publication, Paris, 136 pp (with a geological map, 1:200 000 scale)

Godin L, Brown RL, Hanmer S (1999) High strain zone in the hanging wall of the Annapurna detachment, central Nepal Himalaya. In: Macfarlane A, Sorkhabi RB, Quade J (eds) Himalaya and Tibet: mountain roots to mountain tops, Special Paper 328. Geological Society of America, Boulder, pp 199–210

Le Fort P (1971) Les formations cristallophylliennes de la Thakkhola. In: Bordet P, Colchen M, Krummenacher D, Le Fort P, Mouterde R, Rémi M (eds) Recherches géologiques dans l'Himalaya du Népal, région de la Thakkhola. Centre National de la Recherche Scientifique, Paris, pp 41–81

Le Fort P (1975) Himalayas, the collided range: present knowledge of the continental arc. Am J Sci 275-A:1–44

Le Fort P, Pêcher A, Upreti BN (1986) A section through the Tibetan slab in central Nepal (Kali Gandaki Valley): mineral chemistry and thermobarometry of the Main Central Thrust zone. In: Le Fort P, Colchen M, Montenat C (eds) Évolution des domaines orogéniques d'Asie méridionale (de la Turquie à l'Indonésie), Livre jubilaire Pierre Bordet, Sciences de la Terre, Mémoire no 47, Nancy, pp 211–228

Lombard A (1952) Les grandes lignes de la géologie du Népal Oriental. Bulletin de la Société Belge de Géologie de Paléontologie et d'Hydrologie, Bruxelles LXI(Fascicule 3):260–264

Stöcklin J (1980) Geology of Nepal and its regional frame. J Geol Soc London 137:1–34

Vannay J-C, Hodges KV (1996) Tectonometamorphic evolution of the Himalayan metamorphic core between the Annapurna and Dhaulagiri, central Nepal. J Metamorph Geol 14:635–656

Higher Himalaya of Bagmati–Gosainkund Region

17

The limestone on the crest of the Chendragiri pass between Chitlong and Nepal is somewhat less altered than usual; in it I noticed some small facets of spar having a central puncture, and which I took to be crinoidal; but Dr. Waagen could not say positively that they were so.

—H.B. Medlicott (1875, p. 97)

Hagen (1969) incorporated the elevated terrain north of Kathmandu into his Gosainkund tectonic bridge, which has survived erosion from two mighty rivers: the Trishuli on the west and Sun Koshi on the east (Fig. 10.1). The region also contains to the south, a large doubly plunging megafold, called the Mahabharat Synclinorium. It has a well-developed west closure and a narrow and elongated east wing (Stöcklin 1980). Paleozoic granites preponderate in this region, especially within the synclinorium. Arita et al. (1973) made fairly detailed descriptions of the Higher Himalayan metamorphic mineral assemblages. Nadgir (1976) separated his Kathmandu Group into the Bhimphedi, Chitlang, and Chandragiri formations. He envisaged the Sheopuri Gneisses as intrusives and, contrary to Auden (1935), did not favor their correlation with the Darjeeling Gneiss.

17.1 Kathmandu Complex

The Kathmandu Complex (Stöcklin and Bhattarai 1977), representing the Higher Himalayan and Tethyan sequences, is further subdivided into the Bhimphedi Group and the succeeding Phulchauki Group (Table 17.1), whereas the underlying Lesser Himalayan rocks of the Nawakot Complex are separated into the Lower Nawakot Group and the Upper Nawakot Group (Chap. 10).

17.1.1 Bhimphedi Group

The Bhimphedi Group represents an approximately 8 km thick metamorphic succession (Fig. 17.1), composed of schists, quartzites, marbles, and allied rocks together with Sheopuri Injection Gneisses and Paleozoic granites. The original sedimentary rocks were mainly shales and sandstones with two prominent limestone intervals. The Mahabharat Thrust or Main Central Thrust brings the Kathmandu Complex over the Nawakot Complex. However, on some rare occasions, the thrust approaches the Siwaliks (Chap. 31), concealing the whole Lesser Himalayan sequence.

The Bhimphedi Group begins with the Raduwa Formation, represented dominantly by dark green-gray mica schists of coarse crystalline aspect. Biotite is the predominating mineral; but sericite, muscovite, chlorite, and garnet are also commonly present. Red garnets sometimes reach up to 1 cm in diameter. Amphibole and pyroxene are also locally present, whereas staurolite, kyanite, and sillimanite are observed in the Mahesh Khola, north of Kathmandu, and around Sankhu. The schists usually contain lenses and veins of quartz, which impart a gneissic appearance to the rock. The Raduwa Formation also contains some subordinate bands of gray micaceous quartzite and its pale green or white, purer varieties. The prominent bands of such rocks exposed in a tributary of the Jhiku Khola in its upper reach, are designated as the Chak Quartzite Beds. These quartzites grade locally into coarse-grained gneisses, composed primarily of feldspar and quartz with minor thin alternations of garnetiferous or sericite–chlorite schist (Stöcklin and Bhattarai 1977, p. 24).

The Main Central Thrust is a discordant tectonic contact, commonly associated with a sheared and mylonitized zone between the Raduwa Formation and the underlying Lesser Himalayan sequence of the Upper Nawakot Group. The upper contact of the Raduwa Formation with the Bhainsedobhan Marble is perfectly transitional, and marked by an approximately 20–30 m thick sequence of schist and marble. The Raduwa Formation has a maximum thickness of 2,000 m, but it seldom attains that value.

The main component of the Bhainsedobhan Marble at its type locality appears in coarse to very coarse crystalline (up to a few mm long calcite grains), saccharoidal form. The white marble also contains some pale yellow, pinkish or light brown dolomitic marble lenses and bands. Although the rock seems massive at first glance, close inspection

M.R. Dhital, *Geology of the Nepal Himalaya*, Regional Geology Reviews,
DOI 10.1007/978-3-319-02496-7_17

Table 17.1 Stratigraphic subdivisions of the Kathmandu Complex

Unit	Main lithology	Approximate thickness (m)	Age
2. Phulchauki Group			
Godavari Limestone	Limestone, dolomite	300	Devonian
Chitlang Formation	Slate	1,000	Silurian
Chandragiri Limestone	Limestone	2,000	Cambro–Ordovician
Sopyang Formation	Slate, calc. phyllite	200	? Cambrian
Tistung Formation	Metasandstone, phyllite	3,000	? Early Cambrian–? Neoproterozoic
Transition			
1. Bhimphedi Group			
Markhu Formation	Marble, schist	1,000	Proterozoic
Kulikhani Formation	Quartzite, schist	2,000	Proterozoic
Chisapani Quartzite	White quartzite	400	Proterozoic
Kalitar Formation with: Jurikhet Conglomerate Pandrang Quartzite Bhimsen Dolomite Lower schist member	Schist, quartzite, partly garnetiferous	2,000	Proterozoic
Bhainsedobhan Marble	Marble	800	Proterozoic
Raduwa Formation	Garnetiferous schist	1,000	Proterozoic
Mahabharat Thrust (*Main Central Thrust*)			
NAWAKOT COMPLEX			

Source Modified from Stöcklin and Bhattarai (1977), Stöcklin (1980)

reveals thin banding and foliation defined by biotite, muscovite, and phlogopite. The uppermost and lowermost zones of the Bhainsedobhan Marble are rather thinly banded and contain biotite schist and garnetiferous schist as intercalations. The two zones represent the transitional passage into the underlying Raduwa Formation and overlying Kalitar Formation, respectively. The Bhainsedobhan Marble is about 800 m thick at its type locality (Stöcklin and Bhattarai 1977, p. 24). It is important to note that the Bhainsedobhan Marble serves as a marker horizon, inasmuch as it can be traced continuously for tens of kilometers. The closure of the Mahabharat Synclinorium is excellently delineated by this formation.

Mica schists comprise the main rock type of the Kalitar Formation. There are also some regularly alternating subordinate bands of strongly micaceous quartzite. Owing to the abundance of biotite, the general color of the Kalitar Formation is black with gray-brown weathering shades. Whenever there is some chlorite and sericite, the rock assumes lighter gray-green tints. The schists are generally coarse-grained at the lower portion, and contain garnet crystalloblasts, but they become finer-grained stratigraphically upwards, and the garnets become smaller, or they disappear completely. There also occur alternations of micaceous quartzite, which is finer-grained and more distinctly bedded than the schist. In the schist–quartzite alternations, generally the foliation obliquely cuts the primary bedding in the schist, but the foliation is essentially parallel to the bedding in the quartzite bands. There also crop up sporadic amphibolite bands, some of which are strongly altered to yield epidote. The Kalitar Formation is about 2,000 m thick at its type location, and it includes the following members (Stöcklin and Bhattarai 1977, p. 26).

The Lower Schist Member of the Kalitar Formation occurs between the Bhainsedobhan Marble and the Pandrang Quartzite. This soft-weathering and dark colored schistose interval is highly biotitic and easily discernible in the field against the cliff-forming marble, displaying contrasting properties. In this member, garnet is invariably present and, in places, occurs in profusion; there also locally set in pyroxene and amphibole, especially in its lower end, near the contact with the marble. Towards the upper part of the member, there is a sequence of gray micaceous quartzite alternating with schist, and it transitionally passes into the overlying Pandrang Quartzite.

Carbonate bands are generally uncommon in the Kalitar Formation, however, there are certain areas where they form a distinct horizon. One such zone, reaching a thickness of 100 m, is incorporated into the Bhimsen Dolomite Member, characterized by a brownish marble or calc-silicate rocks, forming sporadic lenticular bands of a few centimeters to 1–2 m thickness. Green, altered amphibolites with much epidote, pyrite, and some hematite are sometimes associated with this member. At the type locality of Bhimsen Danda,

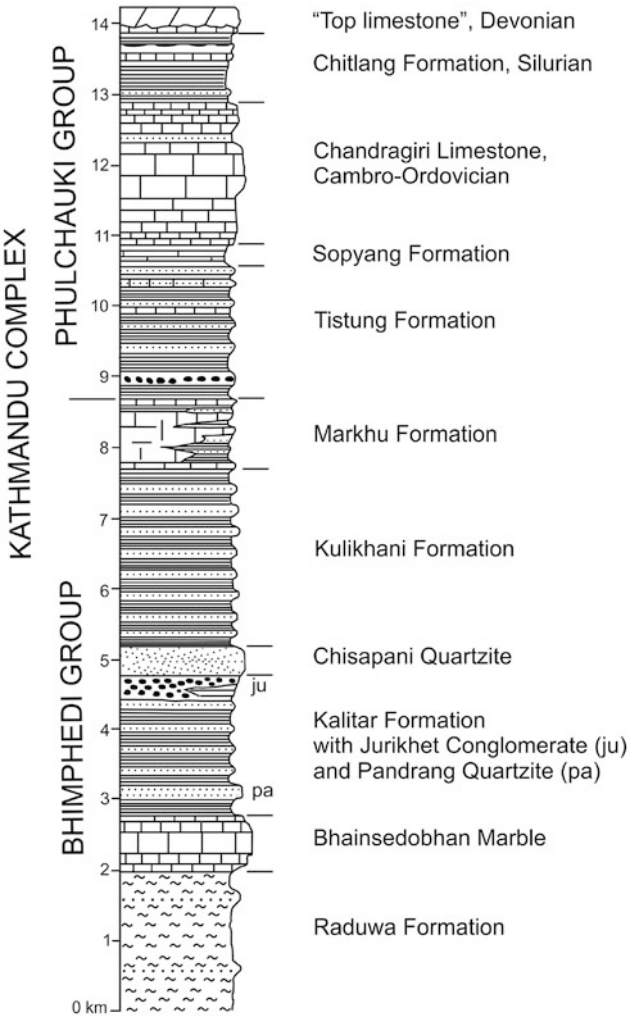

Fig. 17.1 Lithostratigraphic column of the Bhimphedi Group. *Source* Modified from Stöcklin (1980)

the upper part of the dolomite becomes ankeritic, and it contains seams and lenses of a vividly green amphibole–epidote–chlorite rock.

Like the Bhimsen Dolomite Member, the Pandrang Quartzite is also developed locally. It appears about 300 m above the Bhainsedobhan Marble as a strictly parallel band. It is fine-grained, pale green to greenish white colored, and includes partings and interbeds of sericite–chlorite schist, with infrequent biotite and garnet. Indistinct cross-bedding is observed in the quartzite, and it is rather similar to the overlying Chisapani Quartzite in many ways, but is quite thin, and rarely contains those clean and white varieties characteristic of the Chisapani (Stöcklin and Bhattarai 1977, p. 26).

The Jurikhet Conglomerate appears only to the north of Bhimphedi, and it is made up of unsorted and irregularly distributed white quartz pebbles, ranging in size from 1 mm to 2 cm. They occur primarily in a dark gray biotitic quartzite of massive to blocky appearance, without distinct bedding. Apart from them, there are also larger (up to 30 cm across), well-rounded boulders of gray micaceous quartzite and biotite schist. Tourmaline-bearing veins cut across the boulders and matrix of the conglomerate. The Jurikhet Conglomerate attains a thickness of about 200 m and displays gradational contacts with the underlying black schist and overlying Chisapani Quartzite (Stöcklin and Bhattarai 1977, p. 27).

The Kalitar Formation is succeeded transitionally by the Chisapani Quartzite. It serves as a light-colored marker band, separating the underlying much darker schists and quartzites of the Kalitar Formation from the overlying Kulikhani Formation. The Chisapani Quartzite represents a conspicuous, very fine-grained, white to pale green, clean variety with sericite partings or thin sericite–phyllite seams. It is bedded into decimetric bands, displaying frequent cross-lamination and occasional ripple marks. The upper bands of the Chisapani Quartzite are relatively thin-bedded, and the contact with the succeeding Kulikhani Formation is a rapid transition. This formation is about 400–500 m thick at its type locality.

The overlying Kulikhani Formation consists of fine-grained quartz (10–70 %) and mica in various proportions, resulting in the bands of micaceous quartzite and quartzitic schist. In the rock, biotite always predominates over sericite, whereas sporadically occurring fine-grained garnet is rather exceptional and not characteristic of this formation. The Kulikhani Formation exhibits dark green-gray lustrous colors, which become subdued in more quartzitic bands. The beds are generally tens of centimeters thick, but there are also varieties of thin beds as well as laminated sequences of schist and quartzite. Some quartzite beds are graded, and others display cross-lamination. As in the Kalitar Formation, the foliation in the schist is oblique to its bedding, but such an arrangement is less characteristic of this formation. On the other hand, there is a well-developed crenulation cleavage in the schist and a strong lineation in the quartzite of the Kulikhani Formation. Some exceptionally rare bands of carbonate rocks (coarse crystalline marble) and thin dikes and sills of amphibolite are observed at a few places. The Kulikhani Formation is about 2,000 m thick and passes conformably and transitionally into the overlying Markhu Formation (Stöcklin and Bhattarai 1977, p. 28).

The Markhu Formation is composed mainly of three rock types: schists, quartzites, and carbonates, occurring in various proportions. About 50 % of the total rock volume is represented by marbles. The marble bands range in thickness from a few centimeters to tens of meters. They are medium to coarse crystalline; some of them are pure marbles, displaying white and pink colors, whereas others contain much quartz and mica, including biotite. The marbles consist of amphibole and pyroxene at some localities, especially (but not exclusively) near the granite contacts. The schists

and quartzites alternating with the marbles are dark colored, rich in biotite, fine-grained, and also include bands of phyllite and calc-phyllitic rock, where sun cracks and worm tracks are sporadically discerned. Through a decrease in the number and thickness of carbonate bands, the Markhu Formation transitionally grades into the overlying Tistung Formation. The Markhu Formation is about 1,000 m thick at its type locality. At a few places, the Markhu Formation exhibits concentric stromatolitic structures, quite different from those observed in the Dhading Dolomite. A massive lens-shaped body of marble extending for about 18 km in Labang–Khairang could be a reminiscent of a stromatolite reef (Stöcklin and Bhattarai 1977, p. 29).

17.1.2 Phulchauki Group

The Phulchauki Group (Fig. 17.2) is unique in respect to Paleozoic fossil occurrence in the Chandragiri and Phulchauki hills, bordering the Kathmandu Valley on the south. These rocks are part of the Tethyan outlier, positioned to the south of the high Himalayan peaks. The Phulchauki Group is about 5,000–6,000 m thick, and is constituted principally of limestones with a subordinate quantity of shales and sandstones. Presumably, its age ranges from the Neoproterozoic or Early Cambrian to Devonian.

The Phulchauki Group commences with the Tistung Formation, which is comprised mainly of slates, phyllites, and metasandstones. Also noticeable is a distinct decrease in metamorphic grade from bottom to top of this formation. The lower portion of the Tistung Formation consists of dark gray phyllites and fine biotite schists, but while moving stratigraphically upwards, biotite gradually disappears and sericite and chlorite remain as the constituent metamorphic minerals. Similarly, the dark green-gray colors, so characteristic of the schists and quartzites composing the underlying formations, give way in places to conspicuous pink, buff, and purple tints. These colors are more vivid, particularly in metasandstones. As a result, there is frequently red and green color banding owing to the alternation, respectively, of metasandstone and phyllite. There are also a few bands of pale yellow and white clean quartzite. Sun cracks, ripple marks, cross-lamination, and worm tracks are regularly observed in this formation. The fine-grained rocks commonly alternate with thin limestone beds, and the associated sandstones have a slightly calcareous matrix. The sandstones are generally slabby to flaggy, and as such, they can form a single slab of several meters in length and width. The rocks frequently exhibit deep pink, blue, violet, and purple colors in their weathered state. Normally, deep red-purple soil develops on this formation. The Tistung Formation reaches a thickness of about 3,000 m (Stöcklin and Bhattarai 1977, p. 30).

The Sopyang Formation is represented by a mixed lithology of siliciclastic rocks as well as carbonates, and occupies a transitional zone between the Tistung Formation and overlying Chandragiri Limestone. A wide facies variation is noticed within this formation. In its type area, soft-weathering, thin-bedded, argillaceous to marly phyllitic slates contain lenticular beds of argillaceous limestone. The rock exhibits typically dark gray to black colors. Some worm tracks are present on bedding planes of slates. In other places, black slates are intimately associated with a dark gray limestone, and there are also areas where a few isolated limestone beds are found. In the upper part, the limestone bands vary in thickness from a few meters to 20 m or more, and they are intercalated in green or gray sandy phyllites of Tistung affinity. The Sopyang Formation ranges in thickness from 100 to 300 m, and it invariably grades into the Chandragiri Limestone through thin-bedded argillaceous limestones (Stöcklin and Bhattarai 1977, p. 31).

The Chandragiri Limestone, one of the key formations of the Phulchauki Group, forms a number of imposing mountain ranges (Chandragiri, Nagarjun, Phulchauki), overlooking Kathmandu. It is a pale yellow to brown (when weathered) limestone of massive appearance from a distance, but reveals well-developed bedding and platy partings at close inspection. Frequently the limestone is microcrystalline, partly siliceous, and even dolomitic. The fresh rock color varies from pale yellow and white to pale green and pink. There are also thin intercalations, partings, and films of sericite and chlorite. Generally, the lower portion of the limestone is relatively thinly bedded and more argillaceous than the rest of it. On the historic trail from Thankot to the Chandragiri Pass, an approximately 100–200 m thick band of thinly bedded, white quartzite is intercalated in the upper third of the formation. Above this band are thinner-bedded and more argillaceous, bright pink and green colored limestones, which contain conspicuous wave ripple marks on a number of phyllitic intercalations. These strongly rippled beds contain a profusion of well-preserved crinoid and other echinoderm fragments, yielding a Late Ordovician age (Chap. 21). The Chandragiri Limestone varies in thickness from 2,000 to 2,500 m, and the last fossiliferous limestones gradually pass upwards into the slates, belonging to the Chitlang Formation. Because the Chandragiri Limestone is very thick, and the fossils are present in its upper part, its age may range from the Cambrian to Ordovician, as with many other Tethyan sequences developed in Dolpa, Thakkhola, and Manang (Stöcklin and Bhattarai 1977, p. 29).

The Chitlang Formation is found mainly in the core of the Mahabharat Synclinorium. It is made up mainly of dark gray and purple, soft-weathering slates. In its lower part, there is a conspicuous white quartzite band, whereas towards its upper section, some thin limestone intercalations display wave ripples. The Chitlang Formation is a few hundred meters thick.

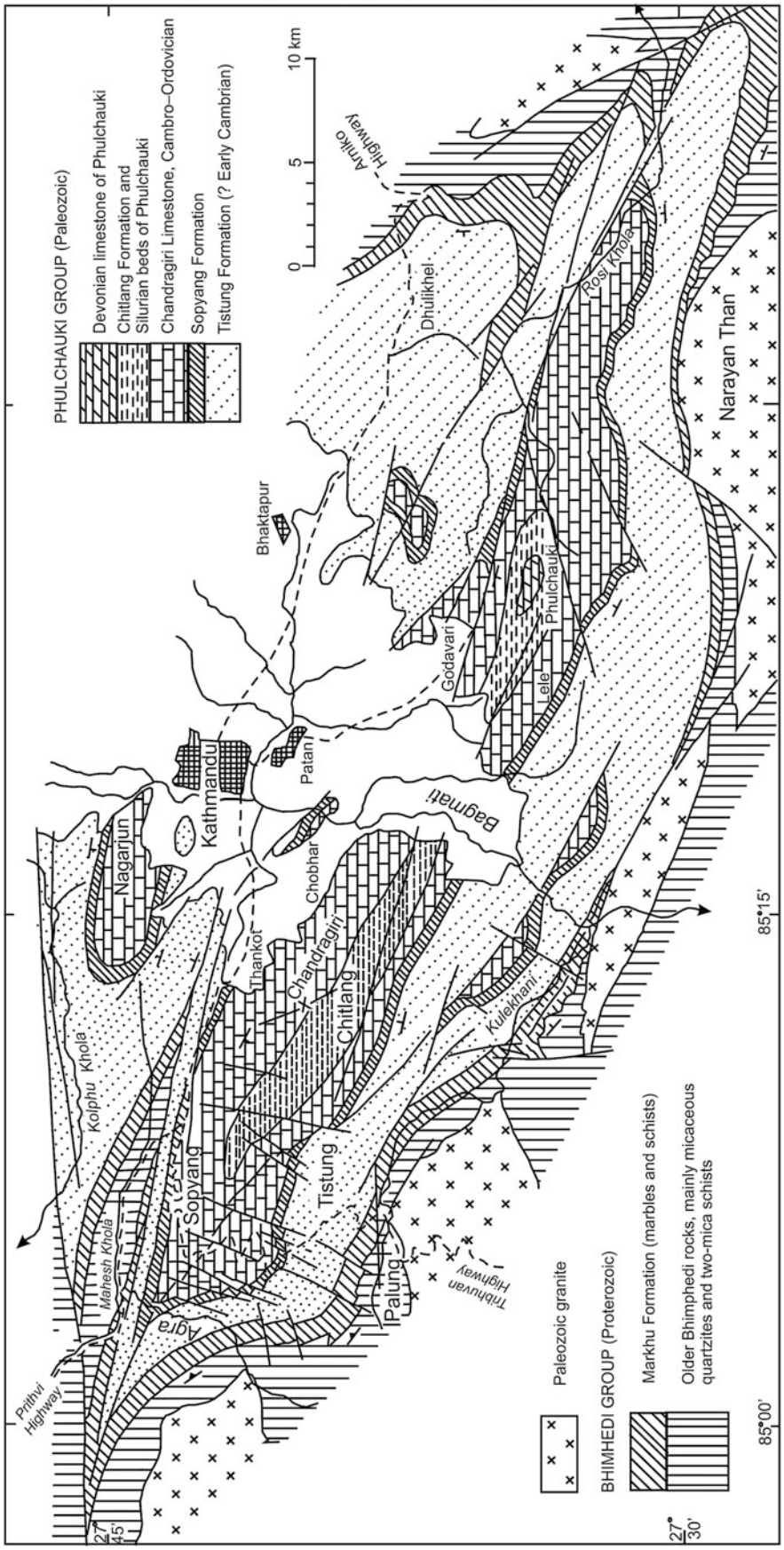

Fig. 17.2 Geological map of the Phulchauki Group in central Nepal. *Source* Modified from Stöcklin (1980)

The Chitlang Formation extends towards the Phulchauki hills, where it is represented by purple slates containing in their lower portion a thick band of white quartzite, followed by a few limestone beds higher in the section. Towards the top part of the slates are intercalated two or three red-purple ferruginous beds, one of which represents the iron ore deposits of Phulchauki (Chap. 21). The iron ores are represented by 10–15 m thick hematitic layers or concretionary bodies. From the ferruginous concretions exposed in the eastern slopes of Phulchauki, Bordet (1961) reported Silurian trilobites as well as other fossils from various locations (Chap. 21). The thickness of these Silurian beds of Phulchauki is about 1,000 m. With the appearance of calcareous slates towards their upper part, the slates of Phulchauki transitionally pass into the lower part of the Godavari Limestone containing crinoids (Stöcklin and Bhattarai 1977, p. 32).

The Godavari Limestone forms the summit of Phulchauki and is the youngest sequence of the Tethyan rocks, constituting the Phulchauki Group in central Nepal. It also forms the core of the Phulchauki syncline as well as the Mahabharat Synclinorium. The lower section of the Godavari Limestone is represented by well-bedded argillaceous limestone of green and purple colors with wave ripples. A number of these beds are packed with crinoids. Overlying the fossiliferous limestone is a massive, coarsely crystalline, white to light brown dolomite. It comprises the main part of the formation and is a few hundred meters thick (Stöcklin and Bhattarai 1977, p. 33).

17.1.3 Paleozoic Granites

In the Kathmandu Complex are found six large Paleozoic granite bodies (Fig. 10.1). Most of them are confined to the Bhimphedi Group, and some are intruded up to the Tistung Formation. Apart from the large intrusives, there are many smaller bodies and some others closely associated with the Sheopuri Injection Gneisses. Generally, these granites are made up of two main varieties. One of them is a biotite-rich granite, which is frequently porphyritic with large (2–3 cm, sporadically up to 10 cm long) idiomorphic K-feldspar crystals, characteristically extremely poor in or devoid of muscovite and tourmaline. The second type is a tourmaline-rich granite, forming irregular bodies within the biotite granite, displaying pegmatitic characteristics with large feldspar, tourmaline, and muscovite crystals, and in it biotite in a very subordinate amount. The granites cut sharply across the bedding planes and fold structures in the Chisapani–Mandu Khola area of south-central Nepal (Stöcklin and Bhattarai 1977, p. 33). Some granite bodies display conspicuously straight alignment, and hence are presumably related to faults. Such folds and faults could have been developed prior to the emplacement of the granites. The contact effects of the granite intrusion on the country rocks are limited to an aureole of a few tens of meters to 200 or 300 m in width, where massive as well as spotted hornfelses are discerned (Stöcklin and Bhattarai 1977, p. 34).

17.1.4 Gneisses and Migmatites

Apart from some gneisses observed to the south of Kathmandu, in the Kathmandu Complex, most of them are confined to the north, where they are called the Sheopuri Injection Gneisses. They are also found around Sindhuli Gadhi in the east and around a small granite complex of Timaldanda, to the east of Kathmandu. The granites of Sindhuli, Timaldanda, and the Shivapuri Range contain from 10 cm to more than 100 m thick granitic or pegmatitic bands, alternating with schists and quartzites. Generally, they are conformably folded. At Sindhuli Gadhi and Timaldanda, the granites occupying the synclinal cores gradually change into granitic gneisses and then to augen and banded gneisses while moving towards the flanks, depicting post-intrusive deformation of granites and formation of gneisses at the expense of their peripheral part (Stöcklin and Bhattarai 1977, p. 36).

17.1.5 Metamorphism

Metamorphism in the Kathmandu Complex gradually increases from nearly unmetamorphic fossiliferous rocks of the Phulchauki Group on top to rocks in the amphibolite facies with kyanite and sillimanite at the base. Sericite and chlorite are common metamorphic minerals in the Phulchauki Group. Very fine biotite flakes are seen in the Sopyang Formation; they become a common mineral in the lower part of the Tistung Formation and continue to be the predominating mineral in the Kulikhani Formation. Although garnets first appear in the Kulikhani Formation, they are abundant in the Lower Schist Member of the Kalitar Formation and the underlying Raduwa Formation, whereas, while crossing the Main Central Thrust, the garnets almost disappear and biotite is changed into chlorite; sometimes small garnets can still be seen in the chlorite schist. This is the zone of inverted metamorphism, and it is generally on the order of 100 m (Stöcklin and Bhattarai 1977, p. 38).

17.2 Rasuwa Gadhi Area

The rocks of Rasuwa Gadhi belong to the root zone of Hagen's Kathmandu and other nappes (Hagen and Hunger 1952). In its vicinity, the Lesser Himalayan sequence is folded into the Great Midland Antiform, which plunges due northeast and contains asymmetrically metamorphosed limbs.

In addition, the rocks also exhibit folds of various scales, strongly developed stretching lineation, and boudinage. The following main lithological units comprise the Lesser and Higher Himalayan successions of this tract (Fig. 17.3).

The Kuncha Formation is widely distributed in the area south of Syaphrubensi, and it also continuously crops out to the north, up to the Chilime village (Fig. 17.3). Here too, the Kuncha Formation is a very thick succession of fine-grained, light gray to dark gray, crenulated schist with a few bands of dark gray quartzite. In the upper part of the formation, there are several thin (5–10 m) zones of fine- to very fine-grained, laminated, light gray to white quartzite, alternating with garnet schists. The grade of metamorphism in the Kuncha Formation increases from south to north, as evidenced from the appearance of chlorite, biotite, and garnet, respectively.

There is a narrow but persistent horizon of calcareous quartzite between the underlying garnet schists of the Kuncha Formation and the overlying graphitic schists. The thickness of this unit varies from about 100 m around the middle loops of the road west of Syaphrubensi to about 20 m at Chilime.

The calcareous quartzites are followed up-section by laminated and intensely deformed graphitic schists with marble bands (Fig. 17.3). In this succession, dark gray to black schists alternate with light gray to white calcareous quartzites or dolomitic marbles. Quartz and calcite veins of several generations crisscross the rock. This unit contains the mineral assemblage garnet + hornblende + plagioclase + quartz + biotite + muscovite + chlorite ± kyanite (accessory: Fe–Ti oxides). Syntectonic garnet porphyroblasts are subhedral to euhedral in shape and reach up to 8 mm in size. They contain helicitic inclusions of quartz, biotite, muscovite, chlorite, and Fe–Ti oxides. These inclusions infrequently display a sigmoidal shape and are aligned parallel to foliation. From 0.11 to 0.4 mm long, subhedral to euhedral hornblende crystals also lie parallel to foliation. Anhedral and polygonal quartz grains, displaying undulose extinction, indicate ductile deformation. Strained plagioclase grains are sericitized at their outer margin.

In this unit, there are mainly three prominent carbonate zones, the thickness of which varies from 50 to 200 m. These zones consist of medium to thick bands of medium- to coarse-grained, white marble containing calcite and dolomite. A strongly folded quartz vein in the graphitic schist about 100 m north of Chilime shows thinned and thickened limbs, where foliation is almost parallel to axial planes of reclined folds. Consequently, the vein was injected obliquely to the principal compression direction and was subsequently involved in folding, rotation, and shearing.

A band of augen gneisses represents the northernmost Lesser Himalayan unit. The band is rather discordant with the underlying formations (Fig. 17.3), and is composed of massive, light gray to gray augen gneisses with schist partings and alternations. The whole sequence is strongly lineated. Near Brabal, the band becomes very thin and disappears below the Main Central Thrust. The augen gneisses usually have the equilibrium assemblage quartz + K-feldspar + plagioclase + biotite + muscovite with varying grain sizes. Mostly anhedral and frequently polygonized quartz grains are up to 0.2 mm in size. Quartz, plagioclase, and K-feldspar are aligned parallel to the foliation plane. Up to 0.65 mm long, anhedral K-feldspar crystals are slightly sericitized and deformed. From 0.5 to 0.9 mm long, euhedral to subhedral plagioclase crystals infrequently show undulose extinction, indicating deformation. Biotite (which is sporadically altered to chlorite) and muscovite define the major foliation plane of the gneiss.

The Main Central Thrust discordantly overrides the Lesser Himalayan succession (Fig. 17.3) and brings with it gray and dark gray, fine- to medium-grained schist and quartzite containing kyanite, garnet, biotite, K-feldspar, muscovite, and quartz. Frequently, the rock is massive to blocky. In the schist, kyanite and garnet crystalloblasts range in size from less than 1 to 5 mm. Generally, they are characterized by the mineral assemblage Kyanite + sillimanite + garnet + biotite + muscovite + chlorite (accessory: tourmaline, Fe–Ti oxides).

In the vicinity of Timure, a thick quartzite succession is exposed. It widens considerably towards the northwest, but extends as a narrow strip to the south, along the Bhote Koshi River. The quartzite is represented by light gray to pale yellow and white, medium to thin bands and laminae. It is sporadically folded and also contains strongly stretched kyanite–garnet schist partings and alternations. The bands also enclose disrupted quartz veins and zones, where stretched garnets have strain shadows of quartz, aligned parallel to foliation.

Banded gneisses and migmatites occupy most of the area north of Timure and east of the Bhote Koshi River (Fig. 17.3). The migmatites are injected into the above quartzite succession and are represented by highly deformed and disrupted leucocratic and melanocratic layers or lenses. The leucocratic layers as well as lenses contain feldspar, quartz, and muscovite, whereas the alternating melanocratic ones are rich in biotite, tourmaline, and hornblende. The gneisses and migmatites exhibit flow structures and many small-scale folds. The gneisses exposed about 2 km north of Nagthali enclose large feldspar-rich boudins and some strongly folded bands. The gneisses contain mainly the assemblage quartz + garnet + biotite + plagioclase + muscovite ± kyanite ± sillimanite (accessory: tourmaline, Fe–Ti oxides). A few undeformed and straight microgranite dikes intersect the migmatites in the direction almost perpendicular to foliation.

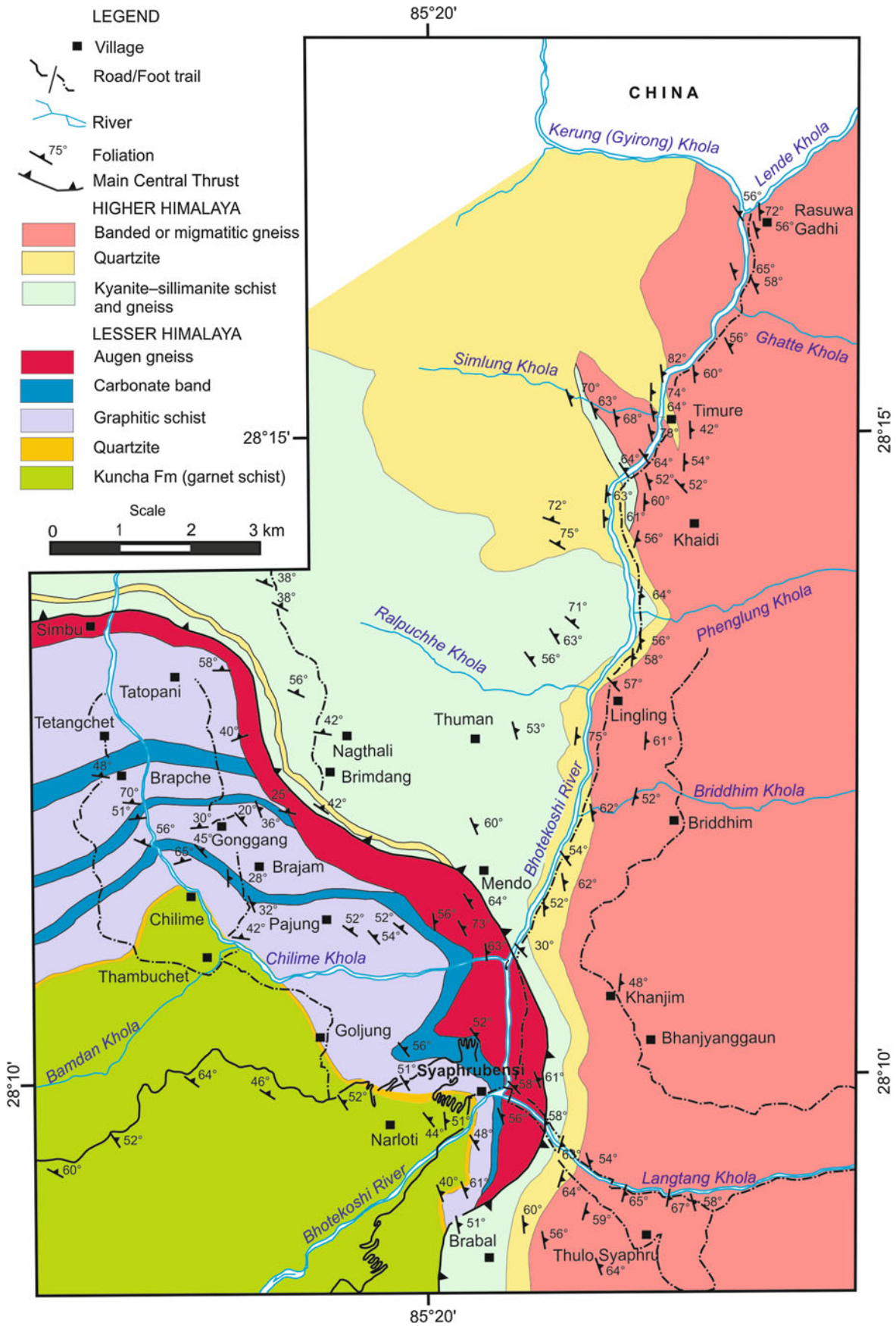

Fig. 17.3 Geological map of the Syaphrubensi–Rasuwa Gadhi area. *Source* Based on field survey in 2009 by MR Dhital, KK Acharya, and N Regmi

17.3 Sundarijal–Melamchi Area

In the Sundarijal–Melamchi area, the Higher Himalayan crystallines contain large masses of augen and banded gneisses, and also record a relatively higher grade of metamorphism than their corresponding formations included under the Kathmandu Complex. The rocks comprise the northeast limb of the Mahabharat Synclinorium and part of the Gosainkund tectonic bridge. Based on lithological characteristics and pre-metamorphic structures, the rocks are classified into the following formations (Dhital et al. 2002).

The Talamarang Formation is made up of light gray to dark gray kyanite–garnet–biotite schists (representing 40–50 % of the total thickness), banded gneisses (30–40 %), and quartzites (10–20 %). There also occur a few bands of white or pale green, clean or sporadically calcareous quartzite as well as sillimanite gneiss or schist. The Talamarang Formation is more than 2,000 m thick, and its contact with the overlying Gyalthum Formation is a gradual transition.

The Gyalthum Formation constitutes the core of the Patibhanjyang Anticline, exposed in the Sindhu Khola. This formation consists of thin- to thick-banded, light gray to gray, laminated quartzites with mica partings (70–80 %), feldspar–garnet–biotite schists (20–30 %), and augen gneisses (5–10 %). This formation too possesses some kyanite- or sillimanite-rich alternations. The quartzites are frequently laminated or cross-bedded, and intensely deformed to yield many conspicuous small-scale folds and faults. The Gyalthum Formation is about 1,700 m thick and transitionally passes into the overlying Bolde Quartzite.

In the Sundarijal–Chisopani area, banded gneisses (80–85 %), augen gneisses (10–15 %), and granitic gneisses (5–10 %) are found within the Gyalthum Formation (Fig. 17.4). They are part of the Sheopuri Injection Gneiss zone. Near Patibhanjyang, banded gneisses are interfingering with laminated quartzites. An approximately 125 m thick zone of mica schist is present to the north of Mulkharka. Protoliths and bands of laminated quartzite are common in the Injection Gneiss zone.

The Bolde Quartzite shows essentially in thick to very thick, massive, medium- to fine-grained, gray bands with mica partings. A few sillimanite-bearing thin schist bands also occur. The quartzite is frequently laminated. Minor cross-bedding and graded bedding can sporadically be seen in the quartzites. The upper part of the Bolde Quartzite imperceptibly grades into the overlying Timbu Formation or the Golphu Formation (in the west). The total thickness of the Bolde Quartzite is about 500 m.

Light to dark gray, intensely deformed, and folded quartzites (10–15 %), schists (5–10 %), banded gneisses (10–15 %), and migmatites (60–70 %) with abundant sillimanite compose the Timbu Formation. It is a discontinuous unit lying between the Bolde Quartzite at the base and the Golphu Formation at the top. The migmatite zone occupies mainly the central and upper levels of the formation, and exhibits various types of ptygmatic folds, small-scale faults, and flow structures. A thick quartzite band occurs in the lower portion of the Timbu Formation, whereas thin quartzite bands are distributed throughout this unit. A few 5–15 m thick garnet–biotite schist bands are also occasionally present. Banded gneisses occupy mostly the lower part of the Timbu Formation, but their thin bands are sometimes seen within the migmatite zone. The maximum thickness of the Timbu Formation is about 1,100 m.

The overlying Golphu Formation contains coarse-grained, thick-banded, dark gray feldspar–garnet–biotite schists (60–70 %) and banded gneisses (30–40 %), with a few laminated quartzite bands (5–10 %). The schists are sometimes crenulated. This formation is crosscut by many pegmatite veins. There are also a few large (several hundred meters long) pegmatite bodies and a zone of augen gneiss. The Golphu Formation is more than 700 m thick.

The moderately (35–50°) northwest dipping Main Central Thrust passes through Majhitar, south of the Sindhu Khola, and crosses the Indrawati River (Fig. 17.4). The thrust is characterized by an approximately 50 m thick zone of garnet–chlorite schist that rests over a 25 m thick fine-grained white quartzite band underlain by the Benighat Slates. The garnet–chlorite schists are followed upwards by the kyanite–garnet schists, belonging to the Talamarang Formation. Although kyanite is observed throughout the Talamarang Formation, yet some sillimanite also sporadically appears in this formation. Sillimanite is rather frequent in the Bolde Quartzite and becomes abundant in the Timbu Formation. The axial trace of the Patibhanjyang Anticline passes through the Sindhu Khola. The fold gently (10–20°) plunges due northwest, and its one limb moderately dips due northeast, whereas the other moderately to steeply dips due southwest. The upper part of the north limb and most of the south limb are invaded by gneisses. Banded gneisses occur either near the Main Central Thrust or adjacent to the core of the anticline, whereas augen gneisses occupy the area beyond the thrust and the core. This type of selective distribution is most probably related to deformation during thrusting and formation of the anticline.

17.4 The Dhulikhel–Panchkhal Area

The Lesser Himalayan sequence of the Dhulikhel–Panchkhal area (Fig. 17.5) is represented by the Benighat Slates. Light green-gray to yellow-gray phyllites and slates, feeble and laminated blue-gray argillaceous limestones together with a massive variety of laminated gray limestone, and sporadic amphibolites constitute this formation. Generally, the rocks are intensely deformed to yield tight and plunging folds.

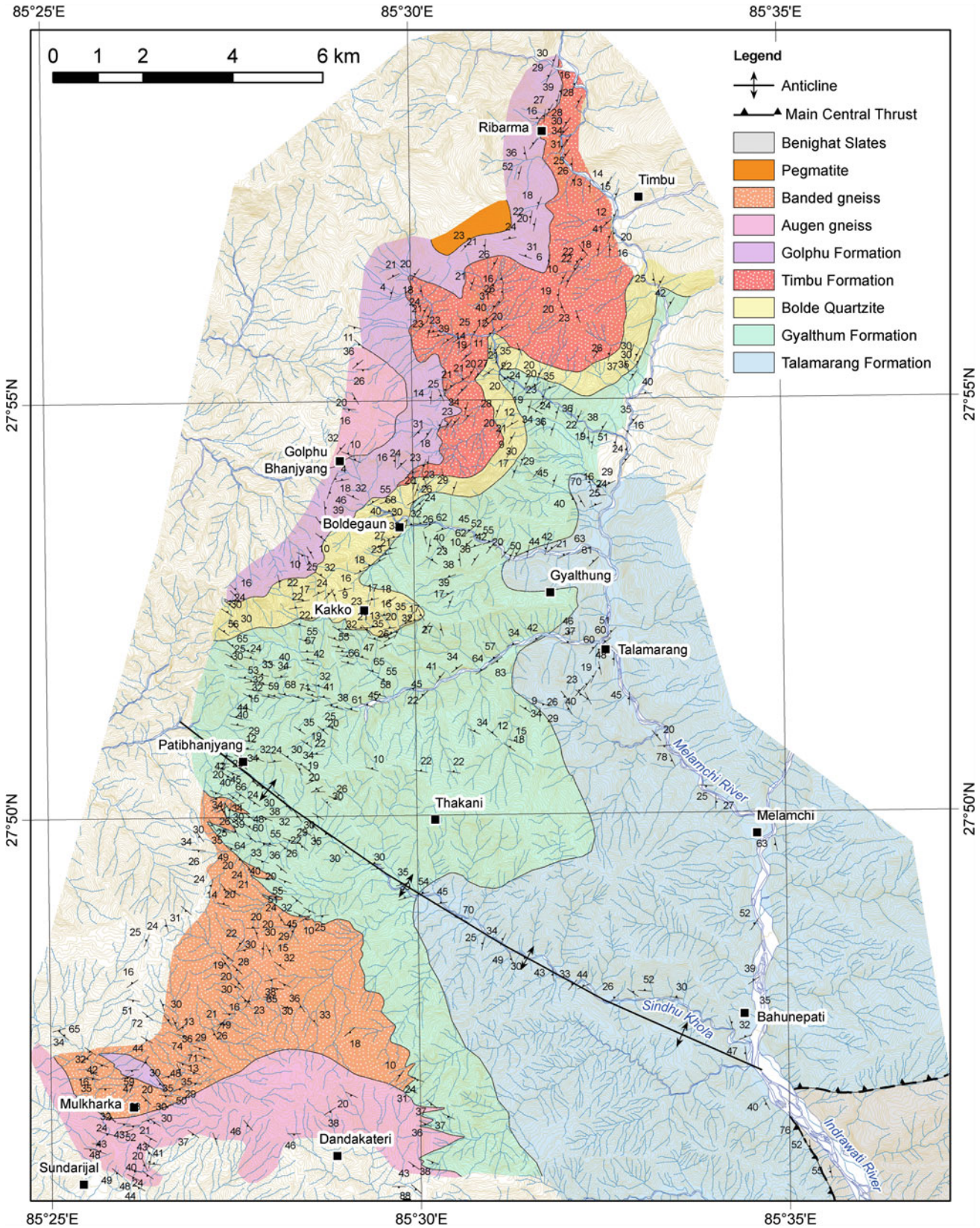

Fig. 17.4 Simplified geological map of the Kathmandu–Melamchi area. *Source* Modified from Dhital et al. (2002)

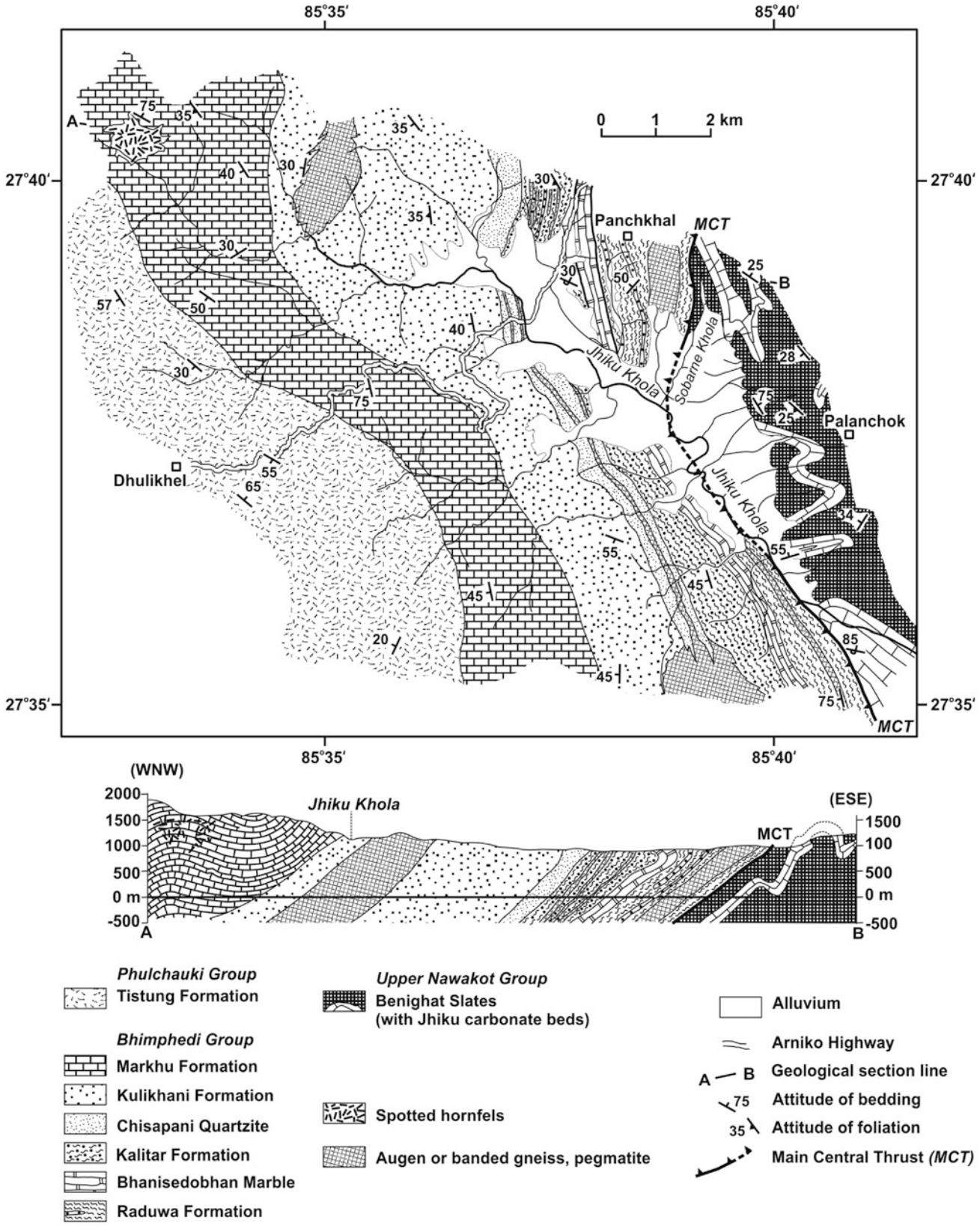

Fig. 17.5 Simplified geological map of the Dhulikhel–Panchkhal area. *Source* Based on field survey in 1997 by NK Tamrakar, KN Paudayal, and MR Dhital

Approximately 250 m thick Jhiku carbonate beds, made up of flaggy as well as massive, laminated, blue-gray argillaceous limestones, are intercalated in slates. Owing to intense folding, the carbonates are repeatedly exposed in a number of places, where their axial traces trend essentially due east–west. At the southeast extremity of the Jhiku Khola, the tightly to isoclinally folded carbonate bands make a gorge, whereas in the Sobarne Khola light green-gray phyllites and slates alternate with dark gray-green amphibolites. The thickness of the Benighat Slates is more than 1,100 m, and its base is nowhere exposed.

The Higher Himalayan crystallines of this area commence with the Raduwa Formation, consisting of green-gray to dark gray, highly foliated garnet–muscovite–biotite schists. There are two major horizons of slabby, micaceous, laminated, white quartzite in its middle and upper parts, and a banded or augen gneiss in the lower part. At the base of the Raduwa Formation, the garnetiferous schists appear to be more chloritic, and also contain many boudinaged and folded quartz veins and lenses. This formation is more than 1,200 m thick.

The overlying Bhainsedobhan Marble is represented mainly by a medium-banded to laminated, coarsely crystalline, white to pale yellow variety, containing phlogopite and accessory pyrite. There are some major alternations of micaceous dark gray quartzite, schist, and thin-bedded to laminated, dark gray calcareous quartzite. The Bhainsedobhan Marble is about 260 m thick.

The succeeding Kalitar Formation is made up of micaceous quartzites, garnetiferous schists, and augen gneisses. In the lower part of the Kalitar Formation, thin- to medium-banded, slabby, micaceous, light green-gray to white quartzites alternate with coarsely crystalline, dark green-gray mica schists. Its upper portion is represented by highly foliated, coarsely crystalline, dark green-gray garnet–muscovite–biotite schists, with a few subordinate intercalations of foliated micaceous light green-gray quartzite and several bands of augen gneiss. The Kalitar Formation ranges in thickness from 650 to 750 m.

The Chisapani Quartzite, which occurs as a marker horizon, is composed mainly of medium to thin, flaggy to slabby bands. Highly foliated, cross-laminated, muscovite- and sericite-rich, light green-gray to white quartzites are also infrequently present. Two major augen gneiss bodies are injected parallel to the quartzite bands, where the gneisses exhibit a more foliated nature owing to their higher mica content. This formation is about 400 m thick.

The overlying Kulikhani Formation is comprised of a relatively monotonous but strongly foliated succession of dark gray, biotite-rich, quartzose schists and flaggy to slabby, dark gray to bluish gray quartzites. Generally, the upper part of the formation is more quartzitic and is invaded by granite sills as well as pegmatite veins and lenses. The formation also consists of augen gneisses at a few places. Owing to a variable degree of interference with granite and pegmatite bands, the thickness of the Kulikhani Formation ranges between 2,400 m to the north and 1,250 m to the south.

The Markhu Formation is made up principally of competent, thick-bedded to laminated, light to dark gray, finely crystalline, calcareous quartzites, and subordinately of thin- to medium-bedded, finely crystalline, blue-gray to dark gray, biotite-rich, calcareous quartzites or quartzose schists. There also infrequently occur laminated light gray siliceous limestones, especially in the lower and upper sections. Granites and pegmatites, forming numerous veins, patches, and lenses, become more prolific towards the northwest, where spotted hornfelses also appear near large igneous bodies. The Markhu Formation ranges in thickness from 1,100 to 1,500 m.

The Tistung Formation delineates the eastern closure of the Mahabharat Synclinorium. Its lower section consists of rather competent, medium-bedded to laminated, light gray to dark gray, biotite-rich quartzites. The sequence continues upwards with an intercalation of light green-gray phyllites and foliated, fine- to medium-grained, light gray, micaceous, laminated metasandstones. The top part is composed of a cyclic sequence of cross-laminated, medium- to fine-grained, light gray, soft, metasandstone, followed by more clayey siltstone with phyllitic thin intercalations. The Tistung Formation is more than 1,700 m thick.

In this area, the Main Central Thrust trends due northwest–southeast and follows mainly the Jhiku Khola. The thrust steepens towards the southeast. Its footwall includes the Benighat Slates, whereas the hanging wall contains garnetiferous schists and quartzites of the Raduwa Formation.

References

Arita K, Ohta Y, Akiba C, Maruo Y (1973) Kathmandu region. In: Hashimoto S, Ohta Y, Akiba C (eds) Geology of the Nepal Himalayas. Himalayan Committee of Hokkaido University, Japan, pp 99–145

Auden JB (1935) Traverses in the Himalaya. Records of the Geological Survey of India, vol LXIX. Part 2, pp 123–167 (with 6 plates including a geological sketch map)

Bordet P (1961) Recherches Géologiques dans L'Himalaya du Népal, Région du Makalu, Expéditions Françaises a l'Himalaya 1954–1955. Edition du Centre National de la Recherche Scientifique (C. N. R. S.), 275 pp

Dhital MR, Sunuwar SC, Shrestha R (2002) Geology and structure of the Sundarijal–Melamchi area, central Nepal. J Nepal Geol Soc 27 (Special Issue): 1–10

Hagen T (1969) Report on the Geological Survey of Nepal. Volume 1: preliminary reconnaissance. Denkschiiften der Schweizerischen Naturforschenden Gesellschaft, Band LXXXVI/1, 185 pp (with a geological map)

Hagen T, Hunger JP (1952) Über geologisch-petrographische Untersuchungen in Zentral-Nepal. Schweiz Miner Petrogr Mitt 32:309–333

Medlicott HB (1875) Note of the Geology of Nepal. Records of the Geological Survey of India, vol VIII. Part 4, pp 93–101 (with a geological map on 1 inch = 6 miles)

Nadgir BB (1976) Tectonics of Nepal Himalaya. Miscellaneous Publication, Geological Survey of India, vol 34. Part 1, pp 109–118

Stöcklin J (1980) Geology of Nepal and its regional frame. J Geol Soc 137:1–34

Stöcklin J, Bhattarai KD (1977) Geology of Kathmandu area and central Mahabharat Range, Nepal Himalaya. HMG/UNDP Mineral Exploration Project, Technical Report, 86 pp (with 15 maps), unpublished

Higher Himalaya of Koshi Region

18

Suddenly, below a little cliff, they came upon a spot of green, Norton's Camp VI of 1924, where Mallory and Irvine spent their last night of life and where Odell came in his great effort to find them. The tent was no longer usable after 9 years of exposure, yet it looked surprisingly new. The men, much cheered by this discovery, rummaged about and found a folding candle-lantern and a lever-torch. The latter worked at the first touch. Then they hurried on downwards, for to remain still in these conditions meant death. The storm continued relentlessly.

—Hugh Ruttledge (1934, pp. 132–133)

The Higher Himalayan succession, that embraces the Okhaldhunga window from the north, belongs to the Khumbu nappe of Lombard (1952). Hagen (1969) mapped these rocks as the Khumbu and Kathmandu nappes, and Ishida and Ohta (1973) included them under their Khumbu migmatites. The Higher Himalayan crystallines also override the window from the south, where they have been classed as the Kathmandu Complex (Chap. 17). From the Bagmati–Gosainkund region, these rocks extend eastwards (Fig. 11.1), forming the close to tight Great Mahabharat Synform, whose core encloses schists, quartzites, marbles, and gneisses, together with some Paleozoic granites. Maruo and Kizaki (1983) identified the Khumbu nappe, Upper Crystalline Sheet, and the Lower Crystalline Sheet from this part of the Higher Himalaya. They also separated the rocks of the Mahabharat Range by a synformally folded thrust, whose structural position is similar to that of the Khumbu nappe.

18.1 Upper Tama Koshi Area

In the upper reach of the Tama Koshi River, the Lesser Himalayan metasediments constitute the footwall of the Main Central Thrust, and its hanging wall contains the medium- to high-grade metamorphic rocks and Miocene granites belonging to the Higher Himalaya (Fig. 18.1). Schelling (1987) divided the Lesser and Higher Himalayan rocks of this area into the following units.

18.1.1 Lesser Himalayan Sequence

The Laduk Phyllites constitute a more than 2,000 m thick pile of gray-green pelitic phyllites, psammitic phyllites, chlorite schists, and graphite schists with garnet and actinolite in abundance, especially near the Main Central Thrust. These rocks are strongly lineated. Schelling (1987, p. 9) reported a foliated dolerite dike, entailing its emplacement prior to the development of foliation in the Laduk Phyllites.

The Suri Dobhan Augen Gneisses crop out in the core of the Tama Koshi Dome, where their thickness exceeds 200 m. The augen gneisses contain muscovite, biotite, quartz, and alkali feldspar. Several centimeter-long feldspar laths are frequently fractured and rotated. A few sporadic bands of quartz-mylonite and sericite-schist are also present within these gneisses.

The Chagu–Chilangka Augen Gneisses range in thickness from 400 to 700 m and they consist of muscovite, biotite, alkali feldspar, quartz, and tourmaline. Quartz frequently shows a bluish tinge. In the gneisses, large (up to 10 cm across) feldspar augen are rotated and fractured with trails of polygonized quartz (Schelling 1987, p. 8). These augen gneisses have a conspicuous C/S fabric, in which the later formed "C" surface is parallel to the foliation in the Laduk and Khare phyllites.

The Khare Phyllites constitute an approximately 2,500 m thick zone of graphite schist, talc schist, chlorite–biotite schist, as well as slate, quartzite, limestone, and magnesite. In them, actinolite and tremolite needles define a lineation. Many small- to meso-scale isoclinal as well as open to close asymmetric folds are common in the Khare Phyllites.

In the Khare Phyllites, the carbonate and quartzite bands (Fig. 18.2) are rather discontinuous, and alternating with black graphitic slates and some infrequent amphibolites. The black slates, equivalent to the Khare Phyllites, continue eastwards from Kharidhunga (Chap. 11) and Kalinchok to the Khimti Khola, and Likhu Khola. Thus, they form an uninterrupted belt representing the Benighat Slates in central Nepal, and are invariably present in the footwall of the Main Central Thrust.

M.R. Dhital, *Geology of the Nepal Himalaya*, Regional Geology Reviews,
DOI 10.1007/978-3-319-02496-7_18

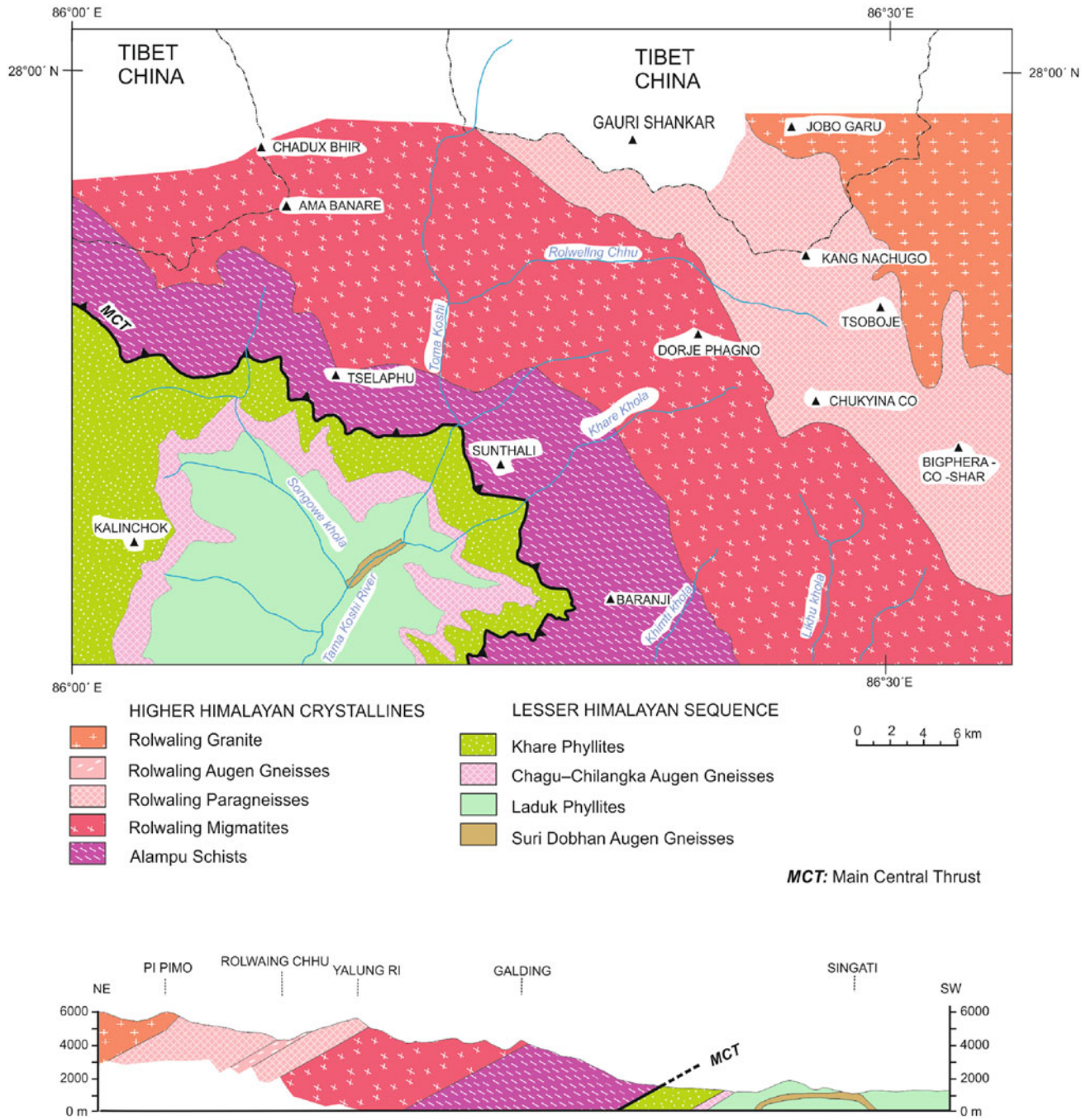

Fig. 18.1 Geological subdivisions of the Upper Tama Koshi area. *Source* Modified from Schelling (1987)

18.1.2 Higher Himalayan Crystallines

The Higher Himalayan rocks override the Khare Phyllites rather abruptly, and they are constituted of the following rock types, respectively, from bottom upwards.

The Alampu Schists are about 6,000 m thick and consist of well-foliated biotite–garnet schists, calcareous schists, quartzites, hornblende schists, feldspathic gneisses, and augen gneisses. The Alampu Schists frequently contain large (up to a few centimeters) garnet porphyroblasts, exhibiting snowball structures, and several centimeter-long blue or green kyanite blades in biotite-rich bands (Schelling 1987, p. 7).

The Alampu Schists are followed upwards by the Rolwaling Migmatites (Fig. 18.1), which attain a thickness of 6,000 m. They are predominantly sillimanite-bearing migmatites with muscovite, biotite, garnet, quartz, feldspar, and tourmaline (Schelling 1987, p. 6). The migmatites are crosscut by a swarm of granitic and pegmatitic veins.

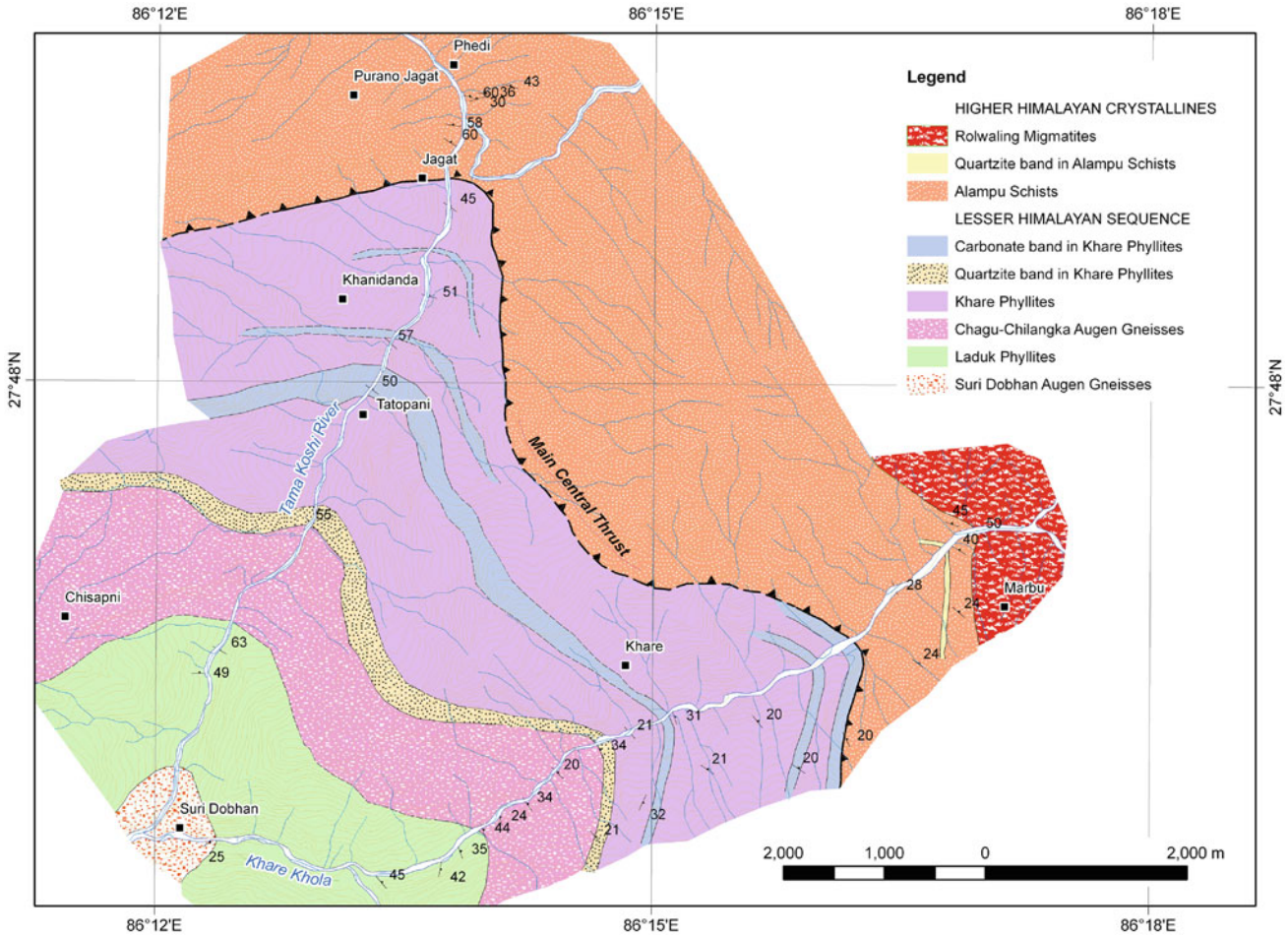

Fig. 18.2 Geological map of the Tama Koshi–Khare area showing quartzite and carbonate bands within the Khare Phyllites. *Source* Based on field survey in 2006 by SC Sunuwar and R Shrestha, and in 2012 by MR Dhital

Farther upwards, the migmatites give way to about 6,000 m thick Rolwaling Paragneisses. The paragneisses are delimited from above by a sharp intrusive contact with the Rolwaling Granites and below by a gradational contact with the underlying Rolwaling Migmatites (Schelling 1987, p. 5). This unit also possesses some biotite schists, calcareous schists, marbles, and granitic gneisses. Sillimanite, garnet, and hornblende are regularly found in the biotite schist. There are also a few, up to 600 m thick, augen gneiss bands in the paragneisses.

The Rolwaling Granites represent a typical Higher Himalayan leucogranite body (Schelling 1987, p. 4). The granites are typically medium-grained and they are composed of quartz, K-feldspar, plagioclase, biotite, muscovite, and tourmaline. Garnet is also infrequently found in the granites, whereas some pegmatite veins contain beryl. The granites cover at least an approximately 50 sq km area and are from 2.5 to 3 km thick in the Rolwaling Valley. The granite body is either undeformed or slightly deformed but the pegmatitic and aplitic veins are strongly folded. Inasmuch as there are no major feeder dikes, Schelling (1987, p. 5) inferred that the source of granite lies farther north, under the Tibetan Plateau, and the granite moved to its present position along the northeast-dipping Tethyan sediment–paragneiss contact.

18.2 Early Expeditions to Mount Everest

The discovery of Mount Everest (Box 18.1) as the highest summit on earth, immediately attracted the attention of mountaineers from many countries. Consequently, various expeditions were organized to ascend this peak and by the prevailing tradition of that time, there happened to be geologists on their team. Heron (1922) was the first geologist to visit the Tibetan portion of the Arun River and carry out a reconnaissance survey of the area, north of Mount Everest. As a member of the first Mount Everest expedition of 1921, his investigations were limited between the river Yaru Chu (Yeru Zangbu) on the east to the town of Tingri and the river

Po Chu (the Bhote Koshi, north of Kodari) on the west. In fact, his work was a westwards continuation of Hayden's (1907) geological research during the Tibet expedition of 1903–1904.

Box 18.1: A Maiden Deity

The Sherpas of Nepal and Tibet call the highest peak *Jomo Langma*, a shortened form of *Jomo Miyo Langsangma*, the name of a maiden deity believed to be resident on the mountain (Sherpa 2003, p. 4). Mount Everest is called Sagarmatha in Nepali.

In the Higher Himalayan zone, Heron identified foliated and banded biotite gneisses with garnets, intimately injected by schorl–muscovite granites or pegmatites. The igneous rocks exhibit every variety of textures, ranging from fine homogeneous granite to coarse pegmatite with graphic intergrowth of quartz and feldspar. Between the sedimentary rocks of the Tethys and the banded gneisses, there are mica schists, tourmaline–mica quartzites, and other metamorphic rocks, which are also penetrated by these youngest igneous bodies. They crosscut almost every crystalline rock in the form of dikes, veins, and sills of varying sizes.

Heron (1922, p. 223) noted that, in contrast to the intense crumpling of the sedimentary sequence comprising the Tethyan zone to the north, the metamorphics overlying the gneisses of the Higher Himalaya are surprisingly gently northwards dipping and are invaded by granite sills injected parallel to foliation.

As a member of the 1924 Everest expedition, Odell (1925, pp. 290–291) described the metamorphic rocks of the Mount Everest region from the valley of the Dzakar Chu, where the Gyachung Chu is confluent from the west. The rocks form a high cliff on the eastern bank of the Dzakar Chu and are composed of horizontal bands of dark biotite gneiss alternating with bands of light granite, representing an example of a large-scale lit-par-lit injection. The granites give way to pegmatites towards the higher part of the cliff. On the other hand, the gneiss itself is composed of feldspathic and biotitic bands, and it predominates in the upper part of the cliff. At the confluence of an eastern head-tributary of the Dzakar Chu, near the snout of the Rongbuk Glacier, the horizontally dipping banded gneiss is invaded by light granite both along the foliation planes and also right across them. The granite is light pink in color, contains tourmaline and garnet, is poor in white mica, and frequently grades off into pegmatite. The biotite gneiss is also garnetiferous.

Higher up in the gorge, there is a porphyritic granite or pegmatite with large (5–7 cm across) muscovite and tourmaline phenocrysts. On top of it is a thick band of hard, variegated (mainly green) crystalline limestone with much epidote, and it is also invaded by the pegmatite. A similar metamorphosed crystalline limestone also crops out at the snout of the East Rongbuk Glacier, where it rests over the schorl granite with its apophyses extended into the limestone. The last limestone band is about 30 m thick and concordantly followed upwards by a banded biotite gneiss with other associated metamorphic rocks. This essentially undisturbed but metamorphosed sedimentary succession continues to the south up to the head of the East Rongbuk Glacier. It persists farther southwards, in the lower part of the northeast ridge of Mount Everest, where the contact with the overlying banded biotite gneiss is excellently exposed. A fault and an anticlinal flexure are also distinct (Odell 1925, p. 291).

The North Col is composed of the metamorphic rocks, ranging from very fine biotite gneisses to hornblende- and tourmaline-bearing rocks, gently (29–30°) dipping due north. While moving up the north ridge, towards the peak of Mount Everest, the siliceous rocks gradually pass into overlying calcareous beds represented by dark calc-gneisses, light limestones, and sandstones. They are injected by various granite dikes and pegmatite veins. The final pyramid of Mount Everest and its northeast shoulder (at an altitude about 8,400 m) rest on an approximately 200 m thick light brown band of calcareous sandstone, which is at times micaceous and injected by pegmatite and granite veins. The pyramid is made up of a very fine-grained and compact, dark calc-schist containing quartz and biotite. It extends some distance along the northeast shoulder as a cap rock to the above calcareous sandstone. This Mount Everest sedimentary series also continues northwards to form the peak of Changtse (Zhangzi) where it rests upon the biotite gneiss with a sharp and straight contact. Here too, the gneiss is profusely veined with light colored pegmatites (Odell 1925, pp. 292–293). Various gneisses, migmatites, and granites constitute the south slopes of Mount Everest (Chap. 19).

18.3 Khumbu Neighborhood

Ishida and Ohta (1973, p. 42) studied the migmatites of Khumbu from the vicinity of Namche Bajar, in the upper reaches of the Dudh Koshi, where they moderately dip due northeast. There are mainly two types of rock: lit-par-lit injection gneisses with several centimeter-thick, tourmaline-bearing granitic pegmatites and various migmatites, showing many minor folds accentuated by biotite-rich layers. Sillimanite, cordierite, garnet, plagioclase, K-feldspar, biotite, and quartz are the main rock-forming minerals. Sillimanite shows in small prisms in the migmatites or fibrous aggregates in injection gneisses. Cordierite occurs in large volumes both in migmatites and gneisses. Biotite is present in two types

(exhibiting essentially green or brown pleochroism). Poikiloblastic garnets 2–3 mm in diameter are less common.

Below the migmatites occur banded biotite gneisses with several thin amphibolite layers and quartz–mica schist bands. The gneisses contain many poikiloblastic garnets with quartz, sericite, biotite, and magnetite inclusions. The amphibolites are made up of K-feldspar, plagioclase, hornblende, epidote, quartz, and biotite.

18.4 Metamorphism in the Dudh Koshi Area

In the Dudh Koshi and neighboring area of east Nepal, Hubbard (1989) investigated metamorphism in the Main Central Thrust zone and also in the contiguous Higher Himalayan crystallines. She identified a 3–5 km thick shear zone, separating the chlorite-bearing schists of the Lesser Himalaya from the overlying sillimanite-bearing migmatitic gneisses of the Higher Himalaya. Here, the metamorphic grade steadily increases through the Main Central Thrust zone towards the structurally higher levels. Hubbard (1989, p. 20) defined the lower boundary of the shear zone associated with the Main Central Thrust as the contact with the lowermost augen gneiss of Phaplu (Chap. 11) with the underlying fine-grained chlorite–muscovite schist of the Lesser Himalaya. She designated the upper boundary of the shear zone within the upper gneiss unit of the Higher Himalaya. The gneiss separates less-deformed, frequently migmatitic gneisses to the north from more deformed biotite gneisses. Most of the Higher Himalayan rocks are represented by pelitic schists, calc-silicate rocks, and gneisses as well as minor amphibolite bands, and granite bodies. The foliation in the gneisses is relatively less penetrative than its mylonitic fabric, which is excellently developed within the Main Central Thrust zone. South of Namche, the foliation moderately (30–40°) dips due N10°–20°E. North of Namche, the foliation outlines many east–west-trending open folds. The granitic rocks of the Higher Himalaya contain an assemblage of quartz + K-feldspar + plagioclase + biotite ± tourmaline ± muscovite ± garnet ± sillimanite.

The predominantly euhedral garnets within the Main Central Thrust zone are generally 1–2 mm in diameter, and the large ones contain helicitic inclusion trails in their cores. Inclusion-free overgrowths surround most of the helicitic cores. Subhedral to anhedral garnets from the Higher Himalaya range in diameter from 2 to 3 mm. Fibrolitic sillimanite occurs as mats and along the foliation plane in the upper part of the Main Central Thrust as well as in the overlying Higher Himalayan crystallines. Kyanite is found mainly within the Main Central Thrust zone, where it is aligned parallel to foliation and also infrequently bent around garnet porphyroblasts, indicating its pre- to syn-kinematic growth (Hubbard 1989, p. 21).

Hubbard (1989, p. 22) discussed three possibilities for the relationship of thrusting and latest metamorphic equilibrium: pre-metamorphic, syn-metamorphic, or post-metamorphic. She eliminated the first case on textural evidence (because metamorphic minerals have not grown across the foliation plane); the second case requires a temperature profile reflecting juxtaposed or overturned isotherms and a normal lithostatic pressure gradient; whereas the third case would result in saw-tooth-shaped temperature and pressure profiles (Chap. 20). The temperature curve (Fig. 18.3a) fits reasonably with the model where the isotherms are overturned as a result of thrust emplacement (Le Fort 1975). The apparent pressure profile within 10 km of the kyanite zone is consistent with the normal lithostatic pressure gradient, which decreases up-section. On the other hand, a frictional heating model would require the peak temperatures within the Main Central Thrust zone, but in this case, the peak temperatures are noted beyond that zone (Fig. 18.3b). Hence, the temperature profile within the Main Central Thrust zone implies a syn-metamorphic thrusting (Hubbard 1989, p. 26).

In this part of the Higher Himalaya, ^{40}Ar–^{39}Ar dating of a hornblende grain from the Main Central Thrust zone indicated the thrust movement and metamorphism about 21 Ma. Granitic intrusion was contemporaneous with movement along the Main Central thrust and metamorphism, where peak temperatures were maintained for a period of less than 2 million years. In this area, regional heating was associated with the granite intrusion. However, there was also relatively recent (about 8 Ma) deformation in the Higher Himalaya (Hubbard and Harrison 1989). Although the average exhumation rate was 1.2 ± 0.6 km/Ma over the time interval from 21 Ma to the present, the exhumation rate could have fluctuated significantly within that interval. The exhumation rate was least sensitive to the details of the assumed initial geotherm, fairly sensitive to the magnitude of radiogenic heat production, and highly sensitive to the nature of boundary conditions applied below the fault zone (Hubbard et al. 1990).

18.5 Metamorphism Within Great Mahabharat Synform

Various metamorphic rocks, such as schists, quartzites, and marbles together with banded and granitic gneisses, constitute this part of the synform (Ishida and Ohta 1973, p. 45). Paleozoic granites with a foliated outer rim occupy its core. They consist of coarse-grained quartz, K-feldspar, plagioclase, biotite, and muscovite. The synform shows a Barrovian type of metamorphism, ranging from the greenschist facies towards the top to the upper amphibolite facies at the bottom, as evidenced from the successive appearance of chlorite, biotite, garnet, staurolite, kyanite, and sillimanite. In this area, the metamorphic isograds are concordantly folded with the Great

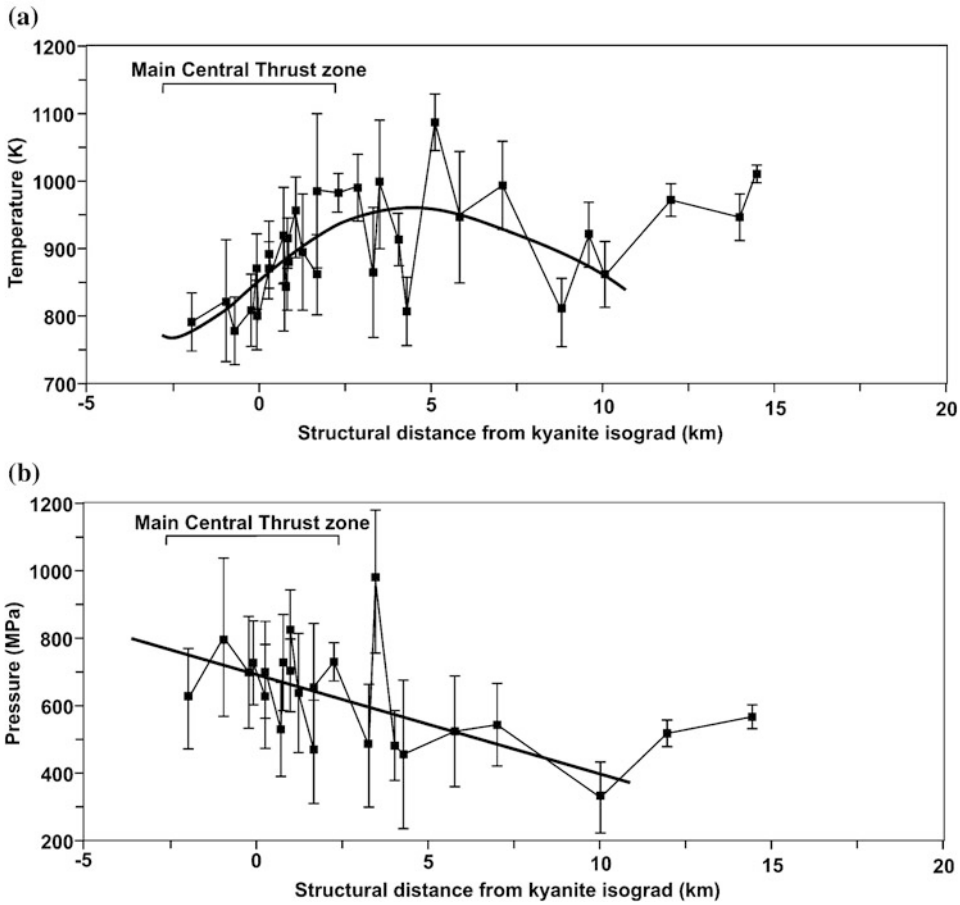

Fig. 18.3 Thermobarometric results from the Dudh Koshi and Hinku–Hongu transects, plotted against the structural distance above the kyanite isograd. Error bars indicate two estimated standard deviations. **a** Temperature and **b** pressure data from the Main Central Thrust zone and the overlying Higher Himalayan crystallines. *Source* Modified from Hubbard (1989). © John Wiley and Sons Ltd. Used by permission

Mahabharat Synform (Ishida and Ohta 1973, p. 62), as they do in the Karnali neighborhood (Chap. 15). But, contrary to the latter area with an inverted grade and the metamorphic thermal peak located above the synform, in this part, the peak lies at the base, near the Main Central Thrust (Maruo and Kizaki 1983).

18.6 Sun Koshi–Kakur Khola Tract

The Higher Himalayan crystallines compose the Mahabharat Range of the Sun Koshi–Kakur Khola tract (Fig. 18.4). Besides, they are part of the Great Mahabharat Synform that extends eastwards from the Bagmati–Gosainkund region (Chap. 17). Here too, the Main Central Thrust is folded around the synform, where the metamorphic grade decreases structurally and stratigraphically upwards from the thrust. The synform gently plunges due east, and its north flank is thrust over the Lesser Himalayan Harkapur Formation, which extends along the Sun Koshi River (Chap. 11). Its south limb overrides the Benighat Slates, distributed along the foot of the Mahabharat Range.

The Raduwa Formation, the lowest stratigraphic unit of the Kathmandu Complex, appears only in the south flank of the Great Mahabharat Synform, because banded and granitic gneisses have taken up its position in the north limb. Gneisses and granitic bodies are emplaced in the south flank of the synform as well, where they partially assimilate the Raduwa Formation and other younger sequences. Gray to green-gray, garnet–biotite–muscovite schists are the principal constituents of the Raduwa Formation, where garnets may exceed 5 mm in diameter (Thapa 1999). Gray to pale yellow, parallel-laminated quartzites occur subordinately in 10–15 m thick bands. Some quartzites are strongly stretched and boudinaged. The Raduwa Formation is more than 1 km thick, and towards its upper end, banded and augen gneisses are injected in several hundred-meter-thick layers.

The Raduwa Formation is transitionally succeeded by the Bhainsedobhan Marble, most of which too is replaced by gneisses. A small portion of it is exposed in the southwest corner, where it is represented by light green-gray to white, coarse-crystalline, impure marbles with schist partings and thin lime-silicate bands (Dwivedi 1997). The Bhainsedobhan Marble is about 200 m thick.

The Kalitar Formation is also developed only in the south flank. It comprises mainly gray to dark gray, two-mica schists and garnet schists, regularly alternating with strongly micaceous quartzites. Biotite is the predominating mineral, however, the schists also include quartz, hornblende, and

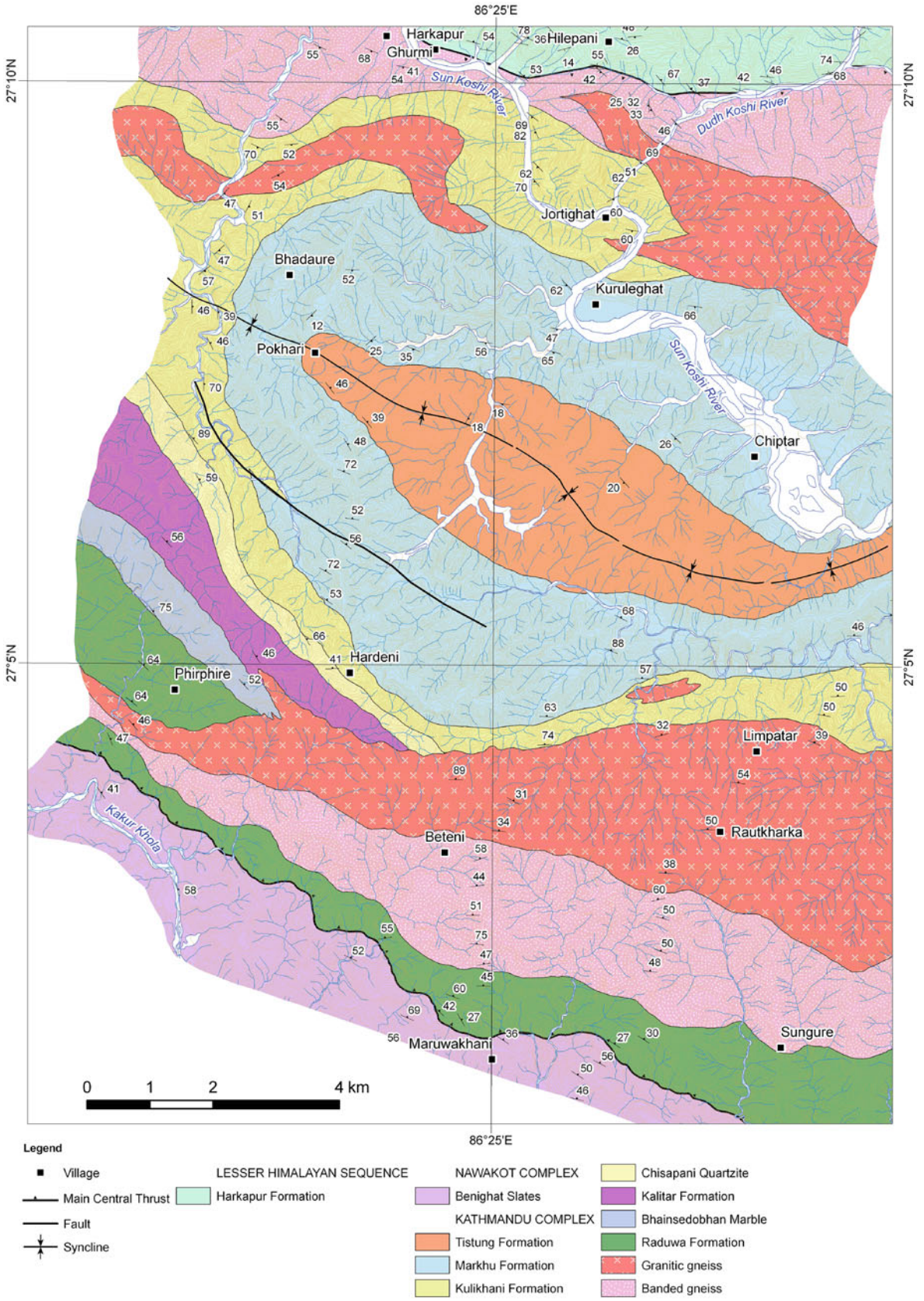

Fig. 18.4 Geological map of the Sun Koshi–Kakur Khola tract. *Source* Modified from Dwivedi (1997) and Aryal (1997)

muscovite. Most of the garnet crystalloblasts exhibit a snowball structure (Dwivedi 1997) with a mica envelope. The size and abundance of garnets decreases stratigraphically upwards. With a rapid transition, the Kalitar Formation passes into the overlying Chisapani Quartzite. The Kalitar Formation attains a thickness of about 300 m.

The Chisapani Quartzite is the most conspicuous formation of the area, but it is also partly replaced by banded and granitic gneisses. The quartzite is usually light green to pale gray, very dense, and massive. It is very fine-grained, thick-bedded, and parallel- as well as cross-laminated. The Chisapani Quartzite is about 250 m thick.

The transitionally succeeding Kulikhani Formation is found mainly around the synclinal closure. It is also crosscut by augen gneisses and granitic gneisses. The Kulikhani Formation comprises fine-grained, dark green or gray-green biotite schists and quartzites. There is a complete transition from a quartzite band to a schist band. This formation also contains tiny garnets, especially in its lower part, and its thickness is about 700 m.

The Markhu Formation is excellently exposed in both flanks of the synform. It is represented by an alternation of quartzite, schist, and marble. The marbles predominate over other lithologies, where their thickness ranges from a few centimeters to tens of meters. The light gray to white and blue-gray to dark gray marbles alternate with thin quartzite bands or gray-green schist partings. The upper portion of the Markhu Formation consists of an alternation of light green phyllite and thin marble or calcareous quartzite. This formation is about 1,400 m thick.

The Tistung Formation of the Phulchauki Group succeeds the Markhu Formation with a rather sharp contact. It constitutes the core of the synform and is made up of gray biotite schists and phyllites, passing upwards into dark gray to black slates and metasandstones, marked by a significant decrease in metamorphic grade. The Tistung Formation is about 500 m thick (Thapa 1999).

Banded gneisses are distributed in both flanks of the synform, where they are concentrated towards its base. They are composed of muscovite, biotite, garnet, and kyanite. Quartz and pegmatite veins are widespread in the gneisses, which also enclose some thin bands of schist and quartzite.

Granitic gneisses are intruded into various formations of the Kathmandu Complex (Fig. 18.4). Most of them exhibit a weakly developed foliation and have been transformed into augen gneisses. They contain quartz, K-feldspar, plagioclase, biotite, muscovite, and tourmaline. A variety of pegmatite veins have also penetrated the granitic gneisses.

References

Aryal A (1997) Engineering geological study of the Katari–Okhaldhunga road, between Km 11 + 500 and Km 28 + 000, Eastern Nepal Lesser Himalaya. Unpublished M.Sc. thesis, submitted to the Central Department of Geology, Tribhuvan University, Kirtipur, Kathmandu, Nepal, 73 pp

Dwivedi SK (1997) Geology of the area between the Sunkoshi River and the Kakaru Khola, Udayapur District, Eastern Nepal. Unpublished M.Sc. thesis, submitted to the Central Department of Geology, Tribhuvan University, Kirtipur, Kathmandu, Nepal, 49 pp

Hagen T (1969) Report on the geological survey of Nepal. Volume 1: preliminary reconnaissance. Denkschiiften der Schweizerischen Naturforschenden Gesellschaft, Band LXXXVI/1, 185 pp (with a geological map)

Hayden HH (1907) The geology of the provinces of Tsang and Ü in central Tibet. Mem Geol Surv India XXXVI(part 2):1–80

Heron AM (1922) Geological results of the Mount Everest reconnaissance expedition. Rec Geol Surv India LIV(Part 2):215–234 (with a map in colors, scale: 1 inch = 8 miles; and three diagrammatic cross-sections)

Hubbard MS (1989) Thermo-barometric constraints on the thermal history of the main central thrust zone and the Tibetan slab, eastern Nepal Himalaya. J Metamorph Petrol 7:19–30

Hubbard MS, Harrison TM (1989) 40Ar/39Ar age constraints on deformation and metamorphism in the main central thrust zone and Tibetan slab, eastern Nepal Himalaya. Tectonics 8(4):865–880

Hubbard M, Royden L, Hodges K (1990) Constraints on unroofing rates in the high Himalaya, eastern Nepal. Tectonics 10(2):287–298

Ishida T, Ohta Y (1973) Ramechhap–Okhaldhunga region. In: Hashimoto S, Ohta Y, Akiba C (eds) Geology of the Nepal Himalayas. Himalayan Committee of Hokkaido University, Sapporo, pp 35–68

Le Fort P (1975) Himalayas, the collided range: present knowledge of the continental arc. Am J Sci 275-A:1–44

Lombard A (1952) Les grandes lignes de la géologie du Népal Oriental. Bulletin de la Société Belge de Géologie de Paléontologie et d'Hydrologie. Bruxelles LXI(Fascicule 3):260–264

Maruo Y, Kizaki K (1983) Thermal structure in the nappes of eastern Nepal Himalayas. In: Shams FA (ed) Granites of Himalaya, Karakorum and Hindukush. Institute of Geology, Punjab University, Lahore, pp 271–286

Odell NE (1925) Observation on the rocks and glaciers of Mount Everest. Geogr J LXVI(4):289–315 (with a map in colors on 1:25,000 scale)

Ruttledge H (1934) Everest 1933. Hodder and Stoughton Limited, London, p 390 (with a topographic map of scale 1 inch = 1 mile)

Schelling D (1987) The geology of the Rolwaling—Lapchi Kang Himalayas, east-central Nepal: preliminary findings. J Nepal Geol Soc 4(1 and 2):1–19

Sherpa LN (2003) Two sides of Everest. In: Sherpa AR, Höivik S (eds) Triumph on Everest: a tribute from the Sherpas of Nepal. Mandala Book Point, Kathmandu, pp 3–10

Thapa SK (1999) Geology of the area between the Kakaru Khola and the Sunkoshi River, Udayapur District, Eastern Nepal. Unpublished M.Sc. thesis, submitted to the Central Department of Geology, Tribhuvan University, Kirtipur, Kathmandu, Nepal, 60 pp

Higher Himalaya of Arun–Tamar Region

19

Across the Buranse Dande, on the path down to the Arun river and Leguwa Ghat, occur gneiss at 3,700 feet and biotite-granite at 3,500 feet.

—J.B. Auden (1935, p. 143)

After visiting the Arun and Tamar valleys, Auden (1935) extended his journey via the Singalila Ridge to Darjeeling. As a result, he confirmed that the Higher Himalayan crystallines of east Nepal are linked up with the Darjeeling Gneiss (Chap. 5; Box 19.1). Although Hagen (1959) had proposed very many nappes in this region, detailed geological mapping by Bordet and Latreille (1958) and further investigations by Bordet (1961) revealed primarily a single Higher Himalayan thrust sheet that had traveled towards the foreland for more than 100 km. Akiba et al. (1973) included the north watershed of the Arun River under their Irkhuwa crystalline nappe. In the Arun–Tamar region, the Higher Himalayan crystallines dip gently due north and are overlain by the Tethyan Himalayan sequence of low-grade metamorphic and sedimentary rocks. Miocene leucogranites, which are magnificently exposed on Cho Oyu, Nuptse, and Makalu, occur at the boundary between the metamorphic and sedimentary sequences (Lombardo et al. 1993).

Box 19.1 Darjeeling Link

On his way from Darjeeling to Tongló, Hooker (1849, p. 433) noted some enormous detached masses of gneiss, which rise abruptly from the ridge. These rocks are strongly deformed and distorted. He was further impressed by the ubiquity of gneiss in this part of the Himalaya as well as in east Nepal, while visiting the Tamar Valley (Hooker 1854).

On the other hand, it goes to the credit of Sherwill (1853), who ventured to verify Hooker's statement that Kanchenjunga and many other summits are composed of granite. Sherwill got this opportunity after an unusually severe earthquake hit Darjeeling in May 1852, and it threw down a very large part of the southwest face of perpetually snow-clad Kanchenjunga, exposing a dark mass of rock. He traveled to the foot of the mountain and observed that Kanchenjunga and many other neighboring summits are also made up of gneiss.

Ghosh (1956, pp. 92–93) reported Daling rocks from the Arun and Tamar valleys in east Nepal, where they dip in three sides under the gneisses and form antiforms, whereas the gneisses form the corresponding synforms, as in Sikkim and Darjeeling. In the Arun and Dudh Koshi valleys, there are metamorphic gradations of the pelitic rocks from the phyllites of the Tamar Valley to the garnetiferous gneisses on the ascent to Dhankuta. On the Hile and Guranse ridges, garnetiferous mica schists are overlain by and grade into sillimanite gneisses.

19.1 Makalu–Arun Neighborhood

The Higher Himalayan crystallines of this tract constitute an approximately 6–7 km thick succession of gneiss and migmatite with large bodies of granitic orthogneiss in its middle part, and biotite paragneiss and mica schist towards the upper end, where there are lens-shaped subconcordant bodies and a network of intersecting dikes belonging to tourmaline leucogranites (Lombardo et al. 1993). Although various investigators have used a variety of classification schemes (Table 19.1), the following units (Bordet 1961, pp. 56–59) are mainly discernible in this area (Fig. 19.1).

19.1.1 Barun Gneisses (Gneiss du Barun)

The Barun gneisses have a sharp tectonic contact with the underlying rocks of Tinjure, and form the base of the Higher Himalayan sequence. They exhibit regular banding, defined by white (quartz and feldspar) and black (biotite) minerals.

M.R. Dhital, *Geology of the Nepal Himalaya*, Regional Geology Reviews,
DOI 10.1007/978-3-319-02496-7_19

Table 19.1 Comparison of various rock units of Arun–Everest region

Nepal				Tibet		
Lombard (1958)	Bordet (1961)	Krummenacher (1967)	Bortolami et al. (1983)	Odell (1925)	Wager (1934, 1939)	Yin and Kuo (1978)
Calcaires de l'Everest	Gneiss noirs	Gneiss Supérieurs du Khumbu	Everest Metapelites	Upper calcareous series or Mt. Everest calcareous series	Mt. Everest limestone series	Jolmo Lungma Formation
Série pélitique supérieure de l'Everest						Yellow band
Série pélitique inferieure de l'Everest			Black Gneiss	Gneissose biotite series or Banded biotite gneiss	Mt. Everest pelitic series	North Col Formation
Ecaille du Nuptse and Nappes du Khumbu	Migmatites du Barun	Migmatites du Khumbu	Island Peak Complex	Lower calcareous series	Lower Mt. Everest limestones	Muscovite gneiss
	Gneiss du Barun	Gneiss inferieurs du Khumbu				Rongbuk Formation

Source Modified from Bortolami et al. (1983)

The extremely thick (6–7 km) Barun gneisses are characterized by a very frequent occurrence of sillimanite and garnet, absence of muscovite, and prevalence of thin banding (1 mm–1 cm). Some yellowish sillimanite-rich bands constitute typical slip surfaces. Certain areas are rich in blue kyanite, others contain impure marbles with pyroxene and black amphiboles. There also occur zones of quartzite devoid of biotite and bands almost exclusively composed of biotite, without any light colored mineral. The gneisses are generally tabular to subhorizontal, and they frequently form immense cliffs (Bordet 1961).

In some locations, the gneisses contain very large idiomorphic garnet crystals, reaching a size of 15 cm, whereas some irregular ones are 20–25 cm. They generally accompany pyroxene, where the gneissic banding is perturbed by their overgrowth. There are also some zones of augen gneisses, where the augen are generally less than a centimeter in size, but sporadically one encounters translucent feldspar crystals reaching 8–10 cm in length.

The presence of impure marbles, the way they are interstratified, and a rapid compositional change in the succession proves the sedimentary origin of the Barun gneisses. Some pegmatite veins have crosscut gneisses, and a number of granite sills have intruded parallel to foliation (Bordet 1961).

19.1.2 Barun Migmatites (Migmatites du Barun)

The Barun gneisses pass into the overlying Barun migmatites by gradual disappearance of garnets, increase in number and size of feldspar crystals, and also diffusion of pegmatite veins. The migmatites resemble Bordet's Lesser Himalayan gneisses very much. They are from 500 to 1,000 m thick. These migmatites are also similar to those occurring in the vicinity of Namche Bajar, studied in detail by Krummenacher (1956) and Lombard (1958). A possible Cambrian age was assigned to the granite protolith found in the Namche migmatitic orthogneiss (Kai 1981; Ferrara et al. 1983). The migmatitic orthogneisses frequently contain cordierite and also include many pods and dikes of granite neosome (Bordet 1961, p. 162).

Bortolami et al. (1983) investigated the south portion of the Mount Everest neighborhood, and stated that Miocene granites constitute the skeleton of the highest peaks, although they are not the axial granite core of the mountain ridge; they are, therefore, a fundamental characteristic of the Himalayan mountain landscape. Their Island Peak Complex (Table 19.1) refers to the rocks cropping out in the basal position, as compared to the other units of the Everest massif that are situated along the east side of the Island Peak (6,189 m). The complex is composed mainly of mica schists, augen gneisses, biotitic gneisses with minor quartzites (which locally grade into microconglomerates), and scarce marbles. Biotitic gneisses possess scattered quartz and sillimanite nodules. Miocene leucogranites are intruded into this unit. They occur in augen gneisses as dikes and a few hundred meter-long bodies.

19.1.3 Black Gneisses (Gneiss Noirs)

The Barun migmatites pass imperceptibly upwards into fine-grained black gneisses. The color is black due to the abundance of biotite. The gneisses are comparatively soft and contorted, especially in their upper part. There also appear sporadic amphibolite bands with hornblende and garnet. The black gneisses contain violet cordierite in grains of a few millimeters across or even in idiomorphic crystals of several centimeters. The gneisses form cliffs with jagged towers and

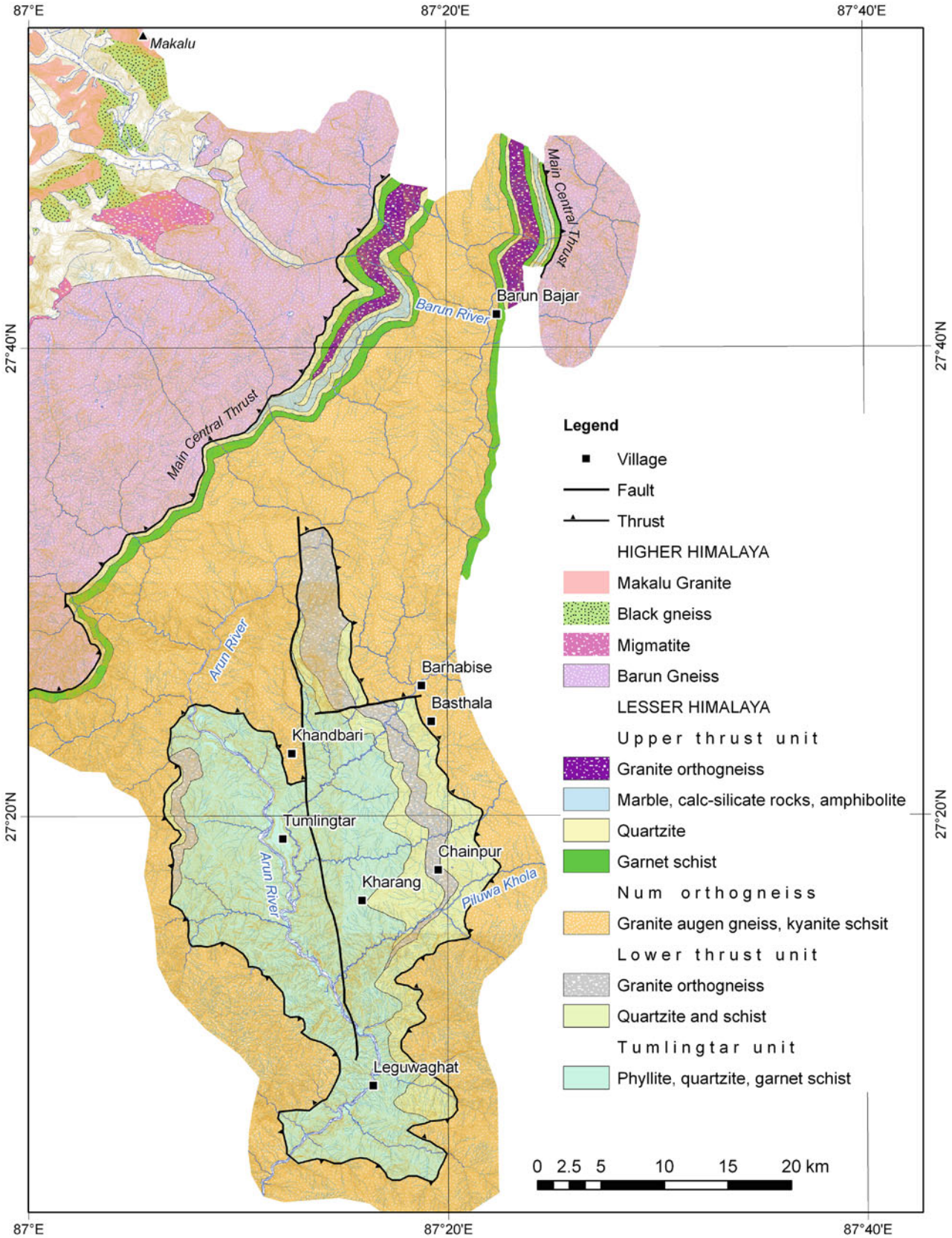

Fig. 19.1 Geological map of Makalu–Arun area. *Source* Modified from Bordet (1961) and Lombardo et al. (1993)

pinnacles, easily identified from a distance. It is difficult to estimate the exact thickness of the black gneisses, as they have a gradual transition from the underlying migmatites and are intimately injected by the Makalu granite in their upper part. Their estimated thickness varies from 1,500 to 2,000 m (Bordet 1961).

In the Everest neighborhood, the black gneisses constitute a thick complex of schist with a high grade (amphibolite facies) of metamorphism. Their lower part is made up mainly of biotite–sillimanite gneisses with local occurrences of muscovite and cordierite. In the gneisses, a few centimeter-long quartz nodules appear rather frequently together with fibrolitic sillimanite (Bortolami et al. 1983).

19.1.4 Makalu Granite

Makalu granite is a conspicuously white, fine-grained, Miocene leucogranite, containing biotite and tourmaline. The latter sometimes forms star shapes of 10–20 cm in diameter. Cordierite is quite frequent, especially in the region of contact with the gneisses. The contacts are abrupt and outlined by a border of pegmatite, consisting of muscovite and tourmaline. There are also veins of aplite and pegmatite, containing pink andalusite. Many large granite veins are frequently found in the underlying Barun migmatites as well as in the overlying Everest series. This passage zone of granitic dikes and apophyses is sometimes thicker than the granite body itself. In the upper reaches of the Hungu Khola, the lower passage zone is from 300 to 400 m thick, the granite is 100 m thick, and the upper zone is 50 m thick. In the Makalu area, the lower passage zone is 1,500–2,000 m thick and the granite above it is more than 200 m thick, whereas in the Pumori area, to the west, the lower passage zone of dikes measures about 3,000 m. Thus, the injected zone of Makalu granite is variable in thickness and forms a thin wedge widening towards the north (Bordet 1961).

In the Everest neighborhood, Miocene muscovite–tourmaline leucogranites intrude into either the upper paragneisses or the lower part of the Tethys Himalaya as large sill-like bodies, accompanied by dikes of aplite and pegmatite, producing widespread phenomena of contact metamorphism (Bortolami et al. 1983).

19.1.5 Everest Series

These rocks overlie the Makalu granite, and they are made up of dark fine gneisses and mica schists with biotite, passing progressively into black phyllites (Fig. 19.2). The formations at the base of this series much resemble the highest beds of the black gneiss of Barun, and a conformable stratigraphic contact is probable. Thus, the Makalu granite seems to be intruded into a tectonic discontinuity (Bordet 1961). The Everest series dips regularly due east at an angle from 20 to 30°. The series continues upwards to include the Permian to Eocene beds of the Tethyan Himalayan sequence (Chap. 26).

The Everest Metapelites belong to the Tethyan Himalayan sequence (Bortolami et al. 1983). These differ from the underlying black gneisses in their lower grade of metamorphism and are constituted of fine-grained biotite–amphibole–epidote schists and diopside–grassular–epidote marbles with varying amounts of quartz, plagioclase, and calcite. Pure marbles and marbles with silicate layers form a strikingly visible band all along the Lhotse south face (yellow bands of Lhotse).

The Jolmo Lungma Formation (Table 19.1) is a complex of mainly carbonate rocks, exposed on the upper part of Mount Everest and more extensively towards the Tibetan side. This complex consists mainly of marbles and calcareous phyllites in the lower part (yellow band) and of crystalline limestones, siltstones, and dolomites in the upper part.

The Everest area contains the largest congregation of leucogranites in the Higher Himalaya (Searle et al. 2003). They are intruded towards the structural top part of the Tibetan slab. One of the most distinctive characteristics of the Miocene Everest leucogranites is their occurrence as large, broadly concordant sill-like bodies, surrounded by a complex network of pegmatite dikes and aplites (Fig. 19.3). The contacts with country rocks are sharp and clearly intrusive, with abundant gneiss xenoliths of any size floating in the granite. Large-scale recumbent folds affecting contacts of the granites with the country rocks (Nuptse) or the swarms of xenoliths floating in the granite (Ama Dablam) are spectacularly exposed in the rock faces of the Upper Imja Khola (Bortolami et al. 1983). The thickest (2,800–3,000 m) granite sill has a ballooning appearance and is exposed on the south face of Nuptse (Searle et al. 2003). The fine- to medium-grained Everest leucogranites contain quartz, microcline or orthoclase, muscovite, biotite, and tourmaline with muscovite prevailing over biotite (Krummenacher 1957). They also contain varying amounts of garnet, sillimanite, apatite, cordierite, monazite, and zircon. They are viscous minimum melts, presumably produced by melting of a quartz + muscovite + plagioclase pelitic protolith, not much different from the underlying black gneisses (Searle et al. 2003).

The Everest area is characterized by a polyphase metamorphism with a thermal and mineral zonation. An early Barrovian-type metamorphism occurred at T = 550–600 °C and P = 0.8–1 GPa related to subduction and crustal thickening during the India–Asia collision. During exhumation, the isotherms rose and the thickened crust underwent partial melting. In the upper crust, migmatites were formed and

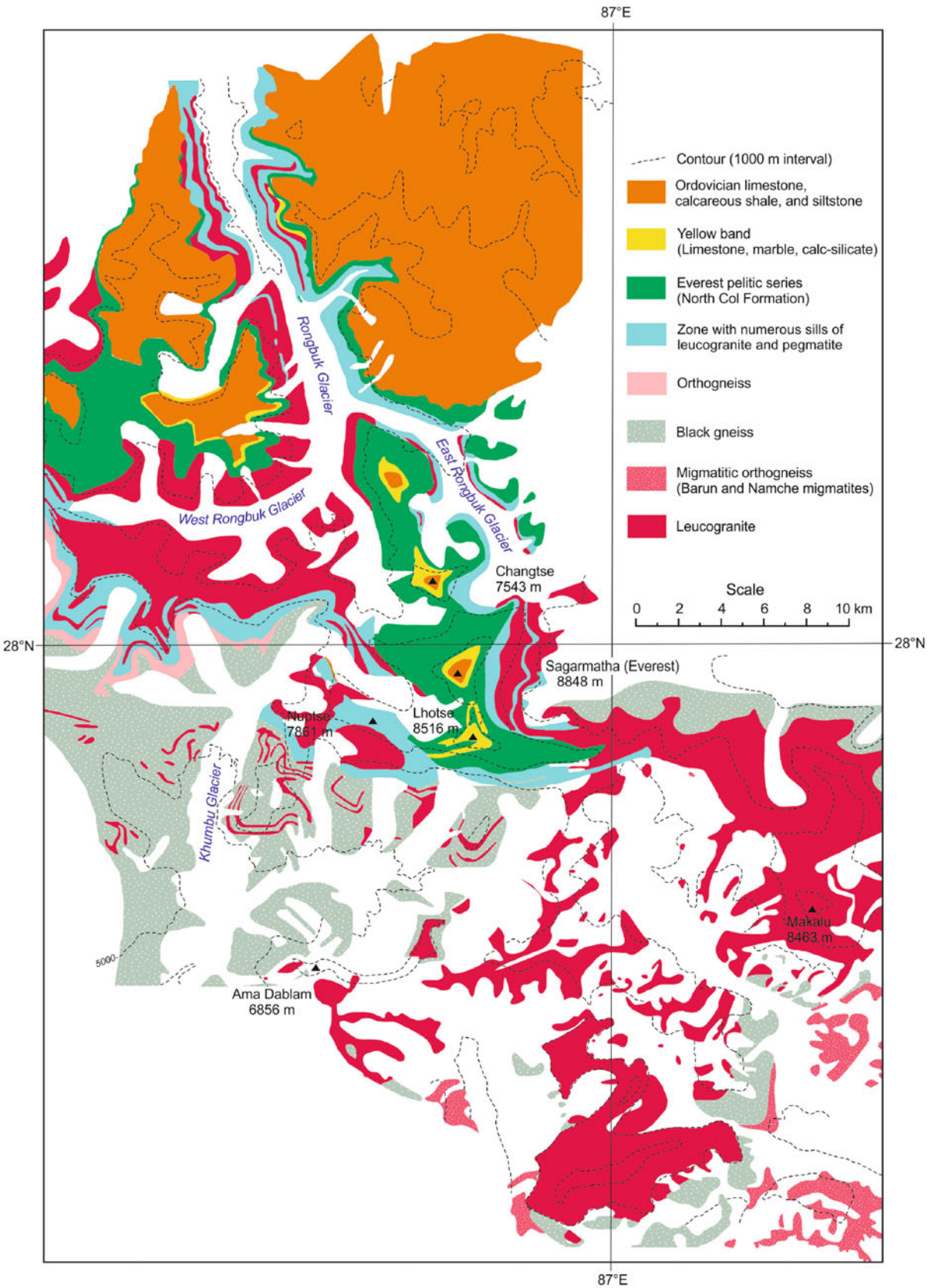

Fig. 19.2 Schematic geological map of Everest–Makalu area. *Source* Modified from Bordet (1961), Bortolami et al. (1983), Carosi et al. (1998), Searle et al. (2003), Mascle et al. (2012), and Geological Map of Tibet (Sheet H 45 C 004002, Scale: 1:250,000)

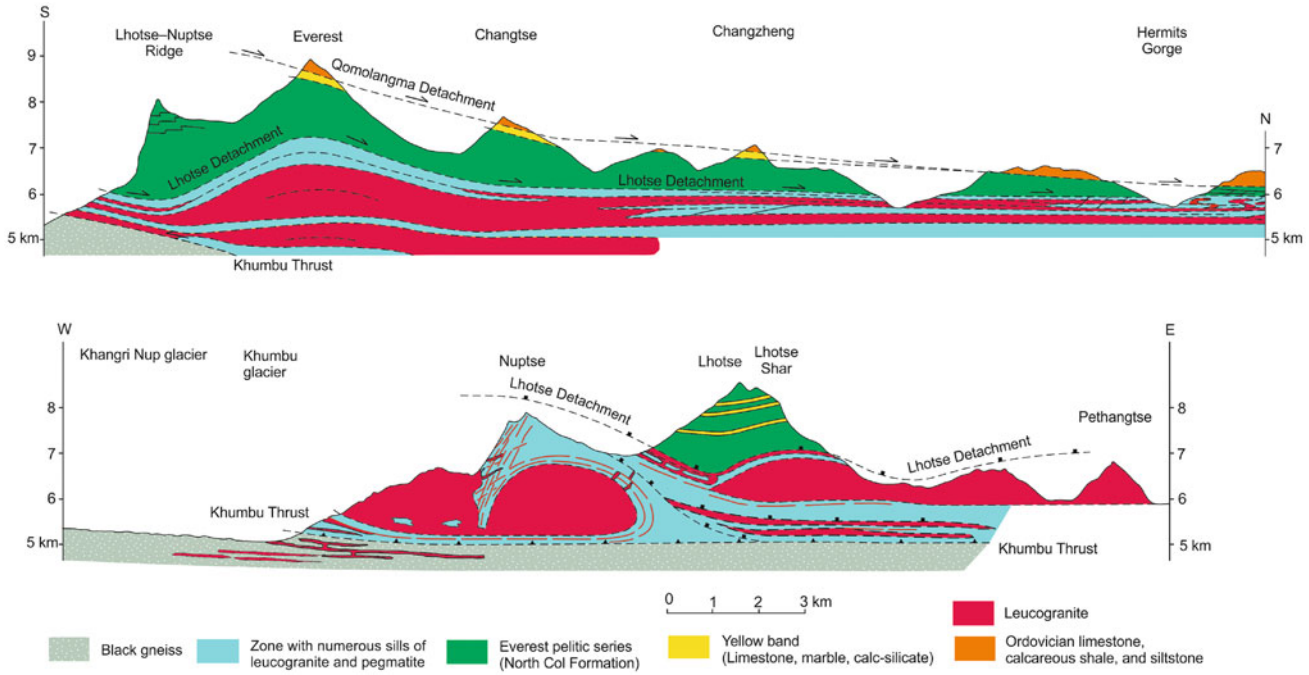

Fig. 19.3 Geological cross-sections across Everest and Lhotse. Large sill-like granite bodies are apparent. *Source* Modified from Searle (2003). © MP Searle. Used by permission

leucogranite magmas were generated from partial melting of the muscovite-bearing metasediments, mainly at medium pressures (T = 650–750 °C; P = 0.4–0.7 GPa). But there was also melting at a lower pressure (T = 600–700 °C; P = 0.2–0.4 GPa). The leucogranite melts segregated as dikes and kilometer-sized bodies in extensional shear zones situated as the uppermost levels of the Higher Himalayan crystallines and at the base of the overlying Tibetan succession (Pognante and Benna 1993).

The orthogneisses developed from early Paleozoic granitoids intruded into a sequence of metasedimentary rocks (Ferrara et al. 1983). During metamorphism, the granites were transformed into migmatized orthogneisses, whereas the metasedimentary country rocks were metamorphosed to give rise to migmatized paragneisses. Water-deficient anatexis generated cordierite-bearing leucosomes in the migmatites. It suggests decompression melting of muscovite-bearing metasediments of the upper Higher Himalayan crystallines. They all gave Miocene cooling ages (Basset et al. 1978; Ferrara et al. 1983; Hubbard and Harrison 1989). Because the leucogranites are voluminous, only vapor-absent melting is not enough to produce them. At first, there was dehydration melting under vapor-absent conditions. This process released aqueous solutions from the upper part and produced large amounts of low-pressure leucogranite melts (Lombardo et al. 1993).

Temperatures higher than 620 °C during sillimanite-grade metamorphism were maintained from 32 to 16 Ma along the top of the Higher Himalayan slab. Two low-angle normal faults cut the Everest massif towards the upper part of the slab. The Lhotse detachment delimits the massive leucogranite sills and sillimanite–cordierite gneisses from above and it is locally folded (Fig. 19.3). Ductile motion along the upper part of the slab was active from 18 to 16.9 Ma. The upper Qomolangma detachment (Burchfield et al. 1992) passes through the summit pyramid of Everest and gently (less than 15°) dips due north. Brittle faulting along the Qomolangma detachment took place after 16 Ma (Searle et al. 2003).

References

Akiba C, Amma S, Ohta Y (1973) Arun River region. In: Hashimoto S, Ohta Y, Akiba C (eds) Geology of the Nepal Himalayas. Himalayan Committee of Hokkaido University, Japan, pp 13–33

Auden JB (1935) Traverses in the Himalaya. Rec Geol Surv India LXIX(Part 2):123–167 (with 6 plates including a geological sketch map)

Basset AM, Kingery FA, Krummenacher D, Layne HF (1978) Petrology, metamorphism and K–Ar age determinations in eastern Nepal. In: Saklani PS (ed) Tectonic geology of the Himalaya. Today & Tomorrow's Printers, New Delhi, pp 151–166

Bordet P (1961) Recherches Géologiques dans L'Himalaya du Népal, Région du Makalu, Expéditions Françaises a l'Himalaya 1954–1955. Edition du Centre National de la Recherche Scientifique (C. N. R. S.), 275 pp (with geological maps and plates)

Bordet P, Latreille M (1958) Esquisse géologique de la région de l'Everest et du Makalu, 1:50,000. CNRS, Paris

Bortolami G, Lombardo B, Polino R (1983) The granites of the upper Imja Khola (Everest region), Eastern Nepal. In: Shams FA (ed) Granites of Himalayas, Karakorum, and Hindu Kush, pp 257–270 (with a colored 1:25,000 scale geological map of the Everest region prepared by Polino)

Burchfield BC, Chen Z, Hodges KV, Liu Y, Royden LH, Deng C, Xu J (1992) The South Tibetan Detachment System, Himalayan orogen: extension contemporaneous with and parallel to shortening in a collisional mountain belt. Geol Soc Am Spec Pap 269:1–41

Carosi R, Lombardo B, Molli G, Musumeci G, Pertusati PC (1998) The South Tibetan detachment system in the Rongbuk valley, Everest region. Deformation features and geological implications. J Asian Earth Sci 16:299–311

Ferrara G, Lombardo B, Tonarini S (1983) Rb/Sr geochronology of granites and gneisses from the Mount Everest region, Nepal Himalaya. Geologisches Rundschau 72:119–136

Ghosh AMN (1956) Recent advances of geology and structure of Eastern Himalaya. Presidential address to Indian Science Congress. In: Proceedings of the forty-third session, Agra, part II, section V, pp 85–99

Hagen T (1959) Über den Geologischen Bau des Nepal-Himalaya mit besonderer Berücksichtigung der Siwalik-Zone und der Talbildung. Jahrbuch der St. Gallischen Naturwissenchaftlichen Gesellschaft 76:3–48 (with 10 figures and 9 plates)

Hooker JD (1849) Notes, chiefly Botanical, made during an excursion from Dorjeeling to Tongló. J Asiat Soc Bengal Calcutta XVIII(Part I):419–446

Hooker JD (1854) Himalayan journals; or, notes of a naturalist (in Bengal, the Sikkim and Nepal Himalayas, the Khasia Mountains, &c.), vol 1. Grand Colosseum Warehouse Co., Glasgow, 408 pp (with 2 maps)

Hubbard MS, Harrison TM (1989) 40Ar/39Ar age constraints on deformation and metamorphism in the Main Central Thrust zone and Tibetan Slab, Eastern Nepal Himalaya. Tectonics 8(4):865–880

Kai K (1981) Rb–Sr geochronology of the rocks of the Himalayas, Eastern Nepal. Part I. The metamorphic age of the Himalayan Gneiss, vol 47, no. 2. Memoirs of the Faculty of Science, Kyoto University, Series Geology and Mineralogy, Kyoto, pp 135–148

Krummenacher D (1956) Contribution a l'étude géologique et pétrographique de l'Himalaya du Népal. II: sur les roches du bassin supérieur de la Dudh Kosi, de l'Imja Khola et de la Bothe Kosi. Archives de Sciences Genève 9:263–281

Krummenacher D (1957) Contribution a l'étude géologique et pétrographique de l'Himalaya du Népal. Pétrographie des éléments structuraux du Népal oriental entre l'Everest et le Gange. Archives de Sciences Genève 10:269–375

Krummenacher D (1967) Géologie et pétrographie des nappes de Kathmandu et de Nawakot et de la série de Khumbu dans l'est du Népal. Bulletin Suisse de Minéralogie et Pétrographie 47:855–871

Lombard A (1958) Un itinéraire géologique dans l'est du Népal (Massif du Mont Everest). Mémoires de la Société Helvétique des Sciences Naturelles 82(1):107

Lombardo B, Pertusati P, Borghi S (1993) Geology and tectonomagmatic evolution of the eastern Himalaya along the Chomolungma–Makalu transect. In: Treloar PJ, Searle MP (eds) Himalayan tectonics, vol 74. Geological Society Special Publication, London, pp 341–355

Mascle G, Pêcher A, Guillot S, Rai SM, Gajurel AP (2012) The Himalaya–Tibet collision. Nepal Geological Society and Société Géologique de France, Paris, 264 pp

Odell NE (1925) Observation on the rocks and glaciers of Mount Everest. Geogr J LXVI(4):289–315 (with a map in colors on 1:25,000 scale)

Pognante U, Benna P (1993) Metamorphic zonation, migmatization and leucogranites along the Everest transect of Eastern Nepal and Tibet: record of an exhumation history. In: Treloar PJ, Searle MP (eds) Himalayan tectonics, vol 74. Geological Society Special Publication, London, pp 323–340

Searle MP (2003) Geological map of the Mount Everest region, Nepal —South Tibet Himalaya. Scale 100,000

Searle MP, Simpson RL, Law RD, Parrish RR, Waters DJ (2003) The structural geometry, metamorphic and magmatic evolution of the Everest massif, High Himalaya of Nepal–south Tibet. J Geol Soc London 160:345–366

Sherwill WS (1853) Notes upon a tour in the Sikkim Himalayah Mountains, undertaken for the purpose of ascertaining the geological formation of Kunchinjinga, and of the perpetually snow-covered peaks in its vicinity. J Asiat Soc Bengal Calcutta XXII (6):540–570 and 7:611–638

Wager LR (1934) A review of the geology and some new observations. In: Ruttledge H (ed) Everest 1933. Hodder & Stoughton, London, pp 312–336

Wager LR (1939) The lachi series of north sikkim and the age of the rocks forming Mount Everest. Rec Geol Surv India 74(Part 2):171–188 (with 5 plates including a geological sketch map)

Yin CH, Kuo ST (1978) Stratigraphy of the Mount Jolmo Lungma and its north slope. Sci Sinica 21:629–644

Models of Himalayan Metamorphism 20

The fundamental ideas with which a science emerges must be clearly formulated and must be reduced to a minimum number.

—Nikolai Ivanovich Lobachevsky (1829)

While carrying out a mineralogical survey of the Northwest Himalaya, between the rivers Sutlej and Mahakali, Herbert (1842) recognized Himalayan metamorphism as early as 1826. He noted that the gneisses in the vicinity of Kedarnath contain kyanite prisms as long as 2.5 cm, whereas the granites from the same vicinity abound in schorl. McMahon (1883, 1887) pioneered in microscopically examining gneisses and other metamorphic rocks, composing the Northwest Himalaya, whereas Middlemiss (1887, p. 136) discerned the association of mica schist and garnetiferous schist with gneissose granite from the Dudatoli area of Kumaun. McMahon (1887, p. 203) invoked a "pressure metamorphism" hypothesis to explain the foliation of the Himalayan gneissose granite. His hypothesis consisted of two parts: the rocks can, under the influence of great pressure, be made to flow for several kilometers; when the rocks are set in motion in this way, shear and friction develop enough heat to fuse, dissolve, or recrystallize them on cooling. He alluded to the conversion of granite into mica schist to the first mechanism, and the conversion of mica schist to granite to the second process.

Auden (1935) attributed the inverted metamorphism in the Darjeeling area to the lit-par-lit injection of granite magma in the upper part of the pelitic succession under stress. He noticed a gradual upwards increase in metamorphic grade from the Dalings into the Darjeeling Gneiss and stated that these two units may represent metamorphic grades, rather than two different stratigraphic entities. Auden (1937, p. 421) also drew attention to lateral variation in metamorphism within the same rock succession.

20.1 Metamorphism and Related Modeling

The insuperable problem of inverted metamorphism has been vexing Himalayan geologists for nearly 15 decades. Medlicott (1864) was troubled by the gradual increase in metamorphism in his unmetamorphic series, which sometimes appeared as schists. Therefore, he stated that the separation of the two series was not solely based on alteration. He wrote (p. 23),

> … the slaty rocks form, without exception, a fringe to the greater area of the metamorphic rocks, and in several places projections from this fringe are deeply inserted into the area. In such positions, however, as well as in the fringing band, the apparent relation of the less altered rock is that of *underlying* the more altered.

Oldham (1883, p. 197) first diagnosed this phenomenon from the Jaunsar area of Kumaun, where he designated the Bawar Formation. The rocks of this formation are far more metamorphosed than the underlying sequence, because they have been converted into schists and gneisses. Gansser (1964, p. 54) succinctly stated that one of the fundamental Himalayan problems is the stratigraphic age of the metamorphics and the age of the metamorphism. Despite the immense progress in radioactive age determination as well as pressure and temperature estimates of metamorphism, the problem of inverted metamorphism is not yet fully resolved. Still hotly debated are the causes and mechanisms of inverted metamorphism, such as its heat source and the relationship of metamorphism with deformation and magmatism. Some of the important theoretical discourses behind these models are the following.

20.1.1 Shear (Frictional) Heating

Ambrose (1936) studied the sedimentary, intrusive, and volcanic rocks exposed along the south border of the Canadian Shield. These rocks are progressively metamorphosed, and their grade ranges from the chlorite zone to the garnet zone. The most intensely metamorphosed rocks are those lying farthest from the large igneous bodies of the area. Inasmuch as all the igneous bodies are metamorphosed to the same degree as the surrounding rocks, igneous activity did not supply the heat. Nor is there any evidence of deeper

M.R. Dhital, *Geology of the Nepal Himalaya*, Regional Geology Reviews,
DOI 10.1007/978-3-319-02496-7_20

burial of high-grade metamorphic rocks than those of low-grade metamorphism. All these rocks are intensely sheared and those of highest grade exhibit the most intense shearing and deformation. Hence the metamorphism was brought about by heat and pressure developed by and during shearing.

Reitan (1968a) investigated the frictional heat along sliding interfaces involved during mechanical deformation. Frictional heat generation is directly related to the load across the interface and inversely related to the initial ambient temperature. As both of them increase with depth, the net effect of these opposing controls is virtual cancellation of each other. Consequently, frictional heat generation is almost independent of depth. He demonstrated that when significant strain is achieved in geologically relatively short time periods of 100,000 to 1 million years, the frictionally generated heat cannot be conducted rapidly away from the deforming zone, and it can increase the temperature at the center of the deforming region by about 100 °C. On the other hand, when the deformation is distributed over a longer period of time (up to 10 million years), the temperature of the deforming region is increased by not more than 10 °C.

Regarding the role of frictional heat in relatively confined zones, Reitan (1968b, p. 274) concluded,

> In rather confined zones of intense deformation – zones 2 km or less across, for example – temperature increases approaching or in excess of 100 degrees may be possible. If these conditions are realized during deformation in tectonically active regions, mechanically generated heat may locally contribute significantly to the total heat budget in dynamothermally metamorphosed volumes of the crust and may be of significance in the attainment of the abnormally steep or the occasionally "reversed" geothermal gradients, sometimes indicated by the application of theoretical and laboratory mineralogical and assemblage equilibrium studies to the interpretation of natural occurrences.

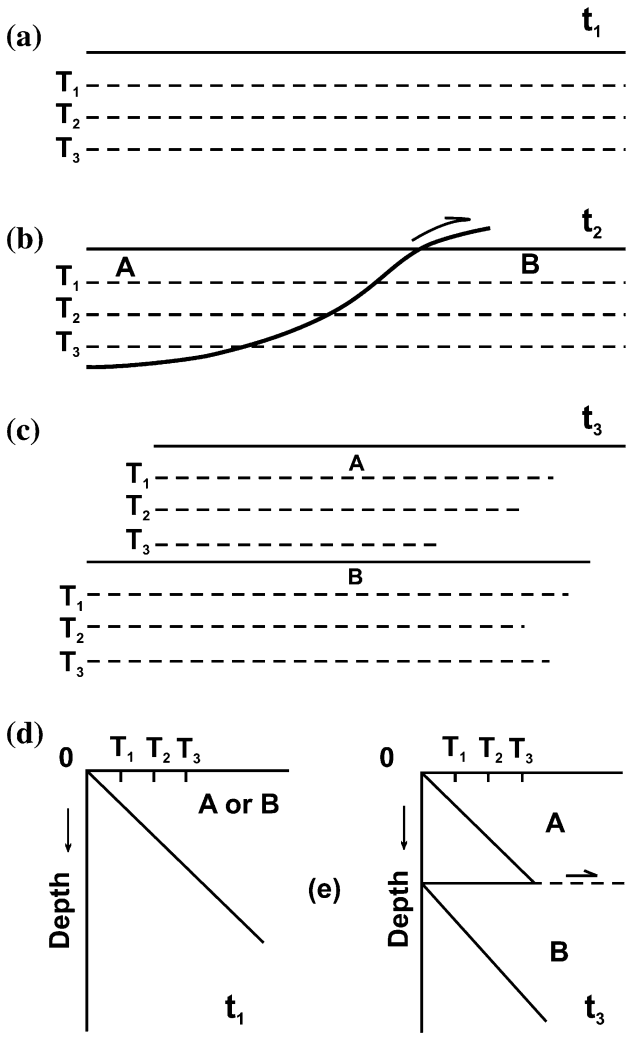

Fig. 20.1 The thrusting model: **a** crustal profile of presumed initial (t_1) condition; T = temperature $T_1 < T_2 < T_3$ with the associated thermal gradient shown in (**d**); **b** incipient thrust; **c** situation immediately after thrusting, giving rise to thermal profile (**e**). *Source* Modified from Oxburgh and Turcotte (1974)

20.1.2 Conductive Heating

Oxburgh and Turcotte (1974) examined metamorphism and thermal gradients in the East Alps, where an approximately 15 km thick thrust sheet covers the European basement. The thrust sheet was piled upon the Mesozoic sediments, experiencing early blueschist facies metamorphism and later stage greenschist to amphibolite facies metamorphism. They considered a steady-state situation (Fig. 20.1a), when at time t_1, the isotherms (T_1, T_2, T_3) are horizontal and increase in value with depth. At time t_2, a thrust fault develops (Fig. 20.1b) and the rocks to the left (A) are rapidly taken over the rocks to the right (B). Hence, the situation immediately after thrusting will be similar to Fig. 20.1c. As a result of thrusting, the former geothermal gradient (Fig. 20.1d) will change to a sawtooth form (Fig. 20.1e). But as soon as the tectonic activity ceases, the sawtooth form will gradually decay with the passage of time and the normal geothermal gradient will be re-established (Oxburgh and Turcotte 1974, p. 644).

In this analysis, the upper surface temperature on both the hanging wall and footwall of the thrust sheet is assumed to be 0 °C. The process of thrusting brings the base of the thrust slab with a temperature T into contact with the footwall basement of zero temperature. Consequently, immediately after the contact, the interface assumes 0.5 T. On the other hand, tens of millions of years are required before the temperature close to the equilibrium (i.e., the initial temperature T of the hanging wall basement) is reached.

Temperature as a function of time at various depths within a 15 km thick thrust sheet is set out in Fig. 20.2. Immediately after thrusting, the slab begins to experience

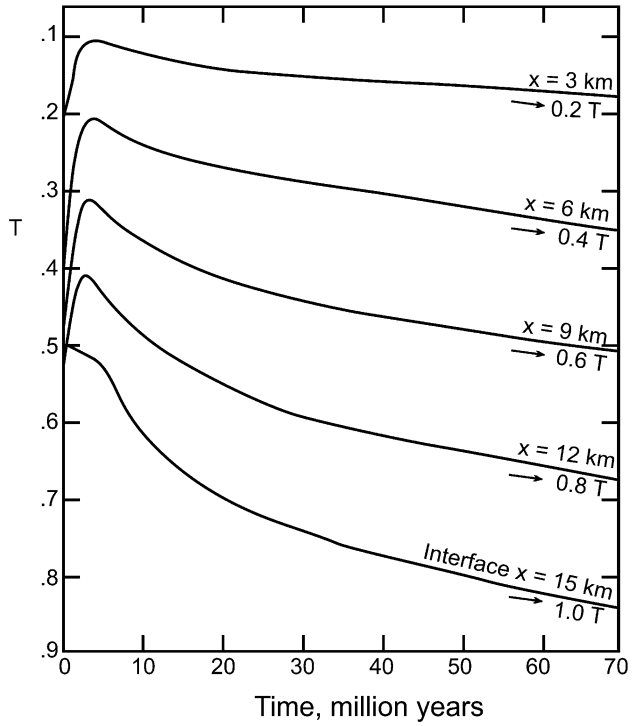

Fig. 20.2 Temperature (T) as a function of time and depth (x) within a 15 km thick thrust sheet. The equilibrium value for T is shown on each depth *curve*. *Source* Modified from Oxburgh and Turcotte (1974)

cooling at all depths, and the temperature tends to about one-half of the initial temperature at that depth. With the passage of time the temperature minimum at each depth propagates progressively upwards through the slab. However, the temperature minimum propagates so rapidly that it takes only 4 million years after thrust emplacement to reach a slab depth of 3 km, and then the temperature begins to increase steadily at all depths. Consequently, the sawtooth isotherm is damped out in less than 1 million years, and by 3.3 million years, the gradient through the slab is nearly linear and has the value about half of its initial gradient. Immediately after thrusting, there is a large heat flux downwards in the basement owing to the negative thermal gradient across the interface. It causes a rapid initial temperature rise, but it slows down considerably after about 25 million years (Oxburgh and Turcotte 1974, p. 647).

20.1.3 Downbowed Isotherms

With the advent of the theory of plate tectonics, it became evident that in the vicinity of the trench and subduction zone, the isotherms must be markedly depressed in the downgoing slab (McKenzie 1969, p. 8). By studying 2D time-dependent heat conduction equations, Hasebe et al. (1970) obtained various heat flow patterns for the subduction

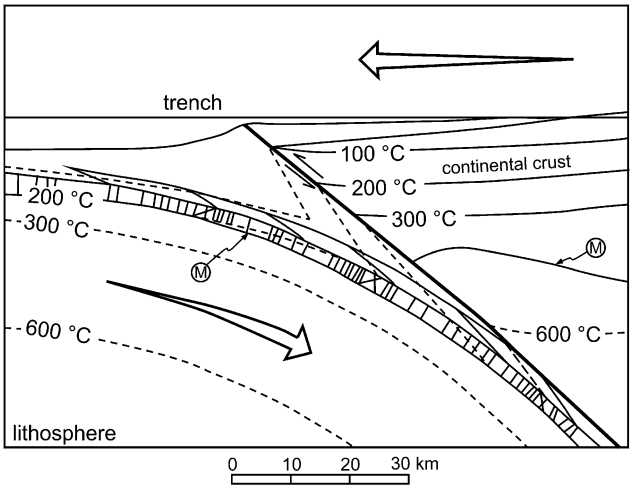

Fig. 20.3 Details of the overall subduction zone model illustrating inferred thermal structure. *M* Moho. *Source* Modified from Ernst (1973)

zone, and pointed out that heat generation four times higher than the mean heat flow at the upper surface and ten times higher heat conduction are required to explain the heat flow pattern across island arcs and marginal seas. Hence, they inferred dissipative heat generation by shear heating to accommodate for such high values. According to Toksöz et al. (1971), the main heat contributors to the downgoing slab in their decreasing order of importance are: conductive and radioactive heating, adiabatic compression, shear heating, and phase changes. Ernst (1973) described in detail such thermal gradients and presented a generalized thermal structural model for the trench and subduction zone (Fig. 20.3). The progressive metamorphic sequence in the subduction zone also marks the direction of lithospheric plate descent (Ernst 1973, p. 264). He also remarked that although the rocks are strongly deformed, and hence have experienced differential stresses, the magnitude of the tectonic overpressure was relatively insignificant (i.e., less than 100 MPa), owing to the insufficient rock strengths to sustain such stresses under prevailing geological conditions (e.g., there are extremely weak shales that have been transferred to metapelites containing high-pressure minerals).

20.1.4 Intracontinental Subduction

In line with the subduction zone, Le Fort (1975) outlined a model of the Main Central Thrust, originating from underthrusting of the continental slab (Fig. 20.4). Through this model, he proposed a unified theory of intracontinental subduction in the Himalaya, and genetically linked large-scale displacement along the Main Central Thrust with the inverted metamorphism and granitization. Based on this model, Pêcher and Le Fort (1986) and Le Fort et al. (1987)

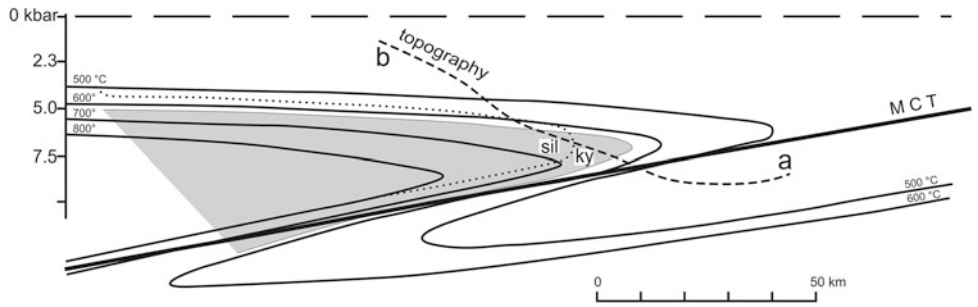

Fig. 20.4 Thermal regime in the hanging wall and footwall during intracontinental subduction; diagram based on field observations of the Main Central Thrust in central Nepal. Temperature isograds are tentatively drawn together with the corresponding kyanite–sillimanite boundary and the muscovite granite excess water solidus. Heat transfer by magma and water movements is not taken into account. The present topographical surface is also indicated (*a*–*b*). *Source* Modified from Le Fort (1975)

were able to explain many features of the Himalayan metamorphism and granitization. In this model, inverted metamorphism results from a rate of thrusting that is greater than the rate of thermal relaxation of the affected rocks undergoing plastic deformation. The deformation, characterized by intracrystalline gliding during thrusting, is parallel to foliation and distributed through a wide zone, marked by the development of stretching lineations in the direction of tectonic transport. England et al. (1992) further investigated this model using rigorous numerical analysis and concluded that dissipative heating at shear stresses of about 100 MPa can account for peak temperatures in excess of 600 °C during slip on the fault and would have contributed as much as 13 °C/km to the inverse gradient.

20.1.5 Shear Heating Accompanying Thermal Relaxation

Graham and England (1976) opined that the downbowing of isotherms during subduction can qualitatively account for inverted metamorphism only on a scale of kilometers. On the other hand, in southern California, the Himalaya, and in the Newfoundland ophiolite sheets, the temperatures (and the inverted gradients) are far higher in the region of thrust than can be explained by the simple conduction of heat from a hot upper sheet into a cool lower one. In such instances, the effects of shear heating at the thrust are significant.

Graham and England (1976) studied metamorphism of the Pelona Schist of the Sierra Pelona in southern California, controlled by an inverted thermal gradient. Metamorphism of the Pelona Schist occurred synchronously with the movement of the Vincent Thrust. The formation of such a transient thermal profile requires large underthrusting of a thick rock pile with contrasted thermal properties, during deep-seated movement along the Vincent Thrust. They used an idealized model in which thermal development of the underthrust plate is dominated by rapid emplacement of cold

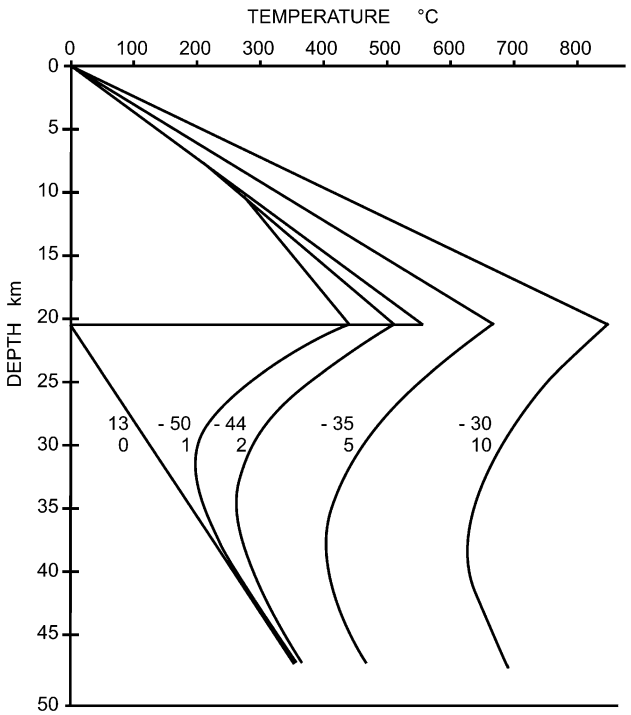

Fig. 20.5 The development in time of the thermal profile of the system described in the text. Lower numbers on each *curve* show the time in millions of years since the commencement of heating. Higher numbers show the gradient in °C/km below the thrust. Heat production due to shear heating at the thrust is equivalent to 4.25 hfu. *Source* Modified from Graham and England (1976)

material beneath an upper thick sheet with normal geothermal gradient and shear heating accompanying it. They considered a model for the underthrusting velocities characteristic of plate convergence (1–10 cm/a), where shear heating is confined to a thin zone at the base of the upper plate and the initial thermal gradients in both the plates are linear. In their model (Fig. 20.5), the temperature in the upper plate rises from zero at the upper surface to 400–600 °C at the thrust, whereas in the lower plate the

temperature gradient is kept constant at 13.3 °C/km, corresponding to a heat flow of 0.8 hfu (= 0.8 × 41.87 mWm^{-2}).

According to Scholz (1980), a sharp inverted metamorphic gradient within the footwall block of a thrust fault can be taken as strong evidence for shear heating. He gave many (more than 17) examples of shear heating in fault zones, such as the fault of the Southern Alps in New Zealand, the Olympus overthrust in Greece, the Glarus overthrust in Switzerland, and a fault in Chile, and also examples of ductile shear zones from France and Afghanistan. He stated that in the Main Central Thrust and plate tectonic boundaries, shear heating is not likely, as it requires a thrusting rate of tens of centimeters per year (not permitted by plate tectonics). But if their shear strength is about 100 MPa, shear heating is possible and the strength of such shear zones could be as high as 350 MPa. For metamorphism, shear stress exceeding 100 MPa or fault displacement of tens of centimeters per year for at least 10 Ma is required. He also gave examples of the Langtang landslide (Scott and Drever 1953; Masch 1979) and the Koefels landslide (Erismann et al. 1977) to show the role of frictional melting and formation of hyalomylonite. Therefore, during earthquakes rocks can melt.

Molnar and England (1990) investigated two-dimensional advective and conductive models of heat transport in a region of thrust faulting. They concluded that a large amount of heat is required to generate granitoid magmas near the Main Central Thrust, having an underthrusting rate of 15 ± 5 mm/a, even for the magmas with comparatively low temperatures of 600–650 °C in the rocks initially not hotter than 700 °C. Because advection quickly carries away heat from these areas, heating from below the lithosphere and radioactive heating are not capable of preventing a large (hundreds of degrees) temperature drop near the Main Central Thrust. Hence, dissipative shear stresses of 100 MPa or more are required to generate the additional heat.

20.1.6 Synmetamorphic Deformation

Heim and Gansser (1939, p. 225) were the first to propose a mechanism of synmetamorphic deformation for the Main Central Thrust zone. According to them, the Higher Himalayan succession represents an enormous (10–20 km thick) deep-rooted body of injected crystalline rocks, overlain by 10–15 km of Proterozoic, Paleozoic, and Mesozoic sediments. The synclinally folded crystalline rocks, overriding the Lesser Himalayan sequences, are the prolongation of the Higher Himalayan thrust sheet towards the south, and have undergone secondary folding after the main horizontal displacement of more than 120 km. The thrusting took place after Cretaceous time when the crystalline basal part of the Higher Himalaya was at a depth of 30 km below the surface. At that depth, at temperatures of 700 °C or higher, injection and migmatization took place partly before and partly during thrusting. The Main Central Thrust slipped easily forward on this fluid substratum. Powell and Conaghan (1973) also put forward a similar model, according to which metamorphism weakened the crust and helped the formation of the Main Central Thrust.

Frank and Fuchs (1970) considered a variety of models to explain metamorphism and tectonics of west Nepal. But it stands to the credit of Frank and his coworkers (Frank et al. 1973, 1977) who proposed multiple ways of formation of inverted metamorphism in the Northwest Himalaya of India. They investigated the Larji–Kulu–Rampur window made up of quartzites, slates, phyllites, amphibolites, and carbonates, belonging to the anchi- to epimetamorphic lower tectonic unit exhibiting a slightly inverted stratigraphic sequence, with the oldest Berinag Formation, occupying the top part of the rock pile. The Crystalline nappe of the Higher Himalaya is thrust over this unit from the NNE. The nappe contains a monotonous succession of metapelitic–metapsammitic rocks with concordantly intercalated augen gneisses and large discordant granitic bodies. At the base of the Crystalline nappe, a thin zone of calc-schists, muscovite schists, and microcline augen gneisses is present on a regional scale. The contact of this Bajaura nappe with the overlying Crystalline nappe is concordant, and its lithology is akin to that of the Berinag Formation (Frank et al. 1977, p. 152).

In this area, folding of isograds is a syn-metamorphic event, caused by rapid tectonic movement and internal deformation in an inverted temperature gradient. There are two possibilities (Fig. 20.6): (1) syn-metamorphic folding of isograds simultaneously with folding of the bedded rock pile, where the forelimb of the fold represents an inverted stratigraphic sequence; and (2) syn-metamorphic shear folding of isograds while the lithostratigraphic sequence remains unfolded. In this case, the isograds are discordant to the s-planes in the hinge zone of the folded isograds.

They reported the first type of inverted metamorphism from the upper Kulu Valley, whereas the second type prevails in the Malana–Parbati Valley (Frank et al. 1977). Searle and Fryer (1986) and Searle and Rex (1989) describe examples similar to the first type from the northwest Himalaya. Jain and Manickavasagam (1993), Jain et al. (2005), and Hubbard (1996) also proposed models analogous to the second type for the Northwest Himalaya.

20.1.7 Delamination of the Lithosphere

Using two-dimensional finite-difference techniques, Bird (1978) numerically analyzed a number of models, relevant to intracontinental subduction along the Main Central Thrust (Fig. 20.7). As the figure depicts, no melting is expected for a velocity of 5 cm/a, notwithstanding the way of stress

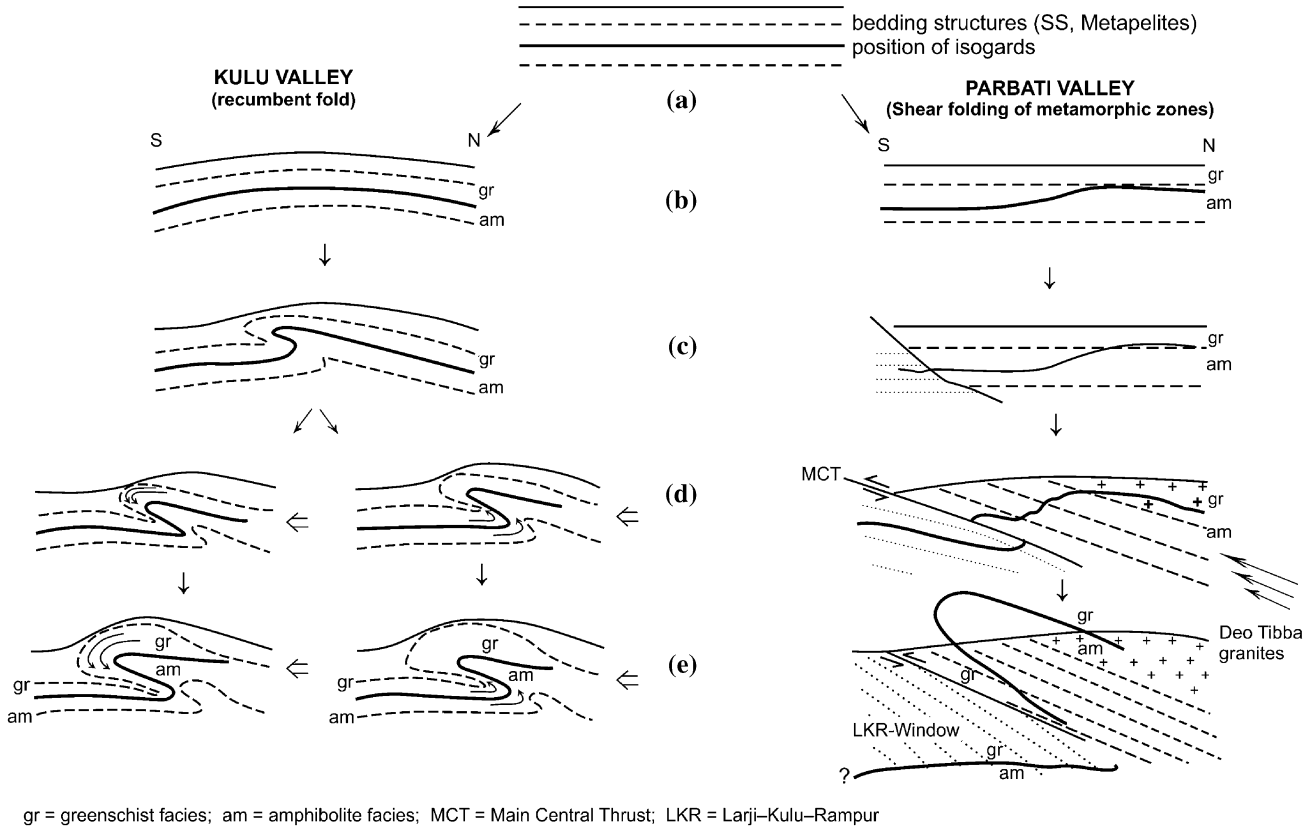

Fig. 20.6 Evolution of inverted metamorphic sections in the northwest Himalaya. Figures **a**–**e** indicate successive stages of folding of isograds as well as bedded rock (*left*), and shear folding of isograds without folding of rock pile (*right*). *Source* Modified from Frank et al. (1977)

distribution or the amount of underthrusting. Hence, either the Himalayan granites were formed by some other mechanism or the required velocity of underthrusting was higher. When the velocity was raised to 25 cm/a, small intrusive bodies appeared at the northern tip of the stressed area, that is, within 30 km of the Indus Suture zone and for the toe stress, it falls within the center of the range. But a reasonably comparable model of granite distribution is obtained only for a velocity of 40 cm/a. However, such high velocities (three times faster than any recorded values) were precluded from the plate tectonic considerations. On the other hand, the total frictional heat production alone also cannot account for the extensive metamorphism covering far wider areas than the granite end-products (Bird 1978, p. 4981). Radioactive heating (Frank et al. 1973) also could not produce crustal melting, unless the thrust sheet is motionless for at least 100 Ma (Bird et al. 1975; Toksöz and Bird 1977). Hence, Bird (1978, p. 4982) proposed that a slab of Indian continental crust was detached from its subcrustal lithosphere, prior to overthrusting the present Lesser Himalaya. He proposed the following three possible causes of detachment (Fig. 20.8): gravitational instability of the lithosphere, tension exerted by excess density of the subducting slab, and moment exerted by rotation of the subducted slab. According to Bird, the delamination model explains the inverted metamorphism better than the frictional heating model. However, Scholz (1980, p. 6177) remarked that Bird (1978) assumed at the outset that the shear stress on the Main Central Thrust could not exceed 20–30 MPa and hence obtained very high slip rates. Subsequently, Bird remarked that, according to this model, all the Higher Himalayan granites in any cross-section should be formed at about the same time. Inasmuch as it is now known that the Higher Himalayan leucogranites range in age from 24 to 17.2 Ma and the granites of the North Himalaya were emplaced around 17.6–9.5 Ma (Harrison et al. 1998), the history was more complex and some other heating mechanism may be necessary. But, he accentuates that this mechanism is still valid and can be the cause of the first melting event and the formation of the Main Central Thrust.

Chemenda et al. (1995, 2000) studied two-dimensional laboratory models of continental subduction, where the subducting continental lithosphere has a strong and brittle upper crust, a weak ductile lower crust, and strong upper mantle. The lithosphere is underlain by a low-viscosity asthenosphere. They concluded that the continental crust can be deeply subducted, and slab break-off, delamination, and tectonic underplating are fundamental processes. For the

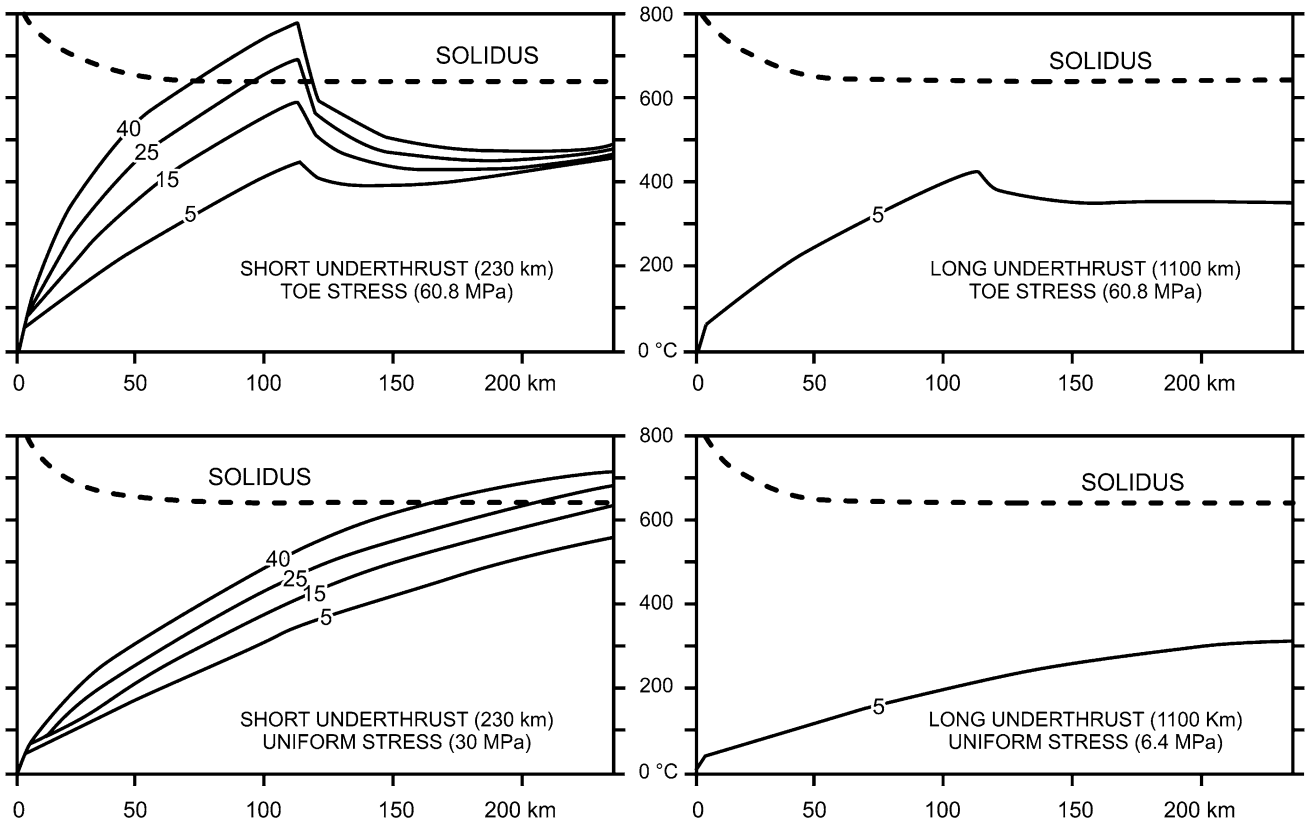

Fig. 20.7 Graphs of maximum temperatures attained on the thrust fault in the finite-difference calculations, as a function of distance down-dip. All models satisfy the stress integral constraint but differ in stress distribution and amount and rate of underthrusting (shown by numbers in centimeters per year attached to *curves*). *Source* Modified from Bird (1978)

Himalaya–Tibet convergence system, they proposed the following events: (1) deep (200–250 km) subduction of the continental lithosphere; (2) failure and rapid buoyancy-driven uplift of the subducted continental crust; (3) break-off of the Indian subducted lithospheric mantle with the attached oceanic lithosphere; (4) underplating of the Indian lithosphere under Asia for a few to several hundred kilometers; (5) delamination, roll-back, and break-off of the Indian lithospheric mantle; and (6) failure of the Indian crust in front of the mountain belt (formation of the Main Central Thrust), and underthrusting of the next portion of the Indian lithosphere beneath Tibet.

20.1.8 Metamorphism in Thickened Continental Crust and *PTt* Paths

England (1978), England and Thompson (1984), and Thompson and England (1984) investigated the effect of thickened continental crust on regional metamorphism. They stressed that it is not necessary to invoke plate motion to explain all types of metamorphic terranes. The metamorphic belts produced during continent–continent collision, such as the Himalaya, characterized by the emplacement of large thrust sheets, may have undergone metamorphism related to the same thrusting mechanism, rather than caused by an abnormal heat flow from the mantle (England 1978, p. 22). In the Alps, the metamorphic conditions are similar to those produced by a normal geothermal gradient through a crust thickened by tectonic processes. England investigated the Tauern Window in the East Alps, and demonstrated that there is a variety of conditions allowing the development of the type of metamorphism observed there, without invoking any other abnormal heat contribution from the mantle. England used finite-difference models to determine the thermal regime that produced the Tauern metamorphism, and concluded that the rate of erosion after the peak of metamorphism and the thickness of the overthrust sheet are sufficient to explain the metamorphism in the Alps.

England and Thompson (1984) described the pressure–temperature–time (*PTt*) paths followed by the rock undergoing burial and exhumation during episodes of continental thickening. They assumed that the major sources of heat during regional metamorphism are radioactivity of the crust and heat transfer at its base from the underlying upper mantle. The main heat transfer mechanism is assumed to be

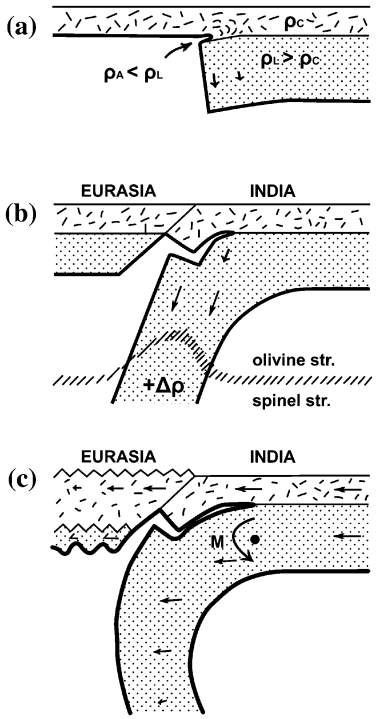

Fig. 20.8 Three mechanisms that might cause continental delamination: **a** spontaneous instability of the dense lithosphere, **b** tension exerted by excess density of the subducting slab, and **c** moment (M) exerted by rotation of the subducted slab as the suture begins to move following a continental collision. Crust is stippled and lithosphere is *shaded*. *Source* Modified from Bird (1978)

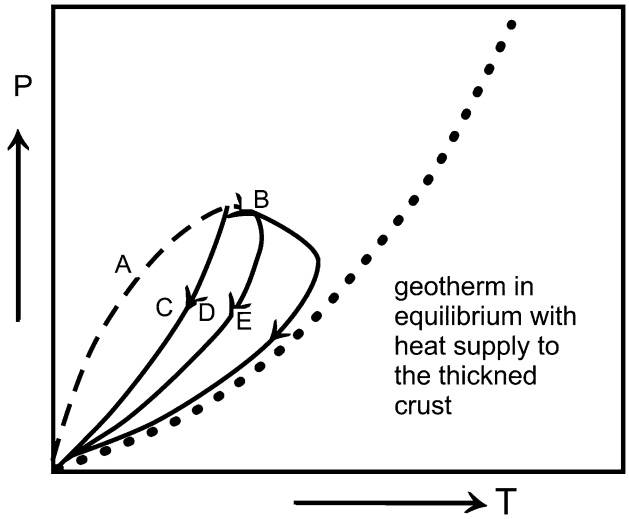

Fig. 20.9 Schematic *PTt* paths of rocks undergoing rapid burial on path *A*, followed by exhumation histories that are progressively longer from path *C* to path *D* and to path *E*. The *dotted line* indicates a geotherm that is in equilibrium with the heat supply to the thickened crust. *Source* Modified from England and Thompson (1984)

conduction. Thickening of the crust in the orogenic belts is supposed to occur without change in the heat supplied to the base of the continental lithosphere. They investigated three types of continental thickening models: thickening due to emplacement of a single thrust sheet, thickening due to homogeneous horizontal shortening of the crust by continental collision, and thickening of the entire lithosphere. They also assumed that the crust, being in isostatic equilibrium, undergoes erosion some time after thickening, and thus comes close to its initial thickness.

They analyzed the models where the continental lithosphere was initially in a steady-state conductive regime and the heat supply from the upper mantle was not altered by the orogenic process (England and Thompson 1984, p. 904). Some schematic *PTt* paths that rocks may undergo rapid burial followed by uplift are shown in Fig. 20.9. It is similar to the case of a nappe emplacement at rates comparable with the plate motions. This phase is followed by a prolonged (20 Ma and more) period of heating, which is ultimately terminated by exhumation or erosion, resulting in a rapid return of the rock to the surface.

Path AC in Fig. 20.9 represents a situation when the rock undergoes rapid burial, and has no period of heating-without-erosion and a quick phase of erosion. The rock encounters a maximum temperature at its maximum burial depth, and returns to the surface following a path similar to that of burial. Because the time required to complete the cycle is short, little heating is expected. Path AD depicts a case of heating with insignificant erosion (at B), followed by a moderate rate of erosion. The rock experiences more heating at or near its maximum burial depth, and also at the same time, its temperature continues to rise owing to a slower rate of erosion, therefore it experiences the maximum temperature at a depth shallower than its maximum burial depth. Path BE portrays a still longer phase of heating with little erosion when the rock has almost reached its equilibrium profile (shown by the dotted line in Fig. 20.9) before the start of appreciable erosion, and it exhumes following the *PT* path that is close to the new steady-state geotherm (England and Thompson 1984, p. 908).

Thompson and England (1984) discussed the *PTt* paths (Fig. 20.10) followed by the rock in continental collision. They also stated that an association diagnostic of continental–collision metamorphism is the metamorphism in or near the kyanite and sillimanite zones, observed in connection with segments of *PTt* paths, recording decompression of several hundred MPa at nearly constant temperatures.

20.1.9 Polyphase Metamorphism

From the Daraundi and Budhi Gandaki valleys in Central Nepal, Hodges et al. (1988) described an early high-temperature–high-pressure event and a later high-temperature–intermediate-pressure event. Pognante and

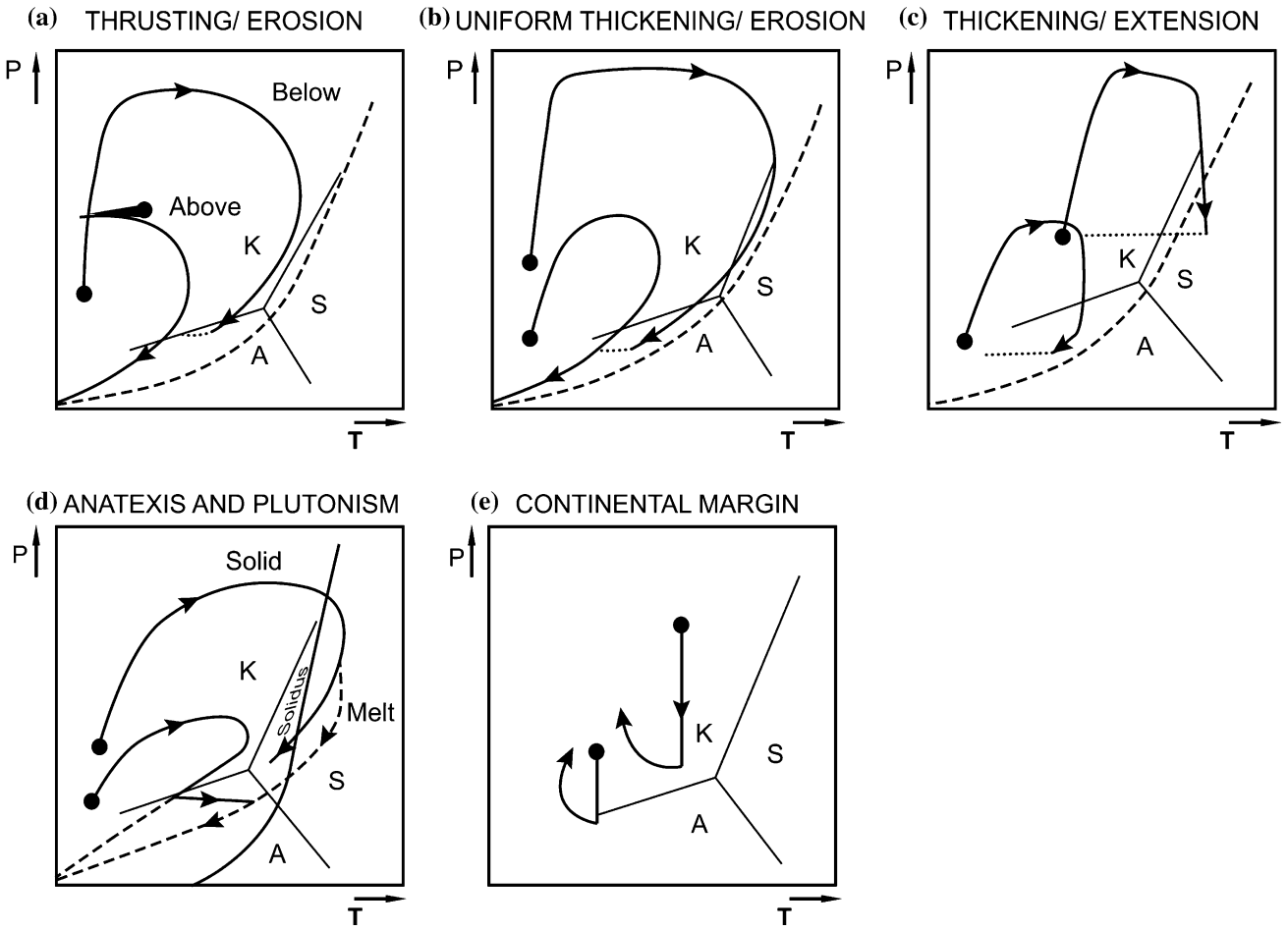

Fig. 20.10 Schematic *PT* diagrams showing the forms of *PTt* paths produced by various tectonic processes. A schematic "dry" solidus is shown in (**d**) as a *solid line* and in (**a**, **b**) and (**c**) as *dashed lines*. *Source* Modified from Thompson and England (1984)

Lombardo (1989) presented a case of polyphase metamorphism from Southeast Zanskar, whereas Stäubli (1989) and Stephenson et al. (2000) described polyphase metamorphism from the Kishtwar window of the Northwest Himalaya. The inverted metamorphism well recorded in the Higher and Lesser Himalaya of Kishtwar is regarded as a product of polyphase metamorphism, combined with ongoing thrusting and shearing. Similarly, Searle and Tirrul (1991) discussed polyphase metamorphism of the Karakoram region, and Neogi et al. (1998) presented a case of polyphase metamorphism from Sikkim. Naha and Ray (1970, 1971) in the Simla area, and Bhargava and Dasgupta (1995) in Bhutan have also described polyphase metamorphism.

20.1.10 Post-metamorphic Imbrication

Brunel and Kienast (1986) as well as Macfarlane (1993) discussed the inverted metamorphism in terms of post-metamorphic imbrication of thrusts within the Main Central Thrust zone. Martin et al. (2010) also proposed a similar variant from the Modi Khola area of west Nepal.

20.1.11 Lateral Extrusion and Channel Flow

Tapponnier et al. (1981, 1982) and Armijo et al. (1986) presented extensive examples of normal faulting from southeast Tibet. They are mainly transverse (perpendicular) to the Mesozoic–Tertiary tectonic structures. The normal faults developed in the last 2 ± 0.5 Ma. These faults are attributed to the eastward extrusion of north-central Tibet.

Bird (1991) stated that because lithostatic equilibrium is different from isostatic equilibrium, rocks are subject to deviatoric stresses in the areas of lateral density contrast, leading to lateral extrusion. He defined lateral extrusion as a Poiseuille flow (planar channel flow) of lower crustal material confined by the motionless but flexible boundaries of the upper crust and mantle lithosphere (Bird 1991). The most probable place for such a flow to take place is near the base of the crust.

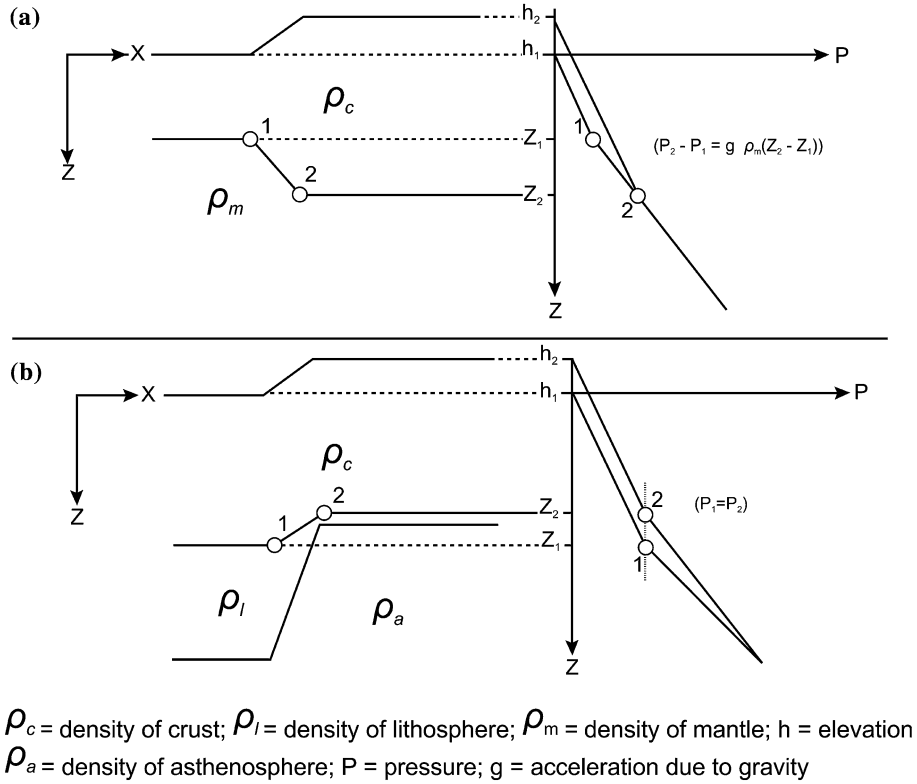

Fig. 20.11 Pressure curves (on *right*) corresponding to two common types of isostatic compensation (on *left*): **a** by crustal roots, **b** by low-density upper mantle. In each case, there is a positive "effective pressure gradient" ($\nabla P - g\rho_c\nabla_z$) when going from the Moho beneath the plains (point 1) to the Moho beneath the plateau (point 2). In both cases, lateral extrusion flow will tend to level the topography. However, only in the case of crustal roots will it also flatten the Moho. (In Fig. a, note that the Moho relief is typically about 6 times greater than the topography; in this figure, the crust/mantle density contrast has been made artificially large to clarify the $P(z)$ diagram. Fig. b is drawn without exaggeration.). *Source* Modified from Bird (1991)

For numerical analysis, Bird took x-axis parallel to the flat earth and z-axis pointing down (Fig. 20.11) and investigated the following two conditions: the margin of a plateau isostatically supported by crustal roots (Fig. 20.11a) and a plateau supported by intrusion of asthenosphere (Fig. 20.11b), instead of the normal mantle lithosphere. However, in both cases, there will be lateral extrusion tending to level the topography, but only in the case of the crustal roots, the Moho will be flattened (Bird 1991). The conditions leading to channel flow, confined to the lowermost crust and induced by the effective pressure gradient, are shown in Fig. 20.12. His analysis results depict that any initial condition with an isolated high characterized by sinusoidal topography tends to flatten as a "spreading pancake" and when such neighboring "pancakes" merge, the relief is obliterated (Fig. 20.13). He also points out that lateral extrusion will be quite significant in the Tibetan Plateau if the Moho temperature is about 979 °C or higher, and any initial topographic relief would have been reduced to 0.2 km within the last 5 Ma for all wavelengths less than 400 km. Because the lower crust of Tibet may resemble a hydraulic reservoir and the information on previous tectonic history is continually lost, the present shape of the Moho cannot be used to make balanced cross-sections to infer its past history (Bird 1991).

20.1.12 Metamorphic Transformation in the Lower Crust

Armijo et al. (1986) observed that Quaternary deformation in Tibet is mainly an east–west extension, expressed in strike-slip and normal faulting, whereas Dewey et al. (1988) did not find there any significant compression in the Neogene. Hence, Le Pichon et al. (1997) proclaimed that although the high altitude (more than 5 km) of Tibet is related to its thick crust, yet the large portion of this uplift cannot be attributed to tectonic shortening, generally believed to be responsible for such thickening. They explored the case proposed by Richardson and England (1979), where crustal buoyancy is increased by phase transition in the lower crust. Le Pichon et al. (1997) theoretically demonstrated that the present altitude of Tibet is incompatible with a gabbroic composition of the lower crust and all

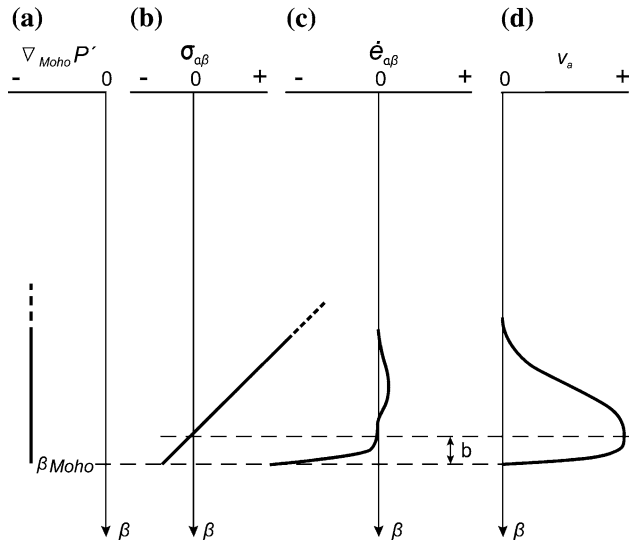

Fig. 20.12 Conditions leading to channel flow in the lowermost crust: **a** effective lateral pressure gradient $\nabla_{\text{Moho}}P'$; **b** shear stress $\sigma_{\alpha\beta}$; **c** strain rate $\dot{e}_{\alpha\beta}$; **d** horizontal velocity v_α. The symbol β indicates a characteristic thickness for the channel, measured from the Moho up to the reversal in shear stress and strain rate. The case illustrated has the diabase rheology and the central North American geotherm. *Source* Modified from Bird (1991)

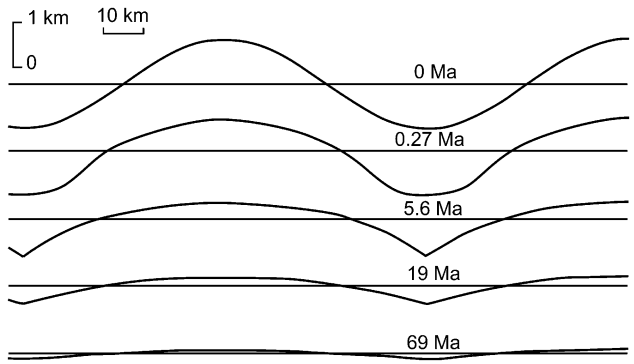

Fig. 20.13 Evolution of initially sinusoidal topography through the spreading pancake phase to eventual flattening. Note the nonuniform time steps. The third profile shows the meeting of adjacent lateral extrusion fronts to form the typical V-shaped valley. The case illustrated has the diabase rheology and the central North American geotherm. *Source* Modified from Bird (1991)

the eclogites, if present there, were subsequently transferred into granulites (Le Pichon et al. 1997).

Based on the INDEPTH I data, Zhao et al. (1993) concluded that there is a single ductile decollement or the Main Himalayan Thrust beneath the Himalaya, dipping at an angle of about 9° and extending for more than 200 km towards Tibet. The Main Himalayan Thrust connects all the active frontal faults and the Main Central Thrust and lies at a depth of 35 km beneath Tibet, and has a seismic velocity akin to that of the upper crust. Henry et al. (1997) remarked that the maximum mean altitude of the Alpine–Himalayan belt between the Alps and Zagros does not exceed 2.5 km, whereas it abruptly reaches a value of more than 5 km in the Himalaya. According to Henry et al. (1997), the altitude difference in the Alps is due to eclogitization of the lower crust at a 55–60 km depth, and they are at the hotter (560 °C at 32 km depth) end of the crustal roots. On the other hand, the Himalaya may represent the cold (less than 500 °C) end member of the evolution where the rate of underthrusting is rapid (15 mm/a), there is a deficit of available water, and the lower crust lies within the blueschist field. Consequently, eclogitization cannot take place and the low-density root of the Himalaya may reach a depth of 70–75 km. The computed isotherms, corresponding to the Himalayan convergence and erosion rates, are depicted in Fig. 20.14. These isotherms also faithfully record the inverted metamorphism observed across the Main Central Thrust, and a high mantle heat flow is unwarranted (Henry et al. 1997).

20.1.13 Late Miocene Activation of the Main Central Thrust

Hubbard (1989), Hubbard and Harrison (1989), and Hubbard (1996) recorded a very young (about 8 Ma) ductile shear zone from the lower part of the Higher Himalaya in east Nepal. According to Copeland et al. (1991), since the beginning of the collision between India and Asia about 50 Ma, the convergence has been taken up along major thrust zones. The dating of Lesser and Higher Himalayan rocks yielded the youngest ages from muscovites (3.1 Ma), biotites (3.4 Ma), and hornblendes (4.1 Ma). All these dates come from within 1 km of the Main Central Thrust zone. There is a marked difference in age between the hanging wall and footwall of the Main Central Thrust. The maximum mica age of the hanging wall is 13 Ma, whereas a muscovite 5 km below the Main Central Thrust, in the footwall, has an age spectrum with a gradient from 400 to 1,400 Ma. They proposed that infiltration of hot fluids through the Main Central Thrust zone at circa 5–4 Ma was responsible for such young ages and corresponding metamorphism. The conditions were such that the fluids heated rocks to temperatures in the range between 470 and 510 °C for less than 1 million years in a region narrower than the entire Main Central Thrust zone. Fluids derived from the footwall rocks of the sole thrust migrated upwards through the Lesser Himalayan rocks, and were subsequently channeled along the Main Central Thrust, producing the thermal disturbance.

Harrison et al. (1997) applied the ^{208}Pb–^{232}Th ion microprobe method of dating on monazite inclusions in the

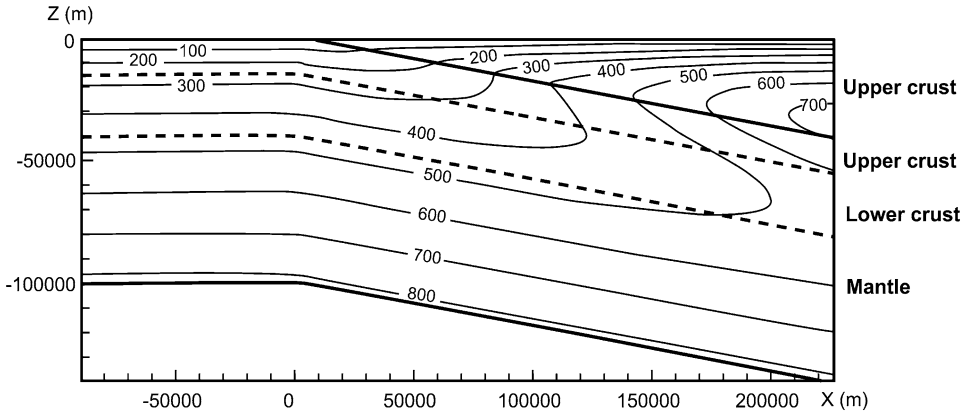

Fig. 20.14 Isotherms in °C computed for a model where mantle heat flow = 15 mW/m^2, upper crust heat production = 2.5 μW/m^2, convergence = 19.5 mm/a, and erosion = 0.8 mm/a. The *thick line* represents the Main Central Thrust. *Source* Modified from Henry et al. (1997)

garnets from the Main Central Thrust footwall and obtained metamorphic ages as young as 6 Ma. Because Pêcher (1989) had obtained *P–T* values of about 600–800 MPa and 500 °C for the pelitic rocks of the Main Central Thrust zone from garnet–biotite–plagioclase–muscovite–quartz thermobarometry, and because monazite and garnet isograds nearly coincide with each other at that temperature, the garnets must have been crystallized at a corresponding depth of about 25 km (Harrison et al. 1997). On the other hand, ^{40}Ar–^{39}Ar biotite ages obtained by Copeland et al. (1991) vary from about 16 Ma in the upper part of the Main Central Thrust hanging wall and then descend to about 4 Ma in its lower part, and finally again reach the pre-Tertiary value, whereas the U–Pb ages of 4.8–4.2 Ma were obtained for the Main Central Thrust zone by these authors.

In their thermal model, Harrison et al. (1997) assumed a fault-bend-fold geometry for the Higher Himalayan thrust sheet (Fig. 20.15). When slip along the Main Central Thrust begins at 8 Ma, hanging wall rocks are first transported along the flat and then they move up the ramp. Sample NL25 (in Fig. 20.15a), which is close to the Main Central Thrust, and hence at the highest peak pressure of about −0.7 GPa, is the first to reach the Main Central Thrust. The sample is followed sequentially up the ramp by U129 (0) and U725 (II), with respective peak pressures of −0.6 and –0.4 GPa. Between 8 and 6 Ma, sample AP332 experiences burial metamorphism, owing to overthrusting by the Tibetan slab reaching 0.7 GPa. At 6 Ma (Fig. 20.15b), the Main Central Thrust zone (modeled as a single fault at the base of the shear zone) is activated, accreting the garnet-grade Midlands rocks, formed by thrusting beneath the Tibetan slab, into the hanging wall, which continues to be transported up the ramp. When slip terminates at 4 Ma, the three reference samples reach the surface, preserving their original lithostatic gradient of 27 MPa/km. Temperature histories (Fig. 20.15c) predicted by the model for various samples indicate that the exposed Main Central Thrust zone reaches the garnet isograd at 6 Ma at a *P–T* of 700 MPa and 550 °C. Biotite ages predicted by the model (Fig. 20.15d) closely match the observed distribution.

20.1.14 Intrusion of Hot Magma in the Upper Part of Main Central Thrust

Brunel and Kienast (1986) studied metamorphism in the Everest–Makalu area of east Nepal and stated that intrusion of leucogranites, confined to the interface between the Higher Himalayan gneisses and the Tethyan sediments, could account for the heat supply. These authors supported late metamorphic thrusting and considered the main phase of Barrovian metamorphism of the Higher Himalayan gneisses, a phenomenon older than the movement along the Main Central Thrust. Hodges et al. (1988) also proposed a similar case of anatexis of crust from Central Nepal, and argued that the widespread anatexis could have effectively buffered the temperature structure of the hanging wall near the solidus temperature for the granites.

20.1.15 Thermomechanical Models Based on Channel Flow and Ductile Extrusion

A fundamentally different approach was taken by Nelson et al. (1996) and Beaumont et al. (2001), who considered the partial melt in Tibet as the main cause of exhumation of the Higher Himalayan crystallines, where erosion allows the continuous flow of material from Tibet towards the Himalaya within a thermally softened “channel”. The model (Fig. 20.16) states that between 35 and 30 Ma (i.e., 20 Ma after collision), the

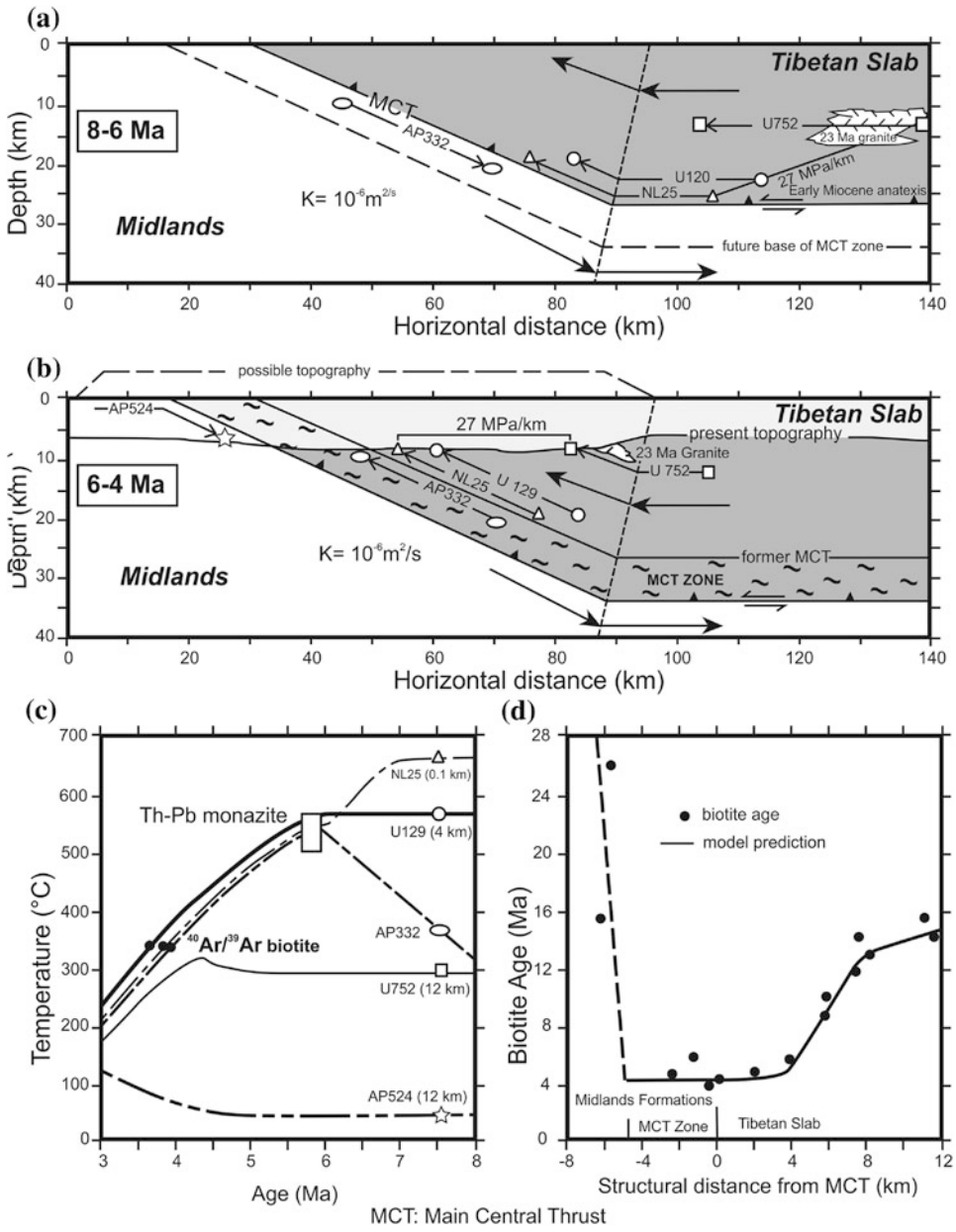

Fig. 20.15 Model illustrating Late Miocene activation of the Main Central Thrust. The model assumes a fault-bend fold geometry. **a** slip along the Main Central Thrust begins at 8 Ma; **b** at 6 Ma, the Main Central Thrust is activated by accreting garnet-grade Lesser Himalayan rocks; **c** temperature histories predicted by the thermal model for the Tibetan slab; **d** biotite ages from a N–S traverse across the Main Central Thrust zone and into the Tibetan slab. *Source* Modified from Harrison et al. (1997). © Elsevier. Used by permission

rocks below south Tibet became quite hot (700–750 °C) and began to partially melt at a depth of 15–20 km, as evidenced by the INDEPTH geophysical observations. The presence of a small fraction of such melt is sufficient to lower the viscosity of the middle crust by one or two orders of magnitude and formation of a channel. The upper crust of the Tibetan Plateau is regionally decoupled from the lower crust and mantle lithosphere below (Nelson et al. 1996). The main driving force to the channel flow is the gravitational potential energy between the thickened Tibet and the Himalayan front. Owing to the intensification of the summer monsoon between 23 and 18 Ma, the erosion rates along the Himalayan front increased significantly. They facilitated the ductile extrusion of the material between the two shear planes (i.e., the Main Central Thrust and the South Tibetan Detachment system). The channel flow (Fig. 20.16) also produced inverted metamorphism as a consequence of the variation in shearing intensity within the channel. This system can operate either continuously or intermittently (Beaumont et al. 2001).

20.1.16 Critical Taper and Underplating Models

In these models, the appearance of sillimanite towards the upper part the Higher Himalayan crystallines and formation of anatectic leucogranites are basically related to isothermal

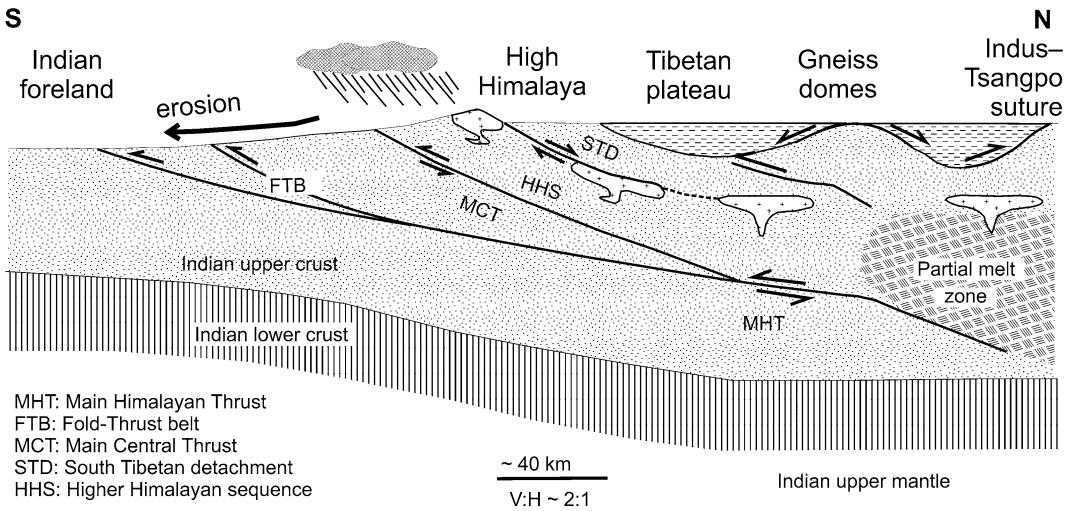

Fig. 20.16 Channel flow model. *Source* Modified from Beaumont et al. (2001)

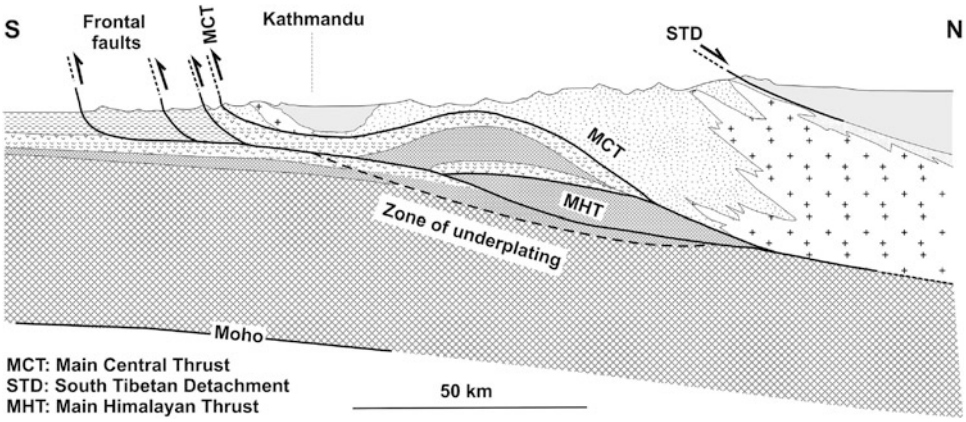

Fig. 20.17 Tectonic underplating model. *Source* Modified from Bollinger et al. (2006)

decompression and melting during the simultaneous movement along the Main Central Thrust and the South Tibetan detachment system. In them, the movement of a southwards extruding wedge (Burchfield et al. 1992; Grujic et al. 1996) or an accretionary prism (Dahlen 1990) is balanced by active erosion at the front of the Himalaya. In other words, in such models, the boundary forces (convergence of India) surpass the volume forces (Mascle et al. 2012). Bollinger et al. (2006) assumed that shortening across the Himalayan Range has occurred essentially along a single low-angle fault, the Main Himalayan Thrust. The growth of the Himalayan wedge has taken place by underplating and formation of a duplex at mid-crustal depth (Fig. 20.17). They demonstrated that these processes can account for the inverted metamorphism observed in the Lesser and Higher Himalaya, the discontinuity of peak metamorphic temperatures across the Main Central Thrust, as well as the variation of exhumation age across the range.

References

Ambrose JW (1936) Progressive kinetic metamorphism in the Missi series near Flinflon, Manitoba. Am J Sci Fifth Ser XXXII:190–286

Armijo R, Tapponnier P, Mercier JL, Han TL (1986) Quaternary extension in southern Tibet: field observations and implications. J Geophys Res 91(B14):13801–13872

Auden JB (1935) Traverses in the Himalaya. Rec Geol Surv India LXIX(Part 2):123–167 (with 6 plates including a geological sketch map)

Auden JB (1937) The geology of the Himalaya in Garhwal. Rec Geol Surv India 71(Part 4):407–433 (with 3 plates including a long cross-section on the scale of 1 in. = 2 miles)

Beaumont C, Jamieson RA, Nguyen MH, Lee B (2001) Himalayan tectonics explained by extrusion of a low-viscosity crustal channel coupled to focused surface denudation. Nature 414:738–742

Bhargava O N, Dasgupta S (1995) Structure and Metamorphism. In: Bhargava ON (ed) The Bhutan Himalaya: a geological account. Geol Surv India, Special Publication 39:191–216

Bird P (1978) Initiation of intracontinental subduction in the Himalaya. J Geophys Res 83(B10):4975–4987

Bird P (1991) Lateral extrusion of lower crust from under high topography, in the isostatic limit. J Geophys Res 96:10275–10286
Bird P, Toksöz MN, Sleep NH (1975) Thermal and mechanical models of continent–continent convergence zones. J Geophys Res 80:4405–4416
Bollinger L, Henry P, Avouac JP (2006) Mountain building in the Nepal Himalaya: thermal and kinematic model. Earth Planet Sci Lett 244:58–71
Brunel M, Kienast J-R (1986) Étude pétro-structurale des chevauchements ductiles himalayens sur la transversale de l'Everest—Makalu (Népal oriental). Can J Earth Sci 23(8):1117–1137
Burchfield BC, Chen Z, Hodges KV, Liu Y, Royden LH, Deng C, Xu J (1992) The South Tibetan detachment system, Himalayan orogen: extension contemporaneous with and parallel to shortening in a collisional mountain belt. Geol Soc Am Spec Pap 269:1–41
Chemenda AI, Burg J-P, Mattauer M (2000) Evolutionary model of the Himalaya-Tibet system: geopoem based on new modelling, geological and geophysical data. Earth Planet Sci Lett 174:397–409
Chemenda AI, Mattauer M, Malavieille J, Bokun A, Alexander N (1995) A mechanism for syn-collisional rock exhumation and associated normal faulting: results from physical modelling. Earth and Planetary Science Letters 132:225–232
Copeland P, Harrison TM, Hodges KV, Maruéjol P, Le Fort P, Pêcher A (1991) An early pliocene thermal disturbance of the Main Central Thrust, Central Nepal: implications for Himalayan tectonics. J Geophys Res 96(B2):8475–8500
Dahlen FA (1990) Critical taper model of fold-and-thrust belts and accretionary wedges. Ann Rev Earth Planet Sci 18:55–99
Dewey JF, Shackleton RM, Chang C, Sun Y (1988) The tectonic evolution of the Tibetan Plateau. Philos Trans R Soc Lond Ser A 327:379–413
England PC (1978) Some thermal considerations of the Alpine metamorphism—past, present and future. Tectonophysics 46:21–40
England P, Le Fort P, Molnar P, Pêcher A (1992) Heat sources for Tertiary metamorphism and anatexis in the Annapurna-Manaslu region, central Nepal. J Geophys Res 97(B2):2107–2128
England PC, Thompson AB (1984) Pressure–temperature–time paths of regional metamorphism I. Heat transfer during the evolution of regions of thickened continental crust. J Petrol 25(Part 4):894–928
Erismann T, Heuberger H, Preuss E (1977) Der Bimsstein von Köfels (Tirol), ein Bergsturz-Frictionit. Tschermaks Mineralogische und Petrographische Mitteilungen 24:67–119
Ernst WG (1973) Blueschist metamorphism and P–T regimes in active subduction zones. Tectonophysics 17:252–272
Frank W, Fuchs GR (1970) Geological investigations in West Nepal and their significance for the geology of the Himalayas. Geol Rundsch 59:552–580
Frank W, Hoinkes G, Miller C, Purtscheller F, Richter W, Thöni M (1973) Relations between metamorphism and orogeny in a typical section of the Indian Himalayas. Tschermaks Mineralogische und Petrographische Mitteilungen 20:303–332
Frank W, Thöni M, Purtscheller F (1977) Geology and petrography of Kulu–Rampur area. Colloques internationaux du C. N. R. S. No. 268. Écologie et Géologie de l'Himalaya, Paris, pp 147–172
Gansser A (1964) Geology of the Himalayas. Interscience, New York, 289 pp
Graham CM, England PC (1976) Thermal regimes and regional metamorphism in the vicinity of overthrust faults: an example of shear heating and inverted metamorphic zonation from southern California. Earth Planet Sci Lett 31:142–152
Grujic D, Casey M, Davidson C, Hollister LS, Kündig R, Schmid S (1996) Ductile extrusion of the Higher Himalayan Crystalline in Bhutan: evidence from quartz microfabrics. Tectonophysics 260:21–43
Harrison TM, Grove M, Lovera OM, Catlos EJ (1998) A model for the origin of Himalayan anatexis and inverted metamorphism. J Geophys Res 103:27017–27032
Harrison TM, Ryerson FJ, Le Fort P, Yin A, Lovera OM, Catlos EJ (1997) A late Miocene–Pliocene origin for the Central Himalayan inverted metamorphism. Earth Planet Sci Lett 146:El–E7
Hasebe K, Fujii N, Uyeda S (1970) Thermal processes under island arcs. Tectonophysics 10:335–355
Heim A, Gansser A (1939) Central Himalaya: geological observations of the Swiss Expedition 1936. Denkschriften der Schweizerischen Naturforschenden Gesellschaft, Band LXXIII(Abh. 1):245 (with maps, sections, and plates)
Henry P, Le Pichon X, Goffé B (1997) Kinematic, thermal and petrological model of the Himalayas: constraints related to metamorphism within the underthrust Indian crust and topographic elevation. Tectonophysics 273:31–56
Herbert JD (1842) Report of the Mineralogical Survey of the Himmalaya Mountains lying between the rivers Sutlej and Kalee. Illustrated by a geological map. J Asiatic Soc Bengal Calcutta XI (126*):i–clv
Hodges KV, Le Fort P, Pêcher A (1988) Possible thermal buffering by anatexis in collisional orogens: Therombarometric evidence from the Nepalese Himalaya. Geology 16(8):707–710
Hubbard MS, Harrison TM (1989) 40Ar/39Ar age constraints on deformation and metamorphism in the Main Central Thrust zone and Tibetan Slab, Eastern Nepal Himalaya. Tectonics 8(4):865–880
Hubbard MS (1996) Ductile shear as a cause of inverted metamorphism: example from the Nepal Himalaya. J Geol 104:493–499
Hubbard MS (1989) 40Ar/39Ar age constraints on deformation and metamorphism in the Main Central Thrust zone and Tibetan Slab, Eastern Nepal Himalaya. Tectonics 8(4):865–880
Jain AK, Manickavasagam RM (1993) Inverted metamorphism in the intracontinental ductile shear zone during Himalayan collision tectonics. Geology 21:407–410
Jain AK, Manickavasagam RM, Singh S, Mukherjee S (2005) Himalayan collision zone: new perspectives—its tectonic evolution in a combined ductile shear zone and channel flow model. Himalayan Geol 26(1):1–18
Le Fort P (1975) Himalayas, the collided range: present knowledge of the continental arc. Am J Sci 275-A:1–44
Le Fort P, Cuney M, Deniel C, France-Lanord C, Sheppard SMF, Upreti BN, Vidal P (1987) Crystal generation of the Himalayan leucogranites. Tectonophysics 134:39–57
Le Pichon X, Henry P, Goffé B (1997) Uplift of Tibet: from eclogites to granulites—implications for the Andean Plateau and the Variscan belt. Tectonophysics 273:57–76
Lobachevsky NI (1829) On the elements of geometry. Kazansky Vestnik 25:178–187, 228–241 (in Russian)
Macfarlane AM (1993) Chronology of tectonic events in the crystalline core of the Himalaya, Langtang National Park, central Nepal. Tectonics 12:1004–1025
Martin AJ, Ganguly J, DeCelles PG (2010) Metamorphism of Greater and Lesser Himalayan rocks exposed in the Modi Khola valley, central Nepal. Contrib Miner Petrol 159:203–223
Masch L (1979) Deformation and fusion of two fault rocks in relation to their depth of formation: The hyalomylonite of Langtang (Himalaya) and the pseudotachylite of the Silvretta nappe (Eastern Alps). In: Conference on analysis of actual fault zones in bedrock, open file report 79–1239, U.S. Geological Survey, Reston, pp 528–533
Mascle G, Pêcher A, Guillot S, Rai SM, Gajurel AP (2012) The Himalaya–Tibet collision. Nepal Geological Society and Société Géologique de France, London, 264 pp
McKenzie DP (1969) Speculations on the consequences and causes of plate motions. Geophys J R Astron Soc 18(1):1–32

McMahon CA (1883) On the microscopic structure of some Dalhousie rocks. Rec Geol Surv India XVI:129–144 (with 2 plates)
McMahon CA (1887) Some remarks on pressure metamorphism with reference to the Foliation of the Himalayan Gneissose-Granitevol. Records of the Geological Survey of India XX(part 4):203–205
Medlicott HB (1864) On the geological structure and relations of the southern portion of the Himalayan range between the rivers Ganges and Ravee. Mem Geol Surv India III(Art. 4):1–206 (with a geological map in colors; scale: 1 in. = 8 miles)
Middlemiss CS (1887) Crystalline and metamorphic rocks of the Lower Himalaya, Garhwal, and Kumaun, section I. Rec Geol Surv India XX(part 3):134–143
Molnar P, England P (1990) Temperatures, heat flux, and frictional stress near major thrust faults. J Geophys Res 95(B4):4833–4856
Naha, H, Ray S (1970) Metamorphic history of the Jutogh Series in the Simla Klippe, Lower Himalaya. Contrib Mineral Petrol 28:147–164
Naha, H, Ray, SK (1971) Evidence of overthrusting in the metamorphic terrain of the Shimla Himalaya. Am J Sci 270:30–42
Nelson KD, Zhao W, Brown LD, Kuo J, Jinkai C, Liu X, Kiemperer SL, Makovsky Y, Meissner R, Mechie J, Kind R, Wenzel F, Ni J, Nabelek J, Leshou C, Tan H, Wei W, Jones AG, Booker J, Unsworth M, Kidd WSF, Hauck M, Alsdorf D, Ross A, Cogan M, Wu C, Sandvol E, Edwards M (1996) Partially molten middle crust beneath southern Tibet: synthesis of project INDEPTH results. Science 274:1684–1688
Neogi S, Dasgupta S, Fukuoka M (1998) High P–T polymetamorphism, dehydration melting, and generation of migmatites and granites in the High Himalayan crystalline complex, Sikkim, India. J Petrol 39(1):61–66
Oldham RD (1883) Note on the geology of Jaunsar and Lower Himalayas. Rec Geol Surv India XVI(Part 4):193–198 (with a Geological Sketch of Jaunsar Bawar, scale: 1 in. = 5 miles, in colors)
Oxburgh ER, Turcotte DL (1974) Thermal gradients and regional metamorphism in overthrust terrains with special reference to the Eastern Alps. Schweizerische Meneralogische und Petrographicscshe Mitteilungen 54(3):641–662
Pêcher A (1989) The metamorphism in the Central Himalaya. J Metamorph Geol 7:31–41
Pêcher A, Le Fort P (1986) The metamorphism in central Nepal Himalaya, its relations with the thrust tectonic. In: Le Fort P, Colchen M, Montena, C (eds) Évolution des domaines orogéniques d'Asie méridionale (de la Turquie à l'Indonésie), Livre jubilaire Pierre Bordet, Sciences de la Terre, Mémoire No. 47, Nancy, pp 285–309
Pognante U, Lombardo B (1989) Metamorphic evolution of the High Himalayan crystallines in SE Zanskar, India. J Metamorph Geol 7 (1):9–17
Powell C McA, Conaghan PJ (1973) Plate tectonics and the Himalayas. Earth Planet Sci Lett 20:1–12
Reitan PH (1968a) Frictional heat during metamorphism. Quantitative evaluation of concentration of heat generation in time. Lithos 1:151–163
Reitan PH (1968b) Frictional heat during metamorphism: 2. Quantitative evaluation of concentration of heat generation in space. Lithos 1(3):268–274
Richardson SW, England PC (1979) Metamorphic consequences of crustal eclogite production in overthrust orogenic zones. Earth Planet Sci Lett 42(2):183–190
Scholz CH (1980) Shear heating and the state of stress on faults. J Geophys Res 85(B11):6174–6184
Scott JS, Drever HI (1953) Frictional fusion along a Himalayan thrust. Proc R Soc Edinb Sect B 65:121–135
Searle MP, Fryer BJ (1986) Garnet, tourmaline and muscovite-bearing leucogranites, gneisses and migmatites of the Higher Himalaya from Zanskar, Kulu, Lahoul and Kashmir. In: Coward MP, Ries A (eds) Collision tectonics, vol 19. Special Publication of the Geological Society, London, pp 185–201
Searle MP, Rex DC (1989) Thermal model for the Zanskar Himalaya. J Metamorph Geol 7(1):127–134
Searle MP, Tirrul R (1991) Structural and thermal evolution of the Karakoram crust. J Geol Soc Lond 148:65–82
Stäubli A (1989) Polyphase metamorphism and the development of the Main Central Thrust. J Metamorph Geol 7(1):73–93
Stephenson BJ, Waters DJ, Searle MP (2000) Inverted metamorphism and the Main Central Thrust: field relations and thermobarometric constraints from the Kishtwar Window, NW Indian Himalaya. J Metamorph Geol 18:571–590
Tapponnier P, Mercier JL, Armijo R, Tonglin H, Ji Z (1981) Field evidence for active normal faulting in Tibet. Nature 294:410–414
Tapponnier P, Peltzer G, Le Dain AY, Armijo R (1982) Propagating extrusion tectonics in Asia: new insights from simple experiments with plasticine. Geology 10(12):611–616
Thompson AB, England PC (1984) Pressure–temperature–time paths of regional metamorphism II. Their inference and interpretation using mineral assemblages in metamorphic rocks. J Petrol 25(Part 4):929–955
Toksöz MN, Bird P (1977) Modelling of temperatures in continental convergence zones. Tectonophysics 41:181–193
Toksöz MN, Minear JW, Julian B (1971) Temperature field and geophysical effects of a downgoing slab. J Geophys Res 76:1113–1138
Zhao W, Nelson KD, The Project INDEPTH Team (1993) Deep seismic reflection evidence for continental underthrusting beneath southern Tibet. Nature 366:557–559

Part V

Tethys Himalaya

Introduction to Tethys Himalaya

21

The folded and crumpled deposits of this ocean stand forth to heaven in Thibet, Himalaya, and the Alps. This ocean we designate by the name "Tethys," after the sister and consort of Oceanus.

—Edward Suess (1893, p. 183)

The Tethyan Himalayan sequence (Box 21.1) mainly occupies the south periphery of the windswept Tibetan Plateau. Despite its towering altitude (above 3,000 m), cold climate, and insurmountable accessibility, the Tethyan realm represents one of the best-investigated sedimentary suites in Nepal. In a celebrated paper of 1893, Eduard Suess gave the name *Tethys* to "the great ocean" that once stretched across part of Eurasia. Argand (1924) further advanced Suess's connotation in his famous work on the tectonics of Asia, and developed the Tethyan tectonics that we understand today (Sorkhabi 1997). Subsequently, Auden (1935, p. 161) suggested that the emphasis should be made on the division of the Himalaya into the Tethys Himalaya and the Peninsular Himalaya. But, his last suggestion was not taken up further, owing to the dispute regarding the peninsular affinity of the Proterozoic Himalayan rocks.

During the breakup of the Pangaea supercontinent, the Tethys appeared as an embayment (Wilson 1963) between the Gondwanaland to the south and the Angaraland (subsequently called the Laurasia) to the north. While discussing the origin of the Himalaya, Dewey and Bird (1970) pointed out that the Alpine–Himalayan system has been developing since early Mesozoic time by multiple collisions, related to the sweeping of microcontinents and island arcs across the Tethyan–Indian Ocean. Crawford (1974) and Gansser (1981) emphasized that the Tethys was actually a narrow zone of complicated island arcs, internal basins, and irregular slivers of continental rocks. Cêlal Şengör (1979, 1985) further introduced the notation of Paleo-Tethys (Paleozoic) and Neo-Tethys (Mesozoic to Eocene) in the geological literature. However, some investigators disagree with this subdivision of the Tethys (e.g., Tozer 1989; Bhat 2001; Torsvik et al. 2009). Tollmann and Kristan-Tollmann (1985) present a good historical review of the various terms related to the Tethys.

Box 21.1: Main Characteristics of Tethyan Himalayan Sequence

- The Tethyan rocks are made up of a variety of terrigenous and carbonate sediments such as sandstones, siltstones, dolomites, limestones, and shales. They range in age from Cambrian to Eocene.
- They were deposited in a variety of marine (from pelagic sediments to coral reefs) and fluvial environments.
- They are strongly folded and faulted, but conformably overlie the Proterozoic succession of the Higher Himalaya.
- Their grade of metamorphism generally increases from west to east.
- Famous as it is, Mount Everest is composed of sedimentary rocks (belonging to the yellow band or slab) of the Cambro–Ordovician age. These rocks were pushed out of the ocean to an altitude of 8,848 m.
- The Tethyan sediments have lateral changes and strong facies differences. The thickness of a given lithostratigraphic unit may change significantly in its lateral prolongation.
- The rocks are intricately folded and frequently verging due north, that is, opposite to the Higher and Lesser Himalayan successions.
- Apart from the South Tibetan Detachment system, occurring at its basal part, there are also north–south trending normal faults that make the half graben of Thakkhola–Mustang.
- There are a few Paleozoic remnants on top of the Higher Himalayan rocks in Nepal and Bhutan.

M.R. Dhital, *Geology of the Nepal Himalaya*, Regional Geology Reviews,
DOI 10.1007/978-3-319-02496-7_21

The Tethyan belt extends from the Alps, through the Mediterranean, Iran, Afghanistan, Salt Range, and the Himalayan arc (Box 21.2), and continues towards Tibet and Burma. The Phanerozoic sediments, accumulated in this vanished ocean, encompass the northern margin of the Himalaya. With a thin intervening strip of the Higher Himalayan crystalline zone, apparently two Tethyan belts compose the Punjab Himalaya of Kashmir (Wadia 1926, p. 345; Gansser 1964, p. 39). There is also a narrow belt of the Tethyan rocks, deposited mainly in Eocene time in the Lesser and Sub-Himalayan zones of Northwest India. Within the Nepalese territory, this group of rocks extends between the Mahakali River and Tinkar Lipu on the west to Langtang Himal on the east. The same sedimentary sequence constitutes the top of Mount Everest and the surrounding tract. A few isolated vestiges of these rocks are also distributed in the Lesser Himalaya, whereas some synformally folded odd outliers cap the Higher Himalayan succession in the vicinity of Kathmandu, Jaljala, and Jumla. Similar outliers are also present in the Higher Himalayan sequence of Bhutan (Chap. 5).

Box 21.2: Historical Background

Strachey (1851) and Stoliczka (1866) made pioneering attempts to investigate the Tethyan rocks of the Spiti Valley in northwest Kumaun, whereas Lydekker (1883) and Wadia (1934) established the Tethyan stratigraphy of Kashmir. The Spiti area was further visited by McMahon (1879), Griesbach (1891), and Diener (1895). Hayden (1904) initiated the first systematic and detailed study of the Tethyan rocks in the Spiti Basin. Heim and Gansser (1939) gave a luminous account of the Tethyan sequence in the Mahakali River valley of Kumaun and Nepal (Chap. 22). Nakazawa and Dickins (1985) succinctly presented the paleogeography and paleobiogeography of the Tethys from Europe and Asia. Kapoor and Tokuoka (1985) discussed the sedimentary facies of the Permian and Triassic rocks of the Himalaya including Dolpa, Thakkhola, Tansen, and Damudas. Bhargava and Bassi (1998) gave a detailed geological description together with a stratigraphic classification of the Spiti–Kinnaur area in the Northwest Tethys Himalaya. On the other hand, Bhargava (2011) gave an overview of early Paleozoic paleogeography, basin configuration, and tectonic setting of the Indian plate.

It was none other than the stalwart of Nepalese geology, Tony Hagen (1959, 1968), who first described the geology of the Tethyan succession from the Thakkhola area. He also prepared a geological map of that region, and described the Saligram Formation (Spiti Shales), the Dangarjong normal fault, and the Mustang granites. In addition, the Austrian expedition to Mt. Dhaulagiri had another diligent and vigilant geologist, named Gerhard Fuchs, on their team. Fuchs (1964, 1967, 1977) was determined to map the incredible and inaccessible Dolpa (Chap. 23) in every detail, when other parts of the country were still far from being understood.

The first detailed geological investigations in the Thakkhola area (Chap. 24) were carried out by P. Bordet, M. Colchen, D. Krummenacher, P. Le Fort, R. Mouterde, and M. Rémi in 1963 and 1966 under the patronage of the French National Center of Scientific Research (Centre National de la Recherche Scientifique, CNRS). The preliminary results are presented in Bordet et al. (1967), and a large-scale (1:75,000) map and detailed observations were published by Bordet et al. (1971). Subsequently, Bordet et al. (1975) extended their investigations to Manang (Chap. 25). Through their latter brilliant publications, the gifted French researchers have brought to light a gamut of stratigraphic, paleontological, petrographic, and structural records of the area together with its impressive geological history and far-reaching tectonic interpretation. Colchen et al. (1986) have incorporated their findings within a regional perspective.

First aerial reconnaissance

On 18 October 1949, A. Heim, D. N. Wadia, and M. R. Sahni, determined to unravel the fundamental structural features of these stupendous Himalayan ranges, took an "unusual and wonderful" mountain flight in a Dakota airplane from Amosi airport of Lucknow (India) to the valley of Kali Gandaki, up to Mustang. The flight began at 5:08 a.m. in the morning and ended at 8:56 a.m. by landing back at Lucknow (Sahni 1958). Probably, this was the first regional geological aerial reconnaissance of the Kali Gandaki Valley.

21.1 Early Fossil Finds

Contrary to the Lesser and Higher Himalayan sequences so wanting in fossils, the Tethys Himalaya contains a bountiful reserve of organic remains. This zone is renowned worldwide for the splendor of its pristine scenery, inherited in a precipitous array of dazzling snow-clad peaks and rolling downs as well as spectacular geological exposures, and above all for the preponderance of ammonites (Box 21.3).

Box 21.3: Ammonite Myth

From time immemorial, *sadhus*, devotees, and pilgrims have picked up from this tract of the country the *Shaligram* (as charms and amulets), frequently concealed in the water-worn rounded concretionary black pebbles of the Kali Gandaki (also known as the Krishna Gandaki or Shaligrami) River. These sacred organic relics are ascribed in Hindu religious epics to the incarnation of Lord Vishnu, representing his *Sudarshan Chakra* (pyritous ammonite whorls), a kind of supernatural weapon in the form of a rapidly spinning brilliant circular disc with a sharp outer edge and a hole in the center for holding it round his forefinger. Consequently, one of the famous Hindu temples is located within this zone of emanating natural gas at *Muktinath* (Emancipator Lord). There is also an equally important Buddhist temple on this peaceful promontory of the Trans-Himalaya, where all gods and goddesses live in perfect harmony with people.

Blumenbach (1803) described an ammonite from the Gandika (Gandaki) River, a tributary to the Ganga, near Patnam (Patna), and stated that Hindus worshiped the ammonites as idols of Vishnu (p. 22). Gray (1830–1832) compiled the meticulous work of Hardwicke on Indian zoology in the form of a book, illustrating a variety of species, where Hardwicke described *Ammonites nepaulensis*, *A. wallichi,* and *A. tenuistriatus.* Similarly, Oppel (1862, 1863, 1865) in his monumental work on the ammonites of the Munich museum described *Ammonites Everesti* Oppel (Oppel 1863, p. 284) and *Inoceramus Everesti* Oppel (Oppel 1863, p. 298). On the other hand, Everest (1833) had earlier tentatively identified the fossils discovered in the Himalaya by Gerard, and also those handed over to him by Sir Charles Gray and James Prinsep. Oppel (1865, pp. 303–304) further gives a register of ammonites where he mentions *Ammonites Nepaulensis, Ammonites Everesti*, and *Inoceramus Everesti*.

Reed (1908) studied 63 Wallich's specimens obtained from Muktinath. These fossils had been lying unnoticed in the collections of the Sedgwick Museum, Cambridge, since 1872 (Holland 1908). They belong mainly to ammonites and belemnites, and Reed (1908, p. 258) provisionally identified the following genera and species.

Belemnites cf. *B. sulcatus* Miller
Hoplites wallichii Gray
Perisphinctes cf. *P. biplex* Sowerby
Perisphinctes cf. *P. torquatus* Sowerby
Perisphinctes aff. *P. frequens* Oppel
Perisphinctes cf. *P. sabineanus* Oppel
Oppelia (*Streblites*) cf. *O. griesbachi* Uhlig
Parallelodon ebertonianus (Stoliczka)
Nucula sp.
Rhynchonella cf. *R. variabilis* Schlotheim.

Reed (1908, p. 261) also identified two other species of ammonites (*Halobia* and *Ptychites*) in the Wallich's collection, belonging to a different horizon and concluded that the Triassic also occurs near Muktinath.

Oppel (1863) also refers to a specimen of *Ammonites sabineanus* Oppel, in a black nodule obtained from the river Gundock (Gandaki), which had been in the collection of the Jardin des Plantes in Paris since 1825; this fossil may possibly have been obtained from the same spot as Wallich's specimens, particularly as the mode of occurrence suggests a "Salagram", and as the same species is most probably represented among the above fossils from Muktinath (Reed 1908, pp. 257–258).

The French Expedition to Mount Annapurna in 1950 gave an opportunity to explore the upper reaches of the Kali Gandaki Valley (Bordet 1961). It was during that expedition when M. Ichac collected many fossils from a rich fossiliferous zone in the Kagbeni area near Muktinath. Subsequently, Ichac and Pruvost (1951) described the following ammonites and belemnites.

Simberskites nepalensis Gray
Paraboliceras himalayanus V. Uhlig
Kossmatia cf. *K. tenuistriata* Gray
Belemnites gerardi Oppel.

Because these fossils are similar to those occurring in the Spiti region of the Northwest Himalaya, they inferred that the Spiti shales make a continuous band, stretching from west to east of the Himalaya. Following these discoveries of "shaligrams" by a team member of the Annapurna I expedition, the team members of the 1954 and 1956 Makalu expeditions with A. Lombard and Pier Bordet arrived. Bordet (1961) prepared a large-scale colored geological map of the Everest area, and showed the yellow band and other formations.

Barthel identified the following species of ammonites collected from the north of Muktinath, around Tange and Tagsa, during the Dutch Himalayan Expedition of 1955 (Helmstaedt 1969, p. 65).

1. From Tange:
Haplophylloceras strigile (Blanford)
Himalayites cf. *H. stoliczkai* Uhlig
(?) *Blanfordiceras* sp.
Belemnopsis sp.
2. From Tagsa:
(a) *Blanfordiceras wallichii* (Gray) in the three variations
Paraboliceras haugi Uhlig
Kossmatia aff. *K. desmidoptycha* Uhlig
Virgatosphinctes aff. *V. rotundidoma* Uhlig
(b) *Mayaites transiens* (Waagen)
Prograyiceras aff. *P. grayi* Spath

Alligaticeras obliqueplicatum (Waagen)
Pachyplanulites subevolutus (Waagen)
Pachyplanulites cf. *P. subevolutus* (Waagen).

Ryf (1962) analyzed the ammonites collected by Hagen from Muktinath and described the species *Hap1ophy11oceras strigilis* (Blanford). Furthermore, he also identified two different forms: *Hap1ophy11oceras* aff. *H. strigilis* (Blanford) and *Hap1ophy11oceras pingue* Ryf from that collection. These species belong most probably to the Late Jurassic Epoch.

21.2 Detailed Investigations of Ammonites

Helmstaedt (1969) investigated the ammonites from the Thakkhola area. According to him, about 50 % of his specimens belong to the genus *Blanfordiceras* Cossmann (1907). He described the genera *Subplanites*, *Substeueroceras*, *Groebericenas,* and ?*Lemenda*, with five species, for the first time, from the Himalaya. He also discovered the following new species: *Blanfordiceras muktinathense* Helmstaed, *B. rotundidoma rotundum* Helmstaed, *Subplanites nepalensis* Helmstaed, *Substeueroceras uhligi* Helmstaed, and *Virgatosphinctes kagbeniensis* Helmstaed. It was found that the majority of the fauna confirms a Late Tithonian (Late Jurassic) age of the Spiti Shales. Genera such as *Berriasella*, *Groebericeras,* and *Thurmanniceras* indicate the presence of the Berriasian Stage. *Thurmanniceras* suggests even the possible occurrence of a younger stage (Valanginian) of the Early Cretaceous.

Krystyn (1982) studied the trachyostracan ammonite fauna from a 350 m thick section, covering the Late Carnian to Middle Norian rocks from an 800 m thick Late Triassic sequence of the Tibetan Tethyan zone in Jomsom (Fig. 21.1). He recognized 67 species belonging to 35 genera and 12 biostratigraphic horizons, which fit well in the ammonite zonation of the west Tethys (Table 21.1). Out of these, 13 species and 6 genera (*Thiniites, Gandakites, Ammotibetites, Tropijuvavites, Projuvavites (Goniojuvavites),* and *Epijuvavites* are newly described. He discovered that the faunal distribution within a single substage is irregular. He also compared the ammonite fossil record from Jomsom with those of the Tinkar Lipu, Dolpa, and Everest regions. On the other hand, Enay and Cariou (1999) provided a paleogeographic setting to the Jurassic ammonite fauna of the Thakkhola area.

21.3 Plant Fossils of Kagbeni

Barale et al. (1976) described the Early Cretaceous plant fossils from Kagbeni. Their collection contains a specimen of *? Taeniopteris* sp. cf. *T. spatulata* McClelland, two species of *Ptilophyllum*: *P. acutifolium* Morris and *P.* sp. cf. *P. cutchense* Morris, and a few petrified araucarian wood fragments, classified as a new species of *Araucarioxylon*, that is, *A. nepalensis* Barale et al. They presumably belong to the basal part of the Early Cretaceous.

The Mesozoic folded formations of the Tethyan Himalayan sequence are exposed at Kagbeni. There is an anticline, and the fossiliferous horizon is exposed on the right bank of the Thakkhola River. The rocks are composed of the Chukh Group (Gradstein et al. 1992; Chap. 24). Bassoullet and Mouterde (1977) divided this group into the Kagbeni Formation of sandstones (Barremian, 150 m thick), and the overlying Dzong Formation (about 600 m), composed of green sandstones and shales, with some intercalations of limestones. The massive, gray colored Kagbeni sandstones, exposed on the right bank, upstream from a bridge, contain plant remains in a horizon of 10 m thickness.

21.4 Paleomagnetic Investigations in Thakkhola

Klootwijk and Bingham (1980) carried out paleomagnetic investigations in the Thakkhola area. They analyzed 750 carbonate and sandstone samples from the Tethyan succession, ranging in age from the Devonian to Early Cretaceous. They identified the following five magnetic components: (1) a predominant component of recent origin, (2) a secondary component probably acquired during early Tertiary collision of India with Asia, (3) primary magnetic components of ? middle Permian to Early Cretaceous age, and two other secondary components. According to them, declinations of the secondary component and the primary components mismatch the declination data from the Indian subcontinent by 10–15 degrees. They related this mismatch to the rotational underthrusting of India along the Main Central Thrust beneath its former leading edge and beneath the Tibetan Plateau. They also inferred underthrusting of the continental lithosphere over 200–350 km in central Nepal.

21.5 Fossils from Phulchauki and Chandragiri Hills South of Kathmandu

During a reconnaissance visit to the Kathmandu Valley in May 1875, Medlicott (1875) identified the synformally folded ridge of Chandragiri and Phulchauki as well as indeterminable crinoidal fossils in the Chandragiri hills. Bowman obtained, for the first time, the determinable fossils from Chandragiri, whereas Auden (1935) revisited the site and assigned the fossils to an Ordovician age. On the other hand, Hagen and B. P. Malla reported Silurian trilobites from the Phulchauki hills.

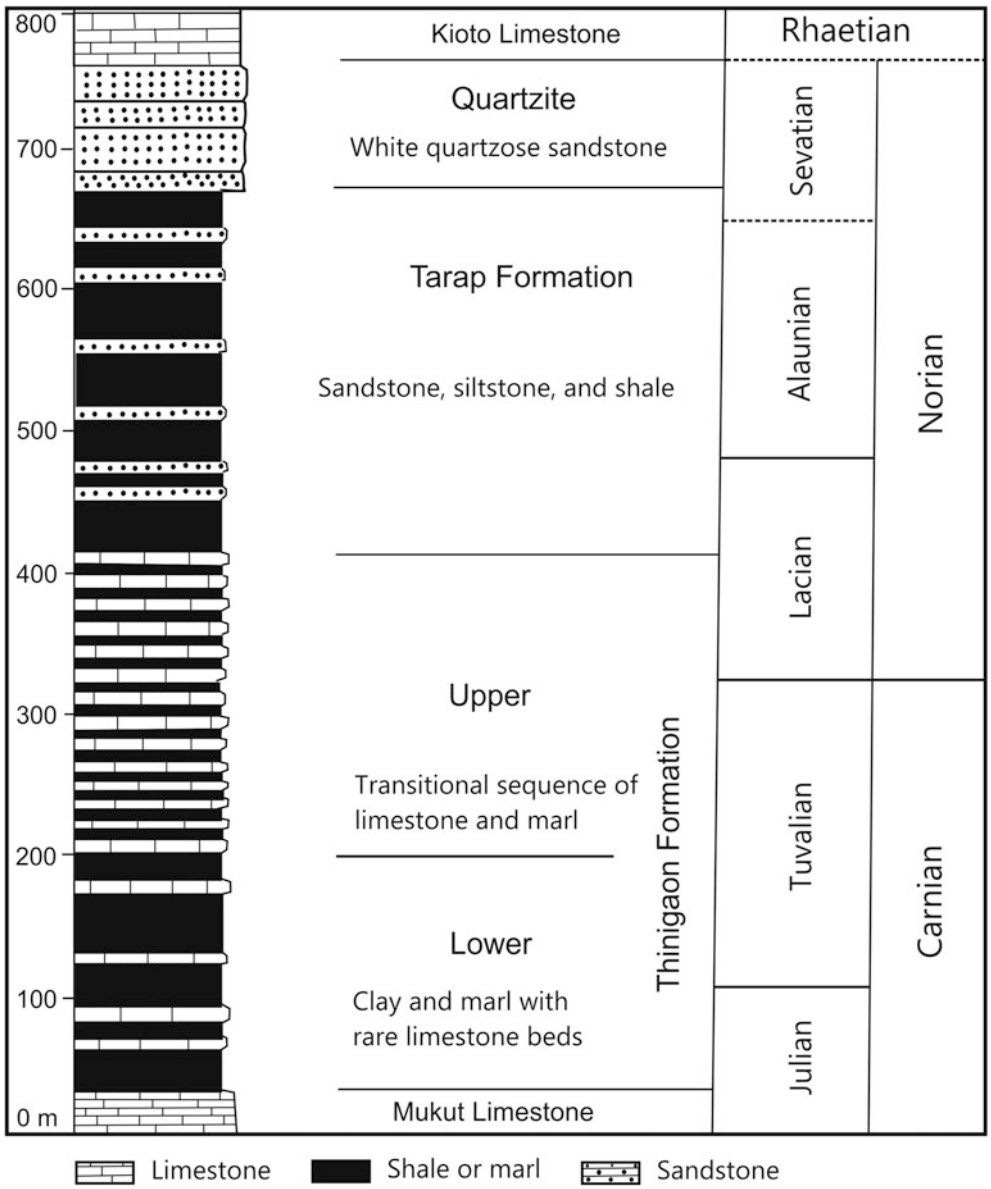

Fig. 21.1 Stratigraphy of Late Triassic sequence in Jomsom. *Source* Modified from Krystyn (1982)

Bordet et al. (1959, 1960) confirmed their findings and reported the following fossils (Figs. 21.2 and 21.3).

Bed 9: There were indeterminable fragments of large crinoids, orthoceras, simple polypora, and some brachiopoda.

Bed 8: It yielded indeterminable bryozoans and the following brachiopods: *Lingula* sp., *Orthis* (?) cf. *O. patera* Salter, *Nicolella* cf. *N. actoniae* Sowerby, *Orthotetes pecten* (?) Linné, *Leptæna rhomboidalis* Wilckens, *Dalmanella elegantula* (?) Dalman, *Dalmanella* cf. *D. rostrata* Dreyfuss, *Harknessella vespertilio* (?) Sowerby, *Atrypa reticularis* (?) Linné, *Atrypa imbricata* Sowerby. The bed also yielded the following bivalves: *Modiolopsis* sp. cf. *M. leightoni* (?) Williams; tentaculites; indeterminable gastropods; cephalopods: *Orthoceras* sp.; echinoderms: *Crinoides* (?*Paleocrinoides*), Cystoides (stem and calices); trilobites: *Phacops* (*Pterygometopus*) *dagon* Reed.

Bed 5 contains compact trilobites in a very large number, but it was possible to determine only the following species: *Phacops* (*Dalmanites*) *longicaudatus* var. *P. orientalis* Reed, *Illaenus* aff. *I. aemulus* Salter (=*Illaenus namshinensis* Reed), *Aristoharpes* sp., *Sphaerexochus* aff. *S. mirus* Beyrich, (?) *Asaphus* sp.

Bed 2: It was not possible to obtain any determinable fossils, but they resembled those of Bed 8.

According to Bordet et al. (1960), these fossils range in age from the Late Ordovician to the Silurian, whereas the overlying unfossiliferous topmost dolomites and dolomitic quartzites could belong to the Devonian, and they can be

Table 21.1 Correlation of Late Triassic fossil horizons in Jomsom with the ammonite zones of west Tethys

			Ammonoid zones	Subzones	Dominant species	Fossil horizon in Jomsom
Norian	Alaunian	2	*Himavatites hogarti*	IV	"catenate *Halorites*"	
				III	*Amarassites s. semiplicauts*	*Trachypleuraspidites*—beds
				II	*Himavatites hogarti*	
				I	*Himavatites watsoni*	
		1	*Cyrtopleurites bicrenatus*			
	Lacian	3	*Juvavites magnus*			*Indojuvavites angulatus*
						lower *Juvavites*—beds
		2	*Malayites paulckei*			*Miltites*—beds
						Malayites grobbeni *Malayites tingriensis*
		1	*Guembelites jandianus*	II	*Dimorphites selectus*	*Guembelites philostrati*
				I	*Dimorphites* Krystyn	*Guembelites jandianus*
Carnian	Tuvalian	3	*Anatropites spinosus*	II	*Gonionotiles cf. G. italicus*	*Microtropites* sp. *? Euisculites* sp.
				I	*Discotropites plinii*	
		2	*Tropites subbullatus*	II	*Tropites subbullatus*	*Discotropites plinii* *Jovites*—beds
				I	*Projuvavites crasseplicatus*	*Margaritropites* cf. *M. margarit.*

Source Modified from Krystyn (1982)

equivalent to the Muth Quartzite in the Northwest Himalaya of India and west Nepal.

From the Chandragiri hills, Stöcklin et al. (1977) identified the thecal plates of Cystoid *Caryocrinites s.l.* ranging in age from the upper part of the Middle Ordovician up to middle Silurian. This fossil also seems to be present in the Phulchauki hills, where it corresponds to Bed 8 with *Nicolella* cf. *N. actoniae*. Furthermore, in the upper part of the Nilgiri Limestone of the Thakkhola area, there are "*Glyptocystida*" plates, resembling this fossil (Chap. 24). The geological section across the Chandragiri hills (Fig. 21.4) contains the following rock sequence of the Phulchauki Group (Chap 17).

Tistung Formation: (1) gray, green, and pink, fine-grained sandstones, siltstones, and slates (cf. 18). Below the Tistung formation are the Markhu Formation (m) and the Bhainsedobhan Marble (b) of the Bhimphedi Group (Chap. 17). Sopyang Formation: (2) dark gray-green argillaceous siltstones and marls with thin and lenticular beds of limestone. Chandragiri Limestone: (3) Thin- to thick-bedded, gray-blue, and light colored limestones, regularly alternating with thin, sericitic slates; (4) very thick-bedded, massive, pale yellow to blue-green, siliceous limestones; (5) argillaceous impure limestones with undulating beds; (6) quartzose sandstones with light gray, thin beds, passing upwards to brown, dolomitic, sandy limestones; (7) undulating beds of thick, very fine-grained, dense, gray-green, brown, and yellow limestone with distinct bedding, in places slightly silty to argillaceous, and containing fragments of echinoderms. Chitlang Formation: (8) resistant beds of medium-grained, light gray quartz arenite; (9) phyllitic slates, alternating with some resistant beds of quartz arenite; (10) very thin, wavy beds of highly argillaceous, blue-gray limestone; (11) thick-bedded, fine-grained, yellow, gray, and pink quartzose sandstones with intercalations of subordinate slate; (12) dark gray-green quartzose slates; (13) pink, yellow, and light gray quartzites; a bit of slate (cf. 11); (14) wavy-bedded, fine-grained, bluish gray, clayey limestones (cf. 10); (15) hard, white quartz arenites constituting the top of the intercalation of gray quartzite with pink and green phyllite (cf. 8 and 9). Chandragiri Limestone: (16) thin-bedded limestone, gray-green, very fine grained, with minor clay partings, passing upwards to an alternation of dark gray limestone, fine-grained sandy–dolomitic limestone, pink sandstone, and clayey–silty slate. The limestone section thickens towards the west–northwest. Sopyang Formation: (17) slates and marls, poorly exposed along this section, but well developed farther to the west–northwest (cf. 2). Tistung Formation: (18) fine-grained quartzose sandstones, siltstones, and slates, mostly green with yellow varieties in the sandy parts (cf. 1).

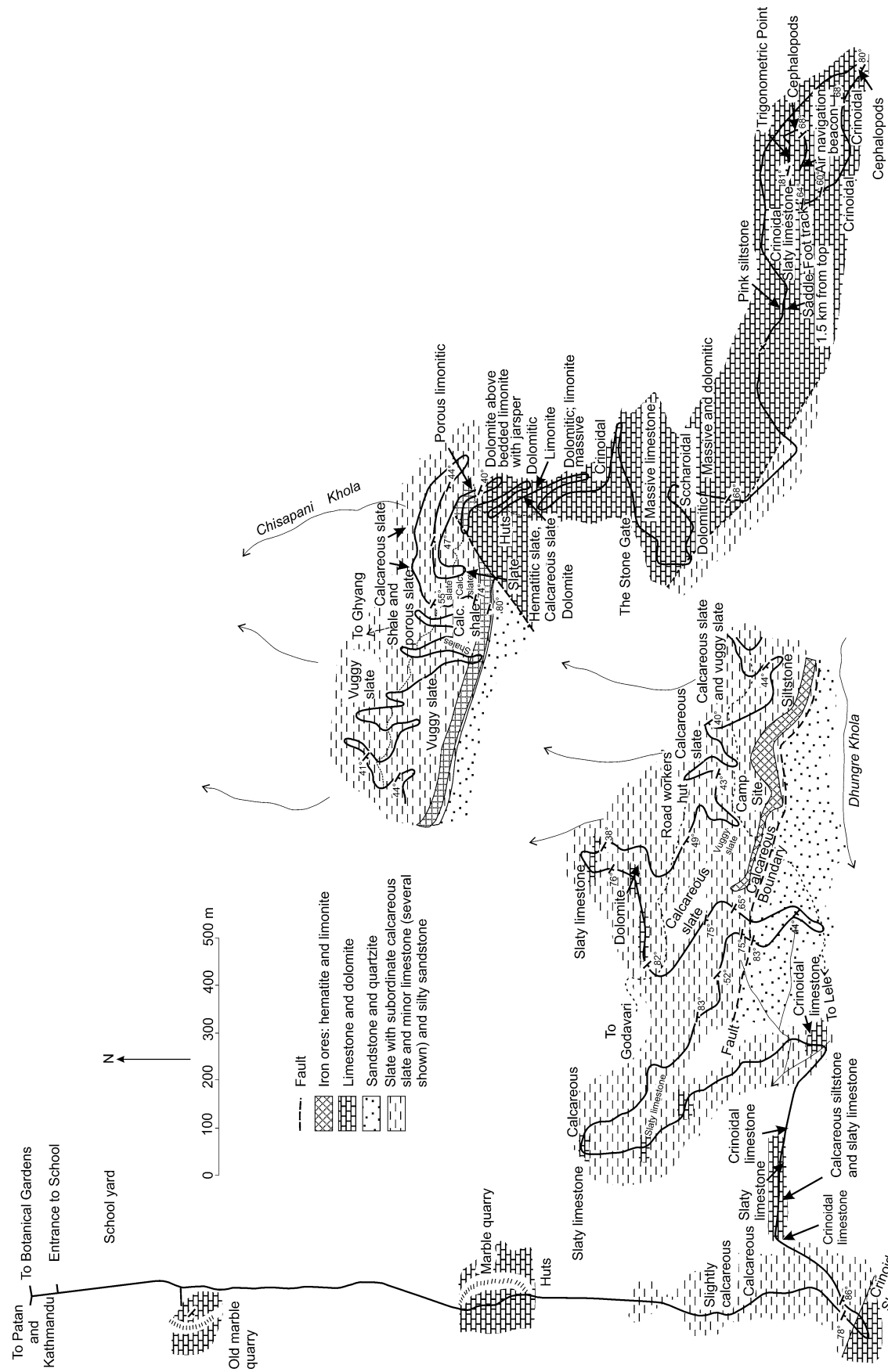

Fig. 21.2 Geological traverse in the Phulchauki area illustrating main rock types, the hematite band, and fossil locations. *Source* Modified from Talent et al. (1988)

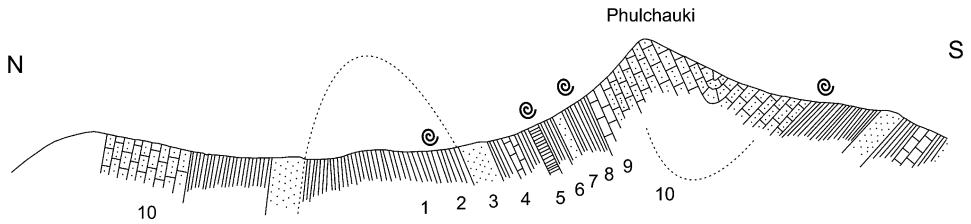

Fig. 21.3 Geological cross-section across Phulchauki. The section is about 3 km long. *1* Gray shales. *2* Graywacke with brachiopods. *3* Quartzites. *4* Green and reddish shales with calcareous layers. *5* Hematitic horizons with trilobites. *6* Gray shales. *7* Quartzites. *8* Graywacke with trilobites and brachiopods. *9* Godavari marbles with crinoids and orthoceratids. *10* Thick dolomites. *Source* Modified from Bordet et al. (1960)

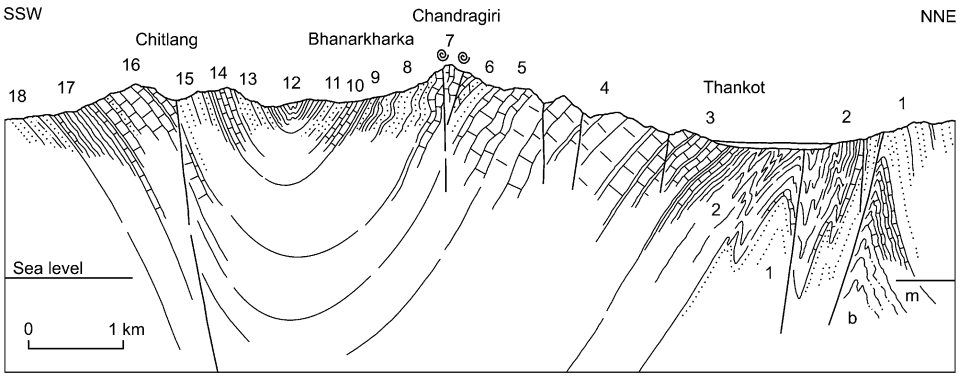

Fig. 21.4 Cross-section across the Chandragiri hills southwest of Kathmandu showing fossil locations. *Source* Modified from Stöcklin et al. (1977)

References

Argand E (1924) La tectonique de l'Asie. Congrès Géologique International, Belgique, Comptes Rendues de la 13ème Session, en Belgique 1922. H. Vaillant-Carmanne, Liège, pp 171–372

Auden JB (1935) Traverses in the Himalaya. Rec Geol Surv India LXIX(Part 2):123–167 (with 6 plates including a geological sketch map)

Barale G, Bassoullet J-P, Bose MN (1976) On a collection of Mesozoic plants from Kagbeni–Muktinath, Thakkhola Valley, Nepal, vol 25. The Palaeobotanist, Lucknow, pp 32–38 (with two plates)

Bassoulle J-P, Mouterde R (1977) Les formations sédimentaires mésozoïques du domaine tibétain de l'Himalaya du Népal, Colloques internationaux du Centre National de la Recherche Scientifique (CNRS), No. 268 - Écologie et Géologie de l'Himalaya, pp 41–52

Bhargava ON, Bassi UK (1998) Geology of Spiti–Kinnaur Himachal Himalaya. Geol Surv India 124:1–210 (with a geological map in colors covering 4 sheets, scale 1:100,000)

Bhargava ON (2011) Early Palaeozoic palaeogeography, basin configuration, palaeoclimate and tectonics in the Indian plate. Memo Geol Soc India 78:69–99

Bhat MI (2001) Untenability of the Neo-Tethys: okeanos was not a polygamist. Himalayan Geol 22(1):5–15

Blumenbach IF (1803) Specimen Archaeologiae Telluris terrarumque inprimis hannoveranarum Alterum, Regitatum in Consessu Societatis Anniversario, vol 1. Gottingen, 28 pp (with 3 plates)

Bordet P (1961) Recherches Géologiques dans L'Himalaya du Népal, Région du Makalu, Expéditions Françaises a l'Himalaya 1954–1955. Edition du Centre National de la Recherche Scientifique (CNRS), Paris, 275 pp (with geological maps and plates)

Bordet P, Cavet P, Pillet J (1959) Sur l'existence d'une faune d'âge silurien dans la région de Kathmandu (Himalaya du Népal), vol 248. Comptes Rendus de l'Académie des Sciences, Paris, pp 1547–1549

Bordet P, Cavet P, Pillet J (1960) La faune silurienne de Phulchauki près de Kathmandu (Himalaya du Népal), 7th Series, vol II. Bulletin de la Société Géologique de France, Notes et Mémoires, Paris, pp 3–18 (with one plate)

Bordet P, Colchen M, Krummenacher D, Le Fort P, Mouterde R, Rémi M (1971) Recherches géologiques dans l'Himalaya du Népal, région de la Thakkhola. Centre National de la Recherche Scientifique, Paris, 279 pp (with two geological maps in colors)

Bordet P, Colchen M, Le Fort P (1975) Recherches géologiques dans l'Himalaya du Népal, région du Nyi-Shang. Centre National de la Recherche Scientifique, Paris, 138 pp (with a geological map in colors)

Bordet P, Colchen M, Le Fort P, Mouterde R, Rémi M (1967) Données nouvelles sur la géologie de la Thakkhola (Himalaya du Népal), 7^{e} Série, Tome IX, No. 6. Bulletin de la Société géologique de France, Paris, pp 883–896

Colchen M, Le Fort P, Pêcher A (1986) Annapurna–Manaslu–Ganesh Himal. Centre National de la Recherches Scientifique, Special Publication, Paris, 136 pp (with a geological map, 1:200,000 scale)

Crawford AR (1974) The Indus Suture Line, the Himalaya, Tibet and Gondwana land. Geol Mag 111(5):369–383

Dewey JF, Bird JM (1970) Mountain belts and the new global tectonics. J Geophys Res 75(14):2625–2647

Diener C (1895) Ergebnisse einer geologischen expedition in den Central-Himalaya von Johar, Hundes, und Painkhanda, vol 62. Denkschriften der Kaiserlichen Akademie der Wissenschaften, Wien, pp 533–608

Enay R, Cariou E (1999) Jurassic ammonite faunas from Nepal and their bearing on the palaeobiogeography of the Himalayan belt. J Asian Earth Sci 17:829–848

Everest RR (1833) Memorandum on the Fossil Shells discovered in the Himalayan Mountains, vol XVIII, part II, chapter V. Asiatic Researches; or, Transactions of the Physical Class of the Asiatic Society of Bengal, Calcutta, pp 107–114 (with two plates)

Fuchs GR (1964) Beitrag zur Kenntnis des Paläozoikums und Mesozoikums der Tibetischen Zone in Dolpo (Nepal–Himalaja) (auch in Englisch), Hefte 1–3. Verhandlungen der Geologischen Bundesanstalt, Wien, pp 6–15 (with a map)

Fuchs G (1967) Zum Bau des Himalaya, Österreichische Academie der Wissenschaften, Mathematisch-Naturwissenschaftliche Klasse, Wien, Denkschriften, 113 Band, pp 1–211 (with 30 plates including 9 large sheets and one geological map in colors)

Fuchs G (1977) The geology of the Karnali and Dolpo regions, Western Nepal. Jahrbuch der Geologischen Bundesanstalt, Wien, Band 120, Heft 2. pp 1–103 (with 9 plates)

Gansser A (1964) Geology of the Himalayas. Interscience, New York, 289 pp

Gansser A (1981) The geodynamic history of the Himalaya. In: Gupta HK, Delany FM (eds) Zagros, Hindu Kush, Himalaya, geodynamic evolution, Geodynamic Series, vol 3. Am Geophys Union, Washington, pp 111–121

Gradstein FM, von Rad U, Gibling MR, Jansa LF, Kaminski MA, Kristiansen I-L, Ogg JG, Rohl U, Sarti M, Thurow JW, Westermann GEG, Wiedmann J (1992) Stratigraphy and depositional history of the Mesozoic continental margin of central Nepal. Geologisches Jahrbuch 77:3–141

Gray JE (1830–1832) Illustrations of Indian Zoology, chiefly selected from the collections of Major-General Hardwicke, vol 1 (Parts I–X), Treuttel, Wurtz, Treuttel Jun., Richter (with 100 colored plates and a lithographic portrait of Hardwicke)

Griesbach CL (1891) Geology of the Central Himalayas. Memo Geol Surv India XXIII:1–232 (with 27 plates)

Hagen T (1959) Geologie des Thakkhola (Nepal). Eclogae Geologicae Helvetiae 52(2):709–719 (with 5 figures and 1 plate)

Hagen T (1968) Report on the geological survey of Nepal. Volume 2: Geology of the Thakkhola. Denkschriften der Schweizerischen Naturforschenden Gesellschaft, vol LXXXVI/2, Druck von Gebrüder Fretz AG, Zürich, Kommissionsverlag von Gebrüder Fretz AG, Zürich, 159 pp

Hayden HH (1904) The geology of Spiti, with parts of Bashahr and Rupshu. Memo Geol Surv India XXXVI(Part 1):129 pp (with Appendix, and 18 plates including a map)

Heim A, Gansser A (1939) Central Himalaya: geological observations of the Swiss expedition 1936. Denkschriften der Schweizerischen Naturforschenden Gesellschaft, Band, vol LXXIII, Abh. 1. 245 pp (with geological maps in colors, sections, and plates)

Helmstaedt H (1969) Eine Ammoniten-Fauna aus den Spiti-Schiefern von Muktinath in Nepal, vol 1. Zitteliana, München, pp 63–89 (with plates 3 to 5)

Holland TH (1908) Note on Jurassic and Triassic fossils from Nepal. Records of the Geological Survey of India XXXVII(Part 1):136–138

Ichac M, Pruvost P (1951) Résultats géologiques et l'expéition française de 1950 à l'Himalaya. Comptes Rendus, Hebdomadaires des Séances De L'Académie des Sciences 232(19):1721–1724

Kapoor HM, Tokuoka T (1985) Sedimentary facies of the Permian and Triassic of the Himalayas. In: Nakazawa K, Dickins JM (eds) The Tethys: her paleogegraphy and paleobiogeography from paleozoic to mesozoic. Tokai University Press, Tokyo, pp 23–58

Klootwijk CT, Bingham DK (1980) The extent of greater India, III. Palaeomagnetic data from the Tibetan sedimentary series, Thakkhola region, Nepal Himalaya. Earth Planet Sci Lett 51:381–405

Krystyn L (1982) Obertriassische ammonoideen aus dem Zentralnepalesischen Himalaya (Gebiet von Jomsom), vol 36. Abhandlungen der Geologischen Bundesanstalt, Wien, pp 1–63 (with 18 plates)

Lydekker R (1883) The geology of the Kashmir and Chamba territories and the British district of Khagan. Memo Geol Surv India XXII:1–344

McMahon CA (1879) Notes on a tour through Hangrang and Spiti. Rec Geol Surv India XII:57–69 (with a geological map in colors; scale: 1 in. = 8 miles)

Medlicott HB (1875) Note of the geology of Nepal. Rec Geol Surv India VIII(Part 4):93–101 (with a geological map on 1 in. = 6 miles)

Nakazawa K, Dickins JM (1985) (eds) The Tethys: her paleogegraphy and paleobiogeography from paleozoic to mesozoic. Tokai University Press, Tokyo, 317 pp

Oppel A (1862) Ueber jurassische Cephalopoden. Palaeontologische Mittheilungen aus dem Museum des Königlichen Bayerischen Staates, Stuttgart, Nr. III, pp. 127–266 (with plates 40–74)

Oppel A (1863) Ueber ostindische Fossilreste aus den secundären Ablagerungen von Spiti und Gnari-Khorsum in Tibet. Palaeontologische Mittheilungen aus dem Museum *des* Königlichen Bayerischen Staates, Stuttgart, no. IV. pp 267–288 (with plates 75–82)

Oppel A (1865) Ueber ostindische Fossilreste (Fortsetzung). Palaeontologische Mittheilungen aus dem Museum des Königlichen Bayerischen Staates, Stuttgart, Nr. IV, pp 289–304 (with plates 83–88)

Reed FRC (1908) Note on some Fossils from Nepal, New series, Decade V, vol. V, no. VI. The Geological Magazine, London, pp 256–261

Ryf W (1962) Über das Genus Haplophylloceras (Ammonoidea) in den Spiti-Shales von Nepal. Eclogae Geologicae Helvetiae, 55(2):317–325 (with 2 plates)

Sahni MR (1958) Geological aerial reconnaissance of the Central Himalaya along the Kali Gandaki (Nepal), as far as the Tibetan Border, on 18th October, 1949. Rec Geol Surv India 85(Part 4):453–470 (with 7 plates)

Şengör AMC (1979) Mid-Mesozoic closure of Permo-Triassic Tethys and its implications. Nature 279:590–593

Şengör AMC (1985) The story of Tethys: How many wives did Okeanos have? Episodes 8(1):3–12

Sorkhabi RB (1997) Emile Argand and Tethyan tectonics of Asia. Himalayan Geol 18:17–32

Stöcklin J, Termier G, Bhattarai KD (1977) A propos des roches fossilifères de Chandragiri (Mahabharat, Himalaya du Népal). Bulletin de la Société Géologique de France 19(2):367–373

Stoliczka F (1866) Geological sections across the Himalayan Mountains, from Wangtu-Bridge on the river Sutlej to Sungdo on the Indus: with an account of the formations in Spiti; accompanied by a revision of all known fossils from that district. Memo Geol Surv India V(Part 1):1–154 (with 1 map, 6 sections in colors, and 10 plates of fossils)

Strachey R (1851) On the geology of part of the Himalaya Mountains and Tibet. Q J Geol Soc London 7:292–310 (with a geological map and two cross-sections in colors)

Suess E (1893) Are great ocean depths permanent? Nat Sci 2(13):180–187

Talent JA, Goel RK, Jain AK, Pickett JW (1988) Silurian and Devonian of India, Nepal, and Bhutan: biostratigraphic and Palaeobiogeographic Anomalies. Cour Forsch-Inst Senckenberg Frankfurt am Main 106:1–57

Tollmann A, Kristan-Tollmann E (1985) Paleogeography of the European Tethys from Paleozoic to Mesozoic and the Triassic Relations of the Eastern Part of Tethys and Panthalassa. In: Nakazawa K, Dickins JM (eds) The Tethys: her paleogegraphy and paleobiogeography from paleozoic to mesozoic. Tokai University Press, Tokyo, pp 3–22

Torsvik TH, Paulsen TS, Hughes NC, Myrow PM, Ganerød M (2009) The Tethyan Himalaya: palaeogeographical and tectonic constraints from Ordovician palaeomagnetic data. J Geol Soc London 166:679–687

Tozer ET (1989) Tethys, Thetis, Thethys, or Thetys? What, where, and when was it? Geology 17(10):882–884

Wadia DN (1926) Geology of India (for students), Revised edition. Macmillan, London, 400 pp

Wadia DN (1934) The Cambrian-Trias sequence of North Western Kashmir (Parts of Muzaffarabad and Baramula districts). Rec Geol Surv India LXVIII(Part 2):121–176

Wilson JT (1963) Hypothesis of earth's behaviour. Nature 198:925–929

Tethys Himalaya of Mahakali Region

22

Today we need machines and computers in order to produce something we think really worthwhile. In earlier times a piece of clay, a sure hand and a good fire were enough to produce astounding works.
—Hansjörg Bloesch (1982, p. 8)

In the Mahakali River valley and mountainous neighborhood (Fig. 22.1), the Proterozoic huge monocline of the Higher Himalaya gives way to the intensely deformed Tethyan zone, distinguished by the abundance of a variety of well-preserved fossils. In contrast to the open folds prevalent in the Spiti region of the Northwest Himalaya, the Tethyan realm of this vicinity displays a more complexly contorted architecture, and it is also ramified by a number of south-directed thrusts (Gansser 1964, p. 119). During the expedition of 1936, Heim and Gansser (1939) not only carried out detailed stratigraphic and tectonic investigations in the area, but also collected a large number of fossils, which were subsequently described by Jeannet (1958, 1959). The Paleozoic and Mesozoic rocks of the Tethys Himalaya in the Mahakali region comprise a very thick (4,000–6,000 m) pile of essentially marine sediments, which are classified in the following formations.

22.1 Garbyang Formation (Neoproterozic–Cambrian)

The rather monotonous Garbyang Formation (Figs. 22.1 and 22.2) occurs above the porphyroblastic biotite schists of Budhi (Chap. 14), and consists of calcareous phyllites with dolomitic and chloritic (tuffaceous) bands. The weathered dolomitic and chloritic bands exhibit rusty brown colors, easily discernible from afar. An approximately 2 km thick lower part of this formation, containing green chloritic bands, gradually passes into the upper portion (about 2.5 km thick), predominated by calcareous phyllites. The lower part is also more calcareous and contains sandy limestones, making high walls, whereas the upper sequence displays more reddish brown weathering. The top section of the Garbyang Formation is represented by green-gray marly schists (Heim and Gansser 1939, p. 99). Sinha (1989, p. 33) subdivided the Garbyang Formation into three members. The Lower Member is made up of shaly dolomitic limestones, dark blue calcareous phyllites, and sericite schists. The Middle Member consists of massive, gray dolomitic limestones with marly bands and shaly horizons. The Middle Member also contains barite and pyrite mineralizations in its lower part. The Upper Member comprises cross-laminated calcareous sandstones interbedded with shales. Heim and Gansser (1939, p. 203) found a crinoidal limestone from the middle part of the Garbyang Formation. They also recovered several large but poorly preserved gastropods from this formation in the Shiala glacier. Consequently, part of the Garbyang Formation is possibly of the Cambrian Period.

22.2 Shiala Formation (Ordovician)

In the Shiala pass, lying to the northwest of Garbyang, the Garbyang Formation is followed upwards by a 400–500 m thick sequence of the Shiala Formation, containing variegated shales intercalated in sandy limestones or crinoidal breccia of brown weathering. The Shiala Formation is intensely bioturbated (Sinha 1989, p. 37). Jeannet identified the following Ordovician trilobite, gastropods, and brachiopods taken from the calcareous sandstone of about 60 m thickness, representing the formation's upper part (Heim and Gansser 1939, pp. 121, 203).

- Trilobite: *Calymene* cf. *C.* douvillei Mansuy
- Gastropods: *Bellerophon* sp. indet.,*? Traconema* sp. indet.
- Brachiopods: *Orthis* (*Dinorthis*) *thakil* var. *O. striatocostata* Salter, *Orthetes pecten* Sow, *Orthetes orbignyi* Dav., *Refinesquina* aff.*? R. subdeltoidea* Reed, *Strophomena chamaerops* Salter, *Sowerbyella umbrella* Salter, *Leptaena sphaerica* Jeannet
- In the moraine was found: *Orthis porcata* M'Coy.

M.R. Dhital, *Geology of the Nepal Himalaya*, Regional Geology Reviews,
DOI 10.1007/978-3-319-02496-7_22

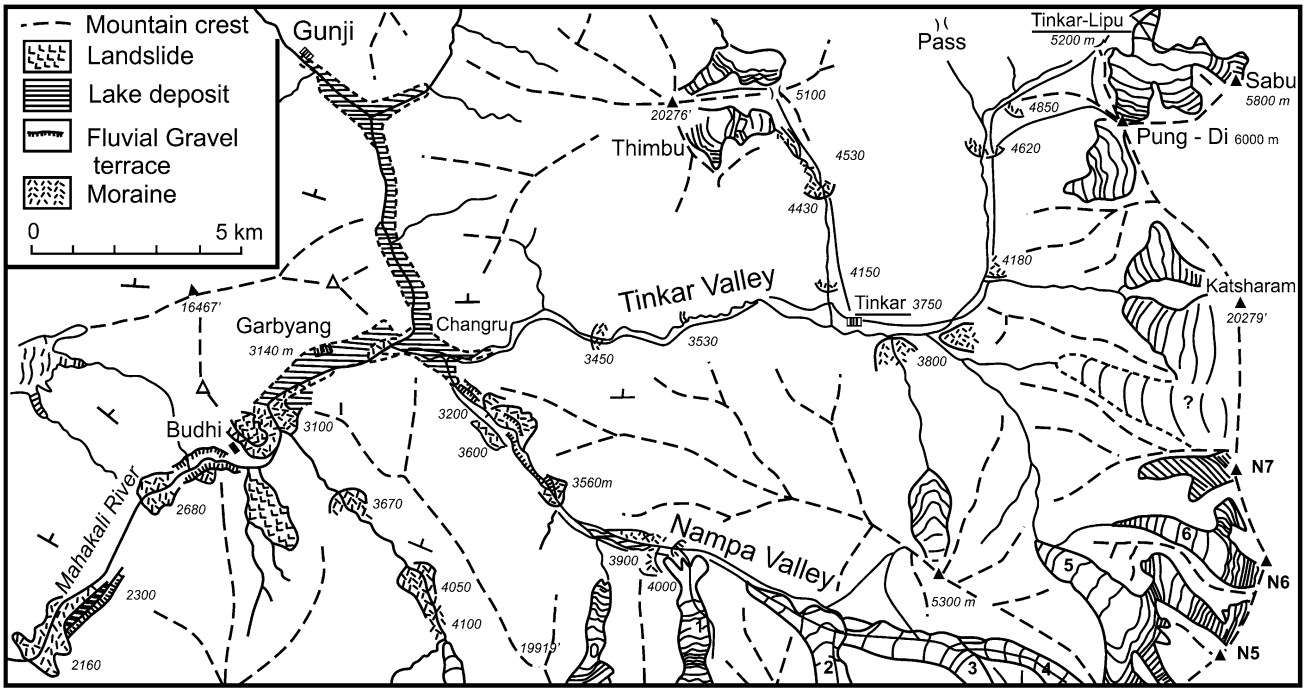

Fig. 22.1 Distribution of Tethyan sequence as well as glaciers and fluvial deposits in the Mahakali River valley. *Source* Modified from Heim and Gansser (1939)

22.3 Variegated Silurian

The Variegated Silurian is a formation with diverse lithology and thickness, represented by an alternating succession of variegated (red and white) limestones and marly to siliceous shales. Heim and Gansser (1939, p. 204) recorded the following sequence in the Shiala pass.

- From 200 to 300 m of red to green and gray shales with beds of white limestone, characterized by smaller, deep-red shale layers, and a rusty weathered dolomite in the upper part
- From 500 to 600 m of shaly lenticular limestone with crinoidal fragments

On the Mahakali River near Gunji, less than 50 m of violet siliceous sandy shales directly overlie the Garbyang Formation. Here, the lower part of the Variegated Silurian is absent. The shales strongly vary in thickness (from 20 to 100 m) and are conformably folded and faulted with the underlying Garbyang shales. In the violet shales, small crinoidal fragments are present (Heim and Gansser 1939, p. 100). East of the Mahakali, the violet shales are again reduced in thickness to less than 100 m (Heim and Gansser 1939, p. 204).

22.4 Muth Formation (late Silurian–Devonian)

The Muth Formation is represented by brown-weathering quartzites with dolomitic beds, and is capped by a massive white quartzite (Figs. 22.3 and 22.4). This formation ranges in thickness from 800 to 1,000 m and its top quartzite band of about 200 m in thickness is replaced by dolomites at Kuti and Tinkar (Heim and Gansser 1939, p. 204). The Muth Formation is regarded to range in age from the late Silurian to Devonian (Hayden 1904, p. 28; Burrard and Hayden 1908, p. 300). In the Spiti area, it has been assigned a Middle Devonian age (Bhargava 2008). Except for some crinoids occurring in the dark limestone of Lipu Lekh, this formation is wanting in fossils (Heim and Gansser 1939, p. 104).

22.5 Kuling Formation or *Productus* Shale (Permian)

The black Kuling shales (Fig. 22.2) conformably overlie the white Muth quartzite with a sharp contact. The basal conglomerate (marking the great gap of Devonian, Carboniferous,

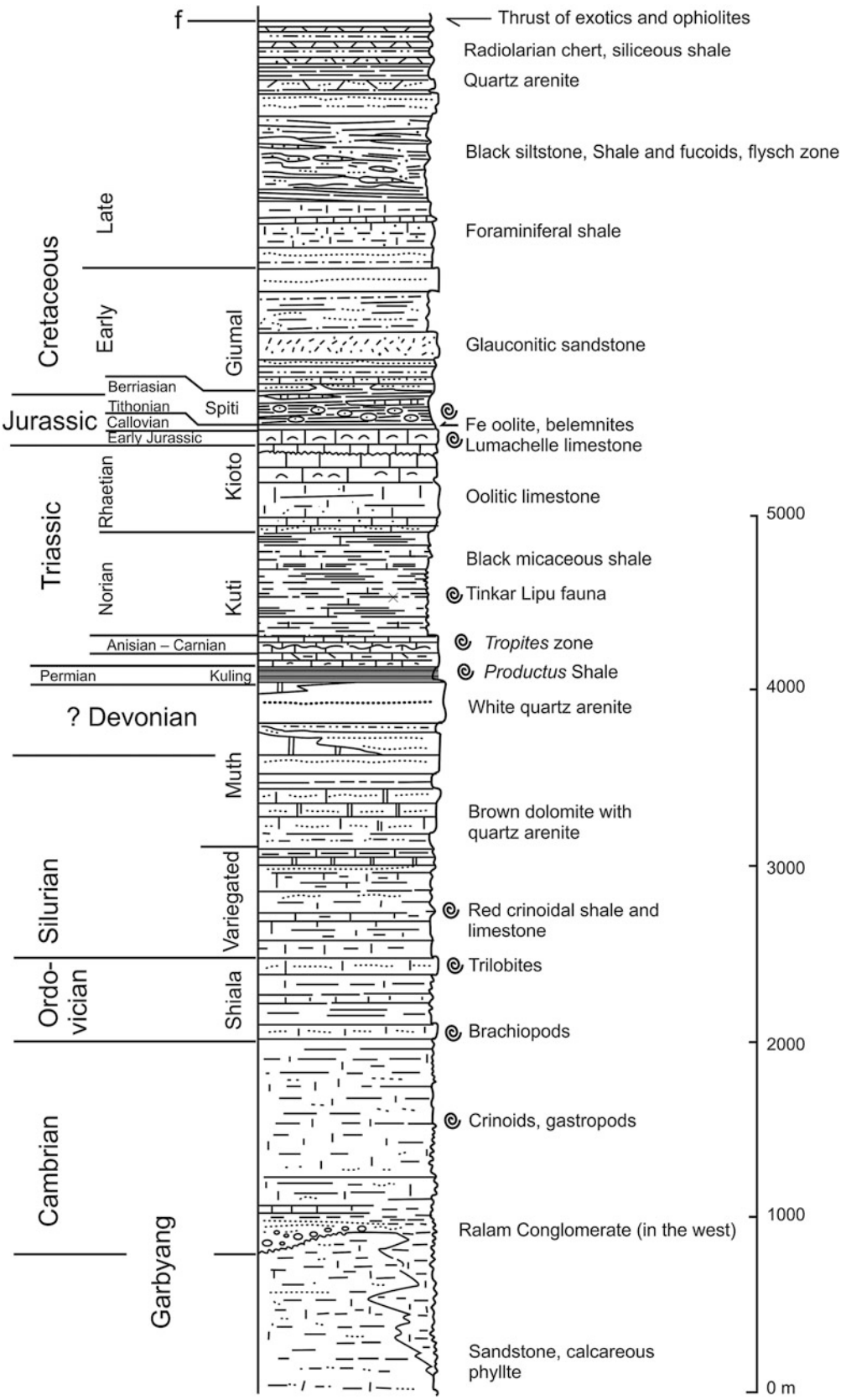

Fig. 22.2 Stratigraphy of the Tethyan Himalayan sequence in the Mahakali River section and surrounding tract. *Source* Modified from Gansser (1964, p. 107)

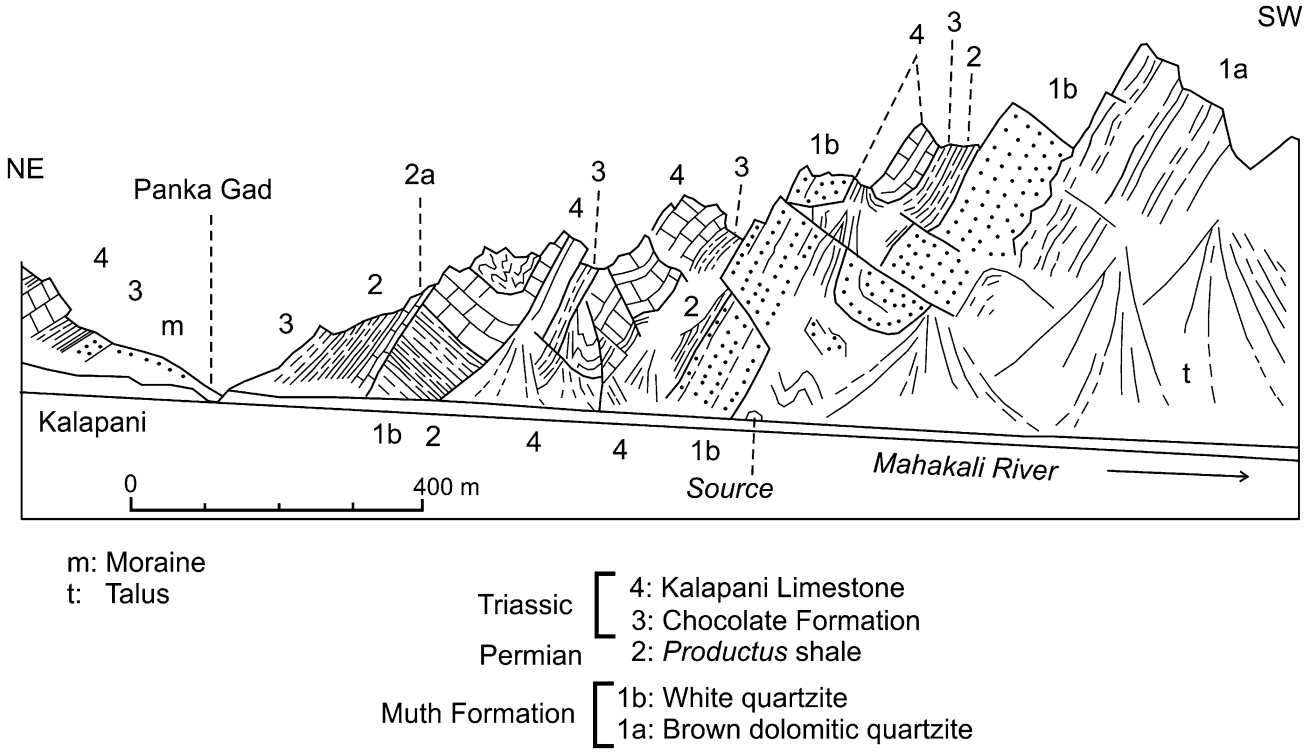

Fig. 22.3 Rocks exposed at Kalapani, on the southeast side of the Mahakali River. *Source* Modified from Heim and Gansser (1939)

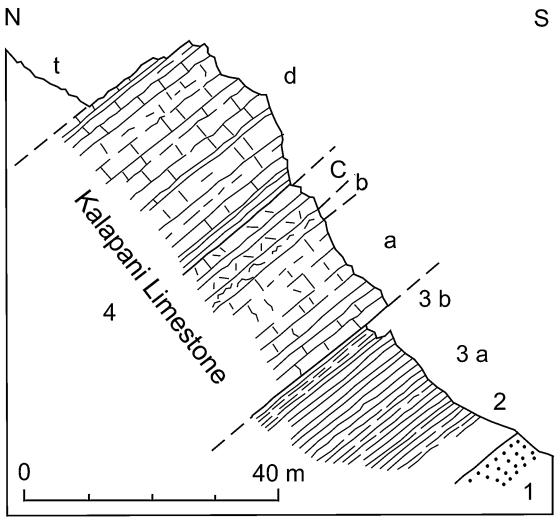

1: Muth quartzite
2: *Producturs* shale – Kuling shale
3: Chocolate Formation
a: 18 m clay–ironstone layers of 10–20 cm with argillaceous shale passing into
b: 3 m band of dark shale with a sharp boundary to
4: a:17 m of compact grey limestone of light brown weathering, upper part coarse-grained with shell fragments
b: 2 m thick limestone spotted with red hematite and large involute ammonites, amongst which *Ptychites cf. rugifer* OPP. and *Paraceratites himalayanus* BLANK
c: 6 of fine-grained limestone
d: 30 m of well-bedded, dense, dark blue limestone spotted with orange colored streaks of ankerite. Upper part nodular and thin-bedded, with numerous ammonites, of which *Tropites subbullatus* v. HAUER
t: Talus on Kuti shale

Fig. 22.4 Kalapani Limestone of Panka Gad, 1 km southeast of Kalapani. *Source* Modified from Heim and Gansser (1939)

and early Permian) observed in Spiti (Hayden 1904, p. 51) is absent in this part of the Tethys Himalaya. Despite a prolonged sedimentation gap, the upper part of the Muth quartzite appears conformable to the overlying Kuling Formation. The Kuling shale is usually 30–50 m thick, but it is a few meters thick at the Tinkar Lipu pass (Fig. 22.5), whereas at Lipu Lekh and Kalapani (Unit 2 in Fig. 22.3), its lower part contains ferruginous (ankeritic to limonitic) limestone beds, full of small brachiopods. On Lipu Lekh, the following fossils were collected from the black *Productus* shale with nodular layers and rusty concretions of clay-rich ironstone (Heim and Gansser 1939, p. 105).

Productus himalayensis DIENER
Productus subreticulatus MARTIN
Productus abichi WAAGEN
Spirifer tibetanus DIENER

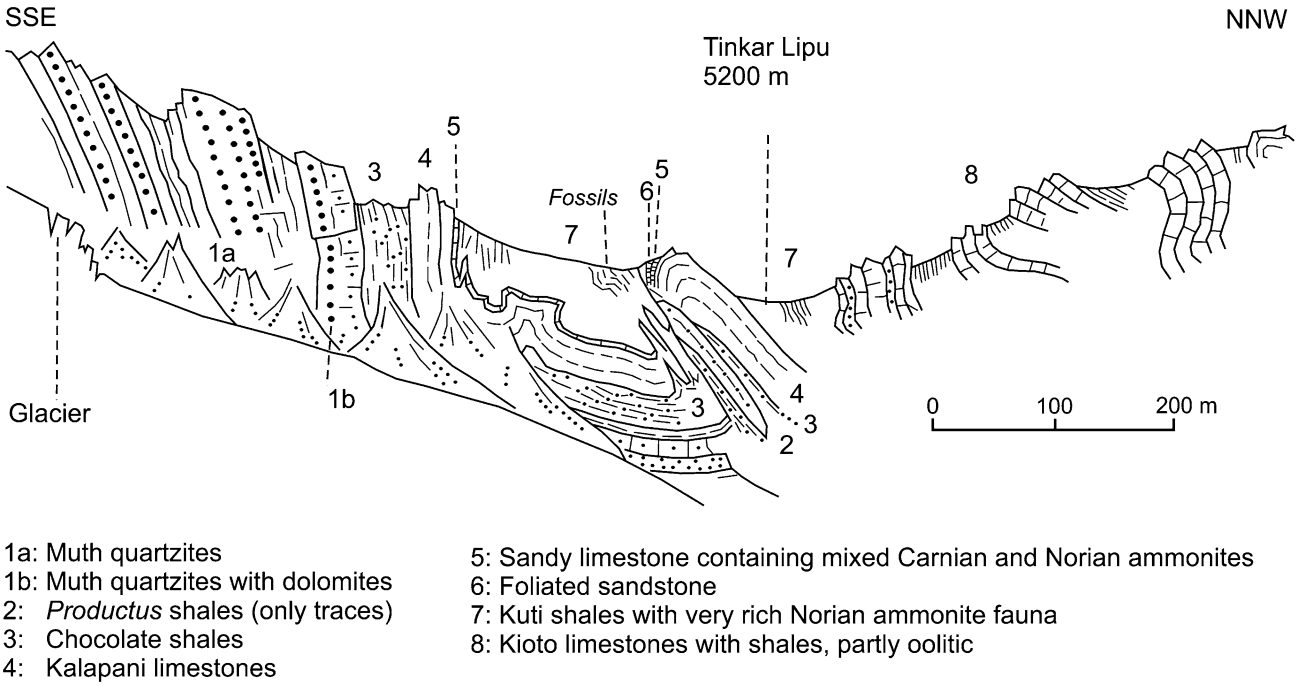

Fig. 22.5 Section across the Tinkar Lipu pass. *Source* Modified from Heim and Gansser (1939)

The black shale also includes some flint nodules. Its lower three meters are rich in brachiopods; especially, there is a 10 cm thick lumachelle horizon, 2 m above the Muth Formation. Except for this horizon, most of the Kuling Formation is of a relatively deep sea deposit. The following late Permian solitary ammonites were found in the formation at the Lebong pass, situated on the headwaters of the Dhauli Ganga River (Heim and Gansser 1939, p. 205).

Cyclolobus oldhami Waagen (*Phylloceras*)
Cyclolobus walkeri Diener

Only at Kalapani, is a lower stratigraphic horizon of the Permian exposed, where it is represented by a platy limestone. Presumably, this limestone is equivalent to the "calcareous sandstone" of the Spiti, where it overlies the basal conglomerate and underlies the black shale (Hayden 1904, p. 52; Heim and Gansser 1939, p. 205).

22.6 Triassic

The Triassic is the most investigated succession in the Himalaya, owing to the similarities with the Alpine fossil-bearing beds. The timeless treatises by Griesbach (1891) and Diener (1912) as well as investigations by von Krafft (In: Hayden 1904) are devoted to the Triassic rocks of Kumaun. Heim and Gansser (1939, p. 206) and Gansser (1964, p. 120) subdivided the Triassic System into the following five formations, respectively, from the bottom upwards (Figs. 22.3, 22.4, 22.5 and 22.6).

22.6.1 Chocolate Formation

This formation was called the Chocolate limestones by Griesbach (1880). It contains brown-weathering shale and limestone. Its contact with the underlying formation is sharp and conformable. Hence, here the marine late Permian is conformably overlain by the marine basal Triassic. Nevertheless, the absence of the lower *Otoceras* horizon may allude to a hiatus (Gansser 1964, p. 119). The Chocolate Formation is from 30 to 50 m thick and subdivided into the following units.

- Streaky or nodular impure ferruginous limestone with shaly beds (3–5 m), rich in imperfectly preserved ammonites of the *Ophiceras* horizon
- Interbedded impure limestone, clayey ironstone, and shale with sporadic and poorly preserved fossils (30–50 m)
- Mainly a shaly bed forming a black wall below the Kalapani Limestone (3–6 m)

From the lower part of the Chocolate Formation at Tinkar Lipu (Unit 3 in Figs. 22.5 and 22.6), Heim and Gansser (1939, p. 110), collected the following fossils, which were identified by Jeannet (1959).

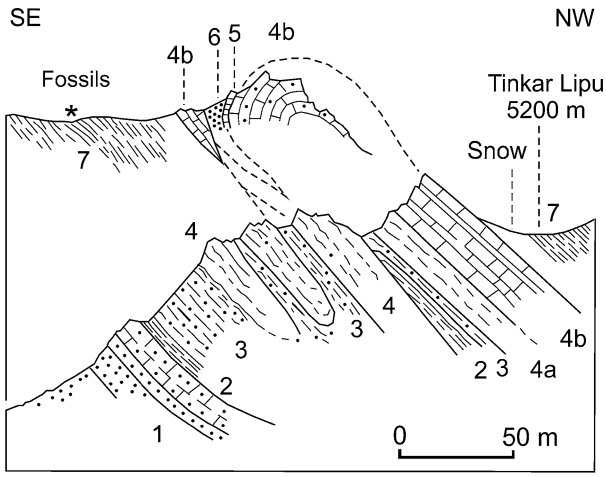

1: A massive dolomite-quartzite of 30–50 m above the Silurian
2: The *Productus* shale (Kuling shale) is not well developed (less than 5 m thick).
3: The Chocolate Formation is 30–40 m thick.
4: The Kalapani Limestone in its lower part (10 m) has yellow to orange rusty patches of weathered ankerite in dense blue limestone with nodular layers and some ammonites. The upper part (20 m) is dark, well-bedded limestone, which contains some brachiopods, corals, and fragments of crinoids. The patchy limestone is piled up four times with three visible thrusts, which dip 40° due N60°W.
5: The top of the Kalapani Limestone is the richest fossiliferous zone. It is a fine, gray, sandy limestone of 1–2 m with full of thick involute and thin sharp-edged ammonites.
6: Foliated gray sandstone with oolitic and sandy calcareous flags of 10–12 m
7: Black shale with calcareous flags, locally rich in deep-sea fauna of Norian age; thickness over 100 m
8: Next higher horizon is a Late Triassic gray oolitic limestone.

Fig. 22.6 Details of the Triassic on the Tinkar Lipu pass (Fig. 22.5). *Source* Modified from Heim and Gansser (1939)

? *Meekoceras* sp. *indet.*
Ophiceras demissum Oppel
Ophiceras cf. *O. demissum* Oppel
Anakashmirites nivalis Diener
? Glyptophiceras kashmiricum Spath
Dictyoconites nepalensis Jeannet

The Chocolate Formation is of Early Triassic (Scythian) age.

22.6.2 Kalapani Limestone

The Kalapani Limestone (Unit 4 in Fig. 22.7) is lithologically rather uniform, but encompasses a relatively wide time span from the Anisian to the Ladinian. The limestone has a varying thickness from 15 to 60 m and is characterized by rusty to orange-colored patches of ankerite, with a dense concentration of ammonites (Figs. 22.3 and 22.4). At Kalapani, this formation contains in its middle part an hematitic layer rich in large involute ammonites, which stick out on a high inaccessible wall. From that wall, Heim and Gansser (1939, p. 102) obtained a leading Anisian ammonite species: *Ptychites* cf. *P. rugifer* Oppel.

From the lower nodular part of the Kalapani Limestone (Unit 4a in Fig. 22.6) of the Tinkar Lipu pass, they reported the following fossils, mainly of Carnian age.

Gymnites cf. *G. sankara* Diener
? Japonites sp. cf. *J. dieneri* Martelli

From the dense, dark blue upper Kalapani Limestone (Unit 4b in Fig. 22.6), the following fossils were recorded, which, most probably, belong to the Early Ladinian ("Daonella limestone").

Traumatocrinus sp.
?Spirigera hunica Diener

22.6.3 *Tropites* Limestone

Succeeding the Kalapani Limestone, there is a few meter-thick limestone bed (Unit d in Fig. 22.4) from which Heim and Gansser (1939, p. 102) recorded *Tropites subbullatus* v. Hauer. From the top 1 m of this famous section, Smith and von Krafft collected numerous species of ammonites and named it the *Tropites* Limestone (Hayden 1904). Later, Diener (1912) identified these fossils and also described 155 ammonite species from the *Tropites* Limestone of Kalapani, Kuti, and surrounding areas. Heim and Gansser (1939, p. 111) also collected a large number of ammonites from the *Tropites* Limestone (Unit 5 in Figs. 22.5 and 22.6) exposed at Tinakar Lipu. Some of the species are the following.

Anatomites cf. *A. brocchi* Mojsisovics
Molengraaffites cf. *M. compressus* Welter
Styrites cf. *S. signatus* Dittm.
Paratibetites adolphi Mojsisovics
Hauerites cf. *H. rarestriatus* Hauer
Sirenites cf. *S. elegans* Mojsisovics
Sirenites cf. *S. alixis* Diener
Cladiscites cf. *C. pusillus* Mojsisovics
Arcestes cf. *A. piae* Diener
Placites sakuntala Mojsisovics
Placites polydactylus Mojsisovics var. *P. oldhami* Mojsisovics
Discophyllites aff. *D. ebneri* Mojsisovics
Proclydonautilus cf. *P. acutilobatus* Diener
Orthoceras sp.
Halobia styriaca Mojsisovics

They include both the Carnian (Arcestidea) and Norian (Paratibetidae) fauna. Von Krafft (In: Diener 1912) and Jeannet (1959) mention a peculiar aspect that Carnian and Norian ammonites are mixed within this horizon with signs

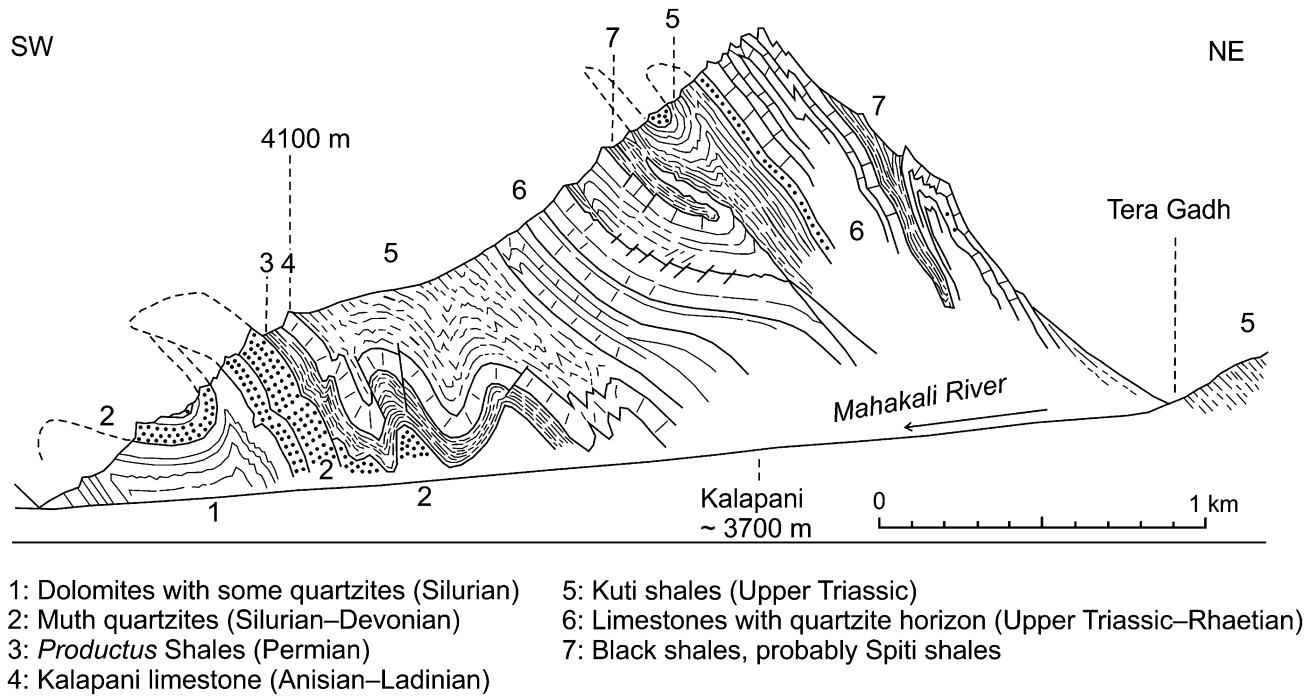

Fig. 22.7 Geological cross-section along the upper Mahakali River. *Source* Modified from Heim and Gansser (1939)

of neither redeposition nor stratigraphic condensation (Gansser 1964, p. 121).

22.6.4 Kuti Shales

The Kuti Shales are well represented by black micaceous varieties and attain a thickness of 300 to 500 m on the Tinkar Lipu pass. Gansser (1964, p. 121) discovered a magnificent ammonite fauna from the black calcareous slabs (Unit 7 in Fig. 22.6), intercalated in shales at Tinkar Lipu. There is a very large list of ammonites described by Jeannet (1958, 1959), and some of them are given below.

Clionites cf. *C. woodwardi* Mojsisovics
Steinmannites lubbocki Mojsisovics (*in*: Diener)
Steinmannites cf. *S. noetlingi* Mojsisovics
Steinmannites tinkari Jeannet
Pseudotibetites tinkari Jeannet
Paratibetites ziegleri Jeannet
Halorites cf. *H. procyon* Mojsisovics
Anatomites cf. *A. brocchi* Mojsisovics
Parajuvavites cf. *P. jacquini* Mojsisovics
Parajuvavites cf. *P. ludolfi* Mojsisovics
Parajuvavites sp. (cf. *P. minor* Mojsisovics)
Metasibirites cf. *M. tietzei* Mojsisovics
Placites sakuntala Mojsisovics

The presence of numerous *Parajuvavites* and *Steinmannites* is attributed to a Norian age for the Kuti Shales.

22.6.5 Kioto Limestone

The Kioto Limestone is one of the consistent formations (Fig. 22.2) between Tinkar Lipu of west Nepal and Spiti in Northwest India. The Kuti Shales transitionally pass upwards through some intervening thin quartzite beds into the Kioto Limestone (Unit 8 in Fig. 22.5). The limestone is usually dark blue and well bedded, and contains conspicuous oolites in its lower part and some ripple marks on the uppermost beds. Its thickness varies from 150 to 200 m at Kuti in the east to 600 m in the west Garhwal, and reaches up to 800 m in Spiti (Hayden 1904, pp. 83–84; Diener 1912; Heim and Gansser 1939, p. 209). Hayden (1904, p. 83) called it the quartzite series, and assigned a Late Triassic (Rhaetian) age for this formation.

22.7 Laptal (or Lapthal) Formation

Heim and Gansser (1939, p. 139) designated the Laptal Formation for the rocks exposed around Lapthal and Kungribingri in Northwest Kumaun. This formation is rather discontinuous, but, based on the description of Hayden (1904, p. 85), extends towards Spiti.

The type sections of this formation are in the Gorge of Chidamu and at Lapthal. In the gorge, about 150 m (at Lapthal, 300 m) below the top of the Kioto Limestone, is a 10 m thick, massive, microcrystalline limestone bed, full of

white spindles or bands, frequently hollow, of up to 20 cm thickness, and 5–40 cm length, irregularly arranged in all directions, called the "horizon of problematics" by Heim and Gansser (1939, p. 139). The "problematics horizon" is like a marker and the succession above it at Chidamu is as follows.

a. Dense, dark gray limestone (120–150 m) with smooth bivalves in the upper part (the Kioto Limestone)
b. 15–20 m of thin-bedded limestone with some bivalves, microbreccia, and oolites (upper part of the Kioto Limestone)
c. A 10 m thick horizon of yellow to reddish spotted dense limestone with layers of lumachelle, some belemnites, and thick shells of pelecypods, sandy top layer
d. 45 m of dense, impure, brown-weathering limestone with nodules and shaly layers
e. 5 m of dark marls with limestone beds
f. 8 m of brown lumachelle with small belemnites and pelecypods
g. About 15 m of well-bedded limestone
h. 5 m of brown limestone with lumachelle, more-or-less sandy, containing belemnites and pelecypods
i. Spiti shales

Heim and Gansser (1939, pp. 139–140) designated the above Units c to h as the Laptal Formation. The Laptal Formation is 60–80 m thick. At Lapthal, it is represented by the following 65 m thick succession.

a. Limestone of brown weathering with layers of fine lumachelle (9 m)
b. Thin-bedded gray limestone (17 m)
c. Brown sandy limestone with lumachelle layers up to 0.5 m thick containing *Mya* and *Gryphaea* (4.5 m)
d. Thin-bedded gray limestone with 1–10 cm thick numerous lumachelle horizons, with small black oysters, *Belemnites*, and *Pecten,* upper part containing 2–10 cm of foliated sandy intercalations (25 m)
e. Mainly brown lumachelle with small belemnites and oysters (8 m)

This formation contains *Ostrea, Arca, Pecten, Lima, Astarte, Trigonia,* and *Belemnites*. Heim and Gansser (1939, p. 209) have tentatively designated an Early Jurassic age to this formation.

22.8 Ferruginous Oolite

This is a thin but important marker bed discovered by Diener (1895, p. 585, 1912, p. 119), on top of the limestone succession. Owing to the abundance of belemnites, it was called the *Sulcatus* beds. Its maximum thickness is 3 m. Its upper and lower contacts are microscopically sharp disconformities (Heim and Gansser 1939, p. 209). This horizon (from bottom to top) is represented by the following succession, exposed to 1 km south of Lapthal (Heim and Gansser 1939, p. 141).

- Laptal limestone of brown weathering, with lumachelle.
- 60 cm of dark dense limestone with shaly beds and small belemnites.
- 185 cm of ferruginous oolite with a sharp lower limit.
- 60 cm of black shale with flat oolite grains; interbedded with layers of dense limestone containing round, gray ferruginous ovoids. In the top layer are belemnites and large ammonites (*Reineckeites*).
- 125 cm of black shales with flat ferruginous ovoid grains.
- 4–6 cm of dense limestone with ferruginous ovoids.
- Spiti shale, black, brittle, with rusty cracks, with very few concretions, more than 35-m thick.

The black shales of the Ferruginous Oolite are hardly discernible from the Spiti Shales, except for microscopic black ferruginous grains. The following ammonites collected from this formation at Lapthal give a Callovian age for this horizon (Heim and Gansser 1939, p. 142).

? Belemnites (*Belemnopsis*) *calloviensis* Oppel
Macrocephalites cf. *M. triangularis* Spath (Early Callovian)
Macrocephalites (*Dolikephalites*) cf. *M. flexuosus* Spath (Early Callovian)
Reineckeites aff. *R. waageni* Till.
Reineckeites douvillei Steinmann
Bonarellia cf. *B. bicostata* Stahl
Rhynchonella and some bivalves

The lower disconformity marks a sedimentation gap between the Early Jurassic and Callovian, whereas the upper one represents a hiatus between the Callovian and Kimmeridgian.

22.9 Spiti Shales

The famous Spiti Shales are generally of black lustrous types and include black ammonite concretions. They reach a thickness of 100 m, but are frequently intensely deformed and may exhibit structural thickening (Gansser 1964, p. 122). Heim and Gansser (1939, p. 144) described the following section of the Spiti Shales from the Kungribingri Pass, where the shale passes into the overlying Giumal Sandstone.

- Upper black Spiti shale with fine-grained calcareous sandstone beds of 2–30 cm each at intervals of 1–3 m
- 30–40 m of rather micaceous and harder shales with layers and lenses of slightly micaceous sandstone of 5–15 cm each
- Gray, fine-grained, sandy, and marly limestone (Lower Flysch of Giumal Formation)
- Greenish, glauconitic Giumal Sandstone

Heim and Gansser (1939, p. 210) collected a large number of fossils from this formation and some of them are the following cephalopods.

Belemnites (*Belemnopsis*) *gerardi* Oppel
Oppelia (*Streblites*) *substriata* Oppel
Hoplites (*Blanfordiceras*) *wallichi* Uhlig

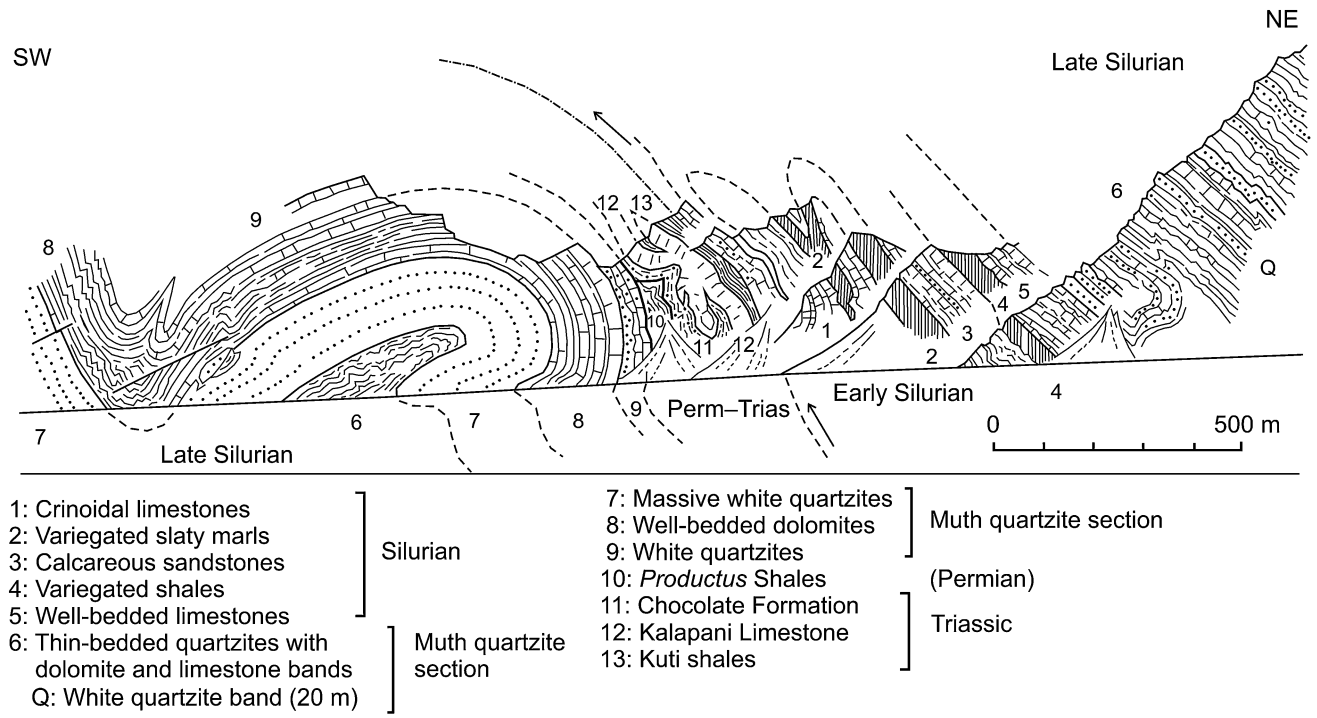

Fig. 22.8 Disharmonic folding and thrusting in the upper Mahakali region. *Source* Modified from Heim and Gansser (1939)

Perisphinctes (*Virgantosphictes*) *kutianus* Uhlig
Haplophylloceras strigile (Blanford) Uhlig

The Spiti Shales range from the Tithonian (Late Jurassic) to Berriasian (Early Cretaceous) in age (Heim and Gansser 1939, p. 210).

22.10 Giumal Sandstone (Lower Flysch)

The Spiti Shales transitionally pass into the Giumal Sandstone. Its basal part is represented by shales with some sandy beds with glauconite (50–150 m), and the upper part contains a green-gray, thick-bedded, massive, lower glauconitic sandstone (80–100 m). It is followed upwards by green, gray, red, and black shales with sandstone intercalations (200 m), and then by the massive, siliceous, greenish gray upper Giumal sandstone (150–250 m) with a shaly band (of about 30 m) in the middle. This formation was called the Lower Flysch by von Krafft (Hayden 1904). The total thickness of the Giumal Sandstone reaches 500–600 m, and is of Early Cretaceous age (Heim and Gansser 1939, pp. 146–147).

22.11 Upper Flysch

The Giumal Sandstone is overlain by red and green shales. But the main part of this formation is made up of black slates with sandstone beds and limestone flags containing fucoids. The succeeding highest and youngest rocks of the Northern Kumaun Himalaya are red siliceous shales and cherts with radiolarian fossils. These rocks are overthrust by the exotic thrust sheet with its basic igneous rocks. The Upper Flysch is more than 1,000 m thick, and is of the Late Cretaceous in age (Heim and Gansser 1939, p. 147).

22.12 Structure

Bordet (1961, p. 210) inferred large-scale north-directed gravity tectonics in the Himalaya, but Gansser (1964, p. 123) denied that. The rocks of this northern sedimentary zone have experienced disharmonic folding and thrusting. Most of the thrusts have developed out of the shale sections, such as those of the Kuling and Kuti. Frequently, the Silurian quartzitic rocks are thrust over the Permian, Triassic, and Spiti shales. The thrusts dip due north, whereas most of the asymmetric folds are south-directed (Figs. 22.5 and 22.7).

A very different structural pattern is observed in the upper reaches of the Mahakali River (Figs. 22.1 and 22.8). In this area, the gray limestone and violet shales of Variegated Silurian (Units 1 and 2 in Fig. 22.8) are followed by a thick succession of folded quartzite of brown weathering. Its upper 400 m thick portion (Units 3–5) is partly made up of regularly bedded dolomite and dolomitic limestone. The last brown-weathering succession is overlain by the Muth Formation, represented by a massive white quartzite (lower part of Unit 6)

of about 150 m in thickness. Then, there follows a crumpled syncline with its disharmonic internal folding. The syncline encloses some alternating beds (each about 150 m thick) of rusty brown-weathering quartzite and dolomite (Unit 6).

One of the most striking structures of this region is the back-folded anticline with its overturned northeast limb. Both the anticline and its complementary syncline to the southwest gently plunge due northwest. The overturned band of white quartzite (Unit 7) is concordantly followed by a thick sequence of well-bedded brown dolomite (Unit 8). Then there occurs another white quartzite band (Unit 9), covered by some compressed dolomite beds of the Muth Formation.

Onwards, there is an intensely deformed but normal succession of the Permian shales (Unit 10) with the Triassic sequence, represented, respectively, by the Chocolate Formation (Unit 11), Kalapani Limestone (Unit 12), and Kuti Shales (Unit 13). This succession is abruptly covered by an overthrust sequence of the older Silurian rocks (Heim and Gansser 1939, p. 101).

References

Bhargava ON (2008) Palaeozoic succession of Indian Plate. Mem Geol Soc India 74:209–244

Bloesch H (ed) (1982) Greek Vases from the Hirschmann Collection. Hans Rohr, Zurich, 105 pp

Bordet P (1961) Recherches Géologiques dans L'Himalaya du Népal, Région du Makalu, Expéditions Françaises a l'Himalaya 1954–1955. Edition du Centre National de la Recherche Scientifique (C. N. R. S.), 275 pp (with geological maps and plates)

Burrard SG, Hayden HH (1908) A sketch of the geography and geology of the Himalaya mountains and Tibet. Government of India Press, Calcutta, 308 pp (with a geological map of the Himalaya in colors, scale 1 inch = 40 miles, and many other maps in colors from various parts of the Himalaya)

Diener C (1895) Ergebnisse einer geologischen expedition in den Central-Himalaya von Johar, Hundes, und Painkhanda. Denkschriften der Kaiserlichen Akademie der Wissenschaften, Wien 62:533–608

Diener C (1912) Trias of the Himalaya. Mem Geol Surv India XXXVI (3):1–159

Gansser A (1964) Geology of the Himalayas. Interscience, New York, 289 pp

Griesbach CL (1880) Palaeontological notes on the lower Trias of the Himalayas. Rec Geol Surv India XIII(2):94–113 and XIV:154–155

Griesbach CL (1891) Geology of the Central Himalayas. Mem Geol Surv India XXIII:1–232 (with 27 plates)

Hayden HH (1904) The geology of Spiti, with parts of Bashahr and Rupshu. Mem Geol Surv India XXXVI(1):1–129 (with 17 plates)

Heim A, Gansser A (1939) Central Himalaya: geological observations of the Swiss expedition 1936. Denkschriften der Schweizerischen Naturforschenden Gesellschaft, Band LXXIII, Abh. 1, 245 pp (with geological maps in colors, sections, and plates)

Jeannet A (1958) La faune Norienne de Tinkar-Lipu (Népal occidental, 5200 m) Céphalopodes. Mémoires de la Société Géologique de France (Nouvelle Série), no. 82, Paris, 50 pp (with 8 plates)

Jeannet A (1959) Ammonites permiennes et faunes triasiques de l'Himalaya central (Expédition suisse Arn. Heim et A. Gansser, 1936). Mem Geol Surv India, Palaeontologica Indica, New Series, XXXIV(1):1–168 (with 21 plates)

Sinha AK (1989) Geology of the higher Central Himalaya. Wiley, Chichester, 219 pp (with a geological map in colors, scale: 1:150,000, a biostratigraphic column, and other plates of maps, sections, and photos)

Tethys Himalaya of Karnali–Bheri Region (Dolpa)

23

... every structure in a rock is significant, none is unimportant, even if, at first sight it may seem irrelevant.

—Ernst Cloos (1946)

Fuchs (1967, 1977) delineated a complexly folded synclinorium, enclosing the Tethyan Himalayan sequence of Dolpa (Figs. 23.1 and 23.2). He also worked out its stratigraphy and recovered many fossils from this remote location (Box 23.1). Waterhouse (1966) described the early Carboniferous and late Permian brachiopods, and Flügel (1964, 1966) identified the Paleozoic corals collected by Fuchs in 1963 from Dolpa. In addition, Siblík (1975) studied the Triassic brachiopods, gathered by Fuchs in 1963 and 1973.

The Tethyan sediments in Dolpa begin with a thick sequence of lime-silicate marbles (Figs. 23.1 and 23.2), frequently injected by leucocratic dikes. The succeeding, presumably Silurian, metamorphic rocks are represented by fossiliferous marls, followed by very thick dolomitic quartzites and siltstones, and dolomites at the top, belonging to the Devonian. Late Devonian fossiliferous limestones appear with a sharp disconformable base. They are further covered by thick dark pelites, deposited in an offshore shelf (Garzanti et al. 1992).

23.1 Dhaulagiri Limestone (?Cambrian–Ordovician)

In east Dolpa, the basal part of the Tethyan zone is represented by the Dhaulagiri Limestone (Fuchs 1967), which rests on crystalline rocks with a gradational contact. The formation is 2,000–4,000 m thick (Fig. 23.3), and metamorphism has altered its basal portion into marbles and calcareous schists (Fuchs 1964). The thick basal succession consists of some thousands of meters of banded, partly arenaceous and argillaceous, and sometimes dolomitic, crystalline limestones and marbles.

During the 1967 expedition, Fuchs and Frank (1970, pp. 49–51) studied the Dhaulagiri Limestone in the south Kanjiroba Range, which lies west of the area mentioned above. In several ways, its lithofacies is different from that in the eastern area (Fig. 23.3). Here the amount of silt is much higher. It is an alternation of fine-grained, gray calcareous sandstone to calcareous siltstone, weathering in a characteristic reddish brown to brick-red color, gray silty limestone, and bluish gray limestone with silver to greenish gray phyllitic to sericitic bands. These rocks alternate rhythmically. Most of the cycles are from 10 cm to a few meters thick, and start with graded and ripple cross-laminated calcareous sandstones that pass upwards to laminated argillaceous limestones. Pure limestones are found only at the top of the cycle. Sporadically, the cyclic units begin with a layer of intraformational breccia. Graded bedding, ripple lamination, load casts, and convolute bedding are frequently observed, and most of the rocks are finely laminated. The Dhaulagiri Limestone of this tract is similar to the Sopyang Formation and the overlying - Chandragiri Limestone of the Phulchauki Group (Chap. 17).

Box 23.1: Contribution from Austria

The far-flung and "mysterious" Trans-Himalayan region of Dolpa (Dolpo) was studied in detail by Gerhard R. Fuchs from the Geological Survey of Austria. Fuchs began investigations in 1963 and completed them in 1973. However, he did not stop at Dolpa, but carried out his research in every part of the Himalaya. His best-known large-scale maps and cross-sections are great assets to the country and the geoscientific community as well. No Himalayan geologist can think without pride and satisfaction of his timeless contributions.

Fuchs investigated east Dolpa as a member of the Austrian Dhaula Himal Expedition 1963 organized by the Austrian Himalayan Society. In 1964 he visited Kashmir, Kulu, Simla, and Kumaun to compare Nepal with these well-known regions of the Northwest Himalaya. Under the Austrian Geological Himalayan Expedition 1967, Fuchs and Frank (1970) investigated west Nepal including a small portion of the Tethyan

M.R. Dhital, *Geology of the Nepal Himalaya*, Regional Geology Reviews,
DOI 10.1007/978-3-319-02496-7_23

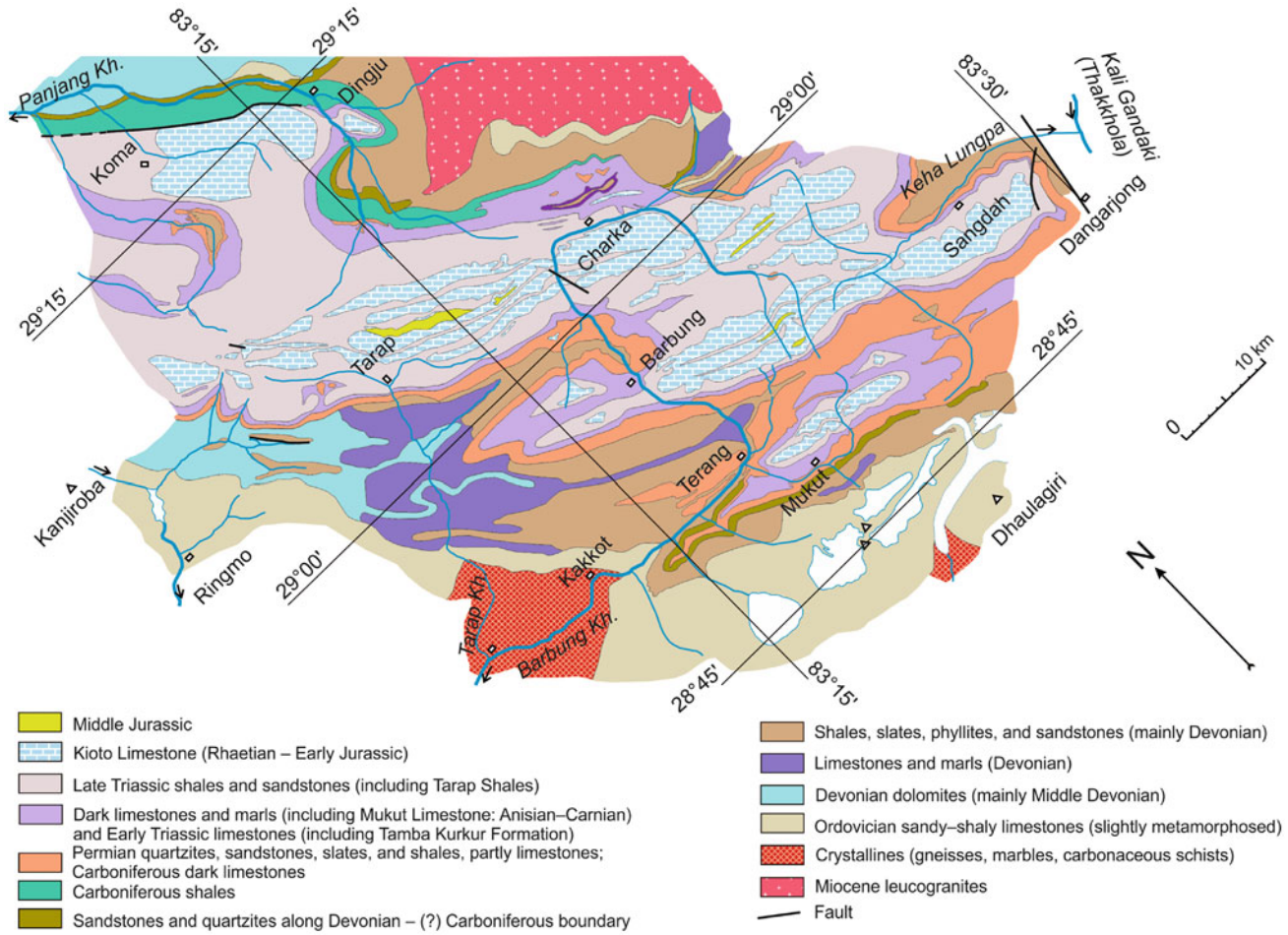

Fig. 23.1 Simplified geological map of east Dolpa. *Source* Modified from Fuchs (1964)

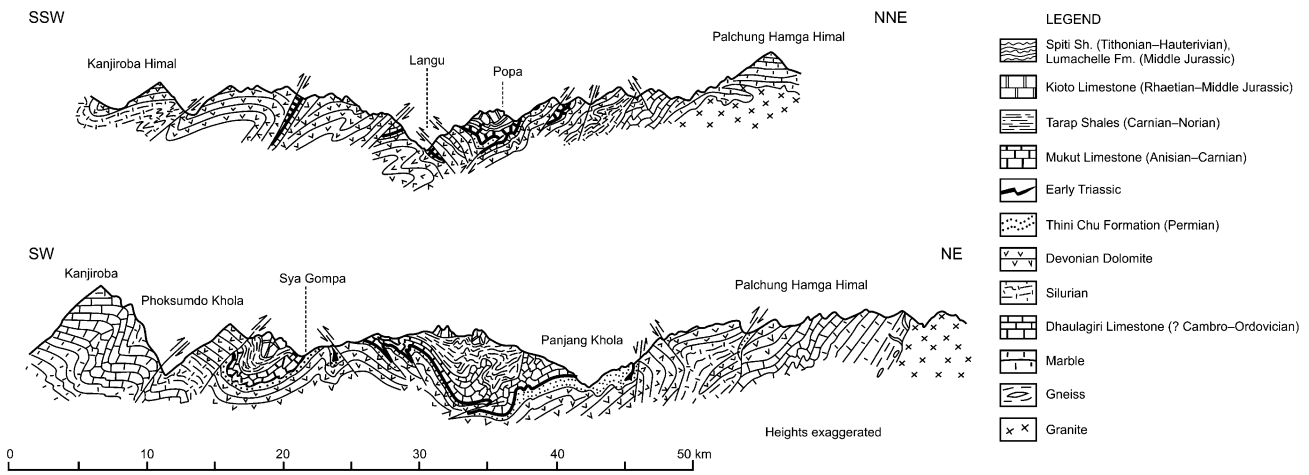

Fig. 23.2 Geological cross-section through the Tethyan succession of west Dolpa. *Source* Modified from Fuchs (1974)

succession. Inasmuch as west Dolpa was still unexplored, one of the main aims of the Austrian Geological Himalayan Expedition 1973, led by Fuchs, was to map it in detail.

As in east Dolpa, the Dhaulagiri Limestone of west Dolpa also passes gradually downwards into the Higher Himalayan crystallines. The carbonates are metamorphosed to calcareous schists and marbles, whereas the argillaceous layers are altered to phyllites (Fuchs 1977).

In the Dhaulagiri Limestone of east Dolpa, Fuchs (1964) discovered brachiopods, crinoids, and bivalves. The fragments of brachiopods included *Dalmanella* (cf. *D. testudinaria* Dalman), *Strophomena*, and *Rafinesquina*. These fossils point to an Ordovician age. Similarly, from west Dolpa, Fuchs (1977) collected poorly preserved lumachelles of orthid brachiopoda, low-spired gastropoda, and crinoids. These fossils are similar to the fossils occurring in the Shiala Formation in the Mahakali Section (Chap. 22) as well as the Nilgiri Limestone in the Thakkhola area (Chap. 24), and they too allude to an Ordovician age.

23.2 Silurian

In the vicinity of Mount Dhaulagiri, there is a conspicuous pale band (50–150 m), comprising light gray dolomitic marls, siltstones, dark limestones, quartzites, and black shales (Fuchs 1967). In the Tarap Khola (Fig. 23.1), the Dhaulagiri Limestone grades into a 300–400 m thick, dark limestone, which is followed upwards by sandstones, psammitic schists, and limestones with crinoids, which are further overlain by black slates (Fuchs 1974).

The graptolite-bearing Dark Band Formation, reported from the Thakkhola area (Chap. 24), is lacking in west Dolpa (Fuchs 1974). Instead, there are either blue limestones and dolomites, or variegated (i.e., purple, pink, cream, green, light gray, and white) calcareous schists and flasery limestones (Fuchs 1977; Fig. 23.3). The limestones are frequently pelletal, intraclastic, or nodular, and contain traces of bryozoans as well as a variety of burrows and hieroglyphs. Sun cracks indicate deposition in shallow water with subaerial exposure. There is a rapid facies change within this unit. For example, the thick variegated limestones, observed in the Sije Khola, are absent in the Khup Khola. In the Phoksundo neighborhood, the red and purple limestones on the northwest are gradually replaced by dark gray to green-gray silty slates to the southeast (Fuchs 1977).

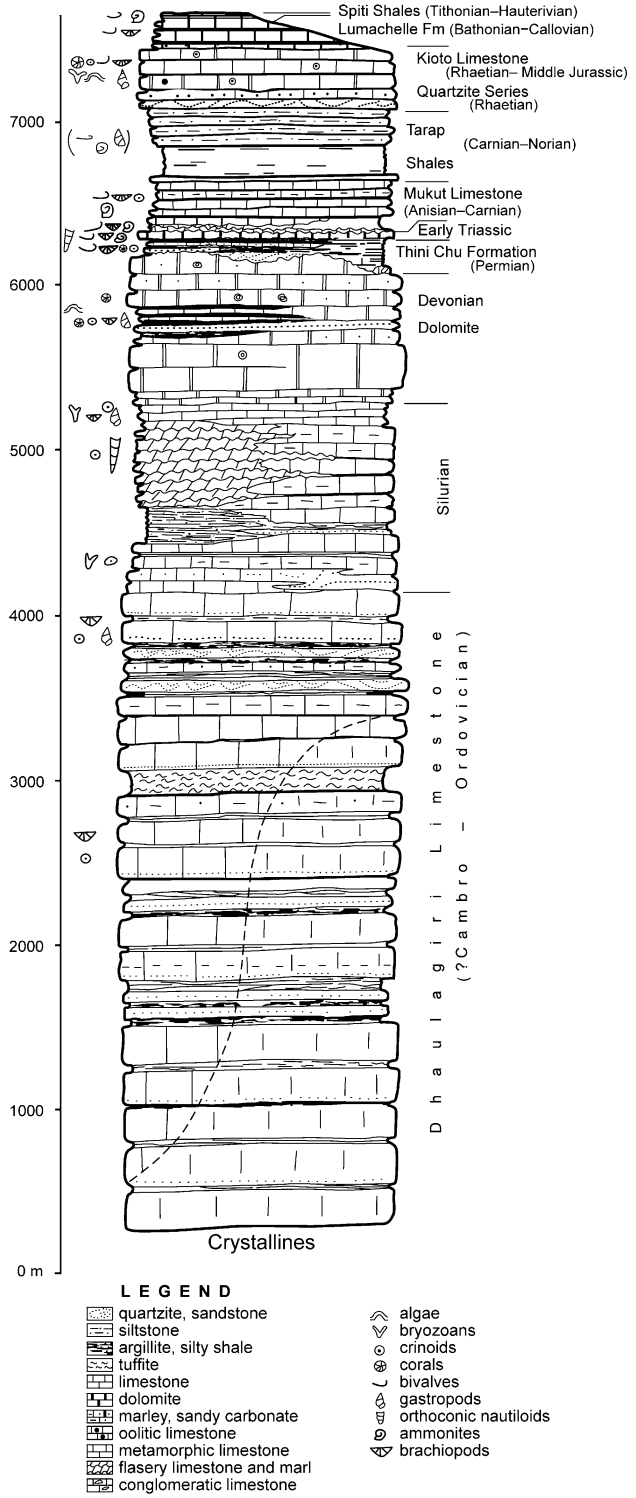

Fig. 23.3 Stratigraphic column of west Dolpa. The *dashed line* shows the varying level of metamorphism in different parts of West Dolpa. The *dotted lines* show the boundary of metamorphism at various locations. *Source* Modified from Fuchs (1974)

Although there is much variation in lithofacies from place to place, blue limestones and dolomites are commonly found at the base and at the top, whereas variegated schistose limestones occur in the central part of the Silurian. However, any of these lithologies may be missing. In the upper Sije Khola, for example, the whole Silurian is represented by just 150–200 m of dark limestones and dolomites, whereas, in other sections, the Silurian is about 1,000 m thick (Fuchs 1977). In Dolpa, the Silurian rocks are rich in crinoids and nautiloids of "*Orthoceras*" type. Because the Dark Band Formation (Early Devonian) is absent in Dolpa, the Siluro–Devonian boundary is lithologically ill-defined (Fuchs 1977, pp. 195–196).

23.3 Muth Formation (Devonian)

West Dolpa is predominantly a dolomite country. Generally, the dolomites are thick-bedded, infrequently massive (Fig. 23.3), and their colors vary from light gray to almost black. The latter varieties give a fetid smell on hammering (Fuchs 1977). The dolomites exhibit conspicuous fine laminae and sporadic grading. In them, oolites, intraclasts, wavy algal mats, and stromatolites are also discerned (Fuchs 1977). There are all gradations from sandy dolomites to calcareous quartzites, and to quartz arenites. Characteristic sedimentary structures include ripple cross-lamination, large-scale cross-bedding, and sun cracks, indicating their shallow water character with occasional subaerial exposure.

As in the Silurian succession, the Devonian rocks also record a considerable facies change, while moving from the east to the west. The Tilicho Pass Formation in the east (i.e., in the Thakkhola area), made up essentially of sandstones and shales, grades laterally westwards into a calcareous and dolomitic formation.

In the vicinity of Lake Ringmo in east Dolpa (Fig. 23.1), there is a succession of gray dolomite (1,000 m) with an intercalation of limestone, shale, and sandstone (Fuchs 1964). Corals of Middle Devonian age (Flügel 1966), bryozoans, brachiopods, and other fossils were recovered from this succession. However, farther east, around the Tarap Khola, occurs a thick series of limestone and marl with only two intercalated bands of dolomite (each about 70 m thick). This calcareous sequence also contains Middle Devonian crinoids, bryozoans, and corals. Farther east, in the Mukut Himal area, a sequence of phyllite, slate, shale, and sandstone appears in place of the limestones and dolomites observed in the west. A bed of gray limestone, intercalated in sandy shale of this unit, yielded ammonites of Late to Middle Devonian age (Fuchs 1964).

Flügel (1966) identified the following Middle Devonian corals from the specimens collected by Fuchs in 1963 from a fossiliferous zone in east Dolpa.

Cyathophyllum (*C.*) *dianthus* (Goldfuss)
Acanthophyllum (*Neostringophyllum*) aff. *A. concavum* (Walter)
Acanthophyllum ? (*Neostringophyllum*) sp.
Stringophyllum (*Stringophyllum*) *isactis* (Frech)
Stringophyllum (*Sociophyllum*) *longiseptatum* ? (Bulvanker)
Favosites goldfussi goldfussi d'Orbigni
Favosites grandis nepalensis Flügel
Pachyfavosites exilis ? Sokolov

Flügel and Tintori (1993) reported Late Devonian (Frasnian) corals from central Dolpa. They described the following species of Rogusa and Tabulata.

Kuanxiastraea pengellyi (Milne-Edwards & Haime)
Scruttonia bowerbanki (Milne-Edwards & Haime)
Scruttonia rota Flügel & Tintori
Sinodisphyllum litvinovitshae (Soshkina)
Fruehwirthia heritschi Flügel & Tintori
Tabulophyllum (?) *implicatum* Tsien
Thamnopora cf. *T. urensis* Dubatolov
Alveolitella cf. *A. rarispinosa* Nowinski

The calcarenitic beds, yielding the fossils, are overlain by a prominent oolitic ironstone bed with thick ferruginous nodules and crusts.

In west Dolpa, Fuchs (1977) collected various fossils from the south limb of the Dolpa Synclinorium, about 300 m below the 800–1,200 m thick Muth Formation ridge. The fossiliferous zone is 150–200 m thick, and it occupies almost the middle portion of the Muth Formation. In fact, this zone is a continuation of the above fossiliferous zone in east Dolpa. The following fossils were identified by Flügel (Fuchs 1977).

Stringophyllum (*Sociophyllum*) *longiseptatum* (Bulv.)
Alveolites cf. *A. parvus* (Lec.)
Thamnopora sp.
Favosites robustum Lec. (?)
Stachyodes (?)
Hexagonaria sp.
Stromatopore

On the other hand, Plodowski (Fuchs 1977) identified the following brachiopods from the same horizon, which gave a Givetian (late Middle Devonian) age.

Indospirifer padaukpinensis (Reed)
Indospirifer sp.
Crurithyris inflata (Schnur)
Emanuella cf. *E. takwanensis* (Kayser)
Stringocephalus sp.
Schiziphoria sp.
Camerophorina sp.

Schnurella cf. *S. schnuri* (Verneuil)
Athyris sp. 1
Athyris sp. 2
Spinatrypa sp.
Productell sp.
Bornhardtina sp.

In west Dolpa, the Muth Formation, constituting the north limb of the Dolpa Synclinorium, is generally barren of determinable fossils. However, a coral sample yielded *Cyathopoedium* sp. (Fuchs 1977).

Flügel and Tintori (1993) noted that the Middle–Late Devonian rocks in Nepal show a wide range of sedimentary environments. From east to west, the following three major areas can be differentiated: the Manang–Thakkhola–East Dolpa subsiding terrigenous basin, the west Dolpa and Kumaun dolomitic platform, and, the Spiti–Zanskar Synclinorium, with sediments accumulated in quartz arenitic beaches.

23.4 Tilicho (or Ice) Lake Formation (Carboniferous)

In east Dolpa, the Tilicho Lake Formation is represented by 50–250 m of dark bituminous, sometimes marly or shaly, limestones (Fuchs 1964). These deposits enclose a remarkably varied and profuse fauna, represented by crinoid stems, bryozoans (fenestellids, etc.), and corals. There are also brachiopods, bivalves, gastropods, and sporadic cephalopods. Near Tarap, the limestone is only 6 m thick. This faunal assemblage indicates an early Carboniferous age (Fuchs 1964). It can be homotaxial with the well-studied Siringothyris Limestone of Kashmir or the Lipak Formation of Spiti, in the Northwest Himalaya (Fuchs 1967). This formation pinches out towards the northwest, and is missing in the western part of the Dolpa Synclinorium (Fuchs 1967, 1974). The specimens collected by Fuchs in 1963 from east Dolpa yielded the following early Carboniferous coral fossils (Flügel 1966).
Siphonophyllia cf. *S. spumosoformis* (Anikina)
Caninophyllum cf. *C. subibicina subibicina* (Mc Coy)
Caninophyllum sp.
Amplexus sp.
Michelina megastoma (Phillips)
Aulopora sp.

Flügel (1966) also determined the following two coral fossils from the samples belonging to the Permo-Carboniferous boundary zone.
Polycoelia (*Polycoelia*) aff. *P. profunda* (Geinitz)
Plerophyllum (*Ufimia*) sp.

Waterhouse (1966) recognized the following eight brachiopods from the east Dolpa samples collected by Fuchs in 1963.
Rhipidomella sp.
Orthotetid gen. and sp. indet.
? Eomarginifera sp.
Linoproductus pollex Waterhouse
Fusella mucronata Waterhouse
Eomartiniopsis cf. *E. helenae* Sokolśkaja
Syringothyris curzoni (Diener) *glaber* subsp.
Punctospirifer sp.

The presumable early Carboniferous is marked by a few-meter-thick shallow marine "fenestellid-rich limestones." The last event is attributed to the onset of continental rifting, and the process continued until the mid-Permian. With a conspicuous unconformity, the Thini Chu Formation, represented by siliciclastics, rests over the Tilicho Lake Formation (Garzanti et al. 1992).

23.5 Thini Chu Formation (Permian)

In east Dolpa, the Thini Chu Formation comprises a series of thick-bedded, light gray quartzites and sandstones with intercalated dark slates and shales. Its total thickness varies from 80 to 300 m (Fuchs 1964). This formation is rich in brachiopods, crinoids, and bryozoans. Its upper 20–50 m is made up of sandy shales, which yielded big brachiopods, crinoids, and tetrapod footprints (Fuchs 1964). In east Dolpa, the Permian is succeeded by the Early Triassic sequence with a slight hiatus, as indicated by an approximately 10 cm thick lateritic layer in between (Fuchs 1977, p. 203).

In west Dolpa, the Thini Chu Formation is generally 30–70 m thick, and becomes about 100–120-m thick in the area east of Phopha (Fuchs 1977). Here, this formation consists of white, gray, green, and rather dark quartzites, and conglomerates with clasts ranging in size from 2 to 5 cm (maximum diameter, up to 25 cm). The conglomerate clasts are made up of quartz, quartzites, and cherts, glauconitic sandstones, calcareous sandstones, calcareous quartzites, blue-gray to black sandy limestones, and gray-green to black silty or sandy shales and siltstones (Fuchs 1977). Here also, the Thini Chu Formation is preponderantly fossiliferous, and contains corals, bryozoans, brachiopods, pelecypods, gastropods, trilobites, and crinoids (Fuchs 1974).

Everywhere in west Dolpa, the Permian Thini Chu Formation transgresses over the Devonian Muth Formation. The basal beds of the Thini Chu Formation disconformably overlie the dolomites of the Muth Formation with a distinct erosional contact marked by a basal conglomerate bed (Fuchs 1977).

Flügel (1966) determined the following late Permian corals from the fossil specimens collected by Fuchs in 1963 from east Dolpa.
Wannerophyllum sp.
Plerophyllum (*Plerophyllum*) *schindewolfi* Flügel
Plerophyllum (*Plerophyllum*) sp.
Gertholites curvatus (Waagen & Wentzel)

Waterhouse (1966) identified the following 20 late Permian brachiopods from the samples collected by Fuchs (1964).

Orthotetes bisulcatus Waterhouse
? Neochonetes sp.
Multispinula indica (Waagen)
Krotovia opuntia (Waagen)
Marginifera sp.
Anidanthus fusiformis Waterhouse
Waagenoconcha purdoni (Davidson)
Costiferina alata Waterhouse
Dictyoclostid sp. indet.
Linoproductus lineatus ? (Waagen)
Neospirifer moosakhailensis (Davidson)
Neospirifer ravana (Diener)
Fusispirifer nitiensis (Diener)
Spiriferella rajah (Salter)
Spiriferella tibetana (Diener)
Martiniopsis sp.
Syringothyris lydekkeri ? (Diener)
Punctospirifer sp.
Cleiothyridina subexpansa (Waagen)
? Hoskingia latouchei (Diener)

Waterhouse (1977, 1978) carried out a detailed investigation of Permian rocks together with their fossils from west Dolpa. He proposed the Namlang Group for Permian sediments and the Langu Group (Devonian) for the underlying laminated shales and limestones of the Dolpa region (Table 23.1).

The Nangung Formation unconformably overlies the Devonian carbonates and dolomites of the Langu Group (Waterhouse 1978, p. 8). The Nangung Formation contains red or pale quartzites, and green or dark gray shales. Siltstones and silty mudstones may alternate with thin cross-rippled quartzites. This formation contains *Lamnimargus himalayensis* (Diener), *Costiferina alatus* Waterhouse, and *Spiriferina rajah* (Salter).

The Senja Formation begins with the Popa Quartzite Member consisting of clean, white, fine- to medium-grained quartzites as well as some of their coarser varieties, alternating with sandstones and shales. The shales contain *Pyramus*, *Neospirifer*, and *Spiriferella* (Waterhouse 1978, p. 12). The following Pija Shale–Siltstone Member incorporates dark shales and siltstones, and yielded *Krotovia arcuata* Waterhouse and *Terrakea* cf. *T. multispinosa* Dear (Waterhouse 1978, p. 14). The overlying Nisal Member is made up of calcareous massive sandstones, standing out as prominent red-colored scarps between the dark shaly or silty Popa and Nambo members. There are numerous shelly horizons. This member contains many brachiopods, such as *Marginalosia kalikotei* (Waterhouse), *Megasteges nepalensis* Waterhouse, *Platyconcha grandis* Waterhouse, *Spiriferella rajah* (Salter), *and Neospirifer ravaniformis* Waterhouse (Waterhouse 1978, p. 16). The succeeding Namdo Siltstone Member consists chiefly of *Cancrinella papilionata* Waterhouse (Waterhouse 1978, p. 17), and it is followed by the Luri Sandstone Member, comprising coarse sandstone and calcareous sandstone with shells of brachiopods so numerous that *Spiriferella,* in particular, makes a significant proportion of the bed. There are *Spiriferella rajah* (Salter) and *Spiriferella oblata* Waterhouse, together with *Marginalosia kalikotei* (Waterhouse), *Megasteges nepalensis* Waterhouse, and *Neospirifer ravaniformis* Waterhouse (Waterhouse 1978, p. 17). The Kuwa Siltstone Member overlies the latter member, and it consists chiefly of dark siltstone and mudstone, with a high carbon content. In this unit, fossils are rare and include the bivalve *Atomodenma* at the type section (Waterhouse 1978, p. 18).

However, Fuchs (1977), and Garzanti et al. (1992) disagree with the lithostratigraphic subdivisions of Waterhouse. They state that it is not possible to trace these subdivisions in the field, and propose to retain the name Thini Chu Formation for this unit.

The middle to late Permian, mainly terrigenous, Thini Chu Formation was deposited in four distinct episodes separated by disconformities. They were "white quartzites," "Costiferina arenites," "Ocher pelites," and "Estuarine Quartzites," respectively, from the bottom upwards. As in other parts of the Tethys Himalaya, the Neo-Tethyan spreading began at the base of the late Permian Kuling Formation (Fig. 23.4), made up of conglomeratic quartzite, ocher-weathering bioclastic marls, and black pelites (Garzanti et al. 1992, p. 294).

Table 23.1 Lithostratigraphic subdivisions of the Namlang group in west Dolpa

Group	Formation	Member	Predominant lithology
Namlang	Senja	Kuwa	Dark shale, siltstone
		Luri	*Spiriferella* sandstone
		Nambdo	Dark shale, siltstone
		Nisal	Red calcareous sandstone
		Pija	Dark siltstone
		Popa	Quartzite
	Nangung		*Lamnimargus himalayensis* shale, quartzites

Source Waterhouse (1978)

23.6 Tamba Kurkur Formation (Early Triassic)

The Early Triassics of Dolpa make a very good marker horizon, characterized by a 15–30 m thick, resistant band, exhibiting yellow-brown and ocher weathering colors, conspicuous from afar (Fuchs 1974, 1977). It consists of thin-bedded, dense, partly flasery, and frequently nodular, light gray to brown limestones, interbedded with rather subordinate shales, appearing mainly in the central part (Fuchs 1977).

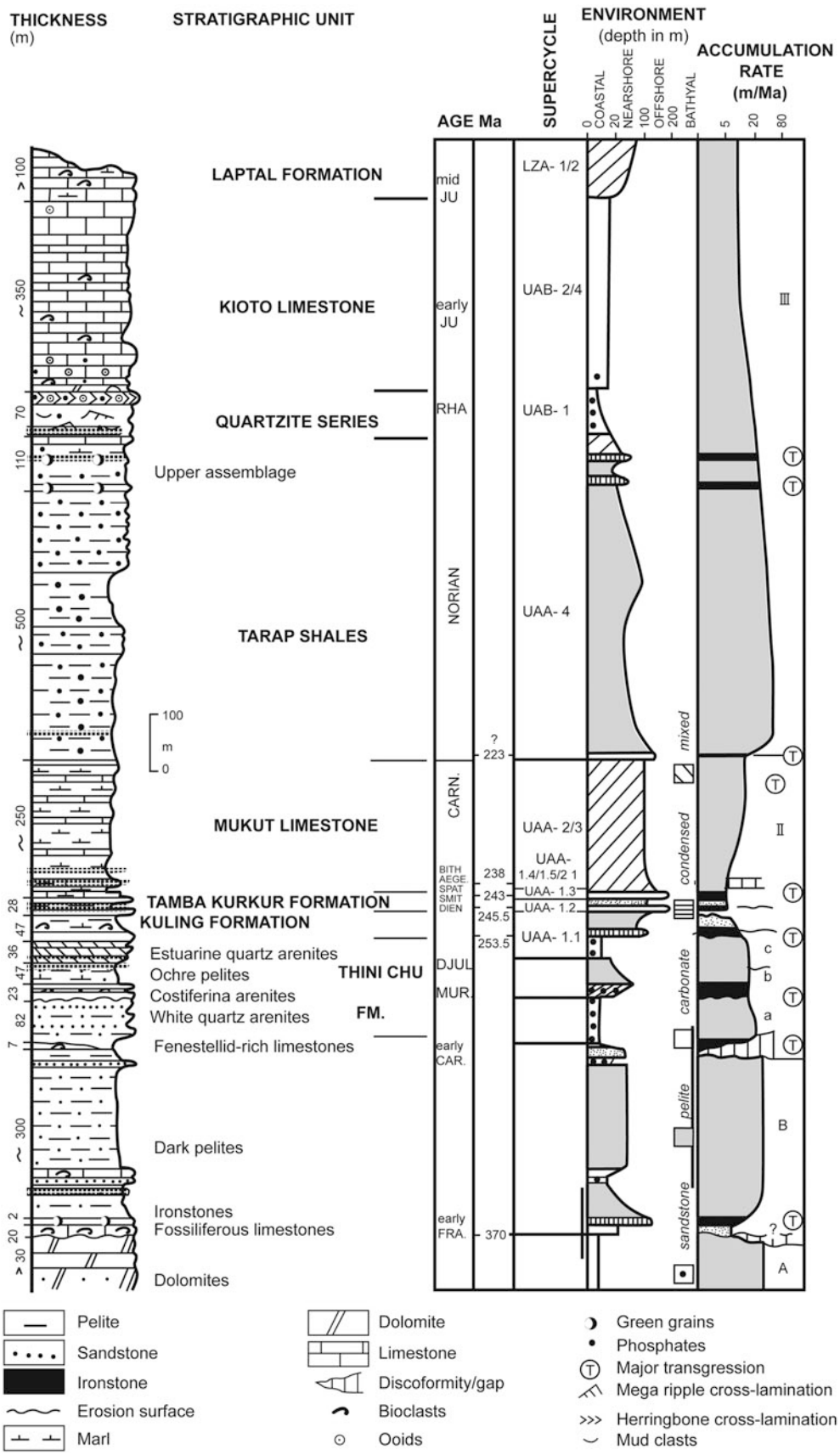

Fig. 23.4 Stratigraphic succession of central Dolpa depicting the depositional environment and sediment accumulation rates. *Source* Modified from Garzanti et al. (1992)

In east Dolpa, the Early Triassic rocks begin with a basal bed of dark limestone (1.5–2.5 m), characterized by ferruginous weathering. Its lowermost part (0–0.8 m above base) is still Permian, as indicated by a rich late Permian fauna, observed in the thin layers of dark limestones, interbedded with sandy shales in the upper Barbung Khola. This fossiliferous zone is separated from the Triassic ammonites by about 1 m of limestone devoid of fossils (Fuchs 1974). In the north, this basal bed is rich in Fe and Mn minerals, exhibiting violet to brown tints (Fuchs 1967). From east Dolpa, Fuchs (1967, p. 173) discovered the following fossils.

Ophiceras serpentinum Diener
Ophiceras sp.
Ophiceras chamunda Diener
Xenodiscus sp.
Meekoceras cf. *M. varaha* Diener
Pseudomonotis aff. *P. painkhandana* Bittner
Meekoceras sp.
Pseudomonotis sp.
Eumorphotis (*? aurita*)
Myophoria sp.

In west Dolpa, the basal part of this marker horizon contains phosphorite concretions of up to 3 cm in diameter. The basal bed is also rich in bivalves and ammonites. Kummel identified the following ammonites collected by Fuchs from the lower 10 cm of the basal bed (Fuchs 1977).

Otoceras woodwardi Griesbach
Ophiceras sp. indet.

Kummel also determined the following ammonites collected by Fuchs from 50 cm above the base (Fuchs 1977).

Otoceras sp.
? Ophiceras sp. indet.

From the lower central portion of the Tamba Kurkur Formation (4–5 m above the base), Kummel recognized the following organic remains (Fuchs 1977).

Pseudosageceras multilobatum Noetling
Prionolobus sp. indet.
Orthoceras sp. indet.
Gyronites sp. indet.
Proptychites sp. indet.

On the other hand, Waterhouse (1977) reported the following Permian fossils from the basal part.

Otoceras concavum
Claraia bioni (Nakazawa)
Glyptophiceras (= *Xenaspis* of Diener).

23.7 Mukut Limestone (Anisian–Carnian)

Except in the region of Phopha, where the lower 30–100 m of the Mukut Limestone (Fuchs 1967) is represented by dark gray to black, bleaching, laminated shales with silty layers, this formation succeeds the nodular Anisian Limestone in many other places (Fuchs 1977). The Mukut Limestone has a total thickness of 100–300 m, and it is composed of well-bedded, dark blue varieties (weathering in ocher colors), sparingly interbedded with dark marls and almost black shales. Some of the limestones are thinly laminated, display nodular structures, and are sporadically bioturbated. Anisian, Ladinian, and Carnian ammonites are frequently scattered in this formation. Also, brachiopods, bivalves, and crinoids preponderate (Table 23.2). Siblík (1975) identified the following brachiopods from Fuchs' 1963 and 1973 collections.

Koeveskallina koeveskalyensis spitiensis (Stoliczka)
Spirigerellina stoliczkai (Bittner)
? *Pexidella* aff. *P. hunica* (Bittner)
Austriellula fuchsi Siblík
Spiriferina cf. *S. stracheyi* (Salter)
"*Rhynchonella*" cf. *R. mutabilis* Stoliczka
Dielasma (?) cf. *D. julikum* (Bittner)
"*Spiriferina*" aff. S. *orophila* (Diener)

Table 23.2 Fossils from Dolpa

Fossil	Age
Daonella lommeli (Wissmann)	Late Ladinian
Daonella indica Britner	
Joannites cf. *J. cymbiformis* (Wulfen)	Early Carnian
Projuvavites sp.	
Arcestes sp.	latest Carnian
nautiloid indet.	
Halobia cf. *H. austriaca* Mojsisovics	earliest Norian
Joannites cymbiformis (Wulfen)	Early Carnian
Joannites sp.	
Tropites cf. *T. acutangulus* Mojsisovics	Late Carnian
Tropites torquillus Mojsisovics	
Anatropites nihalensis Diener	Just below the Carnian–Norian boundary
Euisculites bittneri (Gemmellaro)	
Gonionotites vincentii Gemmellaro	
Projuvavites sp.	
? *Griesbachites* sp.	
? *Anasirenites* sp.	
Arcestes geyeri Diener	
Arcestes schafferi Diener	
Sturia sansovinii (Mojsisovics)	Late Anisian–Ladinian
Monophyllites sp.	
Daonella sp. indet.	
Gymnites sp. indet.	Middle (–Late) Anisian
Ptychites cf. *P. rugifer* (Oppel)	Middle Anisian
Paratrachyceras cf. *P. regoledanum* (Mojsisovics)	latest Anisian
Daonella esinensis Salomon	Anisian–Ladinian boundary

Source Fuchs (1977)

As in the Early Triassic sequence, there are also facies differences in the Mukut Limestone. North of Charka and in the Kahajong Khola, the lowest 30–80 m of the formation are nearly free of lime and contain soft dark shales.

In west Dolpa, there is a 2–5 m thick conspicuous horizon of blue-gray nodular limestone, interbedded with dark gray or green argillite at the highest part of the Early Triassic succession. This horizon is characterized by ferruginous weathering, and forms the top portion of the resistant Early Triassic beds, displaying light brown weathered colors (Fuchs 1977). It contains the following brachiopods (Siblík 1975).

Dielasma himalayanum Bittner
Speriferina stracheyi (Salter)
Speriferina cf. *S. stracheyi* (Salter)
Koeveskallina koeveskalyensis spitiensis (Stoliczka)
Spirigerellina stoliczkai (Bittner)

Krystyn and Gruber (Fuchs 1977) identified the following ammonites and bivalves.

Ptychites rugifer (Oppel)
Buddhaites rama Diener
Nicomedites osmani Toula
Ptychites cf. *P. oppeli* (Mojsisovics)
Trematoceras sp. indet.
Ptychytes sp. indet.

23.8 Tarap Shales (Carnian–Norian)

In east Dolpa, the Tarap Shales (Fig. 23.1) have a somewhat gradational contact with the underlying Mukut Limestone, where the carbonate facies changes into a flyschoid facies of gray, green, brown shaly siltstones, sandstones, and dark shales with black concretions (Fuchs 1967, 1977). In them, graded bedding, flute casts, and load casts are present.

In west Dolpa, the lower boundary of this formation is marked by a 3–5 m (infrequently up to 10 m) thick bed of green, gray, impure, micaceous, quartzose sandstone, exhibiting ferruginous weathering (Fuchs 1977). This horizon is succeeded upwards by 150–200 m thick, dark gray to green silty shales and shaly siltstones. The upper portion of the Tarap Shales is represented by a 150–200 m thick interbedding of thick-bedded clayey siltstone, siltstone, and sandstone. In them, various hieroglyphs, tool marks, load casts, and flute casts are common. The Tarap shales are about 400 m thick, however, in some locations their thickness is reduced to 30 m (Fuchs 1977).

The Tarap Shales are rather poor in organic relics. Krystyn identified *Tibetites* cf. *T. ryalli* Mojsisovics from the ammonite collection of Fuchs (1977).

23.9 Quartzite Series (Rhaetian)

The soft, somber-colored shales of Tarap are overlain by a thick-bedded alternation of light quartzite, sandstone, calcareous quartzite, and siliceous limestone, grading into the overlying Kioto Limestone, without any discernible break (Fuchs 1967). The upper part of the Tarap Shales marks an increase in sand content, and this dark sequence is capped by the conspicuous Quartzite Series. The Quartzite Series (Hayden 1904; Diener 1912) comprises a thick-bedded alternation (about 50 m) of green, white, gray, and brown, thick-bedded quartzites, calcareous quartzites, sandy dolomites, and blue-gray limestones, marls, and gray-green shales (Fuchs 1977). The frequent occurrence of oolites and cross-laminae indicate a shallow water environment (Fuchs 1974).

23.10 Kioto Limestone (Rhaetian–Middle Jurassic)

The Kioto Limestone continues throughout the Tethyan zone, except for the presence of violet, orange, yellow, and green marls and shales towards the top of the Quartzite Series, near Mukut and in the Hidden Valley of northwest Nepal (Fuchs 1974). In east Dolpa, The Kioto Limestone forms many lofty peaks and crests. In west Dolpa, it is from 150 to 350 m thick, and comprises thick-bedded, light to dark gray, blue limestones and dolomites, interstratified with sporadic arenaceous beds (Fuchs 1977). Remains of algae, corals, bryozoans, brachiopods, pelecypods, gastropods, and crinoids are found in various layers, where Megalodon–Lithiotis shell beds are conspicuous (Fuchs 1977).

23.11 Lumachelle Formation (Bathonian–Callovian)

In east Dolpa, the Kioto Limestone transitionally passes upwards into a thin-bedded sequence of gray to dark blue lumachelle limestones (partly weathering into ocher colors), marls, dark shales, and a few layers of light gray calcareous sandstones. Bivalves and brachiopods preponderate and form shell beds (Fuchs 1974). Based on fossil findings, its age is Bathonian–Callovian (Fuchs 1967, 1977). In west Dolpa, it is found only in the core of a syncline south of Sya Gompa, where it is about 150 m thick (Fuchs 1974).

23.12 Spiti Shales (Tithonian–Early Cretaceous)

The Spiti Shales are also confined to the core of the above-mentioned syncline of west Dolpa, where they are represented by an approximately 50 m thick sequence of thin-bedded, black shales with concretions (Fuchs 1977).

In the Mesozoic Era, rapid subsidence after break-up is recorded by the deposition of the condensed carbonate horizons of the Tamba Kurkur Formation. Silty marls become common in the Middle–Late Triassic Mukut Limestone. Its deposition was followed by a short transgression at the base of the Tarap Shale, and then there was a thick accumulation of pelites in the Early Norian. In the upper part of the Tarap Shale ("upper assemblage"), there was another important transgression. The dolomitic or oolitic quartzites (Quartzite Series) cover the Late Triassic succession. They were deposited in a tide-dominated environment. The overlying Jurassic Kioto Limestone and Laptal Formation were accumulated in shallow marine, carbonate to mixed carbonate–siliciclastic subtidal environments (Garzanti et al. 1992; Fig. 23.4).

23.13 Structure of Dolpa

The sedimentary succession of Dolpa is connected with the underlying crystallines. They form one structural unit and are not separated by any tectonic line (Fuchs 1977, p. 211). On the other hand, the pile of Tethyan sediments exhibits the tectonic style, quite different from that of the crystallines (Fig. 23.2). The crystallines underwent northeast–southwest directed strong deformation under metamorphic conditions, whereas the non- to slightly metamorphosed Paleozoic and Mesozoic rocks exhibit open folds with the direction of movement essentially towards the central axis of the Dolpa Synclinorium (Fuchs 1977).

In east Dolpa, the 5,000–7,000 m thick sedimentary succession is folded into WNW–ESE trending open anticlines and synclines (Fig. 23.2). On the north face of the Dhaulagiri, a large north-vergent anticline is observed. Around Mukut, there is a syncline overturned to the north. To the north of Terang, the Barbung Khola crosses a north-vergent anticline, which continues to the east up to Thakkhola. The region south of the village of Barbung is made up of thick Mesozoic sediments, constituting a syncline, which also continues to the east, where it is cut off by the Dangarjong Fault. To the north of Barbung, a complex anticline exposes the Paleozoic rocks. The Charka–Tarap area is built up of thick Mesozoic sediments, belonging to a syncline of large extension. Some kilometers north of Charka, there is an anticline with Paleozoic rocks in the core. The Kioto Limestone southeast of Koma forms the core of a syncline, which ends towards the southeast. The Mustang granite rich in tourmaline is found in the mountains near the Tibetan border. There are also a number of faults, especially in the core of the syncline, within the Kioto Limestone (Fuchs 1964, 1967).

In west Dolpa, there is essentially a complex synclinorium compressed from the northeast and southwest. The Devonian carbonates of west Dolpa are rather resistant rocks, and hence influence the deformation style of the region (Fig. 23.2). Like a fractured bone, the dolomites push into the soft Triassic formations along reversed faults and small-scale thrusts (Fuchs 1974, p. 30). There are mainly two synclines in northwest Dolpa. The syncline south of Sya Gompa is the continuation of the Charak–Tarap Syncline described above. It closes about 15 km WNW of Sya Gompa. On the other hand, the Phopha (or Popa) Syncline joins up with the Koma Syncline of east Dolpa and continues farther northwest. To the east of the Langu–Mugu confluence, this syncline as well as the Dolpa Synclinorium ends.

References

Cloos E (1946) Lineation, a critical review and annotated bibliography. Geol Soc Am Mem 18:122

Diener C (1912) Trias of the Himalaya. Mem Geol Surv India XXXVI (Part 3):1–159

Flügel H (1964) Korallenfaunen aus dem Paläozoicum West-Nepals, Verhandlungen der Geologischen Bundesanstalt, Wien, Hefte 1–3, pp 15–16

Flügel H (1966) Paläozoische Korallen aus der Tibetischen Zone von Dolpo (Nepal), Jahrbuch der Geologischen Bundesanstalt, Wien, Sonderband 12, pp 101–120 (with 4 plates)

Flügel HW, Tintori A (1993) Late Devonian (Frasnian) corals from central Dolpo, Nepal. Rivista Italiana di Paleontologia e Stratigrafia, Milano, vol 99, No 1, pp 3–25 (with 4 plates)

Fuchs GR (1964) Beitrag zur Kenntnis des Paläozoikums und Mesozoikums der Tibetischen Zone in Dolpo (Nepal–Himalaja) (auch in Englisch). Verhandlungen der Geologischen Bundesanstalt, Wien, Hefte 1–3, pp 6–15 (with a map)

Fuchs G (1967) Zum Bau des Himalaya. Österreichische Academie der Wissenschaften, Mathematisch-Naturwissenschaftliche Klasse, Wien, Denkschriften, 113 Band, pp 1–211 (with 30 plates including 9 large sheets and one geological map in colors)

Fuchs G (1974) On the geology of the Karnali and Dolpo regions, West Nepal. Mitteilungen der Geologischen Gesellschaft in Wien, Wien, 66–67 Band, 1973–1974, pp 21–32 (with 3 plates)

Fuchs G (1977) The geology of the Karnali and Dolpo regions, Western Nepal. Jahrbuch der Geologischen Bundesanstalt, Wien, Band 120, Heft 2, pp 1–103 (with 9 plates)

Fuchs G, Frank W (1970) The Geology of West Nepal between the rivers Kali Gandaki and Thulo Bheri. Jahrbuch der Geologischen Bundesanstalt, Wien, Sonderband 18, pp 1–103 (with 9 plates)

Garzanti E, Nikora A, Tintori A (1992) Paleozoic to Early Mesozoic stratigraphy and sedimentary evolution of central Dolpo (Nepal Himalaya). Rivista Italiana di Paleontologia e Stratigrafia, Milano, vol 98, No 3, pp 271–298 (with 1 plate)

Hayden HH (1904) The geology of Spiti, with parts of Bashahr and Rupshu. Mem Geol Surv India XXXVI(Part 1):1–129 (with 17 plates)

Siblík M (1975) Triassic brachiopods from Nepal. Rivista Italiana di Paleontologia e Stratigraphia, Milano, vol 81, no 2, pp 133–160 (including 3 plates)

Waterhouse JB (1966) Lower Carboniferous and Upper Permian Brachiopods from Nepal. Jahrbuch der Geologischen Bundesanstalt, Wien, Sonderband 12, pp 1–99 (with 10 plates)

Waterhouse JB (1977) The Permian rocks and faunas of Dolpo, northwest Nepal. Colloques internationaux du CNRS, no 268—Écologie Et Géologie De l'Himalaya, Paris, No 268, pp 479–496

Waterhouse JB (1978) Permian brachiopoda and mollusca from northwest Nepal. Palaeontographica, Stuttgart, Abt. A., vol 160, pp 1–175 (with 26 plates)

Tethys Himalaya of Gandaki Region (Thakkhola)

24

In this connection, the presence within the gneisses of more or less irregular streaks and pockets of tourmaline-bearing pegmatite—also occurring as dykes in the basal part of the overlying Larjung formation—may be significant, the more so as these pegmatites are only slightly stressed.

—Bodenhausen et al. (1964, p. 105)

The headwaters of the Kali Gandaki have carved the elevated transverse valley of Thakkhola in the Inner Himalaya. The excellently exposed Paleozoic and Mesozoic strata of this tract have remained the center of research since Hagen (1959) brought to light its key position in the interpretation of Himalayan geology. He was able to map the basic stratigraphic units, and to demonstrate their homotaxial relationship with other parts of the Tethys Himalaya. The geologists attached to the Dutch Himalayan Expedition (Bodenhausen et al. 1964; Bodenhausen and Egeler 1971) investigated the stratigraphy and tectonics of the Thakkhola Valley and the neighboring Lesser Himalaya in 1962. They also recovered graptolites and other important fossils that led them to correlate more precisely this region with the Northwest Himalaya. The regional geological work was carried out by Bordet et al. (1971).

The Tethyan Himalayan sequence (Figs. 24.1 and 24.2) of Thakkhola begins with the Paleozoics, constituting a thick shallow-water carbonate succession with some siliciclastics, followed by pelitic units deposited in deeper water environments, and at much higher accumulation rates than in the Northwest Himalaya. During the Carboniferous and Permian Periods, shallow-water limestones and coarse quartzose sandstones were formed, with major unconformities related to the initial opening-up of the Neo-Tethys and associated volcanic activities (Garzanti and Pagni Frette 1991). The Mesozoic sequence continues with shale and carbonate accumulations, containing abundant ammonites in the Triassic and Jurassic, whereas the Cretaceous begins with some continental deposits, succeeded by marine transgression with the deposition of green sandstones, made up mainly of volcanic clasts.

24.1 Augen Gneisses and Larjung Formation (? Cambrian)

There is a zone of impure marbles, containing calcite, garnet, pyroxene, phlogopite, and plagioclase. These lime-silicates and schists then grade up-section into the Larjung marbles. In the river section west of Dhampu (Figs. 24.1 and 24.3), on the right bank of the Kali Gandaki, the following succession is observed, respectively, from bottom to top (Colchen 1971, p. 87).

(a) Augen gneisses injected by pegmatite veins.
(b) Finely banded gneisses, with biotite partings crosscut by pegmatite veins containing tourmaline (100 m).
(c) Banded gneisses with biotite and alternating with colorful impure marble bands, with a total thickness of about 100 m.
(d) The rocks similar to the previous ones but more calcareous and massive with an angle of dip varying between 25° and 30° and dipping due NNE, sparingly injected by pegmatite veins (150 m).
(e) Very fine-grained gneisses with muscovite and alternating with variegated impure marble bands and injected by lens-shaped veins of quartz with muscovite. This unit is about 80 m thick and makes a ledge.
(f) Within the calcareous rocks, there are still a few horizons of gneiss (about 100 m), followed by very finely stratified bands forming a ledge.
(g) The Larjung Formation represented by very thick (about 600 m) and massive marbles that almost completely surround the valley of Kali Gandaki to the north of Dhampu, and in them one can distinguish white, bluish,

M.R. Dhital, *Geology of the Nepal Himalaya*, Regional Geology Reviews,
DOI 10.1007/978-3-319-02496-7_24

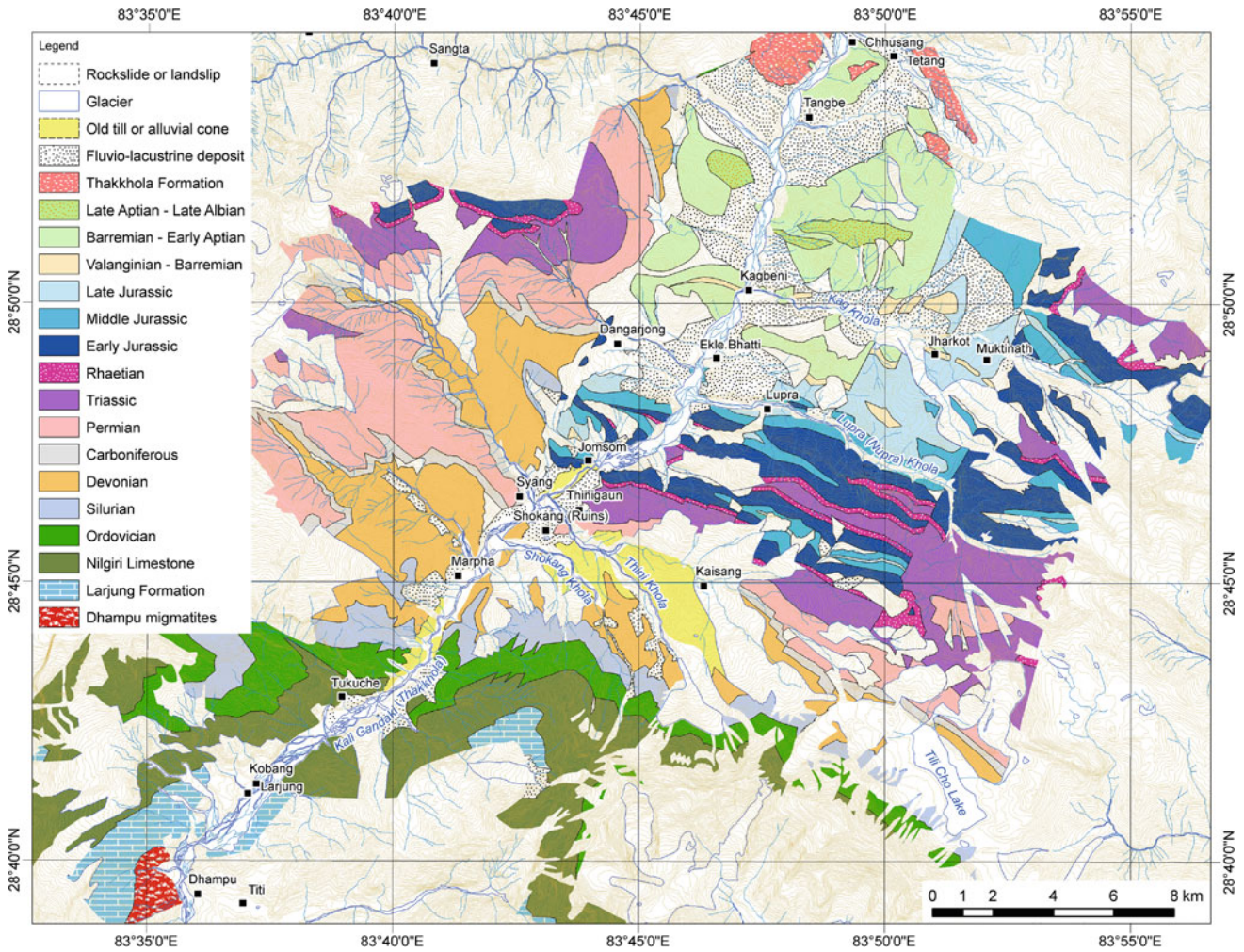

Fig. 24.1 Geological map of the Thakkhola area. *Source* Modified from Bordet et al. (1971)

and yellow bands, constituting mesoscopic (tens of meters) folds verging due north. This sequence is succeeded by about 150 m of rather thinly banded micaceous impure marble, forming a topographic depression.

The Larjung Formation thus constitutes a metamorphic succession, composed of marbles developed on top of the impure marbles and gneisses (Fig. 24.2). Inasmuch as no fossils were recovered from this formation, its assignment to the early Paleozoic is based primarily on the conformable contact with the overlying strata (Colchen 1971, p. 87).

24.2 Nilgiri Limestone and North Face Quartzite (Ordovician)

The Nilgiri Limestone constitutes a very large overturned to recumbent anticline (Fig. 24.4), which closes to the north, and extends essentially in the east–west direction (Waltham 1972). The core of this vast fold is exposed on the west wall of Nilgiri, to the northeast of Chini Gaun, at an altitude of about 4,000 m. From south to north, the succession is as follows.

1. Alternations of fawn and brown slates and limestones, belonging to the Larjung Formation, constitute the core of the Nilgiri recumbent fold.
2. Stratigraphically above the Larjung Formation, lies the Nilgiri Limestone with a transitional contact. The Nilgiri Limestone is made up of alternations of thick (up to 1 m), blue to yellow limestones and medium to thick, yellow-brown, calcareous slates (more clayey), in which cross-bedding can be frequently discerned. These alternations have a total thickness of approximately 900 m. Some very small striated brachiopods were obtained from various horizons, where they form coquina of genus *Aporthophyla*, such as those found in the Early Ordovician. Similarly, a fragment of *Nautiloidae* (probably *Ellesmeroceratidae*) was also discovered (Colchen 1971, p. 88).

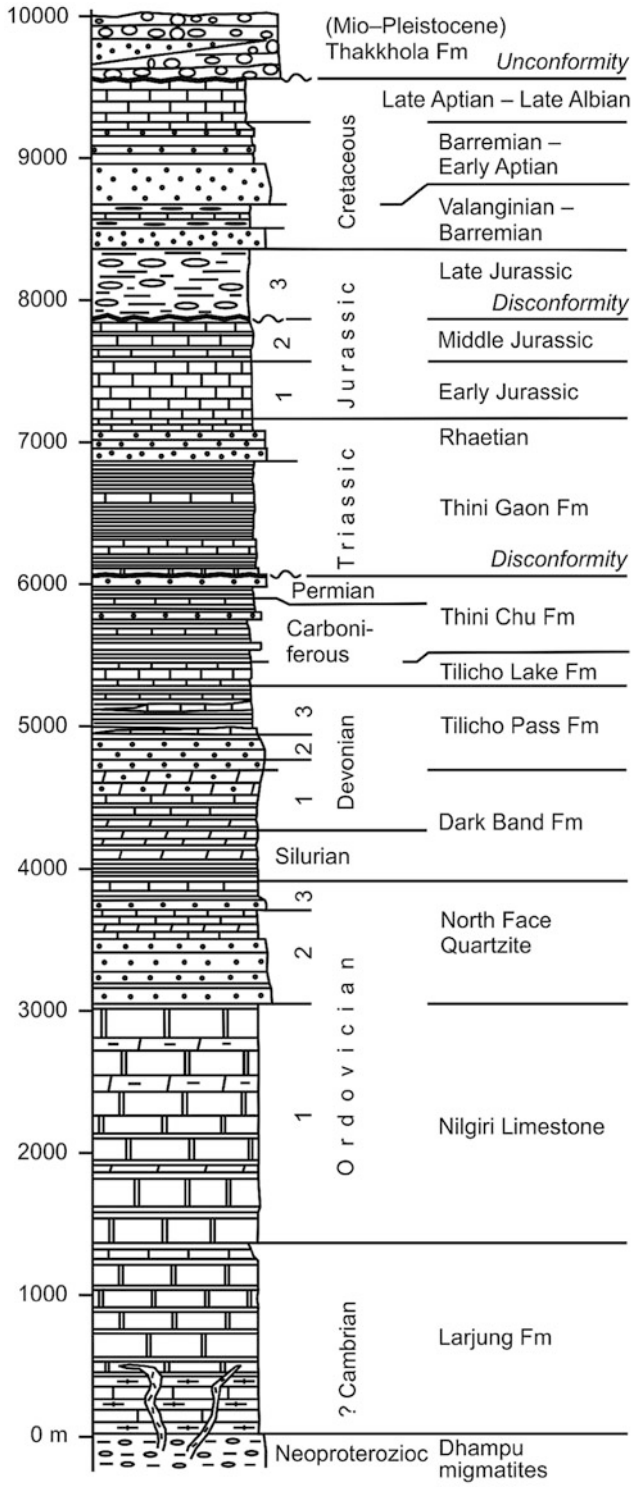

Fig. 24.2 Generalized stratigraphic column of the Thakkhola area. *Source* Compiled from Colchen (1971) and Mouterde (1971)

The limestones of Nilgiri are equally well exposed on the north wall of Nilgiri. The section commences at an altitude of about 5,000 m, and while descending towards the north, the following rock sequence is observed successively (Colchen 1971, pp. 88–91; Fig. 24.5).

(a) The Nilgiri Limestone: There is an approximately 700 m thick sequence of ocher limestones, which are intersected by blue veins, and alternating with ocher-beige horizons, a facies similar to that observed in the west wall. The limestone beds contain brachiopods of family Orthidae, similar to the genus *Aporthophyl*a, frequently deposited in lenticular lumachelle beds. Inside a single bed, parallel as well as cross-bedding is present. A cleavage, which dips 45–50° due south, obliquely cuts the stratification.

(b) The North Face Quartzite: Approximately 400 m of a dominantly sandy succession begins with gray-pink limestone alternations of a facies, rather similar to the preceding rocks, and it is further followed by several-meter-thick beds of beige and green sandstone, alternating with pink and beige dolomitic slates. These sandy dolomitic alternations continue thus for several hundred meters, and constitute the base of the imposing north face of Nilgiri. Hence, Bodenhausen et al. (1964) called them the North Face Quartzite.

(c) A transitional zone: Approximately 120 m of dolomites and limestones alternate with thin clay partings. The limestones are up to 1 m thick, exhibit gray-blue colors, and contain ocher veins, similar to those of the Nilgiri Limestone. They entomb some fragments of brachiopods together with indeterminate trilobites. Colchen (1971, p. 90) has included this and the following horizon "d" into a transitional zone to the Pitted Calc-Schists Member.

(d) The above rocks are followed by sandstones: These alternate with lumachellic limestones containing brachiopods (50 m), and ending in more clayey beds. The limestones are of white color and alternate with blue pelitic beds.

(e) The Pitted Calc-Schists Member: Light pink to green calcareous slates or schists (230 m) constitute the stratigraphic top of this transect. These rocks represent a marker horizon, located towards the upper part of the North Face Quartzite. Generally, a weathered outcrop is characterized by the dissolution of limestone lenses. These pitted calcareous slates represent the last escarpments of the north face of Nilgiri before a first projecting ledge, and a rather significant widening up of the valley. They are profusely fossiliferous, and yielded from several horizons an abundant fauna of brachiopods, crinoids, and echinoderms, in particular, from the middle and higher horizons. The brachiopods are *Orthambonites*, *Aporthophyla*, and *Oepikina,* known in the Ordovician (Colchen 1971, p. 91).

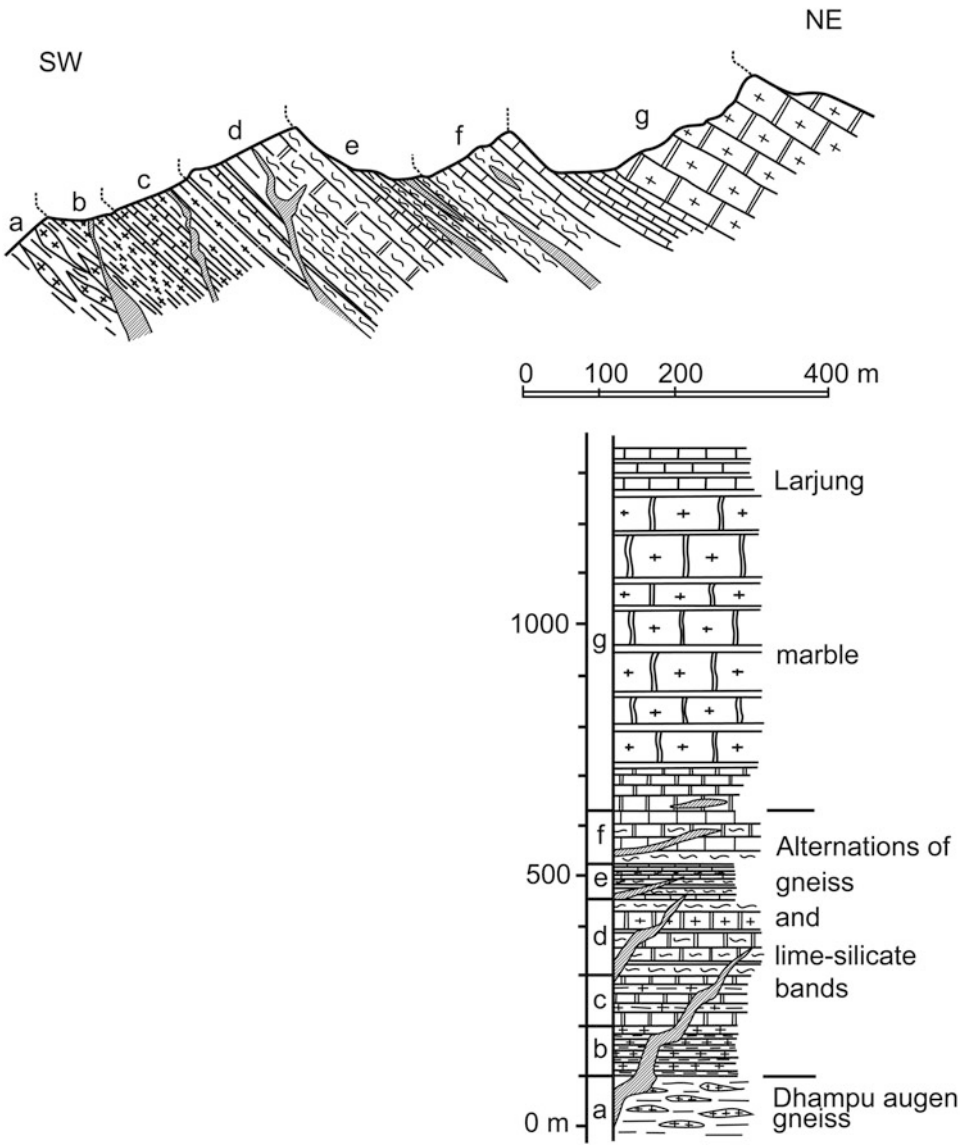

Fig. 24.3 Schematic section depicting the passage of the Dhampu gneiss to the Larjung Formation. **a** Augen gneiss of Dhampu; **b**–**f** alternation of banded gneisses and impure marbles (cipolins); **g** Larjung Formation (limestone and marble); pegmatite veins. *Source* Modified from Colchen (1971, p. 86). © Centre National de la Recherche Scientifique, Paris, France. Used by permission

24.3 Pitted Calc-Schists Member and Dark Band Formation (Middle Ordovician—Early Devonian)

The Dark Band Formation (Bodenhausen et al. 1964) is exposed in the Shokang Khola and on the spur west of Nilgiri. In continuity with the preceding formations, while descending from the right bank in the valley (Fig. 24.6), the following five successive lithological horizons occur Colchen (1971, pp. 91–94).

1. At first, the Pitted Calc-Schists Member of the North Face Quartzite corresponding to Horizon "e" of the preceding section continues.
2. The latter unit is followed by dark gray to black slates and associated rocks (120 m), shaping a protruding ledge and constituting the first horizons of the Dark Band Formation. Its first half section delivered a rich fauna of graptolites in the following stratigraphic order.

a. *Monograptus gemmatus* Barr., *M. gregarius* Lapworth, *Glyptograptus tamariscus* Nich.
b. (19 m higher) *Climacograptus* cf. *C. medius* Törnq.
c. (20 m higher) *Monograptus gemmatus* Barr., cf. *M. communis* Lapworth, *Orthograptus* cf. *O. bellutus* Törnq., *Climacograptus* cf. *C. medius* Törnq.
d. (18 m higher) *Monograptus lobiferus* Mc Coy, *Orthograptus bellutus* Törnq.
e. (6 m higher) *Monograptus lobiferus* Mc Coy, *Rastrites hybridus* (Lapworth).
f. (20 m higher) *Monograptus gregarius* Lapworth,. cf. *M. denticulatus* Törnq., *Climacograptus* cf. *C. medius* Törnq.

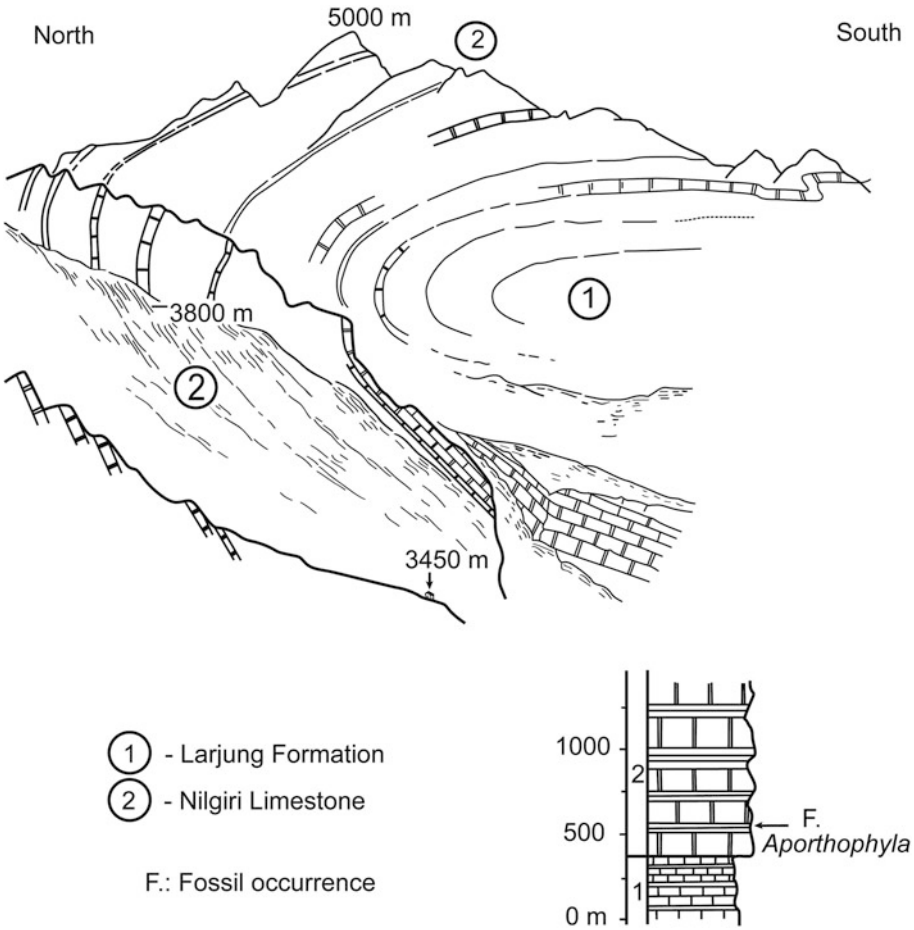

Fig. 24.4 Panoramic view of the west wall of the Nilgiri limestone (*upper* reach of Chini Khola). *1* Larjung Formation; *2* Nilgiri Limestone. *Source* Modified from Colchen (1971, p. 89). © Centre National de la Recherche Scientifique, Paris, France. Used by permission

This section yielded the following species, representing the upper part of the Llandovery (early Silurian): *Monograptus gemmatus* Barr., *M. elongatus* Törnq., *M. involutus* Lapworth, *M. lobiferus* Mc Coy, *M. cygneus* var. *M. incisus* Gort., *Rastrites hybridus* (Lapworth), *R. peregrinus* (Barr.), *Climacograptus medius* Törnq., cf. *C. medius* Törnq., and *Glyptograptus tamariscus* Nich.

3. After the graptolitic horizon, comes a carbonate sequence (320 m), made up primarily of a few-meter–thick sandy dolomite beds, making a morphologically conspicuous cliff, in which indeterminable organic relics of crinoids and orthocerids are found.
4. The succession that follows this cliff comprises an alternation of black limestone and dark gray to black slates (160 m), containing an abundant fauna of tentaculites, associated sometimes with graptolites. Lardeux identified the following tentaculites fossils (Colchen 1971, p. 94): *Nowakia acuaria* Richter, *Nowakia* sp., and *Styliolina* sp., which make it possible to assign them a Pragian (Early Devonian) age. The tentaculites are associated with badly preserved graptolites (*Monograptides*).
5. The above alternations are followed stratigraphically upwards by a few-meter-thick carbonate beds of approximately 120 m in aggregate thickness, representing the following succession.
   (a) An alternation of limestones and black slates passing into a horizon of black limestone with flint in the upper part (6 m)
   (b) Interbedded black slates and limestones (10 m)
   (c) Thick-bedded (up to 1 m) sandy dolomite (15 m)
   (d) Limestone (3 m)
   (e) Thick-bedded (up to 1 m) sandy dolomite separated by medium-bedded slates, constituting a distinct morphological marker (73 m)
   (f) Thin beds of black slate and limestone, exhibiting black sheen, containing some remains of unidentifiable shells, and ending in a more dolomitic horizon (14 m).

The Ordovician–Silurian boundary lies between the above-discussed Horizons 1 and 2. On the other hand, the boundary between the Silurian and Devonian passes somewhere at higher levels of Horizon 3 (Colchen 1971, p. 95).

The spur west of Nilgiri is ramified by numerous faults, and the stratigraphic sequence begins with the Middle to Late Ordovician Pitted Calc-Schists Member, containing many fragments of brachiopods, including genus

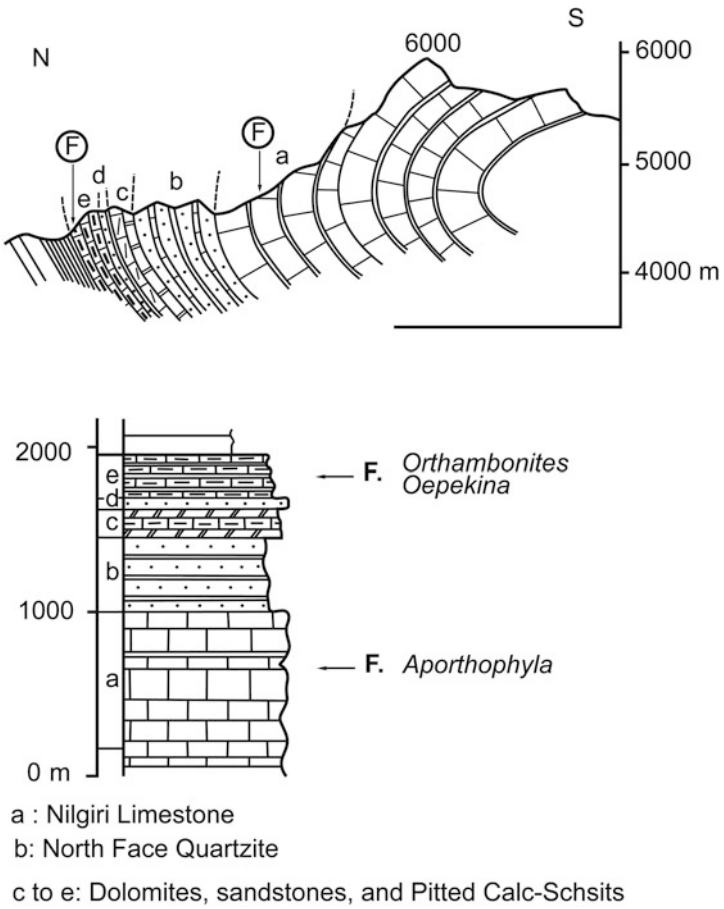

Fig. 24.5 Generalized section of the Nilgiri north face. **a** Nilgiri Limestone; **b** North Face Quartzite (*lower* member); **c–e** dolomites, sandstones, and the Pitted Calc-Schists (*upper* member). *Source* Modified from Colchen (1971). © Centre National de la Recherche Scientifique, Paris, France. Used by permission

Orthambonites, *Aporthophyla*, and *Oepikina* as well as two pygidia of trilobites (cf. *Basiliens* sp.). Then, the Dark Band Formation continues with fine sandy–schistose alternations of the Silurian, containing *Monograptus* cf. *M. concinnus* Lapworth and *Climacograptus* sp. The latter unit extends stratigraphically upwards with black slate and limestone alternations, containing the tentaculites of Pragian age. The preceding sequence is succeeded by a limestone horizon, having black flints of the Early Devonian, and followed further by subordinate limestone beds, containing goniatite and trilobite fragments.

24.4 Tilicho Pass Formation (Middle–Late Devonian)

The following sequence of the Tilicho Pass Formation (Fig. 24.7) crops out in the middle reach of the Shokang Khola (Colchen 1971, pp. 95–96).

1. Thickly bedded sandy dolomite.
2. Slightly calcareous, fine-grained sandstone (10 m).
3. Alternations of coarse sandstones, passing into microconglomerates and micaceous fine sandstones (40 m).
4. Black slates (10 m).
5. Micaceous fine sandstones in decimetric beds, refolded into an anticline, ramified by a north-dipping fault (15 m).
6. Thin alternations of slates and sandstones (20 m).
7. Medium-grained, greenish gray feldspathic sandstones (20 m).
8. Alternations of sandstones, slates, and calcareous sandstones (about 50 m).
9. Lenticular beds of microconglomeratic sandstone with calcareous cement, containing organic debris of crinoids and brachiopods, and interstratified with finely laminated slates (approximately 40 m).
10. Lenticular beds of sandy limestone with remains of crinoids and corals, of which the latter include species belonging to *Favosites* cf. *F. saginatus* Lecompte of Givetian (Middle Devonian) age.
11. In Horizons 11 and 12, fine alternations continue for several hundred meters with identical facies; the lenses of limestone are thin and deliver only crinoid remains. These finely laminated strata frequently constitute north-verging isoclinal folds.

The Devonian sequence continues towards the east, parallel to the Nilgiri Range, and is well exposed at the northern edge of Lake Tilicho, and hence Bodenhausen et al. (1964) named them the Tilicho Pass Formation. Thus, the Early and

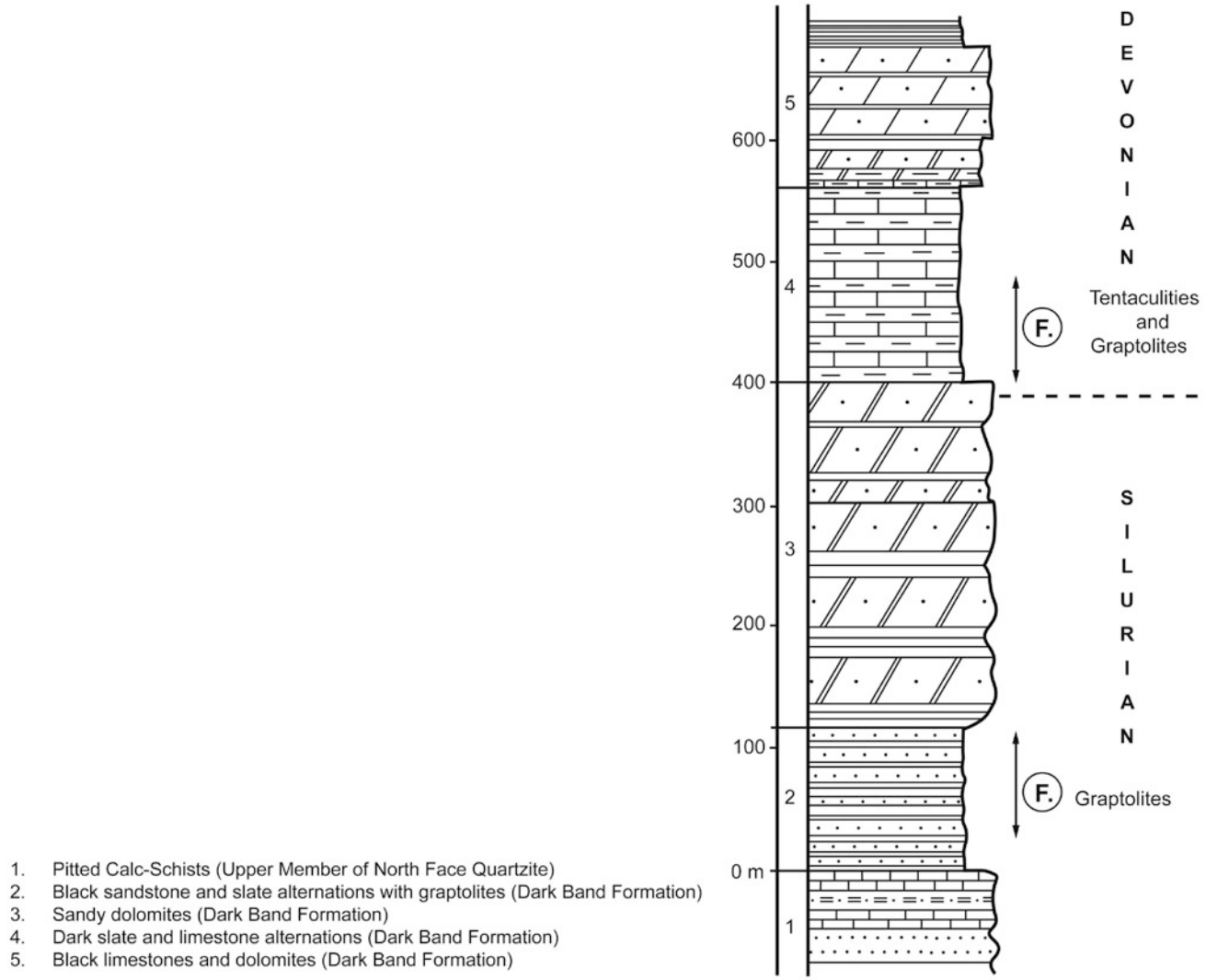

Fig. 24.6 Stratigraphy of the Pitted Calc-Schists Member and Dark Band Formation from the upper reach of the Shokang Khola. *Source* Modified from Colchen (1971). © Centre National de la Recherche Scientifique, Paris, France. Used by permission

Middle Devonian sequences were dated paleontologically, and the last Horizons 11 and 12 may belong to the Late Devonian. The whole Devonian System is about 1,000 m thick in the Thakkhola region. Different from the lower calcareous part, the upper portion of the Devonian is more terrigenous (Colchen 1971, p. 97).

24.5 Tilicho Lake and Thini Chu Formations (Carboniferous–Permian)

The preceding detrital units are abruptly followed by a thin ferruginous horizon and a carbonaceous formation, marking the commencement of the Carboniferous Period. The following Devonian–Carboniferous contact zone is exposed on the left bank of the Shokang Khola, where the sequence is overturned (Colchen 1971, p. 98).

- Alternations of dark gray to black slates with ferruginous nodules and well-bedded granular sandstones (8–10 m).
- Medium to thick strata of cross-bedded calcareous sandstone with a reddish-brown sheen (1.50 m).
- Very ferruginous sandstone of a rusty brown sheen (0.30 m).
- Alternations of slate and dolomitic limestone, and sandy beds of gray-blue color with an ocher sheen (10 m).
- Slates (1 m).
- Alternations of limestone, exhibiting a brown sheen, and slates containing some isolated corals (3 m).
- Gray-blue slates with Orthidae and fenestellids (1 m).
- Gray-blue slate alternations, and crystalline limestones in decimetric beds, containing orthidae, crinoids, and corals (10 m).
- Slates and finely laminated limestones; some thicker beds delivered many fragments of crinoids (12 m).

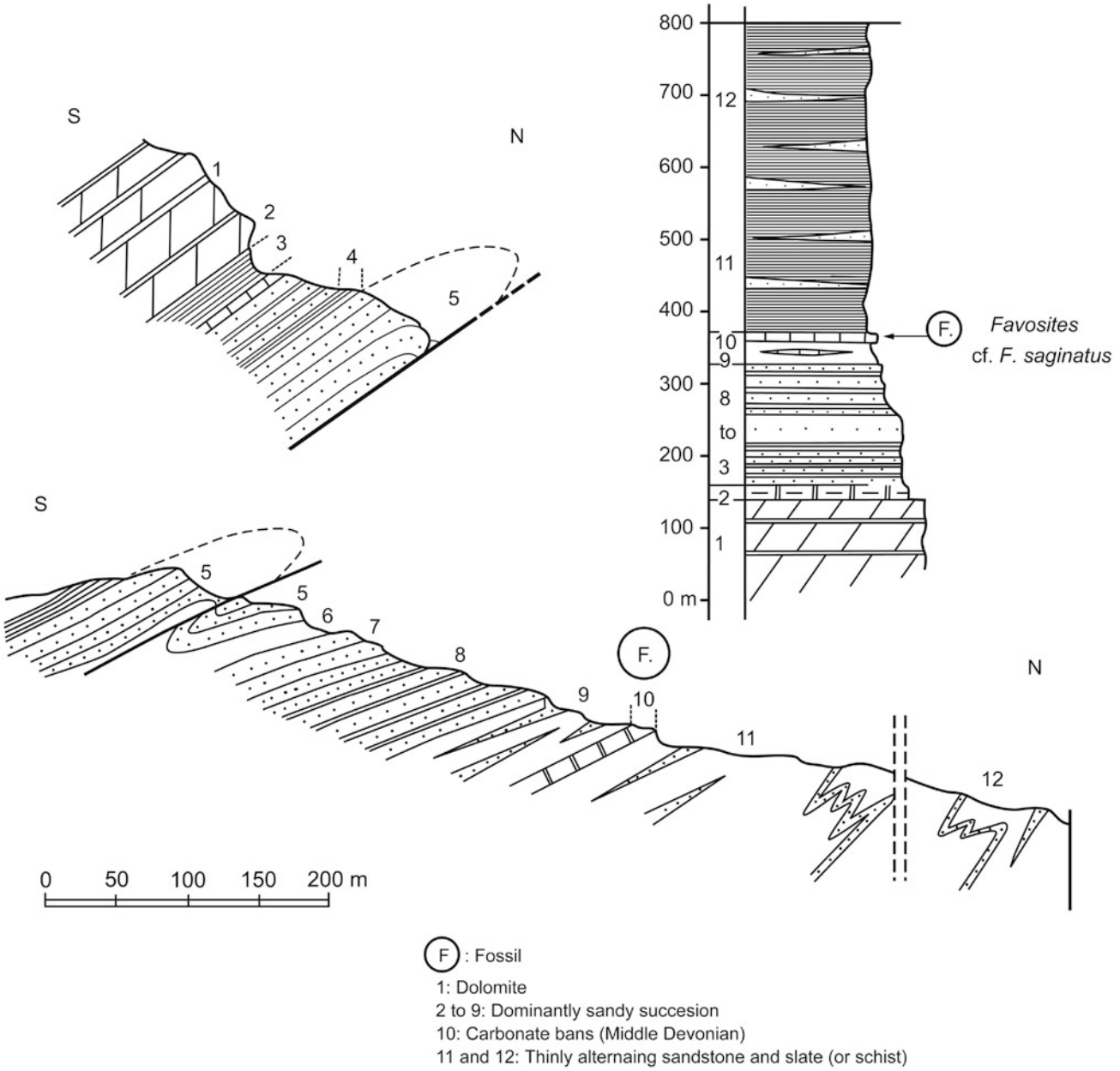

Fig. 24.7 The Devonian succession occurring in the middle reach of the Shokang Khola. *Source* Modified from Colchen (1971). © Centre National de la Recherche Scientifique, Paris, France. Used by permission

- Compact black limestone in decimetric beds, with crinoids and argillaceous limestones with isolated corals and crinoids (5 m).
- Alternations of limestones and black slates in decimetric beds, containing many crinoids (about 25 m).

The first horizons have facies identical to that of the Devonian in the preceding transects. The Devonian–Carboniferous boundary is placed at the first appearance of ferruginous sandstones of a rusty-brown sheen (Colchen 1971, p. 98). The carbonates and slates, structurally located under this horizon, delivered some Orthids as well as many fragments of crinoids and isolated corals.

In the upper reach of the Thini Khola and on the crest of Thini (Thinigaun), the Tilicho Lake Formation contains alternations of limestone and slate (30 m), where the limestone contains many fragments of crinoids, fenestellids *Septopora* cf. *S. ekybastusica* Nekhoroshev, corals, and some brachiopods, such as *Spirifer* aff. *S. attenuatus* Sowerby, or *Neospirifer postriatus* Nikitin or *N. neostriatus* Fredericks. These fossils belong to the early Carboniferous (Colchen 1971, p. 101).

An extension of the last section is found in the north part of the peak of Thini, at the edge of Tilicho, where it intersects the Permo–Carboniferous boundary. In this area, the upper part of the Tilicho Lake Formation is represented by about 30 m thick black slate and limestone alternations. They contain "*Spirifer trigonalis*" (non- MARTIN), *Syringothyris* sp., and *Spirifer,* for example, *attenuatus* SOWERBY, or *Neospirifer poststriatus* NIKITIN or *N. neostriatus* FREDERICKS, M*arginirugus* cf. *M. magnus* MEEK & WORTHEN of the early Carboniferous. The Thini Chu Formation commences, after a faulted crush zone, with black slates with lenses of ocher limestones (100 m) containing brachiopods such as *Syringothyris* aff. *S. lydekkeri* DIENER and *Neospirifer* aff. *N. fasciger paucicostulatus* REED, and *Marginatia* MUIRWOOD & COOPER. These fossiliferous rocks are followed by white sandstones, black slates with marked oblique cleavage (100 m), and coarse sandstones and conglomerates (80 m).

At another transect, farther north of Thini, the Thini Chu Formation yielded an abundant fauna of crinoids, fenestellids, and brachiopods, including *Syringothyris* sp., *S. lydekkeri* DIENER, *Brachythyrina* cf. *B. rectangula* KUTORGA, *Elivina* sp., *Spiriferella* s.l. cf. *S. ?papillionata* SAHNI & SRIVASTAVA, *?Neospirifer* sp., and *Buxtonia* sp.

The same lithotypes crop out farther downwards and to the west of the Thini crest, where they contain *Syringothyris* sp, *Neospirifer postriatus* NIKITIN or *N. neostriatus* FREDERICKS, *Stepanoviella* sp., *Pugilis* sp. (cf. *P. Serpukhovensis* SARYTCHEVA), *Marginirugus barringtonensis alatus* CAMPBELL, *Waagenoconcha* sp., *Buxtonia* sp., *Syringothyris* sp. indet., and *Spirifer* aff. *S. peregrinus* REED. This fossiliferous horizon is followed by *Neospirifer* sp., *Syringothyris lydekkeri* DIENER, *Brachythyrina* cf. *B. rectangulata* KUTORGA, *Buxtonia* sp., *Marginicinctus* sp., and *Ovatia* cf. *O. tenuistriata* DE VERNEUIL. Above these fossils occur *Syringothyris lydekkeri* DIENER, "*Spirifer*" *middlemissii* DIENER.

To the east of Thini, the Late Paleozoic rocks (Thini Chu Formation) constitute part of the peaks, which surround the village. Succeeding normally into the overlying the Early Triassics, the sandy and shaly facies, similar to that of Tilicho, strikes essentially east–west, where the following four fossiliferous zones were discovered (Fig. 24.8) in ascending order (Colchen 1971, pp. 105–107).

1. The sequence begins with intensely folded black schists or slates, containing brown nodules and dolomitic lenses. The slates become more dolomitic towards the top, and pass into fine slate alternations and dolomitic sandstones. Then they alternate with limonitic sandstones in beds very rich in tracks, tubes, and carbonaceous remains (several tens of meters).
2. There are sandstones of light pink color, in decimetric beds, exhibiting cross-bedding, passing towards the top into calcareous sandstones very rich in remains of crinoids, fenestellids, and brachiopods (15 m).
3. This unit is made up of bluish gray folded slates (30 m).
4. There are mainly cross-bedded white sandstones, passing towards the top into calcareous sandstones rich in brachiopods (30 m). This succession is further divided into the following horizons (Transect II in Fig. 24.8).
   (a) Coarse sandstones with irregular stratification covered by a very fossiliferous calcareous sandstone horizon (F7), with following brachiopods: *Syringothyris lydekkeri* DIENER, *Spiriferella* s.l.: cf. *?S. papillionata* SAHNI & SRIVASTAVA, *Spirifer middlemissii* DIENER, *Buxtonia* sp., and *Striatifera striata* FISCHER DE WALDHEIM
   (b) Cross-bedded coarse sandstone (0.5 m)
   (c) Highly limonitic sandstones, very rich in brachiopods, similar to those of "a" (0.50 m)
   (d) Fine alternations of calcareous sandstones and highly fossiliferous gray-blue slates (5 m)
   (e) Grayish blue slates with sandy beds (0.3 m)
   (f) Gray-blue, calcareous, limonitic sandstones with a brown sheen, very rich in crinoids and brachiopods (0.9 m)
   (g) Blue pencil slates and dolomitic sandstone beds, generally rich in small bivalves.
5. This unit consists of gray-blue slates with limonitic and dolomitic nodules (35 m).
6. The cross-bedded, coarse, limonitic sandstones (18 m) of this unit delivered the following fossils (F8).
   - Fragments of crinoids
   - Brachiopods: *Syringothyris lydekkeri* DIENER, *Buxtonia* sp., *Striatifera spinifera* PAECKELMANN, *Alifera* MUIR-WOOD & COOPER
   - Fenestellids: *Fenestella polyseptata* SHULGA-NESTERENKO
   - Trilobites: *Weberides mucronatus* MAC COY, *Griffithides* sp.
7. The section ends with black slates, including remains of brachiopods (35 m).
8. An alternation of fine black slates and medium- to thick-bedded, sporadically lenticular, calcareous sandstones (30 m), contains *Syringothyris lydekkeri* DIENER (F9).
9. Black slates with pink and brown dolomitic lenses (8 m) delivered *Spiriferella rajah* SALTER (Fl0).
10. A horizon of limonitic white sandstone (30 m), which is conglomeratic at the base, rests on an erosional surface. The horizon is very frequently carbonaceous, and its base successively contains (Transect III in Fig. 24.8) the following units.
    - a: Blue-gray slates with limonite nodules
    - b: Coarse limonitic sandstone (0.20 m)
    - c: Slates and finely laminated sandstones of light gray color, with limonite nodules (3 m)
    - d: Coarse sandstones with limonite nodules (0.25 m)

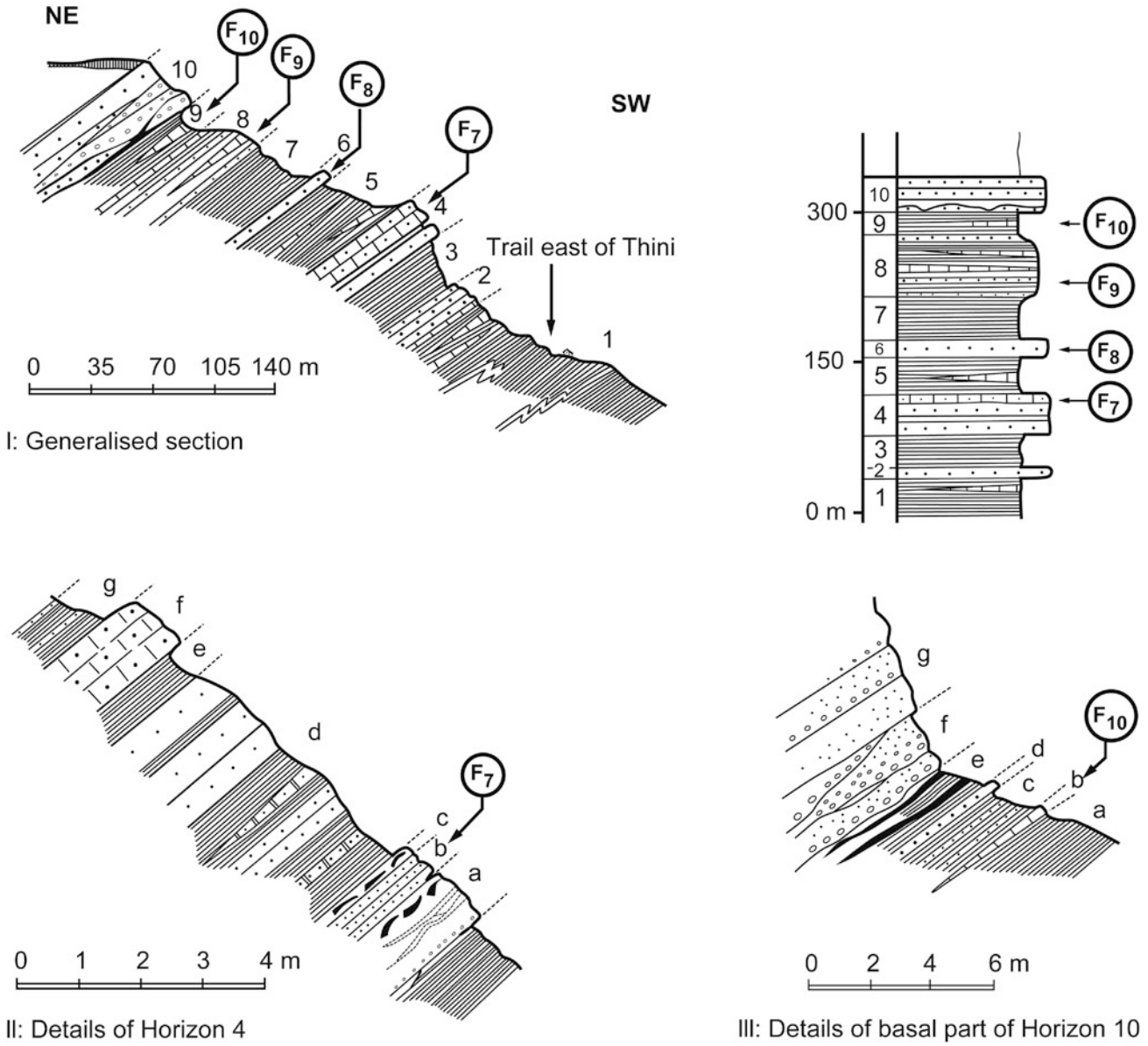

Fig. 24.8 Stratigraphic sections of the Late Paleozoics (Thini Chu Formation), exposed northeast of the village of Thini. *Source* Modified from Colchen (1971). © Centre National de la Recherche Scientifique, Paris, France. Used by permission

- e: Black schists or slates with lenticular coal beds (1.50 m)
- f: Lenses of polymictic conglomerate, followed by coarse pebbly sandstones.

24.6 Permo–Triassic Syn-rift Sediments

Although Colchen (1971) as well as Colchen et al. (1986) infer several depositional gaps in the Thini Chu Formation, von Rad et al. (1994) do not favor any such significant hiatuses. They state that the sediments were accumulated during the opening up of the Neo-Tethys. In the Thakkhola area, the Upper Thini Chu Formation is about 350 m thick, and begins with shales, interbedded with siltstones and cross-laminated quartzose sandstones. This unit is followed by coarse-grained, calcite-cemented, quartzose sandstone with flaser bedding and quartz-rich bioclastic packstone to rudstone with molluscs and brachiopods. The last unit is overlain by a fossiliferous grainstone, containing crinoids, bivalves, brachiopods, and bryozoans. A ferruginous surface is observed above this bed, and it is sharply overlain by shales and siltstones, which are in turn succeeded by a number of sandstone and shale beds. There is an approximately 10 m thick succession of light gray shale with thin

siltstone to very fine sandstone intercalations, followed by 10–20 cm thick coal seams. This unit is succeeded by a 45 m thick quartzite succession, in which the lower 32 m is represented by medium- to coarse-grained quartzose sandstones with shale intraclasts and erosional surfaces in the lower part, and at the top of this unit are *Paleophycus* burrows. The remaining 13 m includes coarsening-upwards cycles of shale and sandstone. This last sequence is overlain by an approximately 32 m thick shale bed, containing pelagic bivalves. The topmost cycle succeeding the shale is about 10 m thick, reddish-brown, pink, and gray, thick-bedded, massive quartzite, containing a quartz-rich grainstone bed with crinoids in its top portion (von Rad et al. 1994).

The strata just below the Permo–Triassic boundary have a conspicuous sequence that begins with about 8 m thick, pink or light gray quartz arenite, sometimes with large-scale trough cross-bedding, and several, up to 3 m thick, quartzitic conglomerates and hardgrounds. They are followed by about 1 m thick, brown, calcareous sandstone, which is underlain by a ferruginous hardground, containing rootlets and tubular structures. The hardground is succeeded upwards by a 20–30 cm thick, dark brown, ferruginous, coarse-grained, pebbly quartz arenite with chloritic matrix, shale clasts and bryozoans. This bed is overlain by a 0.8–1 m thick sandy carbonate with shell debris and some dolomite lenses or ferruginous quartzitic conglomerates with shale and chert pebbles. The topmost bed is a reddish brown nodular limestone with ammonites and shells of Griesbachian age. The lowermost sandstones were presumably accumulated in fluvio–deltaic to marine–deltaic environments. The large trough cross-bedding and channels with conglomerates were developed in a subaerial fluvial environment. The coarsening-upwards sequences indicate a prograding fluvial-dominated delta. The siliciclastic sediments of the Thini Chu Formation are extremely mature, and may have originated from a stable craton that was gradually uplifted during rifting (von Rad et al. 1994).

The Carboniferous and Permian formations are approximately 800 m thick, and always begin with the same lithofacies: a succession, primarily calcareous at the base, constituting the Tilicho Lake Formation, and alternations of black slates and white sandstones above, belonging to the Thini Chu Formation.

24.7 Early Triassic

The Mesozoic succession (Figs. 24.2 and 24.9) in the Thakkhola begins with the Early Triassic rocks, mapped as the Thini Gaon Formation (Bodenhausen et al. 1964) or the Tamba Kurkur Formation (von Rad et al. 1994). The contact between them and the underlying Paleozoic rocks is best exposed in the middle tributary of the north Thini Khola, about 200 m downstream from Thini La. The following stratigraphic units are observed from summit to base of this overturned succession (Mouterde 1971, pp. 124–125; Fig. 24.10).

Paleozoic:

1. Dislodged blocks of coarse sandstone (20–25 m).
2. An alternation of sandstones and carbonaceous slates; the sandstones become conglomeratic in the lower part (3–4 m).
3. Quartzose sandstones (7 m) with slightly undulating contacts, depicting the continuation of the Triassic sedimentation on top of them.

Triassic:

4. Very ferruginous and feebly calcareous coarse sandstones (1.50 m); the beds are irregular and separated by slaty partings. Under the microscope, coarse quartz grains exhibit polygonal overgrowths, and are cemented by chlorite and ankerite.
5. Fine-grained dolomitic limestone with an ocher patina, containing altered remains of echinoderms and bryozoans in a highly recrystallized dolomitic (partly ferruginous) cement (2.65 m).
6. Compact gray limestone with an orange patina, in beds from 5 to 10 cm, containing many sections of ammonites, which are difficult to extract, probably belonging to *?Ophiceras* sp. and *?Xenodiscus* sp. (1.60 m).
7. Alternations of black slates and some limestone beds with an orange patina, containing fossils similar to the previous zone: *?Ophiceras* sp., *?Xenodiscus rotula* Waagen (4 m).
8. Black shales (20–25 m).
9. Irregularly bedded to nodular, compact limestones exhibiting a light gray sheen, containing *Xenodiscus rotula* Waagen, *Xenodiscus* sp. (4 m).
10. A partly dislocated but rather fossiliferous, fissile, black shale bed containing *?Xenodiscus* sp. and *Ceratites* sp., belonging to the group of *C. trinodosus* Mojsisovics, and an imprint of *?Episageceras* sp.

Horizons 6–9 belong to the Early Triassic, more precisely to its lower part. The badly preserved fauna in the shales of Horizon 10 already seems to belong to the Anisian, which would indicate a rather meager thickness for the Early Triassic strata. On the other side of the torrent, separated from the preceding series by a fault, some vertical limestone beds are found together with light gray shales, containing dark or black nodules, which frequently contain ammonites *?Ptychites* sp. and *Flemingites* sp., similar to *F. Griesbachi* v. Krafft, which still indicate the middle or upper part of the Early Triassic.

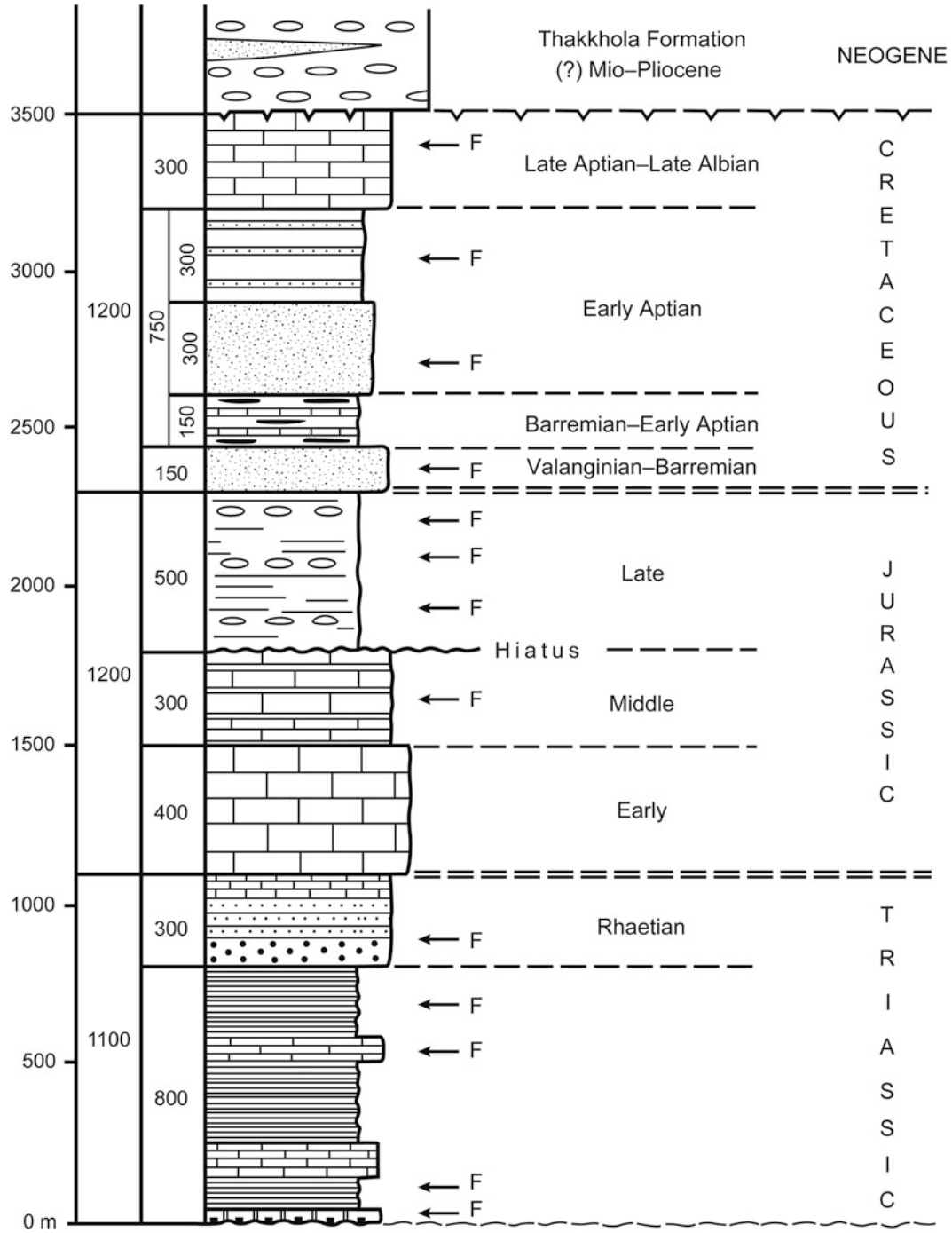

Fig. 24.9 Generalized stratigraphic column of the Mesozoic rocks in the Thakkhola. *Source* Modified from Mouterde (1971). © Centre National de la Recherche Scientifique, Paris, France. Used by permission

The base of the Triassic is well exposed in the vicinity of Thini, about 600 m southeast of the village, and also farther away, close to the trail from Thini. This Early Triassic fauna belongs to a rung, higher than that indicated by the fossils in Horizons 6–9 of the previously described section. This stage thus appears to have a significantly reduced thickness in the area.

24.8 Middle Triassic (Anisian and Ladinian)

The Anisian and Ladinian stages, represented primarily by black shales (100 or 200 m), are affected by many surface failures. Consequently, it was not possible to construct a continuous column. The very fragile and shattered fossils are

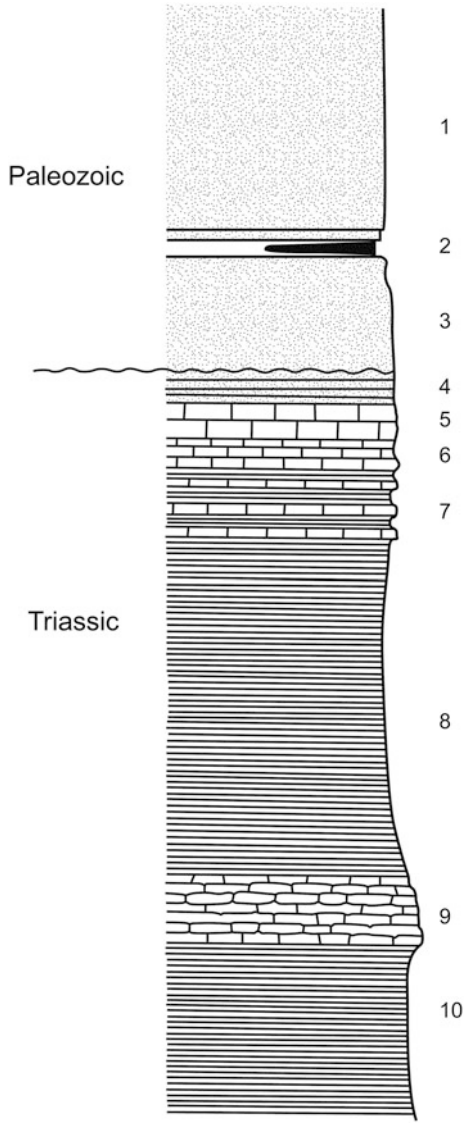

Fig. 24.10 Column of the Early Triassics from the northern Thini Khola. The sequence is reversed. The numbers correspond to the numbers in the text. *Source* Modified from Mouterde (1971). © Centre National de la Recherche Scientifique, Paris, France. Used by permission

frequently represented by Daonellids. On the trail to Thini, compact marls and marly limestones yielded *Proarcestes balfourdi* Oppel, *Ptychites* cf. *P. oppeli* Mojsisovics, and *Balatonites* sp. (Mouterde 1971, p. 126).

24.9 Late Triassic (Carnian and Norian)

This succession is made up of slightly calcareous dark slates, containing some sandstone and sandy limestone beds, ranging in thickness from 15 to about 60 cm. A rather continuous section lies on the west slope of Tilicho Peak, at a high (5,000 m) altitude. The Early Triassic sequence, resting directly on the Paleozoic formations, is represented by nodular limestones, exhibiting an orange sheen. They contain *Ophiceras* sp. To the north of this outcrop, and up to a small ravine, there is an approximately 50 m thick sequence, predominantly of black slates, with the intercalation of sandy limestone beds, containing an Early Carnian fauna, including several *Joannites* or *Arcetes*, *Trachyceras* sp. cf. *T. austriacum* Mojsisovics, and other Trachyceratides imprints. From this section, the following pyritous or calcareous ammonites, ranging in age from the Late Carnian to Early Norian, were also recovered: *Juvavites (?Dimorphinites)* sp. akin to *J. fissicostatus timorensis* Welter, badly-preserved *Juvavites* or *Parajuvavites* sp., *Tibetites* sp. aff. *T. ryalli* Mojsisovics, and numerous fragments belonging to the family Pinacoceratidae (Mouterde 1971, p. 128).

The last succession gives way to about 15 m thick, more cleaved rocks, which are further accompanied by several limestone or sandy limestone beds, exhibiting a brown sheen. The limestones form thick vertical to subvertical bands, separated by dark gray, feeble, micaceous slates (about 80 m). A higher succession of cleaved beds (about 50 m), yielded the following Middle and (?) Late Norian fossils: *Anatomites* sp., *Tibetites* sp., and *Paratibetites* aff. *P. tornquisti* Mojsisovics. On the other hand, an adjacent section yielded *Hypocladiscites subaratus* Mojsisovics, *Anatomites strabonis* Mojsisovics, *Juvavites* sp. aff. *J. interruptus* Mojsisovics, *Trachyceras* sp., *Tibetites* sp., and *Daonella lommeli* Wism. This fauna belongs to the Early Carnian and (?) Ladinian (Mouterde 1971, p. 128).

At a distance of about 1 km to the west, on the edge of a stream, some compact black limestone beds with fucoids are visible in the middle of dark gray, finely micaceous slates, containing pyritous concretions and nodules. This overturned sequence contains the following Early Carnian fauna, respectively, from bottom to top.

1. *Arpadites* sp. cf. *A. ?circumscissus* Mojsisovics, *Trachyceras* sp., *?Joannites* sp.
2. *Paratrachyceras* sp. aff. *P. thous* v. Dittmar, *Joannites* sp. cf. *J. klipsteini* Mojsisovics.
3. *Trachyceras* sp. aff. *T. infudibuliforme* v. Klipst, *Nautilus* (*Syringoceras*) aff. *N. evolutus* Mojsisovics, *Joannites* sp. aff. *J. klipsteini* Mojsisovics, *?Placites* sp.

The top of the Triassic succession lies on the west of the north–south-trending crest of Lupra, approximately 1 km northwest of the preceding point, on the south slopes of a crest separating the two tributaries of the North Thini Khola. It is also an overturned sequence, made up of the following strata.

1. From 20 to 40 cm thick, blue limestone beds with a brown patina, containing many shell remains, separated by finely micaceous black shales and forming topographic breaks.

2. A succession of black or gray micaceous shales containing limestone beds with a red-brown patina, similar to the previous ones (but less frequent), and containing the following fossils (30 m).
   - Firstly: *?Juvavites* or *?Parajuvavites* aff. *P. tyndalli* Mojsisovics and *?Trachyceras* sp.
   - Then: *Guembelites* cf. *G. philostrati* Diener fragment, *G. ?jandianus* Mojsisovics fragment, *Juvavites (?Dimorphites)* sp., *Anatomite*s sp. juv. similar to *A. ducetti* Gem., bivalves, and brachiopods.
   - Finally: *Tibetites ryalli* Mojsisovics, *Melacarnitesfloridus* Wulf., and *Juvavites* (*Anatomites*) sp. indet. fragment.

   This fauna indicates a Norian and perhaps a Late Carnian age (Mouterde 1971, p. 129).
3. The succession becomes then more cleaved with thin brown pelitic to sandy beds, where the limestone beds are generally lenticular. In the higher part, limestone nodules or their black pyritous to siliceous varieties are frequent (about 50 m). It also contains a Norian fauna.
4. Gray to dark gray slates with sporadic beds of pink, purplish, or greenish gray sandstone beds (0.50–2 m thick) displaying a brown patina, with irregular surface, exhibiting animal traces and tracks (70–80 m), infrequent bivalves, and ammonites (ill-preserved imprints of *Tibetites* and *Anatomites*).
5. A series of dark gray micaceous slates with infrequent gray-blue or purplish sandstone beds, appearing at an interval of 5–10 m, and displaying a brown or black patina (about 50 m).

Horizons 4 and 5 presumably belong to the Middle and Late Norian. This section thus represents almost entirely the Norian series whose thickness exceeds 200 m.

The branch of the track that leads to Jomsom from the bottom of Thini, crosses several outcrops of the Triassic with poorly preserved fossils. The way that leaves Thini and continues for about 2 km towards Lupra, overlooking the valley of Jomsom, crosses many fossiliferous Triassic outcrops. From there, Mouterde (1971, p. 130) presented the following overturned sequence, extending from the Late Carnian to Rhaetian.

1. On the right flank of the trail, about 300 m to the village, on both sides of the small peak overlooking the way, there is a more than 100 m thick shaly succession containing soft and fissile, light gray to dark gray, often micaceous, in places calcareous beds, alternating with sandy limestone or compact black limestone beds exhibiting a brown sheen. They abundantly contain daonellids and posidonids. The brachiopods are frequent in the limestones.

   The shales contain some nodules of pyrite and sporadic nuclei of ammonites: *Trachyceras* sp. and badly preserved forms belonging to Trachyceratidae; these beds probably belong to the Ladinian or perhaps to the Early Carnian. The only well-preserved form was that of *Sirenites senticotus* v. Dittmar, representing the Carnian.
2. In the immediate vicinity of the trail, the gray or blue-black slates contain daonellids or halobids, and alternate with thin gray-blue micaceous limestones, exhibiting a brown patina.

   The generally crushed, deformed, and badly preserved ammonites in these slates belong mainly to Trachyceratidae (*?Trachyceras* and *?Protrachyceras*), and they probably represent the Ladinian.
3. It contains a beautiful fauna of the Late Carnian (zone with *Tropites subbullatus*): *Trachysagenites* sp. fragment close to *T. beckei* Diener, *Paratibetites angustosellatus* Mojsisovics, *P.* aff. *P. adolfi* Mojsisovics, *Tibetites* cf. *T. ryalli* Mojsisovics, *Sirenites senticosus* v. Dittmar, *Hannaoceras* (= *Polycyclus*) *leislingensis* Mojsisovics, *Jovites* cf. *J. bosnensis* Mojsisovics, many fragments of brachiopods, bivalves, and particularly of daonellids.
4. Farther upstream in the Lupra Khola, the trail crosses the following continuous section, ranging in age from the Late Carnian to Rhaetian.
   a. At first, there is a sequence of slates, alternating with some sandy limestone beds with a russet-red patina, containing *Tropites* sp. fragments.
   b. After a rather wide cleaved zone, partly covered by falls, there are beds ranging in thickness from 20 to 30 cm of sandy limestone, alternating with thin cleaved slates. These sandy limestones are locally rich in shells, and show some ammonite imprints belonging to *Tropites* sp., *Jovites* sp. aff. *J. daciformis* Diener, spirifers, and crinoids.

   These two horizons above could be allotted to the Late Carnian or perhaps to the beginning of Norian.
   c. Alternations of dark gray to black, finely sandy slates (frequently calcareous and micaceous), and medium- to thick-bedded, rather compact, marly limestones or sandy limestones (about 50 m).
   d. Several intercalations of blue-gray sandy limestone beds displaying a brown patina, separated by the more cleaved sets; the upper 5 m of the calcareous beds (limestones and shales), which is prominent in the landscape, contains badly preserved, infrequent imprints of ammonites (25–30 m).
   e. Micaceous sandy shales with a brown patina contain intercalations of medium-bedded sandy or siliceous limestones with bivalves and brachiopods (approximately 50 m).
   f. A brown-gray colored, rather clean, calcareous sandstone slab, with an ocher patina, rich in intact pieces or fragments of bivalves (2.50 m).
   g. Micaceous gray shales with intercalations of some thin calcareous sandstone beds, displaying an ocher patina

(30 m), containing *Juvavites molengraaffi* Welter, *Juvavites* sp., *Metacarnites floridus* Wulf, and *Tibetites* cf. *T. ryalli* Mojsisovics.

h. Feebly calcareous, compact, brown sandstone, protruding from the topography (6.50 m).
i. Rather soft shales, sometimes a little sandy, with some beds of sandy limestones in the lower part, and gray-pink micaceous and calcareous sandstones in the upper part (approximately 150 m).
j. Beyond the col, there is a soft shaly sequence with a visible thickness of 50–60 m. In the middle of the shales, one finds initially some red calcareous sandstone beds, occasionally with pebbles of black limestone, and farther up, gray or greenish brown micaceous sandstones. At the base of this sequence was found *Distichites* sp.
k. Green siliceous sandstone with some brown or white sandstone intercalations (at least 60 m).
l. White sandstone.

The fauna representing Horizon "g" belongs to the Norian, whereas the fauna of Horizon "j" constitutes the Late Norian. Probably, the compact sandy sequence of Horizon "k" represents the Rhaetian. The limit between the Norian and Rhaetian was placed, for purely lithological reasons, at the base of a thick (80–300 m), green or white, unfossiliferous, sandy sequence. There is a possibility that it still belongs to the Late Norian. It seems, in any case, that there is (from Horizon "a" to "l") a very thick (350–400 m), continuous sequence, comprising the inferred Rhaetian, entire Norian, and perhaps the top of Carnian (Mouterde 1971, p. 131). Krystyn (1982) gives a detailed description of the Late Carnian–Middle Norian ammonite fauna from Jomsom (Chap. 21).

24.10 Latest Triassic (Rhaetian)

The inferred Rhaetian Stage is represented by a relatively massive sandy succession at the base, and, above it, an alternation of thin sandy limestone, marl, and marly limestone (Mouterde 1971, p. 134). This sequence occurs to the north of the east–west-trending Triassic band, extending from Jomsom and Thini to Tilicho. The Late Triassics also form several faulted anticlines in the Kali Gandaki Valley to the north of Jomsom. The sandstones are also well developed in the western slopes of the col of Tilicho.

The lower sandy succession is constituted of white or green sandstones or quartzites, with a total thickness of about 100 m. They are fine-grained, compact, at first gray-rosy, then a little brownish, and sometimes are speckled with rust. They also frequently exhibit cross-lamination, and attain a thickness of 25 m. Under the microscope, the sandstones are predominated by quartz, displaying irregular, polygonal, or subrounded grains. Some of the grains contain hexagonal inclusions. There are also grains of feldspar, biotite, of rare muscovite, colored sphene, zircon, and brown tourmaline. These green sandstones are also quite extensive along the North Thini Khola, where they are more than 100 m thick, and form a cliff on the south bank of the river. On the other bank, along the torrent going down from the east part of the upper col of Thini, these green sandstones are followed by an approximately 15 m thick succession of white or slightly rosy, medium-bedded (20–30 cm), compact, siliceous sandstones. Above them is an alternating sequence of sandstones, shales, limestones, and dolomites of the late Rhaetian. Farther east, near the col of Tilicho, the subvertical, thickly bedded sandstones of the early Rhaetian are 200–300-m thick. At the base, that is, at the contact with the Late Norian, they have a russet-red color, and still alternate with shales or greenish sandstones (approximately 100 m). In certain horizons, they contain lumachelle beds with bivalves.

The late Rhaetian is characterized by a conspicuous stratification of sandy or dolomitic limestones and softer marly strata. The sandstones dominate at the base, then sandy limestones and dolomites alternate with marly horizons, and they gradually pass into bioclastic or oolitic limestones, presumably representing the Early Jurassic. In the upper third of the sequence, a horizon of red-brown nodular limestone constantly appears, accompanied by green and brown mudstones and brownish dolomites. This horizon is visible from afar.

On the slopes between Jomsom and Thini, there is a subvertical to slightly overturned sequence, where stratigraphically above the rosy or brownish sandstones with cross-laminae, the following succession continues from the southwest to the northeast.

(a) A dolomite bed with crystallized dolomite nodules (2.50 m)
(b) A sequence of dolomitic sandstones and limestones (21 m)

The last quartzite bed, in particular, shows many worm tracks, and also contains some plagioclase and dolomite grains. It locally contains an argillaceous cement.

(c) An alternation of green marl and lumachellic limestone (12 m) contains many bivalves, among which *Ostrea* cf. *O. nodosa* Sow. and *Paleocardita* sp., are discernible
(d) Rather thin limestone beds with a brecciated horizon at the base (5 m). Under the microscope, one distinguishes Echinodermata with blurred structure and sparry cement
(e) Sandstones alternating with black shales, followed by micaceous sandstones, containing carbonaceous remains and worm tracks or tubes (9 m)
(f) Red-purple, somewhat nodular limestones and green or orange shales, constituting a softer horizon (4 m)
(g) Thin-bedded sandstones, followed by massive black limestones, at the top an alternation of sandstone and limestone (17 m)

(h) Massive limestones with a brown patina and cross-lamination, which begin with dolomitic horizons and end in thinner gray-blue or black calcareous beds, containing oysters, pectinids, and crinoid ossicles (23.50 m)
(i) Soft marls and sandstones with a brown-ocher patina (2.50 m)
(j) A few-meter–thick, uniformly bedded, calcareous succession, presumably belonging to the Early Jurassic (Mouterde 1971, p. 136).

24.11 Triassic Lithostratigraphy

Resting conformably on the Paleozoics, the Triassics commence with a short sandy episode, whose base is irregular. The Early Triassic deposits are mainly limestones, whereas those of the latest Paleozoic are primarily terrigenous strata. The sandstones with a calcareous cement constitute the base of the Triassic, and they give way, quickly, to marly limestones in nodular beds, which contain a fauna of the lower and middle parts of the Early Triassic (40–50 m): *Ophiceras* sp., *Xenodiscus bittney*, *X. rotula*, *Meekoceras lillangense*, and *Clypeoceras spitiense*. It seems that the horizon below the *Otoceras* zone is not represented. Elsewhere, the similar or more compact limestones gave *Flemingites*, *Meekoceras*, and *Anasibirites,* which mark rather the middle and upper parts of the Early Triassic. The Anisian and Ladinian are made up of thick (about 200 m) shales, often affected by landslips. The lower part of the limestone beds yielded *Ceratites* sp. cf. *C. trinodosus and ?Episageceras* sp. The shales contain ill-preserved imprints of *Protrachyceras, Trachyceras*, and the daonellids are frequent everywhere. The Late Triassic (i.e., Carnian and Norian) is much thicker (at least 500 m), and consists of shales, alternating with rather fossiliferous beds of sandstone and limestone. The Early Carnian of shales and thin-bedded sandy limestones, gave *Trachyceras*, *Joannites*, *Arcestes,* and *Arpadites*. The Late Carnian and Early Norian gave a rather abundant fauna of well-preserved *Juvavites, Parajuvavites, Tibetites, and Metacarnites*. In the middle (and ?Late) Carnian, the shales prevail with graywacke beds, containing the ammonite molds of *cyrtopleurites*, *Helictites Thetidites*, and *Dittmarites* (Mouterde 1971, p. 138).

24.11.1 Tamba Kurkur Formation (Early Triassic)

The Tamba Kurkur Formation is 30–50-m thick in the vicinity of Thini, and is made up of the following five subunits (von Rad et al. 1994).

1. Subunit A is up to 2.5-m thick and comprises a reddish brown-weathering, gray sandy limestone with many ammonites on the knobby surface and conodonts of Griesbachian age. The medium-bedded nodular limestones alternate with black shales. It contains *Glyptophiceras* sp. juv. and the conodonts *Neogondolella nevadensis, N. planata, N.* cf. *N.eflecta.*
2. Subunit B is a more than 20 m thick shale with thin siltstone intercalations. A carbonaceous shale bed of this unit yielded many marine acritarchs (*Veryhachium* sp. and *Micrhystridium* sp.) as well as various spors and Dienerian conodonts.
3. Subunit C consists of two beds of reddish brown grainstone (biomicrite) or mollusc floatstone. The lower 38 cm thick marker bed yields many brachiopods, ammonites, belemnites, molluscs, foraminifera, and crinoids. It yielded the ammonite *Paranannites* sp. juv., indicating a Smithian age. This bed also contains many other ammonites such as *Flemingites* sp., *Meekoceras* sp., and *Anasibirites* sp.
4. Subunit D is about 4 m thick and contains gray to dark gray shale with carbonate concretions and a few sandy or silty intercalations. A thin (10 cm) bed consists of green-gray, moderately sorted, clayey silty sandstone. Another intercalated bed is represented by red-brown parallel- as well as ripple cross-laminated, ferruginous, silty limestone.
5. Subunit E attains a thickness of 10 m and comprises medium-bedded (30–50 cm) gray and reddish brown, nodular marl and clay-rich micritic limestone with very thin (less than 1 cm) flaser-like clay laminae. The limestones represent pelagic wackestone. The top part of the nodular limestone bed yielded conodonts, including *Neospathodus homei, N. gondolelloides, Ellisonia* sp., and *Xaniognathus* sp., indicating a late Spathian age.

Subunits A, C, and E represent a condensed sequence of deep (bathyal) carbonate environments, far from terrigenous influx. On the other hand, the practically quartz-free micritic limestone was formed in relatively deep (several hundred meters) water.

24.11.2 Lower Part of Mukut Formation (? Ladinian–Early Carnian)

It is represented by an approximately 30 m thick succession of thin-bedded micritic limestone, marl, and shale (von Rad et al. 1994). Its lower part comprises a thinly laminated to thin-bedded (5–15 cm) sequence of bluish gray, micritic limestone and gray shale. The limestone includes many pelecypods, crinoids, brachiopods, and small ammonites. The shales and marls are silty, contain plant fragments, and

they sometimes display fining-upwards cycles, having claystone at their top part. The upper part of the formation (i.e., between 14 and 22 m) is composed of rather thick shaly limestone beds, containing pyritous ammonites, such as *Trachyceras* cf. *T. aon* (Münster), *Tibetites* sp., and *Spiriferina* sp., together with crinoids. These fossils record an Early Carnian age. The Lower Mukut Formation was deposited in a low-energy carbonate shelf, with a moderate water depth and without any significant terrigenous influx.

24.11.3 Upper Part of Mukut Formation (Late Carnian)

It is about 350 m thick, and composed of a shale-predominated succession, displaying a gradual transition from the underlying limestone-rich formation. It is composed of a green-gray to blue-gray shale with sporadic thin beds of silty or sandy micritic limestone and marl. Medium-bedded marly limestones, mollusc-rich micritic limestones, and sandy limestones also occur. The shales include dark gray concretions with ammonites. There are also coquinas of pelecypods, gastropods, and brachiopods, including *Spiriferina.* A limestone bed contains *Ptychites* sp. (Carnian–Norian) and *Pinacoceras* sp. (Norian). The Upper Mukut Formation was also deposited on a low-energy outer shelf, presumably in a bathyal zone. The sea was shallowing upwards, as indicated by the floatstones in the upper part of the formation (von Rad et al. 1994).

24.11.4 Tarap Shale (Norian)

This formation consists of: (1) gray silty shale, rich in quartz, muscovite, feldspar, and chlorite; (2) green-gray, fissile silty sandstone, containing chlorite, mica, and quartz; (3) subarkosic sandstone with calcite or clay cement; and (4) quartz-rich bioclastic grainstone to rudstone with pelecypods, gastropods, crinoids, and fish debris. There is also a dark gray coquina with *Monotis subcircularis* Gabb, indicating a Late Norian age. The deposition environment of the Tarap Shale was a terrigenous, storm-dominated shelf or slope (von Rad et al. 1994).

24.11.5 Thini Formation (Quartzite Formation, Late Norian–Rhaetian)

Its type locality lies on the left bank of the Kali Gandaki, about 500 m east of Jomsom, where it is about 130 m thick (Gradstein et al. 1992, p. 17). It gradationally passes into the overlying Jomosom Formation, with an approximately 30 m thick passage zone (Fig. 24.11). There are mainly three lithologies in the Thini Formation. The first predominating component is represented by quartzose sandstones, comprising about 80 % of the exposed thickness. They are white to pale yellow colored with a few red beds. These medium- to thick-bedded sandstones are fine- to coarse-grained, and well-cemented. Generally, they are cross-laminated with trough as well as planar sets. The second rock type is represented by siltstones (85 %) and sandstone (15 %) thin alternations. The siltstones are green to green-gray in color, massive, and contain carbonaceous laminae, whereas some sandstone beds contain mudstone intraclasts. The third unit comprises fossiliferous conglomerates (less than 5 % of the total thickness). They form medium to thin (a few centimeters to 40 cm) lenses and layers with pebbles of red ferruginous clasts, black cherty clasts, and gray mudstone clasts, with rhynchonellid brachiopod and bivalve fragments. *Scolithos* sp. and *Paleophycusheberti* burrows are frequent in several sandstone beds. Generally, a red ferruginous sandstone bed overlies the conglomerates. The Thini Formation shows bimodal paleoflow directions with a pronounced northerly flow (Gradstein et al. 1992, pp. 19–20).

The subarkosic sandstones contain predominantly quartz with some feldspar. They also have a minor amount of plagioclase, microcline, perthite, muscovite, tourmaline, zircon, and phyllite fragments. The ferruginous sandstones are also quartz-rich, but they contain a carbonate cement with abundant hematite (Gradstein et al. 1992, p. 20).

The occurrence of brachiopods and crinoids indicates marine environments. Vertical burrows of *Skolithos* sp. could have been formed in a shallow marine environment, including estuarine point bars, whereas the occurrence of vascular plant debris entails proximity to terrestrial conditions. Hence, the Thini Formation was deposited in coastal conditions characterized by tidal inlets and estuaries (Gradstein et al. 1992, p. 22).

24.12 Early Jurassic

The Early Jurassic Epoch is represented by the Jomosom Limestone (Bodenhausen et al. 1964, p. 109), which forms a thick succession of appreciably east–west trending beds, between Jomsom and the Lupra Khola. These beds envelop the Triassic strata. At the east end of the Thakkhola Valley, these limestones continue as imposing masses with multiple folds. These great compact limestones are constituted of gray-blue or black bioclastic or oolitic varieties, and form extensive cliffs or jagged peaks. Their thickness reaches several hundred meters, and they are about 400 m thick at Jomsom. In spite of the absence of index fossils, they were allotted to the Early Jurassic, because they rest on sandy or shaly alternations and limestones of the late Rhaetian, and are succeeded by the sandy layers or marly limestones,

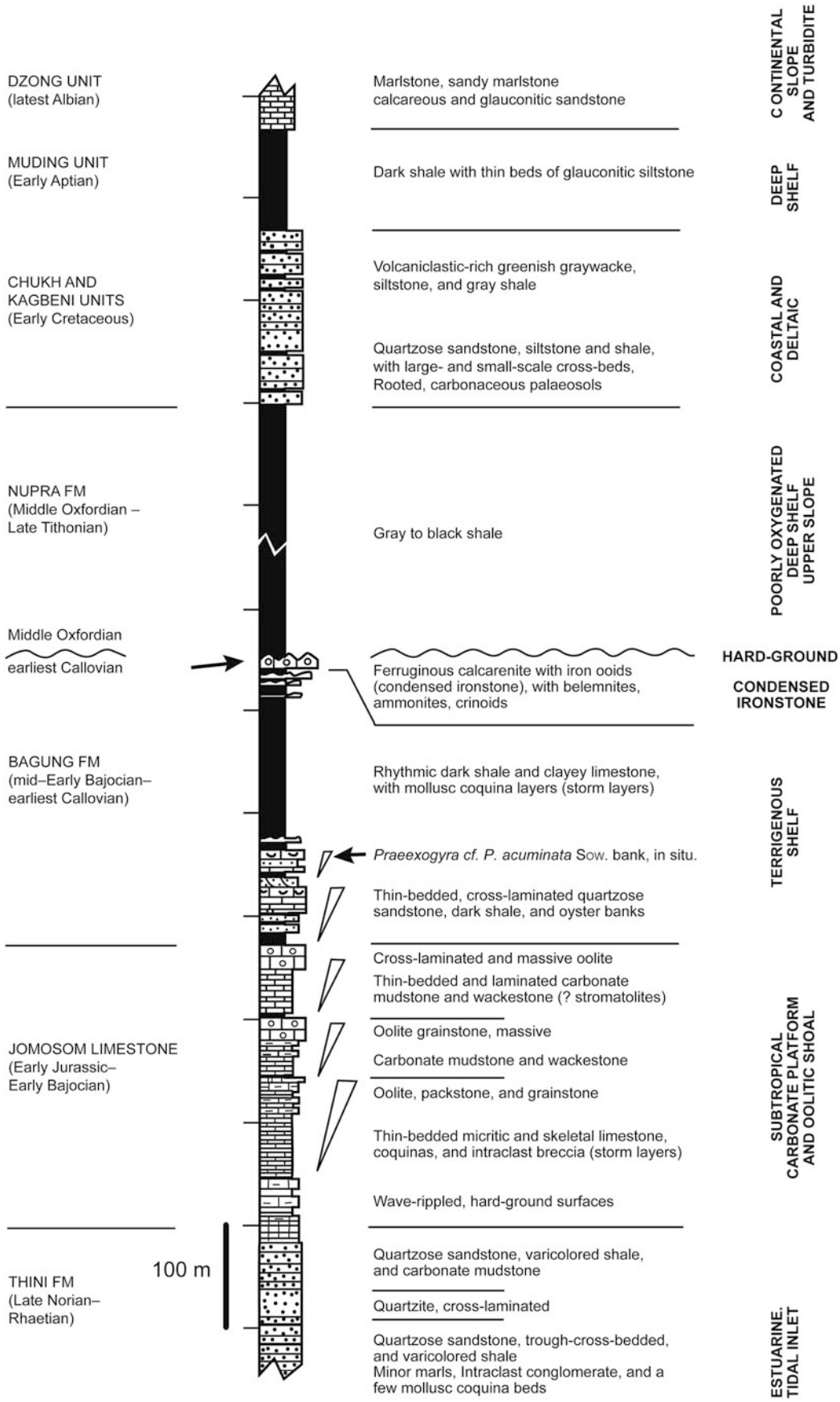

Fig. 24.11 Lithostratigraphy of the Late Triassic–Early Cretaceous sequence in the Thakkhola. *Source* Modified from Gradstein et al. (1992)

which provided two specimens of *Sonninia*, belonging to the Early Bajocian.

On the right bank of the Kali Gandaki, to the south of the bridge of Jomsom, rises an abrupt cliff of some 300 m in height. The rocks forming the cliff regularly dip due northeast, and they are made up of massive limestone beds, alternating with thinner varieties. Towards the south, the cliff turns to the west along a small torrent. The following sequence commences with the lowest horizon on the southwest face.

1. The limestones (40 m) appear first, where they are either thick (0.5–1 m) or thin (0.10–0.25 m), and separated by shale partings or thin bands from marly limestones, containing frequent fucoids. The limestones are generally black, compact, and fine-grained, but, at the base, they are associated with irregular bioclastic lenses or sandy limestones, displaying a brown sheen. In the lower part, they contain remains of bivalves, small gastropods, and sea urchins. Sometimes, the sediments are intimately mixed up. Under the microscope, the rock is a cryptocrystalline, fine-grained, quartzose limestone with bioclastic bands, and it contains *Glomospira* sp., *Globochaete* sp., *Nodosaria, Vidalina martana* Farinacci, and other micro-organisms (Mouterde 1971, p. 140).
2. About 30 m above the base, the limestones, with fine gravels and fragments of rolled organisms, are more frequent, and they contain some small foraminifera and other micro-organisms, replaced by pyrite.
3. On the south slope of the cliff, from 30–50 m above the base, there are very thick (1–3 m) or thin limestones, separated by fine shale partings. Generally, the limestone is black, compact, and fine-grained. It is associated with sandy limestone lenses or cross-laminated beds, occasionally displaying ripple marks. The sandy beds contain bioclastic debris of oysters as well as gastropod molds, whereas the marly beds include fucoids. Under the microscope, the limestones are cryptocrystalline with oolitic or gravelly zones as well as fine remains of molluscs and echinoderms, and light colored fine-grained quartzose limestones. They contain small foraminifera: *Glomospira* sp., *Aeolissacus* sp., and other fossils.
4. Farther up-section, the limestones become more oolitic or gravelly. Beyond two sulfurous hot springs, very thick (1–2 m) limestones alternate with thinner ones and some shale partings for about 40 m. The compact limestones are always associated with some irregularly bedded, lighter colored, rather sandy limestones containing fragments of bivalves, gastropods, and crinoids. They also contain the foraminifera *Glomospira* sp., small Lituolides, Ataxophramoides, or Trochamminides (Mouterde 1971, p. 142).
5. The medium- to thin-bedded limestones continue farther for about 70 m. They are lighter colored at the base, frequently irregularly bedded, and contain many smaller foraminifera. This unit ends at a 4–5 m thick limestone bed.
6. It is a thick- to very thick-bedded (1–5 m) limestone succession, attaining a thickness of 50 m. It is sometimes finely oolitic or gravelly, in places more compact, and occasionally slightly sandy or regularly crystalline. Under the microscope, the limestone is cryptocrystalline, and contains some small foraminifera (*Globochaecte* sp.) and echinoderm and mollusc fragments.
7. This sequence begins with thick oolitic and gravelly limestone beds, associated with more compact varieties (27 m). At the base and the top are alternating limestones and softer marly limestones. They also contain some foraminifera (*Nodosaria*) as well as echinoderm and gastropod remains.
8. It is a rather massive succession of about 100 m in thickness and with less distinct bedding. It includes mainly well-sorted and cross-laminated bioclastic limestones and dolomites. Most of the limestones are replaced by dolomites. They are frequently oolitic, contain a sparry cement and intraclasts, together with some small foraminifera, such as *Haurania*, *Nautiloculina* sp., and *Glomospira* sp., as well as molluscs, echinoderms, and bryozoans.
9. This sequence comprises thinly bedded (10–40 cm) limestones, alternating with shales or soft limestones (25–30 m). There are always bioclastic, gravelly, or oolitic limestones, alternating with finer-grained dolomitic or sandy limestones. Under the microscope, the lumachellic limestone contains microcrystalline cement with small foraminifera, oolites, and oysters. The fine-grained sandy limestone contains echinoderm and molluscan remains.
10. It is an alternation of rather coarse bioclastic limestone, compact limestone, and fawn or ocher sandstone with cross-lamination (17 m). Based on the microfauna, probably, this unit belongs to the Middle Jurassic.

Thus, this thick (350–400 m) succession of bioclastic and finely quartzose limestones (which are locally dolomitic) received ooids and some sandy detritus from time to time. The microfauna suggests that most of it belongs to the Early Jurassic, and the last horizon has affinities with the Middle Jurassic (Mouterde 1971, p. 142). This formation is lithologically equivalent to the Kioto Limestone in the Mahakali region (Chap. 22) and Dolpa (Chap. 23).

24.13 Middle Jurassic

The Middle Jurassic rocks (Fig. 24.12) crop out in east–west trending bands, located to the north of the main Early Jurassic succession. Their most prominent exposures extend from the south of Dangarjong to the banks of the Lupra Khola. The limit between the Middle and Early Jurassic is difficult to establish. Mouterde (1971, p. 146) has designated the boundary at the base of the sandy facies, appearing at Jomsom as intercalations at the top of the Early Jurassic limestones. At Jomsom, the uppermost sandy beds yielded *Sonninia* cf. *S. deltafalcata* Quenst., indicating the top of the Early Bajocian.

The Middle Jurassic contains some sandy beds at several locations (e.g., in the Kali Gandaki Valley, south of the upper spur of Thini), however, it is mainly a calcareous succession, consisting of compact, occasionally sandy or marly limestone alternations in decimetric beds and soft limestones or shales with frequent lumachelle horizons, containing oysters. These alternations are followed by some thick beds of compact limestone with a brown patina, and, in turn, are covered by soft marly limestones, containing ferruginous oolites and Early Callovian fossils.

The above-described Jomsom Limestone, exposed to the south of the bridge of Jomsom, whose last part perhaps already belongs to the Middle Jurassic, is succeeded by the following strata towards the north (Mouterde 1971, p. 147).

1. A rather soft sequence of compact nodular limestone, gravelly and bioclastic limestone, soft marly limestone, and fine sandstone of ocher color or with a dark brown patina. In these rocks, the gravels are generally coarse and irregular, and their debris contains molluscan

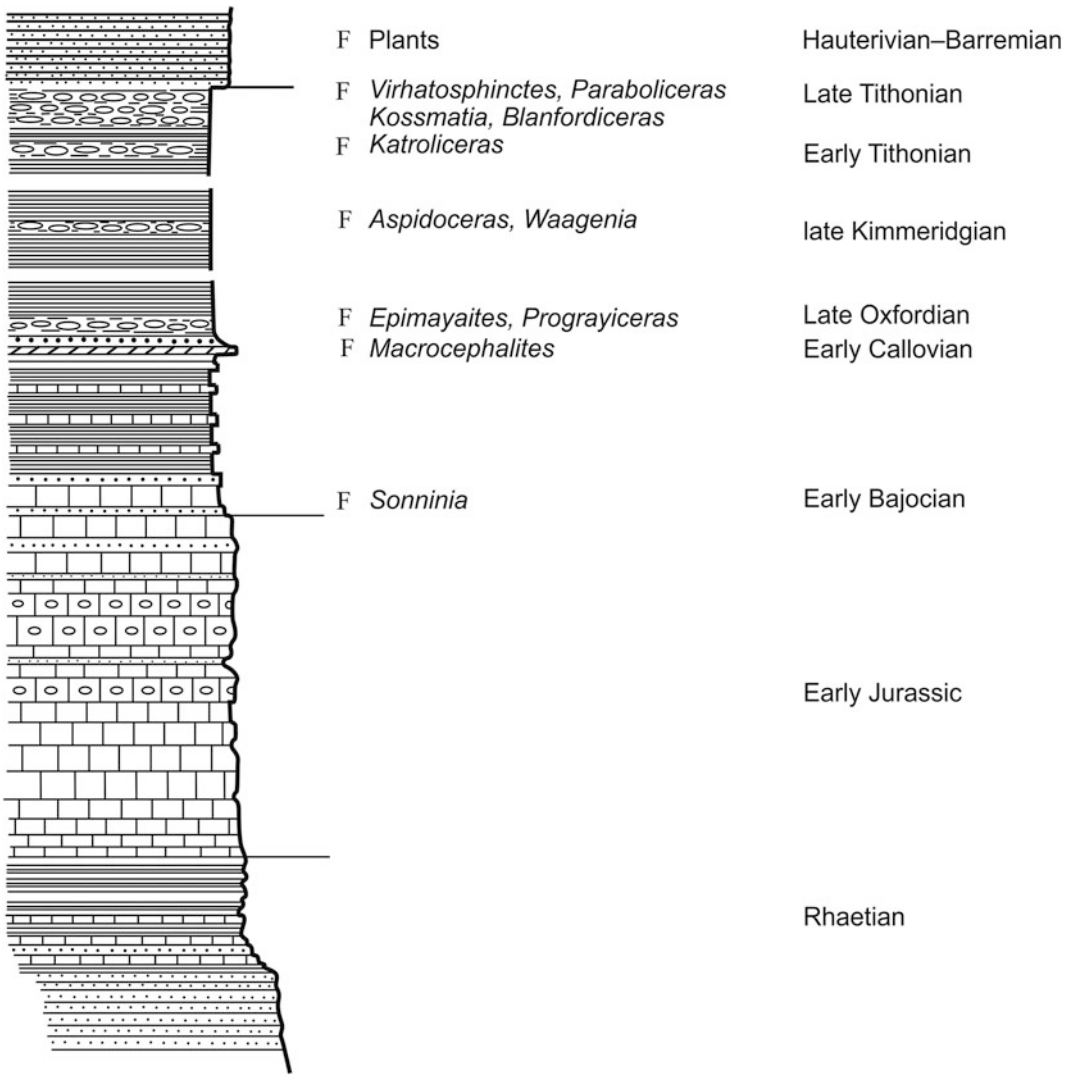

Fig. 24.12 The Jurassic section exposed to the west of Jomsom. *Source* Modified from Mouterde (1971). © Centre National de la Recherche Scientifique, Paris, France. Used by permission

fragments, in particular of oysters, with small foraminifera and incomplete sections of varied Lituolides (25 m).

2. An alternation of lumachelle with oysters, sandstone, and sandy limestone (visible for 5 m). The last sandy limestone bed, which is regularly laminated, contains irregular sandstone clasts in its upper part.

The most suitable point to observe the whole of the Middle and Late Jurassic as well as the Cretaceous sandstones, lies opposite the same Jurassic sequence, exposed on the southwest face of a small tributary torrent of the Kali Gandaki. Beyond the cliff, the marly or shaly limestone beds form a slope with escarpments, and the section is as following.

(a) Rather compact beds of calcareous sandstone with cross-lamination.
(b) Medium-bedded (20–30 cm), bioclastic, calcareous sandstone (2.50 m), containing *Sonninia* cf. *S. deltafalcata* Quenst.
(c) Thick (30–50 cm) beds of gray-brown, compact limestone with oysters and shale partings (5–6 m).
(d) Alternations of thin (10–15 cm), gray, finely quartzose or siliceous, slightly marly limestone, thin (10–20 cm) beds or lenses of sandstone and marl. In the higher part, the calcareous shales prevail with red sandy limestones, containing oysters (30 m).
(e) Thick (30–50 cm) beds of very clean limestone with many oysters, overlain by finely micaceous and sandy blue-gray calcareous shales (6 m).
(f) About 20 cm thick beds of blue calcareous sandstone, with a brown patina, separated by 50 cm thick shale beds (2 m).
(g) Soft marly limestones and marls with some sandstone beds, and very feeble schists at the base, and finely sandy and micaceous beds in the higher part (60–70 m).
(h) Alternations of shales and sandy limestones with a brown patina, full of oysters, especially in the three upper beds (15 m).
(i) Soft shales (5 m).
(j) Limestone beds (5 m), containing at the base an irregular bed (10–15 cm) of ferruginous sandstone with a brown patina. Belemnites are frequent in a coarse calcareous sandstone bed.
(k) Slightly sandy, soft limestone beds with ferruginous oolites (1–2 m), containing *Rhynchonella* sp.
(l) Black shales, exposed for about 150 m, containing septaria and other concretions.

Although Horizon "b" is well dated to the Early Bajocian, it is difficult to place a precise boundary between the Bajocian and Bathonian, because the facies with oysters is rather homogeneous. The sequence is mainly terrigenous and contains many sandstone beds. The summit is dated better: the calcareous Horizon "j" and limestones with ferruginous oolites of Horizon "h" belong to the Early Callovian and the black shales of Horizon "i" can be attributed to the Late Jurassic.

To the south of the confluence of the Lupra Khola, on the right bank of the Kali Gandaki, the Middle Jurassic constitutes the south flank of a faulted anticline. There are about 100 m thick laminated black marls, alternating with brownish limestones rich in oysters, crinoids, brachiopods, and belemnites. At the top, there are some gray and red compact limestone beds (4 m), containing large belemnites that Mouterde (1971, p. 150) has attributed to the Callovian. They underlie the black shales of the Late Jurassic.

Farther north, opposite Bagung, on the left bank of the Kali Gandaki, the Middle Jurassic rocks are extensively exposed. There is an anticline consisting of the following succession.

- Alternations of micaceous shaly marls and compact limestones or lumachelles of oysters with small belemnites, in rather thin beds (visible for about 20 m)
- Some bluish gray limestone beds, exhibiting a brown patina and containing belemnites (2 m)
- A blue-gray marly limestone with a brown patina, containing many fragments of macrocephalitids and belemnites (0.50 m).

These two last units belong to the Callovian.

Beyond the black shales belonging to the Late Jurassic, there is a large anticline, representing a more complete section of the Middle Jurassic. On top of the massive Early Jurassic limestones, the following sequence is exposed successively from north to south.

a. A gray-blue sandy limestone with lumachelles of bivalves (*Grammatodon* cf. *G. virgatus*) and oysters. These medium-bedded (20–30 cm) limestones alternate with brown sandstones containing some shells (10 m).
b. Weathered beds of thin, compact, marly limestone, alternating with shaly marls, generally without fossils, but with some highly fossiliferous sandy limestone intercalations, containing *Ostrea accuminata* Sow., *Ostrea* sp., and *Grammatodon* sp.
c. A succession of soft, marly shale (about 50 m) with light brown micaceous sandstone, irregular-bedded red sandstone, and sandy limestone with lumachelles of oysters (*Hybolites* sp. gr. *fleurianus* d'Orb. and *Lucina* sp.). Towards the middle of the succession, there is about 1 m thick red calcareous sandstone, displaying fine cross-lamination.
d. Thick-bedded (40–50 cm), slightly marly, compact limestone with soft shale partings (15–20 m).
e. Soft shales with some lumachelle beds, marly limestones, or sandy beds, with oysters and pectinids (25 m).

f. Compact marly limestones, alternating with shaly marls. At the top, there are lumachelle beds containing oysters, pectinids, *Belemnopsis*, and *Hybolites* sp. (20–30 m).
g. Shaly marls, alternating with lumachelles of *Ostrea accuminata* Sow., *Ostrea* sp. *Belemnopsis* sp., and pectinids (15–20 m).
h. Massive beds of brown compact limestone, rich in belemnites (3 m).
i. Soft, brown, marly limestone with black-cored ferruginous oolites, with *Indosphinctes* gr. *urbanus* Loczy, *Macrocephalites* sp., large Opellide *Oxycerites* sp. (20–30 cm).
j. Black shales with *Mayaites*.

According to Mouterde (1971, p. 151), the soft succession of about 200 m in thickness belongs almost totally to the Bajocian and Bathonian (Horizons "a" to "f"). He has attributed to the Callovian the compact limestone with belemnites (Horizon "h") and the limestones with ferruginous oolites (Horizon "i"), whereas the marls with *Mayaites* (Horizon "j") to the Late Oxfordian. He obtained an Early Callovian fauna from the exposures on the trail from Jomsom to Dangarjong, where there were marly limestones with a red sheen, containing *Indocephalites chrysoolithicus* Waagen, *Macrocephalites formosus* Spath, and *Macrocephalites* sp.

24.13.1 Lateral Continuity

The calcareous and terrigenous sequences from the Bajocian and Bathonian have an overall constancy in the facies. At the base, there are frequent sandy horizons, which mark a rather abrupt arrival of detritus, corresponding to an interruption between the prevalent bioclastic calcareous sedimentation of the Early Jurassic and that of more argillaceous of the Middle Jurassic with persistent lumachelle horizons of oysters. These conditions extended over vast geographical regions. The lumachelles and marly limestones of the Middle Jurassic are identical to those of the Laptal Formation, only known in the northwest of Kumaun, and which develops even more in the west in the area of Spiti.

The not very thick Callovian is very consistent: it comprises a compact limestone in thick (4–5 m) strata, succeeded by some marly limestone beds with ferruginous oolites and the fauna of Early Callovian. Thus the Callovian marks a relatively abrupt return to a calcareous sedimentation with rather coarse detrital contribution. This mode of sedimentation is established on vast territories, because the lithological facies is identical to that of Spiti, and thus extends on a notable part of the northern fringe of the Himalayan chain. However, close to Tinkar Lipu (Chap. 22), faunas show a well-developed Callovian succession, whereas in the Thakkhola, the Early Callovian alone is present.

24.14 Late Jurassic

In the Thakkhola, above the Early Callovian limestones with ferruginous oolites and after a Middle Callovian–Early Oxfordian gap, there is a very uniform and monotonous succession of black slates and other pelitic rocks (Fig. 24.12) with a variable thickness (150–500 m). These slates are equivalent to the Spiti Shales, contain black concretions with a dark or brownish patina in some horizons, and at certain intervals, quite frequently enclose rather large concretions with septaria structures and ammonites or bivalves.

To the southwest of Jomsom, these slates constitute a moderately inclined slope, and their thickness approximates 150 m. They contain rather large nodules with the following fossils (Mouterde 1971, p. 154).

Epimayaites cf. *E. patella* Waagen.
Prograyiceras sp.
?Grayiceras n. sp.

These fossils belong to the Late Oxfordian, but there are also fragments of *Blanfordiceras* sp. in the debris, representing the Late Tithonian. These shales thus contain nodules, coming from two quite different sources. To about 600 m north, on the prominent slopes of Jomsom, on the south side of the syncline the core of which is composed of the Cretaceous sandstones, the following Late Oxfordian fauna was recovered: *Epimayaites falcoides* Spath, *Prograyiceras* sp. fragment, and "*Perisphinctes*" sp.

On the direct track from Jomsom to Dangarjong, shortly after the passage of the col where Callovian horizons are exposed, the black slates initially contain a fauna of Late Oxfordian (*Prograyiceras* aff. *furoni* Collignon, *Epimayaites* sp.) and 250 m farther north, closer to Dangarjong, there is a zone with Acanthicum, *Aspidoceras* gr. *unispinosum* Quenst., and *Asp*. (*Pseudowaagenia*) *microplum* Oppel, with which were associated *Ulhigites* sp. and *Paraboliceras* sp. fragments, representing a Kimmeridgian fauna. Not far from there, the dislodged large concretions with septaria structures contain many inoceramid bivalves and *Kossmatia* sp. In this area, the nodules belong to the three levels: Late Oxfordian, Kimmeridgian, and Late Tithonian.

To the north of Dangarjong, close to the Dangarjong Fault, a first outcrop to the west of Kagbeni provided *Epimayaites* sp. of the Late Oxfordian. About 4 km farther west, Mouterde (1971, p. 155) collected *Kranaosphinctes indogermanus* Waagen of the Middle Oxfordian, and just near the fault, *Kossmatia* sp. and *Paraboliceras* cf. *P. crytoptychus* Uhlig of the Late Tithonian.

Around Lupra, the Late Jurassic contains higher horizons than those containing P*rograyiceras* and *Epimayaites.* To the east of the village in the valley of Lupra Khola, Mouterde (1971, p. 155) collected *Orthosphinctes* sp. and *Prograyiceras grayi* Spath.

A very good outcrop of the Late Tithonian is present at the village of Chhokhor, where the subvertical beds can be separated into the following three levels (Mouterde 1971, p. 157).

The beds located to the east, probably the lowest, gave: *Aspidoceras* cf. *A. euomphalum* Steuer, *Blanfordiceras* gr. *celebrant* Uhlig fragment, *Bl. subquadratum* Uhlig, *Bl.* cf. *Bl. wallichi* Gray, *Paraboliceras polysphinctum* Uhlig, *Par. cryptoptychum* Uhlig, *Par. fascicostatum* Uhlig, *Par. recticostatum* Uhlig, *Kossmatia tenuistriata* Gray, *Kos. desmidoptycha* Uhlig, *Kos.* gr. *fascicostata* Uhlig, *Aulacosphinctoides* sp. fragment, *Virgatosphincts falloti* Collignon fragment, *and Belemnites uhligi* Stevens.

The middle beds yielded: *Blanfordiceras wallichi* Gray, *Bl. Boehmi* Uhlig, *Bl.* cf. *Bl. tenuicostatum* Collignon, *Paraboliceras haugi* Uhlig fragment, *Substeueroceras* sp., *Kossmatia* sp., *Aulacosphinctes morikeanus* Oppel, *Virgatosphinctes* cf. *Virg. rotundidoma* Uhlig, *Virg.* cf. *Virg. falloti* Collignon, *Uhligites* sp., and *Rhynchonella* sp.

The northern slopes of the Muktinath Valley still contain shales of the Late Jurassic. On the track to Damodarkund, at the col, there are many *Prograyiceras* cf. *P. grayi* Spath and *Epimayaites* sp. of the Late Oxfordian, but some *Blanfordiceras*, probably slipped, indicate the presence of a band, belonging to the Late Tithonian.

Many Late Jurassic ammonites are found in the terraces of the Kali Gandaki and its affluents, in particular around Tangbe. The Holocene alluvial deposits extending beyond Tukuche also contain some ammonites. Among them, there are *Virgatosphinctes* cf. *Virg. raja* Uhlig, *Virg. rotundidoma* Uhlig, *Orthosphinctes* gr. *colubrinus,* and especially a fragment of *Peltoceras* (*Peltoceratoides*) gr. *propinquans* Waagen, which is the only taxa belonging to the Early Oxfordian.

24.15 Jurassic Lithostratigraphy

Gradstein et al. (1992) classified the Jurassic strata of the Thakkhola area into the following lithostratigraphic units.

24.15.1 Jomosom Limestone (Kioto Limestone, Early Jurassic)

The Jomosom Limestone comprises thin to thick beds, alternating with sandy or marly shales. The limestone is oolitic, bioclastic, and micritic. This formation consists of the following nine lithological units (Gradstein et al. 1992; Fig. 24.11).

Unit A is made up of thin-bedded limestone and shale or sandy shale alternations. The dark gray limestone is made up of skeletal carbonate mudstone or wackestone, and contains bivalve and brachiopod debris with infrequent bryozoan, sponge, echinoderm, and coral fragments together with some ooids and oncoids. Their bedding surfaces are flat, infrequently wavy with ripples, and occasionally nodular. The intercalated dark gray to black shales are sometimes laminated and locally bioturbated. The sandy shales and limestones constitute 4–6 cm thick cycles, beginning with bioturbated sandy shale or marl, and grading upwards to skeletal or oolitic limestone, and terminate with a hardground.

Unit B comprises medium- to thin-bedded limestones, represented by dark gray to black calcareous wackestone and mudstone. The limestones are interbedded with white-weathering, fossiliferous shales, oolites, and beds of mollusc coquina.

Unit C represents an approximately 30 m thick succession of thick-bedded micritic, skeletal, and oolitic limestone. The beds are either massive or irregular, and alternate with thin beds of mudstone or wackestone. This unit ends with an approximately 5.5 m thick, massive, oolitic bed, displaying a sharp and locally erosive lower contact. It contains foraminifers, pelecypod fragments, and echinoid spines. The sediments of Unit C are infrequently bioturbated.

Unit D is composed of medium-bedded, white-weathering, organic-rich shale, which conformably overlies the topmost oolitic bed of Unit C.

Unit E is about 35 m thick and contains about 10 m thick, thin-bedded limestone at the base. It is succeeded upwards by irregularly bedded thick limestones.

Unit F appears as an alternating sequence of thin-bedded, massive, oolitic grainstone, and thin-bedded mottled and bioturbated micrite. The oolite beds range in thickness from 2 to 4.5 m, whereas the thin-bedded micrite beds constitute up to 1.5 m thick horizons. At the base of this unit, conspicuous white-weathering shales are found. The ooids have a thick micritic cortex, and there are also moderately to well sorted, skeletal-, oolitic-, intraclast-grainstones. Their skeletal fragments are of molluscs and echinoderm ossicles.

Unit G stands out as a major pelitic horizon, with pelletal carbonate mudstone and shale alternations. It conformably overlies the last massive oolite bed of Unit F, and is about 2 m thick.

Unit H is characterized by an approximately 50 m thick monotonous dark gray succession of medium-bedded (30–40 cm) fine-grained skeletal packstone and a minor amount of peloidal wackestone and packstone. There are also infrequent oolitic beds. The micritic limestone contains planar to wavy laminae, some hummocky cross-laminae, and intraclasts.

Unit I is about 10 m thick and includes two horizons from 2 to 6 m thick of coarse-grained, massive, well-sorted oolitic grainstone, separated by a thin-bedded and parallel-laminated sequence of fine-grained, oolitic grainstone. The coarse

oolitic limestone contains a few large pelecypod shells, algal fragments, and echinoid ossicles as well as some pellets and micrite intraclasts. This unit is rich in foraminifera.

The basal part of the Jomosom Limestone, comprising bioturbated sandy shales, was deposited in a moderately deep subtidal shelf, whereas the skeletal and oolitic limestones were formed on a shallow subtidal shelf. On the other hand, the coquinas represent storm deposits. The cyclic sequences display a shallowing-upwards depositional condition and the top beds record some periods of nondeposition, marked by the hardgrounds.

24.15.2 Bagung Formation (Lumachelle Beds and Ferruginous Oolite, Bajocian–Early Callovian)

The Bagung Formation is composed of a regular interbedding of gray marl or shale with gray-brown limestone. The limestone consists of bioclasts, micrite, or coquina, with some beds having a bituminous smell. It is divided into the following units (Gradstein et al. 1992; Fig. 24.10).

Unit L is an approximately 40 m thick succession of thin-bedded, micritic limestone, fine-grained sandstone, and shale, conformably overlying the topmost oolitic limestone of the Jomosom Formation. The dark gray limestones are fine-grained peloidal packstones and rhythmically interbedded with dark gray and green-gray shales. There are also interbedded successions of medium- to coarse-grained skeletal calcarenite (packstone and grainstone), *Praeexogyra coquina,* and thick quartzose sandstone. The sandstones and shales are frequently bioturbated by *Callianassa*-type burrows and the mollusc coquina contain many east–west aligned belemnites. Generally, the beds are graded, contain densely packed shells at the base and fine-grained skeletal grainstone at the top, and they are scoured by north–south oriented channels.

Unit M is sometimes absent owing to scouring. It is about 10 m thick, and consists of shales and marlstones.

Unit N begins with thick-bedded, yellow-weathering quartzose calcareous sandstone. The siliciclastic rocks become dominant over skeletal limestones and coquinas. There are thick sandstone successions containing shale partings; they are cross-laminated and sometimes bioturbated. This unit is about 50 m thick and shows gradual transition from the underlying unit.

Unit O also commences with a transitional contact with Unit N, and consists of sandstone successions with channel cut-and-fill structures. The sandstones pass stratigraphically upwards into shales and the succession becomes dark gray, and it contains a few 20–40 cm thick beds of bivalve coquina as well as sporadic quartzose sandstones and siltstones. The top part of Unit O is made up primarily of mollusc coquina with a minor amount of sandstone. This unit is more than 80 m thick.

Unit P is more than 15 m thick and begins with approximately 10 cm thick *Praeexogyra coquina* beds, containing very many brachiopod and pelecypod shells, belemnites, and ammonites. These bituminous-smelling "lumachelles" are bioclastic, fossiliferous grainstones or packstones.

Unit Q is represented by the "Ferruginous Oolite," made up of a ferruginous bioclastic limestone or skeletal calcarenite of more than 5 m thickness. It contains a great many belemnites and displays knobbly iron oxide coated surfaces, representing submarine hardgrounds. Under the microscope, 100–200 μ in size iron oxide oolites are present together with irregular clots and patches.

The Bagung Formation was deposited in a moderately deep subtidal shelf, which initially received a significant amount of carbonate mud and then gave way to mixed carbonate–siliciclastic deposits. The topmost Unit Q seems to be deficient in sediment supply, presumably on account of a major transgression resulting in the drowning of the source areas (Gradstein et al. 1992).

24.15.3 Nupra Formation (Spiti Shales, Middle Oxfordian–Tithonian)

There is a disconformable contact with the underlying Ferruginous Oolite of the Bagung Formation and the overlying Nupra Formation, which is more than 115 m thick in the Lupra Khola, but may be as thick as 500 m in other parts of the Thakkhola Valley. The Nupra Formation commences with about 50 m thick gray-black fissile shale, practically devoid of silt, and containing sporadic gypsum blades. But the formation becomes more silty at stratigraphically higher levels. The Nupra Formation includes a profusion of concretions, which occasionally attain more than 1 m in diameter and up to 40 cm in thickness. They display a cracked (septaria) structure with reddish brown exterior and dark gray-brown interior, and contain an ammonite nucleus. Apart from the abundant ammonites, Gradstein et al. (1992) reported a large number of textulariid agglutinated foraminifera from the lower part of the Nupra Formation. It also contains some isolated calcareous benthic foraminifera such as *Lenticulina* and *Dentalina.*

This thick and monotonous, black, pelitic succession generally begins with the Late Oxfordian and continues up to the Late Tithonian, whereas the Oxfordian fauna of Mayaitides is abundant everywhere in the Thakkhola, the Late Tithonian forms are numerous only in the Muktinath Valley and its environs. However, a specimen of *Blanfordiceras* was

collected in Jomsom and of *Paraboliceras* and *Kossmatia*, against the Dangarjong Fault of the valley close to Chukh (Chhusang). In addition to these two very fossiliferous levels, the existence of late Kimmeridgian and Early Tithonian is well established by *Aspidoceras unispinosum*, *A.* (*Pseudowaagenia*) *microplum,* and *Katroliceras pottingeri*. The very fine detrital matter constituting the slates was probably accumulated in a calm and gradually subsiding environment, whose stinking muds were favorable to the precipitation of pyrite and salts, but the micro-organisms were very rare, and the ammonites were preserved at certain levels only in nodules. These black shales are identical to the Spiti Shales, well known more in the west in Punjab, Kumaun, and at the west border of Nepal. In the Thakkhola, the marine series takes place earlier than in India, to the continental facies that marks the beginning of the Cretaceous (Mouterde 1971, p. 159).

24.16 Cretaceous

The Cretaceous System is represented, respectively, by (1) continental sandstones (lower part of Early Cretaceous); (2) a succession of black shales, green sandstones, and dark limestones (Barremian–Early Aptian); and (3) pale limestones (Late Aptian–Late Albian). These formations occupy the northwest flank of the Thakkhola Valley, that is, between Muktinath and the Dangarjong Fault, and they are delimited to the north by the Mio–Pliocene red deposits (Mouterde 1971, p. 159; Garzanti 1999).

24.16.1 Beginning of Early Cretaceous

On the right bank of the Kali Gandaki, opposite Kagbeni, the Early Cretaceous sandstones override the Aptian shales and sandstones with a faulted contact. The subvertical continental sandstones continue to the north with the following sequence.

(1a) Alternations of sandstone with a white or red patina and of black shales
(1b) Thick-bedded, white, arkosic sandstones with a pink patina, separated by some shaly bands, including conglomerates at the base and black carbonaceous shales at the top (15 m)
(1c) Pink quartz arenites succeeded by some thin sandstone beds alternating with shales (6.50 m)
(1d) Light pink quartz arenites, alternating with carbonaceous black shales and thin-bedded white or brown sandstones (7 m)
(1e) Light pink sandstones, followed by a dark wedge-shaped passage zone (6 m)
(1f) A succession of light pink arkosic sandstone (8–10 m)
(1g) A thin-bedded succession of black shales and micaceous sandstones with a brown sheen and sporadic ferruginous, noncalcareous, nodules (10 m)
(1h) Coarse-grained white sandstones (8 m) and black shales (18 m)
(1i) Grayish arkosic sandstones with plant fossils: *Ptilophyllum* (*Williamsonia*) *pecten*, *Otozamites abbreviatus*, and *Nilssonia orientalis* (15–20 m)
(1j) Black shales with a few sandstone beds (15 m)
(1k) Alternations of gray arkosic sandstone and a few shale bands (40 m)
(1l) Two gray arkosic sandstone beds separated by shales (8 m)
(1m) Shales with many nodules (30 m).

Farther up-section appear graywackes with green schists, containing bivalves. This sandy unit thus begins here with sandstones displaying a pink patina (40 m) and continues with alternations of grayish or white sandstones and shales (100–120 m).

Along the Bagung–Muktinath trail, the following succession of vertical beds is observed from south to north, under the Holocene silts and gravels.

(2a) Pebbly sandstones with quartz lenses and black pebbles (0.25 m).
(2b) Light-colored arkosic sandstones with nodules or lenses of ochrous sandy limestone (6.50 m).
(2c) Alternations of decimetric beds of cross-laminated sandstone and blue-gray calcareous shales (8 m).
(2d) Blue-gray pelitic shales with nodules of limestone and coarse sandstone (1.30 m).
(2e) Cross-laminated sandstone with limestone lenses, exhibiting an ocher patina, overlain by finely laminated shales (6.50 m).
(2f) A succession of finely micaceous gray or brown arkosic sandstones, separated by blue-gray pelitic beds (10 m). The sandstones are sometimes coarse-grained and poorly sorted, with cross-laminations; sometimes they are finer-grained. Many remains of plants, various stems, and a rather complete trunk of Araucariaces are found. The southern face of certain beds shows tracks and burrows.
(2g) Thick beds of gray to fawn or greenish gray, compact, arkosic sandstones, alternating with coarse sandstones with convolute bedding, with some sandy shales or sandy limestones (7–8 m).
(2h) Sandstones with large feldspar and quartz veins with soft pebbles, and passing into black and fawn shales (2.30 m); sporadic fossil fragments at the top.
(2i) Sandstones with a brown sheen (20 m).

Thus these continental sandstones (100–150 m) begin locally with gray-brown sandstones and shales (50 m) ("1a"). They include especially pink or white arkosic

sandstones ("1b", "1c", "1d", "1e", "1f"; "2a", "2b", "2e"), which contain horizons of white rounded quartz pebbles or conglomerates ("1b", "2a"). Above appear the finer brownish sandstones, alternating with shaly horizons and enclosing many plant remains ("1g" to "1m", "2d" to "2h"). At the top some sandstones include tests of bivalves, attributing to a marine influence characteristic of the succeeding formation (Mouterde 1971, p. 163).

24.16.2 Barremian–Early Aptian

Above the plant-bearing sandstones, comes a succession of black shales and green or gray-green slightly glauconitic sandstones, with which are intercalated calcareous sandstones or limestones with a fauna of the Early Aptian. This unit crops out in the Kagbeni–Muktinath–Chukh triangle and extends mainly on the right bank of Kali Gandaki (Mouterde 1971, p. 163).

In the Kagbeni transect, on the south slopes of the spur of Dzong, black and soft shales (100–150 m) crop up at the base and are succeeded up-section by the black shales with concretions and nodules, and green glauconitic sandstones in irregular beds. The last sandstones are occasionally rich in volcanic detritus, and the intercalated graywackes contain *Lima*, *Pecten*, and *Mytilus*. The volcanic clasts are present in the form of fine gravels. In the sandstones or the shales are intercalated compact limestones or sandstones containing lumachelles of *Trigonia* and some ammonites. The outcrops, particularly those on the track from Kagbeni to Muktinath, yielded *Deshayesites* sp.

To the north of Kagbeni, the above succession continues with a visible thickness of 150 m, and the limestones exposed on the left bank contain *Prodeshayesites* sp. and allied forms.

A little to the north of the black shales with pyritous nodules, the sandy horizons with lumachelles of bivalves gave an important fauna of *Prodeshayesites* of the group *P. lestrangei* Casey, *P. pseudokilimani* Casey, and *P. fissicostatus* Ph. More to the north still, probably coming from a lower horizon, shales with nodules gave *Tropaeum australe* Moore and a fragment of *Cheloniceras*. These rocks attain a great thickness between Tangbe and Chukh. To the southeast of Tangbe, towards its base are exposed brown or green sandstones, with intercalations of fossiliferous lumachellic horizons with bivalves and *Sanmartinoceras trautscholdi* Sinzow, *Sanmartinoceras* sp., *Deshayesites* cf. *D. calledis-cus* Casey, and *Prodeshayesites* sp.

A thick shaly series follows, towards the top of which Mouterde (1971, p. 165) obtained *Haplophylloceras strigile* Blanford. These shales are succeeded by pink and green sandstones.

The shales, exposed on a small col of the crest to the southwest of the Mio–Pliocene deposits, yielded *Cheloniceras* aff. *cornuelianum*. Thus, all this more than 500 m thick section contains the Early Aptian fossils.

The track from Tangbe to Chukh also crosses this very thick succession, consisting of the following horizons.

- An alternation of black or brown shales with white or pink micaceous sandstones, passing into carbonaceous beds
- Yellow sandstones, succeeded by green shales and sandstones
- Black shales with pyritous nodules
- An alternation of green or purplish shales and green or brown sandstones, containing ripples, worm tracks, plant debris, and bivalves
- A thick succession of black shales
- Relief-forming beds of sandy limestone
- A sequence of dark blue shales with nodules, enclosing *Aconeceras nisoides* Sarasin
- Thick beds of green-gray sandstones and sandy shales with a purplish patina, containing pyritous concretions and limestone nodules.

Thus, this sandstone succession is rather complex and very thick (more than 500 m) in the area of Tangbe. The more shaly lower part did not give any characteristic fauna, and its carbonaceous deposits indicate their continental origin. This sequence was attributed to the Berriasian–Barremian without any paleontological evidence (Mouterde 1971, p. 165). The middle and upper parts are, on the other hand, well dated to the Early Aptian by a varied ammonite fauna. The presence of bivalves and much detritus indicates sedimentation in shallow water. This series of black shales and green sandstones corresponds to the Giumal Sandstones of the Mahakali region (Chap. 22).

24.16.3 Late Aptian–Late Albian

There is a succession of pale limestones in the upper part of the spur of Dzong and the slopes east of the ruins of Muding. At its base are glauconitic sandstones containing some ill-preserved ammonites, such as those found near the track from Kagbeni to Tangbe. Above them come light gray marly limestones with traces of fucoids and rare belemnites. A thin section yielded a microfauna representing *Hedbergella infracretacea* Glas., *H.* sp. aff. *planispira* Tappan, *Globigerinelloides blowi* Bolli, *Schackoina* gr. *cabri* Sigal, and *Globorotalites aptiensis* Bett. This association very precisely indicates the passage of the lower and middle Gargasian (Mouterde 1971, p. 166). The higher part is formed of saccharoidal white limestone with large oyster fragments. However, Gradstein et al. (1992) and Garzanti (1999) have assigned a Late Albian age to this unit.

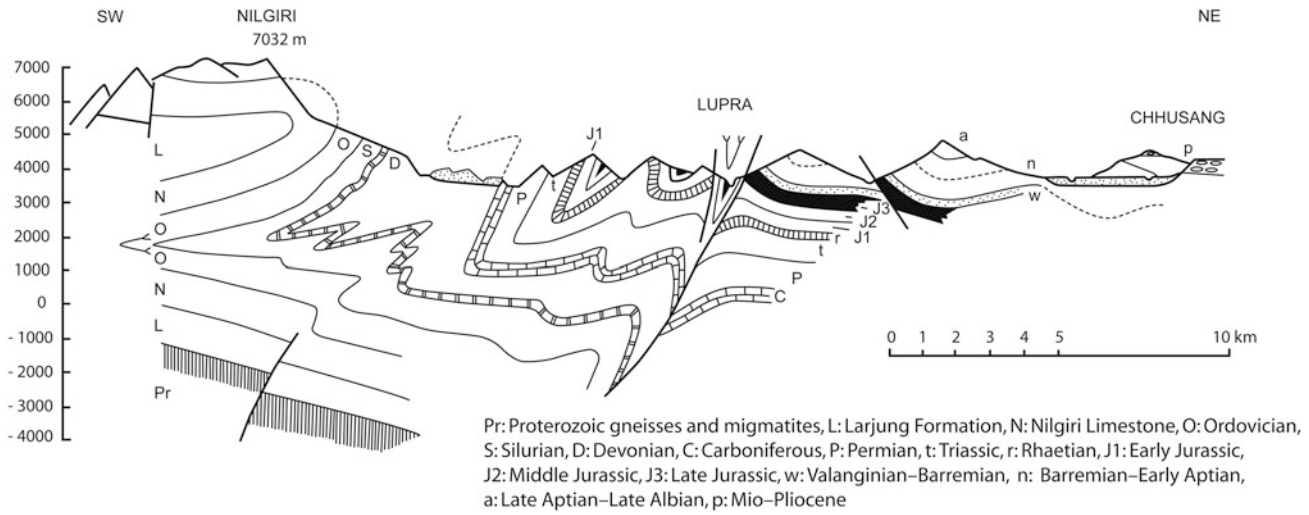

Fig. 24.13 Geological cross-section through Nilgiri, Lupra, and Chhusang, illustrating disharmonic folds and faults. *Source* Modified from Bordet (1971). © Centre National de la Recherche Scientifique, Paris, France. Used by permission

24.17 Depositional Environment of Mesozoic Sediments

The newly formed Indian margin subsided quickly in the Early Triassic (Tamba Kurkur Formation), and was covered by calcareous rocks, accumulated in the Anisian, Ladinian, and Carnian stages (Mukut Limestone). Very fine quartzo–feldspathic sediments (Tarap Shale) were deposited during Norian time, and they can be related to the rejuvenation of the Indian continental block. On the other hand, mainly pure quartz arenites (Quartzite Series), deposited during the Rhaetian, may indicate a more humid climate or subdued relief. The last unit was followed by shallow subtidal Early Jurassic limestones (Kioto Limestone), covered during Bajocian–Bathonian time by bioclastic arenites (Laptal Formation) and capped by widespread condensed ironstones (Ferruginous Oolitic Formation) in the Early Callovian (Garzanti and Pagni Frette 1991, p. 20).

The Ferruginous Oolitic Formation was followed by the black Spiti Shales, containing an abundance of ammonites, indicating their deposition in the outer shelf or slope. In the Early Cretaceous Epoch, represented by the Chukh Group (Gradstein et al. 1992; Garzanti 1999), sedimentation was affected by major geodynamic events, leading to the renewed deposition of quartzose detritus and volcanic eruptions to the south, the clasts of which are found in the deltaic sandstones. The end of the magmatic activity and delta progradation was marked by the deposition of a glauconitic condensed section, covered by Late Albian pelagic marls. This major subsidence was followed by the deposition of glauconite and phosphorite lenses or organic-rich black shales throughout the Tethys Sea (Garzanti and Pagni Frette 1991, p. 20).

24.18 Structure

The north-vergent Annapurna recumbent anticline (Fig. 24.5) is the conspicuous structure of this tract. The anticline extends for several kilometers towards the north and is thrust over other Tethyan strata at least for 15 km towards the east (Colchen 1975). Apart from this large fold, there are many other mesoscopic and small-scale disharmonic folds and north- as well as south-dipping faults in the Tethyan sedimentary sequence of the Thakkhola (Fig. 24.13). The disharmonic folds and thrusts are remarkably similar to those developed in the Tethyan sequence of the Mahakali region (Chap. 22). The north-vergent structures of the Thakkhola are related to the Annapurna Detachment, located towards the base of the sedimentary succession (Chap. 16).

References

Bodenhausen JWA, De Booy T, Egeler CG, Nijhuis HJ (1964) On the geology of central west Nepal—a preliminary note. International geological congress, report of the twenty-second session, India, part xi. Proceedings of session 11: Himalayan and Alpine Orogeny, New Delhi, pp 101–122

Bodenhausen JWA, Egeler CG (1971) On the geology of the upper Kali Gandaki Valley, Nepalese Himalayas. I. Koninkl. Nederl. Akademie van Wetensohappen—Amsterdam. Proc Ser B (Reprinted) 74(5):526–546

Bordet P (1971) La tectonique de la Thakkhola. In: Bordet P, Colchen M, Krummenacher D, Le Fort P, Mouterde R, Rémi M (eds) Recherches géologiques dans l'Himalaya du Népal, région de la Thakkhola. Centre National de la Recherche Scientifique, Paris, pp 205–232

Bordet P, Colchen M, Krummenacher D, Le Fort P, Mouterde R, Rémi M (1971) Recherches géologiques dans l'Himalaya du Népal,

région de la Thakkhola. Centre National de la Recherche Scientifique, Paris, 279 pp (with two geological maps in colors)

Colchen M (1971) Les formations Paléozoïques de la Thakkhola. In: Bordet P, Colchen M, Krummenacher D, Le Fort P, Mouterde R, Rémi M (eds) Recherches géologiques dans l'Himalaya du Népal, région de la Thakkhola. Centre National de la Recherche Scientifique, Paris, pp 85–118

Colchen M (1975) Les séries Tibétaines. In: Bordet P, Colchen M, Le Fort P (eds) Recherches géologiques dans l'Himalaya du Népal, région du Nyi-Shang. Centre National de la Recherche Scientifique, Paris, pp 67–96

Colchen M, Le Fort P, Pêcher A (1986) Annapurna–Manaslu–Ganesh Himal. Centre National de la Recherches Scientifique, Paris, 136 pp (special publication, with a geological map, 1:200 000 scale)

Garzanti E, Pagni Frette M (1991) Stratigraphic succession of the Thakkhola region (central Nepal)—comparison with the northwestern Tethys Himalaya. Rivista Italiana di Paleontologia e Stratigrafia, Milano 97(1):3–26

Garzanti E (1999) Stratigraphy and sedimentary history of the Nepal Tethys Himalaya passive margin. J Asian Earth Sci 17:805–827

Gradstein FM, von Rad U, Gibling MR, Jansa LF, Kaminski MA, Kristiansen I-L, Ogg JG, Rohl U, Sarti M, Thurow JW, Westermann GEG, Wiedmann J (1992) Stratigraphy and depositional history of the Mesozoic continental margin of central Nepal. Geol Jahrb 77:3–141

Hagen T (1959) Geologie des Thakkhola (Nepal). Eclogae Geologicae Helvetiae 52(2):709–719 (with 5 figures and 1 plate)

Krystyn L (1982) Obertriassische ammonoideen aus dem Zentralnepalesischen Himalaya (Gebiet von Jomsom). Abhandlungen der Geologischen Bundesanstalt, Wien 36:1–63 (with 18 plates)

Mouterde R (1971) Les formations Mésozoïque de la Thakkhola. In: Bordet P, Colchen M, Krummenacher D, Le Fort P, Mouterde R, Rémi M (eds) Recherches géologiques dans l'Himalaya du Népal, région de la Thakkhola. Centre National de la Recherche Scientifique, Paris, pp 121–168

von Rad U, Dürr SB, Ogg JG, Wiedmann J (1994) The Triassic of the Thakkhola (Nepal). I: stratigraphy and paleoenvironment of a northeast Gondwana rifted margin. Geol Rundsch 83:76–106

Waltham AC (1972) A contribution to the geology of the Annapurna and Nilgiri Himals. Nepal. Geol Mag 109(3):205–214

Tethys Himalaya of Gandaki Region (Manang) 25

... there may be need of as great a development of subterranean movement as that which in the Alps, Andes, and Himalayas has raised strata containing marine fossil shells and ammonites to the height of 8,000, 14,000, and 16,000 ft.

—Sir Charles Lyell (1875, p. 140)

Although metamorphism has significantly altered the early Paleozoic rocks of Manang (Figs. 25.1 and 25.2), the succeeding strata, and especially the Mesozoic sequences, extend eastwards from the Thakkhola with a very similar stratigraphy. In the upper reaches of the Jarsgeng Khola, however, new facies appear in the Rhaetian and the base of the Early Jurassic (Colchen 1975). In the Marsyangdi Valley, the lower two-thirds of the rock succession are strongly metamorphosed, and the remaining portion is characterized by a gradual decrease in the grade of metamorphism. In this transect, the augen gneisses of Chame, comprising the top of the Higher Himalayan crystallines, give way to a thick Tethyan sequence of calc-gneisses and marbles (Fuchs et al. 1988, p. 594).

25.1 Early Paleozoic

The various peaks of the Annapurna Range are formed of the early Paleozoic strata. They are also exposed on the Marsyangdi River, between Bangba and Chame (Colchen (1975, p. 67). The augen gneisses of Chame disappear at the confluence of the Nar Khola and Marsyangdi, under a thick carbonate succession, dominating the landform of Mutsog. This succession constitutes the south flank of a huge syncline, which plunges 35° due N60°W. On the left bank of the lower Nar Valley, about 500 m upstream from the confluence, where the imposing cliffs of Chame appear to the north, the following landforms with their constituent rock successions are encountered from north to south (Fig. 25.3).

1. Dark and massive cliffs made up of the Chame augen gneisses
2. Topographic depressions corresponding to the banded gneisses, similar to those found on the left bank of the Marsyangdi, in the vicinity of Traglung (about 300 m)
3. Alternating impure marbles and gneisses, where the white carbonate bands stand out clearly in the landscape (about 500 m)
4. Very hard crystalline limestones (about 600 m), in which individual bands form the impressive cliffs to the southeast of Mutsog.

The above sequence discontinuously crops out on the trail from Chame and Pisang, as it is frequently covered by fluvio-glacial deposits. However, to the southeast of Pisang, the following sequence is exposed (Fig. 25.4).

1. Highly recrystallized limestones and marbles, alternating with thin schist bands characterized by crenulated biotite (50 m)
2. Regularly alternating biotite schists and calc-schists, thrown into south-verging, small-scale folds (about 40 m)
3. The same type of alternation as above, but dominated by carbonates (35 m)
4. Calc-schists, followed by gray-green calcareous metasandstones (25 m)
5. Spotted white quartzites with a few alternating bands of biotite schist (60 m)
6. Alternations of calc-schists and white quartzites (30 m)
7. White quartzites, intersected by veins with copper mineralization (30 m)
8. Thin-bedded, green crystalline limestones, passing into pink varieties (30 m)
9. Blue crystalline limestones crisscrossed by ocher veins, and alternating with schists (25 m), and containing completely recrystallized and deformed crinoid stems.

The above two transects represent the succession, overlying the augen gneisses of Chame, and they can be combined into the following three units, respectively, from the bottom upwards (Figs. 25.3 and 25.4).

- The banded gneisses of Traglung
- The calcareous gneisses and lime-silicates of Mutsog
- The sandstones and calc-schists of Pi (or Pisang).

To the northwest of Drongkhang, along the right bank of the Marsyangdi, the jagged south flank of the recumbent syncline of Mutsog consists of the following succession (Fig. 25.5a).

M.R. Dhital, *Geology of the Nepal Himalaya*, Regional Geology Reviews,
DOI 10.1007/978-3-319-02496-7_25

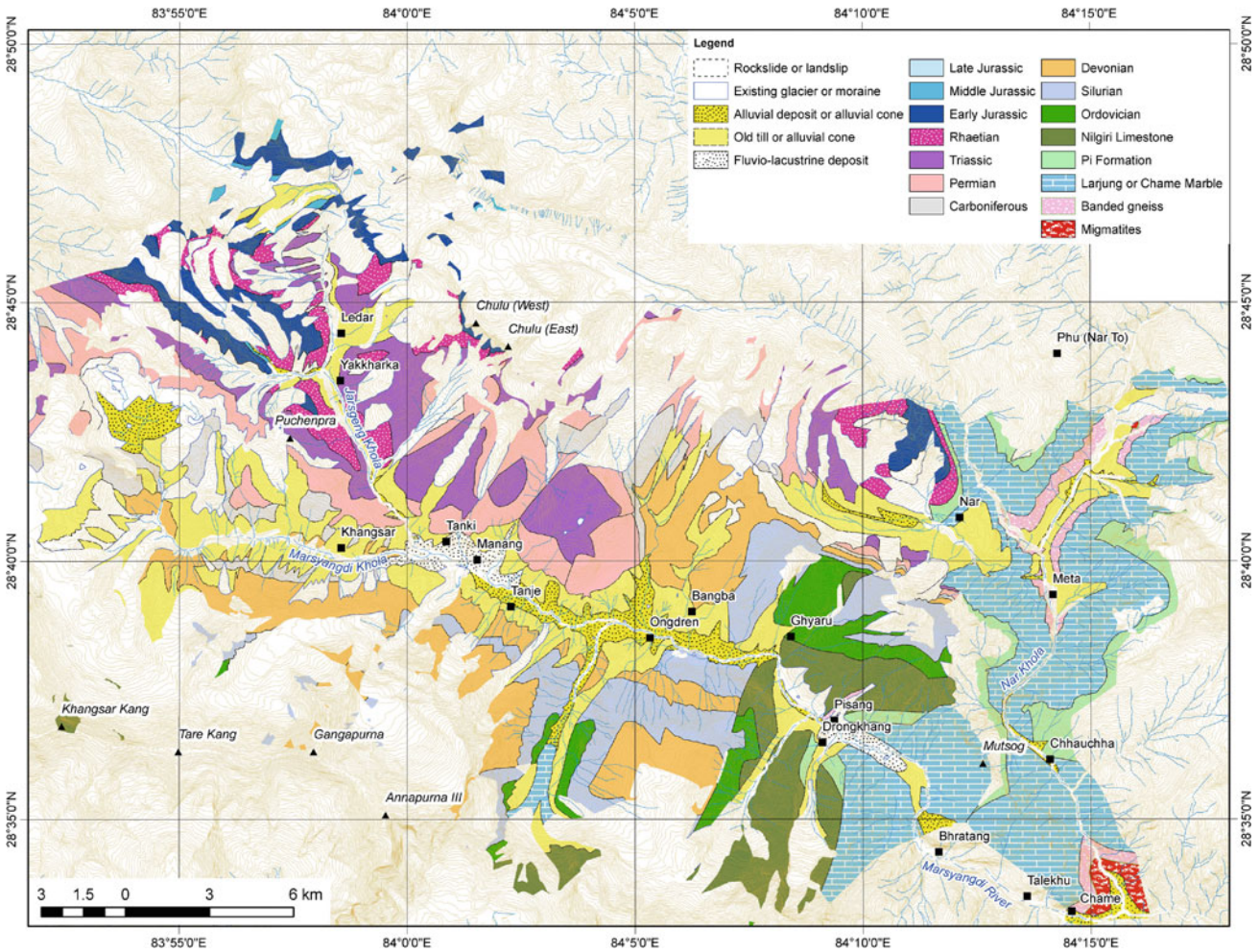

Fig. 25.1 Geological map of Manang and its neighborhood. *Source* Modified from Bordet et al. (1975)

1. Limestones with an ochrous sheen, alternating with more schistose bluish bands (350 m)
2. Mainly black schistose bands, constituting the top of the cliff of Gyaru (Ghyaru).

The overturned sequence, composing the north spur of Annapurna II, is made up successively of the following horizons, respectively, from its base to summit (Fig. 25.5b).

1. Thin to thick beds of black limestone and schist (30 m).
2. Thin-bedded, white limestone, separated by bluish partings, and alternating with medium-bedded, fawn limestones with an ochrous patina (about 20 m).
3. Thinly alternating sandy schists and calcareous schists, exhibiting two sets of lineation (20 m).
4. Very finely alternating black sandy schists with biotite, similar to those of graptolite-bearing horizons in the Thakkhola, but without fossils. This succession continues for several tens of meters with some occasional more sandy beds (about 200 m).
5. This section ends with a new carbonate horizon, consisting of very micaceous calc-schists, alternating with some biotite schists and sandstones.

The upper part of the limestone with an ocher patina and alternating with bluish calc-schists, observed at Drongkhang, also crops out on the right bank of the Gyaru Khola, to the northwest of the village. This horizon continues from south to north, up to the west ridge of Pangla Ri. Departing from the confluence of the stream north of Gyaru and going back to the northwest, along the trail that leads to Bangba, the following sequence is exposed successively.

1. Light blue limestones with an ocher sheen, containing very stretched brachiopoda fragments and alternating with some blue-gray calc-schists crosscut by ocher veins (50 m).
2. White limestones and sandstones, passing upwards into calcareous sandstones (about 30 m).
3. A predominantly carbonate succession with three, more massive, fawn, calc-schist bands with ochrous veins.

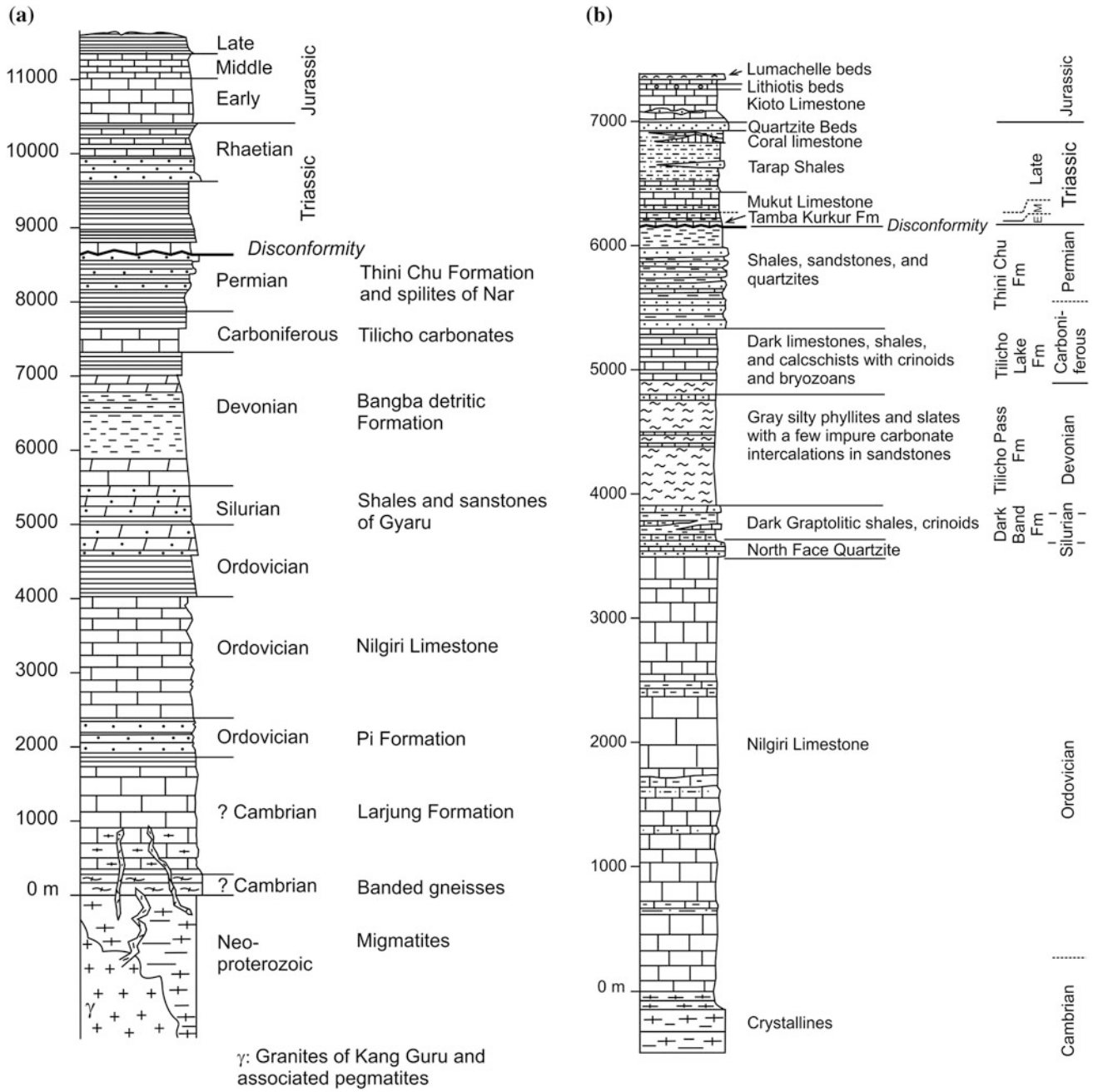

Fig. 25.2 Stratigraphy of Manang. *Source* Classification based on: **a** Colchen (1975) and **b** Fuchs et al. (1988)

The calc-schists are strongly foliated, and contain north-verging small-scale folds and a very tight axial plane schistosity (about 300 m).

4. The succeeding black schists are also thrown into north-verging mesoscopic folds. These black schists are exposed mainly on the west slopes of the spur of Gyaru.

The cirque at the junction of the west ridge of Pangla Ri and the spur east of Bangba is a conspicuous white cliff. It consists of the following succession, respectively, from top to bottom.

1. Fine-grained, black schists, passing into sandstones (similar to Horizon 4 in the previous section)
2. Medium- to thick-bedded (up to a few meters) dolomites, corresponding to a prominent white band (about 70 m)
3. Alternations of calc-schists and black schists, including in their middle portion a blue-gray horizon, rich in *Tentaculites* remains (about 200 m).

In the upper reaches of the Nar Khola, in the north flank of the Nar dome, the following sequence is observed, from south to north, respectively.

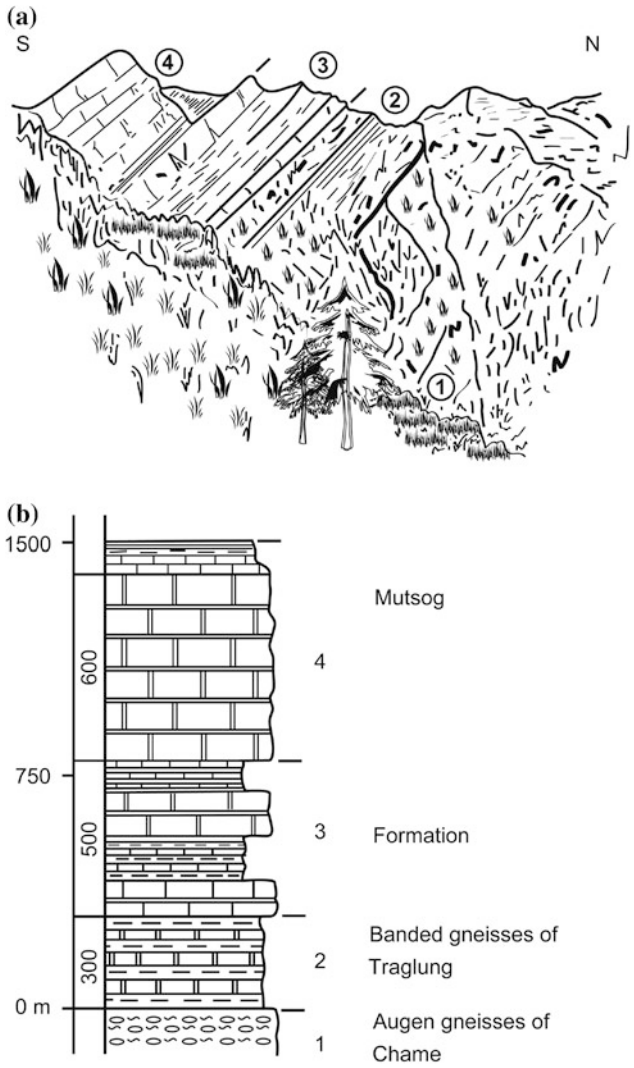

Fig. 25.3 Early Paleozoic sequence of Mutsog. **a** Rocks cropping out in the lower reach of the Nar Khola on its left bank. *Numbers* correspond to the respective horizons described in the text. **b** Restored columnar section representing the above horizons of Nar Khola. *Source* Modified from Colchen (1975). © Centre National de la Recherche Scientifique, Paris, France. Used by permission

1. Top of the augen gneisses of Chago, similar to those of Chame
2. Banded gneisses exposed at the bridge of Nar Ma (250 m)
3. Pyroxene-bearing lime-silicates, forming the dome of Nar (700 m), with pegmatite veins and feeders
4. Black schists and calc-schists (40 m), with crinoid fragments and other indeterminable organic remains
5. Massive limestones, forming the gorge of the Nar Khola, located just downstream from the south entrance of Nar To (60 m)
6. Blue-gray and black schists, followed by the alternations of schists and blue limestones (50 m)
7. Blue limestones with an ocher patina, containing orthocerids (50 m)
8. Black schists and alternations of schist and blue-black limestone, containing Early Devonian *Tentaculites.*

The succession between the augen gneisses of Chago and the black schists with Early Devonian *Tentaculites* has a total thickness of 1,150 m.

25.2 Early Paleozoic Lithostratigraphy

The lithostratigraphic succession in the Marsyangdi includes the following eight separate units, with a total thickness of more than 3,000 m.

1. Augen gneisses of Chame, observed to the south of the map area, on the left bank of the Marsyangdi, which belong to Formation III of the Tibetan slab (Chap. 16)
2. Banded gneisses of Traglung (300 m)
3. Lime-silicates of Mutsog, mainly developed at Mutsog, between Traglung and Pisang (1,250 m)
4. White sandstones, followed by black schists and calc-schists of Pi (450 m)
5. Limestones of Drongkhang, forming a cliff to the northwest of the village, on the right bank of the Marsyangdi (500 m)
6. White sandstones and calc-schists of Gyaru (350 m), well exposed on the right bank of a river, north of Gyaru
7. Black schists of the above river and Bangba (200 m)
8. White dolomites, observed in the same locality (70 m).

The Nar Valley transect yielded a well-preserved *Tentaculites* at its basal part, and this section can be divided up into the following seven lithostratigraphic horizons, which can be compared with those of the Marsyangdi Valley (Table 25.1).

Thus, the aggregate thickness is significantly reduced to about 1/3 in the Nar neighborhood, as compared to that in the Marsyangdi Valley, whereas it is close to 9/10 for the Pi and Drongkhang formations. The early Paleozoic rocks are further divided into the following lithological units.

25.2.1 Marbles of Mutsog and Traglung or Larjung Formation (?Cambrian)

To the early Paleozoic are attributed the lime-silicate rocks and marbles of Mutsog and Traglung that stratigraphically underlie the Pi and Drongkhang formations. This unit is equivalent to the Larjung Formation and Nilgiri Limestone in the Thakkhola Valley (Chap. 24) and the Dhaulagiri Limestone in Dolpa (Chap. 23).

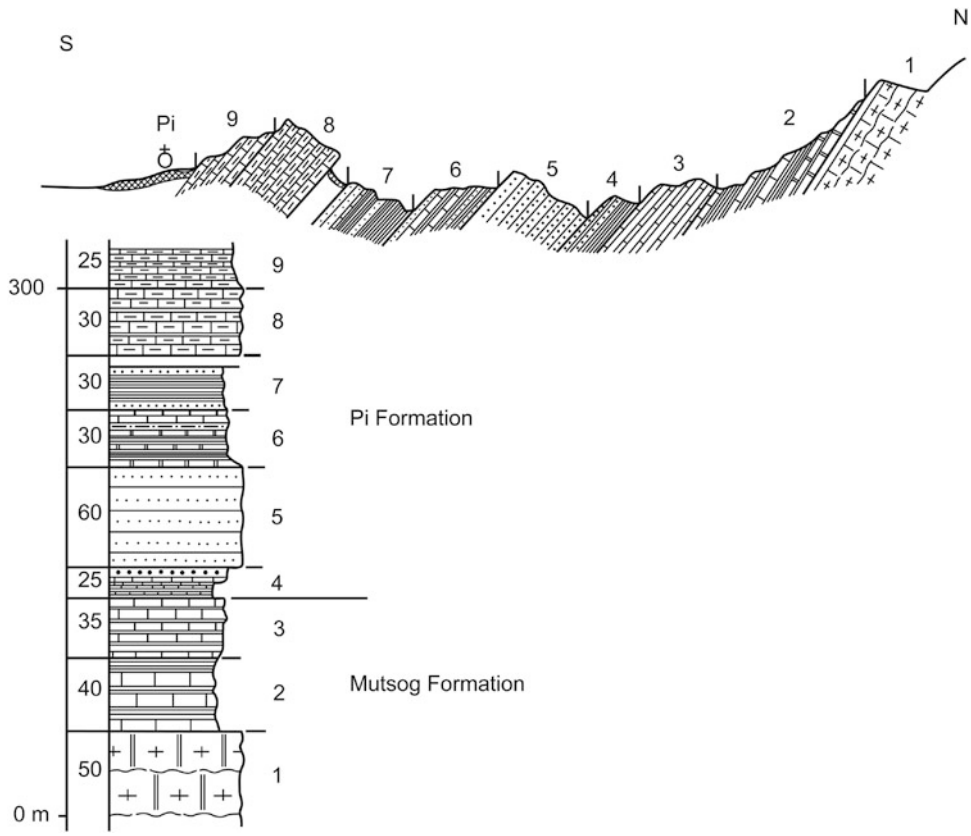

Fig. 25.4 Section through the left bank of the Marsyangdi to the southeast of Pisang. *Numbers* correspond to the respective horizons described in the text. *Source* Modified from Colchen (1975). © Centre National de la Recherche Scientifique, Paris, France. Used by permission

25.2.2 Pi and Drongkhang Formations, Equivalents of Nilgiri Limestone (Early and Middle Ordovician)

By analogy with the lithological succession of Thakkhola, the Ordovician is represented in Manang by the following three rock types: the Pi Formation (white sandstones succeeded by schists and calc-schists), the Drongkhang Formation (fawn and blue limestone alternations), and the Gyaru Formation (white sandstones and calc-schists). The Pi Formation presumably represents the base of the Ordovician, inasmuch as it underlies the carbonates of Drongkhang, which laterally pass into the Nilgiri Limestone in the Thakkhola (Colchen 1975, p. 94).

Fuchs et al. (1988) included the entire Cambro–Ordovician carbonate succession, overlying the crystallines, under the Nilgiri Limestone (Fig. 25.2b). Thus, their Nilgiri Limestone consists of a well-bedded and rhythmically alternating sequence of impure, pelitic or arenaceous, bluish gray carbonates. Its lower part is made up of a medium- to coarse-grained marble with diopside, phlogopite, and hornblende. There are also bands of biotite-rich, calc-gneisses and other lime-silicates. The rock is frequently injected by tourmaline pegmatite veins. The upper part of the Nilgiri Limestone is made up of blue-gray to light gray, finely crystalline limestones with thin pelitic bands. The Nilgiri Limestone is 3,000–4,000 m thick in the Marsyangdi Valley (Fuchs et al. 1988).

25.2.3 Quartzites of Gyaru or North Face Quartzite (Middle–Late Ordovician)

The white sandstones and quartzites of Gyaru are homotaxial with the North Face Quartzite and overlying pitted calc-schists, containing *Orthambonites* of Middle Ordovician age in the Thakkhola (Colchen 1975, p. 94).

This formation displays a well-bedded sequence of light-colored (white, pink, fawn, and gray) rocks, such as very fine quartzites; calcareous, dolomitic, or silty quartzites; siliceous limestones; and quartzitic schists. The sandy beds break into sharp blocks with smooth surfaces. The rocks are either massive or discontinuously laminated. The pelitic beds contain clay gals, whereas the coarser ones display cross-laminae. The North Face Quartzite is about 1,000 m thick in Manang (Fuchs et al. 1988).

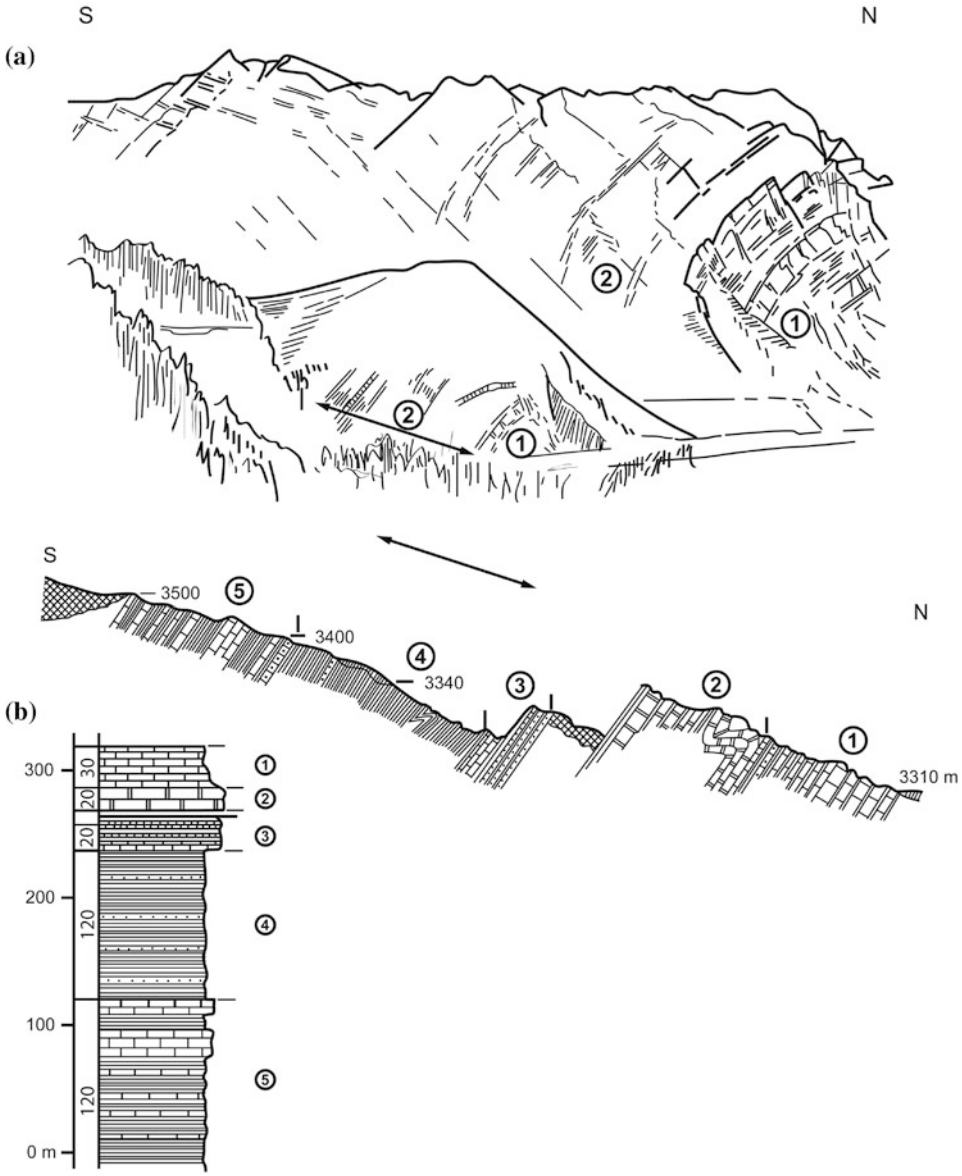

Fig. 25.5 **a** Rocks exposed at Drongkhang (*1*) and at Pisang (*2*) in an overturned succession cropping out to the northwest of Drongkhang. **b** Cross-section and reconstructed column, showing the Pi Formation exposed to the southwest of Drongkhang (details of the *upper horizons*). *Numbers* correspond to the respective horizons described in the text. *Source* Modified from Colchen (1975). © Centre National de la Recherche Scientifique, Paris, France. Used by permission

Table 25.1 Comparison of the Nar Valley and Marsyangdi Valley transects

Unit	Rock succession in Nar Valley	Thickness (m)	Rock succession in Marsyangdi Valley	Thickness (m)
1	Banded gneisses at the bridge of Nar Ma	250	Banded gneisses of Traglung	300
2	Lime-silicates constituting the dome of Nar	700	Lime-silicates exposed at Mutsog	1,250
3	Black schists and calc-schists with crinoids	40	Black schists of Pi	300
4	Massive limestones, composing the gorge of Nar To	60	Massive limestones of Drongkhang	500
5	Blue-black schists and blue limestone alternations	50	All of the calc-schists of Gyaru and black schists of the river east of Bangba	550
6	Blue limestones with an ocher sheen, containing orthocerids	50	White dolomites of Bangba	70

Source Colchen (1975)

25.2.4 Black Schists and Carbonates of Gyaru or Dark Band Formation (Ordovician–? Devonian)

Although the Silurian is not established paleontologically, the black schists and dolomites from the river east of Bangba are attributed to this age, because they underlie the Pragian *Tentaculites* (Colchen 1975, p. 94).

This formation displays wide facies variations, and is composed primarily of light-colored calc-schists and crystalline limestones full of crinoids. The last crinoidal sequence is followed by black slates, siltstones, and carbonates (Fig. 25.2b). There are also some interstratified black slates and light colored crinoidal limestones. Most of the formation was deposited in euxinic conditions, and this facies is intertonguing with the carbonate shelf facies. The Dark Band Formation varies in thickness from 100 m to about 300 m in Manang (Fuchs et al. 1988, pp. 597–598).

25.3 Devonian

The upper part of the paleontologically dated Devonian is exposed on the left bank of the Marsyangdi, to the east and northeast of Bangba, where underlies the white dolomitic succession referred to as the Silurian. The Devonian succession also crops out in the lower reaches of the Sabje Khola, in the upper reaches of the Marsyangdi close to Khangsar, to the east of Lake Tilicho, and close to Nar To and Pangre.

At the Bangba spur, the following stratigraphic sequence is observed.

0. A few-meter-thick, white beds of massive dolomite with a gray-fawn sheen
1. Alternations of finely laminated, black sandstones and slates (20 m)
2. Black calc-schists (5 m)
3. Alternations of rusty-weathering, black schistose sandstones, similar to Horizon 1 above (about 50 m)
4. Fawn and pink, resistant calc-schists, containing a few crinoid stems (20 m)
5. Alternating blue-gray slates and calc-schists (20 m)
6. Gray-black limestones and slates with *Tentaculites* (15 m)
7. Gray-blue slates with *Tentaculites* (20 m)
8. Resistant calc-schists (25 m)
9. Alternations of gray-blue slates and limonitic sandstones (25 m)
10. Resistant limestone beds (15 m)
11. Alternating slaty-sandstones (several tens of meters).

This section corresponds to the Early Devonian sequence with *Nowakia* in the Thakkhola Valley (Colchen 1971, p. 94).

On the right bank of the river, flowing to the west of Bangba, the imposing ridges to the northwest of Nar La consist of well-stratified, medium- to thick-bedded calcareous sandstones, with an aggregate thickness of about 50 m. They correspond to Horizons 8–10 of the previous section, and are followed by more finely laminated black slates and calcareous sandstones, rich in crinoid stems. They represent the higher levels of the Devonian, and are succeeded by some massive limestones, exposed to the northwest of the Bangba Gompa, in which Colchen (1975, p. 78) recovered a brachiopoda fauna of the early Carboniferous.

In the Nar Valley, the Devonian crops out to the south of Nar To, in the vicinity of its south entrance, and on the right bank of the Pangre glacier, located to the south of Pangre. At the proximity of Nar To, the Devonian is reduced to a few schist and black limestone beds of about 20 m thickness, and containing *Tentaculites.* The *Tentaculites*-bearing slates are succeeded by a set of black and greenish slates containing Carboniferous brachiopods.

To the south of Pangre, on the right bank of the glacier, in its south spur, there are a number of horizons, including the black slates with *Tentaculites* at the bottom, and a succession of pelitic sandstones, resembling a flysch at the top, and they attain a total thickness of about 600 m. Hence the Devonian sequence is very thick here, whereas about 15 km to the west in the Thakkhola, it reduces to a few tens of meters.

25.4 Devonian Lithostratigraphy

The section through the spur of Bangba represents a succession of 10 lithological horizons, where only Horizons 6 and 7 yielded some *Tentaculites* (Fig. 25.6).

25.4.1 Bangba or Tilicho Pass Formation (Devonian)

In the Marsyangdi Valley, the Devonian Bangba Formation begins from the top of the white dolomitic band, exposed on the spur of Bangba, and consists of the following horizons.

- Slates and black calc-schists of Horizons 1–3 (75 m)
- Fawn and pink calc-schists of Horizon 4 (20 m)
- Gray-blue slates with *Tentaculites,* representing Horizons 5 and 6 (55 m)
- Alternations of limonitic sandstones, sandy limestones, and calc-schists (Horizons 8 and 9), constituting the higher part to the NW of the col of Nar (50 m)
- Limestones and calc-schists, representing Horizon 10
- Alternations of slates and sandstones with lenses of crinoidal limestones (several tens of meters), succeeding the last horizon, and passing into the limestones of the

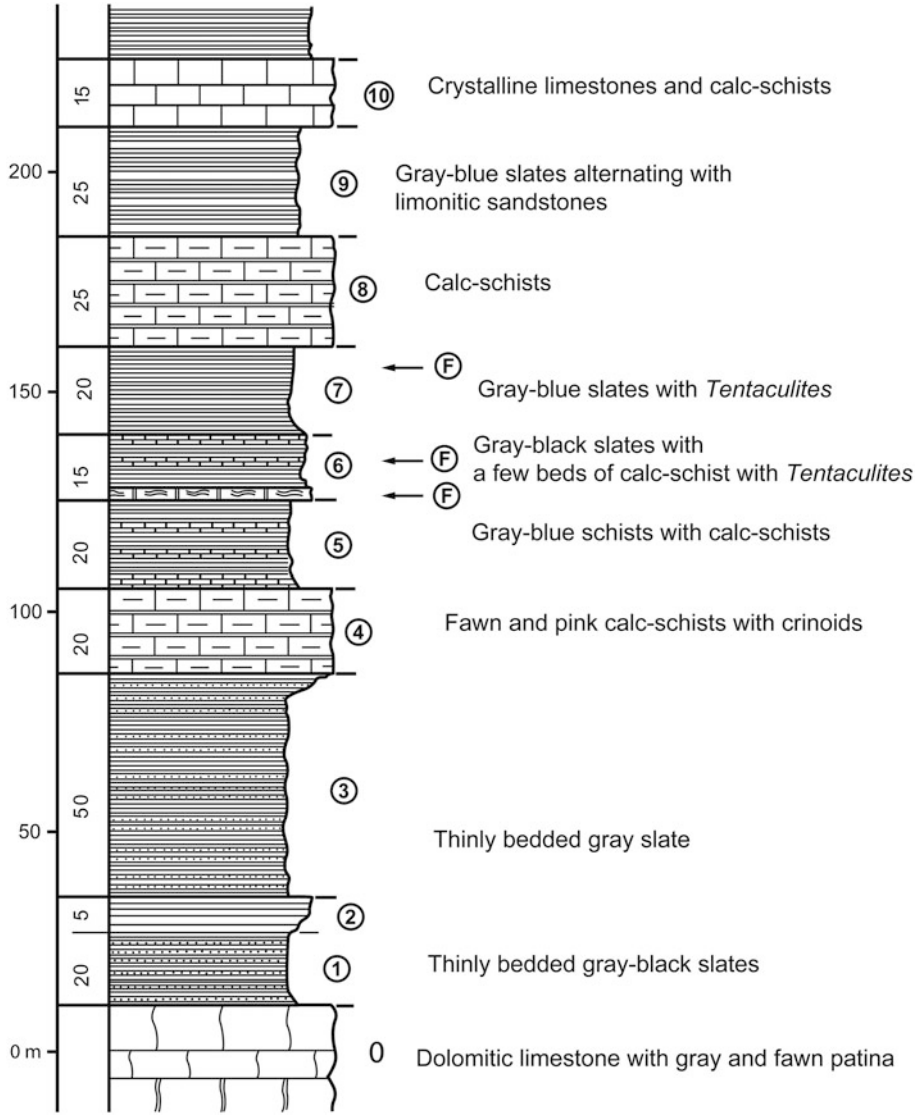

Fig. 25.6 Stratigraphic succession of Bangba. *Numbers* correspond to the respective horizons described in the text. *Source* Modified from Colchen (1975). © Centre National de la Recherche Scientifique, Paris, France. Used by permission

early Carboniferous (cf. Horizon 5 in the section given in Fig. 25.6).

Thus the Bangba or Tilicho Pass Formation comprises gray to black slates, phyllites, and laminated varieties of silty micaceous slates and siltstones. There are also infrequent beds of quartzose sandstone, calcareous quartzite, and gray, green, and white quartzite, reaching a thickness of a few meters and weathering into rusty colors. The siltstone and sandstone beds are irregular to lenticular in shape, and exhibit flute casts and load casts, as well as rill and tool marks. Thus this sequence is presumably a turbidite (Fuchs et al. 1988, p. 598).

At Nar To, the Devonian is represented only by slates, fine sandstones, and calc-schists with *Tentaculites*. It is just about 20 m thick, and separated from the overlying (paleontologically dated) middle Carboniferous horizon by a few meters. However, in the vicinity of Pangre, the Devonian is much thicker (several hundred meters), and is represented by schists and black limestones, containing *Tentaculites* together with pelitic and sandy alternations resembling a flysch facies.

Hence the slates and calc-schists with *Tentaculites* are located approximately 100 m above the top bed of white dolomite, separated from it by black slate and sandstone alternations, and can be attributed to the base of the Devonian. Although the Middle Devonian is not confirmed paleontologically, the crinoidal calc-schists of Bangba may be ascribed to it and they can be the lateral equivalents of the *Favosites*-bearing limestones of the Thakkhola (Colchen 1975, p. 94).

From the middle part of the Tilicho Pass Formation, a 50–60 m thick succession of thick-bedded, gray, blue, pink, fawn, and cream colored limestones, silty limestones, and dolomitic limestones yielded the following conodonts of Late Devonian (Frasnian) age (Fuchs et al. 1988, p. 598).

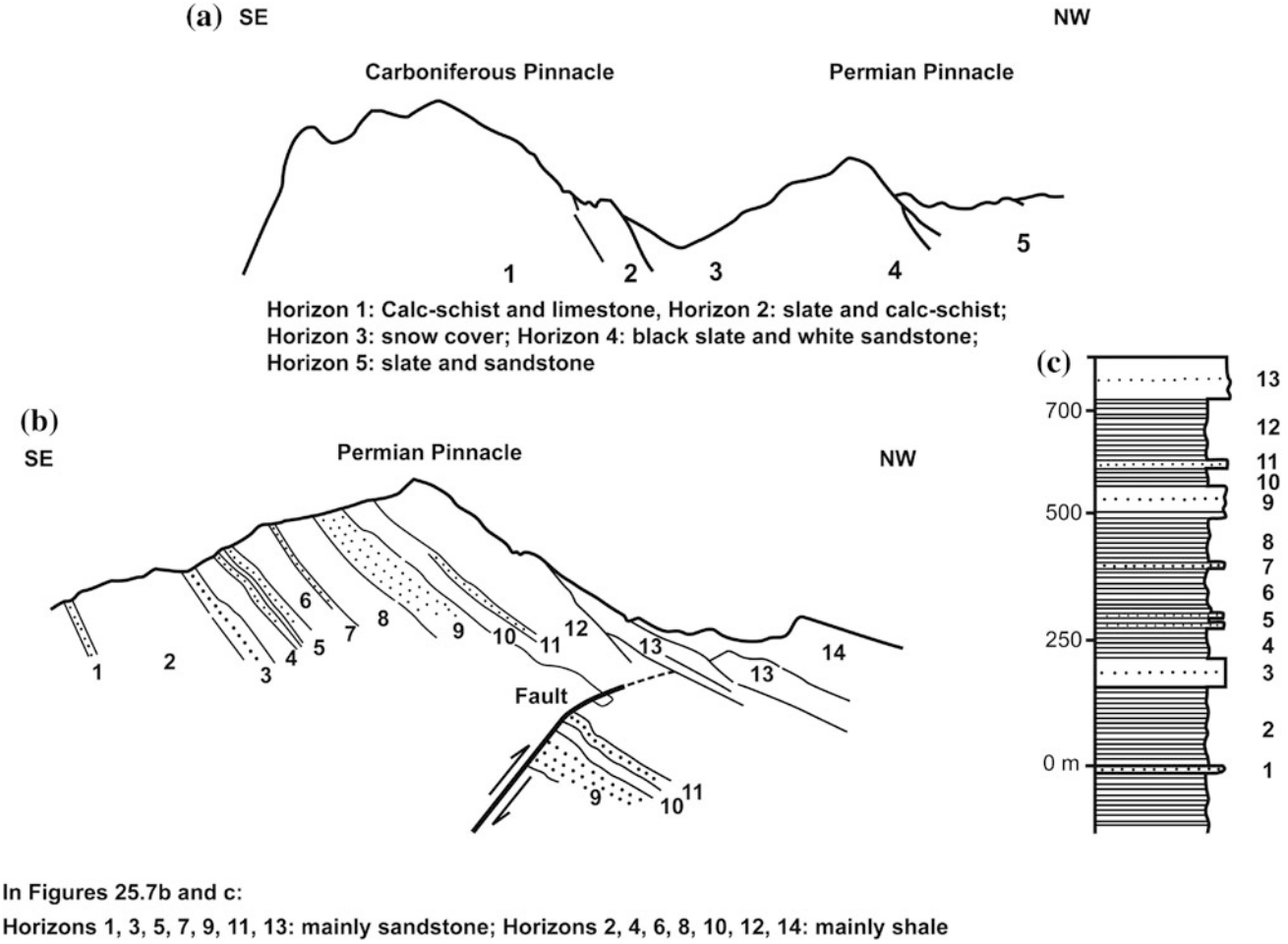

Fig. 25.7 Permo–Carboniferous succession of Tilicho lake. **a** Carboniferous and Permian pinnacles; **b** details of Permian pinnacle; **c** restored column of Permian sequence. *Source* Modified from Colchen (1975).

Ancyrodella curvata (Branson & Mehl.)
Icriodus sp.
Polygnathus linguiformis Hinde
Polygnathus sp.
Palmatolepis sp.

Farther up-section, the following Late Devonian conodonts were recovered from the varicolored, ochrous-weathering, green, gray, and cream dolomites, limestones, and quartzites, alternating with gray and green phyllites.

Ancyrodella nodosa Ulrich & Bassler
Icriodus cf. *I. nodosus* Ulrich & Bassler
Palmatolepis sp.
Polygnathus cf. *P. webbi* Stauffer
Polygnathus cf. *P. linguiformis* Hinde.

Most of the Tilicho Pass Formation was deposited in a deep subsiding basin, which was partly affected by turbiditic currents. The intercalated limestones were formed in adjoining shelf areas, and were subsequently transported to the deeper part by the turbidity currents. The thickness of this formation ranges from a few hundred to 1,000 m (Fuchs et al. 1988, p. 599).

25.5 Carboniferous and Permian

The Paleozoic sequence continues with the Carboniferous and Permian, in which Colchen (1975, p. 80) distinguished the following two main lithotypes.

- A lower carbonate-dominated sequence
- An upper succession, consisting of an alternation of black slates and white sandstones or quartzites.

These horizons continue from west to east, between Tilicho Lake and Bangba, for about 30 km. Colchen (1975, p. 80) studied them on the right bank of Marsyangdi and also on the north side of Nar La. The following general succession is observed through the east crest of Lake Tilicho (Fig. 25.7a).

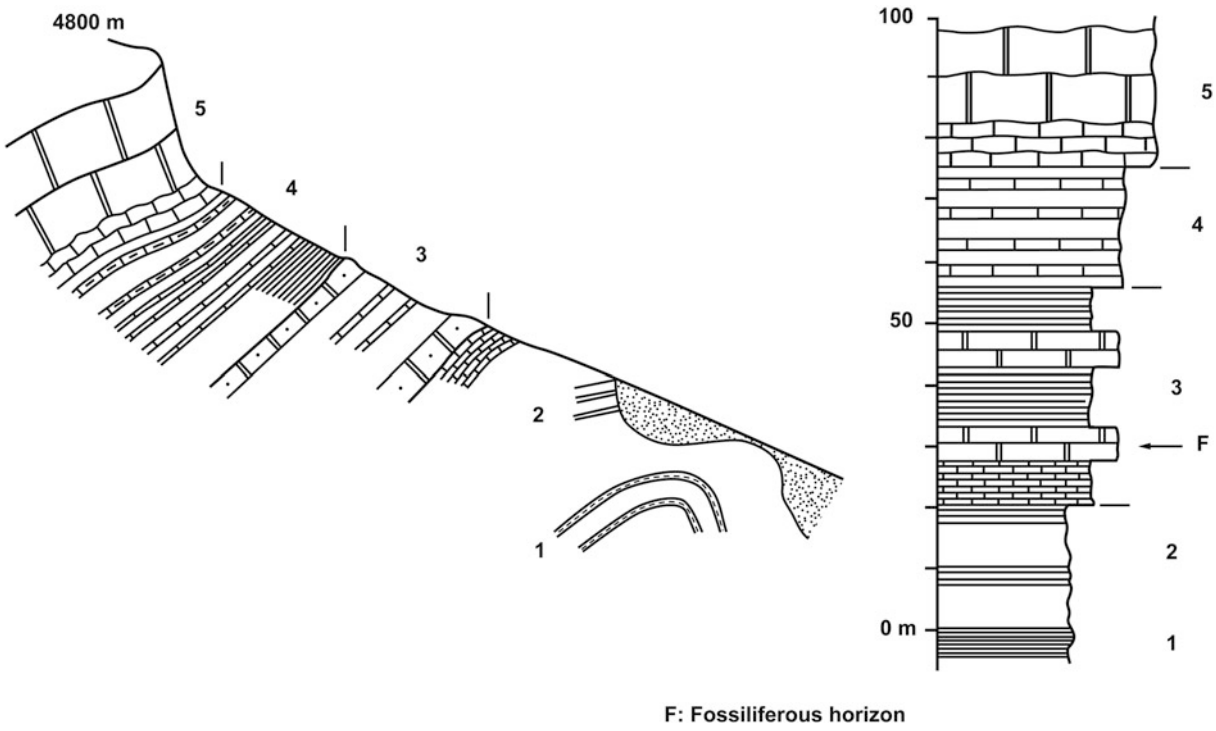

Fig. 25.8 Section through the base of the pinnacle containing Carboniferous rocks, on the left bank of the Marsyangdi. *Numbers* correspond to the respective horizons described in the text. *Source* Modified from Colchen (1975). © Centre National de la Recherche Scientifique, Paris, France. Used by permission

1. The summit composed of Carboniferous rocks, consisting of massive calc-schists, followed by several-meter-thick limestone beds
2. An alternation of slates and calc-schists
3. Snow cover
4. A regularly north-dipping sequence of black slates and white sandstones, ending at the summit made up of Permian strata
5. Alternations of slates and sandstones.

While moving through the base of the pinnacle composed of Carboniferous rocks, along the left bank of the Marsyangdi River, the following sequence is observed from bottom to top (Fig. 25.8).

1. Bluish gray slates, constituting an anticlinal core
2. Blue slates with a few rusty beds
3. Blue limestones with an ochrous patina, and containing crinoids and *Polypora* (5 m), followed by thin alternations of slate and limestone with crinoids, and ending with a new limestone horizon (30 m)
4. Slate and limestone alternations, very rich in crinoids (20 m)
5. At the base, thin-bedded and then massive limestone (several tens of meters).

The second pinnacle representing the Permian rocks (Fig. 25.7a) is essentially an alternation of black slates and white sandstones or quartzites, and they are very similar to those of the Thini Chu Formation in the Thakkhola, notably by the presence of the very remarkable Horizon 5 (in Fig. 25.7b, c) consisting of two quartzite beds separated by a thin, black slate zone.

To the north of the upper Marsyangdi Valley, the section near Black Col, through the crest northwest of Kangsar, consists primarily of a succession of black slates and white quartzites, identical to the Thini Chu Formation in the Thakkhola Valley. The details are the following (Fig. 25.9a).

1. Dark brown quartzites with a wavy surface (6 m), followed by white quartzites (4.50 m)
2. Black limestones and slates with fenestellids and brachiopods, including many *Syringothyris lydekkeri* (6 m)
3. Barren black slates (15 m)
4. A band of white quartzites, showing graded bedding (15 m)
5. Finely laminated black slates with pencil cleavage (16 m)
6. A bed of limonitic quartzite (1.50 m)
7. Black slates similar to Horizon 5, passing into thin-bedded red limestones with sun cracks (40 m)
8. White quartzite (more than 8 m).

A typical Thini Chu Formation of white quartzites and black slates is located slightly east of Black Col (Fig. 25.9b).

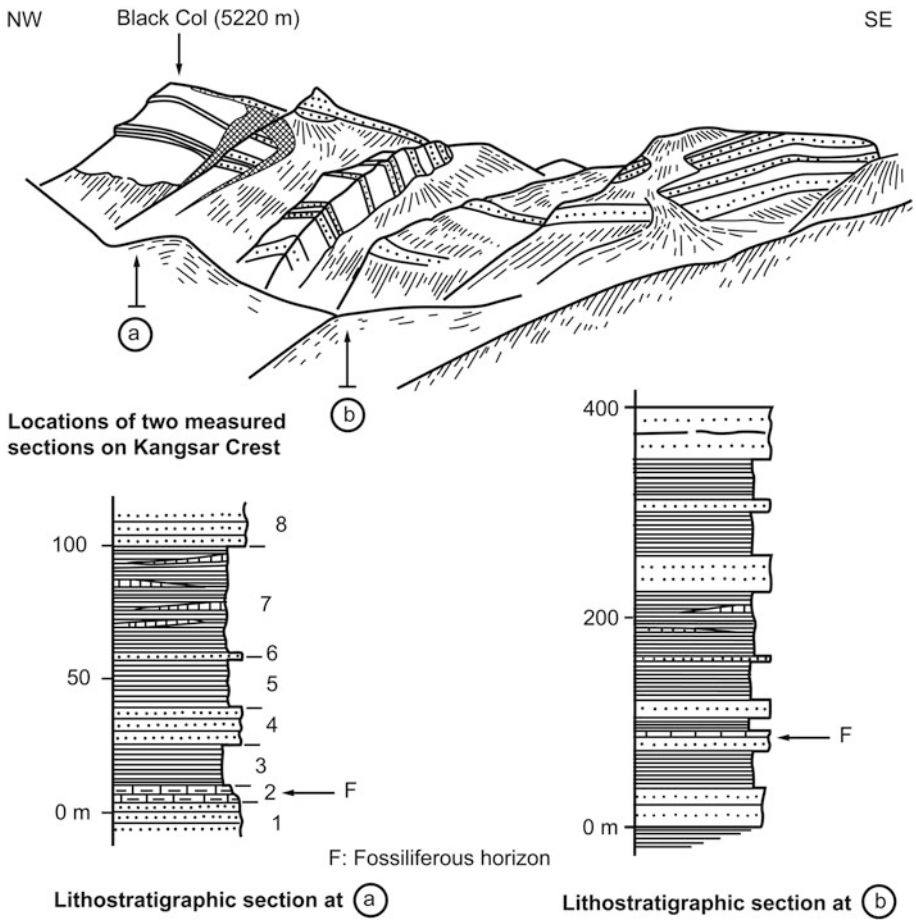

Fig. 25.9 The succession exposed on the Kangsar Crest. *Numbers* correspond to the respective horizons described in the text. *Source* Modified from Colchen (1975). © Centre National de la Recherche Scientifique, Paris, France. Used by permission

To the north of Bangba Gompa, a succession of northeast-verging folds is developed in slates, calc-schists, and limestones. It consists of the following sequence from southwest to northeast, respectively, (Fig. 25.10a).

1. Calc-schists with crinoids (25 m)
2. Light gray slates (30 m)
3. Cliff-forming limestones with a gray sheen (15 m)
4. Alternating slates and calc-schists
5. Calc-schists, followed by highly fossiliferous blue limestones (about 50 m), which reappear farther north in an anticlinal fold. At the level of F_1, there are abundant bryozoans, goniatites, and brachiopods, including *Spirifer* cf. *S. attenuatus* or *postriatus and* "*Spirifer trigonalis*" sensu Diener
6. Blue-green slates and calc-schists, containing brachiopods and fenestellids (Horizon F_2), passing upwards to dominantly pelitic alternations (about 50 m).

To the west of the village of Chulu, the following six units are mainly distinguished (Colchen 1975, p. 85).

1. A sequence consisting of three or four prominent beds of white sandstone
2. A succession of composite beds
3. A very persistent horizon of alternating white sandstones and black slates
4. A heterogeneous sequence, characterized by lenticular bedding with a variable thickness
5. A more regularly stratified horizon
6. A fine-grained succession, composing the upper slopes of the ridge.

The right bank of the river, east of Chulu Khola, has several good outcrops, and it contains the following main units.

(1) This basal unit overlies the calc-schists with crinoids, brachiopods, and bryozoans, belonging to the top beds of the Bangba Gompa, and is composed of fine alternations of black sandy slates, interstratified with some thin limestone lenses (about 150 m). These limestones contain a few crinoids with ill-preserved brachiopoda and bryozoan fragments.

(2) There are mainly three prominently sandy horizons. The first one begins with an alternation of sandstones and black slates (7 m), then is followed by massive sandstones (5 m), which are, in turn, overlain by black slates with many worm tracks. This last pelitic sequence is followed by gray-brown, thin, lenticular, fine sandstones with sporadic pebbly horizons. Laminated to thinly interbedded, black slates and lenticular limonitic sandstones (60 m) overlie the last sequence.

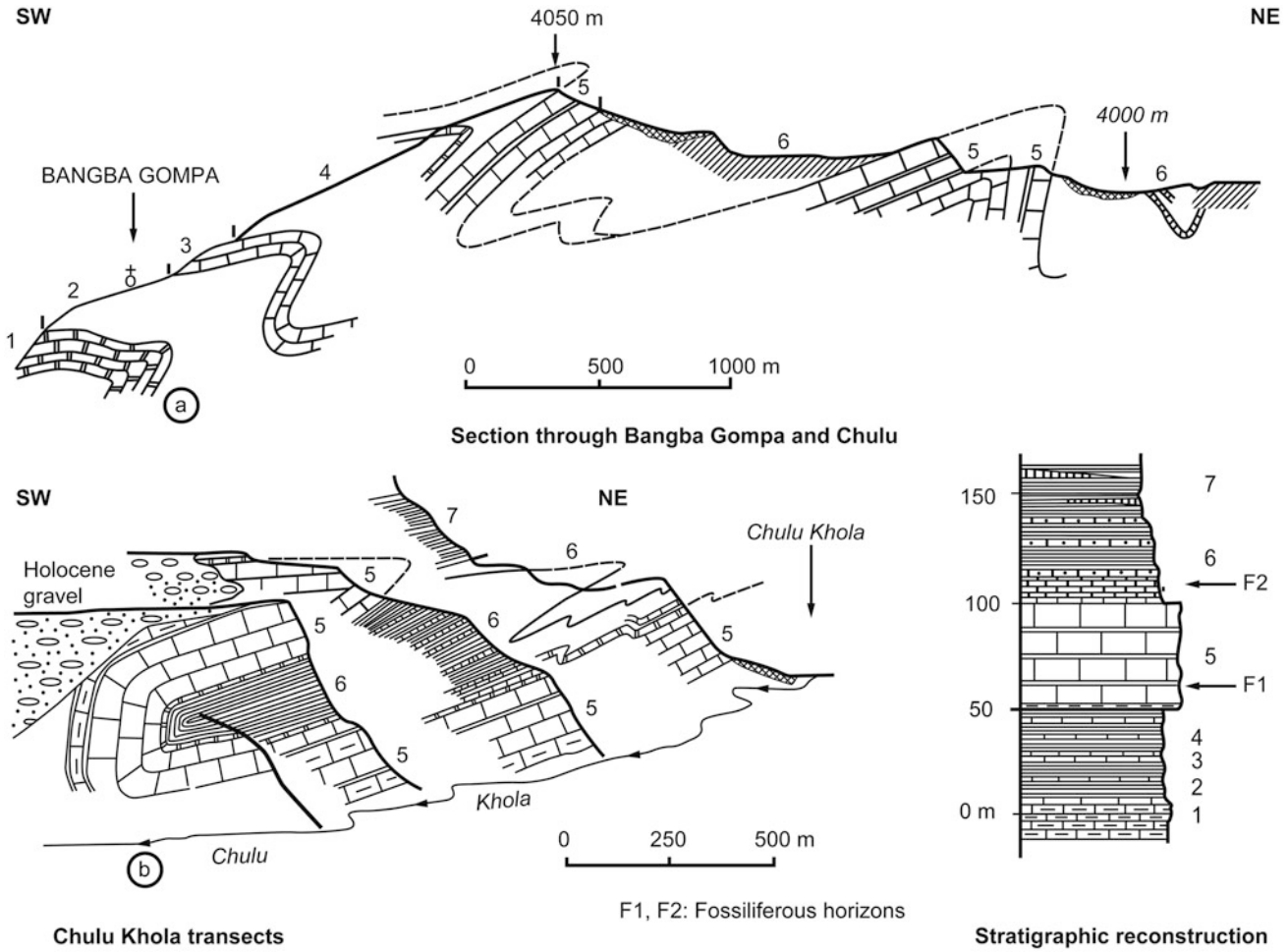

Fig. 25.10 The succession of Bangba Gompa. *Numbers* correspond to the respective horizons described in the text. *Source* Modified from Colchen (1975). © Centre National de la Recherche Scientifique, Paris, France. Used by permission

The second sandy horizon of gray-brown (10 m) color, succeeding the limonitic sandstones is quite friable. It has a calcareous cement and is rich in small bivalves, lingulids, and other brachiopods. This horizon is overlain by black slates with lenticular sandstones (30 m). The third sandy horizon (20 m) begins with limonitic sandstones, containing a calcareous cement and highly compact brachiopods. Finally, there are slate-dominant alternations, passing into calcareous sandstones with numerous worm tracks.

(3) These fine alternations of black slates and lenticular sandy limestones continue for about 150 m.

(4) This predominantly sandy succession begins with a bed of limonitic calcareous sandstone with fossils, and is succeeded by a white quartz arenite (1 m). Then there are successively black slates (2 m), white quartz arenite (6 m), and black slates (5 m). Farther up-section, some more white quartz arenites frequently alternate with black slates. The base of these quartz arenites is irregular and contains black slate pebbles in a lenticular bed of 1–5 m thickness. Then there is a sequence of blue-black slates (about 100 m), which begins with an alternation of fine sandstones and calcareous sandstones full of fossils, such as *Productus,* and *Spirifers,* in particular *Syringothyris* resembling *S. lydekkeri*, *Syringothyridae*, and *Spiriferella* sp. Above the fossiliferous horizon, come lenticular beds of monomictic as well as polymictic conglomerates, alternating with fine slaty-sandstones or diamictites. Their textural features suggest a glacio-marine origin of these sediments. There is a biostratigraphic hiatus between the last fossil assemblage and that occurring above it in Unit 5 (Colchen 1975, p. 88).

(5) The slates and diamictites are overlain by a dominantly sandy succession, consisting of the following rock types, respectively, from the bottom upwards: an alternation of white quartzite and black slate (30 m), black slates (15 m) with lenticular beds of limestone,

containing, in particular, *Neospirifer moosakhailensis, Neospirifer ravana, Spiriferella rajah,* and *Spiriferella tibetana*, white quartzites (5 m), and black slates (8 m). The last slates are succeeded by black slates and blue dolomitic limestones (3 m), containing a lumachelle of brachiopods, fenestellids, and bryozoans, notably the spiriferids analogous to those lying below it. The lumachelle bed is followed by blue slates of about 10 m thickness, and then by calcareous sandstones with coquina, giving way to white quartzites (10 m). The quartzites are overlain by approximately 70 m thick dominantly pelitic alternation, including a few calcareous sandstone beds, yielding some brachiopods (about 70 m). The approximately 80 m thick topmost horizon is represented by slate and limestone alternations, in which there are some fossiliferous calc-schist beds.

25.6 Carboniferous and Permian Lithostratigraphy

Taking the base of the Triassics as a reference level, the successions exposed at the summit of Tilicho Lake, at Bangba Gompa, and the carbonate horizons with *Spiriferella rajah* can be correlated. A closer look at the lithostratigraphic correlation reveals a sudden change in thickness between the section of Manang and that of Chulu, whereas the thicknesses remain almost identical throughout the area of west Manang and Thakkhola. This abrupt change is, thus, represented in the lower carbonate horizons by their reduced thickness, the disappearance of massive limestones, and the predominance of thin limestone or slate–limestone alternations.

In the white quartzite and black slate succession, composing the upper end, the changes are noticed in the increased thickness (from 650 to more than 1,000 m) and the disappearance of rhythmic alternations (which are very characteristic of the corresponding sequence in the Thakkhola), increased number and thickness of sandy beds, the presence of tilloids, occurrence of green spilitic rocks below the last white quartzite bed, and appearance of carbonate horizons at the top of the sequence.

As described above, the Late Paleozoic rocks consist of the following three biostratigraphic horizons. The lower horizon is represented by the Bangba Gompa unit, the intermediate one is intercalated in the middle of the Chulu sequence, and the upper horizon is found at the top of the last sequence. The lower horizon is characterized by the presence of *Spirifer*, already described from the Tilicho Lake Formation in the Thakkhola. This lower fossiliferous horizon represents the early Carboniferous (presumably, the late Tournaisian–early Visean). The intermediate horizon contains a very rich fauna of family Syringothyridae, including *Syringothyris lydekkeri* Diener. This second horizon can belong to the early and middle Carboniferous without, however, excluding the possibility of extending up to the early Permian in its higher levels. The upper horizon, corresponding to the top part of the Chulu transect, separates the tilloid (diamictic) lenticular conglomerate beds from the green spilitic rocks. This upper faunal assemblage occurs about 150 m above the intermediate fossiliferous horizon, and consists of limestones and calc-schists very rich in brachiopods, such as *Neospirifer moosakhailensis, Neospirifer ravana,* and *Spiriferella rajah*. The fossil assemblage is very similar to that of Dolpa (Chap. 23), and represents the Himalayan late Permian, and there could be a biostratigraphic hiatus between the intermediate and upper horizons. The Carboniferous and Permian strata can be classified into the following lithostratigraphic units.

25.6.1 Tilicho Lake or Bangba Gompa Formation (Early Carboniferous)

This formation consists of thin- to thick-bedded, gray, blue, and black, fine-grained, dense limestones, marly limestones, calc-schists, and dark gray to black shales. The beds are even, parallel, or nodular, and some of them are laminated. The weathered carbonate rocks exhibit ochrous colors, and in them crinoidal stems and ossicles (up to 1 cm in diameter) are frequent. There also abundantly occur fenestellids, brachiopods, corals, and bivalves. The following fossils were recovered from them (Fuchs et al. 1988, p. 599).

? Polypora
Spinofenestella
Productus sp.
Remains of Rhabdomesidae and Goniocladiidae
Fenestella
Ultropora
Protoretepora

The following conodonts indicate an early Carboniferous age.

Gnathodus cf. *G. typicus* Cooper
Gnathodus sp.

The Tilicho Lake Formation was deposited in poorly aerated water of a restricted carbonate shelf (Fuchs et al. 1988, p. 599).

25.6.2 Thini Chu or Chulu Formation (Middle Carboniferous–Permian)

The Thini Chu Formation comprises thick-bedded, medium- to coarse-grained, white, gray, and green quartzites and sandstones, alternating with gray-green to black slates and silty slates. It also includes some beds of brown-weathering

calcareous sandstones and quartzites, displaying cross-bedding and containing clay gall breccias. The formation abundantly contains plant debris, corals, bryozoans, brachiopods, cephalopods, bivalves, trilobites, and crinoids. This formation ranges in thickness from 700 to 900 m, and its age spans from the middle Carboniferous to Permian. Hence, the Late Paleozoic hiatus widens to the west of Manang (Fuchs et al. 1988, p. 600).

25.7 Triassic

In the Manang area, the Mesozoics crop out in the Chulu massif, the Jarsgeng Khola basin, and the Thorungse massif. There is apparently a succession from the Triassic to Late Jurassic, in which the lithological characteristics are similar to those of the Thakkhola area. Although the Mesozoics are not well exposed in the Nar Valley, Colchen (1975, p. 92) described them from the ridge west of Nar Ma and from northwest of Nar To.

The Triassic rocks transitionally overlie the late Paleozoic succession, and commence with the ammonite-bearing argillaceous limestones. In the upper portion of the southeast spur of Chulu, the following succession, spanning from the Late Paleozoic to the Triassic is observed, respectively, from bottom to top.

1. White quartzites, succeeded by limonitic calcareous sandstones with brachiopod fragments (10 m)
2. Mainly an argillaceous succession, comprising slates and limestones with lenticular bedding (about 50 m), followed by a quartzite band, and containing the brachiopods of late Permian (60 m)
3. A regular interbedding of green-fawn slates with lumachelles and nodular limestones (10 m)
4. Resistant nodular limestones, containing a few bivalves and ammonites, similar to those of the Early Triassic in the Thakkhola area (5 m)
5. Claystones with limestone lenses (15 m)
6. A limestone-dominating succession of claystones and argillaceous limestones.

25.8 Triassic Lithostratigraphy

The passage from the Permian to the Triassic is observed in a few meters that separate the last Permian horizon (Horizon 2 in the above section) from the green slates with bivalves and ammonite-bearing nodular limestones. Hence there is no sharp discontinuity between the Paleozoics and the Mesozoics, but apparently a gradual transition. The sequence then continues mainly with an argillaceous facies of several tens of meters in thickness. Upwards, the succession becomes more massive and better stratified. Hence, in the Manang area, the Triassic is predominated by an argillaceous facies. The Triassic rocks are further classified into the following formations.

25.8.1 Tamba Kurkur Formation (Earliest Triassic–Early Anisian)

The formation is a conspicuous marker bed of 20–30 m thickness (Fig. 25.2b) and characterized by a resistant band displaying rusty weathering. It is made up of thin-bedded, oftentimes nodular limestone (biomicrite–biosparite or bioclastic wackestone), displaying light gray, blue, or brown colors. There are also some thin gray shale beds. The formation includes many ammonites and conodonts. From the lower part of this formation Fuchs et al. (1988, pp. 600–601) recovered the following ammonites.

Neospathodus cf. *N. dieneri* Sweet
N. dieneri Sweet
N. cristagalli (Huckriede)
N. nepalensis (Kozur & Mostler)
N. cf. *N. pakistanensis* Sweet
N. timorensis (Nogami)
Gladigondolella tethydis (Huckriede)

The Tamba Kurkur Formation was deposited in pelagic conditions and represents condensed sediments (Fuchs et al. 1988, p. 601).

25.8.2 Mukut Limestone (Middle–Late Triassic)

It is made up of medium- to thin-bedded dark gray to blue limestones with marly horizons and dark gray to black shale intercalations. Some limestones are finely laminated, whereas others are nodular and display ochrous weathering colors. Fuchs et al. (1988, p. 602) recovered the following conodonts and ammonites from this formation.

Conodonts:
Gondolella cf. *G. constricta* Mosher & Clark
Gladigondolella tethydis (Huckriede)
Gondolella inclinata Kovacs
Gondolella polygnathiformis Budurov & Stevanov

Ammonites:
Badiotites eryx (Münster)
Gonionotites italicus Gemm.

The Mukut Limestone was deposited in a poorly aerated deep outer shelf. Within this formation, a change from calcareous to silty arenaceous sedimentation took place throughout the Himalaya (Fuchs et al. 1988, p. 602). The Mukut Limestone is more than 200 m thick (Fig. 25.11).

25.8.3 Tarap Shales and Coral Limestone (Late Triassic)

In Manang, this formation comprises dark gray to green-gray siltstones, silty shales, and impure sandstones. There also occur black concretions in the shales. A conspicuous limestone horizon of about 40 m thickness occurs in Manang, and it continues up-section with calcareous sandstones; red, white, and green crinoidal limestones, gray schistose limestones, and fine-grained, green micaceous sandstones. This carbonate succession is followed upwards by the Quartzite Beds. In the Tarap Shale are also found thick-bedded, pink, white, and gray coral limestones (Fig. 25.11) of a few meters thickness. Fuchs et al. (1988, p. 603) obtained the following corals from these last beds.

Parathecosmilia sellae (Stoppani)
Retiophyllia clathrata (Emmrich)
Astraeomorpha crassisepta Reuss
"*Sphinctozoa*" gen. and sp. indet.
Spongiomorpha ramosa Frech
Parachaetetes sp.
Montlivaltia sp. and? *Montlivaltia marmorea* (Frech).

Some part of this formation was deposited in a deeper water environment, however, coral and other fossils indicate a shallow marine environment. As compared to the Mukut Limestone, the production of carbonates was much reduced and the Tarap Shales pass upwards into the more arenaceous succession of the Quartzite Beds. This formation is 400–600 m thick in Manang (Fuchs et al. 1988, p. 602).

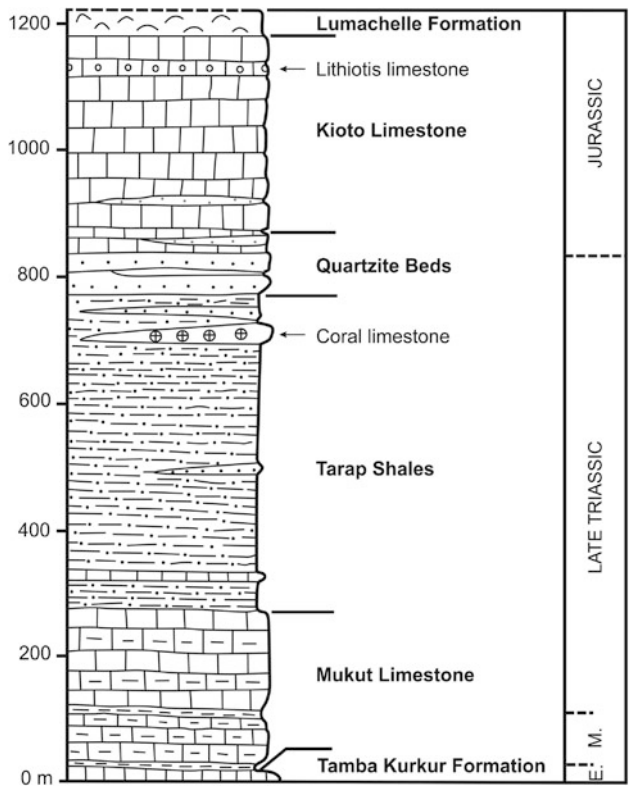

Fig. 25.11 Generalized section of the Mesozoic rocks in Manang. *Source* Modified from Fuchs et al. (1988)

25.8.4 The Rhaetian or Quartzite Beds (Late Triassic)

In the Jarsgeng Valley of Manang, sandy limestone or sandy claystone alternations are very characteristic of the Rhaetian (Fig. 25.11), as was the case in the Thakkhola region. There are mainly rhythmic interbeddings of two or three lithologies: with the lower bed, consisting of a coarse sandstone; intermediate bed with cross-lamination, and frequently containing limestone lenses; and the upper beds of limestone or argillaceous limestone. The only difference is the appearance of a thick (15 m) limestone horizon of pink color, containing abundant fragments of bivalve and *Polypora branchus* (Colchen 1975, p. 93).

25.9 Jurassic

The Jurassic succession, cropping out in Manang, is similar to that of the Thakkhola. It seems, according to some observations made in the sector of the Jarsgeng, that the Jurassic sediments are thinner here than in the Thakkhola, notably the Jomosom Limestone. The black shales with calcareous concretions, equivalents of the Spiti Shales, represent the last beds in Manang. They occupy the core of the syncline of Thorungse North (Colchen 1975). The Jurassic rocks are divided into the following lithostratigraphic units.

25.9.1 Kioto or Jomosom Limestone (Early Jurassic)

The dark colored Tarap Shales grade over an approximately 50 m thick, light- and dark-banded marker horizon of the Quartzite Beds (Fig. 25.2b). The marker horizon consists of white, gray, green, brown, and black, fine- to coarse-grained quartzites, calcareous quartzites, and calcareous sandstones, alternating with bluish gray carbonates and green shales. The marker horizon also contains numerous cross-laminae, clay galls, and worm burrows and pipes (Fuchs et al. 1988, p. 603).

At the expense of the arenaceous beds, the carbonate rocks become prominent in the Kioto Limestone (Fig. 25.12). It consists of blue and gray dolomite and limestone with oolites, pelletal structures, intraformational breccias, and intraclasts. This formation is rich in algae, corals, bryozoans, brachiopods, foraminifera, pelecypods, gastropods, and crinoids. It also contains Megalodon shells

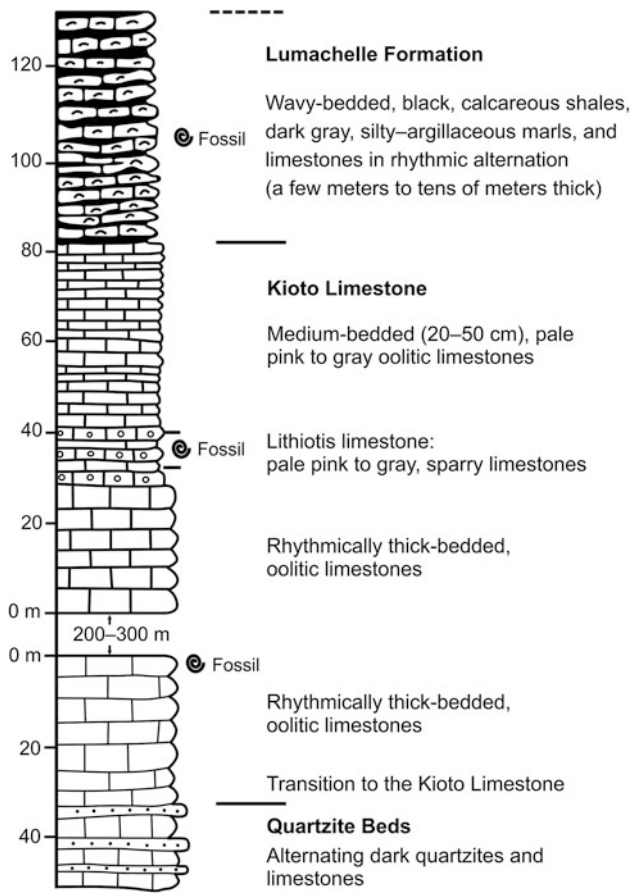

Fig. 25.12 Lithostratigraphic sequence of the Quartzite Beds, Kioto Limestone, and Lumachelle formation in Manang. *Source* Modified from Fuchs et al. (1988)

in the Triassic part and Lithiotis in the Early Jurassic part. Fuchs et al. (1988, p. 603) identified the following Early Jurassic (mainly its middle part) foraminifera from the Kioto Limestone.

Orbitopsella praecursor (Gümbel)
Lituosepta sp.
Lenticulina sp.

Petrographically, the limestones are represented by oomicrite (bioclastic packstone), oosparite (bioclastic grainstone), and biointrasparite (grainstone with aggregate grains). The Kioto Limestone is 300–400 m thick, and it was deposited in an inner shelf area with tidal flats, characterized by warm and shallow water with moderate to restricted circulation (Fuchs et al. 1988, p. 604).

25.9.2 Lumachelle Formation (Middle Jurassic: Bajocian–Bathonian)

The Lumachelle Formation (Fig. 25.12) occurs sporadically in Manang, and occupies the cores of tight synclines. It is composed of wavy-bedded, black calcareous shales with thin layers of ochrous-weathering blue sandstone, arenaceous limestone, marl, and micaceous limestone in rhythmic alternations (Fuchs et al. 1988, p. 604). This formation contains compact bivalves, crinoids, and belemnites together with worm burrows. The Lumachelle Formation is more than 50 m thick in Manang.

References

Bordet P, Colchen M, Le Fort P (1975) Recherches géologiques dans l'Himalaya du Népal, région du Nyi-Shang. Centre National de la Recherche Scientifique, Paris, 138 pp (with a geological map in colors)

Colchen M (1971) Les formations Paléozoïques de la Thakkhola. In: Bordet P, Colchen M, Krummenacher D, Le Fort P, Mouterde R, Rémi M (eds) Recherches géologiques dans l'Himalaya du Népal, région de la Thakkhola. Centre National de la Recherche Scientifique, Paris, pp 85–118

Colchen M (1975) Les séries Tibétaines. In: Bordet P, Colchen M, Le Fort P (eds) Recherches géologiques dans l'Himalaya du Népal, région du Nyi-Shang. Centre National de la Recherche Scientifique, Paris, pp 67–96

Fuchs G, Widder RW, Tuladhar R (1988) Contributions to the geology of the annapurna range (Manang Area, Nepal). Jahrbuch der Geologischen Bundesanstalt (Jb Geol B-A), Wien 131(4):593–607 (with 2 plates containing a map and sections)

Lyell C (1875) Principles of geology (or the modern changes of the earth and its inhabitants), vol I, 12th edn. John Murray, London, 655 pp

Tethys Himalaya of Koshi Region (Mount Everest and Neighborhood)

26

The thickest part of the crust does not lie beneath the main range of the Himalayas but under the low-lying country of the Yalu Tsangpo Valley instead.

—Chang and Chen (1973, p. 262)

The Tethyan rocks of Mount Everest and its neighborhood were first explored by the Geological Survey of India at the beginning of the twentieth century. As early as 1903 and 1904, on his way from Yadong to Gyangze and Lhasa, Hayden carried out an investigation of the Cretaceous and Tertiary strata in the Kamba (Kampa) area of Tibet. Heron (1922, p. 224) observed that the Tethyan rocks, occupying the area north of Mount Everest, consist essentially of a very thick pile of intensely folded and faulted dark brown and black Jurassic shales and argillaceous sandstones. The folds trend east–west, and their tight synclinal cores contain the limestones of the Cretaceous and Eocene ages, belonging to the Kampa system of Hayden (1907). Most of the synclines are overturned with their axial planes dipping due north.

The climbers of the second Mount Everest expedition collected rock specimens from altitudes between 7,000 and 8,200 m. The samples show that the mountain is composed of black to green-gray banded hornfelses and the same colored foliated fine-grained calc-silicate schists together with fine-grained white crystalline limestones. The calc-silicates are slabby and gently dip due north (Heron 1922, p. 235).

Odell (1925) identified the Lower Calcareous series, Gneissose Biotite series, and Upper Calcareous series in the Everest region, and also mapped two faults in the northeast-trending ridge of Mount Everest. Subsequently, Wager (1934, 1939), who was a member of the 1933 Everest expedition, made remarkable observations regarding the drainage pattern of the Arun River (Chap. 3) and the faults (Box 26.1). He also found late Permian fossils on the Lachi Hills and classified the rocks into the following units (Table 26.1).

His Mount Everest Limestone series corresponds to Odell's Upper Calcareous series.

Box 26.1: Discovery of Normal Faults

Regarding faulting, Wager (1939, p. 175) remarks,

> At the entrance to the Rongbuk valley the lower part of the Mount Everest limestone series is injected by granite sills yet, a 100 ft (30 m) above, the only obvious metamorphic effect is a slight hardening, and veining by granite does not occur… No signs of a basement bed to the limestone series are to be seen, nor weathering of the upper part of the gneiss. On the other hand, there are abundant signs of violent movement, so that I regard the junction, which dips north at about 45°, as a fault plane. The Mount Everest limestone is at least a 1,000 ft (300 m) thick in Lhonak, to the west, and probably the same at Dothak in the Chumbi valley, to the east, and it is likely therefore, that on Lachi the fault cuts out much of the limestone. It is noteworthy that the postulated fault is apparently a normal one and not a thrust although it has a relatively low dip.

After such sporadic and cursory reconnaissance, it was left for the Chinese geologists to carry out detailed work in the Mount Everest region, primarily between 1966 and 1968. They covered a vast expanse of about 50,000 km^2, lying between the Himalayan Range to the south, the Yarlung Zhangbo River to the north, Yadong on the east, and Gyirong on the west. Their investigations were confined mainly around Chiatsun, Yali, Naxing, Tulung, Niehnieh Hsiungla section in the Po Chu (Bhote Koshi) River, around Gyirong, Gyagya, Mount Everest, Mount Shisha Pangma, Tingri, Nyalam, Kamba, Shigatse, and Gyangze.

The Tethyan sequence of this tract ranges in age from the Cambro–Ordovician to early Tertiary (Fig. 26.1), and attains a thickness of more than 11,500 m (Wen 1987a, p. 3). The region can be separated into the north and south belts by

M.R. Dhital, *Geology of the Nepal Himalaya*, Regional Geology Reviews,
DOI 10.1007/978-3-319-02496-7_26

Table 26.1 Classification of Wager

Tso Lhamo series	Dark limestones and shales. Probably Triassic
	(Exact relationships to beds below not yet proved)
	Quartzites and shales, the lowest quartzite (ca. 125 m) forming summit of Lachi
Lachi series	Calcareous sandstones, late Permian (ca. 100 m)
	Pebble beds (ca. 200 m)
	Fossiliferous limestones and shales (ca. 15 m)
	Quartzites, hardened silts and shales (ca. 200 m)
Mount Everest Limestone series	Massive arenaceous limestone (ca. 60 m)
	Base cut out by a normal fault

Source Based on Wager (1934, pp. 221–222, 1939, p. 178)

the Zhongba–Gyangze Thrust (Chang and Cheng 1973; Liu 1988). But such a division is quite arbitrary and should not be applied unconditionally (Wang et al. 1987, p. 193). The south belt is rather complete and is composed mainly of carbonates and siliciclastic rocks, whereas the north belt comprises sandstones, shales, and limestones. The Tethyan strata of the south belt have a faulted contact with the underlying Proterozoic rocks of the Jolmo Lungma Group, representing the upper part of the Higher Himalaya (Mu et al. 1973, p. 97).

26.1 Cambro–Ordovician

The Cambro–Ordovician succession of the south belt crops out for about 100 km, between Nyalam on the west and Sar of Dinggye on the east. It was studied in 10 sections, where the strata are gently (20–35°) dipping due NNW. The low-grade metamorphic rocks, constituting the area north of Nyalam, are classed under the Rouqiecun Group (Mu et al. 1973; Yin 1987). This group is conformably overlain by the Chiatsun Group, but is in fault contact with the underlying Jolmo Lungma Group, containing pale yellow to white or pink mylonitic granites or gneisses, passing downwards to muscovite granite-gneisses and marbles (Yin 1987).

The Rouqiecun Group, whose thickness varies from 40 to 160 m, is subdivided into the Lower Formation and the Upper Formation. The Lower Formation consists of dark gray to black diopside-quartz schists, alternating with fine-grained biotite–phlogopite–muscovite schists. The rock is affected by metasomatism and skarns are developed in it. There are also sporadic bands of migmatite and mylonitic gneiss or granite. The Upper Formation comprises gray (yellow-gray, when weathered) crystalline limestones, containing calcite, quartz, plagioclase, biotite, epidote, sericite, and other minerals, oriented parallel to the foliation (Mu et al. 1973, p. 97).

The crystalline limestones, belonging to the Upper Calcareous series of Odell (1925) or the Mount Everest Limestone series of Wager (1939), are equivalent to the Upper Formation of the Rouqiecun Group. The limestone samples of Mount Everest, obtained from an altitude of 8,500 m, were dated at 410–515 Ma by U–Pb methods (Mu et al. 1973, p. 98).

26.2 Ordovician

The Ordovician rocks are described under the Chiatsun (Jiacun) Group and the overlying Hongshantou Formation (Mu et al. 1973, p. 98).

The Upper Formation of the Rouqiecun Group transitionally passes upwards into the Chiatsun Group. The Chiatsun Group is further subdivided into the Lower Formation of gray or yellow-gray (when weathered) medium- to thick-bedded, argillaceous or sandy, banded limestones, oolitic limestones, and calcareous siltstones. This formation varies in thickness from 500 m in Sar of Dinggye to about 300 m in Dotag of Yadong. It contains a large number of fossils, including brachiopods *Aporthophylina intermedia* Liu, *Aporthophyla perelegans* Liu, *Orthambonites* cf. *O. rotundiformis* Cooper, nautiloids *Ordosoceras contractum* Chen, trilobites *Eucalymene tuberculata* Qian, gastropods, and crinoid stems. These fossils indicate an Early Ordovician age (Wang 1987a, p. 38).

The Upper Formation of the Chiatsun Group includes light to vivid purple argillaceous limestones, attaining a thickness of 97 m. It contains cephalopods *Sinoceras chinense* (Foord) and *S. densum* (Yu), crinoidal stems, some brachiopods, and gastropods. These fossils indicate a Middle Ordovician age (Wang 1987a, p. 39).

The Hongshantou Formation conformably overlies the Upper Formation. It is composed of gray, brown, and red calcareous silty shales intercalated with fine sandstones, and has a thickness of about 70 m. No identifiable fossils were recovered from this formation, and it is inferred to belong to the Late Ordovician (Wang 1987a, p. 39).

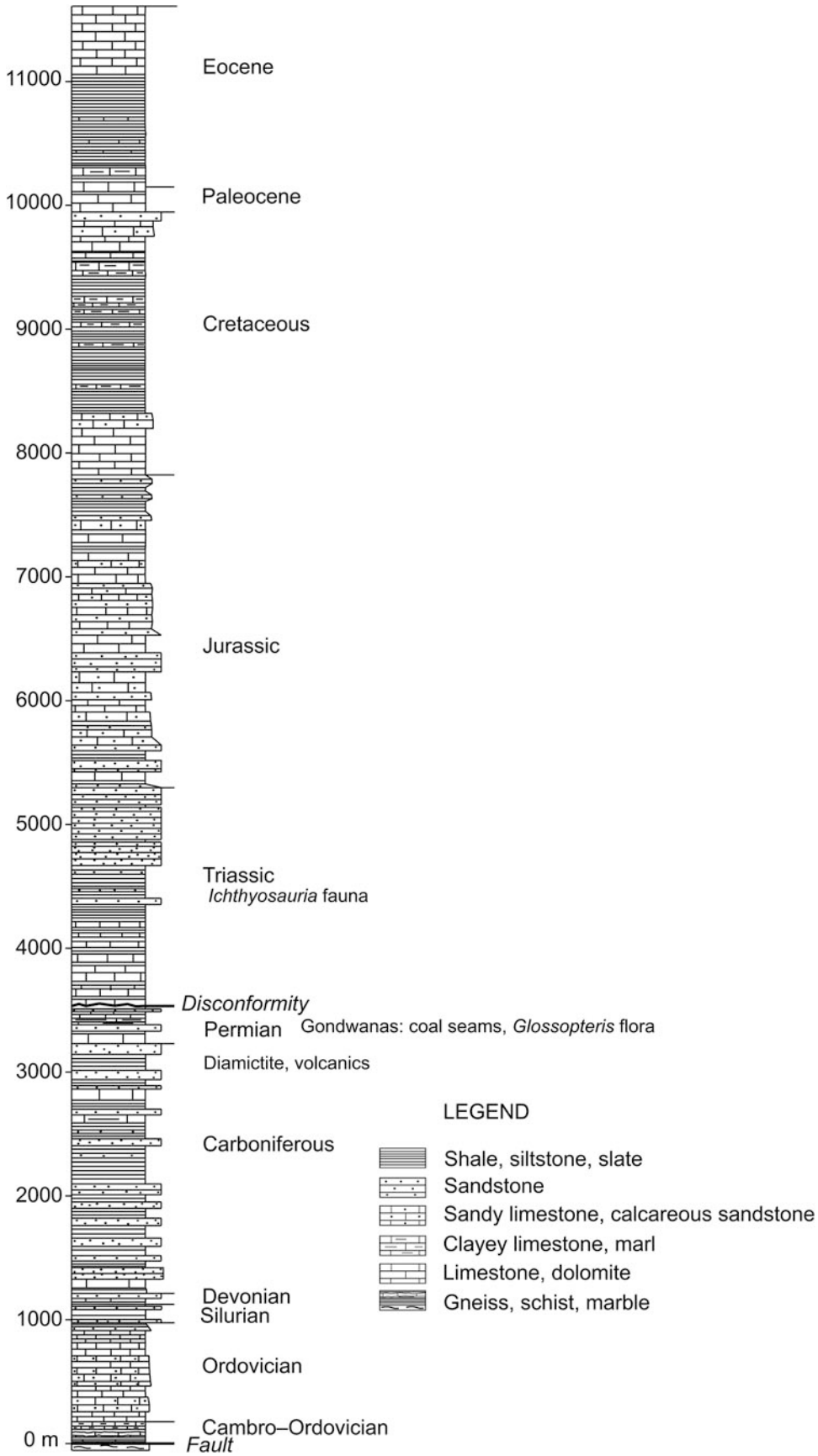

Fig. 26.1 Generalized stratigraphic column of the Tethys Himalaya in the Everest region. *Source* Based on Mu et al. (1973), Wang et al. (1987), and Wang and Mu (1987)

26.3 Silurian

The fossiliferous Silurian rocks transitionally overlie the Hongshantou Formation, and they are classed under the Shiqipo Group, which is again subdivided into the Lower and Upper formations.

The Lower Formation is made up of sandstones at the base, graptolite-bearing black shales in the middle, and limestones with cephalopods and corals in the upper part (Mu et al. 1973, p. 99). The graptolites belong to *Streptograptus lobiferus* (Mc Coy), *Climacograptus normalis* Lapworth, *Cl. rectangulata* (Mc Coy), and *Monograptus priodon* (Bronn). Among the cephalopods, *Michelinoceras transiens* (Barrande), *Michelinoceras* (*kopaninoceras*) *capax* (Barrande), and *Columnoceras priscum* Chen are common, whereas the corals are represented by *Favosites* sp. and *Triplophyllum nyalamense* Yü. This formation is about 90 m thick and belongs mainly to the early Silurian. It is broadly equivalent to the Dark Band Formation in the Thakkhola area (Wang 1987a, p. 40; Chap. 24).

The Upper Formation comprises gray quartzose sandstones, interbedded with dark gray to brown argillaceous limestones, grading towards the upper part into gray limestones. In its lower part are found *Monograptus vomerina subgracilis* Pribyl, *Pristiograptus dubius* (Suess), and *P. dubius latus* (Boucek). This formation also yielded a cephalopod *Michelinoceras* (*kopaninoceras*) *jucundum* (Barrande) from its upper part. The Upper Formation is 46 m thick and ascribed to the middle Silurian. But because its upper part is cut out by a fault, this formation may represent the late Silurian as well (Mu et al. 1973, p. 100; Wang 1987a, p. 40).

Hayden (1907) designated the Dothak series for the limestones with a subordinate amount of sandstones, quartzites, shales, and slates cropping out in Dotag–Akang lying north of Yadong. Although he inferred that most of the 450 m thick limestones belong mainly to the Carboniferous–Triassic, the principal part of the Dothak series is actually the Early Ordovician, and it is equivalent to the Lower Formation of the Chiatsun Group (Wang 1987a, p. 49).

26.4 Devonian

The Devonian rocks comprise quartzites, slates, and phyllites with a total thickness exceeding 500 m. They are classified into the Liangquan Formation and the Pochu (Boqu) Group. The Early Devonian Liangquan Formation is about 40 m thick, and its lower part is made up of gray shales, whereas the upper part contains gray shales, alternating with gray-black thin-bedded limestones (Wang 1987b, p. 51). This formation is very rich in graptolites in its lower part and tentaculites in the upper part. The formation is divided into a graptolite zone and two tentaculites zones. The graptolite zone is predominated by *Neomonograptus himalayansis* Mu & Ni, *Monograptus thomasi* Jaeger, and *Monograptus* cf. *M. yukonensis* Jackson & Lenz. They indicate a Pragian age. The overlying two tentaculites zones contain *Nowakia acuaria* (Richter), *Guerichina xizangensis* Mu, and *Metastyliolina nyalamensis* Mu. The tentaculites indicate a late Pragian age (Wang 1987b, pp. 52–53).

The transitionally overlying Pochu Group consists mainly of medium- to thick-bedded, light gray quartzose sandstones, totaling 256 m in thickness. It conformably underlies the Carboniferous rocks. This group contains some indeterminable plant remains in its upper part. Based on its stratigraphic position, this group is assigned to the Middle and Late Devonian and is equivalent to the Tilicho Pass Formation in the Thakkhola area (Chap. 24).

26.5 Carboniferous

The Carboniferous rocks are divided into the Yali Formation succeeded, respectively, by the Naxing Formation and Jilong Formation (Wang et al. 1987, p. 196). The Yali Formation comprises dark gray to black, medium- to thick-bedded shales in its lower part, followed by argillaceous limestones towards the upper part. This formation is 126 m thick and contains the ammonoids: *Imitoceras orientale* Liang, *I. xizangense* Liang, and *Gettendorfia yaliense* Liang. This formation also includes some brachiopods, such as *Tylothyris* cf. *T. pseudopostrea* (Besnossova), *Pseudosyrinx keokuk* Weller, and *Gyrtiella nyalamensis* Ching. These fossils indicate a Tournaisian age for the upper part of this formation (Zhang 1987a, pp. 63–65). However, its lower part may still belong to the Late Devonian (Wang et al. 1987, p. 193).

The Naxing Formation consists of grayish black shales, intercalated with conglomerates, sandstones, and marls. This formation attains a thickness of 1,888 m, and is subdivided into the following three parts. The lower part is made up of medium- to coarse-grained sandstones, intercalated with thick conglomerates near the base, and there are speriferids with simple costae. The middle part comprises fine conglomerates and quartzose sandstones at its lower level, and they give way to shales upwards and carry primitive dictyoclostids. The upper part is dominated by sandstones and shales, containing bivalves (Zhang 1987a, p. 63).

The lower part of the Naxing Formation contains brachiopods *Fusella holdhausi* (Diener) and *Fussella transversa* Ching. It also contains a conularid *Sinoconularia canaliculata* Chang, and a gastropod *Bellerophon* sp. The middle part yields brachiopods *Tolmatchoffia* sp., *Marginirugus* cf. *M. magnus* (Meek & Worthen), and *Syringothyrix*

ex. gr. *lydekkeri* (Diener), and a lammelibranch *Pernopecten* cf. *P. tenuis* (Koninck). In the upper part of the Naxing Formation are found bivalves *Sanguinolites omalianus* (Koninck) and *Sedgwickia* cf. *S. subregularis* (Koninck), and a gastropod *Retispira nyalamensis* Yu. In Selung, the Carboniferous rocks contain brachiopods *Gigantoproductus shishapangmaicus* Liao, *Balakhonia kokdscharensis* (Grober), and a bryozoan *Meekopora magna* Yang & Hsia. Based on these fossils, the lower and middle parts of the Naxing Formation range in age from the Tournaisian to the Visean, whereas the upper part may represent the remaining Carboniferous Period (Mu et al. 1973, p. 102; Zhang 1987a, p. 66). But the observations of Wang et al. (1987, p. 196) reveal that the Naxing Formation as a whole may belong mainly to the early Carboniferous.

Yin and Guo (1976) investigated the strata of Gondwana affinity, and included them under the Jilong Formation. It contains the Chataje Diamictite Member, and is followed by yellow to green-gray medium- to thick-bedded quartzose sandstones, alternating with light to dark gray shales containing *Stepanoviella.* Some volcanic rocks are also intercalated. The upper part of this formation is designated as the Chaya Quartzose Sandstone Member. This Formation is about 700-m thick and attributed to the late Carboniferous (Wang et al. 1987, p. 196). The Jilong Formation can be correlated with the Umaria marine beds or the *Eurydesma*-bearing deposits of the Indian Subcontinent (Wang and Mu 1987, p. 220).

26.6 Permian

The Permian rocks are classed under the Selung Group, which is widely distributed in Nyalam, Tingri, and Gyirong. It consists mainly of limestones, intercalated with a subordinate amount of sandstones and shales in the lower part. The limestones predominate westwards (i.e., towards Gyirong), whereas to the east (around Nyalam) it comprises mainly marls intercalated with sandstones and shales. Its exposed thickness is 281 m and has a faulted lower contact. The Selung Group contains a variety of fossils, such as brachiopods, bryozoans, corals, gastropods, ammonoids, and bivalves. The brachiopods include *Marginifera himalayansis* Diener, *Waagenoconcha purdoni* (Davidson), *Costiferina spiralis* (Waagen), *Costiferina indica* (Waagen), *Costiferina alata* Waterhouse, *Chonetinella* cf. *C. lissarensis* Diener, *Chonetinella nasuta* Waagen, *Neospirifer ravana* (Diener), *Speriferella tibetana* (Diener), and *Speriferella rajah* (Salter). The bryozoans consist of *Fistuliramus labratulus* (Bassler), *Fenestella* cf. *F. subornata* Schulga–Neterenko, and *Polypora praepluriformis* Morozova. The corals include *Plerophyllum* cf. *P. leptoconicum* (Abich) and *Wannerophyllum dissitum* Wu (Zhang 1987b, pp. 74–75).

The Selung Group is further subdivided into the Qubu Formation and the overlying Quburega Formation (Yin and Guo 1976). The Qubu Formation comprises about 20 m thick sandy shales, containing a *Glossopteris* flora, whose age ranges from the Carboniferous to Early Triassic (Wang and Mu 1987, p. 219). But, based on the stratigraphic position, it is attributed to the early Permian. Similarly, the overlying Quburega Formation, consisting of siltstones, sandy shales, and bioclastic limestones, carries a cold-water fauna, represented by the coral *Lytvolasma asymetricum* and other marine biota, including brachiopods, bryozoans, ammonoids, and bivalves. It ranges in age from the early Permian to late Permian. There is a disconformity between the Selung Group and the overlying Triassic rocks of the Tulung Group (Wang et al. 1987, pp. 196–197).

26.7 Triassic

In the south belt, the Triassic rocks are extensively distributed between Gyirong, Nyalam, and Yadong, where their thickness reaches 1,696 m. They are further divided in ascending order into the Tulung Group, Qulonggongba Formation, and the Derirong Formation. The Triassic succession includes 17 ammonite zones, 3 bivalve zones, and 1 zone of *Ichthyosauria* (Mu et al. 1973, p. 103; Yin et al. 1987, p. 96).

The Tulung Group is subdivided into the Kangshare Formation, Laibuxi Formation, Zhamure Formation, and Dashalong Formation in ascending order (Wang et al. 1987, p. 198). The Early Triassic (Induan) Lower Member of the Kangshare Formation is 63 m thick, and consists of gray to light purple shales, interbedded with gray, medium-bedded, bioclastic limestones with dolomites and dolomitic limestones in its basal part. It includes three ammonite zones, represented by *Gyronites psilopyrus*, *Ophiceras* (*Lytophiceras*) *sakuntala*, and *Otoceras latilobatum.* The Upper Member (Olenekian) is 40 m thick, and comprises red-purple, gray, medium- to thick-bedded limestones with argillaceous beds in the top part. This member contains one ammonoid-bearing bed (*Procarnites–Anasibirites*), one ammonoid zone (*Owenites*), and two conodont zones (*Neogandollela jufata* and *Neospathodus waageni*). The Laibuxi Formation of Middle Triassic age is made up of the 126 m thick Lower Member of gray, yellow, green, shales, alternating with yellow sandy and tuffaceous limestones, which are intercalated in tuffaceous sandstones and gray limestones with a sandy bed in the lower part. This member includes three ammonite zones: *Ptychites rugifer*, *Anacrochordiceras nodosus*, and *Japonites magnus.* The Upper Member of the Laibuxi Formation is 133 m thick, and contains dark gray, medium-bedded limestones, argillaceous limestones, and gray shales. It includes the Ladinian

Protrachyseras–Joanites-bearing beds and the *Daonella indica* assemblage. The Zhamure Formation, corresponding to the Carnian Stage, is 99 m thick, and is represented by bioclastic limestones, siliceous and argillaceous limestones, and siderite-bearing limestones. They are interbedded with sandy shales. The *Halobia comata* assemblage occurs in its lower part, whereas the *Parahauerites acutus* zone, *Hoplotropites* zone, and *Indonesites dieneri*-bearing horizon occur in its upper part (Wang et al. 1987, p. 198). The Dashalong Formation is 179 m thick and comprises medium-bedded, gray, bioclastic limestones and sandy limestones, alternating with calcareous siltstones and sandy shales. It contains the *Griesbachites–Gonionotites* zone and the *Nodotibetites nodosus* zone, and it is of middle–late Lacian (Early Norian) age (Wang et al. 1987, p. 199).

The Qulonggongba Formation contains siltstones and sandy shales, which are intercalated with thinly bedded bioclastic limestones. There are three ammonite zones in it: the *Indojuvavites angulatus* zone, *Cyrtopleurites socius* zone, and the "*Himavatites columbianus*" zone. It attains a thickness of 465 m, and spans from the Alaunian to early Sevatian (Middle–Late Norian) in age (Yin et al. 1987, pp. 102–103).

An *Ichthyosauria* fauna was recorded from the Qulonggomba Formation in Tulung of Nyalam. The discovery of these as well as other fossil vertebrates entails that the sea was intermittent and shallow during Late Triassic time (Yin et al. 1987, p. 108).

The Derirong Formation is made up mainly of quartzose sandstones, intercalated with sandy limestones, carbonaceous sandstones, and coal seams. It yields the Late Triassic *Paleocardita mansuyi*, *Nuculana perlonga*, and *Indopecten serraticostus* (Bittner) fauna and is 591 m thick.

26.8 Jurassic

The Jurassic rocks cropping out in the south belt are divided into the Pupuga Formation (Early Jurassic), Niehnieh Hsiungla Formation (Middle Jurassic), and Menkatun Formation (Late Jurassic), from bottom to top, respectively.

The Pupuga Formation is composed mainly of gray to yellow-green sandstones and shales, with intercalations of gray limestone or sandy limestone. This formation is 421 m thick, and its basal part contains sandy shales or sandy limestones, which grade downwards into the quartzose sandstones of the Late Triassic Derirong Formation. The Pupuga Formation includes a plentiful assortment of fossils; it is especially rich in ammonoids, foraminifers, and bivalves of Early Jurassic age. They include *Schlotheimia* (Hettangian), *Sulciferites* and *Gleviceras* (Sinemurian), and *Nyalamoceras nylamensis* (Toarcian). The Early Jurassic rocks in the vicinity of Gyirong and west of Niehnieh Hsiungla are thinner, and contain more carbonate rocks in their lower part (Wang and Zhang 1987, pp. 120–121).

The Niehnieh Hsiungla Formation is subdivided into the lower, middle, and upper units. The lower unit, belonging to the Bajocian, is 732 m thick and consists of gray to dark gray limestones, alternating with sandstones in the lower part and argillaceous limestones in the upper part, whereas its middle part is predominated by sandstones. It includes ammonites *Dorsetensia haydeni* Arkell, *Dorsetensia xizangensis* Wang, *Witchella tibetica* Arkell, and *Sonninia* cf. *S. dominans* Buckman. The Lungma Limestone of Hayden (1907) is equivalent to the upper part of this unit. The middle unit (Bathonian) is 647 m thick, and comprises medium- to thick-bedded, medium- to coarse-grained, gray quartzose sandstones, interbedded with dark gray to black limestones, oolitic limestones, and sandy limestones. It includes some bivalves and brachiopods. The upper unit (Callovian) is 260 m thick and contains gray, dark gray, and black sandy limestones, alternating with a few beds of gray, black, or yellow-green shales and sandy shales. They are followed upwards by medium- to thin-bedded dark gray limestones, sandy limestones, and quartzose sandstones. The upper unit contains ammonites, such as *Macrocephalites*, *Dolikephalites*, *and Indocephalites* (Wang and Zhang 1987, pp. 122–123).

The transitionally overlying Menkatun Formation contains dark gray to green-gray silty shales, siltstones, and fine sandstones, with concretions in the lower part; a succession of gray siltstones, sandy shales, and gray medium- to thick-bedded quartzose sandstones in the middle part; and an intercalation of dark gray, medium- to thick-bedded limestones and sandy limestones (the Guocuo Limestone) in the upper part. This formation is more than 630 m thick, and includes the *Virgatosphinctes–Aulacosphinctes* bed in the lower part and the *Himalayites–Blanfordiceras* bed in the upper part. The Menkatun Formation ranges in age from the Kimmeridgian to Tithonian, and can be correlated with the Spiti Shales (Wang and Zhang 1987, p. 124; Wang et al. 1987, p. 200).

26.9 Cretaceous

The Cretaceous rocks distributed in the south belt are divided into the Kamba Group, Zongshan Formation, and Jidula Formation in ascending order.

The Kamba Group includes the Giri Limestone, Kampa Shales, and Hemiaster Shales of Hayden (1907). Its thickness varies from 1,187 m at Chajiela to 800 m in the east of Kamba. It comprises shales and sandy shales intercalated with thin-bedded marls and sandstones. Generally, the rocks are dark gray to black in the lower part, and gradually become lighter colored upwards, and weather to gray-green and blue-gray tints (Wen 1987b, p. 137).

The Kamba Group is subdivided into the Kangbadongshan Formation, Chaqiela Formation, and Kangbacunkou Formation in ascending order. The Kangbadongshan Formation is 201–530 m thick, and consists of gray, dark gray, and black shales, alternating with gray limestones and marls. This formation is broadly equivalent to the Giri Limestone of Hayden (1907). There is a significant lithofacies change from east to west. In the east, there are more carbonate rocks that infrequently alternate with shales, whereas to the west, there are mainly coarse-grained siliciclastic rocks. This formation essentially contains three fossil-bearing horizons. The first horizon (Valanginian) has the bivalves *Laevitrigonia cardiniformis* and *Astarte spitiensis.* The second horizon (Aptian) yields the ammonoid *Parahoplites* sp. and bivalves *Pleuromya spitiensis* Holdhaus and ?*Plectomya* sp. The third horizon (Albian) entombs the ammonoids *Mortoniceras* sp., *Dipoloceras crystatum* (Delug), and *Cleoniceras xizangense* Chao. This formation ranges in age from the Valanginian to Aptian or Albian, and can be correlated with the Giumal Sandstone (Wang et al. 1987, pp. 201–202; Chap. 22).

The Chaqiela Formation has a thickness of about 240 m, and contains dark gray to black (blue-gray when weathered) or green-gray shales with subordinate sandstones and calcareous shales in the upper part. This formation roughly corresponds to the Kampa Shales of Hayden (1907). Based on its stratigraphic position, the Chaqiela Formation is attributed to the Late Albian to Early Cenomanian (Wang et al. 1987, p. 202).

The Kangbacunkou Formation is made up mainly of gray shales and calcareous shales, alternating with marls and varies in thickness from 344 to 500 m. It is broadly equivalent to the Hemiaster shales of Hayden (1907), and contains two fossil-bearing horizons. The first one (Cenomanian–Turonian) yields the ammonoids *Acanthocers* sp., *Calycoceras newboldi* (Kossmat), and the foraminifers *Rotalipora* cf. *R. cushmani* (Morrow), *R.* cf. *R. appenninica* (Renz), and *Praeglobotruncana* cf. *P. stephani* (Gandolfi). The second horizon (Coniacian–Santonian) includes the foraminifer *Neoflabellina* cf. *N. ovalis* Wedekind, bivalve *Pycnodonte* (*Phygraea*) *vesiculosa* (Sowerby), and echinoids *Hemiaster front-acutus* Stoliczka and *H.* cf. *H. oldhami* Noetling (Wang et al. 1987, pp. 201–202).

The transitionally overlying Zongshan Formation varies in thickness from 278 to 223 m. The lower part of it is made up of gray argillaceous limestones, passing into a thick-bedded dark blue to gray limestone at the basal part, corresponding to the first scarp limestones of Hayden (1907). The foraminifers *Globotruncana linneiana* (d'Orbigny), *G. carinata* Dalbiez, *G. bulloides* Vogler, *and Heterohelix* sp. were recovered from the overlying succession of gray shales. The middle part of this formation includes the second scarp limestones of Hayden (1907) and overlying gray shales. The thick-bedded limestone abundantly contains the foraminifers *Orbitoides apiculata* Schlumberger, *O. media* (d'Archiac), *Omphalocyclus macroporus* (Lamarck); echinoids *Hardouinia* cf. *H. aequorea* (Morton), *Rhychopygus lapiscaneri* (Leske), *and Petalobrissus lefeburei* (Fourtan); and bivalves *Biradiolites* sp., *Bournonia tibetica* Douvillé, and *B. haydeni* Douvillé. The upper part of the Zongshan Formation begins with the third scarp limestones, which are separated from the underlying second scarp limestones by a 13 m thick, gray, calcareous shale, and is succeeded upwards by the Tüna limestones of Hayden (1907). The third scarp limestones are represented by hard and massive sandy varieties, and contain plentiful fossils, including foraminifers *Orbitoides apiculata* Schlumberger and *O. media* (d'Archiac); ostracods *Bairdia* sp. and *Cytherella tuberculifera* Alexander; echinoids *Domechinus sinensis* Mu & Wu and *Hemipneustes striatoradiantus* (Lesk); and bivalves *Neithea* (*Neitheops*) *qudricostata* (Sowerby) and *Plicatula hirsuta plicata* Douvillé. The Zongshan Formation ranges in age from the Campanian to Maastrichtian, and is followed conformably by the Jidula Formation (Wen 1987b, pp. 138–139).

The Jidula Formation, corresponding to the Ferruginous Sandstone of Hayden (1907), is 188 m thick and comprises brown, grayish, and gray-green quartzose sandstones, intercalated with a few beds of sandy limestone in its middle or lower part. The sandy limestone includes the foraminifers *Verneuilina* sp., Miliolidea gen. et sp. indet., Rotalidea gen et sp. indet.; ostracods *Bairdia acrocaudalis* Huang, *Propontocypris arrosa* Huang & Zhang, and *Xestoleberis kangpaensis* Huang. The Jidula Formation belongs mainly to the Maastrichtian Stage (Wen 1987b, p. 140).

26.10 Tertiary

In the Kamba region, the Tertiary rocks are represented by the Zongpu Group (Wen 1987c), consisting mainly of limestones, but the top part of it contains shales in some sections. It has a total thickness of 383 m, and is divided into the following five members. The first member (78 m thick) comprises medium- to thin-bedded, gray limestones at the base, passing into a thick-bedded, massive limestone at the top. The last limestone contains foraminifers *Keramosphaera tergestina* (Stache) and *Lockhartia* sp.; and gastropods *Campanile ganesha* (Noetling), *Keilostoma multispirallum* Yu, and *Diconomorpha elegans* (Douvillé). The second

member is made up of dark gray limestones with plentiful gastropods, including *Campanile brevius* Douvillé, *Rhinoclavis pissarroi* Vredenburg, *and Velates tibeticus* Douvillé as well as a bivalve *Pseudomiltha* (*Zorrita*) *jidulaensis* Gu & Lan, and foraminifers *Miscellanea miscella* (d'Archiac & Haime), *Fasciolites oblongus* (d'Orbigny), and *Actinosiphon tibetica* (Douvillé). This member varies in thickness from 7 to 73 m, and corresponds to the Gastropod limestones of Hayden (1907). The third member includes gray limestones, interbedded with calcareous shales. Some of the fossils found in it are the foraminifers *Miscellanea miscella* (d'Archiac & Haime), *M. stampi* (Davies), *Lockhartia conditi* (Nuttall), *L. haimei* (Davies), and *Sphaerogypsina globulus* (Reuss); a bivalve *Spondylus rouaulti* d'Archiac & Haime; gastropods *Architectonica vredenburgi* (Cossmann & Pissarro) and *Kangpaya xizangensis* Yu; and an echinoid *Echinolampas* cf. *E. nuclus* Martheron. This member is equivalent to the Operculina limestones, Spondylus shales, and the lower part of the Orbitolites limestones of Hayden (1907), and ranges in thickness from 85 m to more than 150 m. The fourth member is constituted of gray massive limestones, passing into argillaceous varieties towards the top. It mainly bears the foraminifers ? *Opertorbitolites gracilis* Lehmann, *Orbitolites complanatus* Lamarck, and *Fasciolites* (*Glomalveolia*) *subtilis* Hottinger. This member is 33 m thick, and corresponds to the upper part of the Orbitolites limestones. The fifth member comprises gray limestones, alternating with gray-green shales, and its thickness ranges from 111 (with faulted top part) to 114 m. This member is equivalent to the sandy shales and Alveolina limestones of Hayden (1907). It has a profusion of foraminifers, including *Orbitolites cotentinensis* Lehmann, *Nummulites parvulus* Sheng & Zhang, *Fasciolites himalayensis* Sheng & Zhang, and *Rotalia trochidiformis* (Lamarck). It also contains the bivalves *Corbula* (*Bicorbula*) *subexarata* d'Archiac & Haime, *Lithophaga* (*Lithophaga*) *tibetensis* Wen & Lan, and the ostracods *Pokornyella* cf. *P. limbata* (Bosquet), and *Monsmirabilia* cf. *M. subovata* Apostolescu (Wen 1987c, pp. 154–156).

The transitionally succeeding Zhepure Formation is extensively distributed in the Tingri area, where it is over 1,285 m thick, and divided into two parts. The lower part is 967 m thick, and is made up mainly of gray-green shales interbedded with a minor amount of marl. The lower part contains the foraminifers *Orbitolites complanatus* Lamarck, *O. cotentinensis* Lehmann, *Fasciolites* (*F.*) *oblongus* d'Orbigny, *Assilina dendotica, Nummulites gallensis, and Operculina ammonea* Leymerie. The upper part of the Zhepure Formation is 318 m thick, and is represented by massive limestones yielding the foraminifers *Orbitolites complanatus* Lamarck, *Fasciolites* (*F.*) *oblangus* d'Orbigny, *Assilina orientalis* Douvillé, *Nummulites lucasi* Douvillé, and the ostracod *Brachycythere* (Wen 1987c, p. 172).

References

Chang C-F, Cheng H-L (1973) Some tectonic features of the Mt. Jolmo Lungma area, Southern Tibet, China. Scientia Sinica XVI(2):257–265

Hayden HH (1907) The geology of the provinces of Tsang and Ü in central Tibet. Mem Geol Surv India XXXVI(Part 2):1–80

Heron AM (1922) Geological results of the Mount Everest reconnaissance expedition. Rec Geol Surv India LIV(Part 2):215–234

Liu ZQ (1988) Geologic map of the Qinghai-Xizang Plateau and its neighboring regions (scale 1:1,500,000). Chengdu Institute of Geology and Mineral Resources, Geologic Publishing House, Beijing

Mu A-T, Wen S-H, Wang Y-K, Chang P-K, Yin C-H (1973) Stratigraphy of the Mount Jolmo Lungma region in Southern Tibet, China. Scientia Sinica XVI(1):96–111

Odell NE (1925) Observation on the rocks and glaciers of Mount Everest. Geogr J LXVI(4):289–315 (with a map in colors on 1:25,000 scale)

Wager LR (1934) A review of the geology and some new observations. In: Ruttledge H (ed) Everest 1933. Hodder & Stoughton, London, pp 312–336 (with a geological sketch map on scale 1 inch = 10 miles) (Chapter VII)

Wager LR (1939) The Lachi Series of North Sikkim and the age of the rocks forming Mount Everest. Rec Geol Surv India 74(Part 2):171–188, (with 5 plates, including a geological sketch map)

Wang Y (1987a) Ordovician system and Silurian system. Stratigraphy of the Mount Qomolangma region. Xizang Scientific Expedition, Academia Sinica, Beijing, pp 27–49

Wang Y (1987b) Devonian system. Stratigraphy of the Mount Qomolangma region. Xizang Scientific Expedition, Academia Sinica, Beijing, pp 50–60

Wang Y, Sun DI, He G (1987) New advances in the stratigraphy of the Himalayas (China's side). Stratigraphy of the Mount Qomolangma region. Xizang Scientific Expedition, Academia Sinica, Beijing, pp 192–202

Wang Y, Mu X (1987) Some new observations on the Permian biostratigraphy of the Himalayan province in southern Xizang (Tibet). Stratigraphy of the Mount Qomolangma region. Xizang Scientific Expedition, Academia Sinica, Beijing, pp 218–225

Wang Y, Zhang M (1987) Jurassic system. Stratigraphy of the Mount Qomolangma region. Xizang Scientific Expedition, Academia Sinica, Beijing, pp 110–129

Wen S (1987a) Introduction. Stratigraphy of the Mount Qomolangma region. Xizang Scientific Expedition, Academia Sinica, Beijing, pp 1–4

Wen S (1987b) Cretaceous system. Stratigraphy of the Mount Qomolangma region. Xizang Scientific Expedition, Academia Sinica, Beijing, pp 130–159

Wen S (1987c) Tertiary system. Stratigraphy of the Mount Qomolangma region. Xizang Scientific Expedition, Academia Sinica, Beijing, pp 160–180

Yin J (1987) Cambro–Ordovician system. Stratigraphy of the Mount Qomolangma region. Xizang Scientific Expedition, Academia Sinica, Beijing, pp 5–26

Yin J, Wang Y, Zhang M (1987) Triassic system. Stratigraphy of the Mount Qomolangma region. Xizang Scientific Expedition, Academia Sinica, Beijing, pp 81–109

Yin J, Guo S (1976) On the discovery of the stratigraphy of Gondwana facies in northern slope of the Qomolangma Feng in southern Xizang, China. Scientia Geologica Sinica 4:322–330 (in Chinese with English abstract)

Zhang B (1987a) Carboniferous system. Stratigraphy of the Mount Qomolangma region. Xizang Scientific Expedition, Academia Sinica, Beijing, pp 61–67

Zhang B (1987b) Permian system. Stratigraphy of the Mount Qomolangma region. Xizang Scientific Expedition, Academia Sinica, Beijing, pp 68–80

Part VI

Siwaliks

Introduction to Siwaliks

27

The composition of the Siwalik deposits shows that they are nothing else than the alluvial detritus derived from the subaerial waste of the mountains, swept down by their numerous rivers and streams and deposited at their foot.

—D.N. Wadia (1926, p. 231)

The Siwaliks (Box 27.1) represent one of the largest fluvial deposits in the world. They are equally famous globally for the occurrence of vertebrate fossils, leading to the investigation on the evolution of hominid and anthropoid lineages (Wadia 1926; Johnson et al. 1982a). They also enclose a rich collection of plant and mollusc remains. The Siwalik (or Churia) Group of rocks extends from the Mahakali River on the west frontier of Nepal to the Mechi River on the east, making an uninterrupted foothill belt throughout the country. In fact, the Sub-Himalayan belt, made up of the Siwaliks and allied rocks, stretches from the Salt Range (Pakistan) and Kumaun (India) on the west to Darjeeling on the east. With some interruptions in Bhutan (Chap. 5), they continue farther east to Arunachal Pradesh of India, and even beyond.

The Siwaliks (Box 27.2) constitute a very thick (4,000–6,000 m) molasse-like sedimentary succession, comprising a coarsening-upwards sequence as a whole, which reflects the rising history of the Himalaya (Gansser 1964a). The volume of Alpine molasse is double the volume of the present Alps, whereas the Siwalik Molasse represents only a fraction of the Himalayan Range (Gansser 1964b, p. 387).

Box 27.1: Origin of the Term Siwalik

The name Sewalik has been in use for the tract between the Sutlej and the Ganga at Haridwar since as early as 1796 by Rennel (Falconer 1868, p. 6). Concerning the name Siwalik, Falconer and Cautley (1836, p. 38) wrote the following:

> We have named the fossil, *Sivatherium,* from Siva, Hindú god, and *θηριον bellua.* The *Siválik* or Sub-Himálayan range of the hills, is considered in the Hindú mythology, as the *Lútiah* or edge of the roof of Siva's dwelling in the *Himálaya,* and hence they are called the *Siva-ala* or *Sib-ala,* which by an easy transition of sound became the *Sewálik* of the English. The fossil has been discovered in a tract which may be included in the *Sewálik* range, and we have given the name of *Sivatherium* to it, to commemorate this remarkable formation so rich in new animals.
>
> Another derivation of the name of the hills, as explained by the *Mahant* or High Priest at *Dehra,* is as follows: *Sewálik* a corruption of *Siva-wála,* a name given to the tract of mountains between Jumna and Ganges, from having been the residence of Iswara Siva and his son Ganès, who under the form of an Elephant had charge of the Westerly portion from the village of *Dúdhli* to the Jumna, which portion is also called *Gangaja, gaja* being in Hindí an Elephant. That portion Eastward from *Dúdhli,* or between that village and *Haridwár,* is called *Deodhar,* from its being the especial residence of *Deota* or Iswara Siva: the whole tract however between the Jumna and Ganges is called *Siva-ala,* or the habitation of Siva: under *Sewálik.*

Subsequently, Cautley and Falconer, the two pioneers in the study of Siwalik vertebrates (e.g., Cautley and Falconer 1835; Falconer 1837, 1868), applied the term to the entire mammal-bearing zone.

Strachey (1851) and Colbert (1935) also discuss how the name Siwalik (*Siválik* or *Sewalik*) was originally given by Dr. Hugh Falconer. Captain Proby T. Cautley in 1831 was supervising the Ganga canal construction work at Haridwar, India, and discovered the vertebrate fossils (Johnson et al. 1982a) near a Shiva (or Siva) temple (Vaidyanadhan and Ramakrishnan 2008). According to Falconer (1868), laborers working on the canal, under the direction of Feroz the Third, encountered, in the course of their excavation, the bones of human giants in the unbedded mound. Hence, he gave the name Sivâlik to the sedimentary rocks entombing the fossils. But, it was Medlicott (1864, p. 5, 10) who formally designated the rocks constituting a well-marked outer Himalayan geological succession as the Sivâlik series. He also noted that, on the whole, and as not involving an idea of geological age, the most general term of Sub-Himalayan series would be more suitable.

M.R. Dhital, *Geology of the Nepal Himalaya*, Regional Geology Reviews,
DOI 10.1007/978-3-319-02496-7_27

These freshwater soft rocks contain interbedded conglomerates (mainly in the upper part), sandstones, siltstones, pseudo-conglomerates, and mudstones. Their great aggregate thickness and general coarseness give evidence of continuous deposition in a shallow body of water, whose depth kept pace with the accumulation of sediments (Krishnan 1956). These rocks are very fragile and get easily weathered and disintegrate in no time. Hence, good exposures of the Siwaliks are spared mainly along river- or stream-cut banks and in fresh road or canal excavations.

In Nepal, the Siwaliks range in age from the Middle Miocene (about 16 Ma) to early Pleistocene (less than 1 Ma). They invariably have a faulted upper contact with the overriding Lesser Himalayan succession. However, most of the time their lower contact is concealed, yet it represents an erosional disconformity on the Proterozoic slices present in the Siwalik belt of central and east Nepal (Chaps. 10 and 11). In India and Pakistan, there are areas where the Siwaliks transitionally overlie the older rocks (Wadia 1926). In the Punjab and Simla Himalaya, the Tertiary rocks constitute two broad belts, an outer and an inner, formed, respectively, of the Miocene–Pliocene and Paleocene–Oligocene strata.

27.1 Early Investigations in India and Pakistan

Medlicott (1864, pp. 10–11) noted that, because the Siwaliks are separated throughout the Himalaya by a well-marked fault, it is not possible to observe the relationship between these rocks and the older successions. However, he also mapped an extensive outlier of the Tertiary rocks, overlying the older (i.e., Lesser Himalayan) succession and nearly occupying the whole length between the Sutlej and Yamuna Rivers in the Northwest Himalaya. In this area, the bottom beds (Nummulitic strata) of the outlier rest unconformably on a denuded surface of the older rocks, and have been folded up with them in the same contortions.

Box 27.2: Main Characteristics of Siwaliks

- The Siwaliks are made up of mudstones, siltstones, sandstones, and conglomerates. They were deposited in a variety of fluvial environments, including piedmonts, outwash plains, channels, floodplains, and oxbow lakes.
- They comprise a fining-upwards sequence on the scale of individual cycles, but a coarsening-upwards succession as a whole.
- The deposits are frequently divided into the Lower, Middle, and Upper Siwaliks, ranging in age from the Middle Miocene to early Pleistocene. Such lithological subdivisions are diachronous, and the equivalent units become successively younger from the northwest towards the southeast.
- The thickness of a given lithostratigraphic unit of the Siwaliks may change significantly in its lateral direction (i.e., within a few tens of kilometers).
- The Upper Siwaliks exhibit disconformable contacts in a number of places. In a few locations, they are transgressive over the Middle and Lower Siwaliks, indicating past prodigious tectonic movements.
- The Siwaliks are very incompetent (soft), and have buckled into noncylindrical plunging folds with curved hinges in map view (i.e., concave or convex towards the foreland).
- There are areas with overturned Siwalik strata. Such beds are sometimes found just at the boundary with the Terai plain.
- The Siwalik beds are frequently truncated by north- as well as south-dipping thrust faults. Like the folds, the thrusts too are convex or concave towards the foreland.
- Some intermontane valleys are located within the Siwalik belt.
- There are a few Proterozoic outliers in the Siwalik belt of central and east Nepal.
- Contrary to a general belief, there is no single and continuous Himalaya Front Tectonic Line (Nakata 1972) or Main Frontal Thrust (Gansser 1983) outcropping throughout the Nepal Himalaya and beyond; in a number of locations, the Siwalik folds abruptly disappear in the Terai plain.
- The geomorphology of the Siwalik Hills is strongly controlled by their rock texture and structure.

Middlemiss prepared an excellent geological map of the Siwaliks of the Kumaun Himalaya bordering west Nepal. He applied a simple classification scheme of the following equivalent lithostratigraphic terms: Siwalik conglomerate for the Upper Siwaliks, sand-rock stage for the Middle Siwaliks, and Nahan sandstone for the Lower Siwaliks (Middlemiss 1890, p. 19). He minutely worked out their mineralogical and petrographic details, and showed that the rocks are thrown into complex folds (even with overturned limbs) and supervened by various dislocations. Based on the experience gained in this portion of the Sub-Himalaya, he formalized

the concept of the Main Boundary Fault proposed by Medlicott (1864).

The first systematic and detailed stratigraphic investigation of the Siwaliks began in the Potwar Basin of Pakistan at the end of the nineteenth century. While working in the Potwar Plateau, Pilgrim (1910, 1913) divided the Siwalik succession into three units, and assigned them the Middle Miocene, Late Miocene to Early Pliocene, and Late Pliocene to early Pleistocene, respectively. Anderson (1927) and Pascoe (1964) provide detailed descriptions of the Siwaliks in India and Pakistan. Gee (1989) deals with the geology and structure of the Salt Range. Colonel McMahon was one of the earliest researchers to microscopically examine the Siwaliks and associated rocks. In the Siwaliks south of Nainital, he observed mainly angular pieces of quartz, with bits of slate and a little mud. Also present in the rock are flakes of muscovite, greenish mica, and fragments of schorl (McMahon 1883, p. 188). Krynine (1937) investigated the petrography of Siwalik sandstones and pseudo-conglomerates. Gill (1952a, b) carried out a detailed study of the Siwaliks in the eastern side of the Punjab Sub-Himalaya.

27.2 Stratigraphic Classification of Northwest Sub-Himalaya

Medlicott (1864, p. 17) differentiated the Northwest Sub-Himalayan rocks into the following units.

- Upper (Sivâlik: conglomerates, sandstones, clays)
- Middle (Nahun: lignites, sandstones, and clays)
- Lower (Nummulitic Subathu: fine silty clays with limestone, followed by Dugshai: purple sandstones and red clays, and Kasaoli: gray and purple sandstones).

Subsequently, Medlicott and Blanford (1879, p. 524) further proposed the following classification (Table 27.1) for the Sub-Himalayan formations.

In the Salt Range, Wynne (1878, 1880) identified the Miocene (Nahan or Murree) beds and Pliocene (Lower and Upper Siwalik) series. Blanford (1879a) carried out more detailed work in western Sindh, where he classified the Late Miocene rocks under the Lower Manchhar and the Pliocene rocks under the Upper Manchhar beds. Subsequently, he continued further investigations in the hills from Quetta to Dera Ghazi Khan (Sindh and Punjab), and showed that the Manchhar beds are equivalent to the Siwalik beds. From the latter area, Blanford (1883, p. 34) mapped the Late Miocene (Lower Manchhar or Lower Siwalik) and Pliocene (Upper Manchhar or Middle and Upper Siwalik) subdivisions.

Table 27.1 Classification of Sub-Himalayan formations

Sub-Himalayan system	Siwalik series	Upper
		Middle
		Lower (Náhan)
	Sirmúr series	Upper (Kasauli)
		Middle (Dagshai)
		Lower (Subáthu: nummulitic)

Source Medlicott and Blanford (1879)

While studying the Tertiary and post-Tertiary deposits of Baluchistan (Bugti Hills) and Sindh, Pilgrim (1908) described in detail the lithology and fossils of the Lower and Upper Siwaliks. Although he mentioned the name Middle Siwaliks, he did not deal with it in much detail. He also observed that, in the Lower Siwalik sandstones and conglomerates from that area, Nummulitic limestone pebbles are absent, contrary to the case in their upper part. Based on this, he inferred that much of the Nummulitic limestone was covered by other deposits during Lower Siwalik time. Subsequent uplift and erosion of the land area exposed the limestone hills to contribute to the Upper Siwalik boulder deposits.

27.3 The Threefold Classification of Siwaliks

In his classic work on the Siwalik vertebrates and their correlation with European counterparts, Pilgrim (1910, 1913) classified the fluvial deposits in the Potwar Plateau into the Lower, Middle, and Upper Siwaliks from bottom to top, respectively. Gansser (1964a) summarized the Siwaliks of the Punjab Himalaya in two lithostratigraphic columns. Following the earlier workers, he described them in terms of the threefold classification.

27.3.1 Lower Siwaliks

Pilgrim (1908) observed that in the Bugti Hills, the base of the Lower Siwaliks is characterized by red or gray clays, intercalated in soft, gray, brittle, well-bedded sandstones containing "bone conglomerates". These conglomerates are concretionary and contain pellets of red clay and calcareous matter, with occasionally small ferruginous nodules in a sandy matrix.

Actual pebbles, which are infrequent, are invariably of sandstone. The bone conglomerates occur very frequently and, from their superior hardness, give rise to a series of scarps. These concretionary conglomerates continue to occur as lenticular beds in the next higher member of the "series," made up of a massive sandstone, in which the calcareous segregation has taken place to such an extent that Blanford (1883, p. 57) designated it as the pseudo-conglomerate. Presumably, he borrowed this term from the lithological descriptions of similar older sequences, such as the upper

Nummulitic series and Tertiary sandstones, where the term was in wider use (e.g., Wynne 1877, p. 118, 1878, p. 108). This pseudo-conglomeratic sandstone weathers in a characteristic columnar and nodular fashion. In addition to the concretionary conglomerates, there are calcareous nodular beds and clays, the whole deeply tinted red (Pilgrim 1910). Pilgrim (1913, 1925) further subdivided the Lower Siwaliks into the Kamlial (named after a place located at 33°15′ N, 72°30′ E and Chinji (32° 42′ N, 72° 22′ E) "stages." Ironically, Pascoe (1964) noted that the Kamlial village itself is on Chinji rocks, whereas Johnson et al. (1985) stated that the Chinji village is situated on a cuesta of younger Nagri sandstone.

The Kamlial is composed of fine- to medium-grained, gray, green-gray, and sporadically red or brown sandstones. Some of the sandstones are soft, and others are well indurated (Johnson et al. 1982b). The sandstones are interbedded with purple shales, mudstones, and pseudo-conglomerates. Pilgrim (1913) assigned a Middle Miocene age for this "stage," based on the mammalian fossils. On the other hand, Johnson et al. (1985) paleomagnetically dated this unit and defined its lower and upper limits between 18.3 and 14.3 Ma (Early to Middle Miocene), respectively.

The transitionally overlying Chinji stage comprises mainly bright yellow and brown nodular mudstones and claystones, with subordinate amounts of gray to brown sandstones and pseudo-conglomerates (Pilgrim 1910). According to Pilgrim, it belongs to the Middle Miocene. However, further paleomagnetic studies by Johnson et al. (1985) have yielded an age range from 14.3 to 10.8 Ma (Middle to Late Miocene).

27.3.2 Middle Siwaliks

Pilgrim (1910) subdivided the Middle Siwaliks into the Nagri (32° 46′ N, 72° 21′ E) and Dhok Pathan (33° 8′ N, 72° 21′ E) stages. Medium- to coarse-grained, friable, thick sandstones with lenticular, hard, gray carbonate-cemented beds and subordinate gray and brown mudstones and conglomerate constitute the Nagri stage. On the basis of vertebrate fossils, this unit was assigned a Late Miocene age (Pilgrim 1910, 1913; Pascoe 1964). Magnetostratigraphically, it belongs to an interval between 10.8 Ma and about 8.5 Ma (Johnson et al. 1985).

The Dhok Pathan unit consists of very thick-bedded, massive, friable, calcareous, gray and light gray sandstones and sandy beds with fewer mudstones, orange clays, and shales of pale and drab colors (Pilgrim 1910). Based on vertebrate fossils, it was assigned a Late Miocene age (Pilgrim 1910, 1913). On the other hand, Johnson et al. (1982b, 1985) paleomagnetically dated this unit between about 8.5 Ma and about 5.1 Ma.

At the end of Dhok Pathan time, some uplift occurred, and the strata were folded and eroded before the deposition of Tatrot beds. This erosion interval is thought to cover the Late Pliocene (Krishnan 1956). Such an erosional gap is attested by the local geological features, for instance, the distribution of the Upper Siwaliks only along basins and stream channels and not on the Potwar Plateau. This uplift accentuated the Kala Chitta Range and extended it eastwards (Krishnan 1956).

27.3.3 Upper Siwaliks

The Upper Siwaliks in the Bugti Hills rest with a sharp unconformity on the Lower Siwaliks, whereas in Sindh and other parts of Baluchistan, the Middle Siwaliks are observed between them. Pilgrim (1908) subdivided the Upper Siwaliks into the Tatrot (32° 52′ N, 73° 21′ E), Pinjor (30° 47′ N, 76° 55′ E), and Boulder Conglomerate stages, respectively, from the bottom upwards. The Tatrot is made up of conglomerates, soft sandstones, and orange and brown clays or mudstones. The conglomerates contain pebbles derived from igneous, metamorphic, and sedimentary rocks. The sandstones are gray and medium- to coarse-grained. This zone is rich in vertebrate fossils, belonging to the middle Pliocene (Pilgrim 1910, 1913). The Pinjor stage consists of coarse-grained, light gray to white sandstones, light pink siltstones, and conglomerates of Late Pliocene age (Pilgrim 1910, 1913). The Boulder Conglomerate stage consists of boulder- and pebble-conglomerates, containing clasts derived from igneous, metamorphic, and sedimentary rocks. In many places, these deposits are time transgressive (Gill 1952a). Pilgrim (1913) assigned them an early Pleistocene age.

27.4 Problems of Threefold Usage and Terminology

Colbert (1935, pp. 13–19) deals in detail with the issue of nomenclature of the Siwaliks. Following the recommendations of the Committee on Stratigraphic Nomenclature, he alluded to the possibilities of using such terms as system, group, formation, series, or zones. He concludes that the threefold classification is neither purely lithostratigraphic nor biostratigraphic, and recommends applying the terms Lower, Middle, and Upper Siwaliks, without any further descriptive words. On the other hand, to the Kamlial, Chinji, and other subdivisions, he suggested applying the term "zone."

This initially developed threefold classification was based primarily upon vertebrate fossil findings in a set of distinct sedimentary sequences from the Potwar Plateau. Consequently, these units reflected the lithostratigraphic as well as biostratigraphic divisions. Inasmuch as the Siwaliks were

originated from various rivers and streams, operating within a wide geographic span of more than 2,500 km, there are inherent inhomogeneities and lithofacies differences. G.E. Lewis, a prominent American paleontologist engaged in the collection of Siwalik fossils in India (e.g., Lewis 1933a, b), noted in a letter to Colbert (1935),

> Two parallel sections 100 m apart usually give utterly different results as to lithology and fauna; suids predominate in one, proboscideans in the other. At a given level or group of levels, a massive stratum of sandstone up to 20 or 30 m thick may lens out on either side within a distance of 80 m.

Furthermore, the vertebrate index fossils are scanty, and frequently confined to some specific horizons and pockets. As a result, it is not easy to biostratigraphically correlate the distant rock sequences. On the other hand, the paleomagnetic studies have shown a diachronous nature of the lithofacies, essentially becoming successively younger from the west towards the east. Therefore, it is not possible to assign a uniform age to each of these lithological divisions. Despite these limitations, the threefold classification is simple and in wide use throughout the Himalaya. The terms Lower, Middle, and Upper Siwaliks are considered hence as pure lithostratigraphic units.

27.5 Other Classifications

Not all investigators agree with the threefold classification. For example, Glennie and Ziegler (1964) classified the Siwaliks of Nepal into the lower Sandstone Facies and the upper Conglomerate Facies, owing to the difficulty in applying threefold subdivision over the whole country. According to them, the Sandstone Facies corresponds to the lower and middle formations, and is composed of fine-grained sandstone, conglomerate, and pebble-bearing sandstone. The upper portion of the Sandstone Facies consists of claystone or siltstone, and contains leaf imprints and shell fragments. Similarly, the Conglomerate Facies, representing the upper formation, is made up of a very coarse and massive conglomerate with layers of sandstone in between.

Raiverman (2002, 2007) classified the Siwaliks of Northwest India into various "energy sequences." His energy sequences are based primarily on grain-size-trend curves, geomorphic features, seismic reflection properties, and heavy mineral distribution. By applying these criteria, he identified the following nine energy sequences, respectively, from bottom upwards: Dharampur (E1: Late Paleocene to Middle Eocene), Kumarhatti (E2: Late Eocene to Oligocene), Makreri (E3: Oligocene to Early Miocene); Jawalamukhi (E4: Early to Middle Miocene); Kalidhar (E5: Late Miocene); Sadhot: (E6: Late Miocene to early Pleistocene); Batwan (E7: middle Pleistocene); Wah Devi (E8: late Pleistocene); and Sarda (E9: late Pleistocene to Holocene). He applied these sequences to map the entire Northwest Sub-Himalaya of India, primarily for the purpose of petroleum exploration.

27.6 Investigations in Nepal

The first geologist to describe the Nepalese Siwaliks and associated rocks was Medlicott (1875), who identified the Siwalik beds to the south and north of Hetaunda. Auden (1935) investigated the Siwaliks of central Nepal around Hetaunda and Udaipur Gadhi. He classified them into the Lower Siwaliks (Nahans) of brown-weathering sandstones, chocolate clays, and some inconsistent beds of impure limestone; the Middle Siwaliks of thick beds of feldspar and mica sandstones; and the Upper Siwaliks consisting of conglomerates. He also described the foothills of Hetaunda while visiting Kathmandu, and separated the Upper Siwaliks from the Lower Siwaliks by a sharp fault. It was the first record of such an intra-Siwalik (or Dun) fault from Nepal.

Hagen, at first as an employee of Swiss businessmen, then as an employee of the Government of Nepal, and finally as a United Nations expert (Hagen 1994), worked in this mountainous and remote country for a long period of 9 years. Hagen (1951, 1959, 1969), investigated the Nepal Himalaya in detail and adopted the threefold classification. According to him, the Lower Siwaliks are composed of siltstones, red shales with minor sandstones, and pseudo-conglomerates; the Middle Siwaliks consist of sandstones and siltstones with minor conglomerates and red shales; and the Upper Siwaliks contain the conglomerates. Similarly, Lombard (1958), Bordet and Latreille (1955), and Itihara et al. (1972) investigated the Nepalese Siwaliks in some detail. The petrographic classification of Siwalik rocks in Nepal was initiated by Chaudhri (1982). According to him, the sandstones of the Lower Siwaliks are represented by quartz arenites, the Middle Siwaliks are characterized by lithic arenites, and the Upper Siwaliks are composed of boulder-conglomerates, with subangular to subrounded metamorphic and crystalline rock fragments.

After the establishment of the paleomagnetic polarity stratigraphy in the Potwar Plateau in Pakistan by Opdyke et al. (1979, 1982), Johnson et al. (1982b), and others, the Siwaliks have attracted the attention of a wide geoscientific community, resulting in a detailed investigation in the past three decades. Based on fossil findings and preliminary paleomagnetic investigations in west Nepal, West and Munthe (1981), and Munthe et al. (1983) drew a conclusion that the rocks cannot be correlated with the Siwaliks of India and Pakistan solely on their lithological basis. Tokuoka et al. (1986) mapped the Siwaliks of the Arung Khola area (Chap. 30). They also carried out detailed paleomagnetic investigations and correlated the Siwaliks of the Arung

Khola area with those of Potwar Plateau. Further paleomagnetic studies in various parts of Nepal were carried out by Appel et al. (1991), Gautam and Appel (1994), Gautam (2008), Ojha et al. (2000), and many others (Fig. 27.1). Corvinus (1988, 1993) studied the Siwaliks of the Surai Khola, whereas Dhital et al. (1995) worked out its lithostratigraphic and structural details (Chap. 29).

27.7 Fossil Occurrence

Falconer and Cautley carried out the first detailed investigations on the Siwalik fossils (Box 27.3). Pilgrim (1908, 1910, 1913, 1925) and Pascoe (1964) included detailed lists of the Siwalik mammalian fossils. Pilgrim (1932) gave a comprehensive and systematic description of fossil carnivora

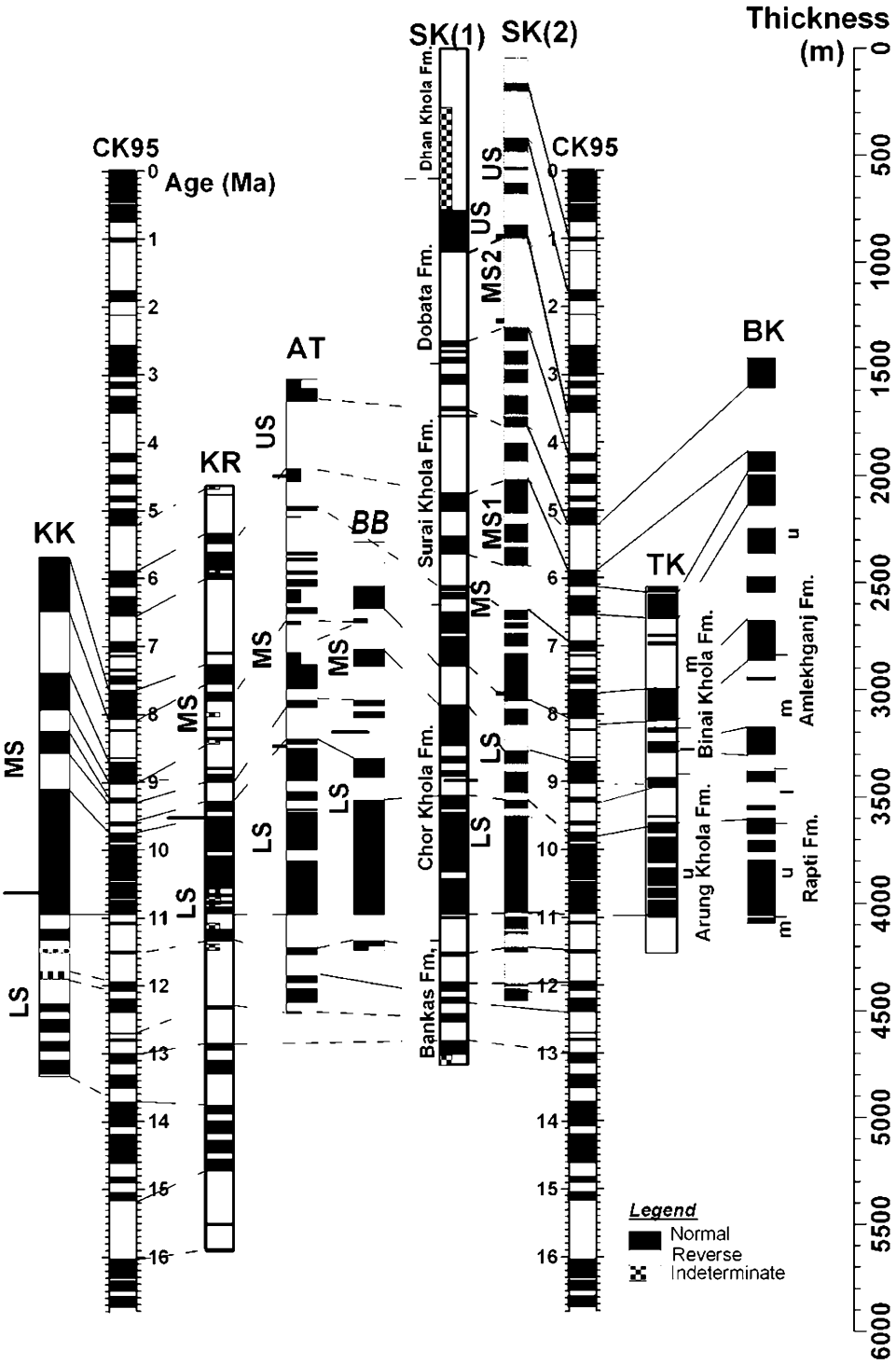

Fig. 27.1 Compilation of magnetic polarity sequences established for the Siwalik sediments in Nepal. Abbreviations for sections (from east to west) and data sources are as follows. *BK* Bakiya Khola (Harrison et al. 1993); *TK* Tinau Khola (Gautam and Appel 1994); *KK* Khutia Khola (Ojha et al. 2000); *SK* Surai Khola (*SK1* Rösler et al. 1997; *SK2* Hoorn et al. 2000); *BB* Bhalubang (Rösler et al. 1997); *AT* Amilia–Tui (Rösler et al. 1997); *KR* Karnali River (Gautam and Fujiwara 2000). CK95 used as standard geomagnetic polarity timescale for calibration is after Cande and Kent (1995). *Source* Gautam (2008). © Nepal Geological Society. Used by permission

from the Siwaliks of India, with impressive sketches and photographs. There is also a complete list of literature on Siwalik mammals. Colbert (1935) provided an exhaustive list of Siwalik mammalian fauna. He also gave a systematic description (with sketches and photographs) of most of the fossils stored in the American Museum of Natural History, New York. The Siwalik fossils are also summarized by Wadia (1926), Krishnan (1956), and recently by Prasad (2001). Barry et al. (1982) discussed the biostratigraphic zonation of the Middle and Upper Siwaliks of the Potwar Plateau in Pakistan. Wadia (1926, 1976) gave a list of some important genera and species of the Mammalia found in the Siwaliks of India and Pakistan (Box 27.4).

Box 27.3: Early Fossil Discovery from Siwalik Range

One of the earliest discoveries of fossils from the Siwalik ranges was made by Lieutenant Proby T. Cautley. Medlicott (1879, p. 522) discusses the discovery of Siwalik fossils by Cautley prior to 1832, as published in the first volume of the *Journal of the Asiatic Society of Bengal*.

Because there arose some confusion when Dr. Royle (Anonymous 1832) reported that Dr. Hugh Falconer was the first discoverer of these fossil bones, Falconer (1832, p. 249) responded with a letter stating the following:

> In No. 3 of the Journal of the Asiatic Society, p. 97, Mr. Royle has announced the discovery by me of the fossil bones in the range of hills which skirts the Valley of Dehra on the south-west… I conceive it necessary to state that Lieut. Cautley, Superintendent of the Doab Canal, is the original discoverer of fossils in these hills. The most perfect portion I have yet seen of these fossil bones, has been in his possession several years…

Murchison (1868) compiled the famous work of Falconer, called the *Fauna Antiqua Sivalensis*. The early summary of fossil vertebrates of India is given by Blanford (1879b) and Lydekker (1883).

27.7.1 Fossils from the Nepalese Siwaliks

Sharma (1973) mentioned the occurrence of vertebrate fossils in the Churia Range of Nepal. West et al. (1978) as well as West and Munthe (1981) reported various fossils from the Lower Siwaliks of the Babai Khola and Tinau Khola areas. Munthe et al. (1983) reported the upper molar of *Sivapithecus punjabicus* from the Tinau Khola area (Chap. 30). West et al. (1991) gave a systematic description of fossils obtained by their team around the Dang Valley and near Butwal (Fig. 27.2, Box 27.5). They compared this fossil record with that of India and Pakistan, and concluded that the mammalian assemblage collected from Nepal was similar to that of the Chinji and Nagri stages.

In the Surai Khola section, Corvinus (1988, 1993) and Corvinus and Nanda (1994) carried out detailed investigation of fossils. On the basis of the fossil record of *Gomphotherium* sp., they correlated the lowest Siwalik beds of the Surai Khola area with those of the Chinji Formation. The massive and very coarse-grained, pepper-and-salt sandstones of the Surai Khola Formation yielded a good collection of fauna, akin to those of the Tatrot and Pinjor zones. The fossils include a large number of mammals, reptiles, fish, and other invertebrates. Most common are the reptiles (Crocodylidae and Trionychidae). A big collection of mammals of the family Elephantidae, Hippopotamidae, Suidae, Cervidae, Giraffidae, and Bovidae was found in these multi-storied sandstones. These fossils point to a thickly forested environment with wide and meandering rivers (Box 27.6). Nanda and Sehgal (2005) describe the mammalian fauna of the Northwest Himalaya and remark that the lithological boundaries of the Siwalik Group are time-transgressive, because the enclosed fossils within a given lithological unit indicate different ages. Takayasu (1988) collected a large number of molluscs from the Nepalese Siwaliks and described their provenance in a regional frame (Fig. 27.3). Gurung (1998) studied various freshwater molluscs from the Siwaliks of the Surai Khola area.

Box 27.4: Some Fossils from India and Pakistan. *Source* Wadia (1926, 1976)

UPPER SIWALIK MAMMALIA

Primates: *Simia, Semnopithecus, Gigantopithecus, Papio*

Carnivora: *Hyaenarctos sivalensis, Mellivora, Mustela, Canis, Vulpes, Hyaena, Viverra, Machaerodus, Felis cristata*

Elephants: *Mastodon sivalensis, Stegodon ganesa, S. clifti, S. insignis, Elephas planifrons*

Ungulates: *Rhinoceros palaeindicus, Equus sivalensis, Sus falconeri, Hippopotamus, Camelus antiquus, Giraffa, Indratherium, Sivatherium giganteum, Cervus, Buffelus palaeindicus, Bucapra, Anoa, Bison, Bos, Hemibos, Leptobos*MIDDLE SIWALIK MAMMALIA

Primates: *Pliopithecus, Semnopithecus, Cercopithecus, Macacus, Sivapithecus*

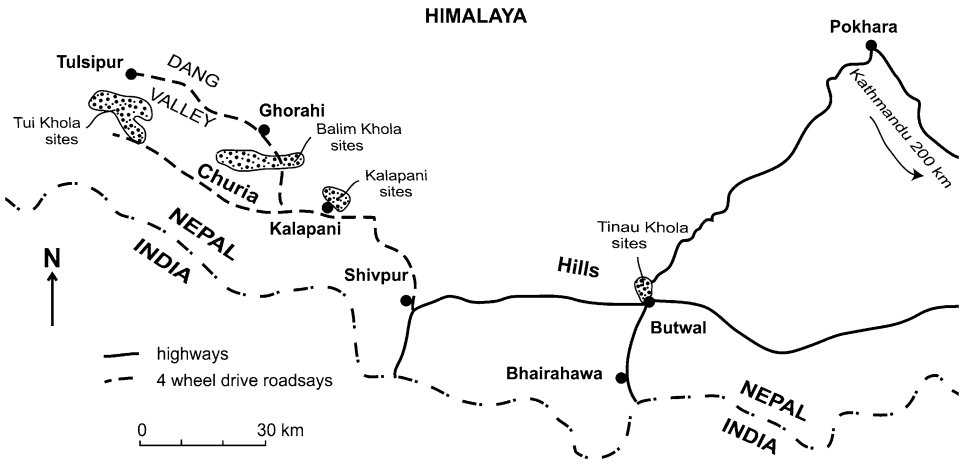

Fig. 27.2 Location of vertebrate fossils in west Nepal. *Source* modified from West et al. (1991)

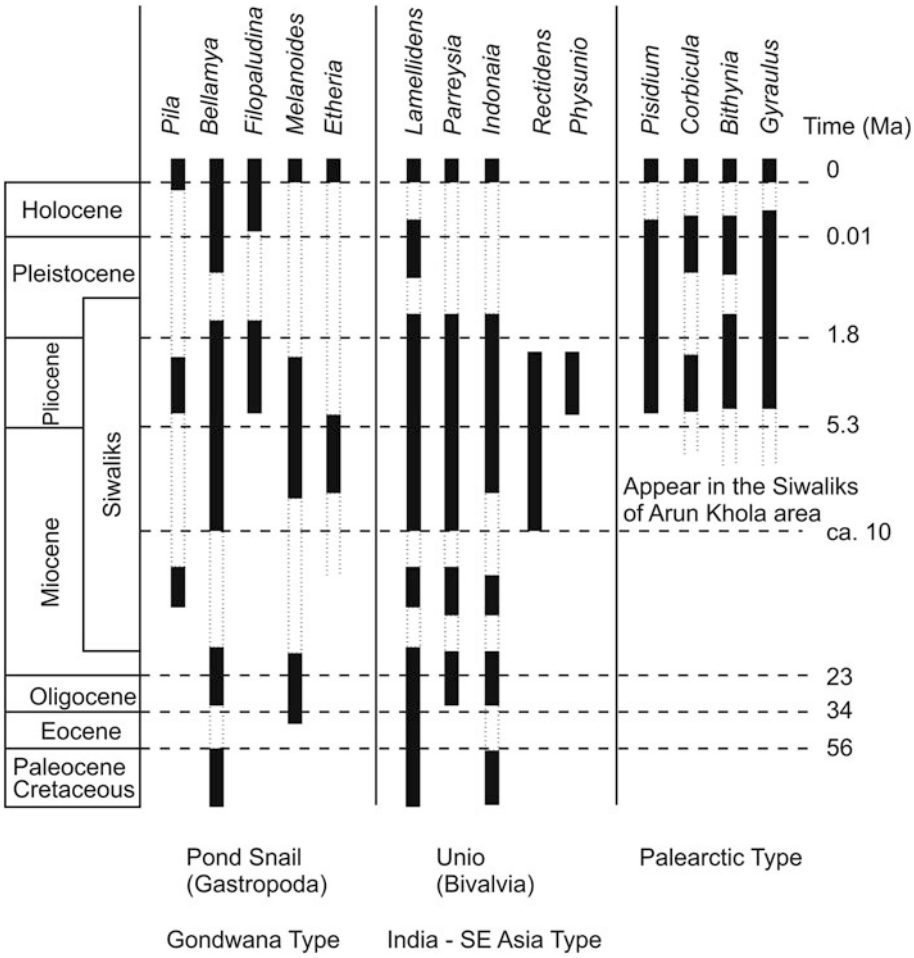

Fig. 27.3 Distribution of freshwater molluscs in the Siwaliks of Nepal. *Source* based on Takayasu (1988)

Carnivora: *Hyaenarctos, Mellivorodon, Lutra, Amphicyon, Machaerodus, Felis*
Rodents: *Hystrix, Rhizomys*
Elephants: *Prostegodon cautleyi* and *P. latidens, Stegodon clifti, Mastodon hasnoti*
Ungulates: *Teleoceras, Hipparion, Merycopotamus, Tetraconodon, Hippohyus, Sus punjabiensis, Hippopotamus irravaticus, Tragulus, Hydaspitherium, Vishnutherium, Cervus simplicidens, Gazella, Tragoceras, Anoa*

LOWER SIWALIK MAMMALIA

Primates: *Sivapithecus indicus, Dryopithecus, Ramapithecus, Paleosimia*
Carnivora: *Dissopsalis, Amphicyon, Palhyaena*
Proboscidians: *Dinotherium indicum, Gomphotherium, Tetrabelodon angustidens, Mastodon*
Ungulates: *Aceratherium, Hyotherium, Anthracotherium, Dorcatherium, Hemimeryx, Giraffokeryx, Conohyus, Listriodon, Telmatodon, Brachyodus, Hyoboops, Sanitherium*

Apart from them, the following vertebrate fossils were also found in the Siwaliks.
Birds: *Phalacrocorax, Pelecanus, Struthio, Mergus*
Reptiles: (Crocodiles) *Crocodilus, Ramphosuchus;* (Lizard) *Varanus;* (Turtles) *Colossochelys atlas, Bellia, Trionyx, Chitra,* Snakes, Pythons
Fish: *Ophiocephalus, Chrysichthys, Rita, Arius.*

Box 27.5: Vertebrate Fossils Discovered in West Nepal. *Source* West et al. (1991)

OSTEICHTHYES

Channiformes *Channa,* n. sp.2

REPTILIA

Testudines *Lissemys punctata*
Chitra cf. *C. indica*
Cuora or *Chinemys* sp. indet.
Geochelone sp. indet.
Squamata *Acrochordus dehmi*
Crocodilia *Gavialis* sp. indet.
Crocodylus sp. indet.

MAMMALIA

Carnivora *Amphicyon palaeindicus*
Creodonta Indeterminate remains of Hyaenodontidae
Proboscidea *Dinotherium pentapotamiae*
Indeterminate remains of Gomphotheriidae
Perissodactyla *Brachypotherium perimense*
Artiodactyla *Conohyus sindiense*
Hemimeryx pusillus
Dorcatherium sp.
Giraffokeryx punjabiensis
Protragoceras gluten
Sivoreas eremita
Rodentia Indeterminate remains of Rhizomyidae
Primates *Sivapithecus punjabicus.*

Box 27.6: Vertebrate Fossils from the Surai Khola and Ratu Khola Areas. *Source* Corvinus and Rimal (2001)

Dhan Khola Formation: Mammalian bone fragments
Dobata Formation: *Elephas planifrons, Equus* sp., *Hexaprotodon sivalensis,* Cervidae, Bovinae, *Crocodylus, Gavialis,* tortoise, and fish
Surai Khola Formation: *Stegodon insignis, St. bombifrons, Hippohyus tatroti,* anthracothere, *Hexaprotodon sivalensis, Cervus* sp., *Giraffa punjabiensis, Proamphibos lachrymans, Crocodylus, Gavialis, Trionys* sp., *Colossochelys, Emyda,* fish, and microvertebrates
Shivgarhi Member of Chor Khola Formation: *Crocodylus,* tortoise, mammalian bone fragments, and microvertebrates
Jungli Khola Member of Chok Khola Formation: Vertebrate bone fragments
Bankas Formation: *Gomphotherium* sp. and tortoise carapace.

Awasthi and Prasad (1990) as well as Prasad (1995) investigated the Siwalik plant fossils from the Surai Khola and Koilabas areas in west Nepal. They classified the leaf impressions into 21 species, belonging to 19 genera and 13 families of monocotyledons and dicotyledons. The assemblage consists mostly of plants growing in tropical evergreen to semi-evergreen forests with a warm and humid climate. Their investigation indicated that the climate gradually changed from humid tropical conditions to dry tropical conditions, respectively, from the Lower Siwaliks to Upper Siwaliks.

27.8 Depositional Environment and Sedimentation Rates

Falconer (1868, p. 33) observed that the Siwalik conglomerates were very similar to the present deposits of the rivers Yamuna and Ganges. He wrote that if their riverbeds were to undergo upheaval in the same manner as those of the

Siwaliks, the appearance of the strata would be quite similar. Medlicott (1864, p. 19) remarked that the Ganga Valley deposits are the temporal continuation of the Siwaliks, and can be ranked as a fourth and uppermost member of this series. Medlicott (1879, p. 541) also pointed out that the Siwalik deposits exposed between the rivers Ganga and Yamuna practically lack fines and are composed mainly of quartzite pebbles, similar to those of the shingles now found in the mountain torrents. He stressed that the Siwalik conglomerates of that tract were laid down on ancient alluvial fans of the rivers Tons, Yamuna, and Ganga.

The Siwalik sediments were deposited in the foreland by numerous rivers originating in the hinterland (and beyond) and flowing into a long narrow depression, called the foredeep (Chap. 3), in front of the rising mountains, that is, towards the side of the Indian Peninsula (Krishnan 1956). Wadia (1976, p. 342) remarked that the Siwaliks on the whole show uniformity of lithological composition for several hundred kilometers with a striking structural unity. This negates any theory of the deposition of these strata in a multitude of isolated basins.

As stated earlier, the depositional environment during the Siwalik time varied significantly in the lateral as well as vertical direction. The fluvial Siwaliks were deposited mainly in these four broad environmental settings: (1) piedmont, (2) outwash plains, (3) channels and floodplains, and (4) lakes (Vaidyanadhan and Ramakrishnan 2008). These environments shifted in space and time and gave rise to the very thick molassic sediments. The Siwalik succession deposited east of the Ravi River in Northwest India exhibits three dominant facies associations: trunk river, piedmont, and alluvial fan (Sinha et al. 2007). The trunk river association consists of multi-storied sandstones of 10–40 m thickness, with a basal erosional contact and a sharp contact with the overlying deposits. The piedmont river displays a heterogeneous facies. In it, the sandstones are less than 4 m thick, have a sharp base, and the grain size increases upwards. The alluvial fan facies is characterized by the deposition of thick conglomerate beds with nonerosive and planar basal contacts, whereas the upper contact is gradational to sharp.

McMahon (1883, p. 192) discussed the source of detritus in the Tertiary rocks. He remarked that much of the material in the sandstones was directly derived from the waste of the granitic and gneissic rocks of the Himalaya. As the Siwalik conglomerates contain boulders of rocks undistinguishable from Himalayan granites and gneisses, he further concluded that these rocks were already extensively exposed and the conglomerates were laid down from these local sources. The freshness of the material also indicated that the detritus was derived from nearby areas (Middlemiss 1890, p. 112). The Lower Siwalik sandstones in the Krol Belt frequently contain fragments of volcanic rock, representing andesites and basalts. They also contain garnet, tourmaline, and microcline (Auden 1934, pp. 388–389).

In Nepal, Hagen (1969, p. 98) found, in the very thick Middle Siwalik sandstones, the detritus derived from the crystalline nappes. He identified feldspar, quartz, muscovite, biotite, hornblende, tourmaline, magnetite, garnet, kyanite, epidote, rutile, and zircon. He also noted that some Middle Siwalik rocks superficially resemble granite.

Raju (1967) investigated the petrography and heavy mineral assemblages (of about 15,000 samples) of the Tertiary rocks from Northwest India. He found in the Siwaliks the following detrital minerals, reflecting a successive exhumation of a progressive metamorphic sequence: (1) epidote and staurolite occur consistently in the Lower Siwaliks; (2) kyanite (with staurolite) occurs frequently from the base of the Middle Siwaliks, and (3) hornblende and sillimanite are prominent in the Upper Siwaliks. Chaudhri and Gill (1981) studied the heavy minerals from the Sub-Himalaya of Nepal. According to them, staurolite serves as an important mineral to identify the Lower Siwalik Formation, and kyanite and sillimanite serve as the markers for the Middle and Upper Siwaliks, respectively. However, this type of normal metamorphic sequence is inconsistent with the observations that a good part of the Himalayan isograds is inverted (Le Fort 1975, p. 16).

In the northern Potwar Basin, near the Indus River, the uppermost 1,000 m of the Middle Siwalik sequence contain thick beds of conglomerate, which die out eastwards and southeastwards into sandstones and clays. Farther eastwards, a clay facies develops at progressively lower horizons, replacing a considerable portion of massive sandstones. The facies change is accompanied by a reduction in thickness. The Lower Siwalik rocks show a development of coarser facies in the opposite direction to that noted in the Middle Siwaliks (Gill (1952a).

In the Potwar Plateau, the Siwalik Group is subdivided into a series of lithostratigraphic units, formalized by the Stratigraphic Committee of Pakistan (Fatmi 1973). The oldest unit is the Kamlial Formation, made up of deep red mudstones and sandstones, representing a combination of upper delta plain sedimentary environment. The Chinji Formation transitionally overlies the Kamlial Formation, and its type section is designated south of the Chinji village (32° 41′ N, 72° 22′ E). This unit consists of a series of lateral accretion sandstones, interbedded with thick dark red vertical accretion silts. The Nagri Formation conformably overlies the Chinji Formation. Its type area is near Sethi Nagri (32° 46′ N, 72° 30′ E). The Nagri Formation is composed of a series of very thick multi-storied sandstones, separated by thin red overbank mudstones and siltstones. The Dhok Pathan Formation has been defined from a region near Dhok Pathan (33° 8′ N, 72° 31′ E). In its type locality, the multi-storied sandstones of

the Nagri Formation pass into the thinner sandstones and more massive overbank muds and silts of light red color. The Upper Siwalik sediments, represented by sandstones, mudstones, and conglomerates (towards the top), were accumulated in a generally well-developed meander belt regime. The stream systems existing at the time of their deposition were characterized by a laterally meandering channel, in association with a trailing floodplain (Fatmi 1973; Opdyke et al. 1979, 1982).

The detailed paleomagnetic and sedimentological investigation carried out by Johnson et al. (1985) near the Chinji village, Pakistan, revealed that the sedimentation in that area spanned about 10.4 Ma. In accordance with the investigation on fluvial systems by Schumm (1977), they are of the opinion that the sedimentation followed a four-stage cyclic pattern. The first-order cycle was on the order of 10^7 years (governed by tectonics); a second-order cycle was about 10^6 years long and produced the large-scale fining-upwards divisions, such as the Lower and Middle Siwaliks; the duration of a third-order cycle spanned 10^4–10^5 years and it produced the basic fining-upwards units; and a fourth-order sedimentation cycle lasting 10^0–10^4 years had a wide-ranging periodicity and was related to river channel shifting and climatic factors.

West et al. (1991) remarked that the depositional environment of the Nepal Lower and Middle Siwaliks was markedly different from that of the homotaxial rocks in India and Pakistan. Most of the Northwest Himalayan Lower and Middle Siwaliks were accumulated as channel bars and overbank deposits of several major braided and meandering river systems, whereas in Nepal the equivalent fossil-bearing rocks were formed in poorly drained areas, characterized by ponds, sloughs, and sluggish streams. The Nepalese fauna are dominated by aquatic taxa, in contrast to predominating terrestrial fauna found in equivalent horizons of India and Pakistan.

Tokuoka et al. (1990), Hisatomi and Tanaka (1994), Ulak and Nakayama (1998), Nakayama and Ulak (1999), and Ulak (2002) carried out detailed paleohydrological analysis of the Siwalik sediments from various sections of Nepal. According to them, the Lower Siwaliks were deposited in a meandering system and a flood-flow dominated meandering system; the Middle Siwaliks were accumulated in a flood-flow dominated meandering system and a sandy braided system; whereas the Upper Siwaliks were laid down in a gravelly braided system, followed by a debris flow-dominated system.

The sediment accumulation rates in the Potwar Plateau during the Chinji, Nagri, and Dhok Pathan interval ranged from 13 to 52 cm/ka (Johnson et al. 1982b). Sedimentation rates in the Chinji village area increased gradually through time, going from 12 cm/ka in the Lower Siwaliks to 30 cm/ka in the Middle Siwaliks (Johnson et al. 1985).

For the Bakiya Khola section of southeast Nepal, Harrison et al. (1993) established highly fluctuating sediment deposition rates (between 10 and 150 cm/ka) in a cyclic fashion, with a period fluctuating between 0.4 and 1.5 million years. According to them, the high accumulation rates may reflect episodic thrusting events in the Himalaya. Gautam (2008) summarized the sedimentation rates from the Nepalese Siwaliks and showed that the rates vary considerably from place to place. In the Nepalese Siwaliks, the mean sediment deposition rate was about 32 cm/ka between 16 and 11 Ma, it increased to about 40 cm/ka between 11 and 5 Ma, attained a peak value of about 55 cm/ka between 5 and 3.5 Ma, and then rapidly decreased to about 27 cm/ka between 3.5 and 1 Ma.

References

Anderson RVV (1927) Tertiary stratigraphy and orogeny of the northern Punjab. Bull Geol Soc Am XXXVIII:665–720

Anonymous (1832) Extracts from Dr. Royle's explanatory address on the exhibition of the collections in natural history, at the meeting of the asiatic society, on the 7th March. J Asiat Soc Bengal I(3): 96–100

Appel E, Rösler W, Corvinus G (1991) Magnetostratigraphy of the Miocene-Pleistocene Surai Khola Siwaliks in west Nepal. Geophys J Int 105:191–198

Auden JB (1934) The geology of the Krol belt. Records of the geological survey of India, vol LXVII, Part 4, pp 357–454 (with 9 plates including a geological map in colors, scale: 1 inch = 2 miles)

Auden JB (1935) Traverses in the Himalaya. Records of the geological survey of India, vol LXIX, Part 2, pp 123–167 (with 6 plates including a geological sketch map)

Awasthi N, Prasad M (1990) Siwalik plant fossils from Surai Khola area, Western Nepal. Palaeobotanist 38:298–318

Barry JC, Lindsay EH, Jacobs LL (1982) A biostratigraphic zonation of the middle and upper Siwaliks of the Potwar Plateau of northern Pakistan. Palaeogeogr Palaeoclimatol Palaeoecol 37:95–130

Blanford WT (1879a) The geology of western Sind. Memoirs of the geological survey of India, vol XVII, Art 1, pp 1–210 (with one colored geological map, 1 inch = 16 miles)

Blanford WT (1879b) Siwalik fauna. In: Medlicott HB, Blanford WT (eds) A manual of the geology of India, Part II: Extra-Peninsular Area. Published by order of the Government of India, Calcutta, pp 572–591

Blanford WT (1883) Geological notes on the hills in the neighbourhood of the Sind and Punjab frontier between Quetta and Dera Ghazi Khan. Memoirs of the geological survey of India, vol XX, Art 2, pp 1–240 (with three plates and a geological map in colors of 1 inch = 12 miles)

Bordet P, Latreille M (1955) La Géologie de L'Himalaya de l'Arun. Bulletin de la Société géologique de France, Paris, vol 5, ser 6, pp 529–542

Cande SC, Kent DV (1995) Revised calibration of the geomagnetic polarity timescale for the Late Cretaceous and Cenozoic. J Geophys Res 100:6093–6095

Cautley PT, Falconer H (1835) Synopsis of fossil genera and species from the upper deposits of the tertiary strata of the Siválik Hills, in the collection of the authors (Prinsep J ed). J Asiat Soc Bengal, Calcutta IV(48):706–707

Chaudhri RS (1982) Petrology of the Siwalik Group of Nepal Himalaya. Recent Res Himalaya 8:424–466
Chaudhri RS, Gill GTS (1981) Heavy mineral assemblage of the Siwalik Group of Nepal Himalaya. J Geol Soc India 22:220–226
Colbert EH (1935) Siwalik mammals in the American museum of natural history. Transactions of the American philosophical society held at Philadelphia for promoting useful knowledge, new series, vol XXVI, 401 pp (with maps)
Corvinus G (1988) The Mio-Plio-Pleistocene litho- and biostratigraphy of the Surai Khola Siwaliks in West Nepal: first results. Comptes Rendus de l'Académie des Sciences, Paris 306(2):1471–1477
Corvinus G (1993) The Siwalik group of sediments at Surai Khola in western Nepal and its palaeontological record. J Nepal Geol Soc 9:21–35
Corvinus G, Nanda AC (1994) Stratigraphy and palaeontology of the Siwalik Group of the Surai Khola and Rato Khola in Nepal. Neues Jahrbuch für Geologie und Paläontologie, Stuttgart 191(1):25–68
Corvinus G, Rimal LN (2001) Biostratigraphy and geology of the Neogene Siwalik Group of Surai Khola and Rato Khola areas in Nepal. Palaeogeogr Palaeoclimatol Palaeoecol 165:251–279
Dhital MR, Gajurel AP, Pathak D, Paudel LP, Kizaki K (1995) Geology and structure of the Siwaliks and Lesser Himalaya in the Surai Khola–Bardanda area, mid western Nepal. Bull Dept Geol Tribhuvan Univ Kathmandu 4:1–70
Falconer H (1832) Dehra Dún fossil remains (letter to the editor of the Journal of the Asiatic Society). J Asiat Soc Bengal I(V):249
Falconer H (1837) Note on the occurrence of fossil bones in the Sewalik Range, eastward of Hardwar. J Asiat Soc Bengal VI:233
Falconer H (1868) Fauna Antiqua Sivalensis. In: Murchison C (ed) Palæontological Memoirs and notes of the Late Hugh Falconer, A. M., A.D., vol I, Robert Hardwicke, London, pp 1–556
Falconer H, Cautley PT (1836) *Sivatherium Giganteum*, a new fossil ruminant genus, from the valley of the Markanda, in the Siválik branch of the Sub-Himaláyan Mountains (Prinsep J ed). J Asiat Soc Bengal, Calcutta V(49):38–50 (with 2 plates)
Fatmi AN (1973) Lithostratigraphic units of the Kohat-Potwar province, Indus Basin, Pakistan. Mem Geol Surv Pakistan 10:1–78
Gansser A (1964a) Geology of the Himalayas. Interscience, New York, p 289
Gansser A (1964b). The Alps and the Himalayas. In: International geological congress, report of the twenty-second session, India, part XI, proceedings of session 11: Himalayan and Alpine Orogeny, New Delhi, pp 387–419
Gansser A (1983) Geology of the Bhutan Himalaya. Denkschriften der Schweizerischen Naturforschenden Gesellschaft (Mémoires de Société Helvétique de Sciences Naturelles, Band/Vol 96, 181 pp), (with 4 plates: a geological map in colors; scale: 1:2,000,000; cross-sections in colors and black, and a panorama of mountains)
Gautam P (2008) Magnetic fabric of Siwalik sediments (Nepal): implications to time–space evolution of stress field. J Nepal Geol Soc 38:39–48
Gautam P, Appel E (1994) Magnetic-polarity stratigraphy of Siwalik Group sediments of Tinau Khola section in west central Nepal, revisited. Geophys J Int 117:223–234
Gautam P, Fujiwara Y (2000) Magnetic polarity stratigraphy of Siwalik Group sediments of Karnali River section in western Nepal. Geophys J Int 142:812–824
Gee ER (1989) Overview of the geology and structure of the Salt Range, with observations on related areas of northern Pakistan. In: Malinconico Jr LL, Lillie RJ (eds) Tectonics of the western Himalaya. Geological society of America, Special Publication No 232, pp 95–112 (with a geological map in colors, based on 1:50,000 sheets)
Gill WD (1952a) The stratigraphy of the Siwalik Series in the northern Potwar, Punjab, Pakistan. Q J Geol Soc Lond, Part 4 CVII(4):375–394 (with Plates XX to XXII)
Gill WD (1952b) The tectonics of the Sub-Himalayan fault zone in the northern Potwar region and in the Kangra district of the Punjab. Q J Geol Soc Lond, Part 4, CVII(428):395–413 (with Plates XXIII to XXV)
Glennie KW, Ziegler MW (1964) The Siwalik formation in Nepal, 22nd international geological congress, 22nd session report, part 25, pp 82–95
Gurung D (1998) Freshwater molluscs from the Late Neogene Siwalik Group, Surai Khola, western Nepal. J Nepal Geol Soc 17:7–28
Hagen T (1951) Preliminary note on the geological structure of Central Nepal. Verhandlungen der Schweizerischen Naturforschenden Gesellschaft, Luzern, pp 133–134
Hagen T (1959) Über den Geologischen Bau des Nepal-Himalaya mit besonderer Berücksichtigung der Siwalik-Zone und der Talbildung. Jahrbuch der St. Gallischen Naturwissenchaftlichen Gesellschaft, vol 76, pp 3–48 (with 10 figures and 9 plates)
Hagen T (1969) Report on the geological survey of Nepal. Volume 1: preliminary reconnaissance. Denkschiiften der Schweizerischen Naturforschenden Gesellschaft, Band LXXXVI/1, 185 pp (with a geological map)
Hagen T (1994) Building bridges to the third world: memoirs of Nepal 1950–1992. Book Faith India, Delhi 386 pp
Harrison TM, Copeland P, Hall SA, Quade J, Burner S, Ojha TP, Kidd WSF (1993) Isotopic preservation of Himalayan/ Tibet uplift, denudation, and climatic histories of two molasse deposits. J Geol 100:157–173
Hisatomi K, Tanaka S (1994) Climatic and environmental changes at 9 and 7.5 Ma in the Churia (Siwalik) Group, west-central Nepal. Himal Geol 15:161–180
Hoorn C, Ohja T, Quade J (2000) Palynological evidence for vegetation development and climatic change in the sub-Himalayan zone (Neogene, Central Nepal). Palaeogeogr Palaeoclimatol Palaeoecol 163:133–161
Itihara M, Shibasaki T, Miyamoto N (1972) Photogeological survey of the Siwalik Ranges and the Terai Plain, southeastern Nepal. J Geosci, Osaka City University, vol 15, Art 4, pp 77–98 (with a geological map of the Siwaliks and 4 plates)
Johnson GD, Opdyke ND, Pilbeam DR, Tahirkheli RAK, Ibrahim Shah SM (1982a) Introduction (to special issue: the geochronology and biochronology of the Siwalik Group, Pakistan), compiled by Opdyke ND. Palaeogeogr Palaeoclimatol Palaeoecol 37:vii–viii
Johnson NM, Opdyke ND, Johnson GD, Lindsay EH, Tahirkheli RAK (1982b) Magnetic polarity stratigraphy and ages of Siwalik Group rocks of the Potwar Plateau, Pakistan. Palaeogeogr Palaeoclimatol Palaeoecol 37:17–42
Johnson NM, Stix J, Tauxe L, Cerveny PF, Tahirkheli RAK (1985) Paleomagnetic chronology, fluvial processes, and tectonic implications of the Siwalik deposits near Chinji village, Pakistan. J Geol 93:27–40
Krishnan MS (1956) Geology of India and Burma, 3rd edn. Higginbothams, Madras, p 555 (with a geological map in colors; scale: 1 inch = 96 miles)
Krynine PD (1937) Petrography and genesis of the Siwalik Series. Am J Sci Ser 5 34:422–466
Le Fort P (1975) Himalayas, the collided range: present knowledge of the continental arc. Am J Sci 275-A:1–44
Lewis GE (1933a) Notice of the discovery of *Plesiogulo brachygnathus* in the Siwalik Measures of India. Am J Sci Fifth Ser xxvi:80
Lewis GE (1933b) Preliminary notice of a new genus of Lemuroid from the Siwaliks. Am J Sci Fifth Ser xxvi:134–138

Lombard A (1958) Un itinéraire géologique dans l'Est du Népal (Massif du Mont Everest). Mémoires Société Helvétique Sciences Naturelles 82:1–107

Lydekker R (1883) Synopsis of the Siwalik vertebrata of India. Records of the geological survey of India, vol XVI, part 2, pp 61–94

McMahon CA (1883) On the microscopic structure of some sub-Himalayan rocks of tertiary age. Records of the Geological Survey of India, vol XVI, pp 186–192

Medlicott HB (1864) On the geological structure and relations of the southern portion of the Himalayan range between the rivers Ganges and Ravee. Memoirs of the Geological Survey of India, vol III, Art 4, pp 1–206 (with a geological map in colors; scale: 1 inch = 8 miles)

Medlicott HB (1875) Note of the geology of Nepal. Records of the geological survey of India, vol VIII, Part 4, pp 93–101 (with a geological map on 1 inch = 6 miles)

Medlicott HB (1879) Sub-Himalayas. In: Medlicott HB, Blanford WT (eds) A manual of the geology of india, part II: Extra-Peninsular Area. Published by order of the Government of India, Calcutta, pp 517–571

Medlicott HB, Blanford WT (1879) A manual of the geology of India, part ii: Extra-Peninsular Area. Published by order of the Government of India, Calcutta, pp 445–817 (with 21 plates)

Middlemiss CS (1890) Physical geology of the Sub-Himalaya of Garhwál and Kumaun. Memoirs of the geological survey of India, vol XXIV, Part 2, pp 59–200 (with 3 plates of cross-sections and a plate of geological map in colors; scale 1 inch = 4 miles)

Munthe J, Dongol B, Hutchison JH, Kean WF, Munthe K, West RM (1983) New fossil discoveries from the Miocene of Nepal include a Hominoid. Nature 303(5915):331–333

Murchison C (ed) (1868) Palæontological Memoirs and notes of the Late Hugh Falconer, A.M., A.D., vol I: Fauna Antiqua Sivalensis, Robert Hardwicke, London, 590 pp

Nakata T (1972) Geomorphic history and crustal movements of the foot-hills of the Himalayas. Sci Rep Tohoku Univ 7th Ser (Geography) 22(1):39–177

Nakayama K, Ulak PD (1999) Evolution of fluvial style in the Siwalik Group in the foothills of the Nepal Himalaya. Sed Geol 125:205–224

Nanda AC, Sehgal RK (2005) Recent advances in palaeomagnetic and magnetostratigraphic aspects of the Siwalik Group of Northwestern Himalaya. Himalayan Geology, Wadia Institute of Himalayan Geology, Dehra Dun, vol 26, no 1, pp 93–102

Ojha TP, Butler RF, Quade J, DeCelles PG, Richards D, Upreti BN (2000) Magnetic polarity stratigraphy of the Neogene Siwalik Group at Khutia Khola, far-western Nepal. Bull Geol Soc Am 112:424–434

Opdyke ND, Johnson NM, Johnson GD, Lindsay EH, Tahirkheli RAK (1982) Paleomagnetism of the Middle Siwalik formations of Northern Pakistan and rotation of the Salt Range decollement. Palaeogeogr Palaeoclimatol Palaeoecol 37:1–15

Opdyke ND, Lindsay E, Johnson GD, Johnson NM, Tahirkheli RAK, Mirza MA (1979) Magnetic polarity stratigraphy and vertebrate paleontology of the Upper Siwalik Subgroup of Northern Pakistan. Palaeogeogr Palaeoclimatol Palaeoecol 27:1–34

Pascoe EH (1964) A manual of the geology of India and Burma, Volume III, Published by order of the Government of India, Published by the Manager of Publications, Civil Lines, Delhi, pp 1345–2130 (with maps)

Pilgrim GE (1908) The tertiary and post-tertiary freshwater deposits of Baluchistan and Sind with notices of new vertebrates. Records of the geological survey of India, vol XXXVII, part 2, pp 139–166 (with Plates 2, 3, and 4)

Pilgrim GE (1910) Preliminary note on a revised classification of the tertiary freshwater deposits of India. Records of the geological survey of India, vol XL, Part 3, pp 185–205

Pilgrim GE (1913) The correlation of the Siwaliks with mammal horizons of Europe. Records of the geological survey of India, vol XLIII, Part 4, pp 264–326 (with 3 plates including a geological map in colors, scale: 1 inch = 1 mile, and cross-sections)

Pilgrim GE (1925) The migrations of Indian mammals, presidential address, section of geology, proceedings of twelfth Indian science congress, pp 200–218

Pilgrim GE (1932) The fossil carnivore of India, Memoirs of the geological survey of India, Palæontologia Indica, vol XVIII, 232 pp (with Plates I to X)

Prasad M (1995) Siwalik flora from Koilabas area in the Nepal Himalaya and its significance on palaeoenvironment and phytogeography. J Nepal Geol Soc 11:203–216 (Special issue)

Prasad KN (2001) An introduction to the mammalian fauna of the Siwalik System. Prasad Publications, Chennai 295 pp

Raiverman V (2002) Foreland sedimentation in Himalayan tectonic regime: a relook at the orogenic process, Bishen Singh Mahendra Pal Singh (Publishers), Dehra Dun, India, 378 pp (with maps)

Raiverman V (2007) Geothermic revolution, mountain elevation, tectonic pulsation and foreland sedimentation in the Himalayan System. Himalayan geology, Wadia Institute of Himalayan Geology, Dehra Dun, India, vol 28, no 2, pp 33–44

Raju ATR (1967) Observations on the petrography of tertiary clastic sediments of the Himalayan foothills of north India. Bull Oil Nat Gas Comm 4(1):5–16

Rösler W, Metzler W, Appel E (1997) Neogene magnetic polarity stratigraphy of some fluviatile Siwalik sections, Nepal. Geophys J Int 130:89–111

Schumm SA (1977) The fluvial system. Wiley, New York 338 pp

Sharma CK (1973) Geology of Nepal. Mani Ram Sharma, Educational Enterprises, Kathmandu 184 pp

Sinha S, Kumar R, Ghosh SK, Sangode SJ (2007) Controls on expansion-contraction of late Cenozoic alluvial architecture: a case study from the Himalayan foreland basin, NW Himalaya, India. Himalayan Geology, Wadia Institute of Himalayan Geology, Dehra Dun, vol 28, no 1, pp 1–22

Strachey R (1851) On the geology of part of the Himalaya Mountains and Tibet. Q J Geol Soc Lond 7:292–310 (with a geological map and two cross-sections in colors)

Takayasu K (1988) Freshwater molluscs in the Churia (Siwalik) Group and Himalayan upheaval. In: Kizaki K (ed) Himalayan upheaval, Tsukiji Shokan, pp 82–92 (in Japanese)

Tokuoka T, Takayasu K, Hisatomi K, Yamasaki H, Tanaka S, Konomatsu M, Sah RB, Rai SM (1990) Stratigraphy and geologic structures of the Churia (Siwalik) Group in the Tinau Khola–Binai Khola area, west central Nepal. Memoirs of the Faculty of Science, Shimane University, vol 24, pp 71–88

Tokuoka T, Takayasu K, Yoshida M, Hisatomi K (1986) The Churia (Siwalik) Group of the Arung Khola area, west central Nepal. Memoirs of the Faculty of Science, Shimane University, Japan, vol 20, pp 135–210 (with a geological map in colors)

Ulak PD (2002) Palaeohydrology of the Siwalik Group along the Bakiya Khola section, Central Nepal Himalaya. J Nepal Geol Soc 26:49–58

Ulak PD, Nakayama K (1998) Lithostratigraphy and evolution of the fluvial style in the Siwalik Group in the Hetauda–Bakiya Khola area, Central Nepal. Bulletin of Department of Geology, Tribhuvan University, vol 6, pp 1–14

Vaidyanadhan R, Ramakrishnan M (2008) Geology of India, Volume 2, published by the Geological Society of India, Bangalore, pp 557–994 (with maps and plates)

Wadia DN (1926) Geology of India (for students), Revised edn. Macmillan and Co. Limited, London 400 pp
Wadia DN (1976) Geology of India, 4th edn. Tata McGraw-Hill Publishing Co., New Delhi, 508 pp
West RM, Hutchison J, Munthe J (1991) Miocene vertebrates from the Siwalik Group, Western Nepal. J Vertebr Paleontol 11(1):108–129
West RM, Lukacs JR, Munthe J Jr, Hussain ST (1978) Vertebrate fauna from Neogene Siwalik Group, Dang Valley, Western Nepal. J Paleontol 52(5):1015–1022
West RM, Munthe J (1981) Neogene vertebrate paleontology and stratigraphy of Nepal. J Nepal Geol Soc 1(1):1–14
Wynne AB (1877) Note on the tertiary zone and underlying rocks in the north-west Punjáb. Records of the geological survey of India, vol X, Pt 3, pp 107–132 (with a geological map in colors on a scale of 8 miles = 1 inch)
Wynne AB (1878) On the geology of Salt Range in the Punjáb. Memoirs of the Geological Survey of India, vol XIV, Art 1, pp 1–313 (with 2 geological maps in colors on the scale of 4 miles = 1 inch, and 31 plates)
Wynne AB (1880) On the trans-indus extension of the Punjab Salt Range. Memoirs of the Geological Survey of India, vol XVII, Art 2, pp 211–305 (with six plates and three colored geological maps, main map is 1 inch = 4 miles)

Siwaliks of Mahakali–Seti Region

28

I believe that, if we could have been present in Siwalik times—nay, even in Nahan or nummulitic times—we should have seen the Himalayan range in all its might standing up very much as it does now.

—C.S. Middlemiss (1890, p. 5)

The lithology and structure of the Siwaliks, cropping out in the Mahakali–Seti region, are facsimiles of their Kumaun counterpart, investigated in detail by Middlemiss (1890). In Nepal, the Petroleum Exploration Promotion Project of the Department of Mines and Geology was engaged in mapping the whole Siwalik Range. The project has published 10 geological maps with many cross-sections, which also include vital subsurface information obtained mainly from seismic survey. Sharma et al. (2007) differentiated the Sub-Himalaya of the Mahakali–Seti region into the Lower Siwaliks, Middle Siwaliks (divided further into the Lower and Upper members), and Upper Siwaliks (Fig. 28.1). From the Siwalik Range and its foothill belt, they also reported four steeply north-dipping imbricate faults, all of which merge with a gently north-dipping decollement, lying at a depth of 7–9 km. Presumably, the oldest Siwaliks in Nepal are exposed in the Karnali River valley, where their lowest stratigraphic horizons gave a deposition age of 16 Ma (Gautam and Fujiwara 2000).

Contrary to the generally accepted piggyback propagation of imbricate faults from the hinterland towards the foreland, frequently there is an active normal fault (Nakata et al. 1984) at or near the north limit of the Siwaliks, implying concomitant and complex tectonic movements in the frontal fold-and-thrust belt. In this regard, the Siwalik prism of the Budar–Jogbudha area (Fig. 28.2) is no exception. To the north, the Budar Thrust delimits the Siwaliks from the Lesser Himalayan sequence, whereas the Jogbudha Thrust divides them into the outer and inner belts. Coincident with or very close to the Budar Thrust, there is an active fault (Figs. 28.2 and 28.3) that crosses the saddle of Budar and passes through Alital and Kalena, living behind a number of sag ponds and lakes in its depressions. To the south of the Budar Thrust, the Lower, Middle, and Upper Siwaliks are distributed in the vicinity of Budar, Godam, Saleta, and in the Puntura Khola. There are also anomalously elevated alluvial terraces around Phaltude and a large alluvial fan in the Kalena Khola.

In the Budar–Jogbudha area, the Upper Siwaliks are characterized by coarse, dissected, and subdued topography. Ephemeral streams running through them produce a huge amount of coarse sediment. In this process, they form valleys wider and straighter than those developed in the Lower and Middle Siwaliks. The Middle Siwaliks are characterized by high hills, steep slopes, deeply dissected gullies, and a dendritic drainage pattern. In them, the sinuosity of streams is higher than that in the Upper Siwaliks. The Lower Siwaliks exhibit smoother and gentler topography, as compared to the Middle and Upper Siwaliks, and their drainage pattern is also dendritic.

28.1 Lower Siwaliks

In the neighboring Kumaun Himalaya, the Lower Siwaliks are made up of dark brown to greenish brown or bluish gray sandstones, which are very micaceous and occasionally feldspathic, and contain secondary ferruginous products. The sandstones are interbedded with purple, dark reddish brown, and green-gray shales. The shales are finely laminated and red color predominates in their lower part. There also occur several pseudo-conglomerate and concretionary layers. Hematite-rich bands appear in some of the lower purple shale beds (Middlemiss 1890, p. 28).

The Lower Siwaliks of the Budar–Jogbudha area consist of fine-grained sandstones and mudstone, ranging in thickness from a few meters to tens of meters, in almost equal proportions. On the Budar–Jogbudha road, gray, green-gray, medium- to fine-grained sandstones contain lithic fragments. They pass upwards into thin (10–20 cm) interbeds of yellow-green siltstone or mudstone. A sandstone succession is 5–15 m thick; it is massive, indurated, and rather hard. There are also very thick-bedded, yellow-green, medium- to coarse-grained sandstones, interbedded with gray, green-gray, brown to orange mudstones, siltstones, and feeble shales. Towards the lower part of the Lower Siwaliks, some

M.R. Dhital, *Geology of the Nepal Himalaya*, Regional Geology Reviews,
DOI 10.1007/978-3-319-02496-7_28

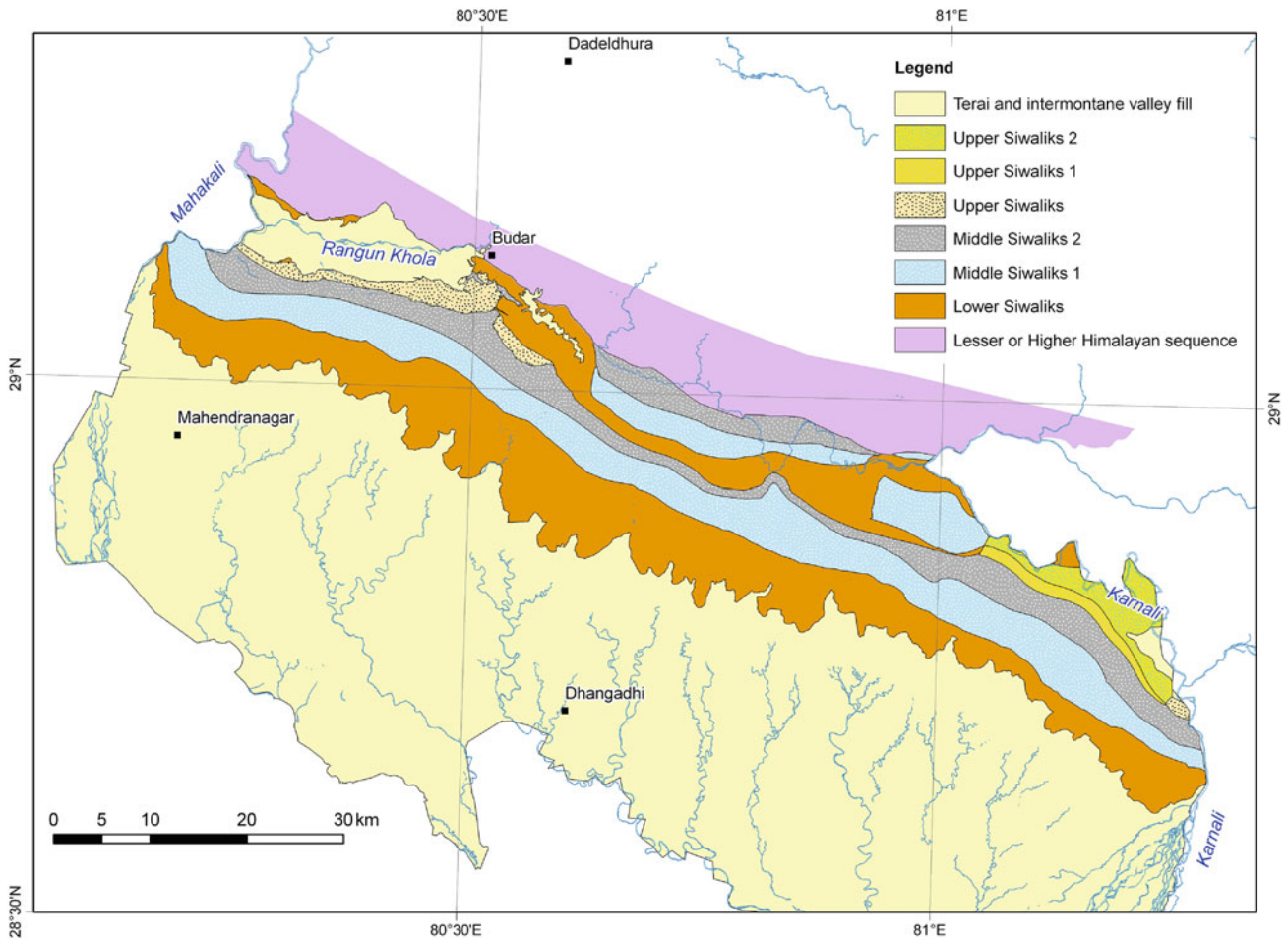

Fig. 28.1 Geological map of the Siwaliks in the Mahakali–Seti Region. *Source* Modified from Sharma et al. (2007)

dark gray-green sandstones are interbedded with brown, yellow, and orange mudstones, which are sporadically mottled. The mudstones are also infrequently calcareous.

28.2 Middle Siwaliks

The Middle Siwaliks of Kumaun are made up of micaceous, slightly ferruginous, sometimes feldspathic, soft sandstone at the base. The sandstone has a sugary texture, pale yellow or blue-gray, brown, and pale purple colors. Reddish brown clays are freely interstratified, and gray clays and mudstones occupy the upper part. One of the characteristic features of the Middle Siwaliks is the presence of numerous nodular layers and concretions. They sometimes constitute a thin layer, ranging in thickness from a few centimeters to tens of centimeters. The Middle Siwaliks also include one or two conglomerate beds, made up of small quartzite pebbles and shale pebbles. They also contain nests and stringers of coal as well as petrified wood fragments. The Middle Siwalik sandstones consist of a good deal of muscovite, quartz (including a significant amount of amethyst), biotite, and feldspar. Some jasper and magnetite grains are also present (Middlemiss 1890, pp. 25–27).

In the Budar–Jogbudha area, very thick-bedded, multi-storied, pepper-and-salt sandstones, interbedded with very thick (up to 20 m) gray mudstones, characterize the Middle Siwaliks. Most of the sandstones are dark gray-green, medium to fine, and alternating with feeble gray to gray-green shales. The lower contact of the fining-upwards cycles is sharp, irregular, and frequently erosional, whereas the upper contact ends with a mudstone or a shale, rich in plant debris and leaf remains. The Middle Siwaliks are truncated by a disconformity, and they abruptly pass into the Upper Siwaliks, represented mainly by a boulder-conglomerate. The disconformity is well observed in the upper reach of Puntura Khola.

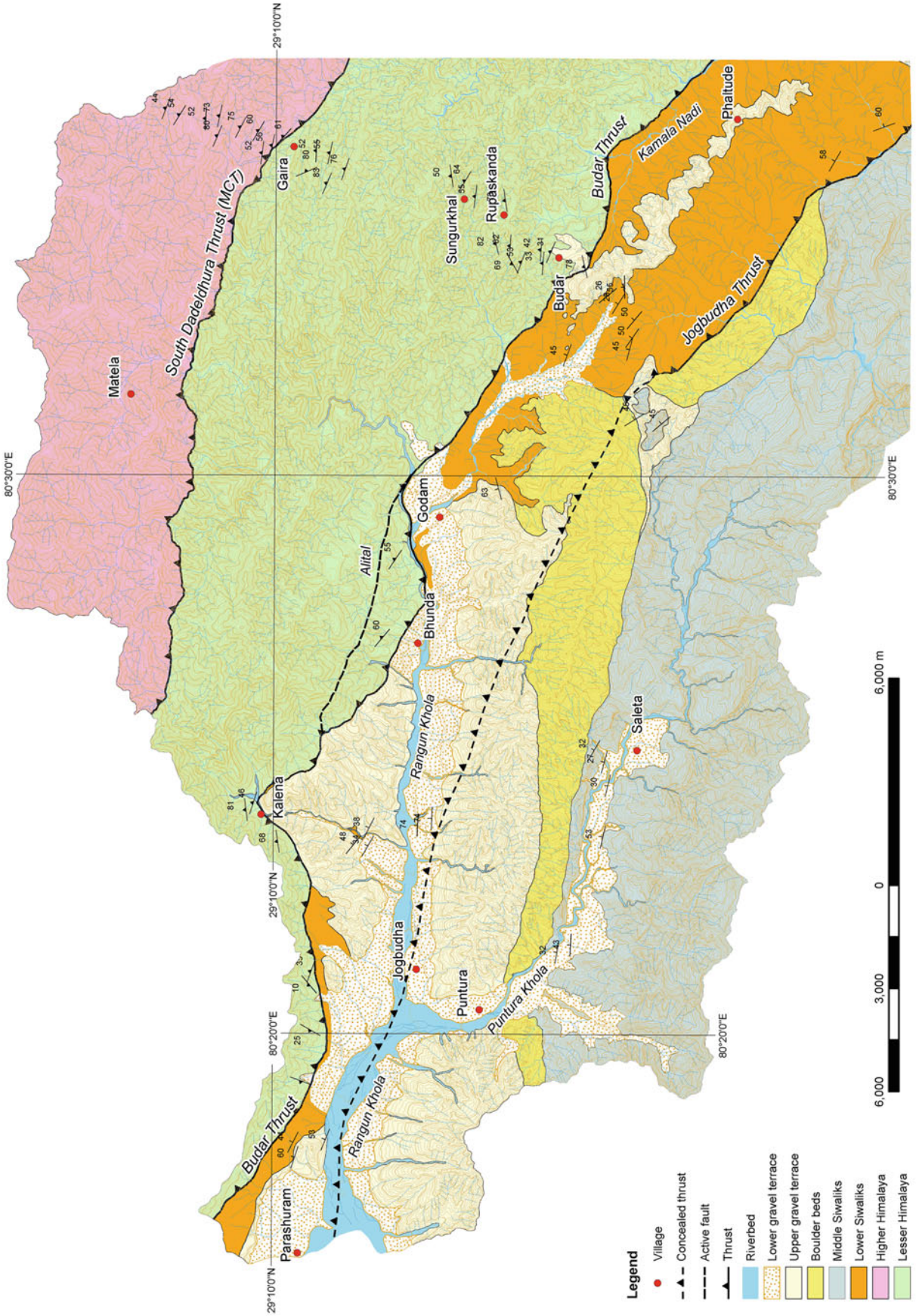

Fig. 28.2 Geological map of the Jogbudha–Budar area. *Source* Based on field survey in 2006 and 2013 by MR Dhital, and in 2006 by AMS Pradhan and MS Dhar

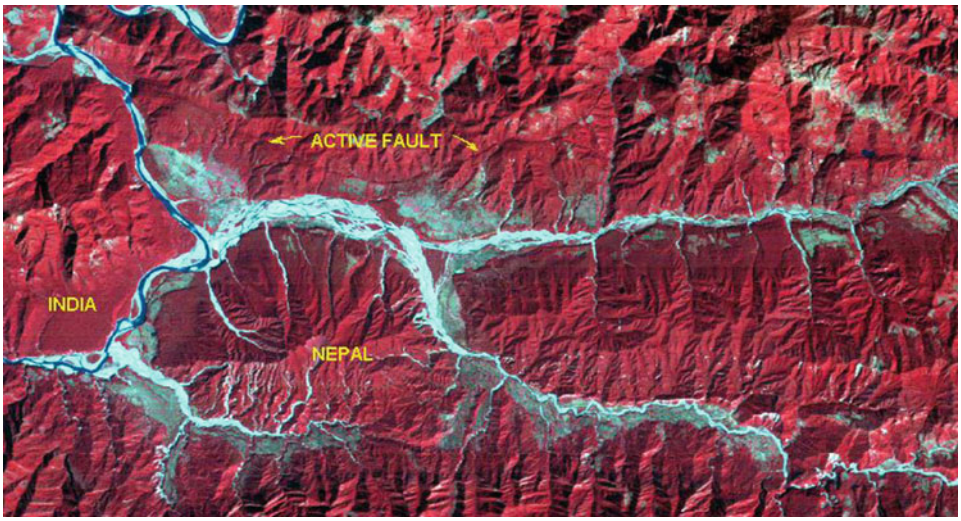

Fig. 28.3 Active fault in the Rangun Khola watershed. *Source* Landsat TM, false color composite

28.3 Upper Siwaliks and Kalena Alluvial Fan

The Upper Siwaliks of Kumaun are composed of conglomerates, consisting of much the same material as that which forms the present streambed. Most of the pebbles are well rounded, and they are represented by Himalayan rocks, with a considerable amount of fawn and dark yellow sand. In some areas, the Upper Siwalik beds are vertical and are almost entirely composed of large pieces of Lower Siwalik sandstone. Many clay and silt beds, of brown and yellow colors, are interbedded with the conglomerates. Cross-bedding is common, and the rock is hardened in places by a deposit of lime between the pebbles (Middlemiss 1890, p. 22).

In the Budar–Jogbudha area, the boulder-conglomerates of the Upper Siwaliks are interstratified with sands and a subordinate amount of clay. The sediments consist of poorly graded materials, including pebbles, cobbles, and boulders, derived from the Lesser Himalaya and the Higher Himalaya.

To the west of Jogbudha, near the confluence of the Puntura Khola and the Rangun Khola, gently north-dipping, pale yellow to orange, fine gravel and sand beds transitionally grade over the boulder-conglomerate (Fig. 28.4). They are composed exclusively of well-rounded quartzite pebbles and quartz sand. Hence, most of them were reworked from the Upper Siwaliks. To the east of Jogbudha, the boulder-conglomerate beds transitionally pass into the large alluvial fan of Kalena (Fig. 28.2). The dip of beds gradually decreases from the Upper Siwaliks to the alluvial fan, implying a progressive unconformity. The Kalena alluvial fan is more than 100 m thick, and it contains boulders of quartzite, gneiss, and granite that reach in size up to 8 m (Fig. 28.5). Such large boulders were derived mainly from debris flows. The Upper Siwaliks and the Kalena fan conceal the Jogbudha Thrust, which includes the Lower Siwaliks on its hanging wall.

Fig. 28.4 Gently (10–20°) north-dipping sand and gravel overlying the boulder-conglomerates on the left bank of the Puntura Khola, near the confluence with the Rangun Khola. View to W. *Source* Photographed by author

28.4 Gravel Veneer East of Budar

An approximately 10 to 30 m thick alluvial gravel veneer covers the ridge east of Budar, where it extends beyond Phaltude (Fig. 28.2). The gravel consists of rounded quartzite boulders, ranging in size from 10 cm to 2 m, and they are not much different from those forming the Kalena

Fig. 28.5 A large quartzite boulder in the Kalena Khola. *Source* Photographed by author

alluvial fan. The veneer also contains a strongly weathered matrix, made up of red-brown to orange, clayey silty sand. These deposits lie at an altitude of about 1,400 m and stretch parallel to the Kamala Khola, whose riverbed is located about 1.5 km north of the ridge, at an altitude of about 1,100 m. Thus, there is an elevation difference of about 300 m between them.

28.5 Structure of the Siwalik Belt

Middlemiss (1890, pp. 77–78) mapped five successive imbricate faults in the Lesser Himalaya and Sub-Himalaya of Kumaun. They are arranged in the following order.

NNE
Schistose group
------Thrust------
Slate and breccia
------Thrust------
Nummulitics
Tal
Massive Limestone
------Thrust------
Lower Siwaliks
------Thrust------
Middle Siwaliks
Lower Siwaliks
------Thrust------
Upper Siwaliks
Middle Siwaliks
Lower Siwaliks
SSW

All these fault-bound blocks are in their right-way-up position, and dip towards the NNE. In this sequence, every formation, when its southern neighbor is younger than itself, is divided from it by a reverse fault; and when the southern neighbor is older than itself, it is in normal superposition on itself. Each fault zone is older than the succeeding zone to the south. In this tract, the older zones show more intense folding than the younger zones. Thus, while moving from the north to the south, each fault-bound block exhibits a set of strata, younger than the predecessor zone. Hence, together with the deposition of strata, there was faulting and upheaval of their neighboring zones to the north. In this way, the disturbance propagated from the north to the south by adding, by an accretive evolution, fresh strata to the mountain mass as the ages rolled along (Middlemiss 1890, p. 79). Thus, Middlemiss accurately described the piggyback propagation model of imbricate faults in the Lesser Himalaya and Siwaliks of Kumaun. He also worked out the development of a piggyback-transported basin. One of his geological cross-sections (Fig. 28.6) clearly demonstrates this concept of simultaneous accumulation, deformation, and thrusting in the Siwalik Basin.

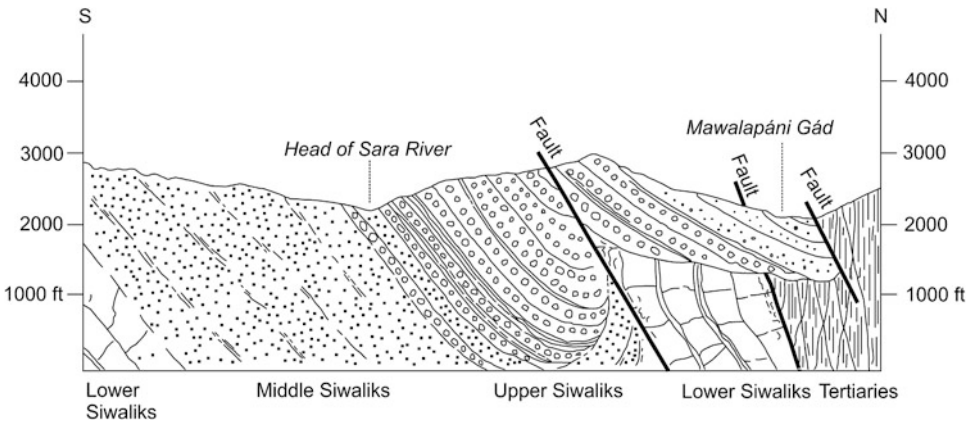

Fig. 28.6 Cross-section across the Patli Dun in the Kumaun Himalaya depicting simultaneous deposition and imbricate faulting in the Lesser Himalaya and Siwaliks. *Source* Modified from Middlemiss (1890)

References

Gautam P, Fujiwara Y (2000) Magnetic polarity stratigraphy of Siwalik Group sediments of Karnali River section in western Nepal. Geophys J Int 142:812–824

Middlemiss CS (1890) Physical geology of the Sub-Himalaya of Garhwál and Kumaun. Mem Geol Surv India XXIV(Part 2):59–200 (with 3 plates of cross-sections and a plate of geological map in colors; scale 1 inch = 4 miles)

Nakata T, Iwata S, Yamanaka H, Yagi H, Maemoku H (1984) Tectonic landforms of several active faults in the western Nepal Himalayas. J Nepal Geol Soc 4(Special Issue):177–200

Sharma SR, Subedi DN, KC SB, Khanal RP, Tripathi GN (2007) Geological map of Petroleum Exploration Block-1, Dhangadhi, Far Western Nepal (Scale: 1:250,000). Petroleum exploration promotion project, Department of Mines and Geology, Kathmandu, Nepal

Siwaliks of Karnali–Bheri Region

29

Geologically all existing mountains are recent; the ancient mountains are gone.
—J.W. Powell (1876, p. 193)

The Siwaliks of the Karnali–Bheri region (Fig. 29.1) form the widest foothill belt in the country, and surround many beautiful intermontane valleys, such as Surkhet, Dang, and Deukhuri. The incompetent Siwalik strata have yielded to a variety of folds, including upright, overturned, and plunging synclines and anticlines. There are also a number of imbricate faults, punctuating and straddling the Siwaliks as well as the neighboring Lesser Himalaya. The Siwaliks of this region also enclose a rich assortment of vertebrate fossils as well as mollusc and plant remains (Chap. 27).

The Siwaliks of the Karnali–Bheri region were investigated in detail in the Surai Khola area (Fig. 29.2), which occupies the east closure of the Dang and Deukhuri valleys. The rocks of the Surai Khola area are divided up into the Bankas, Chor Khola, Surai Khola, Dobata, and Dhan Khola formations, in ascending order (Corvinus 1988, 1993; Dhital et al. 1995), and their total measured thickness is 4,975 m. They are made up mainly of mudstones, sandstones, and conglomerates, with varying proportions (Fig. 29.3).

29.1 Bankas Formation

In the type section, the Bankas Formation (Fig. 29.4) is composed of medium- to very fine-grained sandstones (61 %), variegated siltstones and mudstones (39 %), and infrequently of shales and calcretes. Along the East–West Highway, southeast of Bhalubang, the exposed rock is represented by sandstones (270 m, 46 %), siltstones and mudstones (305 m, 52 %), and calcrete beds (15 m, 3 %). The cumulative thickness plots of sandstone and mudstone beds illustrate their almost equal proportion throughout the formation (Fig. 29.5a, b).

The gray-green to brown and purple sandstone beds range in thickness from 10 cm to 5 m. Most of them are litharenites, and some are sublitharenites. As a rule, the sandstones display gradational contacts with the overlying mudstones. Although the thickness and grain size of sandstones steadily increase from the bottom to top of the formation as a whole, the contiguous sandstone–mudstone duos constitute striking fining-upwards sedimentary cycles. A variety of sedimentary structures, such as cross and parallel laminae, ripple drift laminae, and climbing ripple laminae are universally present in the sandstone beds. Subordinately, load casts and convolute laminae are also discernible. The very thick sandstone beds in the vicinity of Bardanda exhibit spheroidal weathering patterns.

The interbedded mudstones are mostly variegated, and in them colors grade from light yellow, brown, green-gray to gray. Also, red-purple and golden yellow tints are characteristic. Generally, the mudstones are mottled (light gray, blue-gray), and the intensity of mottling gradually decreases from the lower to upper sections of the Bankas Formation. Intense bioturbation is another remarkable feature of the mudstones, where some bioturbation tubes reach from 2 mm to 1 cm in diameter.

Gray and dark gray shales regularly overlie the mudstones. The mudstones (light yellow and green-gray), shales (gray), and siltstones (light brown) include many horizons rich in plant leaves. Particularly, from 5 to 50 cm thick beds of brown and gray calcareous siltstones, overlying thick (more than 10 m) sandstone sequences, yield well-preserved leaves.

The sandstones and mudstones of the Bankas Formation are normally calcareous, owing to diagenetic replacement of their clasts and matrix by calcite, which may sometimes comprise up to 40 % of the aggregate rock volume. There are also a few calcrete and marl beds.

The Bankas Formation is 585 m thick in the Surai Khola, 695 m along the East–West Highway southeast of Bhalubang, and 330 m in the Agge Khola (Fig. 29.6). It transitionally passes into the overlying Chor Khola Formation, and the contact between them is marked at the base of the first very thick (more than 5 m), medium- to coarse-grained, and cross-laminated gray sandstone bed, containing detrital biotite.

M.R. Dhital, *Geology of the Nepal Himalaya*, Regional Geology Reviews,
DOI 10.1007/978-3-319-02496-7_29

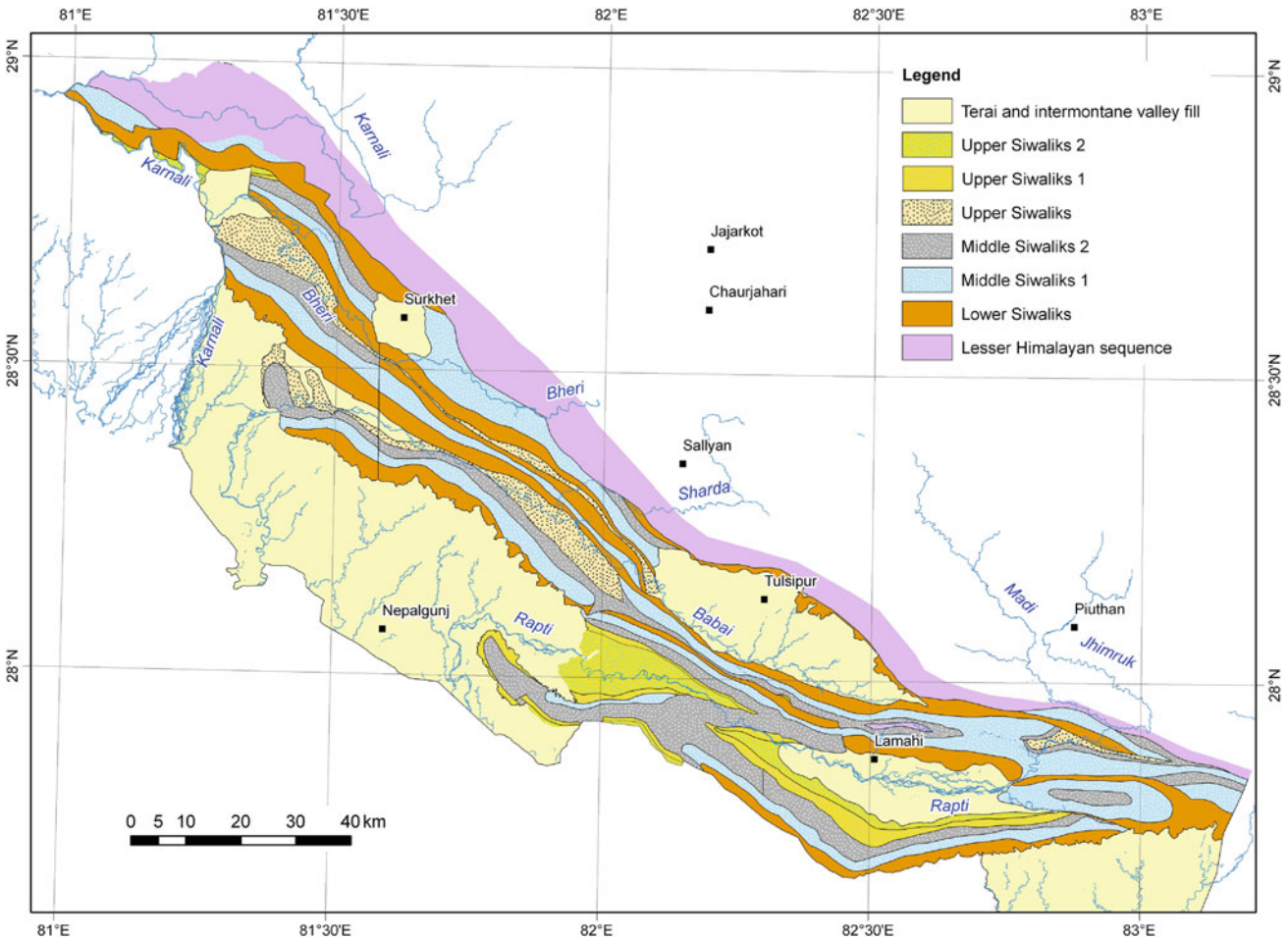

Fig. 29.1 Generalized geological map of the Siwaliks in the Karnali–Bheri region. *Source* Modified from Kayastha et al. (1999), Pradhan et al. (2000, 2003), and Dhital et al. (1995)

29.2 Chor Khola Formation

The Chor Khola Formation has almost an equal amount of sandstone and mudstone, and it is subdivided into the Jungli Khola Member and overlying Shivgarhi Member. The total thickness of the Chor Khola Formation is 1,225 m in its type area.

29.2.1 Jungli Khola Member

The Jungli Khola Member in the type section, in the Surai Khola, consists of sandstones (190 m, 55 %) and mudstones or siltstones (150 m, 44 %), with a trifling amount of marl (5 m, 1 %) as well as a few beds of calcrete and shale (Figs. 29.3 and 29.5c). Along the East–West Highway, southeast of Bhalubang, the exposed cumulative thickness (Fig. 29.5d) of sandstones is 255 m (54 %), those of mudstones or siltstones is 210 m (45 %), and the calcrete beds constitute 4 m (1 %).

Although predominantly fine sandstones are found in the Jungli Khola Member, there are also subordinate medium- to coarse-grained beds (Fig. 29.6). The sandstones are indurated (especially the fine-grained ones), calcareous, and gray and yellow-brown in color. Mostly, the medium-grained sandstones are strongly bioturbated and occasionally include intraformational mud clasts and pseudo-conglomerates in their basal part.

The mudstones are invariably variegated, frequently bioturbated, and commonly mottled. Red-purple mudstones come after yellow colored ones, and these two types are dominant in the lower section, whereas gray and yellow-brown varieties prevail in its upper part, and they contain abundant well-preserved plant leaves. The intensity of mottling in the mudstones gradually decreases towards their upper end and some of them are covered by paleosols.

The Jungli Khola Member is 405 m thick in the Surai Khola (Fig. 29.4), and 530 m thick in the the vicinity of Bhalubang. Its limit with the overlying Shivgarhi Member is

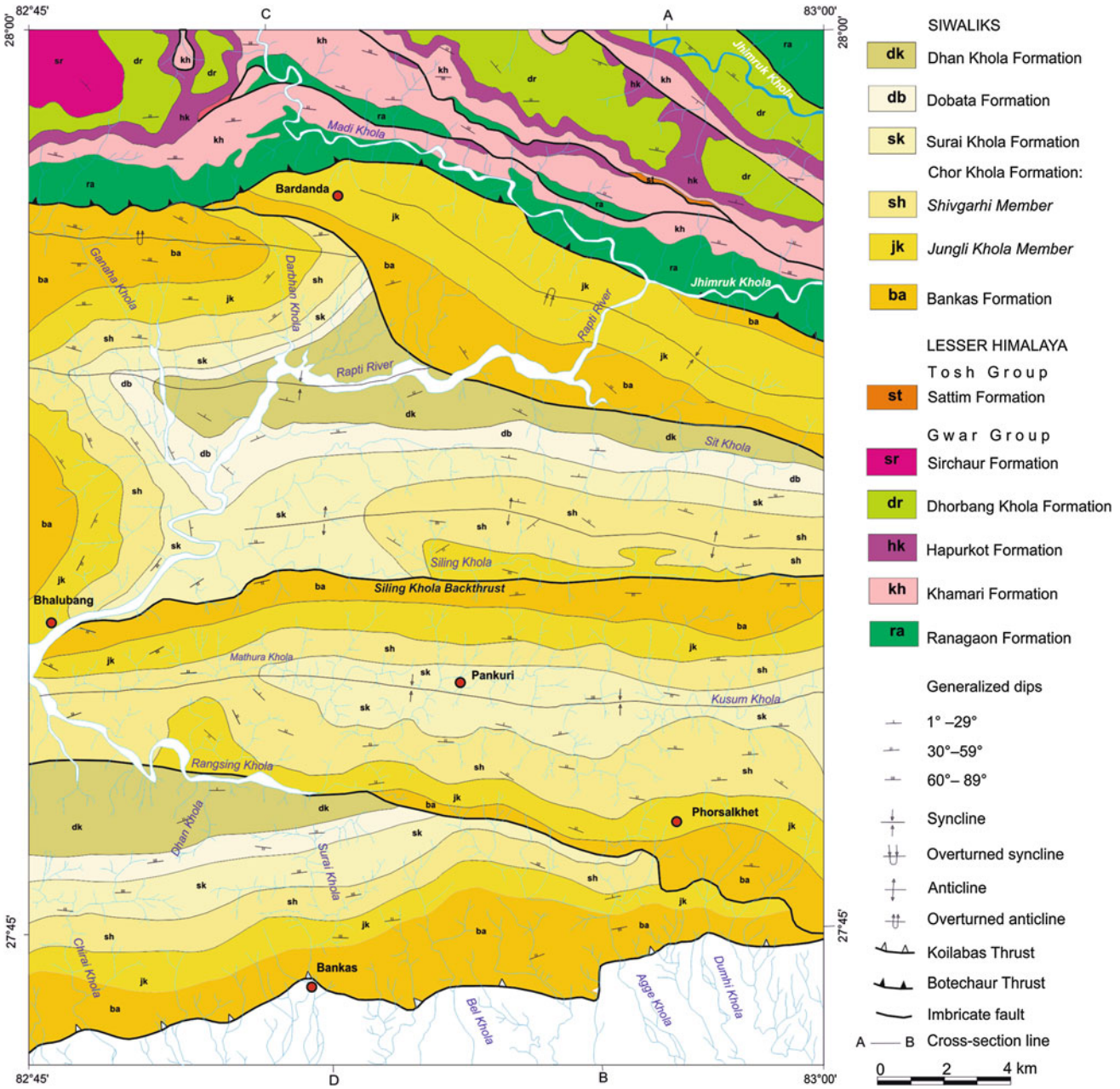

Fig. 29.2 Generalized geological map of the Surai Khola area. *Source* Modified from Dhital et al. (1995)

placed at the base of the first very thick bed of pepper-and-salt colored sandstone (Fig. 29.7).

29.2.2 Shivgarhi Member

The Shivgarhi Member at its type section (Figs. 29.3 and 29.5e) in the Surai Khola is constituted of sandstones (350 m, 52 %), mudstones or siltstones (310 m, 46 %), calcretes (10 m, 1.5 %), and marls (5 m, 0.5 %). The gray sandstones from the Shivgarhi Member are generally medium- to very coarse-grained and calcareous. In them, cross and parallel laminae are more abundant than in those of the underlying Jungli Khola Member (Fig. 29.7). Fine-grained sandstones are less frequent, and they are normally parallel-laminated to thinly cross-laminated. Reworked mud clasts are present at the base of medium- to coarse-grained sandstone beds. Towards the upper section, near the contact with the Surai Khola Formation, the sandstones become very thick-bedded, very coarse-grained, and preponderate in detrital biotite flakes.

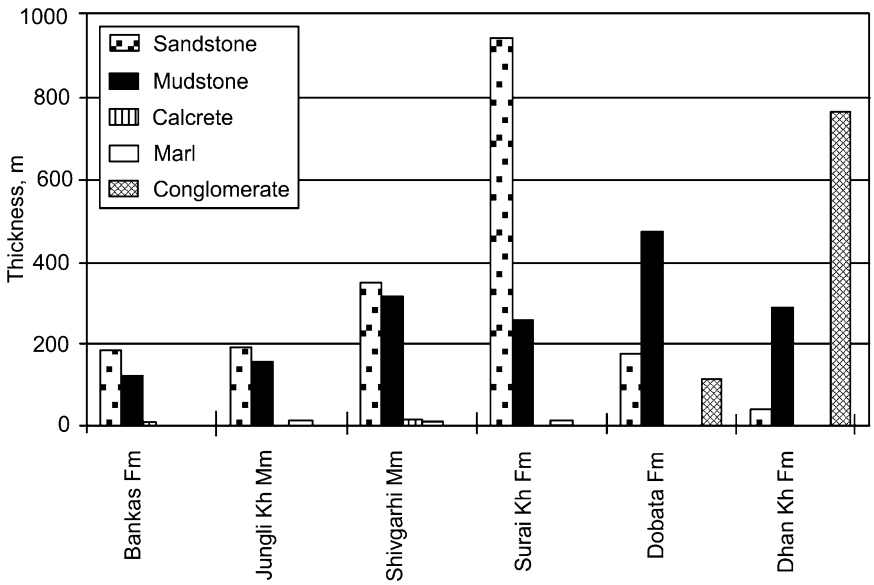

Fig. 29.3 The distribution of various rocks in the Surai Khola area. *Source* Modified from Dhital et al. (1995)

Intercalated light yellow, green-gray, and brown mudstones display spheroidal weathering patterns. There are also infrequent red-purple mudstones and thinly bedded, yellow-brown and gray siltstones, containing shale partings and thin interbeds. From 25 to 50 cm thick light yellow marl beds also sporadically occur in the Shivgarhi Member (Fig. 29.4). In the mudstones, the gray-green color predominates over the red-purple and yellow-brown. Bioturbation (as tubes and irregular bodies up to 30 cm across) is frequent in them, and they also contain calcareous concretions, but paleosols are scant in this formation.

Sandstones and mudstones compose a number of fining-upwards cycles in the Shivgarhi Member. In comparison with the underlying Jungli Khola Member, the sandstone cycles become thicker (up to 30 m) and include a greater amount of biotite and quartz, resulting in their pepper-and-salt appearance.

This member plentifully contains plant leaves, mollusc and vertebrate fossils (especially in its upper part), petrified wood, and thin coal lenses and seams. The upper sections of gray, green-gray, and yellow-brown mudstones as well as light brown siltstones and gray to dark gray shales contain a great amount of dicotyledon plant leaves and stems. Some fine-grained sandstone beds yield petrified wood pieces ranging in length from 5 mm to about 2 m.

The Shivgarhi Member is 820 m thick in the Surai Khola and has a gradational contact with the overlying Surai Khola Formation. Its upper contact is marked at the base of a very thick-bedded, very coarse-grained, cross-bedded, pebbly, pepper-and-salt sandstone.

29.3 Surai Khola Formation

The Surai Khola Formation comprises sandstones (940 m, 79 %) and mudstones (250 m, 21 %) with a minor amount of calcrete, marl, and shale (Fig. 29.3). The cumulative thickness plot (Fig. 29.5f) of successive sandstone and mudstone beds from the Surai Khola Formation reveals a strong predominance of sandstone over mudstone.

The coarse- to very coarse-grained sandstones of the Surai Khola Formation are recognized above all by their striking pepper-and-salt color, owing to the preponderance of detrital biotite and quartz. In addition, they are massive, calcareous, and feeble. Although the sandstone cycles vary in thickness from 0.5 to 50 m, frequently they are tens of meters thick (i.e., multi-storied). Wedge and trough cross-bedding, ripple cross-lamination, parallel-lamination, convolute lamination, and load casts are prolific in the sandstones. Infrequently, ripple marks are present on massive, coarse-grained sandstone beds.

In the Surai Khola Formation, green-gray to dark gray mudstones predominate over light gray to yellow-brown varieties. They vary in thickness from 50 cm to 20 m; regularly contain green and gray mottles; display spheroidal weathering patterns; and particularly, the gray shales are rich in plant leaves, stems, and branches. A few thin to thick calcrete beds are also found in between or at the bottom of the mudstone beds. Infrequently intercalated are 1–2 m thick, gray and yellow-brown calcareous siltstones, which are strongly bioturbated and include tubes of 5–10 cm in diameter.

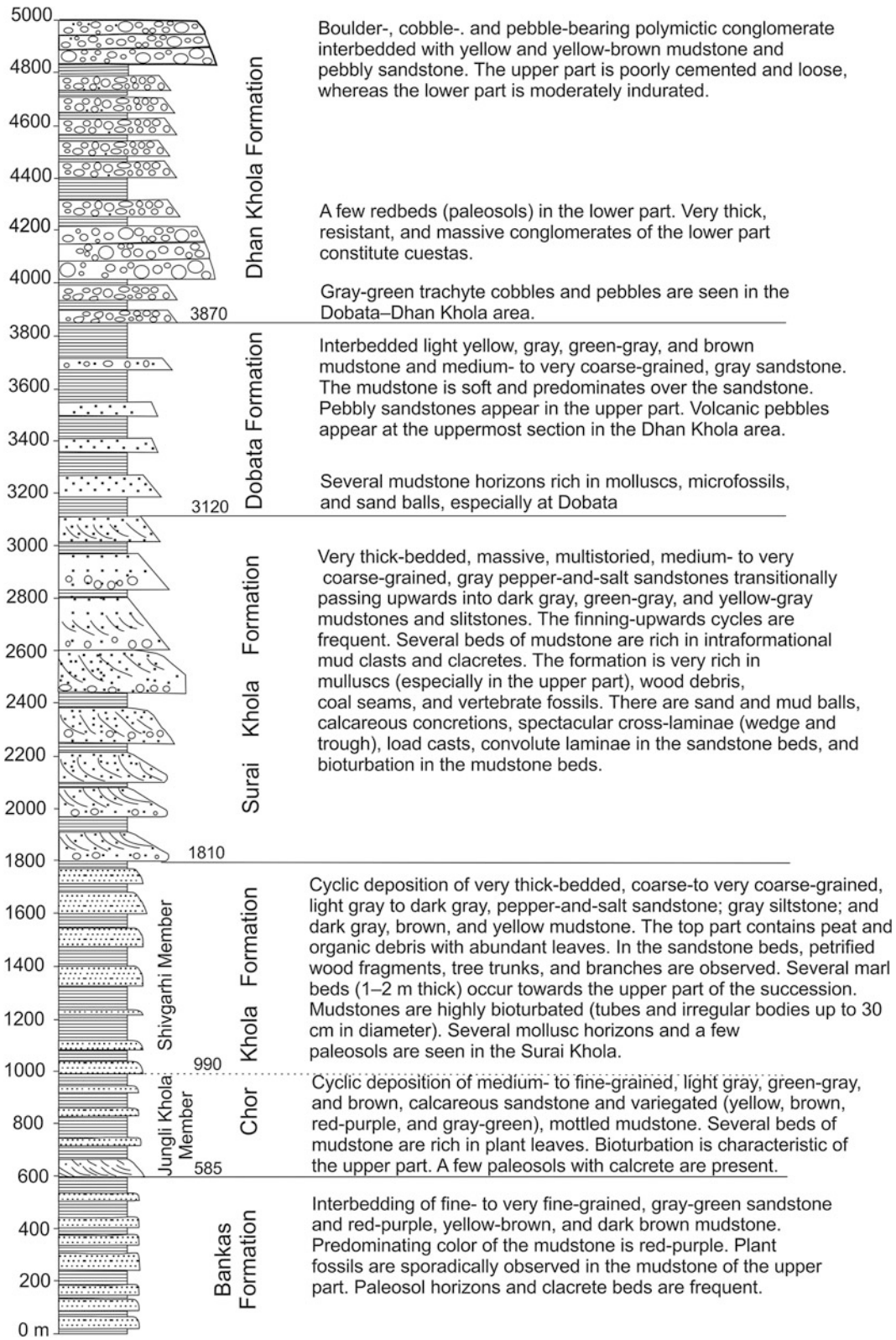

Fig. 29.4 Generalized lithostratigraphic column of the Siwaliks in Mid Western Nepal Sub-Himalaya. *Source* Modified from Dhital et al. (1995). © Central Department of Geology, Tribhuvan University. Used by permission

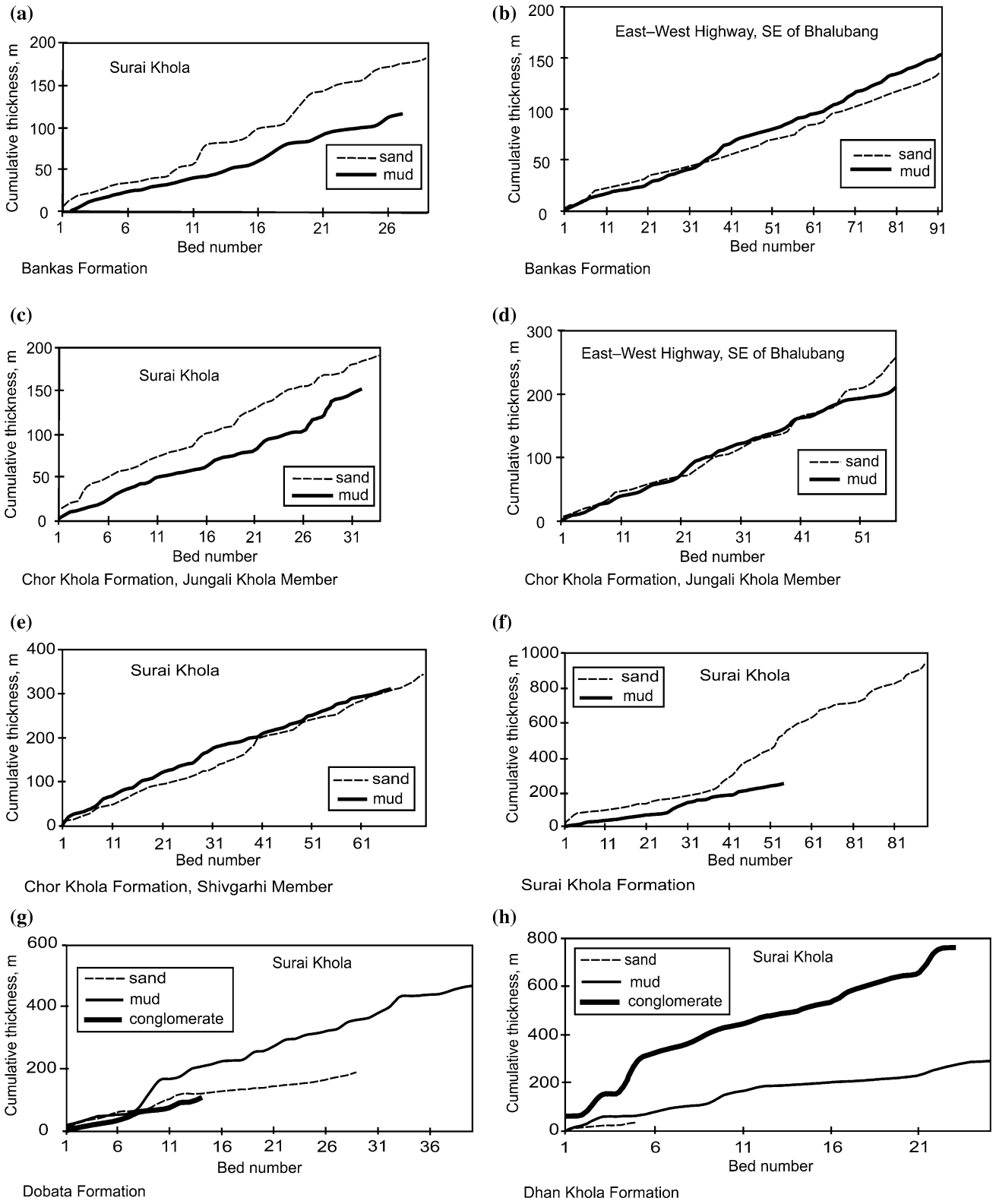

Fig. 29.5 Cumulative thickness plots of successive sandstone, mudstone, and conglomerate beds from various formations and members. **a** and **b** Bankas Formation; **c** and **d** Jungli Khola Member of Chor Khola Formation; **e** Shivgarhi Member of Chor Khola Formation; **f** Surai Khola Formation; **g** Dobata Formation; **h** Dhan Khola Formation. In the lower reaches of the Surai Khola, some mudstone beds are covered by overburden, and hence (**a**) depicts only an apparent increase in sandstone content. *Source* Modified from Dhital et al. (1995)

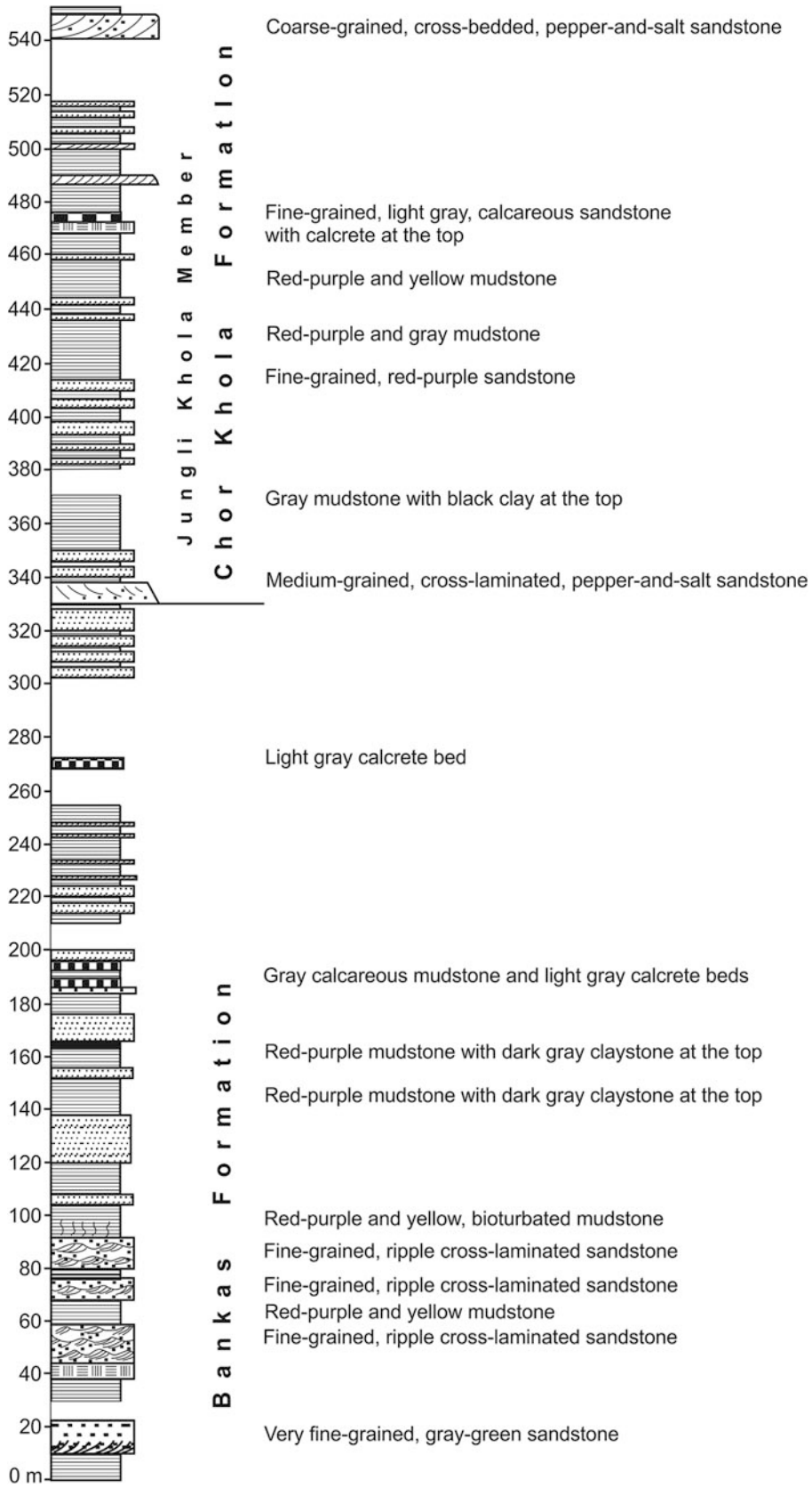

Fig. 29.6 Lithostratigraphic column illustrating the contact between the Bankas and the overlying Chor Khola formations. *Source* Modified from Dhital et al. (1995). © Central Department of Geology, Tribhuvan University. Used by permission

The cyclic fining-upwards sequences in the Surai Khola Formation are made up of very coarse-grained sandy beds at the bottom and grade upwards into thinly laminated gray to dark gray mudstones. The sandstones contain reworked mud clasts of up to 50 cm in size, and there are some pseudo-conglomerate beds at their base.

The lower part of the Surai Khola Formation is composed basically of thick- to very thick-bedded (multi-storied), pebbly, pepper-and-salt sandstones, gray and green-gray mudstones, and pseudo-conglomerates, with a few beds of marl and shale. In this zone, sandstones predominate over mudstones and the latter yield abundant dicotyledon plant leaves, wood debris, and vertebrate fossils. Normally, plant fossils are confined to gray shales, whereas molluscs are recovered mainly from gray shales, siltstones, and green mudstones.

The middle part of the Surai Khola Formation comprises a very thick (more than 20 m) intercalation of cross-bedded, gray, pepper-and-salt sandstone and mudstone in almost equal proportions. There also appear a number of variegated (green-gray, yellow, brown) mudstone beds. The sandstones contain reworked mud clasts (especially at their base), coal seams, and petrified wood.

In the upper part of the Surai Khola Formation, the proportion of sandstone increases considerably (Fig. 29.8) and, with overall coarsening grain size, some sandy beds become pebbly, and even contain thin conglomerate lenses. This sequence portrays conspicuous fining-upwards cyclic deposition (Fig. 29.9) of multi-storied sandstones and mudstones.

The pepper-and-salt sandstones of the upper part are extremely thick (up to 50 m), massive, calcareous, and loose. They develop dip slopes and cuestas, show parallel and trough cross-laminae, and abound in detrital biotite and quartz. The scattered pebbles and pebbly lenses are generally confined to the basal part of the multi-storied sandstones (Figs. 29.8 and 29.9). Some of the pebble-bearing sandstones contain calcareous concretions (10–20 cm in diameter) known as "sand balls" or "nodules." Towards the upper contact of the Surai Khola Formation, the pebbles derived from the Lesser Himalayan sedimentary and low-grade metamorphic rocks (i.e., quartz arenites, dolomites, and slates) preponderate.

The subordinately occurring mudstones of the upper part vary in thickness from 0.5 to 15 m; they are primarily green-gray and dark gray to gray, but light yellow and brown varieties do occur. Sometimes, green-gray or gray and yellow or yellow-brown mudstones are interbedded. A few purple mudstone beds also appear in the Surai Khola. Bioturbation as well as mottling is atypical of the mudstones, comprising the upper part. Excepting a few petrified tree branches in the multi-storied sandstones, it is devoid of plant remains, but is bountiful of fossil molluscs. The Surai Khola Formation is 1,310 m thick in its type area (Fig. 29.4), and transitionally passes into the overlying Dobata Formation. Its upper contact is placed at the base of a very thick mudstone bed (Fig. 29.10).

29.4 Dobata Formation

The sand-dominant Surai Khola Formation passes rather abruptly into the overlying mud-prevailing (470 m, 63 %) Dobata Formation (Figs. 29.3 and 29.5g), which also contains a lesser quantity of sandstone (175 m, 23 %) and conglomerate (105 m, 14 %). The gray-green and gray mudstones vary in thickness from 5 m (in the lower part) to 50 m (in the middle part), and they are frequently calcareous. Bioturbation is confined mainly to gray mudstones (Figs. 29.10 and 29.11), which give way to variegated (i.e., pale yellow, orange, gray-green, and dark gray) varieties towards the upper section. The Dobata Formation is rich in mollusc remains, and the fossil horizons are confined primarily to the gray and dark gray shales and mudstones, composing its middle run.

The sandstones representing the lower part of the Dobata formation are light gray to gray, medium- to very coarse-grained, and contain sand balls approaching 1 m in diameter (Fig. 29.10). In the middle section, the sandstones become medium- to coarse-grained, and they are intercalated with very thick mudstones. The upper portion of the Dobata Formation comprises thick- to very thick-bedded (0.5–20 m), coarse- to very coarse-grained, cross-laminated, pebbly sandstones with conglomerate lenses (Figs. 29.11 and 29.12). The pebbles are rounded to subrounded, made up mainly of yellow and white quartzites and gray dolomites, and are scattered throughout the sandstone, where their higher concentration in its lower part results in a graded bedding. In the road section between the Surai Khola and Dhan Khola, a large quantity of volcanic pebbles occurs in the sandstones and conglomerates of the Dobata Formation and the overlying Dhan Khola Formation (Fig. 29.12). The subrounded and spherical to prolate volcanic pebbles are represented basically by trachyte, and range in size from 5 mm to 5 cm.

In the upper part of the Dobata Formation are intercalated a few conglomerate beds, ranging in thickness from 0.5 to 15 m. They are polymictic (quartzite, limestone, dolomite, and volcanic pebbles), matrix supported, and loose. The Dobata Formation is 750 m thick in the type section (Fig. 29.4). It transitionally grades into the overlying Dhan Khola Formation, and the contact is placed at the base of an approximately 15 m thick conglomerate bed (Fig. 29.12).

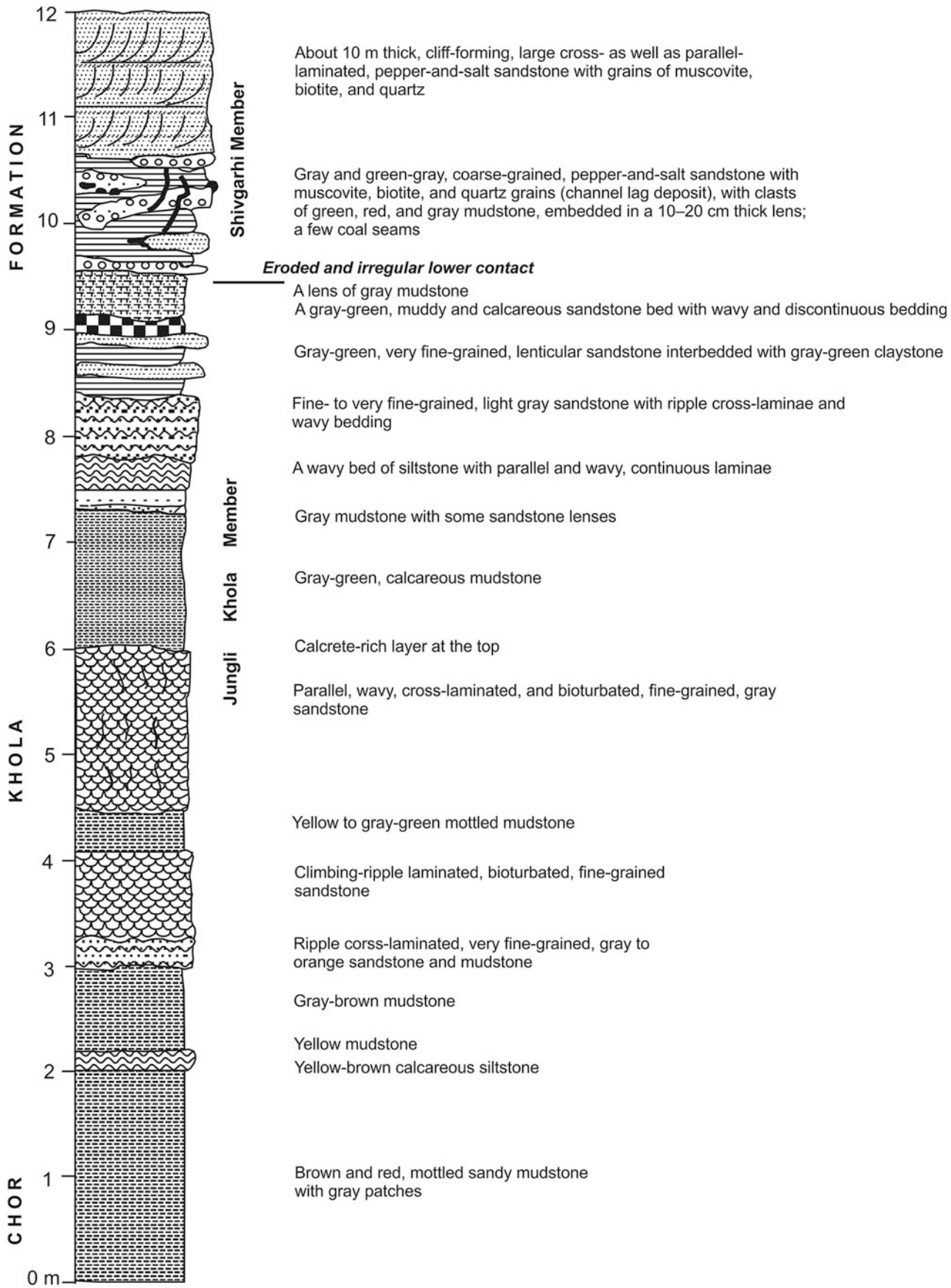

Fig. 29.7 Contact between the Jungli Khola Member and the overlying Shivgarhi Member in the Agge Khola. *Source* Modified from Dhital et al. (1995). © Central Department of Geology, Tribhuvan University. Used by permission

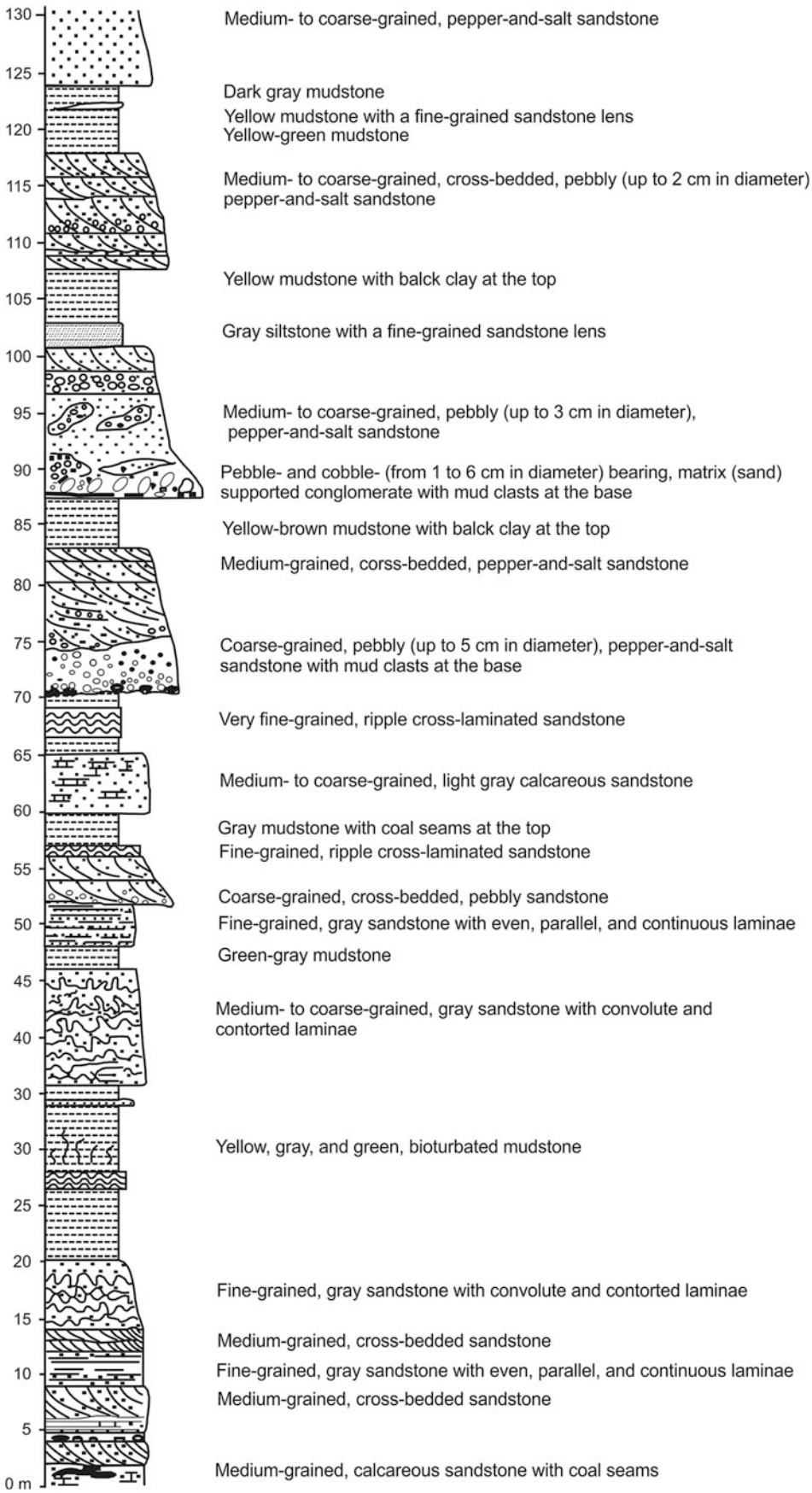

Fig. 29.8 Upper part of the Surai Khola Formation with cyclic deposition of pebbly sandstone and mudstone in the Kusum Khola. *Source* Modified from Dhital et al. (1995). © Central Department of Geology, Tribhuvan University. Used by permission

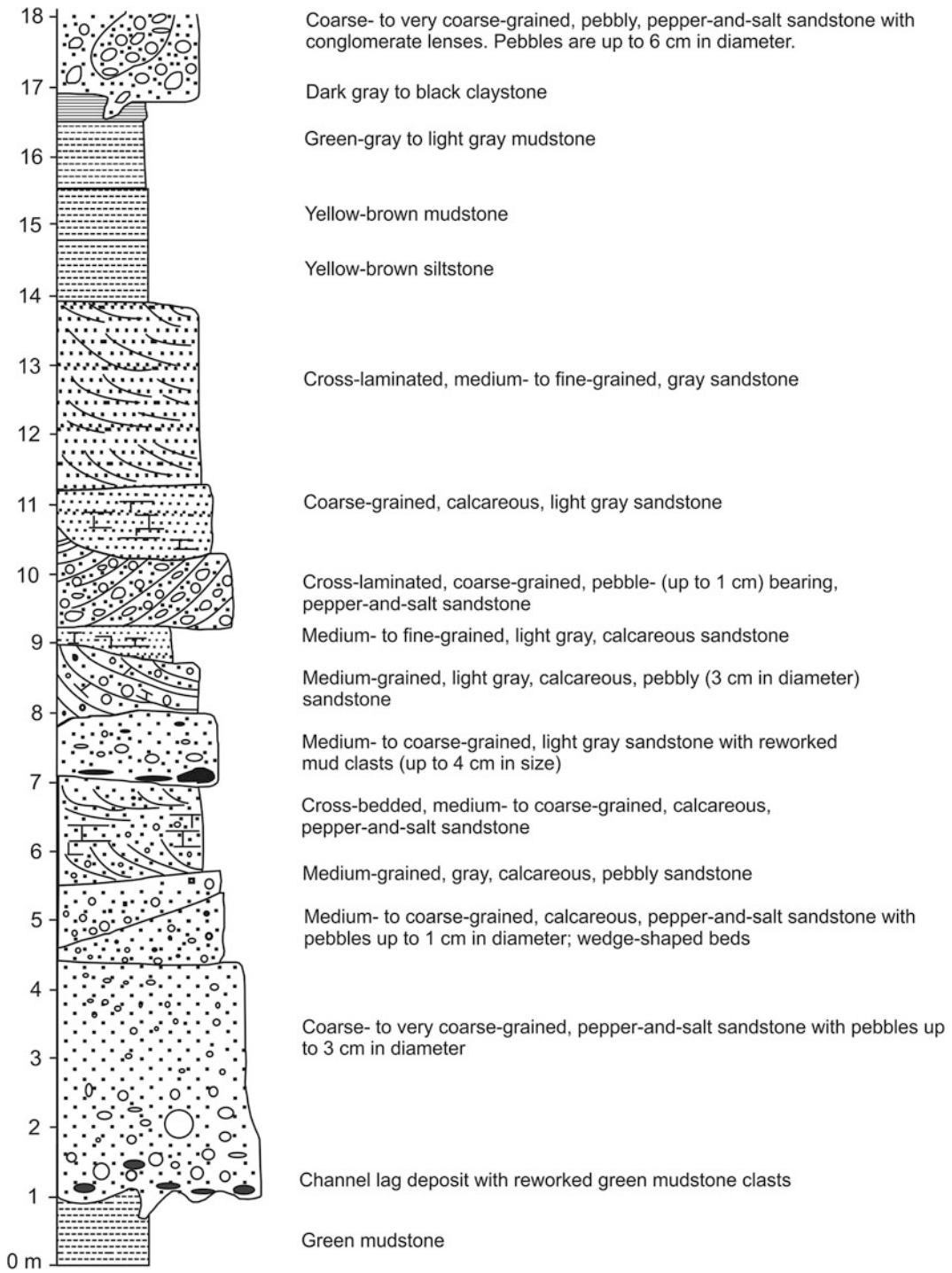

Fig. 29.9 Detailed columnar section of the Surai Khola Formation from the Kusum Khola, depicting a complete cycle of deposition (between 70 and 90 m in Fig. 29.8) from the pebbly sandstone to the dark gray claystone. *Source* Modified from Dhital et al. (1995). © Central Department of Geology, Tribhuvan University. Used by permission

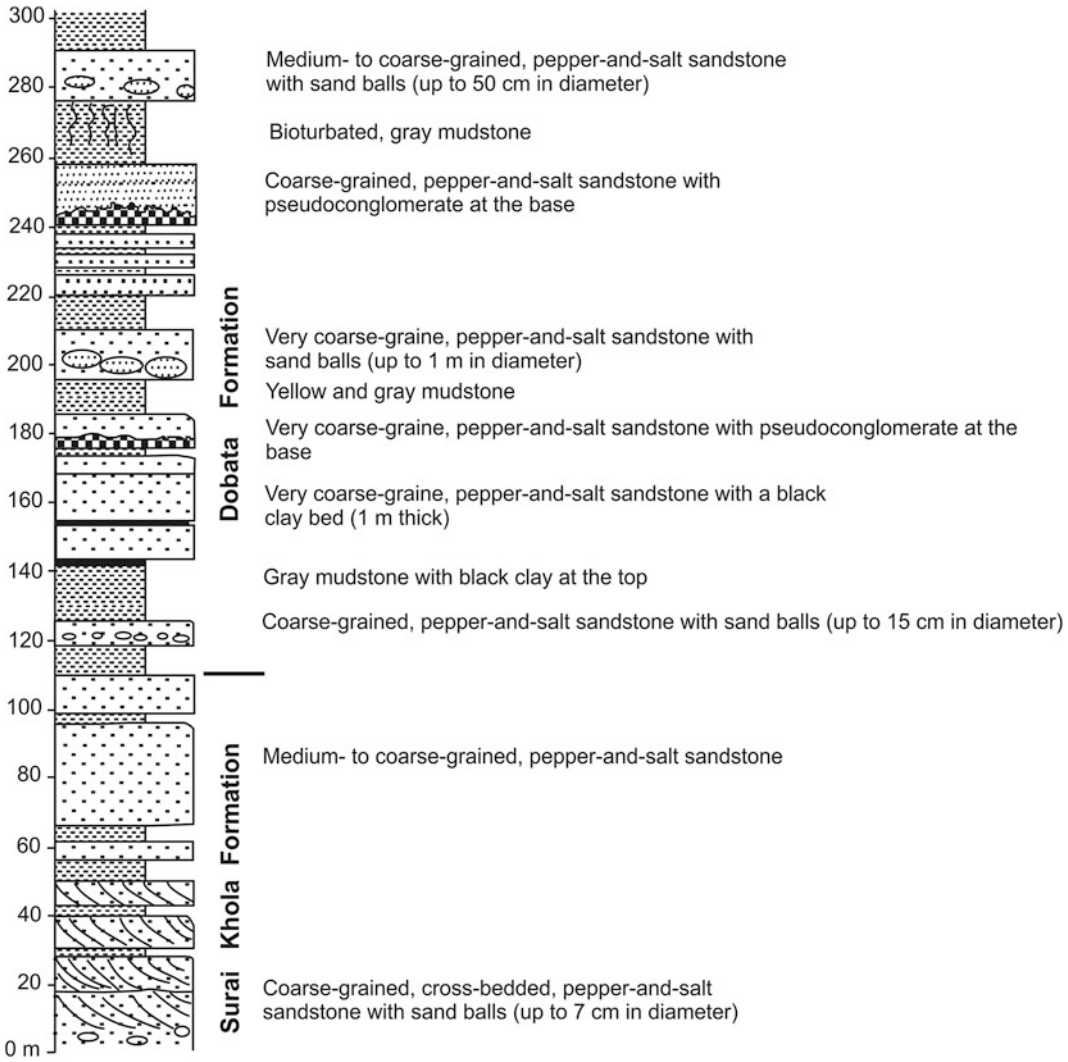

Fig. 29.10 Detailed columnar section at Dobata, showing the contact between the Surai Khola Formation and the Dobata Formation. Notice the large sandballs and pseudo-conglomerate beds in the Dobata Formation. *Source* Modified from Dhital et al. (1995). © Central Department of Geology, Tribhuvan University. Used by permission

29.5 Dhan Khola Formation

In its type section, the Dhan Khola Formation is composed of conglomerate (760 m, 70 %) as a predominating fraction (Figs. 29.5h and 29.13), mudstone (285 m, 27 %), and sandstone (35 m, 3 %). The cyclic deposition of the above three components can be broadly grouped into mud-dominant and conglomerate-dominant types.

The lower part of the Dhan Khola Formation comprises pebble-, cobble-, and infrequently boulder-bearing conglomerates, interbedded with yellow mudstones (Fig. 29.13). The conglomerate consisting of subrounded to well-rounded pebbles of quartzite, limestone, dolomite, volcanic rock, and sandstone, is moderately indurated and contains a matrix of coarse-grained calcareous sandstone. The volcanic pebbles, appearing first in the upper sections of the Dobata Formation, also continue in the lower 175 m of the Dhan Khola Formation. The horizons farther up include conglomerates dominated by cobbles of quartzite and sandstone. In the upper section, a few boulder-conglomerate beds occur together with sandy mudstones and pebbly sandstones (Fig. 29.13). The conglomerates are rather unconsolidated, have a soft mud matrix, and grade into the mudstone, resulting in a number of fining-upwards cycles. In the Dhan Khola section, the light yellow, gray, brown, and red mudstones of its middle part contain gastropod and pelecypod fossils.

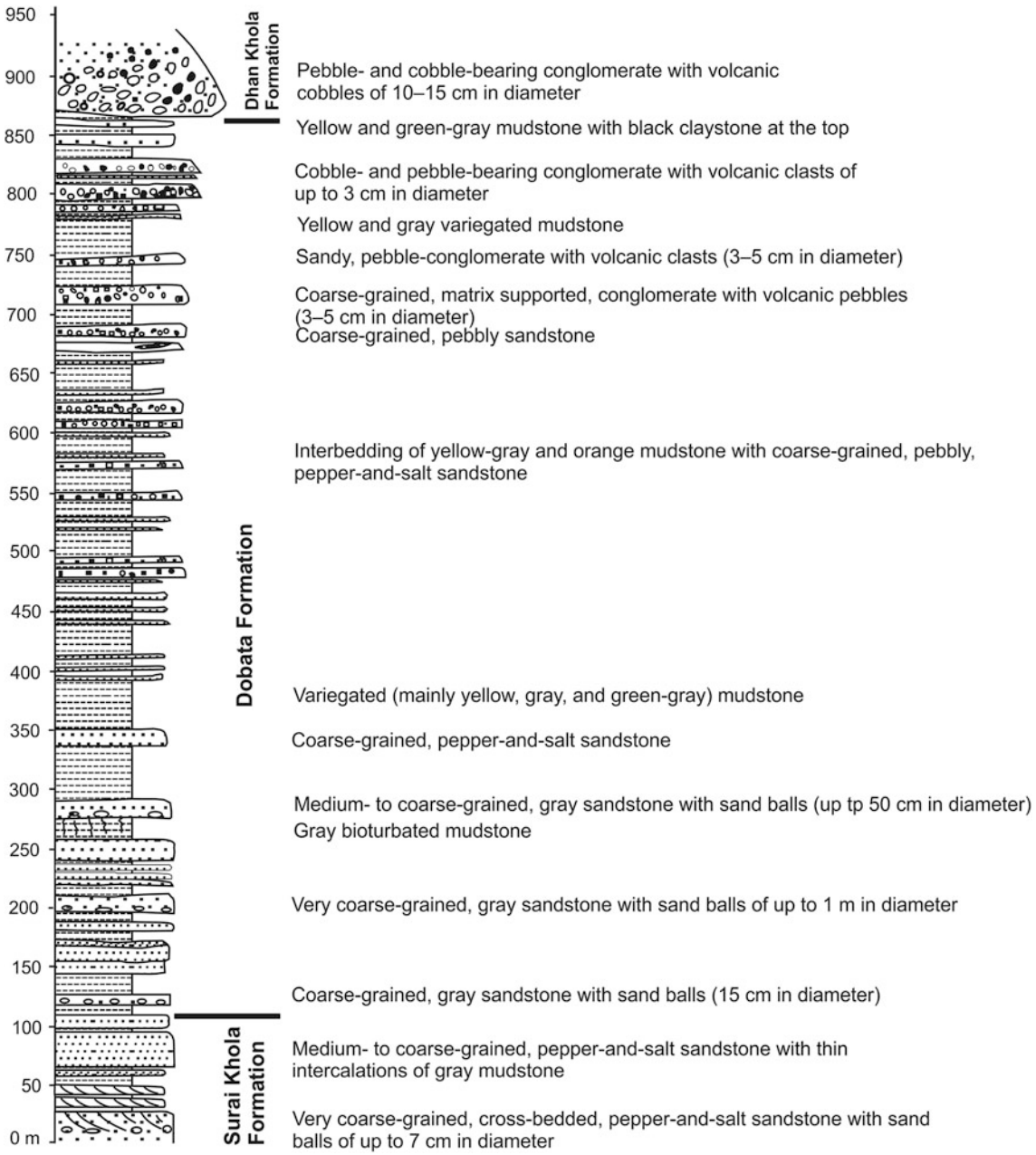

Fig. 29.11 Columnar section of the Dobata Formation prepared from the route map along the East–West Highway. Notice the predominance of mudstone over the sandstone. *Source* Modified from Dhital et al. (1995). © Central Department of Geology, Tribhuvan University. Used by permission

In the Sit Khola, the cobble- and boulder-conglomerates are composed of gray-green sandstone and light yellow to white quartzite clasts, whereas in the Ganaha Khola, the clasts are of sandstone, quartzite, slate, and dolomite.

In the Dhan Khola section, this formation is more than 1,100 m thick. In the south belt, the Dhan Khola Formation is delimited on the east by the Rangsing Thrust, whereas in the Darbhan–Bangesal–Sit Khola area, it is interrupted by the Sit Khola Thrust (Fig. 29.2).

29.6 Petrography of Sandstones

The grain size of the Siwalik sandstones steadily increases from the Bankas Formation at the base to the Surai Khola Formation, and the sandstones are followed by conglomerates in the Dhan Khola Formation. The sandstones are fine- to very fine-grained in the lower part, and successively become coarse- to very coarse-grained (with scattered

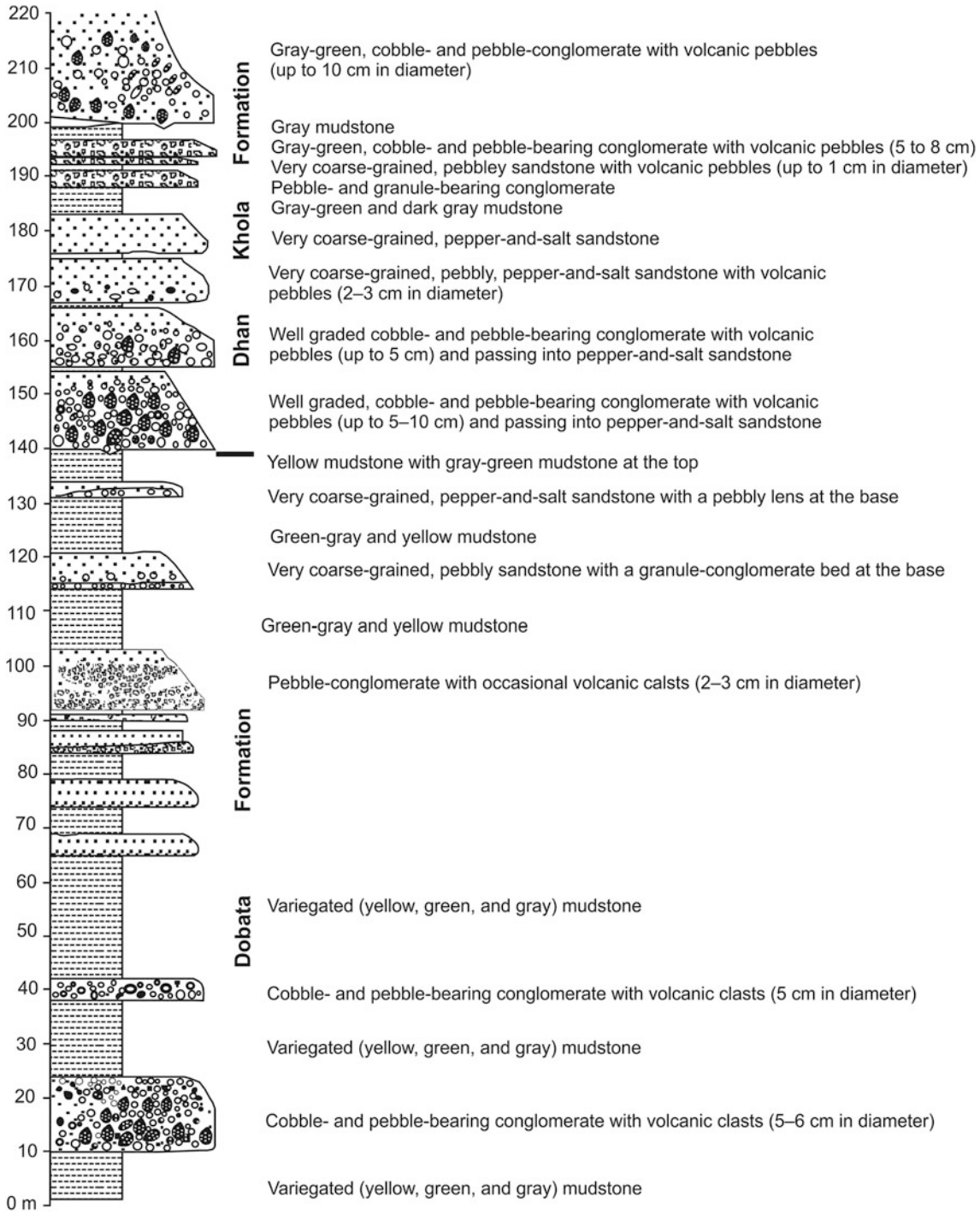

Fig. 29.12 Detailed columnar section depicting the contact between the Dobata Formation and the overlying Dhan Khola Formation at the Dhan Khola bridge. Notice the abundant volcanic pebbles in the sandstone and conglomerate beds. *Source* Modified from Dhital et al. (1995). © Central Department of Geology, Tribhuvan University. Used by permission

pebbles and conglomerate lenses) in the upper part. They contain a considerable amount of matrix, which reaches up to 40 % of the rock volume.

The sandstones belong primarily to lithic graywackes, litharenites, and feldspathic litharenites (Fig. 29.14). The litharenites and sublitharenites are predominant in the

Fig. 29.13 Columnar section of the Dhan Khola Formation prepared from the route maps along the Dhan Khola and the East–West Highway. Notice the considerable amount of mudstone in the middle part of the Dhan Khola Formation. *Source* Modified from Dhital et al. (1995). © Central Department of Geology, Tribhuvan University. Used by permission

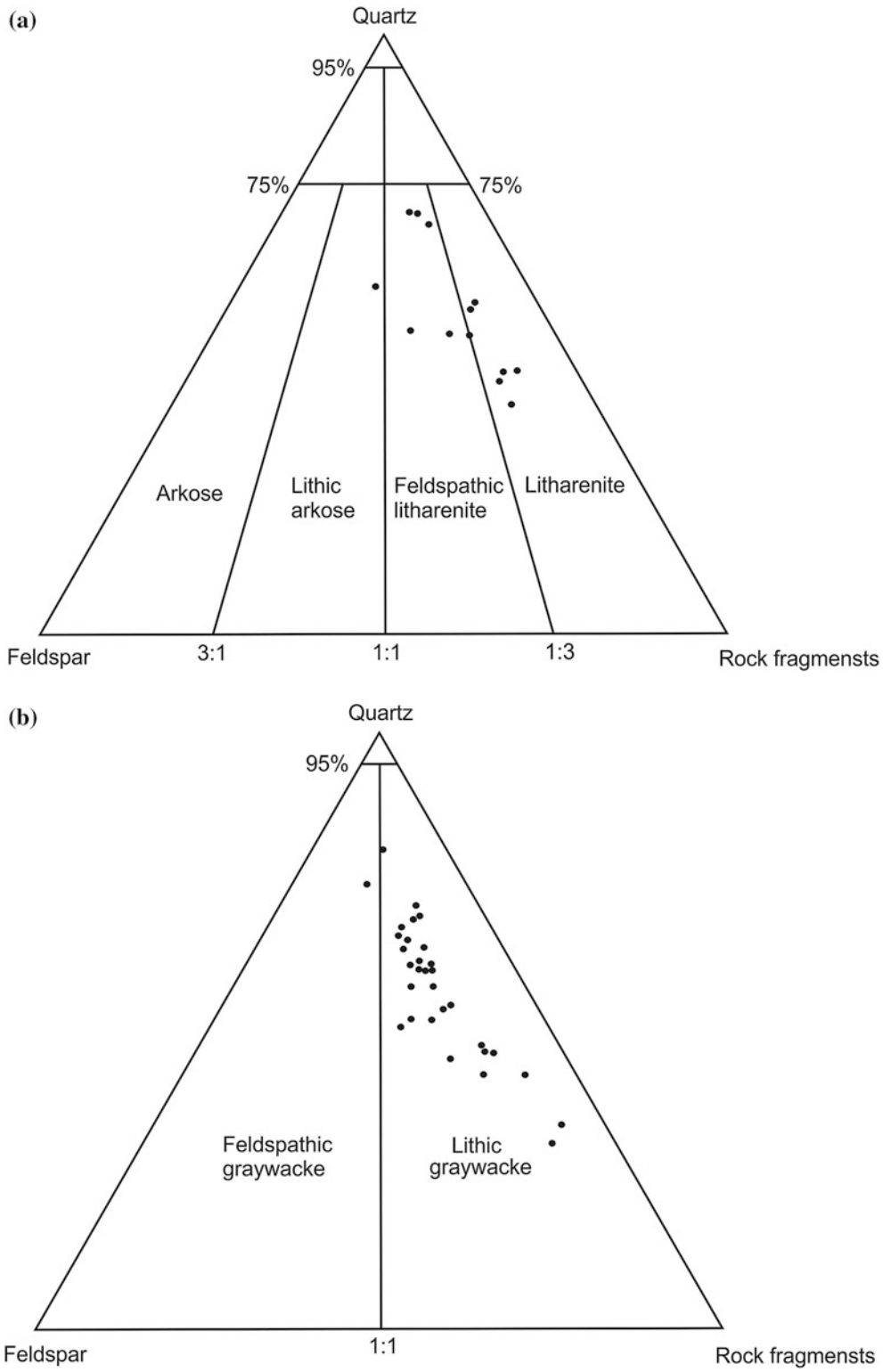

Fig. 29.14 The quartz–feldspar–rock fragment diagrams of sandstones from the Surai Khola area. **a** Arenites, **b** graywackes. *Source* Modified from Dhital et al. (1995)

Bankas Formation, and subordinately occur in the Chor Khola Formation. The prodigiously occurring pepper-and-salt sandstones of the Surai Khola Formation belong to feldspathic litharenites and lithic graywackes (Fig. 29.14). They are also noteworthy for a high biotite content (up to 20 %). Because the detrital grains of litharenites are cemented by calcite, they exhibit a mosaic texture.

Sparry calcite is the predominating cement that occupies from less than 10 % to about 45 % of the total rock volume. Subrounded to subangular grains of quartz, feldspar, and rock fragments are poorly sorted. The sandstones also include the rock fragments of phyllite, quartzite, schist, gneiss, and slate. Often, mica flakes are deformed and bent at the contact with the resistant detrital grains.

The lithic graywackes (Fig. 29.14a) are calcareous in nature, and closely resemble the arenites in composition (Fig. 29.14b). The matrix in the graywackes varies from 15 to 40 %. The rock fragment content in the sandstones increases gradually from the Bankas Formation to the Surai Khola Formation (Fig. 29.15).

29.7 Structures

The rocks of the Surai Khola area are strongly deformed, and many folds and imbricate faults are developed (Fig. 29.16). In the Siwaliks, three imbricate faults (i.e., the Rangsing Thrust, Siling Khola Backthrust, and the Sit Khola Thrust) are seen between the Botechaur Thrust alias Main Boundary Thrust to the north and the Koilabas Thrust alias Main Frontal Thrust to the south. There are also several imbricate faults in the Lesser Himalaya. The imbricate faults extend for tens of kilometers and join with each other, forming a branch line. Most of the imbricate slices of the Lesser Himalaya show eroded trailing branch lines. It is inferred that the imbricates have a common sole thrust at a depth of

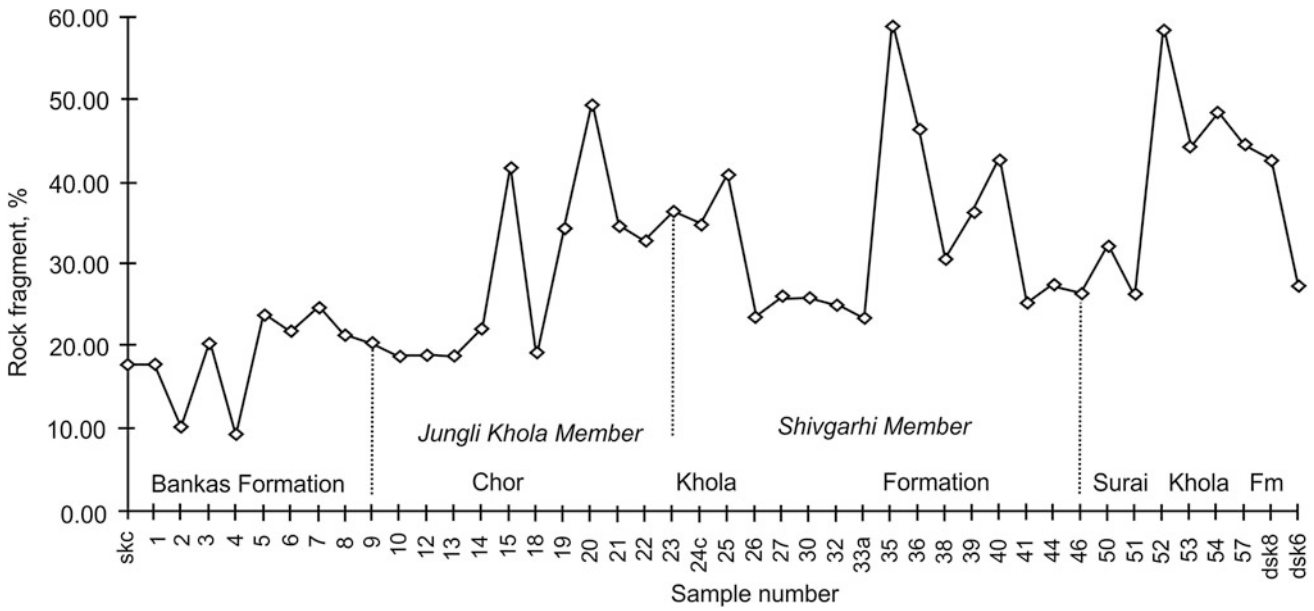

Fig. 29.15 Diagram showing the rock fragment content in the sandstones of the Surai Khola area. *Source* Modified from Dhital et al. (1995)

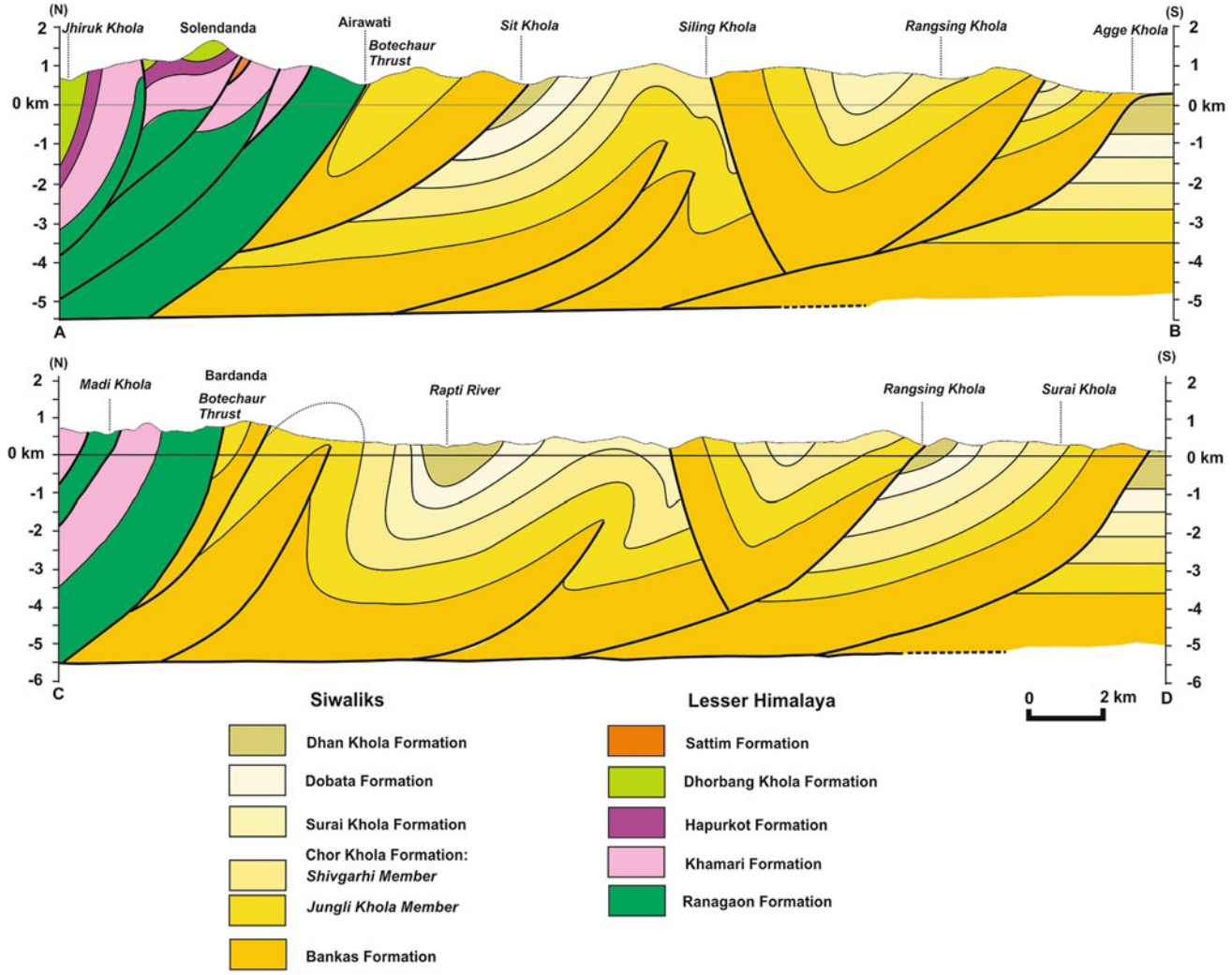

Fig. 29.16 Geological cross-sections of the Surai Khola area. The section lines are shown in Fig. 29.2. *Source* Modified from Dhital et al. (1995)

about 6 km. The Pankuri–Nangal–Kusum Khola Syncline is a pop-up block, uplifted by the Siling Khola Backthrust from the north and the Rangsing Thrust from the south.

References

Corvinus G (1988) The Mio-Plio-Pleistocene litho- and biostratigraphy of the Surai Khola Siwaliks in West Nepal: first results. C R Acad Sci Paris 306(2):1471–1477

Corvinus G (1993) The Siwalik group of sediments at Surai Khola in Western Nepal and its palaeontological record. J Nepal Geol Soc 9:21–35

Dhital MR, Gajurel AP, Pathak D, Paudel LP, Kizaki K (1995) Geology and structure of the Siwaliks and Lesser Himalaya in the Surai Khola–Bardanda area, Mid Western Nepal. Bull Dept Geol 4:1–70 (Tribhuvan University, Kathmandu)

Kayastha NB, Pradhan UMS, Shrestha RB, KC S, Subedi DN, Sharma SR (1999) Geological map of Exploration Block—3, Nepalganj, Mid-Western Nepal (Scale: 1:250,000). Petroleum Exploration Promotion Project, Department of Mines and Geology, Kathmandu

Powell JW (1876) Report on the geology of the eastern portion of the Uinta Mountains, USA. Geologic and Geographic Survey Terry (Powell), Washington DC, 218 pp

Pradhan UMS, Shrestha RB, KC S, Subedi DN, Sharma SR (2000) Geological map of Exploration Block—4, Lumbini, Mid-Western Nepal (Scale: 1:250,000). Petroleum Exploration Promotion Project, Department of Mines and Geology, Kathmandu

Pradhan UMS, Shrestha RB, Subedi DN, KC SB, Sharma SR (2003) Geological map of Petroleum Exploration block—2, Karnali, Far Western Nepal (Scale: 1:250,000). Petroleum Exploration Promotion Project, Department of Mines and Geology, Kathmandu

Siwaliks of Gandaki Region

30

Crude classification and false generalisations are the curse of organised life.

—H.G. Wells

The folds and faults, so prolific in the Karnali–Bheri region, abruptly disappear and a rather simple Siwalik homocline extends in the Gandaki region. Although the Siwaliks of this expanse (Fig. 30.1) form two essentially north–south trending, parallel and contiguous belts, before reaching the Narayani River the outer belt diverges to the southeast, giving way to the Chitwan intermontane basin between them.

Tokuoka et al. (1986, 1988) mapped the Siwaliks stretching between the rivers Arung Khola and Tinau Khola. For the first time in Nepal, they integrated lithology, petrography, sedimentology, paleontology, and magnetostratigraphy to investigate the Siwaliks of this tract. They included these rocks under the Churia Group, which attains a thickness of about 6,000 m. This group is bounded by the Narayani Thrust alias Main Boundary Thrust to the north and Frontal Churia Thrust to the south, whereas Central Churia Thrust separates the area into the north and south belts (Fig. 30.2). There are relatively older rocks in the north belt, as confirmed by paleomagnetic dating. The Churia Group is divided up, lithostratigraphically, into the following four formations, in ascending order, respectively (Fig. 30.3).

30.1 Arung Khola Formation

The Arung Khola Formation is the lowermost unit of the Churia Group. It is further subdivided into the lower, middle, and upper members (Tokuoka et al. 1986). In the north belt, the Arung Khola Formation is extensively exposed in the middle and upper reaches of the Arung Khola (Fig. 30.2). In the lower reach of the Arung Khola, the Lower Member of the Arung Khola Formation (Fig. 30.3) consists predominantly of mudstones with a subordinate quantity of sandstones. The sandstone beds range in thickness from 10 to 50 cm, and the mudstones are 50–100 cm thick. The mudstones are frequently variegated with red and purple tints. In the sandstones, current ripple laminae and planar cross-bedding are widespread. The Middle Member comprises 20–50 cm thick sandstone and mudstone beds in almost equal proportions. They form typical fining-upwards fluvial cycles (Fig. 30.4). The upper half of such cycles is generally from several meters to 10 m thick, and contains black mudstone with plant remains, variegated mudstone, and, in some cases, coal seams, in ascending order (Tokuoka et al. 1986). There are also some composite sequences, made up of two to several sandstone beds. In the Middle Member, fine calcareous sandstones are frequently intercalated, and they form prominent ridges. The Upper Member of the Arung Khola Formation is made up mainly of sandstones with subordinate mudstones, which are sometimes variegated. From 1 to 2 m thick sandstones are sporadically conglomeratic. Some pepper-and-salt sandstones are also intercalated in the Upper Member of this formation (Tokuoka et al. 1986). In the east part of the north belt, the Arung Khola Formation is about 2,100 m thick, whereas to the west it is just 800 m. This discrepancy in thickness is attributed to the slightly obliquely cutting hanging wall ramp of the Central Churia Thrust (Figs. 30.2 and 30.3).

In the south belt, the Frontal Churia Thrust has truncated the Lower and Middle members of the Arung Khola Formation. The Upper Member of this formation is well exposed on the highway, crossing the Churia Hills, where it comprises sandstones and mudstones in roughly equal amounts. As compared with the same member in the north belt, pebble-bearing sandstones are lacking in the south belt (Tokuoka et al. 1986). In the Upper Member of both belts, mudstones are frequently variegated. There also occur fining-upwards sequences passing from large-scale trough or planar cross-bedded sandstones to variegated mudstones.

From the Arung Khola area, Tokuoka et al. (1986) recovered fragmented vertebrate bones and molluscs from two horizons, lying in the lower part of the Upper Member (Fig. 30.3). In as much as Tokuoka et al. (1988) also discovered many molluscs from a bed underlying the *Sivapithecus*-bearing horizon (Munthe et al. 1983; Chap. 27) in the

M.R. Dhital, *Geology of the Nepal Himalaya*, Regional Geology Reviews,
DOI 10.1007/978-3-319-02496-7_30

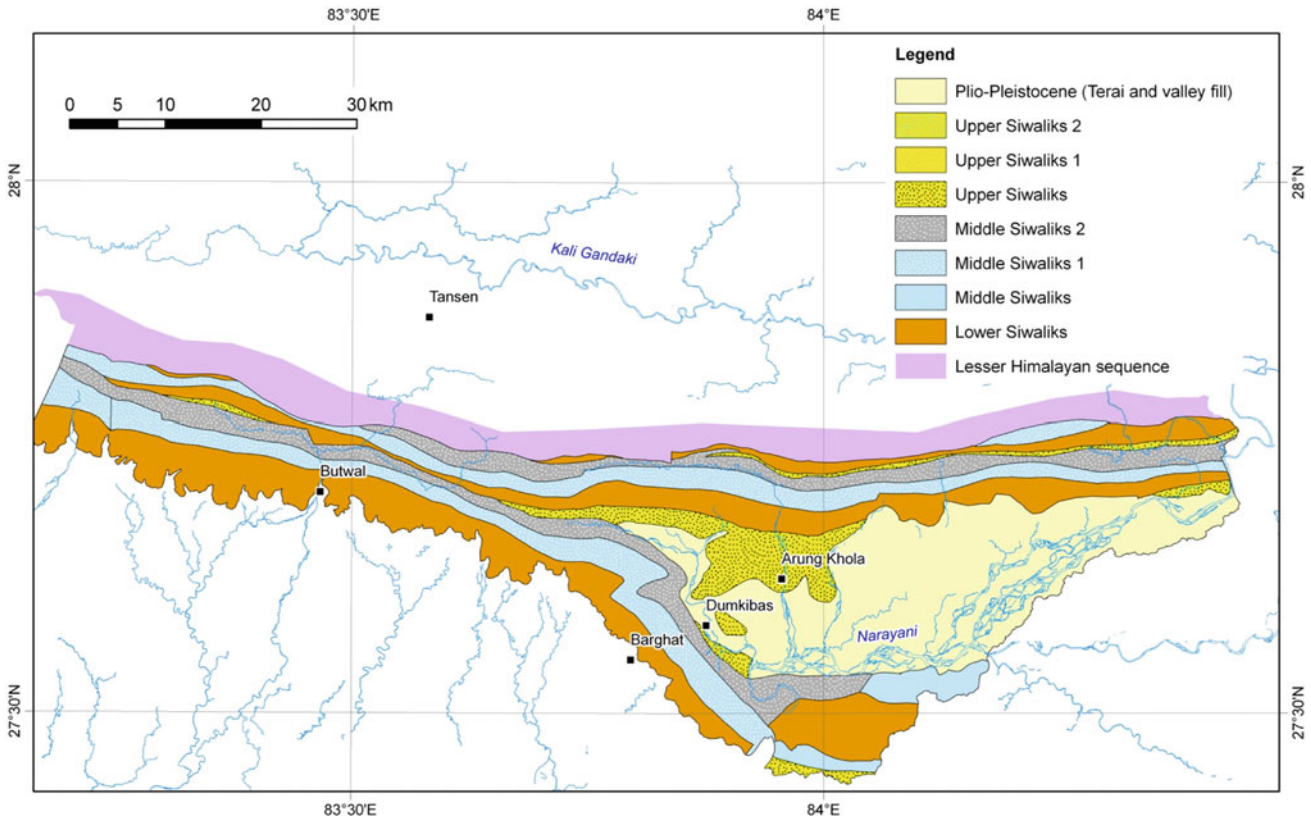

Fig. 30.1 Geological map of the Siwaliks in the Gandaki region. *Source* Modified from Shakya et al. (1998)

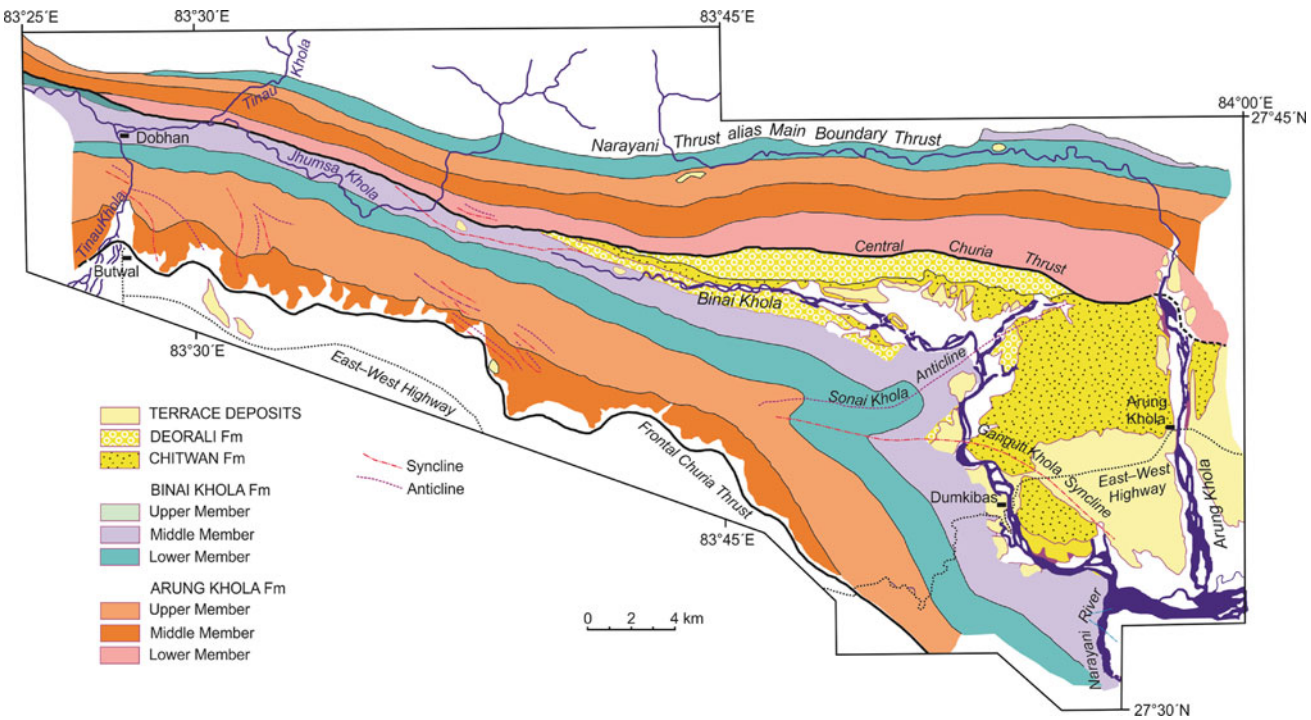

Fig. 30.2 Generalized geological map of the Churia Group of rocks from the Arung Khola–Tinau Khola area. *Source* Modified from Tokuoka et al. (1986, 1988, 1990)

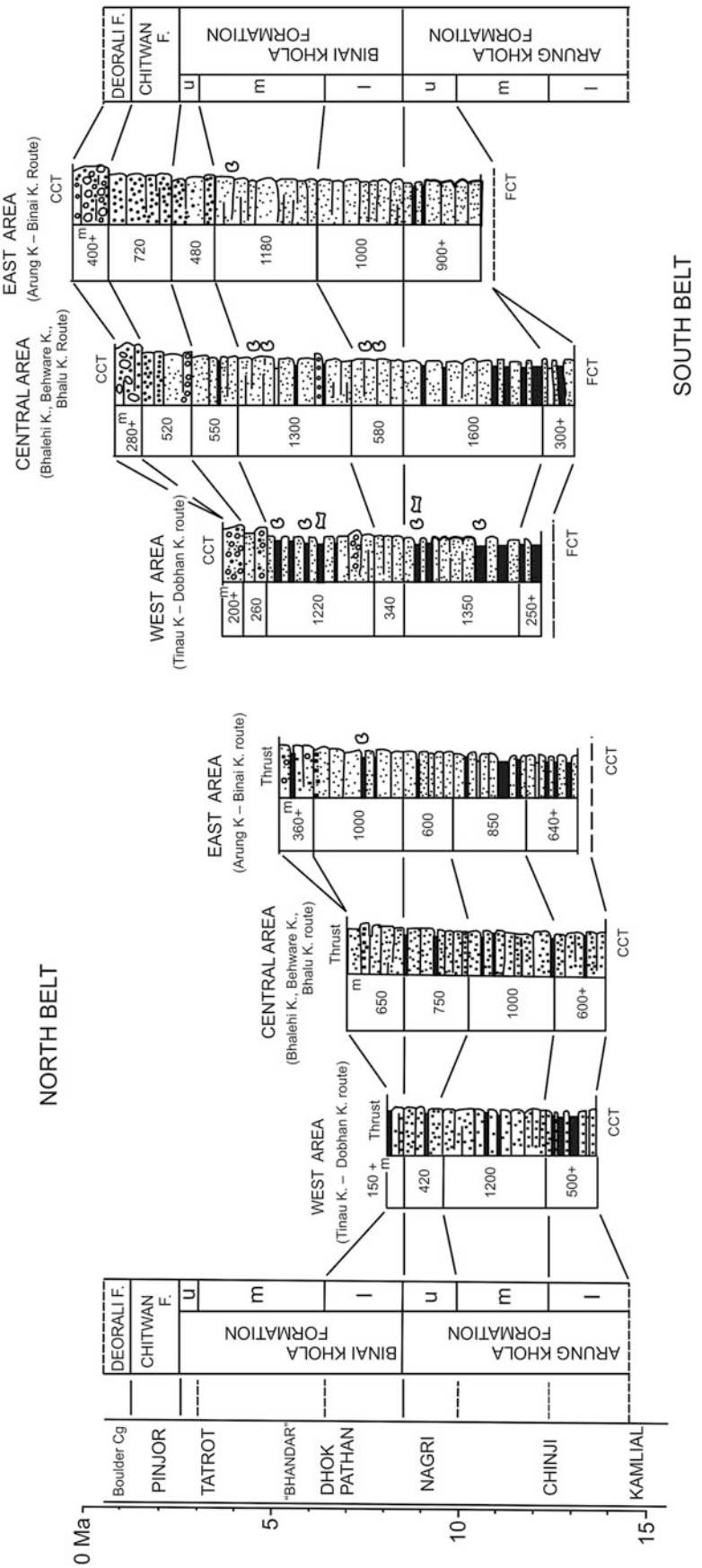

Fig. 30.3 Generalized stratigraphic columns of the Churia Group of rocks from the Arung Khola and Tinau Khola areas. *Source* Tokuoka (1992). © Central Department of Geology, Tribhuvan University. Used by permission

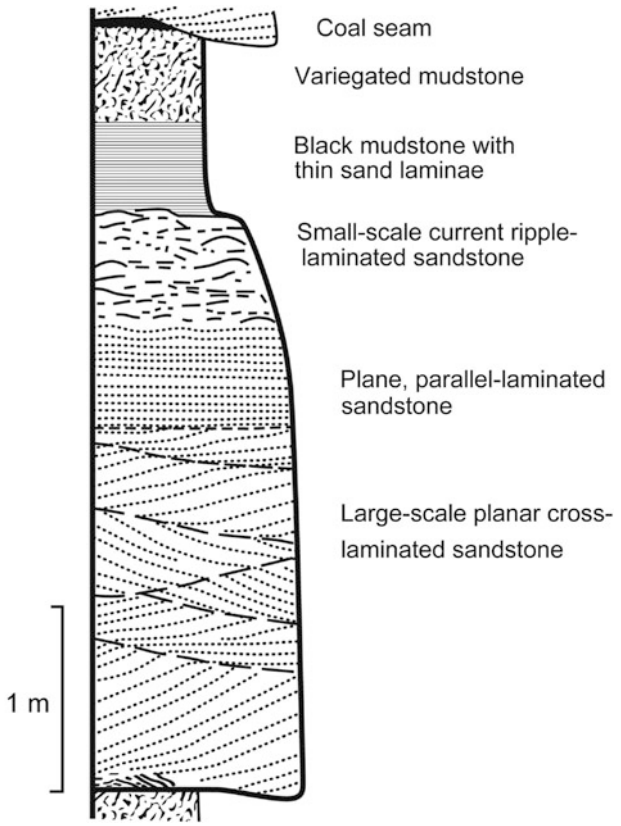

Fig. 30.4 A typical fining-upwards sequence observed in the Middle Member of the Arung Khola Formation in the Arun Khola. *Source* Modified from Tokuoka et al. (1986). © T Tokuoka. Used by permission

Tinau Khola of west Nepal, they are of the opinion that these horizons are homotaxial with each other. The Arung Khola Formation (i.e., its Upper Member) is about 1,000 m thick in the south belt, whereas farther west in the Binai Khola, its exposed middle and upper members measure about 2,100 m.

30.2 Binai Khola Formation

This formation is also subdivided into the lower, middle, and upper members. It crops out mainly in the Binai Khola and its tributaries. In the north belt, The Binai Khola Formation contains very thick-bedded sandstones with frequent conglomerate intercalations. The contact between the Arung Khola Formation and the overlying Binai Khola Formation is a gradual transition, as conspicuously exposed in the Arung Khola section (Tokuoka et al. 1986).

In the north belt, the Lower Member of the Binai Khola Formation is made up of several-meter-thick pepper-and-salt sandstones, which are sometimes pebble-bearing and are interbedded with subordinate siltstones. There are also sporadic beds of calcareous sandstone and sandy limestone. Pebbly sandstones are from 0.5 to 2 m thick and mostly planar cross-bedded (0.5–2 m thick sets), and comprise thick composite sand bodies (Fig. 30.5), as observed in the Murali Khola (Tokuoka et al. 1986). Most of the sandstone beds exhibit conspicuous current ripple laminae and cross-bedding. Tokuoka et al. (1986) also discovered various molluscs from this Member. The Middle Member of the Binai Khola Formation has a limited distribution in the north belt (Fig. 30.2). It is confined mainly to the Murali Khola and the Dang Khola areas in the northeast. It is characterized by pebbly, pepper-and-salt sandstones and conglomerates. There are also infrequent siltstone intercalations of a few meters in thickness. The Binai Khola Formation is about 1,360 m thick in the north belt, and its upper part is truncated by the Central Churia Thrust (Fig. 30.3).

The Binai Khola Formation is well exposed in the south belt, especially in the Binai Khola. In this belt, it forms a syncline and an anticline. This formation is composed mainly of interbedded sandstones and siltstones, and its main feature is the frequent intercalation of pepper-and-salt sandstones. The sandstones become thicker and coarser, giving way to conglomerates towards the top, comprising an overall coarsening-upwards sequence (Tokuoka et al. 1986). The Binai Khola Formation is composed of relatively finer material in the south belt, as compared to that of the north belt. Conglomerates are rather infrequent in the Lower and Middle members. The Lower Member of the Binai Khola Formation is rhythmically bedded in the Deorali area and consists mainly of sandstones with a subordinate amount of mudstone. The prominent sandstone beds are up to several meters thick and form conspicuous cuestas (Tokuoka et al. 1986). Cuestas are also observed in the Middle Member of the Binai Khola Formation, which is made up essentially of very thick (up to several meters) sandstone beds with some conglomerate intercalations. The percentage of conglomerates increases farther up-section in the Upper Member of the Binai Khola Formation, where they constitute beds ranging in thickness from 5 to 25 m. These beds exhibit large-scale planar cross-bedding with scoured lower surfaces (Tokuoka et al. 1986).

In other words, the Binai Khola Formation taken as a whole, represents a coarsening-upwards sequence, although it is made up of numerous individual fining-upwards cycles of a few meters to several tens of meters thickness. The coarse-grained lower half of these cycles is characterized by the presence of some truncated surfaces, followed by two or more sandstone beds (Fig. 30.5), unlike the Arung Khola Formation in which the fining-upwards sequences contain a single sandstone bed (Tokuoka et al. 1986). In the Upper Member of the Binai Khola, many mudstone lumps (from 30 to 100 cm in diameter) are found along a basal scoured surface of each cycle, which is frequently more than 20 m thick.

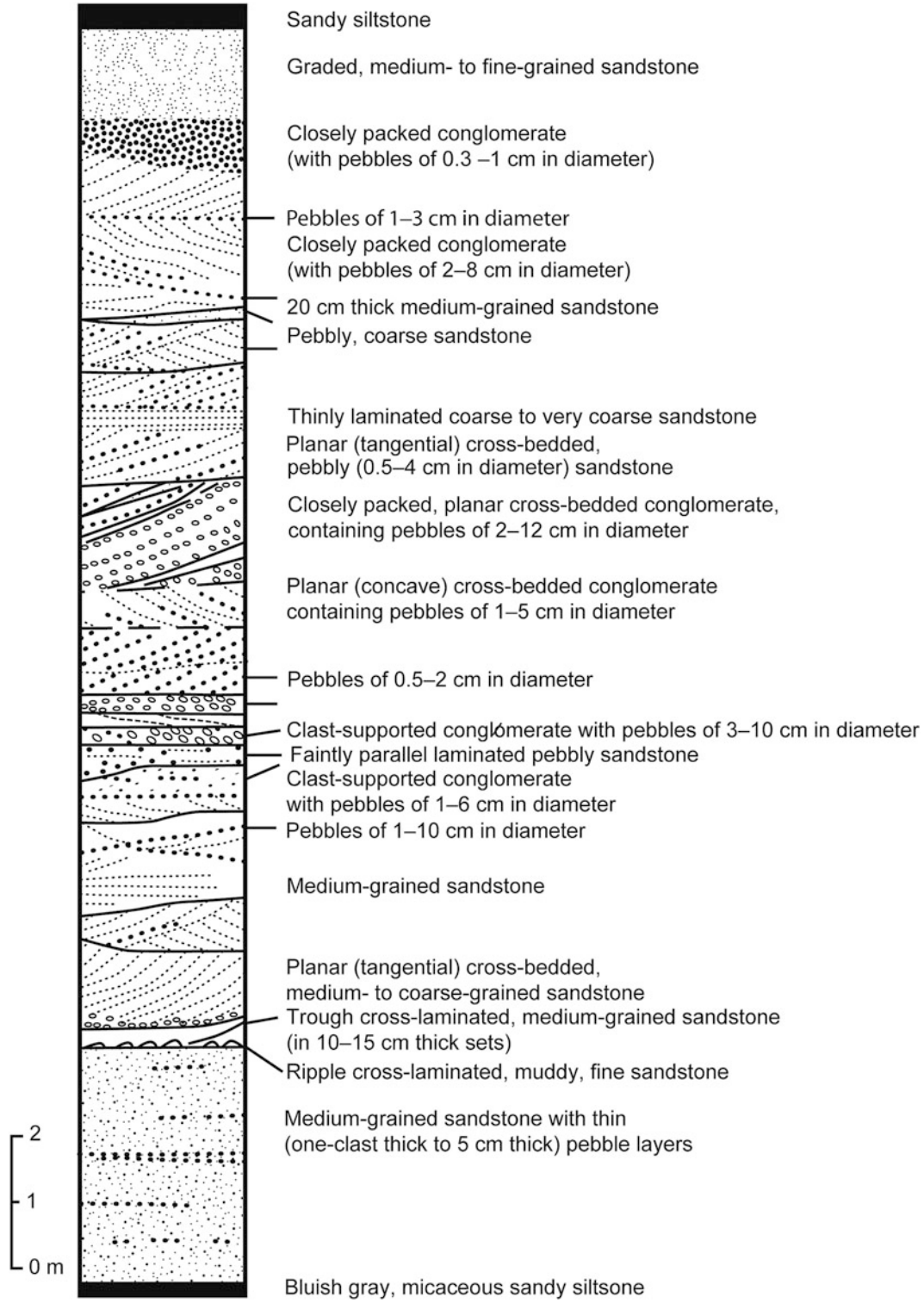

Fig. 30.5 A fining-upwards sequence consisting of composite cross-bedded sandstones. Lower Member of the Binai Khola Formation in the Murali Khola. *Source* Modified from Tokuoka et al. (1986). © T Tokuoka. Used by permission

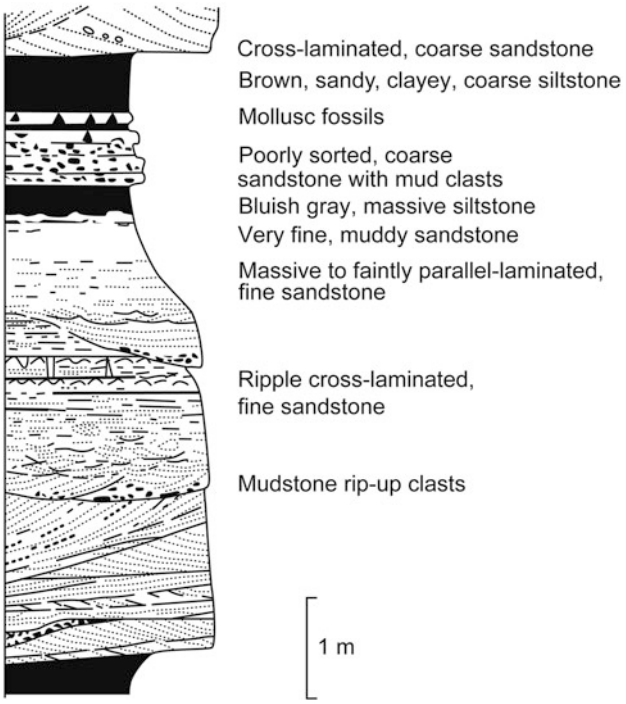

Fig. 30.6 A typical fining-upwards sequence of the Middle Member of the Binai Khola Formation in the Binai Khola. *Source* Modified from Tokuoka et al. (1986). © T Tokuoka. Used by permission

The lower portion of the cycle also contains from 1 to 3 m thick beds of planar cross-bedded pebbly sandstones, which pass up-section into a trough cross-laminated sandstone sequence, grading into the topmost zone of black mudstone (Fig. 30.6). The total thickness of the Binai Khola Formation in the south belt is about 2,800 m, and it transitionally passes into the overlying Chitwan Formation. The Binai Khola Formation is about 2,300 m thick in the western part of the map area (Tokuoka et al. 1988).

30.3 Chitwan Formation

The Chitwan Formation crops out only in the south belt (Fig. 30.2) in the Chitwan Valley. It comprises mainly semi-consolidated conglomerates, some gravel-bearing sandstones, and thin beds of siltstone (Tokuoka et al. 1986). The lower part of the Chitwan Formation contains pebble- to cobble-bearing gravel, gradually passing into the cobble- and boulder-bearing gravel in the upper part. The gravel is made up exclusive of rounded quartzite clasts. A calcareous hardground (marker horizon) is found in the middle part of the Chitwan Formation. The hardground contains many limestone clasts in a calcareous matrix. This horizon is resistant to weathering and traceable for a long distance (Tokuoka et al. 1986). The Chitwan Formation is about 700 m thick (Fig. 30.3) and transitionally passes into the overlying Deorali Formation. The Chitwan Formation is about 360 m thick in the western part of the Binai Khola (Tokuoka et al. 1988).

30.4 Deorali Formation

This formation is distributed only in the northern fringe of the south belt (Fig. 30.2). The Deorali Formation contains very thick beds of disorganized and matrix-supported gravel, in which angular to subangular boulders are predominant. Their bed thickness exceeds several tens of meters, and the boulders are frequently larger than several meters in diameter. A gradual change from the underlying Chitwan Formation is observed at a number of places. In the Deorali Formation, the boulders of quartzite (similar to those of the Chitwan Formation) and the boulders derived from the rocks of the Churia Group are observed in its lower 20 m. Farther up-section, the quartzite boulders disappear and give way to those derived from the Churia Group alone. The Deorali Formation is more than 450 m thick (Tokuoka et al. 1986, 1988).

30.5 Sandstone Petrography

The sandstones of the Churia Group belong mainly to lithic arenites or quartz arenites, and are cemented by calcite (Tokuoka et al. 1986). The sandstones from the Lower and Middle members of the Arung Khola Formation contain quartz (60–90 % of aggregate grains) and some rock fragments (4–30 %), and belong to quartz arenites. The second group of sandstones from the Upper Member of the Arung Khola Formation, and Lower and Middle members of the Binai Khola Formation are mainly lithic arenites, containing quartz (from 35 to 70 %) and rock fragments (12–50 %). The quartz arenites resemble the Lesser Himalayan sandstones in composition (Fig. 30.7), whereas the lithic arenites are characterized by the abundance of biotite, giving the "pepper" in sandstones (Fig. 30.8). The lithic fragments are represented by schistose, gneissic, and granitic rocks. Rarely, in the lithic arenites, grains of garnet, zircon, and kyanite are also found.

30.6 Paleocurrents

Sedimentary structures such as cross-bedding, sole marks, ripple marks, and imbricated pebbles of conglomerate were used to find the paleoflow direction in the Churia Group.

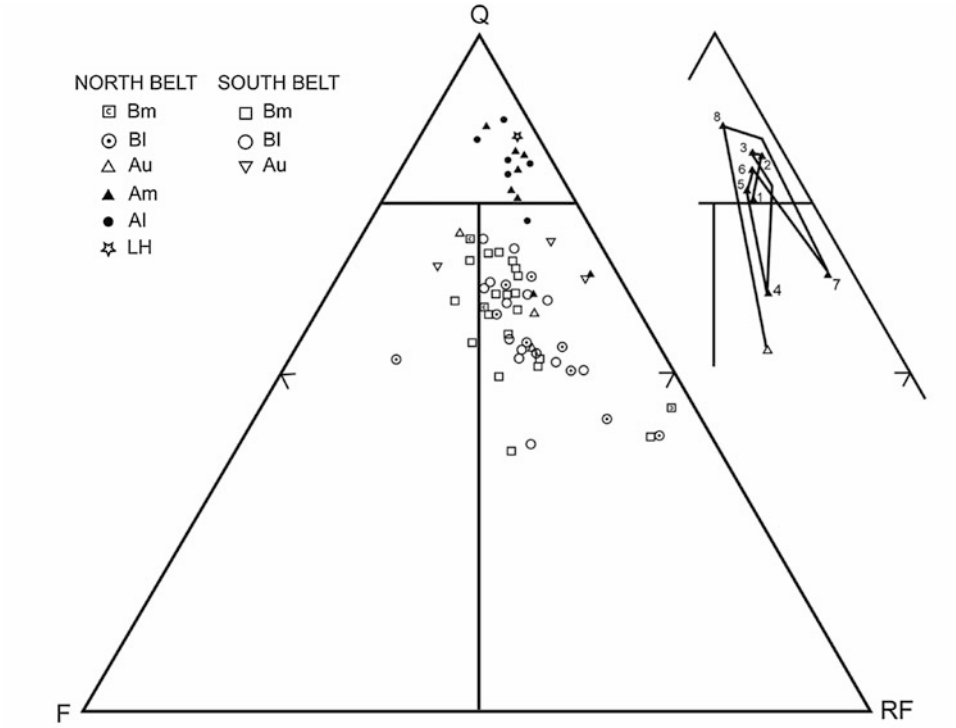

Q (quartz) – F (feldspars) – RF (rock fragments) diagram of sandstones from the Churia Group.
A star symbol indicates the quartize of the Lesser Himalaya. In the additional figure of upper right, successive compositional changes of Am sandstones in the north belt are traced from 1 to 8 in ascending order.
Al: Lower Member of the Arung Khola Fm, Am: Middle Member of the Arung Khola Fm, Au: Upper Member of the Arung Khola Fm, Bl: Lower Member of the Binai Khola Fm, Bm: Middle Member of the Binai Khola Fm, Bu: Upper Member of the Binai Khola Fm, C: Chitwan Fm, D: Deorali Fm, LH: Lesser Himalayan sequence

Fig. 30.7 Q–F–RF triangle showing the distribution of sandstones according to their composition. *Source* Modified from Tokuoka et al. (1986). © T Tokuoka. Used by permission

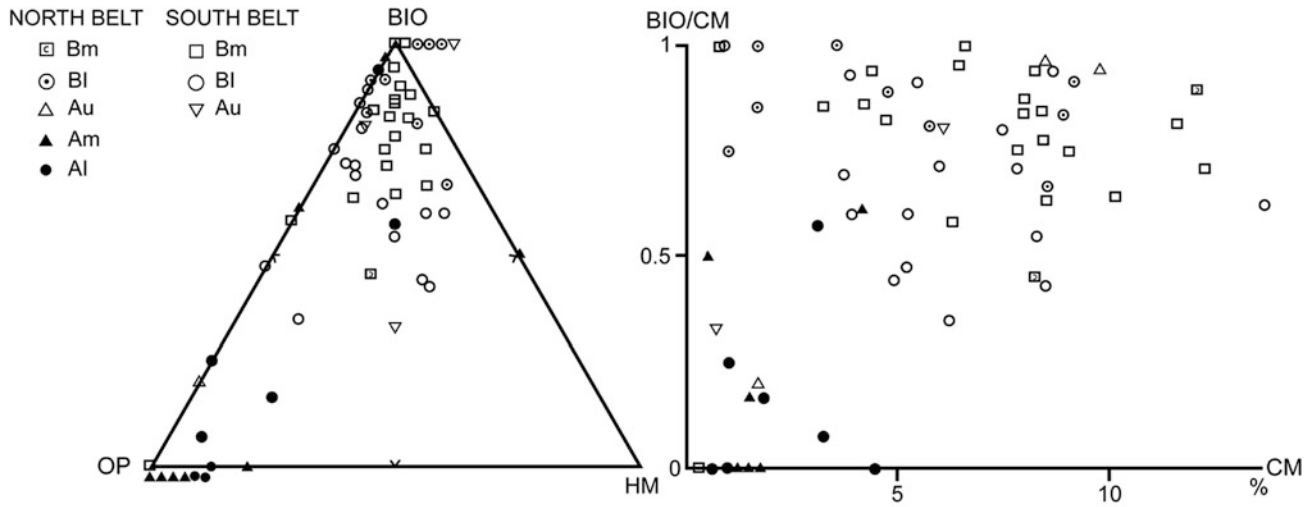

BIO (biotite) – OP (opaque minerals) – HM (heavy minerals) diagram (left) and a diagram (right) showing the relation between BIO/CM (biotite + opaques + heavy minerals) and CM
Al: Lower Member of the Arung Khola Fm, Am: Middle Member of the Arung Khola Fm, Au: Upper Member of the Arung Khola Fm, Bl: Lower Member of the Binai Khola Fm, Bm: Middle Member of the Binai Khola Fm, Bu: Upper Member of the Binai Khola Fm, C: Chitwan Fm, D: Deorali Fm

Fig. 30.8 Triangle diagram and plots of BIO–OP–HM. *Source* Modified from Tokuoka et al. (1986). © T Tokuoka. Used by permission

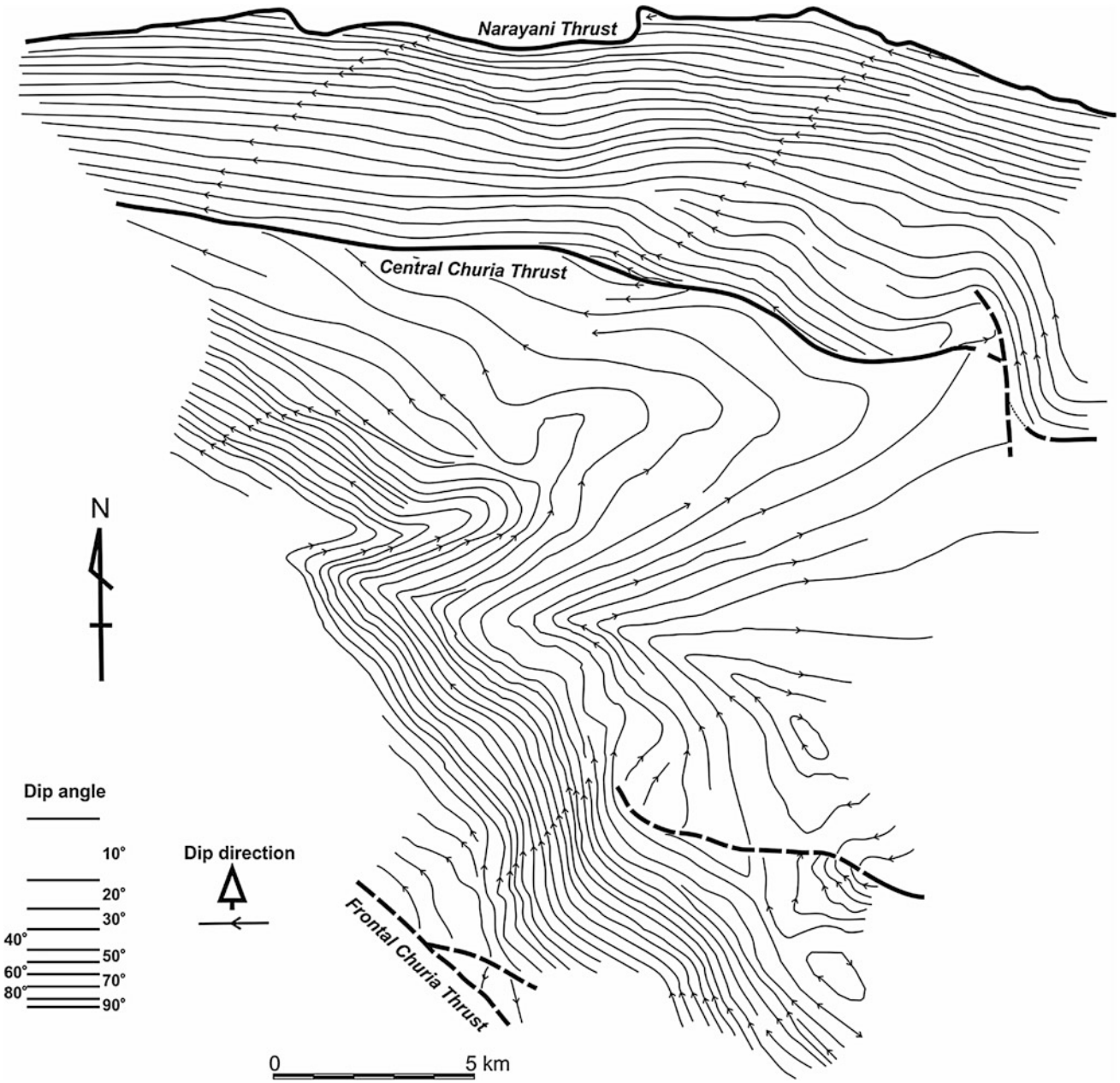

Fig. 30.9 Trend-line map of bedding in the Arung Khola area. *Source* Modified from Tokuoka et al. (1986). © T Tokuoka. Used by permission

The Arung Khola Formation was deposited mainly from northerly sources, whereas the Binai Khola Formation was derived predominantly from NNW to SSW. The paleocurrent direction in the conglomeratic Chitwan Formation fluctuated frequently. The Deorali Formation was basically a fault scarp deposit, derived from the north. In other words, the upheaval of the Midlands was responsible for the deposition of the sediments in the Siwaliks (Tokuoka et al. 1986).

30.7 Fossil Occurrence

Tokuoka et al. (1986) reported crocodile teeth, fish scales, and bone fragments from the Churia Group. Also, they found a very rich collection of molluscs. The molluscs are rich in bivalves and also include some gastropods. Most bivalves are found in a conjoined state, indicating their in situ origin.

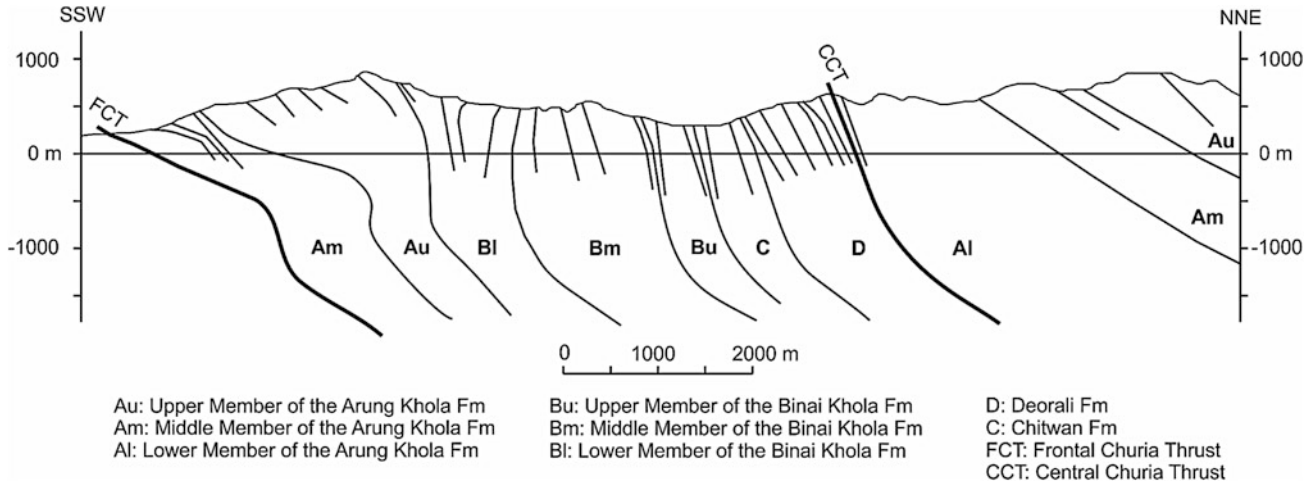

Fig. 30.10 Geological cross-section along the line M–N in Fig. 30.2. *Source* Aurthor's observations

30.8 Paleomagnetism and Regional Correlation

Based on detailed field mapping and paleomagnetic investigations, Tokuoka et al. (1986) have correlated the rocks of the Arung Khola and Tinau Khola with the Potwar Basin of Pakistan (Fig. 30.2; Chap. 27). The correlation was possible mainly owing to the presence of the long and continued normal magnetopolarity chron (C5). This chron was well documented from both the north and south belts. Tokuoka et al. (1986) also prepared an isopolarity zone map. Their paleomagnetic studies revealed that the Lower and Middle members of the Arung Khola Formation are homotaxial with the Chinji zone (Lower Siwaliks), the Upper Member of the Arung Khola Formation is equivalent to the Nagri zone (i.e., the lower half of the Middle Siwaliks), whereas the Binai Khola Formation is correlated with the Dhok Pathan zone (i.e., upper half of the Middle Siwaliks) and the Tatrot zone (i.e., lower half of the Upper Siwaliks), the Chitwan Formation is correlated with the Pinjor zone (i.e., upper half of the Upper Siwaliks), and the Deorali Formation with the Boulder Conglomerates, respectively. Hence, the Siwalik deposits are diachronous in nature. On the other hand, based on their paleomagnetic data, Tokuoka et al. (1986) also inferred a clockwise rotation of the south belt by about 20° with respect to the north belt. The paleolatitude of the Siwaliks ranged from 5° to 21° north, indicating that the terrane was situated about 500 km south of the present position. Their estimated sedimentation rates for the Siwaliks were 0.2–0.5 mm/a (Tokuoka et al. 1986). The sedimentation rate increased from the bottom to top of the Siwalik succession as well as from the north belt to the south belt.

30.9 Structure

The bedding trend line map of the Arung Khola area (Fig. 30.9) clearly depicts the structural differences between the two belts. The Narayani Thrust, Central Churia Thrust, and Frontal Churia Thrust are the imbricate faults (Fig. 30.10), which presumably are part of a single detachment, such as the Main Himalayan Thrust.

References

Munthe J, Dongol B, Hutchison JH, Kean WF, Munthe K, West RM (1983) New fossil discoveries from the Miocene of Nepal include a Hominoid. Nature 303(5915):331–333

Shakya TR, Pradhan UMS, Shrestha RB, Subedi DN, Sharma SR, KC SB (1998) Geological map of exploration block—5, Chitwan, Western Central Nepal (Scale: 1:250,000). Petroleum exploration promotion project, Department of Mines and Geology, Kathmandu

Tokuoka T, Takayasu K, Yoshida M, Hisatomi K (1986) The Churia (Siwalik) Group of the Arung Khola area, west central Nepal. Mem Fac Sci Shimane Univ Jpn 20:135–210 (with a geological map in colors, scale: 1 inch = 1 mile)

Tokuoka T, Takeda S, Yoshida M, Upreti BN (1988) The Churia (Siwalik) Group in the western part of the Arung Khola area, west central Nepal. Mem Fac Sci Shimane Univ Jpn 22:131–140

Tokuoka T, Takayasu K, Hisatomi K, Yamasaki H, Tanaka S, Konomatsu M, Sah RB, Rai SM (1990) Stratigraphy and geologic structures of the Churia (Siwalik) Group in the Tinau Khola-Binai Khola area, west central Nepal. Mem Fac Sci Shimane Univ 24:71–88

Tokuoka T (1992) The Churia (Siwalik) Group in west central Nepal. Bull Dept Geol Tribhuvan Univ Kathmandu 2(1):75–87

Siwaliks of Bagmati–Gosainkund Region 31

The ultimate check of cross sections in deformed terrane is whether or not the process can be reversed and the beds put back into their depositional position without introducing inexplicable bed length anomalies.
—C.D.A. Dahlstrom (1969, p. 753)

The Siwalik sequence constituting the foothill belt of the Bagmati–Gosainkund region recurs several times (Fig. 31.1) inasmuch as it is intensely folded and dislocated by many imbricate thrusts. A large portion of this tract is covered by the Upper Siwaliks and the late Pleistocene–Holocene alluvial deposits of the Narayani and Budhi Rapti Rivers. On the other hand, both the Lesser and Higher Himalayan successions override the inner Siwalik belt (Fig. 31.2), which also encloses a few Proterozoic slivers of the basement (Chap. 10). Lees (1952) described foreland folding from various mountain belts, including the Himalaya. He showed from many borehole data the examples of foreland folding and faulting with the basement involvement. The degree to which basement rocks have been faulted, folded, or flexed in some foreland zones is in marked contrast to more rigid behavior in others.

31.1 Lithostratigraphy

Notwithstanding the widely accepted threefold scheme, there have been various other propositions to classify the Siwaliks of this region. To address their lithological and sedimentological variables, Sah et al. (1994) divided the Siwaliks of the Hetaunda–Amlekhganj area into the Rapti Formation (Lower Siwaliks), Amlekhganj Formation (Middle Siwaliks), Churia Khola Formation (Upper Siwalik conglomerates), and the Churia Mai Formation (Upper Siwalik boulderbeds).

In the vicinity of Hetaunda and Amlekhganj, the Lower Siwaliks consist of a cyclic interbedding of variegated mudstone and green-gray to brown sandstone. The sandstones are generally medium- to fine-grained and indurated. They become more frequent towards the upper part. The lower end of the formation also includes many calcareous claystone or marl beds (Sah et al. 1994). Several paleosol horizons containing pseudo-conglomerates (calcretes) occur in red-purple and orange, mottled mudstones, appearing in the lower portion of the Lower Siwaliks. Frequently, the mottled mudstones are strongly bioturbated (Fig. 31.3).

In the inner belt, the Lower Siwaliks making up the hanging walls of the Kokhajor Thrust and the Bastipur Thrust are comprised of relatively soft, medium- to fine-grained, red-purple mudstones and sandstones. The sandstone and mudstone alternation ranges in thickness from a few meters to tens of meters. Generally, the transition from sandstone to mudstone is imperceptible, whereas the contact between the underlying mudstone and overlying sandstone is sharp as well as wavy to irregular.

The Middle Siwaliks exposed north of Hetaunda and Amlekhganj consist of 20–30 m thick cyclic alternations of very coarse- to coarse-grained pepper-and-salt colored sandstones passing into gray to dark gray mudstones. The relatively soft sandstones of the Middle Siwaliks of this area commonly show large trough cross-stratification (Fig. 31.4). Equally frequent are planar cross-laminae (Fig. 31.5). The Middle Siwaliks are relatively strong and form cuestas or hogbacks. The steeply south-dipping pepper-and-salt sandstones of the Middle Siwaliks near Amlekhganj are overturned. Near the upper part of the Middle Siwaliks, many sandballs (Fig. 31.6) are found. With the appearance of pebbly sandstones (Fig. 31.7) towards its top, the Middle Siwaliks grade into the overlying Upper Siwaliks.

The Middle Siwaliks cropping out north of the Samari Khola are composed of gray sandstone and dark gray mudstone interbeds. This succession also includes a few very thick (several meters) red-purple mudstone and gray sandstone beds. The sequence continues upwards with a few beds of very thick, light pink to gray, pebble-conglomerate (Fig. 31.8). Generally, such thick conglomerates are very rare in the Middle Siwaliks, but they do occur west of Surkhet, in the Karnali–Bheri region.

In the Kokhajor Khola, the pepper-and-salt sandstones consist of detrital muscovite, biotite, feldspar, and quartz. They are generally coarse- to very coarse-grained, moderately indurated, and relatively strong. The extremely thick (more

M.R. Dhital, *Geology of the Nepal Himalaya*, Regional Geology Reviews,
DOI 10.1007/978-3-319-02496-7_31

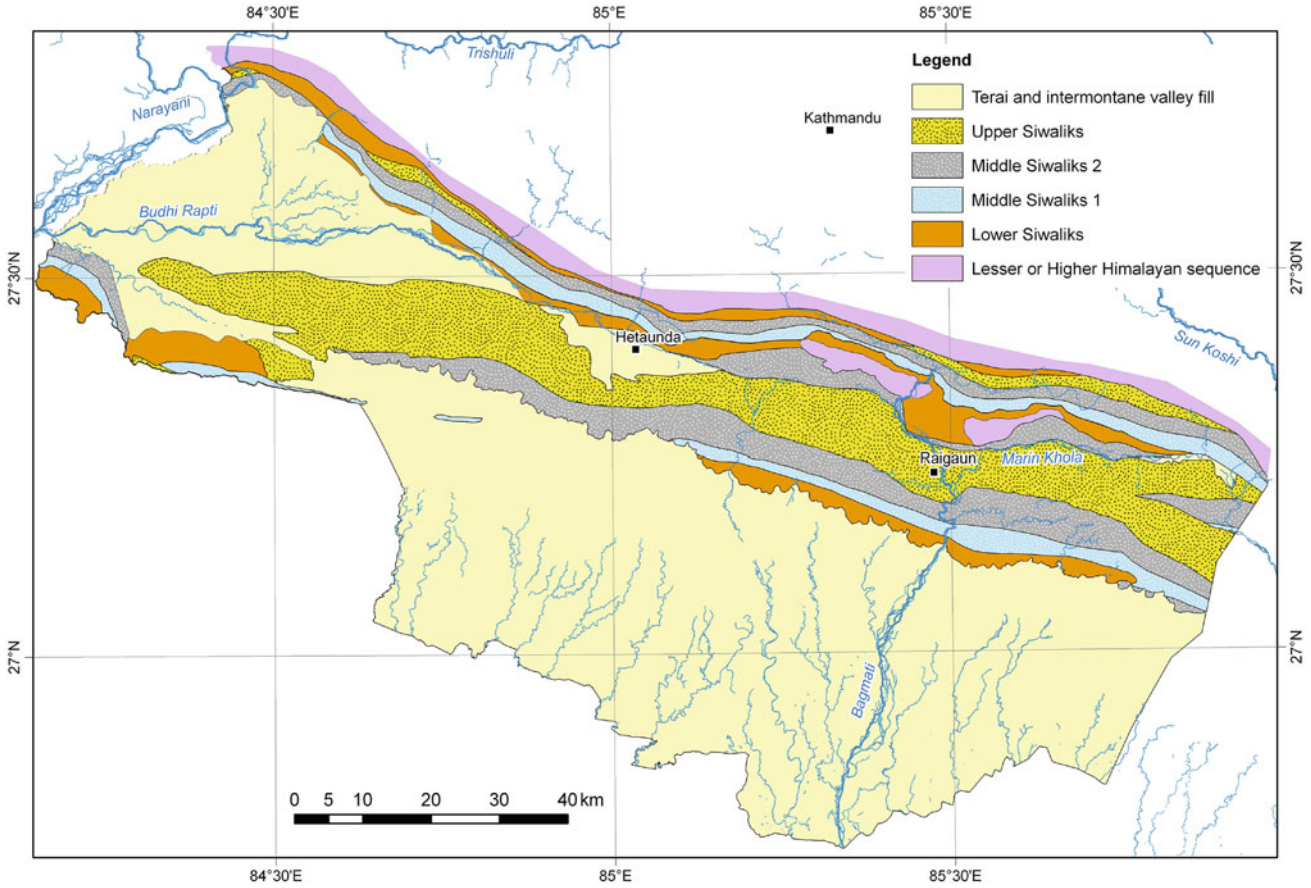

Fig. 31.1 Generalized geological map of the Siwaliks distributed in the Bagmati–Gosainkund region. *Source* Compiled from Pradhan et al. (2001, 2002) and author's observations

than 25 m) Middle Siwalik sandstones are cross-laminated, frequently pebbly, and sometimes calcareous. The multi-storied sandstone beds gradationally pass into soft mudstone strata.

In the Amlekhganj neighborhood, pebble-conglomerates of the Upper Siwaliks succeed the underlying Middle Siwaliks with a gradual transition. In the Upper Siwaliks also infrequently occur yellow-brown mudstone and siltstone. The conglomerates are sometimes cemented by calcite, especially towards the upper part, and they make hard-grounds. The pebble-conglomerates of the Upper Siwaliks grade into boulder-conglomerates interbedded with mud-stones or siltstones.

In the inner belt of the Kokhajor Khola, the Upper Siwaliks comprise mainly soft but sometimes well-cemented and hard (near Bhokteni), pebble-, cobble- to boulder-conglomerates interbedded mainly with pebbly sandstones. Although there are also subordinate mudstone beds, conglomerates and sandstones predominate over the mudstones. The Upper Siwaliks are gray, light yellow to brown in color and an individual conglomerate, sandstone, or mudstone bed ranges in thickness from 5 to 25 m and more. North of Bhokteni, there are extremely thick (2–10 m and more), gray, cobble- and pebble-conglomerates, which are strongly clast-supported and well cemented. The conglomerates are interbedded with 10–30 cm thick lenticular to very thick (1–2 m) beds of cross-laminated, coarse-grained, gray, calcareous sandstone. The conglomerate cliff on the right bank of the Kokhajor Khola is about 25 m high and extends for 100 m along the river course. The beds dip steeply (50–60°) due northeast. On the left bank, a gray sandstone is exposed. Farther downstream, very thick (5 m and more) pebble-conglomerates occur with thin (5–15 cm), gray, coarse sandstone lenses, and gray-green, blue-gray, soft mudstone beds of a few meters thickness. The transitional contact between the Middle and Upper Siwaliks is observed about a few 100 m south of Bhokteni.

The Upper Siwaliks exposed at Devitar (Fig. 31.2) contain a 1–7 m thick conglomerate bed, composed exclusively of subangular to subrounded pebbles derived from red-purple and brown as well as dark green, fine- to very fine-grained, quartzose sandstone or quartz arenite. The conglomerate bed is succeeded upwards by a 20–80 cm thick, gray to dark red

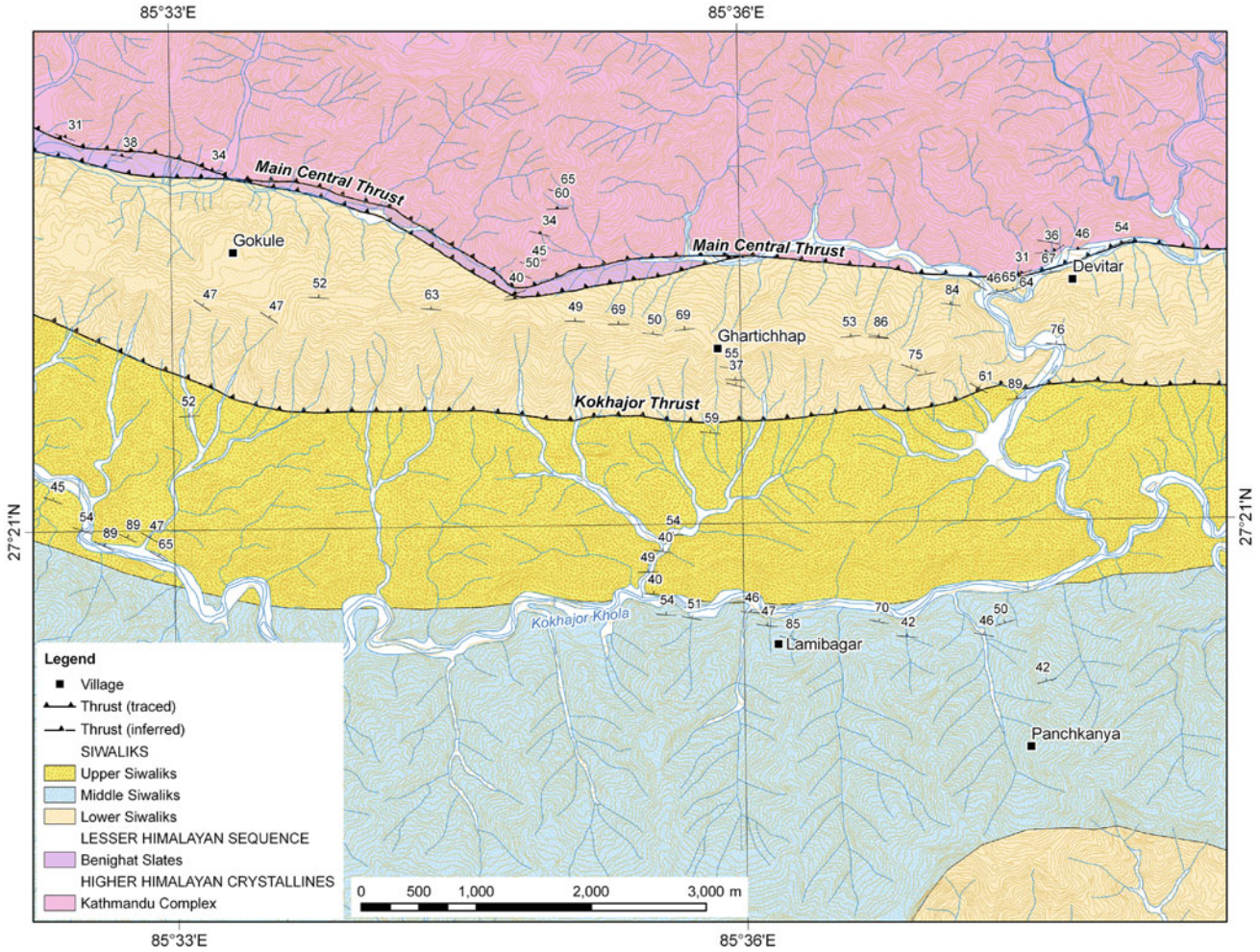

Fig. 31.2 Geological map of the Kokhajor Khola area, depicting the discontinuous Lesser Himalayan belt between the Higher Himalayan crystallines and Siwaliks. *Source* Author's observations

sandstone, followed by a very thick (1–3 m) red-brown mudstone. The imbricated pebbles in the conglomerate indicate essentially a south-directed paleoflow, and their lithology is identical with the Proterozoic rocks of the Bagmati Group. Presumably, the Higher Himalayan thrust sheet has concealed the source rocks of these pebbles, because such rocks are nowhere exposed in the vicinity.

Holocene alluvial deposits are widespread in the region. They are represented by gravel, sand, and silt with sporadic black clay layers deposited in a back swamp. Most of them are concentrated along the main river courses, where they range in thickness from 10 to 30 m and more.

31.2 Lithofacies

The lower part of the Lower Siwaliks consists of very fine-grained sandstones, pigmented and bioturbated mudstones, containing calcareous nodules and paleosols. This facies association was deposited by a meandering river, carrying fine sediments, and with floodplains exposed to weathering for a long time. A second facies association includes medium- to coarse-grained, light gray sandstones interstratified with mottled mudstones. The sandstones contain climbing ripple laminae. This association is characteristic of the upper part of the Lower Siwaliks, and it was laid down by a flood-flow–dominated meandering river system. A third facies association contains medium- to coarse-grained sandstones, fine-grained muddy sandstones, and gray mudstones. There are also some variegated mudstones. This association is found in the lower part of the Middle Siwaliks, and it was deposited by a sandy meandering river suffering from recurrent floods. A fourth facies association is marked by the appearance of coarse- to very coarse-grained, very thick-bedded sandstones with trough cross-stratification. The sandstone beds are extremely thick (up to 25 m), frequently pebbly, and grade upwards to gray mudstones. This association is present in the middle and upper parts of the Middle

Fig. 31.3 Lower Siwalik beds, exhibiting mottled colors and bioturbation structures. West of Hetaunda. *Source* Photo by author

Fig. 31.4 Large trough cross-stratification in the pepper-and-salt sandstone of the Middle Siwaliks. North of Amlekhganj. *Source* Photo by author

Siwaliks. It was deposited in a deep, sandy braided river with much bed load. A fifth facies association is represented by planar lamination, ripple lamination, and less-pronounced fining-upwards cycles. Such associations are found in the middle and upper parts of the Middle Siwaliks, and they were deposited in a shallow sandy braided river. A sixth facies association comprises well-sorted pebble- to cobble-conglomerates interbedded with yellow-brown sandstone lenses and gray mudstone beds. This association is found in the lower part of the Upper Siwaliks, and it was formed by a

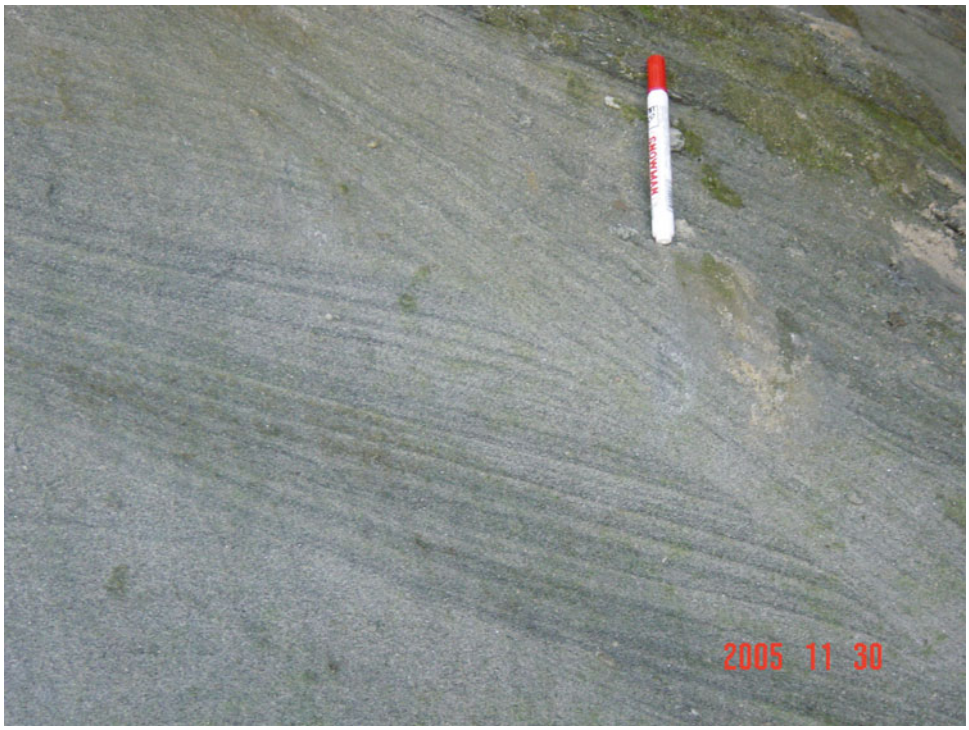

Fig. 31.5 Planar cross-lamination in the pepper-and-salt sandstone of the Middle Siwaliks. North of Amlekhganj. View to WNW. *Source* Photo by author

Fig. 31.6 Sandballs (calcareous concretions) in the sandstone of the Middle Siwaliks. North of Amlekhganj. Hammer on a sandball, for scale. View to W. *Source* Photo by author

gravelly braided stream. A seventh facies association is made up of poorly sorted boulder-conglomerates and well-sorted pebble-conglomerates with a subordinate amount of gray sandstone and mudstone. This facies association is present in the upper part of the Upper Siwaliks, and indicates a debris flow-dominant, braided river system (Nakayama and Ulak 1999).

31.3 Structure

Within the Sub-Himalayan belt, the Kokhajor Thrust, the Basan Thrust, and Marin Thrust occur successively from north to south (Chap. 10). The Kokhajor Thrust has brought the-Lower Siwaliks over the Upper Siwaliks. The Basan

Fig. 31.7 Granular to pebbly sandstone exposed towards the upper part of the Middle Siwaliks. North of Amlekhganj. *Source* Photo by author

Fig. 31.8 Scoured and cross-laminated gray sandstone bed followed by channel deposits (conglomerate) in the Middle Siwaliks. North of the Samari Khola. *Source* Photo by author

Thrust passes north of the Chauda Khola, crosses the Bagmati River, and follows the right bank of the Marin Khola, in the west, central, and east parts, respectively. Some Proterozoic sequences crop out in its hanging wall. The Marin Thrust enters this region from west of Phaparbari, runs through the Chauda Khola, goes over the Bagmati River, and then follows the lower reach of the Marin Khola. In the Siwalik belt as well as in the Terai plains, many blind thrusts are also detected

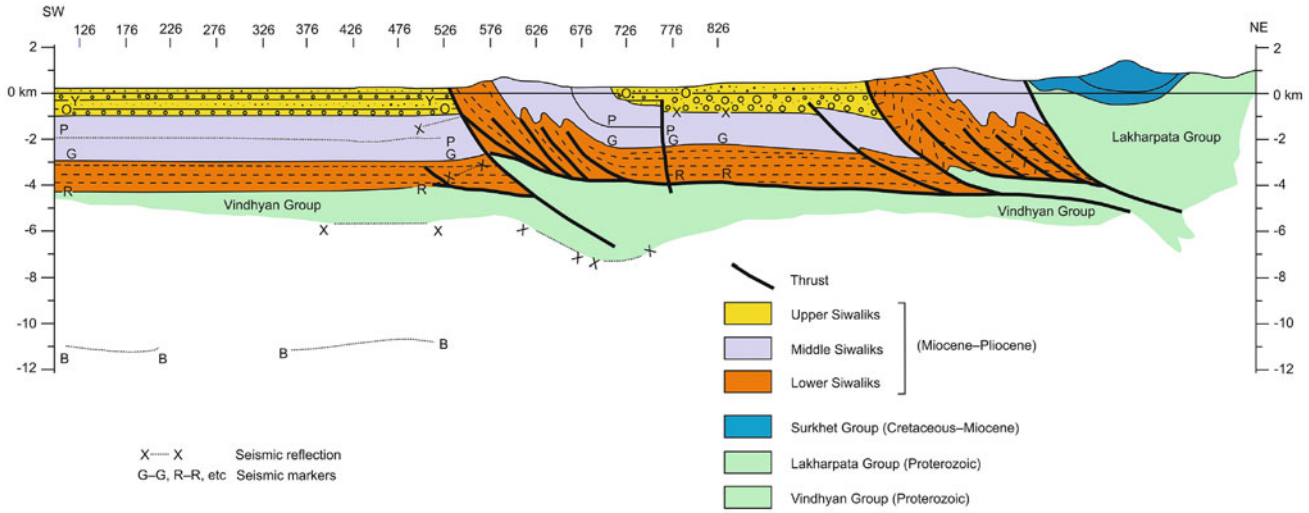

Fig. 31.9 Emergent and blind thrusts in the Siwaliks and Terai of the Hetaunda area. *Source* Modified from Friedenreich et al. (1994)

(Fig. 31.9). In the outer Siwalik belt, an anticline appears parallel to the foothills, near the Bakaiya Khola. The Bakaiya anticline (Pradhan et al. 2002) extends beyond the Bagmati River, and farther east in the Koshi region. The eroded core of the frontal anticline is interrupted by a horizontal alluvial terrace of the Bagmati River (Fig. 31.10).

31.4 Discontinuous Lesser Himalayan Belt

In the upper reaches of the Kokhajor Khola, the Lesser Himalayan rocks form a few 100 m wide strip, where mainly the Benighat Slates of the Nawakot Complex crop out (Fig. 31.9). The slates are frequently black (gray-green, when

Fig. 31.10 The Bakaiya open anticline, exposed at the outlet of the Bagmati River from the Siwalik Hills. A horizontal alluvial terrace is formed on top of the eroded fold. View to E. *Source* Photo by author

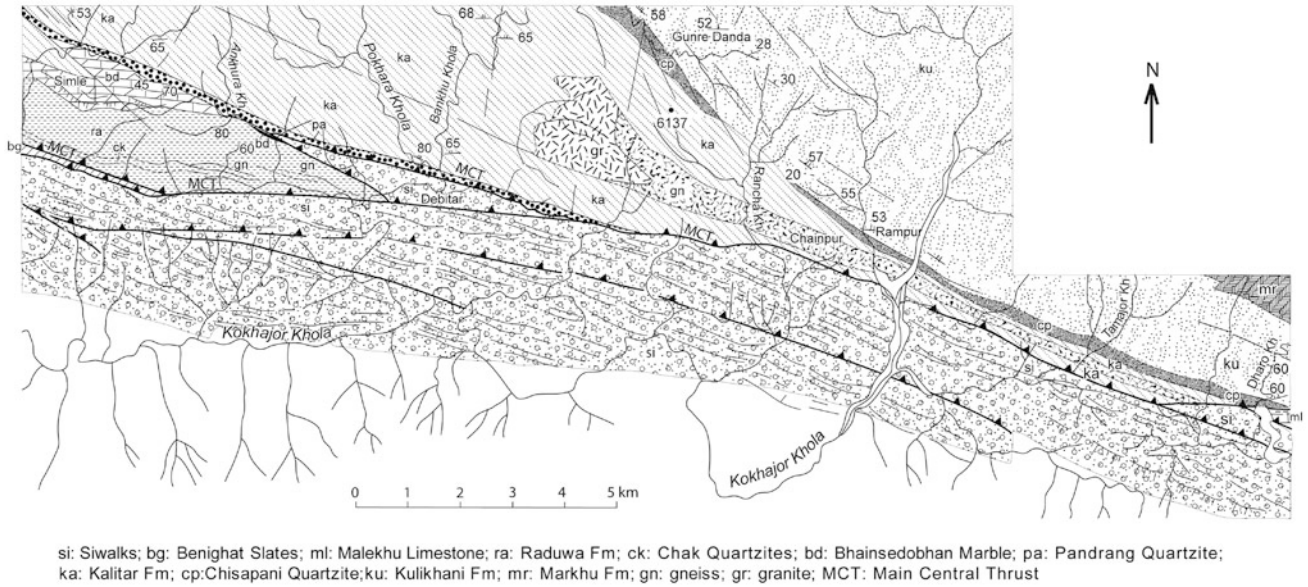

Fig. 31.11 In the upper reaches of the Kokhajor Khola, the Higher Himalayan rocks, represented by augen gneisses, schists, and quartzites of the Kathmandu Complex, are juxtaposed with the Siwaliks. The Narayani Thrust alias Main Boundary Thrust has been overstepped by the Main Central Thrust, forming a frontal duplex. *Source* Modified from Stöcklin and Bhattarai (1977)

weathered) and contain several lenticular (1–30 m thick) Jhiku carbonate beds. This fringe zone is delimited to the north by the Main Central Thrust, carrying the Higher Himalayan rocks of the Kathmandu Complex, represented by banded and augen gneisses, quartzites, garnet schists, and marbles. In the Devitar neighborhood, the Kathmandu Complex is thrust over the Lower Siwaliks (Figs. 31.2 and 31.11). This absence of the Lesser Himalayan sequence along the foothills of the Mahabharat Range (Stöcklin and Bhattarai 1977) clearly indicates quite recent movements of the Main Central Thrust in this area.

References

Dahlstrom CDA (1969) Balanced cross sections. Can J Sci 6:743–757

Friedenreich OR, Slind OL, Pradhan UMS, Shrestha RB (1994) Petroleum geology of Nepal. Can J Explor Geophys 30(2):103–114

Lees GM (1952) Foreland folding. Q J Geol Soc Lond CVIII(Part 1):1–34 (with 4 plates)

Nakayama K, Ulak PD (1999) Evolution of fluvial style in the Siwalik Group in the foothills of the Nepal Himalaya. Sed Geol 125:205–224

Pradhan UMS, Shrestha RB, KC SB, Sharma SR (2001) Geological map of petroleum exploration block—6, Birganj, Central Nepal (Scale: 1:250,000). Petroleum Exploration Promotion Project, Department of Mines and Geology, Kathmandu

Pradhan UMS, Shrestha RB, KC SB, Sharma SR (2002) Geological map of petroleum exploration block—7, Malangawa, Central Nepal (Scale: 1:250,000). Petroleum Exploration Promotion Project, Department of Mines and Geology, Kathmandu

Sah RB, Ulak PD, Gajurel AP, Rimal LN (1994) Lithostratigrphy of Siwalik sediments of Amlekhganj-Hetauda area, sub-Himalaya of Nepal. Himal Geol 15:37–48

Stöcklin J, Bhattarai KD (1977) Geology of Kathmandu area and central Mahabharat Range, Nepal Himalaya. HMG/UNDP Mineral Exploration Project, technical report, 86 pp (with 15 maps), unpublished

Siwaliks of Koshi Region

32

The Eastern Himalayas are fringed by the Piedmont type Foot-hills, the Central Himalayas by the Dun type and the Western Himalayas by the Re-entrant type.

—T. Nakata (1972, p. 49)

The Siwalik belt of the Koshi region (Fig. 32.1) contains several pronged ridges, separated from each other by an imbricate fault. A trunk river in the valley generally follows the trace of such a fault. Hagen (1969, p. 104), remarked that the Siwalik belt of this region and the adjoining Terai are tectonically active, as evidenced from the occurrence of isolated river terraces and great magnetic anomalies in the Terai. Pradhan et al. (2004, 2005) identified three or four north-dipping, emergent splays in the Sub-Himalayan belt and various other blind thrusts in the neighboring Terai (Fig. 32.2). They also documented a few plunging synclines and anticlines, arranged in an en echelon fashion.

Itihara et al. (1972) mapped the Siwaliks between the Rapti River (Hetaunda) to the west and the Lohendra River to the east of Dharan. They differentiated the inner and outer Siwalik ranges situated, respectively, north and south of the Budhi Rapti–Marin–Kamala–Trijuga line. They identified a continuous stretch of the Lower Siwaliks in the inner belt, a number of folds and faults within the outer belt, and a few frontal anticlines in the vicinity of the rivers Bagmati, Bakaiya, and Kamala. They also depicted some discontinuous Siwalik faults that were passing laterally into folds.

32.1 Lithostratigraphy

Based on photogeological investigations (Box 32.1) and field survey, Itihara et al. (1972) subdivided the Sub-Himalaya of East Nepal into the Lower, Middle, and Upper Siwaliks (Table 32.1). The Lower Siwaliks, whose thickness exceeds 2,000 m, are confined mainly to the inner ranges, whereas the Middle and Upper Siwaliks preponderate in the outer range. The Lower Siwaliks are represented by fine sandstones, mudstones, and shales with sporadic, very thin coal horizons and stringers. The Lower Siwaliks of this region also include a few conglomerate beds, accumulated in river channels. The well-imbricated pebbles, composing the conglomerate, were derived mostly from the Lesser Himalayan sequence. The Lower Siwalik sand bodies, formed in river channels and on channel bars, consist of quartz, feldspar, and slightly metamorphosed rock fragments. The sandstones also contain some muscovite, garnet, tourmaline, rutile, zircon, and heavy minerals. The dominant silty clay floodplain deposits of the Lower Siwaliks are frequently capped by calcareous paleosols (Bashyal et al. 1989).

The Middle Siwaliks comprise moderately indurated, soft sandstones, siltstones, and mudstones followed by calcareous paleosols or infrequently appearing calcareous hardgrounds. The sand and mud were deposited by meandering rivers, mainly on channel bars and marshy floodplains. The sandstones are rich in rock fragments, quartz, feldspars, and mica. In this formation, conglomerates are rare, but pebbles of gneiss and granite do occur. Apart from the minerals present in the Lower Siwaliks, the Middle Siwalik sandstones also contain sillimanite, kyanite, and staurolite, implying their Higher Himalayan provenance. The total thickness of the Middle Siwaliks is about 1,200 m (Itihara et al. 1972).

The Upper Siwaliks mainly occupy the outer Sub-Himalayan belt, and they are composed of conglomerates and sandstones interbedded with siltstones and mudstones. The sandstone predominates in the lower part, whereas the conglomerate becomes more abundant towards the top. Such a facies change is related to the passage from a meandering river to a torrential braided stream, forming alluvial fans (Bashyal et al. 1989). The conglomerate is made up of metamorphic and granitic pebbles, cobbles, and boulders, whose size increases stratigraphically upwards. The Upper Siwaliks are about 700 m thick (Itihara et al. 1972).

The terrace deposits or dun gravels are well developed in this region, and they are distributed mainly between the inner and outer Siwalik ranges, whereas some of them are also found in the Terai plain. Itihara et al. (1972) classified

M.R. Dhital, *Geology of the Nepal Himalaya*, Regional Geology Reviews,
DOI 10.1007/978-3-319-02496-7_32

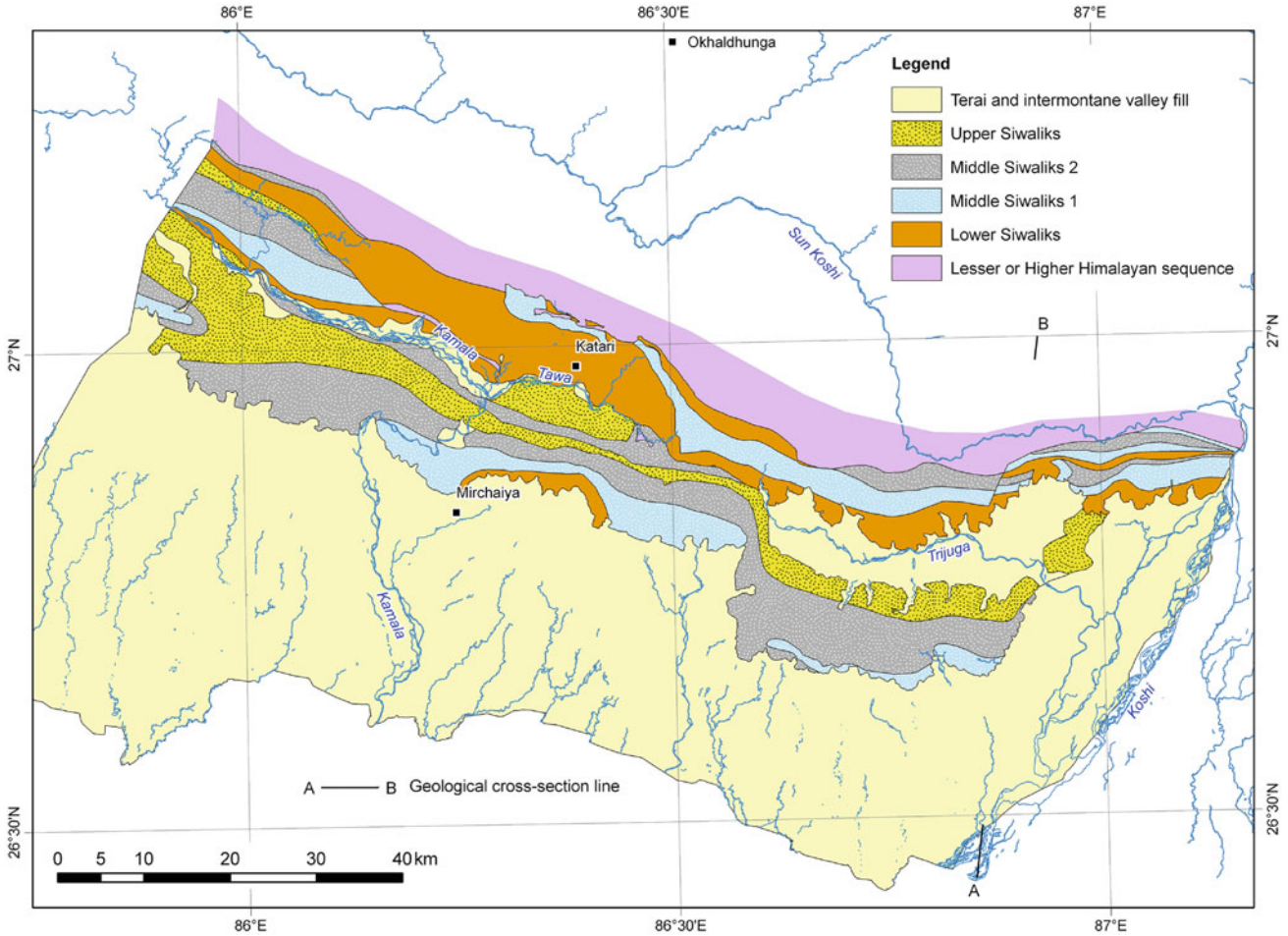

Fig. 32.1 Generalized geological map of the Siwaliks within the Koshi region. *Source* Based on Pradhan et al. (2004, 2005) and author's observations

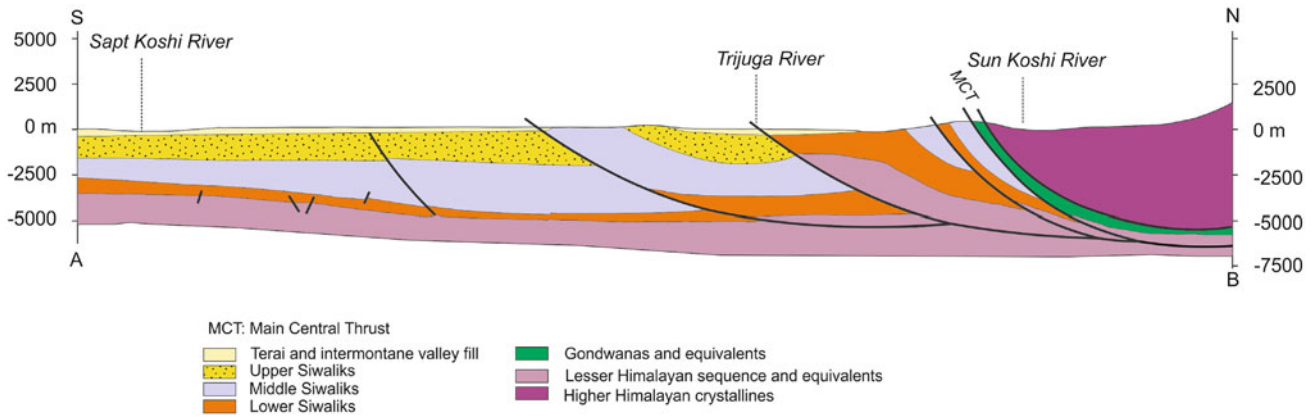

Fig. 32.2 Geological cross-section along *A–B* in Fig. 32.1. *Source* Modified from Pradhan et al. (2005). © Department of Mines and Geology, Kathmandu. Used by permission

them into the middle–late Pleistocene Higher, Middle, and Lower terrace deposits, and the Holocene floodplain deposits. The terrace deposits contain sand and gravel with intercalated thin silt layers. The top part of the Higher and Middle Terrace deposits consists of red lateritic soil. The Holocene deposits form the floodplains of various rivers.

Table 32.1 Classification of Siwaliks and younger deposits of East Nepal

Stratigraphic unit	Age
Floodplain deposits (*Unconformity*)	Holocene
Terrace deposits (dun gravels) (*Unconformity*)	middle–late Pleistocene
Upper Siwaliks	Pliocene–early Pleistocene
Middle Siwaliks	Pliocene
Lower Siwaliks (*Thrust*)	Miocene
Basement rocks	Proterozoic–Paleozoic

Source Itihara et al. (1972)

Box 32.1: Photogeological Properties of Siwaliks and Other Neighboring Rocks. *Source* Itihara et al. (1972)

- The Upper Siwaliks have a rather dark tone, where a dendritic drainage pattern is usually developed. The Upper Siwalik Hills are relatively rounded.
- The Middle Siwaliks have a slightly lighter tone than that of the Lower Siwaliks. As in the Lower Siwaliks, they also show either a grid type or dendritic type of drainage pattern.
- The Lower Siwaliks exhibit a slightly dark tone. If they are steeply dipping with cuesta type of topography, they show a grid type drainage pattern, and if they are gently dipping, the drainage pattern changes into a dendritic type.
- The metamorphic rocks are slightly darker in tone and have a grid type drainage pattern.
- The granitic rocks show a dendritic drainage pattern with a light tone.

32.2 Structure

The Siwaliks of this region are moderately to strongly contorted and imbricate-faulted (Figs. 32.1 and 32.2). Most of the folds show east–west trending hinges. The folds in the Siwaliks are generally asymmetric, and the Lower Siwaliks seem to have undergone more intense deformation and fracturing than the Middle and Upper Siwaliks (Itihara et al. 1972, p. 85). Near Muksar, Auden (1935) recognized an eroded frontal anticline, stretching along the foot of the Siwaliks (Fig. 32.3). In this transect, he mapped the Lower Siwaliks represented by brown-weathering sandstones and chocolate clays, containing some inconsistent impure limestone or marl beds. The Middle Siwaliks exposed at Muksar contain 10–15 m thick sandstone and mudstone alternations with calcareous concretions and lenticular (5 cm in thickness and 1.5 m in length) coal seams. The Upper Siwaliks are represented by conglomerates and mudstones.

The Kamala anticline (Pradhan et al. 2005) crosses the Kamala River and continues farther west, towards the Ratu Khola (Fig. 32.4). The axial trace of this Kamala anticline is about 75 km long and slightly undulating in the vertical section as well as in plan view. The anticline disappears near the Ratu Khola (Fig. 32.5), where there is a complementary syncline and the Bakaiya anticline. The north-lying Bakaiya anticline (Pradhan et al. 2002) plunges due east and it continues to the west, towards the Bagmati River and the Bakaiya Khola for about 130 km (Chap. 31).

The Kamala River has cut through the anticline forming an antecedent gorge, located west of Mirchaiya. Owing to the subsequent growth of the Kamala anticline and its propagation towards the west, the Kamala River has also been deflected to the west (Fig. 32.4). The streams emerging from the Siwalik Range display a coarse texture and rough

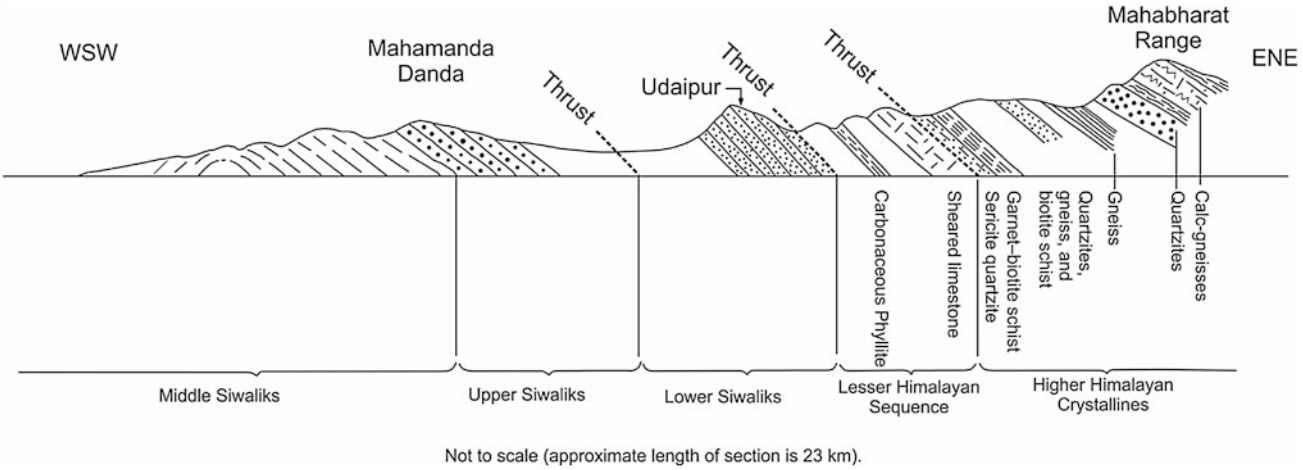

Fig. 32.3 The Siwaliks forming a frontal anticline at Muksar on which is thrust a second series of lower Siwaliks in the Udaipur area of East Nepal. *Source* Modified from Auden (1935)

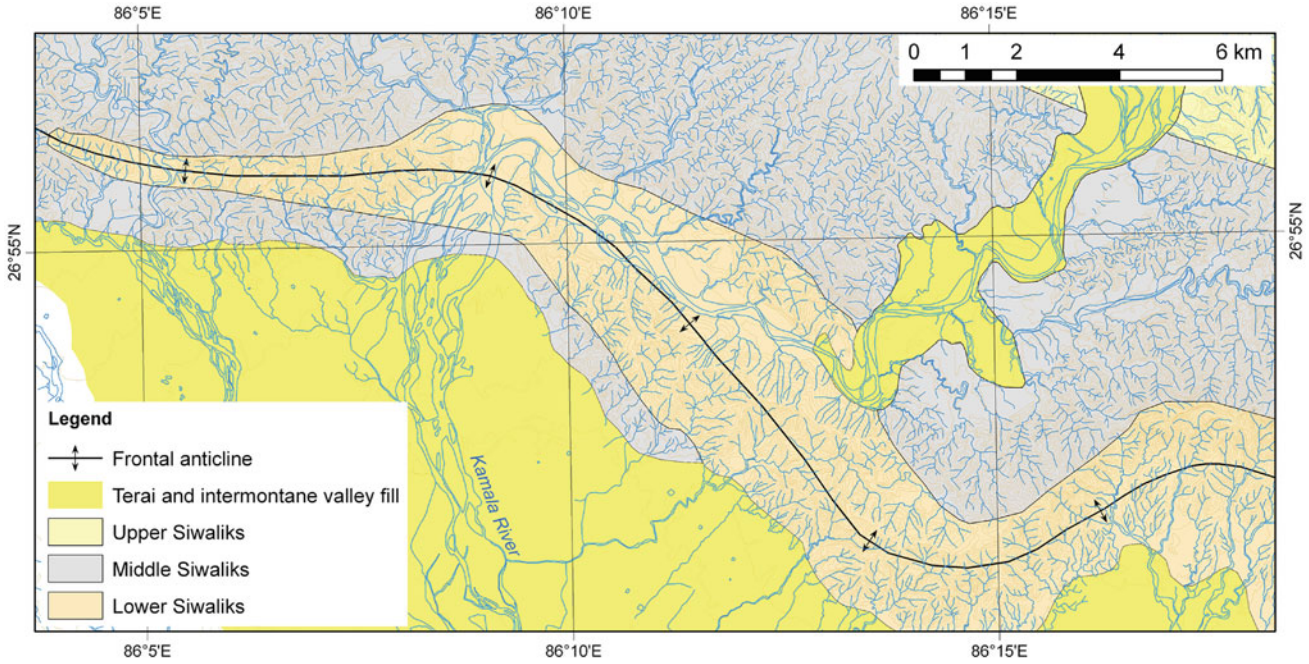

Fig. 32.4 The Kamala frontal anticline, stretched parallel to the foothills of the Siwalik belt in the vicinity of Katari, and the Kamala Khola. *Source* Based on Pradhan et al. (2004) and author's observations

drainage owing to the gentle slope of the alluvial fan constituting the Bhabar zone, where they become essentially parallel for about 10 km and then coalesce with each other (Nakata 1972).

32.3 Development of Siwalik Wedge

The mode of distribution of geomorphic surfaces in the Trijuga River valley is similar to that of the Kota dun in the Kumaun Himalaya (Middlemiss 1890; Nakata 1972) and the Rangun Khola in the Mahakali–Seti region (Chap. 28). The older geomorphic surface is located in the south, whereas the younger one is towards the northern part of the valley. While moving from the south to the north, the older deposits are successively overlain by the younger ones. The amount of tilt in the southern portion of the valley, between the older and younger geomorphic surfaces, was large enough to prevent the younger deposits from covering the older surface. It implies that the formation of the younger surfaces has taken place in the area where the amount of uplift was comparatively small. Hence, the geomorphic surface arrangement in the area suggests that northwards tilting with the warped cliff in the south has been continuing since the formation of the small frontal hill (Nakata 1972).

Hérail et al. (1986) observed that the parallel and successive ridges and valleys (troughs) in the Koshi region were controlled by the imbricate faults running along the river valleys. These structures occurred about 5–4 Ma, beginning with the northernmost fault, as a result of the essentially north–south-directed compressive stresses. The geomorphic surfaces associated with the main inner thrusts are the older ones, whereas the south-lying geomorphic surfaces, associated with the outer imbricate faults, are just a few hundred thousand years old. The coal with a reflectance between 0.75 and 1.05 % (maximum: 0.85 %) is found in the Siwaliks cropping to the north, and the soft lignite or peat with a very low reflectance (0.25–0.45 %) occurs to the south (Bashyal et al. 1989). It indicates that the intensity of deformation decreases from the north to the south. The decrease is also shown by a decline in the dip of strata from the north to the south. Hence, these faults exhibit a piggyback propagation pattern and the valleys are the piggyback basins.

Relatively rapid uplift of the Siwalik strata is also implied by the altitudes and elevations of river terraces. In this region, a number of terraces are developed adjacent to rivers that have cut through the frontal anticline (Delcaillau 1986). Many such terraces, which were formed adjacent to southwards-flowing streams, are now dipping northwards (Delcaillau 1986), indicating a tilt of the front of the range, with the largest vertical displacement at the front. This pattern of tilting suggests that slip occurs on imbricate thrusts that flatten northwards (Fig. 32.2). The Siwalik frontal anticlines are one of the rapidly upheaving structures in the Himalaya. Some such folds grew at a vertical speed of about 1 mm/a or more, as measured in the north limb of the Soan anticline, in the Potwar Plateau, Pakistan (Johnson et al. 1986). Delcaillau (1986) found similar rapid uplifts in the Siwalik belt of the Koshi region.

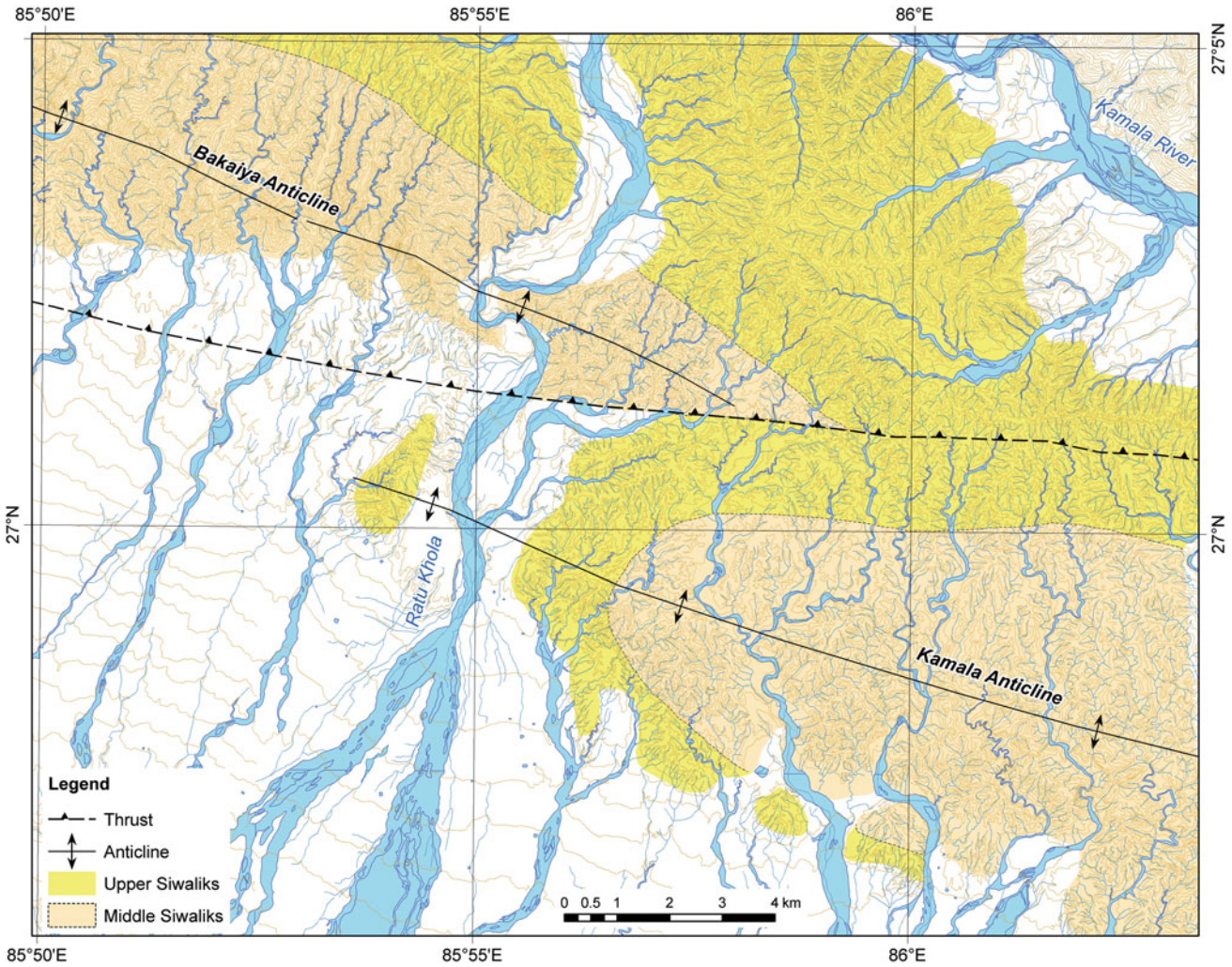

Fig. 32.5 West closure of the Kamala anticline and faulted Bakaiya anticline. *Source* Based on Itihara et al. (1972)

References

Auden JB (1935) Traverses in the Himalaya. Rec Geol Surv India LXIX(Part 2):123–167 (with 6 plates including a geological sketch map)

Bashyal RP, Delcaillau B, Hérail G, Mascle G (1989) Thrusting and orogenesis: the Himalayan front in central Nepal. J Nepal Geol Soc 6:1–9

Delcaillau B (1986) Dynamique et évolution morphostructurale du piémont frontal de l'Himalaya: les Siwalik de l'Himalaya du Népal oriental. Revus géologiques, dynamiques, géographiques, et physiques 27:319–337

Hagen T (1969) Report on the geological survey of Nepal. Volume 1: preliminary reconnaissance. Denkschiiften der Schweizerischen Naturforschenden Gesellschaft, Band LXXXVI/1:185 (with a geological map)

Hérail G, Mascle G, Delcaillau B (1986) Les Siwaliks de l'Himalaya du Népal: un exemple d'évolution géodynamique d'un prisme d'accrétion intracontinental. Sciences de la Terre, Mémoire 47, Nancy, pp 155–182

Itihara M, Shibasaki T, Miyamoto N (1972) Photogeological survey of the Siwalik ranges and the Terai plain, southeastern Nepal. J Geosci Osaka City Univ 15(4):77–98 (with a geological map of the Siwaliks and 4 plates)

Johnson GD, Raynolds RGH, Burbank DW (1986) Late Cenozoic tectonics and sedimentation in the northwestern Himalayan foredeep: 1. Thrust ramping and associated deformation in the Potwar region. In: Allen PA, Homewood P (eds) Foreland basins. Special Publication of International Association of Sedimentologists, vol 8. Blackwell, Oxford, pp 273–291

Middlemiss CS (1890) Physical geology of the Sub-Himalaya of Garhwál and Kumaun. Mem Geol Surv India XXIV(Part 2):59–200

(with 3 plates of cross-sections and a plate of geological map in colors; scale 1 inch = 4 miles)

Nakata T (1972) Geomorphic history and crustal movements of the foot-hills of the Himalayas. Science Reports of Tohoku University, 7th Series (Geography) 22(1):39–177

Pradhan UMS, Sharma SR, Tripathi GN (2005) Geological map of petroleum exploration block—9, Rajbiraj, Eastern Nepal (Scale: 1:250,000). Petroleum Exploration Promotion Project, Department of Mines and Geology, Kathmandu

Pradhan UMS, Shrestha RB, KC SB, Sharma SR (2002) Geological map of petroleum exploration block—7, Malangawa, Central Nepal (Scale: 1:250,000). Petroleum Exploration Promotion Project, Department of Mines and Geology, Kathmandu

Pradhan UMS, Shrestha RB, KC, SB, Subedi DN, Sharma SR, Tripathi GN (2004) Geological map of petroleum exploration block—8, Janakpur, Central Nepal (Scale: 1:250,000). Petroleum Exploration Promotion Project, Department of Mines and Geology, Kathmandu

Siwaliks of Arun–Tamar Region

33

The strength and thickness of the Indian lithosphere are a major reason the Himalayan peaks are so high.
—P. Molnar (1986, p. 75)

The Sub-Himalayan belt of the Arum–Tamar region is reduced to an uneven and asymmetric stretch with discontinuous crests and open valleys, passing into episodic torturous meanders (Fig. 33.1). The region is compressed into tight anticlines and open synclines, interrupted by many imbricate faults. A large part of the belt is represented by the Middle and Upper Siwaliks, where the subordinate Lower Siwalik strata are intermittently distributed. The widest piggyback basin of the region is developed in the Kankai Khola. Its structural position is fairly similar to that of the Siwalik belt in the Budar–Jogbudha area of the Mahakai–Seti region (Chap. 28). Nonetheless, there are some significant differences too, such as it occurs behind a sharp frontal anticline and hardly any Lower Siwalik strata are involved in shaping its southern front.

33.1 Lesser Himalayan Sequence

Lying south of the Higher Himalayan crystallines, the Lesser Himalayan sequence forms a narrow foothill belt of the Mahabharat Range (Fig. 33.2). The Lesser Himalayan rocks are composed of light gray to white quartzites, gray-green and blue-green phyllites, gray metasandstones, and gray-green garnetiferous schists. There also infrequently occur a few bands of dark gray-green amphibolite. The schists contain many folded quartz veins, which are also stretched (boudinaged) parallel to foliation. In the vicinity of Rangapani, a light gray banded gneiss is exposed. The medium- to fine-grained gneiss alternates with chlorite schist bands. The gneiss is strongly lineated, and composed of quartz, feldspar, biotite, and muscovite. Towards the west, the banded gneiss becomes thinner and pinches out in the garnet schist.

33.2 Siwaliks

From the Sapt Koshi River section of this region, Lombard (1958) described regularly north-dipping, massive, and homogeneous sandstones with increasing cross-bedding towards the upper part, together with calcareous concretions. He also documented some intercalated mottled reddish clays and marls, and the upper horizons containing bluish clays with conglomerate beds. Bordet and Latreille (1955) investigated the Siwaliks around Dharan, where Bordet (1961) identified the following cyclic succession (the thickness of a cycle varies from 10 to 20 m) from the bottom to top: (1) cross-bedded micaceous sandstones with small pebbles of quartz or foliated crystalline rocks; conglomerates containing metamorphic pebbles; they constitute a fining-upwards sequence topped by beds of lignite; and (2) greenish gray to pale yellow claystones with yellow calcareous nodules. He also reported some bivalves and gastropods, and remarked that the formation is folded with steep dips towards the north.

The Lower Siwaliks of this region are exposed mainly in the outer belt of the Barahakshetra–Dharan area, and in the inner belt of the Kankai watershed. North of Barahakshetra, the Lower Siwaliks consist of fine-grained, gray-green to blue-green sandstones interbedded with red-purple, yellow-green, or brown mudstones. The mudstones are rich in plant remains. In the lower reach of the Sardu Khola, west of Dharan, the Lower Siwaliks are represented by thick- to very thick-bedded, medium- to fine-grained, light gray-green to dark gray sandstones interbedded with green-gray and red-purple, variegated mudstones. Sporadically, they also contain thin (5 cm) coal seams. In the Kankai Basin (Fig. 33.2), the Lower Siwaliks are confined to the inner belt, where they are represented by fine-grained, moderately indurated, gray sandstones, interbedded with purple and green shales.

M.R. Dhital, *Geology of the Nepal Himalaya*, Regional Geology Reviews,
DOI 10.1007/978-3-319-02496-7_33

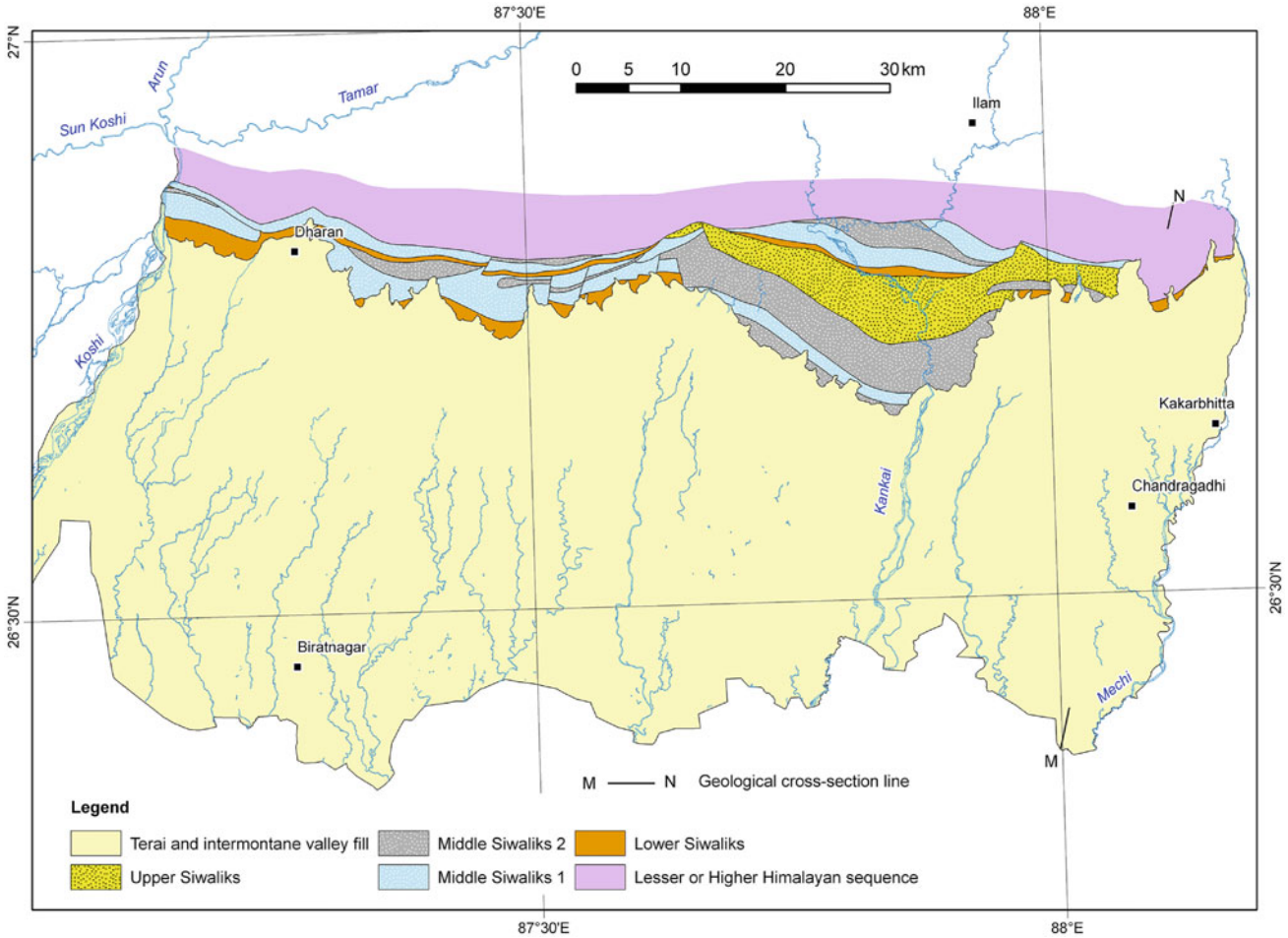

Fig. 33.1 Simplified geological map of the Siwaliks exposed in the Arun–Tamar region. *Source* Based on Pradhan et al. (2006) and author's observations

A thick (more than 3 m) yellow-brown residual soil is generally found on top of the sandstones.

The Middle Siwaliks are widespread in the region, especially towards its eastern half. In the Barahakshetra–Dharan area, they consist of coarse- to very coarse-grained, cross-stratified, biotite-rich, pepper-and-salt sandstones, containing a few conglomerate lenses and thin beds. The sandstones gradually pass upwards to gray or dark gray mudstones containing plant remains. In the Chanjo Khola, the Middle Siwaliks are made up of light gray, cross-stratified, very thick-bedded, coarse- to very coarse-grained and sporadically pebbly, with coal or peat beds, pepper-and-salt sandstones, interbedded with gray to dark gray mudstones. The multi-storied sandstone beds attain a thickness of 10–30 m. There also occur many parallel-laminated sandy strata. The pebbles in the sandstone are made up of white or gray quartzite, gray banded gneiss, and green-gray schist. They range in size from 2 to 5–10 cm. The trough cross-bedded, pebbly sandstones include mud lumps and lenses of dark gray color. Some of the pebbles are aligned along the laminae. Sporadically, the sandstones exhibit climbing ripple lamination. There also occur many sandstone and gray mudstone interbeds, where the mudstone is parallel-laminated.

The Middle Siwaliks of the Kankai Basin are made up of fine- to medium-grained, arkosic, pebbly sandstones with rare gray to dark gray clays, and occasionally silty sandstones and conglomerates. The upper part of the Middle Siwaliks consists of medium- to coarse-grained, fine- to medium-grained, massive sandstones interbedded with green to greenish gray clays, gray shales with thin bands of pseudo-conglomerates, and mudstones. Plant and animal fossils are present in clays and shales. The Middle Siwaliks exposed at Domukha (outer belt) are dominated by thick-bedded, yellowish gray sandstones, siltstone, and greenish gray mudstones. Their lower part consists of coarse-grained sandstones containing petrified wood fragments (diameter: about 20 cm) as well as pebbly lenses or thin discontinuous beds.

In the Kankai watershed, the contact between the Middle and Upper Siwaliks is marked by the appearance of thick interbeds of pepper-and-salt-colored pebbly sandstone and

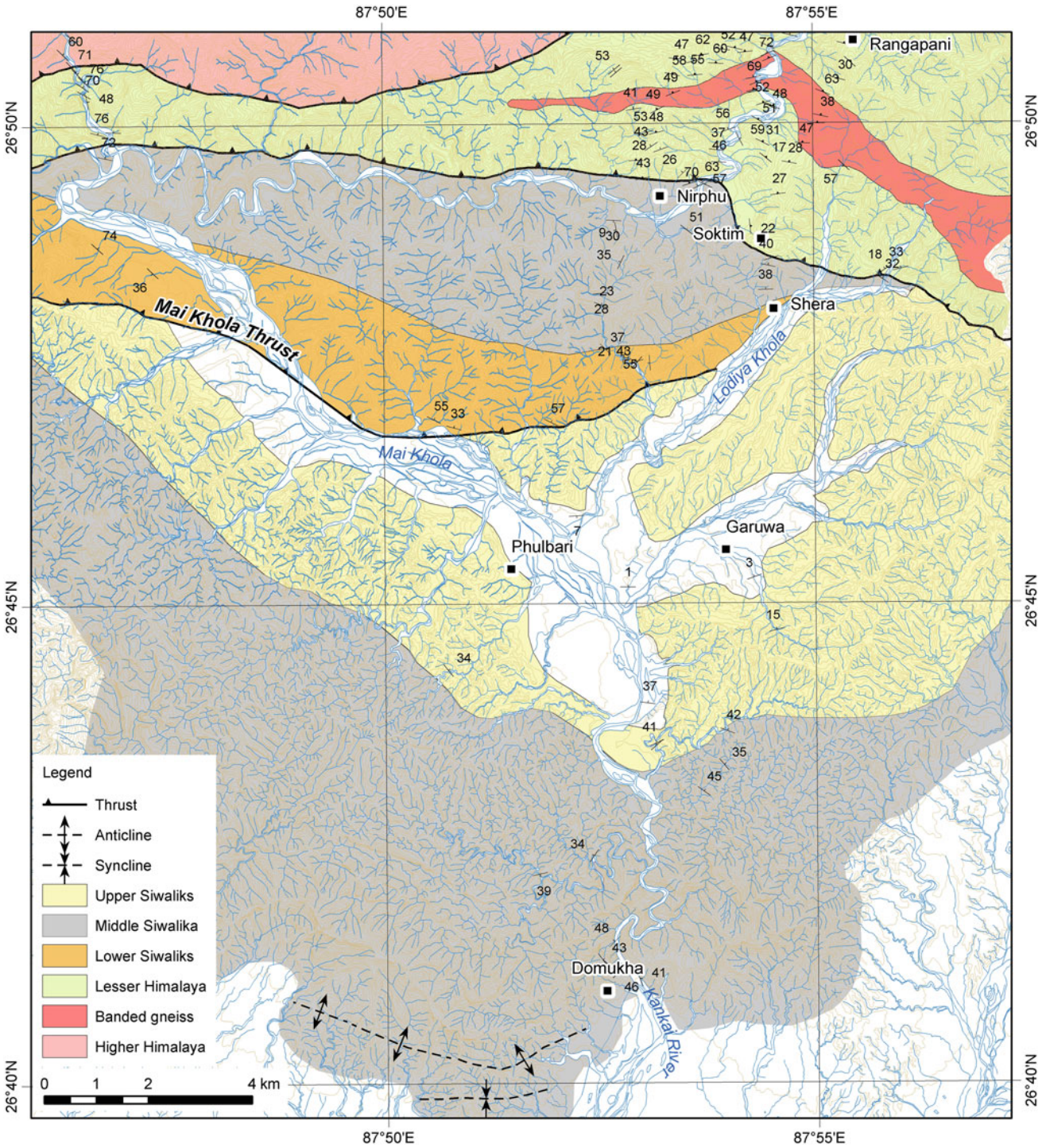

Fig. 33.2 The Siwaliks constituting the Kankai watershed. *Source* Based on field survey in 2009 by A M S Pradhan and A Regmi, and in 2011 by M R Dhital

conglomerate in gray mudstone. The Upper Siwaliks consist of coarse boulder-conglomerates with irregular beds and lenses of sandstones and thin intercalations of yellow, brown, and gray sandy clays. Their lower part contains a few beds of light green, thickly bedded mudstone. The mudstone beds are overlain by conglomerates.

Fig. 33.3 Gently south-dipping Middle Siwaliks exposed on the left bank of the Ratuwa Khola, Ilam. *Source* Photo by author

In the Biring Khola and Barphalyang, very thick (more than 25 m), gently north-tilted alluvial deposits are observed, where the Upper Siwalik gravel beds gradually pass into the late Pleistocene–Holocene alluvial deposits.

33.3 Geomorphology

The Siwalik Range exhibits very rugged terrain with deeply dissected gullies and steep slopes. Low terraces, alluvial fans, badlands, and a thin soil cover are the characteristics of the Sub-Himalayan Range of this region. It contributes a huge amount of sediment to the rivers through gullies and tributaries. A majority of the rivers originating from this range are ephemeral. There is a strong geological control on the physiography of the hills. For example, the Siwaliks consisting of soft sandstones exhibit highly dissected topography; the river valleys are wider and straighter. An open synclinal fold observed in the Siwaliks is responsible for creating typical rolling hills with wide ridges northeast of Domukha. The resistant Middle Siwaliks are characterized by high hills, steep slopes, and deeply dissected gullies. The rivers and streams flowing through the Siwaliks carry much sediment.

33.4 Structure

The Sub-Himalayan fold-and-thrust belt of Arun–Tamar can be divided into the following four sectors, from west to east, respectively (Fig. 31.1).

The west segment between the Sapt Koshi River and Dharan is represented by the gently folded Lower and Middle Siwaliks. The Lower Siwaliks are repeated twice, owing to an imbricate fault passing through the Kokaha Khola. The Lower Siwaliks constitute the hanging wall of various imbricate slices. The stretch between Chatara and Barahakshetra is characterized by open folds, whose wavelength is a few 100 m. Towards the north, the folds gradually disappear, giving way to a homocline running along the left bank of the Kokaha Khola.

The segment between Dharan and Madhumalla is the most complex. It is made up of various imbricate faults, lateral ramps, tear faults, and eroded frontal anticlines. There are also several Proterozoic slivers within the Sub-Himalayan zone. The imbricate faults make a number of trailing branch lines, implying significant erosion. The tear faults disrupt the folds and the faults, indicating their late stage of development.

The Madhumalla–Khudunabari segment includes the gently dipping piggyback basin of Kankai. A wide Upper Siwalik belt is developed on its hanging wall. To the north, the basin is cut out by the Mai Khola Thrust (Fig. 33.2). In the Arun–Tamar region, the Kankai frontal anticline (Pradhan et al. 2006) has mainly a straight axial trace of about 27 km and its sharp hinge plunges essentially due 305° at its western end and due 126° towards its eastern extremity. Its hinge is also undulating in the vertical section. The south limb of the anticline gently dips due south and disappears under the Terai alluvium (Fig. 33.3). The Kankai anticline is well exposed in the Chanjo Khola (Fig. 33.4), where gently

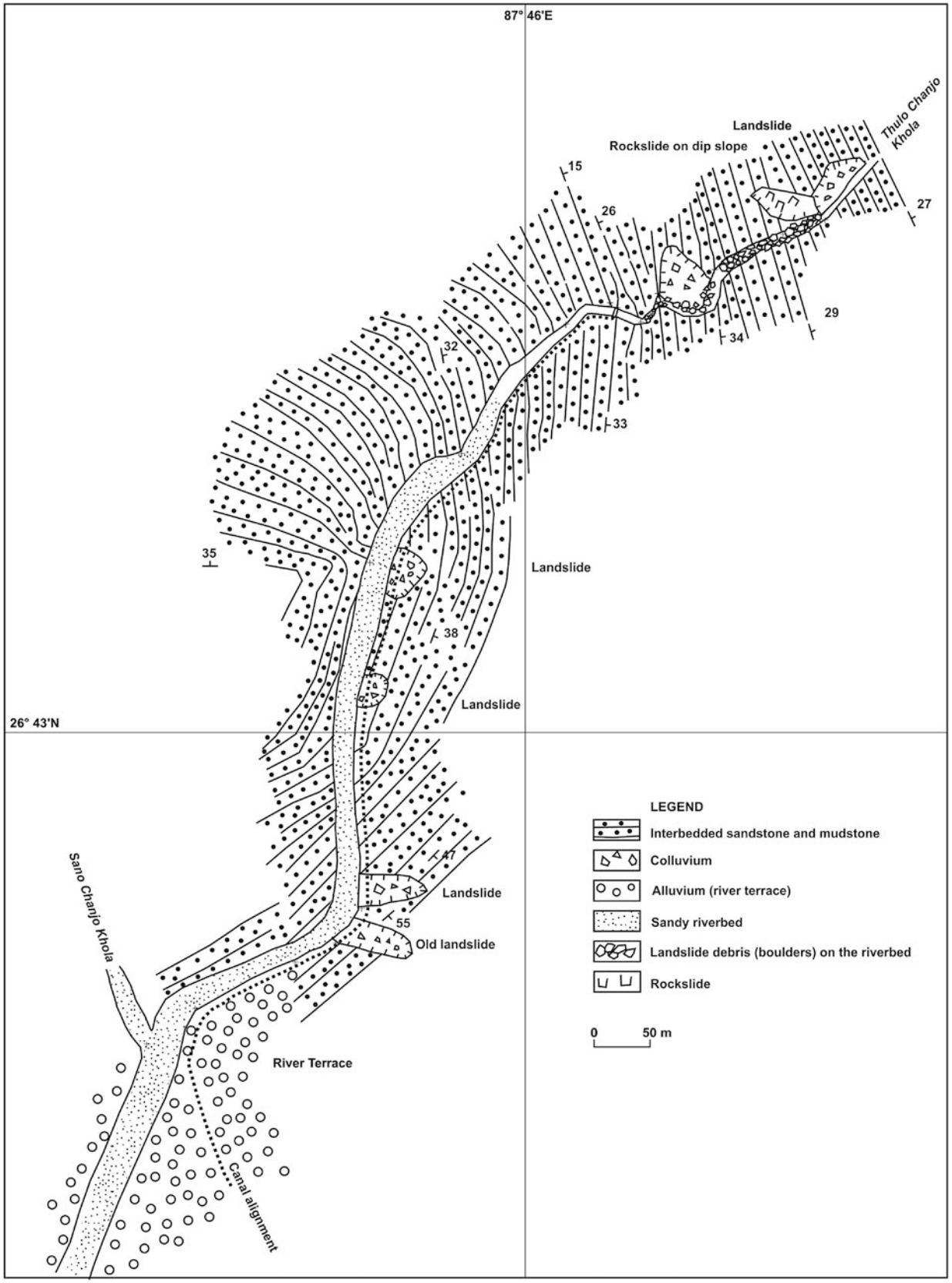

Fig. 33.4 The Ratuwa–Kankai frontal anticline exposed in the Thulo Chanjo River, Ilam. *Source* Author's observations

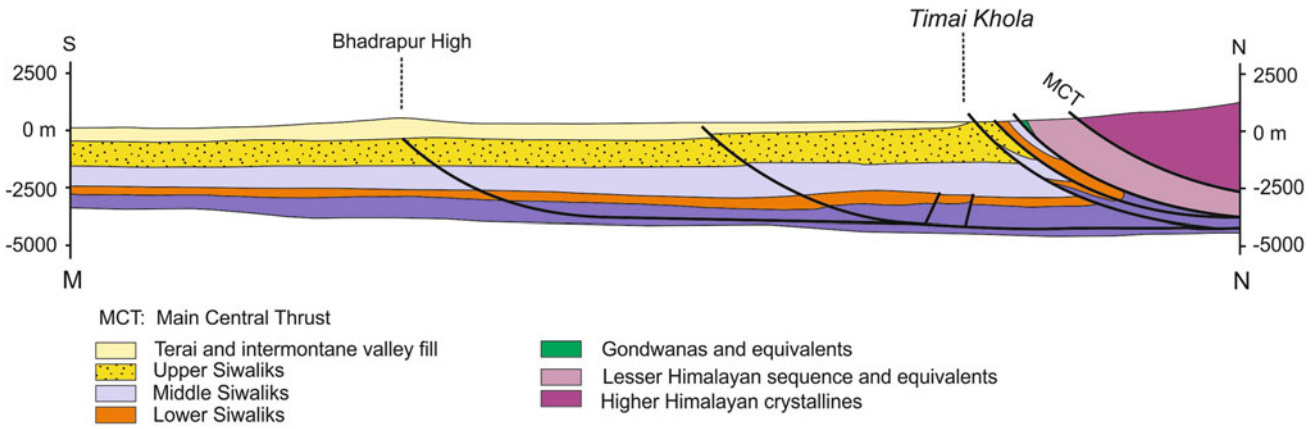

Fig. 33.5 Geological cross-section along M–N in Fig. 33.1, across the Terai and the Siwalik belt of the Bhadrapur–Timai Khola area. *Source* Modified from Pradhan et al. (2006). © Department of Mines and Geology, Kathmandu. Used by permission

dipping Middle Siwalik strata make a beautiful east-plunging arch.

The segment between Khudunabari and the Mechi River is characterized by the proliferation of blind imbricate thrusts. The sharp anticlinal fold of Biring Khola is developed above one such fault (Fig. 33.5). While moving from west to east, the width of the exposed Siwalik Basin is drastically reduced from more than 30 km in the Kankai watershed, to a trifling amount of several 100 m in the Mechi River.

Heim and Gansser (1939) observed a frontal fold in the Tista River, Darjeeling, where the big mass of Siwaliks of about 2,100 m thickness is not only in a normal position, but forms a wide anticlinal arch with its apex at the Sivok railway station. The greater part of its south limb has been removed by recent erosion and covered by alluvial deposits. The Siwaliks of this area are represented by gray sandstones, blue nodular marls and clays with coal seams, and conglomerates. These rocks are very similar to the Siwaliks exposed in the south belt of the Kankai River.

The variation in tectonic style within the Siwalik belt for a distance of less than 100 km, points to a rather shallow nature of deformation and a transfer zone. This region has the thinnest Siwalik succession, less than 4 km. On the other hand, the Bhadrapur High, lying completely within the Terai, about 30 km south of the Siwalik foothills, presumably represents a concealed active fault (Fig. 33.5).

References

Bordet P (1961) Recherches Géologiques dans L'Himalaya du Népal, Région du Makalu, Expéditions Françaises a l'Himalaya 1954–1955. Edition du Centre National de la Recherche Scientifique (CNRS), 275pp (with geological maps and plates)

Bordet P, Latreille M (1955) La Géologie de L'Himalaya de l'Arun. Bulletin de la Société géologique de France 5(6): 529–542

Heim A, Gansser A (1939) Central Himalaya: Geological Observations of the Swiss Expedition 1936. Denkschriften der Schweizerischen Naturforschenden Gesellschaft, Band LXXIII, Abh. 1, 245pp (with maps, sections, and plates)

Lombard A (1958) Un itinéraire géologique dans l'Est du Népal (Massif du Mont Everest). Mémoires Société Helvétique Sciences Naturelles 82:1–107

Molnar P (1986) The structure of mountain ranges. Sci Am 255(1):70–79

Pradhan UMS, KC SB, Subedi DN, Sharma SR, Khanal RP, Tripathi GN (2006) Geological map of Petroleum Exploration Block—10, Biratnagar, Eastern Nepal (Scale: 1:250,000). Petroleum Exploration Promotion Project, Department of Mines and Geology, Kathmandu, Nepal

Part VII

Terai, Intermontane Basins, and Neotectonics

Terai and Intermontane Basins

34

The lack of isostatic equilibrium and the existence of very smooth, inclined substratum suggest that the Himalayas are currently under the influence of large scale tectonic forces, probably due to collision of the Indian plate against the Asian plate.

—Kono (1974, p. 283)

The flatland of Nepalese Terai constitutes the north fringe of the extensive Ganga foreland basin. The Pleistocene and Holocene alluvial accumulations of this strip were laid down by rivers, originating within the Himalaya or beyond it in the Tibetan Plateau. The average thickness of these sediments exceeds 1,500 m (Chap. 2). Burbank (1992) discovered that the sediments of the rising Himalaya no longer accumulate in the Ganga Basin, owing to the lack of space, but are transported directly to the Bengal fan. The Plio–Pleistocene and Holocene sediments also occupy many intermontane basins. Such basins occur mainly in the Himalayan foothills, whereas a few of them also appear in the Midlands, and several others are distributed in the Inner Himalaya of Nepal (Chap. 3).

34.1 Subsurface Configuration of Terai

The subsurface geology is dominated by the sediments from large and coalescing fans, the deposits of the Ganga Basin extending to the north, and the sediments constituting the Siwalik trough. The elevated alluvial terraces as well as subsurface sediments are gently tilted to the south (Figs. 34.1 and 34.2), and are deposited on an irregular surface of the Siwaliks, which, in turn, are thrust over the Gangetic alluvium. It seems that there are a number of blind thrusts, splays from the Main Himalayan Thrust, which become shallower towards the south, and are covered by the alluvial deposits.

34.2 Dang and Deukhuri Valley Fills

The oval Dang Valley (Fig. 34.3) is about 55 km long and 18 km wide. It lies about 10 km north of the Deukhuri Valley, and closes about 30 km west of the latter. The Dang Valley is filled up with Pleistocene to Holocene fluvial sediments, deposited essentially by the north–south flowing rivers. On the other hand, the Deukhuri Valley is about 50 km long in the east–west direction and about 12 km wide in the central part. It is like an elongated trough containing the Plio–Pleistocene deposits of the Rapti River, which flows from east to west, almost through the middle part of the valley.

The Dang Valley is surrounded by the Siwaliks on almost all sides, except for some Lesser Himalayan rocks exposed to the north, at the foot of the Mahabharat Range (Chap. 8). The Main Boundary Active Fault delimits the valley on the north, and the fault is marked by a conspicuous "pressure ridge" (Nakata et al. 1984; Chap. 35). The active fault generally shows a downthrown hanging wall, representing a normal sense of movement, and there are several sag ponds that are sometimes filled up with clay and peat. The pressure ridge comprises strongly deformed fluvial deposits, mixed up with various crush rocks from the Siwaliks as well as the Lesser Himalaya.

All rivers entering the Dang Valley originate from the 1,500–2,200 m high Mahabharat Range lying to the north. These rivers flow essentially due south and thus make a transverse drainage. They are finally confluent with the Babai Nadi (River), the trunk river that flows from east to west along the south margin of the valley. The Dang Valley is separated from the Deukhuri Valley by an intervening Siwalik Range. The altitude of the Dang Valley is about 600 m at the Babai River and gradually increases to about 800 m towards the north and east extremity of the valley.

The fluvial terraces (Fig. 34.3) in the Dang Valley belong mainly to the following six levels (Yamanaka and Yagi 1984). These terraces are well developed, especially in the Gwar Khola, Patu Khola, and their tributaries.

The Highest Terrace is confined mainly to the upper reach of the Bhamke Khola (Fig. 34.3). Its primary landform is obliterated by erosion, and presently a dendritic drainage pattern prevails in this terrace. The fluvial deposits composing this terrace are made up of silty soils with pebbles, cobbles, and boulders (up to 1 m) of quartzite, slate, and

M.R. Dhital, *Geology of the Nepal Himalaya*, Regional Geology Reviews,
DOI 10.1007/978-3-319-02496-7_34

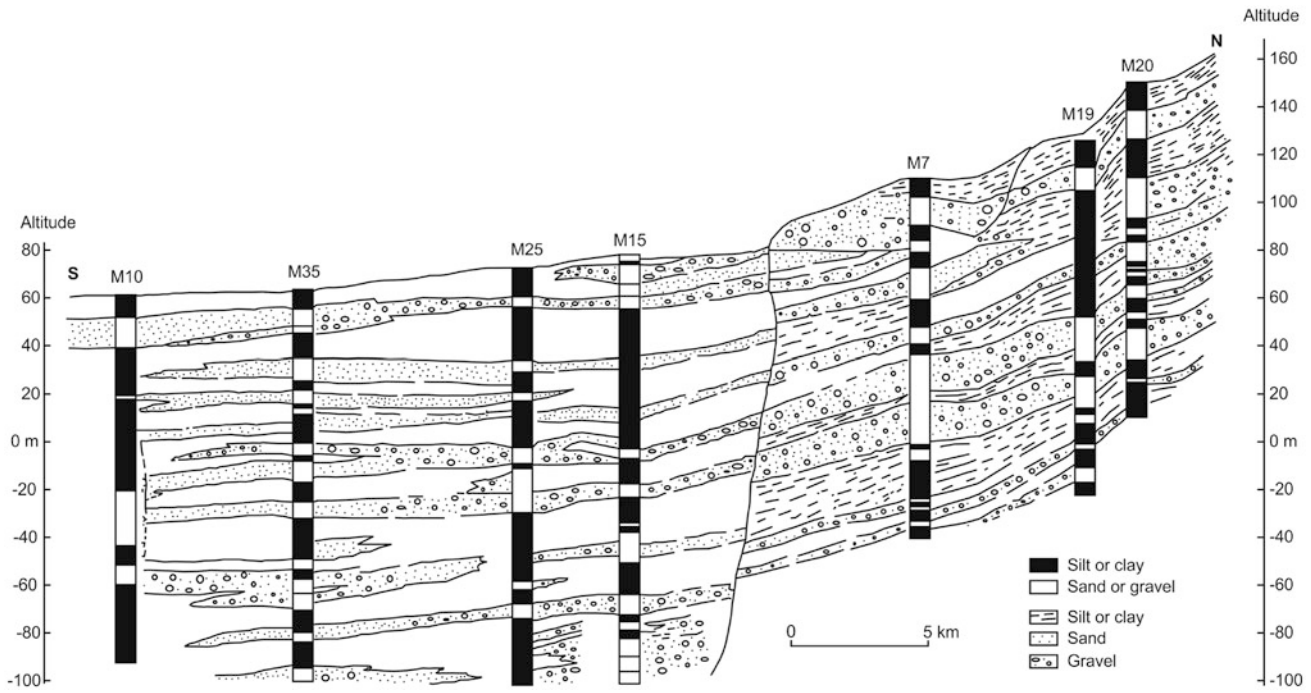

Fig. 34.1 Cross-section of the Terai belt depicting Pleistocene–Holocene sediments in the Mahottari District of east Nepal. *Source* Modified from JICA and DoI (1995)

limestone. Most of the material is highly weathered, resulting in the development of red soils and badlands (Yamanaka and Yagi 1984, p. 154).

The Higher Terrace represents mainly old alluvial fans, strongly reworked by subsequent streams. The Higher Terrace is well developed in the upper part of the Baulah Khola, Bhamke Khola, Patu Khola, and Hapur Khola. Owing to intense erosion, its outer margin is rather smooth, and the terrace as a whole is strongly dissected by gullies. It is a very thick (more than 56 m) filltop terrace whose base is frequently below the present riverbed (Yamanaka and Yagi 1984, p. 156). The fluvial deposits composing this terrace are made up of fining-upwards cycles of gravel, sand, silt, and clay. Most of the clasts were derived from slate, sandstone, quartzite, limestone, dolomite, and other Lesser Himalayan rocks. Generally, the material is strongly weathered, yielding reddish brown colors. The Higher Terrace lies at an elevation of 70 m from the present riverbed, where its height gradually decreases from upstream to downstream, and the terrace is gently dipping towards the downstream.

Like the Higher Terrace, the Middle Terrace, too, is basically the remnant of older fan surfaces developed in the north part of the Dang Valley. These terraces are excellently developed in the Patu Khola, Gwar Khola, Hapur Khola, and Sewar Khola. A few of them are also found in the west margin of the valley. The Middle Terrace can be divided up into two levels in the Gwar Khola. In comparison with the higher terraces, this terrace is less intensely dissected by streams or gullies, and its undulating surface becomes plane at the margins, where some subordinate terraces are also present (Yamanaka and Yagi 1984, p. 155). The Middle terraces also belong to the filltop category and are made up of more than 16 m thick gravels and fines, and their base is below the present riverbed. Towards the upper reaches, the terraces contain rounded to subrounded boulders, cobbles, pebbles, and sand, whereas while moving downstream their grain size steadily decreases, and the material is predominated by sand and silt. Most of the clasts are represented by phyllites, quartzites, slates, sandstones, and limestones. Although the terrace deposits are generally less weathered than those of the higher terraces, 2–3 m thick red soil is infrequently developed, especially towards the north. The Middle Terrace lies at an elevation of about 48 m from the present riverbed, and its height gradually decreases downstream. While approaching the south end, near the Babai River, the Middle Terrace merges with the Lower I Terrace.

The Lower I Terrace is extensively distributed in the Dang Valley and, like other older terraces, it was also developed out of coalescing alluvial fans formed by the rivers flowing from the Mahabharat Range. A narrow strip of these terraces is also found on the left bank of the Babai River (Fig. 34.3). These filltop terraces exhibit well-preserved flat and even surfaces, where their light brown to gray colored deposits have a maximum thickness of 26 m (Yamanaka and Yagi 1984, p. 155). The terrace base lies

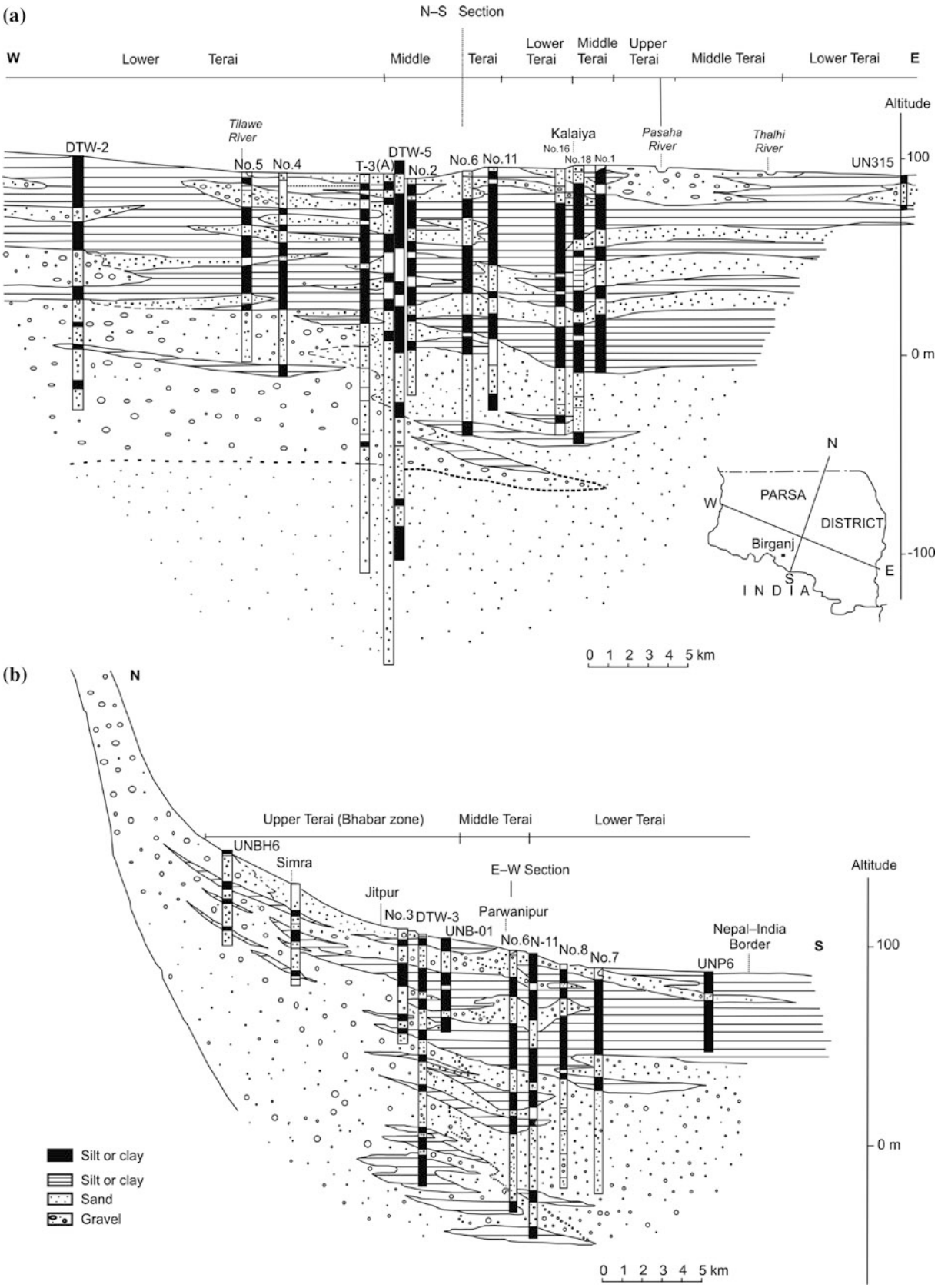

Fig. 34.2 Pleistocene to Holocene sediments deposited on Siwaliks in the vicinity of Briganj, central Nepal. The sediments are gently inclined to the south (*Note large vertical exaggeration* of scale). **a** North–south section; **b** East–west section. *Source* Modified from DoI (1993)

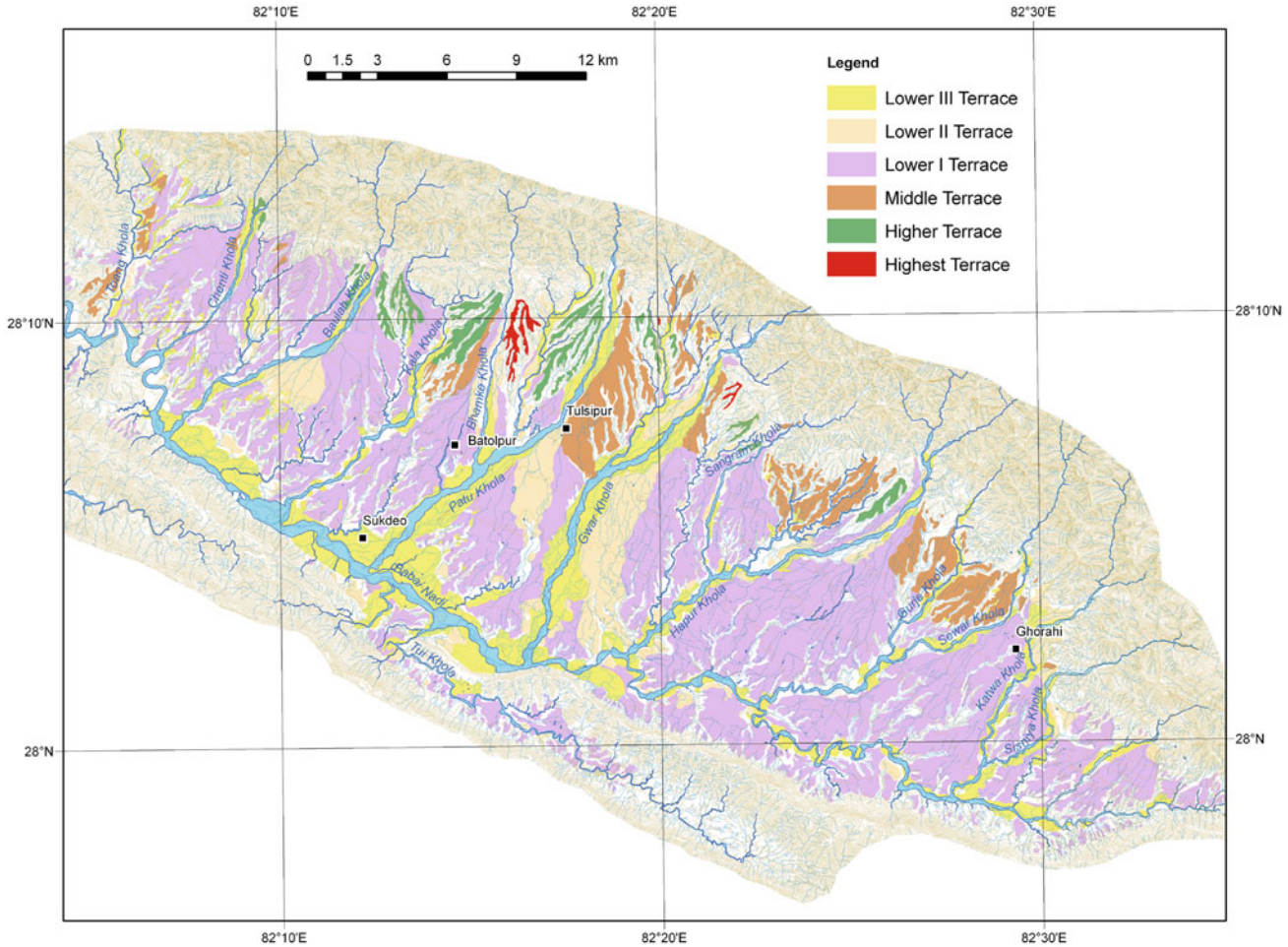

Fig. 34.3 River terraces in the Dang Valley. *Source* Modified from Yamanaka and Yagi (1984)

below the present riverbed in the central part of the valley, but it is exposed as an unconformity on the older terrace deposits along the north edge of the valley (Fig. 34.4). The material composing the terrace is made up of gravels and sands towards the upstream, and they become finer towards the downstream. Most of the material was derived from the Lesser Himalaya with the composition not different from the Middle and Higher terraces. On the other hand, towards

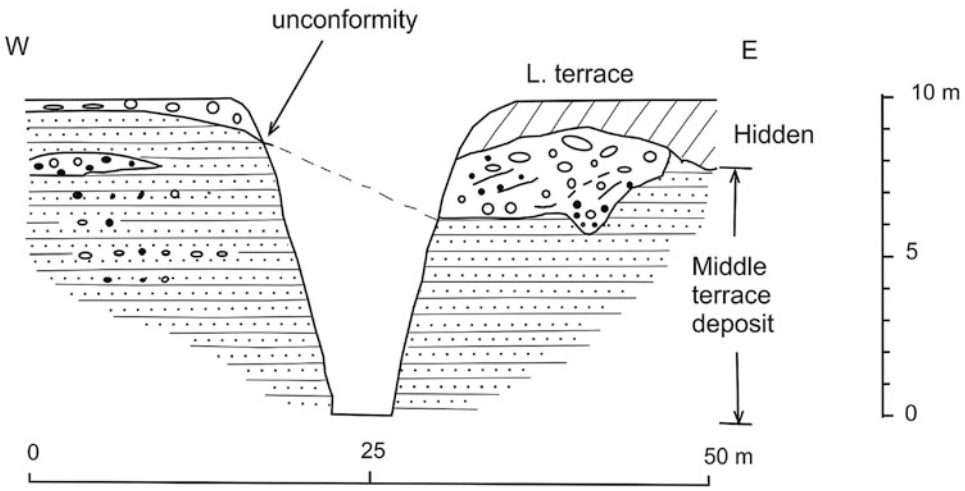

Fig. 34.4 Cross-section across the Bhamke Khola, showing an unconformity between the Middle and Lower terrace deposits. *Source* Modified from Yamanaka and Yagi (1984)

the south end of the valley, the Lower I Terrace is represented by the lacustrine deposits of dark gray to black silt and clay containing plant remains and gastropods. These deposits frequently interfinger with fluvial sequences. The elevation of the Lower I Terrace from the present riverbed ranges from 25 to 5 m. The terrace lies at a relatively higher elevation in the north and south margins of the valley than in its central part, and the north margin of the terrace gently dips due north on the banks of the Babai River. Based on radiocarbon dating, the terrace ranges in age from 16,000 to 26,000 BP, i.e. it was formed during the last glacial age (Yamanaka and Yagi 1984, p. 156).

The Lower II Terrace is developed mainly in the Hapur Khola and Patu Khola, where it lies either within the Lower I Terrace or occupies its outer margins. This fillstrath terrace was carved in the Lower I Terrace and has a flat upper surface. It consists of a few-meter-thick sand and gravel veneer, which is rather fresh and unconformably overlying the Lower I Terrace.

The Lower III Terrace forms the lowest level in the Dang Valley. It is made up of fresh gravels and developed along almost all rivers.

34.2.1 Tectonic Interpretations

As a rule, the terrace slopes become steeper, respectively, from the Lower Terrace to the Highest Terrace in the upstream direction, whereas they merge towards the center of the valley. On the other hand, the relative elevation of the Lower Terrace in the Patu Khola increases towards the downstream between Batolpur and Sukdeo and also towards the upstream between Batolpur and Dandakhuti (Yamanaka and Yagi 1984, p. 157). A similar trend is also observed in the Baulah Khola and Gwar Khola.

In the Dang Valley, younger fans are developed in front of older ones, and the resulting landform is made up of telescoped terraces. These facts indicate tectonic uplift of the Mahabharat Range. Inasmuch as each terrace merges with its stratigraphically subordinate counterpart in the center of the valley, and the base of the Lower I terrace is not exposed, the center of the valley was subsiding before the deposition of the Lower I Terrace (Yamanaka and Yagi 1984, p. 158).

34.3 Sediments of Pokhara and Neighborhood

Pokhara is the most picturesque valley nestled within the Midlands of west Nepal, in front of the snow-clad Annapurna Range. Diversely oriented terraces, deep and narrow gorges with disappearing white rivers, immense cliffs, and blue lakes are the main constituents of the basin landscape. Hagen (1969), Gurung (1970), and Sharma (1975) made early investigations in the area, whereas Hormann (1974) classified various terraces of the valley. Yamanaka et al. (1982) carried out detailed geological studies of sediments and geomorphic classification of terrace landforms, carved by the Seti River in the Pokhara Valley and neighboring tract. They also made paleomagnetic investigations and radiometric dating. The Pokhara Valley lies in the core of the Pokhara–Gorkha–Trishuli anticline (Fig. 34.5). The Pleistocene deposits of the Pokhara Valley overlie the phyllites, metasandstones, quartzites, and slates. They are divided into the following nine stratigraphic units (Yamanaka et al. 1982).

The Begnas Formation is confined essentially to the ridges southeast of Lake Begnas. A few isolated outcrops are also observed in the Seti Khola, south of Pokhara (Koirala et al. 1998). The sediments are conglomerates with ill-sorted, angular to subangular clasts of shale, sandstone, quartzite, and phyllite, derived from the upper or middle part of the Tethys Himalaya. This formation was deposited primarily as a talus during the early stage of basin development. The Begnas Formation is more than 80 m thick (Yamanaka et al. 1982, p. 117).

The Siswa Formation is represented by intensely weathered, loose, vivid red, lateritic conglomerate confined to the hills of Siswa and Khaireni. It contains a fluvial gravel with subrounded pebbles and cobbles of metasandstone, phyllite, and chlorite-sericite schist. The clasts were derived mainly from the Midlands, and were laid down by minor streams dissecting the valley. The Siswa Formation is more than 30 m thick, and it has lost its original depositional surface (Yamanaka et al. 1982, p. 118).

The Tallakot Formation constitutes a strongly cemented calcareous conglomerate succession found in the vicinity of Tallakot, south of Begnas Tal, and on the ridge southeast of Phewa Tal. This formation also occupies the area between the Bijaypur Khola and the Madi Khola. The Tallakot Formation is predominantly comprised of subrounded granules, pebbles, and cobbles bound in light brown calcareous cement. Most of the clasts were derived from the Tethys Himalaya. The clasts are ill sorted, and there also occur infrequent sand beds showing crude stratification. The Tallakot Formation is more than 200 m thick (Yamanaka et al. 1982, p. 118).

The Ghachok Formation is an extremely hardened conglomerate or breccia with a light brown silty matrix and calcareous cement. It contains angular to subrounded clasts of laminated gray limestone, laminated sandstone, and shale derived from the Tethys Himalaya. There also infrequently occur clasts of granite, gneiss, quartzite, and schist from the Higher and Lesser Himalaya. The pebbles and cobbles composing the Ghachok Formation are generally smaller in size than those found in the present riverbed of the Seti Khola.

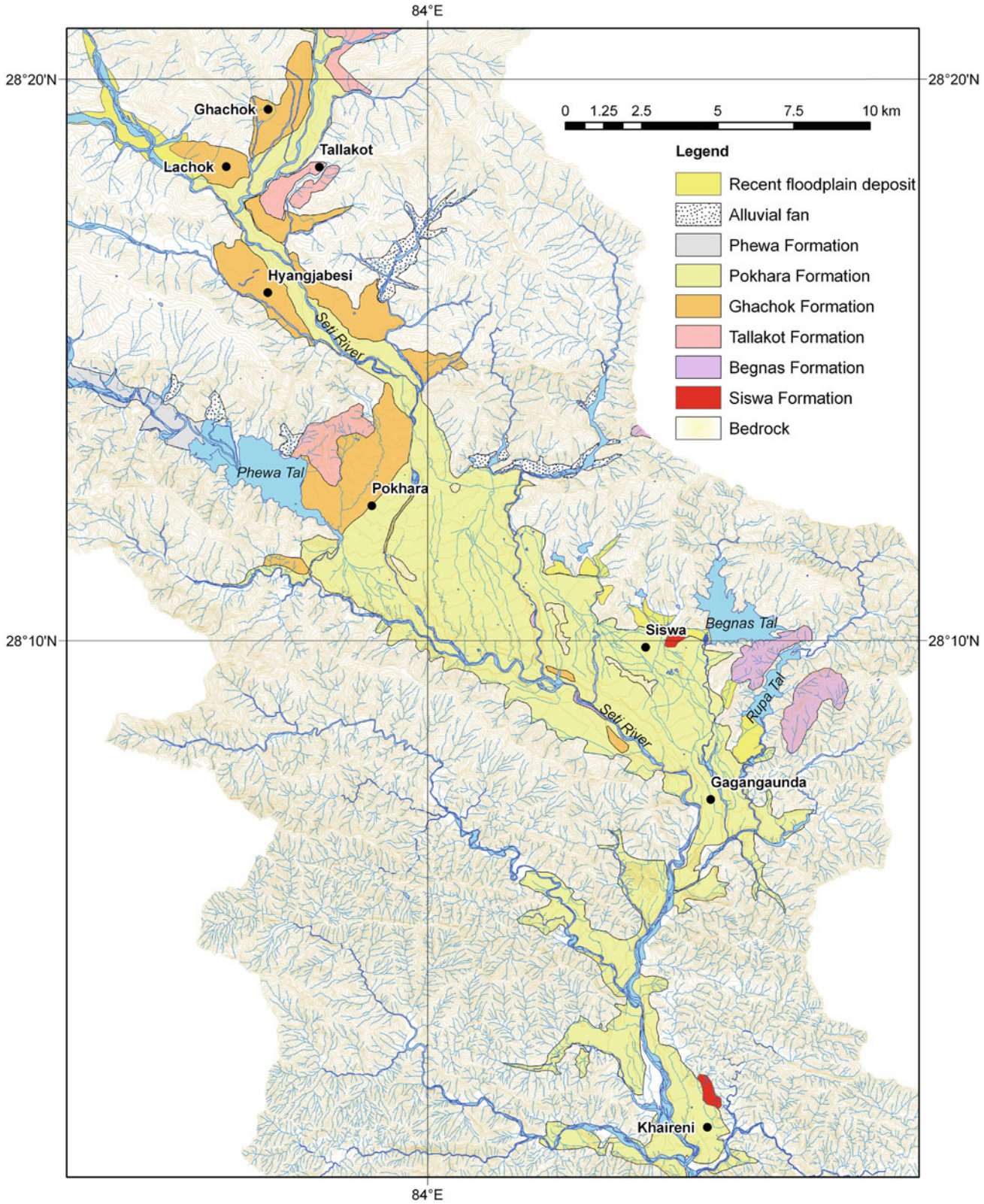

Fig. 34.5 River terraces distributed in the Seti Khola, between Khaireni and Pokhara. *Source* Modified from Yamanaka et al. (1982)

The ill-sorted clasts in the Ghachok Formation are poorly stratified. The lower part of the Ghachok Formation at Ramghat (Pokhara), shows well-developed bedding planes. Most of the material is represented by matrix-supported conglomerate with well-rounded cobbles and boulders (Dhital and Giri 1993). The upper part of the Ghachok Formation contains conical pinnacles covered with dark gray to black crust and the sinkholes between the pinnacles are filled up with soft to stiff yellow soil mixed with granules, pebbles, and even some boulders.

The lithofacies of the Ghachok Formation is similar to that of the Tallakot Formation, but the latter hardly contains any clasts of igneous or metamorphic origin. The Ghachok Formation exceeds 100 m in thickness at Ghachok and it is about 70 m thick at Ramghat. The total volume of the Ghachok Formation is about 9 km^3 (Yamanaka et al. 1982, p. 120).

The filltop Ghachok terrace exhibits a fan-shaped configuration around Lachok, Hemjabesi, Balichaur, and Pokhara (Fig. 34.5), and the Ghachok Terrace deposits enter the tributaries of the Seti River, such as the Yangadi Khola and the Kali Khola. The terrace surface is inclined upstream of the tributaries. This anomalous situation was presumably related to a sudden surge of Ghachok sediments in the Seti Khola and their encroachment into the neighboring tributaries (Yamanaka et al. 1982, p. 120).

There are from 45 to 75 m deep gorges in the Seti River between the K.I. Singh bridge and Ramghat, between Ramghat and Ratopaire, and farther downstream. These gorges range from a few meters to tens of meters wide and contain extremely hard Ghachok Formation as the main constituent. Many longitudinal tension cracks are developed in both bank s of the Seti Khola around the gorge. The tension cracks generate tens of meter wide and hundreds of meter long vertical blocks, which are aligned parallel to the riverbank and are generally toppled towards the river.

In the lower reach of the Harpan Khola and other tributaries debouching into the Phewa Lake, sediments began to settle down in the newly formed lake, synchronously with or immediately after the accumulation of the Ghachok Formation, and the sedimentation in the lake has continued up to the present. The Phewa Formation is made up of sand, silt, and clay and these sediments are assumed to have a conformable relationship with the Ghachok Formation (Yamanaka et al. 1982, p. 120).

The Pokhara Formation comprises fluvial gravel and sand accumulated by the Seti River. It forms a widely distributed filltop terrace. Apart from the fluvial deposits, there are also some interfingering lacustrine sediments. It is one of the extensively distributed formations in the valley and fills the valley, sharply cutting the Ghachok Formation in the north part of Pokhara. The Pokhara Formation is made up of subangular to subrounded pebbles and cobbles of limestone, calcareous shale, gneiss, granite, and schist. The igneous and metamorphic rock fragments are more abundant towards the upper part of the formation. Most of the gravel is ill sorted and crudely stratified. It is rather loose to poorly cemented. A gray to light brown matrix of calcareous silt or fine sand fills in the interstices of clasts. Generally, the top part of the Pokhara Formation is represented by a hard pan. As does the Ghachok Formation, the Pokhara Formation, too, extends into the tributaries at the Begnas Tal and some other locations (Yamanaka et al. 1982, p. 121).

The Pokhara Formation is divisible into three lithological units in the vicinity of Gagangaunda. Its lower and upper parts contain gray limestone gravel with light brown silt and fine sand. The deposits form cliffs facing the Seti Khola. The middle part of the Pokhara Formation includes gravel beds with dark gray calcareous shale pebbles and gray silt. This unit forms badlands with numerous irregular furrows and ribs. It conformably overlies the lower unit, but is separated from the upper unit by a disconformity (Yamanaka et al. 1982, p. 121).

In the Phusre Khola, the Pokhara Formation is represented by an approximately 80 m thick succession of lacustrine deposits containing laminated fine sand, silt, and clay. These light brown beds are infrequently alternating with fluvial gravels. There also occur very thin organic-rich beds with abundant plant fossils. The Pokhara Formation was accumulated between 1,070 and 590 BP (Yamanaka et al. 1982, p. 121).

The Rupakot Formation is similar to the Phewa Formation and consists of laminated fine sand, silt, and clay. These lacustrine deposits were accumulated contemporaneously with the Pokhara Formation. It is believed that there were many lakes in the northeast part of the Pokhara Valley prior to the development of the Pokhara Formation. Most of these lakes are now filled up with sediments, however, sedimentation is still ongoing in the remaining lakes, such as the Rupa Tal. On the other hand, owing to the lithological similarity between the lake deposits of the Pokhara Formation and those of the Rupakot Formation, it is difficult to separate these two formations.

The Pokhara Formation has been reworked by the Seti River, and a gravel veneer is deposited on top of it with an erosional surface. The gravel veneer forms a fillstrath terrace surface (Yamanaka et al. 1982, p. 122). The poorly sorted gravel contains boulders, cobbles, and pebbles of gneiss, schist, quartzite, and phyllite. Their size ranges from 4 mm to 1 m. Sand is present as a layer or in the matrix of the gravel. The gravel veneer is loose and its thickness varies from 3 to 6 m (Dhital and Giri 1993).

Recent floodplain deposits are found in the Seti Khola and its main tributaries. They contain boulders, cobbles, and pebbles of limestone, gneiss, quartzite, phyllite, schist, and granite.

34.3.1 Origin of Lakes

There are numerous small and large lakes in the Pokhara Valley, and the most important ones are the Phewa Tal, Begnas Tal, and Rupa Tal (Fig. 34.5). There also exists some evidence of extinct lakes at Phusre and Bijaypur. Hagen (1969), Sharma et al. (1978), and some other investigators inferred a single large paleo-lake, the remnants of which are the existing ones. Hormann (1974) and Yamanaka et al. (1982) have denied the occurrence of such a big lake and demonstrated that the lakes were formed in consequence of some catastrophic debris flows in the Seti Khola. The flows originating from the lower slopes of the Annapurna Range rapidly approached the wide Pokhara Valley where they dumped most of the debris and simultaneously dammed the tributaries. The first calamitous flow transported the debris constituting the Ghachok Formation and produced the Phewa Tal and other lakes. The second event occurred about 1,000 BP, when again much sediment was rapidly and catastrophically accumulated in the Seti Khola Valley. The second flow cut into the Ghachok terrace upstream from Pokhara. Thus the dammed lakes were formed twice during the Pleistocene.

34.3.2 Tectonic Implications

Although the Ghachok Formation and Pokhara Formation are similar in composition, their terraces are not parallel but partly overlap each other (Hormann 1974). This kind of relationship (Fig. 34.6) is attributed to the tectonic movement. The average gradient of the Ghachok Formation is 3.1 %, whereas that of the Pokhara Formation is 2.4 %. Hence, the relative amount of tilt is 0.7 % or 7 m/km from the time of accumulation of the Ghachok Formation. The relative height between the Ghachok Terrace and the Pokhara Terrace decreases downstream (i.e., to the south) and the Ghachok Terrace crosses the Pokhara Terrace below the city of Pokhara (Yamanaka et al. 1982, p. 123). Thus the relatively higher gradient of the Ghachok Terrace is attributed to the upheaval of the region north of Pokhara.

34.4 Kathmandu Basin Fill

The intermontane valley of Kathmandu (Fig. 34.7) is surrounded by the Phulchauki and Chandragiri mountain ranges, comprising sedimentary rocks of the Phulchauki Group from the south and west, and it is bordered by the Shivapuri (or Sheopuri) Range, containing metamorphic rocks of the Bhimphedi Group together with gneisses and migmatites to its north and east. Its tectonic position is similar to that of the Kashmir Valley in the Northwest Himalaya. The amphitheater-shaped Kathmandu Basin is situated around the headwaters of the Bagmati River with a high valley floor. The Bagmati River originates from the Midlands, whereas other large rivers in Nepal rise in the Great Himalaya or the Tibetan Plateau and cut deep gorges through the Midlands (Yonechi 1973). The valley is filled up with Plio–Pleistocene fluvial, fluvio-lacustrine, and fluvio-deltaic sediments. The monotony of these horizontally disposed sediments is occasionally breached by a few hillocks of bedrock.

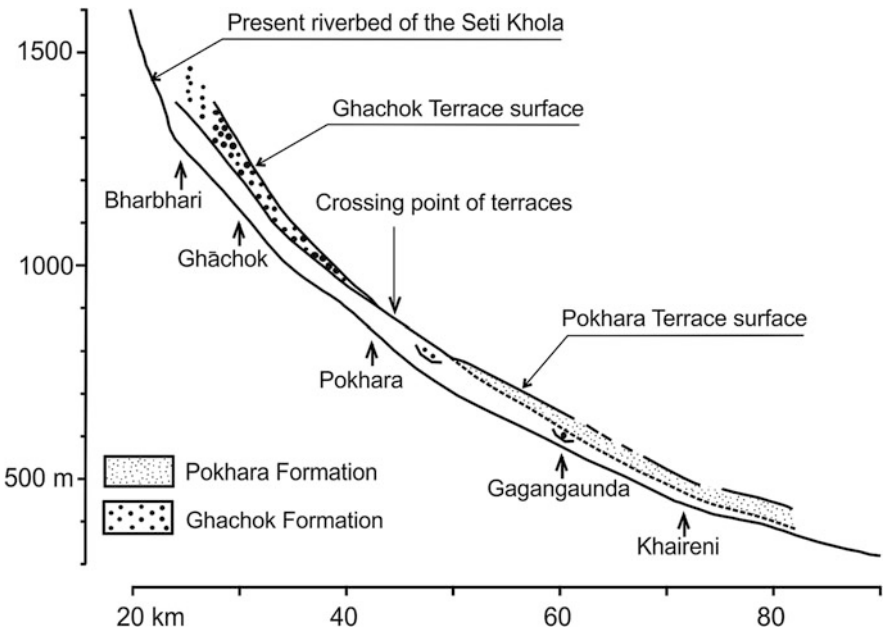

Fig. 34.6 Overlapping Ghachok and Pokhara terraces of the Seti Khola. *Source* Modified from Yamanaka et al. (1982)

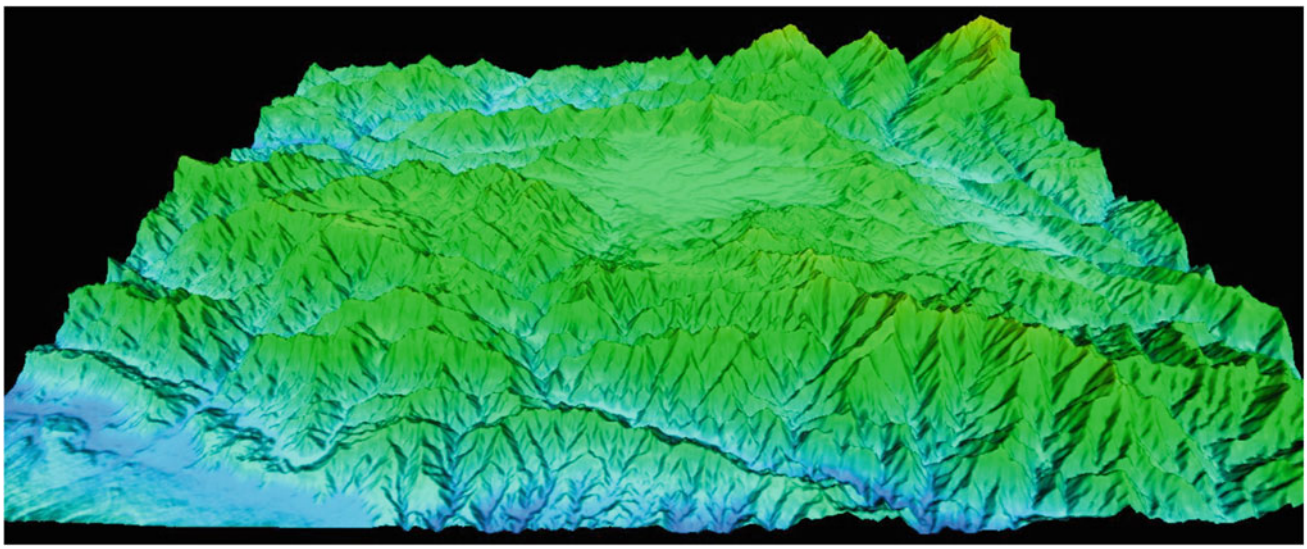

Fig. 34.7 Digital elevation model of Kathmandu Valley and surrounding areas in central Nepal. *Source* SRTM DEM

The oval Kathmandu Basin is about 30 km long in the east–west direction and about 25 km wide in the north–south direction. The valley occupies an area of about 650 km^2, and its altitude ranges from 1,220 m at the outlet of the Bagmati River south of Dakshinkali to 1,380 m towards the north. The Bagmati is the trunk river as well as the only drainage outlet of the valley. The centripetal drainage pattern of the valley is facilitated by many tributaries flowing from every direction. For example, the Bishnumati and Dhobi Khola come from the north, Hanumante from the east, Godavari from the southeast, and Nakhu Khola from the south. However, a detailed examination of streams also reveals a rectangular drainage pattern (Yonechi 1973). Morphometric analysis of the Bagmati River indicates that some of its tributaries have developed relatively stable channels. However, the sixth-order Bagmati River shows some signs of immaturity (Bajracharya and Verma 1989).

Hagen (1969) remarked that the Bagmati River could not keep pace with the rising Mahabharat Range and was dammed to form a lake in the early Pleistocene. Koirala et al. (1993) found interbedded lacustrine and fluvial deposits in the south margin of the basin and inferred multiple episodes of damming. Yonechi (1973) identified the following surfaces in the Kathmandu Basin: (1) Kirtipur Surface, (2) Patan I Surface, (3) Patan II Surface, (4) Kathmandu I Surface, and (5) Kathmandu II Surface, respectively, from top to bottom.

Moribayashi and Maruo (1980) carried out a gravimetric survey to map the basement topography of the valley and came up with a maximum depth of about 650 m in the vicinity of Baneshwar. They found that the lake deposits are of low density and thicker in the central portion of the basin. They also detected an essentially north–south extending trough, which could represent the proto-Bagmati River of Hagen (1969).

Kizaki (1994) divided up the paleo lake of Kathmandu into older and younger types, where the older lake gradually shifted from south to north owing to the upheaval of the Mahabharat Range.

The lacustrine and fluvial deposits of the valley contain peat, clay, carbonaceous clay, sand, gravel, and boulders. They lie unconformably on the rocks of the Phulchauki and Bhimphedi groups. Dhoundial (1966) made early investigations in the Kathmandu Valley and classified the sediments into the Basal Boulder Beds (a thick succession of boulders and pebbles), confined to the south margin of the valley, the Lokundol Formation (lignite, soft carbonaceous clay, silt, and sand), Kalimati Formation (carbonaceous clay, silt, and sand), and Sankhu Formation (pebbly sand, silt, and clay) developed towards the north part of the valley, and the Chapagaon Formation (pebbles, granules, sand, and silt) distributed to the south of the valley.

Yoshida and Igarashi (1984) carried out a detailed mapping as well as paleomagnetic and pollen investigations of the sediments. They divided up these deposits into the following eight stratigraphic units: (1) Lukundol Formation; (2) Pyanggaon Terrace Deposit, (3) Chapagaon Terrace Deposit, (4) Boregaon Terrace Deposit, (5) Gokarna Formation, (6) Thimi Formation, (7) Patan Formation, and (8) Lower Terrace Deposits. Subsequent investigations have documented a complex distribution of sediments in the valley. For example, Sakai (2001) has included the above three terrace deposits under his Itaiti Formation. He also divided the sediments of the Kathmandu Valley into the Tarebhir, Lukundol, and Itaiti formations in the south, and the Bagmati Formation, Kalimati Formation with Basal

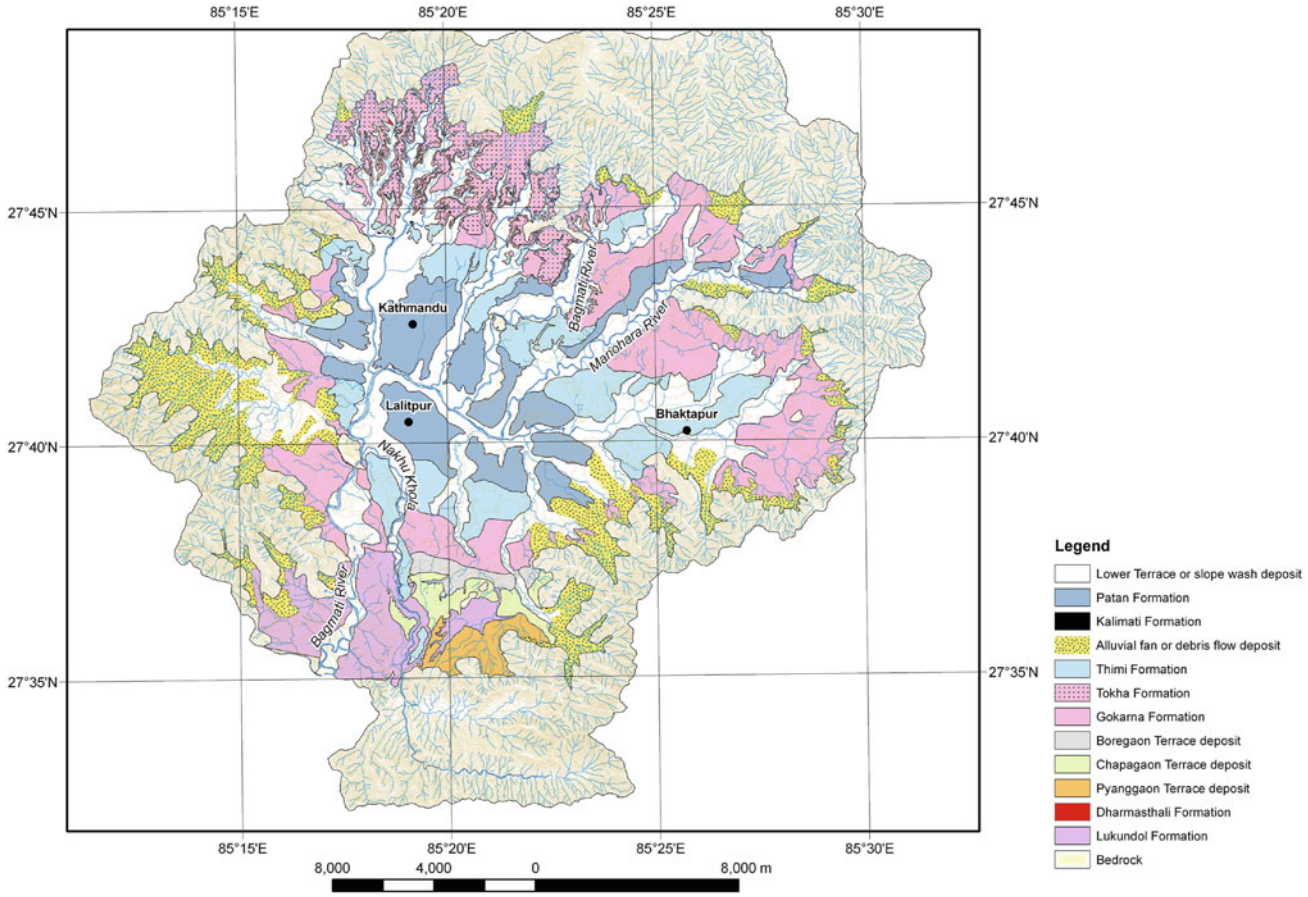

Fig. 34.8 Fluvio-lacustrine deposits of the Kathmandu Valley. *Source* Modified from Yoshida and Igarashi (1984), Shrestha et al. (1998), and Sakai et al. (2008)

Lignite Member, and Patan Formation in the central part of the valley. In the north part of the basin, Shrestha et al. (1998) and Dill et al. (2003) have separated the Tokha Formation, representing primarily braided stream deposits and the Gokarna Formation, predominated by anastomosing streams. The main lithostratigraphic units distributed in the Kathmandu Basin are the following.

The Lukundol Formation (Fig. 34.8) contains weakly consolidated clay, silt, and sand beds with lignite intercalations. The clays and silts are frequently carbonaceous and include plant remains (Yoshida and Igarashi 1984). This formation is developed only in the south fringe of the basin and unconformably rests on the rocks of the Phulchauki Group. The Lukundol Formation is more than 600 m thick and is subdivided into the following members (Dongol 1985).

The Basal Conglomerate Member is well exposed in the Khahare Khola and Tare Bhir. This unit is also defined as the Tarebhir Formation (Sakai 2001). Its exposed thickness is about 60 m at Tarebhir and it is about 350 m thick in the vicinity of Dukuchhap. It contains cobble- and pebble-conglomerates with lenses and thin beds of sand and silt. The rounded to subrounded clasts are made up of gray to green-gray metasandstone, dark green phyllite, pink quartzite, limestone, and granite. The presence of tourmaline granite boulders of up to 2 m diameter indicates that the material was supplied from the Narayanthan or Palung granites. The paleocurrent direction is towards the west to northwest. These conglomerates grade into pebbly sandstone, cross-bedded sandstone, and siltstone, showing a southerly flow direction of the ancient drainage (Dongol 1985, p. 46).

The Basal Member is followed upwards with an erosional contact by a well-bedded succession of sandstone, siltstone, and mudstone, belonging to the Lignite Member. In this member, there are a few lignite seams, ranging from 1.5 to 2 m in thickness. Tuladhar (1982) identified seven lignite horizons from this member. There also occur massive, pebbly, mud beds deposited from the debris flow. This member has also been redefined as the Lukundol Formation (Sakai 2001). It attains a thickness of 115 m. This unit was deposited primarily in a lake with some input from the debris flow and delta (Dongol 1985).

Dongol (1985) reported a number of vertebrate fossils from the Lignite Member. They include teeth of *Elephas* (cf. *E. hysudricus* and *E. planifrons*), teeth of Artiodactyla, a tooth of pig, three horn pieces, and a number of bovid metacarpals. The fossil records mentioned in some earlier or subsequent publications are spurious (Talent et al. 1991). Hence, the fossils described in papers with V.J. Gupta as author or coauthor as well as those referring to his works are omitted.

The Laminated Silt Member succeeds the Lignite Member without any stratigraphic break. It is composed of silt and clay and contains many leaf imprints. This member is about 40 m thick and was deposited primarily in a lake (Dongol 1985).

The Upper Gravel Member is about 50 m thick and overlies the Laminated Silt Member along the Chhampi–Itari Ridge. It is represented by pebble-, cobble-, and boulder-conglomerates, bearing clasts of metasandstone, quartzite, limestone, phyllite, and slate. They represent alluvial fan and fluvial deposits, derived from the rocks of the Phulchauki–Chandragiri Range (Dongol 1985).

The Pyanggaon Terrace Deposit (Fig. 34.8) is found only in the southern part of the valley, where it unconformably overlies the bedrock or the Lukundol Formation. It consists of rounded to subrounded pebbles and cobbles of fluvial gravel derived from limestone, metasandstone, and phyllite. It is more than 5 m thick near Pyanggaon. Its elevation from the Bagmati River ranges from 180 to 240 m (Yoshida and Igarashi 1984).

The Chapagaon Terrace Deposit is also confined to the south of the Kathmandu Valley and disconformably overlies the Lukundol Formation. This terrace deposit is about 10 m thick at Chapagaon and contains subrounded pebbles and cobbles of limestone, metasandstone, and phyllite. The terrace deposit exhibits red weathered colors and its elevation from the Bagmati River varies from 160 to 180 m (Yoshida and Igarashi 1984).

The Boregaon Terrace Deposit, too, is distributed only to the south of the valley and disconformably overlies the Lukundol Formation. It comprises rounded pebbles and cobbles derived from the south mountain range. There are also some silt and sand beds intercalated with the gravel. This terrace deposit is more than 5 m thick and its elevation from the Bagmati River varies from 120 to 160 m (Yoshida and Igarashi 1984).

The Dharmasthali Formation is present only in the northern part of Kathmandu (Fig. 34.9), and consists of silt beds with some intercalations of gravel and sand (Sakai et al. 2008). This formation is about 30 m thick and unconformably overlies the bedrock. Occasionally, the strata gently dip due south, and they may represent the topographic inclination during their deposition. Some thick to very thick, poorly sorted, massive gravel and sand beds contain plant debris. These sediments were deposited in subaqueous slopes and represent debris flow, small-scale grain flow, and meandering river deposits (Sakai et al. 2008). Based on paleomagnetic dating by Gautam et al. (2001), these rocks are older than 780 ka and can be correlated with the Tarebhir, Lukundol, and Itaiti formations distributed in the south margin of the valley (Sakai et al. 2008).

The Kalimati Formation is predominantly made up of black clay or silt (Kalimati in Nepali) beds with some thin beds of fine to very fine sand and diatomite (Sakai et al. 2008). This formation is more than 200 m thick (Dill et al. 2001). The sediments were accumulated in the center of the lake, mainly from suspension and they represent the prodelta deposits interrupted by infrequent turbidity flows from an adjacent delta. Their age ranges from approximately 12,800 BP to more than 29,300 BP. This formation is a basinwards equivalent of the Patan, Tokha, and Thimi formations, and this thick sequence may also include the older Gokarna Formation equivalents, lying at deeper levels (Sakai et al. 2008).

The Gokarna Formation is a fluvio-lacustrine deposit that occupies the north part of the valley. It contains dark brown colored, laminated arkosic sand, silty clay, and peat. There also occur some diatomite-bearing black silt and clay beds. This formation frequently contains fossil wood. The Gokarna Formation is more than 21 m thick at Gokarna, it is about 70 m thick at Mulpani, and more than 50 m thick at its south margin. Its elevation from the Bagamti River varies from 80 to 120 m, and its age ranges from 50 to 34 ka (Yoshida and Igarashi 1984; Sakai et al. 2008). The Gokarna Formation was deposited in a variety of fluvial, deltaic, and lacustrine environments. South of Gokarna, it contains: (1) thick cross-stratified sand interbedded with mud and gravel (about 20 m thick) representing delta front deposits that are followed to the north by (2) black sandy silt (up to 5 m thick) and sand interbeds with wave-ripple and climbing-ripple laminations belonging to the delta succession; (3) parallel beds of prodelta deposits; (4) tabular cross-bedded sand beds (up to 10 m thick) of delta front deposits; and (5) parallel or trough cross-stratified gravelly sand or sandy gravel with silt beds (about 2 m thick) accumulated in both meandering and braided streams (Sakai et al. 2008).

The fluvio-lacustrine Thimi Formation is also distributed mainly in the north part of the valley. It disconformably overlies the Gokarna Formation and grades basinwards to the Kalimati Formation (Sakai et al. 2008). This formation contains gray to light brown colored sediments, represented by arkosic sand, silt, clay, peat, and gravel. The gravel is exclusively made up of gneiss and granite clasts derived from the Shivapuri Range. This formation is about 13 m thick at Pashupati Nath and its elevation from the Bagmati River ranges from 50 to 80 m (Yoshida and Igarashi 1984). Some sand beds exhibit large-scale (up to 20 m thick) cross-

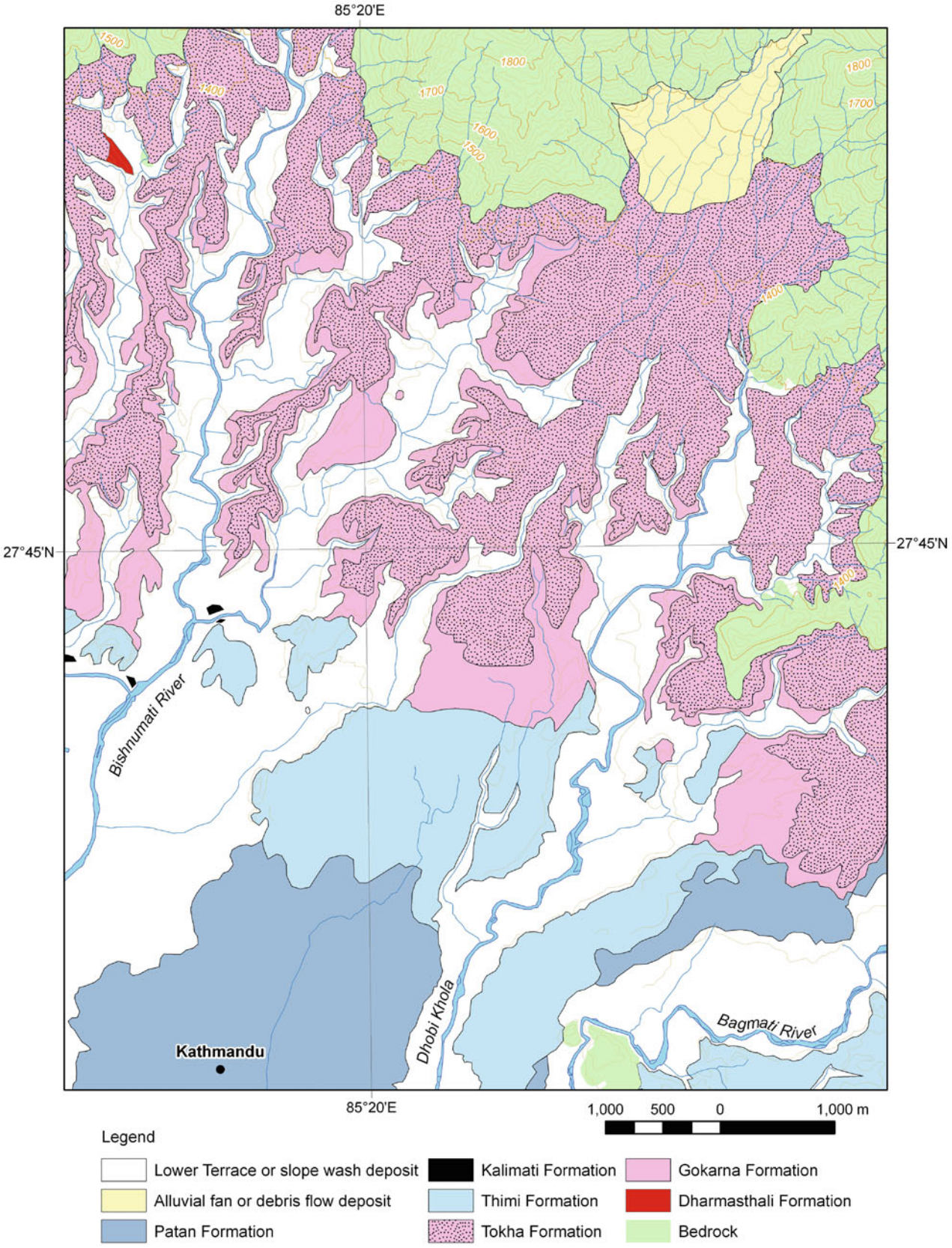

Fig. 34.9 Fluvio-lacustrine sediments comprising the northern part of the Kathmandu Valley. *Source* Modified from Shrestha et al. (1998) and Sakai et al. (2008)

stratification in the southern margin of the Thimi terrace. Its depositional environment is similar to that of the Gokarna Formation and its depositional age ranges from 34 to 24 ka (Sakai et al. 2008).

Shrestha et al. (1998) identified the Tokha Formation in the north part of the valley, whereas Yoshida and Igarashi (1984) had included this formation under their Gokarna Formation. Sakai et al. (2008) identified an erosional hiatus between the Gokarna and Tokha formations. The Tokha Formation has a flat base and begins with pale green silt or silty sand, and some gravel lenses followed by black silt with a thin diatomite horizon. There are also areas where the Tokha Formation commences with very thick (up to 3 m) black silt with diatomite, succeeded by very thick (up to 5 m) sand beds with large-scale cross-stratification and some gravelly sand and black silt beds. This formation was deposited in streams and marshes. The diatomite-bearing black slit and overlying sand were deposited in prodelta and delta front environments, respectively. This formation ranges in age from 20 to 14 ka (Sakai et al. 2008).

The Patan Formation is distributed mainly in the city areas of Patan and Kathmandu, and it conformably overlies the Kalimati Formation in the central part of the basin, but shows an erosional hiatus on the Thimi and Gokarna formations. Some isolated exposures are also seen in the cut banks of the Bagmati and Manohara rivers. It contains gray to light brown fluvio-lacustrine deposits, consisting of laminated arkosic sand, silt, clay, and peat. Its elevation from the Bagmati River varies from 20 to 50 m (Yoshida and Igarashi 1984). The lower part of this formation, containing thick, cross-bedded sand, belonging to a delta front, passes northwards to interbedded mud and sand beds of fluvial channel and floodplain. The Patan Formation ranges in age from 14 to 10 ka (Sakai et al. 2008).

The Lower Terrace deposits are extensive along the Bagmati River and its tributaries. The sediments contain micaceous sand, pebbles, and granules. Their terrace surface is about 5–15 m above the present riverbed of the Bagmati (Yoshida and Igarashi 1984).

34.4.1 Paleoclimate in Kathmandu Valley

A comparison of recent and fossil pollens of *Quercus* and *Pinus* indicates an increase in temperature of the Kathmandu Valley by 4–13 °C since the Pliocene (Nakagawa et al. 1996). Similarly, sedimentological and palynological investigations in the Kathmandu Valley revealed significant changes in the depositional environment of the paleo-lake by about 1 Ma, and such changes are attributed to the upheaval of the Mahabharat Range (Fujii and Sakai 2001, 2002). Palynological investigations of *Quercus* and *Pinus* taxa from the Lukundol Formation indicate an approximate 1,000 m downward shift of vegetation in the Kathmandu Valley during the late Pleistocene (Paudayal and Ferguson 2004; Paudayal 2006). Bhandari and Paudayal (2007) separate three pollen zones in the Lukundol Formation, where Zone I experienced primarily a subtropical climate, Zone II was subjected to a warm temperate climate, and Zone III faced a subtropical to warm temperate climate.

34.5 Thakkhola–Mustang Graben

The valley of Thakkhola (*thak* = red, *khola* = river) lies north of the main Himalayan Range (i.e., on its lee side) in central Nepal. It is an Inner Himalayan Basin (Hagen 1969) located in the upper reach of the Kali Gandaki River, also called locally the Thakkhola. This antecedent river originates from the Tibetan marginal ranges and flows essentially due south. After leaving the Thakkhola Valley behind, the river breaks through the Great Himalayan Range between Dhaulagiri and Annapurna, where it makes the deepest canyon in the world, and flows swiftly towards the Midlands. But, in the neighboring Thakkhola Valley, the Kali Gandaki River forms a wide braided floodplain.

The outstanding upheaval of the Tibetan Plateau is attributed to various mechanisms, such as crustal thickening due to continental subduction (Argand 1924), convective removal of the lower part of the thick Asian lithosphere (Platt and England 1994), and formation of a thick and strong lithosphere (Jackson et al. 2008). Similarly, the widespread development of normal faults is linked up to different processes, including the eastwards extrusion of Tibet (Armijo et al. 1986), isostatic response to removal of the mantle lithosphere (England and Houseman 1986; Platt and England 1994), and lower crustal flow (Royden et al. 1997). This Cenozoic east–west extensional phase of Tibet (Molnar and Tapponnier 1978) has created many small and some large grabens dated about 14 or 8 Ma (Coleman and Hodges 1995; Harrison et al. 1995; Blisniuk et al. 2001). Some of the important ones are the Thakkhola–Mustang Graben, Gyirong Graben, and Yadong Graben.

The Thakkhola–Mustang Graben (Fig. 34.10) is about 90 km long and 20–30 km wide. Its altitude at the bottom varies from 3,000 to 4,000 m, and it is surrounded by many peaks higher than 6,000 m. The graben is delimited to the west by the Dangarjong normal fault zone (Hagen 1968, p. 130) and to the south by the South Tibetan Detachment System (Hurtado et al. 2001). On the other hand, its eastern limit is rather ill defined, and to the north, the graben disappears before reaching the Indus–Tsangpo Suture zone. The Muktinath fault lies at the east border of the basin (Bordet et al. 1971). About 18 Ma old Mustang–Mugu leucogranites are intruded to the northwest of the graben (Le Fort and France-Lanord 1994; Harrison et al. 1997).

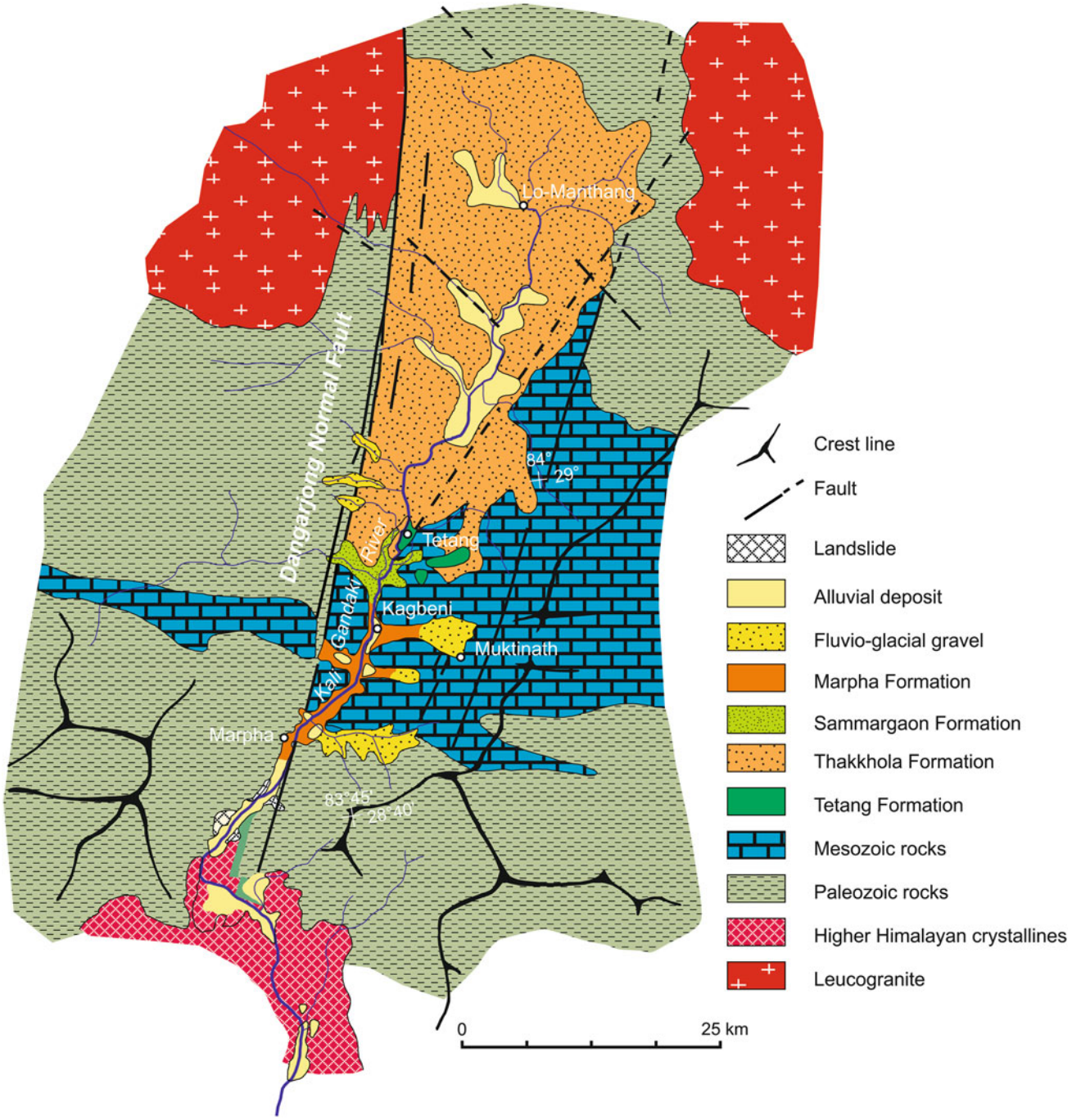

Fig. 34.10 Schematic geological map of the Thakkhola–Mustang Graben. *Source* Modified from Fort et al. (1982) and Hurtado et al. (2001)

Hagen (1959, p. 716) included the sediments filling this syntectonically developed asymmetric basin in his Thakmar (*thak* = red, *mar* = stone) series. The graben fill consists of more than 870 m thick Miocene to Pleistocene fluvial, lacustrine, and palustrine sediments that unconformably rest over the Paleozoic and Mesozoic rocks (Colchen 1999). The sediments of the Thakmar Group are further classified into the Tetang and Thakkhola formations (Bassoullet and Colchen 1974). These two formations are overlain disconformably by the Sammargaon and Marpha formations together with the Lower terrace deposits of the Kali Gandaki River (Fort et al. 1982; Garzione et al. 2003).

The Tetang Formation (Figs. 34.11 and 34.12) is restricted in its distribution to the southeast part of the graben (Fig. 34.10). This formation is well exposed in the vicinity of the village of Tetang and in the Dhinkyo Khola. It

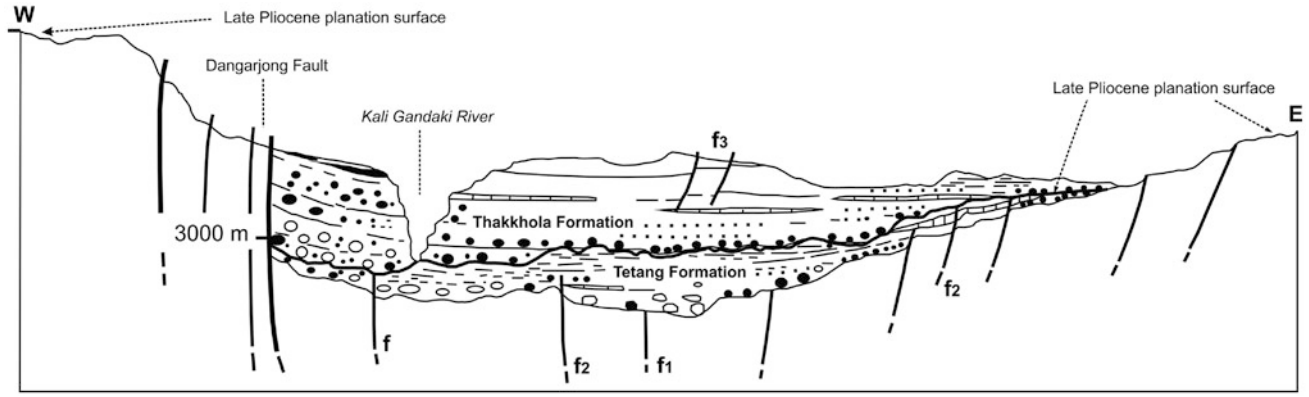

Fig. 34.11 Schematic cross-section of the Thakkhola–Mustang Graben, illustrating important tectonic features of the basin. f1–f2: faults of different phases in the basement rocks. *Source* Modified from Fort et al. (1982) and Colchen (1999)

is composed of fluvial conglomerates and sandstones, with some intercalated lacustrine limestone, calcareous silt, and siltstone. In it, some thin beds of lignite are also present (Yoshida et al. 1984). The conglomerate contains rounded to subrounded pebbles and cobbles of quartzite, limestone, phyllite, shale, sandstone, and granite. The Tetang Formation is more than 200 m thick. This formation is divided into the following four units (Adhikari 2009).

1. The basal unit is about 65 m thick, and it is composed mainly of conglomerates containing pebbles, cobbles, and boulders of quartzite, shale, sandstone, and carbonate rock. Their clasts were derived mainly from the neighboring Mesozoic bedrock. Some massive conglomerate beds attain a thickness of 22 m. A few sandstone lenses are also intercalated in the conglomerate beds containing imbricated pebbles.
2. An interbedded sequence of conglomerate, sand, and silt of about 50 m thickness overlies the basal unit. This sequence also contains some carbonate- and iron-rich concretions. The conglomerate beds range in thickness from a few centimeters to 2 m, whereas the sandstones and siltstones are from 2 to 30 cm thick.
3. The last sequence is followed upwards by a 57 m thick succession, made up of sand-dominated fining-upwards cycles with some conglomerates at the base and siltstones at the top. The sandstones exhibit parallel and cross-laminae, whereas the conglomerates contain imbricated pebbles. There also occur a few fine sandstone or siltstone beds containing plant remains.
4. The uppermost part of the Tetang Formation is composed of a 43 m thick sequence of fine sandstone and siltstone with a minor amount of very fine-grained limestone. The siltstone beds frequently contain plant fossils and the limestones yield ostracods.

A low-angle unconformity separates the Thakkhola Formation from the underlying Tetang Formation (Fort et al. 1982). The Thakkhola Formation covers mainly the central and north parts of the graben (Fig. 34.10). Most of the succession is represented by alluvial fan and fluvial conglomerates with subrounded pebbles and cobbles of limestone, quartzite, sandstone, and granite. Some beds of lacustrine limestone, calcareous siltstone, and sandstone also occur at various intervals. The Thakkhola Formation is more than 600 m thick and younger than 8 Ma (Garzione et al. 2000, 2003). This formation is divided up into the following units (Adhikari 2009).

1. The lowermost unit occurs as a 182 m thick sequence of conglomerate and coarse sand. The pebbles composing the conglomerate were derived mainly from the Paleozoic rocks and the Tertiary granite of Mustang. The conglomerate beds range in thickness from 2 to 20 m.
2. The second sequence is 138 m thick and comprises fining-upwards cycles of conglomerate, sandstone, and siltstone. The conglomerates display a heterogeneous clast composition, and are included in a red and orange matrix. The average clast size in the conglomerates is about 3 cm, whereas the interbedded sandstones are generally coarse- to fine-grained. The siltstone beds are infrequently bioturbated, and some of them contain plant fossils. Carbonate- and iron-rich concretions abound in the sandstone and siltstone beds.
3. The succeeding 180 m thick unit begins with a 15 m thick black siltstone bed, which is followed upwards by a variety of fine-grained sandstone, polymictic conglomerate, lacustrine limestone, and siltstone. The imbricated pebbles in the conglomerate have clasts of Paleozoic and Mesozoic rocks. The limestone is made up of micrite and microsparite with some oncolites and algal mats. On the other hand, the bioturbated siltstones contain sporadic root strands and abundant calcareous concretions.
4. The uppermost 123 m thick sequence of the Thakkhola Formation consists of bioturbated siltstones and sandstones. They are intercalated with conglomerate beds, which generally display imbricated pebbles. In this unit,

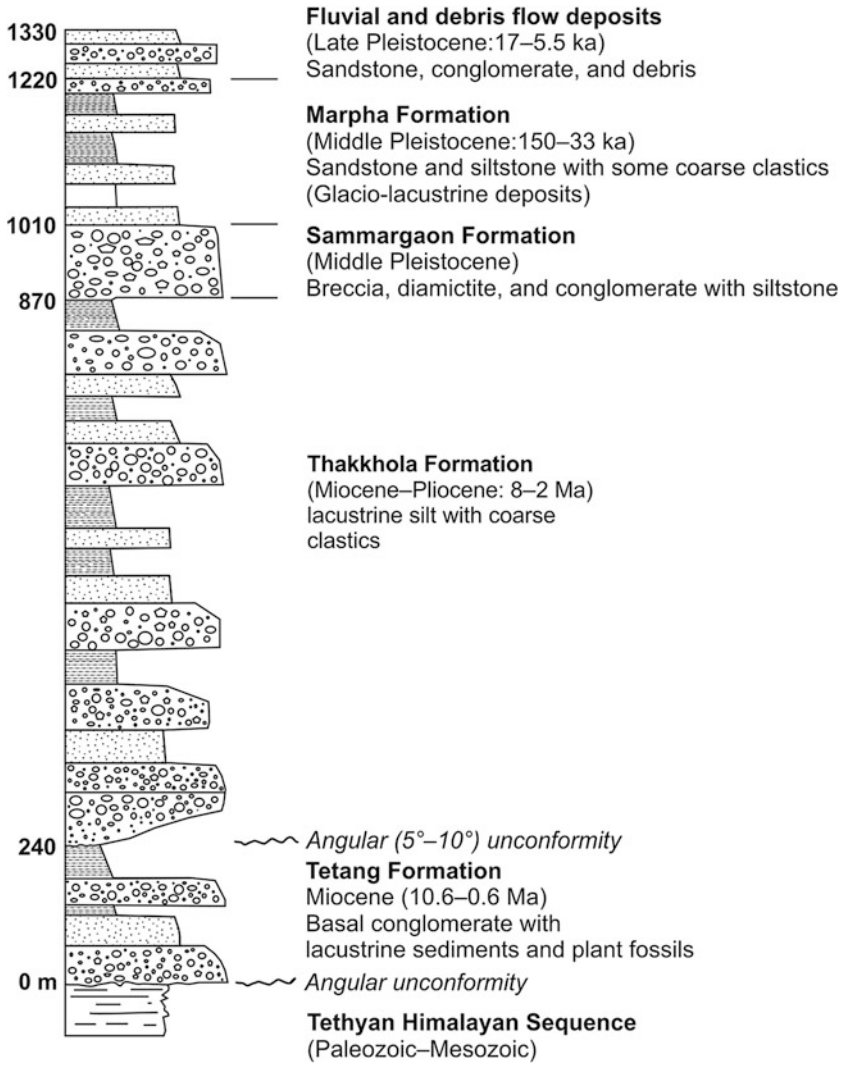

Fig. 34.12 Generalized lithostratigraphic column of the Thakkhola Basin fill. *Source* Modified from Hurtado et al. (2001) and Adhikari (2009)

the clasts derived from the Paleozoic country rock predominate, but Mesozoic rock fragments also infrequently occur. The siltstone and sandstone beds are full of carbonate- and iron-rich concretions.

The Sammargaon Formation (Figs. 34.10 and 34.12) is distributed to the north portion of the graben and it is well exposed near the village of Tangbe. This formation overlies the Tetang and Thakkhola formations with an erosional unconformity. It is represented by a more than 110 m thick succession of conglomerate and breccia. Its basal part consists of fine-grained calcite-cemented sandstone and parallel-laminated siltstone. There are also a few beds of diamictite (Hurtado et al. 2001). This formation was deposited in a glacio-fluvial environment in the middle Pleistocene (Fort et al. 1982).

Iwata (1984) described the Marpha Formation from the vicinity of Marpha and the Syang Khola, where it very gently (5–7°) dips due northeast. It is a more than 200 m thick sequence of mudstone and siltstone interbedded with sandstone and conglomerate (Fig. 34.12). These glacio-lacustrine deposits are also sporadically affected by pene-contemporaneous deformation and slumping. The intercalated conglomerate beds contain imbricated pebbles and cobbles of quartzite, carbonates, granites, and slates. The coarse-grained sandstones generally pass upwards to laminated medium-grained sandstone, which, in turn, give way to muddy conglomerate beds. The lower part of the Marpha Formation could be equivalent to the upper part of the Sammargaon Formation (Fort et al. 1982). Hurtado et al. (2001) have assigned an age of approximately 37–33 ka to the lowermost part of the Marpha Formation.

In the Syang Khola, the fluvial deposits belonging to the lower terrace of the Kali Gandaki River rest on the Tilicho Pass Formation with an erosional unconformity. The lower part of the deposits is made up of sands, followed by gravel beds, and the top part is composed of consolidated angular

gravel with a dark colored calcareous matrix (Iwata et al. 1982). These debris flow deposits were transported from the north wall of Nilgiri (Bordet et al. 1971). Presumably, these deposits range in age from 17 to 5.5 ka (Hurtado et al. 2001).

34.5.1 Dangarjong Fault Zone

The Dangarjong fault zone is marked by a clear topographic depression. To the north, it separates the Tethyan sequence from the basin fill, but towards the south, the fault zone intersects the Higher Himalayan sequence. The fault zone is about 500 m wide and includes a series of essentially parallel but infrequently discontinuous normal faults, which bound the graben from the west. Their strike varies from N20°E to N40°E, and they dip due east at a steep (80–85°) angle. They are the principal growth faults of the graben. Towards the north end of the graben, that is, around the Mustang and Mugu plutons, these faults slightly turn towards the west (Figs. 34.10 and 34.11). The throw of the Dangarjong Fault decreases from the center of the basin to the south. At Sammargaon, its vertical throw is about 4 km and the horizontal throw is about 8 km. But the throw reduces to a few tens of meters near Lete, about 50 km south of Sammargaon (Fort et al. 1982).

The metamorphic grade in the footwall of the Dangarjong Fault progressively decreases from the biotite zone at the latitude of Tangbe to the chlorite zone to the south of Dangarjong, which implies a decrease in footwall exhumation rate towards the south (Hurtado et al. 2001). The Paleozoic and Triassic strata composing the west block of this fault are affected by a low-grade Himalayan metamorphism marked by the appearance of biotite and chlorite, whereas within the downthrown east block, the metamorphism, does not affect the rocks younger than the Carboniferous (Fort et al. 1982).

34.5.2 Tectonic and Environmental Interpretations

The $\delta^{18}O$ values of carbonate rocks from the graben (Garzione et al. 2000, 2003; Adhikari 2009) and paleomagnetic studies of the Tetang Formation (Garzione et al. 2000) indicate that south Tibet had attained its current elevation prior to east–west extension of the graben between 10 and 11 Ma. Palynological investigations of the Tetang and Thakkhola formations revealed the pollens of dominantly alpine trees, such as *Pinus*, *Picea*, *Tsuga*, Quercus, and *Betula* with some steppe elements, such as *Artemisia*, *Ephedra*, *Compositae*, *Chenopodiaceae*, *Plantago*, and *Poaceae*. These pollens indicate a drier and relatively warmer climate during sedimentation. Hence, the Thakkhola–Mustang graben enjoyed significantly warmer than present climatic conditions (Yoshida et al. 1984; Adhikari 2009). The relatively high $\delta^{13}C$ values of the carbonates suggest that the Himalaya existed as an orographic barrier to moisture already during the Miocene (Garzione et al. 2000).

The sediments in the Thakkhola–Mustang graben were deposited in alluvial fan, braided river, glacio-fluvial, and lacustrine environments. The paleocurrent directions measured on imbricated pebbles from all formations of the basin show a generally southwards flow, whereas limestone microfacies analysis indicates a flat and shallow lacustrine environment of carbonate deposition (Adhikari 2009).

References

Adhikari BR (2009) Sedimentology and basin analysis of the Thakkhola-Mustang graben, central Nepal. Unpublished Ph. D. dissertation, submitted to Vienna University, 158 pp

Argand E (1924) La tectonique de l'Asie. Congrès Géologique International, Belgique, Comptes Rendues de la 13ème Session, en Belgique 1922. H. Vaillant-Carmanne, Liège, pp 171–372

Armijo R, Tapponnier P, Mercier JL, Han T (1986) Quaternary extension in southern Tibet: field observation and tectonic implications. J Geophys Res 91:13803–13872

Bajracharya SR, Verma VK (1989) Morphometric analysis of the Bagmati River in Kathmandu valley. J Nepal Geol Soc 6:11–20

Bassoullet JP, Colchen M (1974) Les formations tradi-orogéniques de la Thakkhola, Himalaya du Népal. 2ème Réun. Sc. Terre., Pont-a-Mousson, France, 34 pp

Bhandari S, Paudayal KN (2007) Palynostratigraphy and palaeoclimatic interpretation of the Plio–Pleistocene Lukundol Formation from the Kathmandu valley, Nepal. J Nepal Geol Soc 35:1–10

Blisniuk P, Hacker BR, Glody J, Ratschbacher J, Bi S, Wu Z, McWilliams MO, Calvert A (2001) Normal faulting in central Tibet since at least 13.5 Myr ago. Nature 412:628–632

Bordet P, Colchen M, Krummenacher D, Le Fort P, Mouterde R, Rémi M (1971) Recherches géologiques dans l'Himalaya du Népal, région de la Thakkhola. Centre National de la Recherche Scientifique, Paris, 279 pp (with two geological maps in colors)

Burbank DW (1992) Causes of recent Himalayan uplift deduced from deposited patterns in the Ganges basin. Nature 357:680–683

Colchen M (1999) The Thakkhola–Mustang graben in Nepal and the late Cenozoic extension in the Higher Himalayas. J Asian Earth Sci 17:683–702

Coleman ME, Hodges KV (1995) Evidence for Tibetan plateau uplift before 14 m. y. ago from a new minimum age for east–west extension. Nature 374:49–52

Dhital MR, Giri S (1993) Engineering geological investigations at the collapsed Seti Bridge site, Pokhara. Bull Dept Geol 3(1):119–141 (Tribhuvan University)

Dhoundial EP (1966) Investigation of lignite deposits in Kathmandu Valley, Nepal. Unpublished report submitted to the Geological Survey of India, 34 pp

Dill HG, Khadka DR, Khanal R, Dohrmann R, Melcher F, Busch K (2003) Infilling of the younger Kathmandu–Banepa intermontane lake basin during the Late Quaternary (Lesser Himalaya, Nepal): a sedimentological study. J Quat Sci 18:41–60

Dill HG, Kharel BD, Singh VK, Piya B, Busch K, Geyh C (2001) Sedimentology and paleogeographic evolution of the intermontane Kathmandu Basin, Nepal, during the Pliocene and Quaternary. Implications for formation of deposits of economic interest. J Asian Earth Sci 19:777–804

DoI (Department of Irrigation) (1993) Feasibility study on expanding groundwater development for irrigation in the Birganj area of the Terai. Nippon Koei Co., Ltd. and Nepalconsult (P) Ltd., Kathmandu, vol II: Annexes, pp 1–27 (unpublished)

Dongol GMS (1985) Geology of the Kathmandu fluviatile lacustrine sediments in the light of new vertebrate fossil occurrences. J Nepal Geol Soc 3(1 & 2):43–57

England PC, Houseman GA (1986) Finite strain calculations of continental deformation. 2. Comparison with the India–Asia collision. J Geophys Res 91:3664–3676

Fort M, Freytet P, Colchen M (1982) Structural and sedimentological evolution of the Thakkhola Mustang Graben (Nepal Himalaya). Zötschrift für Geomorphologie N. F 42(Suppl):75–98

Fujii R, Sakai H (2001) Palynological study of the drilled sediments from the Kathmandu Basin and its palaeoclimatic and sedimentological significance. J Nepal Geol Soc 25(Special Issue):53–61

Fujii R, Sakai H (2002) Paleoclimatic changes during the last 2.5 myr recorded in the Kathmandu Basin, central Nepal Himalayas. J Asian Earth Sci 20:255–266

Garzione CN, DeCelles PG, Hodkinson DG, Ojha TP, Upreti BN (2003) East–west extension and Miocene environmental change in the southern Tibetan plateau: Thakkhola graben, central Nepal. Geol Soc Am Bull 115(1):3–20

Garzione CN, Dettman DL, Quade J, DeCelles PG, Butler RF (2000) High times on the Tibetan plateau: Paleoelevation of the Thakkhola graben, Nepal. Geology 28:339–342

Gautam P, Hosoi A, Sakai T, Arita K (2001) Magnetostratigraphic evidence for the occurrence of pre-Brunhes (>780 kyr) sediments in the northwestern part of the Kathmandu Valley, Nepal. J Nepal Geol Soc 25(Special Issue):99–109

Gurung H (1970) Geomorphology of Pokhara valley. Himalayan Rev II–III:37–49

Hagen T (1959) Geologie des Thakkhola (Nepal). Eclogae Geologicae Helvetiae 52(2):709–719 (with one plate)

Hagen T (1968) Report on the geological survey of Nepal. Volume 2: Geology of the Thakkhola. Denkschriften der Schweizerischen Naturforschenden Gesellschaft, vol LXXXVI/2, 159 pp

Hagen T (1969) Report on the geological survey of Nepal. Volume 1: Preliminary reconnaissance. Denkschiiften der Schweizerischen Naturforschenden Gesellschaft, Band LXXXVI/1, 185 pp (with a geological map)

Harrison TM, Copeland P, Kidd WSF, Lovera O (1995) New insights into the origin of two contrasting Himalayan granite belts. Geology 25:899–902

Harrison TM, Ryerson FJ, Le Fort P, Yin An, Lovera OM, Catlos EJ (1997) A Late Miocene–Pliocene origin for the Central Himalayan inverted metamorphism. Earth Planet Sci Lett 146:El–E7

Hormann K (1974) Die Terrassen an der Seti Khola – Ein Beitrag zur Quartären Morphogenese in Zentralnepal. Erdkunde 28:161–176

Hurtado JM, Hodges KV, Whipple KX (2001) Neotectonics of the Thakkhola graben and implications for recent activity on the South Tibetan fault system in the central Nepal Himalaya. Geol Soc Am Bull 13:222–240

Iwata S (1984) Geomorphology of the Thakkhola-Muktinath region, central Nepal, and its late Quaternary history: Geographical Reports of the Tokyo Metropolitan University, vol 19, pp 25–42

Iwata S, Yamanaka H, Yoshida M (1982) Glacial landforms and river terraces in the Thakkhola region, central Nepal. J Nepal Geol Soc 2 (Special Issue):81–94

Jackson J, McKenzie D, Priestley K, Emmerson B (2008) New views on the structure and rheology of the lithosphere. J Geol Soc Lond 165:453–465

JICA (Japan International Co-operation Agency) and DoI (Department of Irrigation) (1995) The master plan study on the Terai groundwater resources evaluation and development project for irrigation. Final report, Sanyu Consultants Inc., vol II, no 6: sector report, pp 9–38 (unpublished)

Kizaki K (1994) An outline of the Himalayan upheaval. Japan International Cooperation Agency (JICA), Kathmandu, 127 pp

Koirala A, Shrestha OM, Karmacharya R (1993) Engineering geology of the southern part of Kathmandu valley. Bull Dept Geol 3(1):151–159 (Tribhuvan University, Kathmandu)

Koirala A, Rimal LN, Sikrikar SM, Pradhananga UB, Pradhan PM (1998) Engineering and environmental geological map of Pokhara valley, scale 1:50,000. Department of Mines and Geology, Kathmandu (map in colors)

Kono M (1974) Gravity anomalies in east Nepal and their implications to the crustal structure of the Himalayas. Geophys J Roy Astron Soc 39:283–299

Le Fort P, France-Lanord C (1994) Granites from Mustang and surrounding regions, central Nepal. J Nepal Geol Soc 10:79–81

Molnar P, Tapponnier P (1978) Active tectonics of Tibet. J Geophys Res 83:5361–5375

Moribayashi S, Maruo Y (1980) Basement topography of the Kathmandu Valley, Nepal—An application of gravitational method to the survey of a tectonic basin in the Himalayas. J Jpn Soc Eng Geol 21(2):30–37

Nakagawa T, Yasuda Y, Tabata H (1996) Pollen morphology of Himalayan *Pinus* and *Quercus* and its importance in palynological studies in Himalayan area. Rev Palaeobot Palynol 91:317–329

Nakata T, Iwata S, Yamanaka H, Yagi H, Maemoku H (1984) Tectonic landforms of several active faults in the western Nepal Himalayas. J Nepal Geol Soc 4(Special Issue):177–200

Paudayal KN, Ferguson DK (2004) Pleistocene palynology of Nepal. Quat Int 117:69–79

Paudayal KN (2006) Late Pleistocene pollen assemblages from the Gokarna Formation, Kathmandu valley, Nepal. J Nepal Geol Soc 33:33–38

Platt JP, England PC (1994) Convective removal of lithosphere beneath mountain belts: thermal and mechanical consequences. Am J Sci 294:307–336

Royden LH, Burchfield C, King RW, Wang E, Chen Z, Shen F, Liu Y (1997) Surface deformation and lower crustal flow in eastern Tibet. Science 276:788–790

Sakai H (2001) Stratigraphic division and sedimentary facies of the Kathmandu Basin Group, central Nepal. J Nepal Geol Soc 25 (Special Issue):19–32

Sakai T, Gajurel AP, Tabata H, Ooi N, Takagawa T, Kitagawa H, Upreti BN (2008) Revised lithostratigraphy of fluvio-lacustrine sediments comprising northern Kathmandu basin in central Nepal. J Nepal Geol Soc 37:25–44

Sharma CK (1975) Natural resources of Pokhara valley. Navana Printing Works Pvt. Ltd., Calcutta, 106 pp

Sharma T, Merh SS, Vashi NW (1978) The terraced conglomerates of Pokhara valley in central Nepal. In: Symposium on morphology and evolution of landforms. Department of Geology, University of Delhi, pp 226–240

Shrestha OM, Koirala A, Karmacharya SL, Pradhananga UB, Pradhan R, Karmacharya R (1998) Engineering and Environmental geological map of the Kathmandu Valley (1:50,000). Department of Mines and Geology, Kathmandu

Talent JA, Dongol GMS, Chhetri VS (1991) Biostratigraphic reports—spurious and dubious—from Nepal. J Nepal Geol Soc 7:9–20

Tuladhar RM (1982) A note to the lignite occurrence in Lukundol, Kathmandu. J Nepal Geol Soc 2(1):47–51

Yamanaka H, Yagi H (1984) Geomorphological development of the Dang Dun, Sub-Himalayan zone, southwestern Nepal. J Nepal Geol Soc 4(Special Issue):151–159

Yamanaka H, Yoshida M, Arita K (1982) Terrace landforms and Quaternary deposit around Pokhara valley, central Nepal. J Nepal Geol Soc 2(Special Issue):113–142

Yonechi F (1973) A preliminary report on the geomorphology of Kathmandu valley, Nepal. Science report, Tohoku University, 7th Series, vol 23, pp 153–161

Yoshida M, Igarashi Y (1984) Neogene to Quaternary lacustrine sediments in the Kathmandu valley, Nepal. J Nepal Geol Soc 4 (Special Issue):73–100

Yoshida M, Igarashi Y, Arita K, Hayashi D, Sharma T (1984) Magnetostratigraphic and pollen analytic studies of the Takmar series, Nepal Himalayas. J Nepal Geol Soc 4(Special Issue):101–120

Neotectonics

35

... the green mountains became white. For 20 to 25 min after the earthquake, visibility was lost in the dust.
—Brahma Samsher J.B. Rana (1935, p. 73)

Neotectonic movements deform or offset river terraces and ancient erosion surfaces. Such movements are manifested as well by earthquakes and associated ruptures, termed active faults. During the Japanese Mount Everest Expedition of 1970, Kono (1974) carried out gravity measurements at 145 locations. He obtained free air, Bouguer, Airy, and Pratt anomalies from the data. The Bouguer anomalies in the Higher Himalaya, Lesser Himalaya, and the Siwaliks of east Nepal did not show any correlation with altitudes, suggesting that isostasy does not prevail in the wavelength of less than 100 km. An increase in the Bouguer gravity gradient from about 1 mGal km^{-1} over the Ganga Basin to 2 mGal km^{-1} over the Himalaya implies a marked steepening of the Moho, and hence a greater flexure of the Indian plate beneath the Himalaya. The flexed Indian plate supports some of the excess mass in the Himalaya and maintains parallel belts of negative and positive isostatic anomalies over the Ganga Basin and the Himalaya (Lyon-Caen and Molnar 1983; Molnar 1986). Cattin et al. (2002) measured two gravity profiles through central Nepal and found a steep gravity gradient across the Higher Himalaya, indicating a locally steep Moho and a 10 km wide hinge in south Tibet.

35.1 Orogeny and Mountain Building

The term orogeny originated in the nineteenth century, when the deformation of rocks and the development of mountainous topography within a mountain were thought to be linked together. But, many geologists consider deformation and mountain building two different processes. According to them, the post-orogenic movements, belonging to the category of epeirogenic processes, are responsible for mountain building (Stille 1936; Gansser 1982). Thus, in spite of its etymology, orogeny is presently used to denote folding of rocks in fold belts and it does not mean mountain building (Ollier and Pain 2000, p. 5). The Himalaya and Tibet are the testing grounds for the theories of orogenesis, and the engine that drives it resides in the mantle (Molnar 1986). Opinions vary regarding the initiation of uplift and formation of the Himalaya (Box 35.1).

Although there were some early views on Himalayan mountain building (Box 35.2), plate tectonics provides a sound theoretical basis to the origin of mountains. According to McKenzie (1969, p. 28), the convective flow in the mantle will continue to move two continents together after they have collided and can produce fold mountains, like the Himalaya, by crustal shortening over large areas. Dewey and Bird (1970, pp. 2625–2626) remarked that mountain belts are a consequence of plate evolution. They develop essentially by the deformation and metamorphism of Atlantic-type continental margins and share some common features, such as:

- They exhibit long linear or arcuate features.
- Their sedimentation, deformation, and thermal patterns are parallel to the belt.
- They have complex internal geometry.
- They show extreme stratal (and crustal) shortening features.
- They have asymmetric deformation and metamorphic patterns.
- There record significant sedimentary composition and thickness changes in the direction normal to the trend of the belt.
- The basement beneath mountain belts is primarily continental but basic and ultrabasic rocks (ophiolites) may occur as basement and as up-thrust slivers.
- Intense deformation and metamorphism are comparatively short-lived in comparison with the time of deposition of the sediments comprising the belt.

Dewey and Bird (1970, p. 2625) classified the mountain belts into the cordilleran (later renamed as Andean) and collision types. Andean-type mountain belts are characterized by paired metamorphic belts (blueschist on the oceanic side and high temperature on the continental side). They grow primarily from thermal mechanisms attributed to the

M.R. Dhital, *Geology of the Nepal Himalaya*, Regional Geology Reviews,
DOI 10.1007/978-3-319-02496-7_35

rise of calc-alkaline and basaltic magmas. They are also characterized by divergent thrusting and synorogenic sediment transport from the high-temperature volcanic axis.

Box 35.1: Contrasting Views on Timing of Himalayan Upheaval

Captain Richard Strachey (1851, p. 306) discovered more than 1,000 m thick Tertiary deposits in the Trans-Himalayan ranges where they are found at an altitude of 4,000–5,000 m, still preserving an almost perfect horizontal surface. He collected a number of mammalian fossil specimens from there. While describing the fossilized remains of large mammals, Falconer (1868) noted a great upheaval of the Himalaya for many thousand meters. An area that formerly bore a tropical fauna has risen up to an altitude of nearly arctic severity, as indicated by the remains of rhinoceros, antelope, hyena, horse, and others found at an altitude of 5,000 m. According to Hagen (1956, 1959), the geomorphic and geological observations indicate recent upheaval of the Himalaya and related neotectonic movements. Powell (1986, p. 89) inferred a pause in the Himalayan convergence during the Middle Eocene to Early Miocene (between 50 and 20 Ma). On the other hand, Armijo et al. (1986, 1989) and Harrison et al. (1992) argued that during the late Cenozoic, the India–Asia collision was accommodated by the sideway extrusion of Tibet.

Gansser (1974, 1981) divided the Himalayan orogeny into various phases, including the time of Indus Suture formation in the Late Cretaceous, Himalayan main orogenic phase (post Eocene–Miocene), the Trans-Himalyan and Sub-Himalayan phase (Early Miocene–Pleistocene), the Sub-Himalayan phase (Pleistocene), and the morphogenic phase (Pleistocene–Holocene), responsible for overall uplift of the mountains. However, Beden and Brunet (1986) remark that although Himalayan upheaval is considered to be a comparatively recent (less than 4 Ma) event responsible for the development of a geographic and ecological barrier between Central and South Asia, it appears that the Late Miocene faunas of Potwar are quite different from those of Afghanistan despite their geographical proximity (300 km). On the other hand, the fossils are similar to those of Nepal and Burma situated more than 1,500 km apart. Hence they conclude that there must be a barrier inhibiting the faunal exchange since the Late Miocene (about 8 Ma). Powell (1986) proposed the continental subduction during 20–5 Ma, subsequent rise of the continental lithosphere (5–2 Ma), and present stage (2 Ma to present) of continental underplating resulting in dramatic Pleistocene and Holocene uplift.

Molnar and England (1990) argue that isostatic compensation of material removed by erosion can elevate the remaining terrain, but the uplift of ridges and peaks with respect to sea level does not necessarily signify an increase in mean elevation. According to them, rapid erosion of mountain ranges could be related to the onset of cooling and glaciation due to global climate change in late Cenozoic time (Zhang et al. 2001).

Box 35.2: Early Views on Himalayan Mountain Building

Burrard and Hayden (1908, p. 61) state that the highest peaks of the Himalaya stand not on the spurs but in the crest zone of a great range. The range resembles a crocodile's back, which is a wide flat arch containing relatively high prominences, called the peaks, and it has no sharply edged crest-line. All the highest peaks fall within a narrow belt running throughout the length of the crest zone. Molnar and England (1990) infer that isostatic rebound could have contributed to developing such an arrangement.

Suess (1909, pp. 706, 722) suggested first that the extensive alluvial plains of the Ganga and Indus Rivers constituted a foredeep in front of the Himalayan fold belt, resulting from the subsidence of the northern part of the Indian Peninsula during the southwards advance of the Himalayan mountains in the form of high crustal waves, as they were obstructed in their southwards migration by the rigid landmass of the Peninsula. However, Hayden (1913) and Oldham (1917) disagreed with that view. Based on the gravity data, Oldham (1917) obtained a gentle northwards tilt of the foredeep floor. Gansser (1964, 1983) mentioned that contrary to the general opinions, the Himalayan foreland, the border area of the Ganga Basin, does not correspond to the foredeep one would expect in front of a mountain range of Himalayan dimensions. According to him, the Indian Shield is depressed in the north and passes into a trough which is filled up mostly by very young detrital sediments, and not by marine geosynclinal deposits. However, the balanced wedge extrusion model is not very different from this view of propagating high crustal waves.

Based on geophysical arguments, Burrard (1916) proposed that the fundamental cause of mountain

building in the Himalaya and subsidence in the Ganga Basin was a crack in the subcrust and the mountains have risen out of the crust from a great depth (100 km), and owe their elevation mainly to the vertical expansion of subjacent rock. He further inferred that granites composing the main range of the Himalaya were protruded upwards due to the expansion of rocks from below (Burrard 1916, p. xcv). Oldham (1917) opposed the deep trough hypothesis. Nevertheless, it was one of the first inferences of a deep root zone in the Himalaya and flow of material from depth. It is remarkable that the hypothesis of Burrard is somewhat similar to the channel flow model.

Collision-type mountain belts result dominantly from mechanical processes. If the continental margin collides with an island arc or with another continent, a collision-type mountain belt develops. Where a collision between an island arc and a continent takes place, the resulting mountains are small, whereas when two continents collide, large mountains develop. The collision-type mountain belts do not exhibit paired metamorphic belts and they generally have a single prominent direction of thrusting, away from the trench over the underthrust plate. The collision mountain belts have a sialic root resulting from the thickening and underthrusting of the continental crust. When the buoyancy of the underthrust continental rocks inhibits further destruction, the descending plate may break off and sink into the asthenosphere (McKenzie 1969; Dewey and Bird 1970).

35.2 Neotectonic Movements in the Northwest Himalaya and Bhutan

In the Northwest Himalaya, Medlicott (1864, p. 20) observed that the mighty Sutlej River flows through Sub-Himalayan rocks for several kilometers. In this process, it cuts through a ridge of massive boulderbeds standing nearly vertical. The materials constituting these beds are identical to the fluvial deposits of the river overlying the vertical beds. Towards the downstream, the low ridge formed on either side of the river by the boulderbeds gradually disappears and the rock itself passes into a pebbly sandstone.

Agrawal and Gaur (1972) measured ground deformation across the Nahan Thrust at Dakpathar, northwest of Dehra Dun. In this area, the Subathu shales override the Siwaliks as well as the Holocene talus. Their tilt measurements indicated that the secular creep rate across the Nahan Thrust was less than 0.4 mm per month.

While investigating the Bhutan Himalaya, Heim and Gansser (1939) and Gansser (1983) noted that Pleistocene to Holocene detrital fans cover or partly replace the Siwaliks along the north edge of the Assam plain. Locally, they are tilted and in the Jaldhoka River area, at the southwest border of Bhutan, they are clearly warped into broad anticlines. In the Hattisar embayment of Bhutan, where the Siwaliks disappear under the alluvium, Nakata (1972) reported an east–west aligned row of southwards tilted gravel terraces with a sharp and steep north scarp 6–12 m high (Chap. 5). The top of the terraces is covered by a red weathered soil. They are cut by antecedent local rivers and on their southern side even the youngest terraces are tilted, indicating recent movements. The sharp east–west aligned north scarp coincides with a structural line bordering the submerged Siwaliks to the South (Gansser 1983). In the Kalonadi River (well known for its coal mines) of Bhutan, Gansser (1983) described from the area nearby the Damudas, a tectonized Siwalik wedge of fine micaceous sandstones with some larger deltaic features and conspicuous horizons of claystone pellets. They border fine sheared lignitic coal seams. The contact against the Damudas is sharp and vertical. Between this tectonized Siwalik wedge and the more normal Siwaliks farther to the south, is observed a thick formation of badly sorted, loosely cemented, coarse fanglomerate, belonging to the Diklai boulderbeds (Jangpangi 1974), which dips gently and transgresses the much steeper Siwaliks. There is a sharp, well-exposed tectonic contact between the Siwalik wedge and the fanglomerate, where a very marked post-Siwalik movement is seen (Gansser 1983).

35.3 Active Faults in Nepal

From various parts of the Nepal Himalaya, Hagen (1956, 1959) reported neotectonic movements that brought the Siwaliks over the Pleistocene–Holocene alluvium (Figs. 35.1 and 35.2).

Nakata (1972, 1982, 1989) and Nakata et al. (1984) studied in detail the active faults of the Himalayan foothills. In Nepal, they distinguished the Main Boundary Active Fault System and the Main Central Active Fault System. Similarly, they also identified some individual active faults, such as the Rangun Khola, Talphi, Bari Gad, and Kolphu Khola faults (Fig. 35.3). Except for a few active faults, extending along the southern margin of the Siwaliks, most of them have not contributed to the Himalayan upheaval, because their north block is downthrown with respect to the south block. Thus these observations are in strong contrast with the records of continued convergence and upheaval of the Himalayan Range (Iwata 1987).

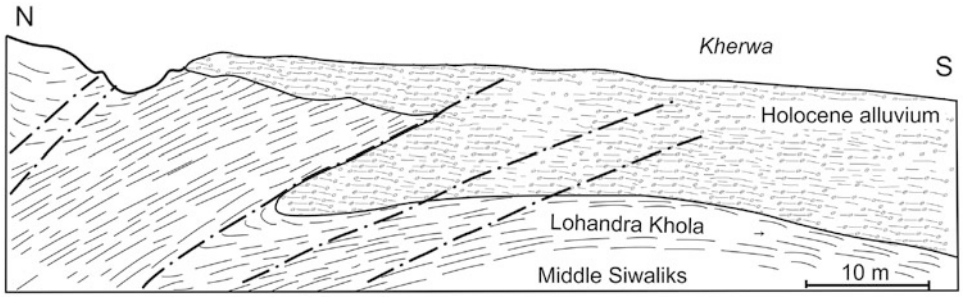

Fig. 35.1 The Middle Siwaliks thrust over the alluvium at Kherwa in the Lohandra Khola, East Nepal. *Source* Modified from Hagen (1956)

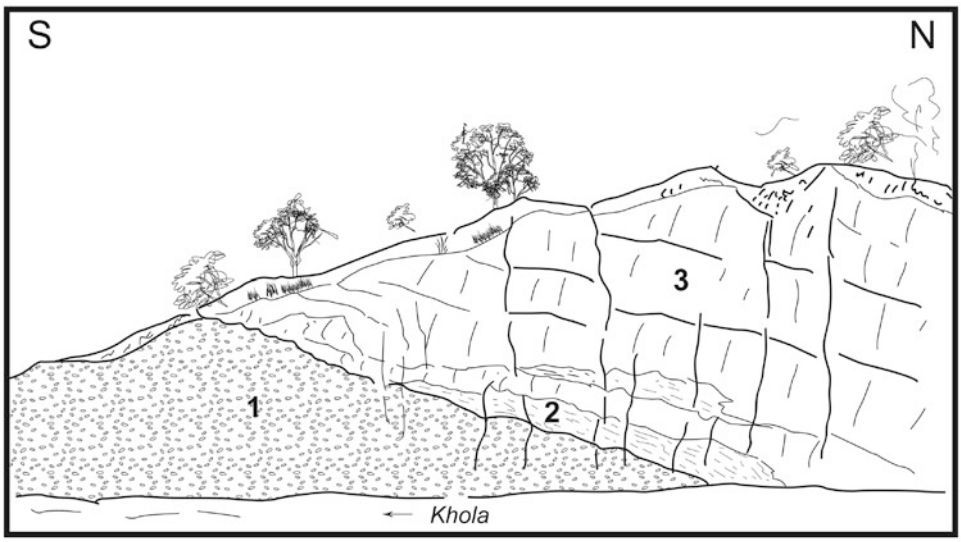

Fig. 35.2 The Siwaliks resting on the Pleistocene alluvial terraces, about 1 km north of Petkot, in the Mahakali–Seti region. *1* Alluvium, *2* Lower Siwaliks (brown shales), *3* Middle Siwaliks (light gray sandstones). The sketch is about 150 m long. *Source* Modified from Hagen (1959)

35.3.1 Rangun Khola Active Fault

A conspicuous active fault (Figs. 35.3 and 35.4) is developed in the Rangun Khola watershed of the Mahakali–Seti region (Chap. 28). Nakata (1982) included the fault within his Main Boundary Active Fault System (Fig. 35.3). Although the active fault runs very close to the Budar Thrust, it diverts significantly from that fault around Alital while crossing the phyllites and quartzites of the Lesser Himalaya. The Budar Thrust lies a few kilometers farther south of the active fault. Except for beautiful Lake Alital, most of the sag ponds developed along this active fault are already silted up. The sag ponds and the "pressure ridge" lying to the south, on the footwall of the fault, imply a normal sense of movement along the active fault.

35.3.2 Talphi Active Fault

The Talphi fault belongs to the Main Central Active Fault System and it is located to the north of Jumla (Fig. 35.3). The fault is marked by a sharp and straight depression, running in the northwest–southeast direction for about 10 km. Several alluvial terraces are tilted to the south and offset by this essentially normal fault, where the south-lying, highest terrace is upthrown by 48 m (Nakata et al. 1984).

35.3.3 Surkhet–Ghorahi Active Fault

The Surkhet–Ghorahi fault constitutes a portion of the Main Boundary Active Fault System, and it extends for about 120 km. The fault marks the north border of the Surkhet and Dang valleys. The fault trace is almost continuous and its dip varies from vertical to less than 30° due north. On the banks of the Bheri River, the fault exhibits a straight trace and displaces several terraces vertically as well as horizontally. They are uplifted to the northeast and dextrally offset. In the Dang Valley, the fault infrequently branches into two parallel traces. The radiocarbon age of a wooden tissue present in the fault zone was obtained at 480 ±90 years BP, whereas a humic layer present in the fluvial deposits offset by the fault yielded an age of 1,400 +90 or −100 years BP (Nakata et al. 1984).

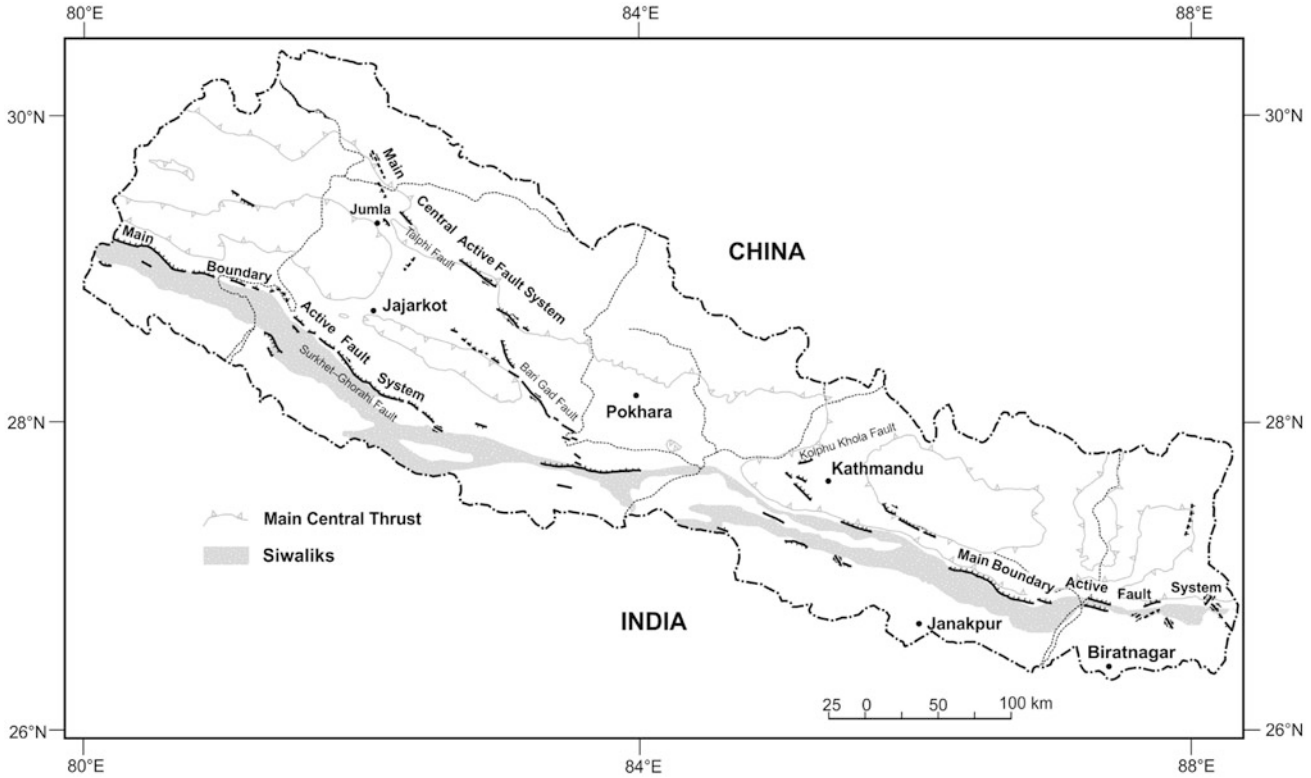

Fig. 35.3 Some prominent active faults of the Nepal Himalaya. *Source* Based on Nakata et al. (1984)

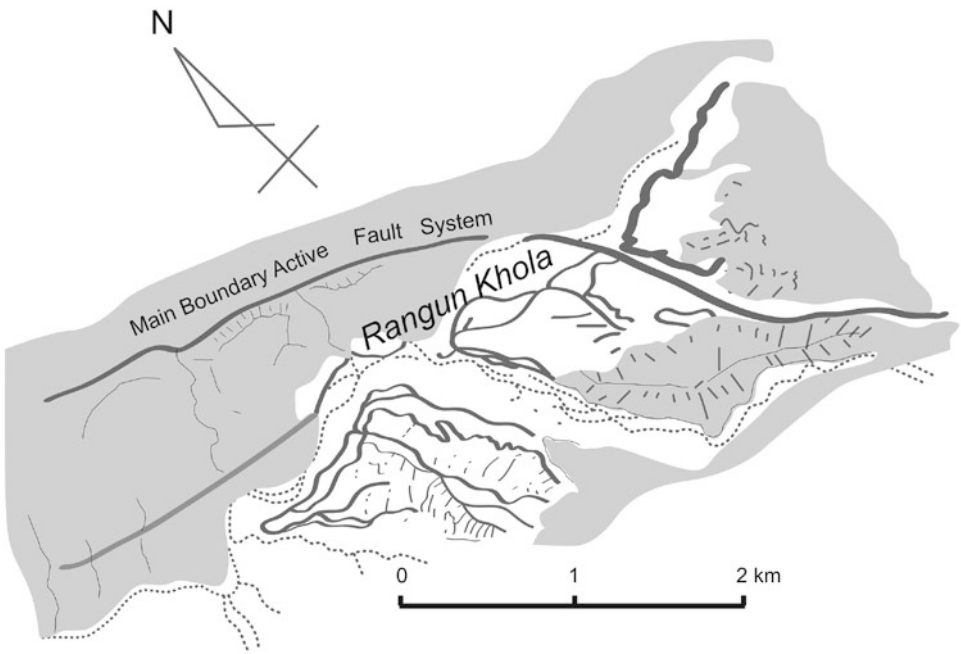

Fig. 35.4 The Rangun Khola active fault occurring in the Mahakali–Seti region (Chap. 28). *Source* Modified from Nakata (1982)

35.3.4 Pressure Ridge Along Main Boundary Active Fault

The Main Boundary Active Fault has a conspicuous "pressure ridge" (Fig. 35.5) that continues to the southeast, along its footwall, parallel to the fault (Nakata 1982). The footwall also consists of shattered Lesser Himalayan rocks spread over the fluvial deposits (Fig. 35.5b). Fault breccia and fault gouge are frequently observed under the shattered rock (Fig. 35.5c). They indicate an initial stage of thrusting along the fault. Subsequently, abrupt uplift of the hanging wall resulted in the formation of the pressure ridge (Nakata et al. 1984), with many sag ponds lying along the fault trace. Most of the sag ponds are already filled up with sediments (mainly silt, clay, and peat).

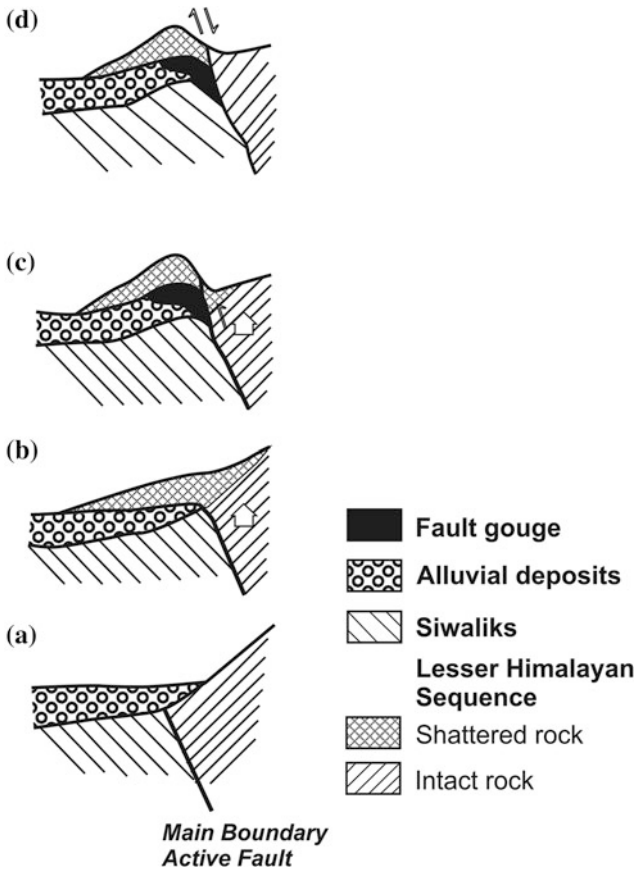

Fig. 35.5 Formation of pressure ridge and active fault recording downthrow towards the north. **a** Deposition of fluvial gravel on the fault; **b** thrusting and movement of shattered rock on the fluvial terrace; **c** further thrusting and development of fault gouge and fault breccia under the shattered rock; **d** subsequent downthrow of the hanging wall and formation of the pressure ridge. *Source* Based on Nakata et al. (1984)

35.3.5 Bari Gad Fault

The Bari Gad active fault extends approximately due northwest–southeast for about 140 km along the Bari Gad Khola and the Sani Bheri River. The fault is marked by uphill-facing scarplets, elongated depressions, and offsets of river courses or ridges. It is essentially a dextral strike-slip fault with some downthrow to the northeast. The amount of vertical and horizontal throw are about 15 and 250 m, respectively (Nakata et al. 1984).

35.3.6 Kolphu Khola Fault

The Kolphu Khola Fault lies to the northwest of Kathmandu, and it is about 10 km long and strikes due ENE–WSW. The fault is steeply (70°) dipping due north and contains many north-facing scarplets, where the hanging wall is downthrown to the north. The fault has displaced only the old terraces, which are covered by red soil, but it has not affected the younger ones. Radiocarbon dating of a humic layer within a displaced terrace gave an age of 34,820 +6,080 or −3,420 years BP, indicating a long recurrence interval of displacement on the fault (Nakata et al. 1984).

35.3.7 Tilted Fanglomerates in the Goyeng Khola, East Nepal

The rocks exposed in the upper reach of the Goyeng Khola, Ilam, are made up of highly crushed and weathered phyllites and metasandstones of the Lesser Himalaya. The area is very close to the Main Boundary Active Fault System. The area is composed of highly to completely weathered and sheared gray-green to brown (weathered colors) phyllite with numerous stretched quartz veins. To the south of the Main Boundary Active Fault, there are highly fractured and sheared Siwaliks up to the Thute Khola, and then one encounters some old gravel beds. The beds are gently tilted to the north in the Thute Khola (Fig. 35.6), and their dip becomes almost horizontal towards the village of Barphalyang. Many large landslides are seen between the Goyeng Khola and the Thute Khola for a distance of about 300 m. They are controlled by two closely lying faults: the Main Boundary Active Fault and a thrust fault within the Siwaliks. Also, the Main Central Thrust lies several hundred meters to the north.

At this location, the Lower Siwalik sandstone is completely milled and fractured (with angular fragments) and the

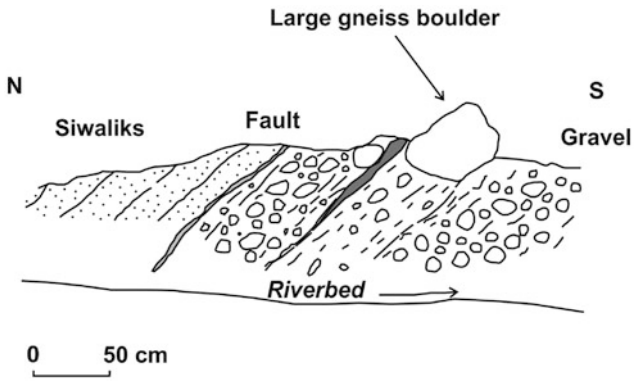

Fig. 35.6 Sketch of the fault on the left bank of the Thute Khola. *Source* Author's observations

clasts range in size from 1 to 5–10 mm. The crush zone is about 50 m thick. There also occur two approximately 50 m thick crushed beds of purple sandstone situated about 30 m upstream from the fault. The fault passes through a gully to the east with many landslides. There is a sharp contact between the sandstone (N) and the boulders (S) along the gully.

35.4 Change in Drainage of Major Rivers

Hagen (1969) inferred significant changes in the drainage pattern of major rivers, such as the Karnali, Gandaki, Koshi, and Arun, due to the rise of the Great Himalayan Range, rapid erosion in the Midlands, and upheaval of the Mahabharat Range. He also related the distribution of Upper Siwalik conglomerates to the ancient drainage pattern of major rivers. Stöcklin (1980) described a change in Bagmati drainage owing to 20–30 km post-Siwalik crustal shortening in central Nepal. Prior to the shortening, the river flowed through the Lesser Himalayan sequence of the Nawakot Complex. Although the Kathmandu complex of the Higher Himalayan crystallines was already thrust over the Nawakot rocks, it was situated beyond the upper reach of the proto-Bagmati River. At that stage, the Nawakot detritus was forming the Upper Siwalik conglomerates. Subsequently, owing to thrusting and imbricate faulting, the Kathmandu Complex was passively transported farther south, and the Nawakot Complex narrowed down to less than 1 km in width. As a result, at present the Bagmati receives detritus from the Kathmandu Complex.

35.5 Elevated River Terraces

Dollfus and Usselmann (1971) prepared the first detailed geomorphic maps of various river valleys in west Nepal, including Pokhara, Kusma, the Budhi Gandaki, and Trishuli. Fort (1976) described the Pleistocene–Holocene deposits of the Middle Kali Gandaki Valley in west Nepal. The deposits have a common occurrence of calcareous conglomerate facies, a rarity of glacial deposits. The Middle Kali Gandaki cuts its course almost at a right angle to all natural geographic units of the Himalaya. It passes between the high peak of Dhaulagiri on the west and Annapurna I on the east. She identified the following three types of sedimentation basins from south to north of the Kali Gandaki, respectively.

The Kusma type of basin has a coarse alluvial fill, which is found at Kusma and Baglung. The basin was developed on schists, calc-schists, and quartzites. It received alluvial and colluvial deposits transformed later into conglomerates. There are five terrace levels distributed on either side of the valley. Conglomerates are specific to the Kusma sedimentation basin. They occur within the third and fourth levels. The contact between the bedrock and the sediments is very irregular. The conglomerate is practically devoid of stratification. The material was derived mainly from debris flow and mudflow. An elevated old fifth-level terrace of the ancient Kali Gandaki was subject to big hollowing. Then an important filling (conglomerates) took place, which was later carved by the river into various fourth-level terraces. The subsequently formed third-level terraces were either alluvial or karstic in nature. Levels 2 and 1 represent successively the younger and youngest surfaces.

The Ghasa type of basin contains alluvial, torrential, and till facies. The deposits are distributed in the Ghasa, Lete, Chooya, and Taglung areas. It contains a multitude of levels and a great variety of facies imbricated into one another. It lies in the Tibetan slab. The highest level is discontinuously overhanging several hundred meters (more than 400 m) above the river. Then there is a main level around Ghasa at about 150 m above the riverbed. It is an alluvial deposit. The deposits consist of conglomerates in other sediments. There are some calcareous conglomerates too. The other deposits contain fluvio-lacustrine, alluvial, debris flow, colluvial, and sporadic till deposits.

The Thakkhola type of basin comprises lacustrine and alluvial deposits. It appears north of Dhampu, where an arid climate prevails. It is on the folded Tibetan series. The main

feature is the appearance of the deltaic to lacustrine deposits above the discontinuous brecciated conglomerate. They become increasingly thin towards the north. There are fine silt and sand of light and dark colors. The second type comprises sandy beds with cross-stratification and ripple marks, probably representing the marginal lacustrine facies. It is assumed that the lake was between Larjung and the north of Jomsom. The lacustrine deposits were cut down by ancient colluvio-alluvial levels, occurring regularly along the sides of the valley from about 400 m above the present wide gravel floodplain.

Sharma et al. (1980) studied the terraces of the Kali Gandaki River in its middle reach, between Behadi and Kusma. They classified them into the T1, T2, and T3 terraces. The T1 terraces stand out from 300 to 400 m above the riverbed, whereas the T2 terraces are from 25 to 60 m lower than the T1 terraces. The T1 and T2 terraces are made up of unsorted, unstratified, and consolidated conglomerates. The T3 terraces rise from 10 to 15 m above the riverbed, and they are composed of Holocene unconsolidated sediments. They inferred that the large volumes constituting the T1 and T2 terraces were fluvio-glacial accumulations, derived from the Great Himalayan Range and accumulated in lake-like stagnant water, caused by damming of the river during the upheaval of the Mahabharat Range.

Yamanaka and Iwata (1982) divided the middle reach of the Kali Gandaki into the Higher, Middle, and Lower terraces. The Higher Terrace is distributed between Beni and Balewa. It is a filltop terrace made up of more than 300 thick conglomerates and its base is situated below the riverbed. The Middle Terraces are found between Baglung and Setibeni. They contain conglomerates of subangular to subrounded cobbles and boulders of limestone, gneiss, schist, and quartzite. There also occur a few extremely hardened conglomerate beds with calcareous matrix. On the other hand, there are also some unconsolidated to semi-consolidated beds of fine detritus (mainly granules and pebbles). The Lower Terraces are restricted in distribution. At Purtighat, they are represented by a fillstrath terrace carved in the younger valley fill deposits.

Iwata and Nakata (1985) investigated the river terraces of the Kali Gandaki in its lower reach. They identified 13 terrace levels, and divided them into 6 groups. The Highest Terraces are covered by scree and red soil. They lie at an elevation of about 150 m from the present riverbed. The Higher Terraces are rather fragmented and covered by red soil. The Middle Terraces are extensively distributed and they are partly reworked by past channels and bars. The Lower Terraces constitute Holocene fans and they are widely distributed in the dun valley. The Higher Terrace situated between Jugedi and Narayan Ghat is slightly inclined to the north, indicating some neotectonic movements after its developement.

In the Hetaunda intermontane (dun) valley of central Nepal, the Highest Erosion Surfaces and the Upper Terraces correspond to the pre-dun phase, when there were piedmont alluvial plains at the foot of the Lesser Himalaya. The Middle Terraces and their deposits were accumulated during the upheaval of the Sub-Himalayan Range and associated paleogeographic changes. In contrast to the older surfaces, the materials constituting the Middle Terraces record paleoflows mainly from the south to the north. At this stage, the Sub-Himalayan Range, lying to the south of Hetaunda, was gradually upheaved and the intermontane valley was formed as a piggyback basin. Subsequently, the Lower Terraces and floodplains, composed of swampy and lacustrine sediments, developed within the valley (Kimura 1994).

35.6 Rupture Due to Great Assam Earthquake of 1897

Oldham (1899, p. 138) noted that the Great Assam Earthquake of June 12, 1897 caused various changes in the landscape. He classified them as (1) faults and fractures, (2) differential changes of level, evidenced by instrumentations of drainage, unaccompanied by faulting, (3) changes in level evidenced by reported changes in the aspect of the landscape, and (4) changes proved by a reobservation of the triangles of the Great Trigonometrical Survey. Of the faults and fractures caused by the Great Assam Earthquake of 1897, the most conspicuous example is the Chedrang Fault (Fig. 35.7) with a NNW trend and about 11 m of upthrow (coseismic slip) on its eastern side. The fault cuts the Chedrang River at several locations and pools were formed wherever the fault blocked the side drainage. On the other hand, waterfalls were created when the river course fell on the downthrown block of the fault (Oldham 1899).

Although Molnar (1987), Cheng and Molnar (1990) and Gahalaut and Chander (1992) interpreted this earthquake as a north-dipping Himalayan thrust fault, Bilham and England (2001) made further studies of past geodetic data of the Great Trigonometrical Survey and concluded that it was due to a rupture of a buried south-dipping reverse fault (which they named the Oldham fault) of about 110 km in length. It formed a pop-up block together with the steeply north-dipping Dauki fault. However, further geophysical investigations to detect the hidden Oldham fault in the region were inconclusive (Saha et al. 2007).

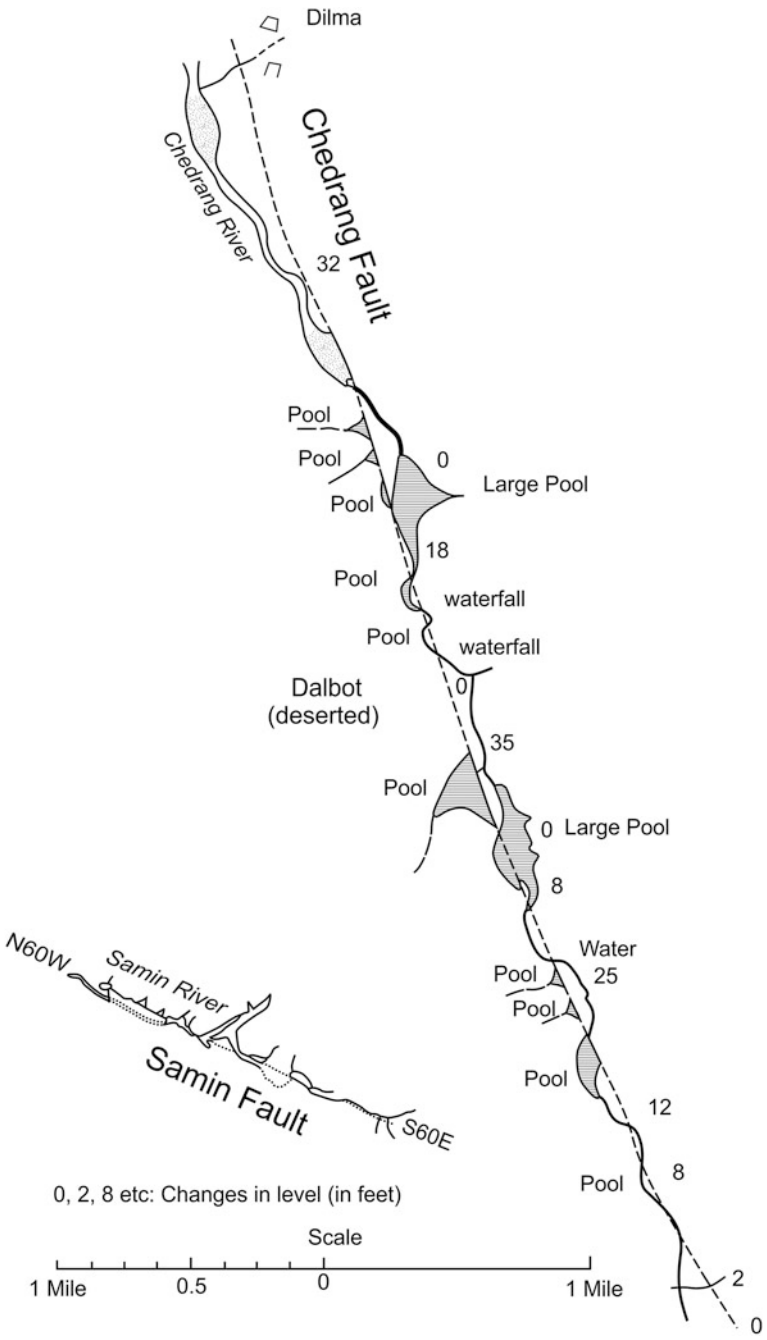

Fig. 35.7 Seismic ruptures (Sumin and Chedrang faults) mapped by Oldham after the Great Assam Earthquake of June 12th, 1897. *Source* Modified from Oldham (1899)

35.7 Deformation Related to the Great Kangra Earthquake of 1905

Middlemiss (1910, p. 348) reported the variation of levels after the Great Kangra Earthquake of April 4, 1905. In 1862, the line between Saharanpur and Mussoorie was first leveled. This was repeated in 1904 between Dehra Dun and Mussoorie. Again in 1905, after the earthquake, the latter portion was leveled to measure the changes. The results showed that Dehra Dun and the Siwaliks had risen and Mussoorie had sunk (Fig. 35.8). It is remarkable that the fault separating the Lesser Himalayan rocks from the Siwaliks exhibited a downthrow towards the Lesser Himalaya. Chander and Gahalaut (1999) summarized six leveling profiles from the same area (Fig. 35.9) and noted that there is a systematic pattern in the interseismic elevation changes. During the coseismic period, the 1905 Kangra earthquake produced uplift all along the leveling line, and gradual subsidence is noted during the interseismic period. The process of

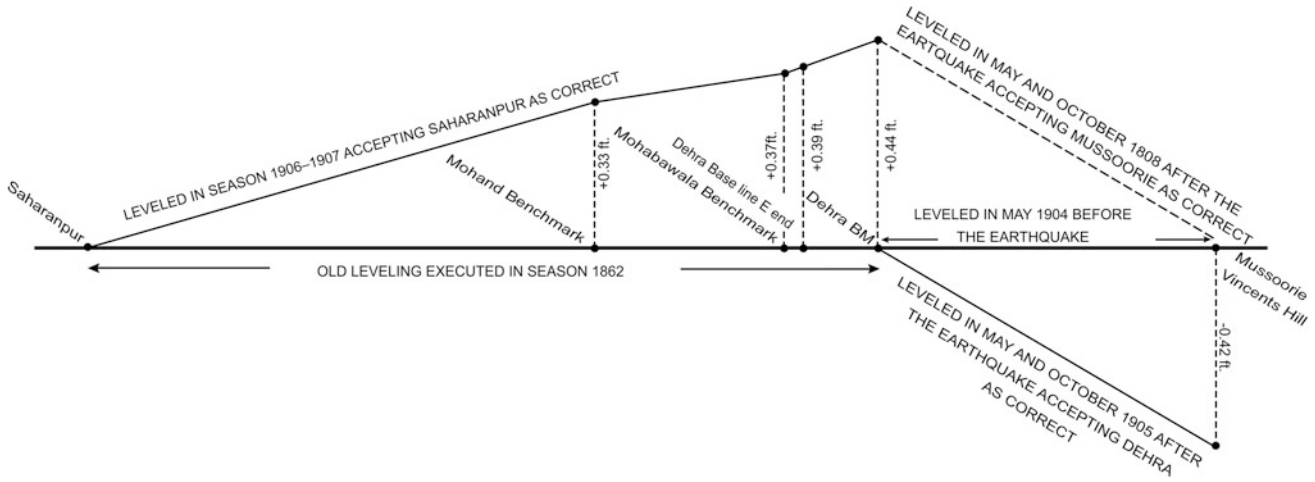

Fig. 35.8 Variation of levels between Saharanpur and Mussoorie after the Great Kangra Earthquake of April 4th, 1905. *Source* Based on Middlemiss (1910)

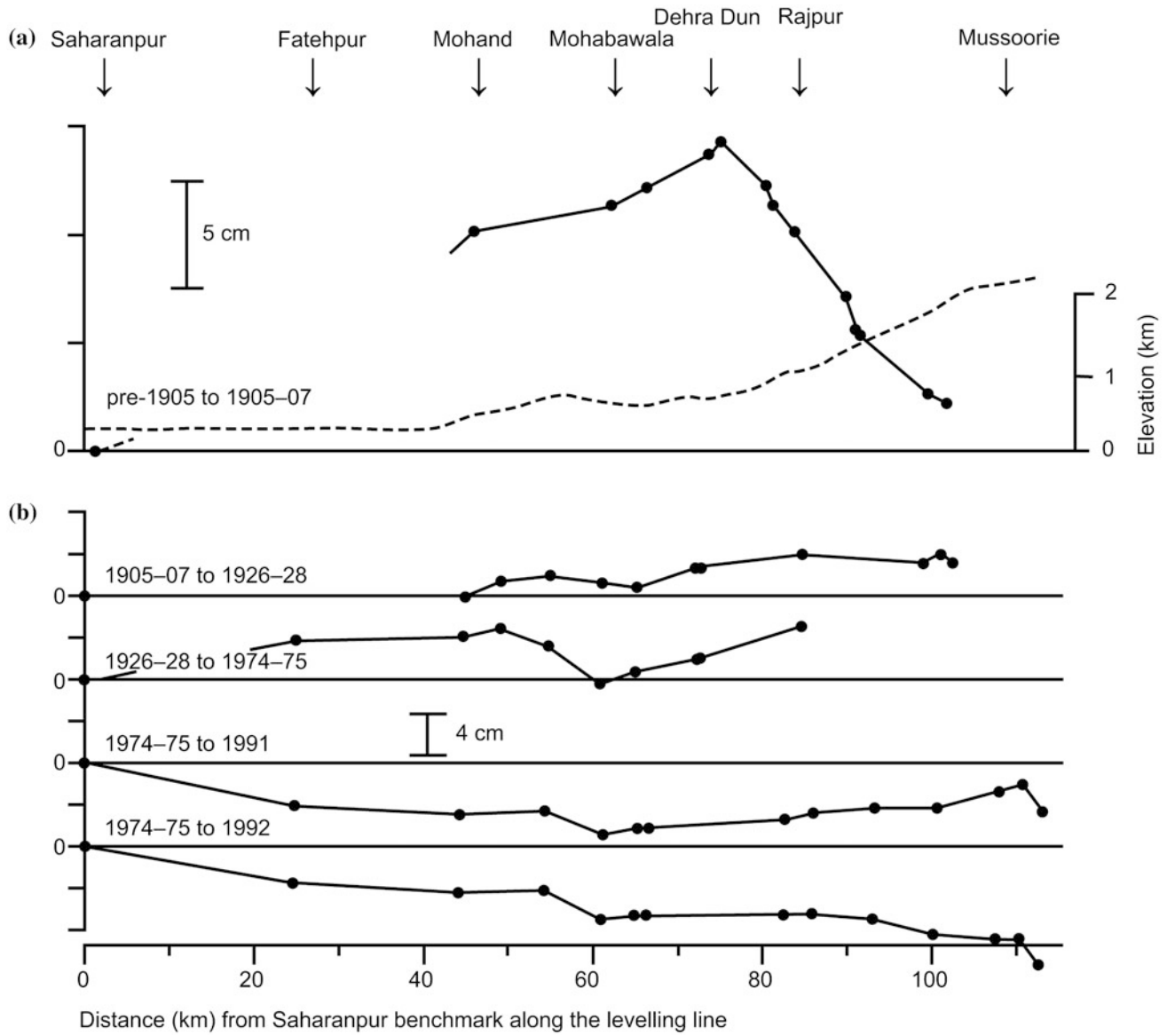

Fig. 35.9 Interepoch coseismic and interseismic elevation changes with reference to Saharanpur benchmark are displayed in parts **a** and **b**, respectively. The *dashed curve* in part **a** denotes the topography along the *line*. *Source* Based on Chander and Gahalaut (1999)

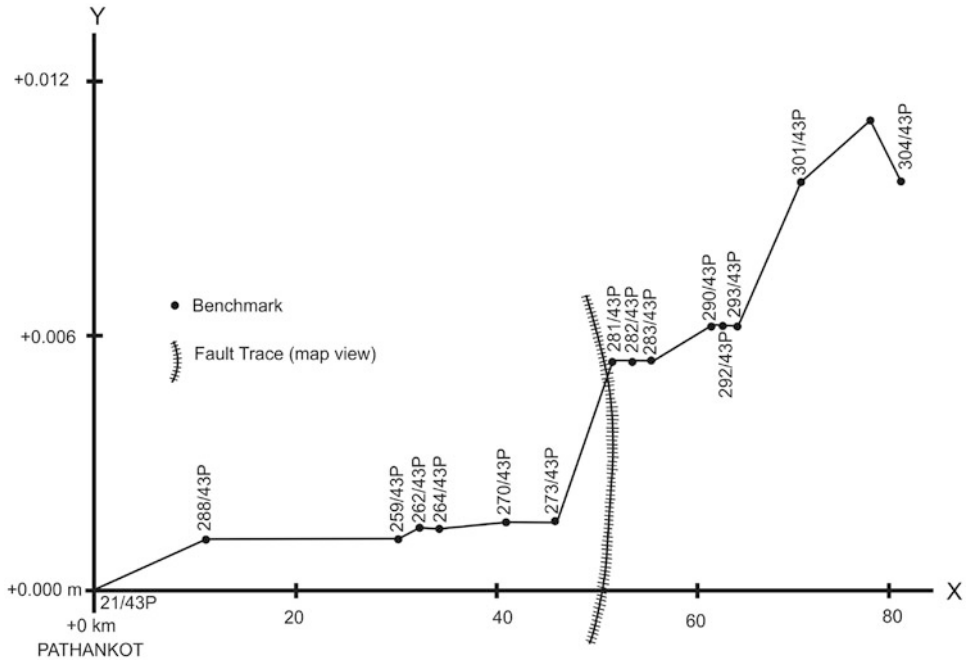

Fig. 35.10 Plot of interseismic slip (coefficient of vertical motion) on the Main Boundary Active Fault between Pathankot and Dalhousie, India, recorded between 1960–1961 and 1972–1973. *Source* Based on Rajal and Madhwal (1996)

interseismic strain accumulation and coseismic release during a great earthquake has a cyclic nature. On the other hand, the interseismic slip measured along the Pathankot–Dalhousie line shows that the velocity is increasing while moving towards the Main Boundary Active Fault (Fig. 35.10).

35.8 Measuring Neotectonic Movements

Bordet (1961) made an early attempt to measure neotectonic movements in Nepal. While approaching Dharan Bajar from the south, he noted the extremely level surface of Terai (consisting of clayey and sandy silt with sporadic pebble beds) with an altitude of about 100 m. Farther north, the surface rises progressively in the Bhabar zone. He attributed this rise to tectonic up-warping and piedmont formation. He also remarked that the rivers flowing on this surface are channeled for a few meters only. Little by little they raise the surface of very flat alluvial cones, which they form on leaving the mountains. Upstream, they are bordered by a succession of terraces. The inclination of these terraces ranges from 5° to 15° to the south and the oldest ones are the most inclined ones (Fig. 35.11). It is notable that the terraces are located within the Bhabar zone and Siwalik belt, just south of the Main Boundary Active Fault.

An attempt to determine accurately the movements along some major active faults of the Nepal Himalaya was undertaken by a team of Japanese researchers in 1980 (Omura et al. 1988; Kizaki 1994). They established a quadrilateral baseline (Fig. 35.12) and leveling stations across the Main Central Thrust at Dana. The measurements were repeated in 1984. The investigation showed that the maximum compressive strain was in the northeast–southwest direction (Fig. 35.13), in a horizontal plane, which is significantly different from the conventional north–south compressive direction. There was also a vertical tilt of 6 mm to the south of the Main Central Thrust along the 3 km long D5–D9 line indicating that the Main Central Thrust was no longer active (Kizaki 1994). On the other hand, similar measurements repeated after four years across the Main Boundary Active Fault at Kerabari (Figs. 35.14 and 35.15) indicated an upheaval of 3 mm for the point lying within the fault zone, whereas a slight northwards tilt of the ground was recorded in the contiguous region lying to the south of the fault zone.

Bilham et al. (1995, 1997), Bürgmann et al. (1999) and Bettinelli (2006) used conventional geodesy as well as Global Positioning System (GPS) to measure crustal deformation in the Nepal Himalaya. Their analysis indicated that the detachment fault (the Main Himalayan Thrust), accommodating about 20 mm/a of the India–Tibet collision, is locked over an approximately 115–150 km width along a more than 500 km reach of the Nepal Himalaya. The accumulating slip deficit will most likely be relieved in future M8 earthquakes. The nonlinear inversions strongly favor shallowly dipping fault planes and do not support any strong variations in dip (Bürgmann et al. 1999). Based on paleoseismological studies in east Nepal, Sapkota et al. (2012) attributed a minimum rupture length of 150 km to the Great Bihar–Nepal earthquake of January 15th, 1934.

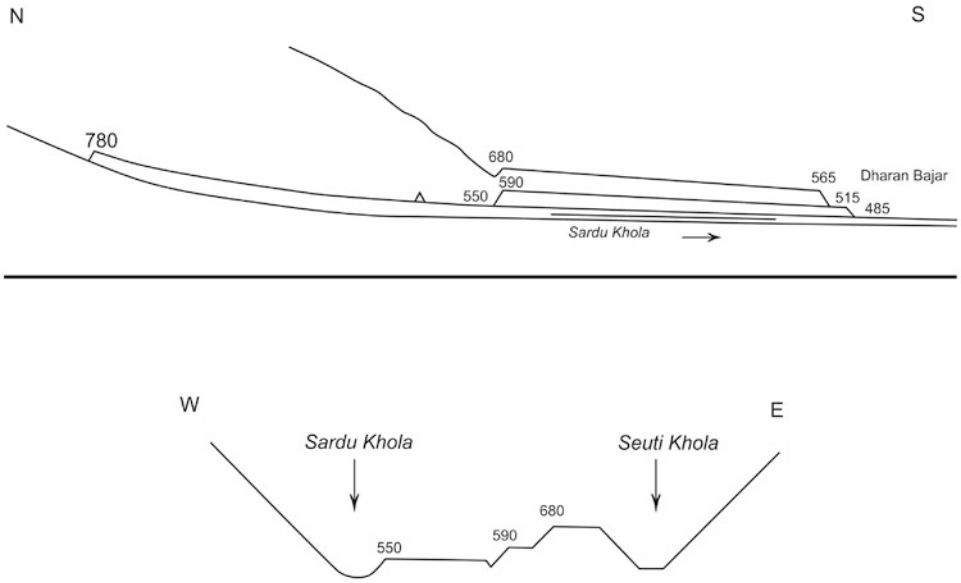

Fig. 35.11 The Sardu Khola terraces near Dharan Bajar (longitudinal and cross-sections). Same *vertical* and *horizontal* scales. The section is 4 km long in N–S direction. *Source* Based on Bordet (1961)

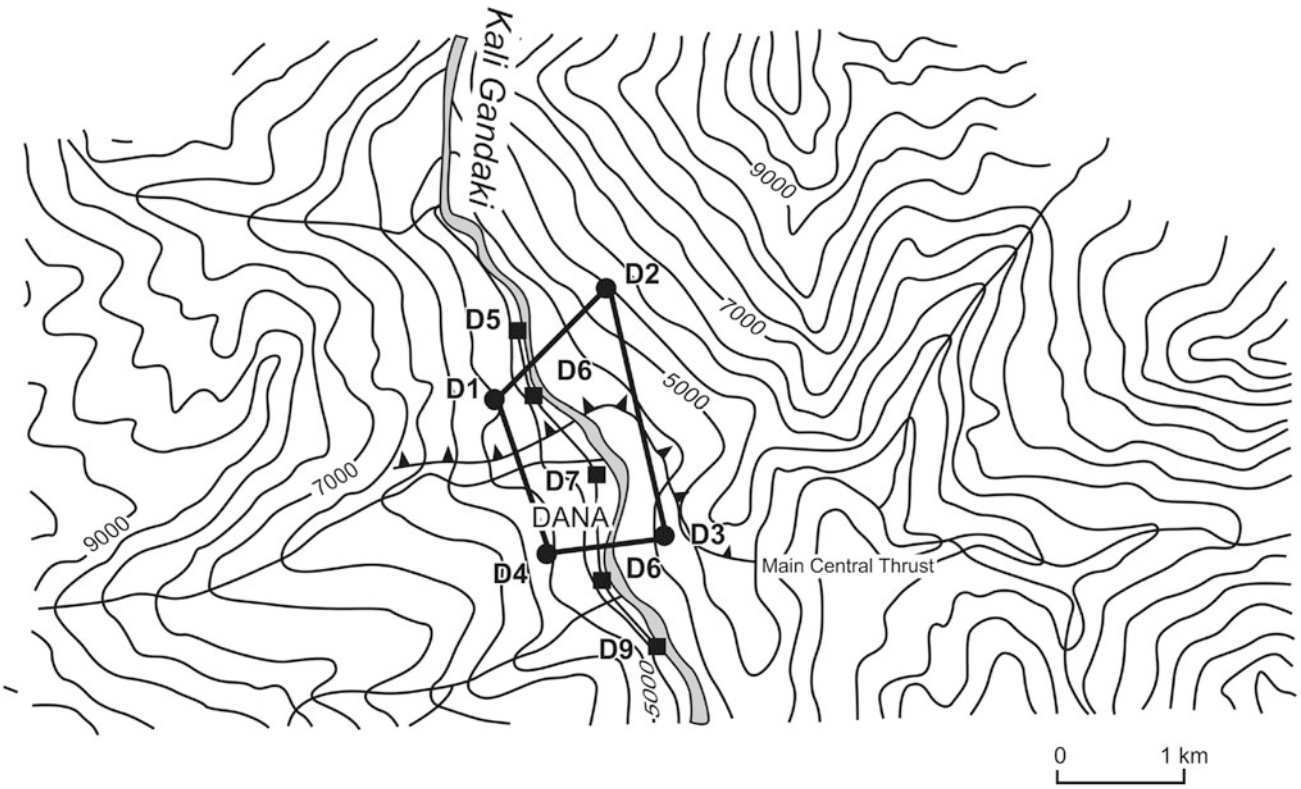

Fig. 35.12 Quadrilateral baseline (*solid circles*) and leveling stations (*solid squares*) at Dana. *Source* Based on Omura et al. (1988)

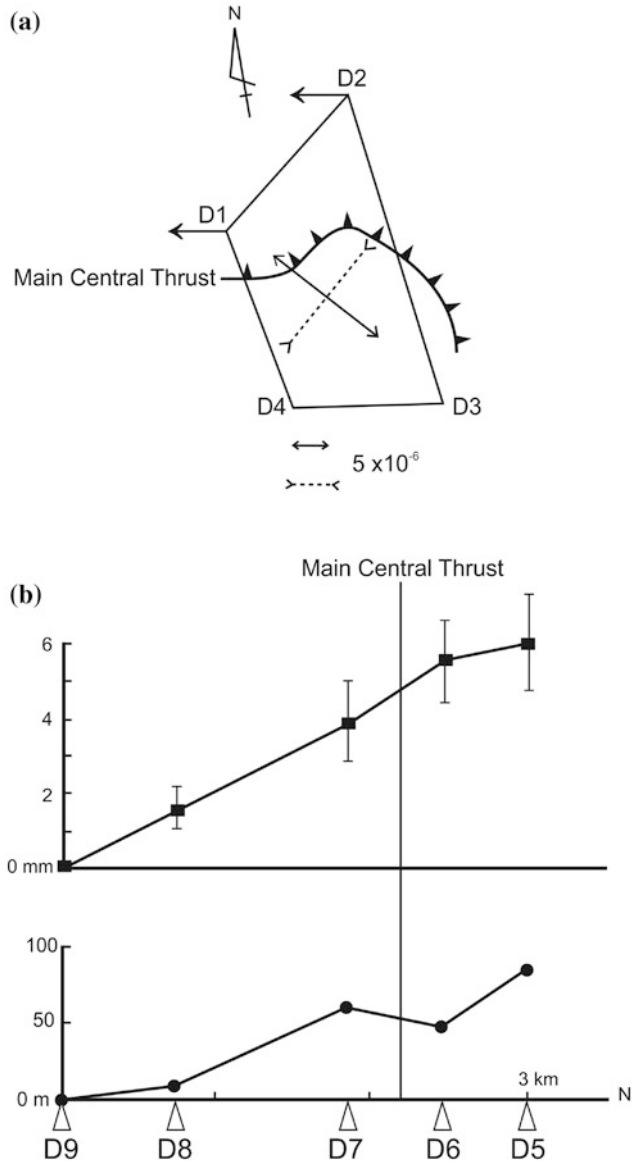

Fig. 35.13 Results of geodetic survey at Dana. **a** NE–SW maximum stress direction and deformation of quadrilateral baseline. **b** The relative variation of leveling stations from 1980 to 1984. *Source* Based on Omura et al. (1988)

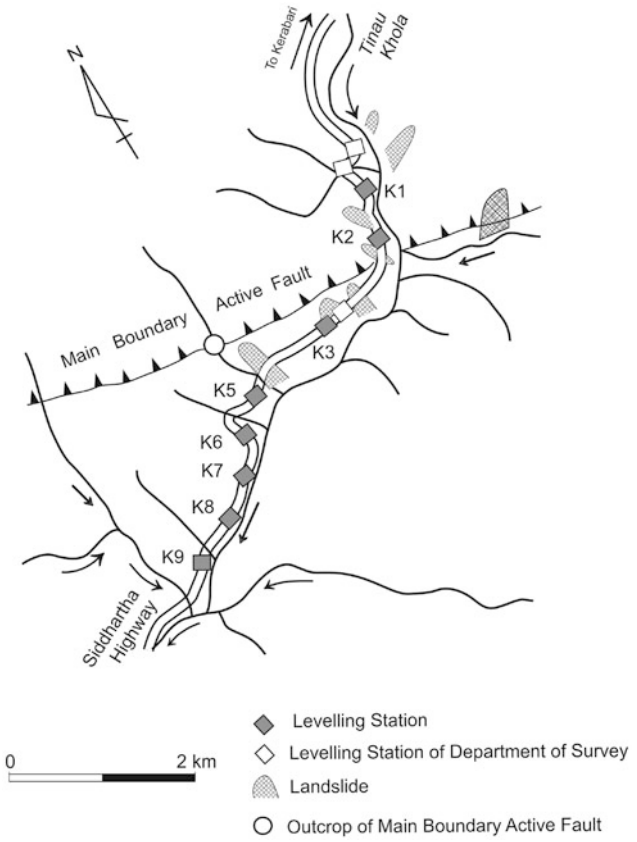

Fig. 35.14 Position of leveling stations near Kerabari. *Source* Modified from Omura et al. (1988)

35.9 Microseismicity in Nepal

The epicenters of microseismic tremors in Nepal (Fig. 35.16) are clustered along the front of the Great Himalayan Range (Avouac 2003; Rajaure et al. 2013). The earthquakes occurring in this region have shallow foci, where the depth varies between 10 and 25 km. But, the M6.5 Udaipur earthquake of 1988 and some others occurring in south Tibet had their foci either in the lower crust or upper mantle. The topographic control on seismicity suggests that at altitudes lower than 3,500 m, the maximum compressive stress is oriented north–south, and it leads to thrusting. On the other hand, where the topographic elevation is higher than 3,500 m, the maximum stress is vertical and the focal mechanisms indicate east–west extension, favoring normal faulting (Avouac 2003; Bollinger et al. 2004).

Pandey et al. (1995, 1999) and Avouac (2003) assumed interseismic stress build-up by elastic straining of the upper crust to be the main cause of microseismicity along the front of the Great Himalayan Range. Avouac et al. (2001) also estimated that the seismicity releases less than 1 % of the accumulated moment of the upper crustal strain.

35.10 A Comparison with the Subduction Zone

Imamura (1929) was the first to note cyclic crustal movements due to the great Nankaido earthquakes. He also pointed out that the slow interearthquake oceanwards tilting

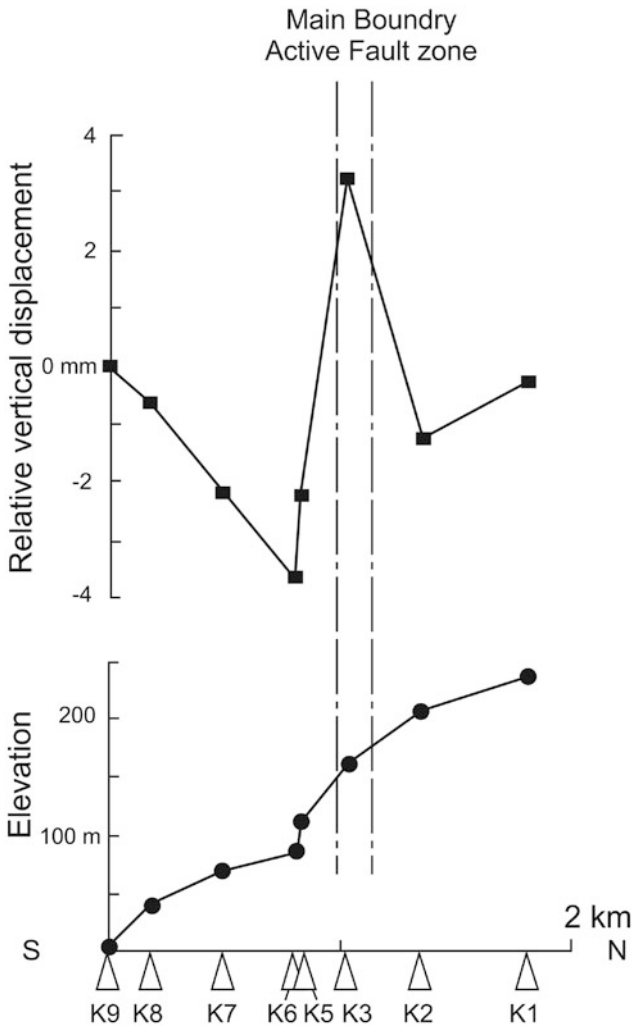

Fig. 35.15 Level variation across the Main Boundary Active Fault near Kerabari from 1980 to 1984. *Source* Modified from Omura et al. (1988)

and coastal subsidence represented elastic strain build-up, whereas the abrupt movements of nearly opposite sense, occurring during the great earthquakes, were related to the release of the accumulated strain.

Thatcher (1984) reconstructed a single complete deformation cycle (coseismic strain release, post-seismic transients, and interseismic strain accumulation) based on the geodetic observations from about 1890 in southwest Japan. There were two great subduction zone thrust earthquakes in 1854 and 1946, and they provided a detailed picture of the strain build-up process. Geodetic measurements show that post-seismic deformation extends more than 300 km inland from the plate boundary, persists for at least 30 years, and has a clear tendency to become longer in wavelength with increasing time. The transient movements have two timescales. The first, of about a year or less, corresponds to deformation, largely uplift, concentrated close to the coseismic fault, and is most easily explained by aseismic slip or much localized deformation downdip of the earthquake rupture plane. The second, longer, timescale is associated with a diffusion-like spread of the deformation farther landwards.

Owing to nonlinearity of strain build-up and the significant permanent deformation, simple recurrence calculations (i.e., dividing the coseismic tilt offset by the interseismic tilt rate) overestimate the true interval between great earthquakes by a factor of 2–3 (Thatcher 1984).

Suyehiro and Nishizawa (1994) described an aseismic contact zone in the subducting plate off the northeast Japan arc. The main features are similar to the aseismic zone in the Siwaliks and Lesser Himalaya. In the Nepal Himalaya, the active faults (Fig. 35.3) that record mainly normal slip are not compatible with the fault-plane solutions of earthquakes. It means that the constituent sediments are incompetent, and this aseismic zone (Fig. 35.16) is deforming plastically. The surface roughness of the ocean bottom near the north Japan trench is well correlated with the large-earthquake occurrence. In the smooth surface region, the coherent metamorphosed sediments form a homogeneous, large, and strong contact zone between the plates. The rupture of this large and strong contact causes great overthrust earthquakes (Tanioka et al. 1997). Similarly, the Main Himalayan Thrust may have a strong contact zone near the Great Himalayan Range, where great overthrust earthquakes can occur. The focus of the Great Bihar–Nepal earthquake was also inferred to fall within this zone (Pandey and Molnar 1988).

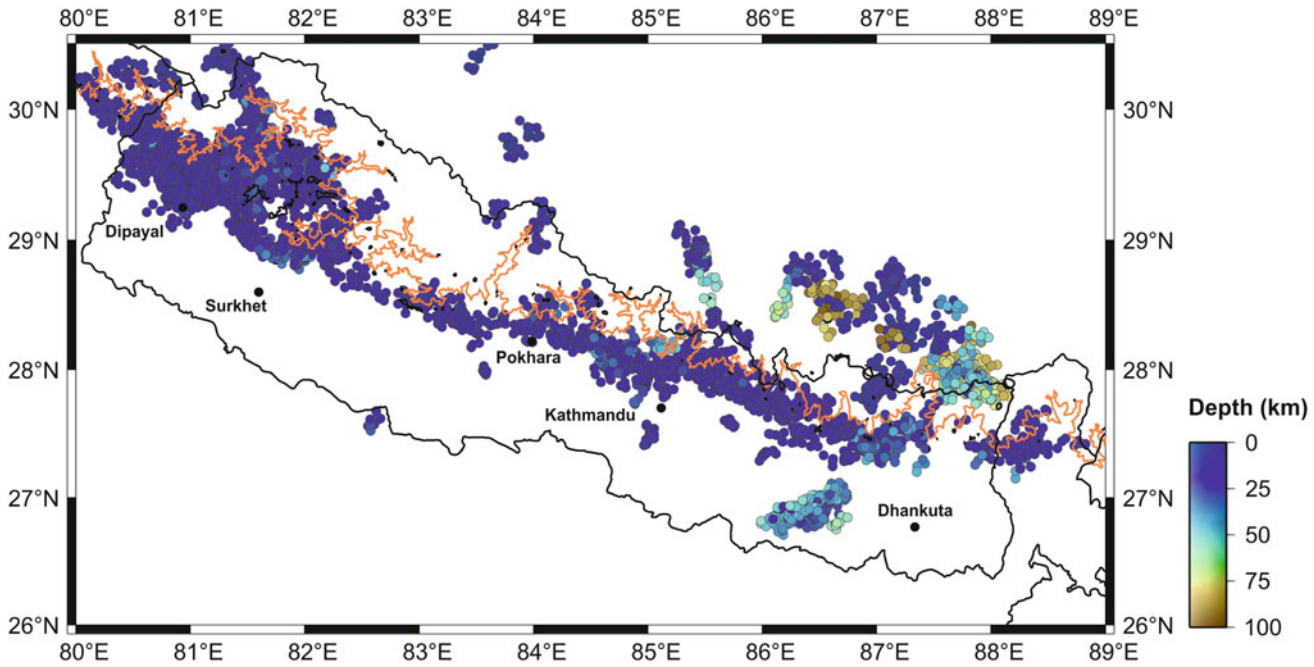

Fig. 35.16 Seismicity of Nepal recorded by the National Seismological Center, Department of Mines and Geology, Kathmandu, Nepal. These earthquakes, with a local magnitude exceeding 1, occurred between 1995 and 2003. The epicenters were relocated using the double difference method. The orange line represents the 3,500 m contour. The shallow earthquakes north of this contour are mostly related to active normal faulting in south Tibet, whereas to the south of it are mainly due to thrust faulting. *Source* Modified from Rajaure et al. (2013)

References

Agrawal PN, Gaur VK (1972) Study of crustal deformation in India. Tectonophysics 15:287–296

Armijo R, Tapponnier P, Han T (1989) Late Cenozoic right-lateral strike-slip faulting across southern Tibet. J Geophys Res 94:2787–2838

Armijo R, Tapponnier P, Mercier JL, Han T (1986) Quaternary extension in southern Tibet: field observations and tectonic implications. J Geophys Res 91:13803–13872

Avouac J-P (2003) Mountain building, erosion, and the seismic cycle in the Nepal Himalaya. Adv Geophys 46:1–80

Avouac J-P, Bollinger L, Lavé J, Cattin R, Flouzat M (2001) Comptes Rendus de l'Académie des Sciences Paris, vol 333, pp 513–529

Beden M, Brunet M (1986) Faunes de mammifères et paléobiogéographie des domaines indiens et péri-indiens au Néogène. Sciences de la Terre, Mémoire no. 47, Nancy, pp 61–87

Bettinelli P, Avouac J-P, Flouzat M, Jouanne F, Bollinger L, Willis P, Chitrakar GR (2006) Plate motion of India and interseismic strain in the Nepal Himalaya from GPS and DORIS measurements. J Geodesy. doi:10.1007/s00190-006-0030-3

Bilham R, England P (2001) Plateau 'pop-up' in the great 1897 Assam earthquake. Nature 410:806–809

Bilham R, Bodin P, Jackson M (1995) Entertaining a great earthquake in western Nepal: historic inactivity and geodetic tests for the development of strain. J Nepal Geol Soc 11:73–88

Bilham R, Larson K, Freymueller J et al (1997) GPS measurements of present-day convergence across the Nepal Himalaya. Nature 386 (6620):61–64

Bollinger L, Avouac JP, Cattin R, Pandey MR (2004) Stress build-up in the Himalaya. J Geophys Res 109:B11405. doi:10.1029/2003JB002911

Bordet P (1961) Recherches Géologiques dans L'Himalaya du Népal, Région du Makalu, Expéditions Françaises a l'Himalaya 1954-1955, Edition du Centre National de la Recherche Scientifique (C. N. R. S.), 275 pp (with geological maps)

Bürgmann R, Larson KL, Bilham R (1999) Model inversion of GPS and leveling measurements across the Himalaya: implications for earthquake hazards and future geodetic networks. Himalayan Geol 20(1):59–72

Burrard SG (1916) The plains of northern India and their relationship to the Himalaya mountains. Presidential Address to the Third Indian Science Congress. J Asiatic Soc Bengal, N.S. XII(2):lxxx–xcviii (with one plate)

Burrard SG, Hayden HH (1908) A sketch of the geography and geology of the Himalaya mountains and Tibet. Calcutta, 308 pp (with a geological map of the Himalaya in colors, scale 1 inch = 40 miles, and many other maps in colors from various parts of the Himalaya)

Cattin R, Martelet G, Henry P, Avouac JP, Diament M, Shakya TR (2002) Gravity anomalies, crustal structure and thermo-mechanical support of the Himalaya of Central Nepal. Geophys J Int 147:381–392

Chander R, Gahalaut VK (1999) On the cyclic nature of active deformation in the Dehra Dun Himalaya. Himalayan Geol 20 (1):87–92 (Wadia Institute of Himalayan Geology, Dehra Dun)

Chen WP, Molnar P (1990) Source parameters of earthquakes and intra plate deformation beneath the Shillong plateau and the northern Indoburman ranges. J Geophys Res 95(B8):12527–12552

Dewey JF, Bird JM (1970) Mountain belts and the new global tectonics. J Geophys Res 75(14):2625–2647

Dollfus O, Usselmann P (1971) Recherches géomorphologiques dans le centre-ouest du Népal. Centre National de la Recherche Scientifique, Recherche Coopérative sur Programme Népal, Paris, 56 pp

Falconer H (1868) Fauna Antiqua Sivalensis. In: Murchison C (ed) Palæontological Memoirs and notes of the Late Hugh Falconer, A.M., A.D., vol I, Robert Hardwicke, London, pp 1–556

Fort M (1976) Quaternary deposits of the Middle Kali Gandaki valley (Central Nepal). Himalayan Geol 6:499–507 (Wadia Institute of Himalayan Geology, Dehra Dun)
Gahalaut VK, Chander R (1992) A rupture model for the great earthquake of 1897, northeast India. Tectonophysics 204:163–174
Gansser A (1974) Himalaya. In: Spencer AM (ed) Mesozoic–Cenozoic orogenic belts: data for orogenic studies. Geological Society Special Publication no 4, London, pp 267–278
Gansser A (1964) The Alps and the Himalayas. In: International geological congress, report of the twenty-second session, India, Part XI, proceedings of session 11: Himalayan and Alpine Orogeny, New Delhi, pp 387–419
Gansser A (1981) The geodynamic history of the Himalaya. In: Gupta HK, Delany FM (eds) Zagros, Hindu Kush, Himalaya, geodynamic evolution. American Geophysical Union, Washington, pp 111–121
Gansser A (1982) The morphogenic phase of mountain building. In: Hsü KJ (ed) Mountain building processes. Academic Press, London, pp 221–228
Gansser A (1983) Geology of the Bhutan Himalaya. Denkschriften der Schweizerischen Naturforschenden Gesellschaft, vol 96, 181 pp (with 4 plates: a geological map in colors; scale: 1:2,000,000; cross-sections in colors and black, and a panorama of mountains)
Hagen T (1959) Über den Geologischen Bau des Nepal-Himalaya mit besonderer Berücksichtigung der Siwalik-Zone und der Talbildung. Jahrbuch der St. Gallischen Naturwissenchaftlichen Gesellschaft, vol 76, pp 3–48 (with 10 figures and 9 plates)
Hagen T (1956) Über eine überschiebung der Tertiären Siwaliks über das rezente Ganges alluvium in Ostnepal. Geographica Helvetica XI (2):217–219 (Bern)
Hagen T (1969) Report on the geological survey of Nepal. Volume 1: preliminary reconnaissance. Denkschiiften der Schweizerischen Naturforschenden Gesellschaft, Band LXXXVI/1, 185 pp (with a geological map)
Harrison TM, Copeland P, Kidd WSF, Yin A (1992) Rising Tibet. Science 255:1663–1670
Hayden HH (1913) Notes on the relationship of the Himalaya to the Indo-Gangetic plain and the Indian Peninsula. Rec Geol Surv India XLIII(Part 2):138–167 (with 2 plates)
Heim A, Gansser A (1939) Central Himalaya: geological observations of the swiss expedition 1936. Denkschriften der Schweizerischen Naturforschenden Gesellschaft, Band LXXIII, Abh. 1, 245 pp (with maps, sections, and plates)
Imamura A (1929) On the chronic and acute earth-tilting in the Kii peninsula. Japan J Astron Geophys 7:31–45
Iwata S (1987) Mode and rate of uplift of the central Nepal Himalaya. Zeitschrift für Geomorphologie NF(Supplement) 63:37–49 (Stuttgart)
Iwata S, Nakata T (1985) River terraces and crustal movement in the area around Narayanghat, Central Nepal. J Nepal Geol Soc 3(1 and 2): 33–42
Jangpangi BS (1974) Stratigraphy and tectonics of parts of Eastern Bhutan. Himal Geol 4(Part I):117–136
Kimura K (1994) Formation and deformation of river terraces in the Hetauda dun, central Nepal: a contribution to the study of Post Siwalikan tectonics. Sci Rep Tohoku Univ 7th Ser (Geogr) 44 (2):151–181
Kizaki K (1994) An outline of the Himalayan upheaval. Japan International Cooperation Agency (JICA), Kathmandu, 127 pp
Kono M (1974) Gravity anomalies in east Nepal and their implications to the crustal structure of the Himalayas. Geophys J Roy Astron Soc 39:283–299
Lyon-Caen H, Molnar P (1983) Constraints on the structure of the Himalaya from an analysis of gravity anomalies and a flexural model of the lithosphere. J Geophys Res 88(B10):8171–8191
McKenzie DP (1969) Speculations on the consequences and causes of plate motions. Geophys J Royal Astron Soc 18(1):1–32
Medlicott HB (1864) On the geological structure and relations of the southern portion of the Himalayan range between the rivers Ganges and Ravee. Mem Geol Surv India III(Art 4):1–206 (with a geological map in colors; scale: 1 inch = 8 miles)
Middlemiss CS (1910) The Kangra earthquake of 4th April 1905. Mem Geol Surv India XXXVIII:1–409 (with 30 plates)
Molnar P (1986) The structure of mountain ranges. Sci Am 255(1):70–79
Molnar P (1987) The distribution of intensities associated with the great 1897 Assam earthquake and bounds on the extent of rupture zone. J Geol Soc India 30:13–27
Molnar P, England P (1990) Late Cenozoic uplift of mountain ranges and global climate change: chicken or egg? Nature 346:29–34
Nakata T (1972) Geomorphic history and crustal movements of the foot-hills of the Himalayas. Sci Rep Tohoku Univ 7th Ser (Geogr) 22(1):39–177
Nakata T (1982) A photogrametric study on active faults in the Nepal Himalayas. J Nepal Geol Soc 2(Special Issue):67–80
Nakata T (1989) Active faults of Himalaya of India and Nepal. In: Malinconico LL, Lillie RJ (eds) Tectonics of the Western Himalayas. Geol Soc Am Spec Pap 232:243–264
Nakata T, Iwata S, Yamanaka H, Yagi H, Maemoku H (1984) Tectonic landforms of several active faults in the western Nepal Himalayas. J Nepal Geol Soc 4(Special Issue):177–200
Oldham RD (1899) Report on the Great Earthquake of 12th June 1897. Mem Geol Surv India XXIX:1–379 (with 43 plates and 3 maps)
Oldham RD (1917) The structure of the Himalayas, and of the Gangetic plain, as elucidated by geodetic observations in India. Mem Geol Surv India XLII(Part 2):1–153
Ollier CD, Pain CF (2000) The origin of mountains. Routledge, London, 345 pp
Omura M, Yokoyama K, Kubo S (1988) Small scale and precise geodetic survey on the Himalayan tectonic lines. In: Kizaki K (ed) Himalayan upheaval. Tsukiji-Shokan, Tokyo, pp 167–175 (in Japanese)
Pandey MR, Molnar P (1988) The distribution of intensity of the Bihar-Nepal earthquake of 15 January 1934 and bounds on the extent of the rupture zone. J Nepal Geol Soc 5:22–44
Pandey MR, Tandukar RP, Avouac J-P, Lavé J, Massot JP (1995) Interseismic strain accumulation on the Himalayan crustal ramp (Nepal). Geophys Res Lett 22(7):751–754
Pandey MR, Tandukar RP, Avouac J-P, Vergne J, Héritier T (1999) Seismotectonics of the Nepal Himalaya from a local seismic network. J Asian Earth Sci 17:703–712
Powell CMcA (1986) Continental underplating model for the rise of the Tibetan Plateau. Earth Planet Sci Lett 81:79–94
Rajal BS, Madhwal HB (1996) Geodetic studies of crustal deformation and fault displacements. Himal Geol 17:17–32 (Wadia Institute of Himalayan Geology, Dehra Dun)
Rajaure S, Sapkota SN, Adhikari LB, Koirala B, Bhattarai M, Tiwari DR, Gautam U, Shrestha P, Maske S, Avouac JP, Bollinger L, Pandey MR (2013) Double difference relocation of local earthquakes in the Nepal Himalaya. J Nepal Geol Soc 46:133–142
Rana BSJB (1935) Nepalko Mahabhukampa (The great earthquake of Nepal), 2nd edn. Published by the author, Kathmandu, 251 pp (In Nepali)
Saha DK, Naskar DC, Bhattacharya PM, Kayal JR (2007) Geophysical and seismological investigations for the hidden Oldham fault in the Shillong Plateau and Assam valley of Northeast India. J Geol Soc India 69:359–372
Sapkota SN, Bollinger L, Klinger Y, Tapponnier P, Gaudemer Y, Tiwari D (2012) Primary surface ruptures of the great Himalayan earthquakes in 1934 and 1255. Nat Geosci 6:71–76

Sharma T, Upreti BN, Vashi NM (1980) Kali Gandaki gravel deposits of Central West Nepal—their neotectonic significance. Tectonophysics 62:127–139

Stille H (1936) The present tectonic state of the earth. Bull Am Assoc Petrol Geol 20:849–880

Stöcklin J (1980) Geology of Nepal and its regional frame. J Geol Soc Lond 137:1–34

Strachey R (1851) On the geology of part of the Himalaya Mountains and Tibet. Q J Geol Soc Lond 7:292–310 (with a geological map and two cross-sections in colors)

Suess E (1909) Das Antlitz der Erde. Wien and Leipzig, vol III(2), 789 pp (with 3 maps in colors)

Suyehiro K, Nishizawa A (1994) Crustal structure and seismicity beneath the forearc off northeastern Japan. J Geophys Res 99 (B11):22331–22347

Tanioka Y, Ruff L, Satake K (1997) What controls the lateral variation of large earthquake occurrence along the Japan Trench? Island Arc 6:261–266

Thatcher W (1984) The earthquake deformation cycle at the Nankai Trough, southwest Japan. J Geophys Res 89(B5):3087–3101

Yamanaka H, Iwata S (1982) River terraces along the middle Kali Gandaki and Marsyandi Khola, central Nepal. J Nepal Geol Soc 2 (Special Issue):95–111

Zhang P, Molnar P, Downs WR (2001) Increased sedimentation rates and grain sizes 2 ± 4 Myr ago due to the influence of climate change on erosion rates. Nature 410:891–897

Conclusions

36

This is called the horizon problem. From one side of the observable Universe, the other side is over the horizon and inaccessible. Yet astronomical observations suggest that the two sides of the Universe were once in contact.

—Robert Jastrow and Michael Rampino (2008)

The foregoing chapters have provided a glimpse of the geological diversity specific to the Nepal Himalaya. Although Himalayan geology has been covered for many years with detailed mapping and painstaking observations in the field as well as in the laboratory, it is still lagging behind the rigor of investigation carried out in other mountain ranges, such as the Alps and Andes. Despite the present trend of narrow specialization and the information boom, regional geological investigations in Nepal are yet quite disorganized and sparse. Hence, it is difficult to present a coherent picture of the broad geological divisions representing the Nepal Himalaya. Nevertheless, an endeavor is made to summarize the main points and to put forward some inferences and critical remarks.

36.1 Lesser Himalaya

An exceedingly thick (more than 15 km) sequence, accumulated within a vast timespan (from Paleoproterozoic to Miocene), and a dearth of fossils, together with strata in tangled juxtaposition, make the geological investigations in the Lesser Himalaya most challenging. The Lesser Himalayan sequence is essentially a northern continuation of the Indian shield, containing shallow marine and continental deposits, bordering the shallow Tethys Sea. This succession records a gradual change from the south shield and Gondwana succession, which is presently disrupted by the Main Central Thrust, conveying the Higher Himalayan crystallines (Gansser 1981). The three broad stratigraphic markers of the Lesser Himalaya in Nepal are the Paleoproterozoic Kuncha Formation, Mesoproterozoic Dhading Dolomite with columnar and branching stromatolites, and the Mesoproterozoic to Neoproterozoic Benighat Slates or their equivalents (Fig. 36.1). Although stromatolites have been used to correlate various Lesser Himalayan formations, they are distributed throughout a wide timespan, ranging from the Mesoproterozoic to Neoproterozoic.

In the Mahakali–Seti region, the Lesser Himalayan sequence comprises the inner carbonate and slate sequence, and outer zone of quartzites and amphibolites with some phyllites. Two conspicuous Paleocene–Miocene slices are observed in the inner zone. Many imbricate faults and some thrust sheets are present below the Main Central Thrust. While moving farther east in the Karnali–Bheri region, one encounters two more thrust sheets that have moved over the outer belt of quartzites and amphibolites. The lower thrust sheet is essentially a carbonate sequence, not much different from the rocks found in the inner zone of the Mahakali–Seti region. The upper thrust sheet is made up of phyllites, quartzites, diamictites, and allied rocks.

On the other hand, the frontal belt of the Karnali River is met with rocks similar to the Krol belt in the Northwest Himalaya of India. It contains slates or shales, which are followed by variegated shales, quartzites, stromatolitic dolomites, and limestones. Cenozoic sediments disconformably overlie the last succession. The sequence continues farther east in the Gandaki region with widespread development of Permo–Carboniferous diamictites, Upper Gondwanas, and Paleocene–Miocene strata. The inner zone of the Gandaki region contains a very thick and rather monotonous sequence of phyllites, metasandstones, and quartzites enclosing some augen gneisses and extremely rare nepheline syenite intrusives. Presumably, these Paleoproterozoic rocks are the oldest outcrops in the Nepal Himalaya. In this area, the intermediate zone abounds in south-dipping backthrusts. There are also north-dipping imbricate faults, whose surfaces are undulating. The backthrusts contain the youngest Miocene rocks of the region in their footwall. The klippe of the Higher Himalayan rocks in the Lima Khola area witnessed an extensive erosion of the Higher Himalayan roof that covered the above imbricate faults, forming a large duplex. The Lesser Himalayan belt becomes quite narrow in the Koshi region and its outer zone is essentially the continuation of the Nawakot Complex. The tectonic widows of Okhaldhunga and Taplejung lie in the inner zone. A few

M.R. Dhital, *Geology of the Nepal Himalaya*, Regional Geology Reviews,
DOI 10.1007/978-3-319-02496-7_36

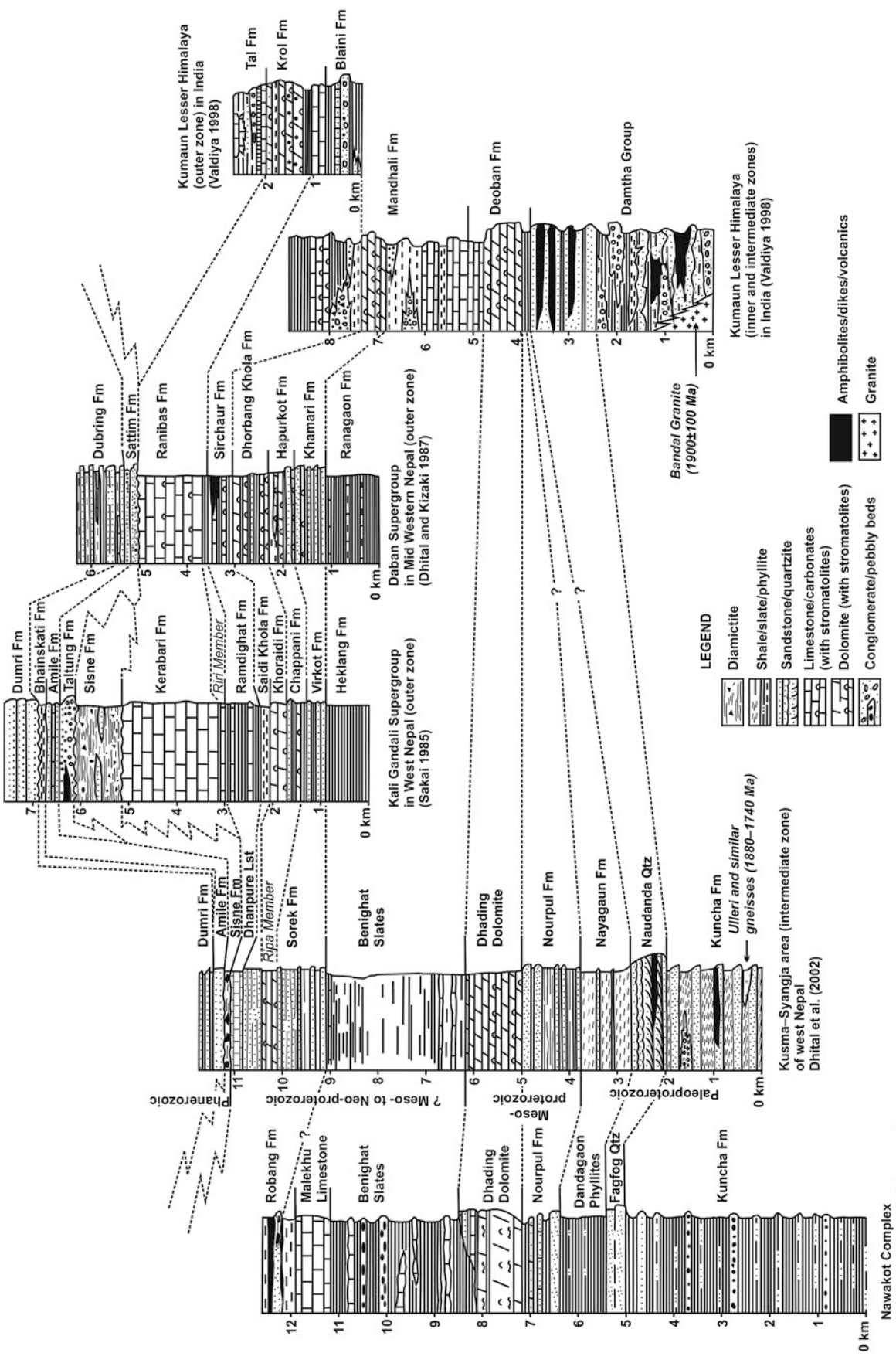

Fig. 36.1 Lithostratigraphic comparison and correlation of various Lesser Himalayan formations of Nepal and Kumaun, India. *Source* Modified from Dhital et al. (2002). © Central Department of Geology, Tribhuvan University. Used by permission

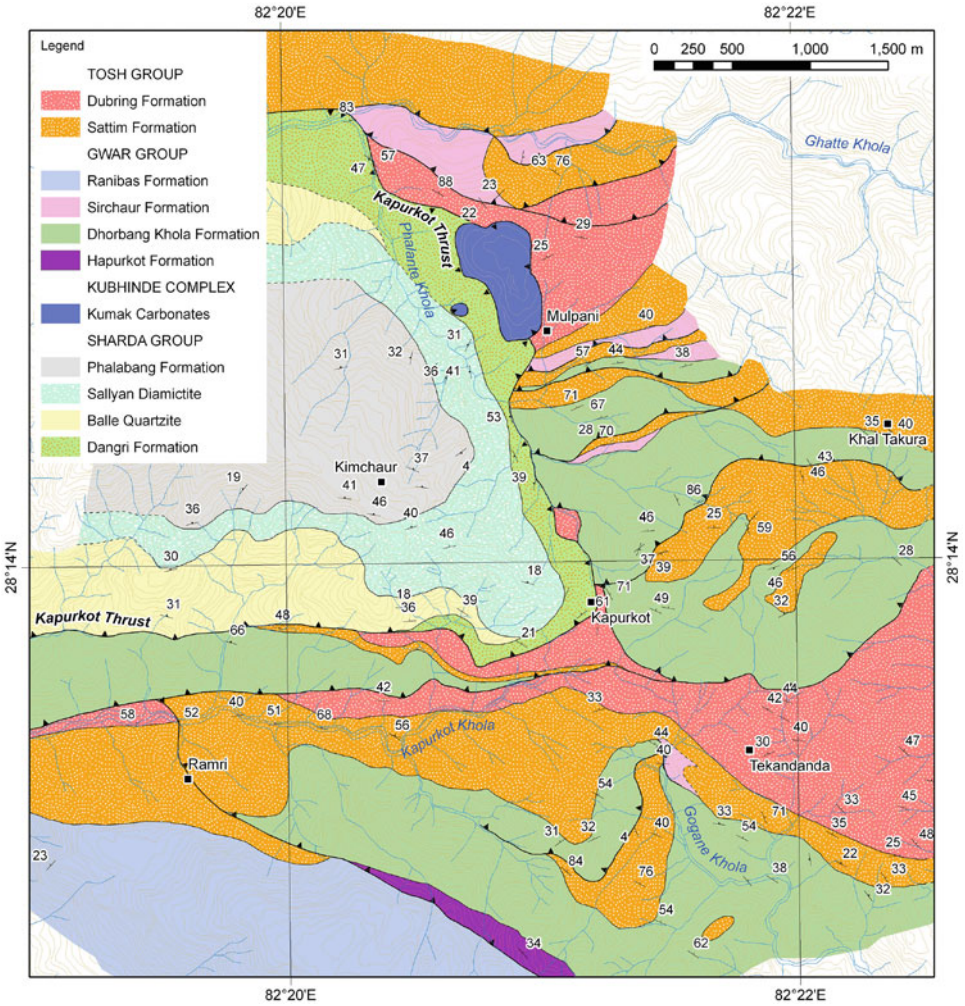

Fig. 36.2 Various imbricate slices exposed in the vicinity of Kapurkot in west Nepal. The Kapurkot roof thrust brings low-grade metamorphic rocks over the sedimentary strata (Chap. 9). *Source* Author's observations

Paleoproterozoic granite bodies are exposed in the Taplejung window. The rocks in the vicinity of Barahakshetra and farther west consist of some diamictites and coal-bearing strata of Gondwana affinity, well investigated in Darjeeling and Bhutan.

The diversity of geological structures in the frontal belt is elucidated by the prevalence of imbricate faults in one area (Fig. 36.2), but a broad syncline (Fig. 36.3) in a neighboring tract, lying in strike continuation with the former. The duplexes and imbricate stacks of the frontal belt form a broad transfer zone, where the displacement along one fault is taken up by another in the adjoining area. Most of the frontal faults contain black slates or phyllites in their hanging wall flats. Such flats are relatively longer and have traveled farther into the Siwaliks than those made up of carbonates or sandstones. The involvement of the Proterozoic basement in some imbricate slices occurring in the Sub-Himalayan belt is characteristic of central and east Nepal. The interruption of the Lesser Himalayan sequence against the Higher Himalayan crystallines, overriding the Siwaliks in central Nepal, demonstrates significant post-Siwalik movements in that tract.

36.2 Higher Himalaya

The Higher Himalayan crystallines form the base of the Tethyan sequence. Their lower boundary is the Main Central Thrust, whereas the upper limit is arbitrarily placed where the Early Paleozoic sediments show a rather independent tectonics, including the remarkable backfolds of Annapurna and where the Himalayan metamorphism is imperceptible (Gansser 1981). The South Tibetan detachment system or a shear zone with top-to-north sense is frequently observed in the north-dipping strata. These rocks have a rather similar lithology. Towards the north, they begin with banded or augen gneisses, which may or may not contain some sillimanite, but they commonly have some kyanite. In places the gneisses are migmatitic. They are followed by quartzites, becoming more calcareous towards the top, and enclosing a

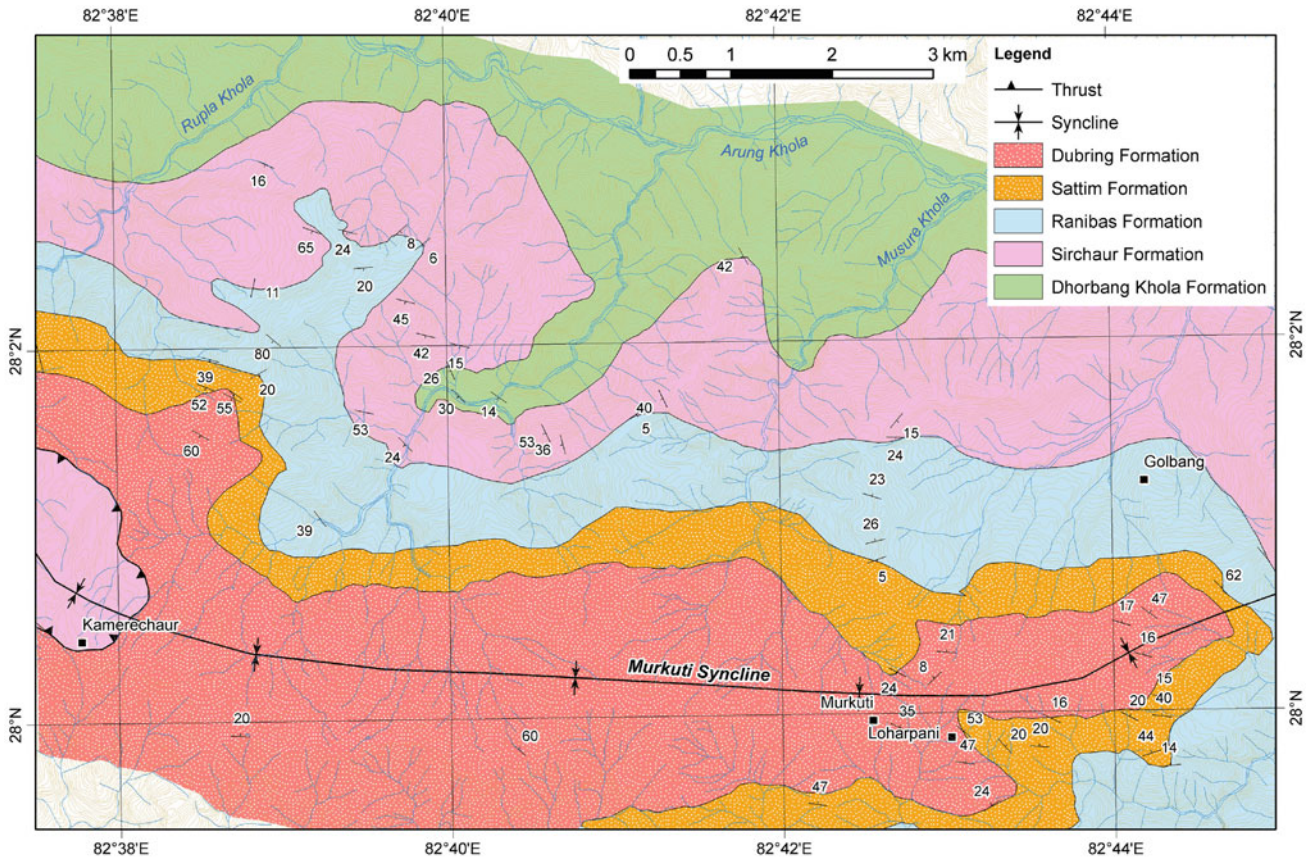

Fig. 36.3 The Murkuti Syncline, extending about 20 km east of the area with imbricate faults (Fig. 36.1). *Source* Author's observations

number of silicate bands. The last sequence gives way to an alternation of marble and lime-silicate rock. The Higher Himalayan crystallines terminate with the appearance of the first fossiliferous crystalline limestone or dolomite. The argillaceous and calcareous basal section is about 10 km thick and the underlying crystalline slab varies in thickness from less than 3 to 15 km. In the middle part of the crystallines, appears a network of complicated dikes of Miocene leucogranite, which give way to larger leucogranite bodies, characterized by similar petrography.

Paleozoic granites are widespread in the Higher Himalayan zone. They are commonly elongated parallel to the Himalayan arc, and some of them have also been transferred into augen and banded gneisses, especially those lying close to the Main Central Thrust. They have a narrow contact metamorphic aureole, but seem to be unrelated to regional metamorphism. On the other hand, the Miocene leucogranites have a limited distribution, but are broadly homotaxial with regional metamorphism. Although inverted metamorphism is widespread in the Lesser and Higher Himalayan successions, the synformally folded klippen or semi-klippen of the Higher Himalayan crystallines on the south slopes of the Great Himalayan Range, are relatively less metamorphosed and record essentially an "uninverted" grade. Hence, the Main Central Thrust must have obliquely cut through the metamorphic isograds.

36.2.1 Some Remarks on Inverted Metamorphism

The Main Central Thrust of Heim and Gansser (1939) became rather arbitrary when Gansser (1964) drew an "out-of-sequence" fault, dividing the thrust into outer and inner segments. This assumption also required that the crystallines bounded by the outer segment be part of a schuppen zone, residing under the inner segment (Gansser 1981). Many subsequent investigators have conveniently drawn the Main Central Thrust or its equivalents at various structural levels (Stöcklin 1980). The model of inverted metamorphism, first proposed by Le Fort (1975), became progressively more complex, involving various new attributes and constraints, such as parallelism (or convergence) of the Main Central Thrust and the South Tibetan detachment system, and their simultaneity of movement for millions of years. Most models also require intense precipitation and wholesale erosion, concentrated precisely at a designated spot or band

throughout the 2,400 km long Himalayan Range, as well as transfer of a large amount of heat and partially molten mass during their displacement for hundreds of kilometers. Some models draw many closely spaced faults, others require shear heating, delamination, underplating, extrusion, or reactivation of the Main Central Thrust, and some others deny even the existence of the fault.

Miyashiro (1994, pp. 64–65) expressed strong doubts over the models that dynamically link metamorphism with thrusting. Geobarometry and geothermometry provide estimates of exhumation and, combined with geochronology, of exhumation rates. The uncertainties involved in these measurements indicate that they cannot provide quantitative information on rates of change of surface height (England and Molnar 1990). It seems equally improbable that such information can be useful to measure quantitatively any horizontal displacement or thrusting.

Because inverted metamorphism is widespread in the Lesser and Higher Himalaya, this phenomenon requires some intrinsic explanation. When the leading edge of the Indian plate was plunging into the Eurasian plate (Lhasa terrane), the heat source rising above the Indian plate generated magma that erupted from volcanos, and created the Trans-Himalayan batholiths (Molnar 1986). The Eo-Himalayan metamorphism is also attributed essentially to the same process. Subsequently, when the Indian and Eurasian plates collided, the readjusted heat source could have caused the "inverted" metamorphism and also be responsible for generating a batch of magma that produced Miocene leucogranites within the Indian plate. During subduction, the Tethyan sediments and oceanic crust were scraped off the descending plate, and, sometime after collision, the Main Central Thrust broke through the Indian crust, topped by Paleozoic and Mesozoic sediments, and it was thrust up onto the oncoming subcontinent (Lyon-Caen and Molnar 1983; Molnar 1986). When the Main Central Thrust became almost inactive, the Main Himalayan Thrust and its splays propagated towards the foreland, in response to the continued convergence of the two plates. On the other hand, newer heat sources were also revealed in their various episodes, some of which led to the formation of quite young (Pliocene) granites.

The development of inverted metamorphism and propagation of the Main Central Thrust could be partly concomitant but independent phenomena. The Himalayan inverted metamorphism is nothing but a progressive (Barrovian) metamorphism imprinted on the inclined Indian plate. Thus, the dip angle of the subducting plate and the configuration of isotherms were the two fundamental parameters that governed the distribution and grade of metamorphism throughout the Himalayan arc.

36.3 Tethys Himalaya

In Nepal, the Tethyan sequence is distributed in a number of isolated regions lying to the north or south of the Great Himalayan Range. These areas differ structurally, however, their stratigraphy is broadly similar. The sediments were accumulated basically on a passive continental margin, and comprise a thick pile of shallow marine sediments, with some deep marine episodes as well as a minor proportion of continental deposits including some volcanics. In them the deformation style is very different from that of the Higher or Lesser Himalayan sequence. The Tethyan realm contains complex disharmonic folds, normal faults, and thrusts. The Tethyan rocks occurring in the Mahakali region are generally strongly deformed to yield various north- as well as south-vergent folds and faults, whereas those of Dolpa constitute a huge synclinorium. There are several other synclinally folded Tethyan outliers lying to the south of the Great Himalayan Range, such as the rocks of Phulchauki in central Nepal and the Jaljala Range in west Nepal.

The Cambro–Ordovician sequence in the Mahakali region is represented by fine detritus to argillaceous strata, whereas in Dolpa the sediments become more calcareous. Farther east, this sequence is made up of limestones with some shales and sandstones in the Thakkhola, Manang, and Everest regions. In the Paleozoic sequence of the Thakkhola Basin and Everest region, also occur some relatively deep marine sediments with poor bottom circulation, marked by the appearance of Silurian and Devonian graptolites. An apparent depositional gap separates the Devonian Muth quartzite of the Mahakali region from the overlying Permian *Productus* shales, whereas in Dolpa, dark limestones and shales of the Carboniferous are delimited from the overlying Permian sandstones and shales by a distinct disconformity. In the Thakkhola, Manang, and Everest regions, the Permian sandstones and shales with sporadic conglomerate beds and coal lenses rest over the Carboniferous strata with a dwindling disconformity. These Permian strata represent the post-rift sediments accumulated during the opening up of the Neo-Tethys Sea (Garzanti 1999). They become more calcareous towards the east, in Manang as well as the Everest region, where the late Carboniferous sequence of Gondwana affinity with some volcanics also occurs.

The Mesozoic Group is remarkable by its great thickness (over 3,500 m) and the abundance of generally fine detrital material, which it contains at all levels. The Triassic sequence of Nepal bears many similarities with the Spiti Basin. The Early Triassic rocks constitute a pelagic succession with a reduced thickness, in often nodular beds, rich in ammonites and alternating with shale horizons. The Triassic System is highly fossiliferous in the Mahakali region,

where several limestone and shale sequences are recognized. In Dolpa, limestones alternate with marls, and they also contain many fossils. Sandstones in them constitute an insignificant amount and they were derived from the distant shores. The Middle Triassic sequence appears much more argillaceous in Thakkhola, and it includes thin and rare limestone beds. During that epoch, there was a progressive increase in aggregate thickness as well as argillaceous content from west Nepal towards east Nepal. Farther upwards, these deposits become increasingly detrital and pass into the Late Triassic. But it is especially in Dolpa and Thakkhola, where a thick series of quartzose sandstone occurs in the early Rhaetian.

The Early Jurassic rocks are made up of compact bioclastic limestones, show a large proportion of fine quartz grains or of silt, and the characters of the deposit are always those of a shallow basin in constant subsidence (Colchen et al. 1986). The lumachelles of lamellibranchs are frequent in the Middle Jurassic and the Early Aptian successions. On the other hand, the Late Jurassic strata of Spiti correspond to a well-known black shale of offshore or continental slope facies with iron-rich nodules containing ammonites (Colchen et al. 1986). At the beginning of the Cretaceous, sandy continental deposits appeared with plant remains in the Thakkhola. They correspond to the Giumal Sandstone and Upper Flysch beds with radiolarian fossils in the Mahakali region, whereas the Cretaceous is represented by a thick sequence of shallow marine carbonates and shales in the Everest region.

The Paleogene sequences occur in the Lesser Himalaya as well as in the Everest region, where they are represented by a very rich assemblage of marine fossils, including the youngest massive limestone beds containing *Nummulites and Assilina*.

36.4 Siwaliks

The Siwaliks constitute the low fringe zone, bordering the Ganga Basin and corresponding to the south molasse belt. They were deposited from the Himalaya and Tibetan Plateau during Middle Miocene–early Pleistocene time. They succeed the Subathu–Dagshai–Kasauli sequence in the Northwest Himalaya or equivalent strata in Nepal. The Siwalik sandstones increase in thickness and grain size, stratigraphically upwards.

The Sub-Himalaya is a typical thrust-and-fold belt. Although in Bhutan, the Upper Siwaliks are found towards the north, at the thrust contact with the Lesser Himalayan rocks, in Nepal, such an arrangement is rare. The incompetent Siwalik strata have been twisted into many noncylindrical, plunging folds. There is an intimate relationship between thrusting and folding. From a glance at the distribution of frontal faults and folds in the Siwaliks and adjacent hinterland region, it is evident that the faults and folds are interrelated and in many instances they pass into one another. The faults are significantly longer than the folds. There are also a few transverse or tear faults interrupting these thrusts in the direction essentially perpendicular to their strike and displacing towards the foreland. Most of the thrusts are north-dipping, but some are south-dipping (backthrusts). Like the axial traces of some frontal folds, the thrusts are undulating in plan view and they are either convex or concave towards the foreland.

In the Karnali–Bheri region, the northeast–southwest trending Babai Backthrust follows the Babai River flowing through the south margin of the Dang Valley (Chap. 34). The fault turns to the south after the termination of the Dang Valley in the west. The backthrust is essentially parallel to the overlying rocks of the Banks Formation in most places. The Tui Backthrust overrides the Babai Backthrust. It leaves the Tui Khola Valley and enters the Deukhuri Valley, obliquely cutting the Siwalik beds and finally terminating at the Rapti Backthrust.

A large region of overturned succession is observed in the area between Tui Khola and Amiliya, and also in the Masot Khola. Sometimes the Siwaliks are overturned right at the south margin of the foothills, bordering the Terai alluvium, such as the Middle Siwalik strata outcropping to the north of Amlekhganj.

Marques (2008) investigated thrust initiation and propagation during shortening of a two-layer model, where a forebulge developed into a buckle with continued deformation. Later, a new fore thrust formed from the forelimb of the buckle. At a later stage, a backthrust formed from the back limb of the buckle, with formation of pop-ups and contractional basins, similar to the intermontane valleys in the Sub-Himalaya.

36.5 Neotectonics

Middlemiss (1890) put forward his classic views on active tectonics, where sedimentation and faulting were going side by side in piggyback basins developed in the outer as well as inner belts of the Kumaun Sub-Himalaya. The gravel veneer lying in the inner Sub-Himalayan belt of Nepal, between Budar and Phaltude, is elevated by about 300 m (Chap. 28), whereas in many other parts of the Sub-Himalaya, such a rapid upheaval is not evident. Hagen (1969) and Nakata (1982) have presented many cases of diverse neotectonic movement in the form of normal, strike-slip, and reverse faults. Many large rivers (Kali Gandaki, Marsyangdi, Madi) in the Midlands are rapidly downcutting their own old

terrace deposits, but have not yet reached the underlying bedrock, implying a protracted, but episodic and irregular upheaval of the Himalaya.

36.6 East Versus West Himalaya

The Nepal Himalaya shares many stratigraphic and structural details with the neighboring regions, however, some differences are apparent. The Lower Gondwanas are well known in Darjeeling, Sikkim, and Bhutan. The coal-bearing beds of Barahakshetra in east Nepal are ascribed as well to the Lower Gondwanas. The Upper Gondwanas are found in west Nepal, whereas no Gondwanas have been recorded so far from the Kumaun Himalaya. The discovery of Cambrian fossils from the Tal Formation in the Northwest Lesser Himalaya has indicated the deposition of the Blaini diamictite in Proterozoic time. On the other hand, in Nepal, the Tal Formation is not yet recognized, but there are Permo–Carboniferous diamictite sequences. Lakhanpal et al. (1958) reported some Permian spores from a carbonaceous shale near Nainital, whereas Ganesan (1972) described fenestellid bryozoa of Carboniferous age from a boulder slate sequence of Garhwal (near Dogadda). Such scattered observations await further detailed study in this part of the Himalaya.

36.7 Some Anomalies

Gansser (1991) opined that there should be an acceptable balance between facts and theories. It is utterly disappointing to spend several days in the field in vain without finding any trace of the geological structure or formation marked on a map. The controversy between William Smith and the first president of the Geological Society, London, George Greenough, over their geological maps is well known (Knell 2009). But, V.J. Gupta (Talent et al. 1991) went so far as to "create" his own fossils, and he polluted the geological literature to the extent that it was reduced to "story telling." V.J. Gupta's voluminous publications have strongly set back the stratigraphic and paleontological investigations in the Himalaya. As Chandrasekhar put it (Wali 1991), probably, some modesty of approach towards the earth science will pay in the long run, and one should be ready to learn from geology rather than to tell how it should be.

References

Colchen M, Le Fort P, Pêcher A (1986) Annapurna–Manaslu–Ganesh Himal. Centre National de la Recherches Scientifique, Special Publication, Paris, 136 pp (with a geological map, 1:200,000 scale)

Dhital MR, Kizaki K (1987) Lithology and stratigraphy of the Northern Dang, Lesser Himalaya. Bull Coll Sci 45:183–244 (University of Ryukyus, Okinawa)

Dhital MR, Thapa PB, Ando H (2002) Geology of the inner Lesser Himalaya between Kusma and Syangja in western Nepal. Bull Dept Geol 9(Special issue):1–60 (Tribhuvan University)

England P, Molnar P (1990) Surface uplift, uplift of rocks, and exhumation of rocks. Geology 18:1173–1177

Ganesan TM (1972) Fenestellid bryozoa from the boulder slate sequence of Garhwal. Himal Geol 2:431–451

Gansser A (1964) Geology of the Himalayas. Interscience, New York, 289 pp

Gansser A (1981) The geodynamic history of the Himalaya. In: Gupta HK, Delany FM (eds) Zagros, Hindu Kush, Himalaya, geodynamic evolution. American Geophysical Union, Washington, pp 111–121

Gansser A (1991) Facts and theories on the Himalayas. Eclogae Geol Helv 84(1):33–59

Garzanti E (1999) Stratigraphy and sedimentary history of the Nepal Tethys Himalaya passive margin. J Asian Earth Sci 17:805–827

Hagen T (1969) Report on the geological survey of Nepal. Volume 1: preliminary reconnaissance. Denkschiiften der Schweizerischen Naturforschenden Gesellschaft, Band LXXXVI/1, 185 pp (with a geological map)

Heim A, Gansser A (1939) Central Himalaya: geological observations of the Swiss Expedition 1936. Denkschriften der Schweizerischen Naturforschenden Gesellschaft, Band LXXIII, Abh. 1, 245 pp (with geological maps in colors, sections, and plates)

Jastrow R, Rampino M (2008) Origins of life in the universe. Cambridge University Press, Cambridge, 395 pp

Knell SJ (2009) The road to Smith: how the Geological Society came to possess English geology. In: Lewis CLE, Knell SJ (eds) The making of the Geological Society of London. Geological Society, London, Special Publication No 317, pp 1–47

Lakhanpal RN, Sah SCD, Dube SN (1958) Further observations on plant microfossils from a carbonaceous shale (Krols) near Nainital, with a discussion on the age of the beds. Palaeobotanist 7(2):111–120

Le Fort P (1975) Himalayas, the collided range: present knowledge of the continental arc. Am J Sci 275-A:1–44

Lyon-Caen H, Molnar P (1983) Constraints on the structure of the Himalaya from an analysis of gravity anomalies and a flexural model of the lithosphere. J Geophys Res 88(B10):8171–8191

Marques FO (2008) Thrust initiation and propagation during shortening of a 2-layer model lithosphere. J Struct Geol 30:29–38

Middlemiss CS (1890) Physical geology of the Sub-Himalaya of Garhwál and Kumaun. Mem Geol Surv India XXIV(Part 2):59–200 (with 3 plates of cross-sections and a plate of geological map in colors; scale 1 inch = 4 miles)

Miyashiro A (1994) Metamorphic petrology. UCL Press, London, 404 pp

Molnar P (1986) The structure of mountain ranges. Sci Am 255(1):70–79

Nakata T (1982) A photogrammetric study on active faults in the Nepal Himalayas. J Nepal Geol Soc 2(Special issue):67–80

Sakai H (1985) Geology of the Kali Gandaki supergroup of the Lesser Himalaya in Nepal. Mem Fac Sci Kyushu Univ Ser D Geol 25 (3):337–397

Stöcklin J (1980) Geology of Nepal and its regional frame. J Geol Soc Lond 137:1–34

Talent JA, Dongol GMS, Chhetri VS (1991) Biostratigraphic reports—spurious and dubious—from Nepal. J Nepal Geol Soc 7:9–20

Valdiya KS (1998) Dynamic Himalaya. Universities Press (India) Limited, Hyderabad, 178 pp

Wali KC (1991) Chandra: a biography of S. Chandrasekhar. University of Chicago Press, Chicago, 341 pp

Index

M.R. Dhital, *Geology of the Nepal Himalaya*, Regional Geology Reviews,
DOI 10.1007/978-3-319-02496-7

H

I

M